CISBAT

PROCEEDINGS VOL. I

INTERNATIONAL CONFERENCE

CLEANTECH FOR SMART CITIES & BUILDINGS
FROM NANO TO URBAN SCALE

4-6 SEPTEMBER 2013 EPFL

LAUSANNE - SWITZERLAND

LESO-PB
EPFL
ÉCOLE POLYTECHNIQUE FÉDÉRALE DE LAUSANNE

Schweizerische Eidgenossenschaft
Confédération suisse
Confederazione Svizzera
Confederaziun svizra

Swiss Federal Office of Energy SFOE

ZKS Fondation ZENO KARL SCHINDLER
ZENO KARL SCHINDLER Foundation
ZENO KARL SCHINDLER - Stiftung

Cambridge University

Massachusetts Institute of Technology

IBPSA CH

LABORATOIRE D'ENERGIE SOLAIRE
PHYSIQUE DU BÂTIMENT

ÉCOLE POLYTECHNIQUE
FÉDÉRALE DE LAUSANNE

CISBAT 2013

PROCEEDINGS VOL. I

CLEANTECH FOR
SMART CITIES & BUILDINGS
From Nano to Urban Scale

4-6 September 2013
EPFL, Lausanne, Switzerland

CISBAT

Schweizerische Eidgenossenschaft
Confédération suisse
Confederazione Svizzera
Confederaziun svizra

Swiss Federal Office of Energy SFOE

IBPSA-CH

Cambridge
University

Massachusetts
Institute of
Technology

CISBAT 2013

International Conference
4-6 September 2013, EPFL, Lausanne, Switzerland

CLEANTECH FOR SMART CITIES & BUILDINGS –
FROM NANO TO URBAN SCALE

ISBN Electronic version: 978-2-8399-1280-8
ISBN Print-version: Vol.I 978-2-8399-1281-5 Vol.II 978-2-8399-1282-2

Conference Host / Editor
Solar Energy and Building Physics Laboratory (LESO-PB)
Ecole Polytechnique Fédérale de Lausanne (EPFL)
Station 18, CH - 1015 Lausanne / Switzerland
leso@epfl.ch
http://leso.epfl.ch
Conference Chair: Prof. J.-L. Scartezzini
Conference Manager: Barbara Smith

Scientific partners
Cambridge University, United Kingdom
Massachusetts Institute of Technology, USA
Swiss Chapter of International Building Performance Simulation Association, Switzerland

Scientific committee
Chairman:
Prof. J.-L. Scartezzini, EPFL, Switzerland

Members:
Prof. Leon Glicksmann, MIT, USA
Prof. Anne Grete Hestnes, NTNU, Norway
Prof. Hans Martin Henning, FhG-ISE, Germany
Dr. Nicolas Morel, EPFL, Switzerland
Rolf Moser, Enerconom SA / SFOE, Switzerland
Dr Jérôme Kaempf, EPFL, Switzerland
Dr Maria Cristina Munari Probst, EPFL, Switzerland
Prof. Brian Norton, DIT, Ireland
Prof. Christoph Reinhart, MIT, USA
Christian Roecker, EPFL, Switzerland
Prof. Claude-Alain Roulet, EPFL, Switzerland
Dr Andreas Schueler, EPFL, Switzerland
Prof. Koen Steemers, Cambridge University, United Kingdom
Prof. Jacques Teller, Univ. of Liège, Belgium
Prof. Thanos Tzempelikos, Purdue Univ., USA

Members IBPSA Switzerland:
Prof. Achim Geissler, FHNW, Switzerland
Prof. Thomas Afjei, FHNW, Switzerland
Dr Stefan Barp, AFC Zurich, Switzerland
Dr Christian Struck, HSLU, Switzerland

Under the patronage of
Swiss Federal Office of Energy (SFOE)
Ecole Polytechnique Fédérale de Lausanne (EPFL)

Generously supported by
Zeno Karl Schindler Foundation

Private sponsor
SwissINSO Holding Inc.

PREFACE

"Clean Technology for Smart Cities and Buildings" was the topic of the international scientific conference CISBAT 2013, which took place in the Swiss lakeside city of Lausanne from 4 to 6 September 2013.

Designed as a platform for interdisciplinary dialog and presentations of innovative research and development in the field of sustainability in the built environment, the conference covered a wide range of subjects from solar nanotechnologies to the simulation of buildings and urban districts.

CISBAT 2013 was the 12th edition of CISBAT, whose vocation is to present new perspectives offered by renewable energies in the built environment as well as the latest results of research and development in sustainable building technology, in a setting that encourages interdisciplinary dialogue and networking at the international level. The conference assembled 270 building scientists and architects from all over the world in an effort to promote clean technologies for sustainable buildings and cities. Close to 200 scientific papers were presented during three intense days of conference.

CISBAT 2013 was organized in scientific partnership with the Massachusetts Institute of Technology (MIT) and Cambridge University. Furthermore, the organizing committee was proud to be able to count on an international team of confirmed scientists to ensure the scientific quality presented papers. This year the conference also teamed up for the second time with the Swiss Chapter of the International Building Performance Simulation Association (IBPSA-CH), to strengthen the subject of “Building and Urban Simulation”, one of the conference's leading topics.

Organised under the auspices of the Swiss federal Office of Energy (SFOE) and generously supported by the Zeno Karl Schindler Foundation, CISBAT 2013 connected researchers and projects and gave an exciting insight into research and development in the field of sustainable buildings and cities. We look forward to seeing you at the next edition.

Prof. Dr Jean-Louis Scartezzini
Conference Chairman
Solar Energy and Building Physics Laboratory
Swiss Federal Institute of Technology Lausanne

CONTENTS VOL. I

Author index see back of book

Keynotes

Nanostructured Materials for Renewable Energies

Sustainable Building Envelopes

Solar Active and Passive Cooling

Daylighting and Electric Lighting

Indoor Environment Quality and Health

Advanced Building Control Systems

Urban Ecology and Metabolism

CONTENTS VOL. II

Integration of Renewables in the Built Environment

Building and Urban Simulation

Information Technologies and Software

KEYNOTES

2013: HOW IS CLIMATE CHANGING AND WHAT ARE THE IMPACTS OF THIS CHANGE?

Summary of Keynote Lecture by Professor Dr Martine Rebetez[1,2]

1: Professor of Applied Climatology, Geography Institute, University of Neuchâtel, Espace Louis-Agassiz 1, CH-2000 Neuchâtel, Switzerland, http://www.unine.ch/geographie
2: Senior Scientist, Swiss Federal Institute for Forest, Snow and Landscape Research, http://www.wsl.ch

SUMMARY

The rise in atmospheric temperature is linked to current and future increases in concentrations of greenhouse gases but it is erratic in terms of both time and space. However, the warming of the climate system since the end of the nineteenth century is unequivocal. It is now evident from observations of increases in global average temperatures not just for the air but also for the oceans, which absorb some of the air's energy. Today's and tomorrow's air temperatures would be much higher if the oceans did not absorb both a large part of the atmosphere's additional energy and a large part of anthropogenic carbon dioxide emissions.

Together with the rise in air temperatures, we are now recording widespread melting of snow and ice across the Earth's surface, which is also consistent with absorption of a significant part of the atmosphere's excess energy by the cryosphere. The temperature increase is widespread across the globe, it is greater at higher northern latitudes, and the land has warmed faster than the oceans. Greenhouse gas emissions over the next few decades are expected to continue at or above current rates, which would cause further warming and induce many changes in the global climate system during the 21st century

The rise in extremes, more than the rise in averages, is likely to affect human populations, vegetation and animal populations most directly. The combined effects of heat and air pollution are also likely to be considerable in urban and suburban areas on account of ozone formation. One degree of temperature rise corresponds to about 150 m altitude, making some areas extremely sensitive to slight changes. If the temperature exceeds a significant threshold, allowing the spread of malaria for example, living conditions may undergo a drastic change. Among the expected positive impacts of temperature rise are a decline in cold-related mortality and morbidity.

As well as causing a sharp decrease in the global surface subject to snowfall or permanently covered by snow, temperature rises are also expected to affect snowfall altitude and melt. This will have consequences for annual water resources and availability in many areas. The dry season could become unbearable for human communities if the glaciers supplying the valleys disappear. The substantial interannual variability of precipitation patterns will play an important part, especially in South America, where the El Nino phenomenon has a considerable impact. And the situation will be all the more critical where water demand is rising as a result of population changes, changing patterns of behaviour and/or irrigation requirements which are putting more and more pressure on water resources.

Current increases in sea level rise are consistent with the increase in temperature. This phenomenon is due both to thermal expansion and melting of the ice. The latter factor was to some extent underestimated in earlier projections for the 21st century and explains their difference from projections published since 2007. The rise observed from the end of the twentieth century is largely due to increased melting in Greenland and Antarctica. Sea level rise will be a long way from stopping in 2100. The rise in sea temperature, together with ice loss in Greenland and Antarctica, will continue to affect the sea level rise for several centuries

at least. The human consequences of rising sea levels in the 21st century must be assessed in conjunction with certain other environmental factors affecting coastal stability, such as the condition of mangroves, wetlands and forests. Furthermore, the issue of sea level rise must be considered not only in terms of disappearing land but also in terms of the salinization of rivers and estuaries. Other factors may have an important impact on river discharge and thus salinization, such as human withdrawals in general, whether for irrigation or power-generation reservoirs.

Consistent with rising temperatures, significant changes have been observed in precipitation patterns, and these are expected to increase in future. These changes will, for example, exacerbate desertification in some regions such as the African Sahel. It has been observed that monsoon patterns are currently changing in several regions of the world. In regions where water supply is already problematic, the decline in total annual precipitation will constitute a major problem. In most regions, however, the threat stems mainly from the interannual variability of precipitation. This variability is generally increasing across the globe, which means that there are to be more and more periods of dryness and of heavy precipitation. The increase in the frequency and intensity of heavy precipitation events are likely to generate more flooding, landslides and mud flows.

The rise in air temperature and its corollary, the rise in ocean temperatures, will theoretically increase the intensity of hurricanes, if not their frequency, as there will be more energy in the climate system. There is observational evidence of a clear increase in intense tropical cyclone activity, particularly in the North Atlantic. Damage, especially in coastal areas, is likely to increase in accordance with an upsurge in storm and hurricane activity over the next few decades. However, actual loss of human infrastructure will depend to a large extent on exposure, the protective measures that may be taken and the state of natural environments with the potential to protect coasts and other vulnerable areas. As hurricane damage is partly due to the associated flooding, sea level plays an important part, which will probably increase in future as the level rises. Hurricane-related risks will thus be greater with a higher sea level and if the hurricane coincides with high tides and a high water period. A combination of various environmental factors and other unforeseen events will thus increasingly determine hurricane related flood risks.

More generally, the final impact of climate change will often depend on a combination of human and environmental factors that are to some extent independent of climatic factors. Temperature rise, sea level rise, hurricane intensity, changing precipitation patterns and changes in snow and ice melting patterns may each have their own individual consequences. But the most problematic consequences will often arise from the conjunction of several factors.

MAIN REFERENCES

IPCC, 2007: Climate Change 2007: The Physical Science Basis. Contribution of Working Group I to the Fourth Assessment Report of the Intergovernmental Panel on Climate Change. Cambridge University Press.

Richardson, K. 2009. Climate Change, Global Risks, Challenges and Decisions. Copenhagen, University of Copenhagen.

EUROPEAN PERSPECTIVES IN RESEARCH AND DEVELOPMENT ON SOLAR THERMAL COLLECTORS AND SYSTEMS

Summary of Keynote Lecture by Dr Gerhard Stryi-Hipp

President of the European Technology Platform on Renewable Heating and Cooling and chairman of the Solar Thermal Technology Panel of the platform

Fraunhofer Institute for Solar Energy Systems, Heidenhofstr. 2, D-79110 Freiburg, Germany

INTRODUCTION

The European Union aims at a fundamental transformation of its energy system to achieve a reduction of greenhouse gas emissions between 80 to 95% by 2050. Today, about half the final energy demand is used for heating and cooling purposes. In future, the heat demand will be significantly reduced through behavioural changes and efficiency measures, e.g. by Nearly-Zero-Energy-Buildings. However, as heat is not only used for space heating in new builds and in the existing housing stock, but also for domestic hot water and process heating, in 2050 there will still be approximately 50% of today's heat demand.

The European Technology Platform on Renewable Heating and Cooling (RHC-platform) is developing concepts showing how renewable energies can meet the entire heating and cooling demand in 2050 [1]. Within the heating and cooling sector, solar thermal energy will play a vital role. Up to now, it has only covered a minor share of less than 1% of the heating demand in Europe, although it has the greatest potential of all renewable energies for heating and cooling. One of the main reasons is that the technological potential of solar thermal has not yet been developed. In the past, public budgets for solar thermal R&D programmes have been relatively small and often solely focussed on demonstration.

On this background the European Solar Thermal Technology Panel (ESTTP) of the RHC-platform published the »Strategic Research Priorities for Solar Thermal Technology«, which describe the relevant research topics and confirms the great innovation potential of solar thermal technology [2].

R&D TOPICS FOR SOLAR THERMAL TECHNOLOGIES

To promote large deployment of solar thermal in multiple market segments, a multi-approach strategy is needed, requiring:

- a considerable increase in the number of annually installed solar thermal systems;
- an increased solar fraction of systems per building;
- a systematic development of market segments with low solar thermal penetration, and;
- a strong support for solar thermal applications in the R&D and pilot phase by increasing both the R&D effort and the number of pilot plants.

This can be attained by means of technological achievements that:

- significantly reduce the costs of solar thermal energy for different applications and for high solar fractions;
- ensure a high system performance and reliability of solar thermal systems, e.g. by system design improvements;
- allow solar thermal to play a more important role in medium temperature applications;
- boost the combination of solar thermal systems with other technologies into hybrid systems, and
- improve the production technology for solar thermal components and systems.

The R&D priorities are described in the research priorities document for applications, components and non-technological issues as follows:

Solar domestic hot water and space heating are the most common solar thermal applications today and have an important development potential for improving the cost-performance ratio and building integration. The 'Solar Active House' concept with a solar fraction above 50% is very promising, since it meets the 'Nearly-Zero-Energy-Building' requirements that will become compulsory in 2020. The R&D priorities aim to reduce costs, increase the solar fraction per building and to improve the reliability of solar thermal systems.

Non-residential solar heating applications are used to provide process heat for industrial and agricultural applications from low up to high temperatures up to 400°C. This includes large-scale solar thermal systems for district heating. R&D is needed on dedicated low, medium, and high temperature collectors, on enlarging the range of applications for increasing solar process heat and optimizing large-scale systems for district heating.

Solar cooling is a very promising application in countries with high radiation and high cooling loads. It has been demonstrated in different configurations and applications, but has only a very small presence in the market yet. A stronger uptake hinges on cost reduction, system quality improvement, energy performance enhancement, and better building and process integration improving components and enhancing system performance.

Further developments on **solar thermal collectors** should focus on new materials, coatings and surfaces, on technical improvements e.g. stagnation temperature limitation, as well as advanced technologies for medium and high temperature applications. New types of collectors such as photovoltaic-thermal (PVT), air and façade integrated should also be considered. R&D aims at increased performance with lower cost, simplified installation and cheaper maintenance, or even increased stability and more reliable long-term performance.

Thermal storage allows the short, medium, and long-term capture of solar thermal energy and enhanced solar fractions. However, it creates additional losses, increases the price of solar heat and can be voluminous if it is used as seasonal storage. R&D is needed to reach more efficient storage through better heat transfer and heat transport, to increase storage density using thermochemical or phase change materials, and to improve its reliability and efficiency.

To improve the management, monitoring and operation of a solar thermal system, **control and performance assessment** have gained in importance and urgency. The R&D priorities in this area should concentrate on new sensors, system integration and communication, as well as the development of advanced algorithms for control and performance assessment.

To encourage innovation in the marketplace, new developments in terms of R&D need to be complemented by **standards and measures for quality assurance.** The development relies also on **non-technological research and supporting measures** like professional training and education and also the necessity to strengthen the research infrastructure related to solar thermal. Furthermore, several socio-economic aspects must be taken into account, such as awareness-raising, the development of new business models for the deployment of solar thermal systems, and the need for effective public support policies.

COST REDUCTION AS KEY TOPIC

In recent years solar thermal energy is losing competitiveness due to stagnating prices for solar thermal systems while other renewable energy technologies like heat pumps and photovoltaic made significant progress in price reduction. Therefore, one main focus of R&D on solar thermal technology is the reduction of solar heat costs.

Competitiveness is not easy to define taken into account that there are many cases where solar thermal energy is already cheaper than heat produced by fossil fuels or electricity. But people usually do not have a clear picture of the competitiveness. Firstly, there is not 'one price' for solar thermal heat, since solar thermal systems vary greatly, reflecting different system types, qualities, and standards by the integration into the building. In addition, the energy yield of a solar thermal system depends on the solar radiation intensity at the installation site and the prices for heat from fossil fuels and electricity vary a lot across Europe. Therefore, competitiveness must be calculated for each system type, for each region of installation, and in comparison with the specific heat costs of the alternative heat source in that region.

Secondly, consumers usually compare today´s price for heat from fossil fuels or electricity with the solar heat costs, which represent the average costs per kWh over the entire lifetime. To achieve a fair comparison, the average costs for heat from fossil fuels or electricity over the next 20 years should be calculated and compared. The result depends greatly on the assumption made for the oil and gas price growth rate over the next 20 years, which is highly unpredictable. Since consumers usually don't take into account the fossil and electricity price increase, they systematically underestimate the competitiveness of solar thermal energy, based on the assumption that fossil and electricity energy prices will rise.

Figure 1 shows typical ranges of solar heat costs for different solar thermal systems in different European regions compared with the costs for useful heat produced by natural gas and electricity in the year 2011. Even though this is an unfavourable comparison for solar thermal energy, it is already in some cases cheaper than heat from natural gas and is in most cases cheaper than heat from electricity. But in the large solar thermal markets in Central Europe, solar heat costs are still significantly higher than the heat price from natural gas.

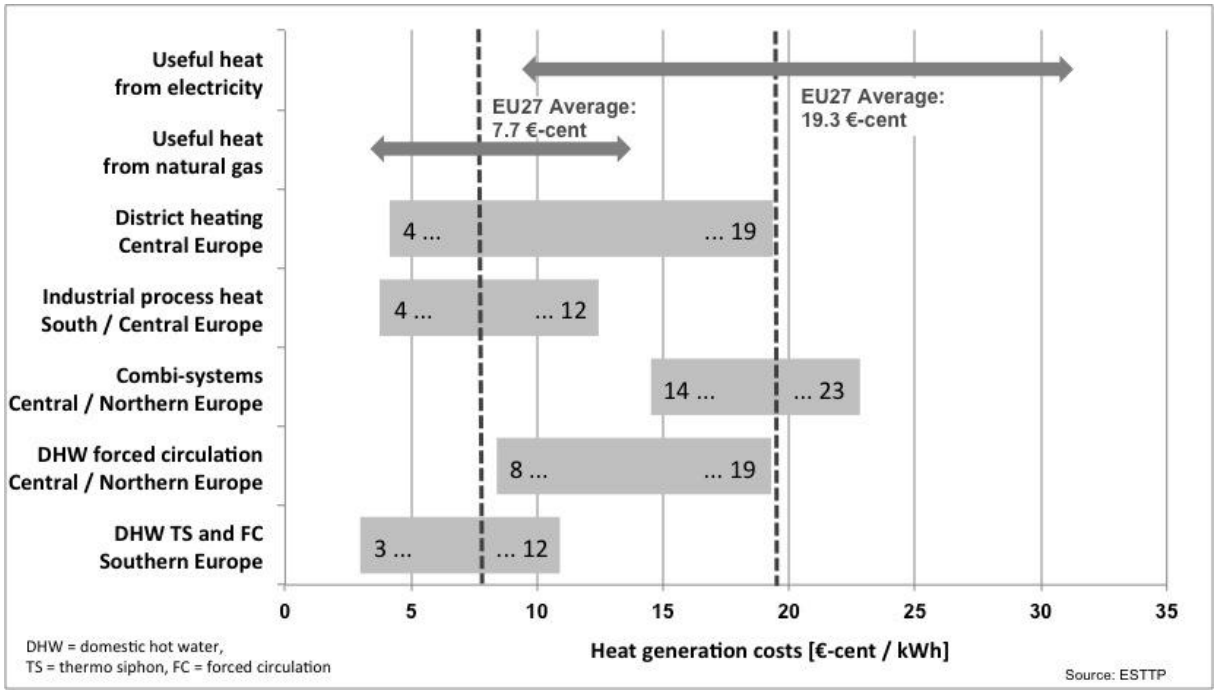

Figure 1: Ranges of heat generation costs of different types of solar thermal systems in comparison to costs for heat generated by natural gas or electricity in Europe (data of 2011)

Many of the R&D priorities described are focusing on cost reduction, which potential is vast, since solar thermal technology is still in its infancy, dating back only 30 years with low budget R&D programmes from the European Union and a few member states. How quickly the cost reduction could materialize if sufficient R&D support is given and the market

develops well can be derived from the solar thermal collector production costs reduction achieved over the past 15 years, which are shown in Figure 2. Since 1995, production costs have been cut by nearly 50%, which corresponds to a learning factor of 23%.

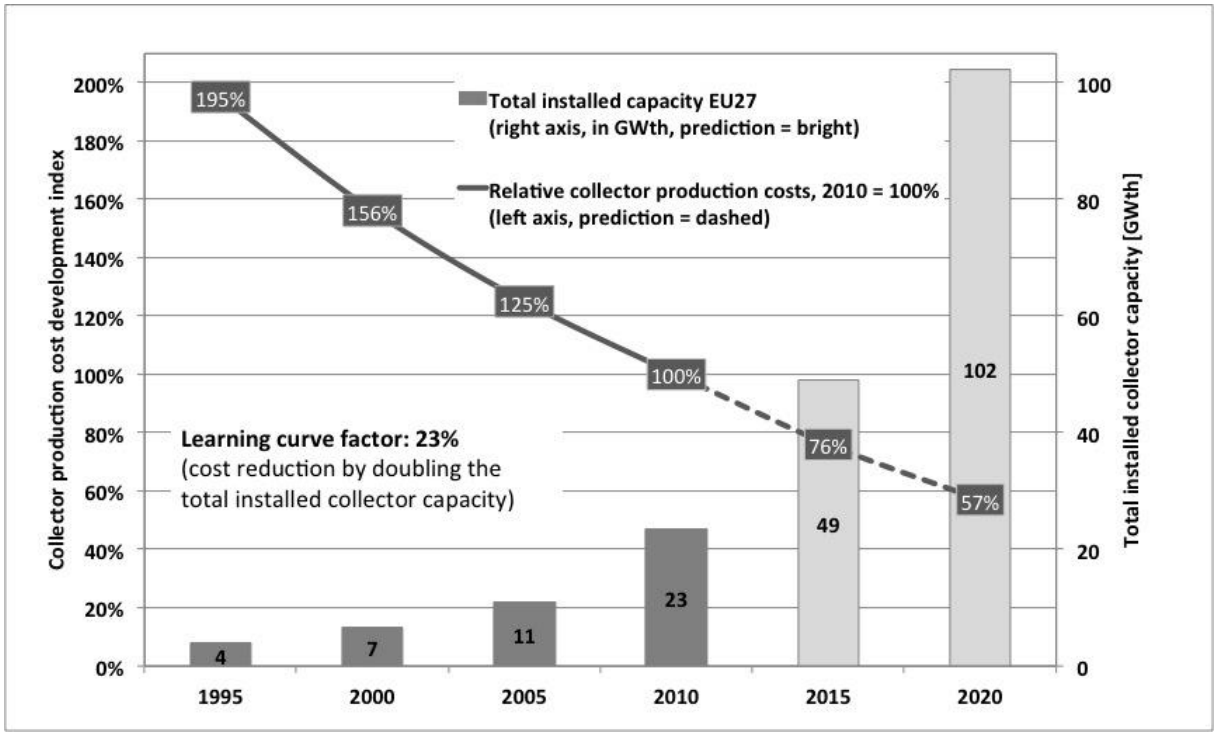

Figure 2: Development of production costs of a Central European standard module collector (flat plate, glass covered, spectral selective absorber coating, size 2.0 to 2.5 m^2) from 1995 to 2010 and projection of the cost development based on the learning curve factor (derived from the 1995 to 2010 data) and the market deployment projections of the EU member states (derived from the National Renewable Energy Action Plans of the member states)

To calculate solar heat costs, the installed solar thermal system price is relevant. Collectors represent typically between 20% and 40% of the whole system costs. Since data are only available on collector costs development they are used as indication on the system price reduction potential. Based on the improvements stimulated by the R&D priorities proposed by the platform it is expected that the price of components and systems, as well as installation, will continuously decrease and can finally be halved by 2020 for solar thermal systems.

CONCLUSION

Solar thermal energy has the potential to become a strong pillar in the sustainable energy system of the future if the solar thermal technology will be further improved. The solar thermal R&D priorities described by the solar thermal panel of the RHC-platform show the huge potential of technological improvements, which will increase the competitiveness of the solar thermal technology by reducing the solar heat costs and enlarge the applications to high solar fractions (Solar Active House), solar process heat, district heating and solar cooling.

REFERENCES

[1] European Technology Platform on Renewable Heating and Cooling, 2020-2030-2050 Common Vision for the Renewable & Cooling sector in Europe, Brussels, 2011

[2] European Technology Platform on Renewable Heating and Cooling, Strategic Research Priorities for Solar Thermal Technology, Brussels, 2012

LOW-COST AND AESTHETIC PHOTOVOLTAIC ELEMENTS FOR THE BUILT ENVIRONMENT: FAILURES, SUCCESSES AND PERSPECTIVES

Summary of Keynote Lecture by Professor Christophe Ballif [1,2]

1: Ecole Polytechnique Fédérale de Lausanne (EPFL), Institute of Microengineering (IMT), Photovoltaics and thin film electronics laboratory (PVlab), 2000 Neuchâtel, Switzerland

2: Swiss Center for Electronics and Microtechnology, CSEM PV-Center, 2000 Neuchâtel, Switzerland

The world photovoltaic market has grown tremendously over the last decade, to reach a world production of over 30 GW in 2012 (> 200 million m^2 of PV modules). Most of the modules are "standard" crystalline Si ones and are deployed in conventional PV systems, such as solar farms, large flat roofs or on regular roofs as building added elements (BAPV). The long awaited emergence of massive building integrated PV (BIPV) is not yet taking place [1]. Indeed, at a time where selling prices for "standard crystalline" modules are in the range of 70 to 90 €/m^2, where some categories of thin-film modules can even be purchased at price below 50 €/m^2, a potential exists for a new generation of PV building elements, which should come in the price order range of tiles or standard façades covering elements.

Over the last ten years, an impressive number of technical and esthetical solutions have been developed for BIPV. This includes flexible PV foils laminated on curved elements, small PV tiles of various colors incorporating crystalline cells, modules and dummies of variable size made out of standard or advanced crystalline silicon cells with dedicated support, small-size thin-film modules used as tiles and large area thin-film modules with customized shapes, size and transparency. However, most of these solutions did not gain a sizable market share and stayed limited to a few demonstration projects, leading to discontinuation of the product manufacturing. Some of the reasons why BIPV could not yet capitalize on the massive cost reduction achieved by the "standard" PV industry include:

- the manufacturing costs for specialty products, strongly linked to the volume, which creates a high entrance barrier for new products,
- the (small) size of individual products, which further increases the manufacturing and the installation costs,
- the absence of standards for roofs and façades for integration of PV elements, and/or the incompatibility of national regulations,
- the usual absence of support schemes for more innovative systems, which need to overcome a higher market entrance barrier because of the low starting volume,
- the inability of engineers, architects and of the building sector to work out common solutions that have a chance to satisfy reasonable final system price and aesthetic criteria.

After showing a few typical examples of market failures, but also successes, we will review some of the products which could gain market shares or make their entrance into the BIPV market. For instance, crystalline modules are under commercialization, in which the busbars are no more visible. This is possible thanks to the use of arrays of thin wires which replace the 2 mm wide metal ribbons, or by using cells made with metallization wrap-through technology. New approaches based on thin-film silicon allow modification of the visual appearance which can be made similar to the ubiquitous terra-cotta tile color with potential costs below 50 €/m^2 and could lead to standard low cost per m^2 PV roofing products. The use of interference filters and textured air-glass interface to create reflection in a specific part of the spectrum is also an approach to vary the color of thin film or crystalline modules, extending the range of possible products by simply modifying the front cover of the modules.

Eventually, we will also consider other urban spaces that can be used for photovoltaics. Beyond "solar carports", new approaches to deploy PV above roads or parking lots are under industrialization and could become part of tomorrow's PV landscape.

[1] P. Heinstein et al. "Building Integrated photovoltaics (BIPV): Review, Potentials, Barriers and Myths", Green 2 (2013) 125-156

Nanostructured Materials for Renewable Energies

ENERGY-EFFICIENT SOL-GEL PROCESS FOR PRODUCTION OF NOVEL NANOCOMPOSITE ABSORBER COATINGS FOR TUBULAR SOLAR THERMAL COLLECTORS

M. Joly[1], Y. Antonetti[1]; M. Python[1]; M. Gonzalez[1]; T. Gascou[1], A. Hessler[2]; A. Schueler[1]

1: LESO PB - EPFL, Station 18, 1015 Lausanne, Suisse

2: CIME – EPFL, Station 12, 1015 Lausanne, Suisse

ABSTRACT

The energy efficiency of production processes for components of solar energy systems is an important issue. Other factors which are important for the production of products such as black selective solar coatings include production speed, cycle time and homogeneity of the coating, as well as the minimization of the quantity of the needed chemical precursors. In this paper a new energy efficient production process is presented for production of optically selective coatings for solar thermal absorbers. The latter should ideally behave as a black body, absorbing a maximum of the incoming solar radiation, while minimizing energy losses by infrared radiation, acting as an infrared mirror. The used method to produce such coatings is sol-gel dip-coating

The optical and morphological properties of the Cu-Co-Mn-Si-O based triple layer have been characterized by spectrophotometry, electron microscopy and time of flight secondary electron microscopy. After optimization of the multilayer design, a solar absorptance of 0.95 and a thermal emissivity of 0.12 at 100°C have been achieved. The intermediate Cu-Co-Mn-Si-O layer was analyzed by high resolution transmission electron microscopy. The likewise obtained images show an agglomeration of crystalline grains with 10-20nm in diameter. Therefore, we can consider that the Cu-Co-Mn-Si-O phase is nanocrystalline. In order to roughly estimate the corrosion resistance of the coating in an acidic environment, a simple corrosion test in harsh conditions was designed. With respect to a commercially available durable black chrome coating, this test of corrosion resistance confirmed the durability of the novel sol-gel coating in an acidic environment.

Moreover, the excellent stability at elevated temperatures in ambient air makes the coating an interesting candidate for solar applications involving concentrated solar radiation, such as the generation of solar electricity (concentrated solar power), industrial process heating and solar cooling. For that reason, prototype coatings consisting of stacks of three individual layers were deposited on 2 meter long stainless steel tubes.

Keywords: selective solar absorber coatings; nanocrystalline spinel; induction heating; receiver tubes for concentrated solar power (CSP)

INTRODUCTION

The energy efficiency of production processes for components of solar energy systems is an important issue. One key element of solar thermal collector is the optically selective coating on the solar absorber, which should ideally behave as a black body, absorbing a maximum of the incoming solar radiation, while minimizing energy losses by infrared radiation, acting as an infrared mirror.

Different types of selective absorbing surfaces exist which are described in detail by Agnihotri et al. [1]. Selective coatings for solar thermal collectors are either produced by

traditional electrodeposition of black chrome [2], as selective paint [3], or by vacuum deposition processes such as reactive evaporation or magnetron sputtering [4-5]. In the electroplating process, toxic Cr(VI) ions are used and care has to be taken to avoid environmental pollution. On the other hand, vacuum deposition leads to large front costs because of the expensive equipment required and can be out of reach for potential producers in certain situations.

This explains the interest in developing a sol-gel process for the production of nanocomposite selective solar absorber coatings. Indeed, sol-gel processing does not require expensive vacuum equipment and allows to completely avoid the use of toxic chrome. Kaluza et al. [6] demonstrated that it is possible to reach a solar absorptance of 0.86 and a thermal emissivity of 0.11 by sol-gel method with a single layer of CuCoMnOx. Using sol-gel spin-coating, Boström et al. [7] obtained competitive properties for multilayered coatings with nitrogen annealing: Al2O3:Ni multilayered coating absorbs 97% of the incoming solar energy for a thermal emittance lower than 0.05. Recently, Bayón et al. [8] obtained highly selective coatings based on Cu-Mn-Si-O oxides that show excellent optical performance. A solar absorptance of 0.95 combined with a thermal emittance of 0.035 was achieved for coatings on aluminium substrates.

Because of its mechanical stability and the possibility of welding, stainless steel is an interesting substrate material. It can be used for cushion absorbers for domestic hot water generation, and also for receiver tubes for applications working with concentrated solar power (CSP) such as power plants for solar thermal electricity generation, co- and tri-generation. Targeting stainless steel substrates, we focus in this work on the development of multilayered sol-gel coatings for solar absorbers consisting of mixed copper, cobalt, manganese and silicon oxides (Cu-Co-Mn-Si-O). Using suitable multilayer designs, we are aiming for a solar absorptance above 0.94 and a thermal emissivity below 0.16. The coatings shall be deposited with satisfactory homogeneity on stainless steel sheets as well as on collector-sized tubes.

METHOD

The used method to produce such coatings is sol-gel dip-coating for which all the solutions have been synthetized at the Solar Energy and Building Physics Laboratory of EPFL. Solutions were obtained by dissolving the precursors in a solution based on a mixture of absolute ethanol and demineralized water. Nitric acid is added as catalyst to influence both the hydrolysis and condensation rates as well as the structure of the condensed polymer.

The solutions described above were deposited on a stainless steel (austenitic 1.4301) substrate using a dip-coating process. This technique allows to produce coatings even in ambient air at a standard room temperature. The dip-coating process comprises three main steps: dipping of the substrate in the solution, withdrawal at constant speed with formation of a liquid film at the surface, evaporation of the solvent and formation of a xerogel [9]. By thermal annealing between 400°C and 500°C in ambient air, the films are hardened and oxidized.

While the sheetlike substrates were annealed in a Vulcan® benchtop furnace during 90 minutes, a novel, fast and energy-efficient process based on induction heating was developed for the thermal annealing of the 2 meter long austenitic stainless steel tubes [10]. The coated tube was passed through a water-cooled induction coil as described in Figure 1a. An alternative (AC) current oscillating in the induction coil at frequencies between 20 kHz and 200 kHz induces a strong AC current in the steel tube, the latter heating up resistively the tubular substrate as well as the film deposited on it. Using this process, the tube and coating reach approximately 400°C within a few seconds. After a single passage of the induction coil,

the radial and longitudinal distribution of the substrate's temperature is sufficiently homogenous as shown by infrared imaging (Figure 1b).

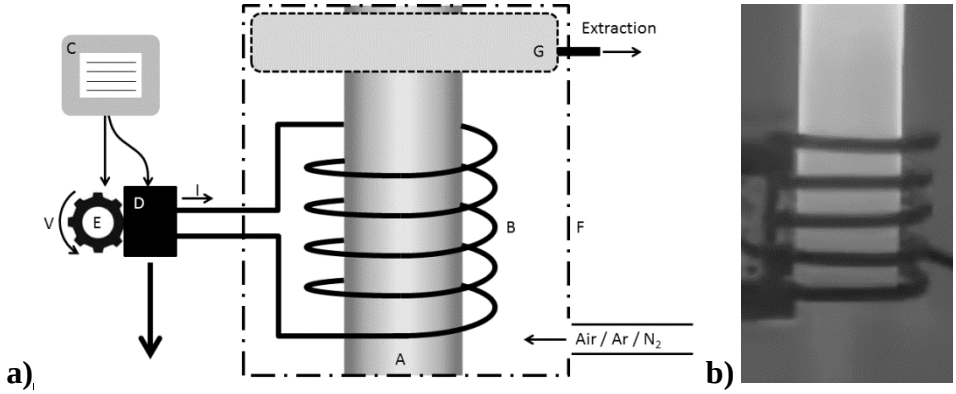

Figure 1a: Schematic representation of the device used for thermal annealing of the coating by induction heating. Austenitic stainless steel tube (A); induction coil (B); control unit (C); AC generator (D); motor (E) rotating at speed V; coil and tube are surrounded by a chamber (F); gasses emitted during thermal annealing are extracted through an exhaust pipe (G). Figure 1b: Infrared imaging of the tube during thermal annealing.

Near-normal spectrophotometric reflectance measurements (380nm – 2500nm) were performed on the produced samples. Using an Oriel MultiSpec 125TM 1/8m spectrograph with Instaspec IITM Photodiode Array Detector and an Optronic Laboratories Monochromator OL 750-M-S coupled to a NIR-sensitive PbS detector (OL 730), the solar absorptance of the coatings can be determined. Additionally, their thermal emittance at 100°C can be measured with an Inglas TIR100 emissiometer.

Structural analysis of different coatings has been performed by high resolution transmission electron microscopy (HRTEM Philips CM300). Bright field images were obtained from cleaved edge single layers deposited on silicon. These images made it possible to obtain morphological information from the deposited films.

In order to know the elemental composition of a multilayered coating on a stainless steel substrate, time of flight secondary ion mass spectroscopy (ToF-SIMS) was performed by means of an IONTOF setup, by reconstructing successive two dimensional (2D) XY measurements from the top-layer down to the substrate. The multilayered coating is composed of three layers of Cu-Co-Mn-Si oxides: Substrate // Cu-Co-Mn-O // Cu-Co-Mn-Si-O // Si-O // air. The layers were deposited successively by sol-gel dip-coating.

In order to roughly estimate the corrosion resistance of the coating in an acidic environment, a simple corrosion test in harsh conditions was designed: a drop of hydrochloric acid 25wt% is deposited on the sample and the degradation time is monitored.

RESULTS

Single layers of Cu-Co-Mn-O on stainless steel were first considered. The solar absorptance of the sample was optimized by varying the withdrawal speed. A solar absorptance of 0.86 ± 0.01 was reached for a thermal emissivity of 0.11 ± 0.01, which is fully appropriate for a single layer coating. The next step consisted in optimizing the solar absorptance of the coating by adding an anti-reflection layer on top of it. The anti-reflection layer used is made of silicon oxide (SiOx). For this double layer configuration, the thickness optimization for individual layers leads to a solar absorptance of 0.94 ± 0.01 for a thermal emissivity of 0.11 ± 0.01.

Optical characterization of the coated samples is shown in Figure 2. The spectral reflectivity is represented as a function of wavelength for a single layer coating (dotted line I) and a double layer coating (dotted line II) on a stainless steel substrate. The same graph also shows the spectral distribution of solar radiation for comparison purposes.

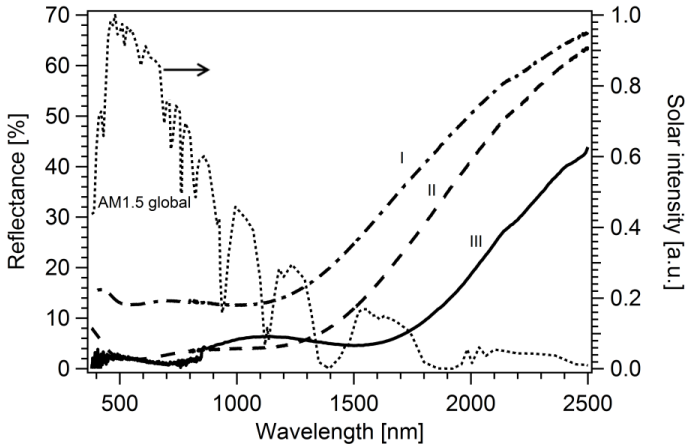

Figure 2: Spectral reflectivity of black selective samples. The dotted line I represents the reflectivity of a single layer coating (substrate / Cu-Co-Mn-O) the dotted line II represents the reflectivity of a double layer coating, (substrate / Cu-Co-Mn-O / Si-O) and the solid line III represents the reflectivity of a triple layer coating on stainless steel (substrate / Cu-Co-Mn-O /Cu-Co-Mn-Si-O / Si-O). The respective solar absorptions are α_{sol}=0.86 for I, α_{sol}=0.94 for II and α_{sol} =0.96 for III.

A graded index coating composed of three distinct layers was then designed. The intermediate layer is a mixture of the bottom (Cu-Co-Mn-O) and the top layer (SiOx). As an intermediate layer favors the light penetration and absorption, it increases the solar absorption of the coating up to 0.96 ± 0.01 with an emissivity of 0.12 ± 0.01.The monitored spectral reflectivity of this sample is also presented in Figure 2 (solid line III). The intermediate Cu-Co-Mn-Si-O layer was analyzed by HRTEM. The figure 3a shows an agglomeration of crystalline grains, 5-20nm in diameter. Therefore, we can consider that the Cu-Co-Mn-Si-O film is nanocrystalline.

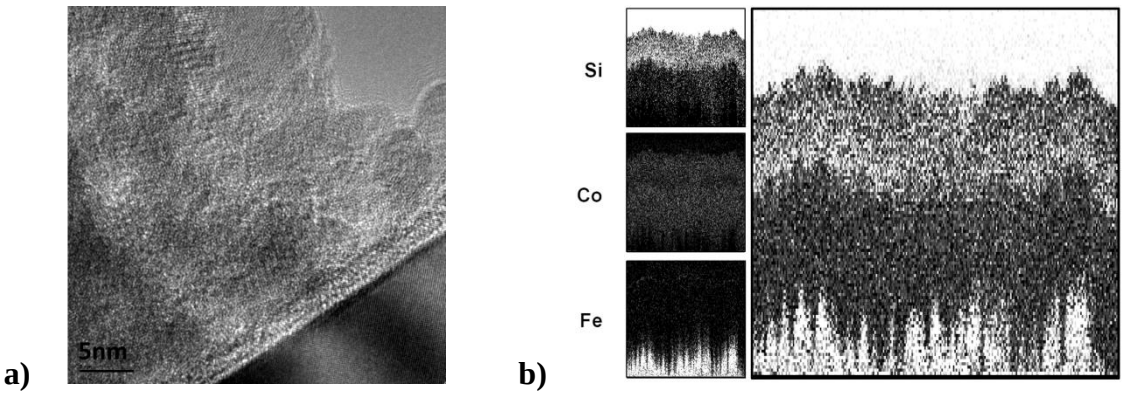

Figure 3a: Nanocrystalline structure of Cu-Co-Mn-Si-O layer by HRTEM. Figure 3b: Analysis of a graded triple layer coating by Tof-SIMS.

Two dimensional (2D) depth profile was performed by ToF-SIMS and element cross section profile is shown in figure 3b. The element specific detection of silicon (Si), cobalt (Co) and iron (Fe) allows the visualization of a stratified coating on stainless steel which confirms the presence of three distinct and superposed layers.

A simple corrosion resistance test confirmed the durability of the novel sol-gel coating in an acidic environment. For the reference black chrome coating, after less than 40 seconds in contact with HCl, a marked variation of colour is observed, reflecting a sharp deterioration of the coating. The sample produced in the laboratory with the sol-gel triple layer coating shows a complete degradation after three minutes instead of less than 40 seconds. These results suggest that the novel coating might be more durable in acidic environments than the conventional black chrome coating for unglazed flat plate collectors.

The excellent stability at elevated temperatures in ambient air [11] makes the coating an interesting candidate for solar applications involving concentrated solar radiation [12], such as the generation of solar electricity (concentrated solar power), industrial process heating and solar cooling. For that reason, prototype coatings consisting of stacks of three individual layers were deposited on 2 meter long stainless steel tubes. Because identical solutions are used for coatings of sheets and the tubes, their chemical compositions remain similar. However, the new production process which is adapted to the cylindrical geometry of the metallic tubes might result in a slightly different phase composition.

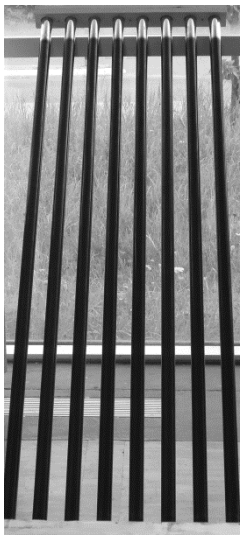

Figure 4: Two meter long black selective tubes produced in our lab using the novel selective coatings applied using the novel deposition-induction process.

For the multilayers obtained by this process, no visible cracks are observed. In addition to that, debonding or peeling effects do not occur, indicating that good adhesion of the individual layers to the substrate and to each other is achieved. The highly reproducible homogeneity of the multilayered coatings on 2 meter long stainless steel tubes is illustrated in Figure 4. The promising results obtained by the novel processing technique demonstrate the commercial potential for sol-gel stacks in concentrated solar power applications.

DISCUSSION - CONCLUSION

Multilayered thin films were designed with the aid of computer simulations based on the method of characteristic matrices. The top-layer used as a corrosion barrier is made of quartz. The challenge was to make this layer very homogeneous with as little porosity as possible. Moreover, controlling the roughness of layers deposited by a wet chemical process was crucial. All these parameters have been mastered to finally produce a coating resistant to hydrochloric acid.

The thermal emissivity of the stainless steel substrate is roughly equal to 0.10 at 100°C. While this value is acceptable for unglazed flat plate collectors, for glazed collectors, a thermal

emissivity below 0.05 is preferable. In order to achieve such values, an infrared-reflecting interlayer would have to be added.

In conclusion, this study describes the development of a black selective coating made by sol-gel dip-coating. The optimization of the optical properties led to a solar absorption larger than 0.95 with a thermal emittance close to 0.12. Corrosion and thermal resistance tests demonstrated that the coating is highly durable and may compete with existing commercial options. Finally, a graded coating consisting of a triple layer was successfully deposited on 2 meter long stainless steel tubes which can be used for concentrated solar power plants.

ACKNOWLEDGEMENTS

The authors would like to thank Prof. P. Oelhafen at Basel University and Prof. L. Zuppiroli at EPFL for their scientific hospitality. The authors are particularly grateful to Dr. L. Marot, Dr. I. Mack, Dr. V. Laporte and M. Schär for their help during measurements and to P. Loesch for his technical support. The financial support of the Commission for Technology and Innovation (CTI) is also gratefully acknowledged.

REFERENCES

1. Agnihotri, O.P., Gupta, B.K., 1981. Solar Selective Surfaces, Wiley, New York.
2. Tabor, H., 1955. U.S. Patent 2,917,817.
3. Orel, B., Vilcnick, A., Šurca-Vuk, A., Jelen, B., Köhl, M., Brucker, F., 2003. Thickness insensitive spectrally selective (TISS) paint coatings for glazed and unglazed solar building facades. Proceedings of the ISES world congress, Göteborg, O2 45.
4. Graf, W., Brucker, F., Köhl, M., Troscher, T., Wittwer, V., Herlitze, L., 1997. Development of large area sputtered solar absorber coating. J. of Non-crystalline Solids 218, 380.
5. Oelhafen, P., Schüler, A, 2005. Nanostructured materials for solar energy conversion. Solar Energy 79, 110-121.
6. Kaluza, L., Orel, B., Drazic, G., Köhl, M., 2001. Sol-gel derived CuCoMnOx spinel coatings for solar absorbers: Structural and optical properties. Sol. Energy Mater. and Sol. Cells 70, 187.
7. Boström, T., Wäckelgard, E., Westin, G., 2005. Experimental and theoretical optimization of a three layer solution chemically derived spectrally selective absorber, Proceedings of the ISES world congress, Orlando, Florida.
8. Bayón, R., Vicente, G., Maffiotte, C., Morales, Á., 2008. Preparation of selective absorbers based on CuMn spinels by dip-coating method. Renewable Energy 33, 348-353.
9. Brinker, C.J., Scherer, G. W., 1990. Sol-Gel Science: The Physics and Chemistry of Sol-Gel Processing, Academic Press, Boston.
10. Joly, M., Schüler, A., 2012. Procédé de fabrication d'éléments de capteurs solaires et éléments obtenus au moyen de ce procédé, PCT Request, P2465PC0P.
11. Joly, M., Python, M., Antonetti, Y., Rossy, J.-P., and Schüler, A, 2009. Optical selective coating for solar absorbers. *CISBAT Proceedings*, 21–28.
12. Selvakumar, N., Barshilia, H. C., 2012. Review of physical vapor deposited (PVD) spectrally selective coatings for mid- and high-temperature solar thermal applications. Sol. Energy Mater. and Sol. Cells, 98(2-3), 1–23.

SYNTHESIS AND CHARACTERIZATION OF POLYCRYSTALLINE $CuGaTe_2$ THIN FILMS

O. Aissaoui[1], S. Mehdaoui[1], M. Benabdeslem[1], L. Bechiri[1], N. Benslim[1], M. Morales[2], X. Portier[2], A. Ihlal[3].

1 : LESIMS, Département de physique Université de Annaba, BP. 12, 23200 Sidi Amar (Algérie)
2 : CIMAP, Centre de recherche sur les ions, les matériaux et la photonique, CEA, UMR 6252 CNRS, ENSICAEN, UCBN, 6 Boulevard du Maréchal Juin, 14050 Caen cedex (France)
3 : LMER, Laboratoire Matériaux et Energies Renouvelables, Faculté des sciences BP 8106 hay Dakhla 80 000 Agadir (Maroc)

ABSTRACT

Polycrystalline $CuGaTe_2$ films were deposited by flash evaporation technique on glass and (100)Si substrates. Morphological, compositional, optical and microstructural properties of polycrystalline thin films are presented. These properties were characterized using various techniques. Microstructure was studied by X-ray diffraction (XRD). Analysis of the XRD data of the powder indicated that (112) is the predominant orientation for a stœchiometric composition of $CuGaTe_2$ with a chalcopyrite structure. The lattice constants corresponding to the powder are a=5.647 Å, and b=11.990 Å. Detailed transmission electron microscopy (TEM) associated with EDXS analysis studies of $CuGaTe_2$ demonstrated that the film composition is a complex mixture of the binary (CG) as well as the ternary (CGT) phases with different compositions. The optical measurements were carried out in the 200–3000 nm wavelength range. The band gap is found at 1.28 eV corresponding to allowed direct transition and the absorption coefficient is close to $7x10^4$ cm^{-1}.

Keywords: chalcopyrite, thin films, optical properties, TEM.

INTRODUCTION

The ternary $CuInSe_2$ and $CuGaSe_2$ are I-III-VI_2 semiconductors. They have attracted much attention and became promising candidates for thin solar cell applications because of their high optical absorption coefficient, low band gap (1.05 eV and 1.68 eV at room temperature, respectively), and owing to their thermal stability [1-2]. In the last few years, much attention has been paid to $CuGaTe_2$ (CGT), another I-III-VI_2 chalcopyrite material. This ternary compound has been studied by various groups [3-7]. It has a band gap energy E_g comprised between 1.22 eV and 1.24 eV at room temperature, which is suitable for solar energy conversion. In addition, its energy gap is direct, it has high optical absorption coefficient, and it is readily made p-type [8-9].
In the present work, we report the fabrication of $CuGaTe_2$ layers on glass and (100) Si substrates by flash evaporation. The flash process was carried out in a vacuum of 10^{-5} Torr in order to investigate the morphological, compositional, and optical properties. The microstructure was analysed by TEM observations.

EXPERIMENTAL

Polycrystalline bulk $CuGaTe_2$ ingots for the flash evaporation technique was synthesized from 99.999% pure elements in evacuated quartz ampoules. Ampoules were inserted in a pipe furnace, heated up to 1200°C, kept at this temperature for 12 hours and then cooled down very slowly as described in previous papers [10]. For XRD and optical properties investigations, $CuGaTe_2$ films were deposited onto glass substrates. The layers thicknesses on glass were determined by using optical measurements. The average thickness of the deposited $CuGaTe_2$ films was about 440 nm. The structure was determined by X-ray diffraction using a diffractometer in a (θ-2θ) Brentano configuration with the $Cu_{K\alpha}$ (λ = 1.54 Å) monochromatic radiation. The cross-section and surface morphology of the $CuGaTe_2$ layers were investigated by scanning electron microscopy (SEM), using a commercial high- resolution JSM JEOL 6400 microscope equipped with an energy dispersive X-Ray spectroscopy (EDXS) analyzer.
For TEM and EDXS analyses, cross-section thin foils were thinned by mechanical polishing down to a few µm. A final ion milling was realized to reach electron transparency with a GATAN ion beam thinning machine with a dual argon ion beam, working at 3 kV, with 7° incidence angle. TEM micrographs were provided by a JEOL 2010 FEG (200kV) equipped with an EDXS analyser. The EDXS analyses were carried out with a probe of less than 10 nm in diameter. The optical properties were studied using the optical a Perkin-Elmer 9 (UV-VIS-NIR) double beam spectrophotometer (500–3000 nm).

RESULTS

1. X-ray characterization of powder

The phase's identification of the starting material was carried out by X-ray diffraction. The diffraction pattern of figure 1 shows the main peaks of the chalcopyrite structure at 2θ= 25.803°, 29.762°, 42.597°, 50.327°, 52.711°, 67.981°, 77.830°, and 83.781°. These peaks correspond to the most intense peaks given in the JCPDS cards. The lattice planes compatible with these angles are: (112), (004), (024), (132), (224), (136), (244) and (336).

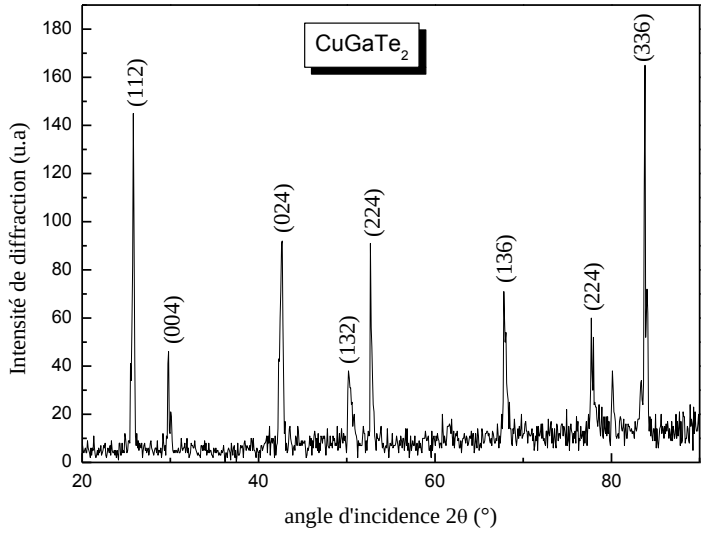

Figure 1: Spectrum of X-ray diffraction of the starting material $CuGaTe_2$

The diffraction peaks observed for the $CuGaTe_2$ films deposited at 350°C reveal that the powder exhibits a chalcopyrite structure. The calculated lattice parameters *a* and *c* are 5.647 Å and 11.990 Å, respectively and these values are found to be in good agreement with the JCPDS data (JCPDS 341500).
The grain size of $CuGaTe_2$ films deposited at 350°C has been calculated using Scherrer's formula [11]:

$$D = \frac{K\lambda}{L\cos\theta}$$

where λ is the wavelength of X-ray used, K is constant, L the full-width at half-maximum (FWHM) and θ the Bragg angle. For 2θ=25.80°, the FWHM is 0.21°. The deduced size of the crystallites is equal to 38.94 *nm*.

2. Morphology and optical characterization of the film

Figure 2a shows an SEM image of CGT layer grown at substrate temperature of 350°C, with composition (determined with EDXS) of the Cu/Ga/Te alloy at the bottom. The grains of the area of 0.24 µm size are uniformly distributed on a densely packed surface. The corresponding EDXS spectrum obtained from region 2 shown in figure 2a is presented in figure 2b. The spectrum is composed of X-ray lines of elements constituting the evaporated material.

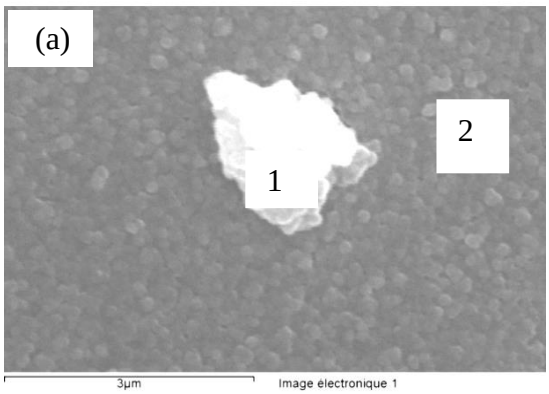

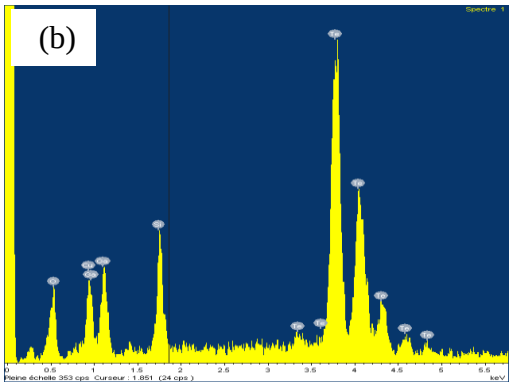

	at % Cu	at% Ga	at% Te
Region 1 :	26.68	38.57	34.75
Region 2 :	24.78	37.99	37.23

Figure 2: a) Plan view of a $CuGaTe_2$ layer obtained by SEM.
b) A typical EDXS spectrum of CGT thin film.

From optical transmission measurements (figure 3), the optical absorption coefficient α (inset of figure 3) is calculated with the equation:

$$\alpha = -\frac{1}{d}\ln\frac{T}{A}$$

where T is the transmission (transmittance of more than 80%); d, the sample thickness and A, a parameter depending of the refractive indices of the layer and the transparent substrate. It is well known that $CuGaTe_2$ is a direct band gap semiconductor. The absorption coefficient spectra close to the fundamental absorption edge can thus be formulated as follows [12]:

$$\alpha h\nu = B(h\nu - E_g)^{1/2}$$

where B is considered independent of the incident photon energy and E_g, the band gap energy. From the α vs. $h\nu$ measurement for each sample, we plot $(\alpha h\nu)^2$ against $h\nu$ (figure 4) to obtain the band gap value. The E_g value is obtained by extrapolating the linear part of the curve near the band edge for $(\alpha h\nu)^2 = 0$. The band gap of the flash evaporated polycrystalline material was found to be 1.28 eV. The band gap of $CuGaTe_2$ thin film prepared using another technique was reported to be 1.23 eV [13]. Similar results have also been reported for flash evaporated $CuGa_xIn_{1-x}Te_2$ films [14-15]. The band gap of our flash evaporated thin films is in good agreement with this value.

3. **TEM observations**

In the cross section geometry, the electron beam is parallel to the layer plane and an observation of the entire film versus thickness is possible. Figures 5a and 5b depicts a bright and dark field TEM images (Figures 5a and 5b, respectively) of a ternary $CuGaTe_2$ thin film obtained by flash evaporation.

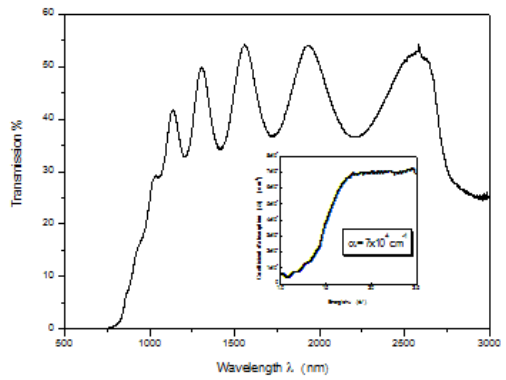

Figure 3: Transmission curve as a function of the wavelength of a $CuGaTe_2$ layer (the inset is the absorption coefficient α versus hν).

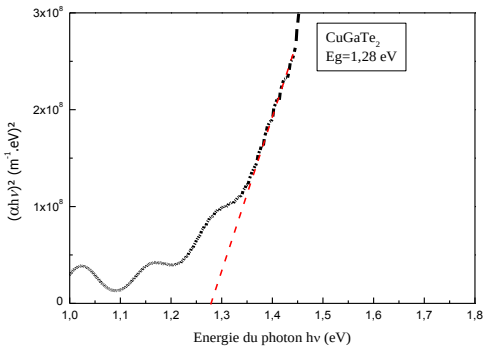

Figure 4: Plot of $(h\nu)^2$ vs photon energy $h\nu$ for $CuGaTe_2$ polycrystals

A columnar growth is observed for the lower part of the film whereas the upper part seems to be less crystalline. Figures 5c and 5d show selected area diffraction patterns corresponding to different regions of the film. Diffraction pattern obtained from the bottom of the layer (Region 1) shows well defined dotted rings, indicating a fine polycrystalline structure with a slight (112) texture. These rings correspond to lattice planes of chalcopyrite structure. These peaks are: (112), (220/024), (132/116), (332/136) and (244/228). For the (112) plane, the lattice parameters were *a*=6.07 Å and *c*=11.56 Å.

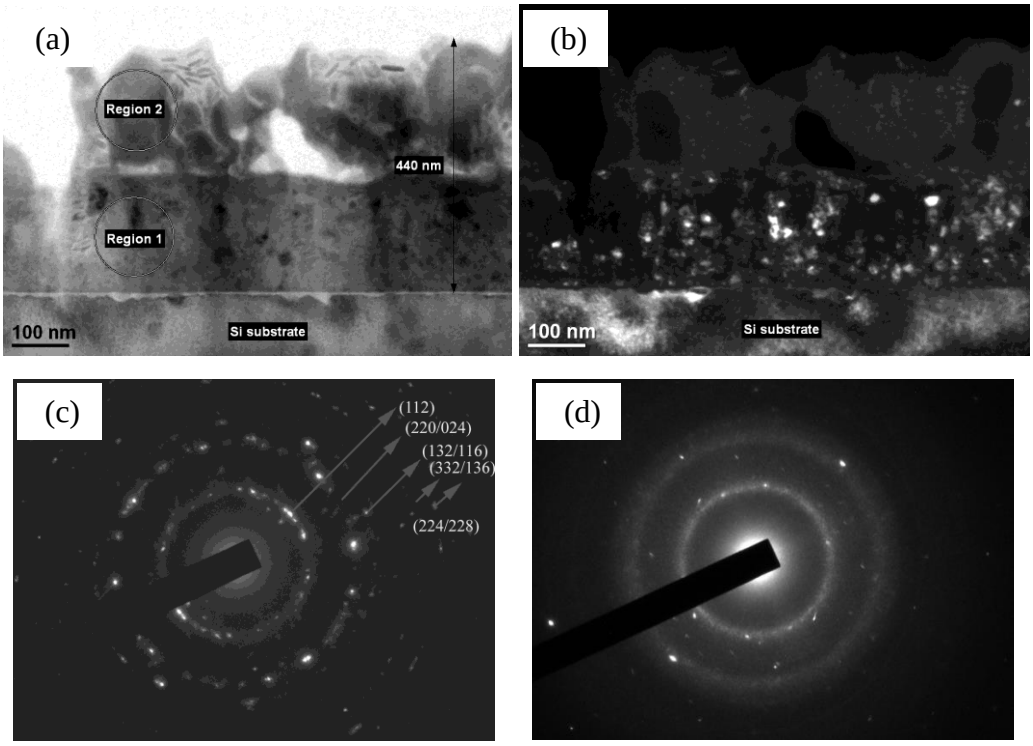

Figure 5: Cross-section transmission electron micrograph of $CuGaTe_2$ thin film grown on (100) Si at a substrate temperature of 350°C. (a) and (b) bright and dark field TEM images. (c) and (d) electron diffraction patterns from regions 1 and 2, respectively.

Figure 5d shows a typical selected area diffraction pattern of the upper layer (Region 2) which is composed of a mixture of amorphous area (diffuse rings) and crystalline grains (dotted rings). It has not been possible to identify this structure.
The upper part of the $CuGaTe_2$ film seems less crystallized than the lower part (near the substrate). It appears that the ternary $CuGaTe_2$ has reacted with the (100) Si substrate to form chalcopyrite. This result is similar to that obtained for the layers prepared by SEL technique [16]. The EDXS composition analysis revealed a small difference from the initial powder composition at% Cu=22.6, at% Ga=30.9 and at% Te=46.5. The chemical composition of binary phase CuGa is: at% Cu=41.3, at% Ga=58.6.

CONCLUSION

Using the flash evaporation technique, $CuGaTe_2$ thin layers with a thickness of about 1.07 µm grown on glass and (100) Si substrates were obtained from powder. It was found that a slight preferred (112) orientation was obtained for both thin layer and powder materials. The optical absorption coefficient α, and optical gap E_g of $CuGaTe_2$ thin films, were determined using only the transmission data. E_g and α values are 1.28 eV and $7x10^4 cm^{-1}$, respectively. A TEM microstructural analysis carried out on the samples revealed that close to the (100) Si substrate, crystallites are of chalcopyrite structure (a=6.07 Å , c=11.56 Å) are formed, and far from the substrate, it was not possible to determine the structure of the Cu_2Ga_3 binary phase due to a lack of crystallinity of the alloy.

REFERENCES

1. Guillen, C, Herrero, J: Sol. Energy Mater. Sol. Cells 43, (1996) 47.
2. Kazmerski, L.I, White, F.R, Morgan, G.K: Appl. Phys. Lett. 29 (1975) 268. Appl. Phys. 83,7867 (1998).
3. Bodnar, I.V and Orlova, N.S: Crys. Res.Technol. 21, 8, (1986) 1091.
4. Bohmhammel, K Deus P. and Schneider, H.A: Phys. Stat. Sol.(a) 71, (1982) 505.
5. Hörig, W, Kuhn, G, Moller, W, Muller, A, Neumann, H, and Reccius, E: Kristall und Technik, 14 (2), (1979) 229.
6. Neumann, H, Peters, D, Schumann, B,. and Kuhn, G: Phys. Stat. Sol.(a) 52, (1979) 559.
7. Sesha Reddy M, Ramakrishna Reddy, K.T; Hussain, O.M; Reddy, P.J: Thin Solid Films, Volume 292, Number 1, 5 January 1997, pp. 14-19(6).
8. Bodnar, I.V, Gremenok, V.F, Viktorov, I.A, and Krivolap, D.D : Tech. Phys. Lett. 24, (1998) 89.
9. Krustok, J, Collan, H, Hjelt, K, Yakushev, M, Hill, A.E, Tomlinson, R.D, Mändar, H. and Neumann, H, J: Appl. Phys. 83, (1998) 7867.
10. Benabdeslem, M, Benslim, N, Bechiri, L, Mahdjoubi, L, Hannech, E.B, Nouet, G: Journal of Crystal Growth 274 (2005) 144–148
11. Scherrer, P: Gott. Nachr. 2 (1918) 98.
12. Kireev, P.S: Semiconductor Physics, Mir, Moscow, (1978) p. 554.
13. Neumann, H et al: Thin Solid Films 61 (1979) 13.
14. Guastavino, F, Berghol, M, Sudibvo, U: Cryst. Res. Technol. 31 Ž . (1996) 489.
15. Lachab, M, Harsono, S, Attia, A.A, Llinares, C: Cryst. Res. Technol. 31 (1996) 809.
16. Bechiri, L, Benslim, N, Benabdeslem, M, Aissoui, O, Mehdaoui, S, Morales, M, Portier, X, Otmani, A, Ihlal, A. M.J Condenced Mater Volume 13 Number 3 (2011) pp 131-134.

NANOMATERIALS FOR BUILDING INTEGRATED SOLAR COOLING THROUGH THE APPLICATION OF THE WATER VAPOR ADSORPTION-CONDENSATION-EVAPORATION-DESORPTION CYCLE

D. Karamanis[1,*], E. Kyritsi[1], E. Vardoulakis[1], G. Gorgolis[1], S. Krimpalis[1], G. Mihalakakou[1], and N. Ökte[2]

1: Department of Environmental & Natural Resources Management, University of Western Greece (currently University of Patras), Seferi 2, 30100 Agrinio, Greece

2: Department of Chemistry, Boğaziçi University, 34342 Bebek, Istanbul, Turkey

ABSTRACT

Ordered mesoporous materials were tested as cooling porous materials through the utilization of the water vapor adsorption-condensation-evaporation-desorption cycle. Materials' morphology and mesoporosity were characterized with techniques like XRD, SEM, nitrogen and water vapor adsorption–desorption isotherms, thermogravimetric and UV-VIS-NIR absorbance measurements. In cyclic experiments inside a tunnel of controllable environmental conditions and simulated low-intensity solar irradiation, the maximum temperature increase in the mesoporous material due to the implementation of the water vapor cycle was much lower than natural materials as soil and marble dust. By in situ preparation of TiO_2 nanoparticles in the mesoporous material, photodegradation and decolorization of a model pollutant was observed. Therefore, different parts of the solar spectrum for simultaneous multifunctional purposes (like UV-VIS for photodegradation and IR for providing the thermal energy for phase changes) can be utilized by supporting semiconducting oxides on the mesoporous materials.

Keywords: solar cooling, nanomaterials, water vapor adsorption-desorption

INTRODUCTION

The urban heat island (UHI) is an environmental problem that results in unfavourable conditions for human health and increases in energy consumption due to the increased cooling demand. In addition, the emission of urban pollutants and the chemical weathering of building materials are higher while discomfort and even the mortality rates are increased. In order to mitigate the UHI adverse effects, several mitigation measures have been proposed like the reduction of the thermal and pollutants emissions of human origin, the increase of the green spaces in the urban environment, the use of cool materials as construction and roof materials and more specialized designs like those associated with humidification and albedo increase, photovoltaic canopies, super-hydrophilic photocatalyst-coated building surfaces with water film [1]. The proposed mitigation strategies have a limited ability for temperature reduction with both advantages and disadvantages.

In the last few years, the use of porous materials for the evaporative cooling of building has been started systematically to be studied as a sustainable and alternative way to cool the roof surface of a building or the pavement of outdoor spaces by taking advantage of the properties of porous materials [2]. According to the principle of evaporation cooling of buildings, stored water or night sorbed moisture are evaporated during the hot day and the porous surface temperature is reduced due to the release of the latent heat. Lower surface temperatures contribute to the reduction of air temperature since the intensity of heat transfer through the

*Corresponding author: dkaraman@cc.uoi.gr

cold surface is lower while the heat flow inside the building is reduced. The principle has been validated with the addition of liquid water in natural porous materials [2], synthetic and aluminum pillared clays [3] or organic polymers [4]. Recently, it was also proved by our group that the principle can be applied by moisture sorption on the highly hydrophilic natural sepiolite [5]. With overnight uptake of water vapor on porous sepiolite in 70% relative humidity (to resemble the night outdoor condition), lower surface temperatures were observed under low simulated solar irradiation in comparison to concrete due to heat absorption for water evaporation and desorption with the accompanied mass reduction. Sepiolite, a fibrous magnesian silicate made up of talk-like layers arranged in long ribbons stuck together to form the fibers, adsorbs water vapor on the external surfaces, in microporous channels and inter-fiber micropores and in larger pores that are also present between fibers [5]. Therefore the solar cooling effect can be maximized by optimizing the pores' characteristics according to the outdoors environmental conditions of solar irradiation, temperature and relative humidity.

Water molecules confined within narrow pores, with pore widths of a few molecular diameters, can exhibit a wide range of physical behaviour. The introduction of wall forces, and the competition between fluid–wall and fluid–fluid forces, can lead to shifts in transitions and a lowering of critical points (e.g. freezing, gas–liquid, liquid–liquid) that are familiar from bulk behaviour [6]. In this context, it is customary to distinguish between water vapor adsorption in the micropores of porous materials (pore widths of less than 2 nm) and mesopores (2-50 nm). In the former, micropore filling (and cooperative filling) is the dominant mechanism. In the latter, the exothermic process of capillary condensation is observed (preceded by a molecular layering on the pore walls) with the appearance of a dense liquid-like state in mesoporous adsorbents for chemical potential lower than its bulk saturating value [7]. In cylindrical mesopores, the adsorbant is confined in two dimensions, the confinement effects are greater and capillary condensation is observed at lower pressures. A similar phenomenon occurs on desorption, with the system persisting in the liquid state at chemical potentials (pressures) below the true equilibrium value. Such metastability is similar to that found in bulk liquids in the gas–liquid coexistence region, but is more pronounced in confined systems. Therefore, the principle of solar cooling with the mesoporous materials can be extended to account for all the phase changes within the adsorption-condensation-evaporation-desorption cycle as: after overnight water vapor adsorption and capillary condensation, liquid water in the mesopores will be desorbed in lower temperatures than the bulk liquids due to solar radiation absorption for providing the sensible and latent heats as well as the heat of desorption (Figure 1). In this way, the temperature of the mesoporous material surface should be highly reduced after these low-temperature solar-heat transformations.

In this work, typical well ordered silicate and aluminosilicate mesoporous nanomaterials were purchased or prepared and tested in a wind tunnel of adjustable environmental conditions in order to investigate the validity of the principle of surface solar cooling. In cyclic experiments inside the tunnel, the maximum temperature increase in the mesoporous material due to low simulated solar irradiation was determined and compared to natural soil. Prior to the tunnel experiments, water vapor sorption isotherms were perfomed while material's optical and thermal properties were characterized by UV-VIS-NIR spectrometry and thermogravimetry, respectively. Additionally, titanium nano-oxides were prepared in situ on the mesoporous structure and were applied for the photodegradation of a model compound under UV irradiation. In this way, the utilization of different parts of the solar spectrum for simultaneous multifunctional purposes (like UV-VIS for photodegradation and IR for providing the thermal energy for phase changes) was investigated.

METHOD

Materials' morphology and mesoporosity were investigates with several techniques like x-ray diffraction (XRD), scanning electron microscopy with energy-dispersive X-ray spectroscopy (SEM-EDX) and nitrogen adsorption–desorption isotherms. The thermogravimetry (TG) and differential thermogravimetry (DTG) measurements were performed on a STA 449C (Netzch-Gerätebau, GmbH, Germany) thermal analyzer. The heating range was from ambient temperature up to 150 °C, with a heating rate of 2 °C min^{-1} under synthetic air flow. Prior to measurements, the samples were put in desiccators of specific relative humidity. The optical characterization of samples with pre-determined adsorbed water vapor was conducted by a UV/VIS/NIR spectrophotometer (Lambda 950 of PerkinElmer fitted with a 150 mm diameter InGaAs integrating sphere that collects both specular and diffuse radiation) over the solar spectrum (200– 2500 nm). The equipment was calibrated with a set of Labsphere certified standards. Moisture sorption isotherms were determined by placing the samples in sealed desiccators with saturated salt solutions for controlling relative humidity while temperature was air-conditionally controlled at 25 °C.

The water sorption properties and the associated surface temperature reduction were conducted in an in-house designed and built wind tunnel of controllable conditions of air relative humidity, temperature and wind flow [Vardoulakis et al.]. The wind tunnel consisted of five parts; the setting entrance, the contraction zone, the diffuser, the test section and the fan housing. Wind flow (m^3 h^{-1}), relative humidity (%) and temperature (°C) of air inside the tunnel, the weight of the sample and the temperatures of the T-type thermocouples at the surface and middle layers of the sample cell were recorded by a CR1000 data logger (Campbell Scientific). The solar radiation was simulated with two 80 W Philips xenon lamps while the reflected radiation and the power stability of the lamps were monitored by an inverted ISO second-class pyranometer on the top of the test section of the tunnel.

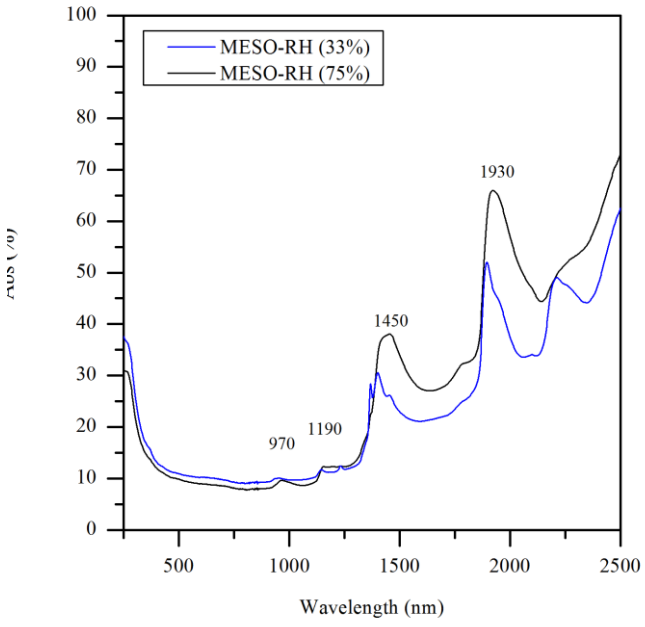

Figure 1: Absorbance spectra of the MESO material after water vapor adsorption at 33% and 75% of RH.

RESULTS AND DISCUSSION

The materials' morphology was of typical well ordered mesostructures with pore diameter between 3.2 to 3.6 nm. In Figure 1, the absorption spectrum of the mesoporous samples after the adsorption of water vapor at different humidity, are shown. In the NIR region of the spectrum for the MESO sample saturated at 75% relative humidity (RH), four main maxima located at c. 970 nm, c. 1190 nm, c. 1450 nm and c. 1930 nm are clearly observed, indicating the water vapor condensation within the mesopores. These maxima correspond to the second overtone of the OH stretching band ($3\nu_{1,3}$), the combination of the first overtone of the O–H stretching and the OH-bending band ($2\nu_{1,3}+\nu_2$), first overtone of the OH-stretching band ($2\nu_{1,3}$) and combination of the OH-

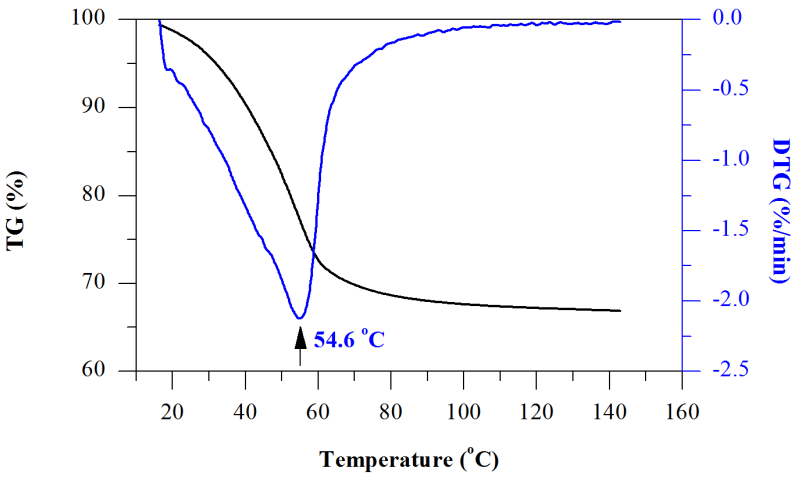

Figure 2: Thermogravimetric curves of the MESO material after water vapor adsorption at 75% RH.

stretching band and the O-H bending band ($2\nu_{1,3}+\nu_2$), respectively [8]. In the MESO sample saturated at 33% of RH, the intensity of the maxima is much lower due to the reduction of the adsorbed water vapor. By normalizing the absorption data with the solar spectral irradiance ASTM G-173, an increase of the NIR to TOTAL absorption ratio from 31% to 42% was calculated for the two samples at 33% and 93% RH, respectively.

According to the thermogravimetric results of Figure 2, there is one major endothermic peak of temperature around 55 °C where the physisorbed and condensed water is released from the mesoporous material. This "free water" bound due to condensation is being removed by the low temperature heating fluxes through evaporation and desorption from the pores. In contrast, water molecules bound to materials like zeolites through the adsorption bonds of physical adsorption demand higher heats of desorption but also higher temperatures for their removal from materials' pores. In the proposed application of materials integration in building surfaces, the temperature rise of an absorbing building surface with 0.05 reflectance can be about 34 -50 °C warmer than the ambient air in full sunlight [9]. Therefore, the mesostructured samples are appropriate for such applications and almost all of the sorbed water is expected to be removed under the summer solar radiation.

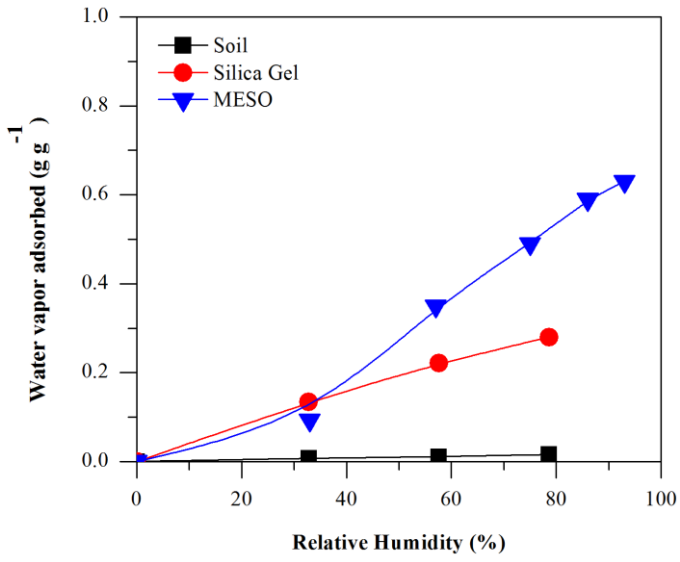

Figure 3: Water vapor adsorption isotherms on MESO, soil and silica gel at 25 °C.

The moisture sorption kinetics of the mesostructures samples followed the pseudo-first-order rate equation yielded with rate constants of 20 hours. Figure 3 shows the water vapor sorption isotherm of the tested materials at 25 °C. For comparison purposes, soil and silica gel isotherm curves are also included. Water vapor sorption in soil is very low in the whole scale of relative pressures. The isotherms of silica gel and MESO samples showed different type behaviour. The silica sorption isotherm was of type I in the IUPAC classification indicating a highly hydrophilic material with water vapor sorption ability up to 0.25 g g^{-1}. The water adsorption isotherm on the MESO sample was of type V. This is indicative of a relatively hydrophobic character in the low-pressure region of the adsorption

isotherm but with a capillary condensation step 0.55 relative pressure leading to a total filling of the pore volume and thus to a type-V isotherm (with maximum uptake more than 0.6 g g^{-1} at 93 % RH). The MESO material was further tested in the wind tunnel under simulated solar irradiation in comparison to soil and marble dust ($CaCO_3$). The radiation was provided by two low paper xenon lamps over the top of the wind tunnel. The incoming radiation at the test cell position (6x6x3cm^3) was measured with a portable digital solar meter at several points of the cell with an average of 300 W m^{-2}.

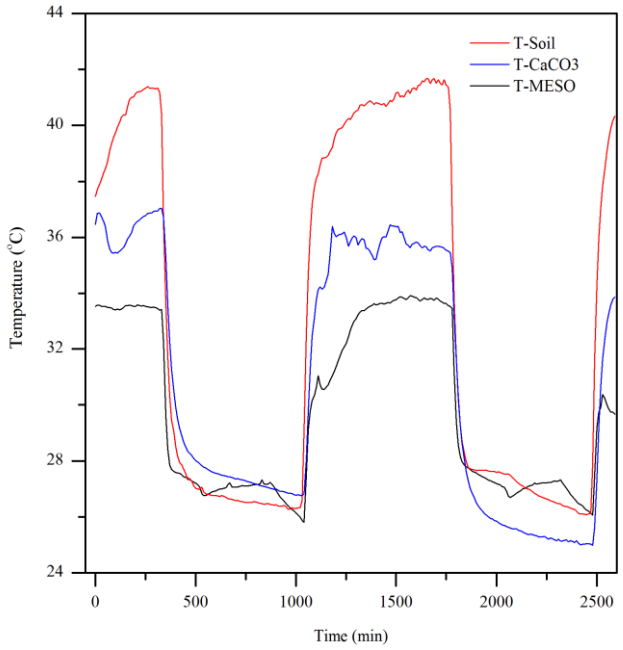

Figure 4: Temperature increase inside the MESO, soil and $CaCO_3$ samples due to low simulated solar irradiation (average 300 W m^{-2}).

Every material test lasted at least for 48 h. In the morning the lamp was turned on for a period of 12 h and the cycle was repeated for one more day. The relative humidity was raised to 70% at night with lamp off. The weight variation curve of the samples revealed that the soil and marble masses remained almost constant at night with increased RH while the MESO mass increased more than 15 % within the 12 hours period. Upon irradiation its mass decreased almost exponentially due to the evaporation and desorption of night sorbed water. Figure 4 shows the measured temperature increase in the cyclic experiments with simulated solar radiation of two continuous cycles, starting from the first lamp on as the zero time. The difference of temperature increase under simulated solar irradiation between the MESO sample and marble dust with comparable reflectance was almost 5 °C in the first irradiation hours and reduced to 2 °C at the end of irradiation. The MESO difference with the soil sample was even higher. By considering a latent heat of 2300 kJ kg^{-1} for water vaporization at the attained material temperatures, the observed MESO mass reduction of 1 g (13% of the initial mass) corresponds to 2.3 kJ of absorbed energy for water evaporation or half of the absorbed incoming radiation. The evaporation term was absent in $CaCO_3$ that exhibits comparable reflectance to MESO and very small in soil with the very low reflectance. These results indicate the material's suitability for the proposed application of evaporative cooling.

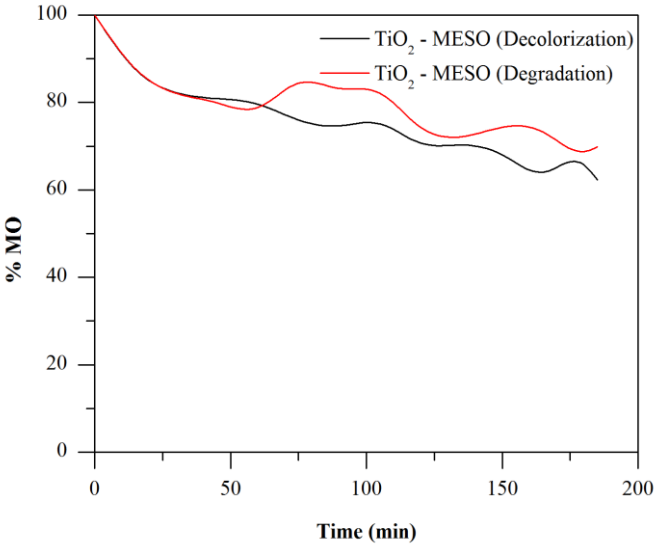

Figure 5: Photodegradation and decolorization of methyl orange in the presence of the TiO_2–MESO composites

In order to test the bifunctional capabilities of the mesoporous sample for pollutants photodegradation in addition to evaporative cooling, TiO_2 nanoparticles were *in situ* prepared in the MESO sample. A nanocomposite of low Ti concentration (7 wt% as deduced from SEM-EDX measurements) was prepared through a sol-gel method [10] and tested for the decolorization and degradation of methyl orange. Reaction systems were set-up by adding 0.1 g of the composites into 100 ml of MO in a pyrex erlenmeyer flask (located in a box with eight UV light lamps) with an inlet for the circulation of air and an outlet for the collection of aliquots. At certain time intervals, aliquots were retrieved from the flask-outlet and after filtering, the characteristic absorption intensity of MO was followed by using UV–VIS spectrophotometer. In the preliminary results shown in Figure 5, the photodegradation and decolarization kinetics are slow due to the low Ti contrentration. However, it is evident that the nanocomposite exhibits photocatalytic activity in addition to the high water vapor adsorption. Therefore, different parts of the solar spectrum for simultaneous multifunctional purposes (like UV-VIS for photodegradation and IR for providing the thermal energy for phase changes) can be utilized by supporting semiconducting oxides on the mesoporous materials.

ACKNOWLEDGEMENTS

This work is supported under the "ARISTEIA" Action of the "OPERATIONAL PROGRAMME EDUCATION AND LIFELONG LEARNING" and is co-funded by the European Social Fund (ESF) and National Resources. Thanks are due to Boğaziçi University Research Foundation (Project No. 11B05P4) and the Horizontal Network of Laboratories of the University of Ioannina for the help in materials' characterization.

REFERENCES

1. Santamouris, M., Synnefa, A., Kolokotsa, D., Dimitriou, V., Apostolakis, K : Passive cooling of the built environment – use of innovative reflective materials to fight heat islands and decrease cooling needs Inter. J. Low-Carbon Tech. 3, 71-82, 2008.
2. Wanphen, S., Nagano, K.: Experimental study of the performance of porous materials to moderate the roof surface temperature by its evaporative cooling effect. Build. Environ. 44, 338–351, 2009.
3. Vardoulakis, E., Karamanis, D., Mihalakakou, G., Assimakopoulos, M.N.: Solar cooling with aluminium pillared clays. Sol. Ener. Mater Sol. Cells 95, 2363–70, 2011.
4. Rotzetter, A.C.C., Schumacher, C. M., Bubenhofer, S. B., Grass, R. N., Gerber, L. C., Zeltner, M., Stark, W.J.: Thermoresponsive polymer induced sweating surfaces as an efficient way to passively cool buildings. Adv. Mater. 2012, 24, 5352–5356.
5. Karamanis, D., Vardoulakis, E., Kyritsi, E., Ökte, N.: Surface solar cooling through water vapor desorption from photo-responsive sepiolite nanocomposites. Ener. Conv. Manag. 63, 118-122, 2012.
6. Gelb, L.D., Gubbins, K. E., Radhakrishnan, R., Sliwinska-Bartkowiak, M.: Phase separation in confined systems. Rep. Prog. Phys. 62, 1573–1659, 1999.
7. Horikawa, T., Do, D.D., Nicholson, D.: Capillary condensation of adsorbates in porous materials. Adv. Coll. Interf. Sci. 169, 40–58, 2011.
8. Büning-Pfaue, H.: Analysis of water in food by near infrared spectroscopy. Food Chem. 82, 107–115, 2003.
9. Berdahl, P., Akbari, H., Levinson, R., Miller, W.A.: Weathering of roofing materials – An overview. Constr. Build. Mater. 22, 423–433, 2008.
10. Ökte, A.N., Sayinsöz, E.: Characterization and photocatalytic activity of TiO_2 supported sepiolite catalysts. Separ. Purif. Tech. 62, 535–43, 2008.

INVESTIGATION OF LIQUID CRYSTAL SWITCHABLE MIRROR OPTICAL CHARACTERISTICS FOR SOLAR ENERGY

P.Lemarchand; J.Doran; B.Norton

School of Physics, Dublin Energy Lab, Focas Institute, Dublin Institute of Technology, Dublin, Ireland.

ABSTRACT

Dynamic optical characterization of a Chiral Liquid Crystal (CLC) mirror manufactured to reflect the visible spectral range is performed to assess their behaviours. CLC mirrors have the advantage over prismatic, electrochromic, and gasochromic technologies of being industrially produced solid state devices with useful lives of over ten years in indoor environments. They electronically switch between a reflective and a transmissive state and can have designed spectral reflection bandwidths from 50nm to 1000nm, in the range from 380nm to 3600nm. A spectrophotometric setup spectrally characterized the transmission and reflection variation in the clear and reflective states and its dependence on light incidence angle. In the 380-780nm range, 78% to 85% average transmission was achieved in the clear state independently of the viewing angle. Average reflection varied from 70% to 45% as incidence angle varied from 0 degree to 62 degrees. In the reflective state, an average photon energy deviation of up to +73nm was observed in transmission and -38nm in reflection. Switching speed from the reflective to the transmissive state occurred in less than 200ms. A switching time back to the reflective state of about ten seconds was measured in transmission from 430nm to 680nm. However, outside that spectral range, 19 minutes was required for the mirror to reach 95% of its fully reflective state. This was also demonstrated by a variation of the reflection bandwidth from 342nm to 287nm at a fixed 20% transmission value. In the reflective state, optimum performance was maintained within a 12 degrees viewing angle; increasing the viewing angle results in increased transmission loss up to 40% and narrowed the reflection bandwidth. Their high transmission and reflection dynamic ranges shows potential for solar heat gain control of building facades, building integrated photovoltaics, solar thermal and for solar concentrator designs.

Keywords: chiral liquid crystal, switchable mirrors, optical performance, concentrator.

INTRODUCTION

Switchable technologies using prismatic [3, 11], electrochromic (EC), polymer dispersed liquid crystal (PDLC or LC) and electrophoretic or suspended particle device (SPD) [5, 6, 7] technologies are already being used for windows in buildings [12] to regulate sunlight transmission and consequently control the daylight and solar heat flow through windows, thus reducing the energy, emissions and costs associated with heating, cooling and electric lighting. Developments apply the switching capability to mirrors [1, 2, 4, 10, 13, 14]. Novel systems incorporating switchable mirrors [8, 9] have the potential to: 1) optically track the sun; 2) accept a wide proportion of the diffuse solar component; 3) optically regulate the solar heat flow; 4) optically concentrate and transfer the reflected energy onto a photovoltaic (PV), thermal (T) or PV/T absorber. These provide economic advantages in building integrated photovoltaic (BIPV) and solar thermal (BIST) applications. For higher concentration designs, effective concentration of insolation requires tracking of the diurnal and seasonal solar path changes. Such mechanical tracking systems can be quite complex and add significant costs - material, installation, use, maintenance and repair; switchable mirrors may reduce such costs [8].

Among all switchable mirror technologies, chiral Liquid crystal (CLC) mirrors (manufactured by Kent Optronics Inc., USA) are presently the only products with useful lives of over ten years in indoor environments. The mirror is built according to Kent Optronics, Inc. patent “Single Layer Multi-State Ultra-Fast Cholesteric Liquid Crystal Device And The Fabrication Methods Thereof” [1]. It is made of a single layer Cholesteric Liquid Crystal (CLC) mixture comprised within two Indium-Tin-Oxide (ITO) electrodes coated with a polyimide layer and two optically transparent substrates. In the absence

of electric field, CLC molecules with a constant pitch in a planar alignment texture naturally reflect light at a central wavelength λ_0 with a narrow bandwidth which is equal to the product of the helix pitch and the CLC birefringence. Creating a pitch gradient along the CLC helix enables the creation of a broadband reflection with a bandwidth $\Delta\lambda$ which is the product of the pitch gradient with the CLC mixture refractive index seen by the light in the reflective state. Non-destructive optical characterization of a CLC switchable mirror made to reflect the 400-700nm range is presented. The device was 5cm long by 5cm wide with two glass panes 2.5mm thick and an active thickness of 20μm. A square wave driver applied 220V at 50Hz with a duty cycle of 1 to switch the mirror to its clear state – a homeotropic texture with all CLC helices unwounded and aligned with the electric field. The driver was switched off to return the mirror to its reflective state - a planar texture with the CLC molecules naturally folding back into their designed pitch distribution. A spectrophotometric setup enabled measurement of the absolute transmission and reflection in the clear and reflective states as a function of light incidence angle. Data analysis additionally provided the switchable active spectral region, the average photon energy (APE) deviation induced by the mirror, the switching speed between clear and reflective states, the variation of the reflective spectral bandwidth and partial information on the device cycling ability and repeatability.

METHOD

Initial measurements of absolute transmission at normal incidence in the clear and reflective states were performed using the PerkinElmer Lambda 900 spectrophotometer. Due to the high transmission accuracy of the Lambda 900 (±0.08% at T=10%) the results were used as a reference to estimate the accuracy of the second spectrophotometric setup.

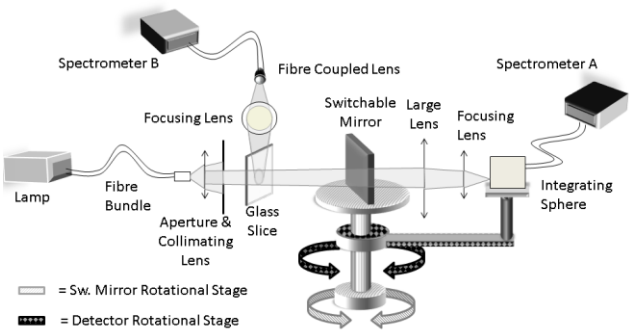

The second spectrophotometric setup consisted of a collimated halogen light source split into two beams being received by two spectrometers (Figure 1). Spectrometer B monitored the source fluctuation while spectrometer A collected the transmitted or reflected light from the CLC mirror. Detector and mirror rotational stages could rotate independently with an angular uncertainty of ±0.5 degrees providing a combined resolution of 0.7 degrees. Reflection measurements could be performed with light incidence angles between 12 and 62 degrees.

Figure 1: Spectrophotometric setup with angular resolution.

Recording the source spectrum with spectrometer B whilst calibrating the spectral intensity response between spectrometer B and A enabled deduction of the spectrum of the source that the detector stage would have recorded in absence of the mirror (A_{source}). Using transmission and reflection measurements by spectrometer A (A_{meas}), the absolute spectral transmission $T(\lambda)$ and reflection $R(\lambda)$ of the mirror were then calculated using equation 1 and the average transmission and reflection in the spectral range $[\lambda_{start}\text{-}\lambda_{stop}]$ by equation 2. Equations 1 and 2 are written for transmission and can be similarly written for reflection. Spectral absorption and absorption percentage were calculated using equations 3 and 4. It is important to note that transmissions and reflections expressed by equations 1 and 2 are the result of multiple Fresnel reflections and transmissions from all surfaces and interfaces. Consequently the absorptions described in equations 3 and 4 are not the addition of the materials' absorption but is the result of the cumulated absorption from multiple internal reflections and transmissions through the mirror.

$$T(\lambda) = \frac{A_{meas}(\lambda)}{A_{source}(\lambda)}; \quad T\% = \frac{\sum_{\lambda start}^{\lambda stop} A_{meas}(\lambda)}{\sum_{\lambda start}^{\lambda stop} A_{source}(\lambda)} \qquad (1)\ \&\ (2)$$

$$A(\lambda) = 1 - T(\lambda) - R(\lambda); \quad A\% = 1 - T\% - R\% \qquad (3)\ \&\ (4)$$

The APE of the source APE_{source} and the measurement APE_{meas} were calculated between λ_{start} and λ_{stop} by using equation 5. The APE deviation, APE_{dev}, between the measurement and the source given by equation 6 therefore expresses a shift of the spectrum's central wavelength induced by the mirror due to a variation of the transmitted or reflected intensity.

$$APE_{source} = \frac{\sum_{\lambda start}^{\lambda stop} \lambda * A_{source}(\lambda)}{\sum_{\lambda start}^{\lambda stop} A_{source}(\lambda)}; \quad APE_{dev} = APE_{meas} - APE_{source} \qquad (5)\ \&\ (6)$$

RESULTS

For light arriving at normal incidence at the mirror, spectral transmission was recorded at time intervals after switching the mirror from the clear to reflective state as shown in Figure 2. Transmission on the clear state is also provided in Figure 2 for reference and shows that the mirror was >78% transparent for all wavelengths above 405nm. At '0 min' the mirror was switched to its reflective state and the CLC molecules re-orientated themselves naturally from the homeotropic texture to the planar texture. Variation of the spectral transmission was recorded between 380nm and 780nm. The change occurred within 10-20s in the spectral range 430-680nm. A much longer time was required to achieve a stable transmission value outside that range.

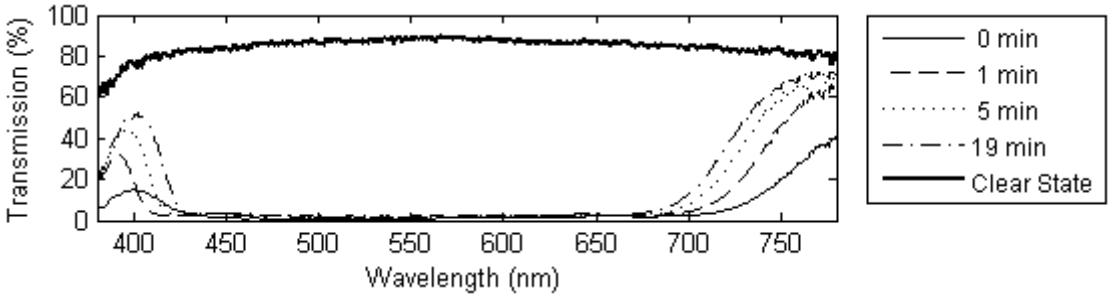

Figure 2: Variation of the spectral transmission in time after switching the mirror into its reflective state in the 380-780nm range.

Measurement of the switching time for the mirror to reach its stable reflective state was performed by calculating the average transmission as a function of time. Monitoring the wavelength bandwidth defined at 20% transmission values was used as a second measurement of this switching time (Figure 3).

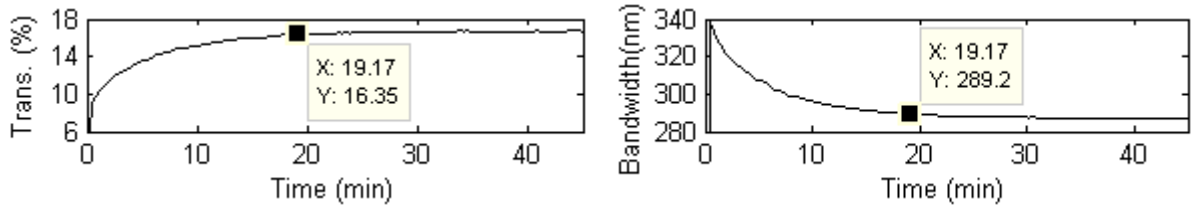

Figure 3: Switching time to reflective state. Left: Variation of the average transmission within 380-780nm range. Right: Variation of the transmission bandwidth at 20% transmission.

A polynomial fit to the transmission and bandwidth curves in time gave 8.6% transmission and a bandwidth of 341.6nm at t =0 minute. In the stable reflective state, transmission and bandwidth, respectively, were 16.8% and 286.5nm. A stability time of 19.2 minutes was defined when transmission and bandwidth reached 95% of the final value. Considering the pitch distribution, natural central wavelength reflectivity and bandwidth of CLC molecules across the active layer thickness, molecules reflecting the 430-680nm range were located in the 'core' of the layer and rotated freely in

about 10-20 seconds. Molecules reflecting outside that range were then located on both sides of the active layer, their rotation was slowed down by the anchoring polyimide coating, taking 19 minutes to rotate fully. Variation of the wings of spectral transmission are explained by the appearance of a focal conic state at a time t+Δt after switching the mirror and a range of angles of the anchored molecules in a tilted planar texture. In comparison, switching the mirror to its clear state forces all molecules to align in a measured time of <200ms.

In the stable reflective state the reflection spectrum strongly varied with light incidence angle as shown in Figure 4. At a 12 degrees angle, above 70% reflection was achieved between 420nm and 700nm. As light incidence angle was increased, the spectrum contracted and shifted towards blue wavelengths as red light was increasingly transmitted and blue light was increasingly reflected. Transmission loss increase resulted in lowering down the average reflection percentage. Molecules reflecting red light have a larger reflection bandwidth than molecules reflecting blue light and the mirror reflection bandwidth is consequently decreasing with increasing angles. The clear state reflection spectrum at a 12 degrees angle is provided in Figure 4 for comparison. One additionally noted that no significant change of the spectral measurements in the fully stable states was noticed approximately after a hundred switches.

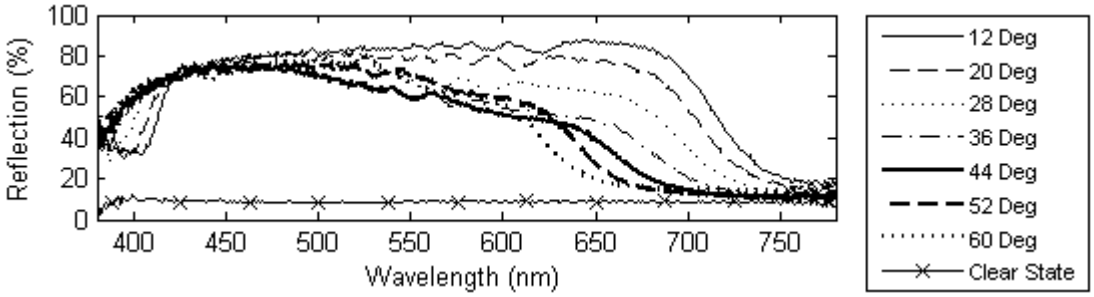

Figure 4: Variation of the reflection spectrum with light incidence angle in the reflective state. Reflection spectrum in the clear state at 12 degrees angle is given for reference.

Average transmission, reflection and absorption percentage of the mirror within the 380-780nm range are given in the reflective and clear states in Figure 5. The mirror absorption at normal incidence was calculated as the average absorption values between 12 to 62 degree angles. In the reflective state, the Lambda 900 measured 1% scattering. Using the calculated 13.4% absorption and the measured 16.4% transmission, 69.2% reflection was found at normal incidence. Moreover, the Lambda 900 measured a far-field transmission at normal incidence of 16.53±0.08% which confirmed the reliability of the angular spectrophotometric setup. The uncertainty of measurement for the latter was estimated to have been about ±0.1%. Beyond 12 degrees incidence angle, reflection continuously decreased down to 46.3% while transmission increased up to 39.7% within a 44 degrees angle.

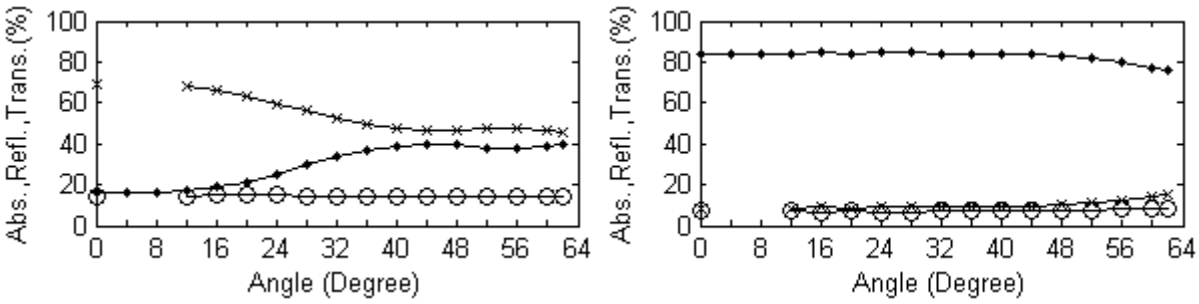

Figure 5: Average transmission (dots), reflection (crosses) and absorption (circles) in the 380-780nm range with light incidence angle in the reflective state (left) and clear state (right).

In the clear state, an averaging 7.3% absorption was found. Transmission and reflection were approximately constant and, respectively, equal to 84.3% and 8.4% up to 44 degrees. The mirror structure is comparable to two glass panes separated by CLC layer of index matching the glass, transmission decreased slowly as reflection increased, following Fresnel reflection laws for

unpolarized light with an extra ~1% reflection induced by the CLC molecules. Effectively, during the 10ms of low voltage of the applied square wave, molecules had sufficient time to rotate partially to give a tilted texture thereby achieving a partial reflective state. Defining the mirror reflection bandwidth at R=50% and considering 13.4% absorption and 1% scattering, the mirror bandwidth measured in transmission at normal incidence was 411-718nm with an average reflection up to 81.6%.

Within the 380-780nm range, covering the entire bandwidth for which the mirror reflectivity was changing within 62 degrees angle, the APE deviation results shown in Figure 6 illustrate that, in the clear state, the mirror was not changing the central wavelength of the reflected or transmitted source spectrum. However, in the reflective state, the combination of the reflection bandwidth shift, contraction and percentage decrease contributed to the APE deviation.

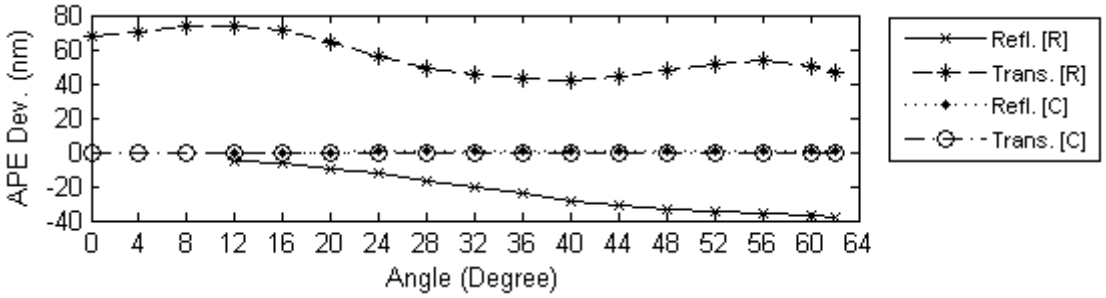

Figure 6: Average Photon Energy deviation in the 380-780nm range in reflection and transmission in the reflective [R] and Clear [C] states.

Independently of the source spectrum, the central wavelength of the reflected spectrum shifted from the source central wavelength by -4.8nm and -37.8nm, respectively, at angles of 12 and 62 degrees. In transmission, a spectral shift variation between +73.5nm and +42.2nm occurred within the 62 degrees angular view.

DISCUSSION

Results of the studied CLC mirror, manufactured to reflect the visible range, showed a strong dependence of reflection and transmission bandwidth with light incidence angle. In the reflective state, the mirror performed best within a 12 degrees angular view, maintaining above 80% reflection in the defined mirror bandwidth 411-718nm. The mirror was, however, showing switchable capability within the 380-780nm range where 69.2% average reflection was achieved and 16.4% transmission loss. In the clear state the mirror was comparable to a single glazing with an extra 1% reflection induced by the CLC molecules' partial reflection. The reflective to clear state transition occurred in less than 200ms, 10s–20s was required to come back to the reflective state in the 430-680nm region, while the mirror required about 19 minutes to reach its fully stable reflective state. Although lifetime tests have not been perform, one noted that after about a hundred switching cycles the mirror appeared to perform the same.

To use CLC mirrors in solar concentration designs it is therefore important to maintain the acceptance angle as close as possible to 12 degrees. Light lost in transmission should ideally be collected, in which case the choice of absorber and its peak efficiency needs to consider the central wavelength shift induced by the mirror. The high transmission dynamic range, potentially from 5% to 86% between reflective and clear states in the most effective spectral region of the designed mirror, enables a high control of the energy transferred through an optical system without mechanical moving parts. Since CLC mirrors can be manufactured with reflection bandwidth up to 1000nm, this is most beneficial for controlling the solar heat transfer to the absorber or for building facades. CLC mirrors designed solely to reflect infrared light and integrated to double glazing can potentially internally reflect and concentrate light to the absorber, lowering the solar heat transfer without visual impair.

A preliminary estimation of 400Wm^{-2} power consumption to switch the mirror in its clear state raises the primary technical concern. For solar concentration applications, considering 84% transmission, 402Wm^{-2} of solar power would be transmitted in the 380-780nm range. Considering the efficiencies of

the optical elements, the absorber and power conversion, such a system would incur a net energy consumption rather than a net solar energy collection. However, conceiving a mirror with a lower power consumption of 230Wm^{-2} that reflects in the 380-1380nm range would yield to 658Wm^{-2} transferred and a net solar gain of 428Wm^{-2}. The size of the CLC mirror in a solar concentration design without mechanical moving parts would then need to be a fraction of the aperture area to further improve solar gain.

Further investigations would consider: 1) optical performances at an intermediary state; 2) power consumption; and 3) lifetime in outdoor conditions to consider using switchable mirrors in solar designs.

ACKNOWLEDGEMENTS

We thank Kent Optronics for their support in this research.

REFERENCES

1. Li, L.: Single Layer Multi-State Ultra-Fast Cholesteric Liquid Crystal Device And The Fabrication Methods Thereof. US Patent US 6,674,504 B1, 2004.
2. Griessen, R., Giebels, I.A.M.E. and Dam, B.: Optical properties of metal-hydrides: switchable mirrors. Vrije Universiteit Amsterdam, 2004.
3. Griessen, R. and Slaman, M. SolSwitch™, owned by VUA. Available from: http://www.nat.vu.nl/~slaman/Optical%20switch/SolSwitch.php.
4. Kent Optronics Inc. e-TransFlector ™. http://www.kentoptronics.com/mirror.html.
5. Lampert, C.M.: Large-Area Chromogenics for Smart Windows. IEEE Circuits and Devices Magazine, 16, 1991.
6. Lampert, C.M.: Optical switching technology for glazings. Thin Solid Films, Vol 236, pp 6-13., 1993.
7. Lampert, C.M.: Chromogenic Switchable Glazing: Towards the Development of the Smart Window. Window Innovations '95, Toronto, Canada, June 5-6, 1995.
8. Norton, B.: Concentrating Solar Energy without Moving Parts. CISBAT 2009, Lausanne, Switzerland, September 2009.
9. Norton, B. and McCormack, S.: Switchable Mirrors for Solar Concentration. Patent, Dublin Institute of Technology, 2009.
10. Richardson, T.J., Slack, J.L., Armitage, R.D., Kostecki, R., Farangis, B. and Rubin, M. D.: Switchable mirrors based on nickel--magnesium films. Applied Physics Letters, Vol 78, (20), pp 3047-3049, 2001.
11. Slaman, M. and Griessen, R.: Solar collector overheating protection. Solar Energy, Vol 83, (7), pp 982-987, 2009.
12. SmartGlass International Ltd, SPD SmartGlass and LC SmartGlass. Available from: www.smartglassinternational.com.
13. Tajima, K., Hotta, H., Yamada, Y., Okada, M. and Yoshimura, K.: Electrochromic switchable mirror glass with controllable reflectance. Applied Physics Letters, Vol 100, (9), pp 091906, 2012
14. Yoshimura, K., Yamada, Y. and Okada, M.: Optical switching of Mg-rich Mg-Ni alloy thin films. Applied Physics Letters, Vol 81, (25), pp 4709-4711, 2002.

Sustainable Building Envelopes

STELA: SMART TOWER ENHANCEMENT LEOBEN AUSTRIA

Markus Bogensberger, Gangoly Hans

Graz University of Technology - Institute of Architectural Typologies, Lessingstraße 25/IV, 8010 Graz, Austria

ABSTRACT

The "smart" city of the future will not be built out of town as a super-efficient artificial city. Instead, the task will be to condense existing urban structures, curtail commuter flows, continue to build where functioning traffic networks are already in place, and at the same time to preserve agrarian and recreational landscapes.

Of particular ecological and economic importance is the fact that condensed settlement forms close to the centre use fewer resources and reduce pollution. Local authorities are therefore facing the challenge of planning and implementing sustainable development in this sense. Intensive, transdisciplinary cooperation of experts and urban facilities will be necessary to tackle this task successfully.

The demonstration and pilot project STELA: Smart Tower Enhancement Leoben Austria is a perfect example of combining high technology and urbanistic/architectural planning. It focuses on extensive thermal and technological refurbishment and enhancement of residential areas planned in the 70s by looking at the example of a residential complex in Judendorf Leoben. STELA is also a prototype for a mobility concept (E-LOBBY) that is an integral part of the building's energy system and which is to enable a new access to e-mobility.

The aim of this project is to formulate strategies for planning sustainable alternatives to the single-family home on the edge of the city. It proposes spaces for living, working and recreation whose surroundings are no longer designed primarily for cars, but once again for people.

STELA meets the conditions of the third call for tenders for further implementation of visible "Smart City" pilot and demonstration projects of the Austrian Federal government's Climate and Energy Fund, in which existing and, to a great extent, already mature technologies, systems and processes are integrated to create interactive overall systems: the aim is for companies, local authorities, and research facilities to undertake further activities towards achieving the European "Strategy Plan for Energy Technology" ("SET Plan").

Keywords: urbanistic planning, facade, Smart Tower, E-mobility

INTRODUCTION

The demonstration and pilot project STELA: Smart Tower Enhancement Leoben Austria focuses on expensive thermal and technological refurbishment and enhancement of residential areas planned in the 70s by looking at the example of a residential complex in Judendorf Leoben. The aim is also to test a mobility concept that forms an integral part of the building's energy system.

The ecological and economic starting-point is the fact that condensed settlement forms close to the centre use fewer resources and reduce pollution. Norman, MacLean and Kennedy [1], for example, demonstrated that a low density (57 individuals/ha) with 8637 kg CO2 equivalent/year compares with a higher density (269 individuals/ha) with 3341 kg CO2 equivalent/year.

But living in multi-storey buildings is only seen as attractive if living quality and amenity can rival single-family homes.

What is more, from the point of view of town planning, the range of dwellings available should cater for the desired lifestyle concepts and thus enable a balanced mix of occupants, taking demographic developments into account.

This demonstration and pilot project involves modifying an existing multi-storey residential building to meet these demands.

METHOD

Three scales

The study analyses the existing building, the adjoining district, and the effects on the urban region at three scales.

1. The urban region of the district capital Leoben
   This part involves an examination of spatial and organisational relationships between the Judendorf peninsula, the (historic) city centre of Leoben, the development area in the east of Judendorf, and the immediate natural surroundings of Leoben. The possible role of the STELA district as a recreational and leisure area is of particular importance.
2. STELA district
   Transforming a residential building into a Smart Tower is the first step in redesigning the district. This refers to the mixture of different uses in the ground-floor zones, use of the outdoor areas, and the mobility concept.
3. The Smart Tower – the real demonstration and pilot project:
   The focus here is on the apartment floor plans, façades, and the building cubage itself, the technical infrastructure, and use of the ground-floor zone including the immediately adjacent outdoor area.

Buffer zone

The building will be fronted by a thermal buffer zone, which will serve as an extension of the living area. The new façade is used to mount hybrid photovoltaic modules which generate electricity.

The integrated solar thermal elements cool the photovoltaic system when required in order to increase its efficiency and protect the buffer zone from overheating. Excess heat is dissipated by downhole heat exchangers. In winter, the geothermal energy is used to keep the new shell at the right temperature.

The new shell will be applied in modular construction and is designed for successive construction for step-by-step renovation of the building.

Additional living area will be created by a structural extension, taking advantage of and at the same time optimising the geometry of the building.

Also, floor plans will be modified by means of efficient interventions. The standard apartment will be replaced by a varied range of apartments with different usable floor areas.

Integrated Mobility concept

As part of the mobility concept, the ground floor zone will be converted into an E-LOBBY car sharing mobility centre with additional public and commercial uses.

In connection with the PV façade elements and the energy storage facilities of the e-mobiles parked in the building, the result is a finely attuned concept for energy supply and energy provision.

The project is conducted by a transdisciplinary team capable of handling both the technical, commercial, aesthetic and sociological questions involved.

This approach can then be extended to the immediately adjoining buildings in the district after the demonstration project has finished. This will allow the urban development effects to become effective.

RESULTS

The aim of the project is to test in practice the adaptability of a specific existing building, taking the current inhabitants and the underlying legal and financial conditions into account. In addition to ecological and economic refurbishment, the focus is above all on amenity and living quality and integrating the measures into an urban context.

The procedure will be documented and evaluated and can be applied as a method for an innovative form of building renovation to numerous residential complexes throughout Austria and beyond.

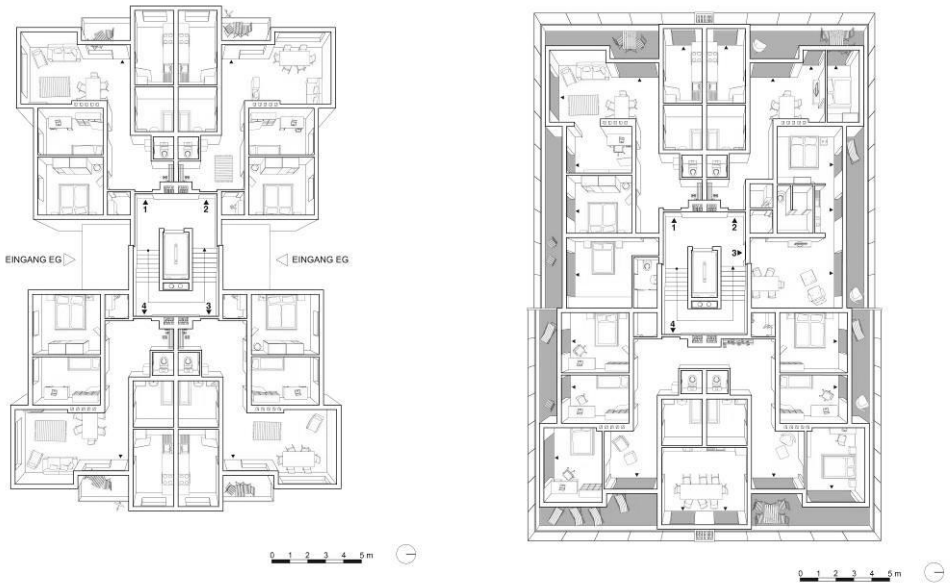

Figure 1: Typical floor plan before and after the transformation

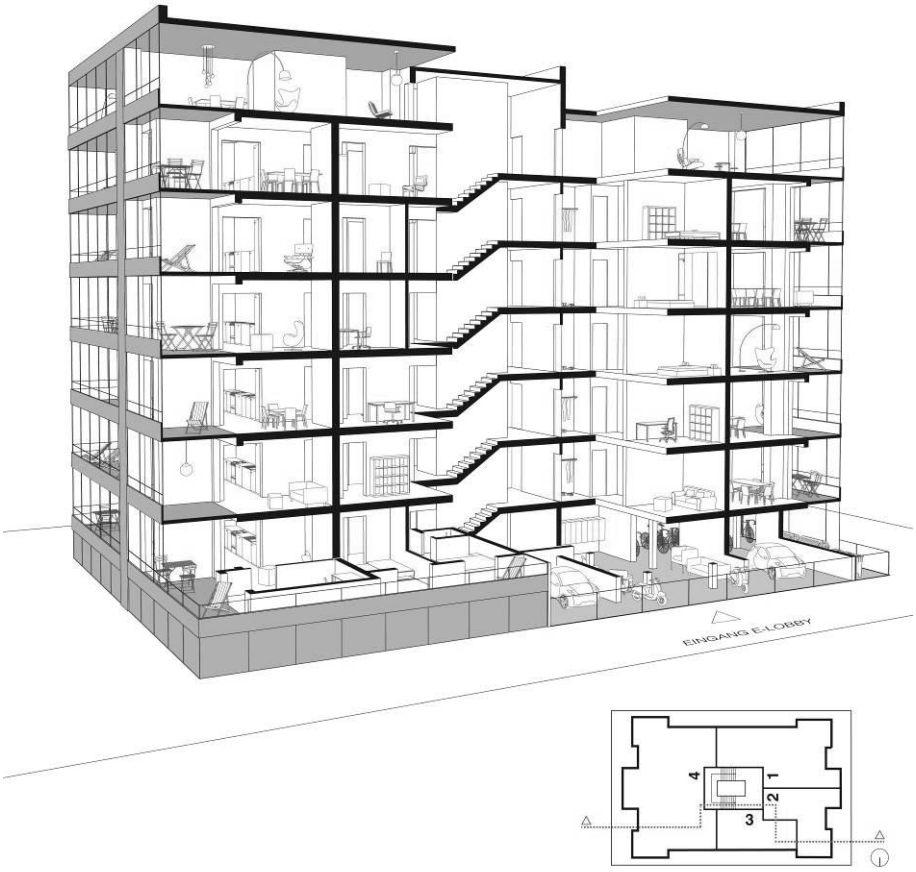

Figure 2: 3D Section Smart Tower

DISCUSSION

The additional value created by the project results from the integrated overall concept of the project, that ensures occupants and citizens greater quality of life with in-house mobility amenities than is currently the case. All in all, this increases the appeal of Leoben as a place to live. Thanks to the stakeholder process and the involvement of inhabitants in designing "Their Smart Tower", the municipality gains additional importance as a citizen-friendly city with future perspectives. The result would be a completely new reference project for combining a residential building, mobility centre, and public use in a "Smart Tower", a project which could spread further in the regional, national and international context.

Thanks to the exemplary renovation, revitalisation and enhancement of a pilot residential building, a showcase example is created for the district of energy-based refurbishment in combination with mobility facilities and new living space design, leading to synergy effects for other smart urban developments. By activating previously unused living space potentials, the lower heat requirements of the buildings thanks to the innovative thermal buffer zones, the mobility centre (E-lobby) in the entrance area, the modular mode of construction, etc., the project will cut CO2 emissions. The possibility of multiplying the project results within the city and outside the region is given thanks to the nature of the project and the use of results from the accompanying monitoring and evaluation.

The project district acts as a prototype for an extensive number of existing buildings that will need to be refurbished in the years to come and that are therefore available for use.

In addition to the ten towers of the STELA district, there is a large number of comparable buildings which could be renovated in the manner described. In terms of the overall area of Austria, several hundred potential residential towers can be assumed, with 120 such buildings in the municipal area of Graz alone.

In the long term, converting part of the existing residential buildings is a viable option above all in Eastern Europe. Owing to the economic situation and the currently reduced pressure of investment, buildings in good residential areas could prove particularly suitable to begin with. In the event of carrying out such projects in larger series resulting in sinking prices, the smart tower system could prove competitive on a large scale.

ACKNOWLEDGEMENTS

Commissioned by:

The Municipality of Leoben, urban planning and urban development section.

Conducted by:

Graz University of Technology - Institute of Architectural Typologies. Head of the institute: Prof. Hans Gangoly.

Project partners:

Energie Steiermark AG, Gangoly & Kristiner Architekten ZT-GmbH, IBO – Österreichisches Institut für Baubiologie und Bauökologie, Institute of Building Theory, Graz University of Technology, Institute of Bearing Structure Design, Graz University of Technology, Montanuniversität Leoben (Chair of Thermoprocess Technology, Chair of Economics and Industrial Management, external institute), neukühn OG, Norbert Rabl ZT-GmbH, Sammer & Partner Ziviltechnikergesellschaft mbH., VATTER & Partner ZT-GmbH Bauphysik / Gebäudezertifizierung, Velo Vital Consulting GmbH

REFERENCES

1. See: “Comparing High and Low Residential Density: Life-Cycle, Analysis of Energy Use and Greenhouse Gas Emissions, Jonathan Norman; Heather L. MacLean, M.ASCE; and Christopher A. Kennedy” Journal of Urban Planning and Development, March 2006.

APPLICATION OF MULTIPLE CRITERIA DECISION MAKING TO RENOVATION OF MULTI-RESIDENTIAL HISTORIC BUILDINGS

N. Galiotto[1,2]; F. Flourentzou[3]; P. Thalmann[4]; L. Ortelli[5]; P. Heiselberg[1,2]; M-A. Knudstrup[1,6]

1: Strategic Research Centre for Zero Energy Buildings, 57 Sohngaardsholmsvej, DK-9000 Aalborg, Denmark

2: Aalborg University, Department of Civil Engineering, 57 Sohngaardsholmsvej, DK-9000 Aalborg, Denmark

3: Estia SA, PSE, CH-1015 Lausanne, Switzerland

4: EPFL, Economics and Environmental Management Laboratory, Station 16, CH-1015 Lausanne, Switzerland

5: EPFL, Construction and Conservation Laboratory, Station 16, CH-1015 Lausanne, Switzerland

6: Aalborg University, Department of Architecture, Design & Media Technology, 6 Østerøgade, DK-9000 Aalborg, Denmark

ABSTRACT

Although the necessity for renovation of the existing building stock is commonly acknowledged, very low renovation rates are observed in practice. With 1% of the buildings renovated annually, it would take 100 years to upgrade the existing building stock to a more sustainable level. In most countries, incentives have so far not had sufficient impact on the rate and depth of the renovations. A very common obstacle in the decision process for building renovation is the conflict between multiple goals. In an early stage of the decision process, stakeholders have the possibility to block a renovation project without any cost. When stakeholders act individually and the project does not meet their goals perfectly, the easiest solution is to reject it. Alongside owner decision makers and authorities, tenants and tenant associations also have a blocking power. Yet, it is rare to find a renovation project, which fulfills simultaneously and optimally all three pillars of sustainability. Multiple criteria decision making methodologies can help to improve the decision environment and handle the whole space of constraints. It therefore leads the stakeholders to find consensual solutions. In this paper, we show on a case study how existing and newly developed evaluation methods were used to determine a convenient renovation scenario accepted by all the stakeholders. The building is a multi-residential historic building constructed in the early twentieth century. EPIQR+ method was used to evaluate the building deterioration, energy performance of refurbishment scenarios and the renovation costs. PETRA method was used to evaluate the quality of the historic building conservation. It was also used to evaluate the economic impact on tenants and the impact on the value of the building. In order to assess the indoor environment quality and the comfort of use, questionnaires were distributed to the tenants. Finally, so as to provide the stakeholders with a comprehensive comparison between different possible scenarios, a synthesis of the evaluation of all criteria was made with HERMIONE multiple criteria aggregation method. The results of the holistic multicriteria analysis change the perception of the stakeholders and their attitude towards the renovation of the building envelope.

Keywords: multiple criteria decision making, building renovation, multi-residential buildings, energy efficiency, historic building conservation, impact on tenants, profitability.

INTRODUCTION

In order to meet durably our society's present and future needs, sustainable development is eventually universally seen as a key. In building construction and renovation, this approach is often interpreted as a reconciliation of numerous conflicting objectives or criteria. While two millenniums ago Vitruvius succeeded picturing architecture as a triad of reconcilable qualities (solidity, utility and beauty), today' sustainability principles are more multifaceted and fuzzy. In this paper, we deal with various pillars of sustainability for the selection process of a historic multi-residential building renovation scenario. The first conflict that one may meet in the process of renovating historic buildings is found in sociocultural values. While individually, building tenants normally prefer maximizing their comfort and health conditions without caring much about heritage preservation, most communities want to preserve architecture heritage. During the decision making process, these sociocultural factors are likely to be in conflict with economic factors. Indeed, building owners seek to maximize the profitability of the operation and tenants to minimize the corresponding impact on the rent level while comfort and architecture heritage preservation generally do not increase the profit or decrease the rent level. Finally, the sociocultural and economic preferences may be in conflict with environmental factors: in order to reduce the impact on the environment, the operation might need to go against an optimal improvement of the occupants' comfort or a total preservation of the architecture heritage. In addition, the operation may not be the most profitable for building owners or for tenants. In this paper, we show how HERMIONE, qualitative multiple criteria aggregation method [1], supported by existing and new evaluation methods, has helped stakeholders to find a consensual solution.

METHODS

Collection of data

The decision making process was iterative and divided into various stages: a collection of data, a generation of scenarios, parallel evaluations and a synthesis. If during the synthesis, no scenario gave enough satisfaction, new scenarios were generated and a new iteration occurred. Quality criteria were selected prior to the collection of data. The criteria were the following: level of deterioration and obsolescence, the energy performance, the impact on the architecture heritage, the economic impact on the tenants, the indoor environment quality and the profitability of the renovation. The collection of data was supported by the EPIQR method [2]. The initial goal of the EPIQR sister method was to support the diagnosis of a building in order to give the level of deterioration and obsolescence of the building, and based on that, give a cost estimation to refurbish the building in a state of pre-deterioration [2]. EPIQR has therefore a triple approach to diagnosis: a visual inspection, complete and systematic, so all sub-elements of the building are examined, a short survey based on a qualitative interviewing and/or a questionnaire sent to the owner or tenants and finally, an analyses of various renovation scenarios. In the studied case, tenants were questioned about their indoor environment. The method has now evolved so it can support more ambitious building renovations.

Generation of scenarios

The generation of scenarios was a stage during which the experts based on their expertise generated renovation scenarios in diverse levels of performance or quality. Only the scenarios with a possible interest were kept for further analysis. If no scenario was agreed on after evaluation and synthesis, new scenarios were generated. This stage was also supported by the EPIQR method [2].

First iteration generated scenarios:

- Scenario 1: the existing building is left as it is.
- Scenario 2: A minimum of measures are applied. The architecture heritage is preserved.
- Scenario 3: Measures are applied to reach a minimum level of comfort and energy performance. The architecture heritage is preserved.
- Scenario 4: Measures are applied in order to comply with the label Minergie [3]. The architecture heritage is still preserved.

Second iteration generated scenario:

- Scenario 5: Measures are applied in order to comply with the label Minergie, keeping a good level of comfort but diminishing the economic impact on the tenants. The architecture heritage is still preserved.

Evaluations

In order to evaluate the quality of each renovation scenario, a combination of methods has been used. The evaluations have been divided into two parts: evaluation of the impact on the building and evaluation of the impact on the tenants or on the profitability of the operation.

Impact on the building – Preservation of the architectural character

Internationally, various buildings are recognized for their extraordinary architectural qualities. For that reason, they are legally protected. In Switzerland as well as in other European countries, specific legal instruments are intended to protect the architectural character of these buildings. In the other hand, others do not have extraordinary architectural qualities but still participate to the feature of an urban context and belong to cultural heritage. These buildings are not as clearly protected legally and therefore, poor preservation works applied on such buildings are unfortunately often seen, justified by a reduction of the economic burden. The main objective of PETRA is to provide reasonable criteria to evaluate the preservation of the general character of such buildings, this without imposing severe rules. The method guides towards the selection of a more optimal balance between beneficial preservation of the architectural character and the corresponding costs [4]. In order to find out those reasonable criteria, it has been chosen to put in foreground the general architectural character, which is to say that all elements contributing have to be maintained, repaired or replaced by similar elements, giving priority to visual and functional aspects. Criteria have consequently been defined as the following: architectural value, authenticity, site integration, uniqueness, representativeness, historical and cultural value and affective value [4]. The evaluation of the present state of historical buildings is to be done by an expert, capable to critically evaluate the work requested. The final result of the evaluation method PETRA is a scale showing the respect of the original architectural feature as well as the energy consumption improvement. Promoters can then easily define the best balance between these two aspects and their financial impact, and orientate their actions according to their scope.

Impact on the building – Deterioration, obsolescence and energy performance

Historic buildings with cultural heritage are often deteriorated and obsolete, in terms of function but also in terms of energy performance. Before renovating, it is therefore important to evaluate the existing building and possible renovation scenarios in order to estimate how the levels of deterioration, obsolescence and energy performance can be improved and at what cost. We have performed such an evaluation thanks to the EPIQR method [2]. The method is based on a collection of data, a questionnaire for the tenants and an inspection of the building. In order to evaluate the level of degradation, the building was decomposed into 50 elements. For each building element, we chose the type that corresponded to the actual building and we decided which level of deterioration fit best the actual state of the building element that we observed during the inspection (see [2] for codes of deterioration). The obsolescence was

evaluated with the same logic than the degradation of the building elements through inspection of each building element and on an expert-based. To evaluate the energy performance of the building, a simplified energy balance calculation based on EN832 has been used through EPIQR+ interface. The method accounts for direct solar gains and natural ventilation and the calculations are performed on an hourly basis from which the annual energy consumption was then estimated [2].

Impact on the tenants – Indoor environment quality of the building

In order to identify the potential problems of indoor environment and the degree of dissatisfaction of the tenants, a questionnaire dealing with indoor environment quality was developed. It was inspired by existing questionnaires [5, 6]. Before being sent to the tenants, the new questionnaire was approved by the realtor. Furthermore, the questionnaire was developed in a very concise form and with a simplified vocabulary to increase the chances of completion. The question themes were sorted in comfort criteria and sub-criteria. The treated criteria were the following: thermal conditions, air quality, acoustics, daylight and artificial lighting and functional comfort.

Economic impact on the tenants and profitability of the renovation

PETRA has been developed to help the building owner with comparing the intervention scenarios defined above on economic criteria. The corresponding tool proposes a list of 50 components describing the building, together with standard time spans before each component must be either maintained or rehabilitated. Maintenance and rehabilitation costs are estimated as a standard proportion of 30%, respectively 50% of construction cost for each component, but the users can replace these standards by their own estimates. They are also invited to indicate the additional cost of rehabilitation at a higher standard, for instance with a higher energy performance. Finally, the users indicate for each component the EPIQR deterioration code, and the degree of urgency. Based on this information, the tool proposes for each component a date of intervention – maintenance or rehabilitation. Again, the users can deviate from these proposals, in particular to group interventions on related components. The tool further plans future interventions based on maintenance and rehabilitation time spans, for a full century. It thus makes it possible to estimate intervention costs for every one of the next 100 years. It can do so for a scenario that has the minimum of necessary interventions, a scenario that selects always the interventions that increase the standard, and a scenario whereby the users select for each component whether they wish to do the minimum or the upgrading. The tool also considers a no-intervention scenario that lets the building gradually degrade with only minimum maintenance that insures building safety. The time series of intervention costs enters, for each scenario, a discounted cash flow (DCF) model of property valuation. Another central element of the DCF is the time path of rents, which is set based on the choice of interventions in each scenario. In the other scenarios, legal rules about rehabilitation costs pass through to rents are applied, with the possibility for the users to postpone rent increases when they consider that these increases are too harsh for the tenants. Combined with a treatment of risks and uncertainties at the level of the cash flows, the DCF model calculates the internal rate of return of the interventions of each scenario compared to the no-intervention scenario. Given a risk-free discount rate, it can also calculate a risk-adjusted present value of the cash flows for each scenario, i.e. the value of building for each scenario. Any of the two indicators can be used by the building owner to select the most profitable scenario.

Synthesis

The synthesis was done thanks to the application of HERMIONE method [1]. HERMIONE is a qualitative and constructivist multiple criteria analysis method. The method is transparent

and unacceptable compensation is made unacceptable. This means that scenarios, not clearly comparable, remain distinguishable. Furthermore, the complexity of the task is reduced to a level where substantial information is not lost. The decision maker is therefore able to interact with the problem and able to aggregate the different factors in his mind or through simple aggregation rules [1]. HERMIONE is capable of dealing equally with both qualitative and quantitative aspects. For more simplicity and a clearer presentation of the results, HERMIONE's evaluation scale has been slightly modified in this paper. Based on a qualitative justification or quantitative thresholds, evaluations have been made for all criteria on each scenario and then directly transposed onto a seven rank colored scale from A to G (Figure 1.a). The seven rank colored scales have been conserved in the construction of the final results to help the stakeholders to aggregate the different factors in their mind. The aggregated result (Figure 1.b) has then been attached to the results in order to stimulate a discussion around the suggested scenarios. To obtain this aggregation, A and B evaluation results have been considered as part of the favorable rank (green), C, D and E results as part of the neutral rank (yellow) and F, G as part of the unfavorable rank (red). The aggregated result for one scenario is therefore given as a color out of a three colored rank scale, green for a favorable scenario, yellow for a neutral scenario and red for an unfavorable scenario (Figure 1.b).

Figure 1.a and 1.b: Respectively evaluation and aggregation scales

RESULTS

The results are presented by a set of scale graphs (Figure 2). Each row represents a scenario. Each column represents a type of evaluation with the last column representing the aggregated results (according to HERMIONE). The four first lines represent therefore the first iteration of scenarios and the fifth line, the second iteration. Through the setting up of the objectives and criteria, the stakeholders agreed that a good renovation scenario shall have no unfavorable evaluation (evaluations F and G) while having a majority of favorable evaluations (evaluations A and B). This was thus converted as an aggregated result being favorable (green result) in the condition where at least half (50%) of the evaluations were favorable (evaluations A and B) and no evaluation (0%) was unfavorable (evaluations F and G). Beforehand, unfavorable, neutral and favorable ranks were defined for every evaluation. This approach corresponds well to the definition of a sustainable renovation since well distributed factors from all three sustainability pillars are represented. During the first iteration of scenario generation, no alternative was good enough. Indeed, scenario 1, scenario 3 and scenario 4 had all at least one unfavorable evaluation (evaluations F and G). Furthermore scenario 1, scenario 2 and scenario 3 had far less than 50% of favorable evaluations (evaluations A and B). This brought all the stakeholders to a new discussion. They finally agreed that the easiest way to generate a compliant scenario was to work from scenario 4 since it had already more than 50% of favorable evaluations and just only one unfavorable evaluation (evaluation G) needed to be converted to a neutral evaluation (evaluation C, D or E). This unfavorable evaluation was a too important economic impact on the tenants. Indeed, despite a reduction of the energy bill, in order to keep the operation profitable, the building owner had to impact some share of his investment on the tenants' rents. Throughout the second iteration, two solutions were therefore suggested to bring the unfavorable evaluation (evaluation G) to a neutral evaluation (evaluation E) without influencing much the other

evaluations. A first solution, not acceptable for the building owner, consisted in replacing progressively the tenants by tenants who are satisfied with the new rent level. A second solution, more progressive and therefore more acceptable, consisted in spreading out the renovation measures over time.

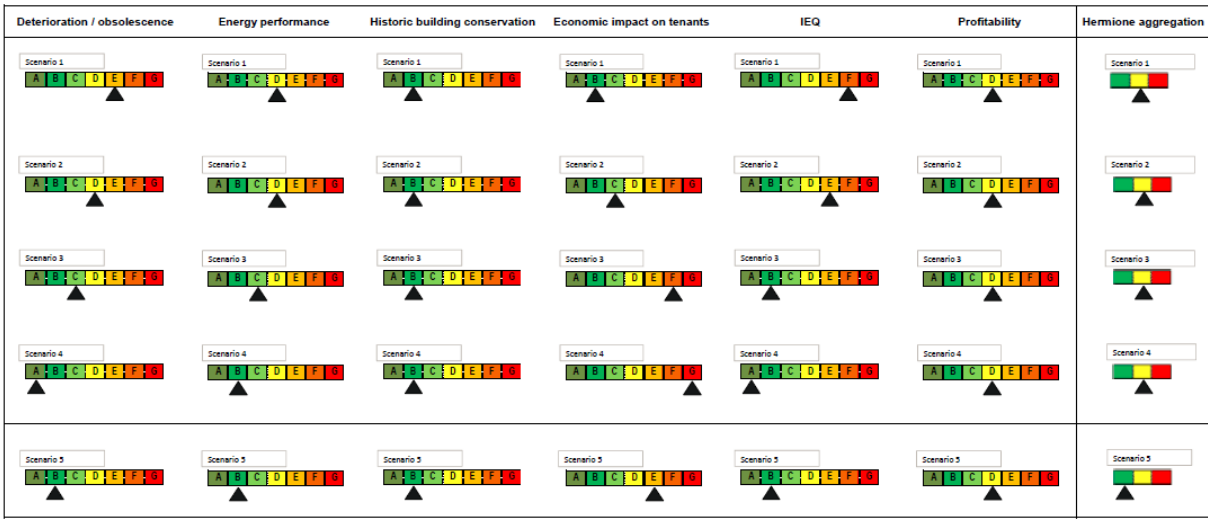

Figure 2: Evaluation and aggregated results

CONCLUSION

Sustainable renovation is a field with numerous challenges. Various contradictory criteria need to be fulfilled simultaneously under unpredictable human influences. A particularly complicated case is the renovation of tenancy buildings with cultural heritage: those projects have often performance criteria in clear opposition and therefore ambitious goals are difficult to achieve. We have showed in this paper how HERMIONE, qualitative and constructivist multiple criteria analysis method, combined with flexible evaluation methods, EPIQR and PETRA methods, lead the stakeholders to find a consensual solution with ambitious goals. The holistic multicriteria analysis changed the perception of the stakeholders and their attitude towards the renovation of the building. The methods used were a support that made the decision making easier and more coherent. They however never decided for the decision makers.

REFERENCES

[1] F. Flourentzou, G. Greuter, C. Roulet, Hermione, une nouvelle méthode d'agrégation qualitative basée sur des règles, Proc.58èmes journées du groupe de Travail Européen Aide Multicritère à la Décision, Moscow (2003) 9-11.

[2] EPIQR Renovation, Estia SA, EPIQR, un outil d'aide à la décision pour la réhabilitation des bâtiments d'habitation. (2004).

[3] http://www.minergie.ch. 2013.

[4] G. Roch, Projet PETRA - Rapport d'activité. 1.1.2011 – 31.12.2011 (2012).

[5] C.A. Roulet, Santé et qualité de l'environnement intérieur dans les bâtiments, PPUR, 2004.

[6] P.M. Bluyssen, EPIQR and IEQ: indoor environment quality in European apartment buildings, Energy Build. 31 (2000) 103-110.

ON THE DETERMINATION OF CLIMATE STRATEGIES FOR A MULTIFUNCTIONAL ENERGY RETROFIT FAÇADE SYSTEM

I.G. Capeluto; C.E. Ochoa

Climate and Energy Laboratory in Architecture, Faculty of Architecture and Town Planning, Technion – Israel Institute of Technology, Haifa 32000, Israel

ABSTRACT

The vast majority of the existing European residential building stock needs energy upgrading to comply with present regulations, reduce consumption and emissions, as well as to improve comfort conditions. Current refurbishment methods are unsuitable to obtain short-term results. Façade retrofitting provides a good solution as residential envelopes account for 20-30% of total building energy consumption. However, common prefabricated systems do not adapt to every situation and climate, and make buildings look the same despite their location.

The European Union FP7 project MEEFS has the objective of developing modular façade retrofit systems that achieve comfort and energy efficiency, while addressing the shortcomings mentioned above. We present here the methodology to determine suitable climatic design strategies for each project location, through diverse technologies that can be supported on a modular construction system.

The methodology had three stages: First, climate characteristics for the European continent were examined for common trends using the Köppen climate classification. Representative cities were chosen for each climate zone. In parallel, data from previous EU projects was used to characterize the existing residential building stock, such as U-values for external walls and windows. Project partners collected and determined information for façade features and dimensions in the representative cities. These elements were used to assemble a basecase typical building and apartment unit for computer simulation in each location.

Second, strategies for each climate were determined based on the psychometric chart for human comfort. These were: glazing type, insulation, shading, ventilation and façade albedo. Based on cost and structural feasibility, ten strategy combinations were also studied. For the third stage, energy consumption from applying each strategy and their combinations on the basecase were calculated and analysed for the representative cities.

As a result of this methodology, strategies were ranked for energy use and presented in an easy to use graphical form. Potential technologies that fulfil the strategies were identified. These will be incorporated into the prefabricated modules according to a cost optimization analysis. The strategy selection method will be abstracted into a computer tool.

Keywords: Retrofit, energy efficiency, climatic design, prefabrication, design method

INTRODUCTION

Highly demanding regulations concerning energy use have been developed in the European Union (EU), Switzerland and Norway, but most of their existing residential building stock does not comply with them [1]. New buildings in Europe grow at only 1% per year [2]; making retrofitting necessary to achieve code compliance, reduce consumption and emissions, as well as to improve comfort conditions of the occupants.

Traditional refurbishment methods are unsuitable to cover the large number of buildings involved. Extended execution times can raise concerns from inhabitants due to prolonged

disruption of their lifestyle. As the residential envelope accounts for 20-30% of total building energy consumption, placing mass-produced prefabricated elements over the existing façade is a viable solution [3].

However, commonly found prefabricated systems have setbacks such as lack of adaptation to variable building geometries and climate zones. Being mass-produced provides the same appearance in every location. An energy retrofit also presents the challenge that most of the variables are already defined, but the solution has to perform as close to a new building.

The EU-funded project MEEFS [4] has the objective to develop a modular façade system for apartment refurbishment, achieving energy efficiency while addressing the shortcomings mentioned previously. The project involves a total of 16 partners. This paper presents initial findings related to the methodology for selecting climatic design strategies the system has to follow according to each location, evaluations for each strategy in terms of energy savings and identification with readily available technologies for competitive cost.

METHOD

Weather classification

The Köppen-Geiger climate classification was used to study weather types across Europe. Observed data for the period 1976-2000 was used [5], taking into account energy-related characteristics such as heating degree days (HDD). This led to identify three main climate distributions, described as follows:

The North climate zone approximates to Dfb, Dfc and Cfa climate types. HDD values are higher than 4000. It is found in Scandinavian and Baltic countries, together with those in eastern and central Europe. The Centre climate zone corresponds to the Cfb climate type, with HDD values between 2500 and 4000. It includes Benelux, Germany, France and the United Kingdom. The South climate zone corresponds to Csa and Csb climate types. HDD day values are lower than 2500, and is located in the Iberian Peninsula and Mediterranean Basin.

Thirteen representative cities spread in the climate zones were selected to study local characteristics, building stock typologies and building regulations (Figure 1).

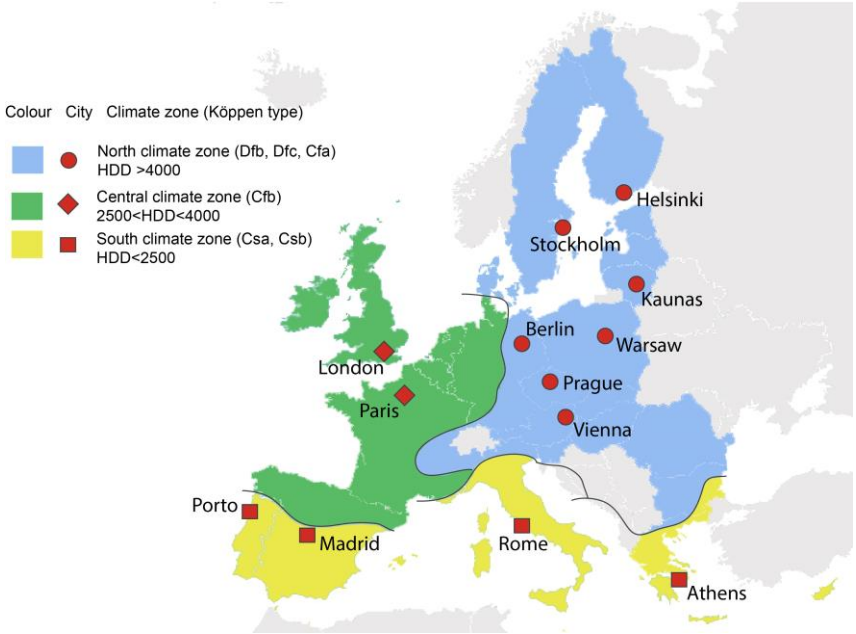

Figure 1: Climate distributions in the European Union and location of representative cities. Parentheses indicate Köppen-Geiger classification. HDD = Heating degree days

Defining characteristics of the building stock

Partners consulted and analysed data from a large number of projects that have characterized the EU building stock erected after 1945, for example TABULA [6]. U-values for opaque and glazing areas, as well as typical wall sections, were determined for the representative cities. It was found that the main materials in exterior walls are clay bricks and concrete. Insulation is present mostly in Central and North regions of Europe.

Dimensions of façade features such as distance between slabs and window areas were measured using a custom-developed BIM tool applied on digital photographs and drawings of apartment facades. Although there is no clear-cut dimension for slab distance, window areas do correspond roughly to each climate zone. For example, large glazed areas are found in southern regions while smaller ones in northern ones.

Databases such as Eurostat were used to determine most widespread HVAC systems. Among them, water-based heating systems are present with different variants (district heating, central boiler, etc.). Independent air conditioning units are frequently found in the south of Europe, with the rest of the continent using mechanical or natural ventilation for summer loads.

Definition of the basecase

From the databases, a typical residential floor size was defined with measurements 14.0x40.0 metres. The apartment unit has dimensions 13.5 (width) x 7.0 (depth) x 2.70 (height) metres, with only one external façade. Partitions and slabs are assumed as adiabatic. The four main orientations (North, South, East and West) were evaluated. Window areas and insulation levels change according to the city being modelled, with smaller openings and higher insulation assigned to climates where heating is predominant.

Definition of climatic strategies and energy calculations

Weather files of the representative cities were used to examine comfort conditions using the psychometric chart. The ASHRAE HOF 2005 [7] comfort model was applied, with indoor effective temperature limits of 20°C to 23.3°C at 50% relative humidity (RH). Analysis between RH and temperature for each location is automated through the software Climate Consultant [8]. An example of the output is shown in Figure 2. A series of façade-based strategies are needed to control internal humidity, regulate solar radiation, ventilation and maintain internal heat gains according to the demands of each region.

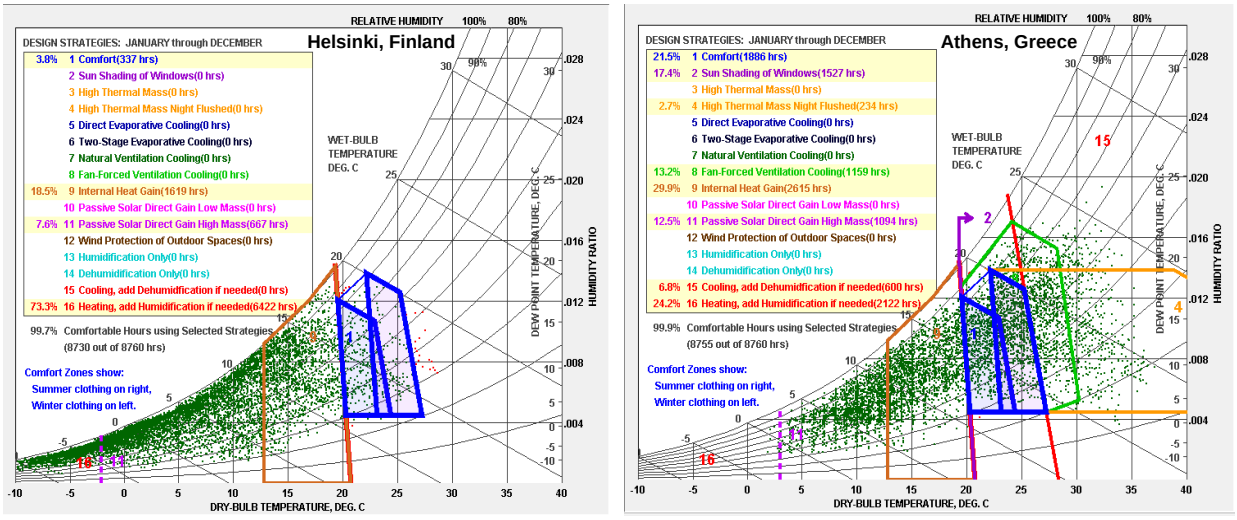

Figure 2: Examples of strategy determination using the psychometric chart for Helsinki, Finland (left) and Athens, Greece (right) using the software Climate Consultant

To perform energy calculations, the strategies were given values through conceptual technologies as detailed below, prior to their identification with specific materials. In this way strategies can be assessed avoiding time-consuming optimization techniques. Values were provided by project partners in order to achieve minimal approval to building code of each location. Ideal loads systems were assumed. Cases considered for simulations were:

a) Basecase: No technologies applied, reflects existing situation in the selected cities.

b) Glazing: improving U-factor of the window system to a value that is specific for each representative city (1.3 to 2.9 W/m2-K). Glazing area remains unchanged (15% to 25% total floor area depending on climate zone).

c) Insulation: Improving insulation in order to comply with minimum EPBD façade U-values for 2010 [9], the latest year with verifiable data for all EU-27 countries.

d) Shading: To avoid effects of specific devices, an idealized "smart" shade is used covering the entire glazing. It changes solar transmittance to 20% during summer, and to 80% during winter.

e) Albedo: changing solar absorptance from 0.65 to 0.25, for all climates.

f) Ventilation: Introduction of 4 air changes per hour (ach) using temperature-controlled openings, increasing the use of outdoor air for cooling. For Helsinki and Stockholm, ventilation in winter uses a mechanical heat recovery system.

g) Combined use of strategies (b) to (f), assuming no interference between them.

h) Ten strategy combinations as pairs, according to the scheme of Figure 3

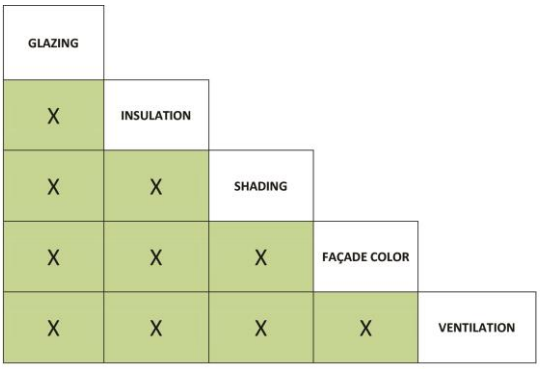

Figure 3: Strategy combinations tested through computer simulations

RESULTS

A combined use of strategies (b) to (f) achieved the lowest energy use. This was 60% to 40% less than the original basecase for all climates. Nevertheless, a number of these strategies have higher influence than others but do not necessarily add up in equal weights when combined. Some technologies can also be combined in pairs to achieve similar savings. It is important to notice them since not all technologies might fit the façade area.

In the South climate zone, strategies with higher impact were using shading (around 40% reduction from initial basecase) and improving glazing (around 20% reduction from initial basecase).

For the North climate zone, the most influential strategies were using ventilation with heat recovery (around 20% reduction from initial basecase), improving glazing (10%-12%

reduction from initial basecase) and improving insulation (10%-5% reduction from initial basecase). Ventilation with heat recovery has a large effect in total consumption in Nordic countries due to savings in the pre-heating of outside air.

For the Central climate area, the most effective strategies were improving insulation (around 12% reduction from initial basecase) and improving glazing (around 15% reduction from initial basecase). Locations within this zone that are closer to the south also benefit from incorporating shading devices. Certain strategies proved counterproductive for all climates, such as applying shading in the north façade, and should be avoided.

Results were organized in a synoptic way, as shown in Figure 4 for two orientations. Strategies were ranked for absolute quantities of energy savings. The graphics are organized by orientation. Climate type and cities are found in the vertical axis and strategies on the horizontal one. The first three strategies with the highest energy-savings are indicated. Many strategies present only very slight variations in terms of absolute consumption, indicating the need to consider other variables such as cost, aesthetics, etc., for a final decision.

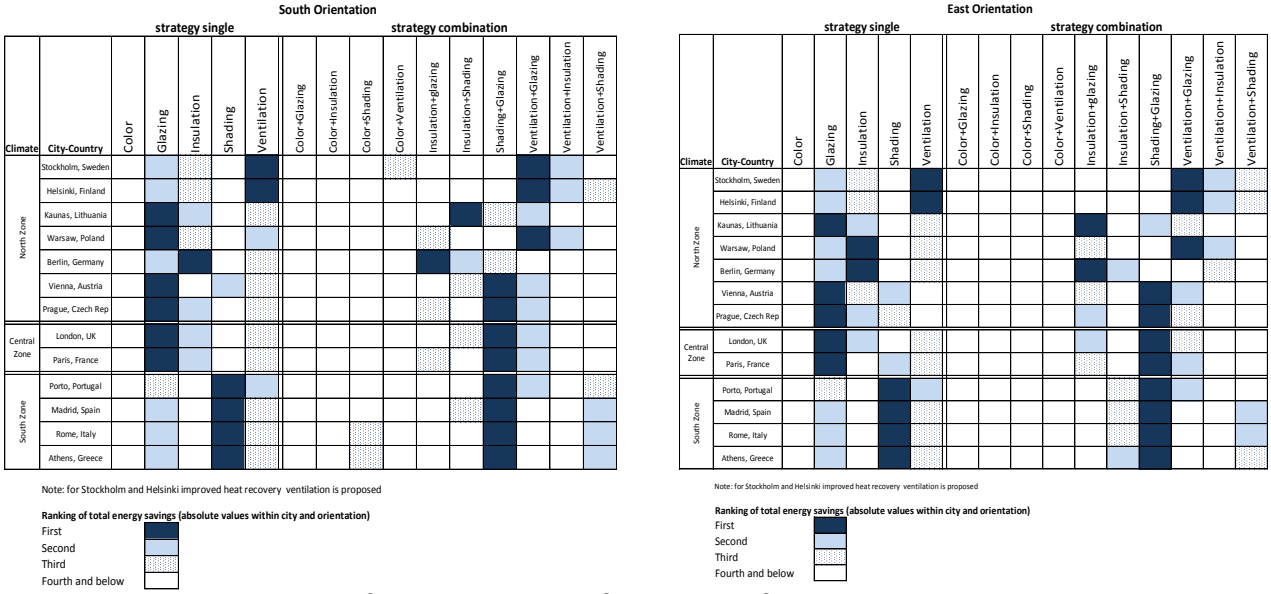

Figure 4: Synoptic table of strategy ranking for South (left) and East (right) orientations

Identification of specific technologies

Based on simulation results, project partners explored existing technologies to carry out the energy strategies, while considering structural and budget constraints. Examples of identified technologies are reflective paints, ventilated walls, green facades, etc. Currently they are being analysed for life cycle assessment, in order to provide specific values and complete the feasibility study. Addition of façade-mounted photovoltaic panels is also being considered.

DISCUSSION

The design method presented here is suitable to analyse a large number of locations and provide energy estimates that indicate which technology to follow. Even though, users need to know previously the correct climate classification of the city they are studying in order to select the right strategies. A proposed solution is using HDDs to achieve the right classification even if the location seems to correspond to another climate zone.

Although combining all strategies produces maximum energy savings, in reality there will be cases where other solutions must be found. Some constrains reside in the existing façade area and contextual conditions, which might limit accommodating all technologies, together with

budget or local laws. For example, in some historical centres large glazed areas are not allowed. In this case, the synoptic table can guide designers on the most effective strategies or their combinations. It is also assumed in the calculations that one technology would not interfere with the performance of another, e.g. combining ventilation with insulation. It is also assumed that there is a communal agreement on façade use to place the modules.

For the preliminary analysis, it was assumed that conceptual technologies were placed optimally within the façade. Further analysis is needed to determine their exact position, such as wind directions and solar irradiation on the plane, according to obstructions such as neighbouring buildings and topography. Rules of thumb can also be used for conceptual massing, such as avoiding placement of shading devices in the north facades. The method to select strategies and technologies will be abstracted into a computer tool to be developed during this project.

ACKNOWLEDGEMENTS

The results presented in this paper are part of the MEEFS project (www.meefs-retrofitting.eu) co-financed by the European Commission in 7th FP, NMP2-LA-2011-285411

Note: The views expressed are purely those of the authors and may not in any circumstances be regarded as stating an official position of the European Commission.

REFERENCES

1. Uhlein, A., Eder, P.: Policy options towards an energy efficient residential building stock in the EU-27, Energy and Buildings. 42 (2010) 791-798
2. Atanasiu, B., Despret, C., Economidou, M., Maio, J., Nolte, I., Rapf, O.: Europe's Buildings under the Microscope. A country-by-country review of the energy performance of buildings. Buildings Performance Institute Europe. October 2011. Available from: http://www.europeanclimate.org/documents/LR_%20CbC_study.pdf (Retrieved March 2013).
3. Spanish Ministry of Housing: Sobre una estrategia para dirigir al sector de la edificación hacia la eficiencia en la emisión de gases de efecto invernadero (GEI). Ministerio de Vivienda (Madrid, Spain2007) Available from: http://www.fomento.gob.es/NR/rdonlyres/7CA1FD2E-1DB9-4F8D-AF52-D61824ED96C6/95543/GEI.pdf (Retrieved March 2013).
4. MEEFS: Project web page http://www.meefs-retrofitting.eu/ (Retrieved April 2013).
5. Rubel, F., and Kottek, M.: World Map of Koppen-Geiger Climate Classification, period 1976-2000 http://koeppen-geiger.vu-wien.ac.at/pdf/1976-2000.pdf (Retrieved March 2013).
6. TABULA Project: Typology Approach for Building Stock Energy Assessment http://www.building-typology.eu/ (Retrieved March 2013).
7. Parsons, R: ASHRAE Handbook: Fundamentals, American Society of Heating Refrigerating and Air-Conditioning Engineers, Atlanta, Georgia, July 2005.
8. Energy design tools UCLA: Climate consultant software, www.energy-design-tools.aud.ucla.edu/ (Retrieved March 2013).
9. Concerted Action EPBD: Energy Performance of Building Initiative http://www.epbd-ca.eu/ (Retrieved March 2013).

EVALUATION OF SHADING RETROFIT STRATEGIES FOR ENERGY SAVINGS IN OFFICE BUILDINGS

Hui Shen; Athanasios Tzempelikos

School of Civil Engineering, Purdue University, 550 Stadium Mall Drive, West Lafayette, IN47906

ABSTRACT

This paper focuses on the energy savings potential of existing office buildings with large glass facades through improvement of shading device properties and control methods, using roller shades as a typical example. A new and improved shading control strategy is proposed as an extension of recent work is. Solar energy utilization is maximized in terms of daylighting and solar heat gains if needed in winter. At the same time, excessive illuminance is avoided to prevent from glare and efficient solar protection is ensured to reduce cooling requirements in summer and other seasons. A transient integrated thermal and daylighting model is applied to investigate the daylighting and energy performance of perimeter zones with automated shading. Using the optimal control strategy, shading properties can be selected to reduce overall space energy use. The "effective transmitted illuminance" concept allows extension of the method to spaces with two or more exterior facades, different climates, glazing properties and orientations. The method can be applied for new construction as well as for retrofitting existing shading systems.

Keywords: shading control, facades, daylighting, energy

INTRODUCTION

The majority of modern office buildings have large glass facades on every orientation. The significant impact of the glass facades on the energy demand for space lighting, heating and cooling should be carefully investigated to determine ways of saving energy while maintaining comfortable conditions for the occupants working in perimeter zones. Previous studies have shown energy savings potential by improving shading device properties or by employing shading control strategies [1]. However, most of the existing studies focus on private office spaces with one exterior façade [2-4]. Shading control studies in spaces with more than one window are quite limited, and the problem becomes more complex for offices with two or more exterior facades.

In most of the existing literatures, automated shading positions (for roller shades) are limited to fully on and fully off conditions. Recently, Shen and Tzempelikos [3] studied shading control methods that move shades to the position of preventing direct sunlight from falling on the work plane surface. The objective is to maximize utilization of solar energy and minimize source energy consumption. However, the methods tend to result in high work plane illuminances (>2000 lux) for a noticeable portion of annual working hours which indicates that glare problems might occur.

In this paper, the previously developed shading control method described in [3] is firstly improved in terms of solar protection and daylight provision. Then roller shade control strategies for spaces with more than one window are discussed. Results are presented for a case study focusing on the energy savings potential of existing office buildings with large glazed surfaces through improvement (retrofit) of shading device properties and control.

A NEW AND IMPROVED SHADING CONTROL STRATEGY FOR ROLLER SHADES

Private Perimeter Offices with One Exterior Facade

The principle of shading control is to maximize the utilization of solar energy in terms of daylighting and offer efficient solar protection. Glare needs to be eliminated, as well as overheating in winter or high cooling requirements in summer. Control strategies developed in [3] well reflect this principle by adjusting shading position according to solar geometry, orientation and occupant protection as shown in Figure 1 and Equation (1).

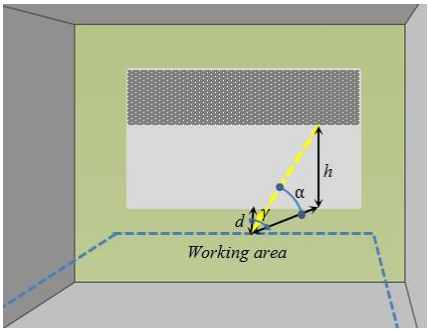

Figure 1: Graph showing automated shading position in [3] (d: defined distance between working area and façade; γ: surface solar azimuth; α: solar altitude; h: shade height over work plane surface)

$$h=d/cos(\gamma)\times tan(\alpha) \quad (1)$$

The issue of high work plane illuminance (above the recommended 2000 lux [5, 6]) for the control procedure shown in Fig. 1 is mainly due to the high solar altitude in summer and the resulting large unshaded window area. Associated with this issue is another problem related to high amounts of solar radiation to entering the space and increasing cooling requirement. To solve these problems, improvements in previous work are made as follows. Assuming that work plane illuminance values below 2000 lx do not result in glare problems (no direct sunlight present), we establish a threshold in transmitted illuminance (through window) using correlations between transmitted and work plane illuminance values (over a grid on the work plane). This is done using TMY3 data and the Perez et al. or a similar method and an interior luminous flux processing engine such as the radiosity method [2] or a mix of ray-tracing and radiosity methods [7]. The shades are controlled using Eq. 1 in these calculations. Using these results, an "upper limit" or threshold is selected, above which work plane illuminances would be unacceptable.

For a typical private office space (5m×5m×3m) with one window occupying 40% of its south facing façade, the resulting variation of work plane illuminance (represented by the maximum value and the minimum value of the nine studied points on work plane surface for each time step) as a function of the "effective transmitted illuminance" through window is illustrated in Figure 2 (a). Data shown is for Philadelphia, using shading transmittance of 0.1, reflectance for two shading sides of 0.6 and 0.3 and a double clear glazing.

In Figure 2, the effective transmitted illuminance through window (E_{eff}) is calculated with equation (2).

$$E_{eff}=(E_g\times A_g+E_{sh}\times A_{sh})/(A_g+A_{sh}) \quad (2)$$

where E_g and E_{sh} are the illuminance transmitted through the unshaded and shaded window parts respectively, lux; A_g and A_{sh} are the areas of the unshaded and shaded window parts, m^2. As illustrated in Figure 2 (a), to maintain work plane illuminances lower than 2000 lx, the effective transmitted illuminance through window should be lower than a threshold E_{esp}

(approximately 8000 lux for the case shown in Figure 2 (a)). Therefore, the shading position is determined by adding another constraint as illustrated in equation (3).

$$h=min\{d/cos(\gamma)\times tan(\alpha),\ (E_{esp}-E_{sh})\times H/(E_g-E_{sh})\ \} \quad (3)$$

where H is the window height.

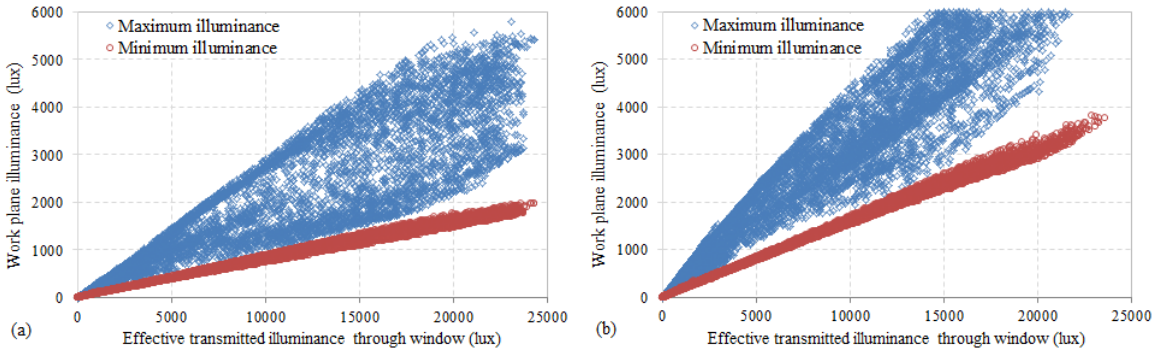

Figure 2: Variation of maximum/minimum illuminance at work plane sensor points as a function of effective transmitted illuminance through window for (a) space with one south window and (b) space with one south window and one west window

This shading control strategy performs better than all previous control methods in terms of daylighting performance, although outside view is reduced to 25% -average value for annual working hours. Table 1 compares the daylighting and energy performance for the private office using the original shading control method developed in [3] and the improved method.

	One-window		**Two-windows**	
	Original	Improved	Original	Improved
% of annual working hours when shades are open	45.4	25.7	45.4/60.7	11.6/21.2
Daylight autonomy (%)	76.8	74.1	91.9	89.9
Continuous daylight autonomy (%)	88.2	87.5	96.6	96.1
Maximum daylight autonomy (%)	0.22	0	4.9	0
Useful daylight illuminance (100-500 lux) (%)	19.8	22.5	7.7	9.6
Useful daylight illuminance (500-1000 lux) (%)	19.3	60	10.1	57.6
Useful daylight illuminance (1000-2000 lux) (%)	40.8	12.3	24.6	31.6
% of annual working hours when work plane illuminance exceeds 2000 lux (%)	48.7	15	76	6.1
Annual lighting demand (kWh/m^2·year)	3.5	3.6	1	1.1
Annual heating demand (kWh/m^2·year)	21	22.1	37.7	48.2
Annual cooling demand (kWh/m^2·year)	61.3	56.7	111	85.6
Annual lighting energy consumption (kWh/m^2·year)	12.2	12.8	3.5	4
Annual heating energy consumption (kWh/m^2·year)	27.5	29	49.3	63.2
Annual cooling energy consumption (kWh/m^2·year)	58.5	54	106	81.7
Annual source energy consumption (kWh/m^2·year)	98.2	95.8	158.8	148.9

Table 1: Daylighting and energy performance for a space with a window occupying 40% of its south facing façade and for a space with a south window and a west window (source-site ratios are 3.34 for electricity (lighting and cooling) and 1.047 for natural gas (heating))

Perimeter Spaces with Two or More Exterior Facades

The same shading control logic presented above can be applied to spaces with multiple windows (exterior facades, different orientations). Extending the previous section, a west window is added to form a space with two windows (corner office). The west window also occupies 40% of the west façade. For such spaces, the same type of shading with the same properties and control strategies (if available) are traditionally installed. However, due to the different amounts (and characteristics) of solar radiation and natural light on different orientations, it is reasonable to study the implementation of variable properties and control on each side of building. Using the shading control strategy described in [3], the variation of work plane illuminance as a function of space effective transmitted illuminance (Equation (4)) through windows is illustrated in Figure 2 (b). To achieve work plane illuminance lower than 2000 lux, the space "overall effective transmitted illuminance" should not exceed 4000 lux (E_{esp}).

$$E_{eff}=(E_{g1}\times A_{g1}+E_{sh1}\times A_{sh1}+E_{g2}\times A_{g2}+E_{sh2}\times A_{sh2})/(A_{g1}+A_{sh1}\ A_{g2}+A_{sh2}) \quad (4)$$

Unlike the single facade case, the E_{esp} limit cannot be used to obtain a shade position directly, but is used to calculate a proper ratio (*eRatio*) of effective transmitted illuminance through the two windows (Equation (5)). Then the shade position for each window can be calculated according to the calculated required effective illuminance for each window (equation (6)).

$$eRatio=E_{esp}/E_{eff} \quad (5)$$

$$h=min\{d/cos(\gamma)\times tan(\alpha),\ (eRatio\times E_{eff}-E_{sh})\times H/(E_g-E_{sh})\} \quad (6)$$

where: $eRatio\times E_{eff}$ gives the required effective illuminance for each window in order to achieve work plane illuminance below 2000 lux.

A comparison of the daylighting and energy performance for the two-window (corner) office using the original shading control method developed in [3] and the improved method is also listed in Table 1. The improved shading control strategy results in better daylighting performance without increasing total energy consumption. Although there is still a small ratio of annual working hours that the work plane illuminance exceeds 2000 lux, the values are always kept below 2500 lux which is a significant improvement comparing to the original higher time portion of working hours with very high values (above 3000 lux). The logic of the improved shading control strategy is optimized for maximizing solar energy utilization on the premise of controlling work plane illuminance below the recommended limit. To further reduce energy consumption, shading properties should be improved according to the characteristics of space energy consumption for lighting, heating and cooling.

THE ROLE OF SHADING PROPERTIES

To reduce energy consumption of existing building by retrofitting shading devices, another option is to select better shading properties and match them with the developed controls. Using the one-window and two-window spaces with automated shading control strategy, this section focuses on further reduction in space energy consumption by improving shading properties. According to Table 1, both the one-window space and the two-window space are cooling dominated. Increasing shade reflectance on front side may achieve lower total energy consumption if the penalty in heating is smaller than benefit in cooling. Before improving shade reflectance, shade transmittance should be firstly improved to optimize daylighting and maintain visual comfort. A proper shading transmittance can be determined by checking the work plane illuminance with closed shades. The value above which the work plane illuminance starts to exceed 2000 lux is the limit for shade transmittance. Shading

transmittance of 10% is a proper value for the one-window space and 8%/10% (south/west) is proper shading transmittance combination for the two-window space as illustrated in Table 2.

	One-window (south)			Two-window (south/west)		
Shade transmittance	0.08	0.1	0.12	0.065/0.08	0.08/0.1	0.1/0.12
% of annual working hours when work plane illuminance exceeds 2000 lux (%)	0	0	0.1027	0	0.05	0.79

Table 2: % of annual working hours when work plane illuminance exceeds 2000 lux as a function of shade transmittance with closed shades.

Variations of heating, cooling, lighting and total source energy consumptionas a function of shade exterior side reflectance are shown in Figure 3 for the one-window space and the two-window space using the proper shading transmittance determined above.

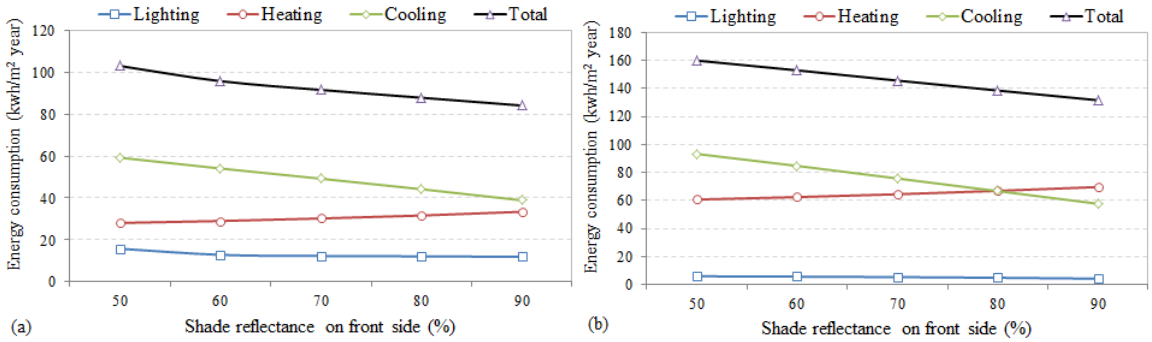

Figure 3: Variation of space total source energy consumption and energy consumption for lighing, heating and cooling as function of shade reflectance on front side for (a) space with one south window and (b) space with one south window and one west window.

Figure 3 indicates that total source energy consumption reduces with the increase of shade reflectance. This is because the developed shading control strategy maximizes daylighting benefits. The selected shading transmittance is the maximum possible value that can be applied without resulting in high work plane illuminance (> 2000 lux). At the same time, this shading transmittance maximizes solar energy entering the space in winter since for this season the shading position is generally low due to low solar altitude. In summer, this shading transmittance results in smaller shading opening time according to the constraint on effective transmitted illuminance through windows. So the only possible option to further reduce space total source energy consumption is to reduce cooling energy consumption by increasing shade reflectance on front side. This trend is applicable to any similar space (space dimension, window size and location) located in other locations with different climate characteristics (except very cold climates) or a space installed with a different type of glazing () or orientation. The reason is that the development of the shading control strategy and the method to select the shading transmittance is general and independent of the above parameters. Results for different locations, orientations and glazing types will be presented in a further study.

CONCLUSION

This paper first presents a new improved shading control strategy (for roller shades) based on previous recent work [3]. The improved shading control can maximize the utilization of solar energy in terms of daylighting benefits. At the same time, excessive illuminance is avoided to prevent visual discomfort, overheating in winter or high cooling requirements in summer.

With the optimal shading control strategy, the procedure of reducing space energy consumption by retrofitting shading properties is presented for perimeter offices with one or more exterior facades. The studied spaces are generally cooling dominated, and the total source energy consumption can be reduced by increasing the shade outside reflectance on front side. The analytical procedure to minimize space energy consumption using the optimized shading control strategy and by retrofitting shading properties is similar. For new buildings, the method is applicable, however several other parameters need to be considered and multivariate optimization is required.

ACKNOWLEDGEMENTS

The authors would like to thank the US Department of Energy for supporting this work through the Energy Efficient Buildings Hub. Thanks also to Lutron Electronics, Kawneer/Alcoa, PPG Industries and Viracon Inc. for their kind support.

REFERENCES

1. Moeseke, G., Bruyere, I., Herde, A.D.: Impact of control rules on the efficiency of shading devices and free cooling for office buildings. Building and Environment Vol 42, pp 784-793, 2007.
2. Shen H., Tzempelikos, A.: Daylighting and energy analysis of private offices with automated interior roller shades. Solar Energy, Vol 86, pp 681-704, 2012.
3. Tzempelikos, A., Shen, H.: Comparative control strategies for roller shades with respect to daylighting and energy performance. Submitted to Building and Environment, 2013.
4. Nielsen, M.V., Svendsen, S., Jensen, L.B.: Quantifying the potential of automated dynamic solar shading in office buildings through integrated simulations of energy and daylight. Solar Energy, Vol 85 757-768, 2011.
5. Nabil, A., Mardaljevic, J.: Useful daylight illuminances: a replacement for daylight factors. Energy and Buildings Vol 38, pp 905–913, 2006.
6. da Silva, P.C., Leal, V., Andersen, M.: Influence of shading control patterns on the energy assessment of office spaces. Energy and Buildings, Vol 50, pp 35-48, 2012.
7. Chan, Y.C., Tzempelikos A.: A hybrid ray-tracing and radiosity method for calculating radiation transport and illuminance distribution in spaces with venetian blinds. Solar Energy, Vol. 86 (11): 3109-3124, 2012.

SMART SKIN AND ARCHITECTURAL INTEGRATION OF PV GLAZED BRICK SHADING DEVICES

Antonella Trombadore[1], Leonardo Scalpellini[2]

[1] *Università degli studi di Firenze, DIDA Department of Architecure, San Niccolò 93,Firenze 50125, Italy, antonella.trombadore@unifi.it*

[2]*Studiosolaris, via gioberti 34 50121 Italy, leonardo@studiosolaris.it*

ABSTRACT

The design and test of a prototype for building envelope integration of PV systems is the focus of this research. The aim is to bridge the gap between architectural integration and cost-effectiveness, fostering a high esthetical value, high energy performance in south facade applications as well as on east / west surfaces. This project is part of a larger research jointly developed by University of Florence and the Palagio Engineering Company, with other Tuscany companies involved in the fields of "*Abitaremediterraneo*" (Mediterranean sustainable living), developing innovative smart façade and double skin, trying to integrate innovative technological systems such as PV concentration with local tradition materials (brick), focusing on passive cooling and energy efficiency strategies in a Mediterranean climatic condition. Developing this idea and trying to get an innovative project we arrived at the design of a solar shading system that uses the parabolic solar concentrator system. The photovoltaic concentrator allows conveying sunlight into a cell of reduced dimensions. The basic unit of photovoltaic concentrator is constituted by an optical system that focuses the light on the cell, a set of photovoltaic cells, a system to disperse the heating surplus heat (due to the concentration), a solar tracking, several connections and components fastening systems. The prototype allows testing and optimizing the design solutions, the brick elements parabolic morphology and especially the correct integration of PV cells and their energy performance, the reflection capacity of the glazing process as well as the optimization of tilt and solar tracking. The cost evaluation of the PV facade construction showed an increase of 20% in comparison to a brick double/ventilated façade market cost but, thanks to the energy saving efficiency (electric solar energy production), we can calculate an investment's payback period of about 4,5 years. It therefore provides a large application in the Mediterranean countries, with a real market penetration of the Arab countries and Latin America, where the climatic conditions require a closer architectural integration of shading devices, solar gains control, natural ventilation, passive cooling strategies and integration of renewable energies.

Keywords: Smart skin, dynamic envelope, renewable energy integration, low energy building, PV concentrator, PV shading devices, brick double/ventilated skin facade

INTRODUCTION

It is not usual that silicon cells are integrated with brick sunshade elements for energy production: the market proposes integrated systems with glass or steel or wood materials. The concept design has focused on the best solution of a mobile shading device form in order to optimize the performance of the photovoltaic concentration system, integrated with a solar tracker. However the brick offers more flexibility allowing to define the more appropriated design of parable configuration for the concentrator unit, using the common production process of shading/wing elements extrusion. The photovoltaic concentrator allows conveying sunlight into a cell of reduced dimensions.

The basic unit of photovoltaic concentrator is constituted by: an optical system that focuses the light on the cell, a set of photovoltaic cells, a system to disperse the heating surplus heat (due to the concentration), a solar tracking, several connections and component fastening systems.

METHOD

In order to optimize the performance it was necessary to modify the curvature as well as the size of the products: the parable was realized with two curved element, allowing the extrusion of the concentrator brick with an operable dimension of 24 cm.

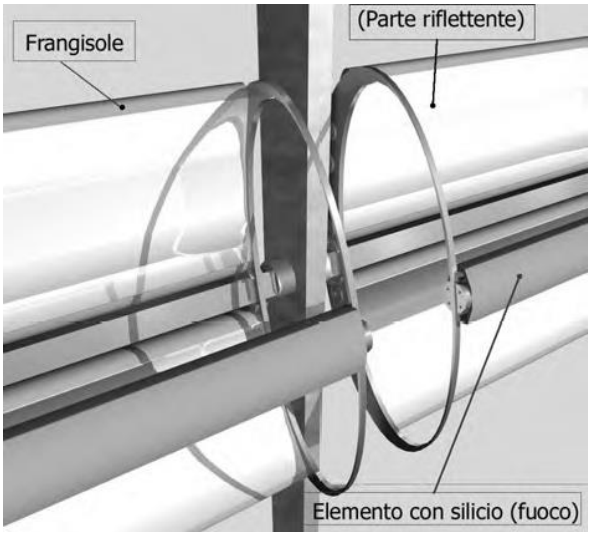

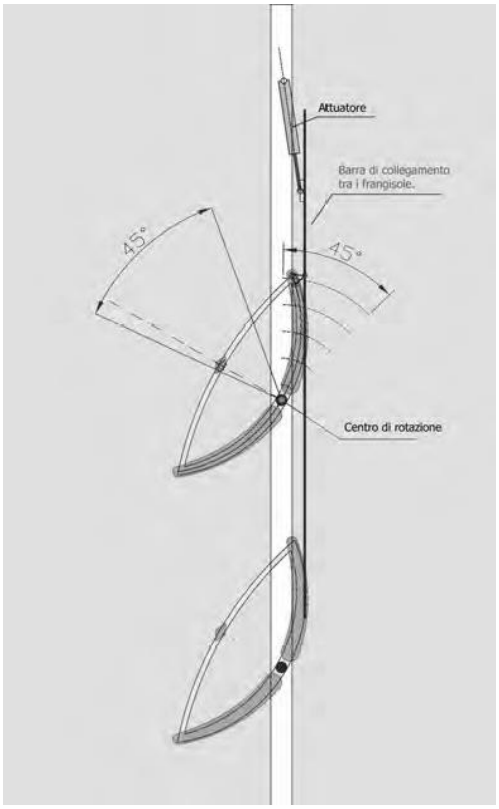

Fig. 1 -2 Design of the shading devices. Selection of the more appropriated architectural solution

Fig. 3 Drawing studio and optimization of brick parabola.

As shown in the drawing the steel structuralelements allow optimising solar tracking and tilt; the concave part of the parabola must be reflective. Palagio Engineering has long experience in glazing of tiles and brick elements: for this prototype the white reflective glazing containing titanium dioxide (TiO2), both to reflect and concentrate the solar radiation in the photovoltaic cells, both to prevent the overheating and reducing thermal load on the building surface.

The earthenware tiles (brick tiles) can be created through modelling or extrusion. The first method, less precise and expensive, useful only for the prototype, consists in bending over a rib a flat element before firing. Once the object has acquired the desired parabola shape, is brought into the oven. Using this method however, the tile, during the firing process, undergoes a curvature change, which differs by a few millimeters compared to the initial configuration.

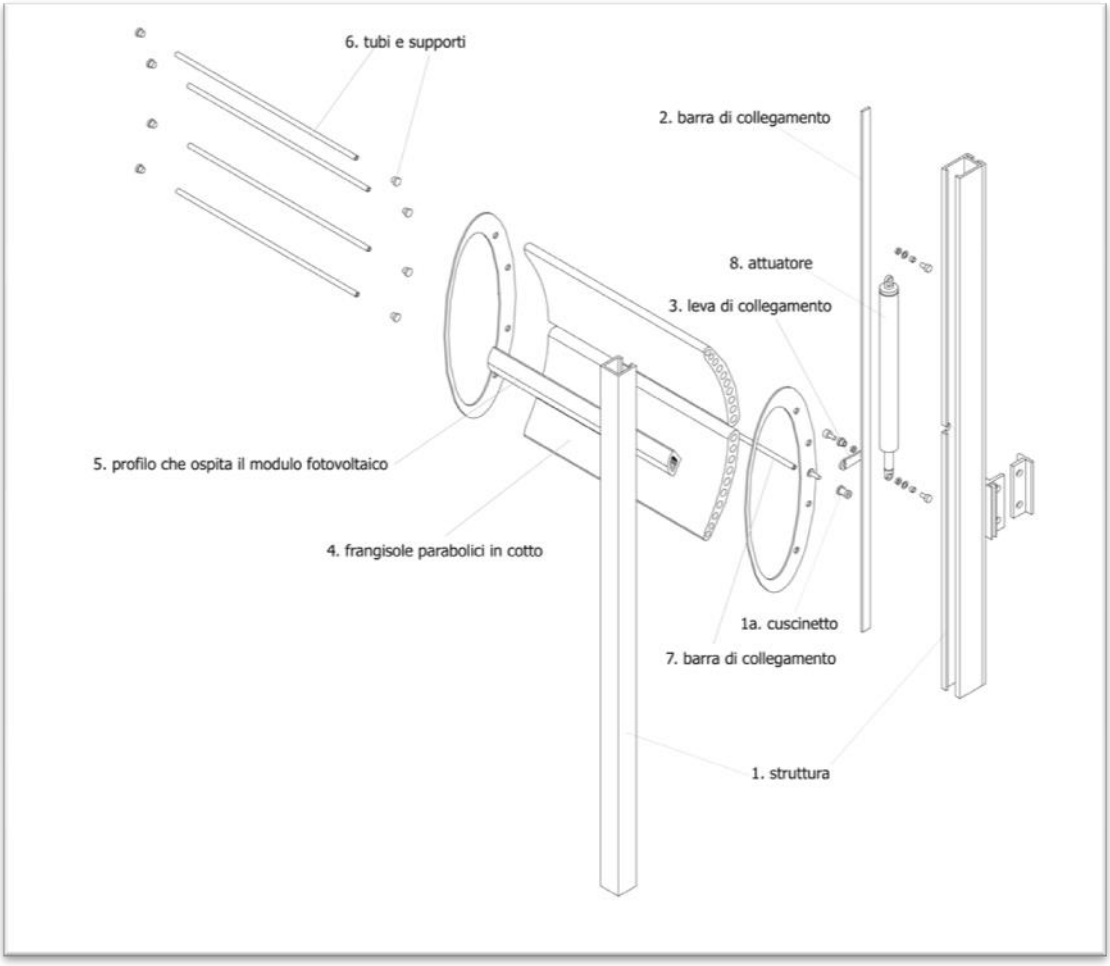

Fig. 4 -View of architectural details of PV concentrator system

The second method consists in the extrusion of the profile and is normally used in the industrial production of all types of bricks. The clay is compressed by passing it through a matrix, which exactly reproduces the external shape to be obtained. This system allows realizing a more precise element, but the cost of a possible prototype is more expensive because it requires a specific production system or supply chain.

The realization of a solar tracking system is essential to ensure that the parabolic solar shadings are always optimally positioned during their rotation, in order to maintain, during the changing in seasons and daylight, the ideal orientation to the sun.

Through a movement controlled by electric actuators, solar concentrators are correctly pointed at the sun, increasing the energy efficiency. In our specific case, the uniaxial tracker used, which performs its rotation around a single axis, is able to change the position exclusively to follow the sun changes in height. Sun tracking can be achieved by adopting two methods: the active system and the passive system.

In our case it may be preferable to use the passive system, set up to know in advance the position of the sun based on (through) date, time and location.

Are commercially available monocrystalline silicon cells with efficiencies of over 21% and the range of operating temperatures from -40° C to 90° C. This type of cell had already been used to create some solar concentrators and therefore its suitability has been tested. The module, assembled with this type of cells, could be mounted in a profile with a section as in the drawing.

Fig. 5 -View of architectural integration in south facades. Different solution for vertical and horizontal PV concentrator - shading systems are provided.

Fig. 6 View of architectural integration in east-west facades.

RESULTS

The prototype allows to test and optimize the design solutions, the brick elements parabolic morphology and especially the correct integration of PV cell and their energy performance, the reflection capacity of the glazing process and the optimization of tilt and solar tracking. The cost evaluation of the PV facade construction showed an increase of 20% in comparison to a brick double/ventilated façade market cost but, thanks to the energy saving efficiency (electric solar energy production is about 70 W for panel , with PV cell of 4,5x120 cm), we can calculate an investment's payback period of about 4,5 years. It therefore provides a large application in the Mediterranean countries, with a real market penetration of the Arab countries and Latin America, where the climatic conditions require a closer architectural integration of shading devices, solar gains control, natural ventilation, passive cooling strategies and integration of renewable energies.

REFERENCES

1. AA.VV. *Costruire sostenibile - Il Mediterraneo*. Alinea Editrice, Firenze, 2001
2. AA.VV. *Verso un architettura nel Mediterraneo*. Ed. L'Epos, Palermo, 2001
3. Bradbury D. *Mediterranean Modern* Thames & Hudson, London 2006
4. M.Sala, L.Ceccherini Nelli, E. D'Audino, A. *Trombadore Schermature Solari*.Alinea Editrice srl, FIRENZE 2007
5. Santamouris M., Wouters P. *Building Ventilation. The State of the Art*. Earthscan Ltd, London, UK 2006
6. Santamouris M. *Energy and Climate in the Urban Built Environment* Ed. Earthscan Ltd, London, UK 2001

A. Trombadore *Processi di trasformazione Urbana e qualità architettonica ambientale: il progetto Med Indo Cities.* In: M.Sala.(a cura di) *100 tesi....sostenibili*. p. 47-52,Ed. Alinea Firenze 2009,

7. Trombadore, P.Gallo, A.P. Lusardi *Potenzialità e prestazioni dell'organismo edilizio esistente*. In: M.Sala. *Recupero Edilizio e Bioclimatica.* p. 59-96,:Sistemi Editoriali - Gruppo editoriale Esselibri - Simone, Napoli 2001
8. Yannas S., Erell E., Molina J. L. *Roof Cooling Techniques: A Design Handbook* Earthscan Ltd, London, UK 2005

RETRO-REFLECTING FILM WITH WAVELENGTH-SELECTIVE PROPERTIES AGAINST NEAR-INFRARED SOLAR RADIATION AND IMPROVING EFFECTS OF INDOOR/OUTDOOR THERMAL ENVIRONMENT

Takashi Inoue[1], Masayuki Ichinose[2] , Tsutomu Nagahama[3]

1: Dept. of Architecture, Tokyo University of Science, 2641 Yamazaki Noda-shi, Chiba 278-8510, JAPAN, Email: SGR03425@nifty.com

2: Dept. of Architecture and Building Engineering, Tokyo Metropolitan University, 1-1 Minamiosawa Hachioji-shi, Tokyo 192-0397, JAPAN, Email: ichinose@tmu.ac.jp

3: Dexerials Corporation, Email: Tsutomu.Nagahama@dexerials.com

ABSTRACT

We proposed and developed a heat-shielding film that had a similar degree of transparency in the visible range to glass, and in addition had retro-reflective properties in the near infrared range. The film embodies an innovative heat-shielding technique that makes it possible to effectively reflect solar radiation towards the sky while minimizing secondary effects on other buildings and the streets around the buildings.

Firstly, we carried out measurements in the urban streets to investigate the impact that heat shielding by high-reflective building envelopes would have on the thermal environment in the neighborhood of the building. The results indicated that solar radiation subjected to mirror reflection from the heat-shielded envelope such as Low-E glass windows would deteriorate the street thermal environment considerably.

Secondly, we carried out comprehensive measurements in order to obtain data on the properties of our newly developed retro-reflecting film and carried out measurements in a state in which the developed retro-reflecting film was attached to glass, thereby verifying its optical performance regarding retro-reflectivity and selective transmission/reflection in various wavelengths. On the basis of the obtained results, we made a comprehensive evaluation regarding energy-saving effects, and the impact on an outdoor radiation environment, when the developed retro-reflecting film was applied to office buildings. The result showed that the film proposed herein could reduce adverse effects on an environment outside a building while ensuring the same level of transmission performance and heat-shielding performance as that of high-performance glass currently available on the market.

It was verified that, with the use of the retro-reflecting heat-shielding film, it would be possible to reduce adverse effects on an outdoor urban environment while reducing energy consumption in a building and enhancing indoor visual and thermal comfort.

Keywords: Solar radiation, Retro-reflecting, Near infrared, Heat shielding, Energy saving, Urban environment

1. INTRODUCTION

According to the IPCC 4th report, it is estimated that the building sector has the highest potential for CO2 reduction, amongst all sectors 1). The majority of CO2 emitted from buildings could be ascribed to the use of building equipment such as air-conditioning and lighting. When discussing the preservation of our environment on a global scale, a critical issue faced is how to confront the expected future increase in energy consumption, mainly

from developing countries in hot and warm regions; this is due to urbanization from the increasing number of people and buildings, as well as a qualitative improvement in the living standard. It is obvious that, in such hot and warm environments, heat shielding against solar radiation at the building envelopes is of greater concern than air-tightness and thermal-insulation properties.

The highly reflective painting, which is a technique for selectively reflecting sunlight in the invisible near-infrared range independent of the visible-light-range properties, is a practical and effective solution. It can be seen in present day high-rise buildings, the number of buildings for which most of the facade consists of glass is increasing. In order to cope with these trends, glass such as a kind of Low-E glass that allows visible light inside, yet keeps solar heat outside, has been developed. In addition, heat-shielding films that can be easily applied to existing buildings have been also developed. The above mentioned glass and heat-shielding film prevents solar radiation heat from entering through the building envelope, thereby decreasing the energy consumption from air-conditioning, while suppressing the rise of building surface temperature; this makes it possible to reduce the heat-island-causing sensible heat flux from the building envelope into the urban area atmosphere.

For heat-shielding measures provided on building roofs such as cool roofs, there is almost no need to take into consideration secondary effects, which include reflected solar radiation to other buildings, humans on the street, etc. Because the facade is on a vertical plane, however, the effect of reflected solar radiation to the ground, particularly due to the mirror-reflecting property of glass, cannot be ignored. Therefore, building envelope performance which satisfies both wavelength selectivity and directivity is highly desired. From the background, we have proposed and developed a novel heat-shielding film, which possesses both retro-reflectivity and wavelength selectivity in the near infrared range, for transparent building envelopes.

2. ACTUAL RADIATION ENVIRONMENT IN THE STREET

In order to investigate the impact that solar heat shielding of a building facade has on its external environment, measurements of the radiant environment around a heat-shielded building facade were conducted by mainly targeting buildings with Low-E double-glazed facades in the central Tokyo area. An on-site spectro-radiometer capable of measuring spectral irradiance within a range of 350 to 2,500 nm was configured and used for the quantitative study. For extracting the direct and reflected solar radiation components, a shielding hemi-sphere and shielding sphere were used, as shown in Fig. 1.

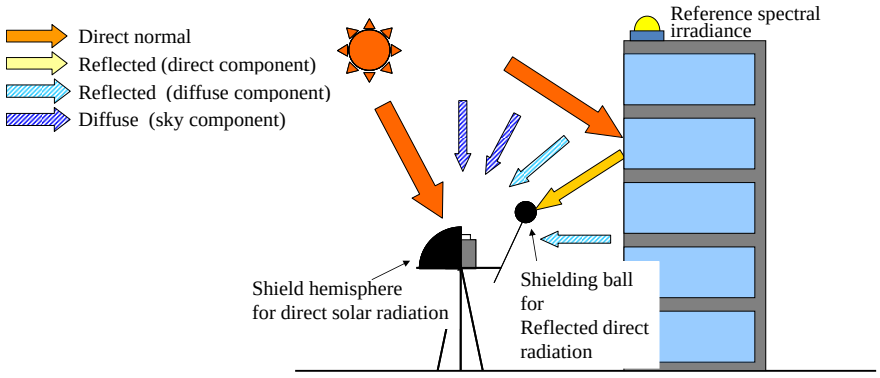

Figure 1: Measurement of solar radiation reflection of facade

2-1 Comparison of spectral solar irradiance for different glazed facades

In order to clarify the influence of the building facade on spectral irradiance to the street, a comparative measurement of spectral solar irradiance was conducted, focusing on two buildings A and B. The glass specifications of the buildings are clearly different, and they are located adjacent to each other. Each building is a 40-story high-rise office building, with air-flow windows over the entire facade. High-transmission glass is used on building A, and Low-E glass is used on building B. The orientation of the external wall surfaces and geometrical factor of the view from the street are equivalent to each other. Therefore, these can be compared directly and evaluated without any differences in solar radiation conditions, measurement time, and so on.

The results of the comparative measurement conducted at culmination time, when the sun faces the facades directly, are illustrated in Fig. 2. From the measurement results, the solar irradiance reflected from the facade for each glass specification is approximately the same in the UV + V wavelength. However, the reflected solar irradiance of Low-E double-glazing, clearly increases in the near-infrared range. The Integrated solar irradiance of the Low-E glass double-glazed is approximately four times larger than that of high-transmission double-glazing. The result shows that, due to heat shielding of the building facade, solar irradiance in the near-infrared wavelengths toward the outdoor space increases, which suggests the potential adverse effects on the thermal environment of the street.

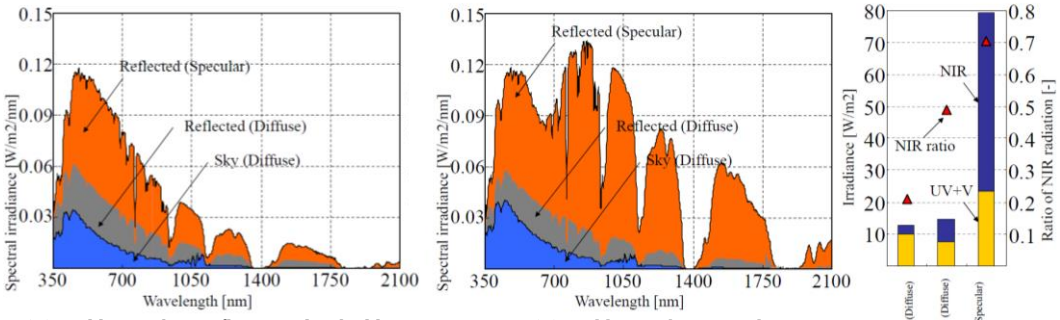

(A) Building without reflective solar shielding (B) Building with Low-E glass

Figure 2: Measured spectral irradiation in the street

2-2 Relationship between heat shielding of the facade and the street environment

The model shown on the left side of Fig. 3 can be derived from the above measurement results. Specifically, only visible sunlight, which is beneficial to the internal building environment, is taken in through the windows, whereas unwanted near-infrared solar radiation is reflected by selective shielding. As a result, a trade-off scheme is established which deteriorates the street environment due to the reflected near-infrared solar radiation. This structure is attributable to the mirror-reflecting property of glass.

If both wavelength selectivity and reflection directivity could be achieved as illustrated on the right side of Fig. 3, it is possible to reduce energy consumption and establish a favorable indoor environment through heat shielding of the building facade, while at the same time not deteriorating the outdoor environment. On the basis of such an inventive concept, we proposed a retro-reflecting film as explained below.

3. OVERVIEW OF RETRO-REFLECTIVE HEAT-SHIELDING FILM

The heat-shielding-type film which is currently being widely adopted uses a method which enhances the heat-shielding performance by increasing reflectivity in the near-infrared range independently of visible sunlight. There are methods which use metal films such as silver coating, as does Low-E glass, and methods which use layers of transparent film with differing optical properties such as refraction.

As an improvement on such existing heat-shielding films, we have devised a new film which enhances heat-shielding performance, by reducing transmissivity in the near-infrared range independently of transmissivity in the visible light range, and also possesses a retro-reflective property due to micro convexes and concaves formed on the transparent film surface. The main feature of the film proposed herein is the potential to avoid the adverse effects of reflected solar radiation onto the ground and other buildings surrounding the building with the film applied, while improving the energy-saving performance and comfort of the indoor environment.

As illustrated in Fig. 3, there are two types of reflectors. One of them is a perfect retro-reflector (3D) that reflects light back in the direction of incidence. The other is an "accordion-fold" reflector (2D) that reflects light in a retro-reflective manner with respect to an incident profile angle, and in a symmetric direction with respect to an incident azimuth angle. The 3D reflector is made of transparent film. Therefore, in the case of perfect retro-reflection, it reflects the beam at least twice. On the other hand, although the 2D reflector does not offer perfect retro-reflection, it can reflect light toward the sky when exposed to incoming direct solar radiation on a vertical plane. Thus, absorptivity of the whole reflector can be reduced by decreasing the number of reflections inside the reflector.

In this paper, therefore, we focused on the 2D reflector.

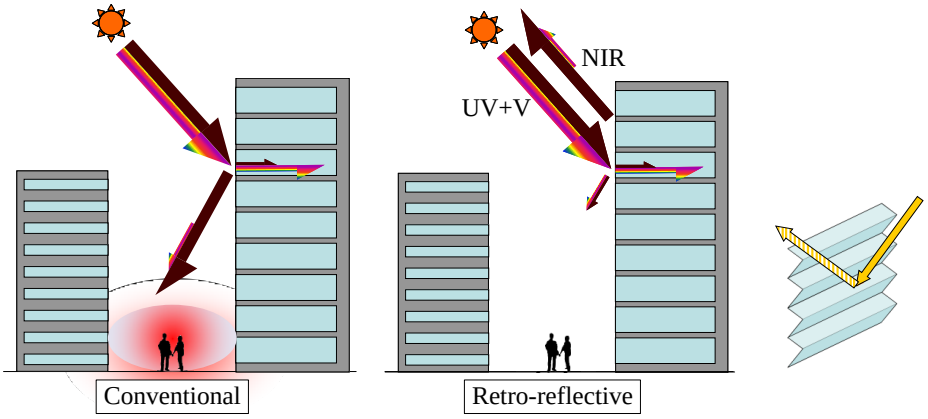

Figure 3: Diagram of solar shielding and influence on the thermal environment in the street

4. EFFECTS ON INDOOR ENVIRONMENT AND ENERGY FOR AIR-CONDITIONING

The heat-shielding retro-reflecting film was compared and tested against the high performing Low-E double-glazing, transparent glass, and glass with heat-shielding film.

In order to evaluate the thermal environment near the window, comparative measurements of the window surface temperature were performed for each glass specifications, using a light-colored venetian blinds in combination therewith. The thermal images shown in Fig. 4 were taken on a clear day with sufficient solar irradiance on the window surface. The temperature on the slat surface of the FL + retro-reflecting film is reduced by approximately 5 degrees, compared to FL glass. Considering the conditions during actual use where a window shade is

used together with the film proposed herein; by reducing the temperature on the window surface and reducing long-wave radiation, it can be expected that the film proposed herein will have an effect on improving the thermal environment, which is roughly equal to that of low-E double-glazing.

In order to grasp the heat-shielding performance of the glass alone, on-site measurements2) of solar heat gain coefficient (SHGC) were conducted. The results of measured SHGC are shown in Fig. 5. According to the result, solar heat gain is reduced to approximately one third during peak solar irradiance; and SHGC is less than 0.6, at the same level as that of FL + Film A, which belongs to the high-end of commercially available heat shielding films.

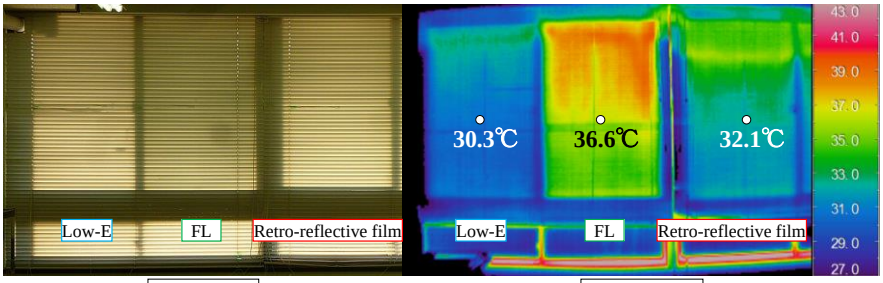

Figure 4: Thermograph of inside surface of various window

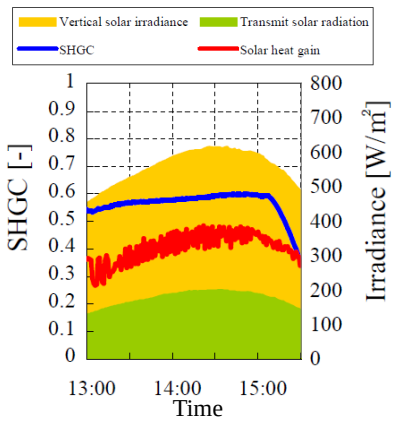

(a) Fluctuation of FL+Retro-reflective film

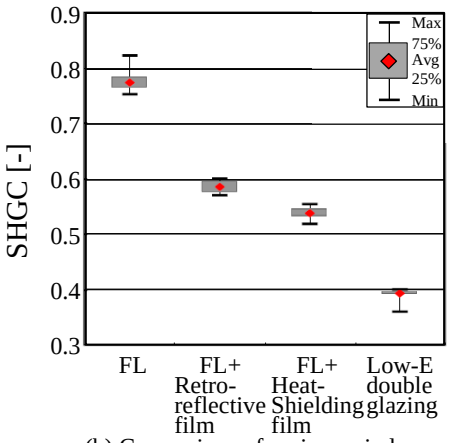

(b) Comparison of various window

Figure 5: Measured solar heat gain and SHGC

5. EFFECT ON OUTDOOR ENVIRONMENT

The comparative measurements were carried out as illustrated in Fig.6. This measurement assumes the situation, as illustrated in Fig. 3, of solar radiation being reflected from a building into the street in front of the building. It is obvious that the film proposed herein can significantly reduce downward mirror reflection in the near-infrared range, compared to both low-E double-glazing.

The daily integrated quantity of downward reflected solar radiation for each of the specifications is shown in Fig. 7. Regarding the ratio of downward reflection quantity, the FL glass + retro-reflecting film is approximately the same as that of FL. On the other hand, the downward reflection of FL+retro-reflecting film could be reduced to approximately half of the FL+heat-shielding film A, and one third of Low-E double-glazing.

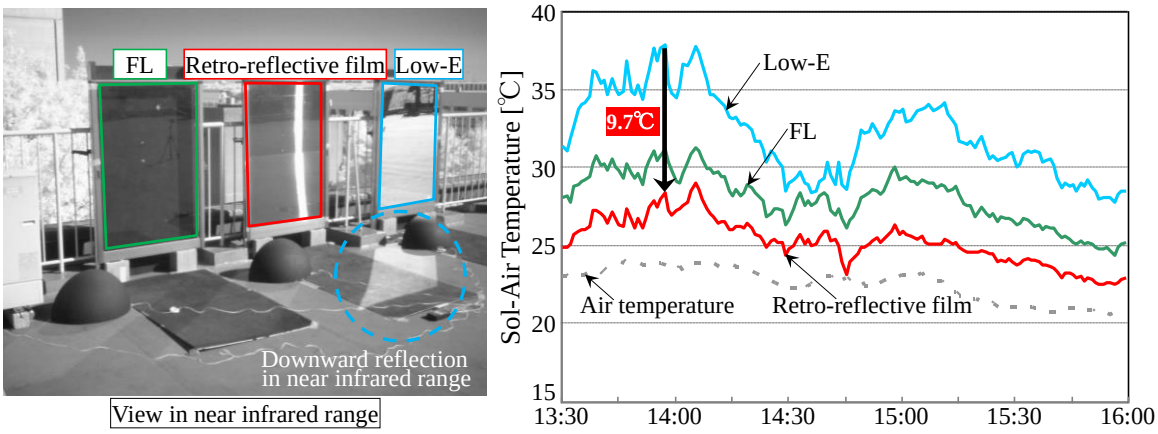

Figure 6: Comparison of downward reflection of various window

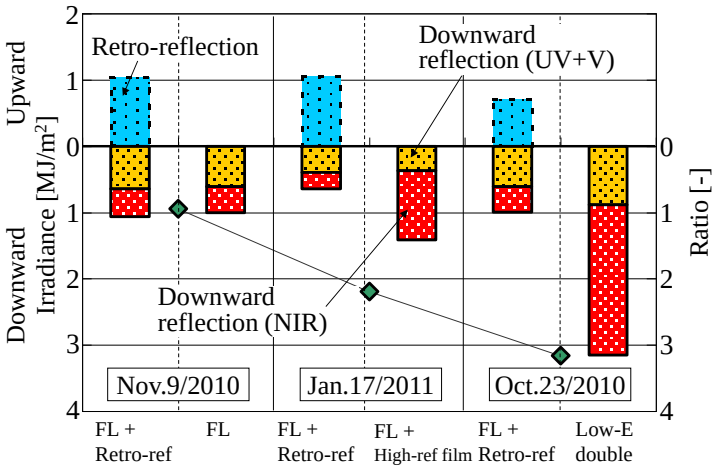

Figure 7: Comparison of directivity of reflected solar radiation between various window

6. CONCLUSION

As a result of the field measurements of a radiant environment conducted on the streets of Tokyo, it was indicated that heat shielding of the building facade had adverse effects on the thermal environment of the streets around the building. It was also verified that, through the use of the retro-reflecting heat-shielding film proposed here, it was possible to reduce the adverse effects on the outdoor urban environment, while at the same time ensuring energy conservation as well as enhancing comfort inside the building.

REFERENCES

1. IPCC Fourth Assessment Report: Climate Change 2007, P11
2. Takashi Inoue and Masayuki Ichinose: Development of a Simplified Method forMeasuring Solar Shading Performance of Windows, Proceedings of International Conference CISBAT, Lausanne, September 2007

TOTAL LIGHT TRANSMITTANCE OF GLASS FIBER-REINFORCED POLYMER LAMINATES FOR MULTIFUNCTIONAL LOAD-BEARING STRUCTURES

C. Pascual[1]; J. de Castro[1]; A. Schueler[2]; A.P. Vassilopoulos[1]; T. Keller[1]

1: Composite Construction Laboratory (CCLAB), Ecole Polytechnique Fédérale de Lausanne EPFL, Station 16, CH-1015 Lausanne, Switzerland.

2: Solar Energy and Building Physics Laboratory (LESO-PB), Ecole Polytechnique Fédérale de Lausanne EPFL, Station 18, CH-1015 Lausanne, Switzerland.

ABSTRACT

Glass fiber-reinforced polymer (GFRP) materials are increasingly used in building construction for the design of multifunctional structures. These composite materials allow the integration of structural functions, building physics functions (mainly thermal insulation) and architectural functions (complex forms and color) in single large-scale building components. GFRP materials also allow the fabrication of translucent structural components with high degree of transparency when optically aligned resins and glass fibers are used, i.e. their refractive indices are identical. In this study the total light transmittance of hand lay-up GFRP laminates for building construction was investigated with a view to two architectural applications: translucent load-bearing structures and the encapsulation of photovoltaic (PV) cells into GFRP building skins of sandwich structures. Spectrophotometric experiments using an integrating sphere set-up were performed on unidirectional and cross-ply GFRP specimens in the range from 20% to 35% fiber volume fraction. Results were compared with the short-circuit currents generated by amorphous silicon (a-Si) PV cells encapsulated in GFRP laminates exposed to artificial sunlight radiation. The total amount of fibers in the laminates was the major parameter influencing light transmittance, with fiber architecture having little effect. 83% of solar irradiance in the band of 300-800 nm reached the surface of a-Si PV cells encapsulated below structural GFRP laminates with a fiber reinforcement weight of 820 g/m^2, demonstrating the feasibility of conceiving multifunctional GFRP structures.

Keywords: Glass fiber-reinforced polymer, Light transmittance, Multifunctional structure, Photovoltaic solar cells

INTRODUCTION

Today, iconic building projects creating lighting effects on their facades are constructed using polymer materials. Visual perception of the building facade is made to change with the illumination conditions, increasing therefore the architectural expression of the building. To this purpose, high light transmittance glass fiber-reinforced polymer (GFRP) laminates are increasingly used due to their low cost, lightweight and impact resistance compared to traditional glass components. Moreover amorphous silicon (a-Si) flexible photovoltaic (PV) solar cells can be encapsulated in the GFRP skins of freeform building envelopes, integrating electric energy production in lightweight and low-cost structures. Reducing the cost of the encapsulation process of PV cells has been a main issue since the early age of photovoltaic energy and for this purpose systems using GFRP composites can constitute a valuable option [1]. The integration of PV cells in multifunctional composite elements has begun to be explored recently for high-tech applications in aerospace [2, 3]. However, in such cases, FRP

composites are used as mechanical support for the PV cells and not as the top encapsulant of the cells. For building applications, recent research [4] has explored the thermal and mechanical feasibility of encapsulating PV cells in the translucent skin of structural GFRP/PUR (polyurethane) sandwich structures, however no optical investigation of the light transmittance through structural GFRP encapsulants was performed. For traditional encapsulants of a-Si PV cells, that is, cells covered with a thin layer of EVA adhesive and front sheets of glass or fluoropolymers, transmittance ranges from 0.89 to 0.95 were reported in [5]. This research investigates light transmittance of GFRP laminates used as translucent load-bearing structures and encapsulants of solar cells. In the first application, the percentage of visible light transmitted through GFRP laminates surrounded by air is investigated. In the second application, where the GFRP laminate is in contact with air on one side and laminated onto a solar cell on the other, the percentage of solar irradiance transmitted through the laminate and reaching the surface of a-Si PV cells is studied.

EXPERIMENTAL WORK

Fabrication of GFRP laminates

Unidirectional (UD) and cross-ply (CP) GFRP laminates were fabricated by a hand lay-up process using a UV-stabilized polyester resin and E-glass fibers, both with refractive indices around 1.56. The laminates cured at room temperature (23 ± 2°C) for one day and were then postcured for another day at 60°C. Five UD specimens (fiber reinforcement weight, *w*, of 410, 820, 1230, 1640 and 3280 g/m^2) and two CP symmetric specimens (of 1230 and 1640 g/m^2) were cut from the hand lay-up laminates. Fiber volume fraction of the specimens ranged from 20% to 35%. Specimens were labeled according to their reinforcement weight and fiber architecture, e.g. 1640CP refers to the specimen reinforced with w = 1640 g/m^2 of E-glass fibers and with cross-ply fiber architecture. In addition, a 1-mm thickness pure resin specimen was fabricated and cured using the same procedure as for the other specimens.

Fabrication of PV modules

Seven PV modules with three serial-connected a-Si PV cells (Flexcell) in each module were fabricated by hand lay-up, as shown in Fig. 1. Additionally, a reference non-encapsulated PV module with three serial-connected bare cells was also fabricated.

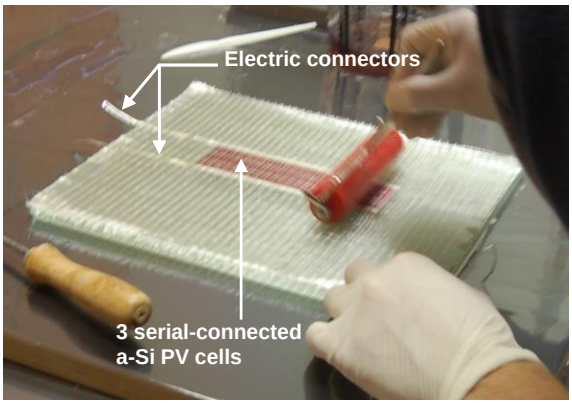

Figure 1: Hand lay-up encapsulation of three serial-connected a-Si PV cells in GFRP

The PV modules consisted of three different components: a rectangular glass pane support (300 x 250 x 10 mm^3), three connected a-Si PV cells (150 x 50 mm^2) and the GFRP encapsulant. One UD layer of E-glass was laminated onto the glass support and the thin PV cells were placed in the wet resin on top of this layer. The upper GFRP encapsulant was

laminated over the PV cells. The fiber architecture and reinforcement weight of the upper encapsulant differed for each module according to Table 1 (from 410 to 3280 g/m^2 in UD and CP architecture). The PV modules cured at room temperature (23 ± 2°C) for seven days.

PV cells encapsulant	None	410UD	820UD	1230UD	1640UD	3280UD	1230CP	1640CP
I_{sc} (mA)	187	164	155	152	140	118	-	136
T_{PVexp} (-)	1	0.88	0.83	0.81	0.75	0.63	-	0.73

Table 1: Short circuit currents for PV modules with different fiber architecture of upper encapsulants and corresponding light transmittance

Spectrophotometric set-up

The total hemispherical spectral light transmittance of the seven GFRP and of the 1-mm thickness resin specimens was investigated by spectrophotometry with a 152-mm-diameter integrating sphere as shown in Fig. 2. The measurements were performed using a halogen light source (Osram 64642 HLX, 150 W, 24 V, Xenophot®), an integrating sphere (LOT RT-060-SF) and a spectrophotometer (Oriel, model 77400, MultiSpec 125TM, type 1/8m) measuring from 400 to 800 nm and connected to a computer equipped with InstaSpecTM II software for signal analysis. Specimens were located at the entrance port A of the sphere and crossed by the beam of light at nearly normal incidence (81°). The specimens were oriented with the reinforcement rovings forming an approximate angle of 45° with the horizontal plane (see Fig. 2). Port B of the sphere remained closed. For each GFRP specimen, four measurements at different locations of the specimen were performed and, in the following, the average spectral curves will be presented.

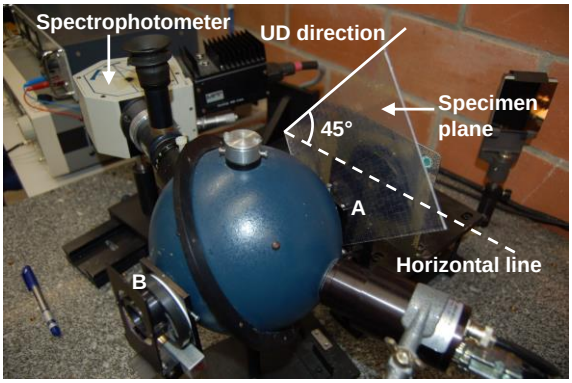

Figure 2: Integrating sphere with GFRP specimen located in port A for total light transmittance experiment

Solar radiation flash set-up

The percentage of solar irradiance reaching the surface of a-Si PV cells encapsulated in GFRP material was investigated subjecting the fabricated PV modules to a standardized radiation flash of 1000 W/m^2 and measuring the generated short circuit current. The flasher reproduced the terrestrial reference hemispherical solar spectral irradiance according to ASTM G173-03 for an air mass (AM) value of 1.5 [6]. The experiments were performed at ambient temperature between 19°C and 20°C.

RESULTS AND DISCUSSION

Spectrophotometric experiments

The measured spectral light transmittance curves of the UD specimens are shown in Fig. 3a. Light transmittance decreased when the reinforcement weight was increased. Light transmittance of UD and CP specimens is compared in Fig. 3b. For CP specimens transmittance was approximately 4% lower than for UD specimens. The transmittance results of the polyester resin specimen are also shown in Fig. 3a. Light absorption in the resin started at 430-nm wavelength and increased linearly until 400 nm. Using another spectrophotometer (Perkin Elmer Lambda 2), measuring regular transmittance from 190 nm to 1100 nm, showed that transmittance disappeared completely at 380 nm, from which point the light was absorbed by the UV additive. The spectral transmittance curve of the resin was therefore linearly extrapolated to zero at 380 nm.

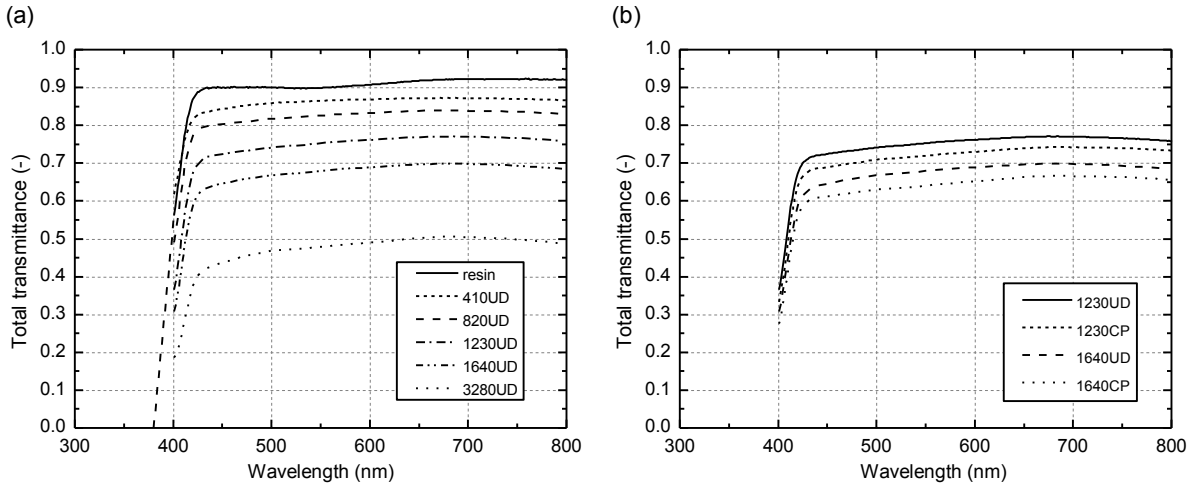

Figure 3: Spectral transmittance of (a) unidirectional specimens at different reinforcement weights and (b) unidirectional and cross-ply specimens

The transmittances at a single wavelength of 555 nm, $T_{t,555exp}$, of the pure resin, and UD specimens are shown in Fig. 4. The 555-nm wavelength was selected because the spectral response of the PV cells and the solar spectral irradiance both have their maximum very close to the 555-nm wavelength.

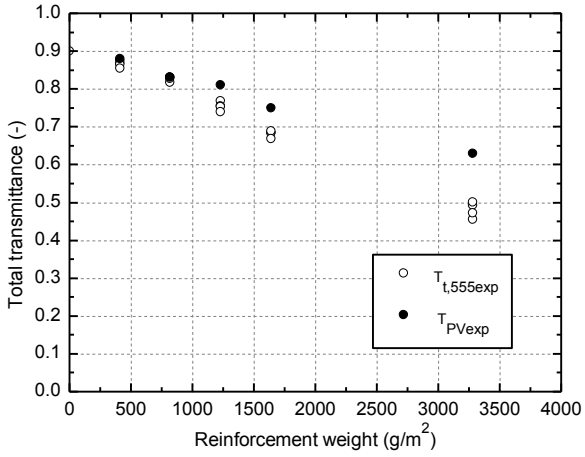

Figure 4: Transmittance measurements at 555-nm wavelength and from solar radiation flash experiments (UD specimens)

Solar radiation flash experiments

The short circuit current, I_{sc}, of a solar cell is directly proportional to the irradiance reaching the surface of the cell [7]. An experimental value of the light transmittance, T_{PVexp}, of the encapsulation system was therefore defined as the ratio between the I_{sc} generated by the encapsulated cells and the I_{sc} generated by the bare cells. The results are shown in Table 1 and Fig. 4. The PV cells with the 1230CP upper encapsulant did not generate any current during the experiment and it was concluded that these cells were damaged during the encapsulation process.

Comparison of experimental results

The light transmittance results obtained from spectrophotometric experiments, $T_{t,555exp}$, and solar radiation flash experiments, T_{PVexp}, are compared in Fig. 4. Both sets of results show that light transmittance significantly decreased when reinforcement weight increased. However, for $w > 820$ g/m^2, $T_{t,555exp}$ decreased much faster than T_{PVexp}. It was concluded that in the spectrophotometric measurements, for $w > 820$ g/m^2, not all of the scattered light inside the specimen passed through port A of the integrating sphere. The results obtained from the integrating sphere are therefore reliable only for low scattering specimens. The observed dependence of the transmittance on the reinforcement weight and, to a lesser extent, on the reinforcement architecture (UD or CP) may be attributed to two effects: 1) Even a small mismatch of the refractive indices of fibers and resin reduces transmittance; this reduction increases with increasing reinforcement weight. 2) Hand lamination cannot prevent the inclusion of some air pores, which represent a "material" (air) with a different refractive index. Locations sensitive to such voids are, in particular, crossings of fibers in CP laminates, which explains the slightly lower transmittance of CP compared to UD laminates.

As shown in Table 1, encapsulant 820UD had a transmittance $T_{PVexp} = 0.83$, which is between 7% and 13% lower than that of traditional encapsulations [5]. The Archinsolar project [8] showed, however, that a 10% loss in efficiency is well accepted for architecturally well integrated PV modules. The slightly lower efficiency of the encapsulation of PV cells into multifunctional GFRP elements with load-bearing capacity presented here thus can be acceptable.

CONCLUSIONS

Total light transmittance of GFRP laminates for building construction applications was measured. The following conclusions were drawn:

- The most important parameter affecting the light transmittance of GFRP is the fiber reinforcement weight of the laminate: transmittance increases with decreasing weight.

- Small-diameter integrating sphere measurements are reliable for low scattering laminates only. Measurements based on the short circuit current generation of encapsulated PV cells lead to more accurate values of GFRP light transmittance, particularly for thicker laminates.

- The solar irradiance in the band of 300-800 nm, reaching a-Si PV cells encapsulated in GFRP, is reduced by approximately 10% compared to traditional encapsulating systems if a structurally significant reinforcement weight of 820 g/m^2 is used for the covering layer. This drawback, however, can be compensated by the possible integration of PV cells into multifunctional load-bearing components, opening up new possibilities in architectural design.

AKNOWLEDGMENTS

The authors would like to thank EPFL Middle East for the financial support of this project, Flexcell for providing the PV cells and performing the artificial solar radiation flashes and Scobalit AG for providing the materials for the laminate fabrication.

REFERENCES

[1] Sawai H, Toshikawa H, Shibata A, Takemoto T, Tsuji T. The development of a low cost photovoltaic module using FRP molded encapsulation. Proceedings of the 16th IEEE Photovoltaic Specialists Conference; 1982 September 28; San Diego, USA. IEEE; 1982. p. 932-937.

[2] Rion J. Ultra-light photovoltaic composite sandwich structures [Ph.D.thesis]. Lausanne: Ecole Polytechnique Fédérale de Lausanne; 2008.

[3] Maung KJ, Hahn HT, Ju YS. Multifunctional integration of thin-film silicon solar cells on carbon-fiber-reinforced epoxy composites. Solar Energy 2010; 84(3):450-458.

[4] Keller T, Vassilopoulos AP, Manshadi BD. Thermomechanical behavior of multifunctional GFRP sandwich structures with encapsulated photovoltaic cells. Journal of Composites for Construction 2010; 14(4):470-478.

[5] Samuels SL, Glassmaker NJ, Andrews GA, Brown MJ, Lewittes ME. Teflon® FEP frontsheets for photovoltaic modules: improved optics leading to higher module efficiency. Proceedings of the 35th IEEE Photovoltaic Specialists Conference; 2010 June 20-25; Honolulu, USA. IEEE; 2010. p. 2788-2790.

[6] ASTM G173-03. Standard Tables for Reference Solar Spectral Irradiances: Direct Normal and Hemispherical on 37° tilted Surface. ASTM International; October 2008.

[7] Markvart T, editor. Solar electricity. 2nd ed. Chichester: John Wiley & Sons; 2000.

[8] Pélisset S, Joly M, Chapuis V, Schüler A, Mertin S, Hody-Le Caër V, et al. Efficiency of silicon thin-film photovoltaic modules with a front coloured glass. Proceedings of CISBAT International Conference; 2011 September 14-16; Lausanne, Switzerland. Lausanne: LESO-PB; 2011. p. 37-42.

SMART ENVELOPE. FROM LOW ENERGY TO NZEB.
ARCHITECTURAL INTEGRATION OF DYNAMIC AND INNOVATIVE TECHNOLOGIES FOR ENERGY SAVING

F. Cambiaso

Urban Planning, Design and Architectural Technology Department, Facoltà di Architettura, Sapienza University of Rome, Via Flaminia 70, 00196, Rome, Italy

ABSTRACT

Growing interest in development of innovative solutions for enhancement of sustainability in the built environments has been observed in recent years. According to the main constituents of buildings particularly in building envelopes, facades are expected to play a significant role towards the promotion of sustainable design in low energy buildings. This study presents a holistic review towards the analysis of 'intelligent facades' according to their types, current implementations, challenges, and ultimate impacts. Intelligent facades need to be responsive and conscious to the local climate, outdoor environment, and indoor spaces with view to parameters such as energy performance, thermal comfort, indoor air quality, visual comfort, etc. The findings demonstrate that energy modelling and simulations should be performed during the early stage of design process of buildings to ensure the practicality and effectiveness of any green implementations in buildings. Considerable attempts and endeavors based on comprehensive research efforts were observed for enhancement of energy efficiency in buildings in order to develop low energy, ultra low energy and zero energy buildings. To expand this goal, researcher efforts are required to focus on all constituents of the built environments and mainly the building envelope. It is clearly stated that innovating energy efficient design could highly reduce the overall energy consumption of buildings. According to Thormark, the 'operation' encompasses the highest rate of energy consumption in buildings; hence, the building envelope is proposed to be significantly reinforced based on enhanced building operations as an indicator of environmental responsiveness in order to contribute to the energy saving concept. In order to improve planning efficiency, Building Information Modeling (BIM) incorporates various information regarding building conditions such as thermographic databases based on laser scanning and infrared thermography in real world. Respectively, BIM-based simulations, specifically with view to building envelopes, can largely contribute towards the prediction of building energy consumptions; hence, resulting in corresponding consequential energy savings. Various energy modeling and simulation software have been developed for the analysis of building energy performances, and in particular the effects of building facades, including ASHRAE 90, DOE-2, MIT Design Advisor, Energy Plus, Etc. According to Maile, two fundamental type of software are utilized today including the "design tools" and "simulation tools". Design tools are predominantly used with focus on HVAC systems while simulation tools are used for the prediction of energy performances. This study highlights that the use of intelligent facades could considerably contribute to the enhanced energy performance of buildings, hence, the effectiveness of such systems is recommended to be verified and confirmed not only during the design stage but throughout the entire building lifecycle through the appropriate energy modelling and simulation software. These facades are not only influential for enhancement of the building energy performance, but also for optimized daylighting, as well as visual and thermal comfort besides the reduction of heat gains, noises and strong winds.

Keywords: high-performance envelope, integrated technologies, energy saving, thermal comfort

INTRODUCTION

Buildings, as the largest users of energy in our society, are also our greatest opportunity for energy conservation and protection of the environment. The rapidly growing world energy use has raised global concerns over continued depletion of energy resources and their negative environmental impacts. Current predictions show that this growing trend will continue. Building facades act as barriers between the interior and exterior environment. To provide building occupants with a comfortable and safe environment, a facade must fulfill many functions, such as: provision of views to the outside; resistance of forces from wind loads; bearing its own weight; implementation of daylighting strategies to minimize use of artificial lighting; protection from solar heat gain; protection from noise; resistance to rainwater and moisture penetration. Moreover, sustainable facades must block adverse external environmental effects and maintain internal comfort conditions with minimum energy consumption.

The location and climate thus are crucial factors in selecting appropriate design strategies for sustainable facades. Different design strategies are required for different climatic regions. Heating-dominated climates benefit from solar collection and passive heating, heat storage, and conservation through improved insulation and use of daylight to reduce lighting demand. For cooling-dominated climates, opposite strategies should be applied; in these climates, protection from sun and direct solar radiation is advantageous, as well as reduction of internal and external heat gains. In mixed climates, combined strategies must be implemented to balance solar exposure and access to daylight.

Different ways of approaching sustainable facade design can be chosen, including proper design and passive strategies based on building orientation; control of solar exposure and self-shading mechanics through tectonic building form; design of external shading elements; selection of facade materials; and design of exterior wall assemblies.

Strategies and technical guidelines for designing environmentally sensitive, energy-efficiency facades based on scientific principles are the basis of this paper, which illustrates with a case study how these approaches have been implemented on real-life architectural projects.

METHOD

Climate-based Design Approach

Designers of sustainable facades should use the specific characteristics of a building's location and climate, as well as its program requirements and site constraints, to create high-performance building envelopes that reduce the building's energy needs. Climate-specific guidelines must be considered during the design process. Strategies that work best in hot and arid climates are different from those that work in temperate or hot and humid regions. Climate encompasses the sum of temperature, humidity, atmospheric pressure, wind, rainfall, atmospheric particles, and other meteorological characteristics over extended periods of time. Climate is affected, in varying degrees, by latitude, terrain, and altitude, as well as by nearby mountain ranges or bodies water. The Koppen Climate Classification System was one of the first methods to categorize different climates. It consists of five major climate groups, each of which is further divided into one or more subgroups. The five primary groups are labelled by the letters A through E, and the subgroups by two and three letter codes to designate relative temperature, average precipitation and native vegetation.

Environmental and Design Criteria

Designers need to consider the external environment, building orientation, space dimensions, and occupants' comfort expectations. In choosing innovative and integrated technologies, we need to consider the conditions of the climate zone to minimize their impacts and reduce energy consumption.

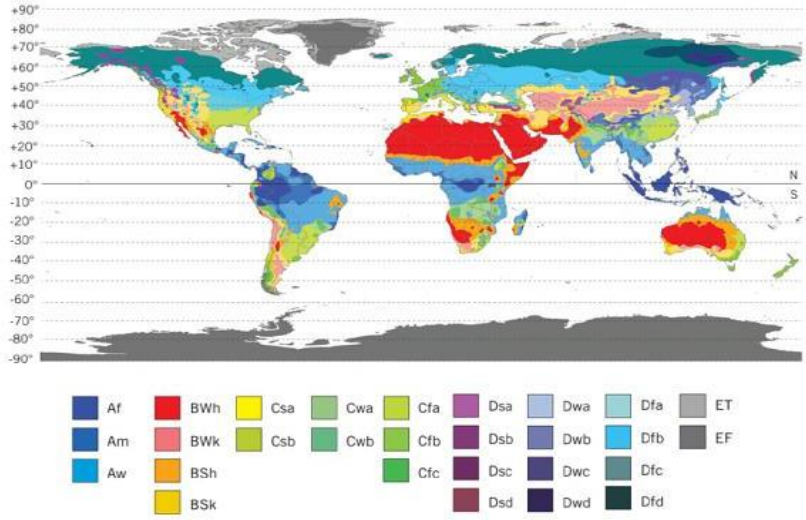

Figure 1: Koppen Climate Classification System.

Climate type	Design strategies for sustainable facades
Heating-dominated climates Zones 5, 6, 7, 8	*Solar collection and passive heating*: collection of solar heat through the building envelope *Heat storage*: storage of heat in the mass of the walls *Heat conservation*: preservation of heat within the building through improved insulation *Daylight*: use of natural light sources and increased glazed areas of the facade, use of high-performance glass, and use of light shelves to redirect light into interior spaces
Cooling-dominated climates Zones 1, 2, 3	*Solar control*: protection of the facade from direct solar radiation through self-shading methods (building form) or shading devices *Reduction of external heat gains*: protection from solar heat gain by infiltration (by using well-insulated opaque facade elements) or conduction (by using shading devices) *Cooling*: use of natural ventilation where environmental characteristics and building function permit *Daylight*: use of natural light sources while minimizing solar heat gain through use of shading devices and light shelves
Mixed climates Zone 4	*Solar control:* protection of facade from direct solar radiation (shading) during warm seasons *Solar collection and passive heating:* solar collection during cold seasons *Daylight:* use of natural light sources and increased glazed areas of the facade with shading devices

Figure 2: Facade Design strategies for different climate zones.

DISCUSSION AND RESULTS

The application of the concepts will be demonstrated and discussed through two case studies.

Case Studies

A) KAFD 4.01

High-performance, low-e double glazing was used for all facades. Three glass types, with visual transmittance values of 25%, 45%, and 69%, were specified.

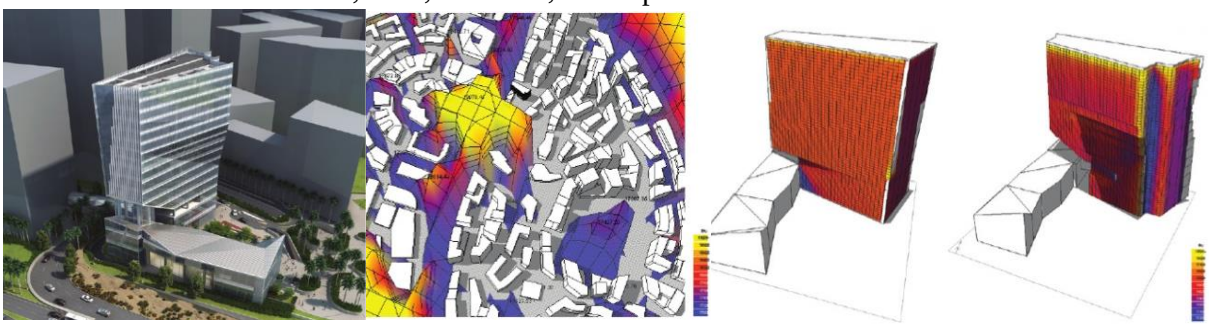

Figure 3 (on the left) KAFD 4.01 south and west facades; (in the middle) Solar radiation on the site; (on the right) Incident solar radiation for flat south facade and self-shaded form.

All insulated glazing units were filled with argon to improve performance. The three glazing types had center-of-glass U-values of 1.1 W/m2-°K). Most of the glazing for the tower facades used the glass type with the lowest visual transmittance (25%), as those facades would receive the highest level of radiation. The glass type with 45% visual transmittance was used on parts of the east tower facade. The glass type with the highest visual transmission (69%) was used for the retail areas on the first two levels, as they would be exposed to the least solar radiation. A number of passive design strategies were incorporated into the design of the facades. The east, south, and west facades are "warped", with parts of the curtain walls sloping outward as they rise higher. The warped facades allow the upper floors of the building to shade parts of the facade below, so the building shades itself. Each facade orientation required a different design solution.

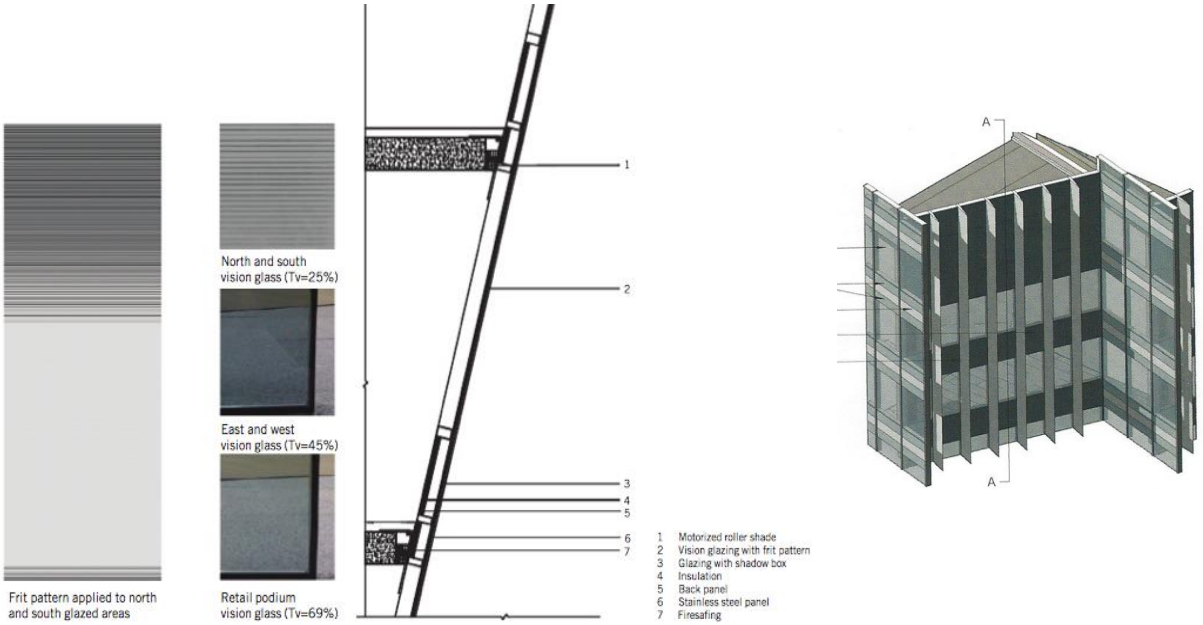

Figure 4: Three glass types and the graduated frit pattern used on the north and south facade glazing. (on the left) Glass selection for different facade orientations; (on the right) Partial south facade curtain wall section.

B) Vincent Triggs Elementary School

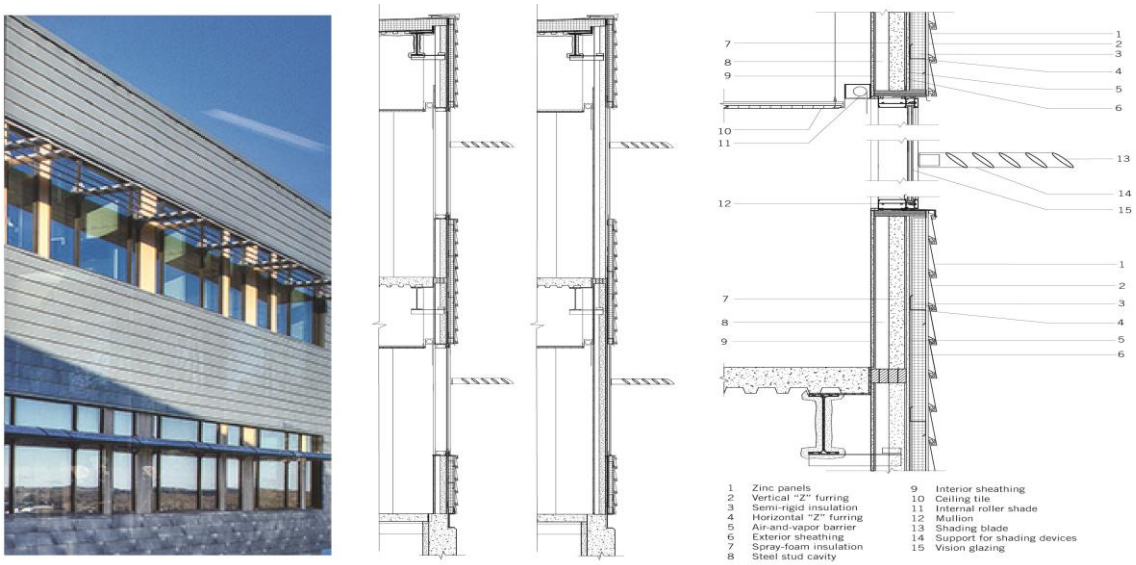

Figure 5: Elementary School showing the zinc siding and horizontal sunshades of the south facade, and the curtain wall of the east and west facade.

The Elementary School in the example, is located in the mixed, arid climate region. The building relies on passive design strategies, including optimized building orientation, climate-appropriate massing, and a thermally improved building envelope to reduce energy use. The building's facade consists of opaque panels containing punched windows, with shading devices on the south and west sides. Insulated tilt-up concrete panels were selected as the opaque facade material. These panels, often used for industrial, warehouse, or big-box retail buildings, were a low-cost way to provide high thermal performance. Each panel is composed of three layers, with the insulation sandwiched between precast concrete skin. This panel construction minimizes the direct transfer of outside heat to the inside. The concrete mass of the panels also provides thermal storage, which is beneficial in this type of climate due to the large daily temperature shifts. All glazing assemblies are composed of high-performance, low-e insulated units set in thermally broken frames.

Instead, the west facade consists of three facade types: zinc panels; curtain wall and composite wood panels. The thickness of the opaque part of the exterior wall has these components: composite wood panels; semi-rigid mineral fiber insulation; sheet air-and-vapor barrier adhered to sheating; fiber-reinforced sheating; spray-foam insulation within a 4-inch steel stud cavity; interior sheating.

The curtain wall consists of thermally broken aluminum frames; low-e, argon-filled and insulated spandrel areas at the upper portion of the curtain wall. The overall U-value of this facade is 0.35 W/m2-°K.

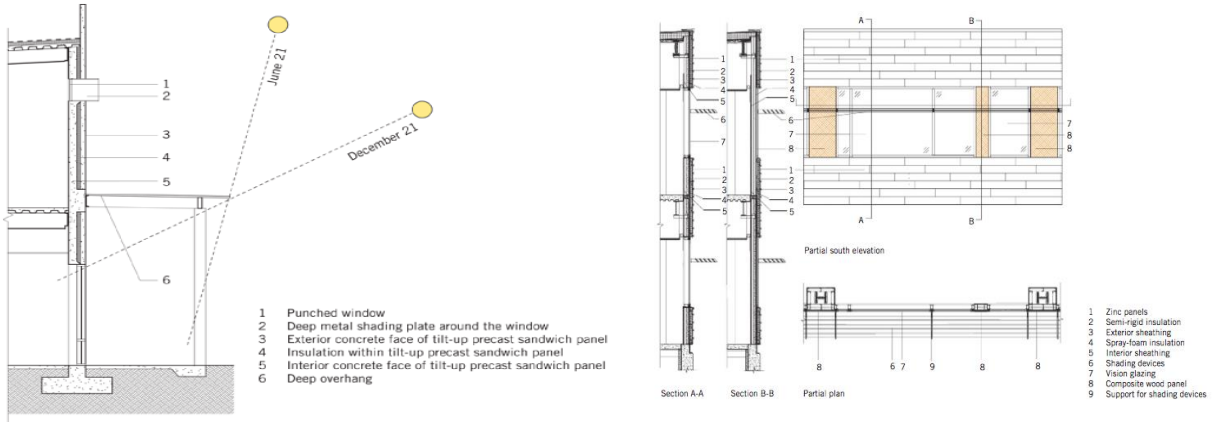

Figure 6: (on the left) Exterior wall section south facade; (on the right) South facade partial elevation, partial plan and sections.

The thickness of the exterior wall is 305mm. The windows consist of thermally broken aluminum mullions and low-e, argon filled, with U-value of 1.36 W/m2-°K. Between the punched windows are resin-impregnated composite wood panels. With 76mm of spray-foam insulation, these opaque wall areas have a U-value of 0.33 W/m2-°K. The 760mm deep overhang consists of five aluminum blades, angled to block high summer sun.

CONCLUSION

The facade is one of the most significant contributors to the energy budget and the comfort parameters of any buildings. As energy and other natural resources continue to be depleted, it has become clear that technologies and strategies that allow us to maintain our satisfaction with the interior environment while consuming fewer of these resources are major objectives for contemporary facade designs. This paper focuses on the strategies and approaches for

designing sustainable, high-performance building facade, and provides technical guidance. This strategies and technical guidelines for designing environmentally sensitive, energy-efficiency and smart envelope are based on scientific principles (such as climate-specific approaches for minimizing energy consumption, thermal behavior of different facade systems, materials and their properties) and also control of physical environment factors (heat, light, sounds) that improve occupant comfort (thermal, visual, acoustic, and air quality). Buildings are not self-contained mechanism functioning independently from their surrounding natural system. Sustainable envelopes are integral parts of high-performance buildings and such buildings require careful planning, design, construction and operation.

The case-study projects illustrate four ways to approach sustainable facade design: building orientation; tectonic sun exposure control; external shading elements; facade properties of materials and wall assemblies.

ACKNOWLEDGEMENTS

I thank the authors whose contributions are of such significant importance for the success of my research. With their buildings, committed clients and designers have created the conditions under which net zero energy buildings can become reality.

REFERENCES

1. Hegger M., Fuchs, M., Stark, T., Zeumer, M., Energy Manual. Sustainable architecture, Detail, Munich, 2008.
2. Thormark, C., A low energy building in a lifecycle – its embodied energy, energy need for operation and recycling potential, Building and Environment, pp. 429-435, 2002.
3. Maile, T., Fischer, M., Bazjanac, V., Building energy performance simulation tools – a lifecycle and interoperable perspective, CIFE working paper, WP107, Center for Integrated Facility Engineering, Stanford University, 2007.
4. Aksamija, A., Context Based Design of double skin Facades: climatic consideration during the design process, Perkins+Will Research Journal, Vol.1, No. 1, pp. 54-69, 2009.
5. Aksamija, A., Analysis and Computation: Sustainable design in practice, Design Principles and Practices: An International Journal, Vol. 4, No. 4, pp. 291-314, 2010.
6. Badinelli, G., Double Skin Facades for Warm Climate Regions: Analysis of a Solution with an Integrated Movable Shading System, Building and Environment, Vol. 44, pp. 1107-1118.
7. Watts, A., Modern Construction Envelopes, Springer-Verlag, Wien, 2011.
8. Lawrence, P., Chase, T., Investigating the climate impacts of Global land cover change in the Community Climate System Model, International Journal of Climatology, Vol. 30, No.13, pp. 2066-2087, 2010.
9. Peel, M., Finlayson, B., McMahon, T., Updated World Map of the Koppen-Geiger Climate Classification, Hydrology and Earth System Sciences, Vol.11, No. 5, pp. 1633-1644.
10. ASHRAE, ANSI/ASHRAE/USGBC/IES Standard 189.1 for the Design of High-Performance Green Buildings, GA: American Society of Heating, Refrigerating and Air-Conditioning Engineers, Atlanta, 2009.

REDUCING EMBODIED ENERGY - A FUTURE CHALLENGE FOR PLANNERS AND MANUFACTURERS

D. Kellenberger

Intep – Integrale Planung GmbH, Dufourstrasse 115, 8008 Zürich

ABSTRACT

Looking at the heating energy demand for new buildings in Switzerland from the time after the Second World War up to today, a reduction from almost 800 MJ/m^{2}a to about 150 MJ/m^{2}a has been documented. That's a reduction of almost 80%. Today, there are plenty of examples pointing towards zero energy heating and even energy producing houses. This effect is based on the introduction of legal requirements in the 1970s which have been tightened in the following years. The introduction of the Swiss Label MINERGIE in 1998, the more stringent MINERGIE-P Label in 2002 and MINERGIE-A in 2011 supported the reduction of the heating energy demand significantly by dictating a high standard for the thermal envelope and the use of locally produced renewable energy. Proofing feasibility resulted again in more stringent rules and regulations. The consequences were an increase of insulation as well as complexity of HVACR (Heating, Ventilation, Air Conditioning and Refrigeration) Systems, both resulting in an increase of embodied energy. Drawing up the relation of non-renewable primary energy for construction and operation in the past and the future shows very clearly where the challenges will be: It won't be operational but embodied energy.

Together with the development of the new labels as for example MINERGIE-A and MINERGIE–ECO, first efforts to reduce embodied energy have been put in place.

In general, there are different ways to improve the energetic and environmental quality of the construction of a building. Instead of targeting a competition between different materials (e.g. timber versus concrete), Environmental Product Declarations (EPD) allow a comparison between different specific products within a certain category based on a large variety of environmental information including embodied energy. Different products within a certain product category have to follow the same calculation and presentation rules (PCR's).

EPD's can also contribute to environmentally improve products/materials by providing a good insight in the production process, the resource usage and the production-related impacts in order to detect optimization potentials in production, installation and operation. Manufacturers can furthermore profit from EPD's when communicating their environmentally sound product in a credible way.

Keywords: Embodied, Energy, EPD, PCR, LCA

INTRODUCTION

Embodied energy and impact on Green Building Labels

A number of existing labels and standards in Switzerland, Germany as well as other international countries require - next to other criteria - a Life Cycle Assessment (LCA) of the building materials.

The Swiss label MINERGIE with its different variants MINERGIE, MINERGIE-P and MINERGIE-A was introduced in 1998 and is mainly assessing the energy efficiency of a building. It is hugely successful as it has achieved a market share of more than 25% in the new homes sector, which is unique even by international comparison. Since 2006, buildings

with healthy and eco-friendly constructions may be awarded the label MINERGIE-ECO which is an addition to the operation-related labels MINERGIE, MINERGIE-P and MINERGIE-A. One of the most important criteria within the assessment is the embodied energy (primary energy non-renewable). The fulfilment of this requirement needs to be proven with the calculation of a Life Cycle Assessment.

In Switzerland, the association "Energiestadt" has successfully introduced the new certificate "2000-Watt-Development-Site" in 2012. At the moment, a pilot phase until 2014 takes place. The certificate is based on the SIA (Swiss Society of Engineers and Architects) Energy Efficiency Path [1] and on the existing Label "Energiestadt". It assesses whole development sites regarding the targets of 2000-Watt-Society. The calculation of cumulative primary energy and Global Warming Potential (GWP) is done with the help of an LCA. A first development site in the city of Zurich (Green City) has been certified in 2012.

The German DGNB-Certificate (German Certificate for Sustainable Construction) was introduced in 2007 by the German Sustainable Building Council (DGNB) and the German Federal Ministry of Transportation, Construction and City Development. In 2012 the process has been adapted by the Swiss Sustainable Building Council for Switzerland. Of the total of 51 SGNI criteria, seven focus on energy and environmental impact as results of an LCA. These are Global warming potential, depletion potential of the stratospheric ozone layer, Eutrophication potential, Formation potential of tropospheric ozone photochemical oxidants and primary energy demand (total, non-renewable and renewable).

A Swiss Standard for Sustainable Construction has been induced by the Swiss Federal Office of Energy and will be released in June 2013. It is based on the SIA recommendation 112/1, Sustainable building construction [2] which includes standard criteria for the most building - relevant topics of the three sustainability dimensions Society, Economy and Environment. It is planned to develop a new Label on the basis of the standard. The environmental impact of construction, operation and building-induced mobility will be assessed on the basis of the indicators primary energy and GWP.

Environmental Product Declaration (EPD)

Ecolabels are the most often used form of environmental product declarations. They offer a coarse information on the environmental impact of single materials, products and services. They can be used as basis for the ecological assessment of buildings. Regarding internationally agreed ISO-Standards, labels are categorized as follows:

- Type I Label (based on ISO 14024)

  Type I ecolabels are committed by independent third parties on the basis of certain criteria over the whole life cycle. They award products and services which fulfill certain qualitative criteria. Common examples are „Blauer Engel" or „natureplus".

- Type II Label (based on ISO 14021)

  Type II ecolabels are, in contrast to type I labels, committed by companies themselves on the basis of certain criteria over the whole life cycle. The certification can, but does not have to be reviewed by a third independent part.

- Type III Label (based on ISO 14025)

  An EPD for building products is a Typ III ecolabel which includes a comprehensive description of the environmental quality without a rating. It is based on an ISO 14040-compatible LCA which systematically includes all material flows from resource extraction to final disposal. The environmental impacts are characterized based on internationally accepted conventions and the results are operating figures like GWP.

An EPD includes a large variety of environmental information including embodied energy and environmental impacts of a specific product (e.g. unlaminated glasswool from Isover). Different products within a certain product category (e.g. insulation materials) have to follow the same calculation and presentation rules, described either in a specific Product Category Rule (PCR) or in the new European Standard EN 15804:2012 (Core rules for the product category of construction products).

Environmental Product Declarations in Labels

There is only one Swiss label accepting EPDs in the calculation of the Life Cycle Assessment of the whole building, the Swiss adaptation of the DGNB label (SGNI):

To calculate the environmental impact of a building for the label DGNB Switzerland the user needs to use either generic data from the German "ökobau.dat" [8] database or if available product specific data from EPDs. Using generic data (e.g. GaBi (http://www.gabi-software.com/databases/) or ecoinvent (www.ecoinvent.ch)) and not verified data (e.g. ökobau.dat) are punished with a 10% surplus on the environmental impact.

The French certification system HQE (Haute Qualité Environmentale) is in use by the HQE-Association since 1997. The certification covers three phases: terms of reference, first draft and implementation. To be successful in achieving the HQE-Certificate, the user needs to work on the categories contaminant-freedom, energy management and water efficiency. Furthermore a minimum of 30 from 110 points have to be achieved in the whole of 14 categories. HQE asks for a LCA for which in minimum 50% of the used components need to have an EPD fulfilling the French or European standards.

Another label used quite often in Switzerland is the US LEED label (Leadership in Energy and Environmental Design). The existing LEED Pilot Credit 63 "Whole Building Life Cycle Assessment" is the basis for the draft version of a new credit in LEED v4. It only requires a reduction of the life cycle impacts compared to a reference building of comparable size and function.

RELATION BETWEEN OPERATIONAL AND EMBODIED ENERGY

A building uses over its entire life cycle both operating and embodied energy. Until a few years ago, the assessment of buildings only looked at the operating energy. This is mainly based on the fact that it wasn't possible to account for the embodied energy and that operating energy was directly linked to operational cost. After calculating the first LCA of buildings and comparing it with the operational energy, it clearly showed that the total energy consumption was dominated by the part of operational energy [3]. Due to mandatory standards and labels (e.g. MINERGIE), new regulations with increasing requirements [4] (e.g. EnEV, SIA Guideline 2031) as well as the use of more efficient HVAC systems and devices [3], operational energy was reduced significantly in the last 30 years.

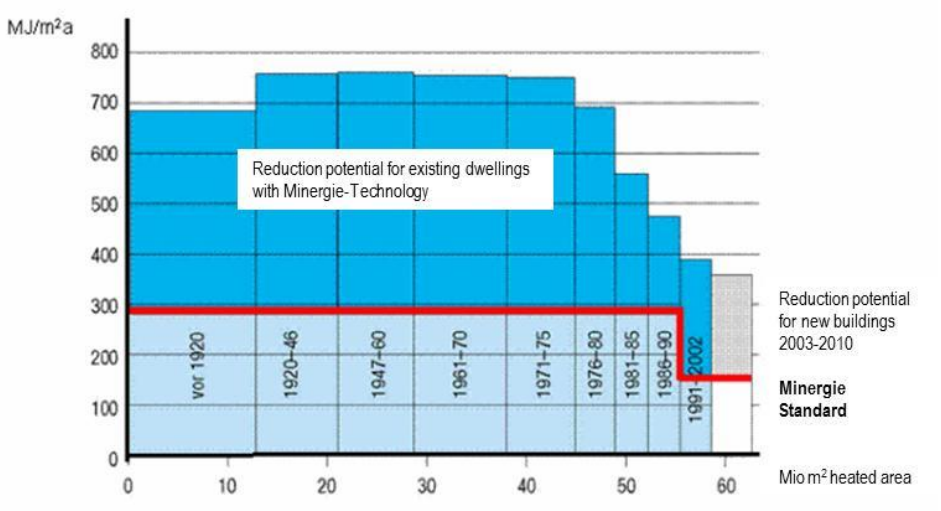

Figure 1: Energy demand for heating and hot water of buildings in the Kanton Zurich [8]

Furthermore, more stringent mandatory standards and labels have been developed in the last years to certify very low (e.g. MINERGIE-P and –A) and even zero operational energy houses (e.g. PassivHaus). Some pioneers have also developed plus energy buildings in the last couple of years [5]. This was mainly possible by reducing or even completely avoiding thermal bridges, using high performance insulation, ensuring maximum air tightness together with very efficient heat recovery systems [4]. All these measures require either additional material or more complex devices leading to an increase in embodied energy. For very low energy houses, the embodied energy contributes to about 75% of the total energy used in a building over its life cycle [6] and [7]. When following the ongoing tendencies on the comparison between operational and embodied energy, the latter is gaining importance in the future.

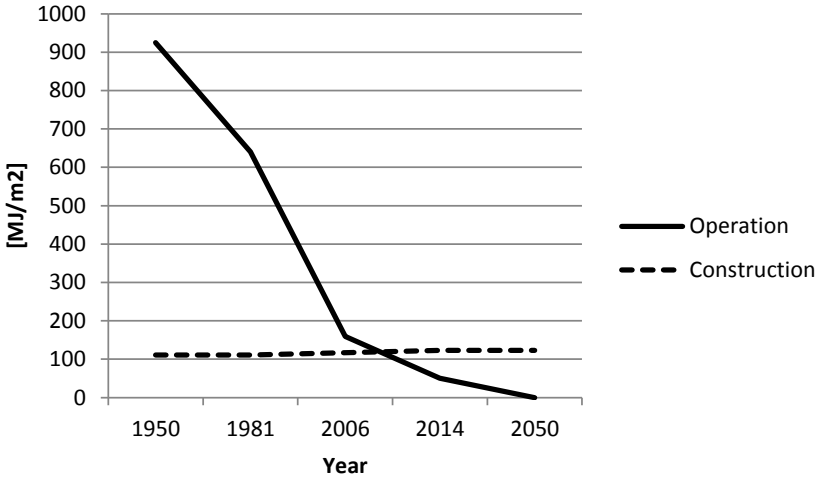

Figure 2: Past and future trend for primary energy non-renewable for operation and construction (embodied energy) of buildings in Switzerland.

This trend is based on the assumption that it will be normal in 2050 to build zero operational energy buildings. Therefore, our future tasks will have to focus on reducing embodied energy. This means motivating building product manufacturers to improve their products from an energetic and environmental point of view.

REDUCING EMBODIED ENERGY

General

In general, there are three different ways to reduce embodied energy and impact on a whole building level:

- When looking at a reduction on a per inhabitant/employee level, reducing the heated area per person/employee is most effective (Sufficiency).
- Reducing the amount (volume or weight) of materials in a building (Optimization by e.g. reducing the thickness of a wall to a minimum) is effective.
- Use of low impact materials based on generic data (Competition between materials as e.g. using raw air-dried, untreated timber instead of concrete when focusing on GWP)
- Choosing a low impact product within a certain product category (e.g. heating system) offered by a certain manufacturer (Competition between manufacturers of comparable products) is the approach on the manufacturer level. At the moment, only EPD schemes are able to present the required information in a credible way.

The basis data for the calculation of embodied energy in Switzerland is the KBOB list (http://www.eco-bau.ch/resources/uploads/KBOB_EMPFEHLUNG_2009_1_Juli_2012.pdf). This list is mainly an extraction of the building related datasets from the Swiss ecoinvent database (www.ecoinvent.ch). The fact that ecoinvent is a generic database based on average datasets for different products (e.g. heat pump air/water SPF 2.8, concrete C 30/37) has led to the situation that improvements regarding embodied energy can only be achieved by using different materials/products (see point 3 in above list). This, for example, has resulted in an often heard general argument that timber buildings are better than concrete buildings. In order to rather focus on the improvement of products than competition between products, different EPD programs have been initiated in the EU in the last years.

Influence of EPDs on a whole building scale

Environmental Product Declarations can be used in different ways in different stages in the production process of a building project.

For manufacturers and product developers, an EPD can provide a good insight in the resource and production-related impacts. This analysis helps detecting optimisation potential in production, installation and operation. This process is also called Ecodesign. Furthermore, the manufacturers can profit from EPDs when communicating product and company information credibly. By a transparent presentation of the information, marketing statements can be backed up and comparisons with similar products in the same product category can be made. EPD's can also be used to present product improvements over time. The calculation of the LCA for EPD's usually use generic data for the resources, energy and waste treatment related to the production process. If existing, specific data (usually from EPDs too) can be used, this makes the impact of a product also more specific.

EPD's can also be used as information source for tender and for the purchasing processes. They give the purchasers the certainty that the environmental quality of a certain product has been proven by a third party reviewer with knowledge in LCA. When used in the planning phase of a building, EPD's can be used to check different options to improve a building from an environmental point of view.

SUMMARY AND CONCLUSION

Based on the fact that research and development of building systems have led to a reduction of operational energy to zero or even below it is time to think about embodied energy. At the moment the only driver for manufacturers to optimize their products is costs which are not directly linked to the embodied energy. The growing market on building labels which are focusing on the overall life cycle of a building are putting even more pressure on manufacturers of building materials/products. First steps to make embodied energy as well as environmental impacts of materials/products transparent for the consumers are EPD's. Transparency is a compellent step towards more energy efficient and more environmentally friendly building products. The information published in the EPDs then would have to be entered in the LCA databases to be available for calculating an LCA of a building.

REFERENCES

[1] Swiss society of engineers and architects: SIA-Effizienzpfad Energie. Merkblatt 2040, Ausgabe 2011.

[2] Swiss society of engineers and architects: Nachhaltiges Bauen – Hochbau, Ergänzungen zum Leistungsmodell SIA 112. Empfehlung SIA 112/1, 2004.

[3] Dixit, M. K. et al.: Identification of parameters for embodied energy measurement: A literature review. Energy and Buildings, Vol. 42, pp. 1238-1247, 2010.

[4] Ding, G.: The development of a multi-criteria approach for the measurement of sustainable performance for built projects and facilities, Ph.D. Thesis, University of technology, Sydney, Australia, 2004.

[5] Kolokotsa, D. et al.: A roadmap towards intelligent net zero- and positive-energy buildings. Solar Energy, Vol. 85, Issue 12, pp. 3067-3084, 2011.

[6] Hernandez, P. and Kenny, P.: Life cycle energy performance: exploring the limits of passive 'low energy' buildings. Paper presented at the World Sustainable Building Conference, Melbourne, Australia, 2008.

[7] Hernandez, P. and Kenny, P.: Integrating occupant preference and life cycle energy evaluation: a simplified method. Building Research & Information, Vol. 38(6), pp. 625-637, 2010.

[8] http://www.stadt-zuerich.ch/content/gud/de/index/umwelt/bauen/energieeffizient_bauen_sanieren.html, 2013

[9] http://www.nachhaltigesbauen.de/no_cache/baustoff-und-gebaeudedaten/oekobaudat.html?cid=1504&did=3021&sechash=72208dd1, 2013

A TOOL FOR THE OPTIMIZATION OF BUILDING ENVELOPE TECHNOLOGIES – BASIC PERFORMANCES AGAINST CONSTRUCTION COSTS OF EXTERIOR WALLS

E. De Angelis[1], D. Pasini[1], G. Pansa[1], G. Dotelli[2], E. Serra[3]

1: Politecnico di Milano, Dipartimento ABC. Mail to enrico.deangelis@polimi.it

2: Politecnico di Milano, Dipartimento CMIC "G. Natta"

3: Università degli Studi di Brescia, Dipartimento DICATAM

ABSTRACT

The configuration of the envelope of a building must answer to many needs. This is even truer nowadays, where the standards for energy efficiency and the crisis of building market require a detailed knowledge of construction technologies and costs to achieve the minimum energetic targets. The present work is focused on exterior wall systems. Among all available technologies, masonry walls have been analyzed (single layer walls with homogeneous insulation, such as clay blocks, flat clay blocks, insulation filled clay blocks, autoclaved aerated concrete (AAC) blocks, and walls with ETICS). Through a systematic data collection of technical information available and declared from the producer, the elementary characteristics and prices of the products are translated in performances and costs of all their possible standard combinations, i.e. every feasible assembly that makes them "a wall". For each solution, with reference to a one square meter building façade in a current section, we performed a multi-criteria evaluation of the following parameters: thermal transmittance, noise rating coefficient, construction costs, and the global warming potential (GWP). Each solution is a point in an n-D space, where n is the number of performance indicators taken into account, but it can be represented in a simplified 2-D or 3-D space where the best solutions are shown as Pareto-optimal curves or surfaces. Moreover, joints between envelope and the building concrete structure (beams and pillars) have been assessed. For each detailed solutions the real cost and the real average performances have been evaluated including thermal bridge effects for a standard façade module. All the Pareto-optimal curves change from starting positions toward new corrected ones. As a last step the results have been applied to a simple case study assessing the EP_H-values for some wall solutions.

Keywords: multi-criteria analysis; construction costs; exterior walls; thermal bridges.

INTRODUCTION

The multi objective optimization is a common practice in building performance analyses [1-3] and aims to identify not only a single optimal solution, but a series of best envelope solutions on the basis of selected parameters. The decision making, in the design phase, is a multi objective optimization problem that is characterized by the existence of multiple and, often, competitive objectives. In fact, the optimal solution cannot be chosen based on just one parameter such as thermal transmittance or costs for realization (as stated in the energy performance building directive EPBD 2010/31 EU [4], with reference to cost-optimal levels of energy performance requirements for buildings and building elements); in many cases, it is of utmost importance to consider also acoustic performances and environmental costs. In this paper, a database of masonry wall technical solutions has been created, including the contribution of main thermal bridges on average performances (thermal resistance and costs) for a standard façade module and considering acoustic and environmental issues.

METHODOLOGY

The considered façade module is 3.1x4.0 m gross size (Figure 1). 70 wall solutions have been analyzed for single layer walls, divided in 57 non-load bearing blocks and 13 load bearing blocks (considering an Italian seismic zone 3). For ETICS walls (External Thermal Insulating Composite System), 57 solutions realized with 3 different blocks (clay, flat clay and AAC) and 7 types of insulation layers (PU, EPS, Kenaf, Mineral Wool, Calcium silicate, Cork, Wood Wool), with different thickness, have been analyzed. The multi-criteria evaluation has been made on the following parameters: thermal transmittance R [(m^2K)/W], noise rating coefficient R_w [dB], construction costs C [€/m^2] and environmental impacts. The effect of wall-window thermal bridge has not been considered in this work. To correct the thermal resistance (R') the reference surface is the gross opaque area (S_{OP}) whereas to correct costs (C') the reference surface is the net wall surface (S_{WALL}).

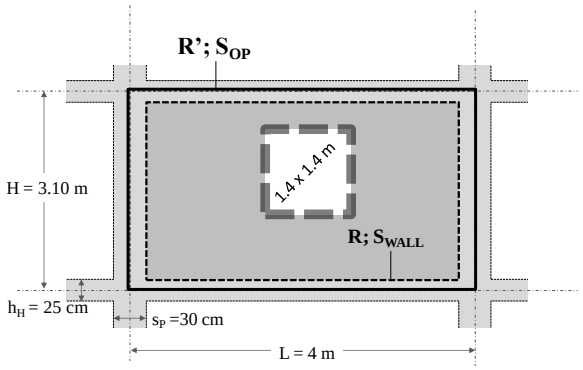

$$R' = R + \psi_{PIL}\frac{H}{S_{OP}} + \psi_{BEAM}\frac{L}{S_{OP}} \quad (1)$$

$$C' = C + C_{PIL}\frac{H}{S_{WALL}} + C_{BEAM}\frac{L}{S_{WALL}} \quad (2)$$

Figure 1: Standard facade module and formulation for correct thermal resistance and cost.

Environmental impact has been calculated using the Life Cycle Assessment (LCA) methodology, limited only to the materials the envelope is made of, in the "cradle to gate" perspective. Each environmental impact (for brevity here only global warming potential is reported [$kgCO_2eq/m^2$]) is calculated according to European standard EN 15804:2012 [5]. Data source is the Ecoinvent 2.0 database and calculations have been carried out using the software SimaPro 7.3. The average R-value has been calculated taking into account main thermal bridges (corrected by insulation material layers in EPS or Wood Wool) contribution assessed by means of a finite element software (COMSOL) according to ISO 10211 [6].

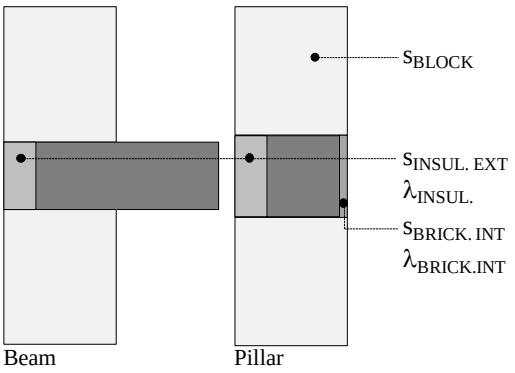

s_{BLOCK} [cm]	$s_{INSUL.\ EXT}$ [cm]	$s_{BRICK\ INT}$ [cm]	$\lambda_{INSUL.}$ [W/(mK)]	$\lambda_{BRICK.\ INT}$ [W/(mK)]
0.300	0.05	0.000	0.04 0.10	0.25
0.365	0.06	0.055		
0.380	0.06	0.070		
	0.12	0.010		
0.400	0.06	0.090		
	0.12	0.030		
0.425	0.06	0.115		
	0.12	0.055		
0.450	0.06	0.140		
	0.12	0.080		
0.490	0.06	0.180		
	0.12	0.120		

Figure 2: Size coordination of load-bearing structures, walls and thermal bridge correction.

Construction costs, including materials, machinery and manpower, overhead costs (safety, site) and contractor's profit (about 32%), have been collected and validated from manufacturers and construction companies.

RESULTS

Thermal Resistance and Cost

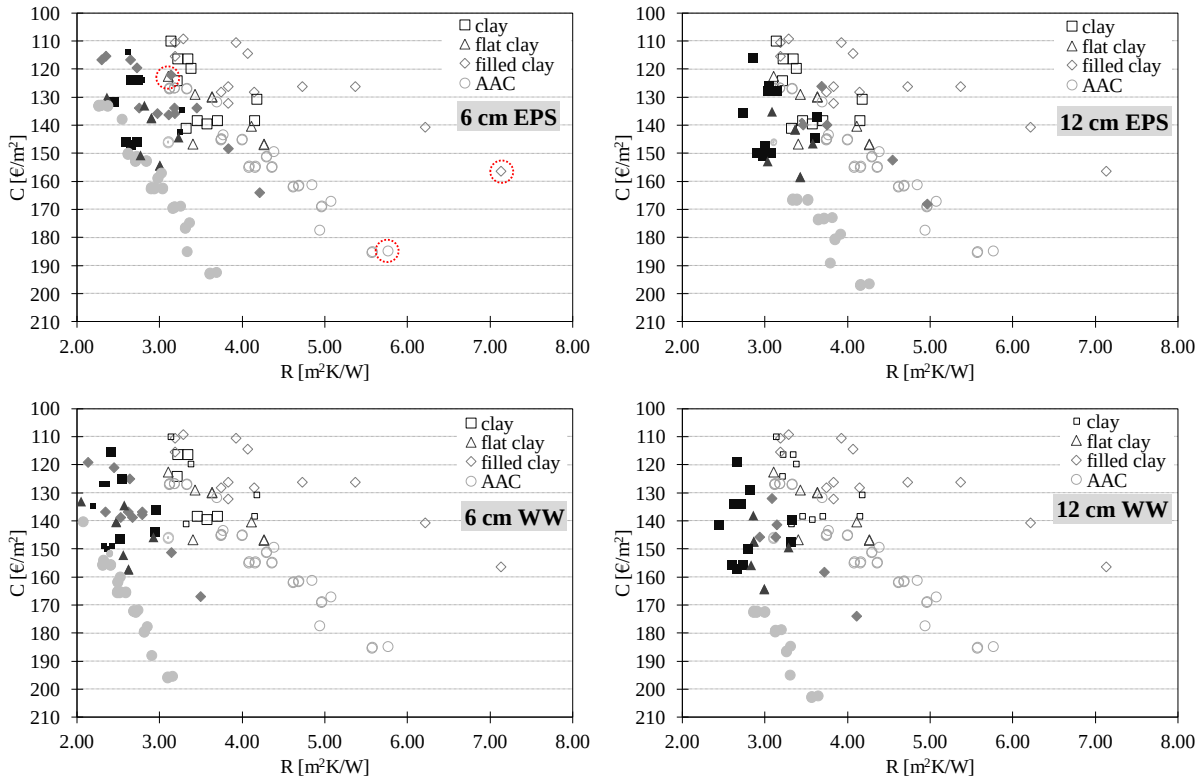

Figure 3: Relations between thermal resistance (R – empty points) in a current section and correct average value (R' - filled points) and realization cost (C and C') for each thermal bridge correction solution.

From all graphs results that thermal bridges assessment brings to a reducing of thermal resistance of about 65% in cases with highest initial thermal resistance values and 50% in cases with the lowest. The correction with insulating materials requires an overhead cost of about 10-15 €/m^2 and it allows limiting the R reduction to 30-35%. Pareto- optimal curves are shifted toward the worst zone of graphs. The best solutions are given with 12 cm EPS thermal bridge correction (see marked points in Figure 3a and Figure 4).

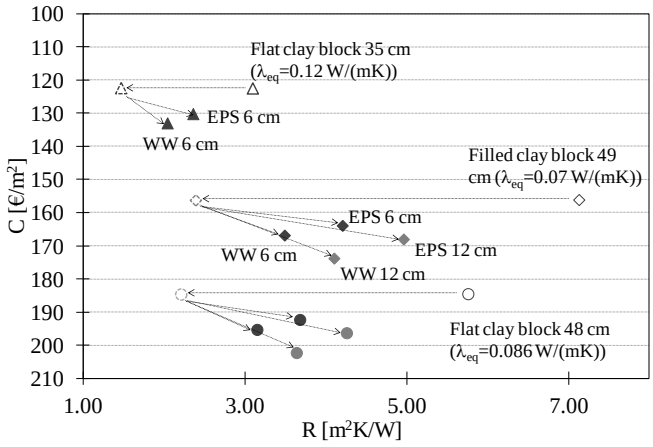

Figure 4: Switch from R to R' and C-C' in case of single layer walls considering thermal bridge corrections.

Noise Rating Coefficient and Thermal Resistance

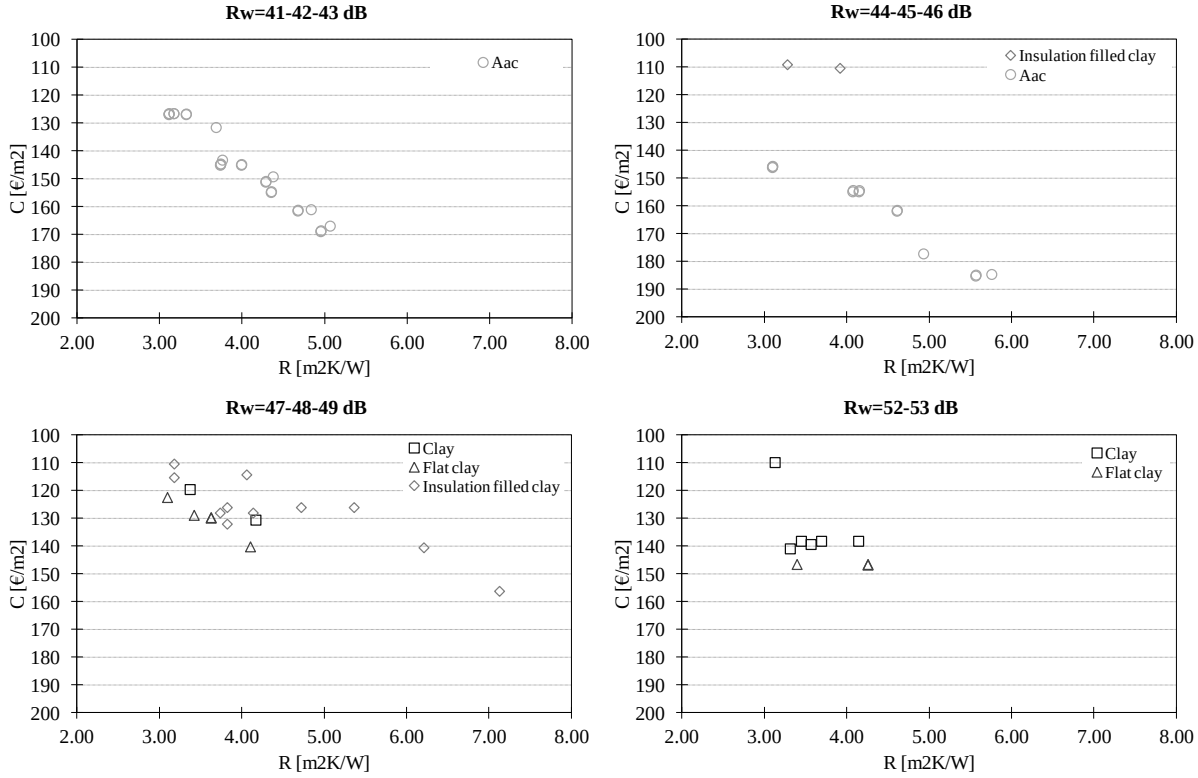

Figure 5: Relations between thermal resistance in a current section (R) and costs (C) for different noise rating coefficient values (Rw).

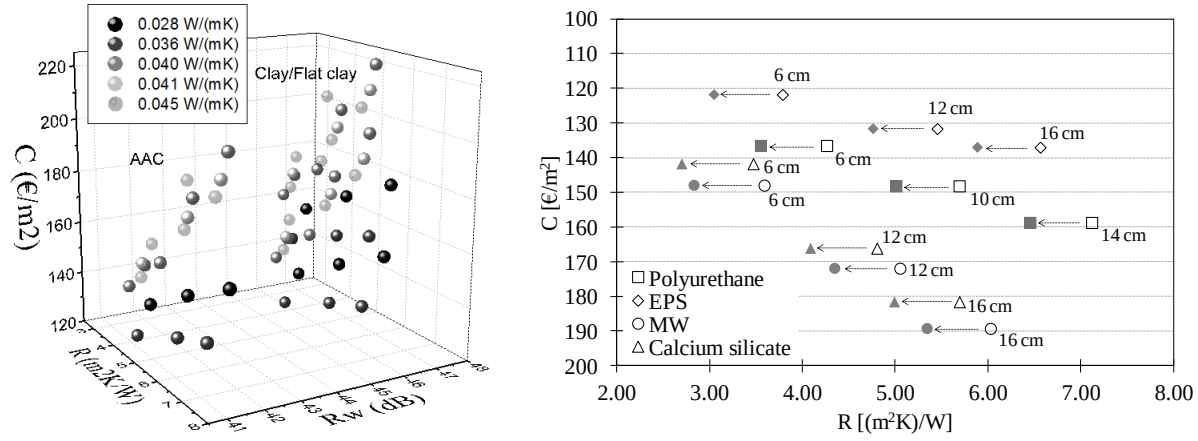

Figure 6: (left) 3D-space with R, Rw and C for ETICS walls with different insulating panels; (right) Reduction of thermal resistance for ETICS walls.

The R_W are calculated according to the mass law (mass values of walls). In this analysis the effects of acoustic bridges are not considered. AAC blocks don't give an optimal acoustic insulation (Figure 5a and b) because they have a low specific mass (m=300÷450 kg/m^3); instead, clay blocks, which have a higher specific mass (m=750÷900 kg/m^3), have improved noise performances at acceptable costs. Insulation filled clay blocks gives the best performances in terms of R and R_w at reasonable costs (Figure 5c). Considering walls with ETICS (Figure 6), thermal bridges effect reduces the thermal resistance of about 5-23%). Pareto-optimal curve is given by EPS insulation. Clay and flat clay blocks give the best R_w; however, absolute values are anyway lower than 50 dB (considered a good R_w-value).

Global Warming Potential and Thermal Resistance

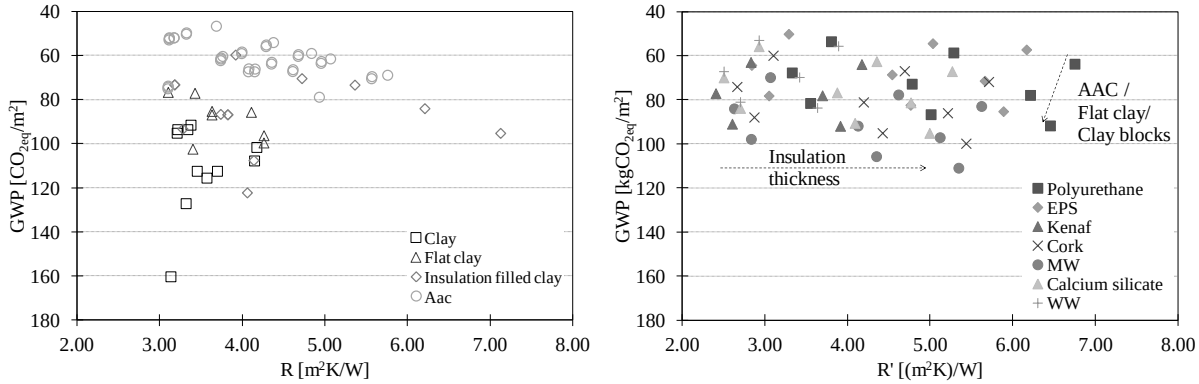

Figure 7: A comparison between the GWP for single layer and ETICS walls. Pareto-optimal curve is given by AAC blocks and insulation filled blocks with R>6 (m^2K)/W for single layer walls. For ETICS the best solution are obtained with PU and EPS insulation and AAC blocks.

Having considered only the materials that constitute the building façade, the total GWP is calculated by multiplying the indicator value of specific material unit mass times the mass of the material contained in one square meter of building façade. This analysis considers only the current section, because the joints between envelope and the building concrete structure (pillars, beams) do not give an important contribution because the correction on GWP is less than the uncertainty introduced by secondary data.

A CASE STUDY

Some results are transposed from the façade module to a real building considered as a benchmark to assess the energy performance indicator for heating EP_H [kWh/(m^2K)] in the "asset rating" evaluation, with reference to the quasi-steady state calculation method standardized by ISO 13790 [7] and Italian standard UNI/TS 11300, for the three different best walls solutions and best thermal bridges correction presented in Figure 4.

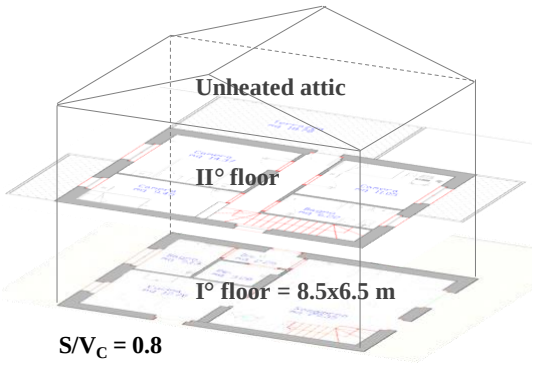

GG	2600	Climate zone E-northern Italy
A_C	104.0 m^2	Conditioned area
A_{WINDOW}	17.0 m^2	Windows surface area
S	349.3 m^2	Thermal envelope area
S/V_C	0.80 m^{-1}	Compactness ratio
U_{GROUND}	0.30 W/(m^2K)	8 cm EPS
U_{ROOF}	0.33 W/(m^2K)	10 cm mineral wool
U_{WINDOW}	1.40 W/(m^2K)	Double glazing, PVC frame
U_{WALL}	variable	(see Table 1)
ε	0.95	Global systems efficiency (condensing boiler)

Figure 8: Building dimensions and U-values for the case study.

At first (step 0) EP_H and costs values are referred to a current section wall, neglecting thermal bridges. Analyzing building geometry, it is possible to see that the adopted façade module well fits with the real building geometry; considering the extension of beams and pillars thermal bridge, this is equal to 75% of the overall length of thermal bridges. A first evaluation (step 1) could be therefore done applying U' value of "standard façade" over the real building envelope (considering only beams and pillars thermal bridges and their correction). At last (step 2) a detailed thermal bridge analysis has been performed, considering all thermal bridges and their corrections (windows, balconies, wall-roof and wall floor junctions).

Table 1: Case study analysis (EP_H and costs) with different levels of calculation detail.

		Flat clay block 35 cm U_w=0.323 [$Wm^{-2}K^{-1}$]		AAC 48 cm U_w=0.174 [$Wm^{-2}K^{-1}$]		Filled block 49 cm U_w=0.140 [$Wm^{-2}K^{-1}$]	
		EP_H [kWh/m²/y]	*C [€/m²]*	*EP_H [kWh/m²/y]*	*C [€/m²]*	*EP_H [kWh/m²/y]*	*C [€/m²]*
Step 0	*Current section (ref.)*	*54.93*	*122.5*	*39.81*	*184.7*	*36.45*	*156.3*
Step 1 (façade)	With thermal bridge	96.55 (+76%)	-	71.55 (+60%)	-	67.84 (+65%)	-
	With corrected thermal bridge	68.60 (+16%)	130.2 (+6%)	48.56 (+13%)	196.4 (+6%)	45.23 (+14%)	168.0 (+8%)
Step 2 (whole building)	With thermal bridge	77.33 (+41%)	-	61.18 (+54%)	-	57.90 (+59%)	-
	With corrected thermal bridge	61.45 (+12%)	129.6 (+6%)	44.01 (+11%)	195.6 (+6%)	41.00 (+12%)	167.2 (+7%)

Comparing the results from the reference façade method (step 1) with the detailed analysis (step 2), it's possible to see that higher values are obtained for the EP_H, since in the whole building there are both less pillar (the incidence of thermal bridges length on total thermal envelope area, L/S ratio, is lower) and there are some negative values for thermal bridges (such as corner, wall-ground and wall-roof junctions). This overestimation effect become less steep when thermal bridges corrections are applied (beams and pillar thermal bridges are the most relevant ones) and when the reference U-value for the current section is getting lower. The cost to correct thermal bridges is not so high, and as a consequence there are no differences between the two methods.

CONCLUSIONS

Thanks to this tool, it will be possible to be aware of technical and economic needs to assess the feasibility of technical solutions in the preliminary design stage. This tool could be used to: set a database of wall technical solutions assessable with multi-criteria strategies; validate commercial data (moving from declared performances to real ones); propose what could be considered – from the adopted point of view – the best available technologies. In conclusion, a method to switch from the thermal transmittance and the cost of the current section to the average thermal transmittance and the average cost of the opaque wall has been put forward. The results are in good agreement with the detailed calculation, leading to a little overestimation of energy performances. This tool could be used to perform a first rough performances assessment for a building with masonry walls.

REFERENCES

1. Hamdy, M., Hasan, A., Siren, K., "Applying a multi-objective optimization approach for Design of low-emission cost-effective dwellings", Building and Environment 46 (2011) 109-123.
2. Shea, K., Sedgwick, A., Antonuntto, G., "Multicriteria optimization of paneled building envelopes using Ant Colont Optimization", EG-ICE 2006, LNAI 4200, pp. 627-636, 2006.
3. Wang, W., Zmeureanu, R., Rivard, H., "Applying multi-objective genetic algorithms in green building design optimization", Building and Environment 40 (2005) 1512-1525.
4. Directive 2010/31/EU of the European Parliament and of the Council of 19 May 2010 on the energy performance of buildings (recast).
5. EN 15804:2012 – Sustainability of construction works-Environmental product declarations-Core rules for the product category of construction products.
6. EN ISO 10211:2008 – Thermal bridges in building construction-Heat flows and surface temperatures-Detailed calculations.
7. UNI EN ISO 13790:2008 - Energy performance of buildings-Calculation of energy use for space heating and cooling.

THE DYNAMIC DOUBLE FAÇADE: AN INTEGRATED APPROACH TO HIGH PERFORMANCE BUILDING ENVELOPES

Edgar Stach[1]; William Miller[2], James Rose[3]

1: Director, Institute for High Performance Buildings, Philadelphia University, 4201 Henry Avenue, Philadelphia, PA 19144, (1999-2012 University of Tennessee), Joint Faculty Oak Ridge National Laboratory – ORNL; stache@PhilaU.edu

2: College of Engineering, Dep. of Mechanical, Aerospace and Biomedical Engineering, UT

3: College of Architecture and Design, UT

ABSTRACT

The U.S. Department of Energy Solar Decathlon 2011 challenged 20 collegiate teams to design, build, and operate solar-powered houses that are cost-effective, energy-efficient, and attractive. The competition was held in September 2011 on the National Mall in Washington, D.C., and demonstrated innovative clean-energy technologies. The University of Tennessee (UT) project LivingLight showcased a state of the art integrated double façade and scored 1st place in Energy Balance, 3rd place in Engineering and 5th place in Architecture.

Keywords: Smart Façade, Double Façade, PV Technology, Auto. Building Control Systems.

INTRODUCTION - SMART FAÇADE

This paper details key features of the integrated façade system developed for the LivingLight house. The project resulted from a collaborative effort between students and faculty of Architecture, Mechanical Engineering, Electrical engineering, Graphic Design, Landscape Architecture, Interior Design, and Business. In addition to meeting the contest criteria of achieving a zero-net energy balance through the use of solar-electric power, the LivingLight house proposes an innovative double façade system to passively harness solar-thermal energy. Although integrated into a small house for the competition, the façade system lends itself well to commercial and residential applications in both retrofit and new construction. The façade resolves the multiple aims of its diverse design team and proposes a new aesthetic expression for an emerging building technology.

AESTHETICS AND EXPERIENCE

In the LivingLight house the ubiquitous glass façade is re-imagined as a transparent wrapper that simultaneously resolves dissimilar interior and exterior design criteria. From the exterior the outer layer of the façade appears taught, flat, and monolithic. Depending on time of day its appearance varies from reflective to transparent, becoming a glowing lantern at night.

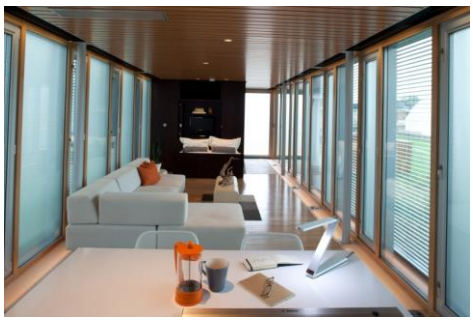

Figure 1: Exterior view of the south Facade of the LivingLight house from the public deck. Cylindrical photovoltaic modules extend over the glazing to provide shade.

Figure 2: Interior view of the open, loft-like, living space. Alternating translucent and transparent glass panels help provide privacy to the public front and more extensive views to the private back. The large expanse of glass also allows the house to be naturally lit during the daytime.

SOLAR PV SYSTEM, MECHANICAL SYSTEMS, HOME AUTOMATION SYSTEM

The integrated roof-top array not only supplies two times the amount of energy to power the home, but it also shades the home's south facade. The 10.9-kW array employs a cylindrical module, so that direct, reflected, and diffused sunlight is captured across a 360° photovoltaic (PV) surface while maintaining a low profile (Figure 3). The home is controlled by a home automation system while providing the user with vital information about the house so they are able to make educated decisions about their energy usage. Lighting and operation of blinds located in the air space of the double facade are also controlled through the automation system (Figure 4/5).

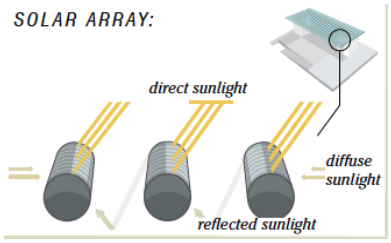

Figure 3: Diagram - Sylindra PV system

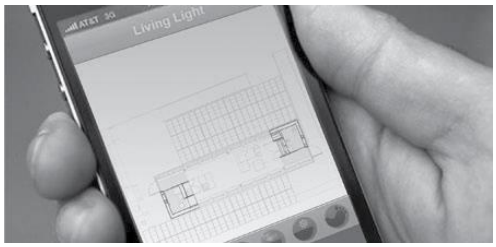

Figure 4: Home Automation System Interface

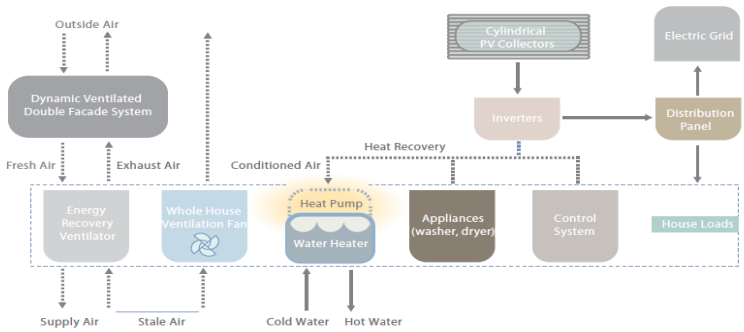

Figure 5: Flow chart for mechanical, electrical, and plumbing systems.

ILLUMINATION

Control of both of natural and artificial light is incorporated into the facades. Daylight is controlled through motorized 2" Somfy blinds mounted between the inner and outer layers of both long facades. These blinds may be adjusted directly by the occupant through the mobile touch pad interface, programmed to follow a schedule, or set to maintain a preset illumination level. The blinds are divided into five-foot units on the module of the exterior layer of the façade and can be controlled simultaneously or in groups. In order that both natural and artificial light come from the outside walls, electric light sources are built into a strip at the floor and ceiling just inside the inner façade.

The ceiling strip lights are high efficiency linear fluorescents with step dimming to provide general, ambient illumination. The floor lights are three-color strip LED fixtures mounted beneath textured and tempered glass panes. The floor mounted LEDs are capable of producing warm white or a full spectrum of colors and can be controlled independently or in groups. The blinds and lighting are linked to the central home automation system. The full functionality of all systems is available to the occupant directly through the mobile touch pad interface or pre-programmed 'moods' may be selected. For instance, setting the *dinner party* 'mood' sets the blinds to open, turns on the LED spot over the dinner table, selects dim warm white floor illumination and edge-lights the canopy over the front door (Figure 6/7).

Figure 6: The lighting can be easily adjusted to pre-set 'moods' from the home automation system. The dinner party mood is illustrated in the interior view to the left. The LED lighting strips help create a unique and memorable ambiance.

Figure 7: LED lights arranged in strips embedded in the floor vary in color and intensity. All light coves and luminaires change colors from a "warm" 2700 k to neutral 4000 k and daylight 5400 k. This allows different lighting actions in different areas, taking care of physiological and psychological needs. For example: Bedroom lighting is activated when the alarm clock sounds.

CONSTRUCTION

Although novel in approach and form, the double façade system is assembled from standard components. The LivingLight team worked closely with manufacturers to make the best use of their existing product lines. The aluminum framing systems for the inner and outer layers of the façade were selected to optimize performance and economy for their particular functions. The outer layer is framed with Kawneer TriFab VG 451 components with concealed vertical mullions. In keeping with the function of the outer layer as air barrier and heat reflector, its framing system is not thermally broken and its 9/16" laminated glass from AGC has low-e hard-coating facing the interior of the façade cavity. In contrast, the inner layer is the primary insulating system. It makes use of thermally broken Kawneer 7500 series curtain wall components and 2" insulated glazed units from Serious Materials. The IGUs are made up of two panes of ¼" tempered glass sourced from AGC with two additional internal films and are filled with argon gas for an R-value of 11 (Figure 8/9).

The primary reason that storefront and curtainwall systems were chosen for this project was their relative ease of customization. These systems allow for facades to be tuned to exact energy efficiency, privacy, and operability requirements. The inner layer of the LivingLight façade incorporates operable thermally broken ISOWEB casement windows, translucent and transparent insulated glazed units, and white oak veneered mullion caps. Additionally, aluminum framing systems lend themselves to retrofit applications and greater ease of maintenance. In the LivingLight house, the layers of the façade are structurally independent of one another with the outer layer being exterior glazed and the inner layer being interior glazed. This allows for the replacement of damaged glass from either side and opens up exciting possibilities for adding a second façade layer to existing buildings with minimal impact on structure or tenants.

THE DYNAMIC DOUBLE FAÇADE

The Living Light house makes extensive use of glass for transparency, daylighting, and spatial connection to the surrounding environment. A dynamic double façade system, made up of suspended film, highly insulated (R-11) interior glass and single-pane exterior glass, is implemented along the majority of the north and south facades of the home. Alternating translucent and transparent panes allow for views of the landscape while maintaining a sense of privacy for the occupant.

Figure 8: Section through the south façade from BIM model
Figure 9: Façade elevation

The north and south facades become the stage upon which the building comes to life. Sandwiched between the two panes of glass is a motorized horizontal blind system which blocks solar radiation, or sunlight, before it reaches the conditioned space. The blind system is programmed to provide proper lighting and shading throughout the year. It also provides more privacy when desired. The cavity within the system is also integral to the mechanical system of the home.

Development of the energy efficiency measures of the double façade required research into four key areas:

- Heat gain in the facade cavity
- Location and type of blinds
- Design of shading overhang
- Integration with ventilation and HVAC

The double façade was designed based on data from both predictive modeling and a constructed prototype. Based on ISO standard 15099, students and faculty developed a code to model heat transfer coefficient and solar heat gain coefficient in the façade. In addition, the WINDOW program (version 6.3.19) created by Lawrence Berkeley National Lab (LBNL) was used to benchmark the new code for SHGC. At normal incidence, WINDOWS predicts a SHGC of 0.70 as compared to the derived number of 0.697. Hence students developed a working code capable of predicting the radiation, convection and conduction occurring in multiple-pane windows (Figure 10). A physical prototype was constructed with south-facing glazing configured in both single and double facades. Both were monitored with thermocouples to measure the temperature gradients between the inner and outer glass surfaces and the air temperature distribution inside the double façade air cavity. Thermocouples were also used to record the exterior and interior temperatures and pyranometers were used to measure the vertical and horizontal solar irradiance incident on the south facing façade. The data shows that for a summer day with strong solar irradiance, the air temperature in the façade air cavity will experience a 10°C temperature gain, under natural convection. In the winter the air cavity showed a 15°C temperature gain due to natural convection (Figure 11). From this data it was determined that a strategy of exhausting the cavity in summer and admitting the warmed air in winter was feasible. Additionally, it was determined that the inner layer of the façade would need to be substantially insulated. The data suggests areas of future study in the areas of variable blind systems incorporating reflective ad low-emittance coatings.

Category	Modeling Tool(s)
Envelope/Heating and Cooling Loads	EnergyPlus
Double Glass Façade	Analytical Computer Code, COMSOL 4.0a, EnergyPlus
Photovoltaic Power Production	Solyndra Energy Yield Forecast Tool
Appliance and Misc. Electric Load Consumption	Excel
Roof Loads	STAR

Figure 10: Energy Modeling Software

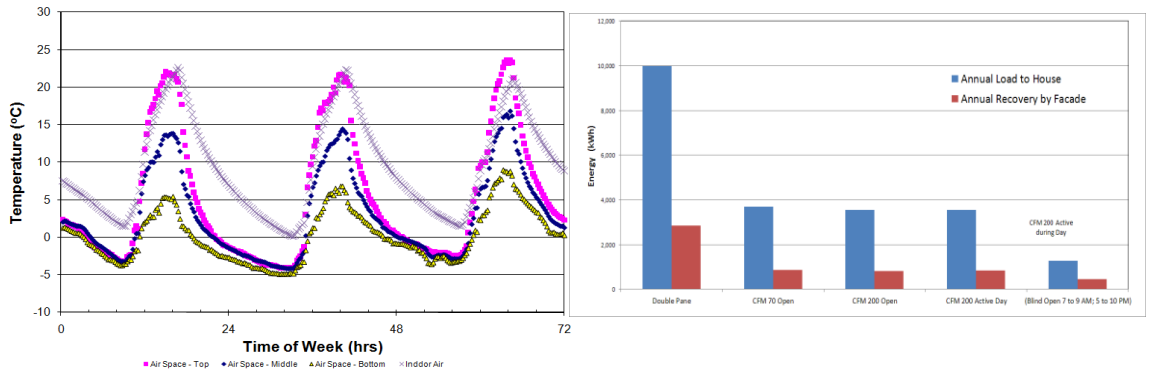

Figure 11: Winter façade cavity temperatures

Figure 12: Optimal façade configurations and energy balance

A model of the LivingLight house was created with EnergyPlus software. The model was first run to simulate performance over a full year with a standard window of double pane glass as control and compared to multiple runs with the double façade in varying configurations of cavity airflow and blinds. The optimum configuration was achieved with the cavity ventilation at 200 cfm (set by the Energy Recovery Ventilator) during daylight hours only with the blinds open from 8 AM to 10 AM and 5 PM to 10 PM only. This scenario seems to track well with actual occupancy of the home and yields a 90% reduction in house load comparable to the control case (Figure 12). All models predict some condensation forming on the exterior façade in the early morning hours. Simulations were created using EnergyPlus software to model the effect of thermal loading on the façade with blinds in the cavity, inside the conditioned space, and without blinds. Contributing interior loads were calculated based on the Building America (BA) Research Benchmark Definition. It is important to note that the software was unable to calculate the active airflow of the unique double façade therefore the model introduces some error by approximating performance with an unventilated cavity. Even so, the study proved that blinds exterior to the conditioned space reduced the cooling energy by 47.4%. Placing the blinds in the cavity allows for the best performance between summer and winter conditions.

The heat radiated to the cavity by the black blinds can be scavenged in winter and exhausted to the exterior in summer. In addition to studying the blinds, the EnergyPlus model was used to predict the effect of horizontal shading on the south façade. The analysis was run with no overhang and again with an overhang of 50% transmittance. The model overhang was based on the LivingLight house's cylindrical CIGS-based photovoltaic panels with a horizontal projection optimized to block summer sun and allow lower angle winter sun. The benefit of the shading provided by the overhang is an additional 18% reduction in cooling energy.[1]

The Living Light house uses a dynamic envelope strategy utilizing an ERV (Energy Recovery Ventilator) and passive solar heating from the double glass façade. The home automation and

control system allows easy control of the three ventilation schemes including heating, cooling, and whole house ventilation. In the cooling mode, fresh air will be introduced to the space through the north façade and the relatively cool air will then exchange heat in the ERV with the stale air being exhausted through the south façade, thus cooling the cavity (Figure 13). In the heating mode, the air flows through the façade cavities will reverse (Figure 14). Solar irradiance will heat the south façade cavity so that fresh air pulled through it will increase in temperature. Stale air will be exhausted through the north façade, heating the cavity, which helps to buffer any additional heat losses. The heating and cooling modes of operation are depicted below.

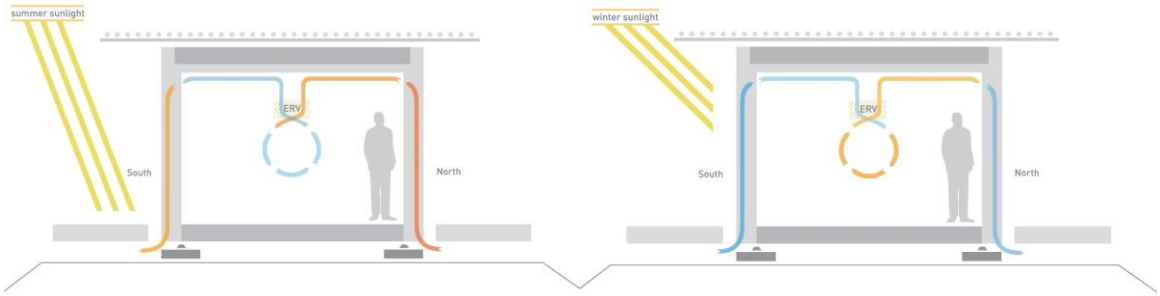

Figure 13: Summer cooling mode showing ventilation through the double façade.

Figure 14; Winter heating mode showing ventilation through the double façade.

The whole house ventilation scheme takes advantage of favorable outdoor conditions during which temperatures are between 60 and 76 °F with relative humidity near 50%. This comprises 25% of the year in Southern Appalachia and is comparable to weather patterns in the competition city of Washington D.C. When these conditions arise, the automation system alerts the occupants that whole house ventilation is an energy saving strategy. Should the occupant wish to use this setting, they may select it and open the operable windows of the north façade to bring in the cooler fresh air while keeping the south windows shut to reduce heat gain. This setting will turn off the mini-splits and allow a small duct fan to ventilate the entire house. About 70 kWh of cooling energy, about 6%, can be saved using this mode.

CONCLUSION

The value of the LivingLight project can be positively measured on three scales. First, as proof of concept for an innovative double façade system, the house has demonstrated a new technology that is functional, robust, aesthetically integral, and scalable. Second, as a pedagogical tool, the project has created a multidisciplinary platform for the collaboration of multiple departments and opportunities for students to gain hands-on experience with emerging building technologies.[2] Third, the LivingLight house proved to be a strong competitor in the 2011 Solar Decathlon. In addition to securing team standing with its first ever proposal, the house ranked first in Energy Balance, third in Engineering, fifth in Architecture, and eighth overall.[3]

REFERENCES

1. Post-competition Mechanical Engineering Report: S. Coley, M. Berwind, I. Bosley, and Professors William S. Johnson and William S. Miller. DOE and NREL 10/242011.
2. E. Stach, J. Rose, A. Howard, “UT Zero Energy House - Sustainable Design-Build as a Teaching Tool”, Purdue University, Ray W. Herrick Laboratories, 2010 Purdue Compressor Engineering, Refrigeration, Air Conditioning and High Performance Buildings Conference, 7/2010
3. Solar Decathlon website, Official Scores and Standings, www.solardecathlon.gov.

AIR-CONDITIONING ENERGY REDUCTION THROUGH A BUILDING SHAPE OPTIMIZATION

G. Caruso[1]; J. H. Kämpf[2]

[1] *Dipartimento di Ingegneria dell'Energia e dei Sistemi, Università di Pisa, Largo Lucio Lazzarino, I-56126 Pisa, Italy*
[2] *Laboratoire d'Énergie Solaire et Physique du Bâtiment, École Polytechnique Fédérale de Lausanne, LE 2 204 (Bâtiment LE) Station 18 CH-1015 Lausanne, Switzerland*

ABSTRACT

The air-conditioning energy consumption, for cooling or heating, has currently a growing trend. The purpose of this work is to develop a method suitable to design optimal three-dimensional building forms to reduce air-conditioning needs in a chosen location by using weather data. The method exploits in particular both diffuse and direct solar radiation; not independently but rather in relation with the external temperature. For this reason this method could be applied in any climatic region. In fact the warmer the region is the more negative the contribution of the solar radiation is in terms of building energy balance. Hence in this case the problem tends to be equivalent to the one of the annual solar irradiation minimization. On the contrary, in the case of cold regions, the problem tends to be equivalent to the one of the annual solar irradiation maximization. The final aim is to guide designers to reduce energy consumptions in buildings, since the first stages of the design process of future buildings.
To achieve that aim, an algebraic cumulative sky is introduced for the computation of the annual useful incident solar irradiation on the building envelope. The methodology consists in using weather data to define in which case the solar irradiation on the envelope gives a positive or negative contribution depending on the external temperature in order to maintain internal comfort of the occupants. The contribution is further associated to the data of the solar irradiation for each hour of a typical year. The algebraic cumulative sky constructed on that basis has the advantage to present particular zones where the solar radiation is useful all year long. Finally we use an hybrid evolutionary algorithm (CMA-ES/HDE algorithm) already applied to maximize solar energy utilization to explore the optimal building forms maximizing the annual useful solar irradiation on the envelope.

Keywords: building form optimization, algebraic cumulative sky, air-conditioning energy reduction

INTRODUCTION

The electricity consumption due to the air-conditioning (AC) in summer is a relevant problem in various warm and temperate climate regions. E.g. the annual electricity peak power in Italy is reached in summer for the first time in recent years and is increasing in intensity, probably due to an increasing diffusion of AC for the summer cooling of buildings [1]. A relevant source of internal gains is solar radiation. This radiation can enter buildings directly through windows or it can heat the building shell to a higher temperature than the ambient, increasing the heat transfer through the building envelope.

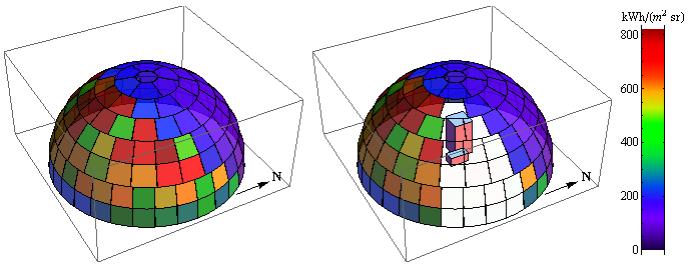

Figure 1: Schema of the cumulative sky, simulated for Basel.

Optimizing the global form of the building envelope is an approach that could be useful to reduce solar irradiation. The optimization of the building form has been studied to maximize the solar energy utilization in cold climatic regions [3, 2] by using a new hybrid evolutionary algorithm (CMA-ES/HDE algorithm) developed in [4].
In this paper, we generalize this method for all climatic regions, by taking into consideration the 'algebraic' solar energy irradiation, i.e. considering solar gains positive or negative respectively in cold or warm hours of the year. The method is applied to two families of possible building forms.

METHOD

The methodology consists in using weather data and RADIANCE [5] in order to build the virtual scene representing the annual solar energy source of algebraic radiation on the building, i.e. considering in which case the solar irradiation on the envelope gives a positive or negative contribution depending on the external temperature. The contribution is further associated to the data of the solar irradiation for each hour of a typical year. The algebraic cumulative sky constructed on that basis has the advantage to present particular zones where the solar radiation is useful all year long.
Finally we use an hybrid evolutionary algorithm (CMA-ES/HDE algorithm) to explore the optimal building forms minimizing the annual air-conditioning energy consumption.

1.1 Algebraic solar potential determination

The backward ray tracing program RADIANCE is used, in order to measure the solar potential of hypothetical buildings. As done by Kämpf and al. [2], a virtual scene is defined by a sky, buildings and a ground. In order to compute the irradiation on buildings over an average year, a cumulative sky is produced for the location [6]. In this study, we have taken two locations to be Basel in Switzerland (47°N,7°E) and Dubai (25°N,55°E) and the corresponding meteorological data from the Meteonorm software [7]. The sky is composed of 145 Tregenza patches with corresponding cumulative radiance ($Whm^{-2}sr^{-1}$), as shown in Fig. 1.

The RADIANCE software is then used to determine the irradiation on surfaces that composes the virtual scene. To realize this, each surface is fitted with virtual watt-meters in order to compute their irradiation. The total irradiation is computed by multiplying the point irradiation (in Whm^{-2}) by the corresponding surface area (in m^2) and summing over all the points.
Solar irradiation is clearly counter-productive only in *warm* conditions, and, not in *cold* conditions. In order to estimate the effect due to solar radiation in a year, an 'algebraic' cumulative sky is reproduced, i.e. an algebraic sum in which solar radiation, at a defined

hour of the year, is taken positive if the atmospheric conditions are *cold* and negative if it is *warm*.
The definition of *warm* and *cold* are here introduced ad hoc for our purpose, as a relation between the monthly average external temperature T_e and the corresponding internal comfort temperature T_c. These two quantities are in fact linked by the following equation [8]:

$$T_c = 13.5 + 0.54 \cdot T_e \tag{1}$$

The software Meteonorm provides the values at each hour of the year, as an average of experimental data, of the external temperature and solar irradiance, and then the sign of the corresponding sky radiance is evaluated for each hour of the year, as shown in Fig. 2. In particular, the following definitions are introduced:

- there are *warm* conditions, in which the sky radiance contribution are accounted for negatively if $T_e > T_c$;
- there are *cool* conditions, in which the sky radiance contribution are accounted for positively if $T_e < T_c$.

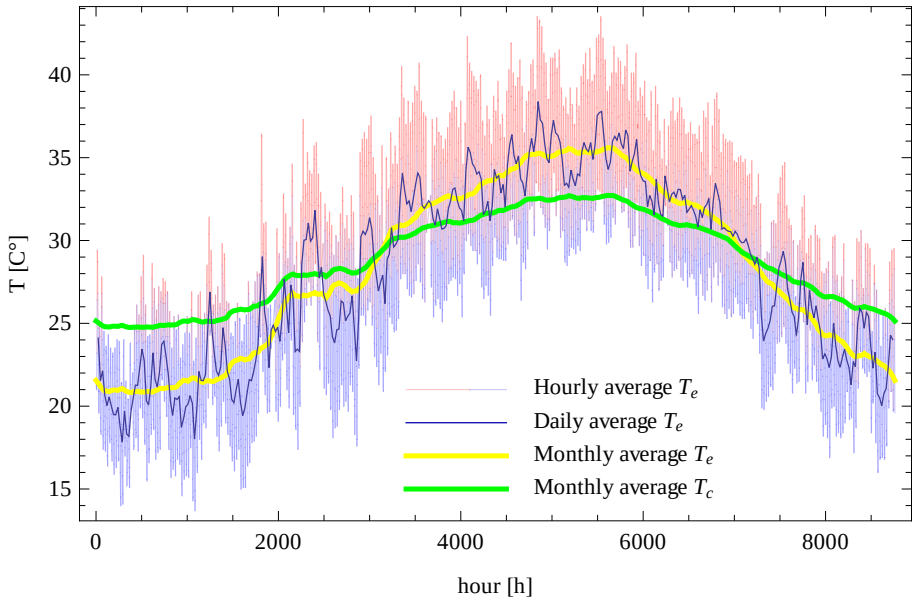

Figure 2: Comparison between the external temperature T_e and the internal comfort temperature T_c, in Dubai.

Finally the 'algebraic' cumulative sky is calculated by summing all positive and negative sky radiance contributions for all hours of the typical year.

1.2 Optimization

The form of the building is described by relevant variables, called 'alleles'. The optimization consists to find the combination of these parameters that minimizes solar irradiation on the envelope. For a few different discrete variables it may be possible to exhaustively test all possibilities, but when the parameter space to explore becomes large to very large, it is desirable to use optimization algorithms.
With these algorithms, we should be able to find the global minimum (or minima) of a function f that depends on n independent decision variables. Put formally, the algorithm

searches for the supremum (the set of variables that maximizes the function) as in Eq. (2).

$$sup\{f(\vec{x})|\vec{x} \in M\sigma\mathbb{R}^n\} \tag{2}$$

with:

$n \in \mathbb{N}$	dimension of the problem
$f : M \longrightarrow \mathbb{R}$	objective function
$M = \{\vec{x} \in \mathbb{R}^n \| g_j(\vec{x}) \geq 0$	feasible region
$\forall j \in \{1, ..., m\}\}, M \neq \emptyset$	
$m \in \mathbb{N}$	number of constraints

The set of inequality restrictions $g_j : \mathbb{R}^n \longrightarrow \mathbb{R}$, $\forall j \in \{1, ..., m\}$ includes a special case of constraints due to the domain boundaries $\vec{L} \leq \vec{x} \leq \vec{H}$, with $\vec{L}, \vec{H} \in \mathbb{R}^n$. $\vec{L}$ is named the lower bound and $\vec{H}$ the upper bound of the domain.
In our case, the parameter space is defined by a geometrical characterization of the buildings and the measure to improve is the received useful irradiation. For this, RADIANCE is used as a black-box together with the 'algebraic' cumulative sky introduced before.

RESULTS

The method is applied to two families of possible building forms. The first one is the family of general three-dimensional surfaces parameterized as Taylor series and the second one is a family of buildings designed as union of cuboids.

1.3 The first parametrization of the building's shape: Taylor series

This first case is based on the idea that consists to use a two dimensional (2D) Taylor series to describe the geometry of the roof. We seek to minimize the algebraic solar irradiation on the envelope throughout a year, on both the roof and the vertical facades. For this application, the two-dimensional Taylor series is expressed as follows:

$$h(x, y) = \sum_{k=0}^{N-1} \sum_{l=0}^{M-1} A_{kl} \cdot \left(\frac{x - L_x/2}{L_x}\right)^k \left(\frac{y - L_y/2}{L_y}\right)^l . \tag{3}$$

where $h : \mathbb{R}^2 \longrightarrow \mathbb{R}$ gives the height as a function of the position (x, y) in the plane, $x \in [o, L_x]$, $y \in [o, L_y]$, L_x and L_y delimit the domain of interest in x and y and A_{kl} are the coefficients of the series, that are used here as parameters in the optimization process. The domain boundaries were chosen to be $L_x = 20\ m$, $L_y = 30\ m$ and $N = M = 5$. The coefficients are limited between a lower and an upper limit as follows:

$$A_{kl} \in [-200, 200]. \tag{4}$$

A minimum cut value was chosen in the height of the surface at 0 m, so that when the surface goes below the ground (placed at 0 m), it is not taken into account in the irradiation calculation.
Further constraints dictate that the volume under the surface must be less than 1000 m^3. The simulations were made for Basel and Dubai, for which results are presented in Fig. 3.

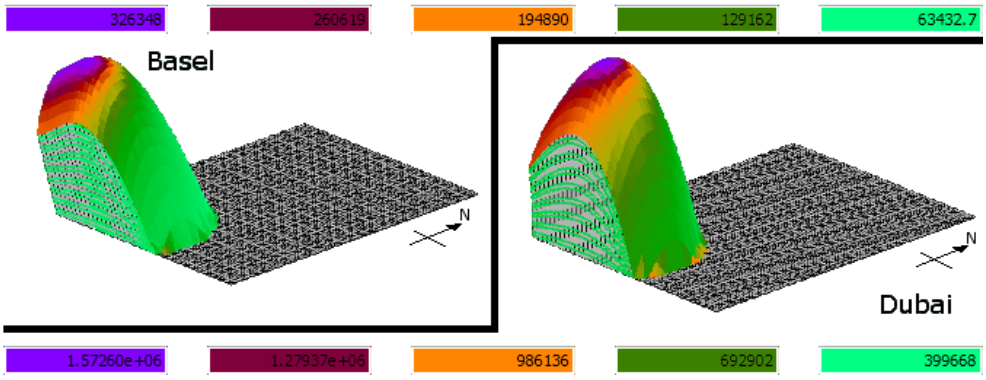

Figure 3: Optimal forms of the first parametrization, with $V_{min} = 1200\ m^3$, in 3D view, with irradiance in Wh, respectively for Basel and Dubai.

1.4 The second parametrization of the building's shape: Cubotron (squared forms)

The second parametrization introduced is closer to the common and widespread constructions, with squared form. In particular, the form is defined by a three floor building, each 3 m high, with a fixed total floor area , and vertical walls. Each floor has a squared form, in particular we use 2 parameters to define with continuity the form of the floor (obtaining rectangular, 'L' or 'Z' shapes), without changing the total area of the floor. In this case the alleles define the form of each floor, how to distribute the gross floor area and the position, rotation and deformation (by homothetic transformation) of each floor. The simulations were made for Basel and Dubai, for which results are presented in Fig. 4.

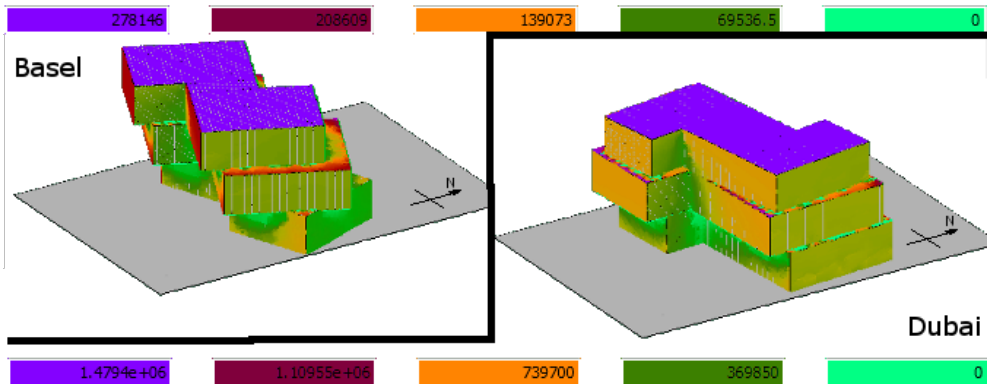

Figure 4: Optimal forms of the second parametrization, with $V = 1200\ m^3$, in 3D view, with irradiance in Wh, respectively for Basel and Dubai.

DISCUSSION

The optimization method is applied to two families of possible building forms. The first one is the family of general three-dimensional surfaces parameterized as Taylor series and the second one is a family of buildings designed as union of cuboids. In both cases we find coherent results in which the optimal forms have more extended portion of the envelope exposed to directions in the sky close to the solar path in the cooler hours of an annual average day. Vice versa the optimal forms tend to have compact sections orthogonal to

directions in the sky close to the solar path in the hottest hours of an annual average day. The final results are shown in Table. 1, where, in particular, it is interesting to note that the optimal forms are inclined to a direction close to the direction of the minimum algebraic solar radiation in the sky, i.e. the direction in respect to which a flat plane should be oriented to minimize the algebraic annual solar radiation.
The method here introduced is applicable to specific architectural projects, to find the optimal solution among a parametric family of potential building forms, previously chosen by the designer. Moreover it could be generalized to study optimized urban settlements to reduce the air-conditioning needs at urban level. Indeed, a building in an urban context cannot see the whole sky, other buildings are shading portions of it, then not intuitive solutions could be found due to the complexity of this scenario.

	BASEL			DUBAI		
Parametrization	V (m^3)	Σ $(60.23°)$	Φ_{sol} $(Wh/year)$	V (m^3)	Σ $(73.65°)$	Φ_{sol} $(Wh/year)$
Taylor $V_{min} = 1200m^3$	1204.58	$70.44°$	$0.57 \cdot 10^8$	1203.56	$82.11°$	$2.97 \cdot 10^8$
Cubotron	1200	–	$0.65 \cdot 10^8$	1200	–	$3.33 \cdot 10^8$

Table 1: Results of optimal forms of Taylor and Cubotron parametrization to reduce energy consumption, in Dubai and Basel, where V, Σ and Φ_{sol} are the volume of, the tilt angle of and the algebraic annual solar irradiation on the optimal forms respectively. The angles in brackets are the zenith angles of the direction of minimum algebraic solar radiation in the sky for the location considered.

REFERENCES

1. Terna s.p.a. (rete elettrica nazionale societá per azioni): *previsioni della domanda elettrica in italia e del fabbisogno di potenza necessario.* http://www.terna.it/linkclick.aspx?fileticket=103363.
2. Kampf, J. H., Montavon, M., Bunyesc, J., Bolliger, R., and Robinson., D.: *Optimisation of buildings' solar irradiation availability.* Solar Energy, 84(2):596 - 603, 2010.
3. Kampf, J.H., and Robinson, D.: *Optimisation of building form for solar energy utilisation using constrained evolutionary algorithms.* Energy and Buildings, 42(6):807 - 814, 2010.
4. Kampf, J.H., and Robinson, D.: *A hybrid CMA-ES and HDE optimisation algorithm with application to solar energy potential.* Applied Soft Computing, 9(2):738 - 745, 2009.
5. Larson, G. W., and Shakespeare, R. A.: *Rendering with Radiance.* Morgan Kaufmann Publishers, 1998.
6. Robinson, D., and Stone, A.: *Irradiation modelling made simple: the cumulative sky approach and its applications.* Plea2004, Eindhoven, The Netherlands, 2004.
7. www.meteonorm.com.
8. Nicol, J.F., and Humphreys, M.A.: *Adaptive thermal comfort and sustainable thermal standards for buildings.* Energy and Buildings, 34:563 - 572, 2002.

SUSTAINABLE LOW COST BUILDING ENVELOPES IN TROPICAL COUNTRIES AND INTEGRATED DESIGN PROCESS: A CASE STUDY IN CAMBODIA

F. Garde[1]; A. Scognamiglio[2]; M. Basile[3]; J. Gorgone[3]; D. Mathieu[1]; M. L. Palumbo[3];

1: Faculty of Engineering ESIROI, University of Reunion, France

2: ENEA (Italian National Institute for New Technologies, Energy and Sustainable Economic Development), Photovoltaic Technologies Area, Portici Research Centre, largo E. Fermi 1, Portici, Italy

3: InArch, Italian National Institute of Architecture, via Gorizia 42, Rome, Italy

ABSTRACT

This paper deals with the integrated design approach that was used by an international team to design a low-cost and sustainable house for Cambodia's future. The main issue was to design houses that promote health, and to allow local people to live in at affordable and attractive conditions. The aim was to find sustainable solutions that take into account the local architectural tradition, the use of renewable materials (clay, bamboo and palm leaves), the local climate conditions, and the use of the solar energy as well. One important feature of the project is the replicability of the prototype to a wide number of sites and conditions common to Cambodia. The first step was a climate assessment of the country in terms of possible and optimum conditions that could be reached with passive means and to collect information about the traditional Khmer houses in terms of architectural, social and cultural aspects. A design *charette* was then organised to taken into account all the aspects (Ecological footprint, optimised solar shading systems, use of cross natural ventilation etc.). The paper presents the evolution of the project until the final stage. It will include the architectural concept, dynamic thermal simulations and the use of the Givoni comfort zones. A comparison was made between the project and a traditional Cambodian Khmer house to assess the improvements in terms of thermal comfort. The final project gets an indoor air temperature which is 4°C lower compare to a traditional house.

Keywords: Design, Sustainable, Low-cost Housing, Tropical Countries

INTRODUCTION

The occasion for the research experience presented with this paper was an international competition for low cost housing in Cambodia, launched by Building Trust International. This is an organisation that works with existing charities and communities in need, and that regularly holds design competitions to raise funds and get the best solution to a global issue. One of the most recent competitions was Cambodia Sustainable Housing. The object of the competition was designs that could propose a sustainable future for housing in the South-east Asian country. Any proposal had to keep below a budget of $2000 and deal with the yearly flooding that effects most residential areas. The winning designs could influence the way they build housing in the region, being a kind of reference models for future developments.

We entered the competition by forming an interdisciplinary international working group (architects and engineers experienced in sustainable design, modelling, use of renewables), having the appropriate expertise for facing the challenge of the competition.

Despite the brief didn't ask for specific energy / ecological requirements, we focused on the design of a house-system that could be self-sufficient from the ecological and energy point of view. We took into account the available lot assigned by the competition brief, and, within the border of this lot, we tried to design a *productive* house, so that it could work as an organism able to produce the energy that the users need (food-energy for metabolism + energy for the building operation), and to collect and re-use the rain water so to that food could be grown all the year long. To do this, we gave a form to what we call "productive footprint" of the building that is necessary area for placing energy generating systems, so to get a Zero Energy Balance of the building. [1]

METHODOLOGY

A design methodology was set-up by the multidisciplinary team composed as we said before by people from different countries and from different backgrounds (architects and engineers/building physicists). We follow an integrated design process based on several steps:

1. Knowledge of the climate and of the traditional Khmer houses, bibliography about the materials used in Cambodia and in close countries;
2. Design *charette* to take into account all the design aspects (Ecological footprint, optimised solar shading systems, use of cross natural ventilation, material etc.);
3. Multiple exchanges between all the team participants to improve the components of the envelope;
4. Design of the final project;
5. Building thermal simulations, CFD modelling;
6. Preparation of the final poster to be submitted.

KNOWLEDGE OF THE TRADITIONAL HOUSES/CULTURE

We started from the study of the traditional Khmer house, in order to understand how the living and the working space can be organized [2]. In a few words, the traditional Khmer house is a wooden two-floor house, organized in a ground level that is generally opened on its sides, and an upper level that is a kind of closed box, often covered by a sloped roof (see Fig. 1a). The kitchen space is in between this two floor, close to the wooden stairs (so to protect food from animals). The structure is made out of wood, and the light walls are made out of palm leaves. The foundation of the building, especially if very close to rivers, is made out of poles.

Figures 1a and 1b : Traditional rural Khmer houses with wooden poles. The building serves as a shelter. During the day the house functions as a large umbrella. Work and life go on at ground level, where the most effective shade is provided. At night, people sleep upstairs

From the analysis, we understood that a very important part of the organization of the traditional Cambodian house is the ground floor, and the contact with the ground itself. On the ground the food is produced, on the ground animals are bred, very often people are seated directly on the ground. Nevertheless this ground often is flooded, due to the presence of rivers that flood in the rain season (see Fig. 1b). As a consequence people who are in river areas use light wooden platform, to create a kind of artificial level, slightly detached from the ground, which protect them and their goods from the water in case of flood. This wooden artificial level is the main living and working space of the Cambodian house, also because it is the most comfortable part of the house, being ventilated and being shadowed by the upper part of the house. In addition to this, the ground floor is also very important in terms of social connections, since it is a relation space that allows people to share the daily life among the community. In terms of thermal comfort, Ono has carried some interesting measurements in different type of houses in Cambodia. He shows that the indoor temperature of the traditional house can reach 38°C, which is a 4°C higher than the outdoor temperature. This is mainly due to the radiant heat from the structure, especially the roof [3].

CLIMATE ASSESSMENT

The latitude of Cambodia ranges from 10° North to 14° North. This country experiences a tropical climate with two seasons: the monsoon between April and September and a dry season the rest of the year. The hottest month is March at the end of the dry season with maximum temperatures that can reach 40°C in the interior of the country. The climate is weakly different between the southwest coast (Kampot) and the interior (Steung-Treng). The differences between the dry and wet season are more pronounced in the interior. In our case, the simulations and design solutions were achieved with weather data from Phnom-Penh (figures below). The climate of the Cambodia's capital is intermediate with a mean monthly dry bulb temperature that range from 25°C to 30°C. The maximum temperature never exceeds 35°C but also never drops below 20°C (see Fig. 2). At this latitude, the sun path is relatively high in the sky all the year. Consequently, the main surfaces exposed to the sunrays are the roof, the east and west walls. The wind rose of this town shows that most of the time blows a wind from the north or from the south. With only a weak part of the time without wind (6.5%), the potential of natural ventilation of buildings is real (see Fig. 3).

Even if the weather is hot and wet the major part of the year, the Givoni's chart [4]. Figure 2 shows that the comfort conditions can be reach 71% of the time with a air velocity of 1m/s.

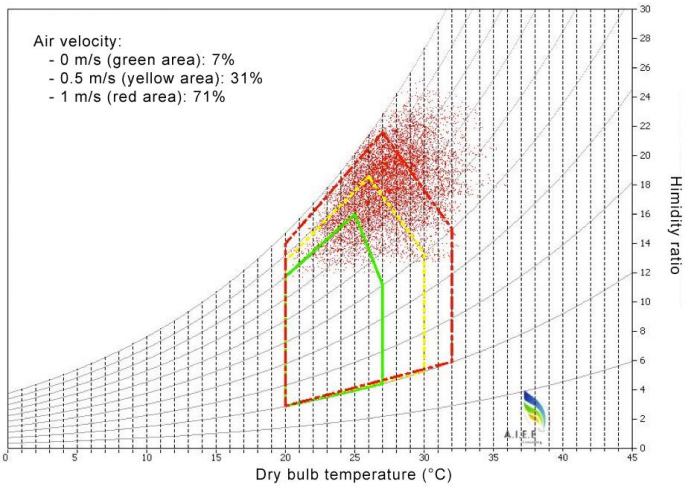

Figure 2 : Temperature and humidity couples for the capital city Phnom-Penh

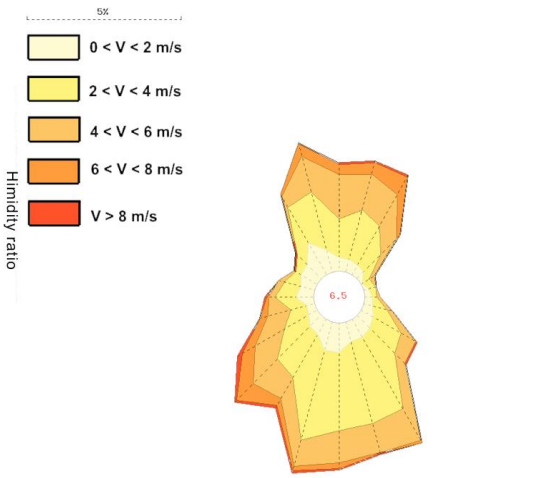

Figure 3 : Wind rose of Phnom-Penh

The Final project

Obviously the main design aim, due to the geographical area where the project is located, was to face the summer challenge. The climate analysis and the understanding of the design of the traditional Khmer house helped us to understand how the thermal behaviour of this kind of house could be improved. So our challenge was in one hand to develop a functional spatial scheme that could reproduce the one of the traditional Khmer house (very effective also in terms of social relationships), and on the other hand to improve its quality and its energy performance by passive strategies. Figure 4 explains in details all our strategies in terms of sustainability and thermal comfort. Basically, the enveloped has been designed to have large solar shadings and big openings to avoid overheating of the roof and the walls and to have an efficient cross natural ventilation, which are the two main passive strategies in a tropical climate [5], [6]. Local materials such as vetiver and bamboo have been used in priority [7].

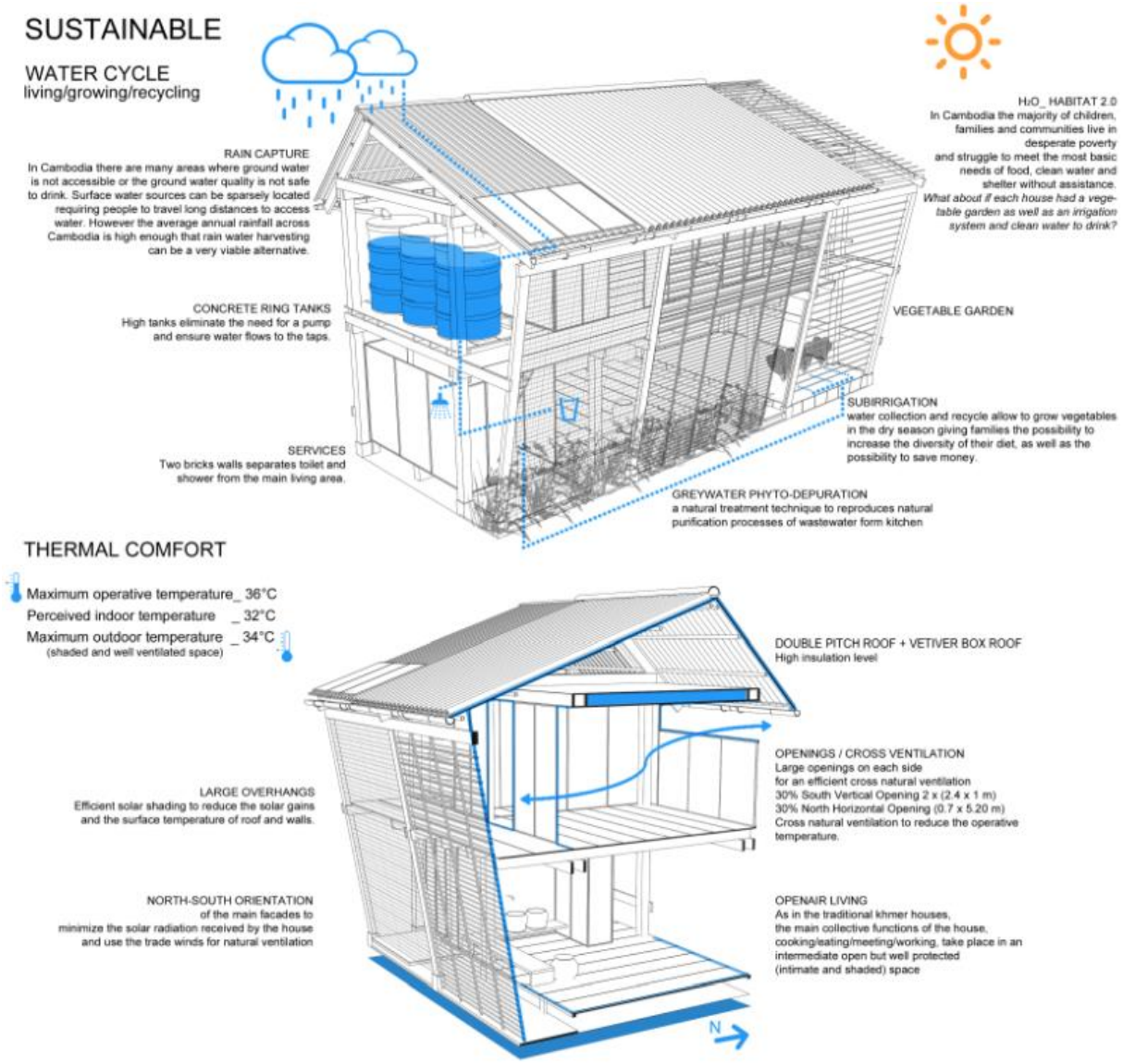

Figure 4 : Description of the passive design and sustainable features of the project. Local materials are mostly used, such as bamboo, vetiver, local timber, palm leaves, with a double skin roof and efficient solar shadings that prevent the light walls from overheating

We designed a two-floor house, characterized by a compact volume on the Northern side, and by a open space on the South side; a sun-shading system protects the East side from overheating, and the openings on the West side walls enhance the natural ventilation. The

roof, made out of bamboo, allows the rain water collection, and the water is stored in tanks, placed on the North side of the building, so to improve the thermal performance of the service block (kitchen + toilettes). The ground floor is characterized by a productive garden where food can be grown for the family's needs, and this, together with the artificial wooden platform, constitutes the main living and working area of the house. At the upper level there are the bedrooms, which face the double height corresponding to the productive garden. We considered that in case on further needs for space, this bedrooms space can be extended over the productive garden.

MODEL AND SIMULATION

Two models of houses have been developed under the Google Sketchup/Open studio environment: the traditional Khmer house and the improved project. The thermal and physical properties of the materials used are detailed in Table 1. The simulations have been run under a whole year at an hourly time step. The outputs were the operative temperature and the Givoni's comfort zones.

Table 1 : Thermal and physical properties of the materials used

Material	Thickness (cm)	Thermal conductivity (W/m.K)	Specific Heat (J/kg.K)	Density	Absorptivity
Nipa palm (Walls)	2	0,14	2000	0.5	0,7
Vetiver (straw)	20	0,07	2000	0,5	0,6
Clay	20	1,5	2085	1.5	0,6
Water (Tank)		0.6	4185	1	
Teck wood (floor)	2	0,19	2390	0.7	0.78
Corrugated iron (Trad)	0.075	45	500	78	0.6
Concrete (water storage)	4	2	1000	2.4	0.6

RESULTS AND DISCUSSION

Figures 4 shows the comparison between the project and a traditional Cambodian Khmer house in terms of operative temperature. The final project gets an indoor air temperature which is 4°C lower compare to a traditional house.

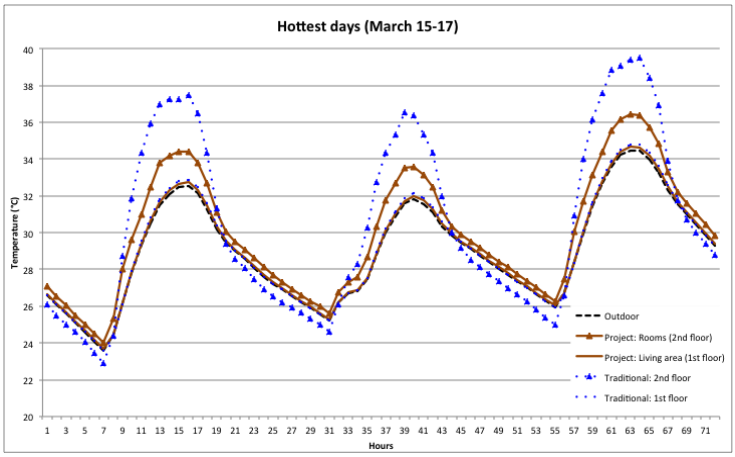

Figure 5 : Comparison of the operative temperature during the hottest days in a traditional Khmer house and in the final project. The difference is approximately 4°C below.

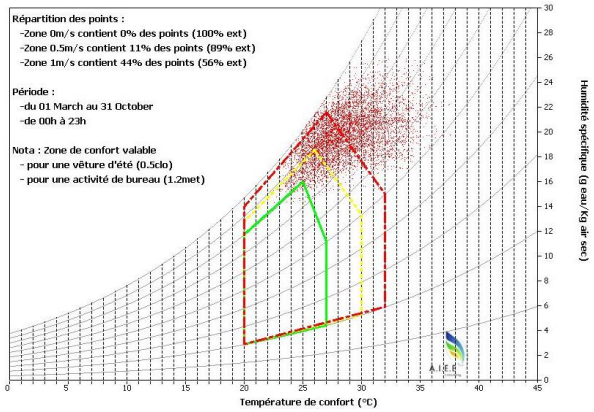

Figure 6: Thermal comfort conditions Project (Roof: Bamboo and Vetiver straw; Walls: Nipa palm; Floors: wood)

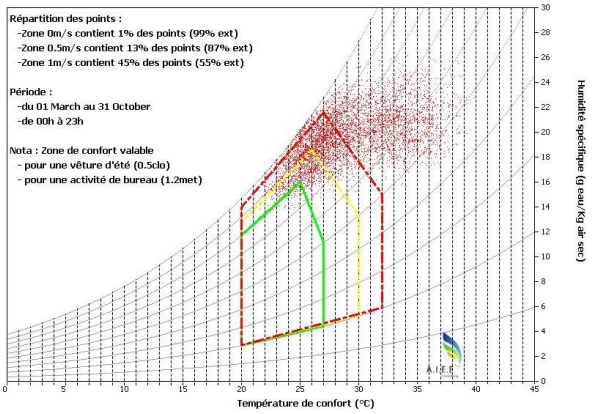

Figure 7: Thermal comfort conditions Traditional rural house: (Roof: Corrugated iron + Nipa Palm; Walls: Nipa palm; Floors: wood)

In terms of thermal comfort, the final project (Figure 6) behaves better than the traditional house (Figure 7). The resultant temperature and humidity couples are closer to the comfort zone. The indoor temperature never reaches 36°C for the project model whereas it reaches 40°C for the traditional house. These results are close to Ono's measurements [3].

CONCLUSION

The IDP approach that was used by the multidisciplinary team to design a low-cost and sustainable house for Cambodia has lead to an efficient house that respond to all of the constraints of the site. The constant interaction between architects and engineers from the early sketch of the project has lead to a final design that behaves well in terms of thermal comfort with a gain in temperature of 4°C and in the same time that responds to the social and living needs of the occupants. The traditional spatial model of the house can be improved by considering the need to contain the ecological footprint within the building's footprint (rain water collection, phyto-depuration system, productive garden, and photovoltaic modules on the roof, together with the use of sustainable materials).

REFERENCES

1. Palumbo, M. L., Scognamiglio, A. Designing material and energy flows for an urban ecosystem. Proceedings of the CISBAT 2011- International Scientific Conference Renewables in a changing climate. From Nano to Urban Scale, Lausanne, Switzerland, 14-16 September 2011, pp. 671-677, ISBN 9782839909068.
2. Rural Khmer house on Wikipedia. http://en.wikipedia.org/wiki/Rural_Khmer_house, October 2012.
3. Ono, K. et al. Investigation of Residential Energy Consumption and Indoor Thermal Environment of Housing in Cambodia. In Proceedings of SUDAC 2010, International Conference on Sustainable Urban Design in Asia City. October 2010.
4. Givoni, B. Comfort, Climate Analysis and Building Design Guidelines. Energy and Buildings, v.18, n.1, p. 11-23, 1992
5. Tantasavasdi C., Srebic, J. Chen, Q. Natural ventilation design for houses in Thailand. Energy and Buildings, 33(8), 815-824. 2001.
6. Garde, F., Boyer, H., Celaire, R., Bringing simulation to implementation : Presentation of a global approach in the design of passive solar buildings under humid tropical climates., Solar Energy, Vol.71, 2001, p.109-120.
7. Hengsadeekul, T. Construction of Paddy Storage Silo Using Vetiver Grass and Clay. Australian Journal of Technology. 7(3): 120-128 (Jan. 2004)

FIELD MEASUREMENTS OF A GREEN ROOF AND DEVELOPMENT OF A SIMPLIFIED NUMERICAL MODEL

Fabio Peron, Ugo Mazzali*, Massimiliano Scarpa,

Department of design and planning in complex environments, IUAV University of Venice, Dorsoduro 2206 – 31023 Venice, Italy

ABSTRACT

In recent years green roofs have increased their application over buildings, both as retrofit and new buildings cladding. Green roofs may be divided into extensive green roofs where the soil depth is thin and the maintenance is cheap or intensive green roofs where the soil is thick, large plants can grow on it and the maintenance is more expensive.

A detailed field measurement campaign was performed on an extensive green roof with the aim to understand the thermal incidence of this kind of architectural cladding and tune a simplified mathematical model for the evaluation of the thermal behaviour of the green roof at different latitudes in the Mediterranean climate and its influence on heating and cooling loads. The measurement campaign was performed on a green cladding installed over an unconditioned industrial warehouse roof in the North-East of Italy. The field measurement was carried out between July 2011 and February 2012. Hourly measurements of surface temperatures, heat fluxes, ambient and internal temperatures, ambient and internal relative humidity, and ambient climatic variables have been collected for the bare and covered roof. The field measurements pointed out a significant difference between internal and external surface temperatures of the bare and covered ceiling. For the internal surface temperatures, differences up to 22°C were recorded. For the external surfaces temperatures, comparing the external bare surface temperature and soil temperature of the green roof, differences around 14°C were monitored. Concerning incoming heat fluxes analysis a great difference has been recorded between the covered and uncovered roof. Values up to 460 W/m2 during a summer sunny day in the early afternoon were monitored.

After the field measurements a simplified finite difference numerical model of the green roof was created. The validation via field measurements of the living wall mathematical model has pointed out a good reliability of the numerical model, with the aim to provide forecasts of the thermal behavior of green roof in various conditions of latitude, Leaf Area Index and insulation.

Keywords: green roof, field measurements, finite difference model

INTRODUCTION

Nowadays the term “green roof” may include some different strategies to improve building impact on urban context. Green roof design aims to reduce storm water runoff, add more green spaces, produce more oxygen and save energy for cooling and heating purpose, but also a green roof strategy can be a cool roof or a roof with solar panels [1]. As far as energy savings are concerned, a detailed study was developed by [2] in Ottawa Campus, Canada. An industrial roof of 72 m^2 was divided in two sections with an extensive roof on one half and a traditional roof on the other. Data was collected for 22 months and great differences up to 45°C were monitored on external surface temperatures of the two sections of the green roof during summer. Energy demand for space conditioning corresponding to bare roof was 6.5

kWh/day – 7.0 kWh/day against 1 kWh/day of the garden roof with an average reduction of 75%. Other studies were developed with the aim to quantify energy consumptions reduction related to green roof installations. Wong et al. [3] used DOE-2 simulation program to determine the energy consumption and cooling load of a five storey hypothetical commercial building with different types of roofs. Results indicates that a reduction in annual energy consumption up to 15% is achievable. Related to energy consumption reduction, the characteristics of the vegetation are very important and strongly related to heat transfer through the green roof. For example according to [4], a higher Leaf Area Index (LAI) increases gas consumption in winter and reduced electricity consumption in summer. Also a correlation with soil thickness was found and in particular when the soil thickness was increased, from 0.2 to 0.3 m, the insulating effects of the added soil reduced wintertime natural gas consumption while also reducing summertime electricity consumption.

Moreover, as far as green roof lifespan is concerned, many studies have been carried out and the green roof lifespan ranges from 40 years to 55 years [1,5] with Net Present Value of the green roof between 20% and 25% less than the conventional roof over 40 years.

The aim of this article is to provide a simplified numerical model validated via field measurements for testing cooling potential with different LAI conditions and structure insulation at different Italian latitudes.

Green roof system

According to standards [6] a green roof may consists in several primary layers namely a structural layer, a waterproof membrane, a protection membrane against root action, a mechanical protection layer, a drainage element, a water storage element, a water filtering membrane, soil and plants. Moreover a green roof classification is made upon a maintenance level as follows: Class 1, low maintenance (extensive); Class 2: medium maintenance (light intensive); Class 3: high maintenance (intensive). The green roof monitored in this article belongs to class 1 extensive.

METHOD

Field measurements

The green roof monitored in this study is located in North-East Italy near Treviso and is installed on a industrial building. It covers an area of 30m^2 on a flat roof protected by an external waterproof membrane.

Variable	Point A, Measured data	Point B, Measured data	Point C, Measured data
Air inside the building	T, UR	T, UR	T, UR
Internal ceiling surface	T	T	T
Waterproof membrane	T	T	T
Soil core	T, URG	T, URG	
Soil surface	T	T	
Air inside the canopy	T, UR	T, UR	
Air external	T, UR	T, UR	T, UR

Table 1. Measured data on the green roof and on the reference. T=temperature, UR= Umidity, HF= heat flux, URG=soil humidity

Three series of probes are installed on the green roof area (A and B) and in the standard original roof area (C) and a data-logger recorded the temperature and humidity behaviors from 1 July 2011 to 31 January 2012. Temperature measurements were obtained by thermal resistances sensors (Pt100) in house constructed and calibrated and humidity measurement by Hobo capacity sensors. The heat flux were evaluated by HukseFlux and Captec heat-flux meters. In the core of the soil layer was measured also the content of water by ECH2O Probe from Decagon Inc.. A weather station mounted on the monitored roof measured air temperature and relative humidity, global solar radiation, wind velocity and direction. The detailed summary of probe positioning is reported in Table 1.

Simplified numerical model

A simplified numerical model has been developed in the frame of this project and validated according to field measurements. The model is based on finite difference equations and a node diagram with domain discretization is visible in Figure 1. The green roof structure corresponding to section A of the reference roof has been described via a RC network and divided into 8 nodes. Node 1 represents the inner surface of the roof, nodes 2 to 6 represent internal thermal nodes of the roof, including air gap of the drainage and soil, node 7 represents outer surface of the soil layer and node 8 represents the vegetation layer. The model calculates hourly heat flows and temperatures using the following boundary conditions: air room temperature, outdoor air temperature, canopy air temperature, sky temperature according to [7], total solar irradiance impinging on the roof.

Finite difference equations of the most representative nodes are reported below. Equation 1 represents node 7 and equation 2 represents node 8, they take into account for several important characteristics of the soil and plants respectively, namely the thermal inertia of the soil, the canopy air temperature (monitored in the field measurements), the solar absorptance of the soil and plants, the solar transmittance of the plants in dependence of LAI calculated according to [8], and the Leaf Area Index (LAI). A Leaf Area Index (LAI) database was proposed by [9]. The corresponding LAI was used for the extensive monitored roof.

$$\frac{\rho_4 c_4 s_4 (T_7 - T_7^0)}{\Delta\tau} = \frac{\lambda_4}{s_4}(T_6 - T_7) + h_{can}(T_{can} - T_7) + \alpha_{gr} rad_{sol} \tau_{pl} + \sigma_n \varepsilon 4 T_{m,1}^3 f_{v,pl}(T_8 - T_7) LAI + \sigma_n \varepsilon 4 T_{m,2}^3 f_{v,sky}(T_{sky} - T_7)(1 - LAI) \quad (1)$$

$$0 = \alpha_{pl} rad_{sol} + LAI h_{ext}(T_{ext} - T_8) + LAI h_{can}(T_{can} - T_8) + LAI \sigma_n \varepsilon 4 T_{m,1}^3 f_{v,gr}(T_7 - T_8) + LAI \sigma_n \varepsilon 4 T_{m,2}^3 f_{v,sky}(T_{sky} - T_8) \quad (2)$$

where λ_n, ρ_n, c_n and s_n: thermal conductivity [W/m K], density [kg/m^3], specific heat [J/kg K] and thickness [m[of the n-layer respectively, T_n [°C] and T_n^0 [°C]: temperature of the n-th node in the current and in the previous time step respectively, $\Delta\tau$ [s] is the hourly timestep, h_{can} [m^2 K/W] is the canopy convection coefficient, T_{ext} [°C] is the external temperature, σ_n is the Stefan-Boltzmann constant [W/m^2 K^4], ε is the mean emissivity, T_m [°C] is the node mean temperature, α_{gr} and α_{pl} are the solar absorption coefficients of the ground soil and plant respectively, rad_{sol} is the solar radiation impinging on the wall, τ_{pl} is the solar transmission coefficient, f_v is the view factor, T_{sky} [°C] is the sky.

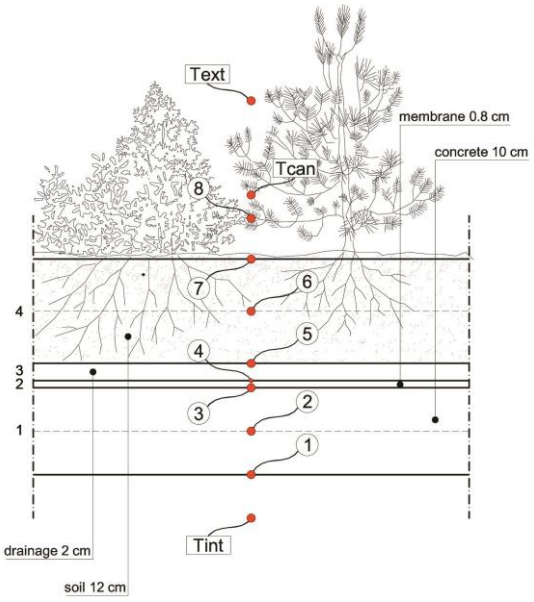

Figure 1: nodes of the numerical model with layer thickness and layer number on the left

RESULTS

The numerical model has been validated via field measurements with the aim to provide forecast of thermal behaviour of the green roof in various conditions. The validation has been performed using data of a week of strong solar radiation from August 18th to August 24th 2011. The comparison against field measurements concerned internal surface temperature at node 1 and internal heat flux as shown in Figure 2. The correspondence is good and confirmed by the calculated Nash-Sutcliff Efficiency Coefficient (NSEC) [10]. This coefficient expresses the accuracy of the model prediction compared against real measurements. A value near to 1 indicates a good correspondence of the model against measured data, a value near to 0 indicates that simulated data are as accurate as the mean of the measured values, and a negative value indicates that the mean of the observed data are more accurate than the model. The calculated NSEC coefficient have been 0.6 for T1 values and 0.9 for heat flux values. The correlation graph is shown in Figure 3, also for node 7 that represents external roof temperature, i.e. soil surface temperature. The correspondence of node 7 with measured data is not as good as the other two cases but external probe was not probably uniformly covered by green roof plants.

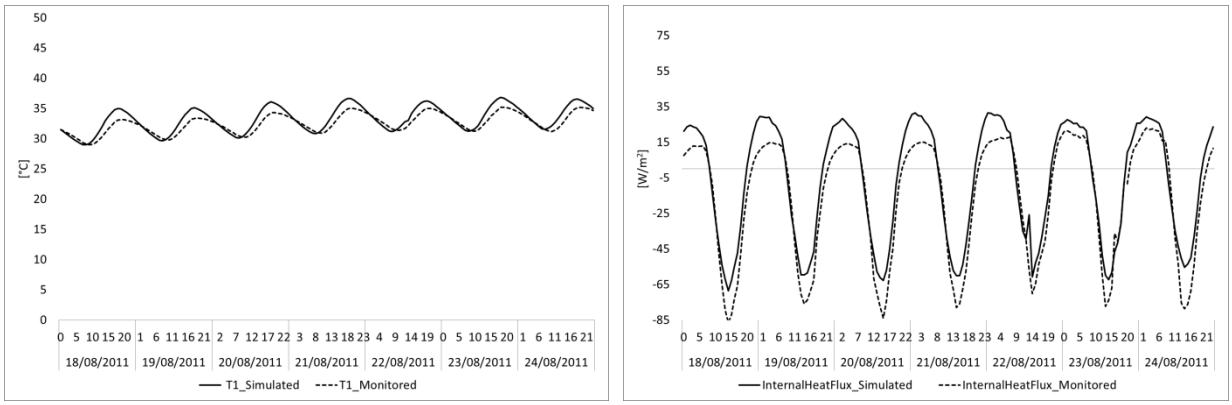

A *B*

Figure 2: comparison between simulated and monitored values. A) node T1; B) Heat flux

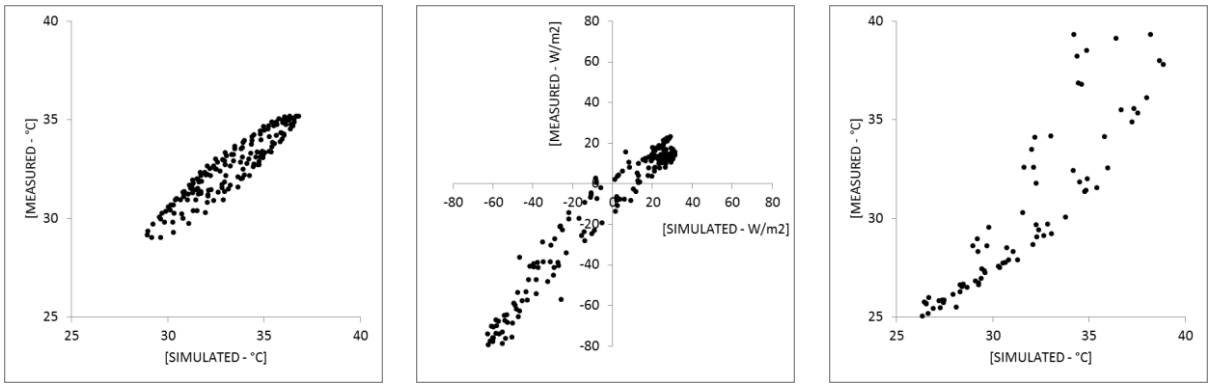

A *B* *C*

Figure 3: correlation graph. A) node T1; B) Heat fluxes; C) node T7

DISCUSSION

Once the model has been validated a parametric analysis has been performed in three different Italian climates with two different roof components and under five different LAI conditions. The three climates are Verona (45° N 26' E), Roma (41° N 53' E), Messina (38° N 11' E) and the two roof components are made up by a structural layer (0.28m) an insulating layer (0.15m), a drainage layer (0.02m) and a soil layer (0.12m) in one case and by the same layers as the first case with a thin layer of light concrete (0.04cm) in place of insulating layer in the other case. Actually many old buildings need to be retrofitted and green roof seems to be an interesting opportunity. The roof component without an insulating layer has been simulated in order to represent old building's roof. As explained before, a further parameter, Leaf Area Index, has been investigated and its influence on heat flux through the roof. Lai values investigated have been 0.5,1,1.5,2 and 3. The inside air temperature condition supposed for the simulation with the numerical model have been 26°C during day hours and 30°C during night hours.

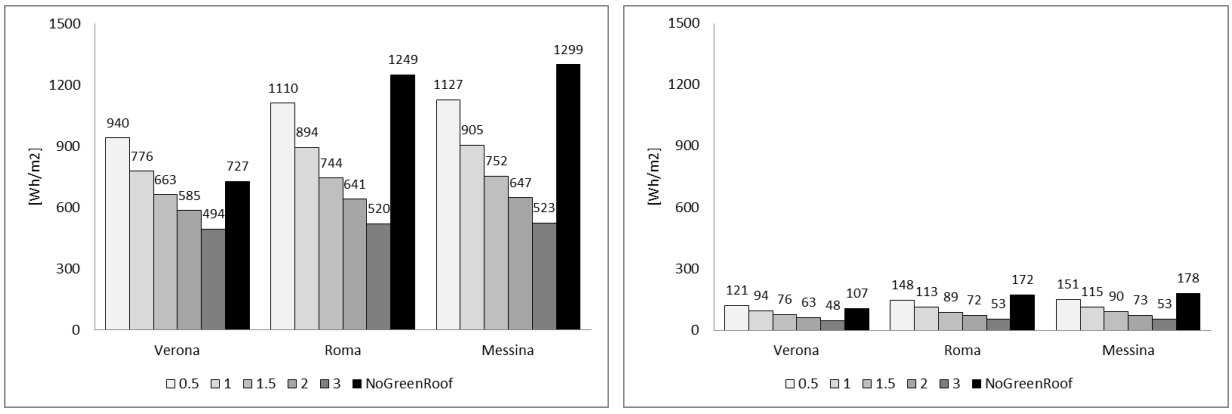

A *B*

Figure 4: Total week heat flux with different values of LAI from 0.5 to 3 and without Green Roof. A) roof without insulation layer; B) roof with insulation layer

Results of the simulation tests are visible in figure 4. In figure 4A the behaviour of the roof, in terms of total week heat flux, without the insulating layer is shown. Incoming (positive) heat fluxes are strongly related to LAI values and latitude. At northern latitudes the effect of the green roof, with respect to the bare roof, becomes positive with a LAI greater than 1.5. This means that incoming heat fluxes through the green roof are reduced if compared with the corresponding heat fluxes through the bare roof. At central and southern Italian latitudes the

effect of the green roof becomes positive starting from LAI values of 0.5. A green roof with LAI value of 3 shows a weekly incoming heat flux of 494 Wh/m^2, 520 Wh/m^2 and 523 Wh/m^2 for the three latitudes respectively, and the corresponding values for the bare roof are 727 Wh/m^2, 1249 Wh/m^2 and 1299 Wh/m^2. The same behaviour can be pointed out for the roof showed in figure 4B, but the effect of the green cover is strongly reduced by the presence of the insulating layer.

ACKNOWLEDGEMENTS

We gratefully thank the Tegola Canadese company and Federico Cais for making available the green roof setup for experimental measurements and for the collaboration and constant availability. We also thank Massimiliano De Bei for the measurement setup and data collection, and Antonio Musacchio and Adriana Casalin for the constant availability.

REFERENCES

1. O Saadatian, K Sopian, E Salleh, CH Lim, S Riffat, E Saadatian, et al. A review of energy aspects of green roofs, Renewable and Sustainable Energy Reviews. 23 (2013) 155-168.
2. KY Liu, A Baskaran. Using Garden Roof Systems to Achieve Sustainable Building Envelopes, Construction Technology Update. 65 (2005).
3. NH Wong, DKW Cheong, H Yan, J Soh, CL Ong, A Sia. The effects of rooftop garden on energy consumption of a commercial building in Singapore, Energy Build. 35 (2003) 353-364.
4. DJ Sailor. A green roof model for building energy simulation programs, Energy Build. 40 (2008) 1466-1478.
5. C Clark, P Adriaens, B Talbot. Green Roof Valuation: A Probabilistic Economic Analysis of Environmental Benefits, Environmental science and technology. 42 (2008) 2155.
6. Ente Nazionale di Unificazione UNI, Istruzioni per la progettazione, l'esecuzione, il controllo e la manutenzione di coperture a verde, (2007).
7. L Adelard, F Pignolet-Tardan, T Mara, P Lauret, F Garde, H Boyer. Sky temperature modelisation and applications in building simulation, Renewable Energy. 15 (1998) 418-430.
8. EPD Barrio. Analysis of the green roofs cooling potential in buildings, Energy Build. 27 (1998) 179-193.
9. Y Chen, The intervention of plants in the conflicts between buildings and climate, (2006).
10. JE Nash, JV Sutcliffe. River flow forecasting through conceptual models part I — A discussion of principles, Journal of Hydrology. 10 (1970) 282-290.

ECO-WALL: MODULAR SOLUTION FOR LOW-COST HOUSES

M. P. Amado[1]; T. Lopes[2]; I. Ramalhete[3]

1: Faculdade de Ciências e Tecnologia, Universidade Nova de Lisboa 2829-516 Caparica e-mail: ma@fct.unl.pt, web: http://docentes.fct.unl.pt/ma

2, 3: GEOTPU – Grupo de Estudo de Ordenamento do Território e Planeamento Urbano Faculdade de Ciências e Tecnologia, Universidade Nova de Lisboa 2829-516 Caparica e-mail: tcl@fct.unl.pt, web: http://sites.fct.unl.pt/geotpu

ABSTRACT

In this paper we discuss the development of modular solutions for low-cost houses based on a pre-fabricated modular wall system that is environmentally sustainable, socioeconomically competitive and geared towards developing African nations who have a marked housing deficit. This deficit is set to increase as the population continues to grow exponentially and moves to urban areas in search of new opportunities. The response to this problem, from governments of different developing nations in Africa, has proved slow and inefficient clearly showing the need to develop a quick, sustainable and low cost housing solution.

The key point for the research of the modular wall solution is that the wall has to be made with local and ecological materials and non-specialized workforce and that it can be adapted to different climates, with good hygrothermal acoustic and mechanical properties and with a competitive cost in local markets. It will fit into the socioeconomic and urban reality of the different countries and should be sustainable throughout its entire life cycle. The modular solution should also offer good safety and interior comfort conditions to its users while maintaining the flexibility to expand the size of the house. African families increase very quickly and subsequently need more living space. To develop an "optimal" wall solution the research goes into the different aspects of construction. Parameters like dimensions, materials and constructive processes of the existing housing stock were studied. Features such as the family size, typology, different uses, common materials, existing regulations, minimal living conditions, safety and comfort have also been studied to find the most efficient solution in terms of construction, use, maintenance and deconstruction.

Keywords: Sustainable Construction: Pre-Fabricated Wall; Ecological Materials;

INTRODUCTION

The developing countries are currently experiencing a strong growth mainly as a result of natural resources exploration and some foreign investment related to it. This developing model has led to a set of social and demographic transformations caused by internal migrations to urban areas who promote the creation of slums without an infrastructures framework. The current African situation reveals a low quality of life related with the public health and poor housing solution.

Public housing programs are difficult to implement due to insufficient funding allied to a weak industry sector and unskilled labour. This context brought out the necessity to adopt a faster and low-cost construction model that promotes a "self building" process with local materials. This model will lead to environmental improvement, to a fair resource management and also to a better quality of life of the population.

The development of a modular prefabricated solution made with concrete and local materials that simultaneously meets hygrothermal, acoustic and mechanical requirements, becomes an interesting solution. The pre-fabrication system, as Stallen, et al (1994) says; can have an important role in solving the housing deficit by combining low cost construction solutions with "self construction" [1]. Prefabrication solutions have environmental and economic advantages, such as: 52% less construction waste [2]; 50% less water and energy consumption [3]; a 35% reduction in construction time [4] and a cost reduction of 30% [4,5].

METHOD

This study belongs to a funding research project, which is due to go on until summer 2014. The current study is constituted of a methodology with 7 steps while the present paper concerns itself only with Steps 1 to 4, who regard the development of low-cost houses and fast on-site assembly [projecto QREN].

Pre-conception Process

The current document has applied a Pre-conception Process [6,7] whose research methodology leads to the optimal modular design.

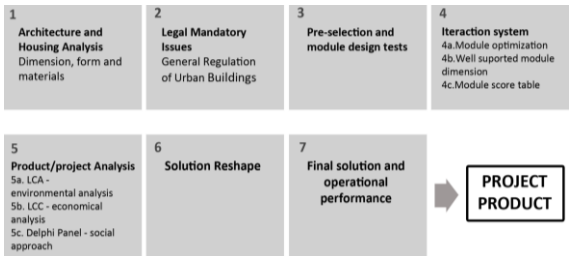

Figure 1: Pre-conception Process Methodology.

The structure of the methodology adopts a sequential process where each steps depends on the preceding one and in the end leads to the best modular product possible to be produced in industrial mode (Fig. 1).

Step 1 corresponds to the survey of the current housing stock in the target countries. This survey considered all the elements that describe the formal architecture concerning the average dimensions, typological geometry and used materials. This survey provides all the information to the database who allows the identification of the available resources for each country in order to find an financially, socially and environmentally viable solution.

The second step deals with legal mandatory issues about housing, namely the required the minimum standards. This is an important step of the Pre-conception Process because it will determine the minimum sizes of the module. This stage, together with Step 1, works possibly as a baseline to next steps.

The following Step three focuses on the pre-selection where decisions are taken regarding the module layers and elements. These elements will be subsequently used in the fourth stage as variables, which will create the optimal module through its interaction. The optimal modular results from the required minimum standards of each country, as well as practical issues like the ease of transport, local implantation and use.

The fifth step is an analysis that considers the selected three sustainable principles: the application of LCA (Life Cycle Analysis) as an environmental analysis; application of an LCC (Life Cycle Cost Analysis) as an financial analysis; and a social approach through a Delphi Panel formed by a group of stakeholders that will evaluate the solution according to the local social reality. These three types of analysis will improve the solution, which refers to the sixth step followed by the final solution reshaped if necessary.

RESULTS AND DISCUSSION

The case study of the method is focused on Africa and in particular on the countries of Cape Verde, Angola, Mozambique and Guinea-Bissau. This option takes into account the fact that these countries have Portuguese as a national language and and legal framework that is similar, which makes it possible to get data about the public housing programs.

Step 1: Architecture and Housing Analysis

The current housing stock analysis in the target countries – Cape Verde, Angola, Mozambique and Guinea-Bissau – allows the creation of an architecture inventory and provides a diagnose about lifestyle, needs and the main problems of the populations. The analysis of the current materials and construction techniques will improve the module concept as well as its adequacy to the social and environmental context.

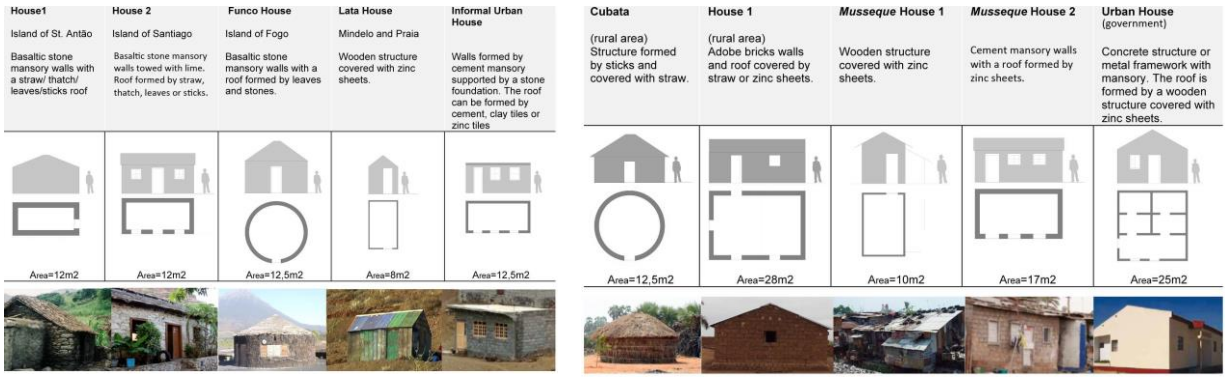

Figure 2: Housing stock analysis of Cape Verde and Angola.

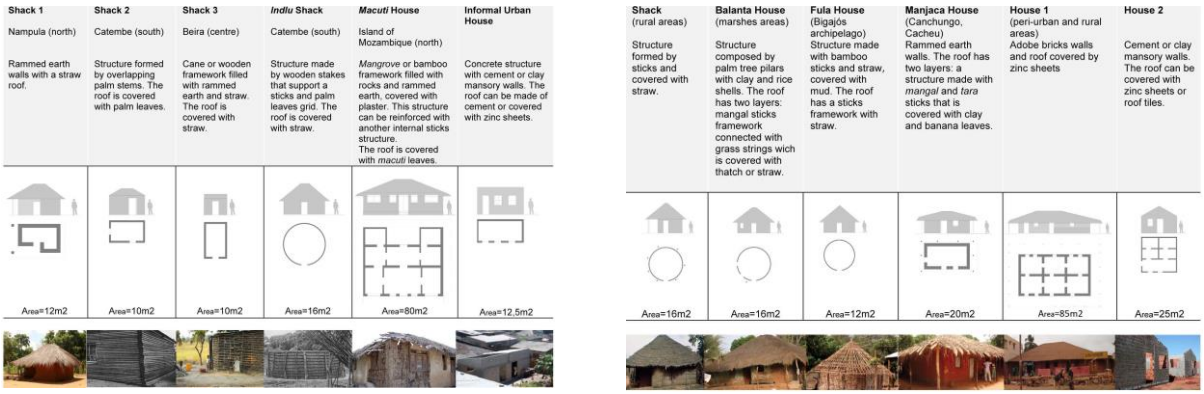

Figure 3: Housing stock analysis of Mozambique and Guinea-Bissau.

The main geometric form of housing stock adopts two types: rectangular and circular in all countries: the rectangular is dominant in Cape Verde, Angola and Mozambique while the circular form is still dominant in Guinea-Bissau.

Figures show that the most used materials in these countries are rammed-earth, adobe, wood and straw although there is a strong presence of basaltic stone in Cape Verde architecture. The analysis of local materials is important in the composition of a modular house because this kind of material offers economic advantages compared with imported materials, a fact to be taken into account in the next steps of the research.

Step 2: Legal Mandatory Issues

The legislation and the regulations about the housing programs are an important database support for the identification of required minimum standards. Principles ensure that all citizens shall have a suitable home. In this context, a house should guarantee the following functional requirements: safety; hygiene, health and hygrothermal comfort; fitness-for-use criteria.

Besides these parameters, there are also technical criteria, like the Building Code of each country that should be respected in the design phase. The following example is about a two-bed house, which established the minimum house area for a family with a child (Table 1).

Country	Typical floor height	Bedroom area	Living room area	Kitchen area	Bathroom area	Frenestration area	Two-bed house area (social housing)
Cape-Verde	2,60m	10,50m2	14m2	6,50m2	4,50m2	1,00m2	52m2
Angola	2,80m	10,50m2	10m2	6,00m2	-	1,08m2	52,m2
Mozambique and Guinea-Bissau	2,80m	9,00m2	12m2	-	-	1,00m2	-

Table 1: Required minimum standards for a two-bed house.

Step 3: Pre-selection and model design tests

The compilation and integration of all variables needed for the modular design phase allows the selection of the materials that will enable establishing the module in its dimension, taking into account the final goal of pre-fabricated modular panels made with a thin concrete sheet fabricated in Portugal, complemented with a local material layer and possibly built with the traditional construction material identified in the research.

One of the materials that should be able to complement this thin panel is rammed earth, like a compressed earth block (CEB) who is common in the four countries and meets the sustainability principles of economical viability, cultural expression who can also be seen in all the informal and traditional architecture, and environmental viability due to its raw material. Furthermore, the application of a CEB layer can improve the wall performance and its sustainability due its natural and ecological proprieties and processes, which means low energy consumption during the production and transport process. This raw material also has the advantage of being easily recyclable and reusable, does not produce construction waste, is not toxic and has a good thermal and acoustic performance due its mass [6,8].

Step 4: Interaction system

The proposed module dimensions are based on the following factors as Figure 4 shows.

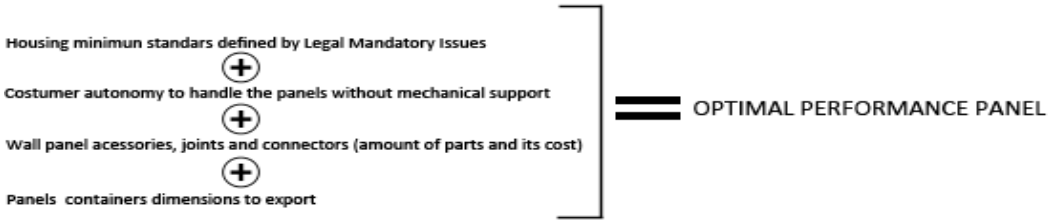

Figure 4: Parameters for dimensioning the modular panel.

The first stage was to define the required minimum standards for room areas, according to the Building Code of each country, taking into account the most stringent values (Table 2).

Typical floor height	Window width	Area$_{min}$ Bedroom	Area$_{min}$ Living room	Area$_{min}$ Kitchen	Area$_{min}$ Bathroom	Area$_{min}$ Frenestration	Area$_{min}$ T2
2,8m	0,90m	10,50m2	14m2	6,50m2	4,50m2	1,08m2	52m2

Table 2: Required minimum standards of each country.

The next step was the creation of standard rooms based on the minimum standards required whose values were optimized (Figure 5).

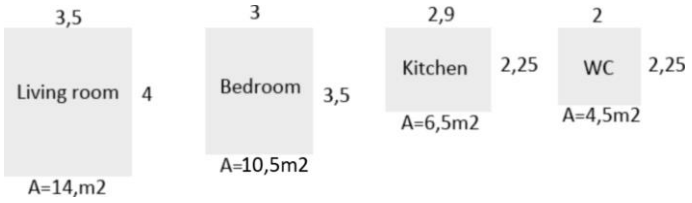

Figure 5: Required minimum standards for the room areas.

The panel height was directly obtained from the minimum standards required with 2,8m. The width calculation considered the panel weight and dimension for its transportation and handling by the user, resulting in 11 types of width between 0,5m and 1,5m. Subsequently, the number of needed panels to form a room was quantified, according to the minimum area standards. After the optimal area calculation for each room a score table between 1 and 11 points to evaluate each panel was considered. The best score was the result between the minimum standards for room area and an optimal width. If the resulting areas are the same but made with different panel widths, the panel that needs less modules to make the area prevails.

The final typologies score was the result of a total sum between all the possible panel widths for all types of room (Table 3).

Panel width	Score for each panel width per room				∑score	Score table
	Bedroom	Living room	Kitchen	WC		
0,5	11	11	8	9	39	2°
0,6	10	8	10	6	34	3°
0,7	7	9	4	5	25	5°
0,8	6	5	6	7	24	6°
0,9	4	4	7	10	25	4°
1,0	8	6	2	4	20	8°
1,1	9	10	9	11	39	1°
1,2	5	3	3	8	19	9°
1,3	1	7	11	3	22	7°
1,4	3	2	5	2	12	10°
1,5	2	1	1	1	5	11°

Table 3: Final score of each panel widths and each typology of room.

The most efficient panel has a width of 1,10m, followed by panels with a width of 0,5m and 0,6m. As Table 3 shows, the panels with a width of 1,1m and 0,5m have the same score but the one with a width of 1,1m has less accessories and connectors, which means that it has less production and assembly costs and is builtfaster. Furthermore, this dimension will allow the integration of windows only with the production of two more panels with the following dimensions: 1,10x1m and 1,10 x 0,8m.

The optimal panel reveals concerns about the transportation; once that the sea containers selected have 12,06m in lenght, 2,34m in width and 2,679m in height, it is possible to export a4 rows of panels in lenght (12,06m/2,80m), multiplied by2 (2,679m/1,1m).

The modular house made with these panels can easily be transformed and expanded because the connectors and joints work mechanically. This modular system allows not only the creation of a residential compact module but also the creation of more open and expansive modules for rural activities.

This kind of modular building maintains African family dynamics: the family has a small house that will evolve over the years according to the family members and its financial situation.

CONCLUSIONS

The present study shows that there is a housing problem that strengthens the importance of efficient solutions to support the current housing programmes promoted in the study countries. The implementation of a pre-fabricated modular wall system, which deals with local materials, will contribute a solution to this housing problem. The present system allows a faster low-cost construction without skilled labour. People's acceptance can promote local employment, which will improve the process.

The modular house resulted from the Eco-Wall modular system also guarantees comfort parameters such as thermal comfort and acoustic insulation as well conditions for a good indoor air quality. The next step of the Pre-conception process will consist in investigating a sustainable solution for the building use-phase, which means creating comfort conditions and ensuring correct resources management system during the whole life cycle.

REFERENCES

1. Stallen, M., Chabannes, Y. e Steinberg, F. : Potentials of prefabrication for self-help and mutual-aid housing in developing countries, Habitat International, vol. 18, n.2, pp 13-39, 1994.
2. Jaillon, L. e Poon, C. S. - The evolution of prefabricated residential building systems in Hong Kong: A review of the public and the private sector, Automation in Construction, vol. 18, no. 3, pp 239–248, 2009.
3. Aye, L. , Ngo, T., Crawford, R. H., Gammampila, R., Mendis, P. - Life cycle greenhouse gas emissions and energy analysis of prefabricated reusable building modules, Energy and Buildings, vol. 47, pp 159–168, 2012.
4. Hsieh, T. - The economic implications of subcontracting practice on building prefabrication, Automation in Construction, vol. 6, pp 163–174, 1997.
5. Waskett, P. - Current Practice and Potential Uses of Prefabrication. Watford: BRE (Building Research Establishment), DTI (Department of Trade and Industry), 2003.
6. Lopes, T., Amado, M.P., Poggi, F. – Construção sustentável – Fase de pré-concepção. In 4º Congresso Nacional da Construção, 2012
7. Amado, M.P., Pinto, A.J., Santos, C.V. – The Sustainable Building Process. XXXV IAHS World Congress on Housing Science, Edited by: R. Wakefield, N. Blismas, RMIT, 2007
8. Torgal, F., Eires, R., Jalali, S. – A construção em terra. Tec Minho. Guimarães: Universidade do Minho, p 174, 2009.

EVALUATING BUILDING ENVELOPES FOR ENERGY RENOVATION – ENERGY- AND MOISTURE PERFORMANCE CONSIDERING FUTURE CLIMATE CHANGE

Björn Berggren*, Maria Wall

Lund University, Dept. of Architecture and Built Environment, Div. of Energy and Building Design, Box 118, 221 00 Lund, Sweden

ABSTRACT

An important strategy for climate mitigation is reduction of energy use in buildings. Especially within the existing building stock. However, increasing the thermal resistance in combination with climate change will result in different hygrothermal conditions within building envelopes. Buildings are expected to have a long life-span. Hence, the effects of climate change in the design of buildings and building elements must be considered.

This paper will present a Multi Criteria Decision Making (MCDM) method developed at Lund University and present a literature review conducted to indentify common buildings and building envelopes.

The literature review show that the majority of the Swedish multi-dwelling buildings built 1966-1975 are slab block buildings with load bearing construction of concrete. There is a rough 50/50 distribution between longitudinal and transverse load bearing systems. For buildings completed 1966-1975, the most common facing material in Stockholm is render, In the Malmö region and Göteborg region only 5 % of the dwellings have render facades. The most common facade materials in Sweden, except the Stockholm region, are clay bricks.

Keywords: Renovation, Multi Criteria Decision Making, MCDM, Climate change

INTRODUCTION

Reduction of energy use constitutes an important measure for climate change mitigation. Buildings today account for 40% of the world's primary energy use and 24% of the greenhouse gas emissions [1].

In Sweden, there are roughly 2 500 000 dwellings in multifamily houses and single family houses [2]. Available statistics show that during the last three years in Sweden new production of residential buildings has only amounted to roughly 10 000 – 20 000 dwellings per year, while demolition of dwellings has been less than 1000 dwellings per year since 2007 [2, 3]. Hence, even if the small share of new production is built as very energy efficient buildings, the overall impact on the energy use in buildings is low.

There is a need to address the energy use within the existing dwellings; especially within multifamily buildings constructed 1960-1975, which accounts for almost one million dwellings or roughly 40 % of the dwelling stock in Sweden.

To decrease the energy use for heating in cold climate, reduction of energy losses through the building envelope in the existing building stock is a fundamental measure. However, increasing the thermal resistance in combination with climate change will result in different hygrothermal conditions within building envelopes [4, 5]. Buildings are expected to have a long life-span. Hence, the effects of climate change in the design of buildings and building elements must be considered.

This paper will present a Multi Criteria Decision Making (MCDM) method developed at Lund University [6] and present a literature review conducted to indentify common buildings and building envelopes. A test of the method evaluating energy performance and risk of performance failure due to moisture, considering future climate change, will be presented at the poster.

METHOD

A literature review is conducted to define common buildings and building envelopes in the Swedish dwelling stock. The investigation is based on data from The Swedish National Board of Housing, Building and Planning and Statistics Sweden [7, 8], focusing on buildings built during the so called "Miljonprogrammet" 1966-1975.

As a basis for future climate conditions data from the Swedish Meteorological and Hydrological Institute [9] is used, using regional climate models developed at the Rossby Centre, RCA3[10]. The RCA3 model covers Europe with a horizontal resolution of 50x50 kilometres. The boundary conditions are from the global climate model ECHAM5.

An initial test of the MCDM-model is conducted, using data from simulations previously presented case studies [4, 11]. The MCDM-model is described below.

Moisture and energy performance is evaluated. An overall main criteria classification is used for which the indicators are sorted under. Aggregation of indicators follows the AHP-method described in [12]. Within each main criterion, the indicators are pairwise compared according to the scale presented in Table 1.

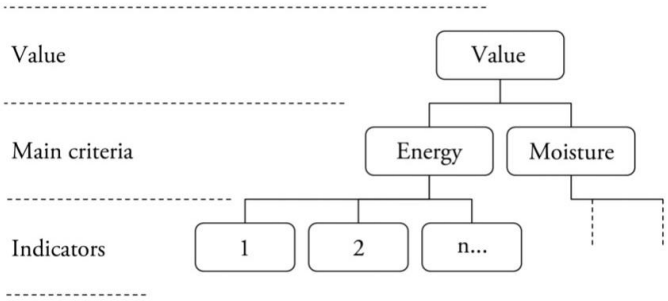

Figure 1 General value tree, describing the evaluation model

Relative importance compared to second indicator	**Grade**
Equally important	1
More important	3
Much more important	5
Very much more important	7
Extremely more important	9
Less important	3^{-1}
Much less important	5^{-1}
Very much less important	7^{-1}
Extremely less important	9^{-1}

Table 1 Grades used for weighting

An example of aggregation of indicators i_1, i_2 and i_3 is presented in Table 2. First i_1 is pairwise evaluated in relation to i_2 and i_3, respectively. Thereafter, i_2 is evaluated in relation to i_3 (i_2 is already evaluated in relation to i_1). The relative importance is translated into grades and arranged in an evaluation matrix to calculate the weighting factor, Table 3.

Indicator	Pairwise priority	Indicator
i_1	is *much more important* than	i_2
i_1	is *much less important* than	i_3
i_2	is *less important* than	i_3

Table 2 Prioritization of indicators using pairwise comparison

Evaluation matrix	i_1	i_2	i_3	Weighting factor, *w*
i_1	1	5	5^{-1}	0.26
i_2	5^{-1}	1	3^{-1}	0.10
i_3	5	3	1	0.64

Table 3 Prioritization of indicators using pairwise comparison

To support the translation of the indicators into relative values, one of the two methods described below may be used, Table 4 and Table 5.

Judgement	Value
Excellent	120 %
Very good	90 %
Good	60 %
Fair	30 %
Not acceptable	0 %

Table 4 Values for indicators based on value judgement

Judgement	Value
Best possible outcome	120 %
Design target	100 %
Lowest accepted level	1 %
Not acceptable	0 %

Table 5 Values for indicators based on design target approach

Before the overall value is calculated, the value of each indicator is calculated.

When the overall value is calculated; a performance failure indicator, *k*, based on the product of all relative values of the indicators is included, see Equation 1. The value, *V*, is calculated as shown in Equation 2.

$$k(a) = 1 \qquad \text{for } v_i(a) \cdot \ldots \ldots \cdot v_n(a) > 0 \tag{1}$$

$$k(a) = 0 \qquad \text{for } v_i(a) \cdot \ldots \ldots \cdot v_n(a) = 0$$

Where

$k(a)$ The performance failure indicator for alternative *a*

$v_i(a)$ Relative value for criterion *i*, for alternative *a*

$$V(a) = k(a) \cdot \sum_{1}^{i} w_i v_i(a) \quad (2)$$

Where

V(a)	The total value of the investigation alternative *a*
k(a)	The performance failure indicator for alternative *a*
w_i	Weighting factor for indicator *i*, for all alternatives
$v_i(a)$	Relative value for indicator *i*, for alternative *a*

The performance failure indicator is used to prevent sub-optimization. By using the performance failure indicator, alternatives where one or more indicators are at a non-acceptable level receive an overall value of zero, regardless of the value of the other indicators.

RESULTS

Literature review

The distribution of different types of multi-dwelling buildings built during the million program is almost equally throughout Sweden; the buildings' are mainly slab block buildings. Across Sweden, 83 % of the dwellings built 1966-1975 as multi-dwelling buildings, are slab block buildings, see Figure 3.

Within the gathered statistics from SCB, data for load bearing systems and number of floors are is only available for 1968-1972. During the middle of the 20th century, industrialized building techniques were introduced in Sweden. The traditional load bearing system, which were longitudinal in situ constructed load bearing system with exterior and interior load bearing walls, were gradually replaced by transverse load bearing systems were the gable and interior, transverse, walls were used as load bearing structure. During 1968-1972, 49 % of the dwellings were constructed with transverse load bearing system.

The number of floors in multi-dwelling buildings built 1966-1975 varies greatly when comparing metropolitan regions and the rest of the country. As high as 81 % of the dwellings in multi-dwelling buildings built outside metropolitan regions was four stories high or lower compared to the Stockholm region; 35 %. Overall, in Sweden, three-storey buildings arethe most common buildings and accounted for 44 % of the dwellings built in multi-dwelling buildings within the "Miljonprogrammet", see Figure 2.

In the beginning of the 20th century, brick masonry walls were the most common type of interior load-bearing walls. During the period 1901-1940 were 76% of all dwellings in multi-dwelling buildings built with brick masonry [13]. Concrete became increasingly more common the next fifteen years, and was during the "Miljonprogrammet", by far, the most common construction in interior load bearing walls, see Figure 2.

In comparison with the materials in load bearing walls and load bearing systems, which show small geographic differences, there are differences of facade materials used, geographically. In the beginning of the "Miljonprogrammet", facades materials were usually clay bricks or render.

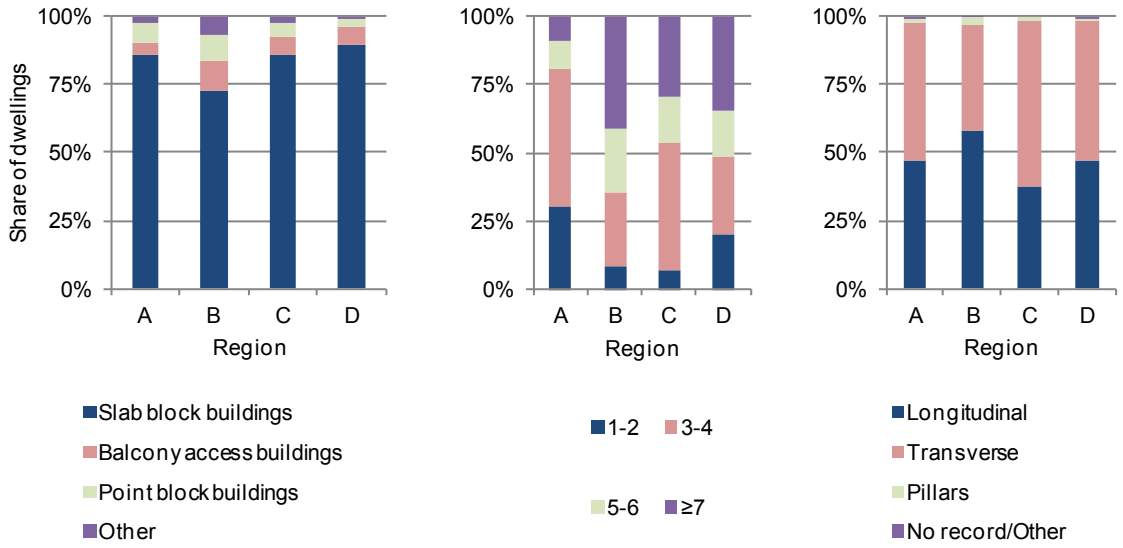

Figure 2 Distribution of dwellings in multi-dwelling buildings in different Swedish regions A: Sweden, excluding metropolitan regions B: Stockholm region C: Göteborg region D: Malmö region [8]. Left: Type of building (1966-1975). Middle: Type of load bearing system (1968-1975. Right: Number of floors (1968-1975).

As can be seen in Figure 3, the use of concrete as a facade material in multi-dwelling buildings was relatively high for a short period; 1968-1970. During the "Miljonprogrammet", the most common facing material in Stockholm was render, In the Malmö region and Göteborg region were only 5 % of the dwellings were given render facades. The most common facade materials in Sweden, except the Stockholm region, are clay bricks.

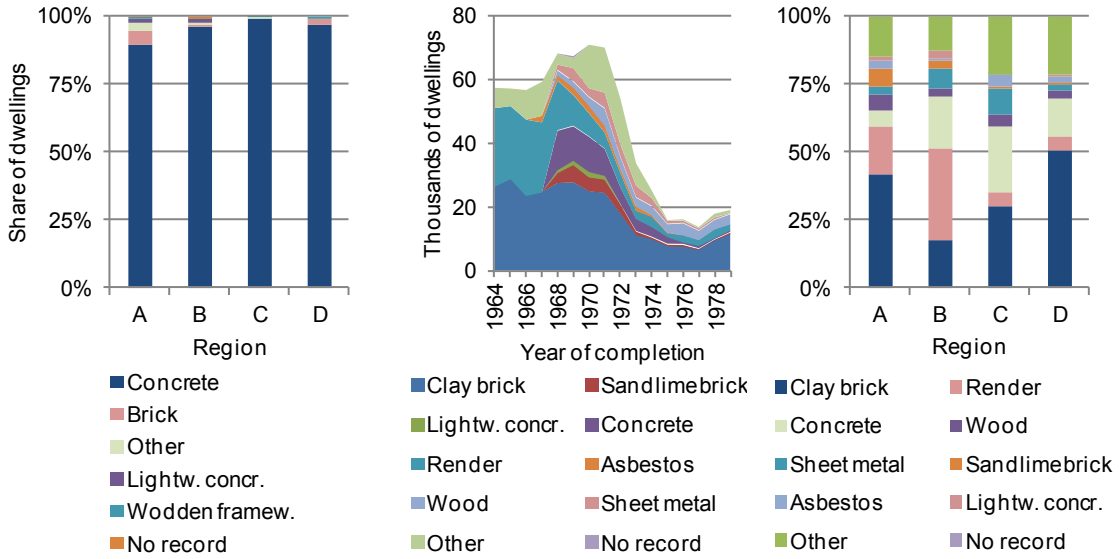

Figure 3 Distribution of dwellings in multi-dwelling buildings in different Swedish regions A: Sweden, excluding metropolitan regions B: Stockholm region C: Göteborg region D: Malmö region [8]. Left: Material in interior load bearing walls (1966-1975). Middle: Facade material (1966-1975). Right: Facade material by year of completion, all regions.

Case study

Results from the case study, using the Multi Criteria Decision Making (MCDM) method, developed at Lund University [6], using data from simulations previously presented case studies [4, 11] will be presented at the poster session.

ACKNOWLEDGEMENTS

This article is part of the project; Klimatskal 2019, a project funded by The Development Fund of the Swedish Construction Industry and Skanska Sverige AB. The aim is to develop a method to evaluate energy- and moisture performance for building envelops.

REFERENCES

1. International Energy Agency (IEA), Towards Net Zero Energy Solar Buildings, SHC Task 40/ECBCS Annex 52 IEA, project fact sheet, 2011.
2. SCB, Bostads- och byggnadsstatistisk årsbok 2012, Retreived (2013-05-01) from http://www.scb.se/Pages/PublishingCalendarViewInfo____259923.aspx?PublObjId=16921, Stockholm, 2012, pp. 240.
3. SCB, Nybyggnad av bostäder, Retreived (2013-05-01) from http://www.scb.se/Pages/TableAndChart____19985.aspx , 2012.
4. B. Berggren, M. Wall, Moisture Conditions in Exterior Walls for Net Zero Energy Buildings in Cold Climate Considering Future Climate Scenario, In proceedings from 7th International Cold Climate HVAC Conference Calgary, 2012, pp. 8.
5. B. Berggren, M. Wall, Hygrothermal conditions in exterior walls for passive houses in cold climate considering future climate scenario, In proceedings from 5th Nordic Passive House Conference, Trondheim, 2012.
6. B. Berggren, Evaluating building envelopes for energy efficient buildings - Energy and moisture performance considering future climate change, Licentiate thesis, Architecture and Built Environment, Lund University, 2013.
7. Boverket, Energi i bebyggelsen – tekniska egenskaper och beräkningar, Retreived (2013-05-01) from http://www.boverket.se/Global/Webbokhandel/Dokument/2011/BETSI-Energi-i-bebyggelsen.pdf , Karlskrona, 2010, pp. 204.
8. SCB, Låneobjektsstatistik Bo-serien (1967-1995), 1967-1995.
9. Swedish meteorological and Hydrological Institute (SMHI), Rossby centre, http://www.smhi.se/en/Research/Research-departments/climate-research-rossby-centre2-552, 2013.
10. P. Samuelsson, C.G. Jones, U. Willén, A. Ullerstig, S. Gollvik, U. Hansson, C. Jansson, E. Kjellström, G. Nikulin, K. Wyser, The Rossby Centre Regional Climate model RCA3: model description and performance, Tellus A, 63 (1) (2011) 4-23.
11. B. Berggren, H. Stenström, M. Wall, A parametric study of the energy and moisture performance in passive house exterior walls, In proceedings from 4th Nordic Passive House Conference, Helsinki, 2011, pp. 9.
12. T.L. Saaty, The analytic hierarchy process: Planning, priority setting, resource allocation, McGraw-Hill International Book Co., 1980.
13. S.-E. Bjerking, Ombyggnad : Hur bostadshusen byggdes 1940-1970, 1978.

LIGHT AND ENERGY PERFORMANCE OF AN ACTIVE TRANSPARENT FAÇADE: AN EXPERIMENTAL STUDY IN A FULL SCALE OFFICE ROOM MOCK-UP

L. Bianco[1]; F. Goia[1,2],V. R. M. Lo Verso [1], V. Serra[1]

1: TEBE Research Group, Department of Energy, Politecnico di Torino, c.so Duca degli Abruzzi 24, 10129 Turin, Italy

2: The Research Centre on Zero Emission Buildings, Faculty of Architecture and Fine Arts, Norwegian University of Science and Technology, Alfred Getz' vei 3, 7491 Trondheim, Norway

ABSTRACT

This paper deals with energy and light performance assessment of two configurations of an Active Transparent Façade (ATF), which are investigated by means of an experimental campaign that makes use of a full-scale mock-up room of an office building. The two configurations of the ATF (a Climate Façade integrated with the HVAC system) differ in the technology of the inner glazing (extra-clear single glass or double pane glazing with low-e coating), while share all the other features – i.e. external glazing, shading system, airflow path and ventilation rate, control strategies.

The aim of the research activity is both to define a methodology to assess energy and light performance of each configuration, through elaboration of experimental data, and an attempt to apply the methodology to the specific case, in order to test it. Experimental investigations in test cells and/or real scale mock-up provide high quality data, but their representativeness and direct application is not always straightforward. Dedicated data analysis procedures and methods need thus to be developed in order to translate experimental data in useful information. Moreover, investigations are usually carried out on either the thermal or the light aspects, while combined analyses are not common, since this increases the degree of complexity of the analysis and measurement requirements are often quite different.

The ATF module equipped with extra-clear single glass pane (Module A) shows, compared to that with a low-e coated double pane glazing (Module B), an increase in the average luminance, over the analyzed surfaces, in the range 20%-52% and 16%-81%, in absence and in presence of the shading systems respectively. A higher amount of daylight is then guaranteed within the indoor space by Module A, but this might result in a higher probability of visual discomfort for the occupants. On the other hand, the Module B determines lower daily energy transmitted toward the indoor environment than Module A: on average, the daily energy gain/loss from/toward the outdoor environment are reduced of about 30%, in summer (with or without the reflective roller screen), and in the range 30-40% in winter (with or without the reflective roller screen).

Keywords: Active Transparent Façades; Energy and Daylight Performance; Thermophysical behaviour; Energy and Daylighting measurements.

INTRODUCTION

Active Transparent Façades (ATF), also known as Advanced Integrated Façades (AIF) [1], are a class of glazing technologies aimed at overcoming the limitations given by conventional transparent façades and at improving the energy performance of the transparent envelope. The characterization of ATFs is not an easy task because their dynamic behaviour is hardly assessed by conventional performance parameters (e.g. *U-value* and *g-value*) [2] – a topic that

is discussed since few years. Light performance assessment of ATFs was also investigated, but to a lower extent than energy performance and thermo-physical behaviour [3]. The aim of the research activity presented in this paper is both to define a methodology to assess energy and light performance of ATFs from experimental data collected by means of measurements in real scale mock-ups. Actually, although this activity provides high quality data, their representativeness and the direct translation into useful information is not straightforward.

The investigation herewith presented focuses upon the role of the glazing components on the overall performance of an ATF, a type of sensitivity analysis that has some precedents in literature [4]. The analysis is carried out on experimental data collected during different seasons, on two modules of different ATF configurations, simultaneously installed on a full scale mock-up. The two modules (named Module A and Module B) share the Climate Façade concept (a Double Skin envelope that works as exhaust air façade), but are equipped with a different indoor-side glazing system. Module A presents a single extra-clear glass pane (10 mm) – a conventional solution for this technology – while Module B has a double glazed unit (10/16/10 mm, clear glass panes with low-e coating, Argon in the gap). The two façade modules share the same shading system in the cavity (reflecting roller screen), the same outer-side glazing (double glazed unit with a selective external glass, 20/16/10 mm), airflow path and rate (25 m^3/h each module) and control strategy.

METHOD

Experimental test rig and data collection

The procedure for data collection used during the experimental campaign is herewith briefly summarized for the sake of brevity. The experimental test rig consists of a full scale office room mock-up (3.20 m width, 5.90 length, 3.45 m height), whose façade, which hosts the two ATF modules under investigation, is south/south-west-oriented.

As far as thermal measurements are concerned, the two ATF modules and both indoor and outdoor boundary conditions are monitored, by means of more than 70 sensors previously calibrated and/or verified in laboratory – i.e. T-type/J-type thermocouples (accuracy: ±0.3°C); heat flux meters (accuracy: ±5%); pyranometers (accuracy ±2%). Thermocouples and heat flux meters are shielded with aluminum foils to reduce the influence of solar irradiation on the measured physical quantities; ventilated thermocouples are used to measure the air temperature in the cavities of the ATF modules. Data are collected by a data logger every 15 minutes and then hourly values are calculated and used for elaboration. Continuous monitoring of the energy performance and thermo-physical behaviour are carried out during summer, autumn and winter season.

Spot light measurements are carried out during a typical late summer day and winter day, under clear sunny sky conditions, from 11 am to 1 pm, both in presence and in absence of the shading system. An Imaging Luminance Measuring Device (Technoteam LMK 98-3, equipped with both a 4.5 mm lens and a fish-eye lens; accuracy ±3%) is used to obtain different luminance maps within the mock-up and to assess the daylight distribution. Measurements are repeated in 3 different positions (close to the modules; at the center of the room; in the back of the room, far away from the modules), positioning the lens of the instrument at a height of 1.20 m (that of a sitting person). The vertical illuminance values on the lens are also recorded by means of an illuminance meter (Minolta LS100; accuracy ±5%).

The configuration of the test facility with both modules installed in the same mock-up presents advantages and drawbacks; the main strength is that the two ATF modules are exposed to the exact same boundary conditions – both outdoor and indoor, where the air

temperature is controlled through a combined air system and radiant heating/cooling panels, with a set point of 26°C in summer and of 20°C in winter. Moreover, this experimental test rig allows the costs of the measurement campaign to be reduced – just one test cell is needed. The main drawback is that the performance of each ATF technology cannot be assessed by measuring the energy delivered to the mock-up, since it depends on the combined behaviour of the two ATF modules – a procedure that however shows some weak spots. Furthermore, daylighting conditions within the room (such as the discomfort perceived by the occupants) cannot be directly assessed either, since the light environment is again determined by the combined effect of the two ATF technologies. As a matter of fact, only the luminance over the glazed surfaces can be directly compared for the two ATF configurations. These drawbacks call for the development of dedicated data analysis procedures and performance parameters that overcome the practical limitations often faced during experimental activities.

Data analysis procedure

In order to analyse the thermal features of the two modules, two sets of 14 days (one for summer, one for winter) are selected. Each data set consists of 7 days during which the roller screen is lowered, and of 7 days during which the roller screen is retracted. In order to be representative the selected weeks contain sunny warm days and cloudy cold days, both in winter and in summer. The detailed information on the days selected in the two datasets are illustrated in Figure 1, where the following boundary conditions are provided: the specific daily solar energy on the vertical plane H_{24} [kWh/m^2], the average outdoor air temperature $T_{av,out}$ [°C] and the temperature range – given by the maximum and minimum temperature during the day.

The energy performance is assessed by comparing the daily total energy transmitted through the façade, e_{24} [Wh/m^2], that is given by the integral over the 24 h (from 8 am to 8 am of the following day) of the transmitted solar radiation I_{in} [W/m^2] (measured on the vertical plane) and the heat flux exchanged at the indoor surface of the façade dq [W/m^2].

$$e_{24} = \int_{24h} (I_{in} + dq) d\tau \qquad (1)$$

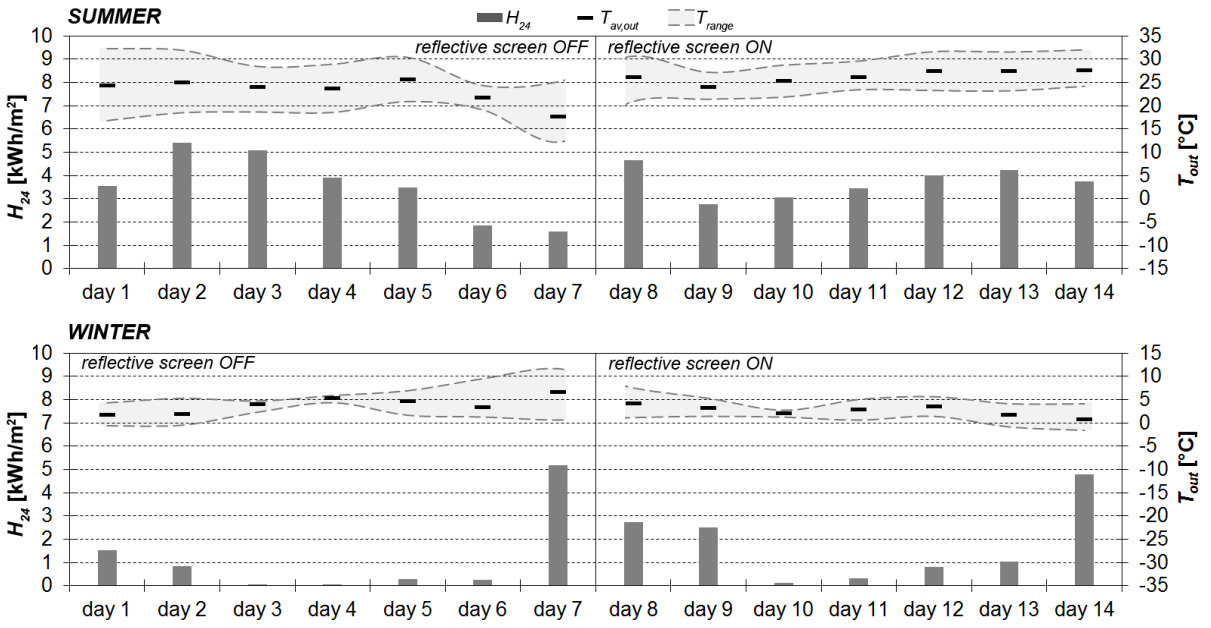

Figure 1: Daily boundary conditions of the analysed periods (winter and summer season).

An attempt is also made to estimate the thermal transmittance (*U-value*) of the two ATF modules, by means of a linear regression method [2], considering both days when the shading system is activated and days when it is retracted.

The solar transmittance τ_e [-] is also evaluated as the ratio of vertical transmitted solar radiation I_{in} and vertical incident solar radiation I_{out} – i.e. $\tau_e = I_{in}/I_{out}$. This parameter is calculated on an hourly basis, and an aggregated value (the average of the hourly values) is then given. The light transmittance τ_l [-] is calculated as the ratio between the illuminance on the vertical plane behind the ATF, E_{in} [lx] and the illuminance on the outdoor vertical plane, E_{out} [lux] – i.e $\tau_l = E_{in}/E_{out}$. The luminance images are analyzed through the Technoteam software "LmL Labsoft", different regions are drawn within the scenes and mean luminance values for each region are returned. The boundary conditions of these days when spot light measurements are carried out are herewith briefly summarized: H_{24} = 5.7 and 6.1 kWh/m^2, and $T_{av,out}$ = 19.0 °C and 5.6 °C, for the summer and the winter day, respectively.

RESULTS

Light and energy façade properties

The solar and light transmittances are reported in Table 1, for different seasons and shading positions. Module B is always characterized by lower values than Module A, in particular approx. 35% lower when the shading is retracted, both in summer and in winter. The small difference in values between summer and winter (max 0.02) can be explained considering the different position of the Sun and the angular-dependent optical properties of the glazing systems. When the screen is lowered the difference between the two solutions and between winter and summer is negligible – about 0.01, i.e. in the same range of the measurement error. The light transmittance follows the same trend – a predictable behaviour, since the ATF modules do not present substantial difference as far as the selective optical behaviour of the glazing systems is concerned.

The calculated *U-values* are 0.62 and 0.33 W/m^{2}K, for Module A and Module B, respectively. However, it is important to mention that the coefficient of determination R^2 of the linear regression for both Module A and B does not reach satisfactory values (i.e. 0.71 and 0.37, for Module A and B, respectively). This is in line with previous studies [2] and reaffirms the limited effectiveness of such a parameter in assessing the thermophysical properties of dynamic building envelope components. The values are however in line with those calculated for the same configuration with dedicated software tools – i.e. WIS/TNO.

	$\tau_{e,\text{summer,on}}$	$\tau_{e,\text{summer,off}}$	$\tau_{l,\text{summer,on}}$	$\tau_{l,\text{summer,off}}$	$\tau_{e,\text{winter,on}}$	$\tau_{e,\text{winter,off}}$
Mod. A	0.03	0.19	0.06	0.50	0.03	0.21
Mod. B	0.02	0.12	0.05	0.42	0.02	0.14

Table 1: Solar transmittance τ_e [-] and light transmittance τ_l [-] for different seasons and shading positions (on = lowered shading; off = retracted shading).

Energy and light performance

The values of the daily energy transmitted through the façade, e_{24}, for Module A and B, are shown in Figure 2. Module A always presents higher values of e_{24}, regardless the season. The low-e glazing in Module B allows both energy loss during winter and energy gain during summer to be decreased. In summer, when the screen is retracted, the energy entering through Module A is 26%-32% higher than that entering through Module B. A very similar

percentage is also observed when the screen is lowered. The screen activation reduces e_{24} by more than 40%, for both the modules – this can be seen by comparing e_{24} of day 5 (screen off) and of day 11 (screen on), two days that show very similar boundary conditions. In winter, e_{24} through Module B is 40% lower than that through the Module A, on average. The absolute difference in e_{24} between Module B and A is lower in winter than in summer, both when the screen is used and when it is retracted, due to the fact that much lower values of e_{24} are always achieved – except in sunny days without screen (day 7, winter), when e_{24} reaches values similar to those of the summer season (e.g. day 2 and 3, summer).

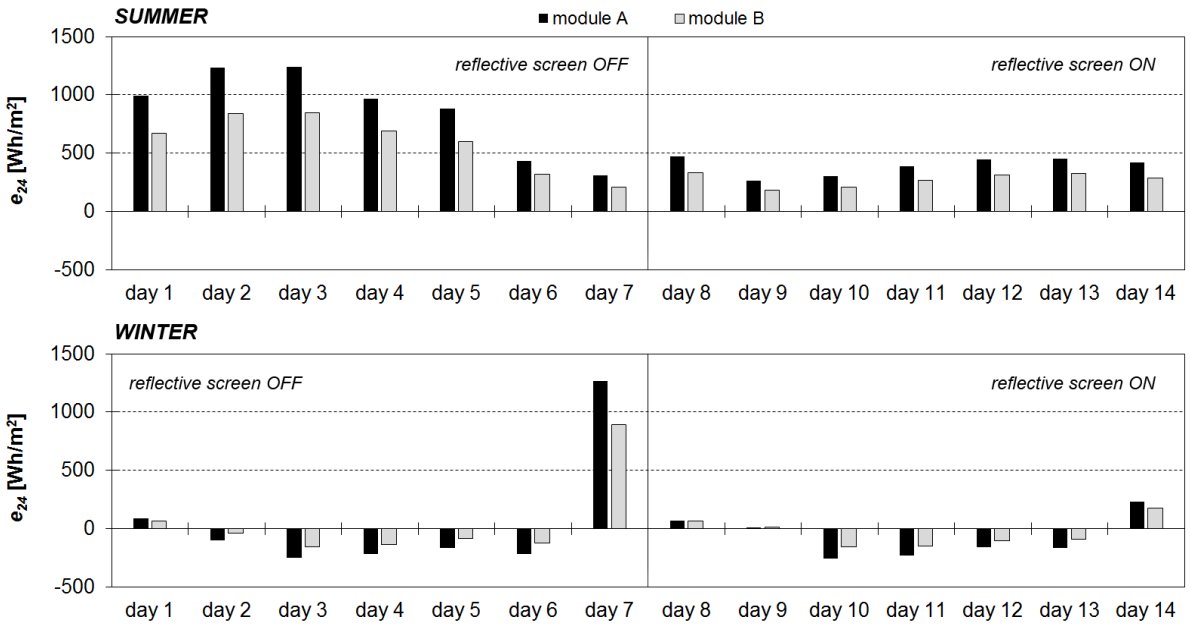

Figure 2: Daily total energy value e_{24} for different seasons and screen configurations.

Winter (shading: off) h12.30; 0-26500 cd/m^2			Winter (shading: on) h12.30; 0-4070 cd/m^2		
Mod B. [cd/m^2]	**Mod. A [cd/m^2]**	**A/B**	**Mod. B [cd/m^2]**	**Mod. A [cd/m^2]**	**A/B**
Glazing $L_{med,15}$ = 1268	Glazing $L_{med,16}$ = 1531	1.21	Glazing $L_{med,12}$ = 265	Glazing $L_{med,13}$ = 326	1.23
Desk in sunlight $L_{med,3}$ = 1225	Desk in sunlight $L_{med,4}$ = 1471	1.20	Desk in sunlight $L_{med,3}$ = 93	Desk in sunlight $L_{med,4}$ = 168	1.81
Desk shaded $L_{med,9}$ = 319	Desk shaded $L_{med,10}$ = 484	1.52	Desk shaded $L_{med,9}$ = 64	Desk shaded $L_{med,10}$ = 74	1.16

Figure 3: Winter luminance images (shading: off and on) and average luminance values. Note: the instrument was positioned pointing at the two ATFs).

Although luminance images are taken both in summer and winter, for sake of brevity just two winter maps are herewith reported, for the point in the back of the room. This choice is done as winter conditions are usually more critical from the discomfort glare risk viewpoint, due to the lower position of the Sun in the sky. In winter, the luminance scenes show higher average luminance values on Module A than in Module B, both over the glazing and the working plane surfaces. The ratio between average luminance on Module A and B is similar for both positions of the screen (off and on). These higher luminance values, due to the higher light transmittance of the glazing package of Module A, might result in a higher discomfort risk for daylighting, as the luminance of the main source (the glazing) is increased. As a consequance, a more frequent use of the shading system might be needed, which in turn would imply an increased energy demand for electric lighting. It should be stressed how the inherent characteristics of the mock-up (two ATF configurations in the same room) do not allow any analysis on the environmental daylight to be performed.

CONCLUSION AND FUTURE WORK

As far as the energy performance is concerned, it is possible to state that Module B, thanks to the low-e double pane glazing, reduces energy loss and energy gain during summer – the reduction being about 30% and about 40%, in summer and in winter, respectively. This is also reflected in different *U-values* for the ATF modules, and in different inner side surface temperature of the glazing systems – the surface of Module B is substantially colder in summer and warmer in winter than that of Module A, with implication on thermal comfort. As a drawback, it has been observed that the air temperature in the cavity of Module B is always higher than that of Module A – up to more than 60 °C, a level that can have negative effect of some sealant materials used in glazing systems. Implications of the ATF configurations on occupant thermal comfort will be evaluated in future by means of thermal simulations, calibrated with experimental data, that lead to the assessment of PMV index.

As far as the light performance is concerned, the higher light transmittance of Module A determines a higher luminance of the glazing (in the range + 20÷80%) which might result in a greater daylight amount within the room, but also in a higher discomfort risk for users. A detailed daylighting analysis cannot be done with the data measured within the mock-up. In order to overcome this limitation, a set of simulation is planned as a future work to calculate the Daylight Glare Probability (DGP) for the different positions within the room. Radiance tool "Evalglare" will be used to assess the DGP of an office room equipped with Module A against that of an identical office room equipped with Module B – measured luminance values over the two ATF configurations will be used to calibrate the models.

REFERENCES

1. Perino, M. (editor): State-of-the-art Review. Vol. 2A. Responsive Building Elements. Aalborg University Press, Aalborg, 2008.

2. Bianco, L., Goia, F., Serra, V.: Energy performance assessment of advanced glazed façades in office buildings. Proc. of CLIMA 2013 - The 11th REHVA World Congress & 8th International Conference on IAQVEC, paper ID 727 pp 1-8, Prague, 2013.

3. Shameri, M.A., Alghoul, M.A., OmKalthum Elayeb, Fauzi, M., Zain, M., Alrubaih, M.S., Halizawati Amir, Sopian, K.: Daylighting characterstics of existing double-skin façade office buildings. Energy and Buildings 2013;59:279-86.

4. Pérez-Grande, I., Meseguer, J., Alonso, G.: Influence of glass properties on the performance of double-glazed facades. Applied Thermal Engineering 2005; 25:3163-75.

DIFFERENT VERIFIED EXAMPLES OF 'NEAR ZERO ENERGY' HOUSES

Josep Bunyesc , Dr. Architecte UPC ETSA Barcelona, Master EPF Lausanne

Arboretum 21, 25198 LLEIDA Spain

info@bunyesc.com +34 609287277

ABSTRACT

With the construction of four houses in Spain, two in Lleida and two in the Pyrenees, following the Passive House standard or Minergie plus and its monitoring system we can study how the houses behave both summer and winter in a Mediterranean climate. It is a lightweight construction with wooden balloon frame structure and low thermal mass, very well insulated with local sheep wool which is helpful during the warm summer.

This building enjoys great energy efficiency; lower than 10kWh/m2 year approximately. The good results are due to the insulation thickness between 18 and 28 cm, the low-emission glass and the good orientation.

The construction system based on the use of wood and sheep's wool as insulation material of organic origin, 100% renewable, has very low embodied energy which turns it into a sustainable building.

The balance of CO2 emissions throughout the buildings are neutral, because the timber stores proportionally the same amount of CO2 generated by construction activity as the use of other materials that are not based on wood.

This construction method drastically reduces the emissions by means of building energy savings.

We present a simple and affordable option in order to score these goals for energy efficiency and global saving of resources.

The results have been very successful as we can observe on the graphs made with the data of the data loggers for temperature.

Keywords: template, conference, paper

INTRODUCTION

We are build and monitoring 4 houses in Lleida and the Pyrenees. Whit this experience we can analyse the real results and well understand the actual building thermal running all year long.

METHOD

After the construction of the houses we install, in its interior and exterior, data loggers which every 30 minutes register the temperature. With the data obtained, we can analyze the real behavior of the building during its use all over the year and compare the results obtained previously with the simulations and calculus. This real verification of the calculations allows to improve or to explain better the results of the simulations in the project phase to approach them more to reality.

The first aim is to evaluate the passive behaviour of climate inside the terraced house constructed with lightweight structure of wood and sheep's wool insulation with thickness between 18 cm into the walls, with a U=0.2Wm2K, and 28cm to the deck, with a U=0.16Wm^{2}K, but low thermal mass. The carpentry is a combination of wood windows and low-emission double glazing, with a U=1.5 Wm^{2}K.

RESULTS

The evolution of the temperature inside the building during the spring and fall is within the comfort zone without energy support. During the winter must promptly provide a total energy of 10kw/h.m^2 year more or less.

During spring and autumn it is stated that the temperature inside is always in the comfort zone, while the outside temperature is the most of the time lower than the temperature of comfort. This average temperature, in the inside is always higher, achieved by the solar provides directly and indirectly as well as internal gains in the use of home.

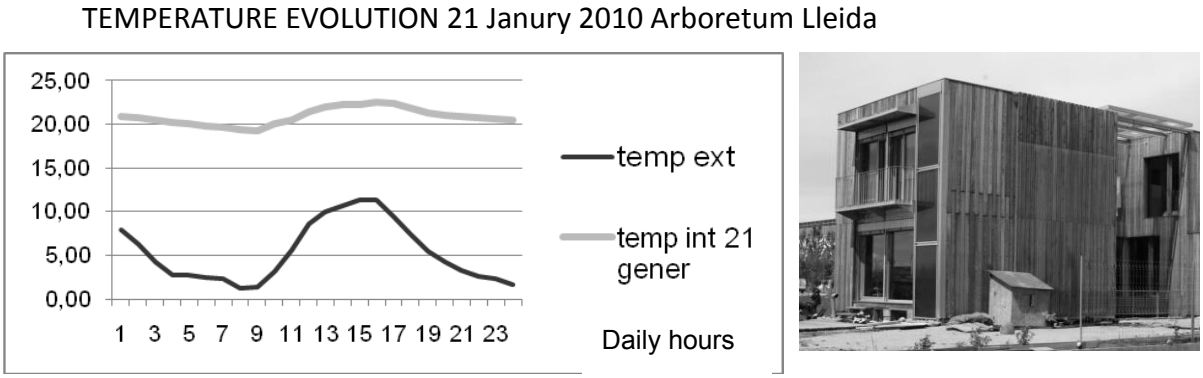

Figure 1: Arboretum House. Graph of daily temperature evolution on January 21th 2010, a typical winter sunny day, without heating. Indoor and outdoor temperature evolution

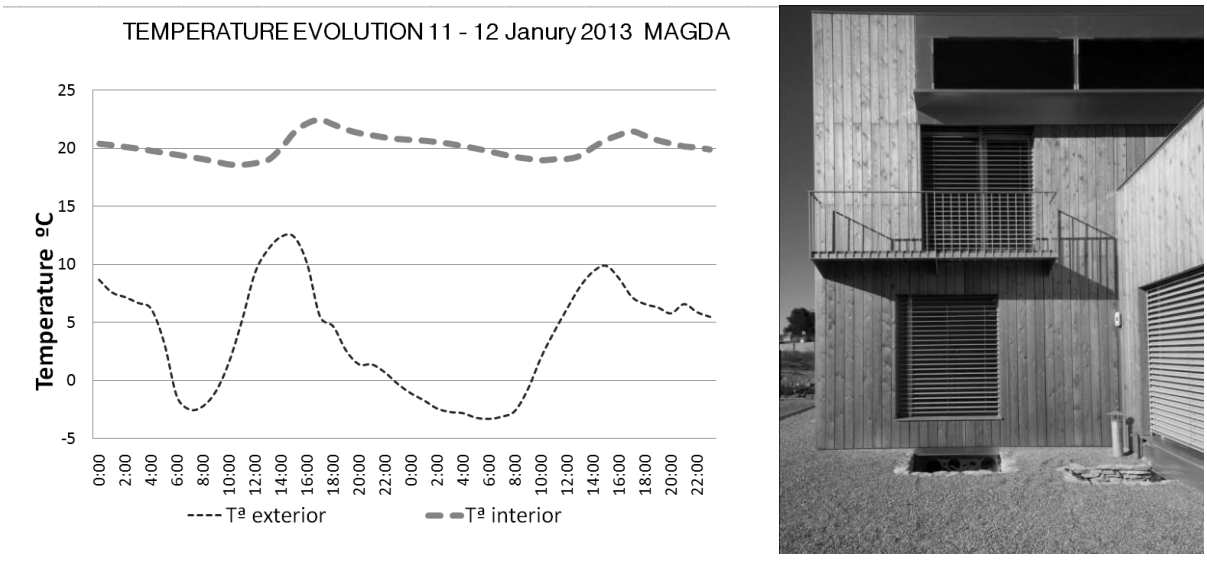

Figure 2: Magda House. Graph of daily temperature evolution on January 21th 2010, a typical winter sunny day, without heating. Indoor and outdoor temperature evolution

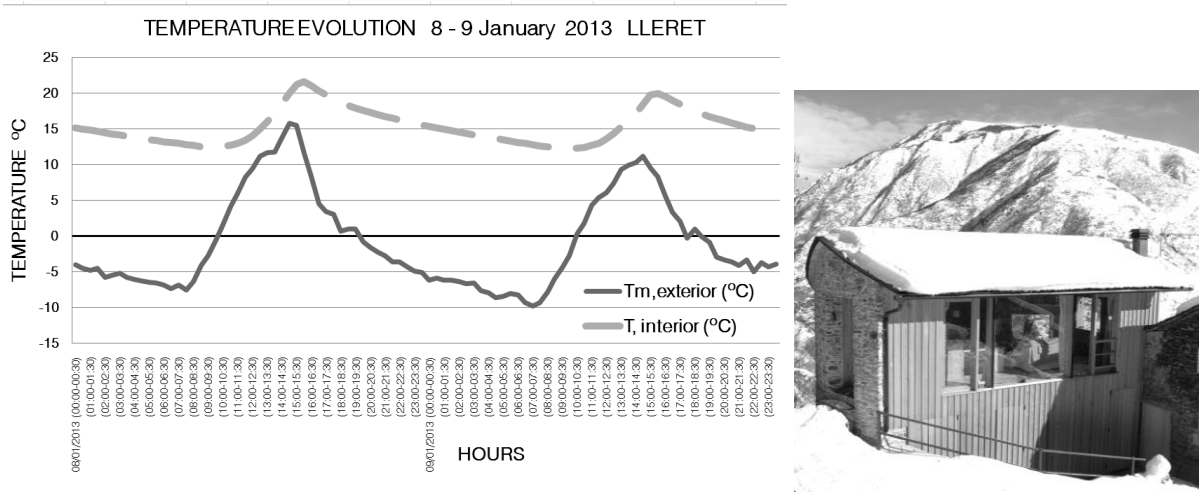

Figure 3: House Lleret 1400m.. Graph of daily temperature evolution on January 21th 2010, a typical winter sunny day, without heating. Indoor and outdoor temperature evolution

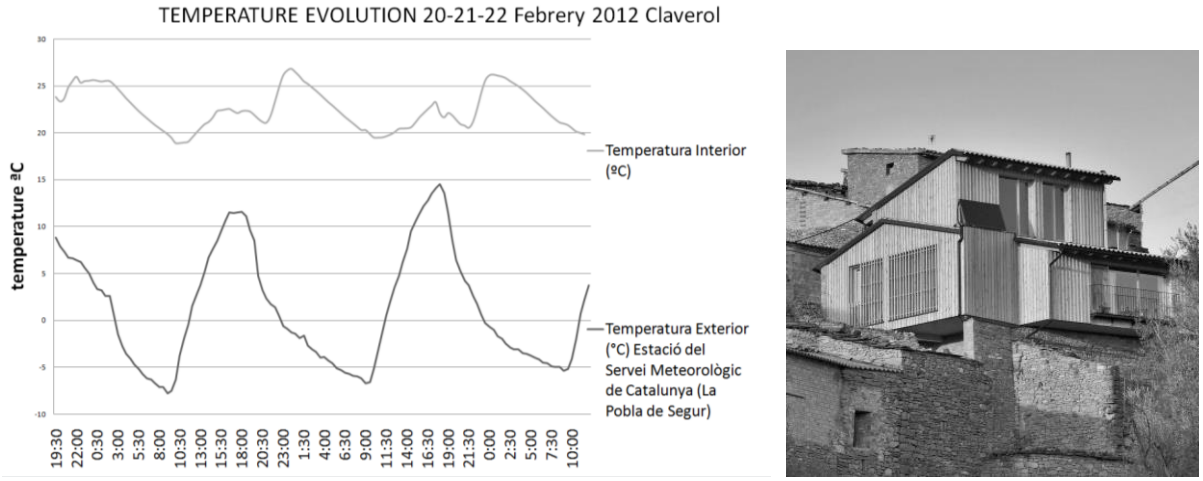

Figure 4: House Claverol 800m.. Graph of daily temperature evolution on Febrery 2012, a typical winter sunny day, without heating. The evening whe are cooking in the wood kichen.

In the two houses in Lleida, during the summer, which is warm and dry with a large thermal jump outside, between 19ºC at night and 37°C during the day, the temperature inside the upper housing ranges between 23 and 27 °C. In the two examples in the Pyrenees the temperatures are 5ºC lower than in Lleida. The low thermal mass means that the building is sensitive to internal or external gains, so to keep all the summer in the comfort temperature needs special attention to avoid solar radiation and to do free cooling at night. This way you can get the average temperature inside to be below compared to the average temperature outside. However, having a lot of insulating material or thermal mass without an active system of ventilation and free cooling during the night, means that the inside temperature of the building will gradually reach the outside average temperature. That means the implication of the users is very important.

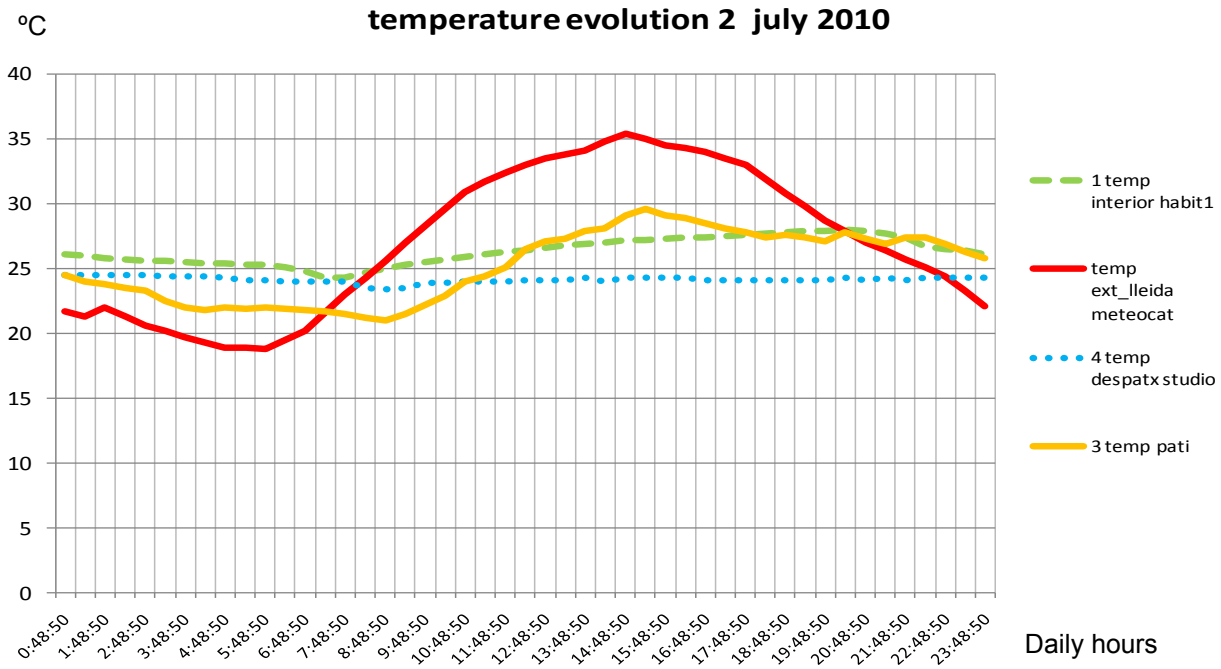

Figure 5: Graph of daily temperature evolution on 2nd July 2010, typical summer day into the arboretum house.

In Figure 5 we can see that there is a comfort zone that corresponds to very stable underground thermal mass much more effectively than other thermal regulation of the land because they are buried and in the fact that cold air floor and settles at the bottom.

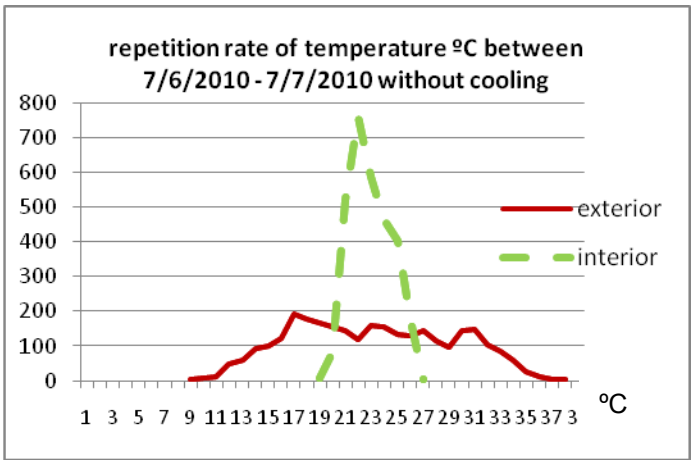

Figure 6, we can see the temperature evolution during a summer month (08/06/2010 - 08/07/2010). Arboretum house.

The average temperature taken each 30 minutes is lower than the outside temperature and major part of time the temperature within the comfort zone.

According to PHPP, the overheating frequency over 26ºC is about 18% and over 27ºC is a 3%. The 27ºC are hardly ever exceeded with a free cooling during the night and closing the house during the day. For this reason is not necessary to install an active cooling system.

In the Pyrenees, as the average temperature is lower, the overheating is less probably.

Furthermore, we observe a delay between the higher outside temperature and the higher internal temperature that we explain by the time necessary for the temperatures of the outer wall surfaces to cross the wall.

In Figure 14, we can see that the patio temperatures, in summer, are not the same that outside: in the patio are from 21 to 31ºC while outside temperatures are from 19 to 36ºC. This fact is important to observe: the patio large windows are not subject to so high external gains.

In winter, the sliding door placed on the east façade (figure 13) is opened during the day to have sunlight into the patio and it is closed during the night to protect the internal space, but it is permeable which means that air can circulate.

We observe that during winter's nights the patio temperature is 2 or 3 ºC higher than outside. For example, 0ºC and not -2ºC : it seems insignificant but it allows to reduce by 20% the patio losses during the night, it represents a decrease of 10% of the losses during the night of the whole building (the patio is the most open part).

DISCUSSION

It is shown that an insulated and very lightweight construction system functions optimally during the winter to reduce heating energy to the buildings.

From building these four examples in Spain, according to the criteria of Passive House or Minergie Plus, we have seen the behaviour of such buildings in hot summer conditions.

The houses consist of ground floor, first floor and, in the two examples in Lleida, a basement used as house and office. All the projects seek to open up to the maximum south to capture passive solar energy free, but also protect itself during the summer. In the two cases in the Pyrenees of building refurbishment the traditional architecture also captured solar energy.

Figure 7: view of the house in construction Figure 8: structure of wood and sheep's wool

The **construction system** used has some self-standing wood panels containing insulation inside composed of sheep's wool, OSB board as interior finishing, and a breathable board in the external surface to prevent condensation and breaking thermal bridges.

Those manufactured panels, prior to the workshop with strict precision planning, are mounted at building work very easily and quickly, which lead to a competitive construction system and a total work duration of less than 5 months.

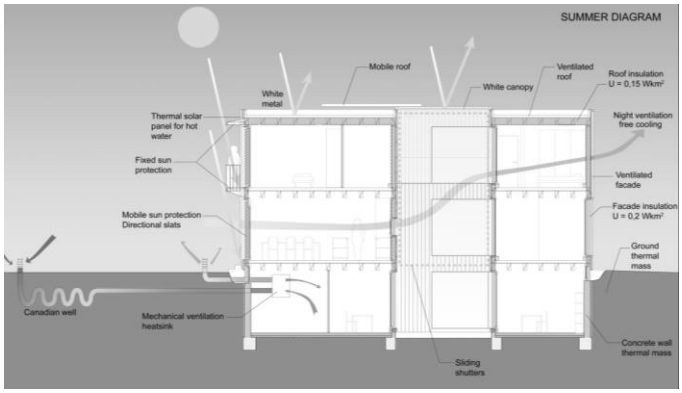

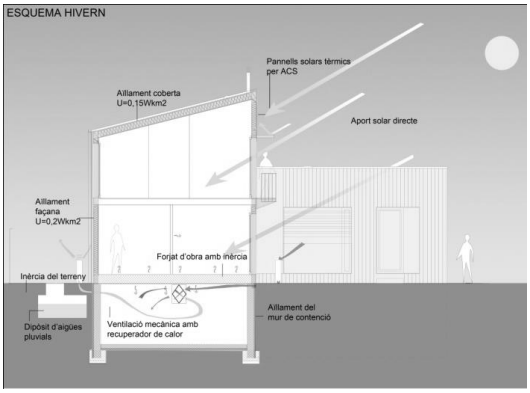

Figure 9: bioclimatic diagram arboretum house Figure 10: bioclimatic diagram magda house

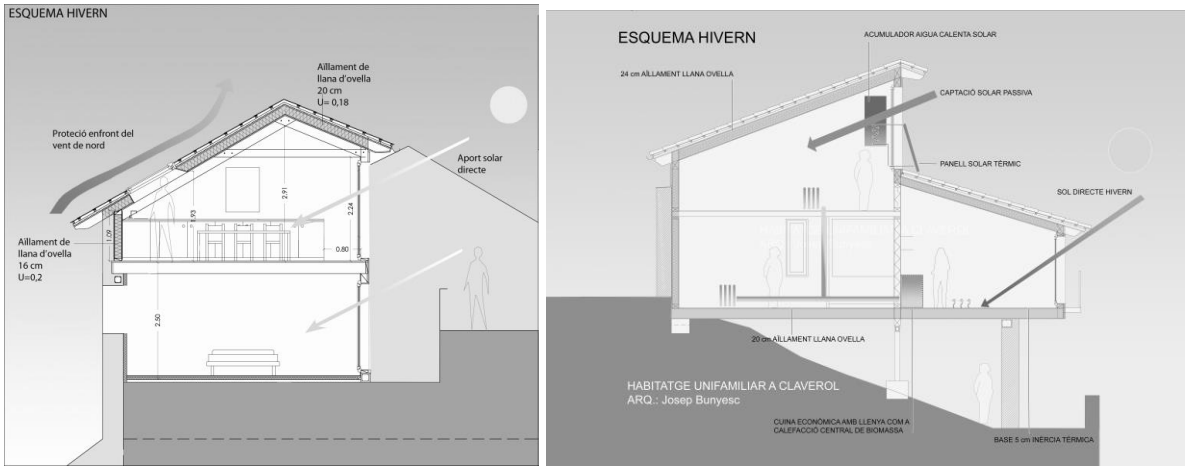

Figure 11: bioclimatic diagram Lleret house Figure 10: bioclimatic diagram Claverol house

They are buildings of great **energy efficiency** with an insulation level between 18 and 28cm, low-emission glass and good orientation. It's interesting to test the performance in summer, the light building, a low internal mass and a good insulation in the Mediterranean climate. The heating system in Magda's house is heat pomp and in the three others are biomass stoves.

This construction system based with the use of local wood and sheep's wool as insulation material of organic origin, 100% renewable, allows it to be a **sustainable** building with a very low embodied energy. The **balance of CO2** emissions throughout the building are **neutral**, because the timber stores proportionally the same amount of CO2 generated from construction activity and the use of other materials that are not wood.

With these examples we demonstrate that is possible a **drastic reduction of emissions from building energy savings**.

CONCLUSION

A light construction with a good insulation allows a large energy saving throughout the year: if we take the necessary precautions to ensure that the sun does not enter directly and with a free cooling, we can keep the temperature comfortable during a hot summer.

The calculations to foresee the building performance during the winter are relatively simple and they approach to reality. But, the calculations to foresee the building performance during the summer have to be dynamic and the results will vary depending on the user's attitude.

ENVELOPE EVOLUTION OF TALL BUILDINGS. AN ENERGY PERFORMANCE COMPARISON

Elettra Cattarin, Dario Marchiori, Fabio Peron, Ugo Mazzali

Department of design and planning in complex environments, IUAV University of Venice, Dorsoduro 2206 – 31023 Venice, Italy

ABSTRACT

Tall buildings have recently spread widely but since early Fifties some questions about their energy consumptions and impact on the environment were asked. The most important issues were about the introduction of new envelope system, namely Curtain Wall, and its influence on tall buildings conditioning energy consumption. New wide glass openings on the building envelope led to high conditioning loads with additional costs of the HVAC systems. The question asked by Henry Wright in 1955 was about the opportunity to invest in new envelope systems reducing opening area and improving thermal features of glass and opaque wall as well. After sixty years the aim of this article is to answer to this interesting question by means of recent energy simulation tools which can provide useful informations about energy consumptions and thermal balance of buildings. A comparison between different typologies of tall buildings has been performed considering the historical evolution of the envelope. One hundred of tall buildings has been analysed in order to identify three envelope classes: massive curtain wall, simple curtain wall and advanced curtain wall. These classes have been simulated with Energy Plus under the same climatic conditions with the aim to provide a more precise comparison of the envelope characteristics. Three climates were considered: temperate, cold and arid. Interesting considerations came out after the simulation analysis. The cooling and heating energy consumptions are mainly in dependence of openings area and internal loads which are usually very strong in office buildings. In temperate climates, the cooling load is more influenced than the heating load from glass opening area because of high solar gains which during winter are balanced from internal gains. This condition changes in cold climates in which heating load is more influenced by the envelope curtain wall and by the opening area because of very low ambient temperatures. In general the simulation analysis shows that the envelope evolution from massive to advanced curtain wall is characterized from a reduction of heating and cooling loads due to improvement in thermal properties of envelope components and airtightness as well.

Keywords: tall buildings, envelope systems, building energy simulation

INTRODUCTION

In general a “curtain wall” system is an external envelope curtain anchored to a structural frame and hence, as a matter of fact, without any kind of structural function and potentially light and transparent. This kind of envelope born officially in 1885 in Chicago when the steel frame made possible to relieve the façade from structural roles.

In 1955 an article titled “What next for the window wall?” [1] published by Henry Wright, made an energy cooling consumption impact analysis relating it with tall buildings design, focusing in particular on transparent envelope. The introduction of new envelope systems, namely Curtain Wall, and the large use of transparent surfaces, led as a matter of fact to a strong connection between transparent envelope and HVAC plants, forcing architects and engineers to spend time, money and building spaces in conditioning systems. Wright

wondered if resources spent for installation and management of HVAC plants could not be invested in improving opaque and transparent envelope performances also by means of minor transparent surfaces design with the consequence of more opaque curtain walls.

The aim of this work is to answer to the interesting question asked by H. Wright, considering tall building envelope evolution. One hundred of tall buildings has been analyzed and classified into 3 envelope classes further compared by means of the simulation tool DesignBuilder (EnergyPlus) in order to give a more accurate answer to the question asked 60 years ago.

METHOD

In order to simplify the historical evolution analysis of tall buildings, 100 envelopes have been classified into three classes. Analyzed buildings are distributed across about 130 years from 1885 and the classification has been done upon previous classification models proposed by [2,3]. The three classes are:

massive curtain wall (from 1885 – 1951)

The façade is usually made up of traditional building elements such as bricks, gypsum blocks, clay tiles and stone claddings. Moreover these opaque strips are reduced to minimum with the aim to let transparent surfaces fill the external curtain. Single glasses and clear glasses are installed on wood frames sometimes covered by aluminum for fire safety. HVAC plants are only for the heating period.

simple curtain wall (1951 – 1973)

The envelope loose completely any of his structural functions. Colored glass become diffuse also for energetic reasons and some examples of double pane windows are visible. HVAC plants are now working also in summer and air handling units for air treatment become visible.

advanced curtain wall (1973 – today)

Energetic crisis of 1973 lead also to new envelope systems much more efficient. Double and triple panes with gas are now available at accessible prices. From ’90 also low-e and spectral selective glasses are available.

A general summary for the average characteristics of tall building envelope during the analyzed historical period (1885-Today) is reported in Table 1.

Period	Curtain wall	Glass	Frame
1885-1951	Massive Curtain Wall	Single pane clear	Wood
1951-1973	Light Curtain Wall	Single pane clear and dark or Double pane clear and dark	Aluminium without thermal break
1973-Today	Advanced Curtain Wall	Double pane clear and dark. Low-e and solar control	Aluminium with thermal break

Table 1: Summary of tall buildings envelope during its historical evolution

After this analysis three types of envelopes were developed, one for each class, in order to make an energy performance comparison. The three envelopes have been simulated under the same climatic conditions with the simulation software. The opaque and transparent characteristics of the three envelopes are reported in the Table 2, together with infiltrations values according to [4]. Values of U-Value, SHGC and Visible transmittance of transparent envelope were obtained according to [5-7].

ENVELOPE COMPONENT	ENVELOPE CLASS 1	ENVELOPE CLASS 2	ENVELOPE CLASS 3
OPAQUE WALL	U-Value: 1.175 W/m^{2}K	U-Value: 0.854 W/m^{2}K	U-Value: 0.854 W/m^{2}K
WINDOW TYPE 1	SINGLE CLEAR (Sgl-Clr) Ug: 5.7 W/m^{2}K SHGC: 0.85 τ_v: 0.9	SINGLE CLEAR (Sgl-Clr) Ug: 5.7 W/m^{2}K SHGC: 0.85 τ_v: 0.9	DOUBLE LOW-E (Dbl-LowE) Ug: 2 W/m^{2}K SHGC: 0.67 τ_v: 0.81
WINDOW TYPE 2	-	DOUBLE CLEAR (Dbl-Clr) Ug: 2.8 W/m^{2}K SHGC: 0.75 τ_v: 0.81	DOUBLE SOLAR CONTROL (Dbl-SlrCntrl) Ug: 2 W/m^{2}K SHGC: 0.38 τ_v: 0.24
WINDOW TYPE 3	-	SINGLE DARK (Sgl-Drk) Ug: 5.7 W/m^{2}K SHGC: 0.44 τ_v: 0.35	-
WINDOW TYPE 4	-	DOUBLE DARK (Dbl-Drk) Ug: 2.8 W/m^{2}K SHGC: 0.43 τ_v: 0.35	-
FRAME	Hard wood U-Value: 2.2 W/m^{2}K	Aluminium U-Value: 3 W/m^{2}K	Aluminium U-Value: 2 W/m^{2}K
INFILTRATIONS	0.3 ach	0.2 ach	0.1 ach

Table 2: Thermophysical and infiltrations characteristics of envelope classes

Location	Geographical Coordinates	Cooling Degree Days	Heating Degree Days
New York	40° 74’ N 73° 98’ W	2.020	2.765
Dubai	25° 13’ N 55° 17’ E	6.254	24
Moscow	55° 45’ N 37° 37’ E	862	4.655

Table 3: Climatic features of the three locations used in the simulations

As far as climate conditions are concerned, three types of climate conditions have been considered: temperate, arid and cold according to [8]. The three associated cities were New York (USA), Dubai (UAE) e Moscow (Russia) respectively and the climatic features are reported in Table 3. The difference in Cooling and Heating degree days is remarkable between the three locations.

Finally, a standard floor has been considered for the simulations. This reference floor has a rectangular section and dimensions of 54x39m. Considered the maximum height of a "Tall building" fixed by the Council of Tall Building and Urban Habitat at 300m, the floor is located at 150m of height. A 2.7 m floor height has been considered and the position of the service core is central with 0.30m concrete walls. Heating setpoint and setback were 22°C and 12°C respectively, cooling setpoint and setback were 26°C and 28°C respectively. A daylight control is active and a reference level of 400lux has been imposed in the computer simulations. Light gains are 5 W/m^2 and equipment gains are 10 W/m^2; the total internal gains are 15 W/m^2. Three Window to Wall Ratio (WWR) options have been considered: 40%, 60% and 80%. Results will be compared in terms of ideal loads which means that no HVAC plant efficiency is considered.

RESULTS

Considering New York climate, annual ideal load for heating reduces passing from Envelope Class 1 to Envelope Class 3 and passing from 80% of WWR to 40% of WWR as shown in Figure 1A. Heating demands for Class 3 ranges from 6.3 kWh/m^2 year to 7.3 kWh/m^2 year. However, dark glasses typical of Class 2, lead to an increase of heating loads due to their very low values of SHGC and visible transmittance. Further, the improvement of the opaque envelope insulation and transparent envelope energetic performances during the 20th century led to a reduction in heating demand but also led to an increase in cooling demand because of high internal loads of office building with high insulation. This behavior is visible in figure 1B and its true for most of WWR conditions. Envelope class 3 cooling demand with double LowE glass and WWR equal to 80% is higher than all previous cases and reaches values of 65 kWh/m^2 year.

As far as Dubai is concerned, no heating ideal load is present and annual cooling load, visible in Figure 2, shows very low differences between envelope Class 1 and Class 3 with double LowE glass. However the double solar control glass reduces cooling loads up to 140 kWh/m^2 year, very close to Class 2 envelope with dark glass.

For the cold Moscow climate the same heating demand trend as New York can be pointed out as shown in figure 3A. In addition in the Moscow case, Class 2 single dark glass lead to an increase of heating demand up to 40% compared to heating demand of the same envelope class with a double dark glass. Class 3 with Double Low-E glass heating demand is the best case with ideal heating loads ranging from 21.7 kWh/m^2 year to 30.6 kWh/m^2 year. Very low values of cooling demand are calculated for the Moscow climate. In addition cooling demand, visible in figure 3B, is again related with colored glass which shows the lowest values of cooling demand among the three classes reaching values ranging from 10 kWh/m^2 year to 13 kWh/m^2 year.

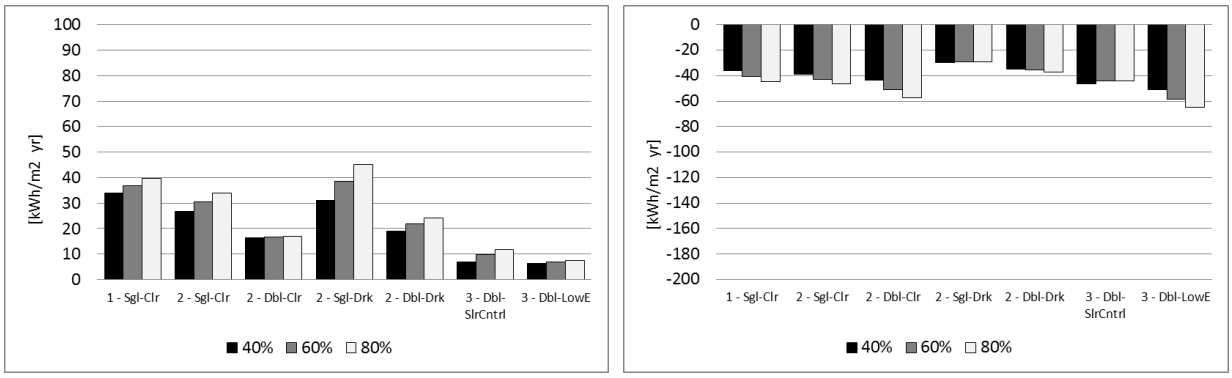

A) *B)*

Figure 1 – New York simulations. A) Annual heating; B) Annual cooling

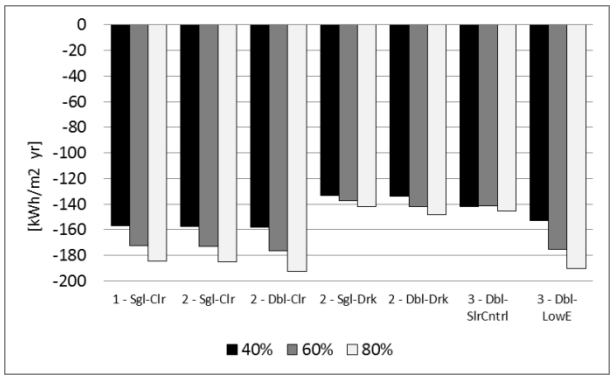

Figure 2 – Dubai simulations. Annual cooling

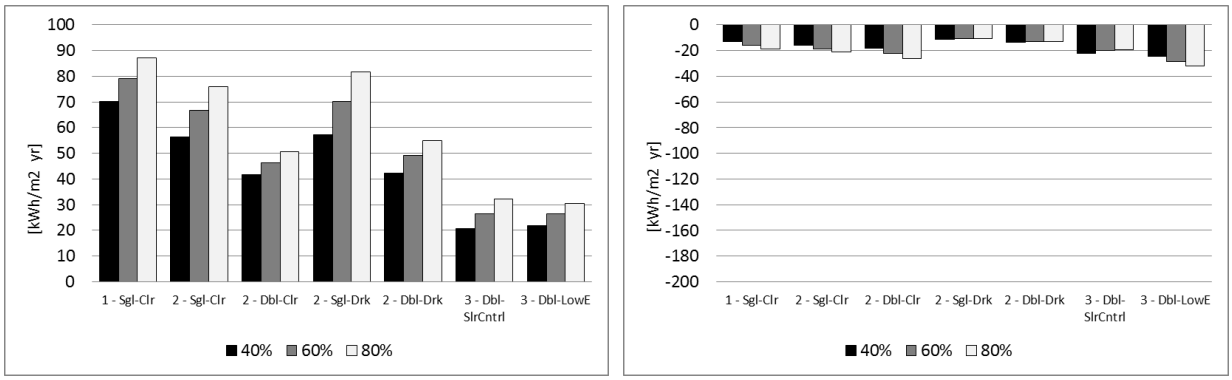

A) *B)*

Figure 3 – Moscow simulations. A) Annual heating; B) Annual cooling

DISCUSSION

Passing from envelope Class 1 to envelope class 3, a reduction in ideal heating loads is calculated at every latitude considered in the simulations. In addition passing from 40% WWR to 80% WWR heating load always increases. A different behavior is founded for single and double dark glass. At all latitudes this particular kind of glass, used from Fifties to Seventies, increases heating loads because of its very low values of SHGC and visible transmittance. In particular, single dark glass (U-Value = 5.7 W/m^2 K) increases heating loads of about 40%-70%, in New York and Moscow respectively, if compared to double dark glass which is characterized by a U-Value of 2.8 W/m^2 K, about a half of the single glass. From a general point of view the opposite behavior is founded for the summer period. Higher thermal

performances, i.e. U-Value of opaque and transparent, lead to higher cooling loads. The worst case is the double LowE glass of the envelope Class 3. However in the class 3 period from 1973, the double solar control glass is diffused and this is a good solution for controlling solar gains in summer, as a matter of fact this is the only solution comparable to dark glass in terms of cooling load reduction.

Concluding, the answer to the question asked by Henry Wright in 1955 is positive. A reduction in heating and cooling loads can be achieved by means of an accurate thermal design of the envelope. In particular, considering the heating period in two different climate conditions, a reduction in heating ideal loads up to 70% can be obtained improving envelope performances in terms of U-Value of opaque walls and U-Value, SHGC and visible transmittances of transparent envelope. A reduction in infiltrations, during envelope evolution, was considered as well. During summer, the improved performances of transparent and opaque envelope lead to an increase of ideal cooling demand in contrast to the heating period. This problem was partially solved by the introduction of solar control glass which helps, in arid climates, to reduce up to 15% the cooling demand compared to other solution of class 3. Finally, attention should be paid with LowE glasses in all simulated climates, because of their excellent performances in winter that turn into a problem in summer, namely very low transmittance and emissivity values. This work is not intended to be exhaustive and more work should be done on tall buildings energy behavior, namely considering for example fresh air flow rates and heat recover.

ACKNOWLEDGEMENTS

We gratefully thank prof. Dario Trabucco for valuable considerations and discussions on tall buildings.

REFERENCES

[1] H Wright, What next for window wall, Architectural Forum. (1955).

[2] P Oldfield, D Trabucco, A Wood. Five energy generations of tall buildings: an historical analysis of energy consumption in high-rise buildings, The Journal of Architecture. 14 (2009).

[3] R Banham. The architecture of the well-tempered environment, (1984).

[4] S Emmerich, A Persily, T McDowell. Impact of Infiltration on Heating and Cooling Loads in U.S. Office Buildings, (2005).

[5] AGC, Glass configurator,.

[6] UNI, UNI EN ISO 10077 - Prestazione termica di finestre, porte e chiusure oscuranti, (2007).

[7] UNI, UNI/TS 11300 - Part1: Evaluation of energy need for space heating and cooling, (2008).

[8] W Köppen, Köppen climate classification, (1936).

INTERNAL INSULATION WITH INTEGRATED RADIANT WALL PANELS: INNOVATIVE INNER INSULATION

G. Cavaglià; I. Caltabiano, C. Curti, M. Mangosio

Politecnico di Torino DIST, viale Mattioli 39, 10125 Torino – Italy

ABSTRACT

Recently in energy retrofit solutions for the built heritage an increasing interest towards the inner shell insulation is arising. In many cases these solutions borrow techniques and products from the most consolidated solutions of outer shell insulation, often revealing difficulties in execution and control of the results. Inner shell insulation is a developing and improving intervention field, both at a technical and productive level. In order to hold costs and duration down and to ensure the required level of energy performance, minimizing installation and setup errors, the research and the market are orienting towards integrated solutions. One of the most interesting features is the chance to refurbish inner spaces, whether with residential or tertiary function, without taking occupiers away from the building.

The aim of the paper is to describe the purpose, the methodology and the former outcomes of a research project, granted by E.U., aimed to experiment an innovative, integrated and active insulation system applied to the inner side of the building envelope. The I.I.I. (Innovative Inner Insulation) project is an industrial research and experimental development national project, which is conducted by three public research universities and three private technical partners selected between small and medium Italian enterprises. The research project allows to perform specific and systematized interventions in a flexible, integrated and active way according to a cross-curricular method. The system consists of a preassembled dry-laid panel, in which structure, thermal and acoustic insulation, heating plant and finish coat are integrated: it is concerned with processing techniques of semi-finished and stratified products, like those used in the refrigerated transport. Choosing a radiant wall heating gives the chance to integrate passive insulation with an active energy contribution at low temperature.

The paper aims to point out the operating procedures and the outcomes of the experimental phase. As a first step the technical solution has been tested in laboratory and later in two sample-rooms within a pilot construction site in Turin. The on-site experimentation includes the monitoring of the energy performances of the envelope and final checks through modelling. The final step is the definition and the production of the I.I.I. insulating and radiant system.

Keywords: built heritage, energy efficient retrofit, inner insulation

INTRODUCTION

The promotion of energy efficiency is listed as one of the seven priorities of the new national energy strategy, launched by the Italian Government in 2012 for the control of energy consumption [3]. The construction sector is far-back recognized both at European and italian level as one of the most responsible of the end-use energy consumption and of the emissions of greenhouse gases. The European Action Plan for Energy Efficiency 2011 highlighted the building sector as the most important field to focus the resources on. The national built heritage is not very efficient and requires different intervention programs, especially in relation to the variety of the Italian climate. The housing and tertiary building stock to refurbish is particularly interesting for its width. The incentives and the support actions of the national government aim to ride out the barriers to the introduction of measures for energy

retrofit, also strengthening minimum standards and regulations according to the EU directives. The achievement of the priority of energy efficiency, however, necessarily requires the support of the research and the development of technologies which consider the different features of the building to transform. According to the 2011 ENEA Report on the energy savings achieved by the recognition of tax deductions, only 2% of redevelopment interventions concerns the opaque envelope. This interventions have proved to be among the most effective to cut down on energy consumption. It is therefore a priority to focus the research on the envelope, because this kind of intervention offers the best opportunities in order to improve the energy efficiency of the building. The aim is to develop new technological solutions to test the integration between the external enclosing and the heating plant, moving the research towards the active building envelope.

In the last twenty years the range of solutions for the improvement of the insulation performances increased. Among these solutions the inner shell insulation stands out for many reasons, as independence from the façade and opportunity of energy refurbishment flat by flat. Also in internal insulation solutions the question of the thermal bridges requests to be carefully planned and not to be solved as a technical intervention without any perceptual interference with the outside. In order to hold cost and duration down and to ensure the required level of energy performance, minimizing installation and setup errors, the experimentation is orienting towards systematized solutions.

The aim of the paper is to describe the purpose, the methodology and the former outcomes of a research project, granted by Regione Piemonte on E.U. funds, aimed to experiment an innovative, integrated and active insulation system applied to the inner side of the building envelope. The methodological premise of this research is the firm belief that an efficient energy retrofit is not able to leave the knowledge of the built heritage out of consideration: it has always to get the technical and energetic potentialities of the existing envelope and enhance them in the technical solution.

The research project aims to develop the potentialities and minimize the disadvantages existing at present in the inner insulation, in order to guarantee: the continuity of the thermal insulation, the minimal amount of space, the reversibility of the intervention, the dimensional adaptability of the system, the accessibility and disassembling for maintenance. The hypothesis object of study and of experimentation is the integration between an inner insulation panel and a low temperature heating plant, providing an active contribution to the main heating system.

THE I.I.I. PROJECT

The main aim of the Innovative Inner Insulation (I.I.I.) project is to find effective solutions to improve the performances of existing buildings. The attention is focalized on the envelope of the buildings and its components. They are analyzed to verify the thermal performance they can guaranty and if it is necessary to add new elements to improve it. The final result underline the importance of the connections among the different parts to avoid the creation of thermal bridges. The I.I.I. project gives the chance to investigate different solutions to reduce thermal bridges. They can be available in the building sector or can be created transforming existing products and systems. In other cases solutions are founded looking at other kind of experiences in other fields such as the refrigerated transport.

The research is funded by the Second Annual Project entitled “Industrial research projects and/or experimental development” funded by Regione Piemonte through the Innovation Pole Polight. These funds are a concrete support given by the European Union, in the period 2007-2013, to promote economic and social cohesion among the local institutions. The rules set for

the funding of this and other types of projects coordinated by Polight push to involve different kind of actors to promote a profitable collaboration. The aim is to support the economic recovery of the Region through the promotion of research and the valorization of the potentialities of Small and Medium Enterprises (SME).

The project is coordinated by professor Gianfranco Cavaglià of the Polytechnic of Turin and involves three university departments and three SMEs. The partners are: Interuniversity Department of Regional and Urban Studies and Planning (DIST) and Department of Energy (DENERG) of Politecnico di Torino; Department of Science and Technological Innovation (DSIT) of Università degli Studi del Piemonte Orientale; Boschis S.p.A (company specializes in the manufacture and installation of wood finished components); NTS Group Srl (company specializes in the sale and installation of technical components for heating and cooling plants) and Cluster Srl (building company). The experiences of studies, analysis and design, collected over time, have been organized in the program of research. It starts from the design and implementation of new products and systems to arrive to verify their performances through a campaign of field experimentation.

METHODOLOGY

From a methodological viewpoint three different levels of successive in-depth analysis can be identified: the general structure of the research, the definition of the thermal insulation system, the setting up and the management of the experimental phase. The research has been structured according a polytechnic interdisciplinary method. The organization of the activities has correlated three different field: the Università and the Politecnico, the production field, the construction field. The cooperation of three different scientific areas was carried out by operating mainly along the border areas and the disciplinary overlaps in a spirit of mutual technology transfer. The synergy between university and small and medium enterprises has been finalized to give a concrete technical answer to the new requests of the building sector. The research was conducted according consecutive stages, arranged in a linear development and was supplemented by cross-checking intermediate stages of the investigation procedures through continuous feedback between the different actors. The general structure of the research involved the identification of a significant case study as field of application and verification of theoretical knowledge and of collection of experimental data.

The built heritage represents a complex reality and is mostly composed by prototypes: to define the ensemble of technical components as a system means working in the field of the complex systems. In this field every variations induced by the change of the boundary conditions must be provided, controlled and absorbed within the system itself.

In the setting up and the management of the experimental phase both deductive and inductive method have been applied. The research questions, the scope of data collection and the analysis techniques have been determined and defined throughout the theoretical framework setting. In the experimental phase in the field the early hypothesis have been verified. In the meantime by means of data analysis and the partners' contribution of experience the early settings have been fine-tuned, generalizing and systematizing what has been observed on site.

INSULATION SYSTEM WITH RADIANT PANELS

The insulation system created and tested during the I.I.I. project is based on the dry laying of a pre-assembled panel, which integrates structure, thermal and acoustic insulation, heating system and finish. It is developed as a reinterpretation of the techniques used in the field of refrigerated transport, associated with heating/cooling systems with radiant panels located below the flooring. The system designed in the research integrates the high performance of

insulating elements, that ensure a passive thermal protection, with low temperature radiating elements in a single component.

The project is based on the use of *insulating/radiant panels* installed vertically on the internal walls of buildings by a dry anchoring system with characteristics of reversibility and inspectability. The system is made of two types of panels: one integrates the insulation and the heating coil, the other, used as coating, can be pre-finished or finished on site. The *insulating/radiant panels* are made of a rigid insulation material coated with a thin plastic laminate glued on the front and back faces.

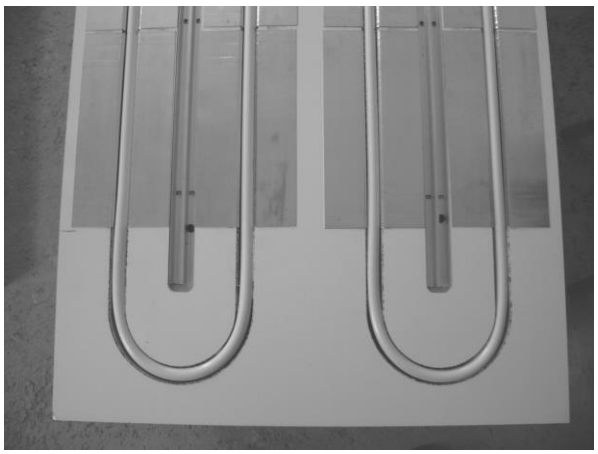

Figure 1: Insulating/radiant panels

Figure 2: Hydraulic connections of the pipes

The panel is milled with numerical control machines in order to produce the necessary space to place the heating coil and the aluminium structure useful for the anchorage of the covering panels. These fastening elements are connected to the panel with self-tapping screws that pass through the insulating layer and the back reinforcement and are anchored to the wooden horizontal slats which constitute one of the elements of fixing of the panels to the wall. In next phase aluminum bent sheets are glued on the front face of the panel, in correspondence of the vertical milling created to position the tubes, in order to make more homogeneous the distribution of heat provided by the radiating elements. After that the heating tubes are trapped within the milling prepared previously and in direct contact with the aluminum sheets. The *insulating/radiant panels* in now complete of all its components. It is ready to be hanged to the wall by a dry anchoring system made of horizontal wooden slats (one on the back of the panel and the other on the wall).

At the end of installation of the *insulating/radiant panels* it is possible to realize the hydraulic connections of the pipes and to assemble the coating panels with a reversible system. These panels can be made of different materials like: wood, aluminium, glass, ceramics. The choose must be done avoiding to compromise the passage of heat from the coils located in the radiant panel to the heated space. When the assembly process of the *insulating/radiant panels* is completed it is possible to finish the installation with the definition of all the elements of finish and the integration of the plants.

A CASE STUDY IN TURIN

During the I.I.I. project the insulating and heating system described has been realized and tested in a pilot case study.

The building company Cluster, one of the partner of the project, has made available as case study a part of one of their construction sites. It is an historic building in the center of Turin (Italy) which they are transforming in an hotel. The construction occupies an entire block and has a big internal court. It consists of several adjacent buildings with different formal values and structural characteristics. The largest and more valuable building, called "ex Casa Gramsci" is facing Piazza Carlo Emanuele II. In this part of the block have been chosen two rooms to measure the thermal performance of the envelope.

Figure 3: Insulating/radiant panels on the wall of the pilot room

Figure 4: Thermal performance monitoring phase of the pilot room

The experimental part of the I.I.I. project has been characterized by four phases: the design of all the components necessary to install the insulating and heating system in one of the two rooms used as sample, the construction of the components of the system, the implementation in the perimeter walls of the room and the monitoring of the thermal performance provided. Each of the these phases has given the chance to verify strengths and weaknesses of the insulation and heating system designed during the project. The design activity required the mediation among the different needs expressed by the partners involved. For example, the choice of the used semi-finished products has to be made according to their thermal, physical and mechanical characteristics. It has brought to select synthetic insulation products instead of those of natural originates previously chosen. During the construction of the different parts of the insulating and heating system there has been to solve the problem of chemical connection between some selected products. It has requested several tests with different products before it was possible to get satisfactory results.

The installation of the *insulating/radiant panels* have showed how each step can hide accidents which must be solved. It confirms the fundamental and useful contribution that only direct experience in the field can offer to a research. In some cases it was necessary to rethink the solutions in order to simplify the process of assembly or make more efficient the whole system. An example has been given by the need to change the hydraulic connection of the panels from the series to the parallel system which ensured a more uniform heating of the coils.

The thermal monitoring of the dynamic operation of the system has allowed to record an innumerable amount of useful data to verify, even through the subsequent modeling, the

impact of several possible choices on its performances, such as: the thicknesses of the different layers of the panels, the geometrical position of their elements (distances, directions,...), the different solutions for the connections among the parts.

CONCLUSIONS

The I.I.I. project has given the chance to develop an interesting and useful research. The main objective has been the creation of a new system to reduce the impact of thermal bridge in the constructions. The use of the *insulating/radiant panels* on the vertical part of the envelope of the buildings has showed different strong points: the presence of an active energy contribution due to the integration of a radiant heating plant, the ability to exercise constant control on the stratigraphy of the isolation system, the systematization of the connection joints and the opportunity to transform the building in a targeted way (for example in the case of the retrofit of a single flat).

A relevant aspect of the system is that the assembly phases of the components of the *insulating/radiant panels* can be performed in a laboratory to minimize the activities to be done in the spaces in which the system is installed. It gives the chance to reduce the interferences with the normal activities carried out by the users of the spaces and makes this system particularly suitable in the case of pre-existing structures. Furthermore, the experience of the I.I.I. project has proved the primary role of the fieldwork in the path towards the fine-tuning of the insulation system. The case study can be considered as an occasion to define critical situations and to work out solutions selected between possible alternatives. The continuous feedback between different partners in the fieldwork allowed the developed of new expertises thanks to different comparisons: the design phase (meetings), the production phase (surveys in laboratory or in the partners' factory) and the layout phase (surveys on site).

Last but not least, the I.I.I. project has represented an opportunity to promote professional partnerships, to subsidize the working world and to confirm the practical utility of the experimentation in the field.

ACKNOWLEDGEMENTS

The research described in the paper has been funded by Regione Piemonte on European Regional Development Fund (ERDF). The project is part of the initiatives promoted by the Innovation Pole Polight.

Six partners have collaborate to the I.I.I. project: Department DIST (Politecnico di Torino), Department DENERG (Politecnico di Torino), Department DSIT (Università degli Studi del Piemonte Orientale), Boschis S.p.A, NTS Group Srl, Cluster Srl.

REFERENCES

1. Settis, S.: *Paesaggio Costituzione cemento. La battaglia per l'ambiente contro il degrado civile*. Einaudi, Torino, 2010.

2. Fasano G.: *L'efficienza energetica nel settore civile*. ENEA, luglio 2011.

3. Ministero per lo Sviluppo economico, *Strategia Energetica Nazionale: per un'energia più competitiva e sostenibile*. Ottobre 2012

IMPROVING THERMAL PERFORMANCE OF RAMMED EARTH WALLS USING EXPANDED GRANULATED CORK

J.J. Correia-da-Silva[1]; J. B. Pereira[1]
1: *University of Évora, Pólo da Mitra, Apartado 94, 7002-554 Évora, Portugal*

ABSTRACT

The use of soil construction dates back to the beginning of our civilization. In the South of Portugal there is still a large number of buildings with rammed earth walls, but this technology has been falling into disuse since the middle of last century. The earth construction is highly sustainable since earth is a local material and is 100% reusable. The buildings with rammed earth walls have a high thermal inertia which, given the climate characteristics Portugal, enjoys its thermal behavior. However, it is desirable that the thermal conductivity of the rammed earth were lower. Environmental concerns related to energy consumption associated with comfort in housing and construction, transportation and application of materials used in construction, has led us to seek new solutions in building typologies on earth.

Considering these aspects and aiming to improve the energy efficiency in buildings with rammed earth walls, this paper presents the results of tests performed in laboratory to characterize phisical properties of several compositions containing soil and expanded granulated cork.

Compositions were considered soil and expanded granulated cork having the following percentages of expanded granulated cork, 0%, 10%, 15%, 20% and 25%. In order to characterize the different compositions from the point of view of mechanical and thermal performance, cubes were produced with 10 centimeters edge and assayed in order to calculate its compression resistance and its thermal conductivity. The results showed that the use of this type of building typologies on earth with the incorporation of expanded granulated cork allows to increase your performance by making it possible to adapt this typology needs of today, including the demands of the Portuguese legislation. The results of this research can be applied, with the appropriate adaptations, both in buildings in rammed earth and in buildings in adobe.

Keywords: rammed earth walls, energy efficiency, expanded granulated cork.

INTRODUCTION

In Portugal, earth construction, and in particular building incorporating rammed earth or *taipa* walls is common in the Alentejo and Algarve regions. However, the use of this construction technique has gradually fallen into disuse, especially since the mid-20th century. As masters of the art disappear, we risk losing a fund of specialised knowledge required for selecting soil, determining optimum moisture content and implementing the technique itself: the placement and compression of the earth between wooden frames.

Portuguese regulations governing the thermal performance of buildings (RCCTE – Regulation of Characteristics of Thermal Behaviour of Buildings, the provisions of which are contained in statute law: Decreto-Lei no. 80/2006 [1]) set out requirements regarding limits on the nominal consumption of energy during the cool season that are not easy to comply with when using the rammed earth technique.

The aim of this paper is to provide a contribution towards the improvement of the thermal performance of rammed-earth walls by examining techniques for reducing thermal conductivity. This study involved the use of granulated cork, which was mixed in different proportions with soil with a number of different particle sizes in order to gauge how thermal conductivity could be reduced without decreasing too much the compressive strength of the mixture.

GEOTECHNICAL AND PHYSICAL CHARACTERIZATION

In order to determine the suitability of soil for rammed-earth construction, the physical and geotechnical properties of soil were determined and the soil characterized in accordance with Portuguese standards and LNEC - National Civil Engineering Laboratory specifications, as well as the information contained in the work entitled "*Construção em terra*" (Earth Buildings) [2].

Water content in soil was determined at the collection site, as well as organic matter content, particle size, and liquidity and consistency ranges; the Proctor test was carried out in order to determine optimum water content.

Geotechnical Soil Properties

We can use Feret's triangle, which takes into account the proportions of sand, silt and clay in soil in order to determine a point in the triangle which characterises the soil. An assessment can be made as to whether soil is suitable for earth building, in the present case using rammed earth, according to whether the point lies within a predefined area [3], as shown in Figure 1.

In this study, the soil contained 58% gravel, 18% sand, 14% silt and 10% clay. Ignoring the gravel content and considering the remaining 42% of sand, silt and clay content as 100% of content, we have 18% sand corresponding to 43% of content, 14% silt corresponding to 33% of content and 10% clay corresponding to 24% of content in the triangle (Figure 1).

These percentages enable a soil intersection point to be found, which in this case falls within the predefined area for rammed earth [3], as can be seen in Figure 1.

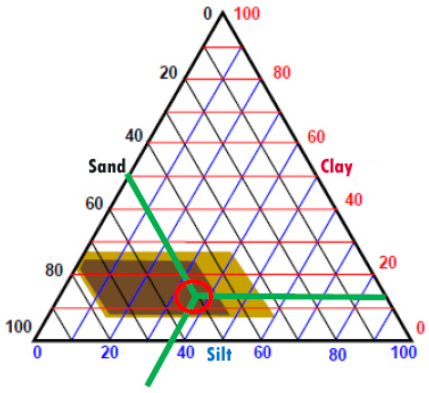

Figure 1 – Feret's Triangle: zone for the use of adobe bricks (dark area) and zone for the use of rammed earth (light area, which includes the dark area)

Mechanical Soil Properties (Compressive Strength)

As regards tests for the uni-axial compressive strength of samples, standard ASTM D 1633 - 00 was applied so that the periodicity used in tests would be adjusted for the time

intervals between readings. Tests were performed after 21 days and after 28 days in order to gauge whether there were significant changes in strength. An increase in mechanical strength was shown to have occurred.

In this paper, only the results of the tests performed after 28 days are presented, which are compared with samples of 100% soil (rammed earth) and soil with various mixtures.

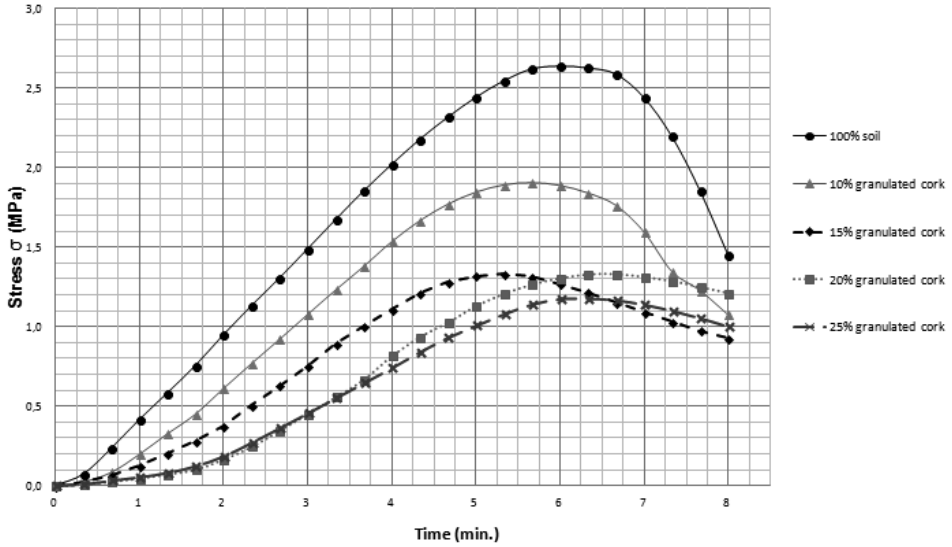

Figure 2 - Uni-axial compression tests on samples of soil with granulated expanded cork 2-10

For samples with a mixture of soil and granulated cork, as the percentage of the latter added to the former increased, the strength of the mixture decreased, and it also decreased with increasing particle size from 3-5 to 2-10 (Figures 2 and 3).

According to New Zealand standard NZS 4297 [4], the minimum value of compressive strength that rammed earth should present is 0.50 MPa. According to the Spanish reference document [5], the average resistance of a no stabilized rammed earth wall should have as compressive strength the value of 1.2 MPa.

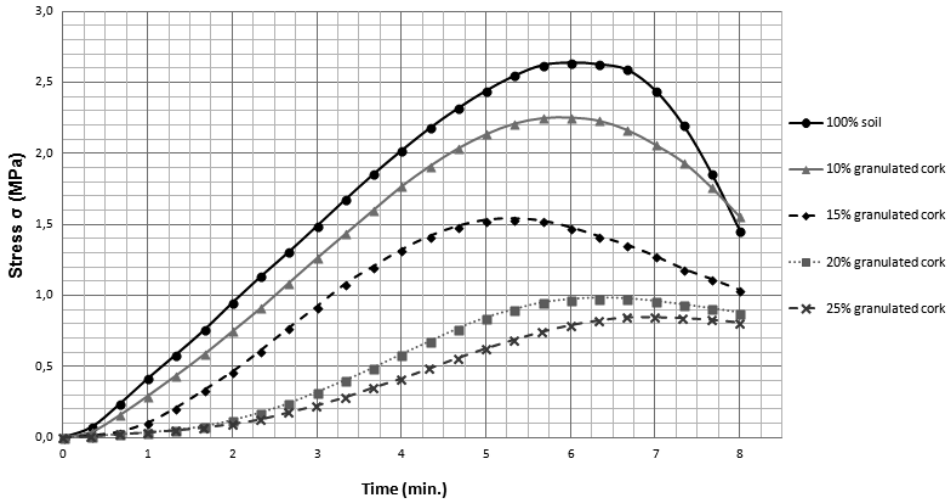

Figure 3 – Uni-axial strength tests for samples of soil with granulated expanded cork 3-5

Thermal Behaviour

The thermal conductivity (λ) of a material is a property, which is essential for the characterization of its thermal behaviour and can be measured *in situ* or in the laboratory. Thermal conductivity was measured using an ISOMET 2104 device, made by Applied Precision. The ISOMET 2104 device allows for the use of various types of probes with different reading ranges. All readings were taken using an API 210412 surface thermal conductivity probe. Probes can be recalibrated using a standard method and each thermal conductivity measurement takes approximately 15 minutes to complete. Readings are stored in the device memory and can be transferred to a computer by means of an RS 232 lead. The cylindrical surface probe used for gauging the thermal conductivity of samples had a diameter of 60 mm (Figure 5), which means that the samples had to be bigger than this.

Thermal conductivity was measured using identical samples to those used to determine compressive strength. Thermal conductivity measurements were taken on the three sides of sample cubes, which corresponded to one of three axes: X, Y and Z. Readings recorded on Side A correspond to the Y axis (Figures 4 and 5). This is the side on which readings are taken perpendicular to compression layers. Sides B and C correspond to the X and Z axes respectively, as shown in Figure 4, and are both perpendicular to compression layers. Of the sides perpendicular to the compression layers, the most regular sides were defined as B because they presented fewer cavities. Three readings were taken for each side of samples.

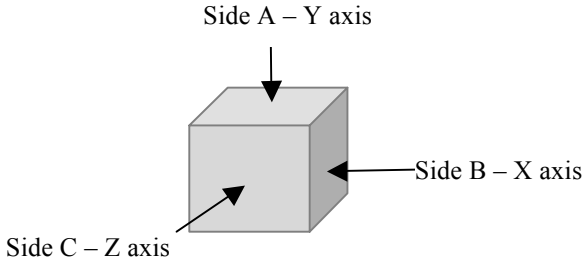

Figure 4 – Configuration of sample readings

Figure 5 – Determining conductibility on the different sides of a sample.

As thermal conductivity may vary from sample to sample of the same material (due to heterogeneity, degree of compaction, particle size) several readings were taken for the various soil samples. Thus, in addition to physical and geological characterization, it was felt that there was a need for characterizing the thermal conductivity of soil samples, which enables a reference value for thermal conductivity to be established for samples where granulated expanded cork was added to soil. On the basis of the various

measurements, an average thermal conductivity value – X axis – of 1.08 W/m.°C was obtained, with a standard deviation of 0.11, as can be seen in Table 1.

In a rammed-earth wall, thermal flux occurs horizontally, hence perpendicularly to the direction in which compression occurs. Thus, the values of thermal conductivity obtained for the X or Z axes that are perpendicular to the direction of compression must be considered. Thermal conductivity values obtained for these two axes are analogous, thus X axis values were considered as this axis corresponds to B sides, which provide a greater level of reliability as they present fewer heterogeneities.

Values recorded for the thermal conductivity of soil samples with added granulated cork 2-10 are presented. Thermal conductivity tests were performed on samples, as was done previously with samples comprising 100% soil (rammed earth) and soil with added expanded cork, corresponding to the three axes: X, Y and Z. The conclusion was drawn that the findings that should be considered are those which relate to the X axis. X axis measurements are similar to the direction of the thermal flux of a wall.

Samples	λ (W/m.ºC)
100% Soil	1.08 ± 0.11
Soil + 10 % Expanded Cork 2-10	0.91 ± 0.11
Soil + 15 % Expanded Cork 2-10	0.73 ± 0.14
Soil + 20 % Expanded Cork 2-10	0.66 ± 0.15
Soil + 25 % Expanded Cork 2-10	0.56 ± 0.16

Table 1 - Thermal conductivity for samples of soil and soil with granulated expanded cork 2-10: X axis (mean values)

For samples of soil with 25% granulated expanded cork 2-10, a decrease in thermal conductivity to 0.56 W/m.ºC was recorded, with a standard deviation of 0.15.

Samples	λ (W/m.ºC)
100% Soil	1.08 ± 0.11
Soil + 10% Expanded Cork 3-5	1.04 ± 0.12
Soil + 15% Expanded Cork 3-5	0.83 ± 0.11
Soil + 20% Expanded Cork 3-5	0.66 ± 0.15
Soil + 25% Expanded Cork 3-5	0.44 ± 0.13

Table 2 - Thermal conductivity for samples of soil and soil with granulated expanded cork 3-5: X axis (mean values).

CONCLUSION

According to the regulations governing the thermal behaviour of buildings (*RCCTE - Regulation of Characteristics of Thermal Behaviour of Buildings,* Decreto-Lei no. 80/2006), the thermal transfer coefficient of the opaque and vertical elements of the exterior envelope in Zone I_1 is 0.70 W/m^2.°C [6]. Let us compare this with the values obtained as a result of the tests carried out. In order to make this comparison let us determine the

thermal transfer coefficient (U) of a rammed earth wall with a thickness of 0.60 m covered with plaster with a thickness of 0.02 m on the inside and outside.

It should be noted that, as a result of the tests performed, a value was obtained for the thermal conductivity of the soil sample equal to 1.08 W/m.°C (Tables 1 and 2). In accordance with the methodology described by Santos and Matias [6], for the rammed-earth wall consisting only of soil and plaster the value U = 1.29 W/m^2.°C was obtained. In this case, the value is below that set by the above-mentioned building regulations, as the maximum thermal transfer coefficient for Climate Zone I_1 in exterior vertical elements which is U = 1.8 W/m^2.°C, but it is above the reference value U = 0.70 W/m^2.°C.

With a mixture of soil and 25% granulated expanded cork 2-10, the following coefficient of thermal transfer was obtained: U=0.77 W/m^2.°C, which is similar to the reference value for the vertical elements in Climate Zone I_1 (nearly the South of Portugal [1].

With a mixture of soil and 25% granulated expanded cork 3-5, the following was obtained: λ=0.44 W/m.°C (Table 2), and the following thermal coefficient was obtained: U=0.63 W/m^2.°C, which is below the reference level of U=0.70 W/m^2.°C.

With regard to compressive strength, if the provisions of standard NZS 4297 [4] were to be applied, all the solutions tested would show a satisfactory level of compressive strength, which means soil with 25% granulated cork 3-5, with a thermal transfer coefficient of U = 0.63 W/m^2.°C, is the best option.

However, more stringent levels are indicated by Guerrero and Delgado [5], so it is best to regard 1.2 MPa as the minimum value for compressive strength. This corresponds to rammed earth which is non-stabilized with average strength. It should be noted that not all samples tested satisfy this condition. In view of this constraint, of all the samples tested the one which produced the lowest value for the thermal transfer coefficient of the rammed-earth wall while complying with the minimum value deemed acceptable for compressive strength is that containing soil with 20% cork granulated cork 2-10, for which U=0.89 W/m^2.°C was obtained, and a compressive strength of 1.33 MPa.

Comparing this with the wall consisting of soil without cork, it was found that the thermal transfer coefficient of the option consisting of soil with granulated cork is equal to 69% of the thermal transfer coefficient of the rammed earth wall without cork, thus, a substantial reduction was achieved.

REFERENCES

1. Decreto-Lei nº 80/2006. *Regulamento das Características de Comportamento Térmico dos Edifícios (RCCTE).* Lisboa: Diário da República, I Série A, nº 67, 2006.

2. Torgal, F.P., Eires, R.M., e Jalali, S. *Construção em terra.* Guimarães: Universidade do Minho, 2009.

3. Moran, E. *Uso del terrocemento en la construcción de vivienda de bajo costo.* Quito: Facultad de Ingeniería Civil - Pontificia Universidad Católica del Ecuador, 1984.

4. NZS4297. *Engineering Design of Earth Building.* Nova Zelândia: Earth Building Association of New Zealand, 1998.

5. Delgado, M.C.J., e Guerrero, I.C. *Earth building in Spain.* Departamento de Construcción y Vias Rurales - Escuela Técnica Superior de Ingenieros Agrónomos: Universidad Politécnica de Madrid, 2006.

6. Santos, C.A.P., e Matias, L. *ITE50 - Coeficientes de transmissão térmica de elementos da envolvente dos edifícios.* Lisboa: LNEC, 2006.

ENERGY RENEWAL OF INA-CASA HERITAGE RELEVANCE OF MOISTURE TRANSPORT

Edoardo Currà[1], Emanuele Habib[2]*

[1]*Dip. di Ingegneria Civile, Edile e Ambientale - Via Eudossiana 18, 00184 Rome, Italy*
[2]*Dip. di Ingegneria Astronautica, Elettrica ed Energetica - Via Eudossiana 18, 00184 Rome, Italy*
** Corresponding author, emanuele.habib@uniroma1.it, tel +39 06 44 585 349*

ABSTRACT

The energy renewal of the INA-Casa Program buildings is guided by the observations of many values expressed about their construction, architectural typology and urban fabric morphology. A study of the energy renewal approaches has been carried out regarding both the way to improve insulation and the heat and moisture transfer analysis approaches needed for the right efficiency check. The study has been carried out on the buildings of the first seven-years period of the Program, which already espoused the framed structure with masonry infill walls and are characterized by a specific quality in the constructive techniques with regards to architecture and building typologies. The analysis of the buildings has confirmed the high thermal transmittance. As is well known, any change of the thermal behavior of a wall modifies the vapor saturation pressure within. This is usually accounted for through the check for interstitial condensation, done together with that of thermal transmittance. In this paper the results of a screening of the possible energy renewal interventions on a significant INA-Casa building, depicting which approaches need a complete check of both effective insulation and moisture transfer and which are not recommended as, even though they could be effective by the thermal point of view, they lead almost surely to interstitial condensation. The coupled vapor pressure and temperature fields are studied numerically, by solving the linear partial differential equations through finite elements method.

Keywords: Energy renewal, Masonry, Interstitial condensation, Thermal bridges, Building renovation

INTRODUCTION

The distinctive features of INA-Casa architecture consist in their homogeneity and specific quality of the constructive techniques with regards to building typologies and architectural quality. A study of the energy renewal approaches has been carried out regarding both the way to improve insulation and the heat and moisture transfer analysis approaches needed for the right efficiency check. It is well known that the housing heritage was formed thanks to the main legislative instrument at the base of the reconstruction in Italy after World War II called "Piano per l'Incremento e l'Occupazione Operaia" (Plan for Growth and Employment Workers), Act n° 43/02-28-1949, known as *Piano Fanfani*, from the name of his proposer, or Piano INA-Casa, named agency established for the management. The built heritage according to the instructions and the means placed at the disposal of the INA-Casa was likely to influence in a decisive way on the configuration of the Italian city. Thanks to the plan they arose 340,000 housing, more than 1,000,000 rooms, designed over two septennia (1949-56,1957-63) by a whole generation of architects and engineers. In this heritage we may encounter some common features which fully justify the definition of appropriate tools of analysis of the construction. The homogeneity of the construction is mainly due to the strong coordination exercised by the INA-Casa agency in the proposition of appropriate modalities to address the issues related to reconstruction, thanks to effective control and to special regulations[1]published in four consecutive dossiers.

[1] The first two regulations dossier are particularly interesting. These includes a formal call to create a list of technicians, architects or engineers, to assign the design task. The compilation of these two were assigned to Mario De Renzi, Cesare Ligini and Mario Ridolfi (Paolo Nicoloso, 2001).

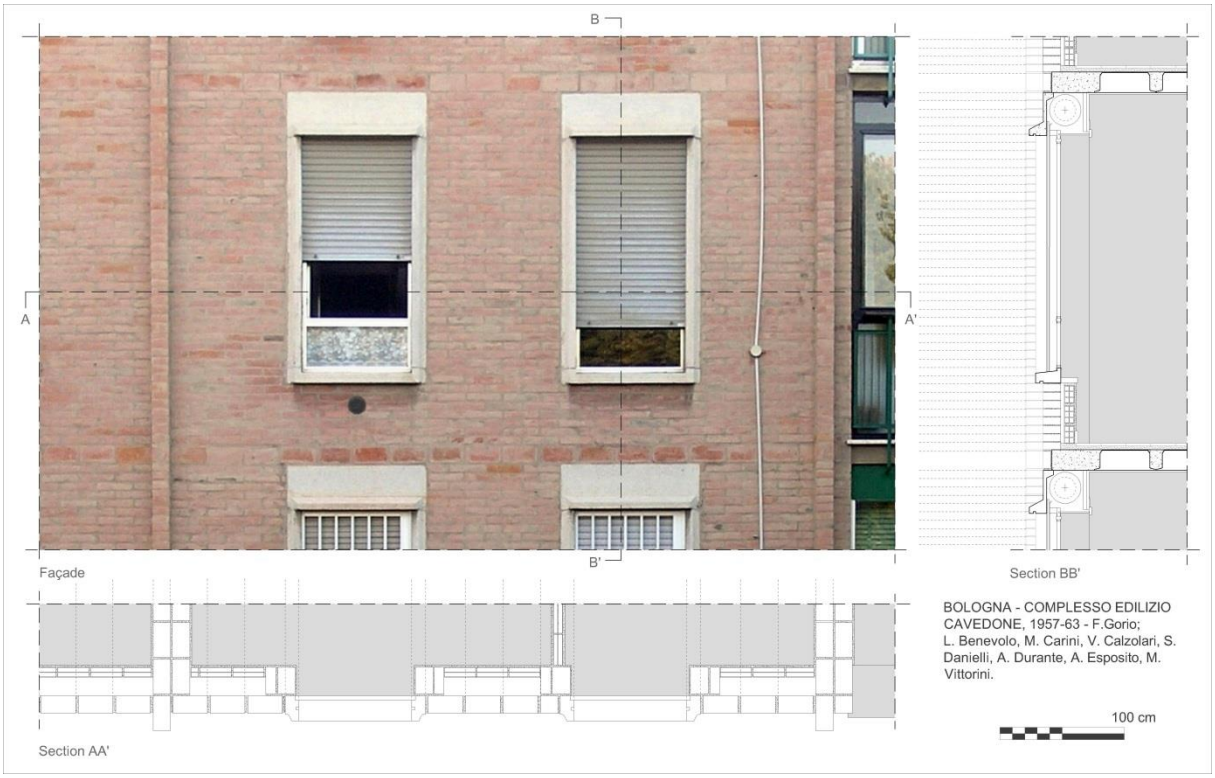

Figure 1: Constructive survey of a building in Cavedone, Bologna.

The apartment, the building type, the neighborhood and the construction have been designed with the strong awareness that building was the main instrument for realizing the essence of living."*The house will have to contribute to the formation of urban environment - taking into account the spiritual and material needs of man,* the real man and not an abstract person.*[…] They will, therefore, the conditions of the soil, the sunshine, the landscape, the vegetation, the existing environment, the sense of color to suggest the planimetric composition so that the inhabitants of the new urban centers have the impression that in them there is something spontaneous, genuine, inextricably fused with the place on which they arise".*[2] It therefore agrees with the proposition of the existence of a "Architecture INA-Casa" by the peculiar characteristics[3]. The INA-Casa heritage on the one hand is so broad as to include a remarkable variety of constructive solutions, on the other hand, thanks to the dirigisme underlying the whole program, we can find in most of works an homogeneity in construction features. Indeed alongside some notable episodes from the great experimental connotation there is a majority of built that responds to the instructions of economy, in techniques and resources, given by the "Gestione INA-Casa" (INA-Casa management board). Particularly right in relation to the realization of the buildings envelope, this is closely connected with the requirements of economy and feasibility in order to encourage the maximum use of unskilled workforce. In terms of materials low houses of the first septennium are almost all made in supporting partitions of brick masonry or split blocks of tuff and brick rows alternated (the masonry called *allaromana*), a minimum thickness of two heads - 28 cm – for the bricks, and 40 cm for the stones. In higher buildings (more than 5 floors) the bearing structure of reinforced concrete is plugged with hollow masonry. For this reason the architecture of the septennium 1949-1956 has a diffuse character of technological backwardness, where only some of the works are actually a reflection of technological progress taking place in the country, while the place of constructive experimentation remains linked to the traditional walls.

[2]"*La casa dovrà contribuire alla formazione dell'ambiente urbano – tenendo presente i bisogni spirituali e materiali dell'uomo,* dell'uomo reale e non di un essere astratto*; […]Saranno dunque le condizioni del terreno, il soleggiamento, il paesaggio, la vegetazione, l'ambiente preesistente, il senso del colore a suggerire la composizione planimetrica affinché gli abitanti dei nuovi nuclei urbani abbiano l'impressione che in essi sia qualcosa di spontaneo, di genuino, di indissolubilmente fuso con il luogo sul quale sorgono"*(PIOO, 1949).
[3] (Poretti S., 2002)

Figure 2: Constructive survey of the building called boomerang in Tuscolano II, Rome

DISTINCTIVE FEATURES OF INA-CASA HERITAGE BUILDINGS

During the second seven years the skeleton of reinforced concrete is mainly adopted even in low houses next to the stronger presence of prefabricated works or parts, and the permanence of masonry. There are significant episodes, such as the project for the district Cavedonein Bologna[4], where the evolution is pursued in the way of rationalization of the wall construction in collaboration with the horizontal elements in reinforced concrete, but are more frequent cases, such as that of Barco in Ferrara[5] or Tuscolano II or Torre Spaccata in Rome, where the infill panels of bricks and the reinforced concrete skeleton, compared with sincerity in the tables[6]. Thus, in framed structures, the building enclosure is made of layers principally aimed to its required quality of lightness. From this it derives therefore a way of constructing based on the hollow walls, where a large cavity is situated between two panels of solid or hollow brick. The nature of the architectural complex INA-Casa and to the large formal value which often makes it impossible to operate with the usual energy renovation based on the thermal coating (outside insulation), especially as throughout the program it has been very prevalent a constructive solution of facades with infill walls or frames, coated or made with brick face view, which is certainly not compatible with that remedial action: in fact, many projects are based on the treatment of facades with infill walls or frames coated or made with brick face view.

This category includes a number of remarkable works and this is amply justified by the formal research during this period. This architectural approach has ennobled, presenting it directly on the façade, the structure of reinforced concrete, and in the name of formal / constructive sincerity has coined the chromatic and material combination of reinforced concrete and exposed bricks. The alternative approach is inside thermal insulation that presents considerable performance issues regarding heat and vapor migration (relevant to ensure that no interstitial condensation occurs).

[4]Cavedone, Bologna. 1957-1960. Design staff coordinator: Federico Gorio. Houses: 968, rooms: 5164. The area is located in the south-est of the town. The context was completely rural and the original master plan would be partially realized. The design is based on the iteration of rectangular court which, sometimes, include the collective services (Currà, 2006).

[5] The district of Barco was coordinated by Pier Luigi Giordani, with Piero Maria Lugli and Alberto Legnani.

[6]But the reinforced concrete elements are usually protected with a coat of plaster. This is right the case of Tuscolano II (Fig. 2) and the plaster protection made possible the optimal state of conservation of the structures.

MATHEMATICAL FORMULATION

Mathematical models of heat transfer and vapor migration through solids are formally identical:

$$\nabla^2 T = 0 \tag{1}$$

$$\nabla^2 p = 0 \tag{2}$$

where T is temperature while p is vapor pressure, thus allowing to use a single solution algorithm for both. Nonetheless, each building material has its thermal conductivity and vapor permeability that are not related each other. Moreover, air-filled cavities behave differently as there is no vapor migration effect similar to radiant heat transfer. The equations are easily solved in the usual one-dimensional hypothesis, where heat transfer in cavities is calculated through the superposition of convection and radiation heat transfer. Where a two-dimensional solution is needed, as at thermal bridges, the partial differential equations could be solved through a finite elements formulation. As long as the cavities are small enough so that there is no boundary layer (Rayleigh numbers smaller than 10^6), a good approximation could be obtained by assuming for air an equivalent thermal conductivity that depends both on convective and radiation heat transfer (dos Santos, 2009). The solution process is iterative, but converges very quickly (usually the third iteration is the final).

Figs. 1 and 2 represent the horizontal and vertical sections of the enclosure of buildings of two significant complexes of the first and second septennium, ideal to illustrate the complexity of the phenomenon. The building of Cavedone (Fig. 1) shows a particular case masonry building where the envelope wall has a cavity. In fact, the constructive solution of Federico Gorio is based on the disposition of all load-bearing walls transversely to the building and consequently the masonry facade appears to have a secondary role in bracing and closing of the mesh, compared with the main transverse walls, upon which all loads horizontal of the floors and roof weigh. So he can thin the wall of the façade, which is composed by only one layer of bricks. Behind the bricks he disposes a cavity and then one layer of hollow bricks.

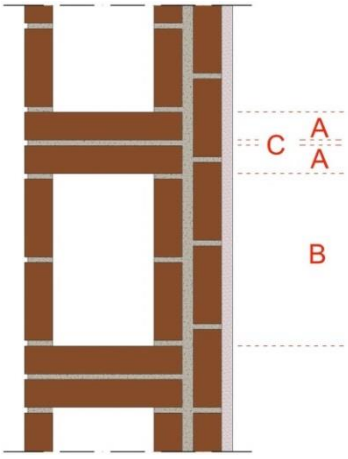

Figure 3 : sketch of the wall and one-dimensional approximations

	Thermal conductivity [W/m K]	Vapor diffusion resistance factor
air (actual)	0,025	1
mortar	0,47	17
brick	0,7	9
plaster	0,9	24
concrete	1,66	148
insulatingplaster	0,056	9
polyurethane	0,028	129
plasterboard	0,21	8
concrete tiles	1,66	148

This makes the solution consistent with the method of concrete frame buildings and useful to our illustration. The main characteristic of the second building is given by the planimetric inclination of the concrete skeleton with respect to the body of the building (called the “boomerang” for this inclination). So the perimetral panels, that close the mesh, are inserted always obliquely and the envelope has numerous thermal bridges. Moreover, the analysis of its composition shows a complex structure made of bricks posed in three different ways with long almost square cavities. The one-dimensional study of walls behavior could be done along three simplified sections: A) almost only bricks, B) through the cavity, C) through mortar and brick. The one-dimensional solution for each section is sketched in Fig. 4 with 0°C outside temperature and 20°C inside (design conditions in Rome). The convective heat transfer through the cavity has been calculated iteratively using the correlating equation given in (Corcione 2010), while radiation heat transfer is calculated through

Hottel's method for view factors with a 0.9 emissivity. Vapor pressure as long as saturation pressure are shown in Fig. 5 for sections B and C as A section is between these, assuming 70% relative humidity inside and outside. No interstitial condensation occurs, even though the outer side of the cavity is critical.

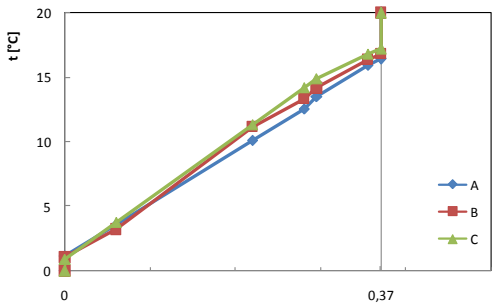

Figure 4: temperature distribution

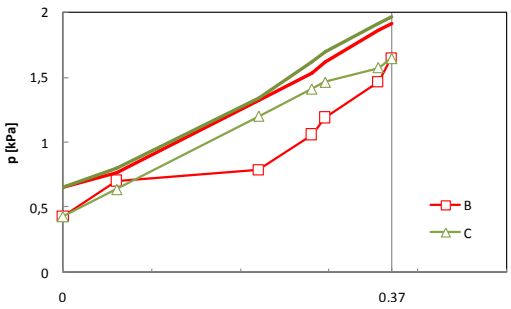

Figure 5: vapor pressure distribution

ENERGY RENEWAL INTERVENTIONS

The overall thermal transmittance (calculated as the mean of the three values weighted with their extension on the front) is a really pour 1.31 W/m^2 K, but an outside thermal insulation is not acceptable, as explained before. Inside insulation could be done either by an insulating plaster or through the installation of insulating boards coupled to plasterboard. The first approach keeps a high vapor transpiration of the wall, while in the second, polyurethane insulating boards act even as a vapor barrier. The use of 6 cm of a 0.056 W/m K insulating plaster reaches 0.55 W/m^2 K thermal transmittance, just as the use of 2 cm of a 0.028W/m K polyurethane. Temperature and vapor pressure distributions for the two solutions are depicted in Figs. 6-9.

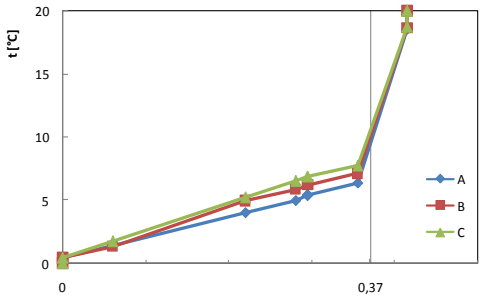

Figure 6: temperature with insulating plaster

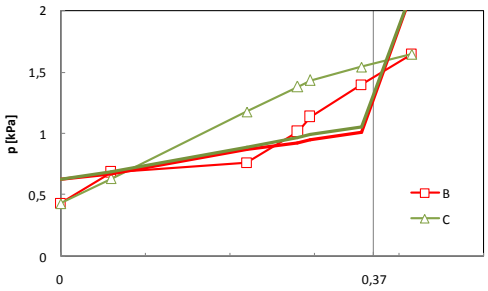

Figure 7: vapor pressure with insulating plaster

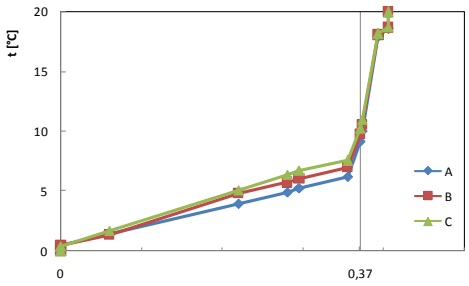

Figure 8: temperature with polyurethane

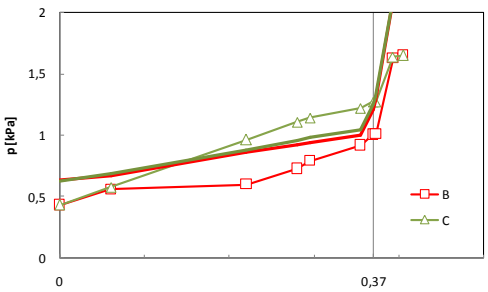

Figure 9: vapor pressure with polyurethane

Fig. 7 shows clearly that interstitial condensation surely occurs with insulating plaster, thus even this is not applicable. On the other hand, Fig. 9 is not definite on whether interstitial condensation actually occurs or not. The two-dimensional solutions of temperature and vapor pressure fields have been worked out for the wall next to the thermal bridge with the floor. Vapor saturation pressures are then computed and used to calculate the nominal relative humidity in the domain as shown in fig. 12. From

the two-dimensional solution it is clear that no interstitial condensation occurs: as vapor would condensate through mortar, it migrates toward the adjacent cavities.

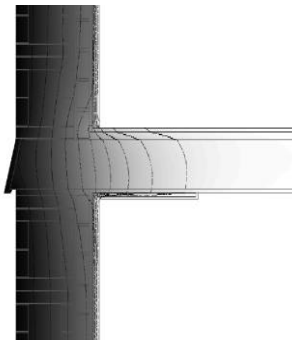

Figure 10: temperature field

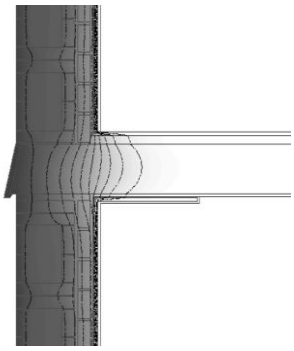

Figure 11: vapor pressure field

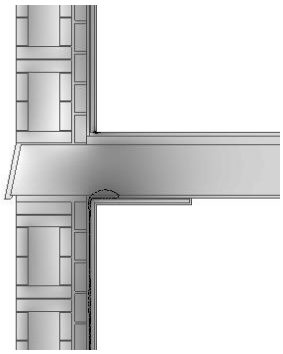

Figure 12: interstitial condensation

CONCLUSIONS

Energy renewal of buildings of the INA-Casa heritage presents many difficulties, as for the exposed bricks facades. Thermal insulation from the inside is possible with low vapor permeability. The two-dimensional analysis of thermal and vapor pressure fields is necessary in order to check for interstitial condensation, as one-dimensional analysis of brick walls my otherwise lead to wrong conclusions.

REFERENCES

Berretta Anguissola L., 1963, *I quattordici anni del piano Ina-Casa*, Staderini, Roma.

Capomolla R., Vittorini R., eds. 2004, *L' architettura Ina Casa (1949-1963). Aspetti e problemi di conservazione e recupero*, Gangemi, Roma.

Curra' E., 2004, *La costruzione a Roma negli anni Cinquanta. L'edilizia residenziale del Piano INA Casa*, Sapienza, Roma.

Currà E., 2006, *Il complesso residenziale di Via Cavedone a Bologna nei progetti e nelle realizzazioni di Federico Gorio.*1st ArTec International Congress, Sapienza, Roma.

Li Q., Rao J., *Fazio* P., 2009, Development of HAM tool for building envelope analysis, Building and Environment 44(5).

Mornati S., Cerrini F., 2004, *Il quartiere Tuscolano a Roma (1950-60),* in Capomolla R., Vittorini R., eds. *L'architettura INA-Casa (1949-1963) Aspetti e problemi di conservazione e recupero*, Gangemi, Roma, pp. 122-139.

Natonyova A. et al, 2013, Hygrothermal properties of building envelopes: Reliability of the effectiveness of energy saving, Energy and Buildings 57(2).

Nicoloso P., 2001, *Gli architetti: Il rilancio della professione*, in Paola Di Biagi, ed., *La grande ricostruzione. Il piano INA-Casa e l'Italia degli anni '50*, Donzelli, Roma.

Poretti S., ed., 2002, *L'INA Casa: il cantiere e la costruzione*, Gangemi, Roma.

PIOO - Piano incremento occupazione operaia case per i lavoratori, 1949, *Suggerimenti, norme e schemi per la elaborazione e presentazione dei progetti. Bandi dei concorsi*, Danesi, Roma.

PIOO - Piano incremento occupazione operaia case per i lavoratori, 1950, *Suggerimenti, esempi e norme per la progettazione urbanistica. Progetti tipo.* Danesi, Roma.

Storelli F., Currà E., 2004, *Il quartiere di Torre Spaccata a Roma (1955-63).* In Capomolla R., Vittorini R., eds., *Op. cit.*, pp. 196-205.

Dos Santos G.H., Mendes N., 2009, Heat, air and moisture transfer through hollow porous blocks, Int. J. Heat Mass Transfer 52.

Corcione M., Habib E., 2010, *Buoyant heat transport in fluids across tilted square cavities discretely heated at one side,* Int. J. Thermal Sciences 49(5).

BIPV-STANDARD MODULE FOR LARGE-SCALE HALLS

C. Ferrara; C. Vicente Iñigo

Fraunhofer Institute for Solar Energy Systems ISE, Heidenhofstrasse 2, 79110 Freiburg, Germany

ABSTRACT

The new targets set by the EU for the building sector such as the EU-Directive on Energy Performance of Buildings (EPBD) open a new field for research and development activities which should focus on giving the best cost-effective innovative solutions in order to reduce the energy consumption in buildings. This contributes to an increase of the market potential for BIPV products and calls for a reduction of the energy needs for heating and cooling of the buildings.

One approach to reduce costs in the building sector is the standardization of products, which helps to improve the quality and reliability of the product. The goal of this project is to develop a Building Integrated Photovoltaics (BIPV) multifunctional façade product which could be used for both retrofitting and new construction. Simplicity of construction and cost-effectiveness are to be kept in focus. A first sketch and prototype of the module is to be developed. Studies are to be run regarding the most suitable measures of the product and the insulation material to be used taking into account costs and energy saving potential.

The selected target group is large-scale halls. Industrial halls represent a large potential BIPV market for both new building and retrofitting purposes. In most cases, these buildings have a poor insulation and need refurbishment. This brings up the opportunity of adding more functions to the building material such as higher thermal insulation and PV electricity production.

The development of this standard product is expected to solve some problems which keep the BIPV market from growing and offer an innovative solution in retrofitting projects to reduce the thermal losses.

Keywords: Building Integrated Photovoltaics (BIPV), thermal insulation, industrial halls, cost-effectiveness, standard module, lifetime.

INTRODUCTION

In 2012 a PV capacity of more than 30 GW was installed worldwide, achieving a cumulated installed capacity of over 100 GW. With this growing PV market, different studies do also state a growing potential of the BIPV market. A study run by EPIA estimates that 40% of the total energy demand in Europe could be supplied by roof and façade PV installations. This means an installed capacity of over 1500 GW with an annual electricity production of 1400 TWh [1].

Another factor that points out this potential is the idea of a future decentralized energy supply system. The Smart Cities idea deals with the integration of living, life, work, mobility, resources and energy concepts in the future cities. In this scenario, BIPV facades and roofs will play an important role in the local energy supply.

Taking into account these numbers and perspectives the actual growth of the BIPV market is still too low. One of the barriers preventing this market to develop faster is the absence of standardized products.

As a first approach to the development of standardized BIPV products, this project focuses on the design and construction of a standard product for a specific building category. Non-residential buildings and especially industry halls with heating and cooling demand represent a large share of the potential market.

INDUSTRIAL HALLS

Factories, retail and warehouses belong to a building category where the integration of BIPV Modules in the facade is very attractive. Due to the simplicity of the architectural design and the large facade surface available, BIPV modules can be easily integrated in these buildings.

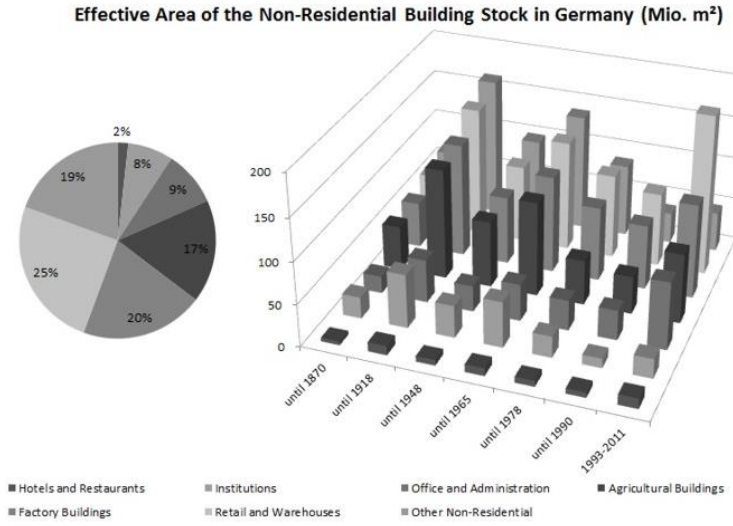

Figure 1: Effective area of non-residential buildings in Germany [2, 3].

In Figure 1it is shown that these building categories represent 45% of the effective area of the non-residential building stock in Germany. A recent study on energy efficiency in halls states that the usable net surface of heated hall buildings in Germany is estimated to be between 508 and 625 million m^2 for the building period 1960-2009 [4]. As a first approach, the total façade surface can be estimated to be of around 400 million m^2 (based on a standard hall for South, East and West facades), which could mean a total installed capacity of 60.000 MWp. Due to shading and other issues, only a fraction of this area would be appropriate for BIPV.

MODULE DESIGN

Approach

Aim of this project is to develop a standard BIPV product with improved thermal insulation properties to be integrated in industrial halls facades. Water resistance, sealing and thermal bridges as well as the different building dimensions should be taken into account from the conception phase.

Whereas for PV roof installations there are already different solutions available in the market (75% of the expected BIPV products for 2014 are for roof integration [5]), the BIPV facade sector is not yet so far developed, and no standard solutions are available. The development of a standard module for BIPV is expected to widen the BIPV market, facilitating the acceptance from the different actors in the building sector.

In relation to the development and study of new BIPV products for integration into steel elements for industrial halls, the first results of the research run within the NASTA project have been published [6]. Results are based on roof solutions and show that the maximum

yield is obtained with standard modules, while the trapezoidal plates produce shadowing in the flexible PV elements, thus reducing the production. This kind of solution would result in a lower yield when installed in the facade due to potential shading. In contrast with the NASTA project, where the research is focused on the use of flexible modules, the approach followed in this case would be to maximize the yield by installing standard modules, thus reducing the losses due to shadowing.

A first sketch is shown in Figure 2 with a trapezoidal plate as the core of the system, which will bring stability, ease of attachment, ventilation and a possible cabling space, while trying to limit the module weight. However, other structures are to be taken into account during the design process.

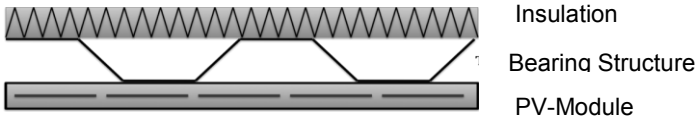

Figure 2: First draft of a standard BIPV module with thermal insulation.

The development of a standard product provides a better quality control and a reduction of the failure rate. As the lifetime for façades should be in the range from 30-120 years, the building process becomes therefore of a great importance here.

Research tasks

Standard module dimensions

An important question is the standard dimensions of a PV product for the building industry. A first approach can be done through the analysis of the module dimensions available in the market. The results of a market analysis of BIPV products show that 79% of them are in the range of 1 – 2 m^2 [5]. But the most important questions have to be answered with regard to the building typology. Therefore, a more detailed study is to be run taking into account façade products dimensions and configurations, available in the market façade systems for industrial halls, mounting systems and transport and handling best suited dimensions.

Insulation system

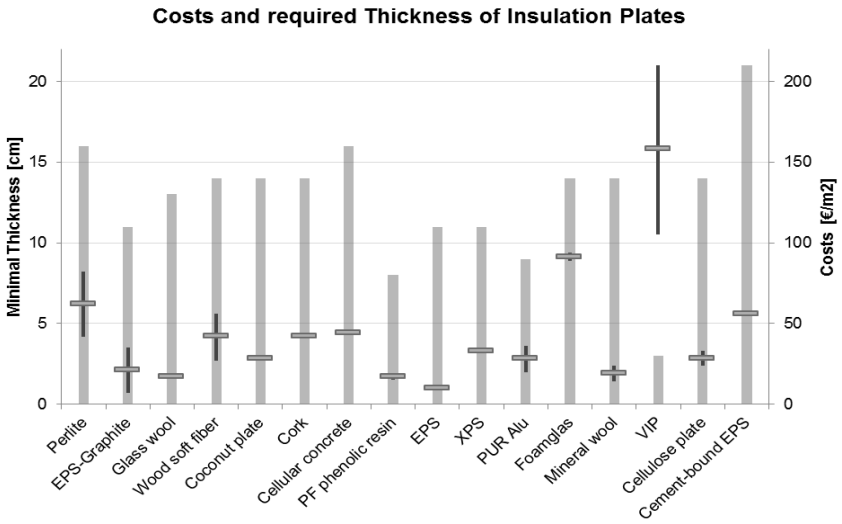

Figure 3: Costs and required thickness of insulation plates based on a U-Value of 0.28 W/m2 K (EnEV 2009 back ventilated facade).

On the other side, there is the need to improve the thermal behaviour of the building stock, reducing the cooling and heating demand. An analysis is to be done in this area regarding costs, thermal conductivity and lifetime of the different insulation systems. In the case of industrial buildings, where the effective surface is not as important in terms of costs as for residential buildings, a cost effective solution is to be expected.

An analysis of the costs and thickness required by the actual regulations is shown in Figure 3. This analysis is based on the German EnEV 2009 Standard for buildings, which requires a U-Value of 0.28 W/m2K for back ventilated façade. Further requirements such as the Passive House Standards, are to be taken into account, and costs and energy savings in different scenarios are to be compared.

Module Configuration

Beyond the economic analysis, there are the technical issues (PV yield and thermal insulation). One yield related issue is the temperature of the module: a good ventilation of the back of the module is important in order to achieve good performances. It should be analysed whether the trapezoidal plate is the best solution or another structure would be more suitable. Further studies regarding the behaviour of the facade as a whole and the effects of the temperature gradient should be simulated and measured.

The thermal characteristics of the solution are directly related to a good design. The mounting system should minimize the thermal bridges, avoiding unnecessary thermal losses. Simulations of the different configurations are to be run in order to help in the decision making process. Analysis of the different photovoltaic technologies, their behaviour under diffuse radiation and high temperature are to be done. In order to realize these measurements, one or more prototypes are to be built, and the selected one is to be installed in a real façade, in order to analyse the characteristics and behaviour under real test conditions.

Lifetime stability

Mechanical Loads			DIN EN 1991 / DIN 1055-4
PV	Mechanical Strength	3 Cycles, >5400 Pa, 1h	IEC 61215
Wind	Wind Pressure / Snow Load	Vacuum Cups Test	prEN 50583
		Air Chamber Test	prEN 50583
		Wind Channel	prEN 50583
	Curtain Wall – Resistance to wind load		DIN EN 12179
Facade	Mech. Durability	5000-50000 Cycles (EN 12400)	DIN EN 1191
	Vertical load	200-800 N/Class 0-4 (EN 13115)	DIN EN 14608
	Torsion	200-350 N/Class 0-4 (EN 13115)	DIN EN 14609
Humidity			
PV	Humidity/Freeze	10 Cycles -40 to >85°C, 85%	IEC 61215
	Damp Heat	1000h, >85°C, 85%	IEC 61215
Facade	Curtain Wall - Water tightness		EN 13050
Temperature			
PV	Thermal Cycling	50-200 Cycles -40 to >85°C	IEC 61215
Fire IEC 61730			DIN EN 13501 / DIN 1055-4 / MBO
Building Product	Non-combustibility	A1, A2	EN ISO 1182
	Heat of combustion test	A1, A2	EN ISO 1716
	Test SBI	A2, B, C, D	EN 13823
	Ignitability Test	B, C, D, E	EN ISO 11925

Table 1: Requirements, Norms and Tests for BIPV

Lifetime stability analyses are as important as the technical or economical due to the high requirements of building products. It is important to keep in mind that building products require a much larger life time than the PV modules. Therefore, it is essential to guarantee the operability, not just of the PV Module but of the product as a whole. This will also secure the investment and ease the growth of the BIPV market.

Table 1 shows a summary of the tests and special requirements for BIVP modules. Due to the special conditions of facade integrated modules, different conditions apply than for ground mounted modules. The action of wind over the whole surface of the façade exposes the buildings to different mechanical loads such as vibrations and resonance processes which can lead to cell breakage and damage of the cell connections. Higher level of humidity due to poor ventilation and high temperatures can be reached in building integrated products, thus, causing an alteration of the viscoelastic characteristics of the polymers. The behaviour of the product under these special conditions has to be analysed in the laboratory in order to guarantee the quality and lifetime of the module.

Another point of conflict is the fire safety requirements for building products. The minimum required in Germany is Class B2 (Class E as for European Standards) for buildings up to 7m. But for higher or special buildings the requirements are set in Class B1 or A2 (C and A2). Due to the higher heat of combustion value of the PV composite films and laminated glass a Class A2 cannot be achieved 7. Therefore, further development of BIPV Standards and test procedures is expected in the coming years in order to be able to expand the BIPV market.

FIRST CALCULATIONS - COSTS

First calculations regarding the cost effectiveness of the solution have been done. This analysis is done for the different insulating materials and the different types of heating energy consumed. The thickness of the insulation plate is calculated for the EnEV 2009 Standards. In order to estimate the costs and benefits, the energy savings are translated into costs depending on the heating energy used, with an estimation of the market price increase. All estimations are done taking as a base a crystalline silicon PV module, and assuming that east, west and south facades will be used. Thus, a mean value of 57% is obtained for the whole facade system electric yield.

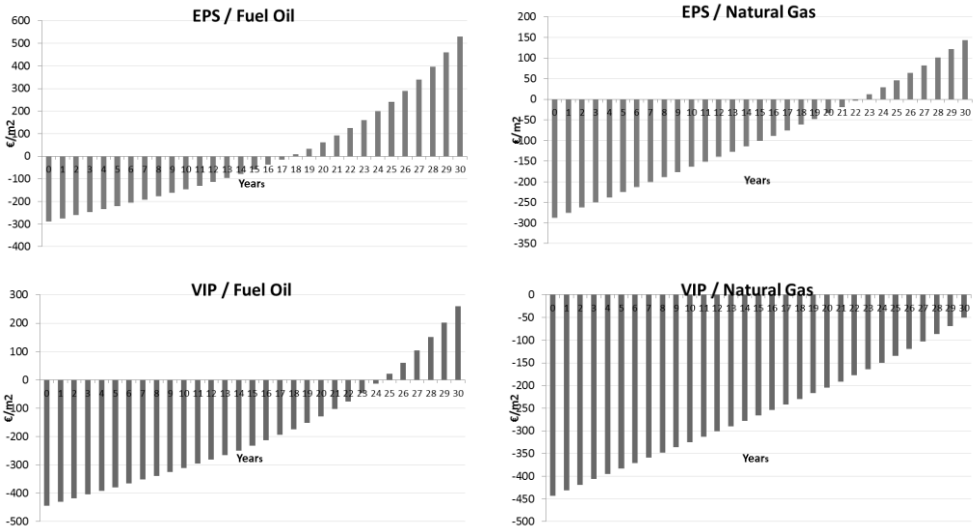

Figure 4: Cash Flow comparison of different insulation materials and energy fuel.

A deeper study should include more detailed information on costs increase per year, and maintenance cost of these installations which are expected to make the product more

profitable. As a first overlook there are the graphs for selected materials and energy supply systems shown in Figure 4. There can be seen how for standard installations where fuel oil or natural gas are used as fuel, the profitability for a common insulation system such as EPS can be high. Benefits are obtained after the 17th year when using fuel oil, or after the 22nd year when using natural gas.

All calculations are done assuming a minimum lifetime of the product of 30 years. On the other side, it is pointed out how high quality materials such as VIP would not be profitable in the case of use of natural gas due to the higher costs of the insulating material. The use of these kinds of materials could be profitable for households where the costs of the useful area per m^2 are higher and this would play an important role in the economic calculations.

CONCLUSIONS

The development of a standard product as well as the added thermal characteristics is expected to contribute to scale up the BIPV market. This is also supported by the increased demand on energy savings for buildings established by the EU- Directive on Energy Performance of Buildings (EPBD).

The standardization of products and regulations regarding BIPV plays an important role when trying to widen the market. Several problems have been pointed out in this paper, such as the absence of standard test for mechanical loads, or the impossibility to achieve the required Fire Class for some products. It is important to further invest in the research and development of these technologies due to their large potential.

When talking about BIPV, lifetime and feasibility of the products are one of the main factors, because of their expected longer lifetime. They require a big initial investment being profitable only in the long term. Therefore, analysis and tests that guarantee the operability of the systems are still needed.

REFERENCES

1. Fraile, D.: Building Integrated Photovoltaics: Closing the gap between the construction and PV sector, EPIA, 11 May 2010.
2. Bauen und Wohnen: Baugenehmigungen / Baufertigstellungen von Nichtwohngebäuden (Neubau) Lange Reihen z.T. ab 1980, Statistisches Bundesamt, 2011
3. Typologie und Bestand beheizter Nichtwohngebäude in Deutschland, BMVBS-Online-Publikation, Nr. 16/2011, August 2011.
4. Oschatz, B, Rosenkranz, J, Mailach, B, Gritzki, R, Kaiser, J, Perschk, A, Rösler, M, Seifert, J, Otto, F: Gesamtanalyse Energieeffizienz von Hallengebäuden, Fraunhofer IRB, ITG Institut für Technische Gebäudeausrüstung Dresden, Universität Kassel, Dresden, 30 June 2011.
5. Schmidt, K-W: Studienarbeit: Markt und Technologieübersicht BIPV Produkte im Rahmen des 10 wöchigen Pflichtpraktikums der Ruhr Universität Bochum, im Studiengang Umwelttechnik und Ressourcenmanagement, Fraunhofer ISE, 2012
6. Rexroth, S: Energieoptimierte Stahlelementfassaden mit Photovoltaik, Hochschule für Technik und Wirtschaft Berlin, 5. Anwenderforum Bauwerkintegrierte Photovoltaik, Bad Staffelstein, March 2013.
7. Roos, M, Misara, S, Henze, N: Untersuchungen zur Baustoffklasse von PV-Bauelementen für den Einsatz in höheren Gebäudeklassen, Fraunhofer IWES, 5. Anwenderforum Bauwerkintegrierte Photovoltaik, Bad Staffelstein, March 2013.

STRATEGY FOR LOW EMISSION REFURBISHMENT, THE OFFICES OF MEYER HOSPITAL. A CASE STUDY IN FLORENCE

P. Gallo

University of Florence, Department of Architecture - Via S. Niccolò 93 , 50125 Florence Italy - Tel. 055/2055568 - e-mail paola.gallo@unifi.it

ABSTRACT

In most European cities there is a vast stock of existing buildings, many of which are getting to the end of their useful life. To replace the stock would take several decades and incur an unrealistic financial burden; so retrofitting actions offer an answer to the problems of the aging building stock of most European countries, including deteriorating building fabric, obsolete mechanical networks, the lack of adequate space for the ever increasing needs, disruptive acoustics, and the need to improve the indoor environment and the user comfort. The overall objective of this paper is to demonstrate how a holistic approach in refurbishment of existing buildings can provide energy efficient system with the only inclusion of some new, not invasive extension (i.e. a greenhouse).

In detail the aims of this work have been to evaluate energy and environmental performances of an old building refurbishment and to obtain significant reductions of primary energy use, CO_2 emissions and peak electricity demand. The case study was the refurbishment of Villa Ognissanti, the old part of the Meyer Hospital in Florence, one of the most important paediatric institutions throughout Italy and Europe: the realization of its new headquarters in the old building retrofitted.

The present retrofitting project has achieved the specific energy targets, as it results, with very substantial total energy reduction, more than 28%. It is estimate that the application of proposed measures to the case study building may easily achieve a very substantial reduction of CO2 emission up to 25%, heating loads up to 31 % and of electrical loads for lighting, cooling and ventilation up to 27 %.

The realization of its new headquarters in the old building retrofitted, has had a great potential for dissemination and for advancing the state of the art on sustainable issues on a National and European scale. The architectural integration of bioclimatic greenhouse and its photovoltaic plant was been the main challenge of this renovation project.

Keywords: Sustainable refurbishment, energy recovery, building office

INTRODUCTION

The Meyer Hospital as one of the most important paediatric institutions throughout Italy and Europe: the realization of its new headquarters in the old building retrofitted, has been a great potential for dissemination and for advancing the state of the art on sustainable issues on a National and European scale. This recovery project participated, as Italian case study, to the REVIVAL[1] project , financed by EU Commission, so the results of this project was to provide also with a direct guidance, complete with architectural and engineering examples, for design

[1] 'Retrofitting for Environmental Viability Improvement of Valued Architectural Landmarks' is a five-year project funded under the European Commission 5th Framework 'ENERGIE' Programme.

professional and hospital authorities, setting a new standard for energy consumption in this special offices buildings [1].

The overall objective of this project was to demonstrate how a holistic approach in refurbishment of existing buildings can provide energy efficient system with the only inclusion of some new, not invasive extension (the greenhouse used as general hall). The architectural integration of bioclimatic greenhouse and its photovoltaic plant becomes the main challenge of this renovation project.

These innovative measures that were implemented in this project, have shown that can be widely used within the office-building sector in financially and functionally attractive mode, especially for the key-decision makers, the constructors and the users. This may only be investigated and documented through "real life situations", meaning that the individual measures must be designed, implemented and monitored in real situations. The application of such innovative features have not applied before in Italy in these kind of building, so there were some problems concerning unforeseeable technical difficulties (i.e. implementation of passive techniques as a greenhouse in an hospital office building). In fact many installed techniques have been already tested but generally in other sectors (in particular in residential buildings, …), thus there was no real life experience of the performance they had in a office building which has specific needs and characteristics. These problems has required an especially careful planning and studies in cooperation with expert in the field, involved in the project, because these features not have been tried in this application before [2].

In particular the project was designed to evaluate energy and environmental performances of the old building refurbishment and to obtain significant reductions of primary energy use, CO_2 emissions and peak electricity demand.

The Villa Ognissanti building had some characteristics of poor insulation standards, an over-provision of glazing, inefficient plant, and degraded fabric. The design teams developed refurbishment packages of fabric and servicing system improvements, aimed at improving energy performance, whilst simultaneously addressing the problem of fabric degradation and the quality of the internal environment. They included both 'design-based' solutions, which has involved re-modelling and re-organisation, and 'product-based' solutions that has applied innovative products newly available from industry.

This project involved the refurbishment of Villa Ognissanti with the global objective to demonstrate that tertiary buildings from post – war and pre- energy conscious era, can be economically improved in their energy performance and environmental impact obtaining significant reductions of primary energy use, CO_2 emissions and peak electricity demand.

DISCUSSION

Historical Background

At the beginning of 1900, in Florence, a new building was needed to be the new hospital as a branch of the existing one which had become insufficient. Careggi estate, a wide beautiful green hill area, was considered a suitable site where the new hospital could be built, thus in the 1912 works started and finished by 1936. The new building took the name of Villa Ognissanti and its plan consisted of three rectangular-shaped pavilions, oriented on the east-west axis: a larger and central one and two symmetrical wings.

The plan of Villa Ognissanti is based on the typology of the triple module, which is no more suitable at present for a purely medical function. Thus, according to the project, pavilion spaces will be converted into a reception and offices for administrative and managerial functions. The central pavilion of the old villa - more than 3000 mq - become the general

administration office of the new adjacent Paediatric Hospital, The Meyer Hospital, that increased in the extended area of the Medical Scientific University Pole of Careggi in Florence (fig. 1).

Figure 1: The building before the refurbishment

Refurbishment strategies

The project was aims at achieving high inner air quality level, thermal comfort and relevant savings in energy consumption, so the strategies adopted to obtain such results can be all synthesized in the following main categories [3]:

Indoor environment improvement

The project has been focused on the detailed planning and design of the healthcare environment and, particularly, the psychological effects of environment. This approach has been considered essential for children ambulatories environment and its subsequent effect on babies, their families and caretakers. All offices and ambulatories are designed in order to obtain the optimal comfort conditions thanks to the application of high efficiency systems, high performance materials and energy saving devices. In each room temperature and humidity levels are regulated in order to guarantee optimal comfort conditions.

Energy and Resource consumption (energy efficiency, renewable energy)

A lot of measures have been adopted in order to improve energy efficiency and integration of renewable energy. In particular for building improvements ventilated roof and insulation has been realized, solar shading and double glazing with super low energy panes have been installed, wood window frames in bad condition have been replaced with low-conductivity ones. Moreover the function of pre-heating, heat storage and reduction of heat loss of greenhouse has been considered. As whom to renewable energy the PV system is integrated on the top of curved surface of the greenhouse, with a southern orientation; this active solar system provide to generate electrical energy (31 kWp that are consumed directly by the same building needs).

Emissions and waste (renewable materials and CO_2 emission)

The main objective of the Villa Ognissanti refurbishment was to obtain significant reductions of primary energy use, CO_2 emissions and peak electricity demand.

The architectural integration of bioclimatic greenhouse and its photovoltaic plant was been the main challenge of this ambitious project. In fact the Meyer's greenhouse is a structure which is not heated or cooled by mechanical means and thanks to his southern exposition and unobstructed solar access to the main solar glazing, the greenhouse makes a net contribution to space heating: up to 17 % of the total heating loads. As far as the materials and the constructive techniques are concerned this greenhouse project aims to use eco-compatible materials: natural paint and wood for structural elements.

Environmental management

The Objective of Meyer's refurbishment activity was the integration into offices and ambulatories of strategies that have the aim of significantly reducing the total energy demand.

This is why Villa Ognissanti complex is characterised by the use of building management devices. Thanks to a control system was been possible to obtin a constant monitoring of the spaces' thermal conditions in order to control temperature, relative humidity and air velocity levels. In each office and ambulatory, the occupants can modify the inside conditions by reducing or augmenting the temperature of about 3 ° C thanks to the presence of temperature sensor-probe on walls. The energy management system, which selects the best operational strategy in order to obtain the optimal indoor conditions, allow optimizing plants use and control, to increase plants safety level, to reduce costs and to plan maintenance activity.

Sustainable Building Technologies implemented

Energy saving and recovery: installation of a HVAC plant equipped with a heat recovery system; construction of a greenhouse which main characteristics are:

- It works as a buffer space in winter, to minimize heat losses;
- It increases natural ventilation through a stack effect, reducing cooling demand in summer;
- It is not heated or cooled by mechanical means;
- It has southern exposition in order to maximize the collection of winter sunshine;

It is protected on three sides by walls, while the southern side is a glazed surface;
According to such proposals the Villa Ognissanti pavilions refurbishment design also deals with the realization of three new volumes: a bioclimatic greenhouse including an integrated photovoltaic plant and two new staircases, whose purpose is that of connecting old volumes (fig.2). The 960 sqm bioclimatic greenhouse - placed along the central pavilion and protected by the two other ones on east and west sides - is the general hall for the whole hospital complex: it has thus great visibility and represents a pilot action for the development of the semi-transparent photovoltaic technology being the first significant example in Italy.

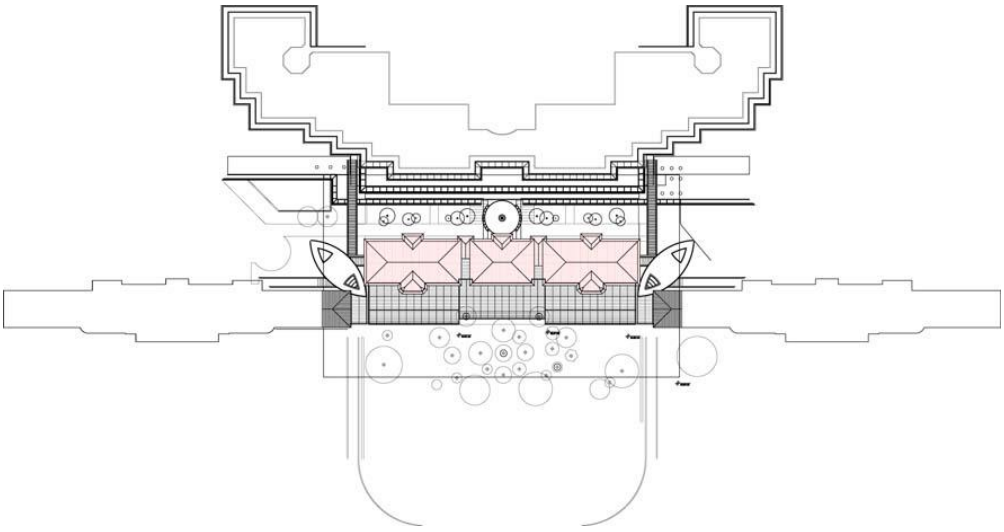

Figure 2: The greenhouse with the integrated photovoltaic plant

Measures to avoid potential overheating problems in summer have been adopted:

- opening area > 40 % of the greenhouse area;
- open able grids provide for heat dissipation (natural ventilation and night ventilation strategies), controlling by sensors;
- 300 m^2 of semi-transparent PV cells installed, reduce the need for shading;

part of the greenhouse roof is opaque and specific grids have been provided in the glazed roof in order to reduce during the night condensation in its internal space.

A special photovoltaic system is integrated on the upper part of the greenhouse and has a southern orientation: cells are inserted in the glazing curved surface, in decreasing density from top to bottom making the upper part of greenhouse almost opaque. Thus this active solar system will fulfil to a double goal: shading the greenhouse' inner space and generating electrical energy. It is a small solar power station (31 kWp) and provided clean electricity will be totally consumed by hospital energetic demand.
So such a solar shading system is able to provide the inner space with very pleasant shade in summer: as cells are placed in the upper part they can guarantee a good protection from high summer rays without interfering with low winter solar radiation. This system also aids the filtration and modulation of daylight, lowering its fastidious glaring effects during summer (fig.3).

Figure 3: The PV plant integration in the greenhouse

Finally specific grids are provided in the glazed roof in order to reduce night condensation on the internal glass surface. If all these measures will be correctly adopted there will be a good habitability in summer as well.
The architectural integration of bioclimatic greenhouse and its photovoltaic plant is the main challenge of the of Villa Ognissanti ambitious refurbishment project.
Under these preliminary considerations, the Meyer's greenhouse is not only a particular type of structure but also a particular kind of space. So, the design objective has not considered only energy and environmental aspects but also social impact: the primary objective is to create a pleasant and "socialising" space which can be used for semi-outdoor activities through much of the year without any extra energy space, a social space well integrated with the adjacent green park.

This greenhouse project has to be evaluated not only the significant energy reduction of the adjacent buildings or for the PV system integration in an existing architecture but especially for its social effect: the improvement of the working conditions, comfort conditions and productivity for staff and consequently quality of life can have a big payoff whenever an office is turned into a eco-building office, the pay back of any expenses is often much quicker than projected because of a great increase in employee productivity. When employees feel that their work environment is healthy and stimulating, it is inspiring what they can accomplish! And it makes their employers more competitive, too [4].

Figure 3: View of greenhouse's interior

CONCLUSION

Today the energy use for space heating, cooling and electricity in the office building is considerably higher per m^2 area than in almost all other building typology. This means that market opportunities for energy conscious building designs and components are present. As consequence of the increasing energy prices the office administrations attention towards these possibilities is increasing too. This proposal has provided thorough information about the possibilities of reducing these costs significantly to the office building administrations in Italy, stimulating that energy conscious designs and components are requested for future office buildings.

In fact the present retrofitting project has achieved the specific energy targets, as it results, with very substantial total energy reduction, more than 28%. It is estimate that the application of proposed measures to the case study building may easily achieve a very substantial reduction of CO_2 emission up to 25%, heating loads up to 31 % and of electrical loads for lighting, cooling and ventilation up to 27 %.

Besides setting up demands from the key-end users with respect to minimised energy use and attractive comfort conditions, the project has helped improving the competitiveness for those designers, manufacturers and contractor witch provide/offer concepts fulfilling these needs set up by the office building administrations

REFERENCES

1. S. Burton: Energy Efficient Office Refurbishment. London, James&James (Science Publishers) Ltd, 2001
2. P. Gallo, M. Sala, A. Lusardi, E. D'Audino, Lo stato dell'arte delle esperienze di retrofitting. Esiti di una ricerca Europea sugli edifici per ufficio, in proceeding of 53° Convegno Nazionale ATI, Firenze 14-18 Settembre 1998, Padova, SG Editoriali.
3. N.V. Baker, The handbook of Sustainable refurbishment, Earthscan, London, 2009
4. M. Sala: Recupero Edilizia e Bioclimatica. Napoli, Esselibri Simone Editore, 2001

INDOOR THERMAL COMFORT EVALUATION OF CLIMATIC RESPONSIVE STRATEGIES IN A TYPICAL CHINESE TRADITIONAL DWELLING IN HOT SUMMER AND COLD WINTER REGION

Shaoqing Gou[1]; Zhengrong Li[1]; Qun Zhao[2]; Xiaobin Li[1]; Haisheng Wang[1]

1: HVAC and Gas Institute, School of Mechanical Engineering, Tongji University, 200092 Shanghai, China

2: College of Architecture and Urban Planning, Tongji University, 200092 Shanghai, China

ABSTRACT

Improving building energy efficiency is one of the most effective ways for most countries to alleviate the present severe situation in terms of global warming and energy shortage and to achieve sustainable development, and adopting passive design strategies is the fundamental way to achieve building energy efficiency. The climatic responsive strategy of the vernacular traditional dwelling all over the world is a typical type of passive design strategies which can provide the construction of new residential buildings with low energy and sustainable design guidelines. In terms of the hot summer and cold winter climatic region of China, the energy consumption of residential buildings here is higher than other climatic regions of the country due to its special climate condition. Hence, aiming to improve the building energy efficiency of residential buildings in this region, the climatic responsive strategies of the local traditional dwelling need to be well investigated and learned. However, the related research is mainly about the qualitative evaluation which still lacks of thorough study and quantitative analysis. In this paper, a typical traditional dwelling of an ancient settlement named Xinye village locating in the middle region of Zhejiang province was systematically studied by the authors. The climatic responsive strategies of the typical dwelling were summarized in terms of nine different architectural features, and they were also classified into three major categories including natural ventilation, solar radiation control and thermal insulation. Furthermore, the indoor thermal comfort parameters of the selected house including air temperature, relative humidity and wind velocity were tested via field measurement both in summer and winter respectively, and the PMV index of the bedroom in the dwelling was calculated based on the measured data. The results of this study shows that the architectural design of the traditional dwelling in Xinye village adapts well to the local summer climate, the indoor thermal environment is comfortable in summer and is not satisfied in winter.

Keywords: Chinese traditional dwelling; climatic responsive strategies; thermal comfort

INTRODUCTION

Improving building energy efficiency is one of the most effective ways for most countries to alleviate the present severe situation in terms of global warming and energy shortage and to achieve sustainable development. At present, although there have been various kinds of building techniques, adopting passive design strategies is still the fundamental way to achieve building energy efficiency. The climatic responsive strategy, which is normally concealing in the vernacular traditional dwelling all over the world, is a typical type of passive design strategies and has the characteristics of low energy and sustainability. In these years, various kinds of studies have been carried out to investigate the climatic responsive strategies of the traditional dwelling in the world aiming to find low energy design guidelines for the residential buildings. As for the hot summer and cold winter region of China, due to its special climate condition the energy consumption of residential buildings here is higher than

other climatic areas of China, thus improving the energy efficiency of residential buildings in this region is relatively urgent. However, the traditional dwelling of this region not only has a beautiful scenery but also has a good climatic adaptability. In these years, although there have been many studies conducted to investigate the climatic responsive strategies of the traditional dwelling in this region, most of the research outcomes are qualitative analysis, and there still lacks of thorough study and quantitative analysis in this area. Aiming to learn from the climatic responsive strategies of the traditional dwelling so as to improve the indoor thermal comfort level, and to enhance the building energy efficiency, of the residential buildings in hot summer and cold winter region of China, a typical ancient vernacular settlement named Xinye village, which is situating in the middle region of Zhejiang province of China and has more than 700 years' history, was thoroughly studied by the authors. In this paper, a typical traditional dwelling of this ancient village was selected to evaluate the indoor thermal performance of its climatic responsive strategies in terms of qualitative analysis and quantitative evaluation.

MATERIALS AND METHODS

The typical traditional dwelling selected in this research is called Shuangmei House, which is located in the centre part of the Xinye village. The Shuangmei House was built in the end of the Qing dynasty (till now it has been nearly 110 years old) and it excellently inherited the architectural design methods of the indigenous traditional dwelling.

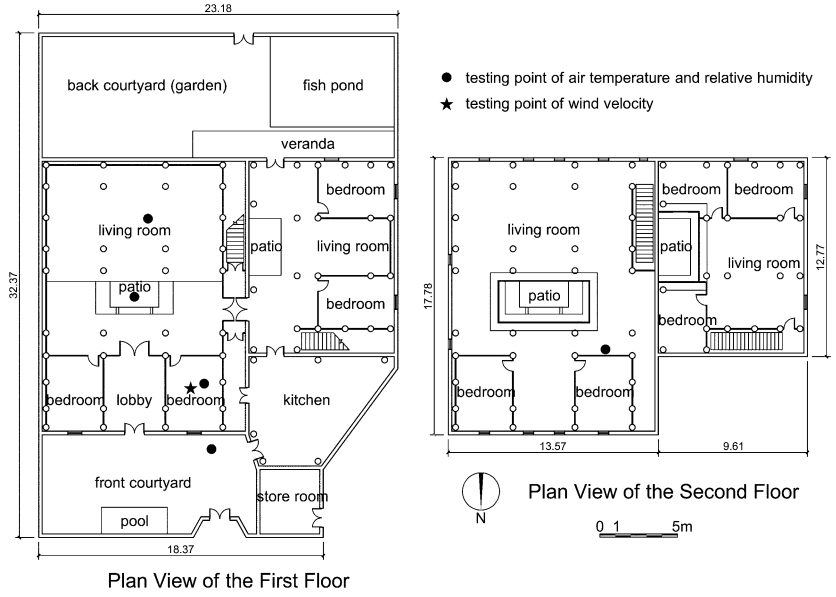

Figure 1: Plan view of the typical traditional dwelling and the distribution of testing points.

As shown in Figure 1, this house has two floors and consists of a folio shape building and a three-wing building, the two buildings represent two typical architectural forms of the village respectively. The house is facing the north which is similar to the orientation of the whole village, this is due to the fact that the local prevailing wind is the north wind caused by the blocking effect of two huge mountains situating around the village. Hence, this orientation enables the house make good use of the natural ventilation in summer time. Furthermore, the architectural form of the house is very high (for about 7 m) and compact, and the inner courtyard (patio), which is the typical architectural feature of the local ancient dwelling, plays a vital role in constructing a good indoor environment in terms of natural ventilation and day lighting. Another architectural feature of the house is its double-layer envelope which consists

of the external hollow wall made up of the local fired-clay brick and the internal timber partition wall made up of the local wooden materials.

The research methods of this paper mainly include field observation, systematic analysis, field measurement and quantitative evaluation. In order to evaluate the indoor thermal comfort of the selected house, the environmental parameters including air temperature, relative humidity and wind velocity were tested in two short terms by field measurement, which was conducted from August 5, 2011 to August 6, 2011 in summer and from January 6, 2012 to January 8, 2012 in winter respectively. The climatic condition of the two test periods are similar to the hottest day and the coldest day of Lanxi City which is the nearest city of Xinye village. As shown in Figure 1, the field test was focused on the folio shape building of the house, the testing points of air temperature and relative humidity were fixed in the bedroom, patio, living room, the attic (in the second floor), and the front courtyard which can represent the outside ambient condition; the parameter of wind velocity was only tested in the bedroom. All the indoor thermal parameters were measured at the height of about 1.1 m. The air temperature and relative humidity were continuously tested by using the HOBO U12 Temp/RH data logger, and the data was recorded every 10 minutes over the test period. The wind velocity was tested manually by using Hot-wire anemometer every 60 minutes, and the data was recorded as the mean value of 3 minutes in every test time. The windows and doors were all kept opening during the summer test period, and in winter they were opened in daytime but were closed during the night hours (the closed hour is between 8 pm to 8 am which is in accordance with the behaviour habit of the local residents).

RESULTS AND DISCUSSION

From the document research, field observation and interview with the local residents, the authors found that the architectural design concept of the traditional dwelling in this ancient village is corresponding to the summer climatic condition. This is due to the fact that the summer here is very hot and humid and the winter is slightly cold, thus the task of thermal protection in summer is the major question of the architectural design here. The authors systematically analysed the climatic responsive strategies of the traditional dwelling of this ancient village in terms of architectural features as summarized in Table 1, and these strategies were classified into three categories including natural ventilation, solar radiation control and thermal insulation. In fact, in addition to the three types of passive design strategies, the buffer space of the dwelling (the outer courtyard, inner patio and the veranda) has the precooling effect on the indoor environment, and the vegetation and water also has the evaporative cooling effect to improve the indoor thermal environment.

Architectural feature	Natural ventilation	Solar radiation control	Thermal insulation
Location selection	Concerning the local prevailing wind resources (the valley wind)		
Building group layout	Guiding the local wind to blow into the buildings effectively	Short spacing between buildings so as to form the mutual shading effect	
Orientation	Oriented to the local prevailing wind direction (facing the north)	Facing the north and arranging fewer openings in the south external wall so as to form a good effect of self-shading	

Architectural form	High and compact enough so as to enhance the stack effect ventilation	High and compact so as to form a good effect of self-shading	
Internal space arrangement	Arranging the major living space (bedrooms) in the windward side (the north side)	Arranging the bedrooms in the north side aiming to minimise the direct solar radiation	Separating the hot indoor space (the kitchen) from the major living areas
Buffer space	Using the outer courtyard and the inner patio to enhance the natural ventilation	Using the patio to shade the inner living space effectively; using the veranda to shade the outer activity space	The attic of the second floor used as an insulation layer of the ground floor living space
Openings	Most windows positioned in the windward side of the building; controlling the wind speed by changing the opening dimension	Positioning most windows in the north side of the building and setting external shading device in the upward of outer openings to reduce the solar heat gain	Designing the low ratio of window to wall so as to reduce the average U value of the building envelope
Construction and materials	Adopting low thermal capacity materials to release heat quickly via night ventilation	Using the white colour lime mortar to plaster the external wall therefore reflecting the solar radiation	The double-layer envelope system combined with the raised ventilated floor has a good effect of thermal insulation
Vegetation and water	Using water to precooling the air temperature of natural ventilation	Appropriately utilising the vegetation to shade the external wall and outer activity spaces	

Table 1: Summary of the climatic responsive strategies of the selected typical traditional dwelling in Xinye village.

Figure 2 shows the results of field measurement during the test periods in summer and winter. It can be found that both the air temperature and relative humidity have a big diurnal variation in summer while those are relatively stable in winter. During the summer time, while the outdoor temperature has a diurnal variation of 8.5℃ i.e., from 27.7℃ to 36.2℃, the simultaneous indoor temperature of living room is varying from 28.4℃ to 31.6℃ showing a diurnal variation of 3.2℃ only. The living room is the coolest place during the daytime, this is because the living room is a semi open space surrounded by three walls without any windows and only connected with the outdoor space by the patio. Hence, even though the natural ventilation here is very limited, the living room is shaded enough so that most of the harsh direct solar radiation can be prevented therefore the air temperature is lower and more stable than elsewhere. However, after sunset the coolest place is shifted into the bedroom, this is due to the good effect of nocturnal ventilation. Furthermore, it was observed that the attic is hotter than the living space of the first floor throughout the test period, this proves that the attic is a buffer space with good effect of thermal insulation. Additionally, it can be noticed that there is a time lag between the indoor and outdoor peak temperature (for about 2 hours), this is caused by the good property of thermal insulation of the double-layer envelope system and the shading-oriented architectural form of the house. Compared with the test results of air

temperature in summer, the relative humidity shows a reverse variation pattern, and it can be found that the living room is the wettest place, this is due to the bad condition of natural ventilation causing the moisture hardly being moved out from the indoor space. And what is needed to be emphasized here is that even though the air temperature of the bedroom is lower than that of the living room in the night, the bedroom is still drier than the living room, this is because the bedroom is built with raised ventilated floor which has a good effect of thermal insulation and moisture protection, and this is partly due to the fact the bedroom locating in the windward side of the house enjoying a good condition of natural ventilation.

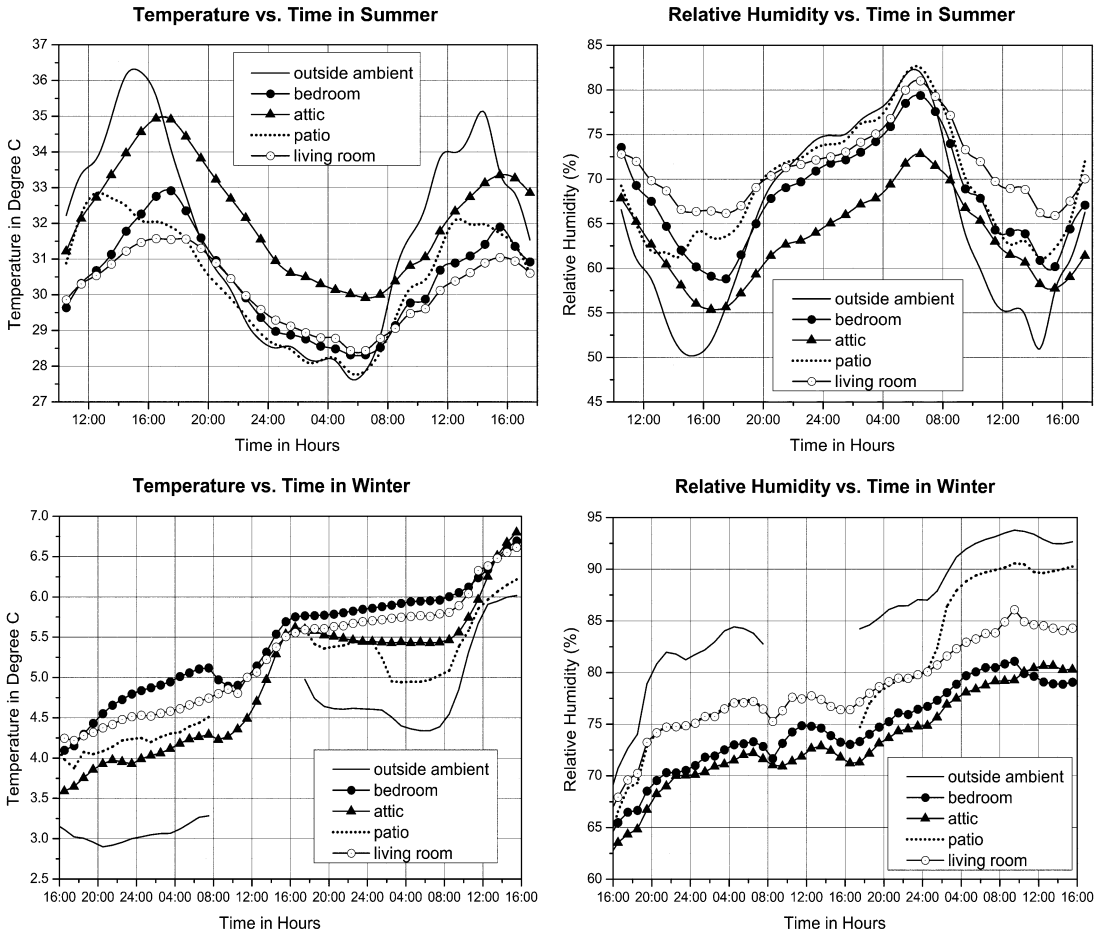

Figure 2: Variation of air temperature and relative humidity at the testing points over the test periods in summer and winter.

From the test results of winter time, it was found that the air temperature of every testing points are rising during the test period and the bedroom is the warmest indoor space even though its air temperature is slightly higher than the outside ambient temperature. And the living room is the second warmest place, followed by the attic. This also proves that, as a buffer space, the attic have a good effect of thermal insulation on the indoor thermal environment in winter. The test results of relative humidity in winter also shows a reverse variation pattern except for the test point of attic. It can be found that the attic is the driest place of the house in winter, this is due to the fact that the attic is relatively far away from the ground level and during the test period its windows were kept opening therefore the condition of natural ventilation here was better. A smoke study was conducted to understand the wind direction of the natural ventilation, and it was found that the wind of the bedroom is always coming from the north regardless of time changes. The test results of wind speed in the bedroom during the test period of summer and winter are merged and illustrated in Figure 3.

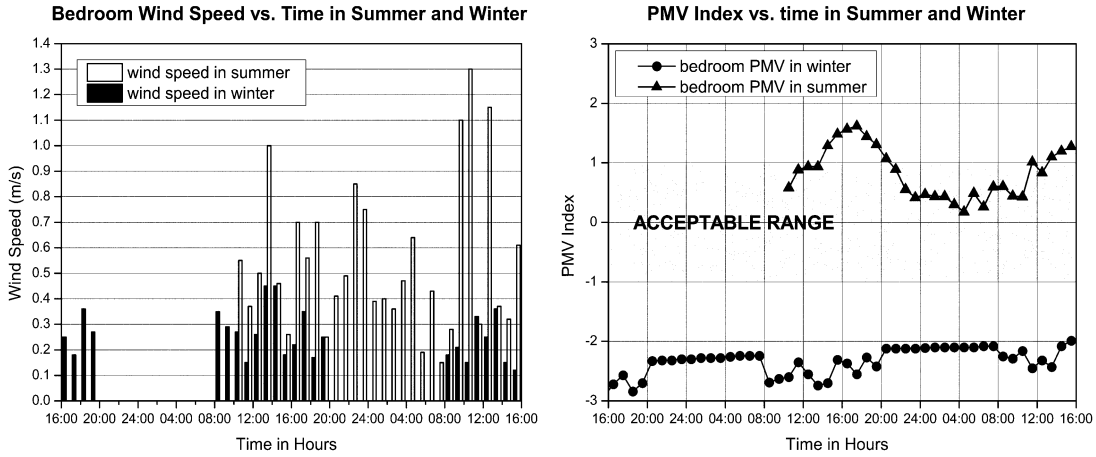

Figure 3: The variation of wind speed and PMV index in the bedroom during the test period.

Aiming to evaluate the indoor thermal comfort of the selected traditional dwelling, the PMV index of the bedroom was calculated using the measured results. In this paper, the PMV index was computed based on the PMV – calculator of professor de Dear [1] and on the following assumptions: average resident's height: 1.65 m, weight: 60kg (subject surface area = 1.65 m^2), wearing clothes at 0.3 col in summer and 1.5 col in winter at sedentary work (70 W/m^2), exposure time of 60 min, mean radiation temperature is also assumed to be equal to the air temperature. For the reason that the PMV-PPD model was assumed to be inaccurate in predicting thermal sensation of the residents in a naturally ventilated building in hot humid climate as it neglects human physiological, behavioural and psychological adaptation [2]. Hence, PMV results of the summer day were corrected by an expectancy factor e = 0.7 (for Lanxi City – assumed to be equal to Singapore) [3]. As shown in Figure 3, the PMV index of the bedroom during the summer test period is mostly in the comfort range except for the afternoon which is the hottest time of the day. However, the winter PMV was just between cool and cold scale. This PMV analysis reveals that the selected traditional house performs well in summer, but in winter the indoor thermal comfort is not satisfied.

CONCLUSIONS

Based on the results presented in this paper it can be concluded that the architectural design of the traditional dwelling in Xinye village adapts well to the local climate and topography especially to the summer climatic condition, and the major climatic responsive strategies of the ancient dwellings here include natural ventilation, solar radiation control, and thermal insulation. It can be observed that owing to these passive environmental control strategies the ancient residential building constructs a good indoor thermal environment in summer, and the winter indoor thermal condition needs to be improved.

REFERENCES

1. De Dear RJ. Thermal prediction calculator. Available at http://web.arch.usyd.edu.au /~rdedear/ [accessd 30.04.13]
2. Brager GS, de Dear RJ. A ASHRAE standard for natural ventilation. ASHRAE Journal; Oct 2000 [version: reprint with permission].
3. Fanger PO, Toftum J. Extension of the PMV model to non-air-conditioned buildings in warm climates. Energy and Buildings, Vol 34, pp 533-536, 2002.

A MULTIFUNCTIONAL, ZERO ENERGY FAÇADE SYSTEM – CONCEPTUAL MODEL AND PHYSICAL PROCESSES

D Heim; M. Janicki; D. Knera; A. Machniewicz; E. Szczepanska-Rosiak; I. Zbicinski

Department of Heat and Mass Transfer, Lodz University of Technology, ul. Wolczanska 213, 90-924 Lodz, Poland, e-mail – corresponding author: dariusz.heim@p.lodz.pl

ABSTRACT

In the following paper a concept model of a façade system is presented. The proposed solution will be dedicated to buildings whose concept goes beyond 2020. According to future, rigorous requirements, a facade concept will be developed and built as an experimental installation. The requirements of the construction sector in the area of energy production from renewable sources make it necessary to integrate selected renewable energy systems (RES) into the building envelope. The external facade system considered in this project consists of several components e.g.: visual, daylight, solar, opaque, airflow. Some of these are individual elements but some can play two or more significant roles. The idea of the presented facade system is to obtain a positive energy balance during a whole year.

The second part of the present paper is dedicated to the definition of different models of thermo-physical properties. Special attention is paid to analyses of advanced coupling processes (in a facade structure) and complex interrelations between them. This study is part of the wider research project devoted to the formulation of a multi objective optimisation task including: energy efficiency, cost and environmental effect. Based on the simulation results the experimental facade system will be constructed and installed on a university building. The energy efficiency of the facade system will be monitored and the proposed solution will be assessed in the future.

Keywords: sustainability, façade, zero energy, model, solar, thermal, photovoltaic.

INTRODUCTION

One of the major challenges to sustainable development in countries of the European Union is how to promote energy efficiency, so as to allow those countries to meet their climate commitments and simultaneously maximise their economic potential of building. One of the means through which this challenge can be met is by fostering energy efficiency in buildings on the one hand, but on the other also by developing innovative approaches to facade technology [1], both helping to reach the goal of "zero emission" buildings.

Requirements defined for buildings in the area of energy production from renewable sources make it necessary to integrate selected renewable energy systems with the building envelope (BIRES). Simultaneously heat transmission has to be minimized to reach a positive energy balance of external partition over a year. The ability to convert surplus energy to the form possible for an on-site use, effective storing or immediate selling to the grid should be also taken into account.

CONCEPTUAL MODEL OF THE FAÇADE

The basic façade construction taken into consideration is a Ventilated Façade Insulation System (VFIS), optionally equipped with photovoltaic panels. Nowadays, the VFI system is less popular than the External Thermal Insulation Composite System (ETICS) because of the cost and versatility for new and existing buildings. However, taking into account future trends

and requirements in building energy performance, this relation would be reverse. The main advantages of VFIS versus ETICS are: easy integration with photovoltaic panels, protection against interstitial condensation through air exchange in a cavity, aesthetics and durability. On the other hand there are some disadvantages to the VFI system. The main problem taking into account the future requirements of thermal transmittance is the limitation in thickness of insulation material. The second one is thermal bridging generated by metal frame constructions.

The main goal of the extensive project is to develop and optimise a new, active façade system for zero energy buildings. The study presented here is a first step of the modelling and numerical analysis of physical processes in a façade, taking into account any form of energy conversion, storage and utilisation. The future façade system will be optimised taking into account some limitations. The total dimension of a one storey façade is 3 m × 3 m. The total area of individual façade systems was divided into 100 elements, numbered from 1 to 100. Each element is characterised by a notation system as follows:

$$N : V - X_1 X_2 - Y - Z \qquad (1)$$

where:

N – number of element, from 1 to 100,

V – façade properties determining solar processes (cases 1÷4);

X_1 – façade properties determining energy conversion into heat (cases 1÷4);

X_2 – façade properties determining energy conversion into electricity (cases 1÷4);

Y – façade properties determining daylight transmittance (cases 1 & 2);

Z – façade properties determining heat exchange (cases 0 & 1).

Graphical representation of the system is presented in Figure 1. Anyone of 100 elements represents a different building structure, defined by selected physical processes defined below.

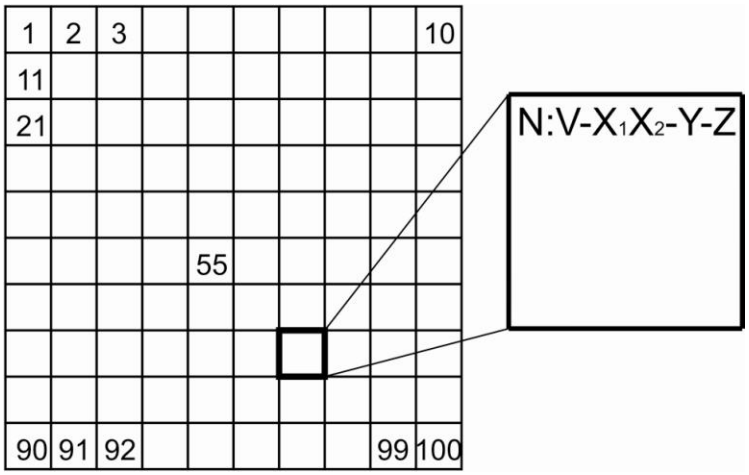

Figure 1: Spatial discretisation of the façade for the purpose of multi-objective optimisation.

SOLAR PROCESSES

The energy performance of a building highly depends on climate conditions, in particular on solar radiation. Solar heat gains significantly affect both heating and cooling demands. The construction of an external envelope and its optical properties directly determines the intensity of solar processes and the amount of solar energy delivered to the conditioned zones.

Solar radiation acting on every surface is comprised of a fraction of direct beam (I_D) and diffuse radiation (I_S). The latter is the radiation that has been scattered out of the direct beam by air molecules, water vapor, aerosols, and clouds or is reflected from the ground. According to the construction of a single layer of the building partition, which can be transparent or opaque, solar radiation is partially reflected (I_ρ), absorbed (I_α) and additionally transmitted (I_τ) - for transparent layers only.

Considering two layered components of a building envelope, if the external wall is opaque, solar processes do not depend on the construction of the internal part of the wall (Fig. 2a & 2b). Application of the transparent structure on the external skin results in partial transmission of solar energy to the surface of the second, internal layer. Similarly as for the external part of the wall, if the second layer is opaque, solar radiation is partially reflected and absorbed (Fig. 2c). As shown in Fig. 3d, an additional part of transmitted solar energy should be considered for the second, transparent construction. The optical properties of the layer can be changeable due to temperature (thermo-), solar irradiation (photo-) or impetus (electro-).

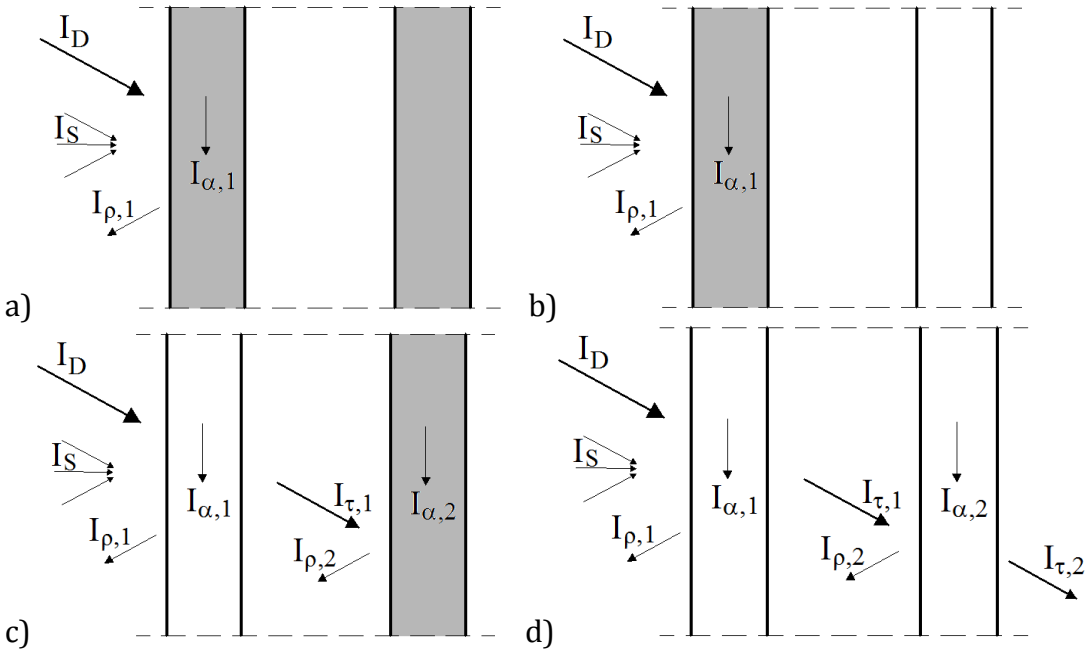

Fig. 2. Solar processes through a) double opaque b) opaque and transparent c) transparent and opaque d) double transparent construction of two layers external wall.Conversion of solar energy

All individual layers from the partition presented in Figure 2 can be considered separately taking into account any processes of conversion and storage of solar energy. The processes can be classified as thermal and electrical, and can occur separately or altogether.

An absorption process can be observed when a ray impacts on a surface of material, is remained within it and solar energy is converted to another form. Absorbed energy can be transformed into heat. In case of a traditional material like brick energy is stored as sensible heat - Q_{TS} (Fig. 3a), and causes an increasing of material temperature. Alternatively, for some special material, e.g. PCM – Phase Change Materials, energy can be stored as latent heat. PCM may charge not only sensible heat but also additional, large amounts of latent heat during the melting process - Q_{TI} (fig. 3b).

The next type of process is conversion of photon energy into electricity - photovoltaic conversion, which is observed in photovoltaic panels (Fig. 3c). PV layers are made from semiconductor matter. Photons that impact on the surface of PV panels send their energy to electrons from semiconductor material causing their liberation . In consequence through the semiconductor material there is an electric current – Q_{El}. The theoretical maximum PV efficiency can be achieved only when solar energy delivered to the photovoltaic panels is equal to the minimum energy necessary for the liberation of the electrons by the photons. On the other hand the remaining energy is transformed into heat, andas a result reduces the PV efficiency. Maintaining delivered solar energy on a level of forbidden bandwidth is impossible in reality, therefore the optimal temperature of a PV system can be assured e.g. by integration of PV and PCM. In that case absorbed energy is transformed into sensible heat, latent heat and electricity (fig. 3d).

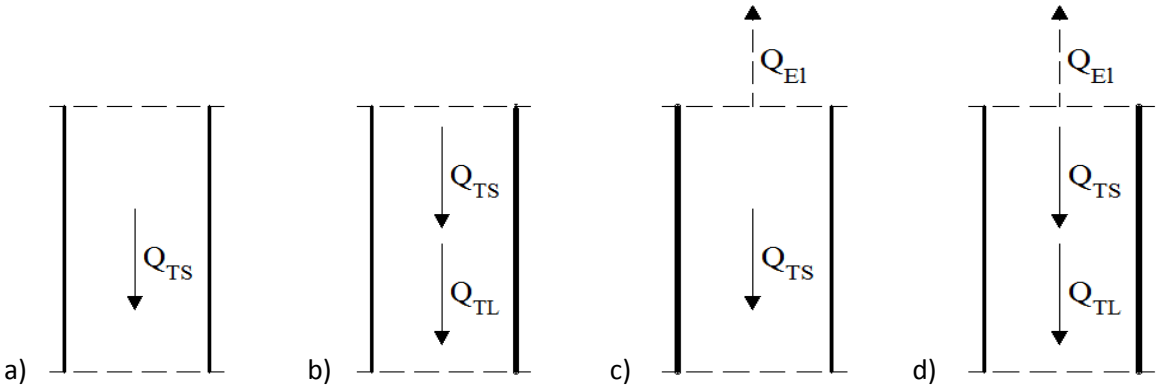

Fig. 3. Conversion absorbed energy for various material a) traditional material, b) phase change material, c) photovoltaic layer, d) photovoltaic layer integrated with PCM.

HEAT EXCHANGE

Division of the façade into two layers with an air cavity between them, provides new possibilities to control heat transfer processes inside the façade as a result of mass exchange – air flow. Ventilation of cavity can be carried out through a variety of technical solutions, ranging from natural ventilation through cracks and openings, ending with advanced hybrid or automated mechanical ventilation systems.

In case of an unventilated air cavity, the thermal insulation of the partition is increased because of an additional thermal buffer forming between both skins (fig. 4). This buffer acts as a solar collector from which preheated air can later be used as an additional heat source (V_0). On the other side, strong ventilation of a cavity during hot and sunny days can lead to the protection of the building's interior against overheating (V_1). To construct an optimized structure for a ventilated façade the analysis should be carried out concerning the physical phenomena occurring at the boundary of the first skin of facade and the external environment, on the interior of the facade and at the boundary of the second skin of facade and adjacent areas.

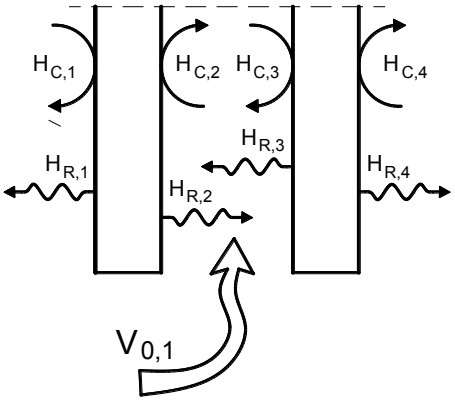

Fig. 4. Heat exchange through convection and radiation.

DAYLIGHT TRANSFER

The light propagation through transparent elements depends on material optical properties which are described by the dimensionless factors: reflectance ρ (defined by the ratio of reflected irradiation to incident irradiation), absorbance α and transmittance τ (defined by the ratio of transmitted irradiation to incident irradiation) that determine the part of incoming light which is reflected, absorbed or transmitted by material. The sum of these three indexes is equal 1. The light beam incident on the surface is first reflected. The amount of reflective light strongly depends on the angle of incidence and refractive indices of the medium. Depending on the nature of the interface, the reflection of light could be specular (mirror-like), for smooth, flat surfaces or diffuse when light reaches a roughness surface or object. The direction and amount of reflected rays is determined, on the basis of respectively, Snell's law and Fresnel's formula.

The part of incoming light is transmitted through transparent materials. This process, dependant on wavelength and incident angle of incoming light, can be accompanied by diffusion (scattering) which caused reflection of a light beam into many directions. Therefore transmission can be divided into 3 types: direct (regular), diffuse or selective. The first type occurs for typical glass or air when light passes through an object without changing direction or quality (no diffusion). For transparent or semi-transparent material with a texture, like frosted glass, diffuse transmission takes place. In this case transmitted light is characterized by less contrast, less intensity and also tends to be softer and generate smooth shadows. Selective transmission is produced when light goes through a coloured object. This process contributes to changing the colour of transmitted light.

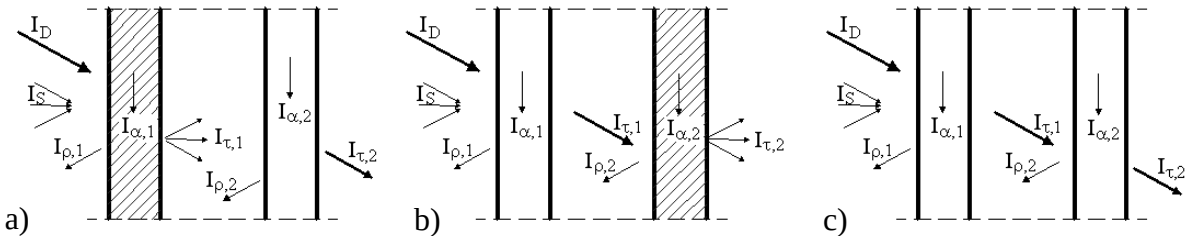

Fig. 5. Daylight processes on the surface of transparent and translucent materials.

The façade under consideration can be constructed from transparent, translucent and opaque layer. Only transparent and translucent elements are able to transmit the light in a form of direct (fig. 5c) and diffuse (fig. 5a&b).

INTEGRATED SIMULATION

The main challenge of the façade performance simulation and optimisation procedure is coupling different domains: energy including RES, lighting and fluid dynamic. The general assumption for coupling of building and system domains were proposed by Clarke [2] and developed by others: Janak [3] method of direct run – time coupling between building energy and building physics simulation (ESP-r) and global illuminance simulation (RADIANCE) and Morrison et al. [4] coupled ESP-r with renewable energy simulation tool TRANSYS.

In the presented projects the following processes are considered:

- Heat flow – Control Volume and/or Finite Element,
- Air flow – Nodal Network and/or Computational Fluid Dynamic,
- Daylight flow – Ray Tracing,
- Electric flow – Nodal Network,
- Energy conversion – Control Volume.

SUMMARY

The concept of a facade for a nearly zero building was proposed as a ventilated façade insulation system. The main physical processes on the external surface as well as inside a partition were described based on physical properties of building elements. The general idea of the system is to obtain a net zero energy balance during the whole year including photo-thermal, photo-electrical energy conversion, air-flow and daylight transmittance.

ACKNOWLEDGEMENTS

This work was funded by The National Centre for Research and Development as part of the project entitled: "*Promoting Sustainable Approaches Towards Energy Efficiency in Buildings as Tools Towards Climate Protection in German and Polish Cities: developing facade technology for zero-emission buildings*" (acronym: GPEE).

REFERENCES

1. Herzog, T., Krippner, R., Lang, W.: Facade Construction Manual, 2004.
2. Clarke, J.A.: Energy simulation in building design, 2nd edition, Oxford: Butterworth-Heinemann, 2001.
3. Janak, M.: Coupling building energy and lighting simulation. Proc. of 5th Building Simulation 1997, Prague, pp. 313 – 319.
4. I. Beausoleil Morrison, F. Macdonald, M. Kummert, T. McDowell, R. Jost, and A. Ferguson" "The design of an ESPr and TRNSYS cosimulator," Proc. of 12th Building Simulation 2011, Sydney, pp. 2333-2340.

NUMERICAL SIMULATION OF METAL FACADE COMPONENTS WITH NEW AND AGED HIGHLY REFLECTIVE MATERIALS

Takeshi Ihara[1]; Arild Gustavsen[2]; Bjørn Petter Jelle[3]

1: Department of Architectural Design, History and Technology, Norwegian University of Science and Technology (NTNU), NO-7491 Trondheim, Norway, and, Takenaka Corporation, Osaka, Japan,

2: Department of Architectural Design, History and Technology, Norwegian University of Science and Technology (NTNU), NO-7491 Trondheim, Norway

3: Department of Materials and Structures, SINTEF Building and Infrastructure, NO-7465 Trondheim, Norway, and, Department of Civil and Transport Engineering, Norwegian University of Science and Technology (NTNU), NO-7491 Trondheim, Norway

ABSTRACT

The purpose of this paper is to study the effect of highly reflective facade materials, which may make fatigue resistance of sealants better because of the less thermal movement caused by reduced surface temperature fluctuations. Surface reflectance usually changes with time due to surface deterioration and dust or dirt sticking to the surface. Important parameters are location and weather. There is however no universal method to predict the change of reflectance with time. At this time, it therefore is useful to investigate the effect of changing reflectance on the temperature fluctuations by performing numerical simulations. This way knowledge about the ageing effect on the surface reflectance may be achieved.

In order to investigate the effect of varying surface reflectance on the sealant fatigue resistance, an exterior wall facing south in Tokyo, Japan, was simulated in the program WUFI. The emissivity and reflectivity were varied. The sealant fatigue test was demonstrated and the sealant internal stress was evaluated by a finite element method (FEM) program. Based on these results of WUFI, the sealant fatigue test and FEM simulations, the possibility of improving sealant fatigue resistant was indicated. When solar reflectance is increased by 0.2, the effect to improve fatigue resistance is increased by about 4.8 times in summer, about 6.4 times in winter respectively. These results are limited only to specific conditions. However, by following the same procedures, it is possible to predict the effect for better sealant fatigue resistance at various conditions. On overall, this discussion focused only on the south wall, i.e. durability is discussed by considering the worst situation. Therefore, highly reflective materials can contribute to improve sealant durability. Other sealant deterioration factors, e.g. moisture, ultraviolet radiation and fatigue caused by wind pressure, are not considered. Hence further work is necessary to estimate how thermal movement affects the total durability of sealants.

Keywords: metal wall, highly reflective materials, reflectance, ageing, lower temperature, sealant, fatigue resistance, thermal movement.

INTRODUCTION

The building envelope often incorporates metal materials from the viewpoint of construction efficiency or architectural design. These metal material layers are usually thin. During daytime, the metal materials can reach high temperatures. In order to maintain a lower temperature, highly reflective materials have been popular in some warmer countries, including Japan. In these areas, roofs or pavements with highly reflective coatings are well

discussed [1] as a good energy saving effect is expected at horizontal parts where the larger intensity of solar radiation strikes. Current research does not present a universal method to predict surface solar reflectance ageing [2-5]. If highly reflective materials are used for walls, this may decrease building energy use and make the durability of sealants better due to lower surface temperatures [6]. However, building walls with highly reflective materials have not been thoroughly studied. Surface reflectance usually changes with time due to surface deterioration and dust or dirt sticking to the surface. Important parameters are location and weather. The purpose of this study is to investigate the effect of highly reflective materials for building metal walls, which may lower surface temperature and make fatigue resistance of sealants better because of the less thermal movement.

METHOD

Heat Transfer Simulations

Numerical simulation was carried out with the simulation tool WUFI 1D [7] in order to investigate the relationship between surface temperature and optical properties of an exterior wall faced toward south in Tokyo, Japan (WUFI is a heat and moisture simulation tool, but in this work only heat transfer was simulated). Fig 1 shows the simulation model and material properties. This composition is typical for an external metal wall in Japan. The main aim of this simulation is to consider the influence of optical surface properties on the surface temperature of the wall. As this was simulated with a 1D program, the metal frame to hang aluminium panels in the air layer was neglected. Total external surface coefficient was set to be 17 W/(m^{2}K) in summer and 23 W/(m^{2}K) in winter. Total internal surface coefficient was set to be 8 W/(m^{2}K). The U-value of the simulated model was calculated to 0.68 W/(m^{2}K). Simulation duration was set to 2 days in summer (9 - 10th of August 2012), winter (9 - 10th of February 2012) respectively. The each second day was analyzed in order to exclude the influence of the initial temperature. The initial temperatures at both exterior surface and interior surface were set to be 20 °C. The analyzed days were those with the temperature range of 26 - 33 °C in summer and 3 - 8 °C in winter. Interior was maintained at 21 °C.

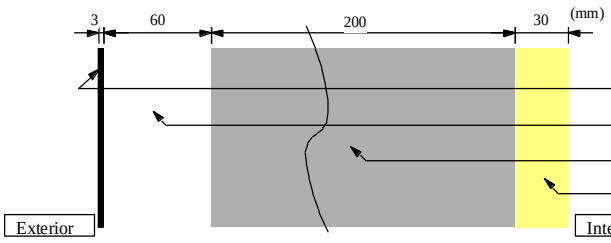

Material	Mass density (kg/m^3)	Specific heat capacity (J/(kgK))	Thermal conductivity (W/(mK))	Water vapor diffusion resistance factor (-)
Aluminum panel	2 700	900	237	15x10^6
Air layer	1.3	1 000	0.337	0.15
Concrete	2 300	850	1.6	180
Polyurethane	40	1 500	0.03	50

Figure 1: Simulation model and material properties.

Sealant Fatigue Resistance

Figure 2 shows the sample used for the fatigue test and FEM simulations. Sealant of two-component polyisobutylene was used after curing according to the sealant manufacture specification. For the sealant section, the width was set to 12 mm, where the depth was 12, 18, 24, and 36 mm. Three samples were made and tested (simulated) at a constant temperature of 20 °C for each size of the sample. The fatigue load was a cyclic load. For every 2 000 counts of fatigue load, the sealant of each sample was checked by observing whether cracks had occurred or not. When the depth of a crack became more than 2 mm, the counts of fatigue load (hereinafter referred to as crack count) were recorded and the fatigue test was terminated. The magnitude of deforming to expansion or shrinkage was set to 30 % of width, because the tested sealant was designed and produced to perform to resist against movements up to 30%

of width. Furthermore, in order to evaluate internal stress in each sample during the fatigue test, the maximum principal stress caused by the sealant shrinkage was calculated by input of optional deformation toward the direction of sealant shrinkage as using FEM simulation tool, Femap with NX Nastran [8]. Young's modulus was calculated from the stress-strain curve of tested polyisobutylene sealant, when strain was 30 % toward the direction of sealant shrinkage.

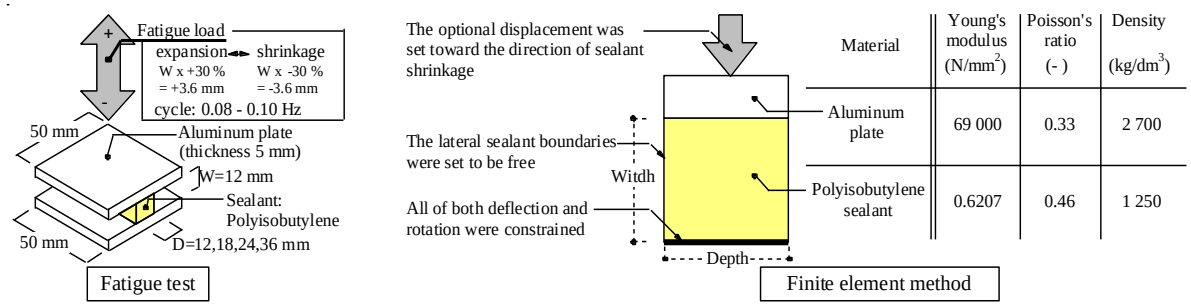

Figure 2: Fatigue test and finite element method for sealants.

RESULTS AND DISCUSSIONS

Heat Transfer Simulations (Effect on Temperature)

Figure 3 shows the maximum temperature of outdoor wall surface in summer and winter as a function of emissivity and reflectivity of the outer facade surface. When solar reflectance of outermost surface was increased from 0.1 to 0.7, the temperature of the outdoor surface was decreased from 47.3 to 34.8 °C in summer and from 36.5 to 16.6 °C in winter, respectively. When solar reflectance is high, the temperature of the outermost surface does not change with emissivity as long as the solar reflectance remained the same value. When solar reflectance was lower, the wall component could get more heat gain from solar irradiation. Maximum temperature in summer was always higher than in winter at the same solar reflectance. That is, the ambient temperature influences the maximum temperature of exterior wall surface predominantly.

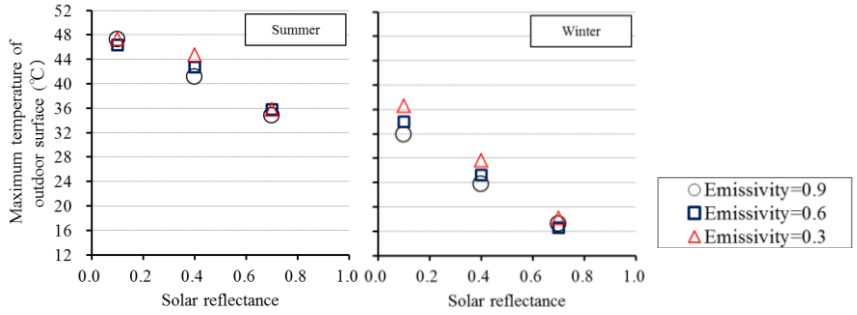

Figure 3: Temperature of outdoor surface related to solar reflectance and emissivity.

The maximum temperature of surface faced toward south for summer and winter were expressed with solar reflectance as the following equations

$$T_{max,summer} = -19.215\rho + 49.431,\ R^2 \text{ (coefficient of determination)} = 0.9366 \quad (1)$$

$$T_{max,winter} = -27.951\rho + 36.834,\ R^2 = 0.9540 \quad (2)$$

where ρ is solar reflectance. Based on simulation results, the temperature difference on outermost surface faced toward south was expressed as following.

$$\Delta T_{out,\,summer} = T_{max} - T_{min} = -17.910\rho + 23.716,\ R^2 = 0.9444 \quad (3)$$

$$\Delta T_{out,\,winter} = T_{max} - T_{min} = -27.356\rho + 31.874,\ R^2 = 0.9812 \quad (4)$$

where T_{max} is the highest temperature of the simulation at outermost surface and T_{min} is the lowest. Solar reflectance could reduce the simulated difference of temperature by about 12 °C in summer and by about 18 °C in winter.

Indication of Sealant Fatigue Resistance

Figure 4 shows the crack count (the uncertainty is expressed as three times the standard deviation of the mean based on three measurement values) and an example result of the FEM simulations. For all samples of fatigue test, sealant cracks occurred near the corner of the sealant section. This fatigue test result was supported by the FEM simulations which show the distribution of stress in FEM was symmetrical around sealant section centre and the largest stress occurred at the sealant section corner. All FEM calculations showed similar results. It was revealed that the cracks during fatigue tests occurred at the largest stress location in the sealant section. That is, all cracks occurred near the sealant section corner, i.e. at the largest stress location. Therefore, crack count was represented, instead of depth/width ratio. The crack count was expressed by FEM results using the largest maximum principal stress caused by the sealant shrinkage to 30 % of width as the following:

$$Crack\quad count = 3.0 \times 10^{14} e^{-79.3\sigma_c} \quad (5)$$

where σ_c N/mm^2 is the largest maximum principal stress calculated by FEM, which is caused by the sealant shrinkage at the sealant section corner. In the fatigue test, crack count can be used as an indicator for the fatigue resistance of sealants. Based on Eq.5, it is possible to assess the fatigue resistance by the FEM calculated stress. However, Eq.5 is applicable only for sealants which are used at a constant temperature of 20 °C.

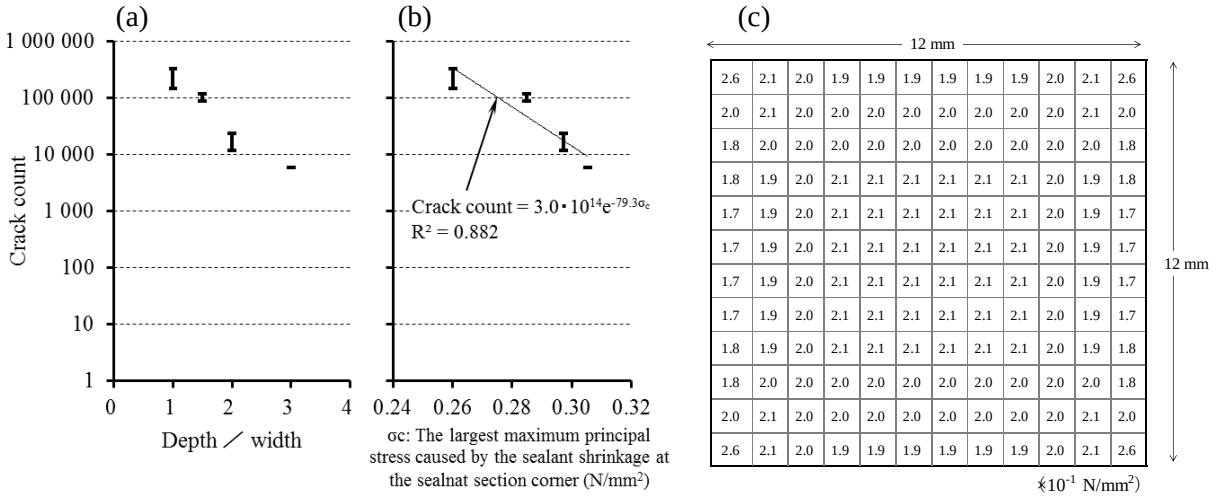

Figure 4: (a) Crack count result of fatigue test with depth/width, (b) Crack count result with σ_c and (c) is an example of σ_c calculated by FEM, where the maximum principal stress caused by sealant shrinkage were shown in a grid by 1 mm.

A Case Study of the Effect to Improve Sealant Fatigue Resistance

The following sealant joint is assumed as a case study model. Sealant type is polyisobutylene, wall components are aluminum whose length is 3 000 mm, wall faces toward south, site is Tokyo, Japan and seasons are considered as either winter or summer. As the sealant is applied

to the gap between two aluminum panels, the thermal expansion of the sealant joint with the aluminum component is expressed as the following:

$$\delta_t = \alpha L \triangle T_{out}(1 - Kt) \tag{6}$$

where δ_t is the thermal expansion (mm), α is the coefficient of linear expansion of aluminum which is 23×10^{-6} (1/°C), L is the length of wall component that is 3 000 mm, $\triangle T_{out}$ is the diurnal difference of outermost surface temperature, and Kt is an empirical value that is stipulated to be 0.2 in Japanese construction techniques [9]. Through three steps, the effect of highly reflective materials to improve durability for the thermal movement of sealant joints is assessed. First step, $\triangle T_{out}$ in winter was assumed as 5, 15, 25 °C and for each $\triangle T_{out}$ in winter, δ_t in winter was calculated by Eq.6. Furthermore, for each $\triangle T_{out}$ in winter, solar reflectance was calculated by Eq.4. Based on the calculated solar reflectance, $\triangle T_{out}$ in summer was calculated from Eq.3. After that, δ_t in summer was calculated by Eq.6. Second step, for each calculated δ_t, the largest maximum principal stress caused by sealant shrinkage was simulated by FEM [8], and then based on the simulated stress, crack count was calculated by Eq.5. Third step, for calculated crack count, the influence to accelerate the ageing deterioration owing to heat and hence increased temperature was added with the following Arrhenius equation[10] :

$$Crack\quad count\quad for\quad heating\quad ageing = crack\quad count \times \frac{e^{\frac{-E}{RT_{lab}}}}{e^{\frac{-E}{RT_{nat}}}} \tag{7}$$

where crack count is the value calculated at the second step from Eq.5, E is the activation energy of sealant that is estimated to 54.531kJ/mol [11], R is the gas constant that is 8.31J/K, T_{lab} is 20 °C. T_{nat} is calculated by the following :

$$T_{nat} = T_{\max,i} - 0.5\triangle T_{out,i} \tag{8}$$

where subscript i means season that is either summer or winter, $T_{\max,i}$ is each season maximum surface temperature calculated by Eq.1 or Eq.2. $\triangle T_{out,i}$ is assumed diurnal temperature difference at first step. Through the above three steps, Fig 5 is drawn. The relationship between crack count for heat ageing and solar reflectance is seen to be linear. That is, the crack count (i.e. the number of cycles before crack occurs) is increasing with increasing solar reflectance as thermal movement is less owing to lower temperature at the outermost surface. The degree of improving fatigue resistance in winter is larger than summer as the decline of diurnal difference of the outermost surface temperature in winter is larger than summer. From Fig 5, it is not possible to estimate how the portion of thermal movement dominates the total durability of the sealants, nevertheless the effect to improve the fatigue resistance depending on thermal movement has been made clear. When solar reflectance is increased by 0.2, the effect to improve fatigue resistance is increased by about 4.5 times in summer, about 7.1 times in winter respectively. These results are limited only to specific conditions of this case study. However, by following the same procedures, it is possible to predict the effect for better sealant fatigue resistance at various conditions. On overall, this discussion focused only on the south wall, i.e. durability is discussed by considering the worst situation. Therefore, highly reflective materials can contribute to improve sealant durability. Other sealant deterioration factors, e.g. moisture, ultraviolet radiation and fatigue caused by wind pressure, are not considered. Hence further work is necessary to estimate how thermal movement affects the total durability of sealants.

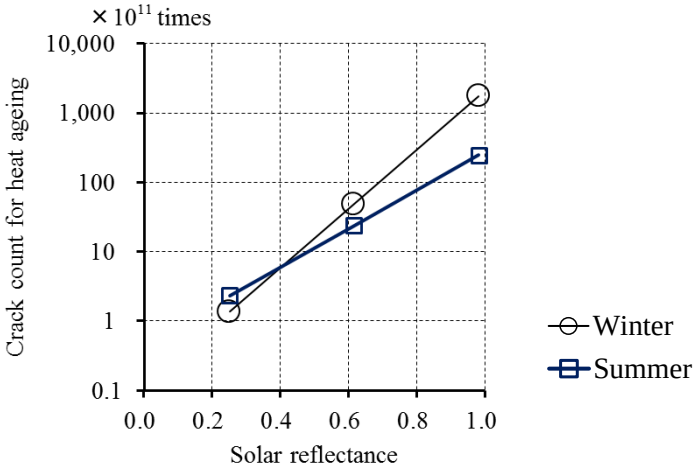

Figure 5: Crack count accounting for heat ageing versus solar reflectance.

CONCLUSION

The effects of highly reflective materials for building walls, which are to keep temperature low and make sealant fatigue resistance better, are represented with the function of solar reflectance of exterior surface faced south, assuming the location of Tokyo, Japan. Highly reflective materials can improve fatigue resistance by several times as comparing to lower solar reflectance materials. These results are limited only to specific conditions of this case study. However, by following the same procedures, it is possible to predict the effect for better sealant fatigue resistance at various conditions. Consequently, highly reflective materials can contribute to improve sealant durability. Other sealant deterioration factors, e.g. moisture, ultraviolet radiation and fatigue caused by wind pressure, are not considered. Hence further work is necessary to estimate how thermal movement affects the total durability of sealants. These effects are useful from the energy efficient point of view because this study implies that highly reflective materials can contribute to less energy and less life cycle cost due to better sealant joints durability.

REFERENCES

1. H. Akbari, H. D. Matthews, "Global cooling updates: Reflective roofs and pavements", Energy and Buildings Vol. 55, pp. 2-6, 2012.
2. Y. Huang, J. L. Niu, T. M. Chung, "Study on performance of energy-efficient retrofitting measures on commercial building external walls in cooling dominant cities", Applied Energy Vol. 103, pp. 97-108, 2013.
3. W. Guo, X. Qiao, Y. Huang, M. Fang, X. Han, "Study on energy saving effect of heat-reflective insulation coating on envelopes in the hot summer and cold winter zone", Energy and Buildings Vol.50, pp.196-203, 2012.
4. M. D. Cheng, W. Miller, J. New, P. Berdahl, "Understanding the long-term effects of environmental exposure on roof reflectance in California", Construction and Building Materials Vol. 26, pp. 516-526, 2012.
5. K. Motohashi, M. Tamura, "Durability evaluation of highly reflective coating materials for roofing", XII International conference on durability of building materials and components, conference proceedings Vol 4, pp. 1891-1898, 2011, Porto, Portugal.
6. A. Synnefa, M. Saliari, M. Santamouris, "Experimental and numerical assessment of the impact of increased roof reflectance on a school building in Athens", Energy and Buildings Vol. 55, pp. 7-15, 2012.
7. WUFI® Pro 5, Fraunhofer-Institut für Bauphysik, Holzkirchen.
8. Femap with NX Nastran, Siemens product lifecycle management software Inc.
9. Architectural Institute of Japan ed, "Japanese Architectural Standard Specification JASS 8 Waterproofing and Sealing (sixth ed) ", Architectural Institute of Japan, 2008.
10. Ding, S., et al. "Polymer durability estimates based on apparent activation energies for thermal oxidative degradation" Thermochimica Acta 367-368, pp. 107-112, 2001.
11. G. K. Kannan, L. V. Gaikewad, L. Nirmala, N.S. Kumar, "Thermal ageing studies of bromo-butyl rubber used in NBC personal protective equipment", Journal of Scientific & Industrial Research Vol. 69, pp. 841-849, 2010.

FAST CALCULATING MULTI-PARAMETER BUILDING OPTIMIZATION FOR EARLY DESIGN STAGES USING THE CLIMATE SURFACE CALCULATION METHOD

Lars Junghans

Taubman College of Architecture and Urban Planning, University of Michigan, 2000 Bonisteel Avenue, Ann Arbor, MI 48109 USA

ABSTRACT

The study presents a fast calculating building optimization method for the early design stages in building renovation. It is based on the Climate Surface calculation method for heating and cooling energy demand calculation. The advantage of the presented calculation method is its short calculation time. The use of this method enables the application of building optimization methods in the early design stages, where optimization methods based on dynamic simulation tools are too time consuming. In the present study, the original structure of the Climate Surface is extended by (1) how the diffuse radiation is calculated and (2) how the influence of the heat transfer is calculated to derive the Climate Surface matrix for cooling.

In this study, the accuracy and calculation time of the Climate Surface method is compared to the dynamic simulation software EnergyPlus. Statistical error indicator methods are used to verify the accuracy of the Climate Surface Method. The equi-marginal building optimization method is applied in combination to the Climate Surface to illustrate its reliable and fast calculation results. Evaluation criteria for the optimization process is the Life Cycle Cost. The results show that the presented optimization achieves reliable calculation results in a reasonable time period for early design stages.

Key Words: Early design stages, building optimization, Climate Surface

1. INTRODUCTION

Large energy demand reductions in buildings can be achieved at early design stages in the planning process through the comparison of different influencing parameter settings for the building envelope and technical systems [1]. When a building is to be designed or renovated, it is often not clear which part of the building envelope or technical system is most effective to renew, improve, or replace. Therefore, a holistic building optimization is the best way to find an economical set of recommendations with the greatest savings [2].

Such algorithms are computationally costly because numerous varying parameter settings must be compared. To meet economic requirements in the early design stages, the algorithm needs to pair a reduced calculation time with reliable precise calculation results.

Optimization algorithms using static calculation methods to predict the energy demand of a building are fast, but do not include building thermal dynamic factors like internal [3]. Also, interactions between different energy demand influencing parameter settings are not considered. Therefore, static calculation methods should not be used for building optimization problems.

To address interacting parameter problems, building optimization algorithms using thermal dynamic building simulation methods, such as DOE2, EnergyPlus, and Trnsys, have been introduced into the scientific community [4]. However, thermal dynamic building simulations are very time consuming because the room condition is calculated for each hour of a reference

year. Building optimization algorithms based on these methods are highly computationally expensive because a large number of simulations is needed to find the optimum.

A promising solution to this dilemma is found in the Climate Surfaces calculation method. This method is a fast energy demand calculating method introduced by Burmeister and Keller [3]. The major advantage of the Climate Surfaces calculation method is that it combines the precision of a dynamic calculation method with a fast static calculation method. The concept is based on dynamic pre-simulations providing climate and building type specific data displayed in a matrix. Once the matrix is calculated, the method does not need weather data information for each hour in the year to predict the energy demand of a building and is therefore much faster than conventional dynamic simulation programs. Employing the pre-simulated matrix, energy demand calculations can be calculated quickly (in seconds) by using only three building specific physical parameters.

In the present study, Statistical Error indicators are applied to verify the results of the Climate Surface method. The method is compared to the thermal dynamic simulation program EnergyPlus. The Climate Surfaces method is combined with a sequential multi-parameter building optimization algorithm to illustrate its calculation speed and performance. The sequential optimization algorithm, based on the equi-marginal principle in microeconomics, is used to find the optimal combination of window type, wall insulation, shading, infiltration and natural ventilation. This approach is tested at a model office building in four climate zones in the United States. Evaluation criterion is the Life Cycle Cost analysis including the Net Present Value [5].

2. METHODS

2.1 Climate Surface Method

The Climate Surface method is a universally valid strategy to predict the heating and cooling energy demand of a room. It is an analytical tool based on the energy balance equation for the calculation of the free run temperature. The idea of the Climate Surface is to extend the heating and cooling degree days used in static calculations, with the dynamic factors of heat gain and internal thermal storage.

To keep the advantages of a fast calculating method in the Climate Surface, the energy balance equation is split into three physical parameters of the building or room: (1) the specific time constant τ, (2) the gain-to-loss ratio γ and (3) the building specific metrological function. The time constant τ and the heat to loss ratio g include fast-to-calculate equations and already include the most relevant parameters for the building optimization. The dynamic metrological function includes external temperature and solar radiation and is calculated in a pre-simulation process as a function of the time constant and the gain to-loss ratio. The energy demand for heating and cooling can be calculated by multiplying the Climate Surface matrix value with the heat transfer value K.

The diffuse radiation is calculated by using the sky model for diffuse radiation on a vertical surface introduced by Perez [6]. The sky model has the advantage over conventional models because it is more precise for the diffuse radiation on vertical surfaces.

The Climate Surface matrix for cooling, which was originally introduced by Burmeister and Keller [3], did not include cooling effects caused by relatively high heat transfer values in time intervals, where the external temperature is below the comfort level. This heat flow is integrated in the here presented Climate Surface matrix for cooling by using an internal load reduction factor.

2.2 Comparison with Energy Plus

The use energy demand for heating and cooling is calculated with the Climate Surface method and the thermal dynamic simulation software EnergyPlus for a test room with identical dimensions and physical properties. The comparison is done for the test room with south orientation in the four locations in the United States. It is calculated for the parameter settings for the building envelope and includes the insulation, infiltration, and glazing type. Each parameter setting is combined to achieve a large variety of data. The parameter settings are listed in Tab.1.

Renovation Strategy			Parameter Settings							
Wall			Not renov.	w U0.76	w U0.5	w U0.38	w U0.30	w U0.25	w U0.22	w U0.19
	U-value	[W/m^{2}K]	1.5	0.76	0.51	0.38	0.30	0.25	0.22	0.19
	Investment	[$ (/1000)]	0	55.6	84.3	113.0	141.8	170.5	199.3	227.9
Shading			Not renov.	internal	external 1	external 2				
	SC	[-]	1	0.45	0.25	0.21				
	Investment	[$ (/1000)]	0	42.4	106.0	169.6				
Glazing			Not renov.	g U2.8	g U2.8	g U1.6s	g U1.6	g U1.2	g U0.7	
	U-value	[W/m^{2}K]	5.20	2.74	2.74	1.57	1.66	1.20	0.70	
	SHGC	[-]	0.72	0.62	0.37	0.31	0.62	0.52	0.51	
	Investment	[$ (/1000)]	0	145.8	145.8	154.9	185.9	241.7	453.6	
Air Tightness			Not renov.	ach 0.25	ach 0.12					
	ACH	[1/h]	0.4	0.25	0.12					
	Investment	[$ (/1000)]	0	5.4	29.6					

Tab.1 Physical properties of not renovated building and building renovation options

The accuracy of the Climate Surface method is determined using the statistical indicators of Mean Bias Error (MBE) and the Root Mean Square Error (RMSE). MBE demonstrates the model's tendency to underestimate or overestimate the outcome of EnergyPlus. RMSE offers a deviation measure from the predicted energy demand calculated by Climate Surface in relation to the values calculated by EnergyPlus.

2.3 Optimization Method

The sequential equi-marginal optimization method (EO) is used as the building optimization method. This method is useful for building renovation because it provides the marginal benefit of the investment of a renovation strategy. It also ranks the recommended renovation strategies according to their reduction of energy demand or Life Cycle Cost. Decision makers are able to find the balance between the long-term Life Cycle Cost and the short-term investment. It is chosen for this study because the results of the optimization process are important in the early design stage where fast calculations are needed.

The equi-marginal optimization method is applied by using energy demand data predicted by the Climate Surface method and the EnergyPlus software. The goal is (1) to compare the calculation time and (2) to compare the recommended renovation strategies.

2.4 Example Office Building

A small office building located on the Central Campus at the University of Michigan in Ann Arbor is used as a reference building.

2.5 Composition of thermal zones

The presented model is designed to operate four pre-calculated Climate Surface matrices. A Climate Surface matrix is prepared for the north, south, east and west orientation. A one-person office room is taken for reference to calculate the Climate Surface matrix for the four

thermal zones of the building. For each parameter study, the heat transfer (K) and the gain (G) is calculated. The total energy demand of the building can be calculated when the area of the thermal zones is known. The heat transfer (K) is extended for rooms with additional area exposed to the external like corner rooms with an opaque sidewall and rooms with an external roof.

2.6 Renovation strategies

The renovation strategies include the replacement of the glazing, the improvement of the wall insulation, the integration of a movable shading device, and the improvement of the façade air tightness. The renovation cost is derived from the commercially available software RSMeans. Table 1 gives an overview of the proposed renovation strategies with the predicted investment cost.

3 RESULTS

3.1 Statistical indicators

Figure 1 a-d) illustrates the comparison of the energy demand values predicted by Climate Surface and the EnergyPlus software. It shows that the deviations are limited for Madison and Ann Arbor for the heating energy demand. The largest deviation can be seen for Houston for the cooling energy demand.

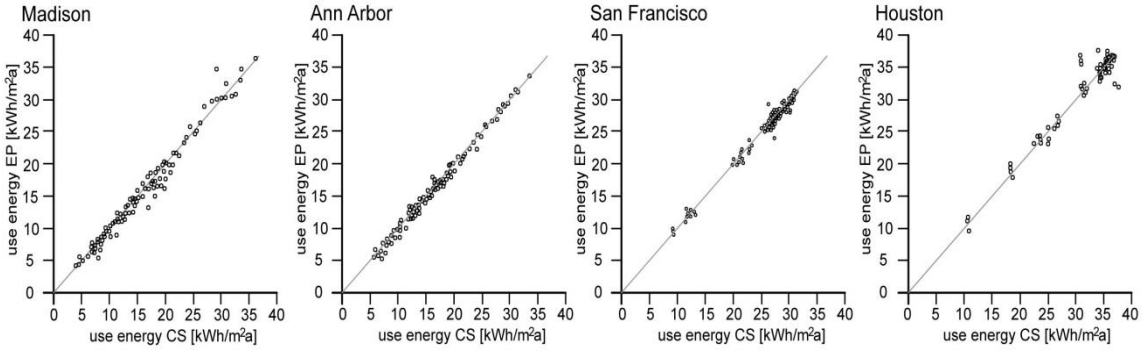

Fig.1 Use energy demand calculated with EnergyPlus and Climate surface method

The Root Mean Square Error (RMSE) indicator illustrates a value of 6.25 for Madison, 4.26 for Ann Arbor, 1.57 for San Francisco, and 4.29 for Houston. The deviation is the smallest in San Francisco. The deviation for the cold climate of Madison is the largest between the two compared calculation methods.

The MPE indicates that the prediction of the energy demand value calculated by CS is underestimated in Madison, Ann Arbor and San Francisco. In Houston the prediction of the energy demand calculated by CS is larger than the calculation of EnergyPlus. The values are illustrated in Tab.2.

Location	Method	Recommend Construction Window U-value [W/m^{2}K]	SHGC [-]	Shading SC [-]	U-value Wall [W/m^{2}K]	Infiltration ACH [1/h]	No. of Simulations	calculation time [sec]
Madison	EnergyPlus	2.8	0.31	0.45	0.5	0.12	78	23.421
	Climate Surface	2.8	0.31	0.45	0.5	0.12	78	312
Ann Arbor	EnergyPlus	2.8	0.31	0.45	0.5	0.12	78	23.423
	Climate Surface	2.8	0.31	0.45	0.5	0.12	78	309
San Francisco	EnergyPlus	2.8	0.31	0.45	0.76	0.25	52	15.632
	Climate Surface	2.8	0.31	0.45	0.76	0.25	52	208
Houston	EnergyPlus	2.8	0.62	0.25	1.7	0.12	65	19.513
	Climate Surface	2.8	0.62	0.25	1.7	0.12	65	260

Tab. 2 Recommended renovation strategies for global optimization with calculation time of Energy Plus and Climate Surface

3.2 Optimization

Table 2 illustrates the global optimal solution for each climate data. Figure 2 illustrates the results of the equi-marginal optimization with the marginal benefit of each investment increment.

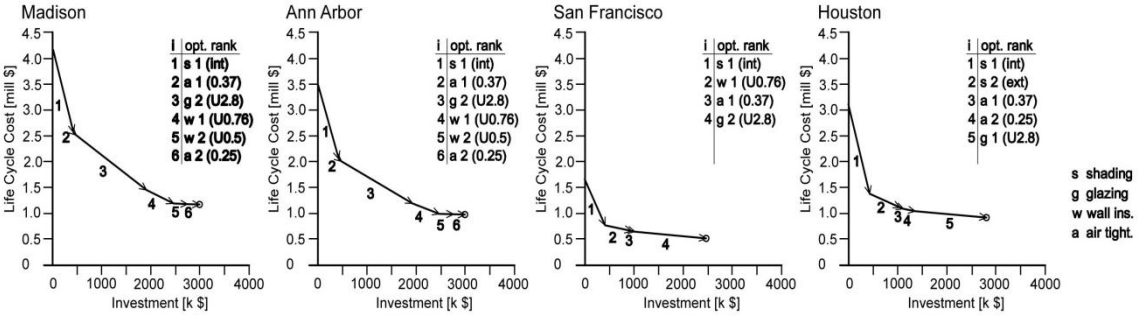

Fig.2 Results of the Equi-marginal building optimization based on the Climate Surface method

For Ann Arbor, as in Madison, the same recommendations were calculated for the most efficient four renovation strategies. The global optimized renovation contains the same renovation strategies in both here investigated cities with mainly heating season. For San Francisco, the most recommended renovation strategy was to add internal shading. The next recommended strategies were to add one inch of insulation, to improve the façade infiltration, and to replace the glazing. These strategies would reduce the LCC, but the marginal benefit of these strategies is diminishing. For Houston, the most effective strategy was to add external shading followed by the building air tightness.

3.3 Calculation time

Table 2 illustrates the recommended building renovation strategies for each location and the computation time of the building optimization method. It shows that both energy demand calculation methods are giving the same recommendations for the building optimization in each climate. For Madison and Ann Arbor, the computation time was 312 seconds for the CS method and 23.420 seconds for the EnergyPlus software. For Houston, with the smallest number of calculations, the optimization calculation needed 19.513 seconds for the CS method and 260 seconds for the EnergyPlus software.

4 CONCLUSION

The Climate Surface energy demand calculation method is compared to the thermal simulation software EnergyPlus. A building optimization method is used to evaluate the climate surface method for accuracy and computation time. The results show that the Climate Surface calculation method delivers accurate results for the heating and cooling energy demand. The computation time for the building optimization is significantly shorter when the Climate Surface method is used. Building optimization based on the Climate Surface calculation method is useful for the application in early building design steps with time constrains.

5 REFERENCES

[1] Schlueter, A., et al., Building information model based energy/exergy performance assessment in early design stages, Automation in Construction, Volume 18, Issue 2, Pages 153–163, 2009

[2] J. Wright, Optimization of Building Thermal Design and Control by Multi-Criterion Genetic Algorithm." Energy and Buildings 2002 34,959-972.

[3] Burmeister H.,Keller B., Climate surface: a quantitative building-specific representation of climates, Energy and Buildings 28 1998 167-177

[4] D. Tuhus-Dubrow,K. Krarti, Comparative Analysis of Optimization Approaches to Design Building Envelope for Residential Buildings", ASHRAE Transactions 2009, 115 554-562.

[5] Marshall H.E., Ruegg, R.T., Principles of Economics applied to investments in energy conservation and solar energy systems, Economics of Solar Energy and Conservation Systems, F. Kreith and R. West, pp 123-173 CRC Press, Boca Raton, FL

[6] Perez R, Ineichen P, Seals R, Michalsky J, Stewart R. Modelling daylight availability and irradiance components from direct ad global irradiance. Solar Energy 1990;44(5):271–89.

[7] R. S. Means. 2005. R.S.Means Residential Cost Data, 24th Annual Edition. Kingston, MA: RSMeans Construction Publishers & Consultants.

DESIGNING REVERSIBLE SEAMS FOR PANELIZED LIGHT-WEIGHT BUILDING SHELL CONSTRUCTION

Dr. J. Ko; L. Widder[2]

1: Rhode Island School of Design 2 College Street Providence RI USA 02903
2: Columbia University The Earth Institute Masters of Sustainability Management 2929 Broadway New York NY 10027 USA

ABSTRACT

Life cycle analysis in buildings argues the need to reuse and/or recycle of as much in-built material as possible. However, typical measures to resist air infiltration in building envelopes rely on mastics and lamination processes, which render envelope components unsalvageable. To address this dilemma, our research considers new strategies for layered building envelope using a multifunctional shell, fabricated in largely bio-based, freely formable materials (ie composite structures with bio-based reinforcing and matrices). Bio-composite panels can resolve infiltration and structural/shear forces in a single layer, reducing material intensity and lowering embodied energy. Panel-to-panel airtight joints can resist infiltration via geometry, not the use of chemical bonding agents. Such joints' reversibility offers greater ability to recapture and reuse building components without waste or downcycling.

Our work on panel-to-panel joints is situated among current studies of joinery and "natural selection" approaches to joint computation; but the form:material reciprocity of composites is fundamentally different. Although reversible joinery leverages the tailoring of composites to localized requirements for strength and flexibility through stranding patterns, this reciprocity between joint form and material engineering creates challenges to formal selection and to prototyping. We are therefore developing alternative computational and typological methods for limiting plausible joint forms in bio-based composites.

Recent affiliated research focuses on the algorithmic generation of joints for optimal resolution relative to structural, material, or fabrication criteria. A common approach is to begin with an initial form-based proposal derived through analogy (ie biomorphic precedents, carpaces) or forms common to traditional mechanical joinery (ie cabinetry). Analysis, such as finite elements modeling, is then used to assess the fitness of each option and to spawn a next generation of prototypes. This ultimately refines the space of options and optimized form.

We adopt the spirit of this approach, but look to different analogies to develop parametric decision trees that can accommodate the interdependent criteria of material and form. For precedents, we seek variants of joinery through involution across materials (ie metal seams, knots, textiles, etc). This paper offers an overview of possible classifications for joint typologies relevant to reversible panel-to-panel joints in engineered materials. Finally, we discuss the design of a decision space for use in identifying the parameters, which will determine the appropriate families of forms.

Keywords: reversible construction, lightweight building envelope, bio-composites, joinery, joint taxonomy

INTRODUCTION

Increasingly, operational energy is recognized as only one of several drivers in "high performance building": material intensity and embodied energy, considered across building and building component lifecycles, must also be included in calculations. Accurate life cycle analysis and the concomitant insight that longer lifecycles offer better ROI on energy and material open the possibility of integrating into the built environment sets of materials that

previously were reserved for other applications for which achieving a high strength-to-weight ratio was of high priority, such as in airplane, sailboat or car production. These include the new generation of largely bio-based composite materials, which permit greatly reduced material intensity while deploying natural fiber reinforcement and soy and other bio-based matrices for improved embodied energy performance.

Advances in digital form engineering offer another boon to building components, allowing for high-precision joinery by milling or forming component edges for fastener-free and mastic-free interlock. To date, this genre of digital form engineering has largely been applied to conventional materials, whose characteristics offer both obvious analogies for seam configuration (e.g. wood joinery) and limiting performance factors to guide digital form-finding processes through "natural selection." Our research develops alternate computational and typological methods for limiting plausible joint forms in the case of materials that can be tailored to localized requirements for strength and flexibility through stranding patterns (i.e. orientation, weft, fiber selection).

Material engineering, an asset to the development of air infiltration-resistant reversible joints, creates obstacles to the adoption of current research focusing on the algorithmic generation of joints for optimal resolution relative to structural, material, or fabrication criteria: the modeling of material performance in environments intended to model forms realized in determinate materials challenges the limits of computation. It necessitates the translation of non-form based criteria into terms that can be understood in available modeling environments. To address this challenge, we have looked to adapt research trajectories developed for joinery in conventional, non-engineered materials.

Nonetheless, the stakes are high for the use of thin-shell, bio-composite construction in the built environment: embodied energy is greatly reduced by light-weighting; building components with appropriately configured joints are reusable, since damage traditionally caused by puncture fasteners or mastics/adhesives is minimized; and the intelligent use of form to integrate response to multiple demands on the building envelope can be maximized.

RESEARCH CONTEXT

The Methodological Context

Digital fabrication has revitalized interest in high precision joinery as a viable method for creating geometrically complex joinery, both structural and ornamental.[1] This interest in joinery often accompanies the ambition to create a geometrically complex panelized structure. A common approach in developing this kind of joinery using conventional building materials is to begin with an initial form-based proposal derived through analogy (i.e. biomorphic precedents, carapaces)[2] or forms common to traditional mechanical joinery (i.e. carpentry, cabinetry, sewing).[3] Analysis, such as the use of finite elements modeling to test structural capacity, is then used to assess the fitness of each option and to spawn a next generation of candidate solutions. This ultimately leads to a refinement of the space of options which can in turn be realistically prototyped and tested. The direct adaptation of these methods to the development of composite joints is not straightforward: composite material properties are variable rather than given whereas formal selection methods typically hold material constant; simulation of material performance within current computational environments requires inputting ranges for material properties which is difficult to a priori quantify; prototyping usually depends on scaling laws and material substitution which is not well supported for composites.

An approach more well-suited for designing composite joints needs to address the highly interdependent relationship between material, form and the mechanical action responsible for fastening and unfastening. Towards this aim, we present a new classification and evaluation system comprising the following components:

1. *Establishing an appropriate taxonomy for reversible joint design.* This involves identifying factors by which a class of joints can be characterized. In our case, these hold primary function (reversibility) constant while traversing material, shape and mechanical properties. Performance and architectural expression may be neutral or conventional.

2. Developing graphical visualizations which can map relative characteristics. These representations are the basis for strategies to identify plausible joint forms in composites as well as for design interfaces that will allow designers to prototype with confidence in the performance of the fabricated end-product.

DEVELOPING A NEW CLASSICATION AND EVALUATION SYSTEM

An Alternate Classification and Evaluation System

Engineered materials can be keyed directly to the forms of the joint, and to the mechanical action which activates the joint in order to optimize performance. The need to consider simultaneously the way in which form, mechanical action and material properties all contribute to a joint's performance requires that all of these three areas of criteria be understood reciprocally. The development of an appropriate classification system is tantamount to the establishment of a precise language in which to frame the design of a new high performance joint, including its material specifications. Ultimately, our goal is to recognize the material-shape-mechanical action reciprocities that can produce a predictive system for reversible joint design, which operates in the more familiar and powerful computational space of parametric form-finding. While the system here is for the family of reversible joints, the process utilized to develop this system has general applicability.

Identifying and Mapping Relative Characteristics

We begin by considering existing reversible joints to understand the key characteristics that contribute to their ability to perform in their intended contexts. Zippers were identified for their strength in resisting force perpendicular to the joint. Ziplocks offered air and watertightness, despite their weakness to force applied perpendicular to the joint line. Snaps, press-fit systems, binder clips, fastener-free wood joinery, and overhand seams and bindings completed our initial family of reversible joints for study. Each joint or genre of joints had to be described in terms that revealed salient differences and similarities across genres. Because material performance, the mechanical action, which activates the joint, and the shape, which facilitates joinery represent the parameters governing the design of our new joints, we decided to use the three as the categories to organize the distinguishing criteria. These criteria and the questions they were designed to answer are as follows:

Category	Properties	Questions addressed
Material Properties	Texture/grain	Is the material stranded or grained? Is it directional? Is this decisive for the joint?
	Rigidity/Shape-holding	Is the material's resistance to force exerted on it decisive for the joint's performance?
	Pliability/Flex	Is the material's ability to flex decisive?
	Tensile or Compressive	Are the material's tensile or compressive properties vital for the joint?
Shape-based Properties	Friction-producing	Is the shape formed to allow for a pinched or friction connection?
	Snap	Is there a shape element that includes male/female or flair/pinch to allow for a snap?
	Pressure-sensitized	Are there such things as ridges, velcro-like hooks, etc that respond to pressure only to make a seal?

	Interlock	Do the two joined pieces interlock as in a tongue and groove?
	Involution	Do the two joined pieces wrap around each other when put together?
Mechanical Action	Deformation	Does the method of joining rely on deformation?
	Self-arresting	Do the parts come to a complete stop?
	Linear	Is the joint continuous along an edge?
	Punctual	Is the joint in series or at a point?
	Penetrating	Does the joint require mechanical fasteners or threads that penetrate the two panels to be joined?

This classification system is intended for use by the architecture and design community so the characteristics are intentionally articulated in a way that can appeal to the intuitive mind. In order to test the power of these characteristics, however, we needed a visual representation that would allow a joint to be mapped against all fifteen variables in a way that could be used to readily make comparisons among precedent joints, reveal dependencies between certain characteristics, and help to identify affinities across different joint genres.

Using Spider Graphs to Define Promising Avenues of Formal Exploration

Because of their ability to depict multifactorial relationships, we use spider graphs to compare precedent joints whose values could be empirically asserted. The categories listed above were translated into radial axes and precedent joints were mapped as shown in Figure 1.

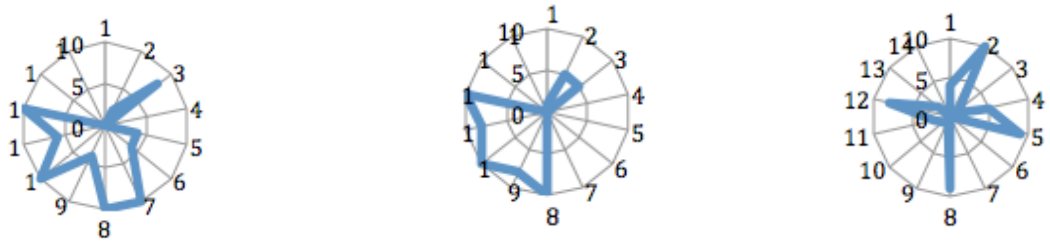

Figure 1: From left to right, spider graph results for a ziplock, a zipper and a scarf joint; axes 8 and 9 represent interlock and involution respectively; 2 and 3 are shape-holding and flex.

By mapping joints that traverse characteristics, these graphs reveal similarities that transcend material in order to help distill salient qualities common to all reversible joints. The emergent reciprocity between characteristics observed in several precedent analyses also indicated promising avenues for future research. For the cases shown in Figure 1, for example, three joints, which use completely different materials and mechanical actions, were compared. The ziplock takes advantage of flexible plastic extrusions to create an interlocking press-lock seal; in the closed position, the two opposing extrusions also involute to give the seal additional air-tightness and resilience. This seal relies to some extent on the material's flex, which allows the extrusions to move out of plane when pressed together, but it relies even more so on the material's ability to hold its shape. The zipper, a hybrid of a rigid (metal) and a flexible (textile) material, creates its seal by virtue of a staggered interlock along the zipper's length, and an involuted male/female seal between teeth. The scarf joint requires only minimal flex from wood, the material for which it was developed; its holding capacity derives almost exclusively from involution, in which the two members wrap around each other, although some penetrating fasteners may be required to hold it in place.

Although advantageous in some respects, this representation has two main shortcomings, both of which limit the tool's use for design purposes: the first is the problem of quantifying salient joint characteristics numerically; the second is the unwieldiness of an excessively large number of variables.

Initial Strategies for Moving from an Analytical to a Design Tool

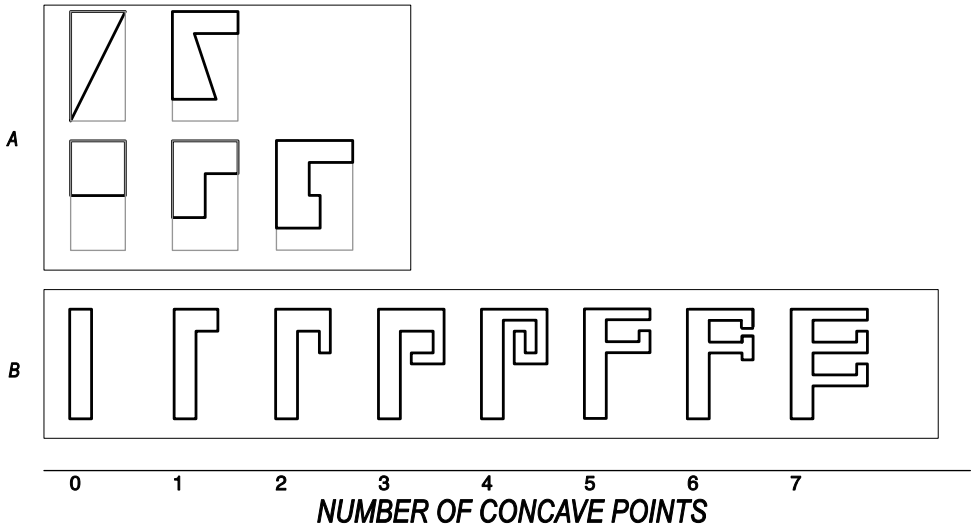

Figure 2: Concavity as a metric to quantify involution. A. Scarf and Dado joints B. A sequence of zip-type joints that includes the zipper and the ziplock.

Addressing the shortcomings of the spider graphs compelled us to develop other methods, which are useful representations in their own right. To make the numerical rankings more precise required translating the characteristics into properties that can be quantified and yet still possess a visual and intuitive quality. An example of this is the characteristic of involution. The geometric property of concavity is a readily quantified characteristic of a geometric figure: a concave point on a plane polygon, for instance, is one in which the interior angle is greater than or equal to 180°. We chose to test the capacity of concavity to measure involution, a quality which the initial spider graphs showed to be significant and recurring for many reversible joints. Figure 2 shows a number of joints represented as plane polygons ordered by the parameter of number of concave points. This diagram not only traverses material and joint genres but also shows natural progressions in joint shape. In fact, the sequence of zip-type joints interpolates between a zipper (1 convex point) and a zip-lock (7 convex points) and shows joint shapes that go beyond existing ones while maintaining other key characteristics. Being able to systematically open up the plausible design space is an important initial step in applying many of the methods in parametric form finding.

The morphology developed to quantify involution also moved us closer to translating all salient characteristics into the language of formal evaluation. In a design context, this allows form to shorthand particular mechanical and material behaviors. The sequential depiction of convexity as a morphological property of reversible joints also offer additional insights about the developmental nature of design from precedents.

To address the problem of an unwieldy number of variables, we focused on only two salient characteristics revealed by the spider graphs to have reciprocity. We used graphs in two dimensions to describe these insights about the unexpected affinities found across joint and joint genres. Recognizing these affinities can in turn support the designation of which particular formal categories can predict appropriate performance in reversible joints, and suggest metrics for comparing characteristics which traverse joint genres. As on-going research reveals further related characteristics, additional criteria for such low dimensional graphs can be mapped. The resulting clusters of like joints can again point to ways to short-hand material and mechanical performance, and to create a design vocabulary adequate to the task of creating material performance specifications while also generating formal properties.

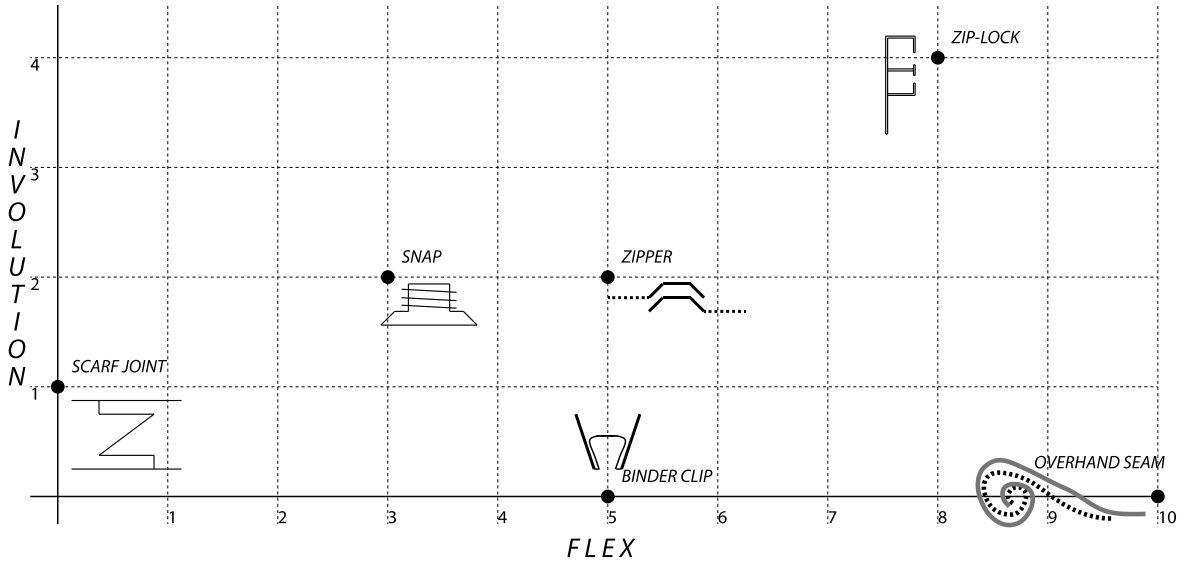

Figure 2: Illustrated graph of reversible joints relative to flex (x-axis) and involution measured in terms of the geometric property of convexity (y-axis). The distribution of reversible joints across the chart demonstrates both unexpected affinities across joint genres and limits to reversibility based upon material rigidity/flex: the rigid scarf joint in wood and totally flexible seam in textiles both require ancillary penetrating fasteners, whereas all the other joints depicted are self-arresting.

CONCLUSIONS AND FUTURE AVENUES OF RESEARCH

As designers have become increasingly comfortable with methodologies developed in response to the potentials of digital fabrication, it behoves us to remember that the "black box" of multifactorial digital calculation bears the direct imprint of the syntax and structures upon which it draws. By moving our design research into a realm in which the number of variables becomes unwieldy for existing methodologies, we have uncovered the need for a new taxonomy that can extract from specific precedents the predictive characteristics from which to derive a design that neither mimics solutions borrowed from other material, formal and performative contexts, nor taxes the limits of empirical and intuitive design. The examples enumerated here are the first of what will doubtless become a whole family of methodological avenues; the test of their efficacy will be the successful production of high-performance, reversible joints for use in a durable, resource-parsimonious panelized envelope system made from engineered materials.

REFERENCES

1. Eigensatz, M., and Schiftner, A.: 2011, Case Studies in Optimization of Glass-panelized Architectural Freeform Designs, in Glass Performance Days Conference Proceedings: Glass and Solar in Sustainable Development, pp. 371-376
2. Knippers, J., Menges, A., Gabler, M., La Magna, R., Waimer, F., Reichert S., Schwinn, T.: 2012, From Nature to Fabrication: Biomimetic Design Principles for the Production of Complex Spatial Structures, in Hesselgren, L., Sharma, S., Wallner, J., Baldassini, N., Bompas, P., Raynaud, J. (Eds.), Advances in Architectural Geometry 2012, Springer Wien New York, pp. 107-122.
3. Ruffo Calderon, E., Schimek, H., Wiltsche, A.: 2011, Seeking Performative Beauty, in Proceedings of the 31rst Annual Conference of the Association for Computer Aided Design in Architecture, ACADIA: Integration through Computation, pp. 300-307

MONITORING THE HYGROTHERMAL PERFORMANCE OF HEMP-LIME BUILDING IN FRANCE

B. Moujalled; D. Samri; F. Richieri

CETE du Sud-Ouest, Rue Pierre Ramond, CS 60013, 33166 Saint-Médard-en-Jalles Cedex

ABSTRACT

Within the framework of the sustainable development, there is an increasing interest in using vegetal fibre materials in construction in order to obtain high environmental quality buildings. The use of hemp concrete (HC) corresponds perfectly to this requirement in new as in renovated buildings. However, there are few works about its hygrothermal performance in real conditions at the building scale.

This paper presents a field study of transient hygrothermal behaviour of a hemp-lime building, located close to Perigueux in South West to France. A protocol measurement has been defined. First, the envelope is examined through air tightness test combined with infrared thermography survey in order to detect thermal defects and air leakages. The North and West-facing walls are instrumented for hygrothermal performance monitoring. Relative Humidity and Temperature (RH/T) sensors are embedded at two depths which allowed temperature and humidity profiles through the wall to be measured over time. Thermocouples are also attached to the internal and external faces. Moreover, RH/T sensors for indoor air have been placed in different rooms in order to evaluate thermal comfort. Weather station is installed near to the house to measure outside temperature and humidity.

Data presented in this paper relate to the period between February and October 2012. Thermographic results show that this construction technique promotes minimal thermal bridging within the building envelope. The dwelling's airtightness level is low, due to leakages located at gaps between envelope elements (wall/roof, wall/wall). In situ monitoring of walls confirms the ability of hemp concrete to almost completely (95%) dampen variations of external temperature with a time shift of 10 hours. Internal relative humidity is maintained at a remarkably stable level, well within the range of good comfort levels for occupants.

Keywords: Hemp concrete, hygrothermal performance, in-situ measurements, thermal comfort, thermal and hygric damping, building envelope airtightness, infrared thermography

INTRODUCTION

In the context of sustainable development, one of the concerns in building construction is the choice of environmentally friendly materials. Indeed, it has some impacts on exhaustion of natural resources, energy consumption (for heating, cooling), and polluting emission. This study deals with hemp concrete (HC) that is told to have a low impact on environment as it is made of hemp shiv (renewable raw) and of lime (lower embodied energy than cement) [1]. HC is characterized by a very important porosity (more than 70% in volume for a ''wall'' mixture) and thus it has low dry density (around 400 $kg.m^{-3}$ for a "wall" mixture). It shows low compressive strength so, it is mainly used as filling material associated with a wooden frame. From a hygrothermal point of view, hemp concrete shows low thermal conductivity (about 0.1 $W.m^{-1}.K^{-1}$), so it can be used without an added insulation layer. The hydric characterization of HC shows high moisture transfer and storage capacities. It was emphasised that this material is an excellent hygric regulator [2].

The researches done until this day allowed us to determine HC physical properties under controlled conditions in laboratory [2, 3]. Numerical studies have shown that its transient hygrothermal behaviour allows reducing energy demand of building while maintaining comfortable indoor relative humidity [4, 5]. However, these last studies are based on experimental data of sorption curve and water vapour permeability; and it was shown that the uncertainty on this kind of data hamper reliable simulations of hygroscopic buffering. There are few works about its hygrothermal performance in real conditions at the building scale.

In order to predict the real hygrothermal behaviour of this material, this paper presents a field study of transient hygrothermal behaviour of a HC building, located close to Perigueux in South West to France. The main objective is to look for more realistic thermal and hydric characterization of hemp concrete at building scale and under real variable climatic conditions.

METHOD

Description of the HC building

The construction is a 2-floor single-detached dwelling that hosts 4 people and has a surface of 250 m^2 (Figure 1). It is located close to Perigueux in South West to France. Its envelope is made of 30cm thick HC sprayed into walls of timber frame structure. HC is also used in roof and intermediate floor in 10cm and 15cm thickness respectively. The walls are internally and externally protected with lime-sand plasters. The properties of the materials are presented in figure 1.

A pellet boiler coupled with 12.6 m^2 of solar collectors provides energy for heating and domestic hot water. The heat is distributed in the house through radiant floor at the ground level and radiant walls at the top level. A balanced ventilation system with heat recovery is used for air renewal.

Material	**Density ($kg.m^{-3}$)**	**Thermal conductivity ($W.m^{-1}.K^{-1}$)**
HC in walls and floor	450	0.100
HC in roof	220	0.060
Lime-sand plaster (exterior and interior finishing plaster)	935	0.190
Lime-sand plaster (exterior coarse)	1200	0.240

Figure 1: View of the south façade of the building on the left panel and thermal properties of hemp concrete and plasters on the right panel.

Building envelope inspection

Thermographic survey and air tightness test have been conducted in order to evaluate the envelope performance. The thermographic inspection helps to detect insulation defects, especially thermal bridging that may occur due to the timber frame structure. The air tightness test helps to evaluate the level of air permeability, and to detect the air leakages through the envelope.

The thermographic survey is done using the FLIR Thermacam E4 infrared camera, and the air tightness testing with Blowerdoor Minneapolis system according to the standard NF EN 13829 [6].

Hygrothermal measurements of indoor climate

In order to evaluate the thermal comfort, 8 Hobo data loggers monitor the air temperature and relative humidity in each room of the house. Data are recorded every 15 minutes.

Hygrothermal measurements of HC walls

Temperature (T) and Relative Humidity (RH) monitoring is done for the West and North-facing walls of the home cinema room. The North-facing wall is sunless; it is monitored for comparison purposes with the West-facing wall. Both walls are made of 30cm of HC, and 3cm of exterior lime-sand plaster. They are uncoated at the interior surface. Each wall is monitored as shown in figure 2.

Two T/RH sensors (type S-THB-M008 from Onset) are placed within the wall at two different depths (15 and 25 cm from the interior surface). The sensors are 12 mm diameter and are inserted into the wall through drilled holes at the specific depths. Once the sensors placed within the wall, the holes are sealed with acrylic sealant. Two thermocouples (type TMC6-H from Prosensor) measure the interior and exterior wall surface temperatures. The thermocouples are fixed with adhesive tape. The indoor air temperature and relative humidity of the home cinema room are measured with a Hobo data logger. A weather station located near to the house measures the outdoor air temperature and relative humidity.

All data are monitored continuously from February 2012 with a time step of 15 minutes.

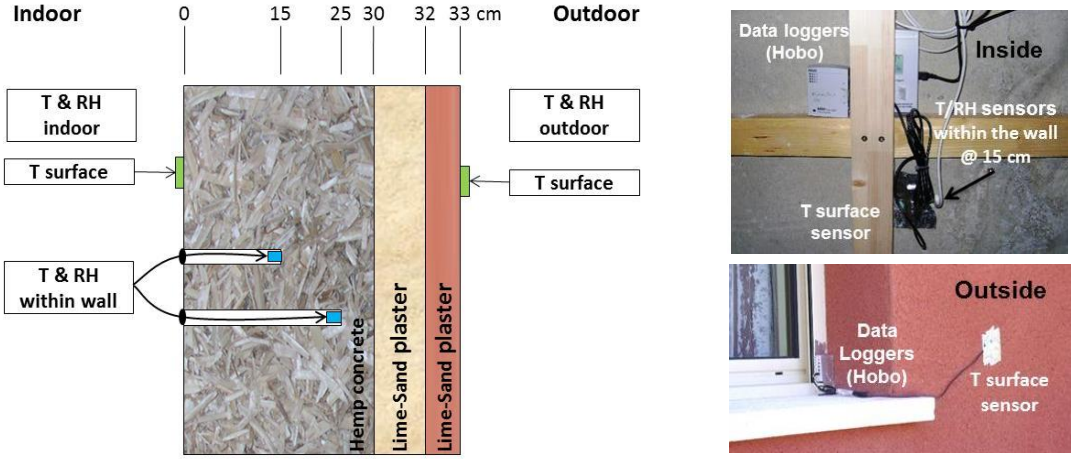

Figure 2: Location of temperature and relative humidity sensors for the monitored walls.

RESULTS

Building envelope performance

The thermographic inspection was performed during February 2013 with covered sky, and adequate temperature differential of 22°C between the interior and the exterior. Figure 3 shows the thermographic image of the exterior surfaces of the north/west corner of the house. The walls of the floor level are heated as being radiant walls. The exterior surface temperatures are clearly homogeneous. We don't observe any structural thermal bridges due to the timber frame covered with the HC walls.

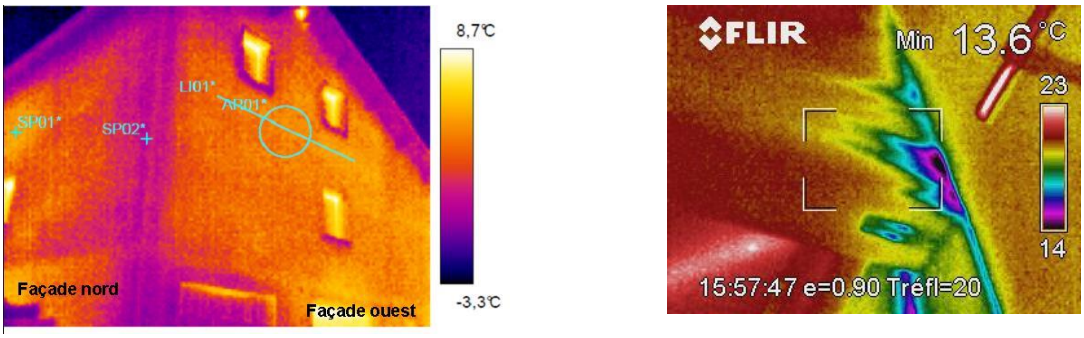

Figure 3: Thermogram of the north and west facades of the building on the left panel. Thermogram from the inside showing air leakages at joints between structural elements on the right panel.

The airtightness test indicates a poor result with an air permeability of 1.32 $m^3.h^{-1}.m^{-2}$, more than twice as the French mandatory level (0.6 $m^3.h^{-1}.m^{-2}$ for dwellings). This can be explained by the shrinkage of the timber frame structure which created gaps at the joints between the frame elements and interior finishing of the walls. Right thermogram of figure 3 shows air leakages at the joints between structural elements.

Thermal comfort analysis

Monitoring results are presented hereafter between February and March 2012 for winter conditions, and between June and September 2012 for summer conditions.

During winter, indoor air temperatures vary between 20 and 24°C with a mean of 21.5°C at the ground level, and 22.5°C at the floor level. Values of relative humidity vary between 25 and 45% with a mean of 35%. During summer, temperatures vary in a wider range from 21°C to 28°C, with a mean of 23°C at the ground level and 24°C at the floor level. Values of relative humidity vary between 40 and 60% with a mean of 55%.

Figure 4 shows the coincidence of the measured psychrometric data and the comfort zones for the living room. The limits of the comfort zones are issued for the standard NF EN 15251 [7]. During winter, T and HR values were in the comfort zone almost all the time (98% of the time). T exceeded sometimes 24°C because the heating systems weren't properly regulated. During summer, T and HR values were in the comfort zone for 55% of the time, but this was because the living room was too cold rather than too hot. T exceeded 26°C during only 2% of the time. However, HR slightly exceeded the upper limit of 60% (18% of the time).

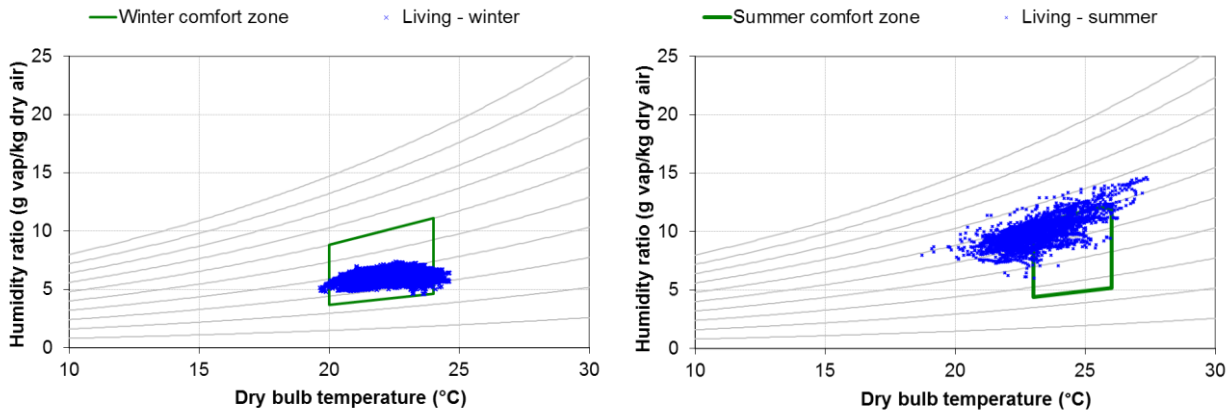

Figure 4: Coincidence of measured psychrometric data with winter and summer comfort zones.

Hygrothermal behaviour of the West wall

Monitoring results of the West-facing wall are presented hereafter for the three coldest days of the winter and the three hottest days of the summer. The sunless north-facing wall presents the same conclusion as for the West-facing wall.

Figure 5 presents the measured T and RH from 5 to 8 March 2012. The indoor air temperature is maintained at 20°C due to the heating system, and the outdoor air temperature varies between -5°C and 10°C. The exterior surface temperature of HC wall follows the variation of the outdoor T reaching a high peak in the afternoon due to the solar exposure. While the amplitude of the exterior surface T reaches more than 20°C, the temperature within the wall (corresponding to 15 cm of HC) varies in a narrower range of 1°C with an average of 15°C. Besides we observe a time shift of 10 hours between the peaks. This means that T within the wall increases when the outdoor T is the coldest. As for T, HR of indoor air and within the wall are stable (40% and 80% respectively), while the outdoor HR varies from 40% up to 100%.

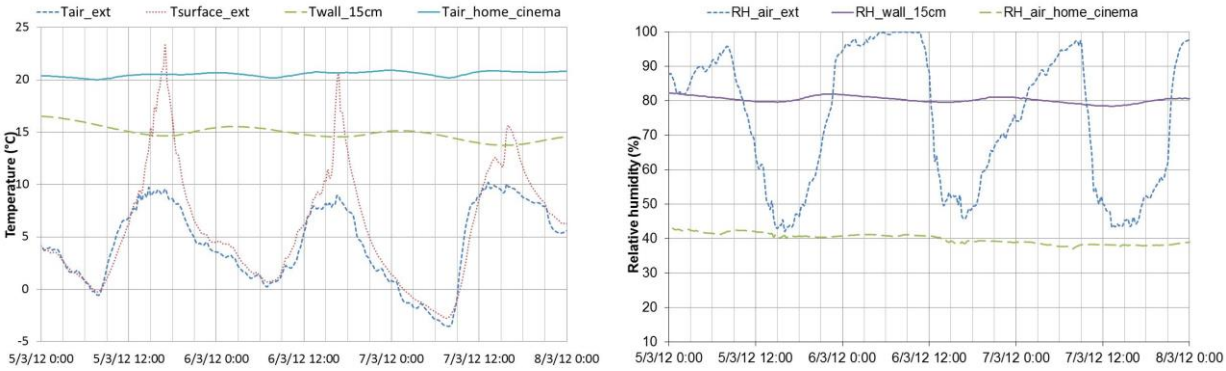

Figure 5: Temperature and relative humidity within the wall from 5 to 8 March 2012.

Figure 6 shows the measured T and HR for summer conditions. The results are the same as above. While the outdoor T and HR vary in a wide range (up to 55°C for the exterior surface T), the variations of T and HR within the wall are limited to 2°C and 4% respectively.

The HC wall shows a high damping capacity (above 90%) and time shift up to 10 hours. These results are in accordance with those obtained by Evrard [5]. However, HR values within the wall are slightly high and need to be further examined in order to evaluate the risk of mold development.

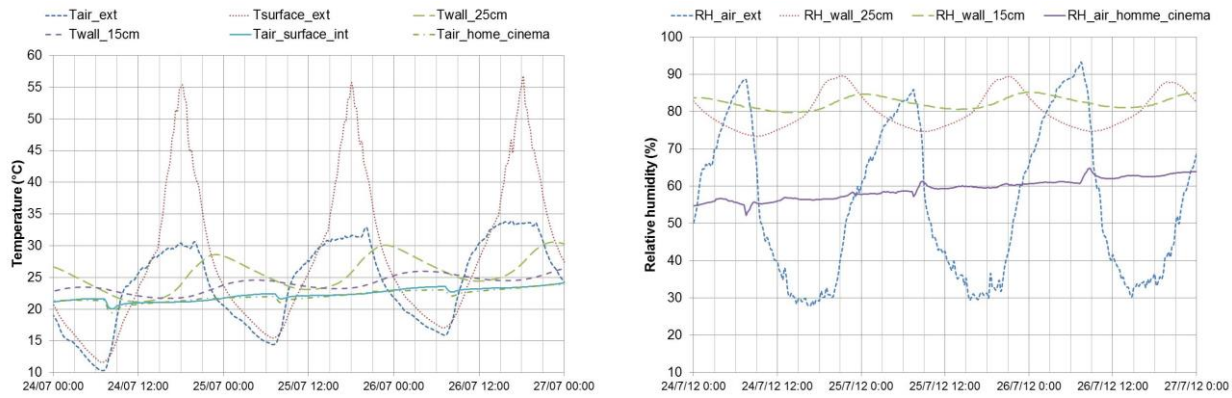

Figure 6: Temperature and relative humidity within the wall from 24 to 27 July 2012.

CONCLUSION

In this paper, we presented a field study of hygrothermal behaviour of a hemp-lime building located in South-West to France, in order to evaluate the transient hygrothermal behaviour of HC under real conditions.

Building envelope inspection showed a good level of insulation for the 30 cm thick HC walls with homogeneous temperature at the exterior surfaces. However, the shrinkage of the timber frame structure created gaps at the joints between the frame elements and interior finishing of the walls. Due to air leakages at these locations, the result of the envelope air tightness test was poor.

The in-situ monitoring of the building has confirmed the ability of HC to maintain hygrothermal conditions at winter and summer comfort levels while outside T and RH daily variations are up to 15°C and 50% respectively. The measurements within the HC walls showed a high inertia which allowed them to dampen the daily variations by 90% and to delay the effects of peak values up to 10 hours. However, HR values within the wall are slightly high and need to be further examined in order to evaluate the risk of mold development.

The monitoring will continue until the end of May 2013 in order to cover a full heating season. Simulation works are actually in progress with TRNSYS and WUFI. The experimental results will be used to compare them with simulation results.

ACKNOWLEDGEMENTS

This work has been financed by the French Ministry of Sustainable Development. The sole responsibility for the content of this publication lies with the authors. It does not necessarily reflect the opinion of the Ministry. The authors thank DB Chanvre Company that provided this construction.

REFERENCES

1. Boutin, M.P., Flamin, C., Quinton, S., Gosse, G.: Analyse de cycle de vie de Compounds thermoplastiques chérgés fibres de chanvre et Mur en béton de chanvre banché sur ossature en bois. Technical report, INRA Lille, 2005.
2. Samri, D.: Analyse physique et caractérisation hygrothermique des matériaux de construction : approche expérimentale et modélisation numérique. INSA de Lyon, Lyon, 2008.
3. Colinart, T., Glouannec, P., Pierre, T., Chauvelon, P., Magueresse, A.: Experimental Study on the Hygrothermal Behavior of a Coated Sprayed Hemp Concrete Wall. Buildings, vol. 3, n°1, pp 79-99, 2013.
4. Evrard, A., De Herde, A.: Hygrothermal performance of lime-hemp wall assemblies. Journal of Building Physics, vol. 34, pp 5-25, 2010
5. Tran Le, A.D., Maalouf, C., Mai, T.H., Wurtz, E., Collet, F.: Transient hygrothermal behaviour of a hemp concrete building envelope. Energy and Buildings, vol. 42, n°10, pp 1797-1806, 2010.
6. NF EN 13829: Determination of air permeability of buildings - Fan pressurization method. AFNOR, Paris, 2001.
7. NF EN 15251: Indoor environmental input parameters for design and assessment of energy performance of buildings addressing indoor air quality, thermal environment, lighting and acoustics. AFNOR, Paris, 2007.

BUILDING PRODUCTS: BEYOND OSTENSIBLE SUSTAINABILITY

I. Oberti

Dept. Architecture, Built Environment and Construction Engineering (ABC) - Politecnico di Milano, ilaria.oberti@polimi.it

ABSTRACT

It was not that long ago when the term green building product did not mean anything in particular other than an ambiguous, but consoling, idea that the product was somehow less harmful to the environment and to people.

Often, however, the lack of clear definitions and standards has supported the sale from many companies of so-called environmentally friendly products, cleverly disguised as green product thanks to an unscrupulous marketing, helping to spread the phenomenon of green-washing.

The objective of this paper is to shed light on the evolution that the concept of environmentally friendly building product has undergone, going beyond the appearance to became concrete due to the following measures:

a. to define unequivocally, and in a more easily verifiable way, whether a product is environmentally friendly or not. This first section deals with the transition from a few criteria, that only a decade ago were considered sufficient to determine the greening of a building product, to the present necessity to have a more refined set of criteria, especially shared. The convergence on shared criteria is fundamental because of the spread of several rating systems which verify the ability of a building to meet the requirements of sustainability.

b. To provide the criteria of certification and to avoid green-washing. The process of environmental product certification is driven, at the international level, by the Technical Committee TC 59, in Europe, by Technical Committee CEN / TC 350, with the development of a set of standards, whose objective is to harmonize the different building environmental assessment tools and to integrate the Environmental Product Declaration (EPD). Recently, the standard EN 15804:2012 was issued to outline the key Product Category Rules (PCRs) for the development of Type III environmental declarations (EPDs) relating to products and services in the construction sector. Interesting in this context is also the work of an American teamwork, whose target is the elaboration of a Health Product Declaration (HPD) to be integrated with the EPD, in order to complete the information of a product relatively to the environmental and human health impacts.

c. To rehabilitate the role of chemistry, that was considered, not long ago, as hostile to the green product. In this last section, the attention is focused on the great work that has been taking place in recent years, at different levels, to revalue the role of chemistry in the green version. Emphasis will be placed on the Responsible Care Program, on the REACH directive and on the international project on the chemical substances managed by the United Nations, WHO and the International Labour Organization.

Keywords: building product; eco-compatibility; green-washing; green chemistry

INTRODUCTION

Only a few years ago, the term green building product did not mean anything in particular except an ambiguous, but consoling, idea that the product was somehow less harmful to the people and to environment.

Often, however, the lack of clear definitions and standards has supported the sale from many companies of so-called environmentally friendly products, cleverly disguised as green product thanks to unscrupulous marketing, helping to spread the green-washing.

Green-washing is a neologism referring to a form of green marketing that is misleading used to promote the perception that a company's policies or products are environmentally friendly. The building industry is not immune to this phenomenon.

Green-washing is one of the greatest dangers for a company's corporate image and, when it is discovered by the public opinion, it has a negative effect on the company's reputation and causes economic damages. This happens more and more often because the consumers, increasingly aware of the environmental question, are proving that some strokes of green do not satisfy them anymore. The customers require that the products they buy are safe for use, that they are made well and that they are produced in a responsible way. With regard to environmental communication they require the use of clear, unambiguous language; confining the use of "green claims" exclusively to the properties of reliable and verifiable products; and avoiding the use of excessively generic expressions, such as "ecocompatible", "ecological", "green".. To this end, information should be accompanied by environmental data obtained by applying well-known, acknowledged, scientifically grounded and reproducible methods.

METHOD

The objective of this paper is to shed light on the evolution that the concept of an environmentally friendly building product has undergone, beyond appearance to concreteness.

To achieve the goal, an analysis was conducted in order to:
1. identify the criteria for evaluating sustainable building materials;
2. define standards of certification;
3. point out initiatives to define the role of green chemistry.

1. Criteria

The first step of the analysis showed that the growing popularity of green buildings and green building programs, such as LEED (Leadership in Energy and Environmental Design), BREEAM (Building Research Establishment Environmental Assessment Method), HQE (Haute Qualité Environnementale), is expanding both the demand for and availability of sustainable products. These changes are providing greater opportunities to improve the environmental performance of many building products. At the same time, assessing the health and environmental impacts of materials is a complex process, which can be further confused due to the green-washing. Although there is not yet a definitive set of materials standards that are intrinsically sustainable from the analysis carried out, it appears that the scientific community converges on some basic criteria, so that the products or systems should have or be:

- *recyclable*. Products are manufactured all or in part with recycled materials, and can also be recycled themselves after use. Using recycled products, or products with recycled content helps the environment and the economy in several ways. A significant effect is that of decreasing the need for manufacture with virgin, non-renewable resources, which saves precious resources and also saves manufacturers money. Material that would have ended in landfills after its useful live, instead can be reprocessed for use in other products. For example, newspapers can be reprocessed into cellulose insulation, plastic milk cartons can be shredded, melted and reprocessed into toilet partitions and rubber from automobile tires can be processed into roofing and flooring materials.

- *Renewable resources*. Products are manufactured with resources that are renewable rather than non-renewable. Depletion of the Earth's resources is occurring at an alarming rate. By utilizing renewable energies, such as wind, solar, tidal, as well as renewable products, such as wood, grasses or soil, it is possible to lessen the impact on biodiversity and ecosystems.

- *Minimum waste*. Products produce as little waste as possible in their manufacture, use and disposal. Buildings are big generators of waste: landfills are overflowing, especially with construction waste, which accounts for 40% of the usage at landfills. By utilizing methods of reuse and recycling of scrap and trimmings, employing strategies that minimize waste through the life cycle of a product, manufacturers can radically reduce the amount of products that are put into the waste stream.

- *Locally or regionally produced*. Products are manufactured closer to their use (within 350 km), producing less pollution in transportation, and also helping to support regional economies.

- *Low embodied energy*. Vast amounts of energy are used in the production of building products. One product's "embodied energy," sometimes involves a complex series of processes that contribute heavily to the pollution of the environment, the depletion of natural resources and the degradation of the Earth. This embodied energy includes the energy it takes to extract minerals and raw materials from the Earth, the fuel it takes to transport the material to the manufacturing site, and the energy used at the plant to make the product. Also included is the energy it takes to use and, later, dispose of the product.

- *Low environmental impact*. Products do not harm the environment, pollute air or water, or cause damage to the Earth, its inhabitants and its ecosystems in their manufacture, use or disposal. They are non-toxic and contribute to good indoor air quality. Pollution caused in excavation, manufacture, use or disposal of a product can have untold consequences on the Earth's ecosystem. Poor indoor air quality, caused by products emitting harmful substances, increases the risks to people's health.

- *Durable*. Products are long-lasting and need little maintenance. Product replacement puts a strain on the earth, its resources and inhabitants. In making products more durable and easy to maintain, manufacturers can help eliminate a costly, damaging and time-consuming process of replacement.

This first level of analysis allowed to identify the main health and/or environmental attributes that must meet the sustainable products.

2. Certification

The second part of the analysis examines the issue of certification of the environmental characteristics of a building product. The green marketplace can be a confusing place, and manufacturers often do not know where or how to even start communicating their products' environmental impacts. Promotional materials may overstate environmental claims without providing reliable evidence.

The process to certify the environmental sustainability of building products is driven by the Technical Committee TC 59, at the international level, by Technical Committee CEN/TC 350, in Europe, with the development of a set of standards, whose objective is dual: to harmonize the different building environmental assessment tools and to integrate the Environmental Product Declaration (EPD). For all those involved in the green building industry, environmental product declarations (EPDs) are becoming a transparency tool of the building product choice and for manufacturers the right way to communicate the environmental impacts of their products. An EPD is a Type III eco-label, as defined under ISO 14025. Type

III eco-labels are summary documents containing both quantitative and qualitative information, provide specific information about a product's life-cycle-based environmental impact by category (e.g., climate change) and require validation by a third party.

Recently, the CEN/TC 350 prepared the standard EN 15804:2012: "Sustainability of construction works - Environmental product declarations - Core rules for the product category of construction products", was issued to outline the key Product Category Rules (PCRs) for the development of Type III environmental declarations (EPDs) relating to products and services in the construction sector. It is also the standard to promote the integration of building life-cycle considerations as an integral part of evaluating the impact of the built environment.

Also interesting are the results of an American teamwork, whose target is the elaboration of a Health Product Declaration (HPD) to be integrated with the EPD, in order to complete the information of a product relatively to the environmental and human health impacts, recognizing that Life Cycle Assessment (LCA) based EPD do not adequately address human health hazards. HPDs and EPDs would improve the transparency and accuracy of sustainable product data reporting allowing manufacturers and design professionals to better understand a product's global and human health impacts.

Finally, as result from this second level of investigation, a recent proposal by the European Commission declared through the Communication "Building the single market for green products" (COM/2013/196) should be noted. The EU action aims to reduce the current uncertainty on what constitutes a green product and a green organisation. It is a step towards a more integrated internal market, where products and organisations that are genuinely green are recognised by consumers. In 2010, the Council of the European Union called on the Commission to develop a harmonised method for the calculation of the environmental footprint of products. Since then, the Commission has been working on the basis of existing LCA approaches and international standards, introducing further methodological specifications necessary to achieve more consistent, comparable and accurate results. This work, supported by a consultation process as well as by a road-testing exercise in collaboration with industry, has culminated in the development of the Product Environmental Footprint (PEF) and Organisation Environmental Footprint (OEF) methods.

The PEF and OEF methods require that Product Environmental Footprint Category Rules (PEFCRs) and Organisation Environmental Footprint Sector Rules (OEFSRs) are developed, as soon as possible, for making comparisons.

3. Green chemistry

In this last section, the analysis focus is on the great work that is taking place in recent years, at different levels, to rehabilitate the role of chemistry, that was considered, not long ago, as hostile to the green product. Emphasis will be placed on some important initiatives, as described below.

- Since the early 1990s, EPA (U.S. Environmental Protection Agency) has promoted sustainable chemical products and practices, primarily through its Green Chemistry Program. Green chemistry, also known as sustainable chemistry, is the design of chemical products and processes that reduce or eliminate the use or generation of hazardous substances; it applies across the life cycle of a chemical product, including its design, manufacture, and use. Green chemistry consists of environmentally friendly, sustainable chemicals and processes whose use results in reduced waste, safer outputs, and reduced or eliminated pollution and environmental damage. It encourages innovation and promotes the creation of products that are both environmentally and economically sustainable.

- Responsible Care is the chemical industry's unique global initiative that drives continuous improvement in health, safety and environmental (HSE) performance, together with open and transparent communication with stakeholders. Responsible Care embraces the development and application of sustainable chemistry, helping the industry contribute to sustainable development. Launched in 1985 by the Canadian Chemical Producers' Association, this dynamic initiative is constantly evolving to meet the challenges facing chemical manufacturers and all those in the value chain. Through the participation of over 50 national chemical manufacturing associations – and through them, thousands of chemical sites around the world – Responsible Care forms an essential part of ICCA's (International Council of Chemical Associations) contribution to the United Nations' Strategic Approach to International Chemicals Management (SAICM). Responsible Care has fostered the development of the ICCA Global Product Strategy (GPS) which seeks to improve the industry's management of chemicals including the communication of chemical risks throughout the supply chain. Through Responsible Care, the chemical industry is reporting and tracking its progress on critical elements of product stewardship and is making further improvements to its current processes.

- In 2007, Europe put into place the Registration, Evaluation, Authorisation and Restriction of Chemicals (REACH) program, which requires companies to provide data showing that their products are safe. This regulation (1907/2006) ensures not only the assessment of the chemicals' hazards as well as risks during their uses but also includes measures for banning or restricting/authorising uses of specific substances. ECHA, the EU Chemicals Agency in Helsinki, is implementing the regulation whereas the enforcement lies with the EU member states. The US Toxic Substances Control Act, passed in 1976, in principle has similar provisions but it is not comparable to REACH as to its regulatory effectiveness.

- The International Programme on Chemical Safety (IPCS), active since 1980, is a joint venture of the United Nations Environment Programme (UNEP), the International Labour Organization (ILO), and the World Health Organization (WHO). The overall objectives of the IPCS are to establish the scientific basis for assessment of the risk to human health and the environment from exposure to chemicals, through international peer-review processes, as a prerequisite for the promotion of chemical safety, and to provide technical assistance in strengthening national capacities for the sound management of chemicals. Among the initiatives promoted by IPCS, there is a regular consultation of international experts for the development of chemicals information, such as the ICSC cards (International Chemical Safety Cards). The International Chemical Safety Cards (ICSC) are data sheets intended to provide essential safety and health information on chemicals in a clear and concise way.

RESULTS

Some thoughts are reported briefly on the results of the analysis, divided into the three areas of investigation.

1. The focus on sustainable building products is increasing. In addition to the features based on performance, aesthetics and cost, the selection parameters are expanded to include both health and environmental impacts. It is ever more urgent to define appropriate and unambiguous criteria for the sustainability of a building product. Compared to the recent past, there has been great progress, thanks to studies and research conducted by both private and public organizations. There is no definitive set of standards recognized at international level, however there is the recognition of basic criteria shared by the scientific community.

2. A fundamental role is assumed by the tools for assessing the environmental sustainability of building products. The manufacturers of building products call for transparency on the methods, evaluation criteria, procedures for the certification of sustainability requirements and issue of environmental labels, to avoid confusion and distrust of the consumer due to the phenomenon of green-washing. To date, the most effective tool is even the environmental label Type III, EPD, although it is working on several levels to make this tool even more complete.

3. Great work is also done upstream, at the level of choice of raw materials, in order to make the finished product more sustainable. The focus is on the role of chemistry, rehabilitated thanks to the design of chemical products and processes that reduce or eliminate the use or generation of hazardous substances, the main goal of Green Chemistry. Government agencies, manufacturers and regulators are working with synergy to make the chemical products more safe and environmentally friendly.

DISCUSSION

The concept of sustainable product has come a long way since it was a very vague term. The need for a more extensive, concrete and less ambiguous definition was the lever to the start of new research, studies and regulatory measures, addressed by both public institutions and private associations. However we must not fall into the trap of believing that the work is accomplished, also considering the new challenges and increasingly ambitious goals, on the way to reaching as soon as possible a sustainable building industry.

REFERENCES

1. AA.VV.: Greendex 2012: Consumer Choice and the Environment - A Worldwide Tracking Survey, 2012
2. Bell, S., Morse, S.: Sustainability Indicators: Measuring the Immeasurable?, Earthscan, London, 2008.
3. EC: Communication from the Commission to the European Parliament and the Council, Building the Single Market for Green Products. Facilitating better information on the environmental performance of products and organisations, COM(2013)196 final, 2013.
4. EC: Communication from the Commission to the European Parliament, the Council, the European economic and social Committee and the Committee of the Regions, Roadmap to a Resource Efficient Europe, COM(2011)571 final, 2011.
5. EC: Regulation No 1907/2006 of the European Parliament and of the Council of 18 December 2006 concerning the Registration, Evaluation, Authorisation and Restriction of Chemicals (REACH), 2006.
6. Edwards, B.: Rough Guide to Sustainability, RIBA Publishing, London, 2010.
7. Kephalopoulos, S. et al.: European Commission's efforts in harmonising the testing and health based evaluation of construction products emissions in relation to CE marking. Proc. of the Healthy Buildings 2012 Conference vol. 1 p. 1D.3, Brisbane, Australia, 2012.
8. Materials Research Collaborative: Health Product Declaration (HPD), 2011, available in www.hpdworkinggroup.org.
9. Sharma, S.K., Mudhoo A.: Green Chemistry for Environmental Sustainability, CRC Press, Boca Raton FL, 2010.
10. UNI 11277-2008: Building sustainability. Ecocompatibility requirements and needs of new and renovated residential and office buildings design, 2008.

ANGULAR DEPENDENT SOLAR GAIN FOR MULTIPLE GLAZING FROM OPTICAL AND THERMAL DATA

G. Reber [1], P. Oelhafen [1], L. Burnier [2], A. Schüler [2]

[1] *Institute of Physics, University of Basel, Klingelbergstrasse 82, CH-4056 Basel*
[2] *EPFL - ENAC - IIC - LESO-PB, Bâtiment GC, Station 18, CH-1015 Lausanne*

ABSTRACT

The angle dissolving determination of the solar gain factor $g(\varphi) = \tau_e(\varphi) + q_i(\varphi)$ of an entire insulation glass (IG) – as described in [1] for a two pane glass – can be generalized for IGs with a pane number n>2. And this lacking the possibility to refer to the thermal reaction of the inner panes (ΔT_1 , … , ΔT_n) on an external signal S (solar source).

The elevated number of inner degrees of freedom of the entire system, corresponding to the heat transfer coefficients (Λ_{12} , … , $\Lambda_{n-1,\,n}$) and the individual absorptances (α_1 , … , α_n) can – regarding the response – be sufficiently represented by means of an equivalent two pane glass with absorptances (A_1, A_n) and Λ as global intrinsic quantities of the glazing. Whose ratio A_1/A_n is again fixed by means of one single thermal measurement alone. Under knowledge of the global absorptance $\alpha(\varphi)$ from an optical measurement their magnitudes (A_1, A_n) follow.

As an intrinsic invariant describing optics, the ratio A_1/A_n provides the possibility of conversion into the response under an arbitrary other boundary condition BC (h_e, h_i). The space these quantities (A_1, A_n) leave open behind concerning an identical response onto a signal S will be specified. This space shows the open margin left designing a glazing.

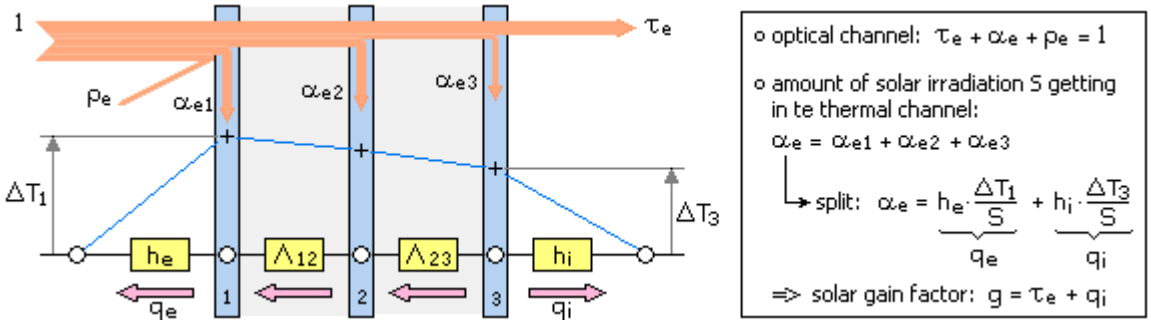

Figure 1: Node-model for a multiple glazing. The absorbed part of irradiation α_e appears in each pane as source, these represented by nodes. The theoretical considerations done with this model show that the information of the outer temperature elevations ΔT_1 and ΔT_3 under known experimental boundary conditions (h_e , h_i) determine the branching ratio $q_e(\varphi) / q_i(\varphi)$ under all other boundary conditions.

INTRODUCTION: MODEL ASSUMPTIONS – THERMAL NETWORK WITH SOURCES

The derivations given concerning the energy flows of the IGs are based on a model of a thermal network according to Fig. 1, in which the panes are represented by nodes:

pc1 The nodes are characterized by their *temperature elevation* (ΔT_1 , … , ΔT_n) towards the environment – e.g. the laboratory.

pc2 *Thermal energy exchange* only takes place between directly neighboured nodes and is described by *conductances* (h_e , Λ_{12} , … , $\Lambda_{n-1,\,n}$, h_i). Those having the property that energy flow *through them* is proportional to the temperature difference *over them*.

pc3 In place of the pane-nodes energy is coupled in by an *external source* S in extent of the *absorptances* (α_1 , … , α_n), which specify the part of S locally reaching the thermal channel. With these *absorptances* α_i are meant those, which are achieved resulting in the given compound of panes in the IG – see EN 410 [3].

pc4 Considered is the *stationary flow equilibrium* tuned in under the source S. Therefore terms in the equations, which describe the inner energy of the panes, can be omitted.

(**pc** = preconditions).

ESTABLISHING THE EQUATIONS FOR A STATIONARY FLOW EQUILIBRIUM

In a system defined as above the entries $S \cdot \alpha_j$ in place of the nodes each can be superposed in their effect, resulting in a linear response ΔT and these scaling with S. The according linear system of equations in an abbreviated matrix notation is:

(1) $\Delta T_i / S = M_{ij} \cdot \alpha_j$, $i = (1 , \dots , n)$, $j = (1 , \dots , n)$, $n =$ number of panes .

The matrix elements M_{ij} contain the thermal quantities Λ_{ij} und (h_e, h_i) by virtue of those the system gets rid of the irradiated energy. Linearity of ΔT in S involves that, with a single measurement under a given irradiation S alone, one acquires knowledge about the system under each other. Vice versa with a further stationary measurement under a changed irradiation S nothing new is emerged. Regardless the fact that *relative errors* of *measured variables* which are scaling with S enter inversely proportional to S.

Without evaluating the system of equations (1) above, for any desired n the following equation is valid at the *system boundary*, describing how this open system exchanges energy in equilibrium and therein gets rid of the irradiated energy:

(2) $\alpha = h_e \cdot \Delta T_e / S + h_i \cdot \Delta T_i / S$, *global absorptance* $\alpha = \alpha_1 + \dots + \alpha_n$,

the two terms on the right side describing the *secondary heat gain* related to irradiation S:

(3) $q_e = h_e \cdot \Delta T_e / S$, $q_i = h_i \cdot \Delta T_i / S$, *secondary heat gain coefficients* .

The useful equation (2) is not an additional equation to the equations (1), while it can be derived from those – in perfect consistence. With the definitions (3) equation (2) has the shape:

(4) $\alpha = q_i + q_e$.

In case the optical value $\alpha(\varphi)$ is already fixed, with (4) one knows already the sum of the two variables: The minimal information missing would be their *branching ratio* q_e/q_i.

GENERAL IMPLICATIONS DERIVED FROM THE EQUATIONS REGARDING THE DETERMINATION OF VALUES

cc1 So far *global absorptance* $\alpha(\varphi)$ is predetermined through an independent experiment – in our case through an optical measurement [2] – with (2) one already knows the irradiation S, that must have been present in the experiment, likewise one knows already the sum (4) of the two secondary heat gain coefficients (q_e, q_i). The value S here appears implicitly in the entire evaluation.

cc2 Nevertheless one could always take the way measuring the value S independently during the thermal experiment at the level of entrance of irradiation into the glazing. In this scenario the value α would follow with (2) and cannot be predetermined additionally. Deciding for one of the two ways is a matter of measuring accuracy. As we have $\alpha(\varphi)$ from a precise optical measurement [2], we decided for a procedure pursuant to (**cc1**), see [1].

cc3 Taking both ways, would contain a certain possibility to validate the reliability of the measurements, also the *boundary conductances* (h_e, h_i). These are modelled in their amount [1] and appear lately as referencing conductances in the entire evaluation procedure of the experiment. This seems to be a subtle point concerning the measuring error. The formal shape of the present discussion will show a certain diminished criticality.

cc4 A priory knowledge of both values (α_1, α_2) in a two pane glass under known boundaries (h_e, h_i) would open the possibility to achieve knowledge of the conductance Λ. This from an independent measurement of S. Measuring one temperature elevation $\Delta T_1/S$ or $\Delta T_2/S$ would be sufficient. The according equation given below (10) resp. (11) determines the conductance Λ. According to (2) the second temperature is not independent. So, measuring the second temperature would here not be from a substantial usability.

(**cc** = conclusions).

OUTER RESPONSE OF A MULTIPLE GLAZING UNDER ARBITRARY BC

Back to the problem originated from a lacking knowledge of the individual absorptances α_j. The proposition whose validity will be shown here reads like:

***Proposition**: A single measurement of the response (ΔT_1 , ΔT_n) of a thermal network defined as above under a signal S and under known boundary conductances (h_e , h_i) and known global conductance Λ determines the response under all other boundary conductances (h_e^N, h_i^N). This is valid for systems of an arbitrary number of panes n.*

Deriving this proposition is not free of charge comparable with direct conclusions getting from the fact that responses are scaling with the signal S: The boundary conductances (h_e, h_i) do not enter as a simple scaling factor. The proposition was already shown in the case n=2 [1]. In the case n>2 now inner degrees of freedom are added.

Anyway, regarding the response again only the outer responses (ΔT_1, ΔT_n) are measured. It has to be shown additionally that the left open degrees of freedom (n>2) can be sufficiently represented by an *equivalent two pane glass* concerning the outer behaving – this under specification the procedure within the parameter of this representing glass can be found.

APPROACH FOR THE SOLUTION: FIND AN EQUIVALENT TWO PANE GLASS

In the case n=2 the proposition follows directly from (1): Two equations determine all absorptances (α_1, α_2). All temperatures are already acquired with the outer pane temperatures (ΔT_1, ΔT_2). An independent measurement of $\alpha(\varphi) \equiv \alpha_1 + \alpha_2$ determines further the irradiation S.

The additional minimal information α_1/α_2 then would be sufficient, to determine both (α_1, α_2). Indeed starting from (1) an isomorphism between this *minimal information* α_1/α_2 and the *temperature detuning* $\Delta T_1/\Delta T_2$ – this interceded by (h_e , h_i , Λ) – can be derived. Consequently complete knowledge over the system is achieved in the case n=2:

$$(5)\quad \frac{\Delta T_1}{\Delta T_2} \xleftrightarrow{(h_e,h_i,\Lambda)} \frac{\alpha_1}{\alpha_2} \qquad , \qquad \alpha = \alpha_1 + \alpha_2 \qquad .$$

The ratio α_1/α_2 herein has the status of a sufficient determining information because it is an intrinsic value of the glass – itself not depending on the interceding values (h_e, h_i, Λ).

Now backwards – from the once determined α_1/α_2 – the *temperature detuning* ($\Delta T_1^N/\Delta T_2^N$) can be calculated for each other BC (h_e^N, h_i^N). Finally the *branching ratio* q_e^N/q_i^N follows with (6) and by means of (4) their amounts (q_e^N, q_i^N):

$$(6)\quad \frac{q_e^N}{q_i^N} = \left(\frac{\Delta T_1^N}{\Delta T_2^N}\right) \cdot \frac{h_e^N}{h_i^N} \qquad , \qquad \alpha = q_e^N + q_i^N \qquad .$$

Now a glass n=2 is the simplest configuration, which is just able at all – this over α_1/α_2 – to tune the *branching ratio* q_e/q_i – particularly capable of an asymmetric behaviour regarding the outflows (q_e, q_i) over intrinsic quantities alone. So, if for all cases n>2 an equivalent glass n=2 could be found, the proposition above would be proved. In this *equivalent two pane glass* the absorptances (α_1 , ... , α_n) will have to be represented by the *representing absorptances* (A_1, A_n), whose direct sum equals again α. So, an isomorphism analogue to (5) has to be found:

$$(7)\quad \frac{\Delta T_1}{\Delta T_n} \xleftrightarrow{(h_e,h_i,\Lambda)} \frac{A_1}{A_n} \qquad , \qquad \alpha = A_1 + A_n \qquad .$$

Such an isomorphism (7) found, the procedure to determine the branching ratio q_e/q_i would follow in a fully analogue way, finally pursuant to (6).

In the cases n>2 however the intrinsic values (α_1 , … , α_n) and (Λ_{12} , … , $\Lambda_{n-1,\,n}$) strike up an alliance regarding the outflow of energy on both sides – resulting in a *branching ratio* (6). From both types of information only their global quantities are known:

$$(8)\quad \alpha = \alpha_1 + \ldots + \alpha_n \qquad , \qquad \textit{global absorptance} \qquad ,$$

$$(9)\quad \Lambda = (1/\Lambda_{12} + \ldots + 1/\Lambda_{n-1,\,n})^{-1} \qquad , \qquad \textit{global heat transfer coefficient} \qquad .$$

The temperatures of the inner panes hidden, the inner degrees of freedom are left undetermined within (8) and (9), of which one only knows the global amounts α and Λ. Nevertheless the parameter A_1/A_n in (7) would – according to case n=2 – represent an intrinsic invariant of the system, whose amount together with $\alpha = A_1 + A_n$ would have a representing meaning concerning the response, but would now leave open a field of equivalent constellations. Therein a manufacturer of glazing has an open field to design a glazing with given properties.

CONCRETE IMPLEMENTATION – DERIVATION OF THE PROPOSITION

To derive equations (5) and (7) and to obtain the concrete shape of (A_1, A_n) establishing the equations (1) is indispensable. Starting from case n=2 subsequently the case n=3 will be treated. The shape of the representing absorptances (A_1, A_3) will in substance be deduced by comparing the coefficients within the two cases n=2 and n=3. The generalization to arbitrary cases n follows by virtue of inductive conclusions:

- In the case n=2 the equations (1) are given by:

(10) $$\frac{\Delta T_1}{S} \cdot \frac{\alpha_1 \cdot (\Lambda + h_i) + \alpha_2 \cdot \Lambda}{\Lambda \cdot (h_i + h_e) + h_i \cdot h_e} \quad ,$$

(11) $$\frac{\Delta T_2}{S} = \frac{\alpha_2 \cdot (\Lambda + h_e) + \alpha_1 \cdot \Lambda}{\Lambda \cdot (h_i + h_e) + h_i \cdot h_e} \quad .$$

Expression (11) corresponds to formula (13) in EN 410 [3] for q_i. This under usage of (3) $q_i = \Delta T_2 / S \cdot h_i$ .The quotient of (10) and (11) delivers the searched shape of (5):

(12) $$\frac{\Delta T_1}{\Delta T_2} = \frac{\Lambda \cdot (1 + \alpha_1/\alpha_2) + h_i \cdot \alpha_1/\alpha_2}{\Lambda \cdot (1 + \alpha_1/\alpha_2) + h_e} \quad \Leftrightarrow \quad \frac{\alpha_1}{\alpha_2} = \frac{h_e \cdot \Delta T_1/\Delta T_2 + \Lambda \cdot (\Delta T_1/\Delta T_2 - 1)}{h_i - \Lambda \cdot (\Delta T_1/\Delta T_2 - 1)} \quad .$$

- In the case n=3 (see Fig. 1) the equations (1) are given by:

(13) $$\frac{\Delta T_1}{S} = \frac{\Lambda \cdot (\alpha_1 + \alpha_2 + \alpha_3) + h_i \cdot [\alpha_1 + \alpha_2 \cdot \Lambda_{12}/(\Lambda_{12} + \Lambda_{23})]}{\Lambda \cdot (h_i + h_e) + h_i \cdot h_e} \quad .$$

(14) $$\frac{\Delta T_2}{S} = \frac{\Lambda \cdot (\alpha_1 + \alpha_2 + \alpha_3) + [h_i \cdot \Lambda_{12}(\alpha_1 + \alpha_2) + h_e \cdot \Lambda_{23} \cdot (\alpha_2 + \alpha_3) + h_e \cdot h_i \cdot \alpha_2]/(\Lambda_{12} + \Lambda_{23})}{\Lambda \cdot (h_i + h_e) + h_i \cdot h_e} \quad .$$

(15) $$\frac{\Delta T_3}{S} = \frac{\Lambda \cdot (\alpha_1 + \alpha_2 + \alpha_3) + h_e \cdot [\alpha_3 + \alpha_2 \cdot \Lambda_{23}/(\Lambda_{12} + \Lambda_{23})]}{\Lambda \cdot (h_i + h_e) + h_i \cdot h_e} \quad .$$

The quotient of (13) and (15) for the two outer panes delivers the searched shape of (7):

(16) $$\frac{\Delta T_1}{\Delta T_3} = \frac{\Lambda \cdot (1 + A_1/A_3) + h_i \cdot A_1/A_3}{\Lambda \cdot (1 + A_1/A_3) + h_e} \quad \Leftrightarrow \quad \frac{A_1}{A_3} = \frac{h_e \cdot \Delta T_1/\Delta T_3 + \Lambda \cdot (\Delta T_1/\Delta T_3 - 1)}{h_i - \Lambda \cdot (\Delta T_1/\Delta T_3 - 1)} \quad .$$

Whereas formal identity between (12) and (16) is reached under absorptances (A_1, A_3), those approaching the searched *two pane glass* with an equivalent behaviour to the outside like this:

(17) $A_1 = \alpha_1 + \alpha_2 \cdot \Lambda_{12} / (\Lambda_{12} + \Lambda_{23}) = \alpha_1 + \alpha_2 \cdot (1 - \Theta)$,

(18) $A_3 = \alpha_3 + \alpha_2 \cdot \Lambda_{23} / (\Lambda_{12} + \Lambda_{23}) = \alpha_3 + \alpha_2 \cdot \Theta$.

The resulting values (A_1, A_3) are achieved by a prorated admixture of the inner absorptance α_2 to the outer absorptances α_1 und α_3. The *admixture ratio* Θ representing the inner degree of freedom ($0 < \Theta < 1$) is weighting this contribution in proportion to $\Lambda_{12}/\Lambda_{23}$.

- First the direct sum of the quantities (A_{e1}, A_{e3}) equals the global absorptance α:

(19) $A_1 + A_3 = \alpha_1 + \alpha_2 \cdot \Lambda_{12} / (\Lambda_{12} + \Lambda_{23}) + \alpha_3 + \alpha_2 \cdot \Lambda_{23} / (\Lambda_{12} + \Lambda_{23}) = \alpha_1 + \alpha_2 + \alpha_3 = \alpha$.

- The quantities (A_1, A_3) and therefore their ratio A_1/A_3 are not sensitive to Λ. The ratio characterizing the system is found to be detached from the amount of the global value Λ:

(20) $$A_1/A_3 = \frac{\alpha_1 + \alpha_2 \cdot \Lambda_{12}/(\Lambda_{12} + \Lambda_{23})}{\alpha_3 + \alpha_2 \cdot \Lambda_{23}/(\Lambda_{12} + \Lambda_{23})} \quad .$$

Independence from Λ still was a property of the invariant in the case n=2 where with α_1/α_2 no thermal property at all is entering. This was given by the simple structure. In the case n=3 now the ratio A_1/A_3 has the meaning to describe the *temperature detuning* $\Delta T_1/\Delta T_3$ outside and this again detached from the global thermal property Λ. In this sense this ratio has again an optical intrinsic meaning, furthermore again not depending from the BC (h_e, h_i).

Starting from the values (A_1, A_3), these once determined under a single BC, backwards by means of (16) the *temperature detuning* under each other BC (h_e^N, h_i^N) is determined. Therewith over (6) the new *branching ratio* q_e^N/q_i^N is determined – interceded by the quantities (h_e^N, h_i^N, Λ). The derivation yields this property of invariance given in A_1/A_3 and this by prescribing in (17) and (18) in which manner the invariance is kept within the constellations (8) and (9). The pane $\alpha_1 + \alpha_2 + \alpha_3 = \alpha$ contains a *solution space* within a glazing exposed to a signal S has an equivalent behaviour to the outside in the sense of indistinguishable responses.

VALUE RANGE DISCUSSION IN THE SIMPLE BUT IMPORTANT CASE N=3

The question concerning the shape of the value range of the absorptances α_j that could have been underlaid for a glazing under an outer measurement leading to (A_1, A_3) can be discussed in an illustrative way for the case n=3. The experimentalist or the manufacturer determines (A_1, A_3) together with the global absorptance ($\alpha = A_1 + A_3$). The possible constellations of values (α_1, α_2, α_3) are in first instance restricted to a pane within the positive octant given by:

(21) $\alpha_1/\alpha + \alpha_2/\alpha + \alpha_3/\alpha = 1$, intercept form of the pane .

Choosing the absorptance α_2 as control variable in equations (17) and (18) under a fixed *admixture ratio* Θ this implies moving on straight lines, whose parametric form is given by:

(22) $\alpha_1 = A_1 - \alpha_2 \cdot (1 - \Theta)$
(23) $\alpha_3 = A_3 - \alpha_2 \cdot \Theta$ } $(0 < \Theta < 1)$.

therein the *admixture ratio*: $\Theta = \Lambda_{23}/(\Lambda_{12} + \Lambda_{23})$ resp. $1 - \Theta = \Lambda_{12} / (\Lambda_{12} + \Lambda_{23})$.

In Fig. 2 the pane (21) is presented containing some straight lines in case (A_1 , A_3) = (0.4 , 0.2):

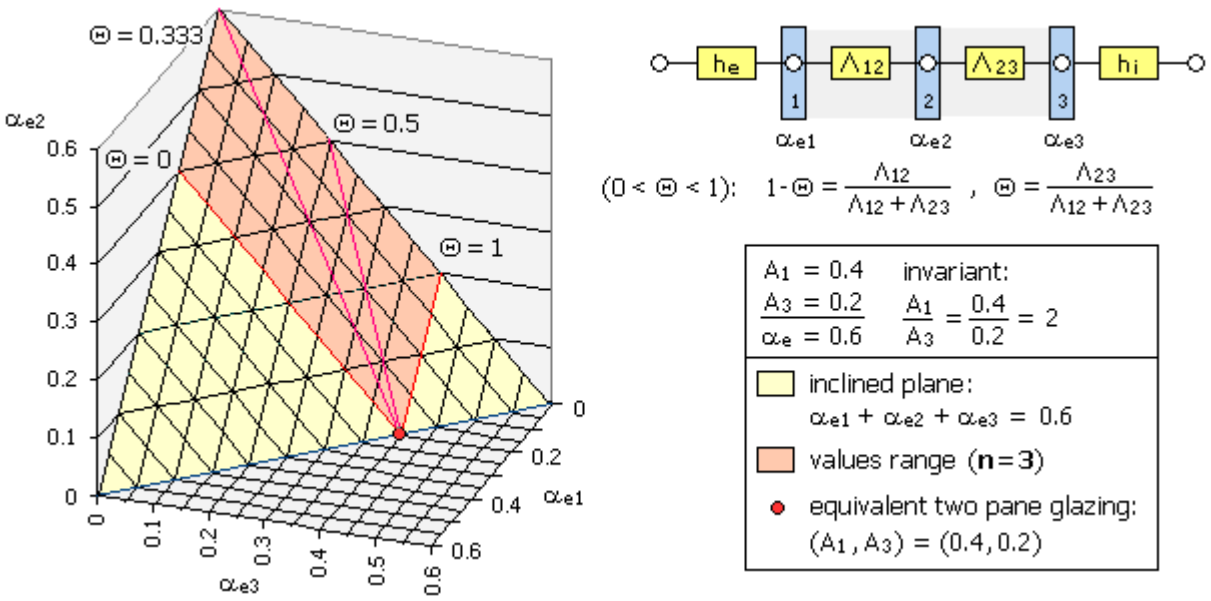

Figure 2: For a given triple glazing (Λ) given boundary condition (h_e , h_i) all these cases give the same answer (ΔT_1 , ΔT_3) to a signal S. They are indistinguishable so long as the temperature of the inner pane ΔT_2 – depending on the ratio Θ – is not accessible.

Under admixture within (0 < Θ < 1) the associated straight lines subtend the permissible value range, in which the system purveys identical responses: Therein the *admixture ratio* Θ is representing the degree of freedom in case n=3, delivering the possibilities to tune in the given values (A_1, A_3) under which outer pane temperatures ΔT_2 (13) and ΔT_3 (15) do not change.

However the temperature ΔT_2 (14) of the inner pane changes, but it remains a *hidden parameter*. In a glazing n=3 with α_2=0 the searched glass n=2 with (A_1, A_3) corresponds directly to (α_1, α_3). In this point, where the admixture Θ has no repercussion, the according straight lines intersect.
If a designer follows the strategy to have no weak link in the chain regarding the conductances Λ_{ij}, he moves on the straight line Θ=0.5. If a designer pursues the extremal constellation of giving an absorptance exclusively to the inner pane – α_2=0.6 in the present example – in agreement with (23) he would choose $\Theta = A_3/\alpha_2 = 0.2/0.6 = 0.333$. With n=3 panes he is able now to obtain a desired asymmetric optical behaviour by tuning with the *admixture ratio* Θ.

EXTENDING THE RESULTS ON ARBITRARY NUMBER OF PANES N

The arbitrary case n is attained by concluding in an inductive way, starting from the case n=3 and equations (17) (18). In the case n=4 the admixtures to α_1 and α_4 have the shape:

$$\left.\begin{array}{ll} (24) & A_1 = \alpha_1 + \alpha_2 \cdot (1/\Lambda_{23} + 1/\Lambda_{34}) \cdot \Lambda + \alpha_3 \cdot (1/\Lambda_{34}) \cdot \Lambda \\ (25) & A_4 = \alpha_4 + \alpha_3 \cdot (1/\Lambda_{12} + 1/\Lambda_{23}) \cdot \Lambda + \alpha_2 \cdot (1/\Lambda_{12}) \cdot \Lambda \end{array}\right\} \quad \Lambda = (1/\Lambda_{12} + 1/\Lambda_{23} + 1/\Lambda_{34})^{-1} \quad .$$

The sum of both equivalent absorptances A_1 und A_4 results in the correct global absorptance:

$$(26) \quad A_1 + A_4 = \alpha_1 + \alpha_2 + \alpha_3 + \alpha_4 = \alpha \quad .$$

And in an analogue way the admixture of each pane j with her particular absorptance α_j takes place to both outer panes for the case of an arbitrary number of panes n.

ERROR DISCUSSION IN THE EVALUATION FOR ENTIRE MEASUREMENT PROCEDURE

The subtle point is given by modelling the boundary conductances (h_e, h_i) these appearing as referencing resistances. Anyhow possible systematic errors compensate each other particulately in the ratio (16) therewith the intrinsic optical invariant A_1/A_n gets fixed. The global absorptance $\alpha(\varphi) \equiv A_1+A_n$ originating from an independent optical measurement [2] opens only just the way to regress on the more harmless behaving ratio A_1/A_n.

CONCLUSIONS

Starting from the question, what can be found out from a glazing regarding its energetical behaviour, without disassembling it that means under an exclusively usage of global characteristic values and available only outer responses in a steady state equilibrium, the *ensemble acting* of panes in compound could be clarified on a principal level. This inversely allows the manufacturer to design the global behaviour in a targeted strategy: The free scope for designing in principle being available as well this in a conclusive formalism, now problems of practicability and feasibility can be treated in a precise way.

Regarding the *response to a signal* and *temperature detuning* of the two outer panes the procedure given here is based on the search for an invariant *intrinsic parameter* which can be attributed to an according *equivalent two pane glass*. This is – as pointed out – the simplest configuration showing all outer possibilities of responses, being capable of an asymmetric behaviour.

The system based was a serial network with nodes in which linear associations between entries and reactions are valid. The deduced propositions are valid in the frame of the model. Nevertheless characteristic values based on simple minimal configurations and the appropriate procedure to find the parameters for the system within the model, open as well opportunities to understand and design systems with a higher complexity. Here i.e. the insight according to which the absorptances are weighted by an *admixture ratio* which corresponds to the two conductances the absorbed energy has to cover on each side.

REFERENCES

1. Angular dependent solar gain for insulating glasses from optical and thermal data, G. Reber, R. Steiner, P. Oelhafen, and A. Romanyuk, CISBAT 2005
2. Experimental determination of spectral and angular dependent optical properties of insulating glasses, R. Steiner, P. Oelhafen, G. Reber and A. Romanyuk, CISBAT 2005
3. Glass in building – Determination of luminous and solar characteristics of glazing, German version EN 410, April 2011

LIFE-CYCLE ASSESSMENT OF ROOF RETROFIT SCENARIOS FOR A SINGLE-FAMILY HOUSE

Carla Rodrigues[1], Fausto Freire[2]

1: MIT Portugal Program, Energy for Sustainability Initiative, University of Coimbra, Pólo II, Rua Luís Reis Santos, 3030-788 Coimbra, Portugal; Tel.: +351 239790739; Fax: +351 239790701; E-mail: carla.rodrigues@dem.uc.pt

2: ADAI – LAETA, Department of Mechanical Engineering, University of Coimbra, Pólo II, Rua Luís Reis Santos, 3030-788 Coimbra, Portugal; Tel.: +351 239790739; Fax: +351 239790701; E-mail: fausto.freire@dem.uc.pt

ABSTRACT

According to the EU's report on Energy roadmap 2050, building retrofit plays an important role to reduce environmental loads associated with the building sector. However, research on retrofit of existing buildings is still limited, especially regarding major refurbishment works. This paper evaluates the influence of the choice of building materials in the environmental life-cycle performance of different roof retrofit solutions. A life-cycle model was developed to assess alternative scenarios for a single-family house located in Portugal. The scenarios were defined combining two types of frame materials (wood and steel), two types of insulation material (expanded polystyrene and rock wool) and three insulation levels (40, 80 and 120 mm). The main stages of the life-cycle model are: removal of the original roof, construction phase and use phase (heating, cooling and maintenance). The functional unit selected for this study is 1 m^2 of living area over a period of 50 years. Life-cycle impact assessment results calculated for six categories (climate change, ozone depletion, terrestrial acidification, freshwater eutrophication, marine eutrophication and primary energy) show that the wood scenarios have the lowest impacts in all the categories. The use phase (maintenance and operational energy) accounts for about 60% of the life-cycle impacts in all categories. The increase of 40 mm in the insulation thickness results in increased embodied environmental impacts (between 10% and 20% in rock wool; between 5% and 25% in expanded polystyrene) and in a 5% increase of the overall LC impacts (for both insulation materials), since there is also a reduction of impacts in the use phase. The reduction of environmental impacts in buildings is commonly focused in energy efficiency measures during the use phase. This paper shows that the entire life-cycle of buildings should be addressed since there are important opportunities to reduce environmental impacts in other phases, namely in the selection of construction materials and insulation levels.

Keywords: Building Retrofit; Environmental Impacts; Insulation Materials; Life-Cycle Assessment; Steel-Frame; Wood-Frame.

INTRODUCTION

Building codes and energy efficiency standards [1,2] have been focused to achieve very low or nearly zero energy building. However, as buildings progress towards low energy performances, the embodied phase starts to play an important role when considering a life-cycle perspective [3]. A wider approach regarding different environmental issues is needed in order to assess the whole building performance during its life span. Furthermore, there is

limited research on retrofit of existing buildings especially major refurbishment works. Literature has been focused on the use phase by applying energy efficiency measures [4,5].

This paper evaluates the influence of the choice of building materials in the environmental performance of different roof retrofit solutions. A comprehensive analysis of alternative frame and insulation materials was performed to assess the environmental performance of the building in five environmental categories (climate change, ozone depletion, terrestrial acidification, freshwater eutrophication and marine eutrophication) and primary energy. Life-cycle assessment (LCA) is a methodology that identifies and quantifies the environmental impacts associated with a product, system or process, according to ISO 14040 [6] and 14044 [7]. The energy needs of the building during the use phase were calculated using an energy dynamic simulation program, Energy Plus.

LIFE-CYCLE MODEL

A life-cycle (LC) model was implemented to evaluate alternative scenarios for the wooden-frame roof retrofit of a single-family house from the beginning of the 20th century (with 280 m^2 of living area distributed in four floors) located in the city of Coimbra, Portugal. The scenarios were defined to assess two types of frame materials (wood and steel), two types of insulation material (Expanded Polystyrene (XPS); Rock wool (RW)) and three insulation levels (40, 80, 120 mm). Figure 1 presents the main stages of the model: removal of the original components of the roof (dismantling and transport for recycling or incineration), construction of the new roof (the production of materials, transport and assembly of the constructive solutions) and use phase (maintenance and operational energy). The functional unit selected for this study was 1 m^2 over a period of 50 years.

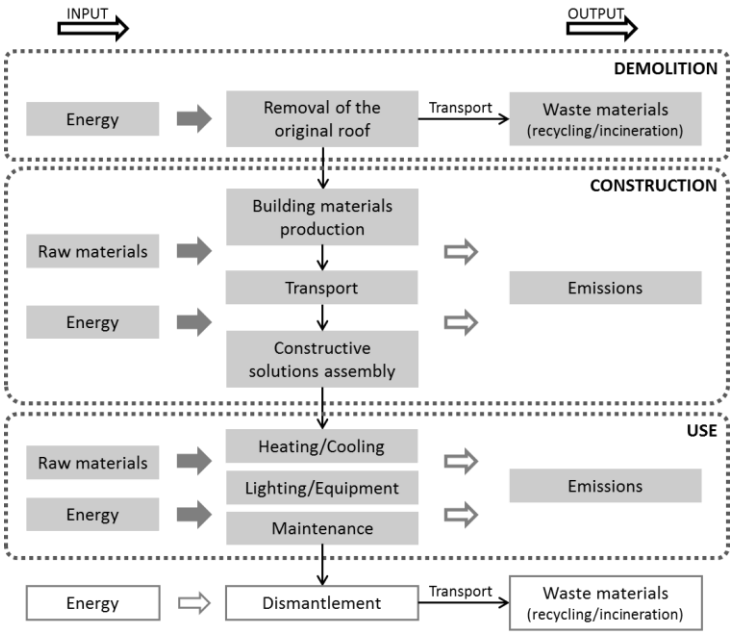

Figure 1. Main processes of the model and system boundaries

This paper is focused on the second floor (attic) of the house because is the most influenced floor by the retrofit of the roof (20% of total energy requirements for heating and about 60% for cooling). The heating and cooling system defined for the house was a 12 kW heat pump with a coefficient of performance (COP) of 3.6 for heating and 3.2 of cooling. The occupancy

type assumed was a 4-people family with a low occupancy level. The low occupancy level was assumed to be especially during the night on weekdays and all day on weekends, with a restricted use of HVAC systems and to be during the night on weekdays and all day on weekends, with a restricted use of HVAC systems. The heating and cooling set-points were define to be 20ºC and 25ºC and the natural ventilation rate of 0.6 air changes per hour was considered, according to the Portuguese building thermal regulation (RCCTE) [2]. Table 1 presents the energy requirements for the alternative insulation level scenarios.

2^{nd} floor (70 m^2)	XPS				RW		
Thickness	0	40	80	120	40	80	40
Heating	12.6	9.4	8.5	8.0	9.6	8.6	8.1
Cooling	1.0	0.9	0.9	0.9	0.9	0.9	0.9

Table 1. Energy requirements per insulation level and material in kWh/(m^2.year)

RESULTS AND DISCUSSION

This section presents the main results of the life-cycle impact assessment (LCIA) of the roof retrofit scenarios. Furthermore, the scenarios were evaluated by performing a sensitivity analysis to frame materials, insulation materials and thicknesses. Results presented in figure 2 shows that W scenario have the lowest environmental impacts. LS scenario has 6% (terrestrial acidification) to 20% (freshwater eutrophication) more environmental impacts than the wood scenario. The impacts of freshwater eutrophication in LS scenario are due to the galvanized steel process.

The construction phase represents 30 to 45% of the total life-cycle impacts in the W scenario and 25 to 50% in the LS scenario. Use phase represents 40 to 70% in W and LS scenarios. Removal phase represents 1 to 3% and maintenance represents 8 to 16%. Ozone depletion and marine eutrophication have the lowest environmental impacts between the analyzed categories. The use phase has 30 to 50% more impacts than the construction phase for terrestrial acidification and freshwater eutrophication, as for the other categories the balance between those phases in 10% to 20%.

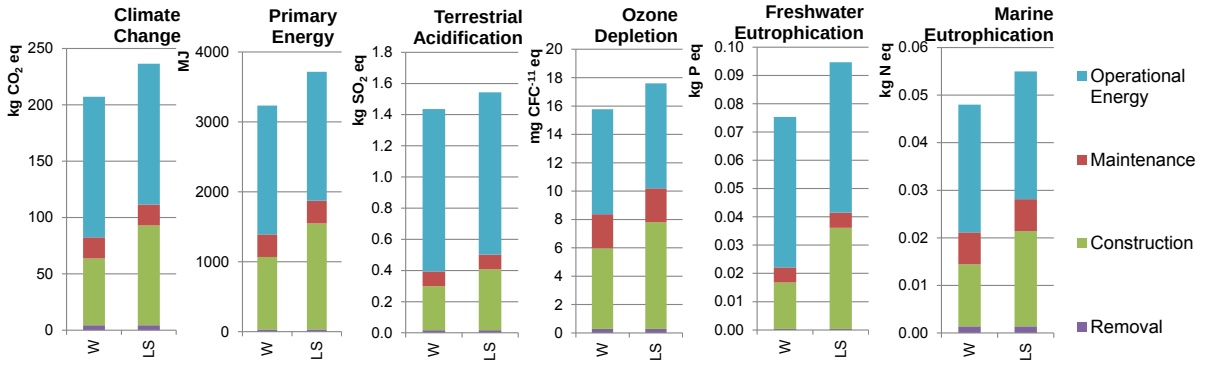

Figure 2: Life-Cycle Impact Assessment of frame materials alternative scenarios (wood and light steel frame; per 1 m^2 of living area for 50 years)

The primary energy analysis shows that the LS scenarios have higher impacts (about 15%) than W scenarios. The use phase of W scenarios is always higher than the construction phase and represents 50 to 60% of total LC primary energy.

Figure 3 shows that RW scenarios have lower environmental impacts than XPS scenarios for climate change and ozone depletion. For marine eutrophication, the difference between insulation materials is only about 5%. For freshwater eutrophication and terrestrial acidification, XPS scenarios have less environmental impacts due to the construction phase. The main difference between the two insulation materials is the use phase (maintenance and operational energy). The use phase accounts for 55% to 70% in XPS scenarios and 60% to 70% in RW scenarios. The results also show that XPS scenarios have lower primary energy requirements than RW scenarios.

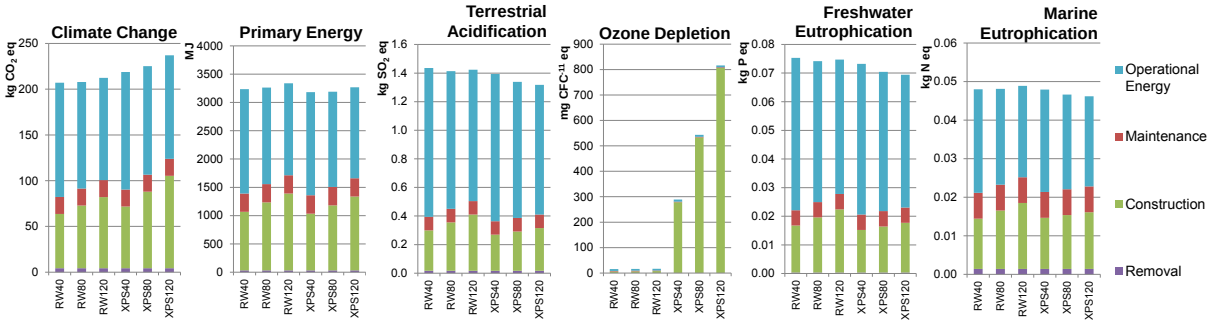

Figure 3: Life-Cycle Impact Assessment of insulation materials and thicknesses alternative scenarios (rock wool and expanded polystyrene; per 1 m^2 of living area for 50 years)

The important contribution of XPS for the ozone depletion is due to the agent used in the extrusion process, the hydrochlorofluorocarbons (HCFCs). Recently some XPS producers have begun to use CO_2 as blowing agent in alternative to HCFCs [8], but this was not considered since there was not inventory data available for this XPS production process,. Nonetheless, a preliminary analysis was performed, showing that the use of CO_2 instead of HCFCs can reduce the contribution ozone layer depletion of the construction phase from almost 97% to only about 11%.

CONCLUSIONS

A life-cycle model was implemented to evaluate alternative scenarios for the wooden-frame roof retrofit of a single-family house. A sensitivity analysis of frame and insulation materials was performed to evaluate the environmental performance of different roof retrofit solutions. It was concluded that the construction phase accounts for 20 to 35% of the overall LC impacts when wood is used as frame material and 25 to 45% when the option is light steel frame. The use phase accounts for 60 to 70% and construction phase for 30 to 40% of the overall life-cycle impacts in both insulation materials. The increase of 40 mm in the insulation thickness results in increased embodied environmental impacts (between 10% and 20% in rock wool; between 5% and 25% in expanded polystyrene) and in a 5% increase of the overall LC impacts (for both insulation materials), since there is also a reduction of impacts in the use phase. The reduction of environmental impacts in buildings is commonly focused in energy efficiency measures during the use phase. This paper shows that the entire life-cycle of buildings should be addressed since there are important opportunities to reduce environmental impacts in other phases, namely in the selection of construction materials and insulation levels.

ACKNOWLEDGEMENTS

The first author (C. Rodrigues) is grateful for the financial support provided by FCT (Fundação para a Ciência e a Tecnologia), under the MIT PORTUGAL program – Sustainable Energy Systems, through the doctoral degree grant SFRH/BD/51951/2012. The presented work is framed under the Energy for Sustainability Initiative of the University of Coimbra and was supported by the FCT, through the MIT PORTUGAL program.

REFERENCES

[1] EPDB (recast), "Directive 2010/31/EU of the European Parliament and of the Council of 19 May 2010 on the energy performance of buildings (recast)," *Official Journal of the European Union*, vol. L153/13–15, 2010.

[2] RCCTE, "Regulamento das Características de Comportamento Térmico dos Edifícios - DL 80/2006," *Ministry of Public Works, Transportation and Communication*, pp. 2468–2513, 2006.

[3] G. A. Blengini and T. Di Carlo, "The changing role of life cycle phases, subsystems and materials in the LCA of low energy buildings," *Energy and Buildings*, vol. 42, no. 6, pp. 869–880, Jun. 2010.

[4] A. Sharma, A. Saxena, M. Sethi, and V. Shree, "Life cycle assessment of buildings: A review," *Renewable and Sustainable Energy Reviews*, vol. 15, no. 1, pp. 871–875, Jan. 2011.

[5] Lollini, Barozzi, Fasano, Meroni, and Zinzi, "Optimisation of opaque components of the building envelope. Energy, economic and environmental issues," *Building and Environment*, vol. 41, no. 8, pp. 1001–1013, Aug. 2006.

[6] ISO 14040, "Environmental Management Life Cycle Assessment Principles and Framework," *International Organization for Standardization*, 2006.

[7] ISO 14044, "Environmental Management Life Cycle Assessment Requirements and Guidelines," *International Organization for Standardization*, 2006.

[8] H.-J. Althaus, C. Bauer, G. Doka, R. Frischknecht, N. Jungbluth, T. Nemecek, A. Simons, M. Stucki, J. Sutter, and M. Tuchschmin, "Documentation of changes implemented in ecoinvent Data v2.1 and v2.2," *Ecoinvent Report n.^{o}16*, no. July, 2010.

ENERGY REHABILITATION ON EXISTING, HISTORICAL, NOT MONUMENTAL BUILDINGS: THE CASE OF THE HIGH PERFORMANCE RETROFITTING OF THE EDIPOWER-CRE IN CHIVASSO (TO) A XIX CENTURY BUILDINGS

A. Rogora, V. Dessì

Politecnico of Milano, Dept. ASTU, via Bonardi 3, 20133 Milano, +39 0223995175, alessandro.rogora@polimi.it

ABSTRACT

The project addresses a critical issue in building retrofitting that until now has not been evaluated by restoration studies; the compatibility between energy efficiency requirements and the traditional objectives of restoration. The need to improve the energy efficiency as well as the necessities to preserve the global value of the buildings in terms of cultural heritage and embodied energy appear to be in contrast with each other. The crucial question is to understand the expected and the required performances to an existing, historical, not monumental buildings (that are largely diffused in Italian small towns and represent a value not for one specific building, but for the set of buildings all together) to evaluate the potential technical transformation to guarantee a satisfactory environmental result - or if possible a high level result -w saving the architectural heritage (that does not necessary mean to preserve completely the building). On the other hand the necessities to upgrade the building to today requirements in terms of facilities, elevator, technical equipments and performances may require a deep modification of the architectural layout.

The case of the ex - Edipower CRE in Chivasso (Recreational Centre for the workers of the Power Plant in Chivasso) is emblematic of this approach. The building was built in the first years of the XX century and in the last years before the refurbishment was completely abandoned and was in a poor state of preservation. Objective of the restoration program was to locate in the building offices and some rooms for guests.
The client invited five Italian architects to submit a project proposal focused on the energy refurbishment of the building. The selected proposal provided different possibilities from the basic to the most efficient solutions. The owner chose the complete proposal (thermal zoning, triple glazing, thin layer insulation, solar greenhouse, PV system) that lead the building to the A+ energy classification and a calculated annual consumption of 8 kWh/m^2 year.

Keywords: Energy retrofitting, Historical building, thin insulation, solar greenhouse

INTRODUCTION

The ex CRE (Recreational Centre for the workers of the Power Plant in Chivasso) was originally built in the early 30 of the XX century. It was a simple rectangular two stories building (plus an underground cellar) of about 200 m^2 surface per floor. It was built in bricks with the horizontal ceilings and the roof made with a wood structure; no specific insulation was used in the envelope. The windows were single glazed with a wood frame and external mediterranean jealousies as protections and shading devices. The building was abandoned for

years and it was in a state of high deterioration when in 2010 the studio TME architects[1] was asked for a renovation project of the building.

ENVIRONMENTAL CONTEXT

The town of Chivasso is located on the left bank of the river Po and it is characterized by a temperate climate typical of mid-latitudes, with hot summer and cold winters, similar to the one of Turin. In winter, as all over the western and souther Piemonte region, develops a "cold buffer" caused by continental air streams which resists to the mild winds that blow at mid-high altitudes such as sirocco. This phenomenon also causes heavy snowfalls.

THE PROJECT

The project concerns the renovation and the extensions of an early 1900 derelict building, in a state of high deterioration that was formerly used as recreation centre for the workers of the power plant and as a nursery school for their children.

Figure 1: Climate in Chivasso (left) and image of the building before the retrofitting (right).

To place a new stair (the old one did not match the legal requirements anymore) and a lift a volume was added to the north side of the building, while on the south facade -facing the park- a three stories greenhouse has been designed. The new volume on the north facade resembles a basalt stone structure with few openings to reduce at minimum heat losses, while the greenhouse on the south resembles a crystal structure. It is completely transparent on the front side with opaque roof and opaque side walls. The two loggias facing east and west, made of decorated cement, have been restored and are visible through the new textile finishing. At the ground floor a small exhibition on the building functioning is located near by the entrance on the north side while the remaining area facing to the south is for offices. At the first floor more offices are located on the south while conference rooms face north. The second floor is completely used as a guesthouse for visitors of the power plant and was located under the existing attic.

Old single glass windows have been replaced with new ones equipped with triple low-e glasses Uw value = 1 W/m^{2}K while a 2 cm thin insulation (infra-red insulation) made of 14 different layers and an equivalent U value = 0,12 W/m^{2}K has has been used to protect the vertical envelope. The inner wall facing the greenhouse is protected with a conventional 10 cm polystyrene insulation, as well as the existing loggias and the first 50 cm of the basement.

1 www.tmearchitects.it

The roof is isolated with a double insulation: a conventional 10 cm insulation in hemp plus the infrared thin insulation described above. The new volume facing north and containing the vertical connections is made of cellular concrete with a thickness of 48 cm finished with plaster. The exterior finishing of the walls (excepted the north added volume and the loggias) is made with a black textile, currently used in agriculture.

Figure 2: North view (left) and South view of the building after the intervention (right).

ENERGETIC STRATEGIES

Having no possibilities to modify the existing form (it is the same than the original except the two added volume), the main energetic strategies regarded the envelope. The interior activities have been organized in order to have the continuously used spaces facing south and the ones for discontinued activities facing north. The former benefits of solar energy gains while the latter bases the comfort conditions on metabolism (natural and artificial). In the attic the south facing guest rooms are primarily used in winter, while the north facing one are the ones primarily used in summer in order to obtain the best inner conditions in each season with the lowest possible energy consumption. A high insulation level was used, but preserving the effective thermal mass due to the brick walls; to reduce the thermal bridges all the insulation is located onto the exterior side of the envelope.

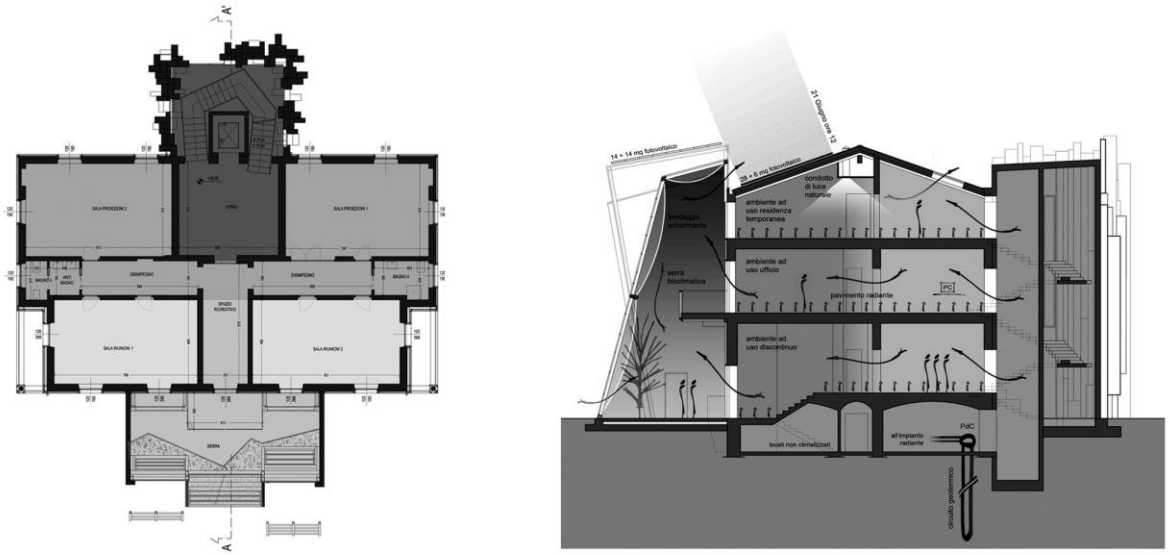

Figure 3: Organization of the activities inside the building in plan (left) and section (right).

Interior walls and ceiling separating the different thermal zones have appropriate U values that have been calculated to guarantee the requested temperature difference in the spaces.

The south facing greenhouse in divided into three different volumes two of them -the ones on the sides- have inclined collecting surfaces to guarantee adequate self shading in summer and prevent overheating. The central volume of the greenhouse is equipped with interior tents to reduce the undesired energy gains in summer. Front openings in the bottom part of the greenhouse and back openings on the top produce cross ventilation powered by stack effect and prevent summer overheating.

A ground heat pump covers the heating and cooling necessities while a 6 zones control reduces to the minimum the unnecessary heating and cooling in the unused spaces. The building heating and cooling system is composed of a geothermal pump, radiant heating and cooling and a dehumidification system.

The 10 kWp PV system, located on the roof guarantee the necessary electrical energy for the building use.

The energy performances of the building have been simulated during the design process using different software like Archisun, Energy Plus and a modified version of 5000 Method. The building functioning is controlled by a home automation system that opens windows when necessary, activates the dehumidification system, etc.

The building has been classified A+ in terms of energy performances, according to the italian standards for the energy performances of buildings, with a calculated consumption of 8 kWh/m^2 year.

Figure 4: View of the greenhouse (left) and thin insulation used in the retrofitting (right).

FIRST RESULTS AFTER ONE YEAR OF USE AND CONCLUSION

The measured energy transfer through the exterior wall was higher than the expected due to the unconventional use of the thin infrared insulation. The use of a textile finishing is not as efficient as a opaque wall and the air movement in the back of the textile finishing was higher than expected. The greenhouse is working greatly and no overheating problems have been

recorded last summer. The windows sealed required openings to guarantee the desired humidity in winter too because of the reduced ventilation (close to 0), while the HVAC equipment required a certain time to be correctly set.

The client was satisfied both by the global image of the building and by its energy performance. The resolution of thermal bridges was difficult and in some cases was impossible to solve completely the thermal discontinuity and to save at the same time the existing moldings and decorations on the facade.

The renovation of existing buildings to obtain high energy performances is complex and requires particular attention in the design of details, nevertheless in most cases the final results can be comparable to the ones of new buildings.

Today energy requirements do not easily fit with the necessity of conservation of existing building, on the other hand it is not possible to imagine a use of an old building for different use and with new comfort requirements without a transformation that should be compatible with the building itself. The ex CRE at Chivasso represents an example of preservation through transformation in which the energy objectives have been reached together with the architectural ones.

REFERENCES

1. Brasca M. Riqualificazione dell'ex CRE Chivasso, Arketipo n.57/11 il sole 24 Ore, Milan 2011.
2. ROGORA A. Progettazione bioclimatica per l'architettura mediterranea, Wolters Kluwert Italia, Milan, 2012.

INNOVATIVE DYNAMIC BUILDING COMPONENT FOR THE MEDITERRANEAN AREA

Marco Sala[1], Rosa Romano[2]

1: Prof. Arch., Director ABITA Inter University Research Centre, University of Florence, via S. Niccolò 89/A, 50125 Firenze, Italy, marco_sala@unifi.it

2: PhD. Arch., Researcher ABITA Inter University Research Centre, University of Florence, via S. Niccolò 89/A, 50125 Firenze, Italy, rosa.romano@unifi.it

ABSTRACT

An appropriate envelope is the main element in sustainable building design, but in mild temperate/mesothermal climates, the rapid changing of outdoor conditions additionally requires a dynamic response of envelope parameters to allow the maintenance of good adaptive interior comfort.

The traditional response of the window components that characterizes the Mediterranean architecture has recently developed by the ABITA Centre into a new range of innovative facade modules and new materials able to play different roles and ensure a dynamic response to climate.

The ABITA Research Centre of University of Florence has a long experience in the field and presents here two prototypes able to modify their performances according to occupants' needs and outdoor conditions, but trying to integrate them into the contemporary architecture.

The design approach focuses on:

- Control of solar radiation (redirect, diffuse or reflect direct radiation)
- Control of air changes (natural and forced ventilation)
- Reduction of energy losses and recover the heat in ventilation
- Increase in security and control in windows frame
- Integration of Renewable Energy in facade components
- Increase of the thermal mass of industrialized building envelopes
- Increase of the overall prefabrication in buildings

The new Directive 2011/27/EC of the European Parliament on the energy performance of buildings, the rising cost of fossil fuels in recent years, high emissions and tiny air pollution particles, led us to the development of new façade systems in the framework of the current project research ABITARE MEDITERRANEO[1]. The façade systems should guarantee considerable energy savings in office buildings. The research is characterized by the development of new building envelope components which can ensure the reduction of heat loss, caused by insufficient building insulation, including glass facades with reduced heat transfer and renewable energy technologies.

In this particular case, the collaboration with a local company has enabled the development of building envelope prototypes, in which the performance is controlled during the year through the integration of shielding, heat exchangers, and phase change materials, ensuring the reduction of energy consumption.

In the following, we introduce the double skin façade DOMINO; an innovative facade system.

The study focused on dynamic envelopes for office buildings with high-energy performances, formed by the dry assembly of advanced facade components; aiming to improve building energy performances.

Keywords: Energy Saving, Dynamic Skin, Smart Envelopes, Renewable Energy

[1] http://www.abitaremediterraneo.eu/

1. INTRODUCTION

The DOMINO facade system described in this paper has been developed with the aim of spreading sustainable building technologies in The Mediterranean Area. The aim is to develop new facade systems to reach the goals of 20/20/20 and to promote regulations that govern energy efficiency in buildings. The European Union established these regulations through the European Directives: 91/2002, 31/2010 and 27/2012. These aim to release local and national regulations to build sustainable buildings, using appropriate policies that consider local climate conditions. In Southern Europe, we must think about winter and summer conditions and avoid copying Northern European energy efficiency architectural solutions, to create appropriate solutions for energy efficient buildings. Southern Europe has specific climatic conditions, with the problems of indoor summer comfort, and the consumption of water resources and natural resources. Therefore it is necessary to improve research into new technologies for envelope solutions with regard to energy consumption in these regions.

In Italy, dependency on fossil fuels, oil and methane gas is still high in the housing and office building sector. At a national level, Italy has adopted the European Directive 2002/91 with the Dlgs. 192/2005, which has been integrated and modified over the years. The new regulation introduces new parameters of evaluation, like the periodic thermal transmittance or the indices of summer energy consumption.

In this paper we describe the a smart facade that we have developed to improve the energy performance of new office buildings in Southern Europe and to reduce the costs of heating, cooling and lighting, responding to national and international energy laws. In particular we show the thermal results that we have analysed for the Domino façade, an innovative dynamic façade system developed for the ICT Centre in Lucca.

2. SMART FAÇADE DOMINO

2.1 Technological features

DOMINO facade is a unitised modular “dry assembled” system that allows an easy installation on building site. This façade system has a simple geometric design made with two modules: transparent and opaque. The modules can be installed with different geometries and different types of materials with different colors can be placed in their frames.

The modules consist of fixed and mobile parts, that can be operated trough automatic or manual controls. The mobile parts, placed in the aluminum frame, are:

- An aluminum shading device;
- A transparent panel with stratified glass 4 + 4.

A vertical mosquito net made with a metallic grid is placed in front of the indoor transparent module and prevents the entering of animals and insects in offices, ensuring night cooling.

The façade system is designed as a double skin façade system, where it is possible to customize the indoor skin, the air gap and the outdoor panel.

The dynamic facade achieves a good performance in the terms of:

- Thermal transmittance: the transparent indoor wall has a U value of 1,2 W/m^2K and the opaque indoor wall has a U value of 0,3 W/m^2K;
- Acoustic insulation: 50dB;
- Mechanical Resistance: the façade has a good fire resistance and mechanical properties and can be tested with accidental and dynamic loads;
- Air and water permeability: the weather strip used in the frame avoids the formation of condensation and guaranteed a good air proof;
- Maintainability: the modular elements enable to repair, with isolated action of maintainability, the facade system without changing the global performance of the façade.

The facade system uses a technological solution with recessed panels. This mechanism allowed hiding in the aluminum box the mobile elements: the glass panel and the shading device. The recessed panel can bear a weight of 180 Kg.

In the opaque outdoor module can be installed:
- Three PV panels that have an electrical energy production between 0,50 and 0,30 kWP. The energy production depends on orientation and localization of the façade system.
- Other types of panels done of: metal or glass or terracotta tiles; so to guarantee the application of this type of façade also in the retrofit of the existent buildings.

In winter the mobile glass panel is placed in front of the transparent module. So the smart facade will have the shape of a double skin facade with a buffer zone that increases its U value to 0.6 W/m^2K. In this configuration the façade guarantees a good thermal insulation and doesn't decrease the natural lighting into the workspaces.

In summer the panel with the shading device is placed in front of the transparent module, regulating direct solar radiation and decreasing heat load in the office. The mosquito net is down so it is possible to obtain natural ventilation in the indoor spaces all day long.
The shading device made with mobile and metallic lamellae or with terracotta tiles, allows regulating the light and minimizing the glare phenomena.

Figure 1: Smart Facade. Prototype with PV panel

Fig. 2. Smart Facade. Prototype with Brick panel

We have realized two prototypes of this type of dynamic facade:
- A prototype with a PV panel in the opaque module and a shading device made of aluminum thin sheets;
- A prototype with terracotta tiles in the opaque module and in the shading device.

2.2 Energy Simulations

We have simulated the energy performance of the facade system using thermodynamic software. The dynamic energy simulations have been made in three different climatic zones in Italy: Milan, Florence and Palermo, and compared for the cardinal directions East, South, West, North. We have built a virtual test room that has a size of 5,00 x 5,00 x 3,00 m and has a wall where it is possible to put the following façade systems (opaque and transparent):

1. Window with double glass and thermal break frame. Size: 3,00 x 1,35 m;
2. Window with double glass and thermal break frame. Size: 3,00 x 2,50 m;
3. Glass curtain wall with double glass and thermal break frame. Size: 5,00 x 3,00 m;
4. Glass curtain wall with double glass, thermal break frame and external fixed shading device system with aluminum venetians. Size: 5,00 x 3,00 m;

5. Glass curtain wall with double glass, thermal break frame and external mobile shading device system with aluminum venetians. Size: 5,00 x 3,00 m;
6. Double skin façade (unitized system typology) with natural ventilation of the buffer zone. Internal and external layers have size: 5,00 x 3,00 m;
7. Double skin façade (unitized system typology) with natural ventilation of the buffer zone and fixed shading device system located inside the buffer zone. Internal and external layers have size: 5,00 x 3,00 m;
8. Double skin façade (unitized system typology) with natural ventilation of the buffer zone and mobile shading device system located inside the buffer zone. Internal and external layers have size: 5,00 x 3,00 m;
9. Opaque curtain wall made with an insulated panel with rock wool (thickness 8,00 cm) and a window with double glass and thermal break frame. Window size: 3,00 x 1,35 m;
10. Smart façade. Winter configuration
11. Smart façade. Summer configuration without shading device
12. Smart façade. Summer configuration with shading device

The thermal simulations have been done with TRNSYS (TRaNsient System Simulation Program), analyzing for each situation the following parameters:

- Primary energy for heating (H_{eat}, kWh)
- Primary energy for cooling (C_{ool}, kWh)

Then we have calculated:

- The total primary energy supply (kWh)
- Heating and cooling consumptions (€)
- Heating and cooling CO_2 emissions (kg)

The simulations show that:

- In winter months for the smart facade, the primary energy supply for heating is lower than that required by a brick wall (Case 2, 50% of transparent module and 50 % of brick wall: 4422 kWh). The primary energy for heating supplies for the three cities chosen and the four cardinal directions is, in fact, of 4187,69 kWh. However in the smart facade the primary energy need is bigger than that required by a glassed curtain wall and transparent double skin (Case 3: 3447 kWh and Case 6: 3759 kWh) because the solar heat gain decreases with the decrease of transparent surface. **When the mobile glass panel is placed in front of the transparent module the heating needs decreases by the 5%.** In the future, aiming improve the summer energy performances could be interesting to evaluate the input given by the use, in the mobile panel, of TIM or other phase change materials. The smart facade should be oriented toward south to improve the solar heat gains and decrease the energy consumption for heating.

- In summer months the smart facade guarantees good energy performance and in the configuration with the shading device placed in front of the transparent module the primary energy need is of 770,16 kWh (reduction by the 70% for the cooling), lower than that performed by a brick wall with a central window (Case 1: 1049,00 kWh) and also lower than that of a glass curtain wall or of a double skin with fixed or mobile shading device (Case 4: 1509,21 kWh, Case 5: 1527,41 kWh, Case 7: 895,01 kWh and Case 8: 899,87 kWh). The smart facade should be oriented toward south or north so to reduce the thermal loads and the solar heat gains and decrease the energy consumption for cooling.

- The best orientation during all year, in Florence and Palermo, is south, with a 40% reduction of primary energy for heating and cooling.

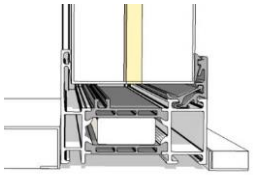
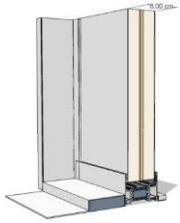
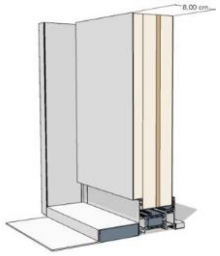
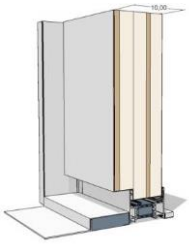

Thickness insulation panel (mm)	60	80	100
Thickness Aluminium panel (mm)	4	4- 5	5
Peso (Kg/m^2)	9,2	10,6	12,1
K (W/m^{2}K)	0,38	0,24	0,21
kcal/m^{2}h°C	0,28	0,21	0,18

Tab.1: Opaque component: analysis of energy performance increasing the insulation

The lighting simulations have been made with the software Relux, with which it has been possible to evaluate the average of natural lighting in the test room. The simulations have shown that the smart façade, which has a transparent module of size 1,50 for 3,00, allows achieving the following results:

- good performances in summer months, with an illumination of 592 lux;
- inadequate performances in winter months, when the glass panel is placed in front of the transparent module, with an illumination of 300 lux.

In order to reduce the energy consumptions for lighting, the smart façade should be located in spaces where it is possible to have two windows located in opposing walls. It is also necessary to install an electronic light system that controls the artificial light and allows switching on only the lights in areas that are not reached by solar radiation.

Heating [kWh]

	South			**West**			**East**			**North**		
	Milan	**Florence**	**Palermo**	**Milan**	**Florence**	**Palermo**	**Milan**	**Florence**	**Palermo**	**Milan**	**Florence**	**Palermo**
Case 1°	5623.49	3717.68	220.95	6920.75	5179.38	1291.08	6842.05	4829.31	1295.46	7677.02	5795.49	2058.26
Case 2°	5699.82	3801.07	1196.59	6989.62	5228.12	1424.44	6886.81	4793.86	1394.48	7860.29	5995.17	2000.78
Case 3°	4236.16	2010.35	0.00	5969.93	4239.26	432.94	5266.03	2991.65	198.96	8415.29	5995.17	1609.28
Case 4°	6642.46	4300.99	274.02	8365.59	6245.95	1547.20	8249.08	5754.34	1490.25	9357.63	6920.01	2535.22
Case 5°	4242.27	2010.46	0.00	6873.96	4889.39	511.52	6656.44	4019.74	454.96	8460.04	6011.71	1609.35
Case 6°	4154.47	2216.08	12.63	6251.55	4576.83	664.18	7130.74	4733.41	954.79	7419.38	5389.49	1613.78
Case 7°	6130.47	4146.44	439.53	7392.31	5565.96	1548.50	7314.63	5221.57	1553.05	8088.85	6051.86	2280.86
Case 8°	4171.02	2216.38	12.63	6306.97	4581.42	665.10	6135.66	3903.94	607.44	7459.12	5409.39	1613.97
Case 9°	5818.40	4003.39	514.80	6860.98	5186.23	1500.03	6814.46	4922.76	1544.64	7487.31	5609.53	2146.36
Case 10°	5460.94	3716.63	1055.99	6552.45	4952.50	1418.03	6476.16	4611.02	1405.68	7246.00	5398.41	1958.42
Case 11°	5503.10	3614.84	1050.06	6840.09	5105.12	1337.65	6742.80	4667.49	1322.77	7743.73	5700.68	1956.20
Case 12°	5336.66	6951.59	6903.99	6951.59	5106.11	1322.77	6903.99	4668.05	1322.77	7766.60	5708.96	1956.26

Table 2: Primary energy analysis for heating (H_{eat}, kWh) for the twelve cases of facades.

Cooling [kWh]

	South			West			East			North		
	Milan	**Florence**	**Palermo**	**Milan**	**Florence**	**Palermo**	**Milan**	**Florence**	**Palermo**	**Milan**	**Florence**	**Palermo**
Case 1°	519.73	907.76	1651.09	688.08	1034.23	2348.83	672.17	1447.16	2283.56	30.69	211.97	792.74
Case 2°	1892.85	2312.13	2841.99	2206.75	2516.00	4052.64	2181.17	3248.79	3962.74	484.21	797.67	1401.92
Case 3°	3786.70	4640.05	5608.35	4624.43	5185.82	7957.79	5224.40	7358.30	8516.51	967.28	1607.85	2728.58
Case 4°	864.76	1374.48	2212.54	1085.18	1522.33	3221.04	1072.71	2114.04	3157.52	85.85	366.92	1033.14
Case 5°	865.09	1374.66	2225.76	1085.63	1524.62	3336.91	1073.03	2119.77	3237.45	85.86	366.97	1033.23
Case 6°	2044.40	2688.81	3507.43	2620.70	3126.09	5393.42	2368.42	3921.08	5077.34	450.24	923.93	1733.31
Case 7°	377.34	703.01	1417.06	559.05	882.77	2103.89	523.69	1265.67	2039.78	15.91	158.22	693.69
Case 8°	377.40	703.44	1417.44	559.52	883.26	2145.05	523.87	1266.44	2054.02	15.91	158.24	693.82
Case 9°	240.84	464.10	1164.26	362.55	647.72	1677.27	317.58	915.25	1581.49	0.00	89.70	558.14
Case 10°	1022.03	1337.73	1818.49	1287.72	1540.09	2757.48	1254.69	2047.67	2669.14	226.66	456.50	916.39
Case 11°	1892.92	2312.41	2868.47	2204.09	2513.60	4090.96	2180.63	3248.59	3992.27	484.59	798.28	1413.60
Case 12°	422.89	682.12	1177.31	506.30	749.16	1736.90	453.99	1047.39	1676.28	43.38	179.84	566.29

Table 3: Primary energy analysis for cooling (C_{ool}, kWh) for the twelve cases of facades.

3. CONCLUSIONS

The research Abitare Mediterraneo has involved companies, leaders in the engineering and production of facades: Schueco, Metra, Permasteelisa, Focchi, Cotto Imprunetta, Palagio Engineering. The advice of industrial companies has improved the technological solutions of the production process and of the construction phase. The smart façade prototype was developed and realized by DAVINI, a Tuscan company. The advice of the industrial companies has improved the technological solutions of the production process and of the construction phase. The façade system has a thermal break frame by Schueco and glass panels by Pilkington. This choice allowed us to reduce the cost of the smart façade, bringing it, without PV panels, to 850,00 €/m2. This cost is the same as that of a traditional double skin. The Domino Facade was used in the construction of the south and east facades of the New Centre in virtual environments and ICT of Lucca Chamber of Commerce. The research has showed that is possible to realize dynamic façade systems that can change their technological configuration during the year, decreasing the energy needs of the building for heating and cooling.

REFERENCES

1. Oesterle L., Lutz H., Double-Skin facades: integrated planning, Prestel, Munich – London – New York, (2001)
2. Poirazis H., Double Skin facades for office buildings, Division of Energy and Building Design, Department of Construction and Architecture, Lund Institute of Technology, Lund University, (2004)
3. Romano R., Smart Skin Envelope. Integrazione architettonica di tecnologie dinamiche e innovative per il risparmio energetico, Firenze University Press, Firenze (2011)
4. Schumacher M., Schaeffer O., Vogt M., Move: Architecture in Motion - Dynamic Components and Elements, Birkhauser, Hardback, 2010

INVESTIGATION AND DESCRIPTION OF EUROPEAN BUILDINGS THAT MAY BE REPRESENTATIVE FOR "NEARLY ZERO" ENERGY SINGLE FAMILY HOUSES IN 2020

G.C.J.Skarning[1]; S.Svendsen[1]; C.A.Hviid[1]

1: Department of Civil Engineering, Technical University of Denmark, Section of Building Physics and Services, DK-2800 Kgs. Lyngby.

ABSTRACT

As part of European energy politics and strategies for reduction of fossil fuels all new buildings should have a "nearly zero" energy consumption in 2020. This creates a strong need for research in cost-effective technologies and solutions that will contribute to the fulfilment of the ambitious energy reductions without compromising desirable daylight conditions and indoor climate. This development requires knowledge about the demands and possibilities of the low energy building mass of the future. An important basis for the research within this field will therefore be the establishment of a set of reference parameters that can be expected to be representative for the behaviour of the "nearly zero" energy building of 2020 in different European climatic zones. This paper provides an overview of how single family houses with a very low energy demand for space heating and cooling can be approached by rational and conventional means in three different European climates: Rome, Bratislava and Copenhagen. Special attention is paid to the role of windows and their contribution to solar gains in these well-insulated buildings of the future. By a neutral treatment of the window configurations towards different orientations, where the windows in all rooms are dimensioned based on the diffuse daylight access at the specific location, it is shown that an equal window distribution will allow fulfilment of an ambitious energy target, while simultaneously enabling a balanced daylight access across the building and a comfortable indoor climate. Furthermore, the analyses indicate that the ability of these well-insulated buildings to utilise solar gains is highly restricted, even at the location of Copenhagen. Window panes with a solar control coating seem to be an appropriate protection against overheating for all three locations.

Keywords: Building parameters, European climates, energy, daylight, windows, solar gain.

INTRODUCTION

The establishment of cost-optimal levels for energy requirements is a task requiring several considerations, spanning from future energy prices and discount rates to local possibilities. According to the guidelines accompanying the Commission Delegated Regulation (EU) No 244/2012 on the energy performance of buildings, it is the responsibility of the member states to set minimum energy performance requirements for their buildings with a view to achieving cost-optimal levels. This paper aims at providing an example of how buildings with a low energy demand for space heating and cooling can be achieved based on a selected target. The analyses are the first step towards a more detailed study on how windows with optimal properties for the energy frame in 2020 can be developed. For this reason, special attention is paid to the link between the building behaviour and the windows. The overall building performance must be transparent to the effect of orientation, window configuration and room distribution, and it must be possible to trace both the heating and cooling demand back to a specific room with a specific orientation and window fraction. Furthermore, daylight conditions, energy demand and thermal environment must be evaluated at room level and the behaviour of rooms with different orientation must be comparable.

The daylight access is considered an unquestionable aspect of the building performance, thus all solutions are created in accordance with an ambitious daylight target. The analyses will lead to a suggestion on low energy solutions for each location, followed by parameter variations on how these solutions are affected by different glazing properties.

METHOD

In accordance with the criteria above, the symmetrical building set up in Figure 1 is chosen.

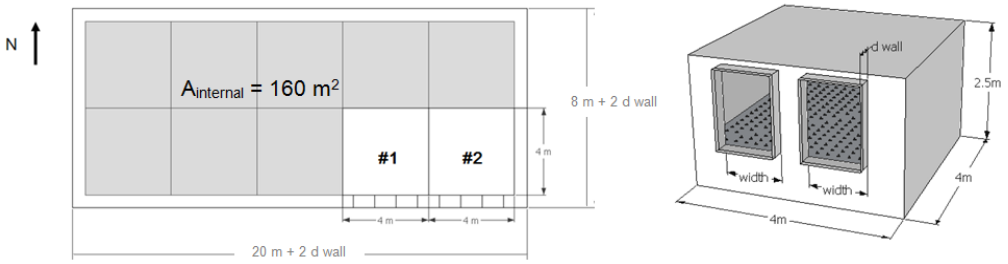

Figure 1: Building set up. The building is composed by equal quadratic rooms and oriented South-North for neutral treatment of room composition, window distribution and orientation.

A building with internal floor area of 160 m^2 is composed by 10 equal quadratic room modules with the internal dimensions 4 x 4 x 2.5 m. All modules are side-lit by two windows and the variable dimensions are the wall thickness and window width. These will depend on the amount of insulation and window size needed in order to reach the selected targets for both energy and daylight. The building is oriented South-North and the relevant room types are evaluated separately. As the transmission area in rooms located at a building corner (#2) is significantly larger than in the rooms positioned in the middle (#1), all results will be derived from the individual area weighted performance of these two room types. The heating and cooling demands are given for the two building halves facing South and North respectively and for the building in total.

Locations and climate

The locations Rome, Bratislava and Copenhagen are selected for the study, representing three different latitudes and two different longitudes at the continental part of Europe (Figure 2).

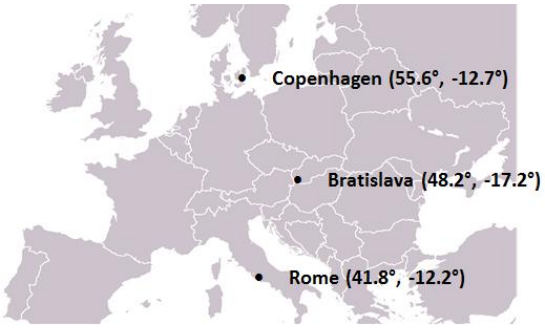

Figure 2: The three different locations.

Both a room's heating and cooling demand and its access to daylight are climate-dependent. The access to light and solar gains decreases nearly linearly from Rome in South to Copenhagen in North, while Bratislava is positioned in between. Moreover, Rome and Copenhagen represent coastal climates with rather small temperature differences between summer and winter, whereas Bratislava, which is located in the central parts of Europe, experiences large temperature variations from -20°C in winter to 30°C in summer [1].

Windows dimensioned according to the availability of diffuse light at the location

In order to create building solutions with comparable daylight conditions across the different climates, the windows are dimensioned for an occurrence of 300 lux in 50 % of the light hours at 50 % of the work plane under the diffuse daylight availability at the given location. Target and methodology are selected with reference to the on-going discussions on how European daylight standards can be upgraded in a way that approaches climate-based daylight modelling (CBDM), which delivers daylight predictions under realistic sun and sky conditions [2]. For the purpose of these comparative studies, a simplified methodology from these proposals is chosen, where the effect of the sun and its position is neglected. Under the assumption that the diffuse light access at the locations follows the same graduation in brightness as the CIE overcast sky model, a target daylight factor (DF_{target}) can be derived for the different locations based on the median daylight level required indoors and the diffuse median illuminance available outdoors ($E_{median\ diffuse}$):

$$DF_{TARGET} = \frac{300\ lux}{E_{MEDIAN\ DIFFUSE}} \quad (1)$$

The DF target values for the different locations and the window fractions required in order to meet the selected target are given in Table 1, along with an illustration of the spatial daylight distribution in the rooms. All calculations are performed with Daysim for comparability with fully climate-based approaches. A diffuse reflectance of 70 % is assumed for walls and ceiling and a reflectance of 30 % for floors.

Heating and cooling demand based on EN ISO 13790

For comparison across the countries, all buildings are optimised with off-set in the same energy target. After subtraction of energy needed for ventilation fans, pumps and domestic hot water, the target for the annual space heating and cooling demand is set to 13 kWh/m^2.

The heating and cooling demands are calculated according to the hourly method with simplified input-parameters described in EN ISO 13790. The method simplifies the heat transfer between the external and internal environment, but distinguishes between the internal air temperature and the mean radiant temperature. This enables its use in principle for thermal comfort checks [3]. Standard set-points of 20°C and 26°C are used for heating and cooling respectively. Venting is controlled based on a set-point of 23°C and solar shadings are modelled by means of a simplified shading factor. Movable solar shadings are activated when the irradiation on the external window surface exceeds 300 W/m^2. The calculations are performed with the program WinDesign, developed at the Technical University of Denmark. Climate files are collected from the U.S. Department of Energy's homepage [2].

General building specifications and assumptions

Mechanical ventilation with heat recovery and the constant air change rate of 0.6 h^{-1} is applied all year in order to ensure an indoor air quality in accordance with EN 15251. A high heat recovery efficiency of 90 % with bypass during the cooling season favours comfortable supply temperatures and keeps the ventilation losses to a minimum. As a simplification the infiltration rate is set to 0. Natural ventilation with a maximum venting rate of 3 h^{-1} is used in order to reduce the overheating and cooling demands. The internal gains from people, equipment and lighting are 5 W/m^2 and the thermal capacity 260,000 J/K m^2. In general the building envelope holds a high quality and all connections are constructed for minimum heat losses (see footnote in Table 1).

RESULTS

The building parameters that are directly related to the fulfilment of the energy and daylight targets are now restricted to *insulation thickness*, *window size* and *glazing properties*. Reasonable values for these parameters are selected through iterations between window optimisation for daylight, insulation thicknesses required for energy and reasonable choices of glazing properties. The suggested set of building parameters are given in Table 1 and Figure 3 illustrates the heating and cooling demand of the solutions.

Variable building parameters		**Unit**	**Rome**	**Bratislava**	**Copenhagen**
Insulation*	Insulation thickness	mm	125	300	250
	Wall thickness	m	0.325	0.500	0.450
	U-value, wall	W/m^2 K	0.20	0.10	0.12
	U-value, roof/floor	W/m^2 K	0.14/ 0.11	0.06/ 0.05	0.07/ 0.06
Window size	Fraction of internal floor area	%	24	30	32
Glazing	Type	-	2-layer	3-layer	3-layer
	U-value	W/m^2 K	1.0	0.5	0.5
	g-value	-	0.27	0.27	0.27
	TL	%	50	50	50
Daylight	DF target	%	1.56	1.84	2.11
	Spatial distribution of daylight target. Dark area: DA 300$_{diffuse}$ < 50 %		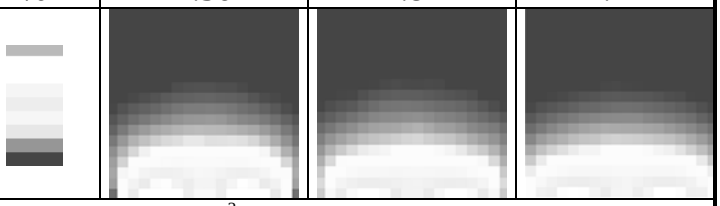		

*) Additional properties of the building envelope; U_{frame} = 1.34 W/m^2 K (width = 0.057 m, ψ = 0.33 W/m K), $\psi_{window/wall}$ = 0.01 W/m K and $\psi_{foundation}$ = 0.13 W/m K. Insulation in roof/floor is the double amount as in walls.

Table 1: Suggested values for the climate-dependent building parameters.

Triple glazings are needed in Bratislava and Copenhagen, whereas double glazings are found sufficient in Rome. Although Bratislava is located in a southern climate relative to Copenhagen, the large variations between summer and winter force the insulation thickness to exceed Danish levels. Glazings with a solar control coating and a g-value of 0.27 are selected as a cheap mean for control of overheating. In Copenhagen, where there are no traditions for mechanical cooling, the decision is based on whether the comfort limits can be met without additional solar shadings or not. This was found possible with the selected g-value of 0.27.

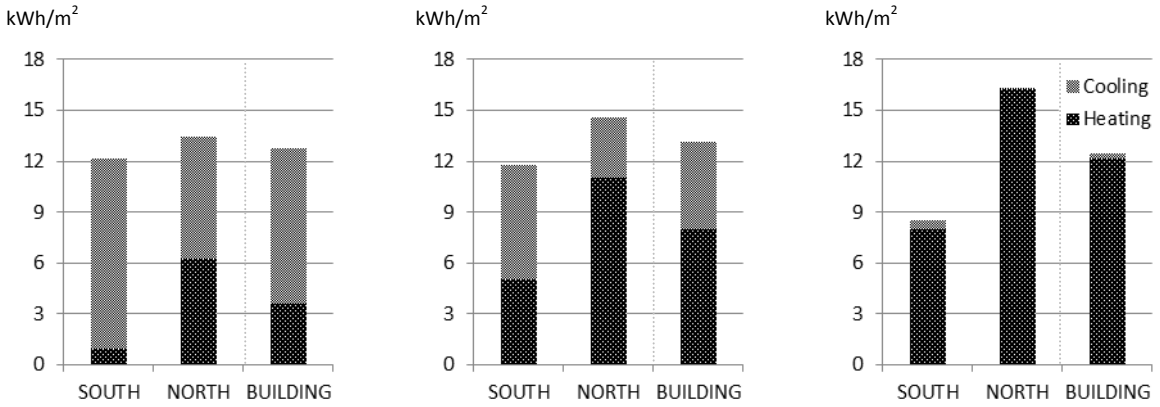

Figure 3: Energy demand of the solutions. From left: Rome, Bratislava and Copenhagen.

Figure 4 and Figure 5 show parameter variations on the window glazing properties, with the building solutions suggested above indicated with the grey line labelled "ref".

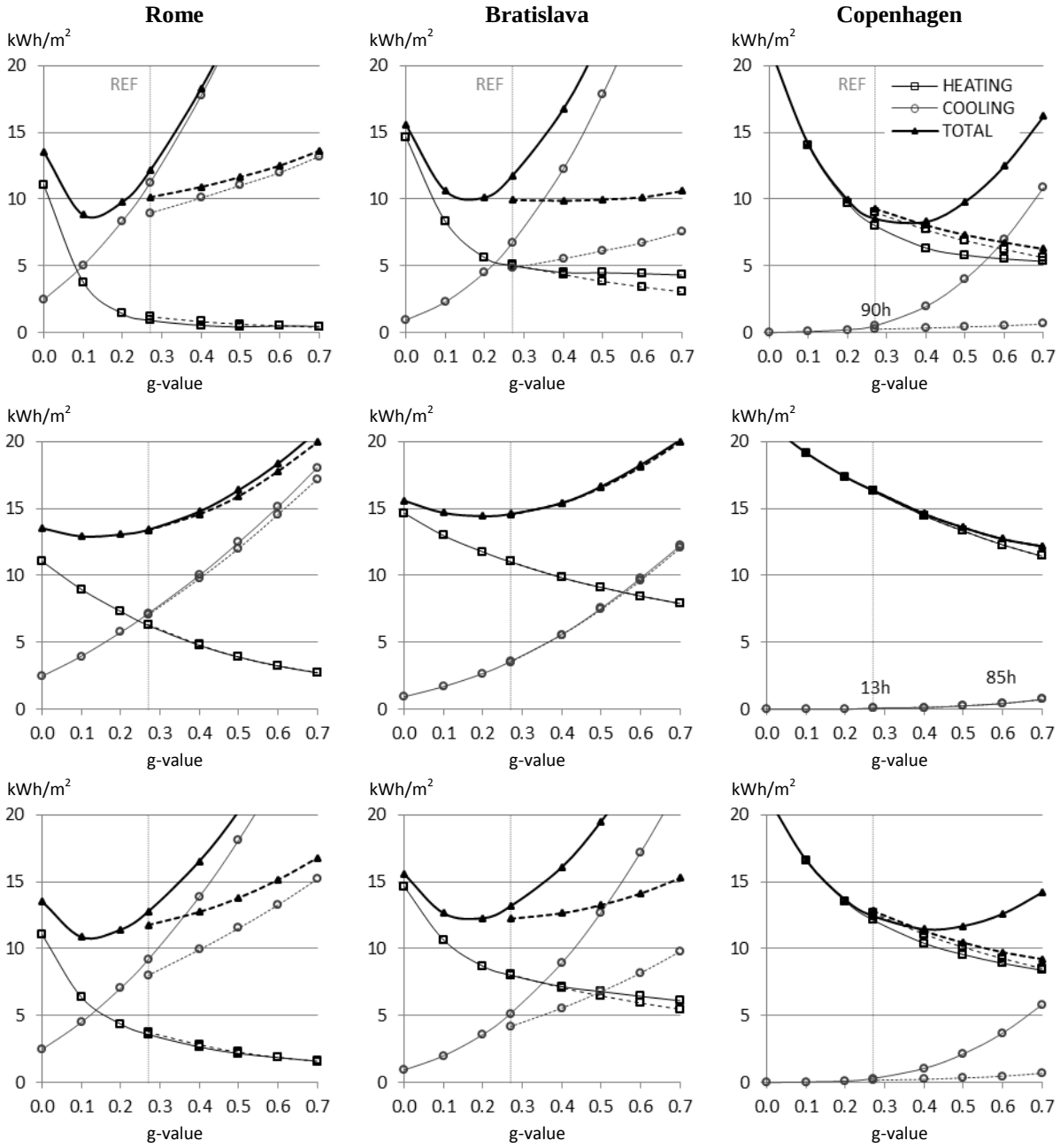

Figure 4: Heating and cooling demand as a function of g-value. From top: South, North and the building in total. Dashed lines represent the addition of movable solar shadings with shading coefficient 0.2 when activated. Equivalent overheating is indicated for Copenhagen.

DISCUSSION

In Rome and Bratislava the optimal g-values are found in the range of 0.1 - 0.2 for both orientations. This indicates that even the diffuse solar gains in rooms facing North contributes to more overheating than they reduce the need for space heating. The g-value's effect on the heating demand stagnates around this level in rooms facing South. Furthermore, the positive effect of low g-values seems to override the potential energy saving by choosing smaller windows with higher light transmittances. Smaller windows would however be favourable if the solar loads could be kept down by movable solar shadings or other means. For this

purpose a potential may be found in the use of fully climate-based methods for daylight optimisation. This may allow further reductions of window area in the rooms that are most exposed to direct and indirect sun. In Copenhagen the optimal g-value is found at 0.4 for the building in total. This contradicts the current practice in Denmark, where high g-values are favoured by the energy rating system for windows. Furthermore, the flexible range of this optimum may open new development possibilities for the related glazing parameters. In a room oriented towards the North, higher g-values are still favourable and movable solar shadings may in general enable energy savings in Copenhagen. For further conclusions, the cooling demands must be verified by a reliable program. Moreover, the robustness of the findings to changes in internal gains and other building parameters must be investigated.

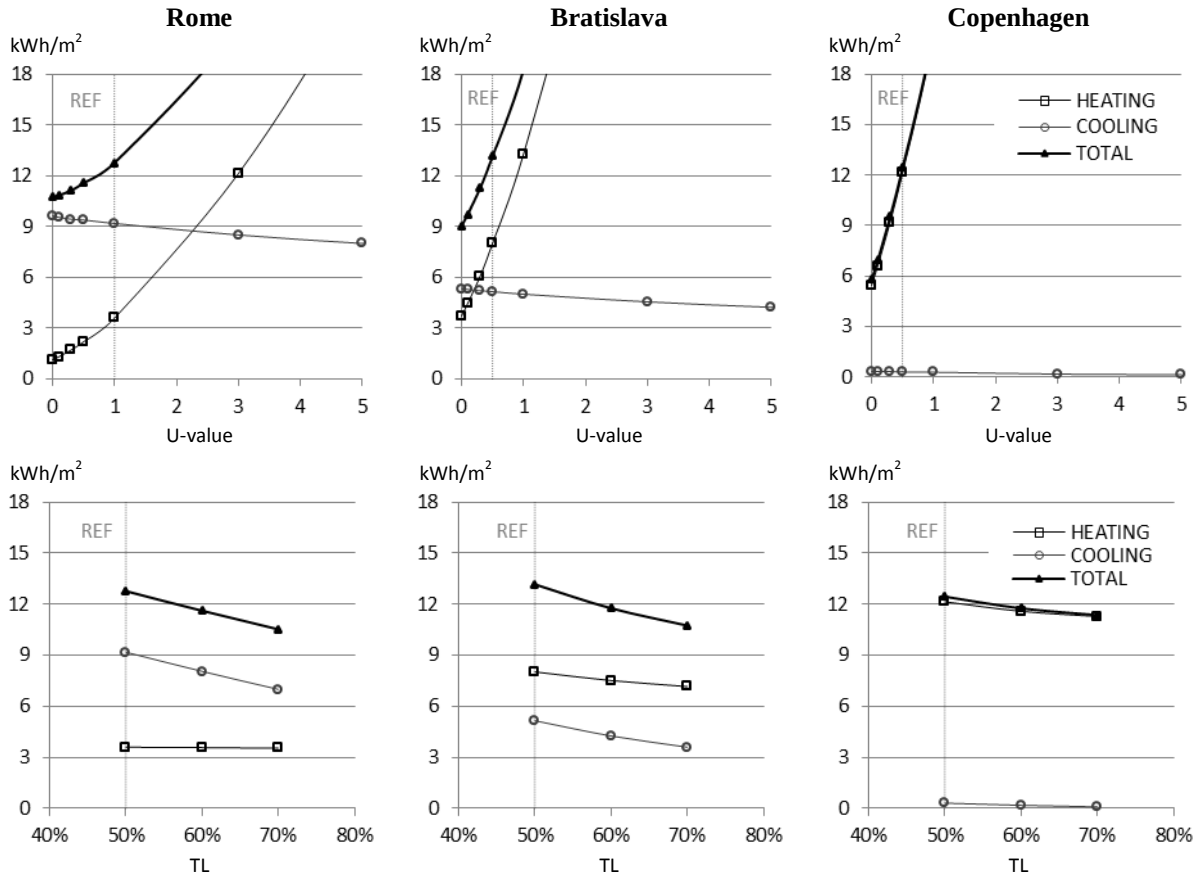

Figure 5: Building heating and cooling demand as a function of glazing U-value (top) and light transmittance (bottom), given that the window fraction is adjusted for sufficient daylight.

ACKNOWLEDGEMENTS

The work is funded by VELUX A/S and the author gratefully thanks colleagues at VELUX for fruitful discussions and their important contributions to the investigations.

REFERENCES

1. The U. S. Department of Energy: EnergyPlus Energy Simulation Software. Weather Data. *http://apps1.eere.energy.gov/buildings/energyplus/cfm/weather_data.cfm*, accessed 2013.
2. Mardaljevic, J. and Christoffersen, J.: A roadmap for upgrading national/EU standards for daylight in buildings. Proc. of the CIE conference, Paris, 2013.
3. EN ISO 13790 : Thermal performance of buildings. Calculation of energy use for space heating and cooling.

TRANSPORTATION OF BUILDING MATERIALS: AN ENVIRONMENTAL ISSUE?

Sophie Trachte

Architecture et Climat, Université catholique de Louvain (UCL),

Place du Levant, 1, B-1348, Louvain-la-Neuve, Belgium.

E-mail : sophie.trachte@uclouvain.be

Phone: +32/10.47.26.36

ABSTRACT

In the context of sustainable design of buildings and selection of building materials, where reduction of environmental impact is a key issue, it's interesting to analyze the influence of the transportation on the environmental impact of building materials throughout its life cycle. Indeed, the life cycle analysis (LCA) [4] considers the transportation step between the extraction phase and manufacturing phase but rarely other steps. If this transportation step is undoubtedly the most important in terms of kilometers covered, the other steps are mainly by road (truck and van) and may have a significant environmental impact.

The present contribution aims to answer to a simple but current question: does the use of a local building material really reduce the environmental impact of transportation and thereby lower the environmental assessment of this building material? This work is performed by analyzing through different transportation scenarios based on seven specific distances, the influence of the distance covered and the influence of the means of transport.

Keywords: building material, transportation of building materials, environmental impact assessment of building materials

INTRODUCTION

Transportation is an inherent demand of the construction sector especially for the production and distribution of building materials. Transportation is a part of the life cycle of building materials. Each transportation step is characterized by the use of mode(s) of transport and a number of kilometres covered; but also by a demand of energy and by emission of atmospheric pollutants.

The environmental impact of transportation, mainly long distance, is often seen as a negative element in the overall environmental assessment of a building material or product. Indeed, in terms of sustainable choice of building materials, people, in building sector, argue for the short distance - building material locally produced rather than fare away - as a positive element to reduce the environmental impact and embodied energy requirement of a building material.

The paper aims to ensure the accuracy of this statement. If selecting building materials produced locally can meet specific and local climate and can promote local economy, is this selection really interesting in terms of energy requirement and environmental impact? Does it really reduce energy consumption? Does it significantly lower the environmental impact of building material?

METHOD

Goal and scope of the research

This contribution highlights the environmental impact of various modes of transport and tries to establish different transportation scenarios depending on the origin of the building material, the number of kilometers covered and the mode(s) of transport used. The environmental impact of various modes of transport and the results of the scenarios are assessed through five LCA indicators (see table 1).

Seven geographical areas have been selected (from 90 km to 10 000 km covered). For each area, various scenarios were proposed. The scenarios are based on transportation step between the manufacturing plant where building materials is produced and the building site where building material is implemented. The building site is located in the center of Brussels.

Environmental impact assessment of transportation modes

Modes of transport consume fossil energy resources and thereby have an impact on energy requirement and atmospheric air quality. Environmental impacts generated by the different modes are shown in the table 1. They are based on the ton-kilometers (tkm) through five mandatory LCA indicators: grey energy consumption, global warming, acidification potential, eutrophication and photochemical ozone creation potentials.

Mode of transport	Data base	Environmental impact				
		Grey energy *MJ/tkm*	Global warming *kCO_2/tkm*	Acidification *$kgSO_2$/tkm*	Eutrophication *$kgPO_4$/tkm*	Photochem. Ozone *kg C_2H_2/tkm*
truck 16t	Ecosoft	5,9	0,37	0,00264	0,00046	0,00009
	KBOB 2007	5,27	0,318	/	/	/
	ECOINVENT	5,511702	0,33384	0,0017912	0,0033337	0,000059612
	CLIMAT	5,511702	0,333840	0,001791	0,000460	0,000060
truck 28t	Ecosoft	3,7	0,22	0,0016	0,00027	0,00008
	KBOB 2007	3,76	0,223	/	/	/
	ECOINVENT	4,595289	0,19439	0,0010596	0,0019749	0,000037076
	CLIMAT	3,760000	0,212463	0,001059	0,000270	0,000037
truck 40t	Ecosoft	2,7	0,15	0,00108	0,00016	0,00007
	KBOB 2007	2,84	0,165	/	/	/
	ECOINVENT	1,977356	0,11727	0,00056487	0,0010044	0,000019357
	CLIMAT	2,700000	0,150000	0,000565	0,000160	0,000019
van (<3,5t)	Ecosoft	27,1	1,65	0,00844	0,00115	0,0014
	KBOB 2007	19,5	1,16	/	/	/
	ECOINVENT	/	1,5718	0,0056272	0,0072329	0,00079057
	CLIMAT	19,500000	1,571800	0,007356	0,001150	0,000791
freight train	Ecosoft	1,2	0,06	0,0004	0,00004	0,00001
	KBOB 2007	0,606	0,0138	/	/	/
	ECOINVENT	0,716884	0,039543	0,00021161	0,00022926	8,8767E-06
	CLIMAT	0,716884	0,039543	0,000212	0,000040	0,000009
inland waterway	Ecosoft	0,9	0,06	0,00041	0,00006	0,00001
	KBOB 2007	0,657	0,0457	/	/	/
	ECOINVENT	0,650593	0,046401	0,0003361	0,00061414	6,5004E-06
	CLIMAT	0,657	0,050700	0,000336	0,00006	0,000007
sea waterway	Ecosoft	0,1	0,01	0,00026	0,00001	0
	KBOB 2007	0,17	0,0106	/	/	/
	ECOINVENT	/	0,0090391	0,00022775	0,00017264	7,1141E-06
	CLIMAT	0,100000	0,010000	0,000228	0,000010	0,000000
freight plane - europe	Ecosoft	/	/	/	/	/
	KBOB 2007	/	/	/	/	/
	ECOINVENT	32,943769	1,6689	0,0064768	0,0085938	0,00027032
	CLIMAT	32,943769	1,668900	0,006477	0,008594	0,000270
freight plane - world	Ecosoft	/	/	/	/	/
	KBOB 2007	16,4	1,08	/	/	/
	ECOINVENT	16,334347	1,0675	0,0041314	0,0054769	0,00017271
	CLIMAT	16,3343465	1,0675	0,004131	0,005477	0,000173

Table 1: Environmental impact of transportation modes – five environmental indicators

Unlike other European countries, Belgium does not have database related to the environmental impact of products. Considering the difficulty of obtaining complete and valid data for all modes of transport, the author has used several databases [8 to 10].

Scenarios of transportation

Transportation steps considered

Transportation of building materials can consist, like the life cycle of a product, of several steps:

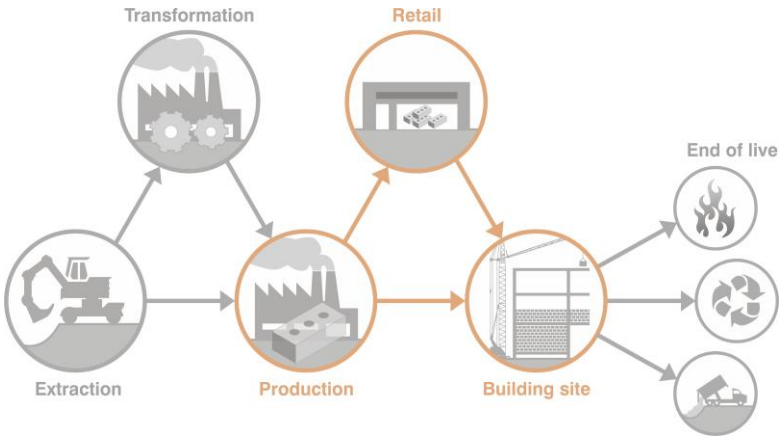

Figure 1: Steps of transportation in live cycle of building material

For the evaluation of environmental impact of transportation, the author only considered the transport step between the manufacturing plant and the building site, located in the center of Brussels.

If this phase transportation is not always the most important in terms of kilometers, it takes into account the transport of various materials such as certain types of wood, metals and certain raw materials. For this step of transportation, the author has considered two alternatives:

- Building materials are directly carried from the manufacturing plant to the building site ;
- Building materials go through a retailer before they are carried to the building site. In this case, an average distance of 30 km covered by van has been considered [5]. This alternative was included in the scenarios.

Geographical zoning

Seven geographical areas have been identified for the establishment of scenarios. These areas and distances covered should be considered as an estimation. It is obvious that some materials coming from China, Russia or from the rest of the world can travel higher distance than 10000 km. The seven areas and the average distance covered are presented below:

- **Area « Belgium »** with an average distance of 90 km to cover;
- **Area « Benelux »** with an average distance of 200 km to cover;
- **Area « Neighbouring regions »** with an average distance of 500 km to cover;
- **Area « Neighbouring countries»** with an average distance of 1000 km to cover;
- **Area « Nearby Europe »** with an average distance of 2000 km to cover;
- **Area « Enlarged Europe »** with an average distance of 4500 km to cover;
- **Area « World »** with an average distance of 10 000 km to cover.

Distribution of transportation modes

In terms of transportation, it is important to consider the mode or the different modes of transport used to cover a given distance. Indeed, over the same distance, the use of a truck, a freight train or inland waterway transport or a mix of them will not lead to the same amount of carried material, nor the same cost nor the same energy consumption, nor the same emission of air pollutants.

Except for the "Belgium" area where only two scenarios were established, over ten different scenarios were developed for each area, considering that the more the distance covered is important, the more the transportation by rail, by inland ou sea waterway are used. For example, scenarios selected for the "Neighboring countries" area are presented below, with the results for each scenario and an average score (green line on the graphs).

- **Area « Neighbouring countries »**

  scenario 1 : 100 % van
  scenario 2: 100 % truck 16t
  scenario 3: 100 % truck 28t
  scenario 4: 100 % truck 40t
  scenario 5: 100 % freight train
  scenario 6: 100 % inland waterway
  scenario 7: 95 % truck16t et 5 % van
  scenario 8: 95 % truck28t et 5 % van
  scenario 9: 95 % truck 40t et 5 % van
  scenario 10: 90 % freight train et 10 % truck 28t
  scenario 11: 90 % inland waterway et 10 % truck 28t
  scenario 12: 50 % freight train et 50 % truck 28t
  scenario 13: 50 % inland waterway et 50 % truck 28t
  scenario 14: 55 % inland waterway, 40 % truck 28 t et 5 % van

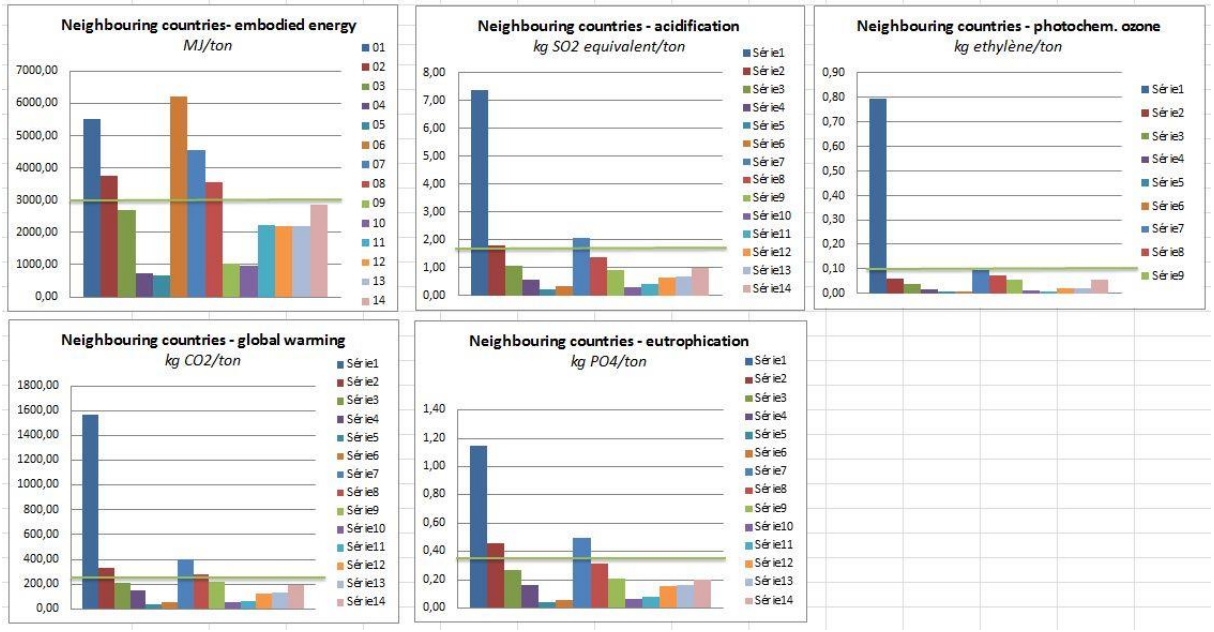

Figure 2: Environmental impact of scenarios – Neighbouring countries

Systems boundaries

This contribution only takes into account the step of transportation between the manufacturing plant and building site. It would be interesting to analyse the transport step between extraction and manufacturing plant but the kind of analysis can only be achieved for a specific building material as it requires knowledge of all the components (raw materials) and their origin.

An estimation of environmental impact of transport step between the building site and the treatment unit at the end of life has been achieved. This estimation has considered a distance of 35 km covered by 16t truck following a study of localization of processing units of

construction waste in Belgium [3]. In addition, to complement this first contribution, the environmental impact of a full transport cycle has been studied for two materials produced by Knauf and Knaufinsulation, in the area of Liege [3]. The results of this second study are not included here but have confirmed the results below.

RESULTS AND DISCUSSION

While those different scenarios are relatively rough, especially in the distribution of transportation modes and the estimated number of kilometers covered, they offer some interesting conclusions:

1. *Influence of the distance on the environmental impact*

More the distance covered is important, more the transportation phase will require energy and have higher impacts on the environment but the energy requirement and the environmental impact are not linear results: their increase is not proportional to the number of kilometers.

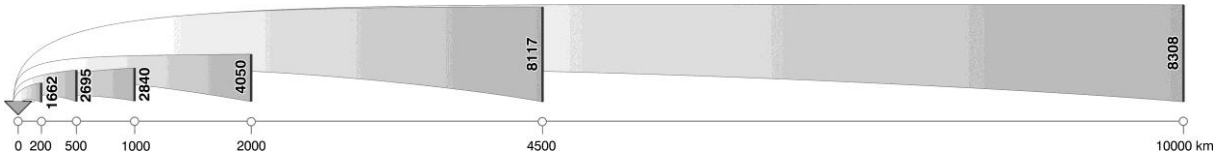

Figure 3: Consumption of grey energy for «1 ton x number of kilometers covered", calculated on the basis of the average of the scenarios for each geographic area - [MJ]

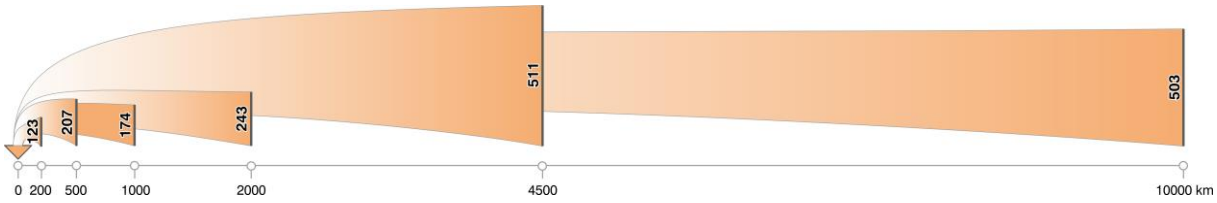

Figure 4: Emission of greenhouse gases for «1 ton x number of kilometers covered", calculated on the basis of the average of the scenarios for each geographic area - [kg CO_2]

In fact, when the distance increases, the mode of transport changes from the truck to the freight train, inland waterways or to sea waterways. The consequence of this change is a significant reduction of the environmental impact.

2. *Influence of the mode of transportation on the environmental impact*

This contribution highlights that the mode of transport strongly influences the energy requirement and the environmental impact, especially over short distances where road transport (especially vans) is predominant [6], [7].

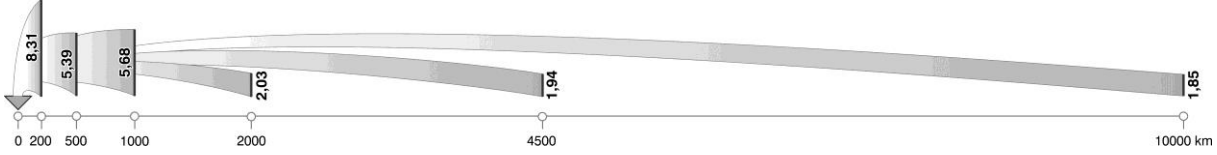

Figure 5: Grey energy consumption for "one ton travelled one kilometer" - [MJ]

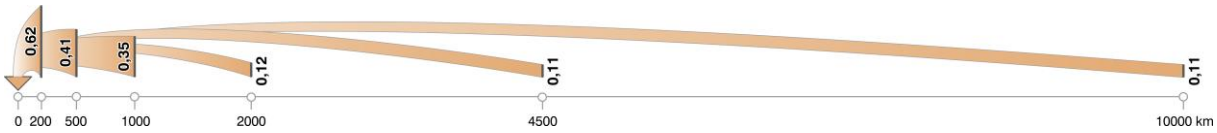

Figure 6: Emission of greenhouse gases for "one ton travelled one kilometer" - [kg CO_2]

This contribution also demonstrates that the combination of several alternative modes of transport with road transport could significantly reduce energy requirement and environmental impact of transport in general, over short and long distances.

So, with the objectives of reducing the environmental impacts related to transportation and encouraging the use of local, regional and / or European materials, it is therefore essential to consider not only the distance, but even more, the modes of transport used to carry the raw materials and buildings products. Some Belgian manufacturers, aware of the challenges of sustainable construction, have chosen to follow this goal and thus have chosen alternative modes of transport (train or inland waterways) to carry their raw materials and products.

REFERENCES

1. TRACHTE SOPHIE, MASSART CATHERINE, Reducing the environmental impact of new buildings: Analyzis of the balance between heating energy saving and environmental assessment of the building materials, Proceedings PLEA 2011
2. TRACHTE SOPHIE, DE HERDE ANDRE, Choix des matériaux, Ecobilans de parois, élaboration d'un outil d'aide à la conception de maisons à très basse consommation d'énergie réalisé pour le compte de la Région Wallonne, Louvain la Neuve, 2010
3. TRACHTE SOPHIE, Matériau, Matière d'Architecture Soutenable ; Choix responsable des matériaux de construction, pour une conception, thèse de doctorat, 2012 Faculté LOCI, Université Catholique de Louvain.
4. EN ISO 14040: Management environnemental - Analyse de cycle de vie - Principes et cadres, 2006.
5. Bepalingsmethode Milieugerelateerde Materiaalprestatie van gebouwelementen, étude réalisée par le CSTC, VITO et la KUL à la demande de l'OVAM, rapport de mai 2010
6. Climate for a transport change, TERM 2007: indicators tracking transport and environment in the European Union, EEA Technical report No 1/2008 disponible sur http://www. eea.europa.eu/publications/technical_report_2008_5/at_download/file
7. HERTVELDT, HOORNAERT, MAYERES, Perspectives à long terme de l'évolution des transports en Belgique :projection de référence, ouvrage publié par le Bureau fédéral du Plan, mai 2009, téléchargeable sur www.plan.be/admin/uploaded/200904211523080.pp107_fr.pdf
8. Database Ecoinvent : http://www.ecoinvent.ch
9. Database KBOB : http://www.bbl.admin.ch/kbob.
10. Database Ecosoft : http://www.ibo.at/de/oekokennzahlen.htm

OPTIMIZED THERMAL BRIDGES IN EARTHQUAKE RESISTANT BUILDINGS

S. Wyss[1]; W. Hässig[2]

1: Hässig Sustech GmbH, Weiherallee 11a, 8610 Uster

2: Hässig Sustech GmbH, Weiherallee 11a, 8610 Uster

ABSTRACT

In energy-efficient buildings, thermal bridges can be the cause of up to 40% of the total heat loss of the building envelope. As building trends move towards widespread implementation of very low energy buildings, this issue grows in importance. At the same time, a revision of earthquake codes for structures in many parts of Switzerland has resulted in increased demands on structural elements. These factors contribute to conflicts between structural integrity and the minimization of thermal bridges. A number of solutions to these conflicts exist, are often not implemented due to a lack of communication between building physics experts and structural engineers and of timely identification and discussion of the problem. This project's aim is to create a leaflet to present the problem and indicate the many existing solutions to architects, engineers and contractors.

The most critical and commonly occurring thermal bridges are identified and their Ψ-values determined for a theoretical base case and for each possible solution. The base case is defined as every connection being constructed from reinforced concrete. This produces the basis upon which the relative improvement of the Ψ-value of each solution can be compared. Calculations are carried out with a two-dimensional FEM (finite element model) computer program. Furthermore, a simplified typical Swiss apartment building is conceived and simulated to demonstrate the effectiveness of the various solutions and provide a basis for structural load distribution.

Solutions consist of various market products and strategies such as cantilever slab connections, specialized high thermal resistance bricks, insulation along the sides of construction elements, etc. The calculated Ψ-value of each solution is placed into three load categories: low, medium and high. These solutions are presented in a simplified and detailed table in the finished leaflet. The simplified table shows which solution is possible for which load category and the detailed table shows the calculated Ψ-value of each solution for the specific base case. Using the example building, several possible combinations of solutions are presented and their effect on the overall energy consumption illustrated.

Since each building and building owner has different priorities, it is left up to the engineers, architects and building physics experts to determine which solution is right for a given project. Care and attention should be given to the choice of materials or products, as well as detailed calculations of structural integrity and moisture performance.

Keywords: thermal bridge, earthquake resistance, energy efficiency, building envelope

INTRODUCTION

Thermal bridges can make up to 40% of the total heat loss of a highly energy efficient building (passivhaus, MINERGIE-P, etc.). Structural building elements sometimes come into conflict with a continuous thermal insulation layer, particularly in unheated basement floors or underground garages. As requirements on energy efficiency and earthquake resistance

increase, these conflicts become more pronounced. A number of products and techniques to minimize thermal bridge effects at the junctions of structural members exist already, but are not widely implemented due to a lack of knowledge on the importance of thermal bridges in energy efficient buildings and how these solutions may be implemented.

As the U-value of a building component decreases by placing more or better insulation, thermal bridge effects become more pronounced. In addition to heat loss, thermal bridges can lead to problems such as discolouration, mold or condensation. Any method of reducing thermal bridge effects must not compromise structural integrity and building safety. This paper aims to illustrate construction techniques and products that satisfy both the requirements of structural integrity and energy efficiency.

METHOD

Thermal bridges

This paper examines thermal bridges in typical newly constructed apartment buildings between three and six stories, which represent a large portion of the built infrastructure in Switzerland. The most common areas where structural members create discontinuities in thermal insulation are defined along with the associated boundary conditions in order to examine possible solutions. The thermal bridges examined are placed into five groups: indoor wall-to-floor/ceiling connections (1), outdoor wall-to-floor/ceiling connections (2), wall-to-wall connections (3), cantilevers (4) and connecting members to underground garages (5). Figure 1 shows the locations of the various types of thermal bridges with numbers denoting their groups.

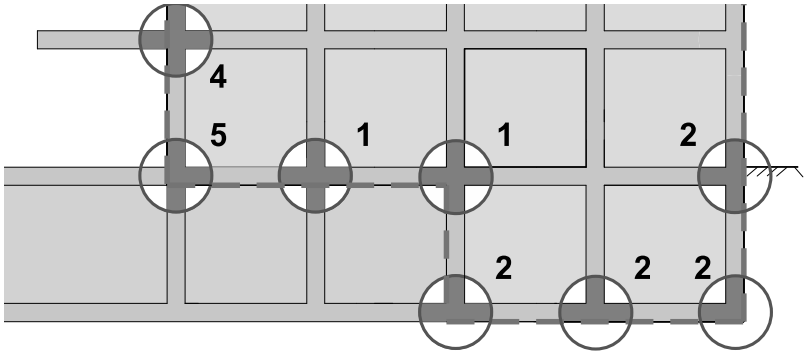

Figure 1: Cross-section of basement and ground floor showing locations of thermal bridge types

Reference building

In order to illustrate the proper application of the various solutions and their effects on the Ψ-values of the thermal bridges, a simplified typical example was developed, shown in Figure 2.

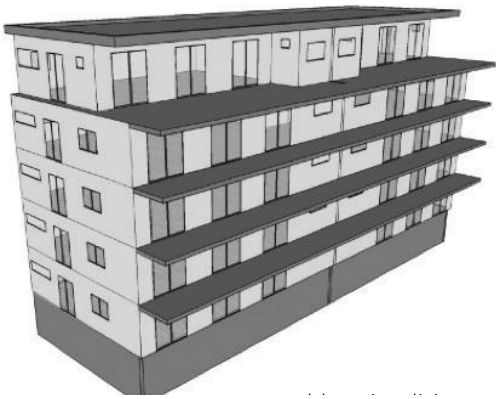

Figure 2: Reference building

This example was optimized to meet the requirements for high energy efficiency in all aspects excluding the thermal bridges. The resulting value for the total heat energy required, Qh, was found to be 104 MJ/m2a, which was 69% above the heat energy limit for highly energy efficient buildings which is 60% of the base heat energy limit $Q_{h,li}$ (according to passivhaus, MINERGIE-P). This case was referred to as the base case to which all improvements in Ψ-values could be measured.

Structural analysis was performed on the reference building and the loads grouped into low, medium and high according to Table 1 below.

Load case	Compression (-kN/m)	Tension (+kN/m)	Horizontal shear (+kN/m)	Vertical shear (+kN/m)
1 – low	<350	<30	<30	<30
2 – medium	350-750	30-100	30-100	30-100
3 – high	>750	>100	>100	>100

Table 1: Load cases for walls in reference building

The areas on the ground and basement floors where the loads from Table 1 are located are shown in Figure 3 below.

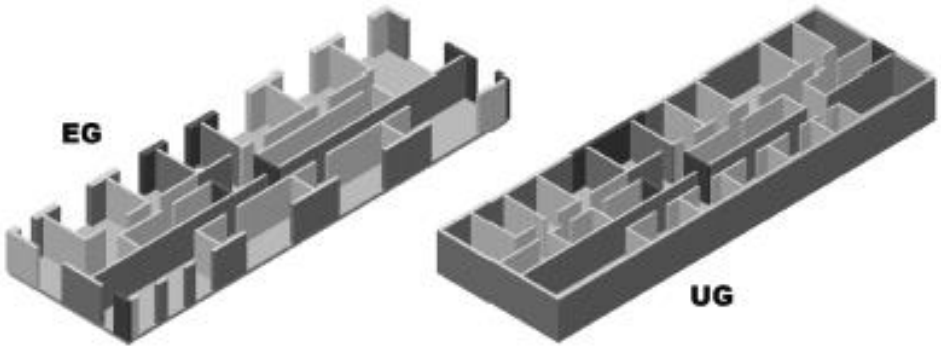

Figure 3: Locations of load cases from Table 1 (light/medium/dark grey = low/medium/high loads; EG – ground floor, UG – basement)

RESULTS

The following strategies for improving Ψ-values were examined in this project, summarized in Table 3.

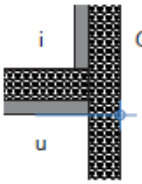	**Connections constructed with reinforced concrete (base case)** All structural members constructed entirely of reinforced concrete	Ψ Ψ Ψ
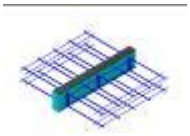	**Cantilever slab connecting members** Reinforced and insulated special connecting members that simultaneously transfer loads and reduce heat transfer for cantilever slabs	√ √ x
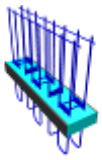	**Reinforced stainless steel connecting members** Reinforced, stiffened and insulated special connecting members that simultaneously transfer loads and reduce heat transfer for wall connections	√ √ √
	**Insulated wall connecting member for reinforced concrete walls** Reinforced, stiffened and insulated standardized special connecting members that simultaneously transfer loads and reduce heat transfer for wall connections	√ √ √
	**Concrete wall connection with insulating bricks** Insulating bricks placed at wall-floor or wall-ceiling junctions	√ x x
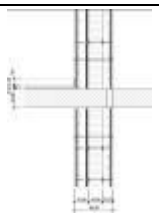	**Concrete with lower thermal conductivity** Walls built using a specialized system consisting of thermal insulation between insulating concrete slabs	√ √ √
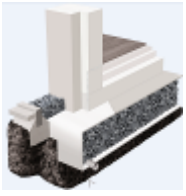	**Ground-side insulation under foundation slab** Foundations constructed using one monolithic slab with insulation continuous underneath the slab and along walls	√ √ √
	**Insulation along sides** Minimal insulation placed along the sides of connecting members	√ √ √

	**Bricks** Walls constructed using bricks (clay or sand-lime as required) as opposed to reinforced concrete	√ x x
	Structural members detached Members are thermally detached from one another * loads must be transferred through alternate members	√* √* √*

Table 3: Methods to improve thermal bridges (light/medium/dark grey = low/medium/high loads; √ - strategy may be applied at this load level, x – strategy may not be applied at this load level, Ψ – strategy may be applied at this load level, but thermal properties are not desirable)

For the case study building, Ψ-values were calculated for each thermal bridge and each construction strategy. The resulting table is printed in the finished leaflet, but is too large to include in this paper. In the following section, the effect of choosing certain strategies is evaluated based on its effect on the total heat energy required, Q_h.

DISCUSSION

In order to demonstrate the flexibility the above solutions allow designers and architects to implement, a few strategies were chosen and the total heat energy required calculated and compared to the base case in Table 4.

Strategy	**Qh (MJ/m2)**	**Improvement of Qh**
Base case – all thermal bridges constructed with reinforced concrete	104	-
Best possible Ψ-value for all thermal bridges	56	46%
Best possible Ψ-value for all thermal bridges with exception of thermal bridges at stairwell*	61	41%
Best possible Ψ-value for all thermal bridges with exception of outer walls*	64	38%
Best possible Ψ-value for all thermal bridges with exception of balcony connections*	71	30%
Best possible Ψ-value for all thermal bridges with exception of underground garage*	60	42%
Minimal strategy: base case Ψ replaced with highest Ψ-value from Table 3	89	14%

*Table 4: Selected strategies used to illustrate many methods to improve overall thermal energy efficiency of a building by improving structural thermal bridges (*exceptions are left with the original Ψ-value of the base case scenario)*

As evidenced by the many possibilities in Table 4, it is possible for architects and designers to choose appropriate solutions according to additional criteria. It must be remembered that these solutions do not guarantee freedom from damage that may be caused by moisture.

Considerations relating to moisture damage are separate from thermal bridge criteria and outside the scope of this project. It is recommended that all strategies be checked by a structural engineer and building physics expert prior to implementation.

Additional criteria such as costs, permeability, fire safety, acoustics and others may narrow the possible solutions for a given building component. These are to be examined prior to implementing any solution. Naturally, it is necessary to assure quality construction on site to ensure the solutions perform as expected.

ACKNOWLEDGEMENTS

This project was carried out by hässig sustech gmbh and Buchmann Partner AG with financial and technical support from the following industry partners: Debrunner Acifer AG, Misapor AG, Spaeter Zug AG (ebea AG) and Stahlton Bauteile AG. The project was financially supported by the Swiss Federal Office of Energy (SFOE) and the Office of Waste, Water, Energy and Air (WWEA) of the canton of Zurich.

REFERENCES

1. Arbeitskreis kostengünstige Passivhäuser: Wärmebrücken und Tragwerksplanung - die Grenzen des wärmebrückenfreien Konstruierens. Passivhaus Institut, Darmstadt, 2007
2. Infomind GmbH: Wärmebrückenkatalog. Bundesamt für Energie BFE, Ittigen, 2002
3. Notter, G; Menti, U.-P; Ragonesi, M: Wärmebrückenkatalog für Minergie-P-Bauten. Bundesamt für Energie BFE, Ittigen, 2008

DOUBLE FACADES A MORE SUSTAINABLE SOLUTION THAN A OPTIMAL SINGLE FACADE

Wim Zeiler, Joep Richter, Gert Boxem

Department of Built Environment, Eindhoven University of Technology, Netherlands

ABSTRACT

Facade parameters influence the energy flows coming through the facade, in order to optimize the indoor environment for the comfort of the individual building occupant with minimal energy use. How can the facade make optimal use of the free incoming energy flows to maximize the comfort level of the individual building occupant at minimal energy use? The type of façade described as a second skin façade is characterised by a single glass layer on the outside and an isolated façade layer on the inside, which often includes an insulated glass layer. The application of the single glass layer as a second skin around the insulated layer results in an air cavity between these two layers. The property that distinguishes a second skin façade from other DSF is that it relies on natural ventilation of the cavity, in comparison to other facades which use mechanical systems to induce the airflow. The advantage of merely using natural ventilation in the façade cavity is the lower energy consumption. However, it also results in some unresolved issues which require further attention. This project is concerned with the behaviour of a highly complex shaped second skin facade on a Dutch office building, and the thermal comfort impact on the building user. During 3 weeks different measurements were done to determine the main characteristics of the glass and the facade. These measurements were related to earlier measurements done by other buildings with a second skin facade. A key difference between a second skin facade, as well as other climate facades, and more traditional opaque facades is its dynamic behaviour.

Keywords : double skin façade, thermal comfort

INTRODUCTION

The façade of a building is one of its most distinct features, defining not only a buildings aesthetics, but also separating the indoor environment for the outdoor climate as a large part of the building shell. As a result of this, a façade strongly affects the comfort level and energy use of a building. Improving the performance of the façade is therefore aspired in order to further improve the quality of a buildings indoor environment while also reducing its energy consumption. In modern buildings the facade is often considered as part of the climate system, since its performance greatly affects the indoor climate and thus comfort and energy use. The second skin principle offers excellent possibilities to improve the comfort level and energy use of existing buildings, by applying the second skin to its current facade. Despite all these positive effects associated with the application of the second skin façade to buildings, sometimes realized applications are linked with comfort problems [1-4]. The inducement for this study originates from a building in the Netherlands, displayed in figure 1. Occupants of this building complained about the quality of the indoor environment, especially the thermal environment. It was discovered that the behavior of the applied second skin was not in accordance with its design, and the presumption is made that this could be the cause of a part of the comfort complains. Considering all the positive and negative implications associated with a second skin facade made it a very interesting subject for further study.

Figure 1: Outside of the façade, the cavatity of the DSF and the atrium behind the DSF

METHODOLOGY

The aspect of thermal comfort is one of the key facets of the indoor climate, which has an essential part in the quality of the indoor climate of a building. And it is also strongly related to the energy household of a building. The objective is to determine the interactions of a transparent facade with the comfort perception of a occupant. In order to do this it must first be determined how the thermal comfort of the indoor environment should be assessed, and how the façade impacts this. The comfort aspect can be subdivided into four aspects according to the European standard EN-15251: Thermal environment; Lighting; Air quality and Acoustics. From these four aspects the thermal environment (Constant and Warmth) is discussed because of their relationship to the dynamic chancing conditions of the façade and their higher contribution to the overall comfort perception of a building user according to [5], which is displayed in table 1.

Table 1. The relative importance of six indoor comfort aspects in European offices

	Coefficients	SE	*t*	*p*
(Constant)	1.24	0.062	20.0	<0.001
Warmth	0.39	0.023	17.0	<0.001
Air movement	0.16	0.024	6.6	<0.001
Humidity	0.12	0.024	4.8	<0.001
Light	0.05	0.023	2.3	0.020
Noise	0.13	0.019	6.6	<0.001
Air quality	0.36	0.021	17.2	<0.001

Currently, the most common method to determine the quality of the indoor thermal environment is based on the predicted mean vote (PMV) and percentage people dissatisfied (PPD), which expresses the mean thermal sensation vote of the building user, and the number of building users that is expected to be dissatisfied with the thermal environment in the building based on the PMV, respectively. The PMV is determined according to four thermal environmental factors and two personal factors: Air temperature, mean radiant temperature, air velocity, relative humidity, activity level and clothing.

CALCULATIONS

When considering the influence of the surface temperature of the façade on the MRT only the long wave radiation is taken into account. The range of this effect can be determined by finding the maximal range in view factors and surface temperatures in order to calculate the resulting effect on the MRT. The range in view factors is derived from previous work conducted by Rizzo [6]. The difference of the façade temperature compared to the rest of the indoor surface temperatures has been derived from manual calculation of the indoor surface temperature for various cases.

Table 2: Indoor surface temperatures(Tsi) of the glazed area as a result of various external temperatures (Te), which correspond to extreme outdoor conditions (30 and -10) or assumed cavity temperature (45, 60, 5) and indoor surface temperatures (Tsi) of the glass

T_e (°C)	T_i (°C)	R_e (°C)	R_c glass(°C)	R_c frame(°C)	R_i (°C)	T_{si} glass(°C)
-10	22	0,04	0,75	0,42	0,13	17,5
5	22	0,04	0,75	0,42	0,13	19,6
30	24	0,04	0,75	0,42	0,13	24,8
45	24	0,04	0,75	0,42	0,13	27,0
60	24	0,04	0,75	0,42	0,13	29,1

The calculated surface temperatures above apply to the surface temperature of the glass surface on the inside of the building. In case a shading device is present and deployed on the inside a considerable difference can be present, because the temperature of this device can increase to temperatures much higher than the calculated indoor surface temperatures of the glass, and therefore affect the MRT to a greater extent. Although the temperature differences are greater, as can be seen in table 2, it must be kept in mind that the surface area, and therefore the view factor in regard to a building occupant is also considerably lower. Another part of the facade of which the temperature can differ of the glazed material is the frame in which the glazing is held. The thermal resistance of this part is often considerably lower than that of the glazing. As a result, the local surface temperature on the inside of the facade differs from the above calculated glass surface temperatures. For the effect of long wave (infrared) radiation on the MRT the indoor surface temperature and view factor are key parameters.

MEASUREMENTS

During a period of nearly two weeks, from April 5th till April 17th 2013, the temperatures within the cavity were measured as well as the indoor solar radiation in the horizontal plans as well as parallel to the window. The surface temperatures (T_s) of both sides of both panes are measured in one line and not too close to the window frame. The different sensors that are used for the measurements can be found in table 3. Since the measurements continue for one week, the data is stored with data loggers. Two different data loggers are used. One data logger is used for the parameters that are measured in the office space and one for the parameters that are measured in the cavity and outside the building. This data logger has a wireless connection with transmitters that are connected to the sensors, which makes it possible to station the data logger inside and the sensors and transmitters outside and in the cavity.

Table 3: Sensors used by measurements

Parameter	Sensor	Accuracy
Temperature	NTC thermistor Sensor data DC 95	calibrated sensitivity
Solar radiation	Pyranometer (CM5 and CM11)	1 %
Air velocity	Dantec 54R10	calibrated sensitivity

The air temperatures (T_a) in the cavity are measured at three levels: 2nd floor, 3th floor and 4th floor. The pyranometer and air temperature sensor to measure the outside conditions are placed on appropriate positions on the roof, where there are no obstructions. The air temperatures inside are measured at 0.5 m from the façade at a height of 1.10 m. The air velocities are measured on the same positions as the air temperature at 0.5 m from the façade at a height of 1.10 m. The horizontal radiation asymmetry (T_{ra}) is measured at 0.5 m from the façade at a height of about 1.1 m and the vertical radiation asymmetry is measured at the same distance from the façade at a height of about 1.1 m. The solar radiation inside is measured vertically at a minimum distance of the façade, see Fig. 2.

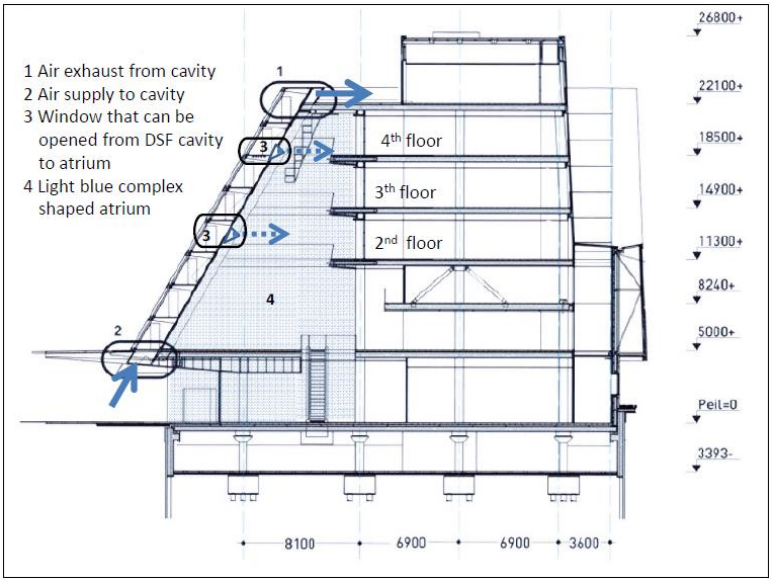

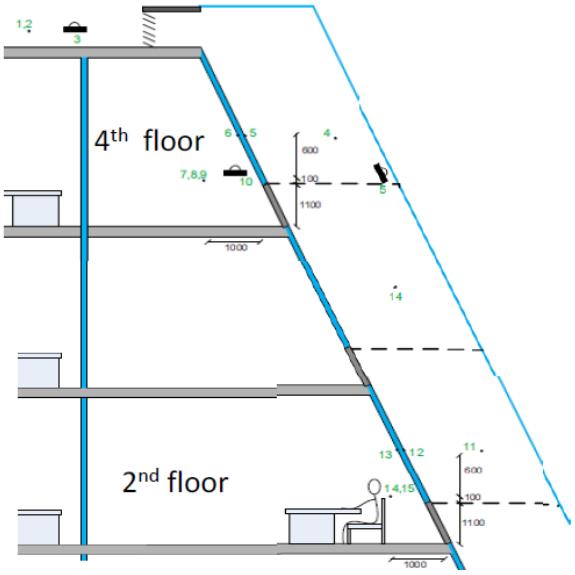

Figure 2: The schematic representation of the ventilation supply from the cavity to the atrium and the schematic measurements setting on the 2nd and 4th floor

RESULTS

Here the focus is the cavity temperature increase and the inner glass temperature due to the solar radiation and the fast changes to the thermal indoor conditions for the occupants. Beside the MRT the radiation asymmetry is also a comfort indicator related to the facade. The Fig. 5 and 6 provided previously correlated dissatisfaction between radiant temperature and air temperature. This corresponds to the difference between the indoor MRT and the surface temperature on the inside of the facade. In the Fig. 5 & 6 the comfort lines are drawn related to the approach by Lusden and Freymark [7] to indicate the range of perceived thermal comfort.

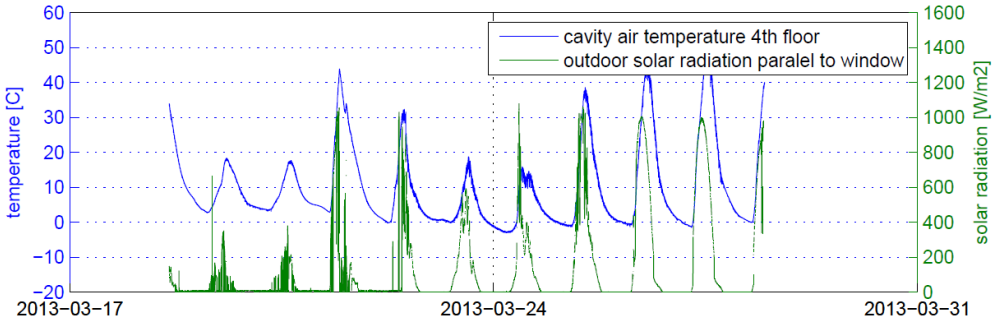

Figure 3: Cavity temperature 4th floor versus outdoor solar radiation

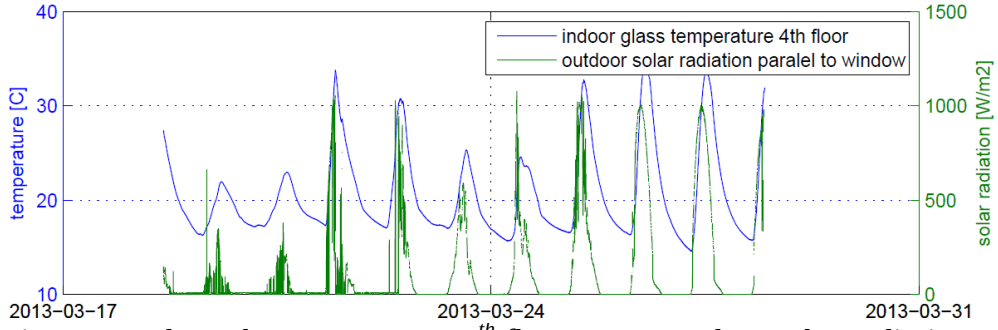

Figure 4: Indoor glass temperature 4th floor versus outdoor solar radiation

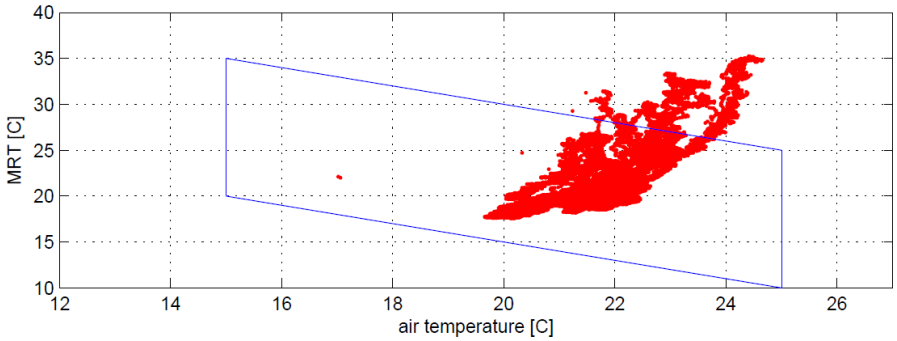

Figure 5: Ration between radiant temperature and air temperature of 2nd floor

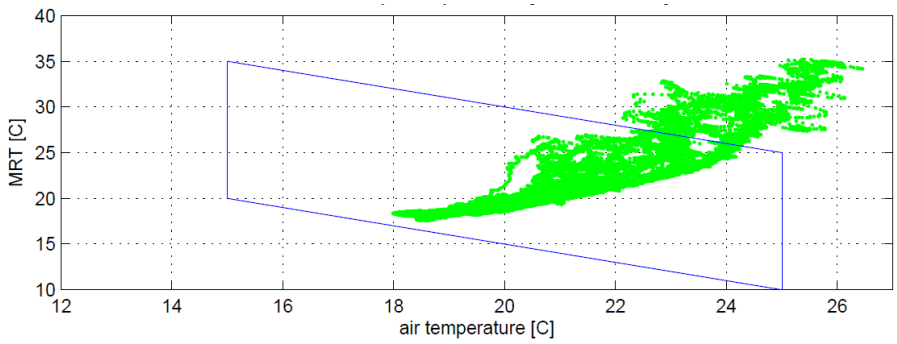

Figure 6: Ration between radiant temperature and air temperature of 4th floor

DISCUSSION AND CONCLUSIONS

Concerning moderate environments the mean radiant temperature is a very significant factor even though the surrounding air may be at a comfortable level may lead to the asymmetry of the radiant heat flow around the person with the consequent onset of local thermal discomfort [8]. When comparing the results of this study with results of two other buildings with double facades [9], as shown the case study building is tending to a ration between radiant temperature and air temperature which is too warm already in some periods in winter.

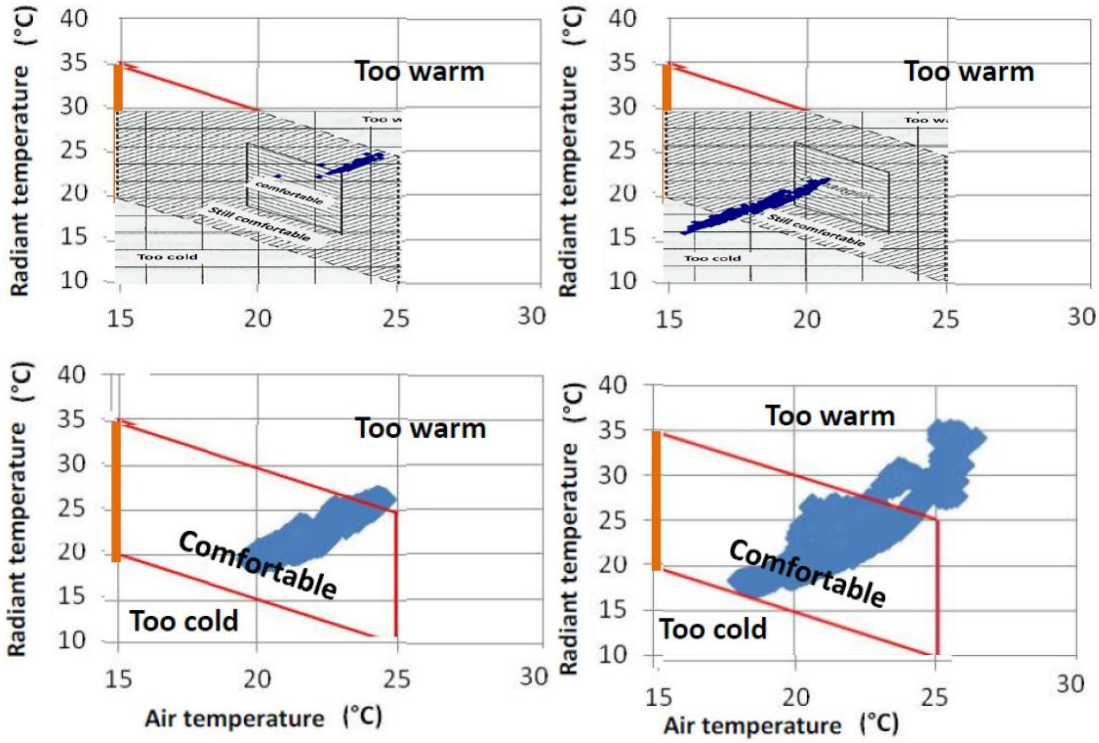

Figure 7: Comparison between radiant temperature and air temperature of projects[9].

The case study building with its double skin facade showed the strong effect of solar radiation with an average temperature increase of 20°C and peak increases reaching 40°C. The high increases of cavity temperature in the case study during the cold period indicate that the risk of the increased cooling load is very plausible during warm periods. Therefore, the effect of the additional air cavity to the façade by the application of the second skin is questionable for the optimization of thermal comfort and energy use. In this case more energy is needed to cool the occupants than will be saved by the reduced energy losses in winter.

REFERENCES

1. Lyons P.R.: Window performance for human thermal comfort, ASHRAE Transactions. 2000:594-602
2. Poirazis H.: Double skin facades, a literature review, IEA SHC Task 34 ECBCS Annex 43, 2006
3. Hwang R., Shu S.: Building envelope regulations on thermal comfort in glass facades buildings and energy-saving potential for PMV-based comfort control, Building and Environment 46:824-834, 2011
4. Joe J., Choi W., Kwon H., Huh J.: Load characteristics and operation strategies of building integrated with multi-story double skin facade Energy and Buildings, 60:185-198, 2013
5. Humphreys M.: Quantifying occupant comfort: are combined indices of the indoor environment practicable? Building Research & Information(2005): 317-325
6. Rizzo G. C.: Algorithms for the calculation of the view factors between human body and rectangular surfaces in parallelepiped environments. Energy and Buildings, 1992, 51-60.
7. Leusden F. P., Freymark H., 1: Darstellung der Raumbehaglichkeit für den einfachen praktischen Gebrauch. Gesundheits Ingenieur 72(16): 271-273, 1951
8. Atmaca I, Kaynakli O, Ygit A. Effects of radiant temperature on thermal comfort. Build Environ 2007;42:3210-20.
9. Verdonschot, J. (2006). Performance of ventilated double façades compared to a single skin façade, Masterthesis Technische Universiteit Eindhoven.

THE INFLUENCE OF SURFACE IRREGULARITY OF BUILDING FACADE ON ITS THERMAL PERFORMANCE

Alan Lai[1]; Edward Ng[2]

1: School of Architecture, The Chinese University of Hong Kong, Rm 505, AIT Building, HK

2: School of Architecture, The Chinese University of Hong Kong, Rm 504, AIT Building, HK

ABSTRACT

Urban heat island effect has been intensified due to rapid urbanization. The intra-urban temperature rises resulted in a higher energy demand for temporal thermal comfort inside the building. Anthropogenic heat is further released worsening the urban heat island effect. Inhabitants of urban areas are trapped in such a vicious circle. The aim of this study is to reduce energy generation demand for mechanical air-conditioning system, especially in summer, by means of optimising overall urban and building albedo through modifying surface geometry, and hence thermal performance, such as reflectance, emittance, transmittance and admittance of each building envelope. This study at first examined the influence of surface irregularity of external vertical wall on its temperature gradient so as to establish an understanding about the effect of geometrical structure of building facade on its thermal admittance and transmittance.

Keywords: albedo, surface irregularity, building façade, surface temperature, urban heat island

INTRODUCTION

Urban heat island has been identified as a phenomenon whereas air temperature in the urban area is higher than that in the surrounding rural area. Figure 1a illustrates the air temperature gradient across the distance from the rural to the centre of the urban area with cloudless skies and light winds, just after sunset [1]. The high intra-urban temperature is obviously due to urbanization causing thermal stress to the inhabitants. This introduces a greater electrical energy demand for air-conditioning within the buildings in the hot days and nights. Anthropogenic heat released is thus getting larger from the mechanical air-conditioning system. The air temperature in the urban area is even prompted intensifying the heat island effect. Inhabitants are being trapped in such vicious cycle unless the effect is alleviated from the fundamental aspects.

Surface geometry control of urban city could be one of the strategies to reduce solar heat gain from the very beginning of the aforementioned process. Geometrical structure does affect its albedo, or reflectance of solar radiation, and hence the solar heat gain and the surrounding temperature [2]. This study aims at investigating how the geometrical structure of building envelope affects its surrounding temperature in the first place so as to study its thermal behaviour, such as albedo, admittance, and so on in the near future for both indoor and outdoor thermal comfort.

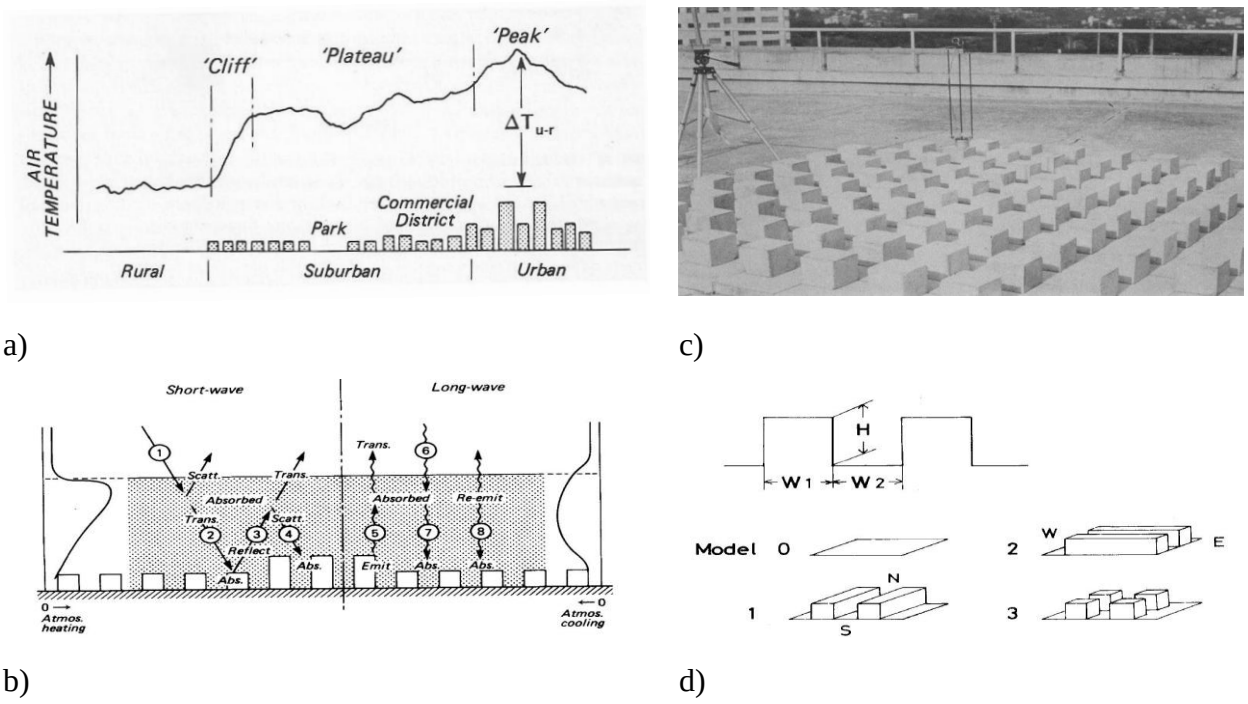

Figure 1: Studies of precedent concerned the heat island effect and urban albedo: a) generalized cross-section of a typical urban heat island (Oke, 1987); b) Schematic depiction of radiative exchanges in a polluted urban boundary layer (Oke, 1982); c) View of block-canyon model experiment, and d) Illustration of block-canyon models (Aida, 1982).

BRIEF LITERATURE REVIEW

To reduce direct solar radiation, construction materials of higher albedo, or reflectance are usually used for the buildings surfaces, such as roof, and envelopes reducing the surface short-wave absorption, thus reducing direct solar heat gain. In fact, the term, albedo can be referred as either the characteristics of the materials itself; or the characteristics of the final product as a whole [3]. For the first meaning, Prado (2005) discovered that certain roof materials of high albedo not only could absorb little solar radiation, but also could attain a lower surface temperature if only they were of high emittance resulted in transmitting little thermal radiation to their surroundings [3]. Moreover, Simpson (1997) had revealed that white roof had the lowest surface temperature which was around 20℃ cooler than gray or silver roof. Also, one of the important things is that both gray and silver roof had similar surface temperatures, though the silver roof is more reflective, i.e. higher albedo, than the gray one [4]. The above results show that a high value of albedo is not decisive enough to attain a lower ambient temperature, hence the thermal comfort.

Since the understanding of characteristic of the material itself is not sufficient enough to achieve thermal comfort, surface geometry control could be alternative. For another meaning of albedo, Aida and Gotoh (1982) studied the urban albedo, the effective reflectance of an urban city, decreased due to canyon geometrical structure because of its surface irregularity had introduced an anomalous absorption of direct solar radiation (see Figure 1c and 1d) capturing more photon by multiple reflections within the canyon [5]. It is evident that the geometrical control did affect the albedo of a given surface, like the urban surface. Aida's research result is correlated to Oke's statement that urban geometry is a fundamental control on the urban heat island [1].

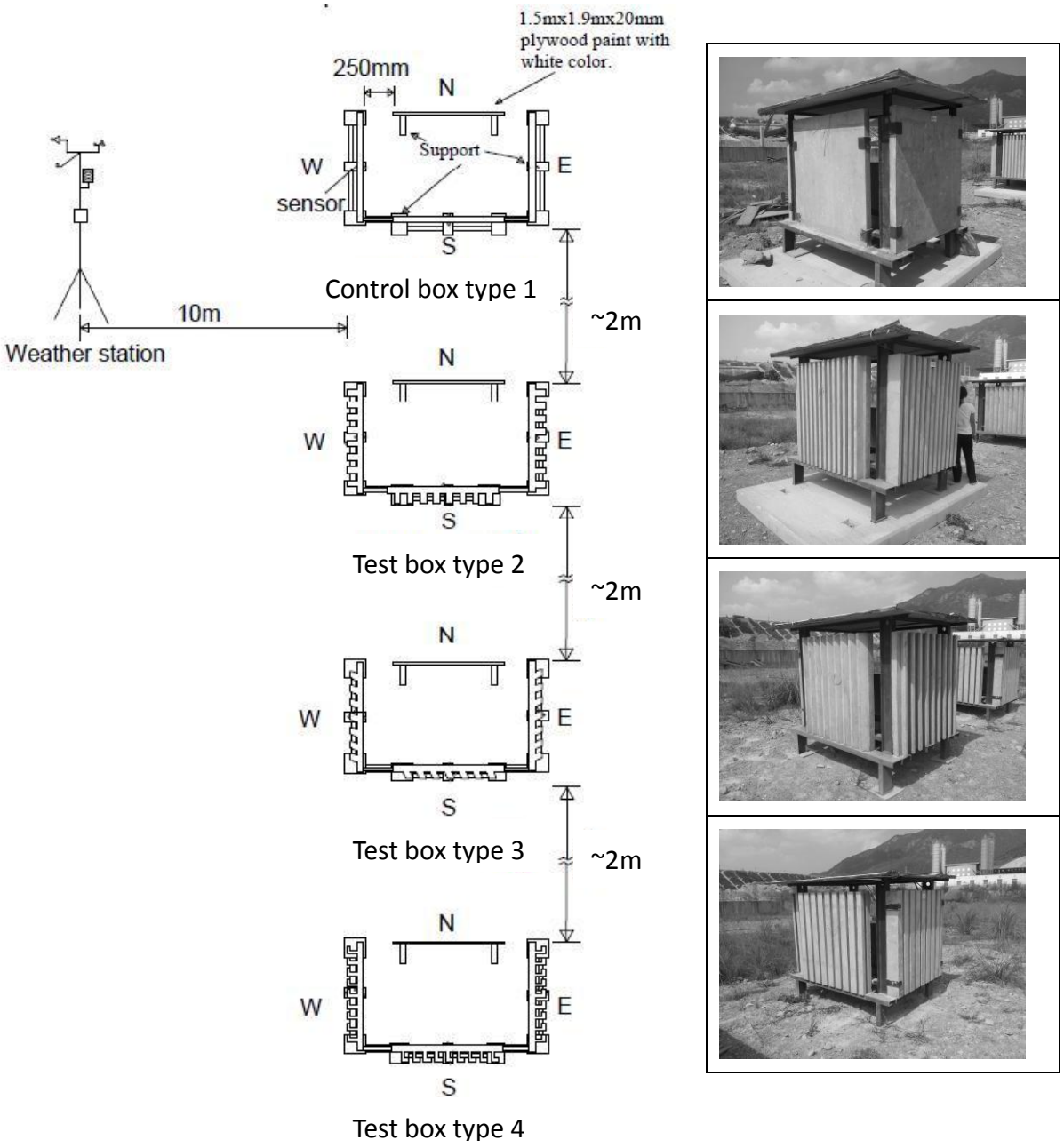

Figure 2: The schematic diagrams of the experimental setup are shown.

METHODOLOGY

For the sake of simplicity, four small house models have been represented in Figure 2 with each consists of three concrete walls facing east, south, and west. The experimental models aligned in a row along the north-south direction on an unobstructed horizontal terrain with canyon width of about 2 m so as not to block the direct solar radiation on each south-facing wall. The walls were pre-cast concrete wall in nature of at least 75mm width. The house models were named as type 1 to 4, respectively as in Figure 2. Type 1 walls were fair face flat concrete wall working as control; while other three types, namely type 2 to 4 had different

surface geometrical irregularities which can again refer to the corresponding figure. Besides, there were sensors, which are thermocouple in principle, mounted on the centre of each wall to measure the exterior (outside) and interior (inside) surface temperatures. For each wall, both ‘outside’ and ‘inside’ temperatures were recorded for the whole day with a time step of 5 minutes. In other words, the equipment recorded both temperatures for each wall every 5 minutes. The temperatures and the temperature gradient of the same wall could be plotted on different graphs against the time and date.

The thermal performance discussed in the following text is the thermal admittance, which measure how easily the heat is transferred from outside to inside. And one thing should be noted is that when the model performed better means the admittance is low, i.e. it is relatively not easy for the heat transferred into interior environment.

RESULT AND DISCUSSION

For the west facing wall, type 2 wall achieved the best thermal performance by day, while the least is the type 1 wall design. Type 3 and type 4 had similar thermal behaviour. Their performances were in between type 1 and type 2. From figure 3 and 4, both outiside temperatures of type 1 and 2 were similar, but the inside temperature of type 2 was smaller than that of type 1 by about 2 °C. Hence, the temperature difference between outside and inside temperature of type 2 were about 2 °C larger than that of type 1 (see Fig. 5 and 6). This showed that the geometry of the wall improved the thermal performance of type 2 in this preliminary study.

For the south facing wall, the thermal performance of type 4 is better than that of type 1. Meanwhile, results of type 2 and 3 were not resonable which might suffer from serious instrumental error or human error, etc. The outside temperature of type 4 was less than that of type 1 by 2 °C. And the inside temperature of type 4 was about 4 °C smaller than that of type 1 (see Fig 7 and 8). Thus, temperature difference between outside and inside temperature of type 4 were about 2 °C larger than that of type 1 (see Fig. 9 and 10). The geometrical design of type 4 enhanced its thermal performance.

For the east facing wall, the thermal performance of type 2 was better than that of type 1. But, type 3 and 4 had their outside temperature much lower than that of inside, which might be due to instrumental error. The outside temperature of type 2 was less than that of type 1 by about 1 °C (Fig. 11) . And the inside temperature of type 2 was less than that of type 1 by 3 °C (Fig. 12). The temperature difference between outside and inside of type 2 was larger than that of type 1 by about 2 – 3.5 °C (Fig. 13 and 14). Hence, the geometically modified type 2 was better than the control type 1 in thermal performance.

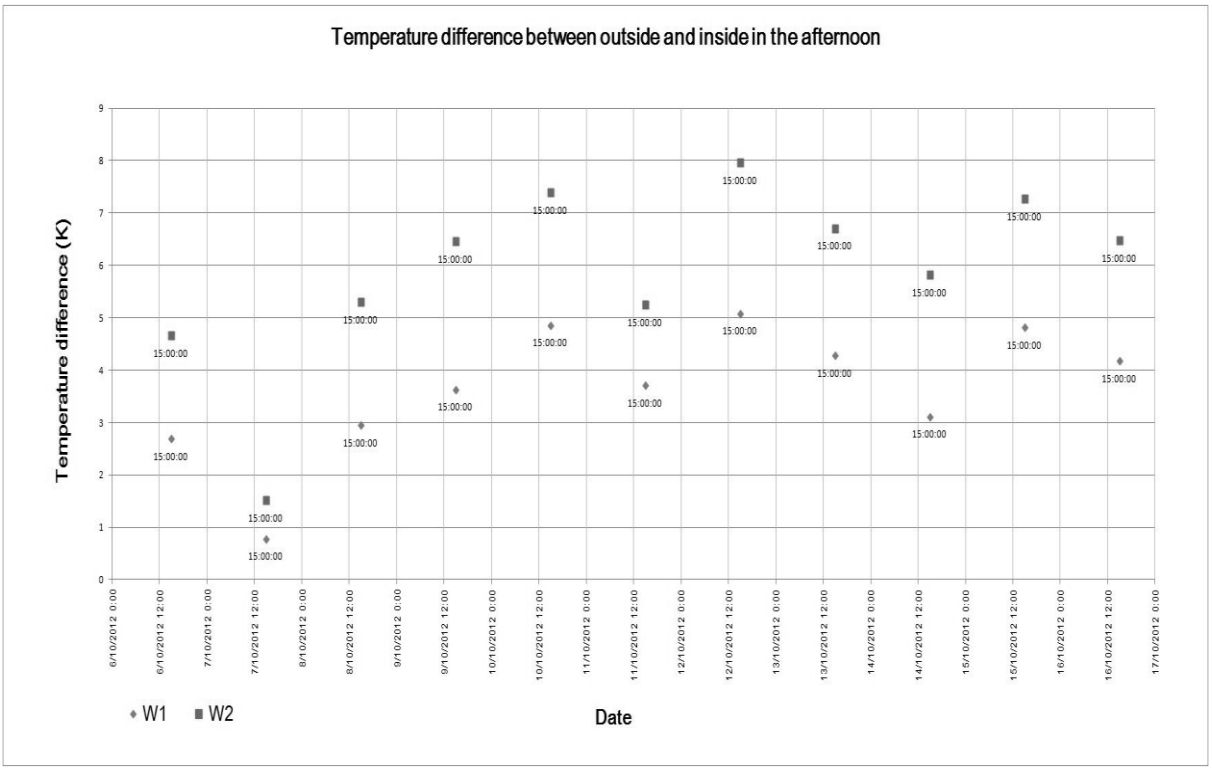

Figure 6: The temperature difference relative to inside temperature of type 1 against the date for the west wall.

CONCLUSION

Desipte of the orientation of the walls, the concrete walls with geometrical modification on their surface behaved better than the concrete wall with flat surface in terms of thermal behaviour. The interior surface temperature of geometically modified walls was kept cooler than that of the flat one by 2°C in most of the cases, and even by 3.5 °C in some cases. As a matter of fact, it will reduce 9% energy use in air-conditioning if the room temperature is raised from 22.5 °C to 25.5 °C. In order words, the geometrically modified walls will reduce the need to lower room temperature by 2 - 3.5°C and, thus prompt occupants not to use air-conditioning system so as to save both energy and money.

Last but not least, the modified geometrical surface of the concrete walls does affect and even enhance their thermal performance. It is verified that type 2 model was the best among other types in this preliminary study.

FUTURE STUDIES

This study only preliminarily verified the geometrical treatment did affect its thermal admittance such that it is not so easy for the heat energy transferred from the exterior surface to the interior surface. Further studies are needed to investigate the difference between the sol-air temperature and the exterior surface temperature for each wall. In order to do this, meteorological data should be collected properly by the local micro-station. For another thing, the dimensions of the surface irregularity should be recorded and testified as a new set of parameters so as to scrutinize the influence of surface geometry on thermal performance. All of the above in fact require future works.

REFERENCES

1. Oke, T.R.: Boundary Layer Climates (2nd Ed.), Methuen, Inc., USA, 1987.
2. Aida, M.: Urban Albedo as a Function of the Urban Structure - A Model Experiment, Boundary-Layer Meteorol., 23, 405 – 413, 1982.
3. Prado, R.T.A., and Ferreira, F.L.: Measurement of albedo and analysis of its influence the surface temperature of building roof materials', Energy and Buildings, 37 (2005) 295 – 300, 2005.
4. Simpson, J.R., and McPherson, E.G.: The effects of roof albedo modification on cooling loads of scale model residences in Tucson, Arizona, Energy and Building, 25 (1997) 127 -137, 1997.
5. Aida, M., and Gotoh, M.: Urban Albedo as a Function of the Urban Structure - A Two-Dimensional Numerical Simulation, Boundary-Layer Meteorol., 23, 416 – 424, 1982.

Solar Active and Passive Cooling

PROMOTING ENERGY EFFICIENCY IN COMMERCIAL BUILDINGS BY USE OF NATURAL VENTILATION

Leon R Glicksman[1, 2]; FA Dominguez Espinosa[2]; MA Menchaca-Brandan[2]; Stephen Ray[2]; Haofan Cheng[1]

1: Building Technology Program, Department of Architecture, Massachusetts Institute of Technology. 77 Massachusetts Avenue, room 5-418, Cambridge, MA 02139, USA.

2: Department of Mechanical Engineering, Massachusetts Institute of Technology. 77 Massachusetts Avenue, room 5-418, Cambridge, MA 02139, USA.

ABSTRACT

The use of mechanical cooling is rising in many parts of the world leading to substantial increases in energy consumption and greenhouse gas emissions. This is particularly true in fast-growing areas of the developing world. Natural ventilation holds the promise to provide comfort during the cooling season while minimizing energy use. There are key issues of design and control that must be met to assure successful application of this new technology. These must be based on an understanding of the air flow behavior found from simulations and real building data. New insights into the behavior of naturally ventilation systems will be presented based on monitoring of multistory commercial buildings in the US, UK and Japan. A new design tool, CoolVent, using an airflow network, refined by CFD simulations, and building data will be described. The program has been used in the design of a new office building in central Tokyo that uses a hybrid natural ventilation/ air condition system. Initial results of the building performance will be presented. A key challenge to the successful operation of this building lies in the control system. Proper control can extend the duration of interior comfort conditions while also dealing with instances of multiple equilibrium states.

Keywords: Natural ventilation, design tools, monitoring

INTRODUCTION

The use of mechanical cooling is rising in many parts of the world leading to substantial increases in energy consumption and greenhouse gas emissions. For example, in US commercial buildings, cooling and ventilation account for close to 20 percent of the total yearly energy use. This is particularly true in fast-growing areas of the developing world that are located in cooling dominated climates. Natural ventilation holds the promise to provide comfort during the cooling season while minimizing energy use. In its simplest form natural ventilation uses wind or buoyancy forces to induce high air exchange rates in the building interior. The internal gains are balanced by the enthalpy increase of the airflow. Elevated air circulation rates result in an interior temperature close to the exterior conditions. The actual design of a natural ventilation system must consider a number of challenges. The airflow must be circulated uniformly through the building interior to ensure adequate comfort throughout the space. The system must be flexible to account for changing weather conditions and interior loads. When properly used, the thermal mass of the building can moderate exterior temperature fluctuations. Additional control strategies are needed to properly operate hybrid systems that combine natural ventilation with mechanical fans and conventional chillers.

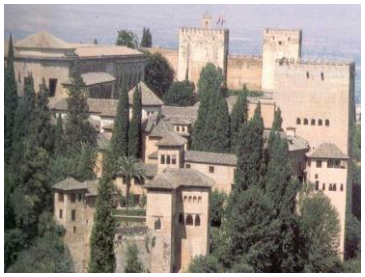

a)

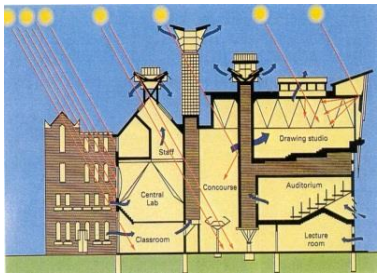

b)

c)

d)

e)

f)

Figure 1: Examples of natural ventilation designs: a) wind towers, b) individual ventilation "chimneys", c) wind driven cross ventilation, d) combined wind and buoyancy ventilation, e) fan assisted ventilation, f) hybrid buoyancy / air conditioning.

NATURAL VENTILATION SYSTEMS

Figure 1 illustrates a range of different natural validation designs that have been employed. Traditional wind towers used in the Middle East are shown in figure 1a. De Montfort University building, figure 1b, has a series of vertical stacks to promote buoyancy flow. The San Francisco Federal building, figure 1c, uses wind driven cross flow to ventilate the upper floors. An office building at Luton in the UK uses a combination of cross flow and buoyancy through a central atrium, figure 1d. The Artists for Humanity building in Boston, figure 1e has a fan assisted natural ventilation for night cooling and the Hulic headquarters building in Tokyo, figure 1f, has buoyancy driven natural ventilation with multiple floors connected to a common vertical stack. This latter building also has a conventional air conditioning system; in extreme conditions the natural ventilation vents are closed and the conventional system is used to maintain comfortable conditions.

For architects and consultants to consider using one of these various designs, they need to have a means to simulate their performance under a number of operating and weather scenarios. Although there have been studies of specific buildings, each new building design has unique considerations; thus, it is difficult to apply the results of these specific studies to a new case. The designer must turn to more generic simulation tools first of all to at least determine if natural ventilation is a feasible option. The simulation should encompass an estimation of the airflow through each specific buildings zone as well as the average temperature in that zone for a specified internal heat gain. For a very small building that can be modeled as a single zone, prediction of airflow and temperature is straightforward. However, for larger buildings with multiple zones that may be interconnected such estimation becomes more challenging. This situation is common in buildings with multiple interconnected zones which rely on buoyancy to produce the pressure difference that creates

the airflow. In such instances, the buoyant flow is a function of the temperature difference between the interior zones and the ambient surroundings. At the same time the temperature of the zones is proportional to the flow rate in each individual zone. Thus, the momentum balance and energy balance equations are coupled and must be solved simultaneously for all of the zones.

DESIGN TOOLS

One widely used tool to study airflow in buildings is computational fluid mechanics, CFD. CFD will predict detailed temperature and velocity distributions within a given building zone. However, a CFD simulation of the entire array of interconnected zones requires considerable time, effort and care to set up. To maintain a reasonable computation effort that predicts time resolved behavior over a single day requires the use of simplified turbulence models of limited accuracy. In addition, the CFD calculation requires as input the thermal boundary conditions which in turn, are part of the solution for buoyancy induced flows. On balance, CFD is more properly employed in the later stages of the design to determine detailed aspects within a single zone or at the interface between zones.

There are also tools that will predict the flow rate between zones where each zone is represented by a single value of pressure temperature and flow rate. CONTAM is one such nodal model that allows designers wide latitude in specifying zone dimensions and interconnections. However, this tool also requires the thermal conditions as a prerequisite to the solution. For purely wind driven cross ventilation, the tool will be a valuable method of simulation but is of limited use when buoyancy is important.

Physical scale models have also been used to study the overall flow behavior of a proposed building design. In most instances water is used as the modeling fluid so that high Reynolds numbers typical of interior building flows can be simulated. The flows cannot simultaneously simulate the corresponding thermal conditions so once again thermal boundary conditions must be prescribed at the initial point of the experiment. A number of studies have used water models to simulate the evolving flows within single building zones. One drawback even when the thermal boundary conditions are known is that the water is opaque to infrared radiation, Menchaca-Brandan [1]. This leads to erroneous predictions of the temperature and flow distributions of the air within the zone.

CoolVent

CoolVent is a natural ventilation design tool that has been developed to allow users to quickly simulate the conditions within a proposed building design. Early development of the tool was by Tan [2] and Yuan [3]. More recent contributions have been made by the current authors. It is intended as a tool to be used in the early design stages to demonstrate the advantages of natural validation in a particular design situation. CoolVent models each building zone as a single node assuming a well-mixed air temperature. It assumes an open plan space within each zone with negligible obstructions for the airflow. The airflow can be a result of wind, buoyancy, and fan assist at the exhausts. Airflow resistances are established at the exterior openings of the façade and between adjacent zones. The airflow resistances are represented by a power law relationship with the pressure differences across adjacent zones. CoolVent includes thermal gains due to lights, plug loads and solar gains though fenestration. The program simultaneously solves for the airflow and thermal balance for each zone by use of an iterative process that rapidly converges in most cases. In some instances there is not a single unique solution to the set of equations but rather several solutions for the temperature and flow distribution throughout the zones that are dependent on the initial assumed temperature

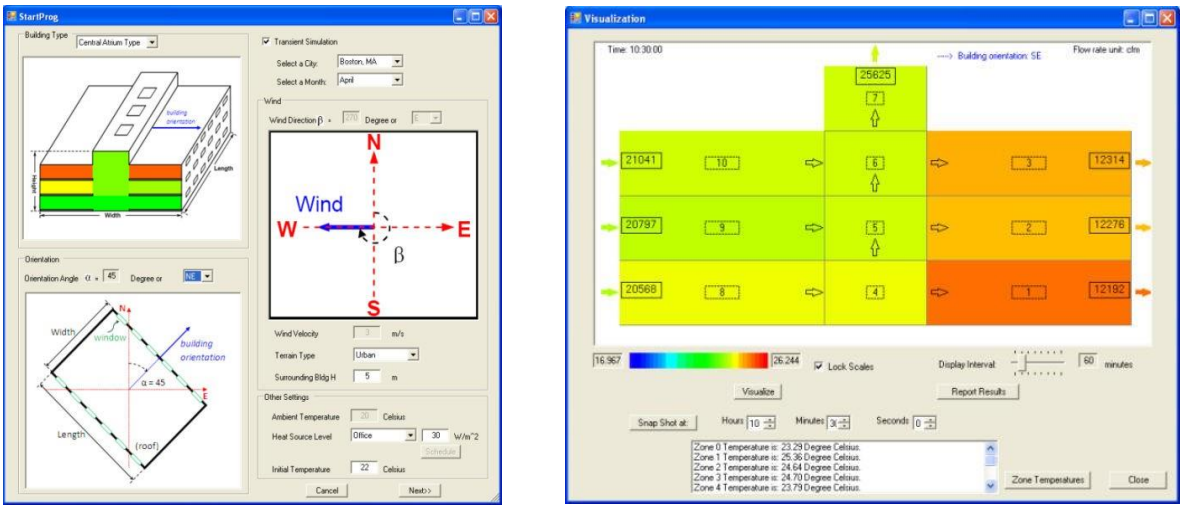

a) b)

Figure 2: CoolVent interface. a) Input window for general information of the building (type, orientation, occupancy and weather information). b) Visualization of results: a chromatic scale indicates the temperature of each zone and the air flow; arrows represent the direction of the flow; black rectangles show ventilation rates.

distribution. For given hour by hour monthly average weather conditions, the program predicts the transient behavior of multiple zones over one or more days. This includes heat transfer between the zone air and surrounding thermal mass; the thermal mass conditions are found from a solution to one-dimensional transient conduction through its thickness. Recent additions to the tool include a prediction of vertical temperature distribution within a zone based on a general dimensionless correlation of multiple CFD simulations. Also, realistic fan characteristic curves simulate fan flow versus pressure difference and the influence of momentum to enhance entrained air flow in a vertical stack connected to multiple floors, Ray [4]. The user can choose from several comfort criteria.

The interface of CoolVent is designed to allow users to easily enter design geometry and other operational parameters. Figure 2a taken from Menchaca [5] illustrates some of the graphical inputs. To maintain a simple input structure, users can choose from several generic designs layouts which can be modified to simulate the specific application. For example, the user can choose a simple wind driven cross flow arrangement. Another choice is a combined wind driven and buoyancy driven flow in a multi-story design where the open floors are connected to a common atrium. Results are displayed graphically showing hour by hour variation throughout the building, figure 2b. Also the hourly results within each zone can be compared to the ambient conditions and the temperature and humidity compared to comfort criteria.

RESULTS

The results of CoolVent have been compared to exact closed form solutions for simple internal geometries. It also has been compared to actual measured conditions in building monitored by the team. Figure 3 shows a comparison of measured and predicted temperature for the Luton, UK building shown in figure 1d. These measurements were made during a particularly warm period in the UK. The floor slab and ceiling are exposed for night cooling whose effectiveness in moderating peak daytime conditions is evident. Recent measurements were made in the Artists for Humanity Building in Boston, MA shown in figure 1e. Figure 4 shows the measured zone air temperature (figure 4a) as well as the temperature of the upper surface of the floor slab (figure 4b) over a 24 hour period compared to the CoolVent

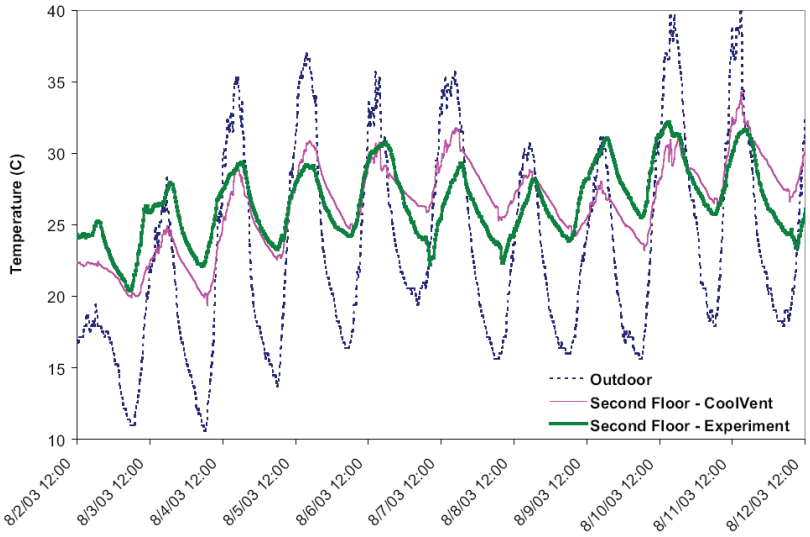

Figure 3: Temperature on the second floor of the Luton, UK building shown on figure 1d during ten days in August 2003. Shown are the outdoor ambient temperature, the average zonal temperature and predictions of CoolVent. This building is cooled by a combination of wind and buoyancy induced flow.

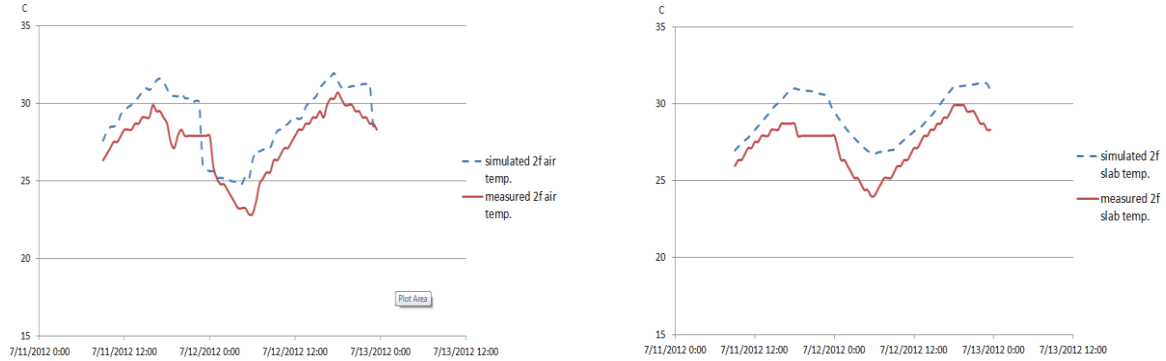

a) b)

Figure 4: Measured and predicted air temperature and floor slab temperatures in the Artists for Humanity Building in Boston.

predictions. In this building, an exhaust fan is used at night to help cool the floor slab. The results suggest that the fan should be turned on earlier in the night to further condition the concrete slab.

Several of the present authors assisted in the design of the Hulic Head Office Building in Tokyo, shown in figure 1f. This building uses buoyancy driven natural ventilation with several floors jointly connected to a vertical exhaust shaft. In addition, there is a fan near the upper end of the shaft that can be used to assist the air flow. Figures 5a and 5b show comparisons between measured zonal temperatures and airflow rates, respectively, taken from the building on October 19, 2012 and simulated values from CoolVent. Airflow measurements were made in accordance with ASHRAE Standard 111-2008 following the equal area method and only allowed snapshot comparisons between the office building and CoolVent. This snapshot allowed for the use of detailed input data, such as equipment and lighting loads from the building control systems, ambient weather conditions from the onsite weather station, and detailed occupant count. With this accurate input data, CoolVent predicts

average zonal temperatures and airflow rates within the experimental error of the measurement devices.

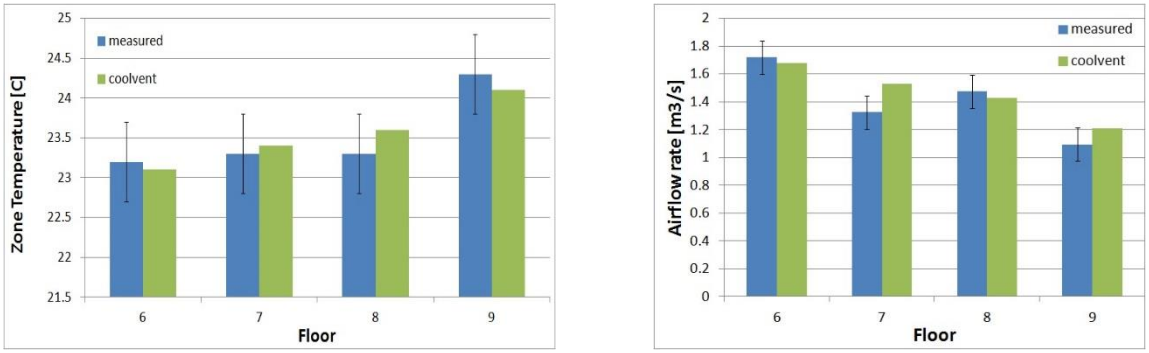

a) b)

Figure 5: Comparison of simulation results using CoolVent and measured performance of a hybrid ventilation office building in Tokyo: a) zonal temperatures, b) airflow rates.

CONCLUSIONS

A new design tool, CoolVent, using an airflow network, refined by CFD simulations and building data allows designers to quickly and accurately simulate natural ventilation operations. It has been used in the design of a new office building in central Tokyo that uses a hybrid natural ventilation/ air condition system. Results of building performance measurements in several natural ventilated buildings show good agreement with the design tool predications. A key challenge to the successful operation lays in the future development of simple, effective control algorithms. Proper control can extend the duration of interior comfort conditions while also dealing with instances of multiple equilibrium states and hybrid operation with a conventional air conditioning system.

ACKNOWLEDGEMENTS

This work has been supported by the Cambridge MIT Alliance, the Hulic Company Ltd. and the US-China Clean Energy Research Center-Building Energy Efficiency Consortium

REFERENCES

1. Menchaca-Brandan, M.-A, and L. R Glicksman. “The Importance of Accounting for Radiative Heat Transfer in Room Airflow Simulations.” In Proceedings of RoomVent 2011. Trondheim, Norway., 2011.
2. Tan, Gang and Glicksman, L.R., “Applications of the Integrated Multi-zone Model and CFD Simulation to Natural Ventilation Prediction” Energy & Buildings Jrnl, v 37, issue 10, ISSN: 0378-7788, I10, pp 1049-1057, Oct-2005.
3. Yuan, J. and L. R. Glicksman, “Validation of a Multi-zone Model with Integrated Energy Equation and Impact of Thermal Mass Modeling Methodology” Proc. SimBuild 2006, MIT Cambridge MA. (2006)
4. Ray, Stephen Douglas. “Modeling Buoyancy-driven Airflow in Ventilation Shafts.” Massachusetts Institute of Technology, 2012. http://dspace.mit.edu/handle/1721.1/74930.
5. M. A. Menchaca-Brandan and L.R. Glicksman, “CoolVent: A Multizone Airflow and Thermal Analysis Simulator for natural ventilation in Buildings,” Proceedings of SimBuild 2008, IBPSA-USA National Conference (2008).

NATURAL VENTILATION AND COOLING TECHNIQUES FOR THE NEW NICOSIA TOWNHALL

Flourentzos Flourentzou[*1], Dickon Irwin [2], Margarita Kritioti [2], Tasos Stasis[3], and Nicholas Zachopoulos[3]

1 *Estia SA, Parc Scientifique EPFL, 1015 Lausanne, Switzerland, flou@estia.ch*

2 *irwinkritioti.architecture, 10 Gregoriou Xenopoulou, 1061 Lefkosia Cyprus*

3 *Eliofotou, Zinieris & Stasis Partners, 77 Strovolos Ave., Strovolos Center 4th Floor, 2018 Strovolos, Cyprus*

ABSTRACT

The new Nicosia Town-hall is a very particular building. On the site where it is built, important antiquities were discovered during the first day of construction and the whole design was completely modified to fit to the new situation. The archaeologists continued to excavate 2/3 of the entire site and created an archaeological park in the centre of the town. The building area was constraint to the remaining land, and co-exists with the uncovered findings.

As a consequence, the building was split into 5 smaller units, 4 office and public service buildings and a municipal hall. Foundations were changed to a combination of piling between findings and large raft slabs sitting above the level of undisturbed ground. The design of office buildings followed the rules of bioclimatic architecture to meet the passive standards and the building is on process for Minergie® (Swiss) labelling. Massive buildings, naturally ventilated and cooled, offer a natural comfort with minimum energy consumption.

The article explains the ventilation concept, bioclimatic principles and the simulated and measured comfort and energy performances, showing that Minergie standards are possible also in climates with higher cooling energy demand .

Keywords: Potential for ventilative cooling strategies; design approaches for ventilative cooling and case studies; summer comfort and ventilation;

INTRODUCTION

The new Nicosia town hall (Cyprus) is not a simply green building showing several bioclimatic architecture principles. It is the first contemporary building in the island applying all the bioclimatic principles, which are necessary to meet the passive building standards (primary energy consumption for heating, ventilation, air conditioning and hot water production less than 30 kWh/m^{2}y).

The "town hall" is not a single building. Archaeological findings restricted the available land to the 1/3 of the initial available surface and the unique initial building is split to smaller units in order to fit in the remaining complicated site. 4 office buildings and a municipal hall, able to receive the council meetings in presence of 250 people, form a neighbourhood in Nicosia old town, just 100 m from the green line, where the war divided the city several decades ago.

Bioclimatic and sustainable architecture starts from the site use. The buildings respect the old town scales and they are integrated in the archaeological site not only preserving cultural heritage, but also making it available to the population, through walk paths, squares, and shaded patios. They create a public space with a social environment, where urban life meets culture and municipal services, in a marginalised district of the city, where social life is stopped for many years now. Orientation and disposition of the buildings group similar uses,

separate polluting and noisy activities from office spaces, create natural shading to public space and neighbouring buildings.

Figure 1. Panoramic virtual view of the building complex from the green roof of building 1.3; view of the municipal hall from the antiquities, view of the shaded patio between buildings B1.2 and B1.4. Only building B1.3 is finished. The other buildings are under construction.

BIOCLIMATIC DESIGN, OF OFFICE BUILDINGS

The basic condition for a confortable thermal environment of offices is good insulation and solar protection. In south climatic conditions, with very hot summers and relatively cold winters, energy performance is necessary for both winter and summer seasons. A well-insulated building, with reasonable glazing orientation and solar protection, consumes 15-25% of the total thermal demand for heating and 75-85% for cooling. In the past, where buildings where not insulated, this ratio was inversed, with heating demand representing more than 75% of the total demand. This is illustrated on table 1 and Figure 3.

Insulation	Heating demand	Cooling demand	Total demand
A. 0 cm, single glazing	149 (78%)	43 (22%)	192
B. 4 cm, double glazing - 3.5 W/m^{2}k	21 (25%)	64 (75%)	85
C. 10 cm, dbl glazing-1.3 W/m^{2}k, shading	8 (19%)	34 (81%)	42

Table 1. Heat and cooling demand of 3 scenarios simulated dynamically with DIAL+[1] software.

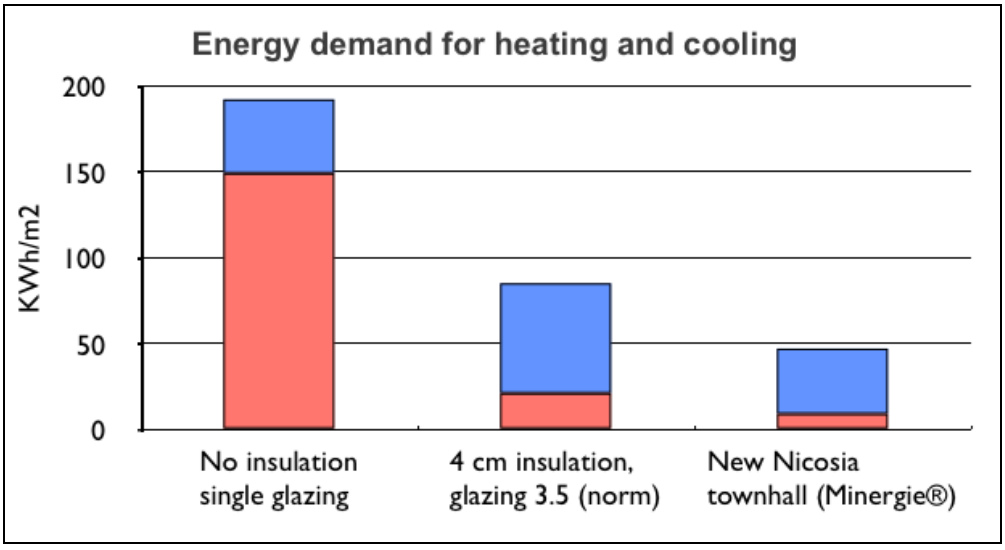

Figure 2. The graph shows heating and cooling demand, according to the 3 basic scenarios.

As it is seen in Figure 2 and Table 1, Cyprus Energy Law reduces the energy needs to the 44% of those of a building, without any care for solar protection. Additional thermal insulation (10 cm instead of 4) and more insulated windows (U value 1.3 instead of 3.5), with

60 cm passive solar protection on the south façade, reduces the energy needs to the half of those of a building meeting the minimum legal insulation values. Passive buildings (C) have only 22% of the energy needs of non-insulated buildings (A).

Thermal insulation, thermal mass and solar protection of building B3

Thermal Insulation

Thermal mass

Solar Shading

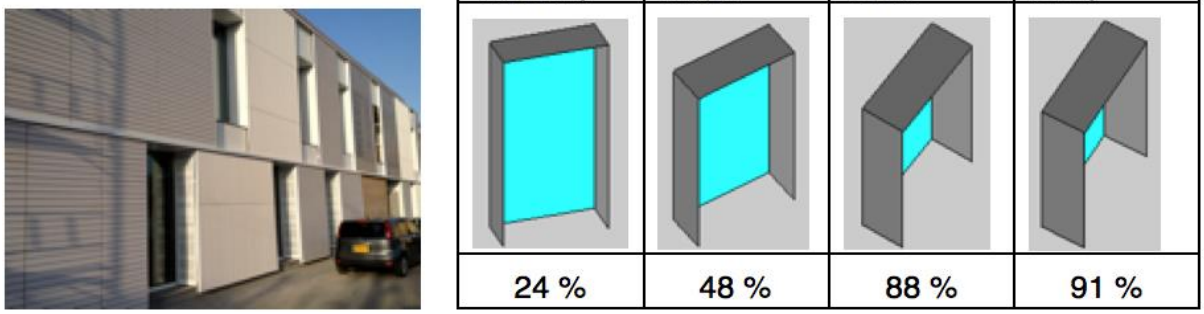

Figure 3. Outside thermal insulation with minimised thermal bridges is composed mostly by 10 cm rockwool. Foundations are insulated with 5 cm xps. Floor and ceiling are composed by massive materials with high thermal mass, The south façade (15° South – West) at 14:00 is shaded with 60 cm static top and side solar protection. The choice of a glazing with g value of 0.4 is a good compromise between summer solar protection and winter useful solar gains. The façade white ceramics is a robust, inert, self-cleaning material with low sun absorption, offering low façade temperature rise to prevent overheating of incoming air during summer. The table shows the solar shading during the year. In winter solar shading is minimum and in summer maximum.

After several optimisation dynamic simulations with DIAL+ software [1], we decided that the optimum insulation characteristics to meet the passive standards are 10 cm of rockwool for the roof and the facades, 5 cm for the periphery of the building and a U value of the windows of 1.3 W/m^2K. Thermal insulation on the ground does not change anything, as the mean ground temperature in Cyprus is high. A careful analysis and treatment of every joint between constructive elements minimises thermal bridges and heat losses in winter. External insulation gives the advantage of thermal mass inside the building.

An apparent cladded concrete ceiling and a floor composed with 4 cm anhydride screed over the concrete slab and rough concrete screed, offer a high thermal mass, absorbing excess heat during the day and restoring it during night. This optimises the use of internal heat gains during winter and reduces the peak temperature during summer.

As building B3 is north - south oriented, static solar protection of 60 cm overhangs is sufficient. As we see from table 1, comparing scenario B with scenario C, solar protection reduces cooling demand in summer by nearly 50% (additional wall and window insulation plays a small role for the cooling demand).

Ventilation and cooling strategies of office buildings

Before we adopt a ventilation strategy, we put on the balance 4 aspects: air flow necessary to provide air quality and occupant's health, energy consumption by fans or by thermal losses or gains because of excess ventilation and occupant's wishes / well-being. Some people, influenced by good practice in the North and Central Europe countries, concentrate on the possibility of heat recovery. They a priori consider that mechanical ventilation with heat recovery is a good practice for every climate and for every building use, extrapolating intuitively this conclusion from what happens in the cold climates.

Without excluding any solution, before adopting a ventilation strategy, we answered to 3 questions:

1. what are the wishes of the users and how do they feel in regards to the control of their environment;
2. what is the real impact of different ventilation strategies on heating, cooling and electricity demand;
3. what is the real risk of wrong use and bad ventilation control by the users ?

Question 2 and 3 may have a different answer according to climatic conditions, building function, physical characteristics of construction elements.

Users wishes and feelings in regard to ventilation systems.

The objective was not only a high-energy performance and a confortable building. A municipal building is a professional tool for public service. Well-being of the users is a key factor on productivity and service quality. Before the building design, the great majority of the municipality personnel answered to a questionnaire about their current indoor environment quality and their expectations from their new place of work. The personnel showed a high degree of environmental consciousness with low CO2 emissions being their second concern. 63 people imagine an exemplary building of natural comfort and only 23 an exemplary fully air-conditioned building. 30% of the people consider mechanical ventilation as problematic. Less than 5% considered natural ventilation from the window as problematic. These results confirm the results of European research, showing higher acceptance and lower building sick syndrome index in naturally ventilated buildings.

NATURAL VENTILATION DESIGN AND VENTILATION STRATEGIES

Vents are vertical, opening on the whole room height, in order to maximise stack effect. With 5°C temperature difference between inside and outside, a 40 by 300 cm vertical vent creates a stack effect of 611 m^3/h, while the same vent in horizontal position 300 by 40 cm creates only 223 m^3/h. The right disposition of the vent opening may boost ventilation airflow by 275%! High airflow rates are necessary only during night. During the day only 36 m^3/h per person are necessary. An opening of 40 by 140 cm height may provide 75m^3/h at a ΔT = 5°C and 47m^3/h at ΔT = 2°C. These dimensioning calculations leaded us to divide the high vent in two parts and to make it open right or tilted. The user instructions become simple and easy to understand: "tilt the top vent during working hours winter or summer. During winter, you close it when leaving the office and during summer, you open completely one or both vents, according to your cooling needs; you put it back to the tilted position in the morning."

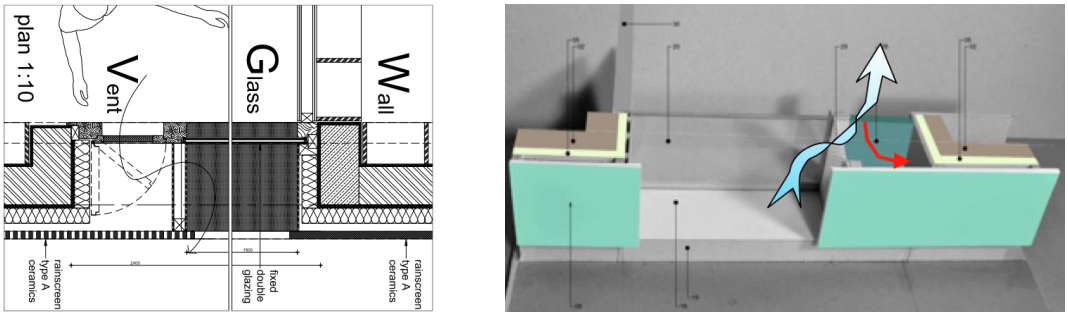

Figure 5. South façade vent. Air enters from the side of the glazing through a perforated sheet metal protection.

opening 60X300	m^3/h	
60X300	914	100 %
60X300 with grid	548.4	60 %
60X160	356	39 %
60X160 + 1X60X90	752	82 %
15X160 regular opening	139	15 %
7X160 regular opening	91	10 %
15X160+15X90 à la Fr.	235	26 %
15 cm tilted (5.4°)	109	12 %
10 cm tilted (3.6°)	70	8 %

Figure 6. top: tilted north façade vent, north façade open regular, bottom: south window from outside, south vent from inside.

Table 2. Air flow of different opening modes according to DIAL+ simulation at 5° inside-outside ΔT

As we can see from the photos of Figure 6, lighting openings are dissociated from air vents. This makes it possible to treat correctly the glazed part, hiding frames or any obstacles and divide, protect or hide the vent part. In the south façade, air comes from the side after passing through a perforated sheet metal. On the north light and façade air comes directly after the protection.

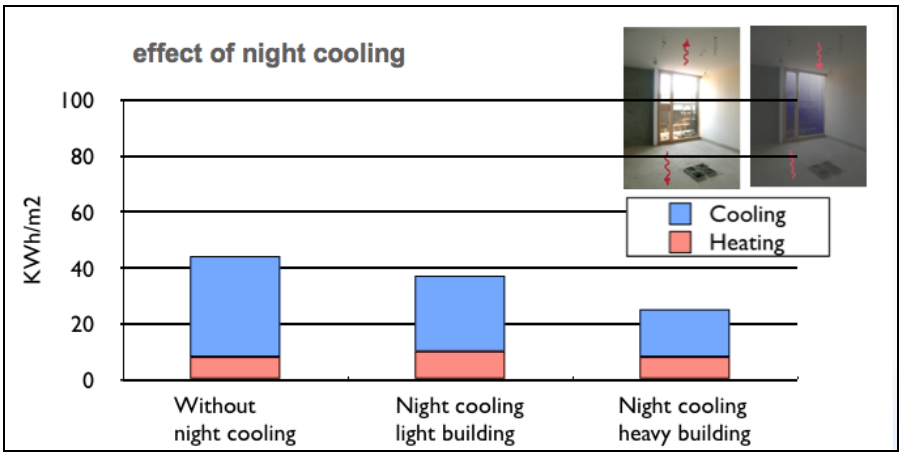

Figure 7. DIAL+ simulations show that with a heavy building, the already low cooling demand is reduced by 53% (17 kWh/m2 instead of 36). A light building offers also some cooling potential but only a 25% potential reduction.

As we can see on the second picture of Figure 6, all offices are equipped with a ceiling fan. This offers the possibility to the users not to use air conditioning up to 28°C of internal temperature and use the ceiling fan instead, reducing drastically the hours of use of air conditioning. It avoids also a bad use of the window, left completely open, when external temperature is around 30°C and users seek for a wind breeze. If the user wishes an air movement, he may use the ceiling fan, avoiding excessive heat and dust entering in the office. DIAL+ simulations showed that for every °C of set point temperature decrease, we have 15% rise of cooling demand. It was observed that more than 60% of occupants choose a temperature set point 26°C or over with some of them at 28°C

CONCLUSION

After thermal insulation and solar shading, free ventilative cooling is the key issue for low energy passive buildings in Mediterranean climate. Issues like high air-tightness and heat-recovery, which are important for North and Central Europe, have minor importance for southern Europe, simply because in the mild climates, most of the time the building should be open to benefit from the outside air, which is within or near the comfort zone.

Free cooling by natural night-ventilation is the simplest strategy, but it needs special design attention. Standard windows are not always the best way for natural ventilation. When ventilation strategy depends from the occupant's behaviour, simple smart windows with many opening possibilities, equipped with protections from insects, dust and vandalism, ensure the users and encourage a correct use. Nicosia town hall is a good example illustrating both natural ventilation design principles on a very low energy consumption building. One year monitoring showed that thermal comfort and energy consumption meet the design targets: perfect thermal comfort with primary energy consumption less than the Minergie® standards.

REFERENCES

[1] B. Paule; F. Flourentzou; S. Pantet; J. Boutillier : « DIAL+ : A complete but simple suite of tools to optimize the global performance of buildings openings ». Proceedings of the CISBAT'11 Conference : Cleantech for sustainable buildings, Lausanne, Oct. 2011.

SIMULATION AND ANALYSIS OF PREDICTIVE CONTROL STRATEGIES IN BUILDINGS WITH MIXED-MODE COOLING

Jianjun Hu, Panagiota Karava

School of Civil Engineering, Division of Construction Engineering and Management, Purdue University, 550 Stadium Mall Drive, West Lafayette, IN 47907-2051

ABSTRACT

This paper aims to demonstrate the potential performance bounds of model predictive control (MPC), in terms of energy savings within thermal comfort constraints, through its comparison with standard heuristic rules used in current practice. To achieve this goal, a multi-zone dynamic building model has been developed in MATLAB, based on thermal and airflow network representation and it is solved with the finite difference method. A linear time-variant state space model is also developed (based on the same network representation), which approximates the nonlinearity caused by natural ventilation with very good accuracy, and can be used for the development of reduced order models for use in real supervisory controllers. The dynamic building model is used within an offline MPC framework with PSO (embedded in GenOpt) as an optimizer. An optimization method based on binary integer linear programming with progressive refinement is also used. The MPC decision space includes different modes of operation for space cooling and the objective is to find the optimal operation schedule for mixed-mode cooling over a 24-hour planning horizon.

Simulations are conducted using Montreal TMY3 data for six consecutive days during summer for a generic section of a high performance building, optimally designed for natural ventilation, with high levels of exposed thermal mass and a highly glazed atrium façade that assists buoyancy-driven flows. Results show that control sequences decided by the MPC optimizer can significantly reduce the cooling requirement by 75% with the operative temperature maintained in an acceptable range (23-27.6 °C). Mixed-mode cooling schedules based on heuristic rules result in energy reduction of 83% but could overcool the space, with a maximum daily mean deviation of operative temperature from the desired range by 0.7 °C, which corresponds to occupant acceptability of approximately 60%. The optimal control sequences presented in this paper, although limited to a short period of time, demonstrate intelligent mode switchings with superior overall performance. These sequences are significantly different than those based on heuristics and could not have been developed without the use of an optimization algorithm and a carefully tuned building model that captures the relevant thermal and airflow dynamics. Simulations with the linear time-variant state-space model and a three stage progressive refinement optimization method show similar results with those obtained with the non-linear model and PSO as well as significant reduction in the calculation time enabling real-time implementation (on-line MPC) in mixed-mode buildings.

Keywords: Mixed-mode cooling, model predictive control, natural ventilation, state space model, optimization

INTRODUCTION

Mixed-mode cooling refers to a hybrid approach for space conditioning, employing free cooling by natural ventilation, where the flow is driven by wind or thermal buoyancy forces sometimes assisted by a fan, and mechanical systems, along with smart switching, to minimize building energy use and maintain occupant thermal comfort [1]. Existing control strategies for mixed-mode buildings are heuristic and may lead to increased operating costs or

occupant discomfort since they are not optimized for the local climate and particular building features such as thermal mass, façade orientation, building construction, etc. These problems can be avoided by employing model predictive control (MPC) strategies [2, 3]. The present study (a) establishes physical models that capture the relevant thermal dynamics for buildings with mixed-mode cooling; (b) demonstrates the potential performance bounds of MPC through its comparison with standard heuristic rules used in current practice.

MODEL DEVELOPMENT AND METHODOLOGY

This study is based on previous work by Karava et al. [4] in which extensive measurements were conducted in an institutional building (located in Montreal, Canada) to assess the performance of mixed-mode cooling using natural ventilation with heuristic control strategies, based on fixed schedules, and to identify opportunities for additional energy savings from night cooling with variable low temperature set points. The natural ventilation design concept of the building (Figure 1) includes: (a) inlet grilles with motorized dampers located at the end of the corridors in the southeast and northwest façade of each floor, and (b) five three-storey atria (located on the SW façade) that are separated with a floor slab and connected with grilles equipped with motorized dampers to enhance buoyancy-driven flow. The building has high levels of thermal mass in the form of exposed concrete floor slabs in the atrium (10 cm thick) and the corridors (40 cm thick), which are located adjacent to the inlet grilles on the southeast and northwest ends and extended all the way to the atrium.

Thermal and airflow model

The present study focuses on a generic section of the mixed-mode building (described above) with an atrium connected to six corridors as shown in Figure 1 (right). Each corridor has one exterior façade where the inlet grilles are installed thus it acts as long air "duct" for delivery of outside air into the atrium zone. Thermal dynamics of the interior building zones are predicted by applying the heat balance method, which explicitly models the heat transfer rate to the interior and exterior surfaces and to the zone air. Due to the corridor's large dimension (30 m long) a significant temperature difference is anticipated in the slab surface, thus, the surfaces are divided into 4 sections but are connected with the same corridor air node. The thermal model for the corridor zones has been verified using data from an experimental study [4, 5]. The atrium is modeled with three zones to account for the temperature stratification [4]. Therefore, the thermal model includes three atrium zones plus six corridor zones (three in southeast and northwest orientation). A multi-zone airflow network model (Figure 1) has been developed in MATLAB using the Newton-Raphson method to solve the non-linear airflow problem by iteration of solutions of linear equations. The "Multiple Opening Model" [6] was used to model the air exchange between zones connected with large openings. An assisting exhaust fan is located on the roof of the atrium that operates in case of insufficient natural ventilation. The airflow network model was compared with CONTAM and the predicted differences of both flow rates and pressure drops were less than 5%.

Numerical solver

The heat balance for the nodes in thermal network can be mathematic formulated as follows:

$$C_i \frac{dT_i}{dt} = \sum_{k=1}^{n} \frac{T_{k,i} - T_i}{R_{k,i}} + Q_{aux} + \dot{m} c_p (T_j - T_i) \quad (1)$$

in which, the last term calculates the advective heat transfer due to the airflow exchange between neighbor zones, thus it should be eliminated when T_i denotes wall temperatures but has to be included when T_i denotes zone air temperatures. $\dot{m}$ is the airflow rate through openings connecting zone j and zone i. The airflow rate is calculated with an airflow model which in turn, requires the zone temperatures as inputs. Thus, the "onion" coupling method [7]

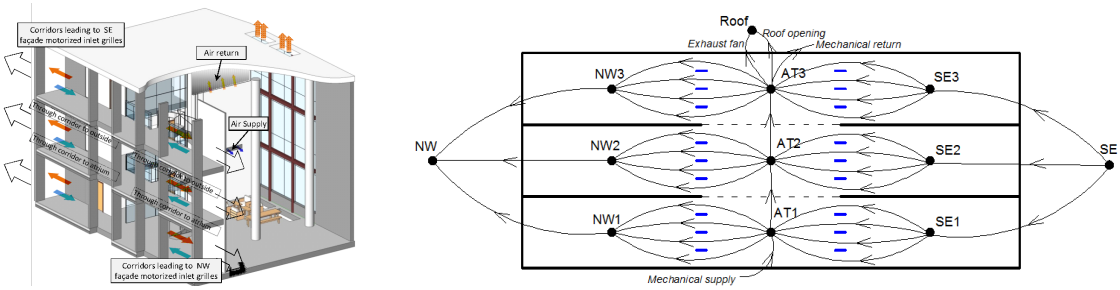

Figure 1: Mixed-mode cooling concept (left); Schematic of the airflow network (right)

in which thermal and airflow simulation iterate on each time step is implemented. To solve the ODEs, an implicit finite difference method is used:

$$C_i \frac{T_i^\tau - T_i^{\tau-1}}{\Delta\tau} = \sum_{k=1}^{n} \frac{T_{k,i}^\tau - T_i^\tau}{R_{k,i}} + Q_{aux}^\tau + \dot{m} c_p \left(T_j^\tau - T_i^\tau\right) \quad (2)$$

There is one heat balance ODE for each thermal node, which results in a large system of ODEs for a multizone building that need to be solved simultaneously, requiring extensive computing resources. Therefore, the full-scale model solved with the finite difference method is not suitable for implementation of predictive control in real buildings. One way to simplify the model is order-reduction, which requires a state-space representation for the building thermal dynamic system. Rearranging terms in Eq. (1), the thermal dynamic system for a building with mixed-mode cooling can be formulated into the state-space representation as follows:

$$\begin{aligned} \dot{X} &= AX + BU + f(X, U, \dot{m}) \\ Y &= CX + DU \end{aligned} \quad (3)$$

in which, *A, B, C, D* are coefficient matrices derived from building material properties. *X* is the states vector that represents the temperature of each thermal mass node. *U* is the inputs vector that includes the outside temperature and solar heat gain and *Y* is the outputs vector (e.g. zone air temperature, wall temperature). The state-space model is nonlinear due to the term $f(X, U, \dot{m})$ that represents the advective heat transfer caused by the airflow. In order to conduct model-reduction, a linear state-space model is required. Thus, the nonlinear state-space model has to be linearized, i.e. instead of finding the air mass flow rate $\dot{m}$ using zone temperatures at the current time-step, the airflow rate can be calculated using zone temperatures from the previous time-step. In this way, the $\dot{m}$ term becomes known in the current time step. The solution flow chart is illustrated in Figure 2. Rearranging Eq. (3), the nonlinear model becomes a linear time-variant model (LTV-SS) that can be expressed as follows:

$$\begin{aligned} \dot{X} &= \overline{A(t)} \cdot X + \overline{B(t)} \cdot U \\ Y &= \overline{C(t)} \cdot X + \overline{D(t)} \cdot U \end{aligned} \quad (4)$$

MPC framework

The MPC framework for buildings with mixed-mode cooling developed in the present study is deterministic, i.e., based on the assumption that future predictions are exact. The decision space is the operating schedule of the motorized openings and the objective is to minimize energy use with comfort constraints. The problem can be mathematically formulated as:

$$\text{Minimize: } J\left(\overrightarrow{IO_t}\right) = E \quad (5)$$

Subject to:

$\overrightarrow{IO_t} = \{0, 1\}$; $W_{speed} < 7.5$ m/s; $T_{dew} \leq 13.5$ °C; $T_{ope} \in$ [23 °C, 27.6 °C] and $T_{setpoint} \in$ [21 °C, 24 °C] during occupancy hours.

E is the energy cost (mechanical cooling and mechanical fan) determined through energy simulation, $\overrightarrow{IO_t}$ is the vector of binary (open/close) decisions for the motorized openings, W_{speed} is the wind speed, T_{dew} is the outside dew point temperature, T_{ope} is the operative temperature, and $T_{setpoint}$ is the setpoint air temperature. The operative temperature constraint is not applied when the building is not occupied while the setpoint air temperature fluctuates between 13 and 30 °C. The meta-heuristic search technique particle swarm optimization (PSO) (embedded in GenOpt [8]) was used to solve the optimization problem for searching the discrete decision space [9]. For the cases under consideration, one optimal control sequence which is the hourly operation schedule of the motorized openings is formulated over a 24-h planning horizon beginning from 20:00 at night to 19:00 in following day. Details of this method are presented in Hu and Karava (2013) [10]. An optimization method based on binary integer linear programming with progressive refinement (three-stage) was used in order to speed-up the calculation process. With this method two-hour decisions blocks were used during the night (20:00-5:00) and hourly decisions blocks during the occupancy period. A few heuristic rules derived based on initial simulations (offline MPC) were used as shown in Figure 2 (right). The thermal history of the building is preserved by running the simulations for a historical horizon of seven days that was found to be sufficient.

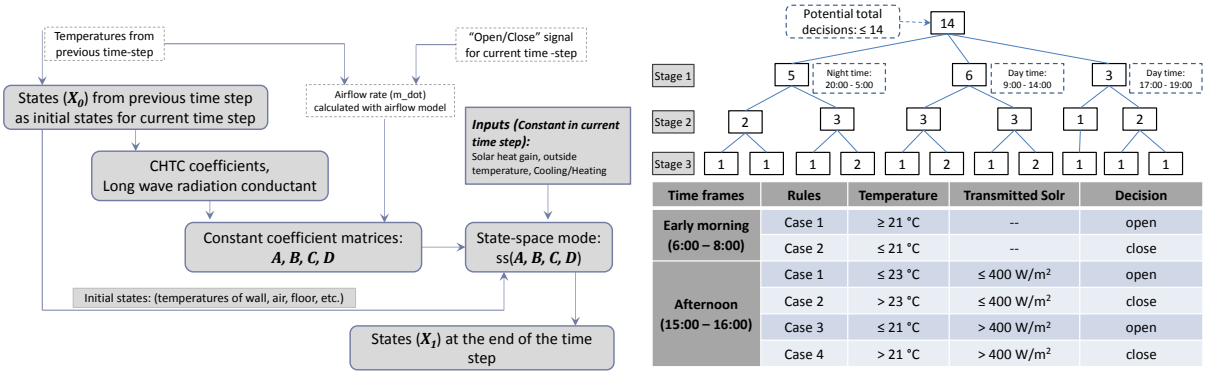

Time frames	Rules	Temperature	Transmitted Solr	Decision
Early morning (6:00 – 8:00)	Case 1	≥ 21 °C	--	open
	Case 2	≤ 21 °C	--	close
Afternoon (15:00 – 16:00)	Case 1	≤ 23 °C	≤ 400 W/m²	open
	Case 2	> 23 °C	≤ 400 W/m²	close
	Case 3	≤ 21 °C	> 400 W/m²	open
	Case 4	> 21 °C	> 400 W/m²	close

Figure 2: Flow chart of the linear time-variant model (left); optimization environment (right)

SIMULATION RESULTS

Simulations were performed using Montreal TMY3 data (Figure 3) for six consecutive days during summer to demonstrate the potential performance bounds of MPC strategies through its comparison with (a) baseline simulations (mechanical cooling with night set back); (b) standard heuristic rules used in current practice ($T_{amb} \in [15°C, 25°C]$, $T_{dew} \leq 13.5$ °C, $W_{speed} <$ 7.5 m/s). The main assumptions are: (a) Mean velocity and turbulence intensity were not used in the thermal comfort evaluation; (b) Local controllers were ideal such that all feedback controllers follow set-points exactly; (c) Internal heat gains (occupancy, lighting) were not considered; (d) An idealized mechanical cooling system with a COP value of 3.5 was modeled. The operation schedules obtained based on heuristic and MPC strategies are shown in Table 1 with the corresponding energy consumption and mean operative temperature deviation from the desired range predicted by the linear time-variant state-space and the finite difference mode shown in Figure 4. Table 1 indicates that the heuristic strategy leads to more cooling hours during early morning (Day 1, Day 4 and Day 5) which would cause higher risk of over-cooling (Figure 4). Th Results show that the LTV-SS model can predict the thermal behavior of the building using either heuristic or predictive control strategies, with very good accuracy. Simulations with the LTV-SS model and the three stage progressive refinement method show similar results with those obtained with the non-linear model and PSO with significant reduction in the calculation time (e.g. for the six days simulation, the time is

reduced from 3 days to 3 hours) which enables real-time implementation (on-line MPC) in mixed-mode buildings. Compared with the baseline case, the mixed-mode cooling strategy effectively reduces building cooling energy by 83% for the heuristic case and 75% for the MPC case. However, the heuristic strategy can lead to mean operative temperature deviation up to 0.7 °C, which may decrease the comfort acceptability from 80% to 60%. The trade-off between thermal comfort and cooling energy reduction resulted in natural ventilation during hours with lower temperatures with the MPC optimizer (Table 1, Day 5), thus eliminating the need for overcooling.

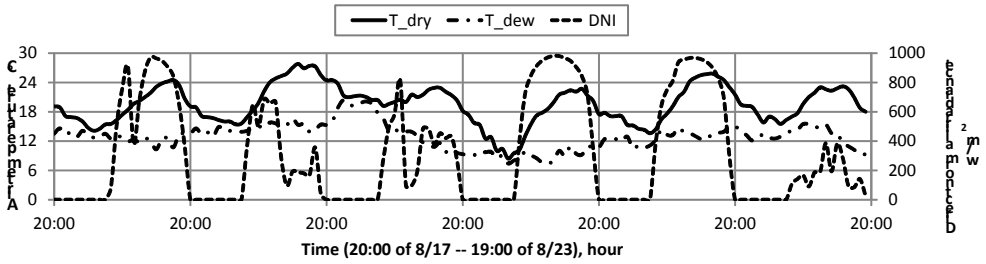

Figure 3: Weather conditions used for the simulation study

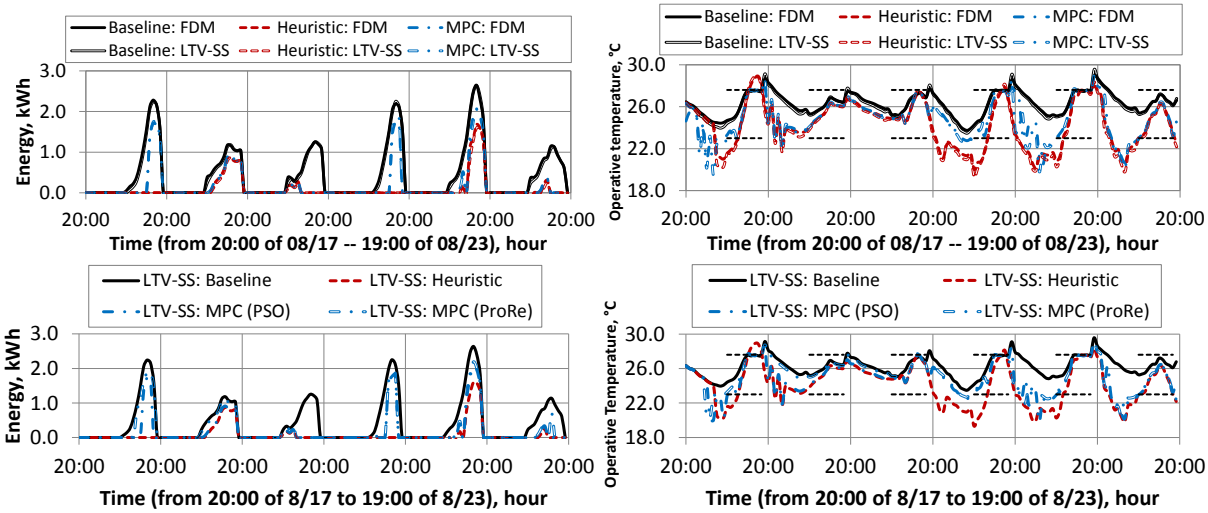

Figure 4: Simulation results for the cooling energy consumption (left) and indoor operative temperature (right) using finite difference (FDM) and state-space (LTV-SS) models with PSO and progressive refinement (ProRe) as optimizer for three cases: baseline night set back control, heuristic control, and MPC

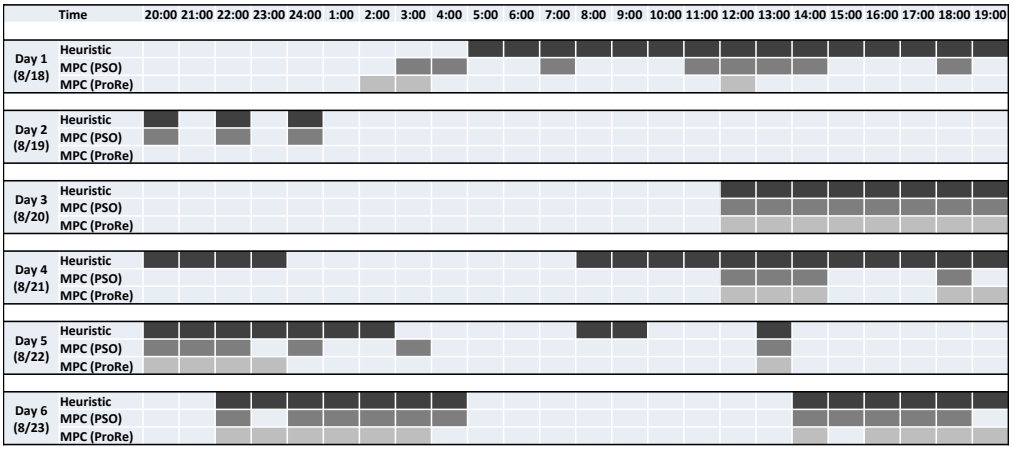

Table 1: Operation schedule using heuristic and MPC strategies (hours during which windows are open are illustrated by cells with grey background)

CONCLUSIONS

The paper shows optimal control sequences for mixed-mode cooling in a multi-zone building optimally designed for natural ventilation. Two different physical prediction models, based on the heat balance method, solved with finite difference, or formulated using a state-space representation are developed and used within an MPC framework. Results show that the linear time-variant state-space model can predict the thermal dynamics of a mixed-mode building, which could be either controlled with heuristic or predictive strategy, with very good accuracy. A simulation study of the building operation over a period of six consecutive summer days using Montreal TMW3 data showed that MPC can significantly reduce the cooling requirements compared to baseline night setback control while maintaining the operative temperature during the occupied period within acceptable limits. On the contrary, rule-based control strategies for the window opening position, based on simple heuristics for the outdoor conditions, create an increased risk of overcooling with lower thermal comfort acceptability. The three-stage progressive refinement method showed very good agreement with the PSO and significant reduction in calculation time. Current research efforts are focused on the development of reduced-order models which are necessary for real-time application of anticipatory control strategies in buildings.

REFERENCES

1. Brager, G., Borgeson, S., Lee, Y., 2007, Summary report: control strategies for mixed-mode buildings. Technical Report. University of California, Berkeley, CA: Center for the Built Environment, 81p.
2. Spindler, H.C., Norford, L.K., 2009b, Naturally ventilated and mixed-mode buildings – part ii: optimal control, Building and Environment, vol. 44, no. 4: 750-761.
3. May-Ostendorp, P., Henze, G.P., Corbin, C.D., Rajagopalan, B., Felsmann, C., 2011, Model-predictive control of mixed-mode buildings with rule extraction. Building and Environment, vol. 46, no. 2: p. 428-437.
4. Karava, P., Athienitis, A.K., Stathopoulos, T., Mouriki, E., 2012. Experimental study of the thermal performance of a large institutional building with mixed-mode cooling and hybrid ventilation. Building and Environment, vol. 57, no. 11: 313-326
5. Hu, J., Karava, P., 2012. Modeling and analysis for mixed-mode cooling of buildings, 2012 Annual ASHRAE conference in San Antonio, TX. July 2012.
6. Stuart, W.D., Walton, G., Denton, K., 1997. CONTAMW 1.0 User Manual, Gaithersburg, MD, NIST.
7. Hensen, J.L.M., 1999. A comparison of coupled and decoupled solutions for temperature and air flow in a building. ASHRAE Transactions, vol. 105, no. 2: 8 pages
8. Wetter, M., 2011, GenOpt(R) Generic Optimization Program. User Manual Version 3.1.0. Simulation Research Group, Building Technologies Department, Environmental Energy Technologies Division, Lawrence Berkeley National Laboratory, Berkeley, CA, 109p.
9. Kennedy, J., Eberhart, R.C., Shi, Y., 2001. Swarm intelligence. Morgan Kaufmann Publishers.
10. Hu, J., Karava, P., 2013. Simulation of anticipatory control strategies in buildings with mixed-mode cooling. 13th International Conference of the International Building Performance Simulation Association, Chambéry, France August 2013.

VENTILATED HOLLOW CORE SLAB TOWARDS ENERGY EFFICIENCY OF THE BUILT ENVIRONMENT

F Mirakbari; L Brotas

Low Energy Architecture Research Unit, Sir John Cass Faculty of Arts, Architecture and Design, London Metropolitan University, 40-44 Holloway Road, London N7 8JL, UK
Emails: e.mirakbari@yahoo.com; *l.brotas@londonmet.ac.uk*

ABSTRACT

Buildings are responsible for almost 50 per cent of the UK's energy consumption and carbon emissions. Therefore improving the energy efficiency of the built environment is fundamental if the UK is to meet the proposed objectives of reducing energy consumption and the depletion of fossil fuel resources without harming the environment. Thermal energy storage in buildings plays an important role as one of the energy conservation strategies and the use of Ventilated Hollow Core Concrete Slab (VHCS) is now considered an efficient and cost-effective way to reduce the energy consumption of buildings. Space conditioning systems using VHCS show considerably higher thermal capacities than conventional systems and are therefore able to decrease and normalize extremes of high and low temperatures indoors.

This paper discusses the positive effect the VHCS has on the thermal environment of buildings and thus on the thermal comfort of occupants; likewise how this system influences the energy consumption of buildings. This research mainly focuses on further and higher educational buildings in UK. However, the techniques used and the results obtained from this study may be transferable to other countries with similar climates and building codes.

A summer investigation in one university building located in Norwich and one college building located in Luton using VHCS system with exposed thermal mass is presented. Indoor and outdoor air temperatures, slab temperatures and supply air temperature in different rooms in both buildings were recorded over a two-week period. A post occupancy survey was done to the occupants of the Luton College to assess their thermal comfort levels.

Results of this study confirm the effectiveness of the VHCS in reducing the daily temperature swing and also increasing the ability of a space to handle daytime heat loads. Comparing the overall energy consumption of the buildings with the CIBSE benchmark indicates reduction up to 10% can be achieved.

Keywords: Ventilated hollow core slab (VHCS), thermal mass, energy efficiency, thermal comfort

INTRODUCTION

During the last few years comfort requirements, indoor air quality and energy efficiency have shown an increasing importance. In consequence, highest numbers of passive techniques have been reintroduced in order to decrease or eliminate the need for mechanical ventilation, cooling and heating thereby reduce energy consumption.

One approach that decreases energy consumption in buildings and maintains the thermal environment within the comfortable range is utilizing the building fabric as thermal storage. In this case the maximum and minimum indoor temperatures are reduced and so is the energy consumption. Total energy saving potential can be increased by the active utilization of the building mass. One of these active strategies is utilizing Ventilated Hollow Core Slab

(VHCS). The VHCS is a precast slab of pre-stressed concrete that has tubular voids extending the full length of the slab. In this technique, ventilation air is passed through the hollow cores of the floor and ceiling slabs, thereby increasing the airflow and the convective heat transfer between the air and the building fabric. This system can be used for heating and cooling buildings. Energy savings from this system have been reported of between 13% and 70%, depending on the building type and the prevailing weather conditions [2].

This study is specific to the further and higher education sector of the building industry where a significant proportion of the energy use is for heating and cooling of the buildings. The intention of this study is to demonstrate that by utilizing the VHCS, the thermal performance of the building can be improved; also heating and cooling energy demand within these buildings can be significantly reduced and consequently the overall energy consumption of the building can be cut down.

METHOD

To achieve the aim of this study, a summer investigation has been conducted over 10 days in one College (Luton Sixth Form College) and one university building (Thomas Paine, University of East Anglia, Norwich). Placing a couple of iButtons (temperature data loggers) in various spaces within the buildings and one of the loggers outside each building produced valuable information of hourly indoor and outdoor ambient temperature. Furthermore, the temperature of the hollow core slab has been recorded by placing the iButtons on the ceiling. Recorded data has been used to produce several graphs, which permitted an evaluation of the thermal performance of the buildings.

Additionally, an assessment of energy performance of the buildings has been conducted based on the annual electricity consumption of the buildings which was compared against figures of a typical practice and good practice published by the Charted Institution of Building Services Engineers - CIBSE benchmark.

VHCS CONTROL STRATEGIES APPLIED IN THE CASE STUDIES

The VHCS system delivers heating, cooling and ventilation. A number of air handling units (AHU) serve the VHCSs utilized in different zones of the buildings. The AHU's supply heated or cooled air into the respective zones through a system of ductwork, thermal planks and supply air diffusers. The ductwork from each AHU is separated into the independent thermal zones. Generally, the air will be supplied to each slab and discharged through soffit-mounted diffusers. The AHU's can be started either manually or automatically controlled by the Building Management System (BMS). There are temperature sensors in each zone, which show when the AHU needs to start in order for the average temperature to reach its desired set point. When the temperature reaches the suitable value or at the end of the occupancy time, the AHU reverts to normal temperature control. When the AHU is started, both supply and extract fans are activated by the control system with a constant speed.

A series of temperature sensors recorded the slab temperature of different zones. In order for each AHU to determine the supply air temperature for that zone, the highest 'zone average slab temperature' is considered. The temperature set point for the slabs is 22^{o}C in winter and 21^{o}C in summer. A dead band of 1.5^{o}C is placed around the set point of (+0.5^{o} C / -1.0^{o}C) during both seasons. The only different between Thomas Paine building and the Luton college is the way air is supplied to the spaces within the Thomas Paine building. Basically when the supply air is passing through the slab, instead of being diffuse from the ceiling, air is distributed from the walls.

ANALYSIS CONSIDERATIONS

- As mentioned before, to monitor the temperature, iButtons are used. They have an accuracy of ± 0.5°C that is taken in to account when analyzing the results.
- In order to assess thermal performance of the building regarding occupant comfort, Thermal Comfort Zone (TCZ) is assumed to be between 22°C and 26°C.
- In the final, total energy consumption of the buildings is considered to equate to the energy performance of the buildings. Therefore, these values do not display the part played by the VHCS in this achievement.

This paper only presents part of a much larger investigation. Further complementary information is available in the thesis that this paper is based on [2].

RESULTS AND OBSERVATIONS

Considering the overall results of the recorded temperature, a significant amount of information related to the thermal environment of the Luton Sixth Form Collage could be pointed out. Figure 1 shows relatively small temperature variation within the rooms though the outdoor ambient temperature is highly fluctuating and the rooms are located in different orientations. Also the indoor temperature remains fairly constant due to the effect of the VHCS utilized in these spaces.

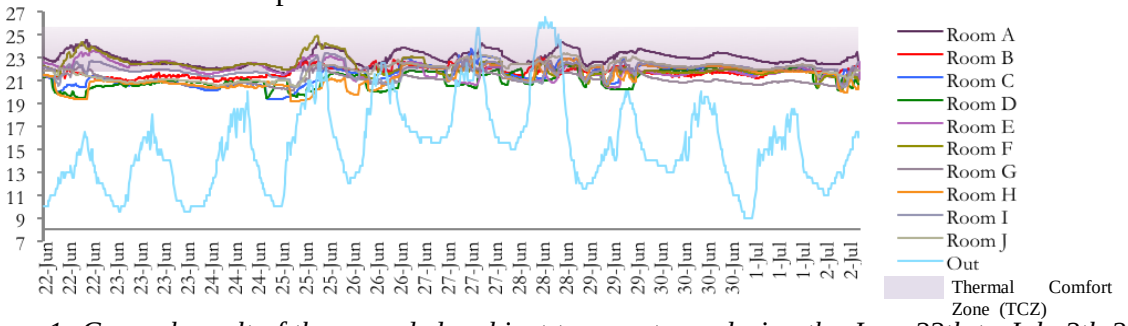

Figure 1: General result of the recorded ambient temperatures during the June 22th to July 2th 2012 (Luton Sixth Form College)

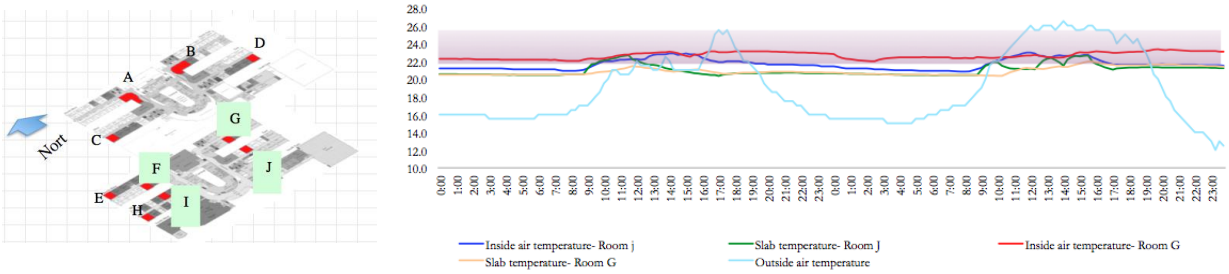

Figure 2: Comparative temperature results room G and room J during 27th and 28th June 2012

Figure 2 illustrates the thermal performance of two classrooms during the warmest days of the recorded period, when one is north facing (room G) and another is south facing (room J). The slabs temperatures are relatively constant and within the same range, whereas the ambient temperature inside the room G is approximately one degree higher than the room J. This can be as a result of more solar radiation entering the room G. Higher temperature of the room G results in higher percentages of time within the TCZ. Although during the working period from 8 AM till 9 PM, room J is also within the TCZ, but the inside temperature is around the minimum level of TCZ. It can be concluded that the system is over cooling, by pumping the air in the higher temperature thereby raising the slab temperature, a more thermally comfortable environment can be achieved. Looking at the indoor temperature of the room J, In the morning 27th it is clear that by raising the slab temperature, the indoor temperature is increased. The interesting point in this growth is that the slab reaches the peak at 11:30 AM,

whereas the indoor temperature peak occurs only at 2:30 PM. This phenomenon is due to the time lag created by the VHCS.

Looking more deeply at the thermal performance of two rooms with the same dimensions, orientation and occupancy pattern during the first three days figure 3, the slab temperature and ambient temperature in the room F are higher than room I, the difference between the slab temperature and the room temperature is around 2°C. The possible reason is that the control system of this wing was probably reduced or even shut down during this weekend therefore the temperature of the slab went up but remained relatively stable because of its thermal mass, and the effect of thermal mass is detectable in the much reduced temperature swing. Because the building is highly insulated with high thermal mass even if the control system is shut down not only will the indoor temperature remain stable but the slab temperature will also remain relatively stable and the effect of the outdoor temperature is minimal.

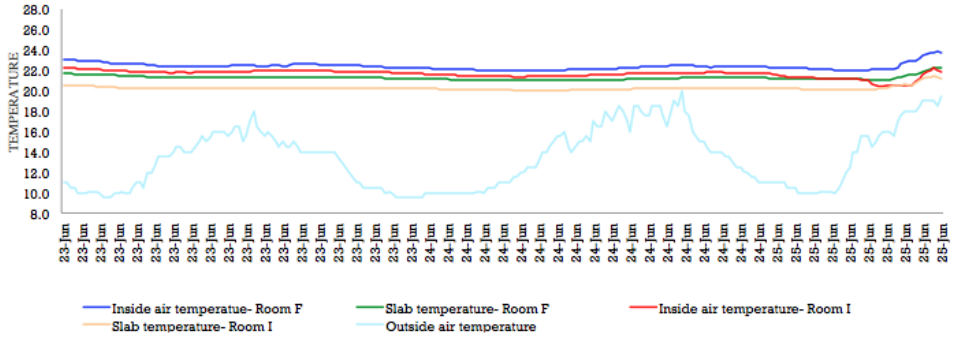

Figure 3: Comparative temperature results room F and room I during 23th, 24th and 25th June

Figure 4 displays the overall ambient temperatures recorded over ten days during July. It is clear that indoor temperatures are fairly steady and most of the time within the TCZ while the outdoor temperature is highly fluctuating. The maximum outdoor temperature is recorded on July 15th and it is 22°C while the lowest temperature occurred on July 13th it is around 12.5°C. Furthermore, the maximum and minimum temperatures have been measured in the rooms F and B, with the temperature of 27°C and 19.5°C, respectively.

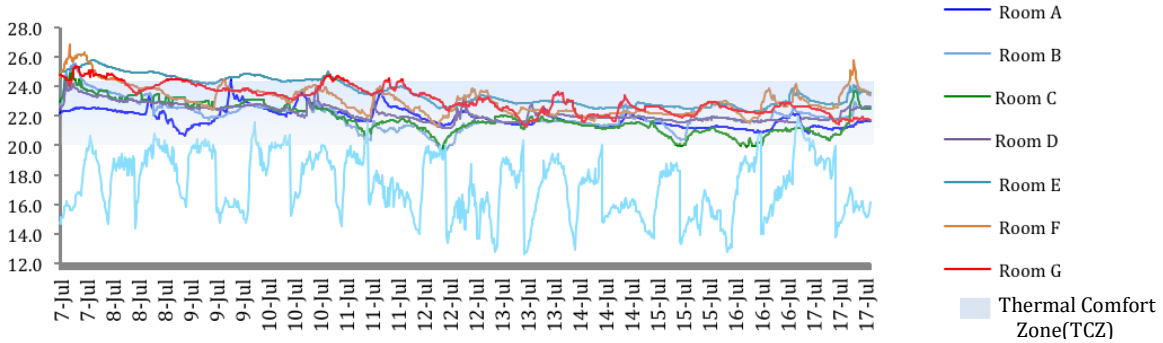

Figure 4: General result of the recorded ambient temperatures during the July 7th to 17th 2012 (Thomas Paine Building)

The results of the recorded temperature in three rooms in Thomas Pain building are presented in table 1. Outcomes indicate the outdoor temperature fluctuates widely whereas the indoor temperature is relatively steady. Comparing the rooms, it is clear that in the rooms A and B the slab temperatures and the room temperatures are very similar and the peaks that have occurred during the week days could be a result of internal gains. Room E is providing the thermally comfortable environment for over 90 per cent of the time. While for room A and B the temperature within the TCZ is around 40 per cent. It can be concluded the higher the

temperature the more the rooms are thermally comfortable. The average slab temperature for room E is one degree higher than the room A and slab temperature in room E has a wider range than the others. The average supply temperatures for the rooms are very similar, but in room E the temperature of the supply air is fluctuating over a wider range. Looking at room E, though the supply air temperature is varying a lot during the period, the inside air temperature and the slab temperature remain very constant. This possibly has happened because the air flow rate was highly reduced. This means that when the air flow rate is minimal it does not affect the temperature of the space significantly.

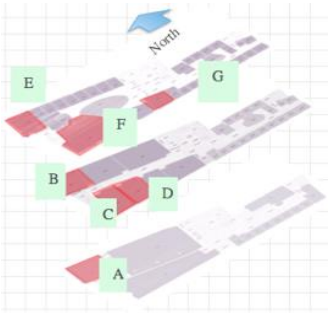

Figure 5: Key map of Thomas Paine building, showing the rooms that have been monitored

July 7th 2012 to July 17th 2012	Room A Ground floor	Room B First floor	Room E Second flooe
Ave. Ambient Outside Temp. °C	17.5		
Ambient Outside Temp. Range °C	12.5 to 22		
Time Ambient Outside Temp. within TCZ, as %	0.0		
Ave. Internal Room Temp. °C	22.5	22	23.5
Internal Temperature Range °C	20.5 to 24	19.5 to 25.5	22.5 to 26
Time Internal Temp. within TCZ, as % Internal Temperature Range °C	41.5	44	99.9
Ave. Slab Temp. °C	21.5	22	22.5
Slab Temperature Range °C	21 to 22.5	21 to 23.5	21 to 25
Ave. Supply air Temp. °C	21.5	21.5	21
Supply air Temperature Range °C	20.5	20 to 23	13to 25

Table1: General results of the analyzing the recorded temperature in room A, B and room E

ASSESSMENT OF ENERGY PERFORMANCE OF THE BUILDINGS

Since colleges and universities are comprised of a wide range and mix of spaces such as classroom, lab, library, catering and offices, it seems wise to use a modified benchmark in order to appropriately assess the energy performance of the building. For this reason, the buildings are divided into different categories with the same function and occupancy characteristics. Furthermore, dividing the buildings into different space types by percentages of their total area provides greater insight into the energy usage of each sector and highlights the potential for energy saving in each space category. Figure 6 shows schematically the process of analysing the energy performance of the buildings using the modified benchmark.

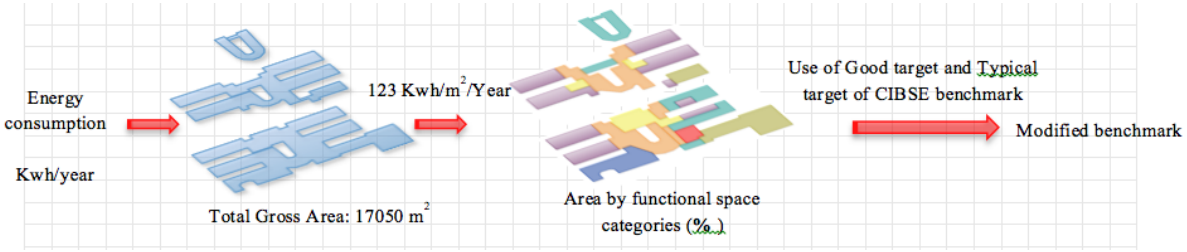

Figure 6: Schematic plan of the process of energy assessment

Tables 2 and 3 show the calculated values for each space category along with the energy consumption from the CIBSE benchmark, Guide F [3]. The highlighted values are the modified targets for typical and good practice. Comparing the electricity consumption of the building (kwh/m^2/y) with the modified benchmark. Real consumption for the Luton college is calculated as 123 kwh/m^2/y: 33.5% lower than the typical target and 10.5 per cent less than the benchmark for the good target. The Thomas Paine building in terms of energy performance is 182 Kwh/m^2/y. This value is 11 per cent lower than the modified benchmark for typical practice (205 kwh/m^2/y) in electricity consumption. However in comparison to the modified good practice benchmark (147 kwh/m^2/y) the real electricity consumption of the building is 4 per cent higher. These values indicate that the buildings perform reasonably well in terms of energy consumption.

Space Type	Areas covered %	Energy consumption (Good Practice) Kwh/m²	Energy consumption (Typical Practice) Kwh/m²
Teaching	31	113	129
Research	17	155	175
Lecture hall	2	67	76
Library	8	292	404
Office	21	128	226
Catering	8	137	149
Leisure	13	127	194
Total building	100	140	188

Table 2: Modified benchmark for Luton Sixth Form Colleae

Space Type	Areas covered %	Energy consumption (Good Practice) Kwh/m²	Energy consumption (Typical Practice) Kwh/m²
Teaching	29	113	129
Lecture hall	15	67	76
Office	25	234	358
Catering	4	137	149
Services	27	128	226
Total building	100	147	205

Table 3: Modified benchmark for Thomas Paine building.

Because of the limitations of this study it was not possible to accurately estimate the influence of the VHCS in this performance, however taking to account the utilization of the VHCS in considerable portions of the whole buildings it can be concluded that the VHCS amongst another strategies implemented in these buildings play an important role in the total energy performance of the building.

CONCLUSION

Based on the findings from all the previous research and the results of the investigation in these two buildings, the following results can be highlighted as the final conclusions.

Utilizing the VHCS in the building can reduce the peak temperature during the day and the temperature fluctuation. The VHCS also has a great influence on the reduction of the total hours with excessive temperatures and also the ability of the building to handle diurnal heat loads from the internal gains and solar gains.

The effectiveness of the VHCS is influenced by several parameters most importantly the amount of thermal mass and ventilation strategy. It is also important to take to account the role of the climate, set-point temperature, occupancy pattern and ventilation rates. Results from the college confirm the high potential of the VHCS to be set for higher temperature resulting in a higher thermal satisfaction of the occupants and lower energy demand.

The results also confirm that the VHCS could contribute to decrease the cooling/heating demand in buildings thereby improving the overall energy performance of the building.

Finally, it can be concluded that VHCS can meet the net energy frame for further and higher educational buildings, and significantly enhance the thermal performance and increase the level of thermal comfort without consuming extensive and expensive energy.

REFERENCES

1. Mirakbari, F. Ventilated Hollow Core Slab: A low energy strategy to improve energy efficiency of the built environment. MSc Thesis in Architecture, Energy and Sustainability, London Metropolitan University, 2012
2. Zmeureanu, R. A. *Thermal performance of a hollow core concrete floor system for passive cooling*. Building and Environment, 23 (3), 243-252, 1988
3. CIBSE. Energy Efficiency in Buildings, Guide F, 3rd edition, The Chartered Institution of Building Services Engineers, London, 2012

Daylighting and Electric Lighting

ASSESSMENT OF CIRCADIAN WEIGHTED RADIANCE DISTRIBUTION USING A CAMERA-LIKE LIGHT SENSOR

Borisuit A* ; Deschamps L ; Kämpf J ; Scartezzini J-L ; Münch M

Solar Energy and Building Physics Laboratory, School of Architecture, Ecole Polytechnique Fédérale de Lausanne (Switzerland)

ABSTRACT

Suboptimal light distribution in a room can cause visual discomfort and glare. Next to rods and cones, perception of light is also governed by a third class of photoreceptors, important for circadian rhythm regulation and non-visual functions such as alertness, mood and hormonal secretion. These receptors show greatest sensitivity in the blue part of the visible light spectrum. In order to assess light distribution with respect to non-visual sensitivity functions, we aimed at validating a new device to create light distribution maps with a circadian weighted radiance (L_{ec}) which accounts for this difference in sensitivity.

We utilized a camera-like light sensor (CLLS) to assess the distribution of L_{ec}. For this purpose, we equipped the device with customized filters to adapt the camera's spectral sensitivity to circadian sensitivity, similarly, as we had previously reported for the photometric calibration with the same device [1]. After spectral calibration and circadian weighted radiance calibration, we validated the CLLS in real scenes. The results showed that circadian luminance maps of a room can be efficiently assessed in a very short time (i.e. within 100 ms) under electric lighting as well as under daylighting conditions. We also used the CLLS to compare the L_{ec} values between two rooms, equipped with different daylighting systems such as LightLouver™ and standard venetian blinds. Our results showed different dynamics of luminance and L_{ec} in the course of the day with highest values at noon. We also found higher luminance and L_{ec} values in the test room with the venetian blinds, when compared to the room equipped with LightLouvers™.

Taken together, the validation of circadian luminance maps under real dynamic lighting conditions offers new possibilities to integrate the CLLS into advanced (day-) light sensors systems. This would allow to instantly adapting ambient lighting conditions with respect to tailored biological user needs.

Keywords: Light distribution, circadian weighted radiance, daylighting system, camera

INTRODUCTION

Conscious light perception via rods and cones is important for visual functions, visual comfort, glare and contrast in humans; it also depends on luminance distribution. A decade ago, a new class of photoreceptors in the retinal ganglion cells has been described, mainly responsible for non-conscious light perception to regulate circadian functions, the pupil light reflex and hormonal secretion. One important indirect marker for activity of these cells in response to light is suppression of the pineal hormone melatonin during night time. It has been shown that this light induced melatonin suppression is greatest in response to blue light exposure (446-477 nm) [2,3]. Sensitivity to different wavelengths of light was tested and subsequently a specific circadian sensitivity function created. This function is called C-lambda curve ($C(\lambda)$) [4] and differs from the V-lambda curve which reflects the photopic eye sensitivity ($V(\lambda)$).

Several new tools assessing (photopic) luminance maps were developed within the last ten years [5-8]. We recently described the different calibration processes of the camera-like light sensor (CLLS), developed by the Centre Suisse d'Electronique et de Microtechnique, and demonstrated its potential in creating luminance maps in real scenes under highly dynamic daylight conditions [1]. In order to also evaluate light distribution from an observer's perspective at the eye level, and with respect to non-visual functions, we intended to create light distribution maps with a circadian weighted radiance (L_{ec})[4]. We used our CCLS, equipped with customized filters enabling to adapt the camera's spectral sensitivity to the C(λ) function. We finally compared the distribution of L_{ec} using circadian luminance mapping under electric and daylighting conditions at different times of day.

METHODS

Spectral sensitivity calibration

In our previous work, the CLLS was calibrated based on the photometric sensitivity function (V(λ))[1] and corrected also for vignetting effects. The aim of this project was to use the CLLS device for circadian luminance maps: we thus first performed the spectral calibration with respect to the circadian sensitivity function (C(λ)). Narrow-bandwidth monochromatic light beams were used as a reference light source. The CLLS captured the photos of the light beams at 470 nm with different intensities. Simultaneously, we measured L_{ec} of the emitted light beams with a calibrated spectrophotometer (Specbos 1201, JETI, Jena, Germany). We then correlated the values obtained from the CLLS and the L_{ec} from the spectrophotometer. The camera provided a single value per pixel on a greyscale (in arbitrary units from 0 to 1024 digits); we used an exponential function ($R^2 = 0.9986$) in order to fit the greyscale and the respective L_{ec} ($W/sr.m^2$).

The same CLLS measures and those of the spectrophotometer were then taken at a constant light intensity, while modifying the wavelength of the light beam in 5 nm steps from 380 to 780 nm. The relative raw spectral sensitivity of the CLLS and the circadian sensitivity curve taken from the literature [4], are shown on Figure 1a). This sensitivity curve is based on the action spectrum for light-induced melatonin suppression, performed by Brainard *et al.*[2], and Thapan *et al.* [3] with a peak at 464 nm.

To implement customized filters in the camera, we calculated their optimal thickness to correct for the spectral response of the CLLS. We then performed the same steps as described above to determine if the filter corresponds to the circadian sensitivity function (Figure 1b). In order to assess the error between the relative spectral sensitivity from the CLLS and the circadian sensitivity (4), we applied the CIE standard error (F') of the V(λ) function [9] on the modified formula for C(λ) [see equation (1)]. We obtained a standard error of 10.4% for C(λ) by using the modified formula:

$$f' = 0.93584 \int_0^{\infty} \left| s(\lambda)_{rel} - C(\lambda) \right| d\lambda \% \qquad (1)$$

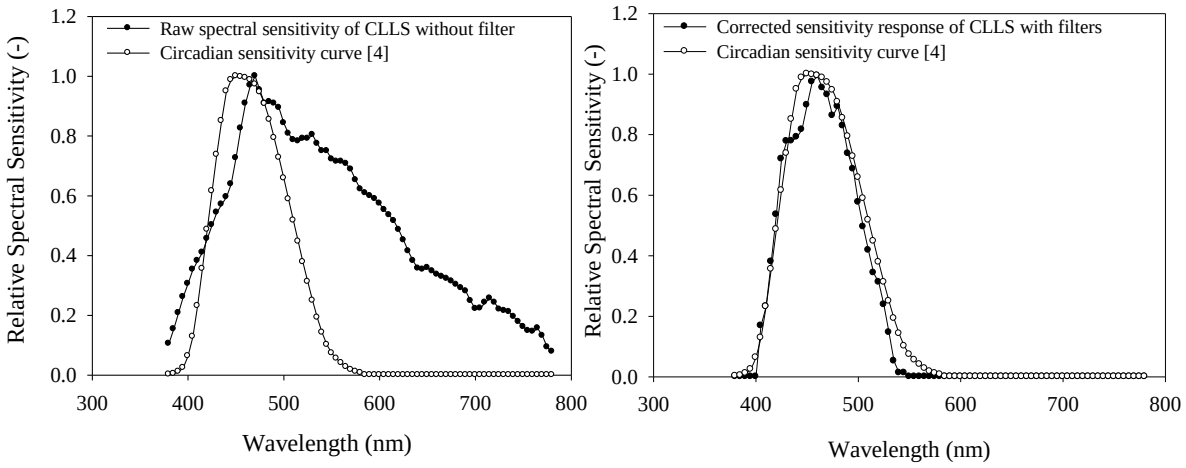

Figure 1a-b: Relative spectral sensitivity assessment of the CLLS; 1a) Relative raw spectral sensitivity of the CLLS (normalized data; black circles) and circadian sensitivity function (C (λ)[4]; white circles). 1b) Corrected spectral sensitivity response of the CLLS, equipped with filters (black circles) and circadian sensitivity function C (λ) (white circles [4]).

Circadian weighted radiance calibration

To perform the photometric calibration, a total of 83 measurements (from 0.04 cd/m^2 to 23'871cd/m^2) were made by using simultaneously the CLLS and a luminance meter (Minolta LS-110) as the reference sensor. Polychromatic white light from a 1000 W Xenon lamp and a 1200 W metal halide spotlight were used as reference light sources for the photometric calibration. The camera and the calibrated spectrometer monitored the emitted radiance values: the camera provided the associated pixels on a greyscale (in arbitrary units from 0 to 1024 digits); the luminance meter gave the corresponding luminance (cd/m2). The best fit between the pixel greyscale values and their associated luminance was determined [10] by using two different functions: for greyscale values which were lower than 425 (arbitrary units), we used an exponential function (R^2=0.97); for greyscale values higher than 425 (arbitrary units), a polynomial function was used (R^2=0.98; Figure 2). Both functions were finally implemented in the CLLS software.

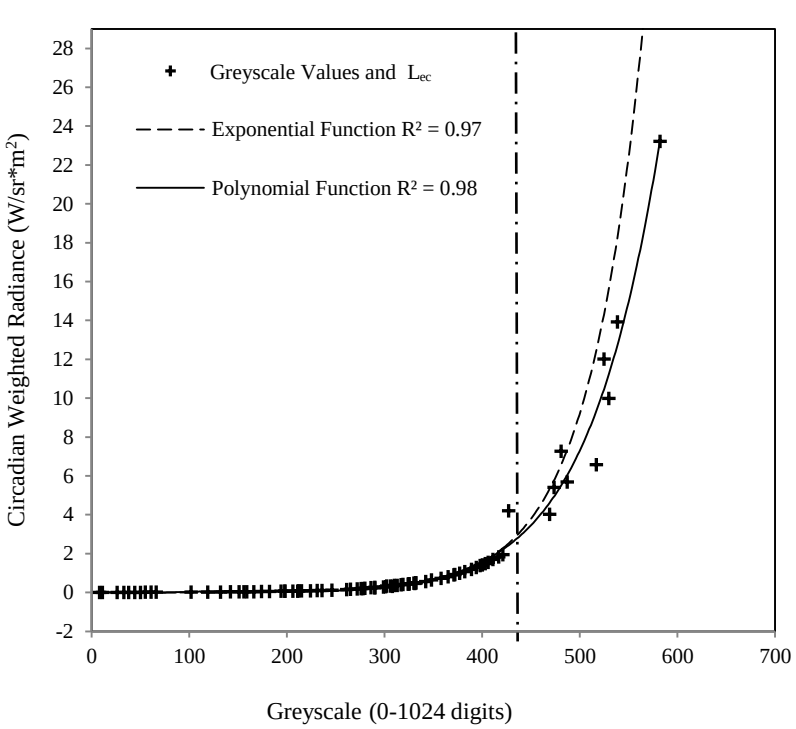

*Figure 2: Correlations between pixel greyscale values (arbitrary units from 0-1024) and associated luminance (W/sr*m^2). The black crosses indicate measurements taken with the CLLS and the spectrophotometer; the solid line indicates the regression line for the two functions (R^2=0.97 and R^2=0.98). The vertical dashed line depicts the border for the two regression functions at greyscale value 425 (arbitrary units).*

RESULTS

Circadian weighted radiance mapping

We tested the CLLS in an office room located in the LESO solar experimental building on the EPFL campus (Ecole Polytechnique Fédérale de Lausanne, Switzerland). We used 20 different room elements as targets for measurements (Figure 3). A set of pictures was taken under electric lighting conditions (2 x 36 W fluorescent tubes; 3000K) and under daylight conditions (clear sky). The L_{ec} values of the room elements were simultaneously assessed by the spectrophotometer and by the CLLS. Both data sets were then compared with the luminance meter values, as shown on Figure 4. The coefficients of determination (R^2) between L_{ec} measured with CLLS and the spectrophotometer across all room elements were: 0.96 for electric lighting and 0.91 for daylighting.

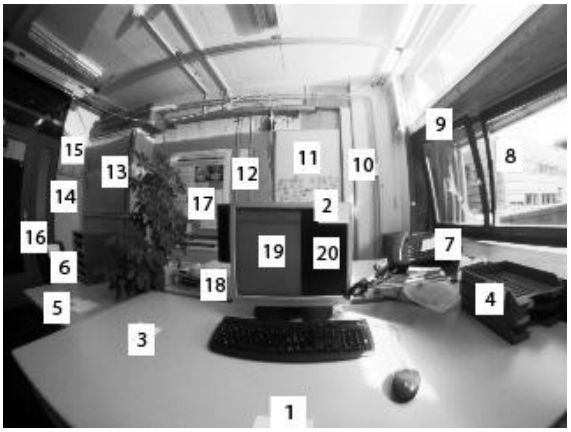

Figure 3: Locations of different room elements for the validation of the CLLS. 1=desktop, 2=PC screen, 3=desktop left side, 4=desktop right side, 5= second desk left side, 6 = chair, 7= telephone, 8= window, 9 upper window, 10 = back wall 1, 11 = white board, 12=back wall 2, 13 = closet, 14 = wall left side, 15= door, 16=bottom of the door, 17= poster, 18=behind PC screen, 19=document on PC screen, 20=black wallpaper on PC screen.

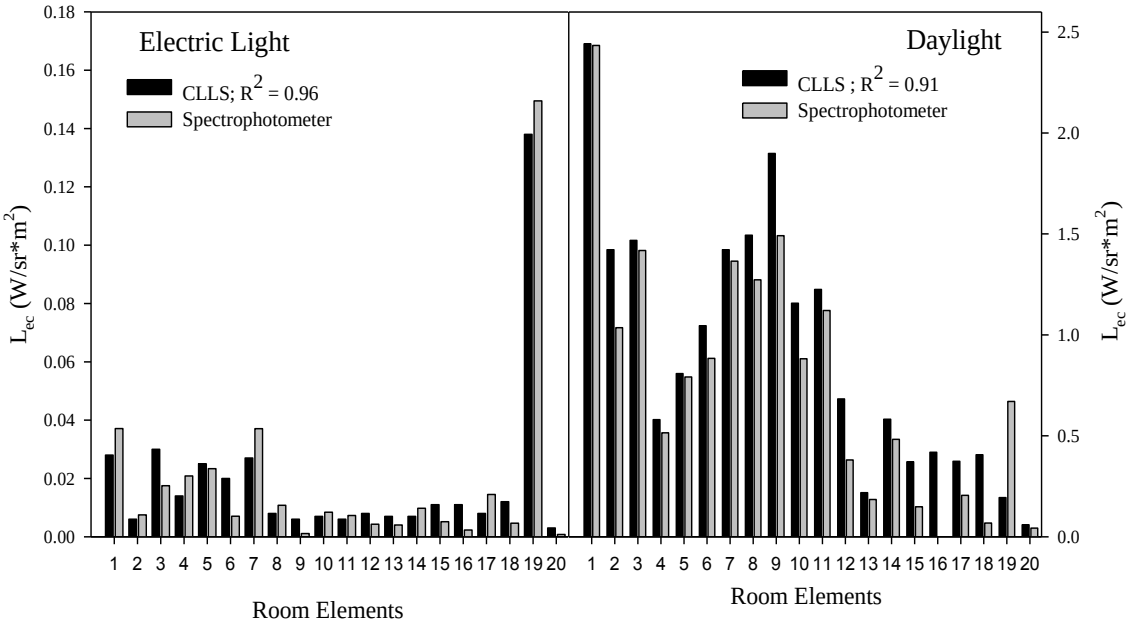

Figure 4: Luminance mapping derived from L_{ec} values of different office room elements (see Figure 3). The data points were extracted from CLLS (black bars) and the reference luminance measurements (spectrophotometer; grey bars). Left: assessment under electric lighting conditions; right: assessments under daylight conditions.

Circadian weighted radiance mapping at different times of day

After these calibration steps, the CLLS was tested in two test rooms at the Lawrence Berkeley National Laboratory (LBNL; CA, USA), during a short term stay of the first author. The two rooms (A and C) are equipped with standard venetian blinds (room A) and Light Louvers™ (room C). Both daylighting systems were located in the upper part of the windows, whereas the lower parts of the windows were completely covered. A set of pictures was taken with the CLLS at 9AM, 12PM and 3PM. Luminance and L_{ec} were measured for the same reference points in both rooms (walls, windows, task area, and ceiling). The ratio of L_{ec} and luminance (L_{ec}/L) was then determined to assess the circadian efficiency of the light distribution in the room: a higher ratio indicated a higher circadian efficiency. A total of 84 measurements were taken under clear sky conditions; extracted luminance, L_{ec} and ratio on log-transformed values were analysed with 2-way rANOVA with factors 'time' and 'room'.

We found higher luminance and L_{ec} in room A (venetian blinds) than room C (LightLouver^{TM}) for all three time points. For both rooms, luminance and L_{ec} were higher at 12PM than at 3PM and lowest at 9AM (Figure 5a-b, 'room' x 'time'; $p<0.05$). The ratio of L_{ec}/L was overall higher in room A than C ($p<0.05$; main effect of 'room'); the ratio for both rooms was higher at 3PM than 9AM ($p<0.05$; main effect of 'time'). First comparisons between two different locations in the room (near by the window and deeper in the room) did not reveal any difference in circadian efficiency of light distribution ($p>0.20$).

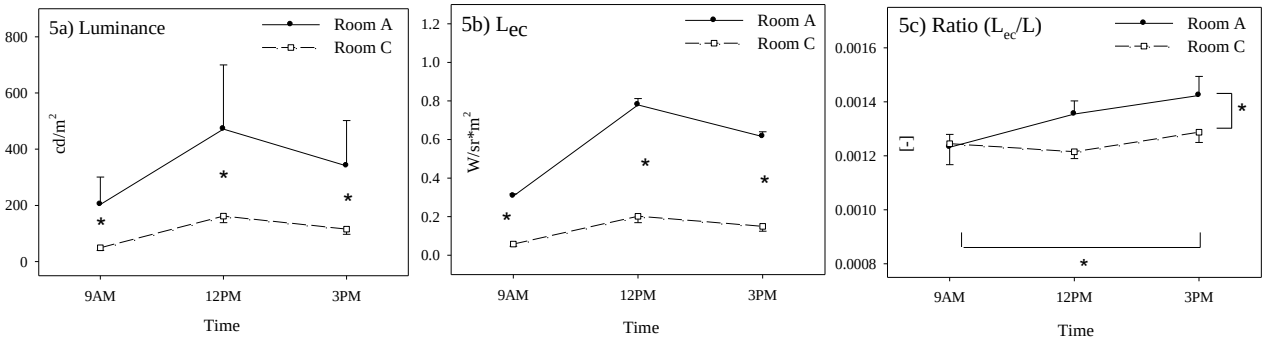

*Figure 5a-b: Photopic luminance (5a) and L_{ec} (5b) for room A (black circles) and C (white squares) at 9AM, 12PM, and 3PM. The Ratio between L_{ec} and Luminance was higher in room A than C; and larger at 3PM than 9PM; *=p<0.05; mean ± SEM).*

DISCUSSION

The CLLS was successfully calibrated and tested in real scenes: the calibrations resulted in high correlations with a reference device. The validation in real scenes revealed that the correlation of L_{ec} between CLLS and values monitored with spectrophotometer was high for constant electric lighting conditions and daylighting conditions under clear sky. The room equipped with standard venetian blinds provided higher luminance and L_{ec} than the room equipped with LightLouver^{TM} throughout the day, with highest values at noon. The most likely reason for the dynamics of luminance and L_{ec} is due to the change in the angle of incoming sunlight. Interestingly, circadian efficiency was highest at 3PM: one reason for this might be that the different angle of daylight did not provide only different light levels, but also accounted for changes in the spectral composition of daylight.

One important question remains: what does a higher or lower circadian efficiency mean? It can be used as a proxy for biological functions. Future experiments should also test other variables, for example circadian efficiency of light for human alertness, mood or performance.

The first experimental assessments of circadian weighted luminance maps of two complex fenestration systems were also carried out in this work: the latter provided different circadian weighted light distributions. Therefore it will be important to further analyse those systems also with respect to circadian weighted luminance at different locations in the room and at varying times. Using the CLLS for circadian luminance mapping is thus innovative in particular for the assessments of light with respect to non-visual biological functions in architectural settings.

ACKNOWLEDGEMENTS

The authors thank the Centre Suisse d'Electronique et de Microtechnique (CSEM, Switzerland) for their collaboration and Pierre Loesch (LESO-PB EPFL) for technical support. The authors are grateful to Eleanor Lee and Dr. Anothai Thanachareonkit at Lawrence Berkeley National Laboratory (USA) for inviting and hosting the first author. The work was financially supported by the Velux Foundation (Switzerland) and a PhD mobility award from the doctoral school (EDCE, EPFL, Switzerland).

REFERENCES

1. Borisuit, A, Münch, M, Deschamps, L, Kämpf, J, Scartezzini, JL: A new device for dynamic luminance mapping and glare assessment in buildings. Proc. of the SPIE 2012 Optics+Photonics Conference conference. San Diego, 2012.
2. Brainard, GC, Hanifin, JP, Greeson, JM, Byrne, B, Glickman, G, Gerner, E, Rollag, MD: Action spectrum for melatonin regulation in humans: evidence for a novel circadian photoreceptor. Journal of Neuroscience. Vol.21(16) pp 6405-6412, 2001.
3. Thapan, K, Arendt, J, Skene, DJ: An action spectrum for melatonin suppression: evidence for a novel non-rod, non-cone photoreceptor system in humans. Journal of Physiology. Vol.535(Pt 1) pp 261-267, 2001.
4. Gall, D: Circadiane Lichtgrössen und deren messtechnische Ermittlung. Licht. Vol.11-12 pp 1292-1297, 2002.
5. Bellia, L, Cesarano, A, Minichiello, F, Sibilio, S: Setting up a CCD photometer for lighting research and design. Building and Environment. Vol.37(11) pp 1099 - 1106, 2002.
6. Inanici, M: Evaluation of high dynamic range photography as a luminance data acquisition system. Lighting Research and Technology. Vol.38(2) pp 123 - 134, 2006.
7. Beltrán , LO, Mogo , BM: Assessment of luminance distribution using HDR photography. Proc. of the 2005 ISES Solar World Congress conference. Orlando, FL, USA, 2005.
8. Borisuit, A, Scartezzini, JL, Thanachareonkit, A: Visual comfort and glare risk assessment by HDR imaging technique. Architectural Science Review. Vol.53(4) pp 359-373, 2010.
9. CIE: CIE Technical support. Methods of characterizing illuminance meters and luminance meters - Performance, characteristics and specifications. Vol. CIE 069-1987, Vienna, CIE Central bureau, 1987.
10. Andersen, M: Innovative bidirectional video-goniophotometer for advanced fenestration systems. Ecole Polytechnique Fédérale de Lausanne (EPFL), 2004.

EFFICIENT VENETIAN BLIND CONTROL STRATEGIES CONSIDERING DAYLIGHT UTILIZATION AND GLARE

Ying-Chieh Chan[1]; Athanasios Tzempelikos[1]

School of Civil Engineering, Purdue University, 550 Stadium Mall Drive, West Lafayette, IN 47906, USA

ABSTRACT

Optimized control of venetian blinds, including consideration of thermal loads, lighting energy use and occupant comfort, has not been achieved despite the recent efforts on identifying important variables and comparison of common control strategies. This paper presents the development of new venetian blind control strategies considering daylight provision, lighting energy use and visual comfort for different slat material properties. A hybrid ray-tracing and radiosity method is used to calculate transmission through the window-blind system and interior illuminance distributions. The specular and diffuse characteristics of the louvers are treated separately. Work plane illuminances are used to extract daylighting metrics (such as continuous daylight autonomy), while directional light distribution and respective luminance values are used to calculate glare potential using the daylight glare probability index. The developed control strategies consider the specular characteristics of slats in detail. Using the common "cut-off" angle may result in a strong second reflection from the bottom surface of slats that might significantly affect visual discomfort depending on the direction of view and profile angle. A proper rotation of the slat angle can help to avoid this effect and redistribute daylight deeper into the space. Appropriate set points for control actions are determined based on work plane illuminances and glare probability. Annual results of daylighting metrics, lighting energy use and glare probability are presented along with a comparison between commonly used blind control strategies.

Keywords: venetian blinds, daylighting, control, visual comfort

INTRODUCTION

Previous studies have showed that occupants do not frequently change the blind position and slat angle [1-3]. The correlation between occupants' control behaviour and environmental variables such as temperature, illuminance, solar radiation etc is not obvious [4]; however, annual operation has an impact on energy use and potential energy savings. Glare form daylight is bound to occur when direct light falls on or near the work plane area –or directly on occupant's eyes- as well as in cases where high surface luminance values exist within the field of view. The typical blind control strategy to avoid direct illuminance is to rotate to a "cut-off" angle which can be calculated from the solar profile angle and blind geometry [5-6]. Recent studies presented blind control algorithms based on slat geometry, cut-off angles, ANN and genetic algorithms, as well as model-based controls with high computational time [7-11]. A thorough work on blind controllers with multi-objective optimization processes [12] with extensions to user wishes [13] provides advanced and promising solutions. To account for glare, several glare models focusing on daylighting were developed such as the daylight glare index (DGI) [14] and daylight glare probability (DGP) [15,26]. Operational algorithms to reduce energy use while maintaining proper DGI values can be found in [16-17]. Pfrommer et al. [20] extended the pioneer ray-tracing method [19] then used a "shining factor" to separate the portion of diffuse reflection and specular reflection. Ray-tracing techniques and software [22], advanced experimental approaches and bi-directional transmission distributions functions [26-27] can be used to characterize the distribution of transmitted light through

complex fenestration systems; however, the process is complex and requires intensive calculations or measurements [25]. A recently developed hybrid ray tracing and radiosity method for light transport through blinds [21] was extended to the room scale for obtaining illuminance results and annual daylighting metrics. This paper presents newly developed venetian blind control strategies and comparative results using the latter method. Daylight metrics and visual comfort for different slat material properties are considered.

METHOD AND SIMULATION APPROACH

Hybrid Ray Tracing and Radiosity Daylighting Model

In the hybrid model [21], three components – direct-specular, direct-diffuse, and diffuse are treated separately. The direct-specular component transmitted through the window-blind system is traced using forward ray tracing until the ray reaches a "diffuse" sub-surface or until the intensity decreases to a specific threshold. The direct-diffuse and diffuse-diffuse components inside the blind cavity are modelled by a 2-D radiosity method as suggested in ISO 15099 [23]. The amount of direct-diffuse illuminance generated in the inter-reflecting process is estimated from the shining factor, surface reflectivity, and number of bounces. The final amount of illuminance (and luminance) on work plane, other interior surfaces, and vertical illuminance on occupants' eye are predicted by a 3-D radiosity method where each room interior surface is separated into smaller sub-surfaces –here, every surface is separated into 9 elements. The inter-reflection process inside then room is then solved by a gathering algorithm and the entire calculation is repeated for every time step for an annual analysis.

Daylight Glare Probability

To evaluate glare, the daylight glare probability index (DGP) is used [24] as shown in Eq. (1). To calculate vertical illuminance, a reference point and a view direction vector are needed. In this paper, the glare source is defined as having 4 times the average work area luminance, which is defined as a 0.2m x 0.2m virtual surface in front of the occupant, at a height of 0.8m. The configuration of occupant's position and viewing directions is presented in Fig. 1.

$$\boldsymbol{DGP} = 5.87\times10^{-5}\boldsymbol{E}_v + 9.18\times10^{-2}\log(1+\sum_i \frac{\boldsymbol{I}_{s,i}^2\omega_{s,i}}{\boldsymbol{E}_v^{1.87}\boldsymbol{P}_i^2}) + 0.16 \quad (1)$$

Development of Control Strategies

The base case presented here has flat blinds of equal width and distance between them, and negligible thickness –variations of these parameters can be studied following [6]. The cut-off angle in conventional blind control is calculated from Eq. 2 [5].

$$\beta_{cut-off} = 90° - 2\Omega \quad (2)$$

where β is slat angle (0° when horizontal; positive when it rotates counter-clockwise, and Ω is solar profile angle. There are two problems when applying the "cut-off angle control" to slats with specular properties. The first problem is the second reflection originating from the bottom surface of slats as shown in Fig. 2(a). The second problem has to do with the direction of reflected rays, as this is directly related to glare. As shown in Figure 2(b), following the cut-off angle control strategy, the (direct) reflected rays would be horizontal, causing direct glare from daylight. This problem happens with high profile angles and specular slats at the top surface. To solve these two problems, first we need to check if there is a second reflection when slats rotate to the cut-off angle. The conditions are defined in Eq. (3):

$$[\delta < 90 \,|\, \cos\beta\tan\delta > 1+\sin\beta] \rightarrow \text{ second reflection occurs} \quad (3)$$

where δ is ray's reflected angle which can be obtained from Eq. (4)

$$\delta = \Omega + 2\beta \tag{4}$$

If there is a second reflection, the slats are set perpendicular to the profile angle (Figure 2(c)). Otherwise, the second problem is considered. The design of reflected angle depends on both the blind material characteristics and slat angle as well as on the occupants' position (Fig. 1). In this paper, the redirection angle is set to 30° to cover most cases shown in Figure 2(d). The slat angle that redirects the rays to the desired angle can be obtained by:

$$\beta_{design} = \frac{\delta_{designed} - \Omega}{2} \tag{5}$$

If the original cut-off angle ($\beta_{cut\text{-}off}$) is larger than β_{design}, then the cut off angle is selected since extra rotation would result in direct-direct transmission. A solution to reduced light transmission is having "double –sided" slats. For such cases, blinds can remain in the cut-off angle when $\beta_{cut\text{-}off} > \beta_{design}$. Finally, a different control approach can be used to correlate between interior light levels/glare indices and sky conditions. By using a reference sensor reading (e.g. transmitted illuminance) and simulated correlation results, it is possible to determine a set point for directly controlling the blind tilt angle. When the measured illuminance exceeds the set point, DGP would be unacceptable so the blinds would rotate to 70° (glare is minimized for that tilt angle). Otherwise, the slats will remain horizontal.

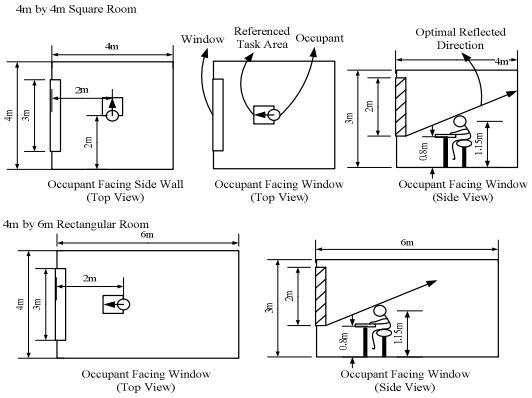

Figure 1: Occupant position and viewing directions.

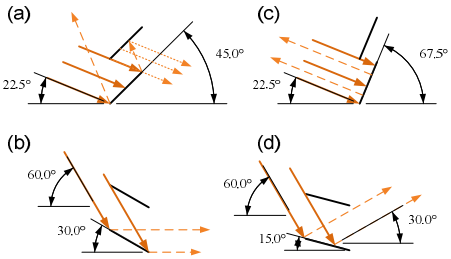

Figure 2: Reflected rays' direction with different profile angle and slat angle configurations.

SIMULATION RESULTS

Two perimeter office spaces are modeled in Philadelphia: 4m x 4m and 4m x 6m together with three materials (Table 1). The slat reflectivity is all 70% and the slat width and distance are equal to 0.05m. The window is 3m by 2m and is double-glazed clear. The window lower side is 0.8m above the floor. The reflectivity of interior floor, ceiling and walls are equal to 45%, 80% and 50% respectively. The installed lighting power density is 10 W/m^2.

	S1 - Diffuse	S2 - Specular	S3 – Double Sided
Slat Bottom	Shining Factor – 1.0	Shining Factor – 0.2	Shining Factor – 1.0
Slat Top	Shining Factor – 1.0	Shining Factor – 0.2	Shining Factor – 0.2

Table 1 – Blind specular characteristics

Comparative results are presented for seven different blind tilt angle settings/controls: Fixed blind angle - 0°, 45°, 70°; Cut-off angle control; R1 "blocking" control - Set blinds perpendicular to profile angle when a second reflection is possible/ redirect transmitted rays to 30° when $\beta_{cut\text{-}off} < \beta_{design}$; R2 control- Set blinds to cut-off angle when $\beta_{cut\text{-}off} > \beta_{design}$ / redirect transmitted rays to 30° when $\beta_{cut\text{-}off} < \beta_{design}$; Sky conditions/glare control: blinds are controlled based on correlations between transmitted illuminance and DGP.

Variation of Blind Tilt Angle Using Different Controls

Fig. 5 shows the comparative blind tilt angle results for the case of south and west facing windows for representative days in summer and winter. Higher profile angles allow redirection strategies to become more efficient. More profound differences are observed for west facing facades; R2 control allows more view to the outside and efficient light redirection.

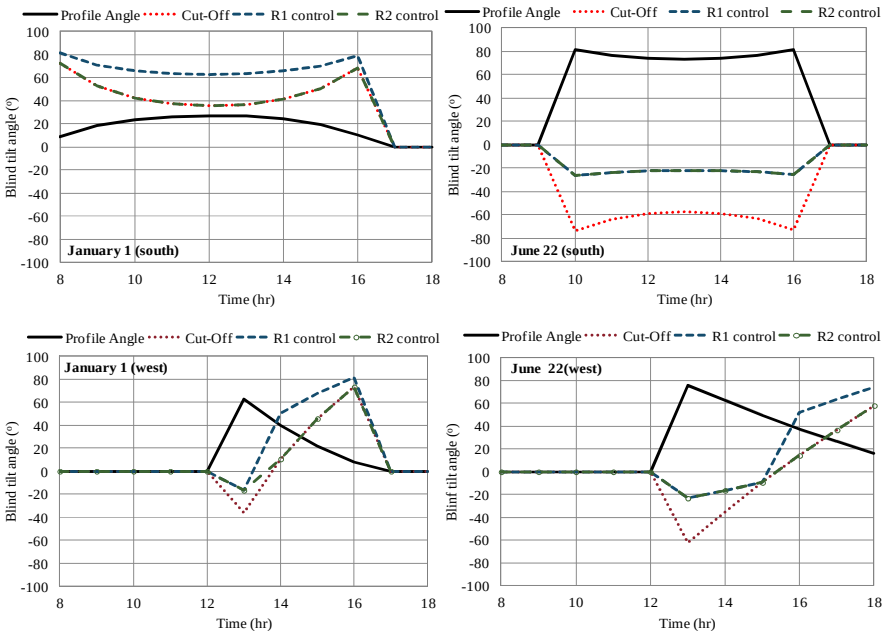

Figure 5: Blind tilt angle variation for representative days in winter and summer for south facades (top) and west facades (bottom) using the different control strategies.

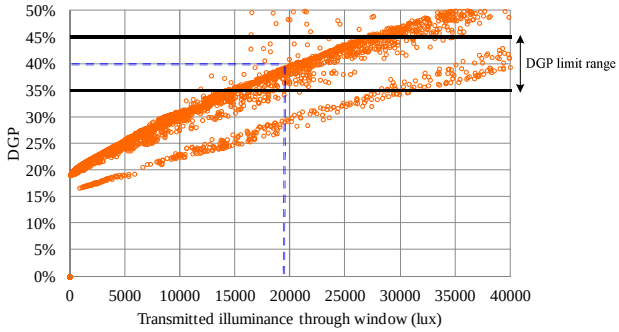

Figure 6: Correlation between DGP and transmitted illuminance for the full year with horizontal specular blinds.

Sky Condition/Glare Control Analysis

In this case the set point to open/close blinds is pre-determined. A correlation between transmitted illuminance and DGP with fixed horizontal blinds is first performed. Figure 6 presents the correlation results for a full year. Aiming at DGP values lower than 40%, the transmitted illuminance set point (for rotating to 70^{o}) is 19000 lux. Specular slats were used.

Impact of Control Strategies and Slat Properties on Daylighting Metrics and Glare

The graphs below present results of continuous daylight autonomy (cDA) as well as the percentage of time within office hours during which DGP is greater than 40% (noted as "annualDGP") for both viewing directions: facing the window and facing the side wall. The cut off angle control results in unacceptable glare values. The three developed control strategies (R1, R2 and sky/glare control) show good daylighting performance. Nevertheless, diffuse blinds will cause glare problems for R1 and R2 controls when facing the window –this becomes less significant with specular or double-sided blinds. The sky conditions/glare control method eliminates glare and maintains high cDA levels. Interestingly, when facing the side wall, diffuse blinds perform better then specular blinds, because specular reflections on the wall will result in high luminance that affects DGP. The results for a west facing office are shown in Fig. 8 and follow a similar trend -with lower values. Figure 9 shows the results for the 4m by 6m room. In this case, R2 control with specular and double-sided slats shows better results due to stronger light redirection. This effect would be more obvious for even deeper spaces. Glare is still considerable, especially for diffuse blinds, but better glazing types and could solve this problem.

CONCLUSION

This study presented the development of new venetian blind control strategies for maximizing daylight penetration considering the risk of glare. Depending on the occupant relative position and window size and orientation, light redirection angles may be used for controlling blinds to eliminate direct light on the work plane or at the eye level. This method works well for high profile angles. For lower profile angles, either total blockage of direct light or double-sided blinds with the cut-off control may be used. Diffuse blinds are more likely to cause glare but the advantage of specular blinds is only evident for deeper spaces, and R2 control shows promising results, especially for double-sided blinds. Alternatively, blinds can be controlled based on sky conditions, using correlations between DGP and transmitted illuminance.

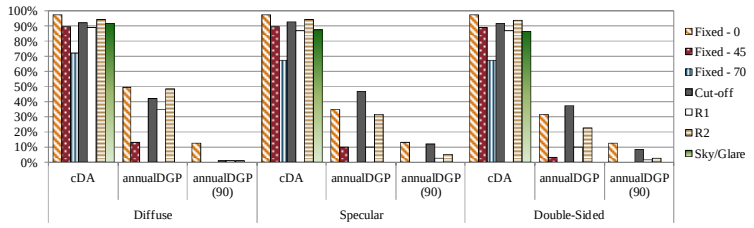

Figure 7: Impact of blind control strategies – 4m by 4m south facing room

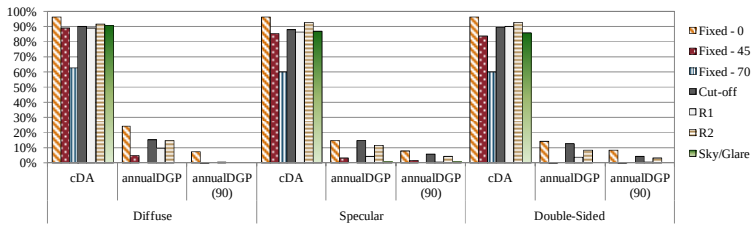

Figure 8: Impact of blind control strategies – 4m by 4m west facing room

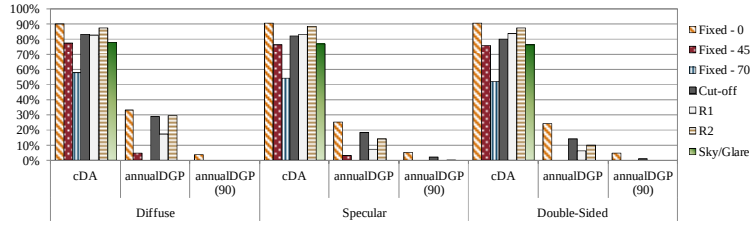

Figure 9: Impact of blind control strategies – 4m by 6m south facing room

REFERENCES

1. Foster, M. and T. Oreszczyn, *Occupant control of passive systems: the use of Venetian blinds.* Building and Environment, 2001. **36**(2): p. 149-155.
2. Zhang, Y. and P. Barrett, *Factors influencing occupants' blind-control behaviour in a naturally ventilated office building.* Building and Environment, 2012. **54**(0): p. 137-147.
3. O'Brien, W., K. Kapsis, and A.K. Athienitis, *Manually-operated window shade patterns in office buildings: A critical review.* Building and Environment, 2013. **60**(0): p. 319-338.
4. Correia da Silva, P., V. Leal, and M. Andersen, *Occupants interaction with electric lighting and shading systems in real single-OCCUPIED offices: Results from a monitoring campaign.* Build.and Env., 2013.
5. Athienitis A. K., Tzempelikos A., 2002. A methodology for calculating room illuminance distribution and light dimming for a room with a controlled shading device. Solar Energy 72 (4), 271-281.
6. Tzempelikos, A., *The impact of venetian blind geometry and tilt angle on view, direct light transmission and interior illuminance.* Solar Energy, 2008. **82**(12): p. 1172-1191.
7. Zhang, S. and D. Birru, *An open-loop venetian blind control to avoid direct sunlight and enhance daylight utilization.* Solar Energy, 2012. **86**(3): p. 860-866.
8. Koo, S.Y., M.S. Yeo, and K.W. Kim, *Automated blind control to maximize the benefits of daylight in buildings.* Building and Environment, 2010. **45**(6): p. 1508-1520.
9. Hu, J. and S. Olbina, *Illuminance-based slat angle selection model for automated control of split blinds.* Building and Environment, 2011. **46**(3): p. 786-796.
10. Čongradac, V., et al., *Algorithm for blinds control based on the optimization of blind tilt angle using a genetic algorithm and fuzzy logic.* Solar Energy, 2012. **86**(9): p. 2762-2770.
11. Kim, D.-W. and C.-S. Park, *Comparative control strategies of exterior and interior blind systems.* Lighting Research and Technology, 2012. **44**(3): p. 291-308.
12. Guillemin A., Molteni S., *An energy-efficient controller for shading devices self-adapting to the user wishes*, Building and Environment 37 (2002) 1091 – 1097.
13. Daum D., Morel N., *Identifying important state variables for a blind controller*, Build. and Env. 45 (2010) 887–900.
14. Osterhaus, W.K.E., *Discomfort glare assessment and prevention for daylight applications in office environments.* Solar Energy, 2005. **79**(2): p. 140-158.
15. Wienold, J., *Dynamic Daylight Glare Evaluation*, in *Building Simulation 2009*2009: Glasgow, Scotland.
16. Chaiwiwatworakul, P., S. Chirarattananon, and P. Rakkwamsuk, *Application of automated blind for daylighting in tropical region.* Energy Conversion and Management, 2009. **50**(12): p. 2927-2943.
17. Oh, M.H., K.H. Lee, and J.H. Yoon, *Automated control strategies of inside slat-type blind considering visual comfort and building energy performance.* Energy and Buildings, 2012. **55**(0): p. 728-737.
18. EnergyPlus, *EnergyPlus Engineering Reference*—2007, Lawrence Berkeley National Laboratory (LBNL).
19. Parmelee, G.V. and W.W. Aubele, *The Shading of Sunlit Glass: an Analysis of the Effect of Uniformly Spaced Flat Opaque Slats.* ASHVE Transactions, 1952. **58**: p. 377-398.
20. Pfrommer, P., K.J. Lomas, and C. Kupke, *Solar radiation transport through slat-type blinds: A new model and its application for thermal simulation of buildings.* Solar Energy, 1996. **57**(2): p. 77-91.
21. Chan, Y.C. and A. Tzempelikos, *A hybrid ray-tracing and radiosity method for calculating radiation transport and illuminance distribution in spaces with venetian blinds.* Solar Energy, 2012.
22. Ward, G. and R. Shakespeare, *Rendering with RADIANCE.* 1998: Morgan Kaufmann Publishers.
23. ISO, *ISO 15099:2003(E)*, International Organization for Standardization: Geneva, Switzerland.
24. Wienold, J. and J. Christoffersen, *Evaluation methods and development of a new glare prediction model for daylight environments with the use of CCD cameras.* Energy and Buildings, 2006. **38**(7): p. 743-757.
25. Kämpf J.H., Scartezzini J.-L., *Ray-tracing simulation of complex fenestration systems based on digitally processed BTDF data*, Proc. of CISBAT 2011, pp. 349-354.
26. Klems J.H., Warner J.L., 1995. *Measurement of bi-directional optical properties of complex shading devices*. ASHRAE Transactions 101, 791-801.
27. Andersen M., Rubin M., Powles R., Scartezzini J.L., 2005. *Bi-directional transmission properties of venetian blind: experimental assessment compared to ray-tracing calculations*. Sol. Energy 78 (2), 187-198.

LIGHTING PERFORMANCE AND ENERGY SAVING OF A NOVEL FIBRE OPTIC LIGHTING SYSTEM

D Lingfors[1], R Hallqvist[2]; T Volotinen*[1]

[1] *Div. of Solid State Physics, Dept. of Engineering Sciences, Uppsala University, The Angstrom Laboratory, Box 534, 75121 Uppsala, Sweden.*
[2] *Parans Solar Lighting AB, Kampegatan 4C, 41104 Goteborg, Sweden*
* *Correspondence: ttvolotinen@gmail.com*

ABSTRACT

The abundant luminous flux of 3000 - 4600 lm at 100 000 - 130 000 lx direct sun illuminance at a 10 m fiber distance was obtained from Parans fiber optic solar lighting system SP3. The illuminance of 2400 lm at 100 000 lx, after a 20 m distance, was higher than specified. The illumination performance and energy savings of a solar fiber optic lighting system have been verified in a study hall - corridor interior within the EU FP7 NMP project Clear-up at Uppsala University in Sweden. The system provides the intensive full spectrum white light with the color temperature (that describes the light color perceived) being 5800 ± 300 K, i.e. close to the direct sunlight outside. The color rendering index (85) (that describes how well colors are rendered under the light source) is higher for the solar lights than for the supplementary fluorescent lights (77). Thus this high quality solar lighting improves the visibility of all kinds of objects compared to the fluorescent lights. Annual lighting energy savings of 19 % in Uppsala, Sweden and 46 % in southern Europe were estimated for a study hall interior, as well as 27 % and 55 % respectively for an interior illuminated 16 h per day all days of a year. The efficacy (the total output flux divided by the consumed electric energy) of 300 lm/W was obtained at sun illuminance over 100 000 lx is significantly higher than for any artificial light sources available. Furthermore, the spatial light distribution was noticed to be wider than the expected, and a new .ldt-file was developed from the data for lighting simulation tools. The illuminance distributions were studied in the study hall under various sunlight conditions and the experimental data was found to correspond to the simulated light scenes. This solar lighting technology would have the greatest impact in offices and other commercial environments where human beings would work under these lights.

Keywords: daylight, optical fibers, solar light, energy saving, fluorescent lights, illuminance, correlated color temperature, color rendering index, luminous flux, luminous efficacy.

INTRODUCTION

Lighting stands for 25-45 % of the electric energy consumption of the commercial building sector today [1]. Solar fiber optic lighting systems can reduce the energy consumption and at the same time provide excellent light quality close or similar to sunlight outside [2-5]. Such a light is known to have a positive impact on the working efficiency and well-being [6]. The fiber optic solar lighting technique has been fairly expensive ever since it was introduced during the 80s [7], making it unmotivated as an energy saving technology. However, during recent years a significant price drop on solar lighting systems has been

seen [8]. The most recent generation of the solar lighting system studied here, the SP3 system from Parans Solar Lighting, costs less than half of the previous system (SP2) [4], but the light output power (luminous flux) has more than doubled [2-3]. The illumination performance (illuminance vs. sunlight intensity, luminous flux, light color) and energy savings of the SP3 have been investigated at Uppsala University within the EU FP7 NMP project "Clear-up" during past two years [2-5], and the main results are briefly reported in this paper. The new result is the wider, and thus more relevant, spatial distribution data for the fiber luminaires of SP3 system, developed to a data file that can be used for DIALux and other lighting simulation software. In earlier tests [2-3] it was noticed that the data from the product supplier shows a distribution which is too narrow.

METHOD

Illumination performance

The novel fiber optic solar lighting system SP3 from Parans has been tested in a study-hall-corridor test site at Uppsala University, The Angstrom Laboratory, for the illumination performance and energy saving as a supplement for fluorescent electric lights. The solar light collector, consisting of 36 lenses that couple the direct sunlight into the 36 optical fibers, is shown in Fig. 1(a). The 10 m fibers transport the light into the six fiber luminaires that are installed in the ceiling of the study-hall-corridor interior (Fig. 1(b)). Another SP3 system with 20 m fibers was installed in offices [5]. Fig. 1(b) shows the lighting conditions in the study hall area during a sunny day. The electric lights have been dimmed down in this case. The daily, seasonal and weather based variations have also been examined.

(a) (b)

Figure 1: (a) The sun-tracking solar light collector of the SP3 system. (b) The study hall area, where the solar fiber optic light luminaires of the Parans SP3 system have been installed, shown during a sunny day in May 2012. The electric lights have been dimmed down.

The illuminance, temperature and electric power consumed have been monitored continuously with sensors coupled to a web logger in the study hall test site. The fluorescent lights have been automatically dimmed down when the light from the solar lighting system has been available. The direct solar illuminance was measured by a sensor, attached on the

solar light collector and the signal was used to control the electric lights. The illumination performance has been simulated by DIALux software and compared with the measured illuminance maps. The luminous flux of the fiber luminaires was measured by using Hagner EX-4 lux meter and a custom made integrating sphere (CMIS), calibrated at the SP Technical Research Institute of Sweden [2,5]. The spectra of the fluorescent light, direct sunlight outside and the solar light obtained from fiber luminaires were measured with an optical spectrum analyzer (OSA) consisting of a Jarrel Ash monochromator (JA-150) and a Princeton Instrument detector (IRY 1024/L). The color rendering indexes (Ra) were calculated according to the method described in CIE 15:2004. The color temperatures (Tc) were calculated through to the polynomial method developed by McCamy [9].

To ease the work of lighting designers in planning of the lighting for an interior, luminaire manufacturers provide polar diagrams describing the spatial distribution and the luminous intensity of the luminaires. Illuminance schemes take into account all walls, ceiling, floor, furniture, windows and light sources are created by the lighting planning software, such as DIALux, Relux or 3ds Max Design. When characterizing the light distribution for optical fiber luminaires, it is important to consider the numerical aperture (NA) and intensity distribution of the in-coupled light including the non-parallel part of the sun beam, as described in Ref. [5]. At the test site, it was noticed that the spatial distribution was wider than expected from the system specs. The specified .ldt files had been defined through measurements with a goniophotometer using an artificial light as the light source. In order to get the relevant and meaningful output distribution for the fiber luminaires, we used the light provided by the solar collector of the SP3 system itself into the fibers. The light distribution from the fiber luminaires were measured at the work plane (85 cm above floor and 155 cm from the luminaire), starting at nadir and in steps of 5 cm linearly away from nadir. The light output was considered symmetrical around its vertical axis, which is not entirely true, since the luminaire is a bundle of six pentagonally arranged fibers. The measured distribution was converted to match the format used in the .ldt-files using the photometric distance law [10-11]. The simulated lighting conditions with the old and new .ldt-files were compared with the measured illuminance distributions over the entire test site under varied sun light conditions [2-3, 5].

Energy savings

The consumed electric energy for all the test equipment including the solar light system, sensors, web logger and fluorescent lighting, as well as the direct sun illuminance outside and the temperatures in several locations of the test site were continuously monitored every 10 seconds for several months. The energy savings were calculated from the measured data and by using the information of the annual sunny hours for the locations of interest: Uppsala, Stockholm, Italy and Dubai, as described in Refs. [2-5].

RESULTS

The illuminance with the solar lights was at least as high as when using the artificial lights and even higher at very clear sunny days (Fig. 2). The luminous flux output was 500 lm per luminaire at 100 000 lx direct sun illuminance and at 130 000 lx it was 770 lm per luminaire for a 10 m fiber distance. However, for a 20 m SP3 system the luminous flux output (400 lm per luminaire) at 100 000 lx was higher than specified (350 lm).

The illuminance is highest at the nadir location under the fiber luminaires (Fig. 2), and

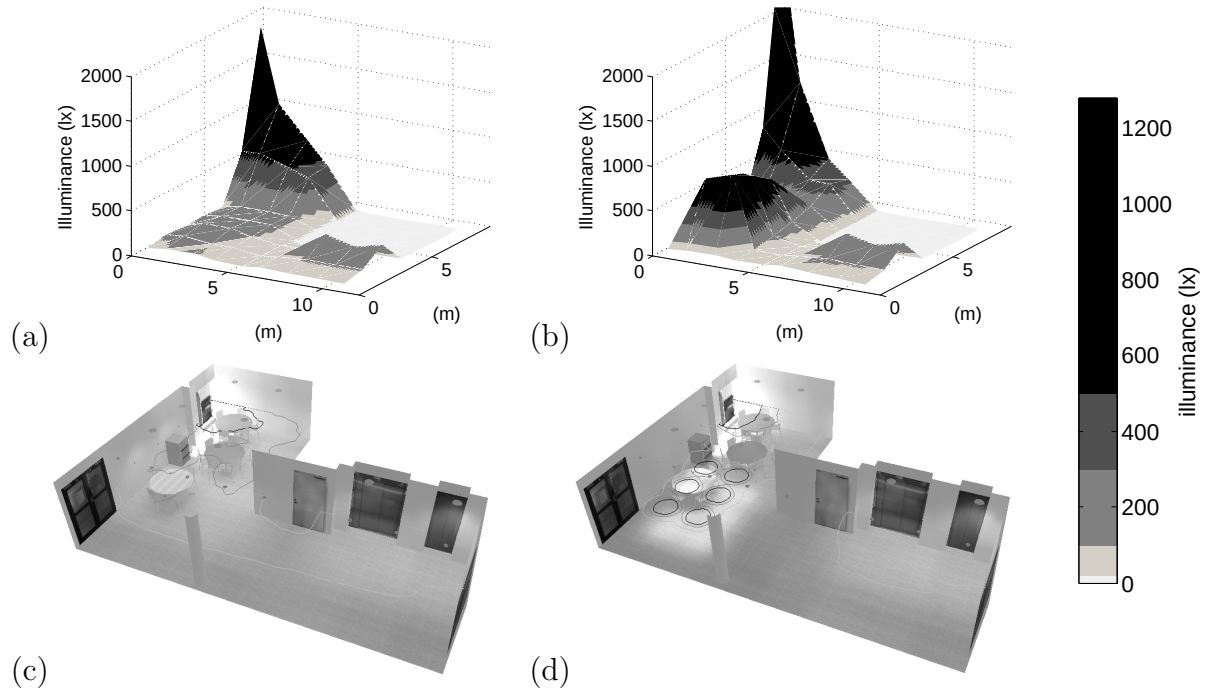

Figure 2: The measured (a-b) and simulated (c-d) illumination scenes at 85 cm distance from the floor for the test site during two different sunshine conditions.

the light spread-out could have been increased. The light distribution, measured as the illuminance at 85 cm above the floor for the 10 m system luminaires, is shown in Fig. 3. The polar diagram for the improved .ldt-file is shown in Fig. 3(c). The simulated illumination schemes shown in Fig. 2 (c-d), corresponding to the sunlight conditions of Fig. 2 cases, are calculated by using the new distribution data file. They match well with the measured data.

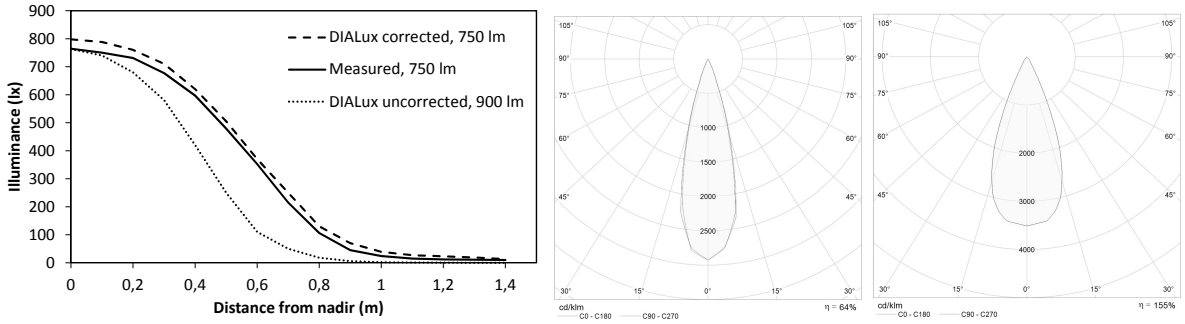

Figure 3: (a) The measured and the for DIALux fitted illuminance distributions under a fiber luminaire. The (b) old and (c) new polar light diagrams for the bare fiber luminaires of SP3.

The SP3 system provides high quality solar light of almost full visible spectrum, close to the spectrum of the sun. The spectrum of the fluorescent lights at the test site consists of a few narrow peaks. The correlated color temperature of the light from the SP3 system was 5800 ± 300 K and the color rendering index 85 at the 10 m fiber distance. The corresponding values for the fluorescent lights of the test site are 3180 K and 77

respectively, and for the sunlight outside 6500 K and 98. Thus the quality of the solar light is high and the visibility of details and color nuances is improved because of the fuller spectrum compared to the fluorescent lights.

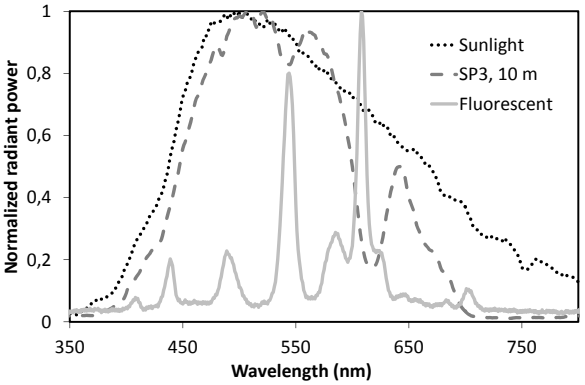

(a)

Light source	T_c (K)	R_a (0-100)
SP3, 10 m	5800±300	84.9±0.5
SP3, 20 m	7000±300	74.5±0.3
Fluorescent	3180±10	76.9±0.1
Sunlight	6500	98

(b)

Figure 4: (a) The spectra of sunlight and the SP3 fiber luminaires (10 m) for 125 000 direct sun illuminance. Also the spectrum of the fluorescent light source. (b) The color rendering index (Ra) and the color temperature (Tc) for the light sources in (a).

The lighting energy saved due to decreased need for artificial light was estimated in the study hall - corridor interior to 19 % in Uppsala [2-3]. There are 1790 annual sunny hours in Uppsala. The saving is calculated for 13 h usage time during the holiday free week days. The savings in a similar type of interior in Italy, where 3400 yearly sunny hours are available, is 46 %. Higher savings are achieved in offices, where the electric lights can be switched off instead of dimming down during sunny weather [2-3]. The luminous efficacy of the solar lighting system is thus in the order of 260 - 460 lm/W for the 10 m system, and 200 - 300 lm/W for the 20 m system. These are much higher values than known for commercially available electric light sources. One SP3 system can be used for lighting 6 one-person offices. The test results also suggest that an additional saving, especially in warmer countries, can be obtained due to decreased need for cooling in the building, as the solar luminaires provide negligible heat to the surrounding air. The economical saving could also be realized by improved productivity and well-being of the human beings working under the solar luminaires [2-3, 5].

DISCUSSION

The solar lighting system tested has a new type of sun-tracking solar collector. The daily duration when the system can provide the sunlight, is improved from the earlier version of Parans systems. The solar light output is not any more limited by the sun-tracking function. A limitation is the availability of the direct sunlight, i.e. the weather.

The system was shown in this study to provide abundant luminous flux at direct sun illuminances above 100 000 lx. The direct sun illuminance was measured by the Hagner EX-4 sensor of type SD2 that was fastened on the top of the sun tracker. No tube was used to limit the side light or the numerical aperture of the sun light into the illuminance detector, as automatic measurement set-up and the accurate sun-tracker of the SP3 system were used. The protruding tube attached to the lux detector was tested for several weeks, but it was noticed not to provide any significant improvement. Instead, it caused other

problems because some birds wanted to sit on it, disturbing the tube position. The angular accuracy of the solar tracker was noticed to be good enough to guarantee repeatability better than ± 3 % in the sun illuminance data in the range 20 000 - 140 000 lx. However, it might be the case that our direct sun illuminance data is slightly (a few %) higher than accurately measured data with a side light limiting tube would be.

The other possible inaccuracy may be included in the luminous flux data, measured with the CMIS integrating sphere. The calibration was made with an artificial light source, which had a different spectrum and spatial intensity distribution than the solar light. The light source provided a slightly smaller numerical aperture of the light coupled into the fibers and bundles, than the solar light system SP3 does. However, this fault is estimated to be conservative and small. Thus the luminous flux results shown here are not overestimated.

CONCLUSIONS

The illumination performance and energy savings have been examined for a solar fiber optic lighting system, Parans SP3. Abundant output flux, excellent light quality, significant energy savings and very high luminous efficacy have been obtained under direct solar illuminances above 100 000 lx. The system gives very good light, which is especially suitable as working lighting for human beings and for interiors where artificial lights are used in daytime.

ACKNOWLEDGEMENTS

The Angstrom Material Academy, The "Energihuset" project, Akademiska Hus AB, Bravida, EU FP7 NMP Project Clear-Up, Prof. G. Niklasson, and PhD student A. Mattson are all warmly acknowledged.

REFERENCES

1. Dubois, M-C and Blomsterberg, A.: *Energy saving potential and strategies for electric lighting in future North European, low energy office buildings: A literature review.*. Energy and Buildings (2011), doi:10.1016/j.enbuild.2011.07.001.
2. Lingfors, D: *Illumination properties and energy savings of a solar fiber optic lighting system balanced by artificial lights.* MSc thesis at Uppsala University, (2012).
3. Lingfors, D and Volotinen, T: *Illumination performance and energy saving of a solar fiber optic lighting system.* Shortly to be published in Optics Express, (2013).
4. Volotinen, T, Nilsson, N, Johansson, D, Widen, J and Krauchi, Ph: *Solar fibre optic lights -daylight to office desks and corridors.* Proceedings CISBAT2011, 491-496 (2011).
5. Volotinen, T and Lingfors, D: *Benefits of glass fibers in solar fiber optic lighting systems.* under review for Applied Optics (2013).
6. Edwards, L and Torcellini, P: *A literature review of the effects of natural light on building occupants.* National Renewable Energy Laboratory, Colorado, USA, NREL/TP-550-30769 (2002).
7. Himawari solar fiber optic light systems: *Specification data sheet.* http://www.himawari-net.co.jp.
8. Parans Solar Ligting AB: *Specification data sheet.* www.parans.com/products.
9. McCamy, C S: *Correlated color temperature as an explicit function of chromaticity coordinates.* Color Research Application **17** (2), 142-144 (1992).
10. CIE Technical report 70-1987: *The Measurement of Absolute Luminous Intensity Distributions.* Photocopy 2008, Vienna, Austria.
11. Ashdown, I: *Thinking photometrically, part II.* Lightfair 2001 Pre-Conference Workshop.

RESULTS FROM A PARAMETRIC STUDY TO ASSESS THE DAYLIGHT AMOUNT IN ROOMS WITH DIFFERENT ARCHITECTURAL FEATURES

S. Cammarano, V.R.M. Lo Verso, A. Pellegrino, C. Aghemo

Politecnico di Torino, Department of Energy, TEBE Research Group,
Corso Duca degli Abruzzi 24, 10129, Turin, Italy

ABSTRACT

This paper describes the research activity carried out by the Lighting Team of the TEBE Research Group on the daylight availability in interiors. The analysis was done through a parametric study, running a high number of Daysim simulations of a single target room whose architectural features were changed (orientation, window size, room depth and height of an external obstruction). For each case-study, referring to an illuminance of 500 lux and a glazing visible transmittance of 70%, the values of Dynamic Daylight Performance Metrics DDPM and of the energy use for electric lighting (in presence of either a manual on/off switch or a daylight responsive control system) were calculated and the obtained results analyzed to understand how the DDPM and energy demand values change as a function of the architectural features. As a next step, to provide an overall representation of the DDPM results for all simulated case-studies, a graphical tool was developed. The tool was intended to be used by the design team since the earliest design stages to quickly verify the influence of preliminary design solutions on daylight amount. As a further step, which is currently in progress, a set of mathematical models are being developed to predict the daylight availability within a space or the corresponding energy demand for lighting. New sets of simulations were run for this purpose so as to expand the database including more latitudes, illuminance levels and glazing visible transmittances. The final step will deal with the implementation of the models into an interactive software that will allow practitioners getting DDPM and lighting energy demand values by directly inputting the site, spaces architectural features and illuminance threshold. The different steps of the research, the main results which have been obtained during each step and the future developments are described in the paper.

Keywords: Daylight amount, Dynamic Daylight Performance Metrics, room architectural features, tools for early daylighting design stage.

INTRODUCTION

The importance of skylight and sunlight for both building energy performance and ambient quality implies the need for a more accurate design approach which takes into account the dynamic behaviour of daylight. Within this frame, taking advantage of the potentials of a Climate Based Daylighting Modeling (CBDM) and DDPM [1], a research is being carried out at the Politecnico of Turin (Italy), to provide architects and building engineers with information and tools to quickly estimate, since the earliest design stages, the indoor daylighting and the related electric lighting energy demand. The paper has the objective of presenting the research activity carried out during the last years as well as the remaining part of the work which is still ongoing. In particular some basic results about how architectural features influences the daylight amount in a room and how to convert the huge database of results obtained from the parametric study into simple tools to be used during the early daylighting design stages are presented**.**

METHOD

The analysis of the daylight amount within a considered space as well as of the related energy demand for lighting has gone through the following phases.

As a first step, the parameters influencing the daylight amount within a space and its related electric lighting energy need were identified and the daylighting conditions were analyzed by estimating, through simulations, the values of DDPM (Daylight Autonomy, Continuous Daylight Autonomy, Maximum Daylight Autonomy, Useful Daylight Illuminance, Annual Light Exposure) and of the annual energy need for several configurations of a target room. Daysim, a Radiance-based software that calculates daylight through a dynamic climate-based annual simulation, was used for this purpose. A single room was used as 'case study'. Its width, height and reflection properties were kept constant (width: 12 m; height: 3 m; reflectances: 80% for the ceiling, 50% for the walls, 30% for the floor), as well as the glazing visible transmittance (set to 70%) while other parameters were changed to assess their influence on the space's daylighting, namely: room depth, RD (assumed equal to 3, 4.5, 6, 7.5, 9, 10.5 and 12 m); window area, expressed in terms of window-to-wall ratio, WWR (0.6, 0.5, 0.4, 0.3, 0.2); obstruction angle 'seen' by the window, γ (0°, 15°, 30°, 45°, 60°, 75°); orientation (south, west, north). For south-facing rooms both the absence and the presence of a moveable shading system was modelled (a Venetian blind with a diffuse transmittance of 25%, when closed, automatically pulled down whenever an irradiance of 50 W/m^2 hits any point of the working plane, this latter set at a distance of 75 cm from the floor and covering the whole room minus a peripheral strip of 50 cm). During this phase, all rooms were assumed to be located in Turin (Italy, latitude: +45.2°N), continuously occupied Monday through Friday from 8:30 a.m. to 6:30 p.m, and considering a target illuminance of 500 lux. The database of results was then analyzed to understand how the DDPM change as a function of the architectural features. Some considerations are presented in the section 'Results'.

As a later step, with regard to DDPM values, a graphical tool was developed to visualize the huge database of data and thus to allow an immediate reading of daylight conditions within the considered room, without consulting the full database of numerical values from Daysim simulations. The tool is conceived to be used by the design team since the earliest design stages in two possible ways: either to predict the daylight availability for a particular combination of architectural features for the considered room or to identify which combinations of architectural features would correspond to specific classes or thresholds of daylighting performance. The tool is briefly described in the section 'Results'.

As a further development, currently in progress, a set of mathematical models are being developed to predict during the earliest design stages on the one hand the daylight availability within a space as a function of its architectural features and on the other hand the corresponding energy demand for lighting. For this purpose, further simulations were run to expand the database including more latitudes, illuminances and glazing visible transmittances.

The final step of the research will deal with the implementation of the databases into an interactive software that will allow practitioners to get DDPM and lighting energy demand values by directly inputting the spaces architectural features, site and illuminance threshold.

RESULTS

Variation of daylight availability depending on room architectural features

In this section, a synthesis of results concerning the influence on daylight availability of varying room features is presented.

The results shown in the following graphs are expressed in terms of Annual Light Exposure (ALE), to describe the cumulative amount of daylight on the horizontal plane over the course of a year [Mlxh], Daylight Autonomy (DA), to assess the percentage of the occupied times of the year when the illuminance requirement is met by daylight alone [%] and Maximum Daylight Autonomy (DA_{max}), to account for the occurrence of potentially glary conditions during the year [%]. Results are presented to analyze the effect of each variable (orientation, RD, WWR and γ) on daylight availability. For the orientation, data are referred to unobstructed spaces (γ= 0°), considering all RD and WWR, while for room depth, WWR and external obstructions data are referred to rooms facing north and south (this latter with blinds).

Effect of orientation (Figure 1)

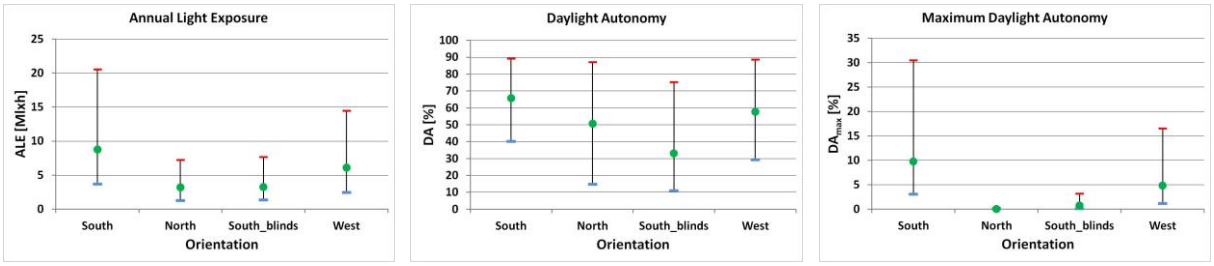

Figure 1: ALE, DA and DA_{max} ranges (maximum, minimum and mean values) as a function of orientation.

The daylight availability is higher for south-facing rooms without blinds (ALE_m= 8.7 Mlxh) compared to west-facing (ALE_m= 6.1 Mlxh) and north-facing rooms (ALE_m= 3.2 Mlxh), while ALE values are similar for south-facing rooms with blinds and north-facing rooms, in terms of both mean values and range of variation. If the daylight availability within the space is evaluated in terms of Daylight Autonomy, results are slightly different. South-facing rooms still have higher values (DA_m= 65.7%) than west-facing (DA_m= 57.7%) and north-facing rooms (DA_m= 50.6%). However the DA_m value for south-facing rooms with blinds drops to 33% (lower than north-facing rooms). As for potentially glary conditions (expressed through DA_{max} metric), north-facing rooms have lower values ($DA_{max,m}$= 0.03%) than south-facing rooms with blinds ($DA_{max,m}$= 0.8%), west-facing rooms ($DA_{max,m}$= 4.8%) and south-facing rooms without blinds ($DA_{max,m}$= 9.8%). In the latter two cases the range is very wide, with maximum values of 16.5% and 30.5%.

Some considerations can be drawn from these results: a) high daylight amount mainly occurs for south-facing and west-facing rooms. At the same time, if blinds are not used, glare and overheating may occur, as expected and already stated in other studies [2]; b) daylighting performance is better for north than for south-facing rooms with blinds. For both orientation the risk of glare is low but DA values are higher for north rooms which may result in a lower lighting energy demand.

Effect of room depth, RD (Figure 2)

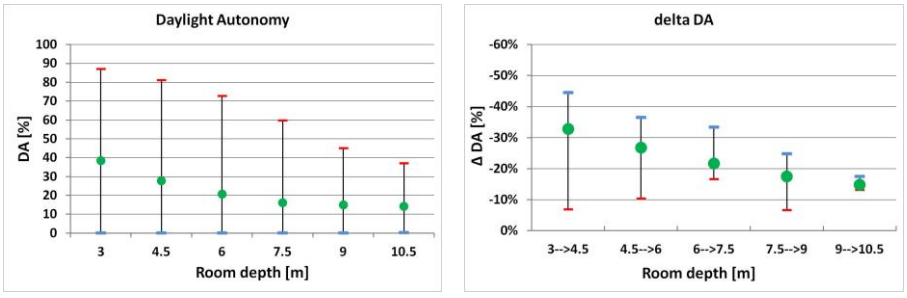

Figure 2: DA (maximum, minimum and mean values) and ΔDA ranges as a function of RD.

Increasing the room depth results in a decrease of DA and the DA reduction appears to be greater for small and medium RD (the average percent difference when increasing room depth from 3 m to 4.5 m and from 4.5 m to 6 m is ΔDA_m= -30%) than for RD over 6 m (ΔDA_m= -18%). These results are consistent with what shown in [2].

Effect of Window-to-Wall Ratio, WWR (Figure 3)

Increasing the WWR results in an increase of DA, higher passing from WWR 0.3 to 0.4 (ΔDA_m = 61%), than passing from WWR 0.4 to 0.5 (ΔDA_m = 30%) and from WWR 0.5 to 0.6 (ΔDA_m = 21%).

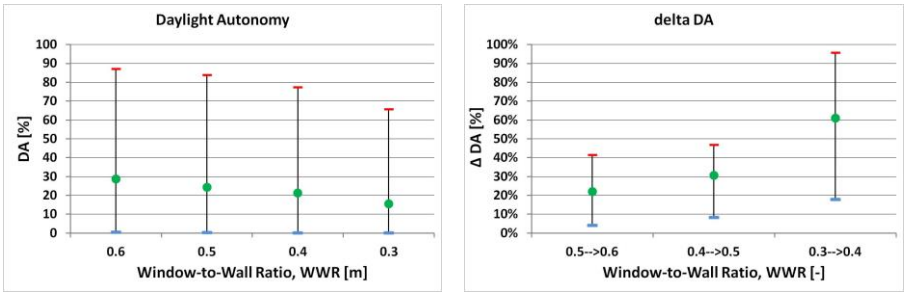

Figure 3: DA (maximum, minimum and mean values) and ΔDA ranges as a function of WWR.

Effect of external obstructions, γ (Figure 4)

Increasing the obstruction angle results in a linear decrease of DA_m. The DA range for γ between 0° and 30° is wider (6%<DA<87.2%) than for γ over 45°. The DA decrease is lower for γ between 0° and 30° (ΔDA_m = -25%), than for γ over 30° (ΔDA_m = -49%).

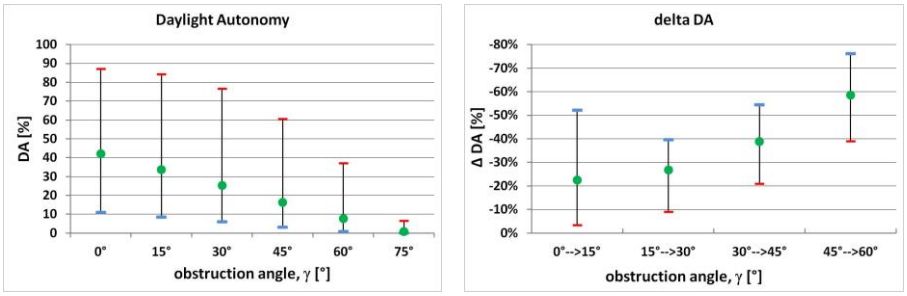

Figure 4: DA (maximum, minimum and mean values) and ΔDA ranges as a function of γ.

Graphs and data presented above are representative of the range of results obtained from a large number of room's configurations (all WWR, RD, γ, and for north and south with blind orientation). The information achievable from this data are quite general and self-evident, while to have more detailed information a different approch in representing the whole database of result should be used.

A graphical tool to express the daylighting performance depending on room architectural characteristics

Figure 5 shows the rationale on which a graphical tool to present the results of the parametric study was developed; it represents all variables involved in the study: room depth (on the x-axis), obstruction angle (on the y-axis) and WWR, from 0.6 to 0.3 (represented by side-by-side circles for each room depth and obstruction angle). The circles' diameter is proportional to the metric absolute value and the colour shows the interval in which the metric value lies. The possible scale of values of each DDPM (0-100%) was divided into five ranges (<20%; 20-40%; 40-60%; 60-80%; >80%). This type of tool can be used by professionals to quickly

verify the influence of preliminary design solutions on daylight availability within the room, identifying the daylighting performance of a specific room's configuration or for which combination of the room architectural features the corresponding daylighting performance will be above or below target values, that might be user-defined or, in the future, set by recommendations and standards. In a past paper three classes of performance, in terms of daylight quantity, were assumed by the authors: "low" (DA≤40%), "acceptable" (40%<DA<60%) and "high" amount (DA≥60%) [3]. By defining ranges of performance, practitioners can quickly verify, on the tool, which are the combinations in terms of architectural features able to provide high, acceptable or low daylight amount within a room.

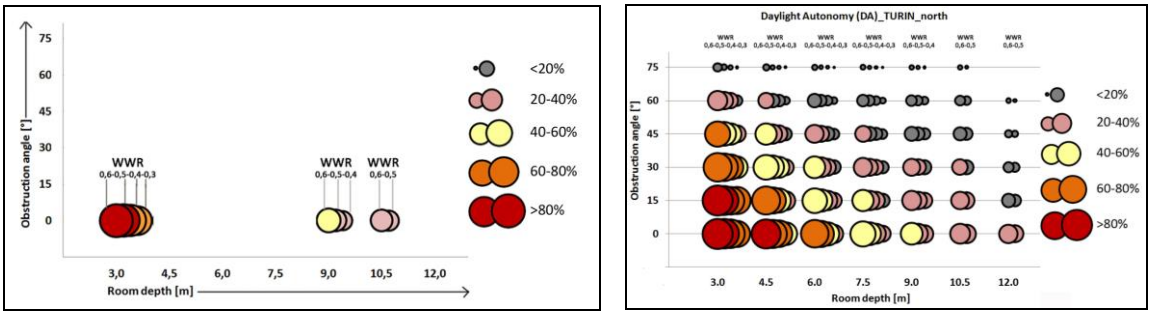

Figure 5: Schematic representation of the format of the graphical tool which was developed to visualize the daylighting conditions within the rooms as a function of the variation of their architectural features.

Figure 6 highlights the combinations of the examined architectural features which fell within the three performance classes considering both north and south (with blinds)-facing rooms.

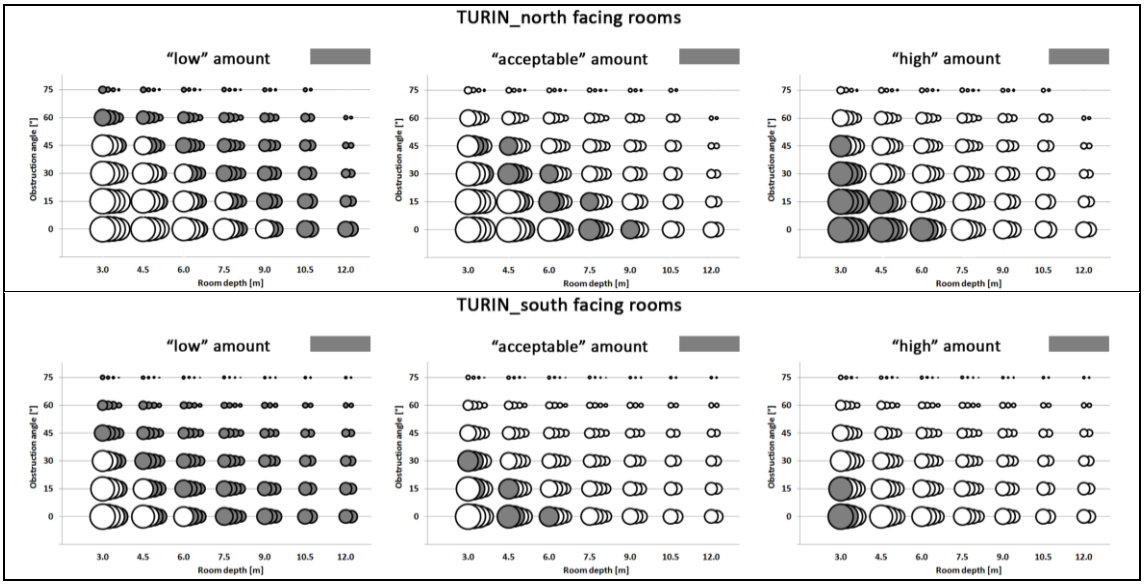

Figure 6: Combination of architectural features falling into the daylight performance classes (case-studies: north/south-facing rooms in Turin; τ_{vis}=70%; E_{target}=500 lx).

Development of a set of mathematical models for the earliest design stages

The developed graphical tool presents some limitations: first of all, it visualizes the results of DDPM for a restricted number of configurations, relative to spaces in Turin, with a τ_{vis} of 70% and in which activities requiring an illuminance of 500 lux are carried out. Moreover, the DDPM data are given in ranges, which implies that rooms with different characteristics might result in the same range. In order to overcome these limitations, a set of mathematical models

are being derived from the database to link the daylight availability within the considered space (in terms of DDPM values) or the lighting energy demand to the space architectural features and, for the energy demand values, to the installed control systems and lighting power densities. For this purpose, new sets of simulations were run to expand the databases including more sites (Catania, Italy, latitude: +38.3°; Berlin, latitude: 52.3°N), target illuminances (E = 150, 300, 750 lux) and glazing visible transmittances (τ_{vis} = 90%, 50%, 35%). The definition of the mathematical models in their final version is underway, in particular with regard to the testing and validation phase. Some first results were presented in [4], concerning a multivariate non-linear regression model for the lighting energy demand.

DISCUSSION AND CONCLUSION

The huge research activity presented in this paper does not cover every possible site or building configuration, but it still makes available a set of information, graphical tools or equations that can be useful to inform the design team on the impact of their architectural choices on both the DDPM values for the considered space and on the energy demand for lighting during the very first stages of the building design process, when the use of simulation tools for more detailed calculation is still premature. According to the authors' intent, designers are assisted in crucial decisions concerning the window and the room sizing and under which conditions the choice of a daylight responsive control system is worthwhile: for instance, for a given urban settings (for which room obstruction angles are known), designers can find out how room depth and window area influence the room energy performance; or, the other way around, they can size window and room geometry so as to guarantee a desired value of DDPM values or energy demand for lighting.

On the other hand, it's worth noting how the proposed tools and equations are valid for the assumed boundary conditions (sites, architectural features, building usage and lighting system characteristics, etc.). The daylight availability and the lighting energy demand for the room would vary if, for instance, it would be located in sites with different latitude, or with same latitude but with quite different annual climates or if it would have a different use (in terms of illuminance, occupation profile or user behaviour) or a different type of lighting and control system or if the blind would have different characteristics. Furthermore, the results are based on the use of Daysim as tool to run annual climate based daylight/electric lighting simulations. Again, if a tool other than Daysim was used to complete the parametric study, the result database would change and so would the graphical tool and the mathematical models. Anyway, the considered variables cover a wide range of possible scenarios and the obtained models represent an effective starting point in the direction of providing designers with easy to use tools for the early stages of the design process.

REFERENCES

1. Reinhart, CF, Mardaljevic, J, Rogers, Z: Dynamic daylight performance metrics for sustainable building design. Leukos. 2006. 3 (1): 1-25.
2. Dubois, MC, Flodberg, K: Daylight utilization in perimeter office rooms at high latitudes: investigation by computer simulation. Lighting Res. Technol. 2013. 45: 52-75.
3. Pellegrino, A, Lo Verso, VRM, Cammarano, S, Aghemo, C: A climate-based graphical tool to predict the daylight availability within a room at the earliest design stage. Proc. of CIE Centenary Conference, Paris, France, April, 15-16, 2013.
4. Aghemo, C, Lo Verso, VRM, Pellegrino, A, Pellerey, F: Prediction of energy demand for lighting in buildings with different architectural features. Proc. of COBEE, pp 152-159, Boulder, Colorado, USA, August 1-4, 2012.

EXPERIMENTAL STUDY OF DAYLIGHT SPECTRAL FILTERS INFLUENCE ON CIRCADIAN STIMULUS IN THE SIDELIT INDOOR SPACES

L. Mankova[1]; P. Hanuliak[1]; P. Hartman[1]; J. Hraska[1]

1: Slovak University of Technology, Radlinskeho 11, 813 68 Bratislava, Slovakia

ABSTRACT

Daylight is the primary stimulus for synchronizing the human circadian photobiological system. Deficiency of daylight or its spectral anomaly in indoor environments is related to several health problems such as hormonal unbalance, sleep disorder, depression and so on. Permanent spectral filters in windows can modify full daylight spectrum in a large amount. Colours of interior and external finishing, shading devices, curtains and other materials and surfaces can also contribute to the modification of indoor daylight spectral composition. So, it is obvious that the daylight in a room is spectrally filtered. Different spectral filters were monitored and statistically processed in dependence on photopic and circadian daylight data measured under real climate conditions. Some glazing systems, for example tinted glazing or some foils, can change daylight spectrum and circadian stimulus distinctly.

Keywords: daylighting, glazing, spectral filters, circadian stimulus

INTRODUCTION

For a long time in the scientific field increased attention has been paid to non-visual effects of light on the human body. Discoveries of circadian rhythm mechanisms in human body [1 - 3] increased the interest of non-visual lighting in technical and professional public. Traditional parameters and criterions based explicitly on photopic vision are being critically re-evaluated. Basic principles of circadian photometry have been developed in theoretical level. It is well known, that the impact of lighting environment on vision, physiological and psychological processes in human body significantly differs in term of light intensity and spectrum, time and directional effect. Despite a number of studies focused on non-visual impact of light on human health, still many questions remain and it will take some more time to apply this issue into technical standards and design practice. This paper deals with the influence of daylight spectral filters on circadian stimulus defined in [4]. In general daylight is considered to be a healthy light, practically from all points of view. In fact daylight in interiors could considerably differ to daylight in exteriors, mainly in term of intensity and spectral composition. These values define circadian stimulus, which was experimentally monitored in scaled room models with side windows placed under real climate conditions.

METHOD

Circadian stimulus

There are fundamental differences between responses of the visual and circadian human systems to optical radiation. Rea et al. [4] proposed a mathematical model for quantifying circadian light for any spectral irradiance distribution. Subsequently a device named Daysimeter [5] was developed in Rensselaer Polytechnic Institute in the USA. This device was used for measurements of specific light levels in our research.

The Daysimeter is an electronic device, which process the data from two independent sensoric systems as an input for a circadian stimulus [CS] calculation, which is described in a mathematical model for description of human circadian phototransduction, proposed by Rea, et. al. [4]. Because the amount of light entering the eye is the most important for circadian entrainment, circadian stimulus was monitored by Daysimeters on a vertical plane at eye level (1.20 m), imitating a person sitting by the work desk facing the window at a distance 3 m from the window.

Circadian action spectrum function *C(λ)* used in graphs (Fig. 2-4) was determined in this paper by [6], where the maximum of *C(λ)* is set as 100 % at 450 nm. Evaluation of circadian properties in environment, in particular it is the circadian transmittance of transparent materials and circadian reflectance of surfaces, can be expressed using this action spectrum (1).

$$\tau_c = \frac{\sum_{\lambda=380nm}^{580nm} D_\lambda . \tau(\lambda) . C(\lambda) . \Delta\lambda}{\sum_{\lambda=380nm}^{580nm} D_\lambda . C(\lambda) . \Delta\lambda} \quad (1)$$

Where D_λ is relative spectral distribution of the light source D_{65}; $\tau(\lambda)$ is spectral transmittance of glazing system; $C(\lambda)$ is action spectrum of melatonin production suppression in humans; $\Delta\lambda$ is range of wavelength.

Experimental rooms and measuring devices

The influence of spectral filters of daylight was measured in two scaled models of rooms, see Fig. 1. These models were constructed in a scale 1:5 and represent real office room with internal dimensions 3 × 3 × 9 m, while the size of the window is 2 × 1.5 m with a sill in 1m distance from a floor. Windows of both models were equipped by a simple, clear glazing with a thickness of 4 mm and models were placed on a roof of the Slovak University of Technology in the centre of Bratislava (Slovakia) while windows were facing east. During the measurement two office models were used. Model room A – a reference room was equipped with neutral matt internal surfaces and clear glazing at the window. The alternations were made in the modified room B – where particular components were changed in every course of measurements. Several types of glazing, shading curtains and wallpapers were used in modified room to change the spectral composition of the light in internal space of a model

Figure 1: The view of two models, reference room (left) and modified room (right)

office. Spectral transmittance and reflectance of light through glazing, shading curtains and wallpapers were measured by spectrophotometer Konica Minolta CM-5. Horizontal and vertical external illuminance was measured by standard luxmeters (LI-COR photometric sensors LI-210SA).

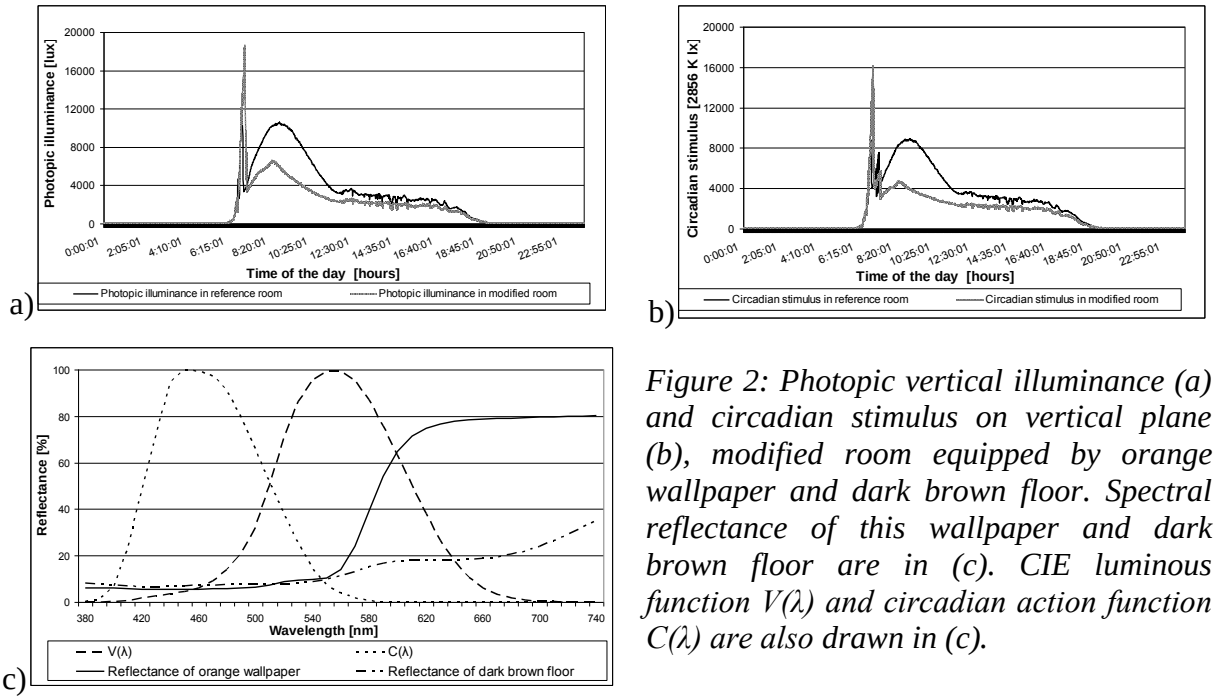

Figure 2: Photopic vertical illuminance (a) and circadian stimulus on vertical plane (b), modified room equipped by orange wallpaper and dark brown floor. Spectral reflectance of this wallpaper and dark brown floor are in (c). CIE luminous function V(λ) and circadian action function C(λ) are also drawn in (c).

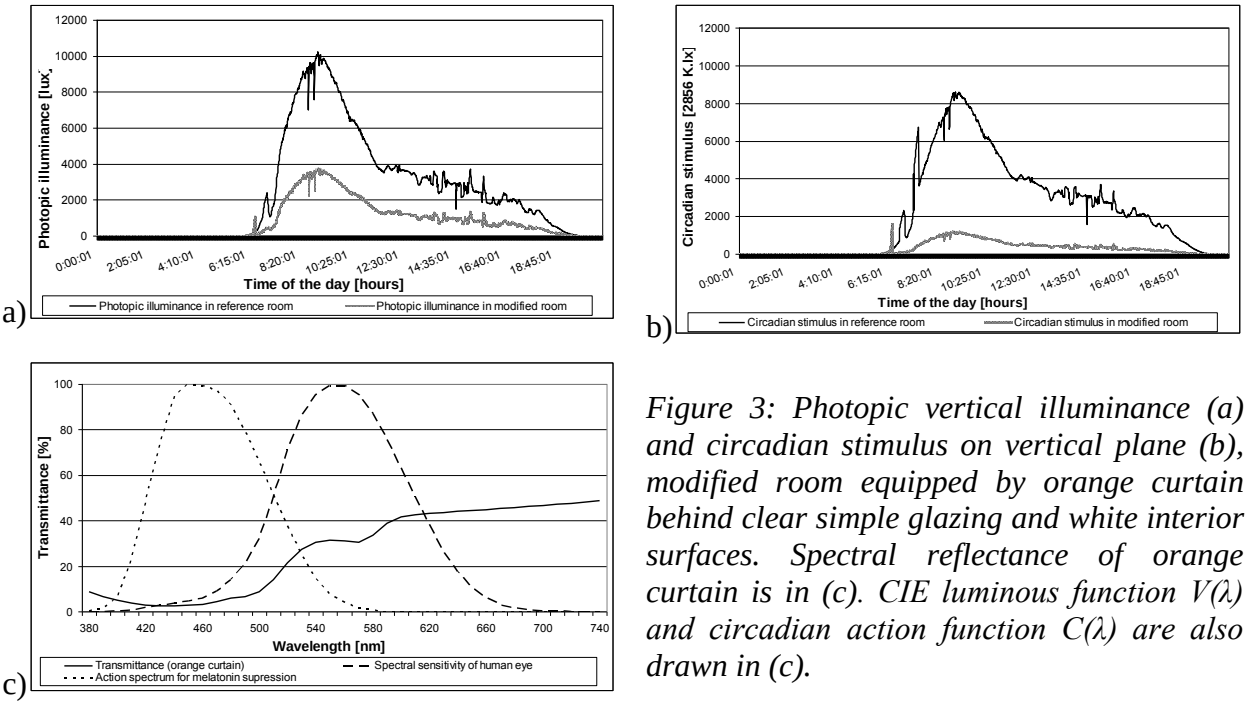

Figure 3: Photopic vertical illuminance (a) and circadian stimulus on vertical plane (b), modified room equipped by orange curtain behind clear simple glazing and white interior surfaces. Spectral reflectance of orange curtain is in (c). CIE luminous function V(λ) and circadian action function C(λ) are also drawn in (c).

RESULTS

Measurements were made during 8th, 9th and 10th April 2013 when the sky was partly cloudy. Results of photopic illuminance and levels of circadian stimulus are presented in Fig. 2, 3, 4.

In the Fig. 2 spectral filter in modified room was represented by orange wallpapers in combination with dark brown floor, while the ceiling stayed white.

In the Fig. 3 orange shading curtain and simple clear glazing were used in modified room. Transmittance of light through the curtain was relatively low (Fig. 3c), but stayed very low in the range of blue spectrum. These facts are expressed by very low levels of circadian stimulus in the modified room. In the Fig 4 spectral filter was made by orange foil on a simple clear glazing in modified room.

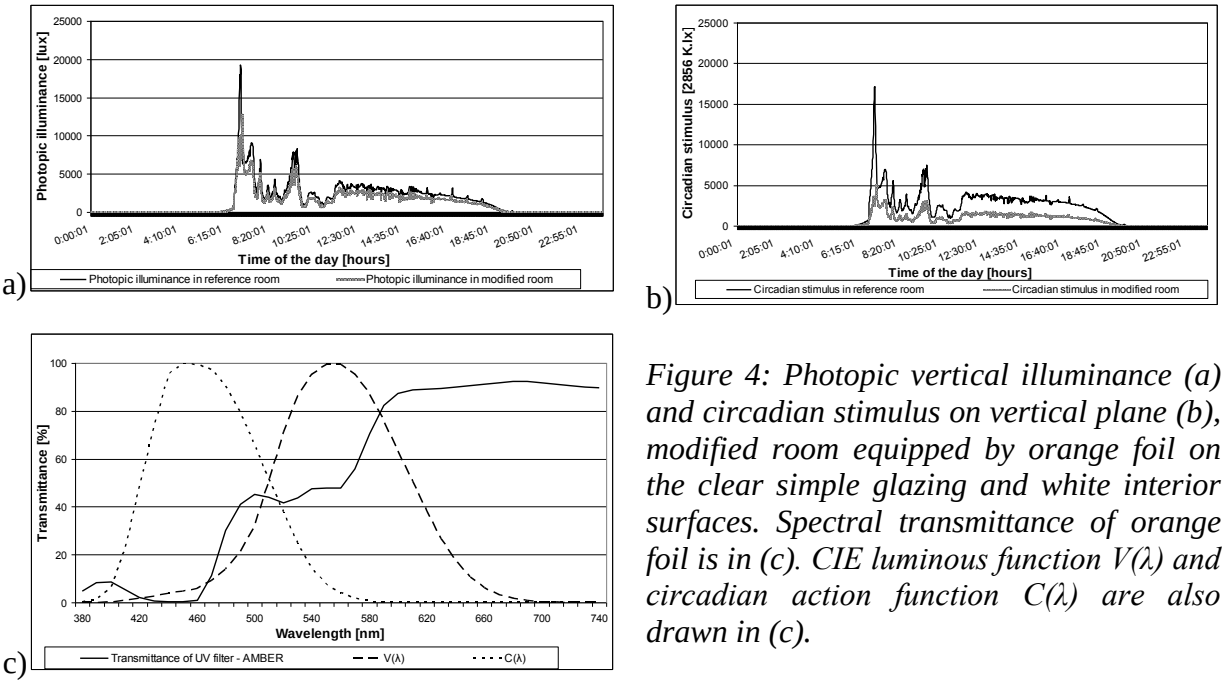

Figure 4: Photopic vertical illuminance (a) and circadian stimulus on vertical plane (b), modified room equipped by orange foil on the clear simple glazing and white interior surfaces. Spectral transmittance of orange foil is in (c). CIE luminous function V(λ) and circadian action function C(λ) are also drawn in (c).

Ratios	**Orange wallpaper on the walls**	**Orange curtain**	**Orange foil**
Ratio of photopic illuminance in the modified room to the illuminance in the reference room	0.69	0.35	0.74
Ratio of circadian stimulus in the modified room to the circadian stimulus in the reference room	0.65	0.13	0.39

Table 1: The ratios of the vertical photopic illuminances and circadian stimulus in the room with a spectral filter to the reference, i.e. spectrally neutral, room.

The comparison of ratios of vertical photopic values of illuminance and circadian stimulus in reference room to the values measured in the room modified by spectral filters is presented in Table 1. These data clearly point out, that measured photopic illuminance cannot be directly used to determine the impact of spectral filter on the levels of circadian stimulus.
Photopic and circadian transmittance and reflectance of spectral filters installed in modified room are presented in Table 2.

Sample	**Day**	**Photopic reflectance ρ_v [-]**	**Circadian reflectance ρ_c [-]**
Orange wallpaper	8.4.2013	0.271	0.062
Dark brown floor	8.- 10.4.2013	0.118	0.074
Sample	**Day**	**Photopic transmittance τ_v [-]**	**Circadian transmittance τ_c [-]**
Orange curtain	9.4.2013	0.29	0.07
Orange foil	10.4.2013	0.57	0.18

Table 2: Measured values of transmittance and reflectance by $V_{(\lambda)}$, $C_{(\lambda)}$. Standard light source represented by D_{65} was used.

It should be noted that particular spectral filters were measured by spectrophotometer with a light source D_{65} with intensity of 1000 lx. This laboratory conditions cannot be compared to data measured under the real clear sky conditions with variable spectral composition and with the intensity of 70000 lx. As the results point out, levels of circadian stimulus is not directly proportional to the values of circadian transmittance of the materials used in the model. The reason is probably, that spectral composition of daylight is significantly different to a spectral composition of light source D_{65} and also the CS values from Daysimeter rely not only on the sensor recording short wavelengths of light, but also on the input from the photopic sensor, while circadian transmittance was calculated only using $C(\lambda)$.

DISCUSSION

The results of measurements, presented above, point out the impact of spectral daylight filters on circadian stimulus in internal building environment. This impact cannot be neglected because non-visual influence of daylight on human is obvious. Table 1 shows that vertical photopic illuminance is modified by spectral filters in considerably different ratios than circadian stimulus. In this study we used orange spectral filters, which significantly influence mostly the blue part of the light spectrum, which is the most capable for circadian entrainment. Circadian properties of internal environment cannot be directly and sufficiently derived from photopic parameters based on a photopic vision. Daylight environment quantification based on circadian photometry would enable the evaluation of „circadian potential“ of spaces. In theory, the basics of circadian photometry are already in progress (e. g. 7). However, the question is, whether current scientific knowledge could provide sufficient and proven basis for the introduction of circadian photometry. This relates with a current lack of standards and design guidelines for the evaluation of circadian parameters of space in general practice. As the first approach to this, the relation between the photometric and circadian effect of a light source, which is given by the circadian action factor a_{cv} [8], is used.

In practical terms, the presented results of measurements are applicable to avoid the use of strong spectral filters in spaces, where it is important to maintain the circadian quality of architectural environment. This is particularly the interior spaces with a long-term stay of elderly, hospital rooms, etc. In these spaces we strongly recommend spectrally neutral glazing with high light transmittance and the use of spectral neutral surfaces and shading devices.

ACKNOWLEDGEMENTS

This article was supported by Slovak Research and Development Agency under the contract No. APVV 0150-10.

REFERENCES

1. Brainard, G. C., Hanifin, J. P., Greeson, J. M., Byrne, B., Glickman, G., Gerner, E., et al. Action spectrum for melatonin regulation in humans: evidence for a novel circadian photoreceptor, Journal of Neuroscience, 2001, 21 (16), 6405-6012.
2. Thapan, K., Arendt, J., Skene, D. J. An action spectrum for melatonin suppression: evidence for a novel non-rod, non-cone photoreceptor system in humans, Journal of Physiology, 2001, 535 (1), 261-267.
3. Berson, D. M., Dunn, M. F., Takao, A.: Phototransduction by retinal ganglion cells that set the circadian clock, Science, 2002, 295, p. 1070–1073.
4. Rea, M. S., Figueiro, M. G., Bullough, J. D., Bierman, A.: A model of phototransduction by the human circadian system. Brain Research Reviews, 2005, 50, p. 213-228.
5. Bierman, A., Klein, T. R., Rea, M. S. The Daysimeter: a device for measuring optical radiation as a stimulus for the human circadian system, Measurement Science and Technology, 2005, 16, 2292–2299.
6. DIN V 5031-100 Strahlungsphysik im optischen Bereich und Lichttechnik – Teil 100: Über das Auge vermittelte, nichtvisuelle Wirkung des Lichts auf den Menschen – Größen, Formelzeichen und Wirkungsspektren. Juni 2009. In German.
7. Bellia, L., Bisegna, L. From radiometry to circadian photometry: A theoretical approach, Building and Environment, 2013, 62 (4), 63-68.
8. Gall, D., Lapuente, V.: Beleuchtungsrelevante Aspekte bei der Auswahl eines förderlichen Lampenspektrums, Licht, 2002, vol. 54, no. 7/8, s. 860–871. In German.

DIFFUSE DAYLIGHT AUTONOMY: TOWARDS NEW TARGETS

B. Paule, S. Pantet, J. Boutiller, Ch. Sergent[2], E. Valentin, N. Roy[3]

[1] *Estia SA, Lausanne, Switzerland*
[2] *Saint-Gobain Glass, Paris, France*
[3] *Velux AS, Hørsholm, Denmark*

ABSTRACT

To quantify the building daylighting performance, most standards dealing with environmental quality and energy efficiency, such as LEED, BREAM, CERTIVEA or DGNB, mainly rely on daylight factor values (DF). Besides the fact that this approach is not intuitive, it also does not take into account the orientation nor the localization of the project.

There is a serious need to provide building owners and designers with concrete notions such as the number of hours during which the use of artificial lighting is not necessary and, thus, gives them the opportunity to estimate the energy consumption due to electric lighting, which is key information.

A lot of work was done on this subject within the last decades: CIE charts [1] and Swiss contributions based on diffuse daylight (ASE [2], DIAL-Europe project [3]), developments from Nabil, Mardjalevic and Reinhart based on global daylight [4],[5].

Nevertheless, it appears that, in practice, building professionals actually do not know what are the affordable targets to match. The common sense suggests that the potential for an office building located in the northern part of Germany should dramatically differ from the one of a primary school in Portugal, but information simply does not exist.

This paper focuses on Diffuse Daylight Autonomy (DDA), which excludes the sun contribution and thus, leads to estimate, on an annual basis, the probability that diffuse daylight will help to achieve or exceed the required indoor illuminance.

The outcome of this work is a set of charts allowing building professionals to answer to questions such as:

"*Does a 48% average diffuse daylight autonomy correspond to a "Very Good" daylighting performance for a west-oriented office-room in Paris?*"

METHODOLOGY

Case-studies

We decided to study five typical rooms: Individual office (19 m^2); Medium-size open-office (65 m^2); Classroom (72 m^2); Bedroom (12 m^2); Living room (30 m^2) (see Fig. 1-5).

As far as the purpose of this work is to give target values for DDA, we had to define reference cases-studies with an *upper limit*, corresponding to a "Very high" daylighting performance and a *lower limit* corresponding to a "Very low" daylighting performance. The proposed configurations had also to take into account the objective of thermal performance and to involve a significant portion of opaque façade. In addition, we assumed that all the premises are equipped with outdoor mobile shading devices such as movable blinds or fabric screens.

- ***Upper limit***

We based on our own experience to define typical rooms with "largely but not fully" glazed façades and, for indoor reflection coefficients, a "bright" but not extreme set of values: ρ_{Floor}: 0.30; ρ_{Walls}: 0.60; $\rho_{Ceiling}$: 0.70. The glazing transmittance has been set to 70%, which may correspond to a triple-glazing for northern countries or a double-glazing with solar control for southern countries.

- ***Lower limit***

To simplify the study, we decided that the only difference between "Upper limit" and "Lower Limit" cases-studies would be the global glazed area. For Lower Limit, we took the minimum requirement set by the French regulation [14], which states that the windows should exceed 1/6 of the room surface area (including frame). Figures 1-3 show that to achieve this reduction of the glazed area in the 2 office rooms and the classroom, we have lowered the window's height, which clearly leads to a "poor" daylighting solution.

Individual office 19.3 m²		Upper limit	Lower limit
Room Height: 2.70 m	Frame area: 20 %	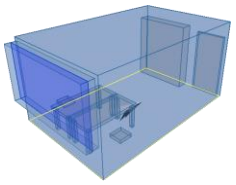	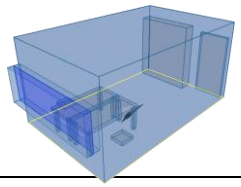
Room Width: 3.50 m	Glazing index "Upper limit": 23 %		
Room Depth: 5.50 m	Glazing index "Lower limit": 14 %		
Wall thickness: 0.35 m	Required illuminance: 500 lux		

Figure 1: Individual office characteristics

Medium-size open-office 65 m²		Upper limit	Lower limit
Room Height: 2.70 m	Frame area: 20 %	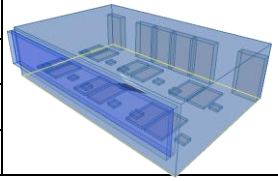	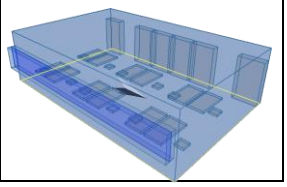
Room Width: 10.00 m	Glazing index "Upper limit": 21 %		
Room Depth: 6.50 m	Glazing index "Lower limit": 13 %		
Wall thickness: 0.35 m	Required illuminance: 500 lux		

Figure 2: Medium size open office characteristics

Classroom 72 m²		Upper limit	Lower limit
Room Height: 3.00 m	Frame area: 20 %	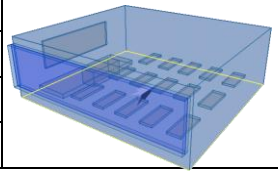	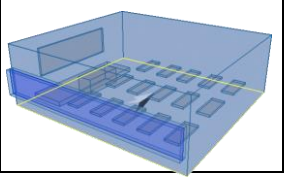
Room Width: 9.00 m	Glazing index "Upper limit": 20 %		
Room Depth: 8.00 m	Glazing index "Lower limit": 12 %		
Wall thickness: 0.35 m	Required illuminance: 500 lux		

Figure 3: Classroom characteristics

Bedroom 12 m²		Upper limit	Lower limit
Room Height: 2.50 m	Frame area: 20 %	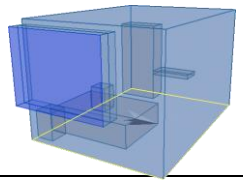	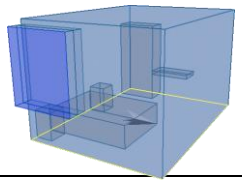
Room Width: 3.00 m	Glazing index "Upper limit": 20 %		
Room Depth: 4.00 m	Glazing index "Lower limit": 13 %		
Wall thickness: 0.40 m	Required illuminance: 300 lux		

Figure 4: Bedroom characteristics

Living-room 30 m²		Upper limit	Lower limit
Room Height: 2.50 m	Frame area: 20 %	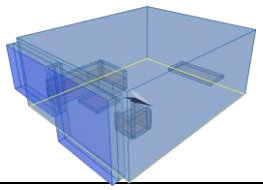	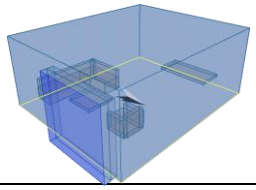
Room Width: 5.00 m	Glazing index "Upper limit": 20 %		
Room Depth: 6.00 m	Glazing index "Lower limit": 13 %		
Wall thickness: 0.40 m	Required illuminance: 300 lux		

Figure 5: Living room characteristics

[Editorial note: for better legibility of these figures please refer to the colour images in the electronic version of the proceedings].

Diffuse daylight autonomy (DDA)

This work is based on simulations made with DIAL+Lighting software [6],[7]. For each configuration, daylight factor values are calculated on the work plane (0.80 m above the floor level) with Radiance [8]. Then, hourly meteo-data from Meteotest [9] are processed using the Perez [10],[11] model in order to calculate:

- The hourly value of outdoor horizontal diffuse illuminance.
- The hourly value of inclined diffuse illuminance.

The diffuse daylight autonomy (DDA), weighed by orientation factors, is then calculated between 8:00AM and 6:00 PM, according to the method described by Paule & al [12],[13] (ground reflection coefficient = 0.10). The results take into account the daylighting saving time due to European summer time.

We decided not to consider an upper threshold for indoor illuminance, as far as we look at diffuse light. Moreover experience shows that if the user moves the blinds down due to an excessive illuminance level, this does not mean that it will switch on the electrical lighting.

This approach has 2 main advantages:

- The first one is linked to the fact that it is based on DF calculation and thus requires short computing time.
- The second one is that it is independent from the type of shading devices and the users behavior regarding visual comfort and glare.

This work looks at the average DDA values for each of the 5 rooms, according to the latitude and the orientation. It is limited to the European zone.

Latitude : We focused this study on the following European cities :
Oslo (N), Stockholm (S), Aberdeen (UK) Copenhagen (DK), Hamburg (D), Berlin (D), London (UK), Paris (F), Geneva (CH), Milano (I), Toulouse (F), Barcelona (SP), Roma (I), Athens (G).

Orientation : Simulations were performed for the 4 cardinal points.

RESULTS

Single office room

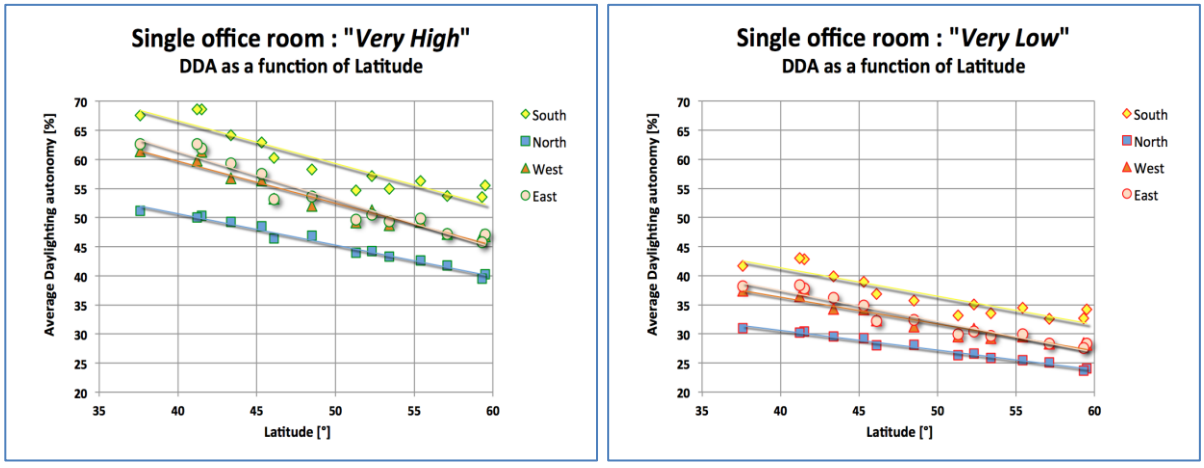

Figure 6: Average DDA for a single office room as a function of the latitude and the orientation. Left: "Very High" daylighting performance; Right: "Very Low" daylighting performance.

Figure ***6*** confirms that, on an annual basis, the diffuse daylighting performance of a given office room highly depends on the location and orientation. On one hand, DDA = 69% in the

Mediterranean area (Roma, south orientation) and, on the other hand, DDA = 39% in Scandinavia (Stockholm, North orientation). Obviously we can not conclude that we should increase the glazed area in Norway, as far as the design this office room is considered as "Very good" from a daylighting point of view.
Nevertheless, this information is useful to understand what are the reasonable targets to reach in terms of diffuse daylight autonomy.

To go one step further, we have used these results to establish performance charts for the five rooms typologies (because of the limited number of pages available for this article, we present here only the results for the individual office and the classroom. The results for other rooms are available at the following web address: www.estia.ch/dial/dda.php.

For each orientation, if the average DDA value is higher than the "Upper limit", we consider that the daylighting performance is "Very High". On the other side, if the average DDA is below the "Lower limit", the daylighting performance of the room is regarded as "Very Low".

In between, we have built 3 intermediate classes : "Good", "Average" and "Low", as described in *Figure 7* hereafter. For example, for a north-oriented individual office located in the Milano area, (latitude 45°) the daylighting performance is considered as :

- "Very Good if the average DDA is above 48%,
- "Good" if the average DDA is somewhere between 42 to 48%,
- "Average" if the average DDA is somewhere between 35 to 42%,
- "Low" if the average DDA is somewhere between 29% to 35%,
- "Very Low" if the average DDA is below 29%.

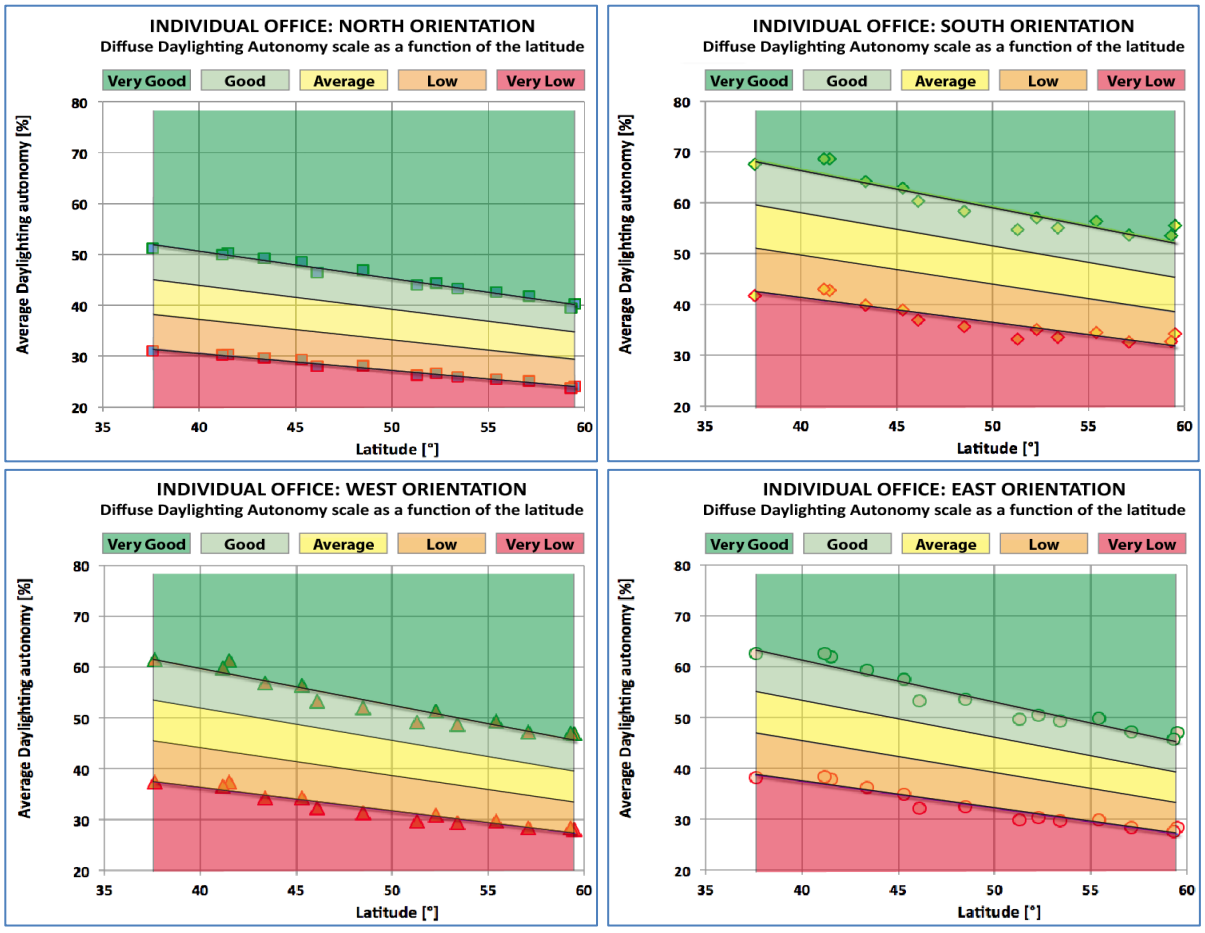

Figure 7: Performance charts characterizing the diffuse daylight autonomy of an Individual office.

Classroom

Furthermore, *Figure **8*** below shows that, for a south-oriented Classroom located in the Copenhagen area, (latitude 55°) the daylighting performance will be considered as :

- "Very Good if the average DDA is above 53%,
- "Good" if the average DDA is somewhere between 45 to 53%,
- "Average" if the average DDA is somewhere between 37 to 45%,
- "Low" if the average DDA is somewhere between 29% to 37%,
- "Very Low" if the average DDA is below 29%.

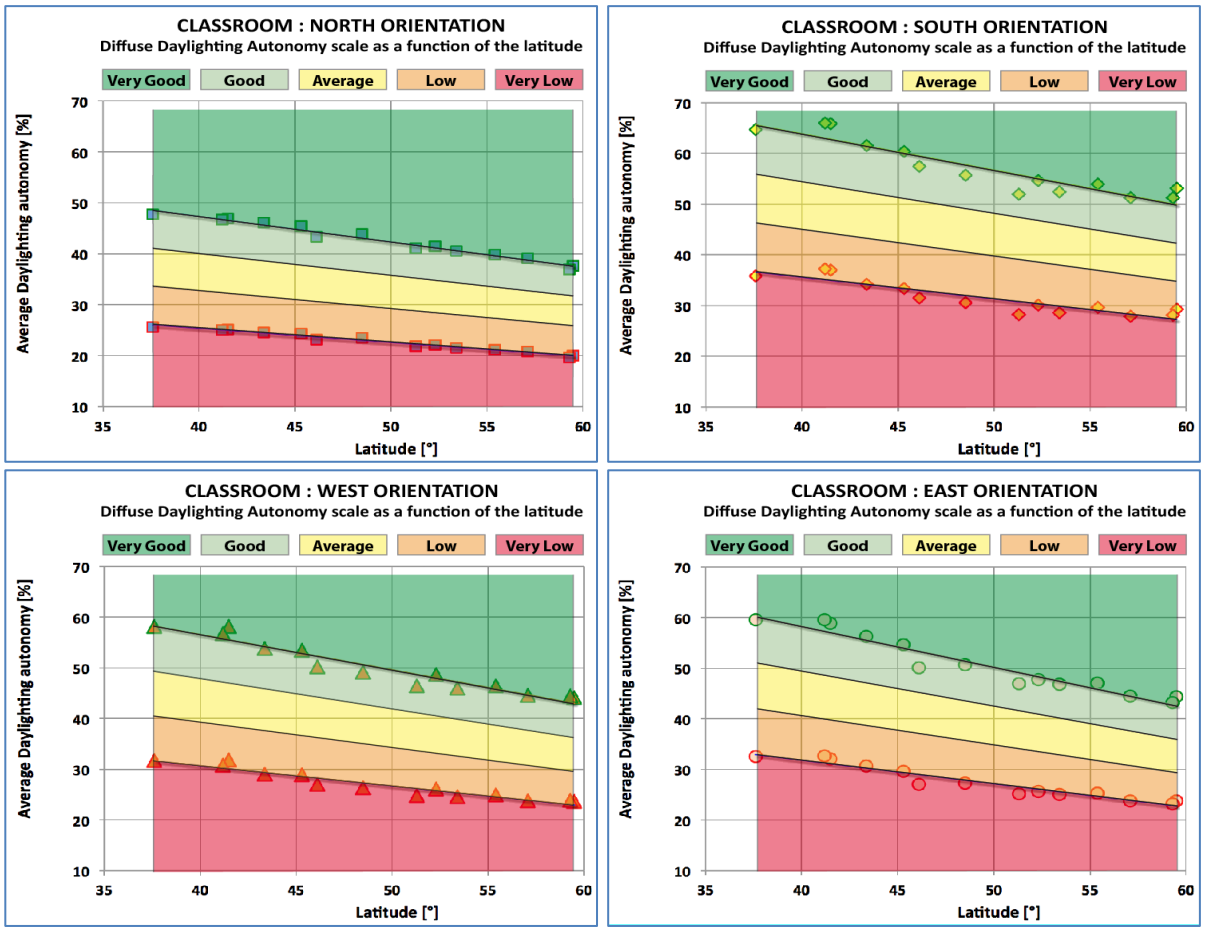

Figure 8 : Performance charts to characterize the diffuse daylight autonomy of a classroom

CONCLUSION

We have seen that it was possible to build a set of charts aiming to describe the relationship between latitude & orientation and the potential of diffuse daylight autonomy.

We are then able to answer the question mentioned in the abstract and to say that:

" For a west-oriented office-room in Paris, a 48% DDA corresponds to a "Good" daylighting performance"

We believe that it should be very useful to improve daylighting performance within the first stages of the design process, by fixing clear and intuitive targets for diffuse daylight autonomy.

Moreover, if applied to the analysis of several variants of the same project, this approach could also be used to estimate the difference in electricity consumption for lighting.

Future research will consist in integrating the impact of direct radiation and the use of blinds in the calculation of daylight autonomy, with a low computation time, which would lead to use this information in the early design stage.

BIBLIOGRAPHY

[1] CIE Technical Committee E-3.2. "Daylight: International Recommendation for the Calculation of Natural Light", CIE, Pub. N°16, Paris, 1970.

[2] Association Suisse des Electriciens: "Eclairage intérieur par la lumière du jour", ASE-SLG, Norme Suisse SN 418911, Zürich, 1989.

[3] Paule B et al: "DIAL-Europe: An European Integrated Daylighting Design Tool ", Proceedings of the PLEA -2002 conference, Toulouse, France, July 2002.

[4] Nabil A, Mardaljevic J: "Useful Daylight Illuminance: A New Paradigm to Access Daylight in Buildings". Lighting Research & Technology, 37(1), 41-59, 2005.

[5] Reinhart C F, Mardaljevic J, Rogers Z: "Dynamic Daylight Performance Metrics for Sustainable Building Design", Leukos 3:1, 2006.

[6] Paule B, Flourentzou F, Pantet S, Boutillier J, Heeren N: "DIAL+Suite: a new suite of tools to optimize the global energy performance of room design" 17. Status-Seminar «Forschen für den Bau im Kontext von Energie und Umwelt», Zürich, 2012.

[7] Paule B, Flourentzou F, Pantet S, Boutillier J: « DIAL+ : A complete but simple suite of tools to optimize the global performance of buildings openings ». Proceedings of the CISBAT'11 Conference : Cleantech for sustainable buildings, Lausanne, Oct. 2011.

[8] The Radiance software (http://radsite.lbl.gov/) is developed by the Lawrence Berkeley National Laboratory (http://www.lbl.gov/).

[9] METEONORM 6.1; www.meteonorm.com

[10] Perez R, Seals R, Ineichen P, Stewart R, Menicucci D: "A new simplified version of the Perez diffuse irradiance model for tilted surfaces" Solar Energy 39 (3), 221–232, 1987.

[11] Perez R, Ineichen P, Seals R, Michalsky J, Stewart R: "Modeling daylight availability and irradiance components from direct and global irradiance" Solar Energy 44 (5), 271–289, 1990.

[12] Paule B, Bouvier F, Courret G: « Eclairage naturel », Techniques de l'Ingénieur, CC 3315, Fév. 2008.

[13] Damelincourt JJ, Zissis G, Corbé Ch, Paule B: « Eclairage d'intérieur et ambiances visuelles », Editions Lavoisier, Col. Optique & Vision, 2010.

[14] RT-2012: "Réglementation Thermique 2012 : Principes et exigences, cadre réglementaire, méthodes de calcul"; "Règles Th-L pour la détermination du facteur de transmission lumineuse des parois vitrées du bâtiment".

DAYLIGHT AND PRODUCTIVITY IN A SCHOOL LIBRARY

A Pniewska; L Brotas

Low Energy Architecture Research Unit, Sir John Cass Faculty of Arts, Architecture and Design, London Metropolitan University, 40-44 Holloway Road, London N7 8JL, UK
Emails: agl0048@my.londonmet.ac.uk ; l.brotas@londonmet.ac.uk

ABSTRACT

Artificial light is reliable and can be accurately estimated making it easy to comply with building regulations and codes of practice. Daylight due to its variability requires much more thoughtful design. At the same time daylight is a free light source and has a positive effect on the health and productivity of human beings. Moreover significant energy savings are possible in lighting and cooling loads. For these reasons daylight has become one of the primary topics in energy conscious design in particular for buildings with daytime occupancy. This is the case in offices and educational buildings.

This paper gives an overview of aspects associated with lighting design, its regulations and recommendations applicable to a library school. Constraints and opportunities associated with the use of daylight and its impact on the occupants' productivity are addressed. Lighting design as a holistic approach can be beneficial for the occupants' satisfaction and provide energetic and economic savings. However, several studies confirm that lighting design is not an easy process and involves many different elements, namely legal requirements, visual function and amenity, integration with architecture, energy efficiency as well as sustainability, installation, maintenance and cost.

Productivity can be assumed as an important aspect of sustainability. Daylight provides a less stressful environment, contributes to our sense of well-being and comfort and has been shown to improve learning rates. Nowadays, staff salaries can be the highest cost in a company, up to 85%. Even small increases in workers' productivity may induce more money savings than savings on energy.

A post-occupancy evaluation was designed to collect real data on the occupants' behaviour in relation to the lit environment. The survey involved 100 occupants of the library in the Learning Centre at London Metropolitan University. Simultaneous recording of the illuminance next to the subjects also allowed the judgment of the light conditions in regards to the lighting requirements.

Results showed a preference for daylight against artificial light, despite the satisfaction with the light levels (combination of both light sources). They also highlighted the importance of daylight to productivity in comparison to other factors such as temperature, ventilation, crowding and noise. Issues such as glare and user control were not significantly perceived as unsatisfactory to the respondents. This may be a result of the reduced range of illuminance recorded (average 633lx, maximum 1056lx and minimum 277lx). Suggestions for improving the current situation in the Learning Centre are presented.

Keywords: daylighting, post-occupancy evaluation, user satisfaction, comfort, productivity

INTRODUCTION

Light can be perceived as the richest experience our senses have to offer. Light supplies people with information and awareness of the world around us.

Lighting Guides list seven distinct aspects of lighting design that need to be considered: legal requirements, visual function, visual amenity, architectural integration, energy efficiency and sustainability, installation, maintenance and costs. A holistic approach to lighting design can give all possible benefits for human health and comfort, energetic and economic efficiency [1].

The main aim in lighting design in buildings such as libraries is to allow the users of the space to carry out their work quickly and accurately, without discomfort. When designing such a scenario it is necessary to identify all of the functions that lighting is expected to fulfil.

According to Lighting Guide 5: Lighting for Education [2], in libraries the designer needs to allow for users to carry out a few important tasks such as finding the correct book, reading or studying, using a computer and for displaying purposes.

Therefore recommendations are different for specific areas, activities and tasks. See table 1.

	Recommended maintained illuminance	Recommended maintained illuminance for special situations
Library/ information centres	300 lx (general)	200lx (vertically on bookcases) 500 lx (on reading desks and counters)

Table 1: Places of public assembly [3]

Daylight can be an essential contribution to lighting and its design and so should be an inherent element of the educational environment. According to IEA/OECD Light Labours Lost 2006 electric lighting currently consumes 19% of the total global electricity which accounts for 1.9 Gt of CO_2/year. Lighting design should maximise the use of daylight to promote energy savings [2].

Because there is no substitute for electric lighting during the hours of darkness it is imperative to save electricity during daylight hours. Controlled daylight can replace up to 80% of electrical consumption associated with lighting during daytime hours. A successful integration of daylight and artificial light will encompass a thoughtful zoning of electric lighting as well as light controls that account for daylight. Higher satisfaction of occupants is the ultimate aim for successful solutions combining daylight and electric light.

The assumed relationship between daylight and productivity express the idea that a well daylit room is instinctively more welcoming and contribute to our sense of well-being and comfort and has an important role in regulating our circadian system. It has been shown that daylight provides a less stressful environment for students and staff, improves learning rates and saves energy [2].

Despite the fact that energy prices are increasing, staff salaries are still the greatest cost in a company: up to 85% [4]. Thus it can be assumed that even a small increase in the workers' productivity may induce more money savings than savings on energy. From another perspective daylight has a positive effect on human's psychology and health and influences occupant's attendance rates. Happier and healthier occupants have higher attendance rates at work/school. This may result in more productive and creative people in the working environment, which is a very positive aspect of sustainability. There is a strong correlation between daylight and health and well-being because people perceive a working space with daylight as being more attractive and feel they have a better mood and attitude towards work. Lastly, task performance can improve due to higher and clearer visibility [5].

RESEARCH AND POST OCCUPANCY EVALUATION

This paper presents the findings of a case study undertaken at the Learning Centre of London Metropolitan University [6]. A questionnaire was designed to assess the occupants' perception of the lit environment. Simultaneous illuminance readings collected at the work plane allowed an analysis of the acceptable levels identified by the occupants. 100 library

Figure 1: Pictures of library's interior (londonmet.ac.uk, Photographer: Pniewska)

users participated in this Post Occupancy Evaluation that took place over two days.

Information about the participants' gender, age and vision defects was anonymously collected. 93% of the subjects are younger than 40 years of age so no significant age degenerative eye diseases are expected. No statistical significance is given to the high rate of young people which can be seen as representative of the population that use the library space in a university. 45% of the subjects are females and the remaining percentage of valid responses is men. The survey collected information about the average number of hours per day in the library, on a desk at other work and in front of a computer. The study also reported preferences between daylight, artificial light and daylight in relation to productivity, in comparison to other factors such as: temperature, ventilation, crowding and noise. Maximum and minimum illuminance were calculated. Subsequently lighting level preferences were displayed.

DISCUSSION

Results from this research drawn the following points:

- **People can adapt quickly to the lighting environment they work in and typical ranges of indoor light levels** (in this case 277-1056 lx) **are acceptable and satisfy most people** More than 65% of the participants were satisfied with lighting conditions overall in the library and over 60% said 'no change' was required to the light conditions in the work area;
- **The preferred illuminance level in the library varies a lot from one individual to another** There is no significant correlation between illuminance levels and user preferences. Lighting levels in the work area were found to be bright for most of the people (58%), with 14% finding the level to be very bright. No one considered the lit environment to be slightly dim, dim nor very dim. Only 14% of the people considered the light in the library to be unsatisfactory and 55% considered it to be satisfactory. The remaining gave a neutral response. 43% (valid responses) of the people considered that the light environment in the library has increased their productivity

and 42% considered the light to have a neutral impact in their productivity. 14 out of the 100 participants did not respond to this question;

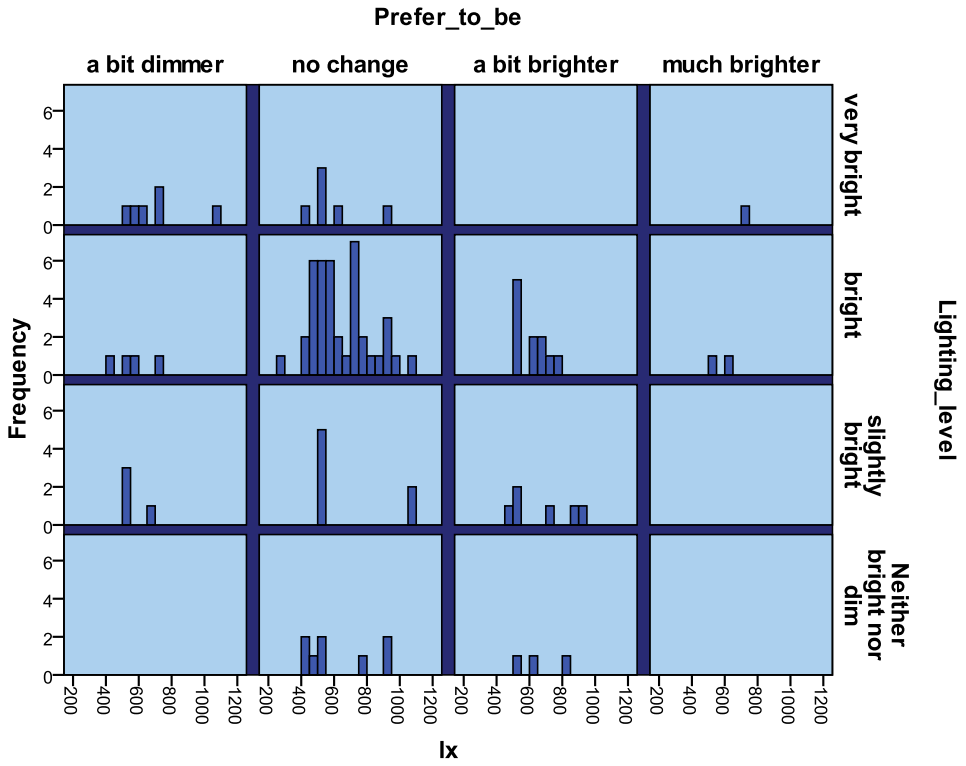

Figure 2: Figure 3 Graph comparing lighting level, preferences and illuminance

- **There is a clear preference for daylight**, associated with opinion that daylight supports psychological comfort (67% voted for daylight against 11% for electrical light), general health (68% voted for daylight against 7% for electrical light), healthy vision (63% voted for daylight against 17% for electrical light), colour appearance of people and furnishing (37% voted for daylight against 11% for electrical light) and for building appearance and pleasantness (51% voted for daylight against 20% for electrical light). In case of work performance daylighting was marginally preferred (35%) than electric lighting (33%). Only for jobs requiring fine observation electric lighting (45%) had more voters than daylight (32%);
- **Lighting is the 'most important' (42% of responses) and 'important' (22% of responses) aspect according to the productivity** Crowding was considered the less important by 28% of the valid voters. Temperature was considered to be most important by 25% and ventilation had the highest percentage of the neutral responses (25%). Sound was considered the most important by 28% of those who voted. Leaman and Bordass [7] results show that noise and then heating and cooling produces the strongest association with productivity.
- **Glare from sun and sky and from artificial light was not assumed problematic** 51% of those who voted considered that the quality of light in the library was neutral from glare from the sun and sky and from artificial light. The quality was considered satisfactory for 32 and 34%, respectively;

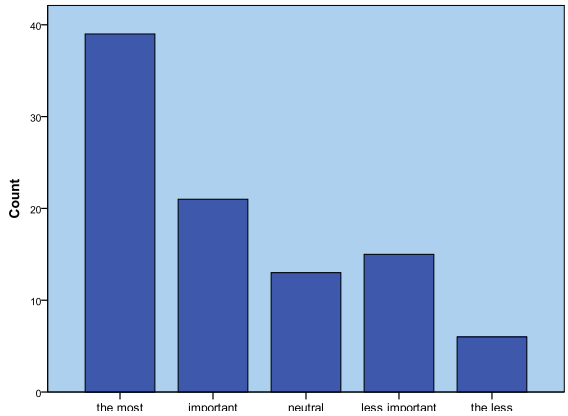

Figure 3: Lighting according to the productivity

- **Light controls can lead to occupant's comfort and energy-efficiency.** Giving control of lighting to the users of a building was suggested as a way to promote sustainability and increase the percentage of people satisfied with the lit environment. To integrate daylight sensors to switch/dim artificial light might reduce the electrical bill. The plan of the library could be sectioned into zones where daylight may contribute to the overall visual environment and the light levels. Some parts of the library such as techno booths or individual-groups tables could have occupancy control or PIR sensors to be switched off when not in use. But the overall light scheme must take into consideration all the requirements and how energy savings can be obtained while still promoting an exciting and appealing general appearance.

CONCLUSION

Although this research seemed very concise, a significant number of occupants have been surveyed and some interesting conclusions emerged. Further studies could have been undertaken to substantiate the indicative findings presented.

Ideally measurements and POE should be undertaken with and without artificial lights to separate both components. This was not feasible in the space surveyed to minimise annoyance or disruption to the occupants. A possible solution to identify the contribution of daylight and artificial light would be to measure the space at night with only artificial light. However this was not possible during the surveyed days as these took place during summer and there was always daylight on opening hours. Electricity bills could have been collected and analytical calculations or simulations could have been carried out to estimate the daylight and/or electrical light impact on the energy consumption of the building and to assess possible improved scenarios. Nevertheless the lighting scheme in place seems to satisfy the majority of the participants of the survey. Light seems to have the biggest impact on the perceived productivity of the occupants and should therefore be given the biggest thought in space design. Daylight is usually identified as the preferred light source for several reasons.

In other studies light quality does not assume such an extreme importance in comparison to other factors such as: noise, temperature, ventilation. This may be a result of people being oblivious to the lighting conditions around them provided they are above minimum lighting levels [8]. In other surveys the other environmental conditions are within acceptable ranges and therefore not raise annoyance.

This survey measured a relatively small range of illuminance on the working plane. No one reported the light level to be slightly dim to very dim. With the exception of one recording of

277lx all the illuminance levels surveyed are above 404lx and 18% are above 500lx. Given the recommended values on lighting guides this may indicate that lower lighting levels may be acceptable on the working plane. This might be true, particularly at the level of justifying more costly lighting choices. Likewise the maximum illuminance level recorded next to the occupant is not sufficient to indicate the potential for problems with glare.

A high percentage of disagreement with the statement that "The lighting in an office is not important to me" suggests that lighting does matter to the ordinary occupant, at least at the simplest level. The problem remains that we are only slowly identifying the lighting conditions that would satisfy most people, a problem that is further complicated by the fact that preferred conditions vary widely from one individual to another [9]. Therefore we may be better judging acceptable light levels on a set of ranges and not based on absolute minimum values. The human eye has a good capacity to adapt to a wide range of light levels.

Given the daylight variability throughout the day and the year as well as the influence of weather conditions it is still difficult to predict the daylight contribution using simple metrics. This should not be however a justification to privilege artificial light. Architects should cooperate with experts in daylight to successfully integrate daylight from early phases of design. Delaying this to later design and construction stages may significantly compromise daylight exploitation in future.

Daylight must be included in a holistic design together with the building form, orientation function and program, integrating in the electric light design and control strategy. This will result in proven user satisfaction, increased productivity, health and beauty of the indoor space as well as energy savings and a more sustainable environment.

REFERENCES

1. CIBSE The SLL Lighting Handbook. The Chartered Institution of Building Services Engineers, London, 2009
2. CIBSE Lighting Guide 5: Lighting for education. The Chartered Institution of Building Services Engineers, London, 2011
3. BSI British Standard Light and lighting - Lighting of work places Part 1: Indoor work places. BS EN 12464-1:2011 BSI British Standards Institution, London, 2011
4. Carter, D.J., Mayhoub, M.S. *The costs and benefits of using daylight guidance to light office buildings* Building and Environment, 2010
5. Veitch, J.A., Newsham, G.R., Boyce, P.R., Jones, C.C. *Lighting appraisal, well-being, and performance in open-plan offices: a linked mechanisms approach* Lighting Research and Technology, v.40, no.2, 2008
6. Pniewska, A. Daylight Performance and its vital effect on building occupants. MSc Thesis in Architecture, Energy and Sustainability, London Metropolitan University, 2012
7. Leaman, A., Bordass, B. *Productivity in buildings: the `killer' variables* Building Research & Information 27(1), London, 1999
8. Boyce, P. R. Lighting quality: Proceedings of the First CIE Symposium on Lighting Quality CIE-1998 Vienna Austria: Commission Internationale de l'Eclairage, 1998
9. Veitch, J.A., Newsham, G.R. *Preferred luminous conditions in open-plan offices: research and practice recommendations* International Journal of Lighting Research and Technology, v.32, no.4, 2000, Ottawa, Canada, 2000

MULTI-POINT SIMULTANEOUS ILLUMINANCE MEASUREMENT WITH HIGH DYNAMIC RANGE PHOTOGRAPHY

Xiaoming Yang; Lars O. Grobe; Stephen K. Wittkopf

Lucerne University of Applied Sciences and Arts

ABSTRACT

Daylight illuminance uniformity is a common criterion when assessing the performance of fenestration and solar control. To evaluate a design according to this requirement, a grid of horizontal illuminance readings for a given time is required. In simulation based assessments, this can be calculated by defining sensor points at working plane level and running a simulation for a single time step, or an annual simulation to assess the uniformity for a typical year. Backing such predicted assessments with measured data has been a task involving installation and calibration of sensors, cabling and data acquisition systems, which typically render the assessed space unusable for the time of assessment. Using sequential readings from handheld devices as a convenient alternative ignores the dynamics of daylight, as the sky conditions cannot be assumed constant during the time required to record the illuminance at the required amount of locations.

We propose instantaneous image-based measurements of horizontal illuminance for assessments of daylight uniformity. Instead of cabled sensors, near-Lambertian reflectors are placed at working plane level in the assessed space. High Dynamic Range (HDR) images of the working plane with markers are taken and the luminance of the marker surfaces is extracted from the corresponding pixel values. These luminance values can be used to calculate horizontal illuminance for each marker location, assuming Lambertian reflection. As direct sunlight at working plane is considered to exceed the range of acceptable illuminance for uniformly lid spaces, only readings below a threshold of 3000 lm/m2 are considered.

Keywords: Illuminance, daylight, Lambertian diffuser, Goniophotometry, high dynamic range imaging

INTRODUCTION

Horizontal illuminance requirements have been related to tasks and have been established for planning with artificial and natural light. Handheld devices for point-measurements of horizontal illuminance are available and commonly found in practice. National and international standards however impose requirements of horizontal illuminance over the occupied area of buildings. LEED IEQ8.1 e.g. requires horizontal illuminance in an acceptable range for at least 75% of the occupied space [1]. Daylight uniformity as a separate metric addresses the spatial distribution and is credited e.g. in the BREEAM rating system as a minimum uniformity ratio Emin/Emax of 0.4 [2]. The distribution of horizontal illuminance however cannot be evaluated using measurements for only one point due to the uneven distribution of illuminance in typical environments. Handheld illuminance meters, which are not suitable for simultaneous measurements, could be used for sequential measurements at given locations. However, the dynamics in daylight would heavily affect the results of such measurements. The effort to equip a space with wired sensors and a data acquisition system, which typically limits the usability of the assessed space, is hardly acceptable to occupants especially for extended assessment periods.

Researchers have investigated the usage of digital cameras as commonly available devices for luminance measurements [3]. Stacked exposures of low dynamic range images, as captured by the image sensors of typical consumer cameras, have been assembled into HDR images to cover the dynamic range of daylight environments [4, 5]. The dynamic range of the resulted HDR image is mostly limited by the number of images that can be taken in a short time. The time span available for the image series is determined by the variability of the lighting conditions, which are assumed as constant in the assembly process. Research has shown that HDR techniques are an accurate method for luminance measurements [6, 7, and 8].

For perfectly Lambertian diffusion, luminous flux through transmissive objects can be calculated from observed luminance if the diffusor is placed between a calibrated camera and a light source. The method has been demonstrated for assessment of luminous flux through fenestration systems and light pipes, and also as a method to capture total-horizontal and diffuse-horizontal illuminance [9]. The almost perfect Lambertian bidirectional scatter distribution function (BSDF) for transmission through paper allows its application in flexible and low-cost measurements within an accuracy range reasonable for daylighting applications.

We extend the method of using paper as a diffusor for illuminance calculations using HDR imaging techniques to illuminance calculations from luminance measured on the reflecting side of the diffusor. While the deviation from an ideal Lambertian BSDF is higher for reflection than for transmission, this allows the application of the method for multipoint illuminance measurements, addressing the lack of measured data backing requirements for daylight uniformity. Markers made of low-cost paper are placed on existing surfaces. The area covered by the markers included in the measurement is limited only by the view angle of the camera lens and the image resolution, as wide angle lenses lead to lower pixel resolutions for each marker. Besides allowing a simultaneous measurement of illumance at many locations, potentially over an extended time span, the resulting images contain relevant information for documentation such as marker locations, changes in the setup and shadowing effects.

METHOD

A Lambertian diffuser [10], with its perfect diffuse reflection properties, has a constant luminance independent of the viewing direction. A marker made of a Lambertian diffuser would be ideal for our method. Regardless the location of the marker in the field view of the luminance acquisition camera, illuminance *E* on an ideal diffuser could be calculated as

$$E = \frac{1}{\rho} * \pi L \qquad (1)$$

where ρ is the reflectance of the diffuser and *L* is the luminance from the viewing direction.

Acquisition of luminance maps

The camera used in this project, the “LMK mobile advanced” by Technoteam, is a luminance acquisition system based on a calibrated Canon EOS 5500 DSLR. A proprietary software reads in raw image data and applies the calibration data for the combination of lens and camera as supplied by the manufacturer. This results in luminance maps that can be processed and exported in a tabular format of pixel coordinates and corresponding luminance. These luminance values were used to assemble HDR images in Radiance RGBE format using the *pvalue* program as part of Radiance.

Selection of the Marker

The marker for the presented method should have properties as close as possible to those of a Lambertian diffuser. To obtain illuminance values at multiple positions in a scene, a number of markers are required so it must be inexpensive and easy to attach to surfaces. Industry diffuse standards, typically made of Polytetrafluoroethylene (PTFE) such as used in integrated spheres would be much too expensive. Hence, an alternative material needs to be found that still presents desired reflection property.

To quantify how close the reflection of a real material comes to that of the Lambertian diffuser, a Goniophotometer is used. A Goniophotometer measures the light that is reflected off and/or transmitted by surfaces and materials (optical scatter) at any point in space [11]. In addition, the angle of the light that is incident on the surface or material can be varied from the standard normal (perpendicular to the sample plane) to very oblique angles (up to 85°) to quantify the optical scatter as a function of the incidence angle. The outgoing angles are defined by an orbital mesh around the sample with an angular resolution of less than 0.1°. The characterization follows the format of Bidirectional Scattering Distribution Function (BSDF), in which light intensities for each angle of incidence are measured for all outgoing angles (direct-to-direct reflection/transmission). In this paper, only reflectance property is investigated, therefore the term Bidirectional Reflectance Distribution Function (BRDF) is used instead of BSDF. The results were presented in polar plots as shown in Figure 1. The polar plots show the BRDF in common logarithmic scale for the scatter plane (Φ_i=0°). Each polar plot shows the scatter of the sample in reflection. The logarithmic scale is marked by concentric rings whose values represent a ratio of the power of light leaving a unit area of the sample in a given direction to the power of light incident on that area.

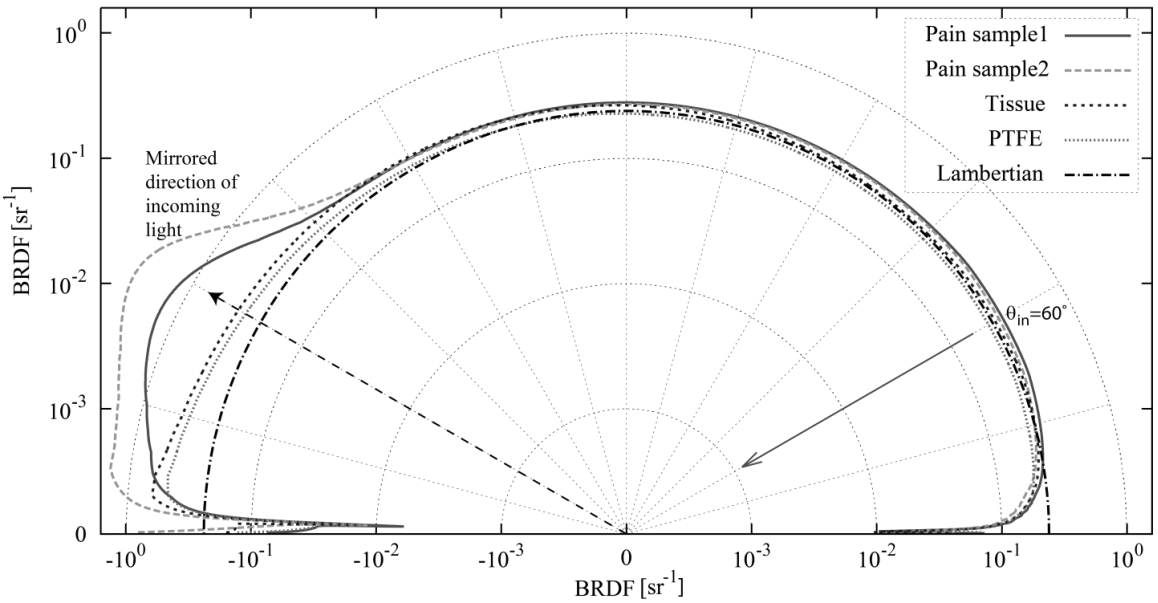

Figure 1: Polar plot showing the reflection properties of two pain samples, tissue paper and PTFE at 60° incident angle compared to a theoretical ideal diffuse reflection of a Lambertian surface with reflectance the same as PTFE.

Eight materials were measured including two spray matt pains, four kinds of matt paper, tissue paper and Polytetrafluoroethylene (PTFE). The PTFE sample is a reflectance standard for optical experiments which has nearly ideal diffuse reflection properties over a wide range of wavelengths from UV to infrared (250 – 2500 nm). All materials were measured with Goniophotometer at incident angle (θ_i) equals to 0°, 15°, 30°, 45° and 60°. Results for 60° are

shown in polar plots comparing to the theoretical Lambertian diffuser (Figure 1). All materials expect paint sample 2 present reflection properties that are very close to the theoretical Lambertian surface when incoming light is close to the normal of the material surface. However, when incoming light is at a more oblique angle (θ_i = 60°) the reflection pattern of all the materials become asymmetrical along the surface normal. Among all the materials, PTFE shows the closest result to the theoretical Lambertian diffuser follows by the tissue paper. The four matt paper samples have similar reflection pattern and shows larger value near the mirrored direction of incoming light. The two pain samples show bulging along the light exit angle which suggests strong directional diffuse components in their reflection properties. As shown in the above results, tissue paper, with its desired reflection property, was selected as the material for the diffuse marker.

Validation and error analysis

The directional diffuse component in the reflection property of a marker leads to the errors in the presented method. This error is dependent on light incident direction and viewing angle. With directional light at oblique angle, the error is considerable as shown in Figure 1. However, the presented method is proposed for useful daylight monitoring. As the highly directional sunlight which always result illuminance values exceeding the desired range, it need not to be quantified for this method. In order to validate the method in diffuse daylight conditions for various incident light direction, a marker was placed one meter away from a façade with French windows. The marker was made of tissue paper pasting on an opaque rigid corrugated-core sandwich panel. The panel ensured the flatness of the tissue paper and it could also maintain the reflection property of the marker independent from the background. With a movable blind next to the windows, the façade working as a diffuse light source could be changed for its elevation angle to the marker. With a correction factor *f* introduced to equation 1, the difference between the calculated illuminance from a HDR image and the illuminance from a lux meter could be quantified. As shown in Figure 3 left, the factor remains in a limited range which implies that under diffuse daylighting condition, the luminance value reflected from the marker can be considered independent from the direction of incident light.

$$E = \frac{1}{\rho} * \pi L * f \qquad (2)$$

For a fixed set up of the camera and markers, the factor *f* could be calculated for each marker to correct the error from viewing direction. Using the same setup with the blind fully open, a series of HDR images of the marker were captured with half hour step. During the entire process, the weather was dominated by overcast sky. The illuminance values calculated from the HDR images was compared to the illuminance value recorded with lux meter (Figure 3 right). With the same camera-marker position, the factor *f* was applied to correct errors result from the viewing angle in this set up. The difference between the image and lux meter is within 12% for the sequence expects the value recorded at 15:45 which is 19%. The error is beyond the 10% range which is acceptable for daylighting monitoring. The experiment will be repeated for further investigation.

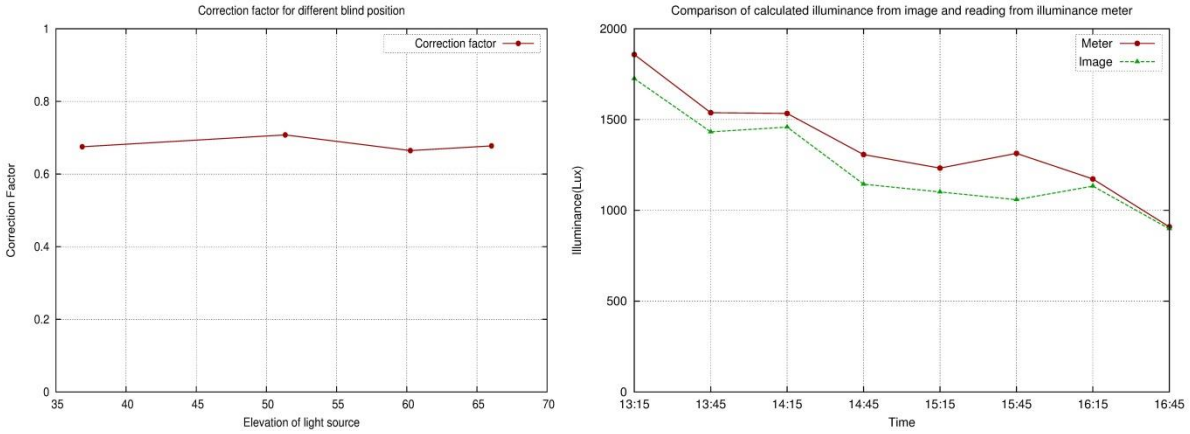

Figure 2: Left: Correction factor calculated for different blind positions. Right: Comparison of calculated illuminance from images and readings from illuminance meter.

CASE STUDY: OFFICE SPACE

The presented method was applied to capture daylight distribution in an occupied office (Figure 3 left). Ten markers in two rows were equally spaced along the working plane away from the façade. The camera position and direction was fixed to take a series of images. A correction factor for each marker was calculated and applied to the readings from the images. Two rounds of photo shoot were taken place in the office with one hour step. Each round consists of two images taken one minute apart to capture instant daylight variance. The results are shown in Figure 3 Right. It is clear that daylight level on the working plane decrease gradually with the distance from the façade. For the first round, the daylighting condition kept constant and there is a 10% variance of illuminance level in the second round. With an extended assessment period, the set up could be used as a daylighting monitoring system for the office space.

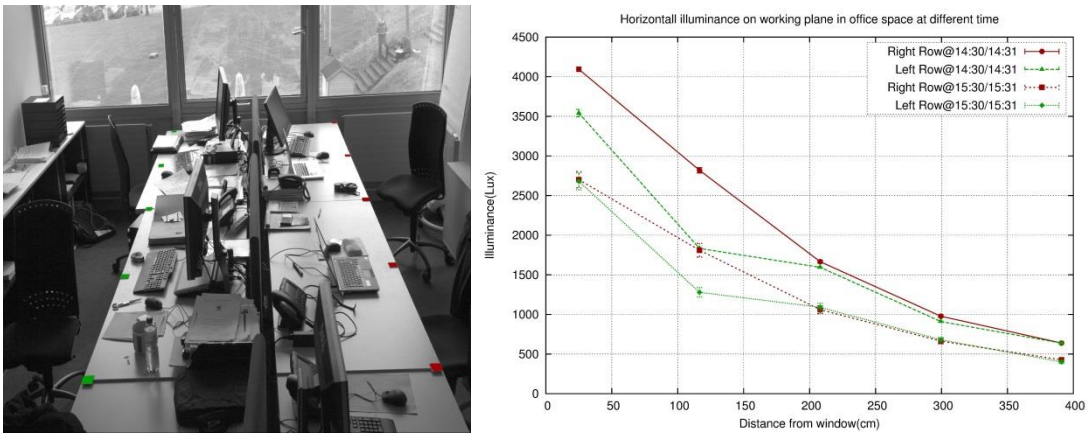

Figure 3: Left: Experiment set up in an occupied office space with 10 markers on the working plane. Right: Daylight distribution in office space at different time using the presented method.

CONCLUSION

This paper addresses the lack of measured data backing requirements for daylight uniformity by introducing a method for measuring daylight illuminance at many points simultaneously. The method uses HDR techniques to capture the luminance of markers located at the measurement points.

A Goniophotometer was applied to identify a marker material that exhibits nearly Lambertian diffuser properties allowing the calculation of illuminance from the luminance values captured in HDR images.

Inexpensive tissue paper is found to be a suitable material for the markers, presenting reflection properties very close to those of perfect Lambertian diffusers. The deviation from a perfect Lambertian diffuser is corrected by a factor for each marker in the set up. The highly directional sunlight is not covered, as areas receiving direct sunlight would not contribute to a uniformly daylight space and thus do not need to be quantified. The non-Lambertian reflection occurs only for extreme incident angles and can be neglected for predominantly diffuse lighting conditions. Within this scope, relevant for assessments of daylight uniformity, the presented method has potential to provide sufficient accuracy to be used for simultaneous multi-point illuminance acquisition of daylight in buildings. We believe, that digital photography could become an integrated capturing and display system for luminance, illuminance and surface material properties of an architectural scene and as such helps lighting planners/engineers in quantifying and visualizing the lighting milieu of a scene.

REFERENCES

1. U.S. Green Building Council. LEED 2009 for New Construction and Major Renovations. 2007
2. BRE Global Ltd. BREEAM New Construction Non-Domestic Buildings Technical Manual SD5073 – 3.2 :2011
3. L. Bellia, A. Cesarano, F. Minichiello, S. Sibilio, Setting up a CCD photometer for lighting research and design, Building and Environment, Vol.37, 2002, pp. 1099-1106.
4. Paul E. Devec and Jitendra Malik. Recovering High Dynamic Range Radiance Maps from Photographs. In SIGGRAPH97, August 1997.
5. Axel, J. Advances in Building Energy Research, Volume 1, Number 1, pp. 177-202(26), 2007
6. Anaokar S, Moeck M. Validation of high dynamic range imaging to luminance measurement. Leukos. 2(2):133-144, 2005
7. Inanici M. Evaluation of high dynamic range photography as a luminance data acquisition system. Light Res Technol. 38(2):123-136, 2006
8. Moeck M. Accuracy of Luminance Maps Obtained from High Dynamic Range Images. Leukos; 4(2), 99-112, 2007
9. Mardaljevic J, Painter B, Andersen M. Transmission illuminance proxy HDR imaging: a new technique to quantify luminous flux. Light Res Technol. 41(1):27-49, 2009
10. Bass, M., Mahajan, V. N., & Optical Society of America. Handbook of optics (3rd ed.). New York: McGraw-Hill, 2010
11. Grobe, L. O., Wittkopf, S., Apian-Bennewitz, P., Johnson, J. C., & Rubin, M. Experimental validation of bidirectional reflection and transmission distribution measurements of specular and scattering materials. Photonics for Solar Energy Systems Iii, 7725, 2010

SIMULATING DAYLIGHT PROPAGATION THROUGH COMPLEX FENESTRATION SYSTEMS IN A URBAN CONTEXT USING A VARIABLE SAMPLING SUBDIVISION SCHEME

Chantal Basurto, Jérôme Kämpf and Jean-Louis Scartezzini

Solar Energy and Building Physics Laboratory (LESO-PB), Ecole Polytechnique Fédérale de Lausanne (EPFL), CH – 1015 Lausanne (Switzerland)

ABSTRACT

The use of Complex Fenestration Systems (CFS) within buildings can contribute to a significant reduction of cooling loads by the way of two assets: the redirection of daylight and the shading of sunrays. In order to back-up these features, daylight performance evaluations need to be performed individually in each case according to the geographical location, outdoor conditions, building orientation and design as well as indoor material properties. The use of computer simulations can make this assessment easier than on-site CFS monitoring requiring the availability of testing facilities, materials and equipment transportation as well as the physical installation of a CFS. Computer simulations can be carried-out using the RADIANCE lighting software, which allows the estimation of the daylight propagation through the CFS using monitored light transmission properties. Those features named BTDF data (Bi-directional Transmission Distribution Function) are assessed using a bidirectional gonio-photometer and stored in an internationally standardized format. In order to perform such simulations, BTDF data are assigned to a planar polygon that models the CFS and/or a window becoming a secondary light source in the virtual model. The accuracy of the simulation results is generally relying on the computer simulation parameters that drive the lighting calculation in the virtual model, as well as the BTDF data resolution assigned to the polygon mimicking the CFS. In an urban context moreover the shadowing effects due to adjacent buildings have a significant impact on the incoming daylight flux transmitted by the CFS. It is important accordingly, to subdivide such a polygon - which may be a large glazed area - in an optimal way in order to enhance the simulation accuracy. Computer simulations were carried-out for that purpose using a virtual model of an office room placed in an urban-context. The BTDF data of a Laser-Cut Panel (LCP), made of a 6 mm thick acrylic panel with 4 mm spaced parallel laser cuts, were applied for that purpose to: i) a single pane representing a full-size office window and ii) subdivided polygons of the size of the LCP sample benefitting from BTDF monitoring. All results are compared in order to determine the influence of the polygon subdivisions referenced to the BTDF data on the final computer simulation accuracy.

Keywords: Daylighting, Complex Fenestration Systems, Bi-directional Transmission Distribution Function (BTDF), RADIANCE Lighting Software, Bidirectional Gonio-photometer.

INTRODUCTION

The use of CFS in buildings signify important benefits for the users by allowing a more even redistribution of direct sunlight, improving the visual comfort and contributing to the mitigation of the final energy demand [1, 2]. The ideal way of obtaining an assessment of the daylight propagation through Complex Fenestration Systems (CFS) in a room would be to perform on-site evaluations in a full scale building. However, to test CFS in real buildings represents several difficulties such as the availability of a testing facility, materials and

equipment transportation as well as the CFS installation. To overcome these drawbacks, the use of computer simulations based on virtual models provides significant advantages. Computer simulations are essential for making an effective selection of the CFS in every particular case. The ray-tracing software RADIANCE [3] allows the simulation of the daylight propagation through CFS [4] by applying BTDF data (Bi-directional Transmission Distribution Function) [5-7] to a previously selected planar polygon acting as a window in the virtual model. Two RADIANCE procedures are mainly applied today to perform such simulations. Both use the BTDF data of a CFS stored in an XML format to model the propagation of daylight in a room. A first procedure uses the pre-process mkillum to model the daylight distribution through the CFS; a second procedure uses the *bsdf* material function to perform such simulation [2, 8]. As a common practice, the BTDF data is applied to a single polygon representing the full pane of a window in the virtual model. However, when using the mkillum procedure, the calculation of the daylight distribution through the CFS is performed from the center of the polygon, taking into account its full area assigned to the BTDF data. This might lead to inaccuracies in the simulation results when the shadows of adjacent buildings are projected on the building's façade. The objective of this study is to investigate the impact that the resolution of the subdivision of the polygon assigned to the BTDF data representing the window, might have in the accuracy of the simulation in the presence of exterior obstructions. This study proposes that the use of a subdivided polygon leads to more precise calculations.

METHODOLOGY

An office room located in the city of Zacatecas, México (22° 783' N., 102° 583' W, Altitude: 2543m) was used to carry-out simulations using RADIANCE [3]. The room is part of a buildings complex of a public university dedicated to Humanities and Social Sciences. Its dimensions are typical of an office room (5.50 x 4.17m and 2.46m height). For the purpose of this study the equipped building façade was orientated to south in the virtual model. The interior material properties (reflectance and transmittance) were assigned to the latter using optimal values. Thus the surface reflectance's were based on the IESNA recommendations [9] (floor 0.40, walls 0.70 and ceiling 0.80), while the glazing transmittance was set to 0.75. The BTDF data [2, 6] of Laser cut panel (LCP) [10] was assigned to the polygon that accounts for the upper window in the office room. In order to test the accuracy of RADIANCE simulations regarding the resolution of the BTDF data, the latter were carried-out first using the full-size polygon that accounts for the upper window in the office room. Secondly, such polygon was subdivided into small sections of 10cm x 10cm, which are the dimensions of the original LCP sample monitored with the gonio-photometer [5, 11] to assess its photometric properties [12, 13]. In total, the east upper window was subdivided into 150 sections of 10cm x 10cm plus 6 sections of 6cm x 10cm for the remaining space next to the column located in the middle of the room; the west-upper window was subdivided into 72 pieces of 10cm x 10cm plus 6 sections of 4cm next to the west wall. Since the objective of this study is to test the accuracy of the simulated daylight propagation through CFS when external obstructions are present, three buildings were included in the virtual model, placed 7m away from the façade in order to create shadows in the office room.

When modelling the daylight distribution through CFS in a room, the pre-process mkillum performs the calculation from the center of the polygon assigned with the BTDF data. Therefore, when a combination of light and shadow falls over such polygon, the calculation might be performed taking into account the entire polygon as if it was fully lit or fully shadowed, which might lead to inaccurate results. In order to investigate that, a daylight situation in the virtual model was created with exterior obstructions partly projecting a

shadow over the entire polygon; such situation was created for winter solstice at 11h 50. Simulations were then carried-out using first the mkillum procedure [2], and secondly using the *bsdf* material function [8], in order to compare the results obtained with the two RADIANCE procedures. The simulations were carried-out first with the full-size polygon and later with a subdivided polygon. Since the *bsdf* procedure reproduces the propagation of daylight through the CFS directly using the BTDF data stored in the XML file, the use of a subdivided window will not represent any difference in the calculation. Hence, when using the *bsdf* procedure the simulations were carried-out only with the full-size polygon. Three situations were then assessed: i) using mkillum with the full size window; ii) using mkillum with the subdivided window and iii) using the *bsdf* procedure. The final assessment was performed in two steps: a visual assessment was performed first by comparing visualizations in the interior of the room from three different viewpoints. A second assessment was performed by comparing the simulated daylight distribution through the office room on the basis of illuminance ratio (IR)[14]. Illuminance was estimated for that purpose by placing points in the middle of the room, every 10 cm from the window up to 2.5m and every 20cm from there to the back of the room, at task level height (0.75m).

RESULTS

Visual Assessment

A straight view of the larger window in the office room is shown in Figure 1. It shows that when using the mkillum procedure with the full-size polygon, the light is projected on the ceiling as if the entire area was lit (left). However, when using mkillum with a sub-divided polygon, the visualization shows that a more accurate calculation is performed (center): the light is redirected to the ceiling only for the lit area on the façade. In case of use of the *bsdf* procedure (right), the visualization shows that the calculation is performed taking into account only the lit area. However, when using the *bsdf* procedure, the CPU time is larger than when using the mkillum procedure using similar radiance parameters. In order to obtain simulation results in a reasonable time using the bsdf procedure, the values of the parameters have to be reduced and even so the quality of the pictures.

Figure 1. Visualization of the office room using mkillum with the full-size window (left); the visualization using mkillum with the subdivided window (center)and the visualization obtained with the bsdf procedure (right).

A second visualization shows the office room viewed from the back of the room. It allows the comparison of the modelling of the daylight distribution through the LCP in both windows (Figure 2). The picture shows a well-defined lighting redirection on the ceiling when the simulation is performed using mkillum with the subdivided window (center). A similar result is also achieved using the bsdf procedure (right). However, in the latter the redirected light shows a less defined pattern due to the low picture quality. This is due to the limited CPU time

allowed to the bsdf procedure by the values of the rendering parameters. In this case the rendering of a picture can take from 20min to one hour in low quality with the corresponding simulation parameters (-ab 2, -aa 0.2, -ar 32 –ad 512); while when using mkillum it takes about 10 minutes in both cases (full-size window and subdivided window) in medium quality with the corresponding simulation parameters (-ab 6, -aa 0.1, -ar 64 –ad 1024).

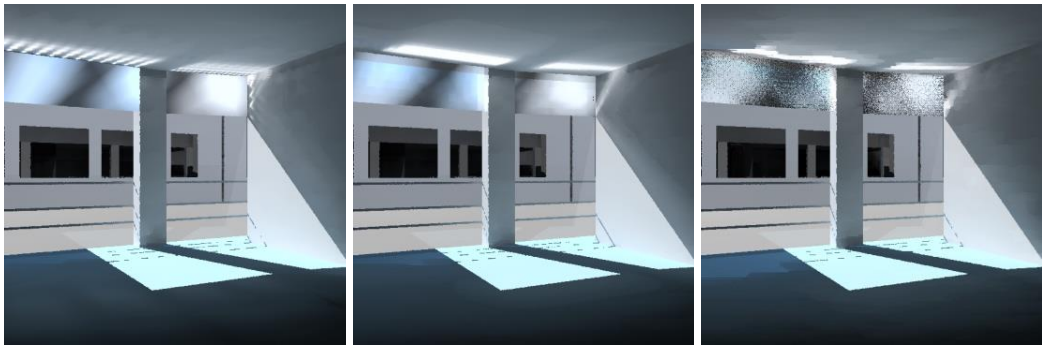

Figure 2. Visualizations of the interior of the office viewed from the back. Modelling of the daylight distribution through the LCP using mkillum with the full-size window (left), using mkillum with the subdivided window (center) and using the bsdf procedure (right).

A third visualization was obtained, which shows a closer view to the window as shown on Figure 3. It allows observing how daylight is redirected on the ceiling. When using mkillum with the subdivided polygon (center) the light pattern is regular and defined, while when using the full-size polygon it shows a discontinuous light projection (left). The simulation carried-out with the *bsdf* procedure shows an undefined light redirection due to the low quality of the picture (right).

Figure 3. Transversal view of the window allowing detailed observation of the daylight propagation through the LCP using mkillum with the full-size window (left), with the subdivided window (center) and with the bsdf procedure (right).

Assessment of daylight distribution through CFS in the office room

A second assessment was performed by analysing the daylight distribution through the room by comparing the illuminance ratio (IR) profile obtained in the shadowed area of the room (at the middle of the larger window). Different points were placed for that purpose at 10cm distance from the window up to 2.5m and from there at 20cm to the back of the room. The results are illustrated on Figure 4; they show a very similar IR profile across the room with values in between 9-10% next to the window. However, the IR profile obtained using mkillum with the full-size window shows larger values at a distance of 1m to 1.8m from the window. When calculations are performed with the mkillum process using the subdivided window and the *bsdf* procedures, the IR values shows a continuous profile, meaning that no

daylight is modelled in the shadowed area of the façade. For all, the IR profile using the three conditions is within a range of 10% accuracy. The larger values obtained using mkillum with the full-size window are not considered as significant in regards to the daylight distribution. The CPU computing time using mkillum was equal to 2 hours when using the full-size window and about 14 hours when the window is subdivided. With the *bsdf* procedure, the CPU time is equal to 2 hours. The simulations were carried-out using the same simulation parameters in all cases (-ab 4, -aa 0.1, -ar 64, -ad 1024).

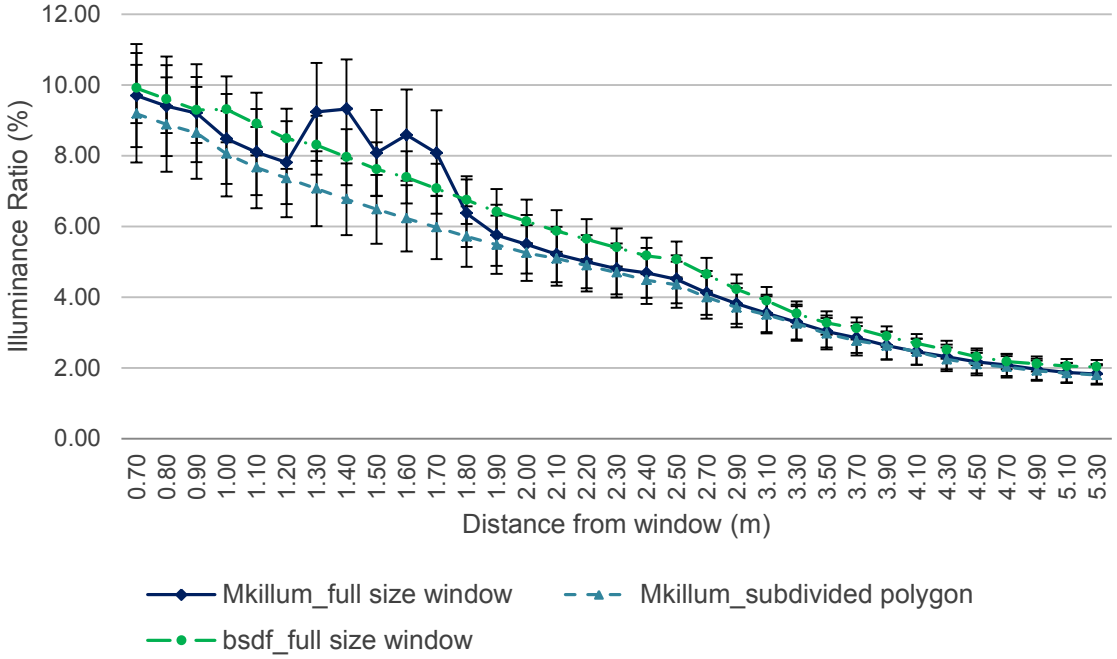

Figure 4 Illuminance Ratio through the room obtained using mkillum with the full-size, the subdivided polygon and the bsdf procedure at 11h 50 when shadows are projected on the façade.

CONCLUSION

The aim of this study was to investigate the impact that the BTDF data resolution assigned to a polygon representing a CFS has on the accuracy of simulations when exterior obstructions are present. Simulations were carried-out using two RADIANCE routines: the pre-process mkillum and the *bsdf* procedure. A full-size polygon was used first and then a subdivided polygon associated to the BTDF data of LCP, in order to compare the renderings and the illuminance ratio distribution. The former, showed that when simulations are carried-out with the full-size polygon, mkillum performs a calculation overlooking the shadow effect of the adjacent buildings, leading to inaccurate results. On the other hand, when the polygon is subdivided, the daylight distribution is calculated taking only in to account the areas that are not shadowed by the exterior obstructions; the same situation is observed when using the *bsdf* procedure. However, the assessment of the daylight distribution with the IR profile showed no significant differences in the simulation results when using the two procedures. In summary, if the daylight interior environment needs to be assessed regarding visual comfort, risk of glare, then the subdivision of the polygon assigned to the BTDF data of the CFS is advisable. If the quality of the interior environment requires a quantifiable evaluation, such as illuminance ratio (IR) or daylight factor (DF) [15], the subdivision of the polygon associated to the BTDF data does not lead to a significant improvement.

ACKNOWLEDGEMENTS

This work has been financially supported by the National Council for Science and Technology (CONACYT), México and by the Swiss Federal Office of Energy (SFOE). The author thanks Eng. Carsten Bauer for his comments during the 11th International RADIANCE workshop in Copenhagen, Denmark, the origin frame of the present study.

REFERENCES

[1] McHugh, J., P.J. Burns, and D.C. Hittle, *The Energy Impact of Daylighting.* Ashrae Journal, 1998. 40(5): p. 31-35

[2] Kämpf, J.H. and J.-L. Scartezzini. *Ray-Tracing simulation of Complex Fenestration Systems Based on Digitally Processed BTDF data.* in *CISBAT 2011*, Lausanne, Switzerland.

[3] G.Ward and R. Shakespeare, *Rendering with Radiance, The Art and Science of Lighting Visualization*. 1997: Morgan Kaufmann.

[4] Ruck, N., et al., *Daylight in Buildings*. 2000: International Energy Agency (IEA).

[5] Andersen, M., *Light distribution through advanced fenestration systems.* Builiding Research & Information, 2010. 30(4): p. 264-281

[6] Kämpf, J. and J.-L. Scartezzini Integration of BT(R)DF data into Radiance Lighting Simulation Programme, Technical Report Record Number Lausanne EPFL

[7] Kämpf, J. and J.-L. Scartezzini, *GERONIMO: the CFS Daylighting Wizard*, in *4th VELUX Daylight Symposium*. 2011: Lausanne, Switzerland.

[8] G. Ward, R.M., E. S. Lee, A. McNeil, J. Jonsson, *Simulating the Daylight Performance of Complex Fenestration Systems Using Bidirectional Scattering Distribution Functions with Radiance.* Journal of the Illuminating Engineering Society of North America, 2011

[9] America, I.E.S.o.N., *Lighting Handbook.* 2006, New York: IESNA.

[10] Edmonds, I.R., *Performance of laser cut light deflecting panels in daylighting applications.* Solar Energy Materials and Solar Cells, 1993. 29: p. 1-26

[11] Scartezzini, J.-L., et al. May 2000 Bi-directional photogoniometer for the assessment of the luminous properties of fenestration systems Record Number Lausanne EPFL

[12] Andersen, M., *Innovative bidirectional video-goniophotometer for advanced fenestration systems*, in *Architecture; Faculté Environnement Naturel, Architectural et Construit*. 2004, Ecole Polytechnique Fédérale de Lausanne: Lausanne, Switzerland.

[13] Tharin, J. Remise en état du Photogoniomètre Record Number Lausanne Ecole Polytechnique Fédérale de Lausanne, LESO-PB

[14] Thanachareonkit, A., *Comparing physical and virtual methods for daylight performance modelling including complex fenestration systems*, in *LESO-PB*. 2008, École Polytechnique Fédérale de Lausanne.

[15] IESNA, *IES Lighting Handbook, Reference Volume*. 1984: Illuminating Engineering Society of North America (IESNA).

ASSESSING LIGHTING APPEARANCE USING PICTURES: INFLUENCE OF TONE-MAPPING PARAMETERS AND LIGHTING CONDITIONS IN THE VISUALIZATION ROOM

C. Cauwerts[1]; M. Bodart[1]; R. Labayrade[2]

[1]*: Université catholique de Louvain (UCL), Architecture et Climat, Place du Levant 1 bte L5.05.02, B-1348 Louvain-la-Neuve, Belgium*
[2]*: Université de Lyon, Lyon, F-69003, France. Ecole Nationale des Travaux Publics de l'Etat (ENTPE), Laboratoire Génie Civil et Bâtiment, Rue Maurice Audin, F-69120, France*

ABSTRACT

Appearance of lit environments is often studied using pictures, both in lighting research and in architectural design context. With high dynamic range (HDR) imaging techniques and physically-based renderings, it is nowadays possible to reproduce or predict accurately real world luminances and so, to create images achieving a high level of physical realism. However, conventional displays are not able to produce the large range of luminances encoded in these HDR pictures and the dynamic range of the pictures should be compressed. Among the commonly used algorithms developed to realize that compression, the photographic tone-mapping operator gives satisfying results. However, this algorithm leaves to the appreciation of the user the setting of some important parameters whose key value, a parameter which greatly affects the overall luminosity of the picture.

This paper raises the question of the determination of the most appropriate key value for reproducing perceptions of light level, glare and contrast experienced in the real world. Influence of the lighting conditions in the visualization room is also discussed.

Three experiments are presented. The first two experiments compare perceptions of light level, glare and contrast experienced in four actual corridors with those experienced when visualizing pictures of the same rooms displayed on a conventional display. In the first experiment, the default key value of the photographic tone-mapping operator is used. In the second experiment, the key value minimizing the relative error between luminances extracted from the tone-mapped picture and from the HDR picture is determined. The third experiment evaluates the influence of the ambient light conditions in the visualization room.

The first two experiments show that, as expected, key value of the photographic tone-mapping operator greatly influences the perception of light level. But these experiments also highlight that the proposed method for determining the optimized key value has proved satisfactory. The third experiment shows that light level, risk of glare and contrast are perceived as being higher in a dark room compared to a lit visualization room.

Keywords: lighting perceptions, tone-mapping, key value, visualization conditions.

INTRODUCTION

This study is part of a wider research aiming at evaluating several modes of presentation of images (2D, 3D, HDR displays) for assessing lighting and space appearances of daylit rooms. In the frame of this study, questions linked to the choice of a tone-mapping operator, and to its setting, were raised. The impact of the lighting conditions in the visualization room was also questioned. This paper presents the results of three experiments. The first two experiments investigate the influence of the key value of the photographic tone-mapping operator which modifies the overall luminosity of the picture, as explained in [1]. The third

experiment evaluates the influence of the room lighting conditions on the perceptions of light level, glare and contrast.

METHOD

The first experiment took place in Louvain-la-Neuve (Belgium) in February 2012. Twenty-two students from the Faculty of Architecture at UCL were recruited. They were aged between 21 and 24 years (mean: 22.3 +/- 0.7 years). All the participants visited first the real rooms and then visualized the panoramic pictures captured in the rooms the day of the visit. Eleven days in average separated the visit of the actual rooms and their visualization on a conventional display. In order to minimize uncontrollable variations of natural light in the rooms during the experiment, the visit was organized around noon and by groups of five to six people. The visualization was individual. In average, the visit took 60 minutes while the visualization of pictures, about 45 minutes. Pictures of the actual rooms were realized at half the experiment in the real world, between the visit of the second and the third group, in order to capture the luminous ambiance experienced the day of the visit.

The second experiment was organized in March 2012, in the same rooms than those presented in the first experiment and following a similar procedure. In order to avoid the bias introduced in the first experiment and linked to the fact that all the participants visualized first the rooms and then the pictures, a first group of forty-three participants visited the actual rooms while another group of thirty-nine people visualized the pictures realized the day of the visit. All the participants were students from the Faculty of Architecture at UCL. They were aged between 18 and 25 years (mean: 21.6 +/- 1.5 years).

The third experiment was organized in December 2012, at ENTPE in Lyon (France). Forty participants were recruited among the students of the school of engineering. They were aged between 20 and 24 years (mean: 21.2 +/- 1 year). Participants visualized three tone-mapped pictures under two lighting conditions: a dark visualization room and an artificially lit visualization room (presenting luminances around the display similar to the average luminance of the displayed scenes). In order to reduce the bias linked to the order of lighting conditions, half the participants visualized first the images in the dark room and then in the lit room, and vice versa.

Rating scales

This paper discusses participants' perceptions of light level, glare and contrast assessed through the three following questions: (Q1) Corridor is: dim-bright, (Q2) Corridor is: comfortable-glaring, (Q3) Contrast in the corridor is: high-low. Participants responded to these questions on 6-grade scales.

Stimuli

In the first two experiments, participants rated actual rooms (corridors) and their pictures. In order to reduce the bias between real world room experiment and visualization of pictures, the point of view in the real rooms was fixed and identical to the picture point of view.

Figure 1 shows the rooms assessed in the three experiments.

Figure 1: Rooms rated in the first two experiments (4 rooms) and in the third one (3 rooms).

For the three experiments, pictures were realized using HDR imaging techniques to capture luminances of the actual rooms. Photographic tone-mapping operator [1] which according to [2, 3, 4] gives satisfying results was applied to reduce the dynamic range of these HDR pictures to those of the conventional display.

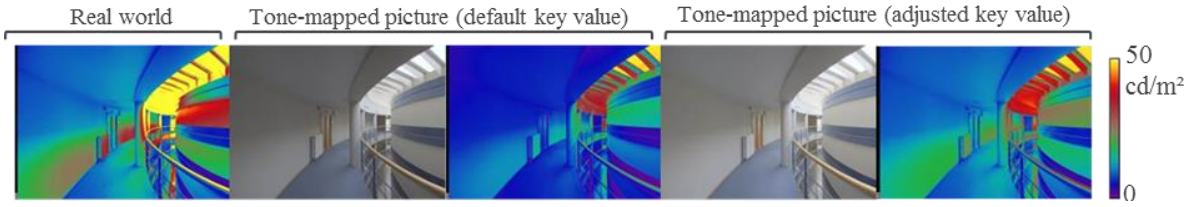

Figure 2: Influence of the key value (exp2-room1)

Default key value was used for the first experiment. For the second and third experiments, rather than working with default parameter, the key value minimizing relative error between real world luminances and luminances extracted from the tone-mapped image was determined. Mean maximum luminance and mean minimum luminance of the monitor were first measured. On the basis of these values, luminances of the tone-mapped image were then calculated. Relative error between real world luminances and tone-mapped luminances was determined at each pixel. Finally mean relative error for the entire picture was calculated. The key value minimizing this error was determined using an iterative process. The influence of the key value on the overall image luminosity is illustrated in Figure 2.

RESULTS

Statistical analyses were performed using R software [5].

Figure 3 presents, for the first experiment, mean ratings for each question, collected in the real world and when the same participants visualize pictures.

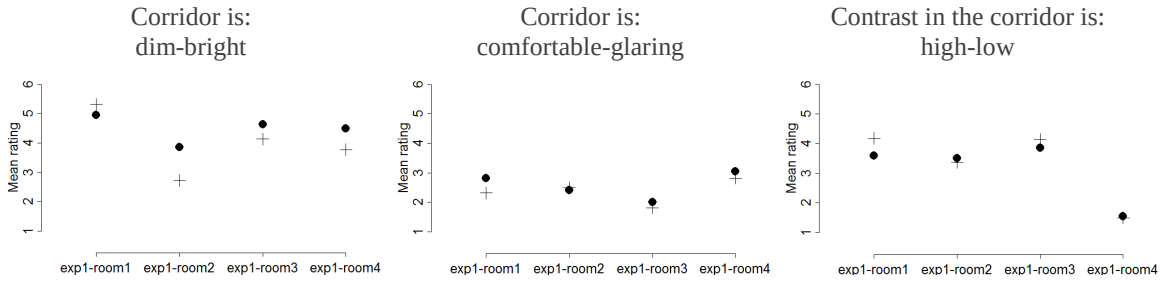

Figure 3: Experiment 1(default key value). Mean ratings. (+ Real world ● Picture)

A two-way ANOVA with a repeated measure on one factor (room) was performed on the collected data to test the effect of presentation mode on perceptions of light level, glare and contrast. As shown in Table 1, for the question related to light level (Q1), a significant interaction (presentation mode x room) was detected which indicates that the effect of presentation mode varies according to the room.

	Presentation mode	Room	Presentation mode x Room
Q1	F=28, p=3e-05 ***	F=25.86, p=1.8e-09 ***	F=8.54, p=7.7e-05 ***
Q2	F=2.68, p=0.12	F=6.98, p=0.00039 ***	F=0.905, p=0.4330
Q3	F=1.4058, p=0.2490	F=42.93, p=3.1e-15 ***	F=1.7020, p=0.1756

* = p≤ 0.05; ** = p≤ 0.01; *** = p≤ 0.001

Table 1: Results of the ANOVA performed on data collected in the first experiment.

Questions related to glare (Q2) and contrast (Q3) present neither interaction effect nor significant effect of presentation mode.

Analyses of variance were repeated on each room separately in order to determine the effect of presentation mode on perceived light level. P-values for significance were adjusted using a Bonferroni correction. These analyses indicate that two rooms are perceived as significantly brighter on the basis of pictures (room#2: $F=22.44$, $p<0.001$***; room#4: $F=19.77$, $p<0.001$***).

In the second experiment (adjusted key value), similarity of mean profiles is observed for the first question between ratings from the real world experiment and those from the picture visualization (see Figure 4).

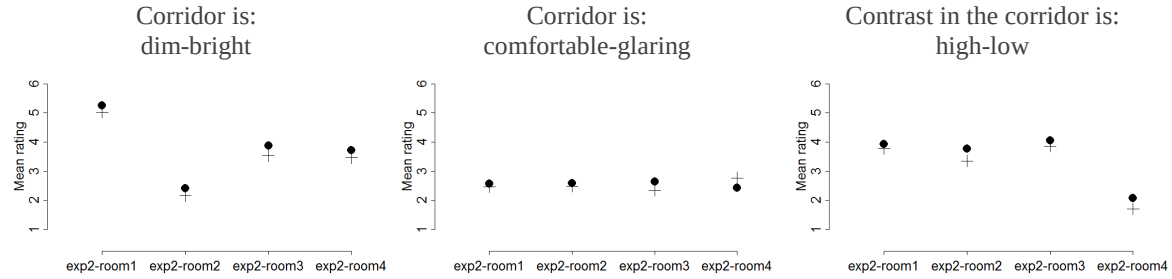

Figure 4: Experiment 2(adjusted key value). Mean ratings. (+ Real world ● Picture)

An analysis of variance was realized on the collected data to determine if the effect of presentation mode on the perceptions is significant. In order to better take into account that subjects are a random sample of a population, a mixed model analysis was performed. The fixed effects are the mode of presentation and the room. Subjects are treated as random-effect variable. The AIC criterion was used to judge whether adding interaction between mode of presentation and room improves the model [6]. The smaller the AIC, the better the fit, the preference is for the model without interaction. Results of the mixed model analysis are presented in Table 2.

	Estimate	MCMCmean	HPD95lower	HPD95upper	pMCMC	Pr(>|t|)
Q1	0.2676	0.2672	0.0381	0.4726	0.0158	0.0145 *
Q2	0.0392	0.0382	-0.2025	0.2713	0.7458	0.7804
Q3	0.2745	0.2764	-0.0174	0.5414	0.0588	0.0943

* = $p \leq 0.05$; ** = $p \leq 0.01$; *** = $p \leq 0.001$

Table 2: Results of the mixed model analysis performed on data of the second experiment.

The analysis reveals that all the rooms are judged as significantly brighter on the basis of images. No significant difference is observed between the two modes of presentation for perceptions of glare and contrast.

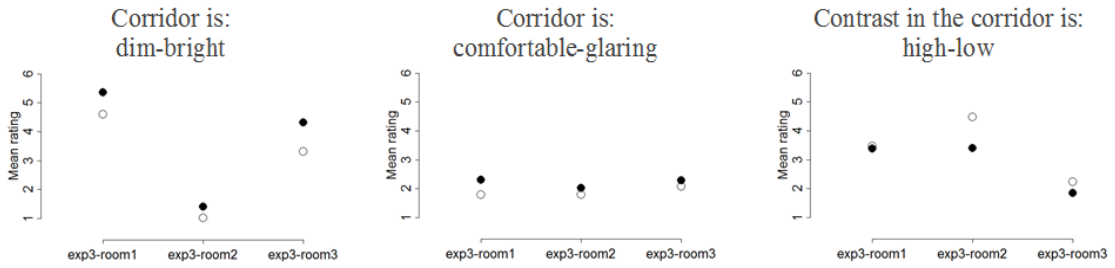

Figure 5: Experiment 3 (lighting conditions). Mean ratings. (○ Lit room ● Dark room)

Figure 5 presents mean ratings for the third experiment. As expected, the ambient light conditions in the visualization room influences perceptions, in average.

A two-way ANOVA with a repeated measure on two factors (lighting conditions and room) was performed on the collected data (see Table 3). A main effect of the lighting conditions was detected for the question related to glare (Q2): the rooms are perceived as being slightly more glaring when viewed in the dark. Interaction effects were observed for the questions related to light level and contrast (Q1 and Q3). ANOVA's performed on each room separately revealed a significant effect of the lighting conditions in each room (Room#1: F= 24.718, p=4.11e-05***; Room#2: F= 16.402, p=7.07e-04***; Room#3: F=35.286, p=2.06e-06***; p-values for significance were adjusted using a Bonferroni correction).

	Lighting conditions	Room	Lighting conditions x Room
Q1	F=77.2, p=1.1e-10 ***	F=363.5, p<2.2e-16 ***	F=5.54, p=0.0077***
Q2	F=6.20, p=0.0185 *	F=0.93, p=0.40	F=0.59, p=0.56
Q3	F=8.89, p=0.0057 **	F=21.91, p=2.5e-06 ***	F=3.14, p=0.05 *

* = p≤ 0.05; ** = p≤ 0.01; *** = p≤ 0.001

Table 3: Results of the ANOVA performed on the data collected in the third experiment.

At last, a significant effect of the lighting conditions on the perception of contrast (Q3) was observed in the second room which is the darkest corridor (Room#2: F=19.022, p=2.75e-04***).

DISCUSSION

Influence of the key value

In the first experiment, three rooms were perceived as being brighter on the basis of pictures than in the real world. One room was perceived as being dimmer than in the real world. In the second experiment, similar mean profiles were observed between real world and pictures. But mixed model analysis detected a significant over-evaluation of the perceived light level on the basis of pictures in comparison to real world. These two experiments show that, as expected, perception of light level is widely influenced by the choice of the key value. These two experiments have also shown that perception of light level experienced in the real world is better reproduced using the adjusted key value rather than the default parameter. But the observed over-evaluation of light level suggests than the key value could also be adjusted according to the lighting conditions in the visualization room.

Influence of lighting conditions in the visualization room

The third experiment highlighted the influence of lighting conditions in the visualization room on perceptions of light level, glare and contrast. Rooms were perceived as brighter and more glaring when assessed in the dark room than in the lit one. The second room (the darkest one) was perceived as presenting a lower contrast when viewed in the lit visualization room.

HDR pictures of the monitor displaying each room in each lighting condition were realized. On the basis of these HDR pictures, mean luminance, ratio of mean luminance to background luminance and local contrast were calculated. These measurements, presented in Figure 6, match with our observations. Mean luminance of the pictures increases in the lit room, influencing the perception of light level. Contrast between the picture displayed on the monitor and its background is higher in the dark room, increasing risk of glare. And

finally, local contrast in the second corridor (the darkest) is strongly reduced when the visualization room is lit.

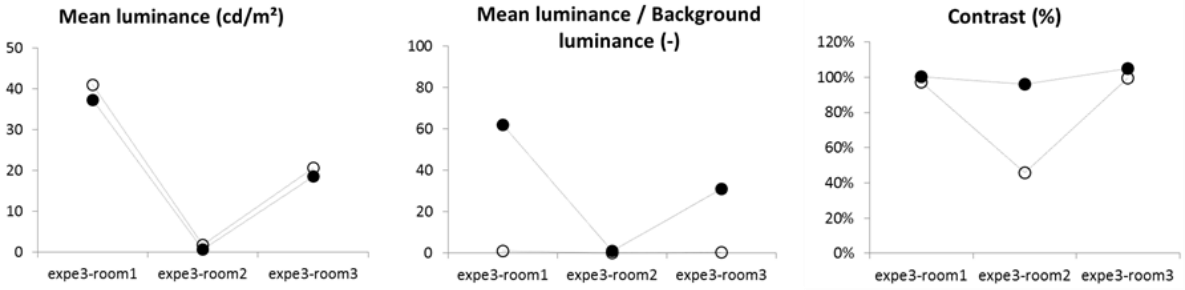

Figure 6: Influence of room lighting conditions on physical measurements (○ Lit ● Dark).

CONCLUSIONS

The first two experiments show that key value of the photographic tone-mapping operator greatly influences perception of light level. Our method for determining the key value based on the minimization of the relative error between luminances of the HDR picture and luminances of the tone-mapped picture has proved satisfactory. However, the method should be repeated on a wider range of rooms to be validated.

At last, the third experiment shows that lighting conditions in the room of visualization also influence perceptions of light level, glare and contrast. Working in a dark room increases perceived light level, risk of glare and contrast in comparison with working in a lit visualization room.

Finally, to reproduce, using pictures, perceptions of light level, glare and contrast experienced in the real world, the work should continue in determining the best key value according to the lighting conditions in the room.

ACKNOWLEDGEMENTS

This work was partly supported by the Belgian Research National Foundation (FNRS). The authors also thank students who have participated in the experiments.

REFERENCES

1. Reinhard, E., Stark, M., Shirley, P. & Ferwerda, J. Photographic tone reproduction for digital images. ACM Transactions on Graphics (TOG), 21-3, pp 267-276, 2002.
2. Cadík, M., Wimmer, M., Neumann, L. & Artusi, A. Evaluation of HDR tone mapping methods using essential perceptual attributes. Computers & Graphics, 32-3, pp 330-349, 2008.
3. Ledda, P., Chalmers, A., Troscianko, T. & Seetzen, H. Evaluation of tone mapping operators using a high dynamic range display. ACM Transactions on Graphics (TOG), 24-3, pp 640-648, 2005.
4. Yoshida, A., Blanz, V., Myszkowski, K. & Seidel, H.-P. Perceptual evaluation of tone mapping operators with real-world scenes. Proc. SPIE 5666, Human Vision and Electronic Imaging X, pp 192-203, 2005.
5. R Development Core Team. R 2.11.1. 2010.
6. Pinheiro, J. & Bates, D. Mixed effects models in S and S-PLUS. Springer, New York, 2000.

INVESTING IN BUILDING ENERGY RETROFITS FOR ECONOMIC, ENVIRONMENTAL AND HUMAN BENEFITS – THE TBL

R. Srivastava; V. Loftness; E. Cochran

Carnegie Mellon University, 5000 Forbes Avenue, Pittsburgh, PA 15213, USA

ABSTRACT

The combination of net present value (NPV) and return on investment (ROI) calculations are critical for overcoming first-least-cost decisionmaking patterns that prevent owners and tenants from investing in high performance low-cost retrofits. While the 5-15 year energy payback analyses alone could be sufficient to prompt greater investment, the addition of triple bottom line (TBL) calculations that capture the economic, environmental and human cost benefits (also described as profit, planet and people) make the life cycle arguments significant. The challenge is the quantification of environmental gains and human factors, including health, productivity, and organizational performance. This paper focuses on strategic electric lighting retrofits, given that lighting energy is over 30% of site and source energy loads in commercial US buildings and in critical need of upgrading specially with the changing nature of work. For each lighting retrofit options – installing vacancy sensors; daylight harvesting controls; DALI controls and vertically integrated LED lighting controls, the first cost per employee (employees being the critical unit of health and productivity) was evaluated against the 15-year life-cycle benefits in a TBL calculation.

The first bottom line relates to the known cost-benefits of energy and facility management savings resulting from the retrofit. The second bottom line relates to the environmental cost-benefits that are directly linked to electric energy savings: reductions in CO_2, SO_X, NO_X, particulates, and water, and could include peak power shaving (capacity cost-savings). The third bottom line relates to the human cost benefits that are directly linked to improved lighting quality for today's predominantly computational work tasks, as well as a number of other human benefits identified from laboratory and field studies. In addition to iterative and cumulative NPV calculations, ROI and simple paybacks were calculated to provide professionals and manufacturers compelling arguments for inspiring investment in energy retrofits that will improve the quality of the indoor environment for workers. The analyses reveal ROIs between 15 to 350%, and show installation of vacancy sensors for closed spaces had the highest ROI when the economic and environmental impacts alone were considered. The human health and productivity benefits of lighting energy retrofits, establish a different set of investment priorities. In this case, any action that increases daylighting or simulated daylight patterns with electric lighting yields the highest ROI.

Keywords: Triple bottom line, Lighting controls, Life Cycle

INTRODUCTION

Analysis of the commercial building stock in the Mid-Atlantic and Northeast region of the U.S reveals that lighting consumes more than 30% of the building's source energy demands, generating the highest energy costs in offices, and the second largest site energy load after heating [1]. The CBECS data base of measured energy use and the attributes of over 450 representative US buildings offer additional explanations for why lighting loads are so high in commercial buildings and the current conditions. Less than 1% of the buildings surveyed in CBECS have sensors or automatic controls for their lighting. 60% of office buildings were found to be lit when unoccupied after business hours, a statistically significant factor for

Lighting Energy Use Intensity (EUI) for entire set of buildings ($p < 0.0001$) and 20% of the predominantly recessed fluorescent fixtures are still using T-12 lamps with magnetic ballasts.

Findings from several post occupancy evaluations in commercial office buildings completed by Carnegie Mellon University's Center for Building Performance and Diagnostics (CBPD) reveal a wealth of significant arguments for office lighting retrofits, including the dominance of lighting loads in office buildings, the age and poor performance of the lighting systems, the poor utilization of daylight, and the human benefits from improving lighting quality for today's predominantly computational work tasks.

Four TBL studies are summarized in this paper, focused on strategic retrofits for lighting control that can save upto 85% of the lighting energy in conventional US offices. Along with NPV calculations, ROI and simple paybacks were calculated for each of the lighting control actions to provide professionals and manufacturers with compelling arguments for investment in energy efficient retrofits.

FRAMEWORK FOR ANALYSES

The CBPD made a decision to complete cumulative NPV and ROI calculation for the selected lighting controls. The United Nations ICLEI Triple Bottom Line standards (2007), in which benefits are categorized in one of three categories relating to the three E's (1) Economic (2) Environmental (3) Equity, also often discussed as the three P's (1) Profit (2) Planet and (3) People was used as the framework. For each of the lighting retrofit option, the first cost per employee (the critical unit of health and productivity) was evaluated against the 15-year life-cycle benefits in a TBL calculation.

The first bottom line calculations include the hard **economic** cost-benefits of energy and facility management savings resulting from each of the four retrofit actions, with ROI's ranging from 15 to 52%. The cost of energy was set at \$0.103/kwh, the average all-inclusive commercial fixed rate in the U.S. [2].

The second bottom line calculations capture the **environmental** cost-benefits that are directly linked to electric energy savings: reductions in CO_2, SO_X, NO_X, particulates, and water demands. CMU's CBPD has undertaken a multi-year effort to build baselines on the environmental benefits of electric energy savings. CO_2, SOx, NOx, PM are four pollutants that represent a majority of the environmental damage from burning fossil fuels to generate electricity [3]. In addition to global warming, these pollutants cause respiratory illness, cancers, and developmental impairment.

The third bottom line relates to the **human** (i.e. equity) cost-benefits that are directly linked to improved lighting quality. The human benefits associated with each recommendation have been drawn from the ongoing work of the CBPD captured in the BIDS tool that aggregates research linking the quality of buildings to health and productivity and reduced absenteeism outcomes[4]. The specific research findings that have been included, include gains in human health, productivity, and reduced absenteeism.

The life-cycle benefits of each of the recommendations have been calculated in three successive "return on investment" groups to offer decision-makers the choice of where they are willing to draw the line, with: 'hard' economic cost benefits in the first bottom line; environmental cost-benefits that may be legislated or incentivized in the second bottom line; and the human cost-benefits that should drive standards and investments in buildings in the third bottom line.

FOUR LIGHTING CONTROLS TBL STUDIES

Identification of lighting control strategies is based on a number of efforts by the research team. In-depth investigation of existing U.S commercial building stock was undertaken to find critical factors that contribute to a high energy use index (EUI): percent of office lit when unoccupied; and the rarity of lighting automation (less than 1%) [1]. The CBPD has completed several building post occupancy evaluations (POE) in commercial buildings and federal workplaces over two decades and identified lighting and daylighting as two significant retrofit actions for buildings[5]. In 2010, the CBPD contributed to a two year controls research project with Siemens Corporate Research funded by the US Department of Energy, which identified a range of lighting system investments that can save upto 70% energy.The control strategies discussed in this paper, are part of a 2012 research project completed by CBPD for the Department of Energy's EEBHub, an energy innovation hub led by the Penn State University. The team developed economic, environmental and human cost-benefits of investing in energy efficient lighting building components and integrated systems as part of the project.

For each retrofit, investment costs as well as performance benefits were identified. Costs were collected from both the literature and from direct communications with manufacturers and professionals who specify lighting components and systems. The team collected average technology and labor costs for each retrofit recommendation, assuming a medium size office of 100,000 square feet on 3-5 floors with 500 employees. Energy saving calculations are based on Mid-Altantic CBECS average energy use of 6.8 kWh/sqft for the annual lighting energy [1]. For the benefits, an extensive literature review was undertaken to identify lab and field studies that statistically linked lighting quality with energy, facility management benefits, and human health and productivity. Selected studies that link high performance lighting solutions to outcomes are employed in the TBL calculations. The selected recommendations listed from lowest first cost to highest are described below along with the ROIs, payback periods and an example field/laboratory study used in the calculations.

1. Install occupancy/vacancy sensors for closed spaces.

The lowest cost high payback lighting retrofit action for building owners and managers is to install occupancy sensors in all closed spaces on the occupied floor. These spaces include closed offices, conference rooms, copy rooms, bathrooms, and storage areas, and account for over 25% of the floor area in most office buildings. Occupancy sensors can be used as "vacancy sensors" to turn off lights when no presence is detected, while avoiding automatically turning lights on in daylit spaces. Vacancy sensors and switches can be installed without full automation systems, making them cost effective retrofits for all closed spaces, and even stairwells (where allowable by law) to save up to 50% lighting energy in 25% of the office spaces [6].

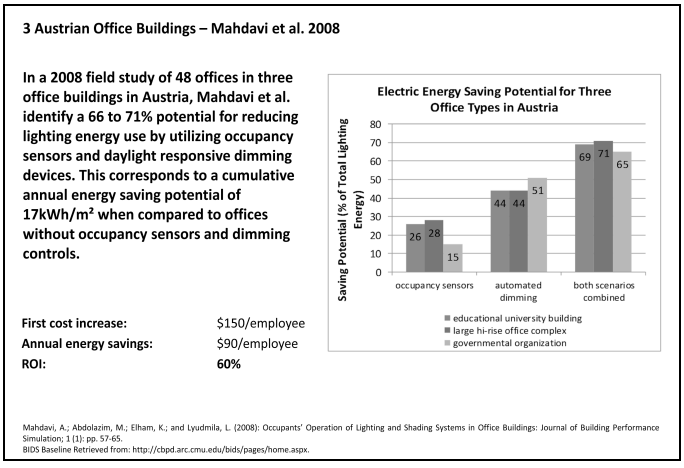

***Figure 1**:Occupancy sensors & dimming devices save energy*

	Profit	Planet	People
ROI	52%	68%	n/a
Payback	2 years	1.5 years	n/a

2. Install daylight harvesting for perimeter lights.

The second cost-effective retrofit action for lighting energy savings is the installation of daylight sensors for on/off or dimming controls of the first and second rows of lights on each building facade. This modest investment in new controls for groups of lights ensures up to 35% energy savings through 'daylight harvesting', savings that are possible even in large, deep buildings with windows [7].

Daylight sensors can be installed without full automation systems, and can be introduced with wireless interfaces to existing fixtures, making them cost effective retrofits. Critical attributes for selection of daylight sensor include: programmable thresholds for acceptable daylight minimums, relocatable sensors to address variations in office layout, and assurance of gradual light level changes through dimming or time limited switching.

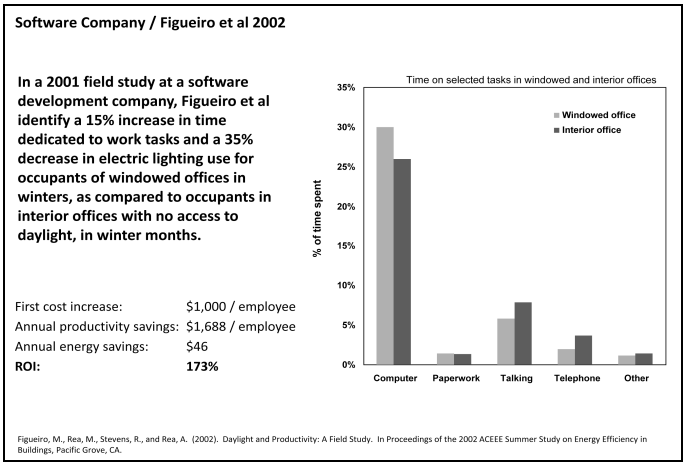

***Figure 2**: A field study shows 15% increase in productivity and energy savings due to daylighting*

	Profit	Planet	People [8]
ROI	21%	28%	354%
Payback	4.5 years	3.5 years	9 months

3. Install individually addressable ballasts with lighting automation system.

Third retrofit strategy for upto 65% energy savings is to invest in individually addressable dimming ballasts combined with automated lighting control systems. DALI controls (Digital Addressable Lighting Interface) combine digitally addressable ballasts with distributed controllers for 2-way communication between occupants and building automation systems for local lighting control. This strategy can bring operating lighting power densities below 1 watt per square foot; create ambient lighting levels appropriate for computer work; maximize daylighting; maximize occupancy/vacancy control of unoccupied spaces; give controls back to occupants.

The quality of the ballasts is critical, it needs to be continuous dimming from 100-10-off, with energy use profiles that match dimming profiles and no parasitic energy demands when off.

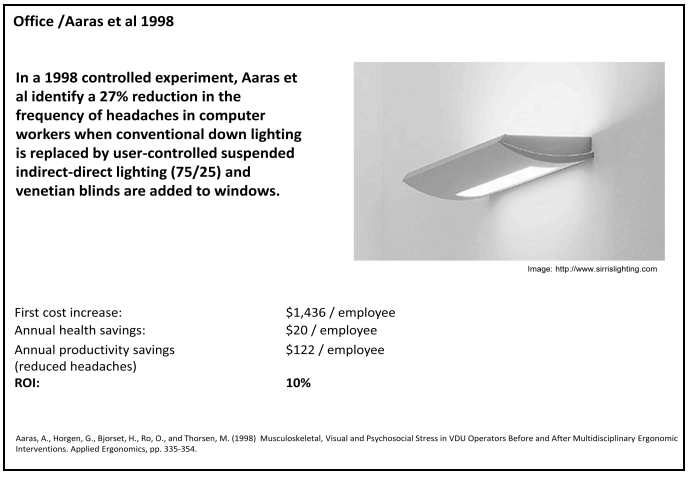

***Figure 3:** A controlled experiment reveals that user controlled lighting reduces headaches amongst workers*

	Profit	Planet	People [9]
ROI	15%	19%	260%
Payback	7 years	5 years	10 months

4. Install LED light fixtures with dimming and IP addressable controls.

The final lighting retrofit recommendation is to invest in high performance fixture upgrades that include replacement of existing 2'x4,' 1'x4,' or 2'x2 ' troffers containing between two to four T12 or T8 lamps with "vertically integrated" LED light fixtures (lamp, ballast, fixture) with add-ons for dimming and IP controlling. Carefully specified LED lamp sources can save upto 85% lighting energy, and significant environmental and human benefits.

When selecting LED light sources, it is important to specify: lamp efficacy, measured in lumens per watt, as well as the correlated color temperature and the color rendition index of the LED sources. While CRI above 80 (on a 100 point scale) is considered acceptable for interior applications, CRI's above 90 provide the excellent color quality we have come to expect from incandescent lamps.

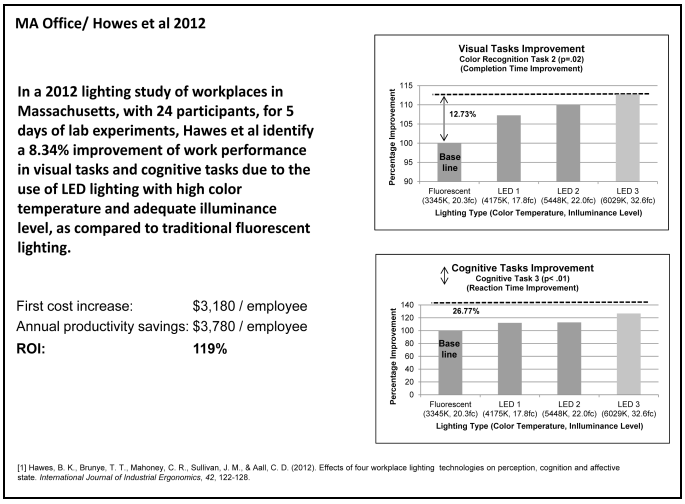

***Figure 4**: High color temperature LED lighting improves individual productivity*

	Profit	Planet	People [10]
ROI	18%	22%	300%
Payback	5 years	4.5 years	2 months

FINDINGS

The installation of vacancy sensors in closed offices, conference rooms, toilets and shared spaces has the highest ROI, followed by daylight harvesting for perimeter lights when "hard"economic benefits are considered. The environmental benefits of reducing electricity use for lighting in our calculations mirror the energy benefits, so the priorities remain the same. Adding the human health and productivity benefits of lighting retrofits, however, establishes a very different set of investment priorities (Figure 5). In this case, any action that increases daylighting, or simulates daylight variability with electric lighting, yields the highest ROI when triple gains of energy, environmental and human benefits are considered.

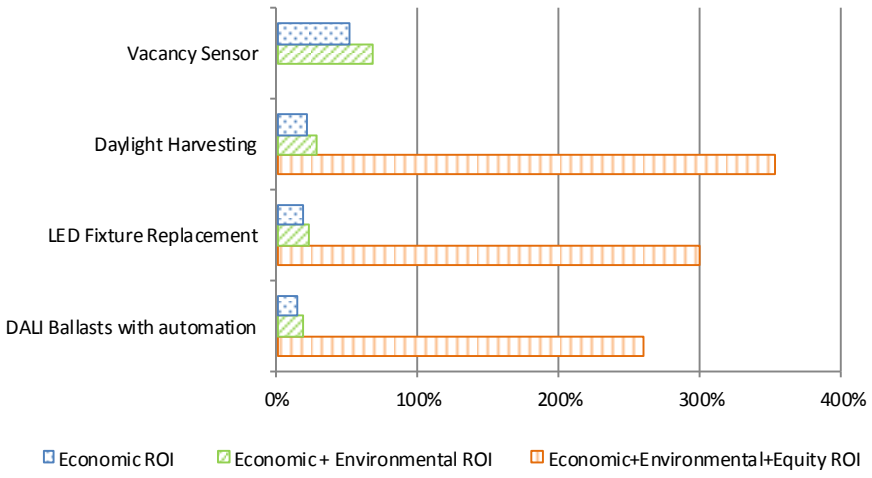

***Figure 5:** Lighting retrofit priorities based on economic, environmental and human cost-benefits*

CONCLUSION

Lighting is the most strategic investment for conserving energy and for improving the quality of visual conditions for task performance and human health. The prioritization of investments will depend significantly on the condition of the existing lighting and daylighting assemblies, the ability to invest based on NPV (carrying costs) rather than first cost, and the commitment to environmental and human cost-benefits as well as the "hard" energy cost benefits.

The addition of environmental benefits accelerate payback of the investment, and can be monetized if the organization is required to meet energy reduction goals for city, state or federal mandates; or the organization has made sustainability a centerpiece of their market growth. The addition of environmental and human factors including health, productivity, and organizational performance will be useful for professionals and manufacturers who seek compelling arguments for inspiring investment in energy retrofits that also have the potential of improving the quality of indoor environment for workers.

ACKNOWLEDGMENT

This work was performed under the US Department of Energy's Energy Efficient Buildings Hub led by Penn State University and located at the Navy Yard in Philadelphia, Pennsylvania.

REFERENCES

[1] EIA.(2003).*Commercial Building Energy Consumption Survey*. U.S. Department of Energy.

[2] EIA. (2012). September 2012 Monthly Energy Review (2011 data). EIA.

[3] Kats, G., & Capital, E. (2003). The Costs and Financial Benefits of Green Buildings. California: California's Sustainable Building Task Force.

[4] CBPD. (2008). *BIDS - Building Investment Decision Support Tool*. Retrieved from http://cbpd.arc.cmu.edu/bids/login.

[5] GSA. (2009). *Energy Savings and Performance Gains in GSA Buildings Seven Cost Effective Strategies.* GSA Public Buildings Service

[6] Mahdavi, A.; Abdolazim, M.; Elham, K.; and Lyudmila, L. (2008): Occupants' Operation of Lighting and Shading Systems in Office Buildings: Journal of Building Performance Simulation; 1 (1): pp. 57-65.

[7] Verderber, R., and Rubinstein, R. (1984) Mutual Impacts of Lighting Controls and Daylighting Applications. Energy and Buildings 6:2, pp. 133-140.

[8] Figueiro, M., Rea, M., Stevens, R., and Rea, A. (2002). Daylight & Productivity: A Field Study. Proceedings 2002 ACEEE Summer Study on Energy Efficiency in Buildings, CA.

[9] Aaras, A., Horgen, G., Bjorset, H., Ro, O., and Thorsen, M. (1998) Musculoskeletal, Visual and Psychosocial Stress in VDU Operators Before and After Multidisciplinary Ergonomic Interventions. Applied Ergonomics, pp. 335-354.

[10] Hawes, B. K., Brunye, T. T., Mahoney, C. R., Sullivan, J. M., & Aall, C. D. (2012). Effects of four workplace lighting technologies on perception, cognition and affective state. International Journal of Industrial Ergonomics, 42, 122-128.

“DOOR – WINDOW” DAYLIGHTING EVALUATION IN TRADITIONAL HOUSES OF IRAN

Mansoureh Tahbaz, Shahrbanoo Djalilian, Fatemeh Mousavi

School of Architecture, Shahid Beheshti University, Iran

ABSTRACT

In Middle East, Iran is one of the places with lots of daylight all year round. Because of its long term civilization history, Iranian traditional architecture has seen a great amount of daylighting experiences, including 6 daylighting systems with 20 kinds of wall and ceiling windows [1]. One of them, called “door – window”, is the most common used in different places such as halls and their adjacent rooms in traditional Houses in all parts of Iran. Uncover the daylighting design principles used in this kind of window is the subject of this article.

To achieve this aim, “Ameri House Complex” in Kashan with an appropriate diversity of rooms and spaces has been chosen as a case study [2]. In days during May, July and Jan of 2011-12, the field study was performed to gather all needed daylight data from 13 different chosen rooms of this house. The illumination data were gathered on the roof (as the reference point) and inside the rooms. Data such as the reflectance of the interior surfaces, the dimensions and other properties of the rooms were recorded as well.

Subsequently, using the criteria and calculating methods introduced in handbooks of lighting and daylighting, all the information were analyzed in four steps of: room specification and geometry, neighbourhood condition, analyzing the field data and the illumination distribution of each room in a pattern year that was simulated using Radiance Software.

The results showed that in Ameri House - as a sample of traditional houses in hot arid climate of Iran - daylighting design was performed in 4 levels. 1) Neighbourhood conditions to have at least 40-degree “visible sky angle” for the main spaces. 2) Specification of the main spaces and their adjacent rooms to have the best view and daylighting condition. 3) Depth and geometry of the rooms and details of the windows to help appropriate visual uniformity or diversity of illumination according to the function of the room.

Keywords: door – window, Useful Daylight Illuminance (UDI), Perimeter Zone, No sky line

INTRODUCTION

The aim of this research is to evaluate daylighting system of door-windows in the different rooms of a traditional house of Iran. Ameri House Complex in the middle of Iran next to the desert is chosen as a case study. Kashan has very bright sky illumination and arid-hot climate in summer and cold sunny winters [3].

Through field photometry at various sites of the house, the study attempts to illustrate the lighting condition at door-window rooms from the following aspects: the extent of interior lightness, interior light distribution and glare control during the year from physical aspect of lighting. Since natural lightness could be evaluated by visual lightness and visual interest [4, 5, 6], investigating the features from this view would determine the best activity for each site [7]. The correspondence between sites proximity, geometry, place and shape of skylights and its attachments and interior lightness from visual lightness and visual interest point of view is a subject which could inspire designers in natural lighting in contemporary architecture.

RESEARCH METHODOLOGY

"Ameri House Complex" in Kashan with 7 yards, 85 rooms in different sizes such as "3-door room", "5-door room", "7-door room" and halls located in north, south, south east and south west directions, has been chosen as a case study for this research. In some days during spring (25-26 May) and summer (12 July) of 2011 and winter (12 Jan) 2012, the field study was performed to gather all needed daylight data from 12 different chosen rooms of this house. (Fig 1)

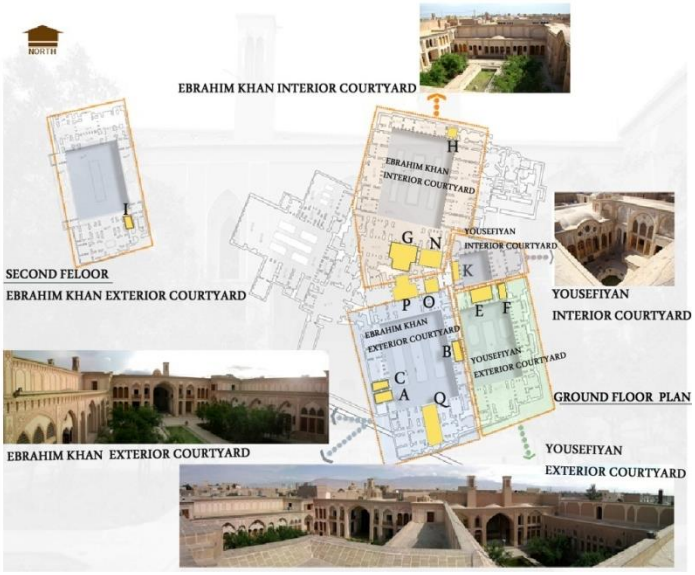

Figure 1: 13 selected rooms of Ameri house in Kashan

A digital Lux meter data logger [8] was used to gather the illumination data on the roof as the reference point. A simple Lux meter [9, 10] was used to measure the illumination data inside the rooms in a mesh of 60*60 cm in the height of 70 cm as the reference plane. A color analyzer [11] was used to determine the reflectance of the interior surfaces as their RGB color. The exact size, dimension and the ceiling shape of each room were measured by a digital 3D meter [12].

Other properties of selected rooms such as its location in the House, its geographic orientation, its place in the yard and so on are shown in the information table of each room such as Fig 3. The location of the window in the room wall, ratio of the window area to the room area, ratio of the window glazed area to the frame area, and other details such as the materials, colours and shapes of the frame and glazed part of the window are presented as well. To predict the illumination inside the selected rooms, the collected data where analyzed as the illumination contours by excel program in the observation days. To expand the results to a whole year, simulation was performed by radiance software. True color and false color pictures of light distribution in each room was illustrated in three times of the day at 9 am for morning, 12 pm for noon and 15 pm for afternoon condition. (Fig 2)

Using the criteria and calculating methods introduced in lighting and daylighting handbooks, all the information were analyzed in four steps:

1- Room specification and geometry: By calculating "Room Index", "Room Depth Criteria", "Perimeter Zone" and "Orientation Factor" of the room. The "Room index" is calculated by equation 1 where L is the room length from window to the end of the room, W is the room width parallel to the window surface, H is the height of the window from the floor, R_b is mean reflectance of the room surfaces [13].

$$\text{Room Index} = \frac{L}{W} + \frac{L}{H} \leq \frac{2}{1-R_b} \qquad (1)$$

The "perimeter zone" is predicted according to the room dimension and height of the window [14]. The "orientation factor" of the window is calculated by equation 2 where E_s and E_{out} are

indoor and outdoor illumination respectively, F_o is the orientation factor and df_{min} is the minimum daylight factor inside the room [15].

$$E_s = E_{out}(f_o \times df_{min}) \quad (2)$$

2- Neighbourhood condition: by drawing "No Sky Line" area, "Visible Sky Angle" in section and façade and "sky Mask" of the window. "No sky line" is shown in the section of the room and the sky line of the opposite façade in front of the window [13, 7]. "Visible sky angle" in section is determined as vertical section of the room for a window located in a canyon [13]. In traditional houses of Iran the room is located in a central yard. Here the "visible sky angle in façade" of the room toward the yard is determined to find out the "sky mask" of the window [16]. This information will show how much the room is benefiting from sky light.

3- Analyzing the field data: by drawing the "Illumination" contours in plan (on the reference height) and section of each room using the collected data in spring, summer and winter. 4- The illumination condition of each room in a whole year that was simulated using Radiance Software. In steps 3 and 4, the data were analyzed by "Useful Daylight Illuminance (UDI)" [17,18]. It shows the percentage of the room area which is in "UDI Achieved" (100-2000 Lux), "UDI Autonomous" (300-2000 Lux), "UDI Supplementary" (100-300 Lux), UDI Exceeded" (> 2000 Lux), and "UDI Fell-Short" (< 100 Lux) in different months of the year in 9 am as morning, 12 pm as noon and 3 pm as afternoon. (Fig 2)

At the end, the "Uniformity Ratio" of Illumination in each room was calculated to determine the variation of the light pattern in two conditions of closed and open "door – window". It shows that according to "visual amenity", door - window daylighting system will be suitable for "visual interest" by 0.3 – 0.5 and "visual acuity" by 0.6-0.7 "Uniformity Ratio" with regards to the function of the places [7]. "Uniformity ratio" is calculated by equation 3 where U_o is the uniformity ratio, E_{min} is the minimum illumination and E_{Ave} is the average illumination inside the room. [19]

$$U_o = {}^{E_{min}}/_{E_{Ave}} \quad (3)$$

INFORMATION ANALYSIS

The information of each room and its interpretation are shown in tables that one of them is presented here as a sample for the room G (Fig 2). The other 12 tested rooms (A, B, C, E, F, H, I, K, N, O, P and Q) in this research have the same detail analysis presented in the main research report. [20]

Room G: definition and geometry

Room G is a combination of two squares of 5.37X3.33 and 9X4.37 meters and the doom ceiling with height of 8.40 that is located in the south part of one of the large yards of Ameri Hosue, face toward the north. The windows toward the yard are in the larger side of the room with a combination of an "orosi" of 3door-windows with a tall head with colored glass, two doors in two sides and 3 small circle windows in the top of the wall. The greatest height of the window is 4.21 meters. This room has other windows toward its adjacent rooms in both sides that present indirect light. The ceiling is covered by some decorative mirrors that can reflect the light.

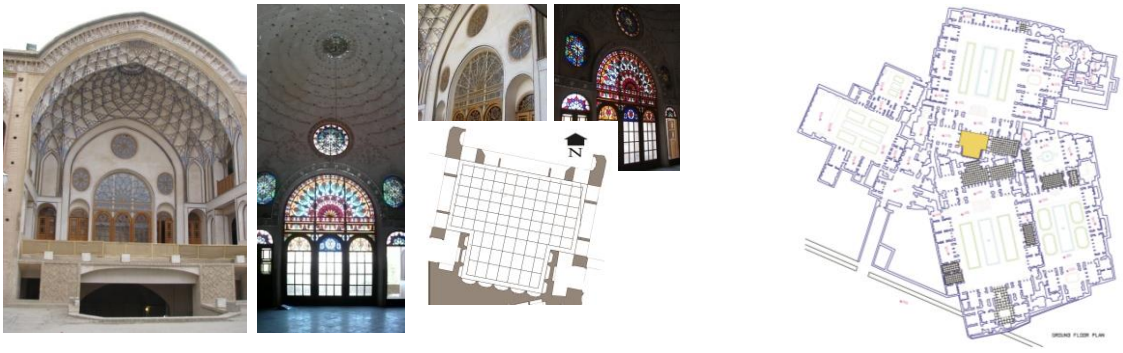

Room G: Neighborhood condition

Visible sky angles in section and façade are 51◦ from 90◦ and 121◦ from 180◦ respectively. It means that 15% of skylight is receiving to it from sky hemisphere. In all parts of the room from floor to the height of 2.30 meters sky light is available from the Orosi door-windows. The perimeter zone of the room is 7-11 meters for the short and long depth of the room (4.90-8 meters) respectively. It shows that the depth of the room and its geometry is appropriate to prepare enough daylight from skylight.

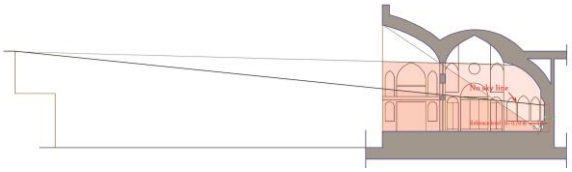

No sky line area

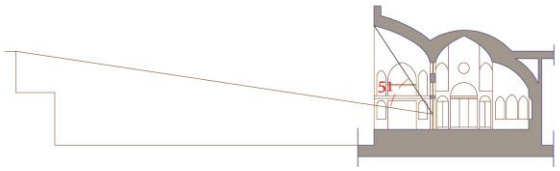

visible sky angle in section

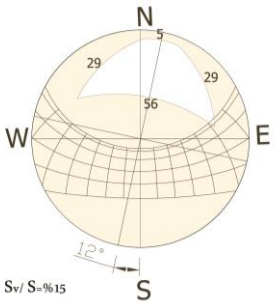

Sky mask

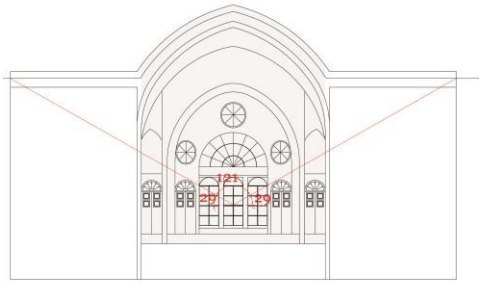

visible sky angle in facade

Room G: Field data analysis

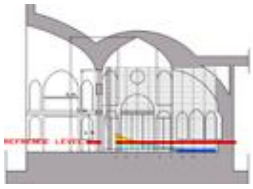

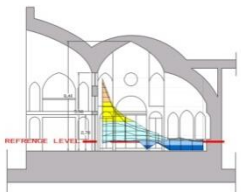

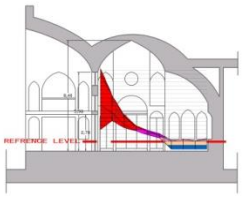

Legend of the illumination contours

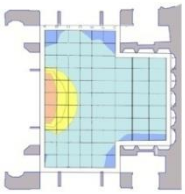

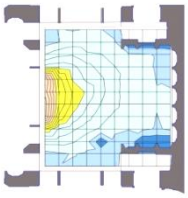

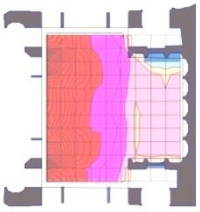

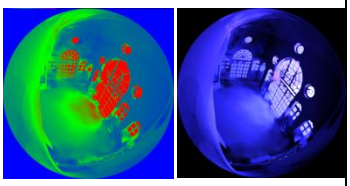

Day: 26 May 2011
Time: 2:10-2:50 pm
Reference light on roof: 75-85 Klux
Room temperature: 22 C
Room humidity: 40%
Closed windows

Day: 12 July 2011
Time: 5:25-5:40 pm
Reference light on roof: 56 Klux
Indoor E_{Ave}: 177.83 Lux
Indoor E_{min}: 72 Lux
Uniformity ratio: 0.4
Closed windows

Day: 12 July 2011
Time: 5:05-5:20 pm
Reference light on roof: 55-62 Klux
Indoor E_{Ave}: 2900 Lux
Indoor E_{min}: 900 Lux
Uniformity ratio: 0.31
Open windows

Day: 12 Jan 2012
Time: 1:30 pm
Simulated perspective
Left: false color
Middle: true color
Right: legend

In spring afternoon with reference illumination on the roof of 75-85 Klux and closed windows, almost all parts of the room has achieved UDI (more than 100 Lux). Summer afternoon with reference illumination on the roof of 56 Klux and closed windows the uniformity ratio is 0.4. In the same condition with open windows the uniformity ratio is 0.31 and more than half part of the room in front of the window has exceeded UDI (more than 2000 Lux) and glare may happen.

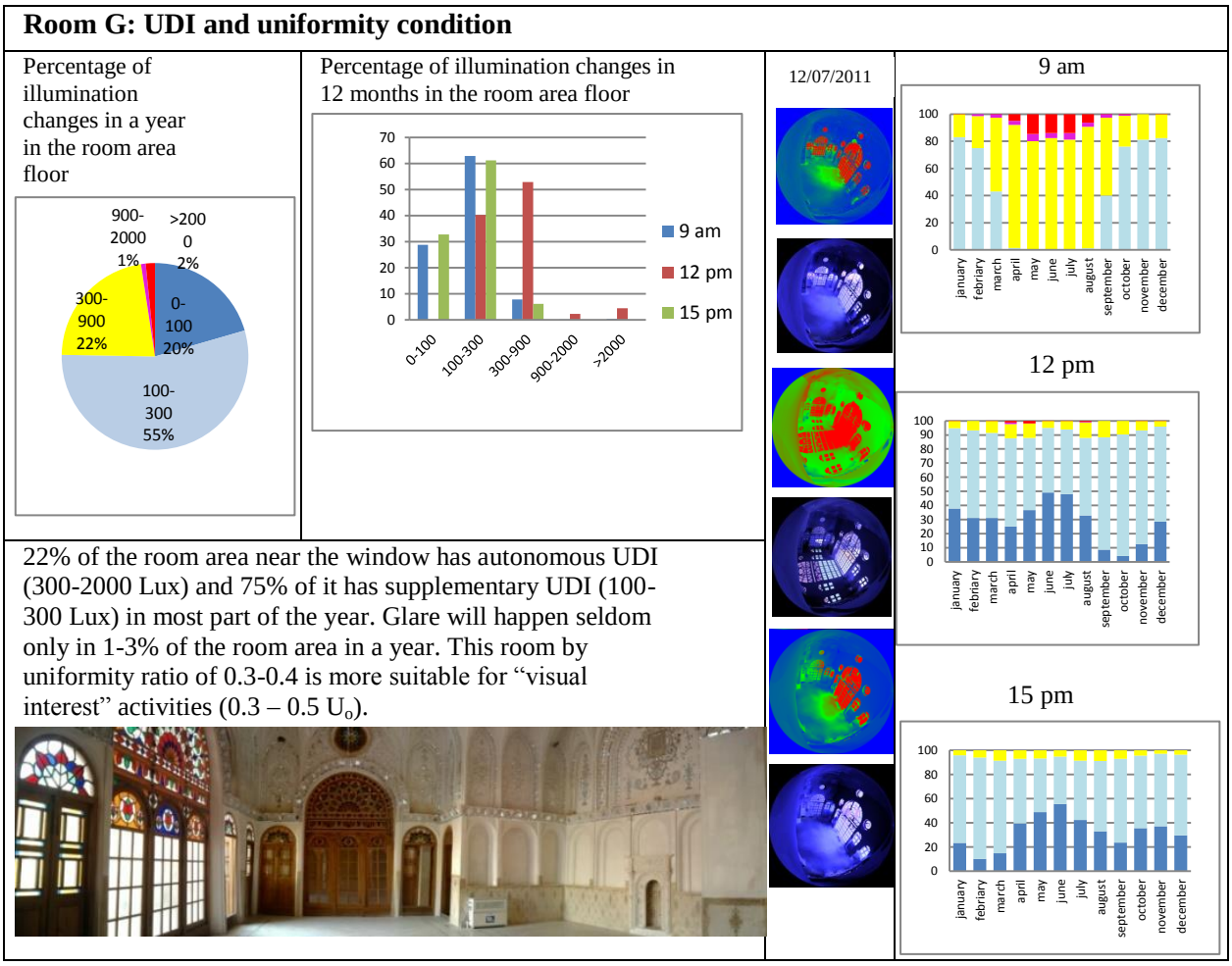

Figure 2: field information and daylight analysis of one of the sample rooms: Room G

THE RESULTS AND DISCUTION

The study investigates door/window rooms in Ameri house in Kashan from two aspects: 1) Site proximity including site geometry and skylight features, 2) The extent of interior lightness and how it distributes

1- The studied rooms in Ameri house were the same in respect of natural lighting-dependent proximity where natural lighting standards were met, that is to say, all the rooms, even in their very depths, have the view of the sky and the opposite view has the appropriate height considering the distance from window wall. Thus, the "no skyline" is always set with respect to the yard width. The rooms also had a "visible sky view angle" in section not less than 40° (of 90°) and in façade not less than 75° (of 180°) and on average 15% to 25% sky hemisphere was visible from window center.

2- According to skylight features, the light was distributed evenly through the rooms, making there a suitable place for visual activities. The reason is large bright surface in proportion to the interior of the room, high ceiling, and large crown of top of the window. Therefore, "uniformity ratio" in I, F, C, B, A,G, K - more than half of the rooms under study - lies between 0.3 to 0.5, making them suitable for "visual interest" activities. Rooms P and E with "uniformity ratio" 0.6-0.7 provide the potential for "visual acuity" activities at all parts of the room. Rooms H and Q with "uniformity ratio" less than 0.3 are not suitable for visual activities because of glare problem or darkness in some parts. Rooms O and N which were in the middle and received illumination from the ceiling, were the dimmest sites under study with lightness lower than 100 Lux most of the year. These sites are suitable for rest or passing by.

Ultimately, what is so special about Ameri house is that it was built under specific rules and there are a few points which can be used in contemporary architecture: 1) Controlling site proximity 2) Controlling depth and geometry of the room 3) Designing special sites (halls-…..) located on the main and long axis 4) Using ceiling skylight in the middle where there is no access to daylight. In other words this study shows that natural lighting - contrary to artificial lighting - should be focused from the early designing concepts to the latest details.

ACKNOWLEDGEMENTS

The authors would like to express their appreciation to all responsible people of Ameriha House and Ezam Co. Ltd. who helped us to carry out the field study in this historical building. Also we need to thank Shahid Beheshti University as the sponsor of this research.

REFERENCES

1. Tahbaz, Mansoureh and Fatemeh Moosavi. (2009). Daylighting Methods in Iranian Traditional Architecture (Green Lighting). CISBAT 2009 Proceedings, Lausanne, 2-3 SEP, pp. 273-278.
2. Ezam, Co Ltd., Brochure of Ameri House Complex. Ezam Co. Ltd., 2011.
3. Tahbaz, Mansoureh, Shahrbanoo Djalilian and Fatemeh Moosavi. (2011). Assessment of Iranian Traditional Door-Windows, A Proposal to Improve Daylighting System in Classrooms. CISBAT 2011 Proceedings, Lausanne, 14-16 SEP, pp. 273-278.
4. LaGiusa, F.F. and L.R. Perney. (1974). Further studies on the effects of brightness variations on attention span in a learning environment. Journal of the Illuminating Engineering Society, No. 3, pp. 249–252.
5. Loe, D.L., K.P. Mansfield and E. Rowlands. (1994). Appearance of lit environment and its relevance in lighting design: Experimental study. Lighting Research and Technology, No. 26, pp. 119–133.
6. Loe, D.L., K.P. Mansfield and E. Rowlands. (2000). A step in quantifying the appearance of a litscene. Lighting Research & Technology, No. 32, pp. 213–222.
7. The SLL lighting Handbook. (2009). London: The Society of Light and Lighting. CIBSE.
8. TES Electrical Electronic Corp: website: http://tes.com.tw/1339re.htm
9. Radio Parts Group: website: http://www.doss.com.au/st8809a-light-meter-wlcd-display-usb/
10. Superior Value Products Inc.: website: http://www.superiorvalueproducts.com/Light-Meter-Measure-in-Foot-Candle-or-Lux-Over-a-Wide-Range-ST-1301_p_584.html
11. LUTRON ELECTRONIC: website: http://www.instrumentsgroup.co.za/index_files/colour_analysers.htm
12. Leica Geosystems: website: http://www.leica-geosystems.com/en/Leica-DISTO-D3a_81046.htm
13. Lighting Guide 5. (2011). Lighting for Education. London: The Society of Light and Lighting. CIBSE.
14. CIBSE TM37. (2006). Design for Improved Solar Shading Control. London: Chartered Institution of Building Services Engineers (CIBSE).
15. Lighting Guide 10. (1999). Daylighting and Window Design. London: The Society of Light and Lighting. CIBSE.
16. Olgyay, Victor. (1957). Solar Control and Shading Devices. Princeton, New Jersey: Princeton University Press.
17. Nabil, A. and J. Mardaljevic. (2005). Useful daylight illuminate: A new paradigm for assessing, daylight in buildings. Lighting Research and Technology, Vol. 37, No. 1.
18. Mardaljevic, John. (2010). Climate-Based Daylight Modelling –IESD. Retrieved from: www.iesd.dmu.ac.uk/~jm/doku.php?id=academic:climate-based-daylight-modelling
19. The SLL Code for lighting. (2012). London: The Society of Light and Lighting. CIBSE.
20. Tahbaz, Mansoureh, Shahrbanoo Djalilian and Fatemeh Moosavi. (2012). Daylighting Evaluation in Traditional Houses of Iran – Ameri House in Kashan, Research Report, Tehran, School of Architecture and Urban Planning, Shahid Beheshti University

Indoor Environment Quality and Health

THE HUMAN BODY AS ITS OWN SENSOR FOR THERMAL COMFORT

M. Veselý, W. Zeiler, G. Boxem, D.R. Vissers

Department of Built Environment, Eindhoven University of Technology, Netherlands

ABSTRACT

To reduce the energy consumption for thermal comfort it is important to be effective as possible. The hands are probably the most responsive body parts of the body's thermoregulatory system. In cool conditions, the hand is fully vasoconstricted and the fingertips are the coldest areas of the hand. In warm conditions this pattern is reversed. Interpreting earlier results obtained by Wang, it seems to be possible to recognize cool body thermal sensations by a transition of the finger skin temperature out of the neutral range to slightly cold. The effects of hand-warming and hand recovering on overall thermal sensations and comfort were earlier investigated through experiments focused on thermal conditions in automobiles. In these experiments the body was perceived as cold. However in an office environment, the level of body cooling is often quite small that only the extremities will become cold. So the hands (and feet) may be the only source of discomfort. In this situation, local hand heating could directly remove the only source of discomfort and may therefore have a strong effect on overall sensation and comfort. This required further investigation. The hypothesis, that the finger temperature could be used as feedback control signal for automatic regulation of the radiant hand-heating system, was tested for different finger temperature bandwidths. Thereby, the objective was to determine whether the system was able to keep the conditions within the user's thermal preferences. Two healthy young subjects (male and female) participated several times in these experiments. This pilot study showed the possibilities for including the human body in the control loop of personalized heating systems using the IR thermography. The obtained results could however only be applied to the two subjects (male and female) who participated in this research. It is already known that individual differences such as body fat percentage and age, can have a significant influence on the thermal sensation and upper-extremity skin temperature. By modeling the preference that arises from the interactions with the user, this small bandwidth might be applicable to other individuals. New measurements will be done in the next month's to have a more thorough basis for our conclusions. The limitations of the previous study and from them arising future research directions are discussed in the present paper.

Keywords: thermal comfort, heating, personalized conditioning

INTRODUCTION

It is essential to develop more energy effective thermal comfort conditioning. The traditional approach to heating, ventilation and air conditioning (HVAC) design aims to create uniform conditions in the entire conditioned space. The requirements for indoor environment prescribed in the currently used standards like ISO 7730 or ASHRAE 55 [1], [2] are based on the average values for a large group of occupants. However, in practice the individual differences based on many factors including age, gender, clothing, activity or individual preferences make it impossible to satisfy the comfort needs of all the occupants using a total volume conditioning. Furthermore only few body parts are usually the source of thermal discomfort, typically head in warm environments and hands and feet in cool environments [3], [4]. These facts led many researchers to designing of a personalized conditioning system.

Different personalized conditioning systems were introduced, including personalized ventilation [5], combination of personalized ventilation with local convective and radiant heating [6], [7] or personal environmental module [8]. These systems not only have positive impact on thermal comfort and indoor air quality, but also have a good potential for energy reductions. Personalized ventilation with a proper control strategy makes it possible to reduce energy use in hot [9] as well as in cold climates [10].

A crucial aspect influencing the performance of any personalized conditioning system is the individual control provided to its user. The users are often provided with the control over their personalized air flow, temperature of this air flow or temperature of the heating elements. However, this way of control is still highly dependent on the occupants' behaviour and can often lead to decreased comfort level and increased energy use. It is therefore desirable to control the conditioning by a critical parameter predicting the changes in occupants' comfort.

Since the hands dictate the thermal comfort in cool environments [11], the hand skin temperature can become a critical parameter for control of a local heating system. This paper presents results of a study of a "human in the loop" control approach, where the remotely sensed fingertip temperature is used as a control signal for the local radiant hand heating. The limitations of the presented study and future research directions are discussed.

HUMAN THERMOREGULATION AND THE IMPORTANCE OF THE BODY EXTREMITIES

Although the human body can be exposed to a wide range of thermal environments comprising temperatures from about -40 °C in arctic areas up to +100 °C in sauna it normally keeps its core temperature in a small range of 36 – 38 °C. Human skin representing the boundary between the human body and its surrounding environment is the major organ which plays a role in the body thermoregulation. The human thermoregulation consists from three main components – thermoreception, its integration through neural pathways and effective response of the organism in terms of heat loss or heat production [12].

The body does not sense directly the temperature of its environment. The thermal sensation is instead coded in the fire rate of cold and warm receptors contained in human skin [12]. The temperature information is then passed to the hypothalamus in the brain, where the autonomic thermoregulation is activated. Each of the thermo receptors is activated in a specific range of temperatures, the textbook of medical physiology [13] states that the maximum fire rates lie for cold receptors at 25 °C and for warm receptors at 44 °C. Moreover, the thermal sensation is influenced by time dependent change in skin temperature. The active falling or rising of the skin temperature causes much colder or warmer sensation compared to steady conditions. This overreaction is called 'overshoot' [11].

Different thermoregulatory principles are applied within and outside the thermoneutral zone. The thermoneutral zone is defined as the range of ambient temperatures without regulatory changes in metabolic heat production or evaporative heat loss [12]. The main thermoregulatory principle applied within the thermoneutral zone is thus vasomotion (vasoconstriction and vasodilatation), while outside the thermoneutral zone the human body either produces more heat via shivering or loses more heat via evaporation of the sweat. Vasomotion represents a principle of controlling the heat flow within the body by dilating (vasodilatation) or constricting (vasoconstriction) of the blood vessels, more or less heat is then transported by the blood to the skin where it dissipates to the environment. Since staying within or close to thermoneutral zone is essential for the thermal comfort, vasomotion is important aspect to be considered while designing personalized conditioning systems.

The hand is probably the most active body part in responding to the body's thermoregulatory requirements. In cool conditions, the hand is fully vasoconstricted and the fingertips are the coldest areas of the hand. This pattern is reversed in warm conditions [11]. Wang et al. reported that the finger is a good indicator of the thermal sensation and comfort in cool conditions [14]. The fingertip temperature (of the 4th finger) of 30 °C was indicated as a threshold for cool discomfort possibility, while above this temperature the thermal sensation is neutral or higher and no cool discomfort occurs.

Thermal sensation and comfort for whole body and local body parts vary greatly in subjects exposed to uniform environments [11], [15], [16]. Under colder environments the overall thermal sensation and comfort follows the hands and the feet which are perceived as the coldest and the most thermally uncomfortable. Similarly under warmer environments the overall thermal sensation and comfort is determined by the head which is perceived as the warmest and the most thermally uncomfortable. Wang et al. [14] reported a substantial improvement of the thermal comfort in cool environments achieved by warming the hands, but the thermal comfort vote was not brought to a positive level. However, these tests covered fairly extreme conditions as found in automobiles. It is likely that under milder conditions hand warming will be able to compensate for the only source of the thermal discomfort.

"HUMAN IN THE LOOP" APPROACH EXPERIMENTS

A study by Vissers [17] tested the hypothesis that cold thermal discomfort can feed forwarded by the drop in the skin temperature of the body extremities such as hands or head. An experiment using two infrared cameras for skin temperature measurements and local radiant heating system for providing a local thermal comfort was set up at Eindhoven University of Technology. The radiant heating panels used in earlier phase of the experiments were later replaced by a pair of radiant heating lamps. An impression of the experimental setup is shown in Figure 1.

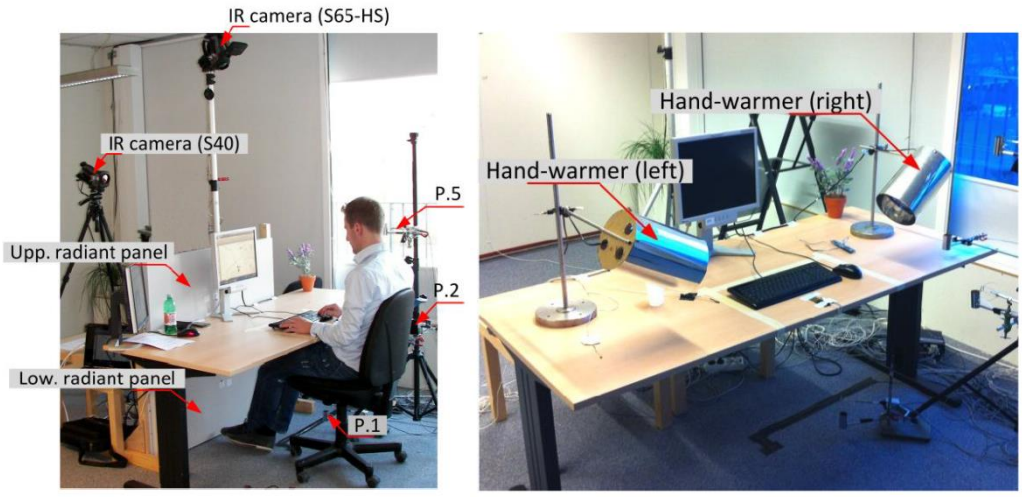

Figure 1 An impression of the experimental setup with the radiant heating panels (left side) and the radiant heating lamps (right side) [17]

The fingertip temperature was identified to have the most decreasing trend under mild cool office conditions, similar trend with smaller temperature drop was observed for the hand and the nose (Figure 2). Furthermore the skin temperature drop of the body extremities was observed before the actual thermal discomfort was reported by the subject.

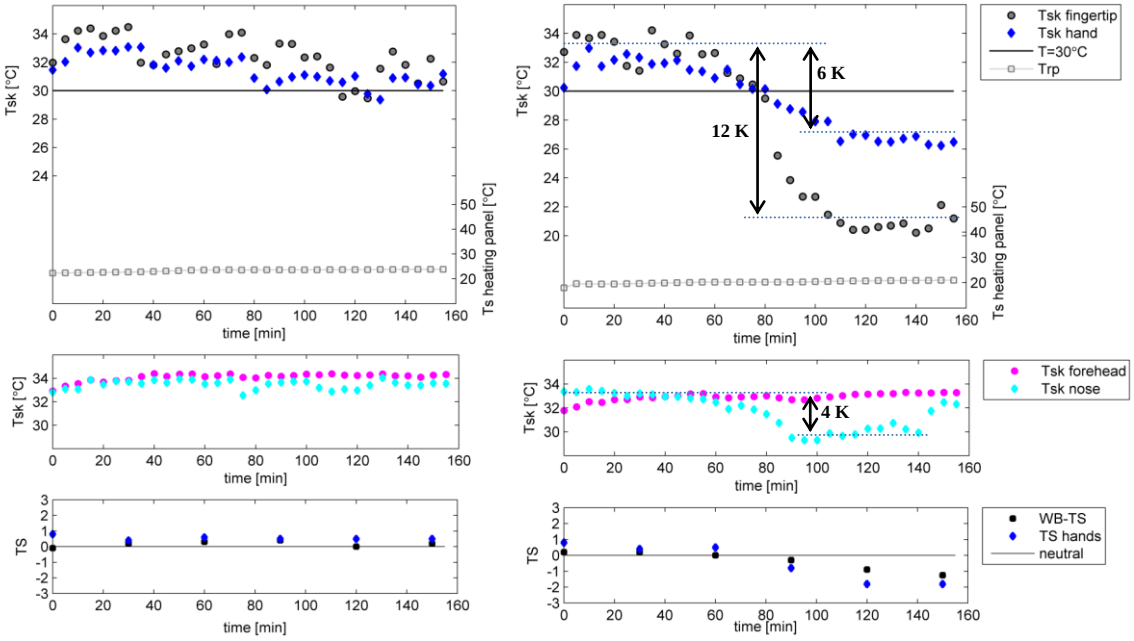

Figure 2 Comparison of the skin temperatures under neutral (left side; PMV = 0.0) and mild cool (right side; PMV = -0.9) conditions, the temperature drops under mild cool conditions are highlighted [17]

The fingertip temperature remotely measured by the infrared thermography was then tested as a signal for a local radiant heating system. Different fingertip temperature bandwidths were tested, but only by controlling the fingertip temperature in a small bandwidth of 29 to 31.5 °C it was generally possible to keep the thermal sensation above the neutral and the subjects did not prefer any change in their thermal environment (Figure 3).

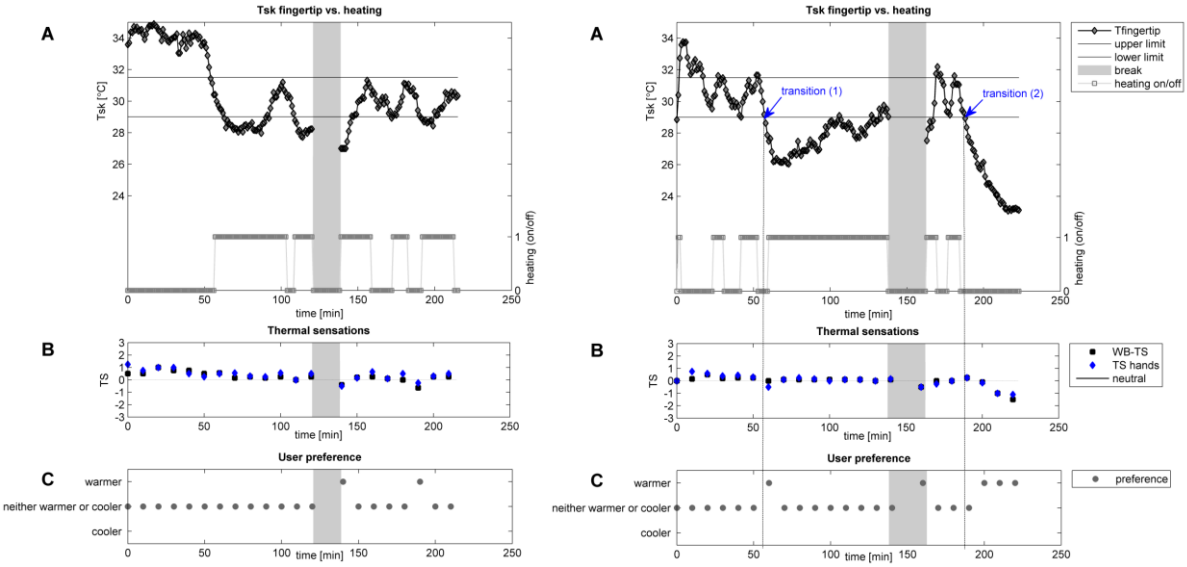

Figure 3 Upper-extremity skin temperature controlled in a small bandwidth: male (left side) and female (right side) subject. [17]

DISCUSSION

Figure 4 presents a comparison of the overall thermal sensation and fingertip temperature as measured in the studies by Wang et al. [14] and Vissers [17]. This comparison is complicated due to different ranges of ambient temperatures (17.5 – 20.7 °C in Wang's study and 19.6 – 19.9 °C in Vissers') and different heating principles (convective in Wang's study and radiant

in Vissers'). However, both studies show an agreement in the fact that keeping the fingertip temperature above 30 °C under mild cool conditions is able to bring the thermal sensation close to neutral and thus avoid the cold discomfort.

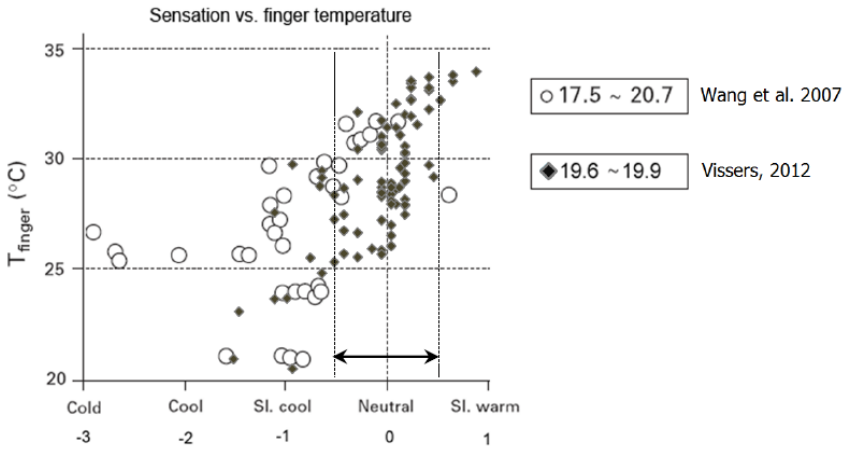

Figure 4 Comparison of the studies by Wang et al. [14] *and Vissers* [17]

The previous study [17] did show a potential of using remotely sensed skin temperature as a control for local radiant heating. However, this study was limited to just two test subjects. Since the individual preferences regarding thermal comfort vary greatly among the population it is needed to perform the tests with a larger group of persons.

The way of automatic control represents another limitation of the previous study. In these experiments the following approach was applied. The real-time infrared video signal was observed by the researcher. A certain area of the picture representing the fingertip was then chosen and followed by a computer mouse during whole experimental session. Based on observation of the temperature in the fingertip area the researcher was turning on or off the local radiant heating system to keep the fingertip temperature in a certain bandwidth. This approach served as a proof of a principle and the control was fully automatic from the user point of view. However, the human factor in the control loop could lead to some bias in the experimental results. Moreover, the on/off control can cause an overshoot in thermal sensation. Further tests will thus be performed with automatic finger tracking and using a PID control.

The current experimental setup uses a very sophisticated thermo camera which is because of its size and high price not suitable for use in the building practice. Therefore the applicability of low cost infrared arrays will be investigated.

REFERENCES

[1] International Standard Organisation, "ISO 7730: Ergonomics of the thermal environment - Analytical determination and interpretation of thermal comfort using calculation of the PMV and PPD indices and local thermal comfort criteria," 2005.

[2] ASHRAE, "Standard 55-2004 (2004) Thermal environmental conditions for human occupancy, Atlanta, GA," *American Society of Heating, Refrigerating and Air-Conditioning Engineers*.

[3] Y. Yao, Z. Lian, W. Liu, and Q. Shen, "Experimental Study on Skin Temperature and Thermal Comfort of the Human Body in a Recumbent Posture under Uniform Thermal Environments," *Indoor and Built Environment*, vol. 16, no. 6, pp. 505–518, Dec. 2007.

[4] H. Zhang, E. Arens, C. Huizenga, and T. Han, “Thermal sensation and comfort models for non-uniform and transient environments, part III: Whole-body sensation and comfort,” *Building and Environment*, vol. 45, no. 2, pp. 399–410, Feb. 2010.

[5] A. Melikov, “Personalized ventilation,” *Indoor Air*, vol. 14, no. s7, pp. 157–167, Aug. 2004.

[6] A. Melikov and G. Knudsen, “Human response to an individually controlled microenvironment,” *HVAC&R Research*, no. February 2013, pp. 37–41, 2007.

[7] S. Watanabe, A. K. Melikov, and G. L. Knudsen, “Design of an individually controlled system for an optimal thermal microenvironment,” *Building and Environment*, vol. 45, no. 3, pp. 549–558, Mar. 2010.

[8] M. Demeter and P. Wichman, “PERSONAL ENVIRONMENTAL MODULE,” 1993.

[9] S. Schiavon, A. K. Melikov, and C. Sekhar, “Energy analysis of the personalized ventilation system in hot and humid climates,” *Energy and Buildings*, vol. 42, no. 5, pp. 699–707, May 2010.

[10] S. Schiavon and A. K. Melikov, “Energy-saving strategies with personalized ventilation in cold climates,” *Energy and Buildings*, vol. 41, no. 5, pp. 543–550, May 2009.

[11] E. Arens and H. Zhang, “The skin’s role in human thermoregulation and comfort,” *Office*, pp. 560–602, 2006.

[12] B. Kingma, “Human thermoregulation: a synergy between physiology and mathematical modelling,” NUTRIM School for Nutrition, Toxicology and Metabolism of Maastricht University Medical Center, 2012.

[13] A. Guyton and J. Hall, “Textbook of Medical Physiology,” *WB Saunder’s Co., Philadelphia*, 2000.

[14] D. Wang, H. Zhang, E. Arens, and C. Huizenga, “Observations of upper-extremity skin temperature and corresponding overall-body thermal sensations and comfort,” *Building and Environment*, vol. 42, no. 12, pp. 3933–3943, Dec. 2007.

[15] E. Arens, H. Zhang, and C. Huizenga, “Partial- and whole-body thermal sensation and comfort— Part I: Uniform environmental conditions,” *Journal of Thermal Biology*, vol. 31, no. 1–2, pp. 53–59, Jan. 2006.

[16] E. Arens, H. Zhang, and C. Huizenga, “Partial- and whole-body thermal sensation and comfort—Part II: Non-uniform environmental conditions,” *Journal of Thermal Biology*, vol. 31, no. 1–2, pp. 60–66, Jan. 2006.

[17] D. R. Vissers, “The human body as sensor for thermal comfort control,” Eindhoven University of Technology, 2012.

FIELD ASSESSMENT OF CO_2 REMOVAL EFFECTIVENESS WITH UNDERFLOOR AIR DISTRIBUTION

T. A. Baker; J.A. Love

Faculty of Environmental Design, University of Calgary, Calgary, Canada

ABSTRACT

Underfloor air distribution (UFAD) is gaining popularity, because many believe it provides better CO_2 removal effectiveness, reduced energy use, improved occupant satisfaction with thermal comfort, and easier reconfiguration relative to conventional overhead mixing ventilation (MV) systems. This paper reports a field assessment of CO_2 removal effectiveness in offices, on which few articles have been published. In the study building, many diffusers were initially misaligned (e.g., placed under furniture), because furnishing plans were only available after installation. Measurements were made before and after relocation of the diffusers. Evaluated spaces included open plan offices and a private office. Thermal comfort parameters at head, body and foot levels were also measured. The CO_2 removal effectiveness was generally lower than the value nominally assigned for UFAD systems in ASHRAE Standard 62.1-2010. In most cases, CO_2 removal effectiveness was similar or lower after relocation of the diffusers. Thermal comfort conditions were improved after diffuser relocation.

Keywords: underfloor air distribution, UFAD, stratified ventilation, ventilation effectiveness, carbon dioxide

INTRODUCTION

Stratified ventilation systems supply room air around 18 ^{o}C and close to floor level. Occupants and equipment generate thermal plumes that entrain buoyant contaminants so that, above occupant head height, temperatures and contaminant concentrations are higher. This allows greater selectivity in extracting contaminants. CO_2 has been considered an indicator of other indoor contaminants, but evidence is emerging that it may have adverse effects at concentrations below 1000 ppm, which have generally been considered acceptable [1]. With uniform CO_2 source distribution, zone air distribution effectiveness can be defined [2] as

$$E = (C_r - C_s)/(C_b - C_s) \quad (1)$$

where

E	=	zone air distribution effectiveness
C_r	=	CO_2 concentration at the room ventilation extract (ppm)
C_b	=	CO_2 concentration at the breathing height (ppm)
C_s	=	CO_2 concentration at the supply air diffuser (ppm)

In ideal MV, C_b and C_r would be the same (E=1.0). E values higher than 1.0 ($C_r > C_b$) correspond to the putative superior selectivity of stratified ventilation noted above.

Underfloor air distribution (UFAD), one form of stratified ventilation system, has gained popularity, because many believe it provides 1) better effectiveness at removing CO_2 exhaled by occupants, 2) reduced energy use, 3) improved occupant satisfaction with thermal comfort, and 4) easier reconfiguration relative to conventional overhead mixing ventilation (MV) systems [3]. However, [4] concluded in 2004 "valid and reliable field data from UFAD systems are not available to conclude that ...UFAD performance is superior to" MV.

UFAD swirl diffusers (SW) supply air at velocities that generate a swirl like airflow pattern, so a fully mixed condition is approached up to the diffuser throw height. UFAD horizontal diffusers (HD) supply air at lower velocities and parallel to the floor, producing a displacement-like airflow pattern. Stratification depends on factors such as the diffuser discharge velocity; [4] gave a range of 1.0-1.2 for UFAD *E*., consistent the values in the version of ASHRAE 62.1-2004 published that year [5]. Based on lab measurements and simulation, [2] argued in 2009 that *E* values specified in ASHRAE 62.1 neglected the impact of space type (e.g., office or classroom), supply airflow rate, supply air temperature and thermal loads. They proposed, based on lab measurements and computational fluid dynamic (CFD) analysis, values of 1.05-1.15 for offices with low velocity systems and 1.05 for those with high velocity systems.

Only a couple of reports of *E* based on field measurements in UFAD offices have been published. In 2006 [6] reported an average *E* of 1.13 at 7 workstations/private offices for an open plenum UFAD system with SW, with variations from 1.05 to 1.20 and higher. The outdoor air flow rate was about 30 L/s per person, about three times the minimum [7]. [6] also undertook an internet-based occupant survey of work environment satisfaction. 45 occupants (47% response rate) completed the questionnaire. The response regarding thermal comfort was very positive.

[8] reported median *E* of 1.23 (table 1 and figure 1) for open plan and private offices with HD. [8] found 75% of diffusers were under furniture and/or further from or closer to occupant seating positions than manufacturer guidelines, because the construction schedule required completion of the floor prior to availability of tenant fit-out drawings. In many cases, the diffuser was below the occupant foot position. Some occupants worked with blankets or coats over their laps to reduce discomfort from draft.

In this study, measurements in the spaces evaluated by [8] were repeated to evaluate performance after relocation of diffusers to 1) meet manufacturer guidelines for diffuser-chair distance and 2) to eliminate obstruction by furnishings. In particular, many diffusers were moved from the occupant foot region to an area sufficiently far behind the occupant chair to meet manufacturer guidelines. A limitation of the studies by [6] and [8] was that, due to the cost of the high precision CO_2 analyzer used, only a single point was sampled in the breathing zone. In this study, a second analyzer was deployed so that up to 4 breathing zone points could be sampled during a test. Thermal comfort parameters were also measured.

METHOD

Test Spaces

The University of Calgary's Child Development Centre (CDC) is a 12,000 m^2 four-storey building. Levels 2-4 have a ducted UFAD system with zone variable air volume (VAV) boxes, allowing automated zone occupancy-based control of air flow.

[8] limited testing to level 2, the only completed floor during testing. Because so few measurements have been conducted in operating buildings with UFAD systems, [8] selected test spaces to provide a variety of occupancy densities, heat generation rates, diffuser locations relative to occupants and furniture, room type (open space, individual office, meeting room and break out room), and orientation (core and perimeter spaces).

In this study, many of these spaces were re-tested to compare performance before and after diffuser relocation. Results are reported for perimeter private office 2018, core open plan offices 2143 and perimeter open plan offices 2115, 2147 and 2189 [9 see "Interactive Room

Finder" for plans]. As in [8], tests were conducted during office hours when workstations were occupied.

Errors

Relatively small measurement CO_2 measurement errors may generate substantial differences in *E*. For example, the CO_2 sensor used by [10] for a field study of displacement ventilation in schools, had a specified maximum error of 1) 2% of range plus 2) 2 % of reading. On a measurement range of 2000 ppm with CO_2 concentrations of 400 ppm (supply), 900 ppm (breathing) and 1000 ppm (extract), *E* could range from 1.0 to 1.4, depending on error, in particular because the denominator values are typically much smaller than the numerator values. Evaluation of this model by author 2's research group showed an error that exceeded the manufacturer's specification, even after recalibration by the manufacturer. [6] reduced measurement error by 1) using a gas analyzer with a total accuracy of 1% of range and 2) multiplexing the air samples drawn from the supply, breathing zone, and extract to reduce instrument-related errors. The same procedure was used in this study.

Since changes in occupant numbers during a multiplexing cycle could affect the representativeness of air samples, [8] established and used criteria for steady-state conditions. In the study reported here, the further step was taken of research assistants assuming occupant seats when vacated while a test was in progress, since participants left their seats intermittently.

Measurement Procedures

Flexible tubes were used to sample air from 1) 2.9 m above floor level, which was 0.1 m below the ceiling (C_r), 1.1 m above the floor (C_b), and inside the diffuser nearest to the sample workstation (C_s). A standard tube length of 15 m was used for all sampling points; testing showed that the air pump in the CO_2 analyzer cleared this length of tube in less than 1 min. Equipment was placed to avoid interference with the normal activity in the test areas. The data were compiled and treated according to the following procedure:

1. The CO_2 analyzer was set to a 5 second time step (12 readings/min).
2. Each point (C_s, C_b, and C_r) was sampled to obtain 60 readings. Three sequential 5-min periods constituted a measurement "round".
3. Readings for min 1 at each sampling point were excluded (clear previous point), and the median of readings for the last 4 min (48 readings) was used as the CO_2 ppm.
5. Linear interpolation between rounds was used to approximate CO_2 levels at the midpoint of a round.

As noted above, two high precision gas analyzers were deployed. Prior to each test, each multiplexer simultaneously sampled a C_s points to provide a correction factor.

Thermal comfort conditions were evaluated in terms of head-foot temperature for seated occupant (from 0.1 to 1.1 m) and standing occupants (from 0.1 to 1.7 m). Air temperature, air velocities, relative humidity were measured at 0.1, 0.6 and 1.1 m above floor as per [11]. Predicted Mean Vote (PMV) and Predicted Percentage Dissatisfied (PPD) were used to evaluate thermal comfort conditions [11]. Because of temperature stratification, PMV and PPD were calculated using the average occupied zone temperature following [12]

$$Toz,av= (1/1.7-0.1) *[(1.7-1.1)/2*(T1.7+T1.1)+(1.1-0.1)/2*(T0.1+T1.1) \quad (2)$$

where Tx presents the temperature value measured at height x.

RESULTS AND DISCUSSION

On a room by room basis, pre- and post-reconfiguration *E* were similar (figure 1 and table 1) except that post-reconfiguration *E* was lower for workstation 2115. Figure 2 shows the horizontal pattern of *E* across each test area. The highest value of *E* was measured away from the occupants (*E*1.1D) while the other *E* values were measured close to occupants. The maximum variation of *E* across a space was 0.70 (0.86 to 1.55) for open plan office 2189; the low value of *E* being for the occupant position, while the highest was away from the occupant. The pattern was similar for the other rooms. This suggested that the location of the CO_2 intake relative to the occupant substantially affected *E*; moreover, this suggests that *E* close to occupant may be lower than field values reported by [8] and [8]. Values as low as 0.8 were found. Overall, *E* near occupants was close to the nominal maximum (1.0 [7]) for MV.

Several thermal comfort indices were calculated (table 2.) The median temperature difference from 0.1m to 1.1m (TD1.1-0.1) and 0.1 to 1.7 (TD1.1-1.7) were below the 3°C limits specified in [11]. Thermal discomfort due to draft was not an an issue in the investigated spaces as very low air velocities (below 0.2 m/s) were measured in the occupied zone. The reason for these low air velocity values is the low discharge air velocity of the HD. Calculated PMV and PPD were also within acceptable ranges specified in [11]. The metabolic rate used for calculating these two indices was assumed to be 1.1 met based on [11] as the main activities observed were reading and typing. Most occupants were females with clothing varying from knee length skirts with short sleeves to trousers with long sleeved shirts. Thus, clothing insulation was assumed to be 0.6 clo and an addition 0.1 clo was added for standard office chair insulation as prescribed in [11]. Overall, conditions met [11].

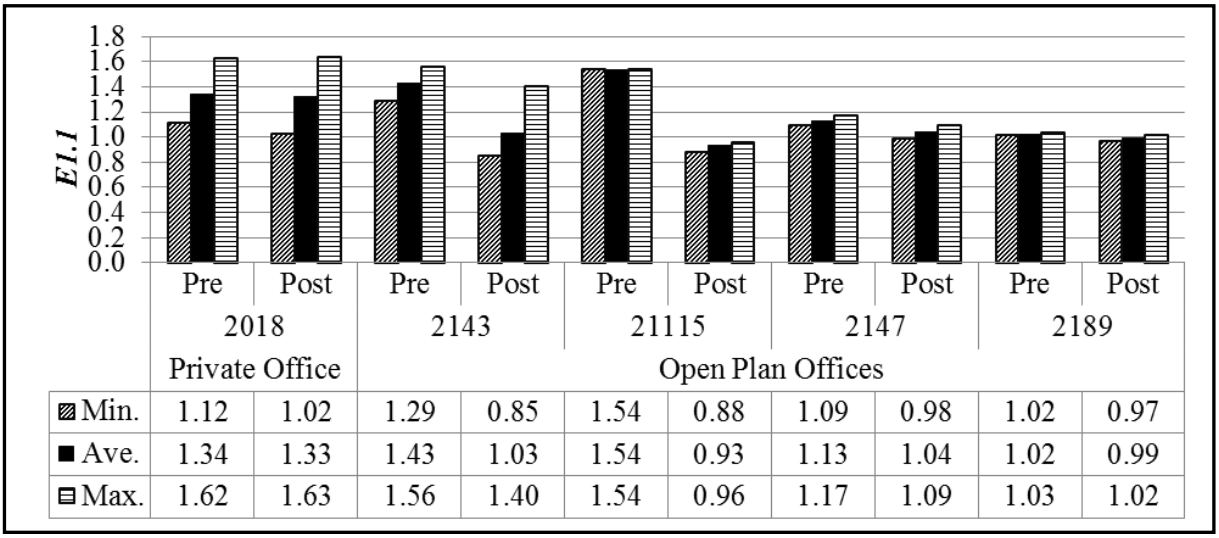

	Pre	Post	Pre	Post	Pre	Post	Pre	Post	Pre	Post
	2018		2143		21115		2147		2189	
	Private Office		Open Plan Offices							
Min.	1.12	1.02	1.29	0.85	1.54	0.88	1.09	0.98	1.02	0.97
Ave.	1.34	1.33	1.43	1.03	1.54	0.93	1.13	1.04	1.02	0.99
Max.	1.62	1.63	1.56	1.40	1.54	0.96	1.17	1.09	1.03	1.02

Figure 1: Pre- and post-reconfiguration E by test area.

Study	***E* Statistics**				**Test Statistics**		
	Median	**Median Absolute Deviation**	**Min.**	**Max.**	**No.**	**Median Test Length (hr)**	**Min Test Length (hr)**
pre [8]	1.23	0.17	1.02	1.62	10	1.50	0.75
post (current)	0.98	0.04	0.85	1.63	16	1.25	0.50

Table 1: Summary of results for pre- and post-reconfiguration E.

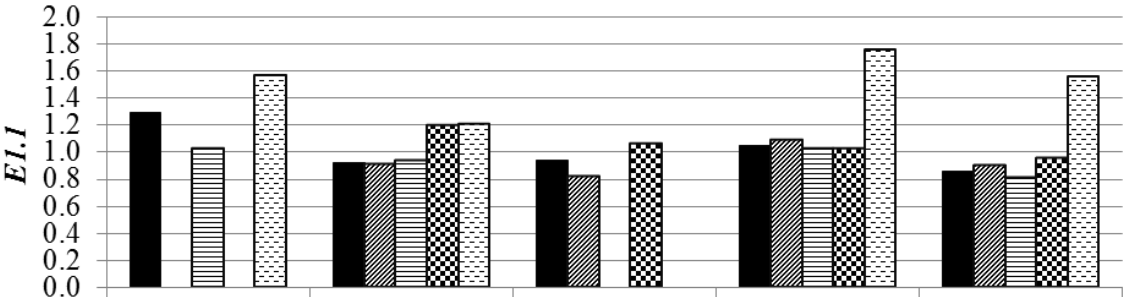

	2018	2143	21115	2147	2189
	Private Office	Open Plan Office			
■E1.1 Ave.	1.29	0.92	0.94	1.05	0.86
▨E1.1A		0.91	0.82	1.08	0.90
▤E1.1B	1.02	0.93		1.02	0.81
▩E1.1C		1.19	1.06	1.02	0.95
▣E1.1D	1.56	1.21		1.75	1.55

Note: Letters (as in E1.1A) indicate measurement position. E1.1D presents C_s measurements away from occupants.

Figure 2: Ai distribution effectiveness (E) across each test space.

Variable	**Median**	**Median Absolute Deviation**	**Min.**	**Max.**
Operative Temperature (Toz_av) (°C)	23.1	0.4	22.0	24.0
Vertical temperature difference				
0.1m to 1.1m (TD1.1-0.1) (°C)	1.5	0.2	1.0	2.0
0.1m to 1.7m (TD1.7-0.1) (°C)	1.6	0.2	1.0	2.0
Air velocity, occupied zone (Voz,av)(m/s)	0.01	0.00	0.01	0.15
Relative humidity (Roz,av)(%)	21	34	19	22
Predicted Mean Vote (PMVoz,av)	-0.3	0.10	-0.7	0.0
Predicted Percentage Dissatisfied (PPDoz,av)	6.6	1.0	5.0	15

Table 2: Summary of thermal comfort parameters for the test spaces.

DISCUSSION

The results showed that air distribution effectiveness (*E*) was generally lower at the occupant position than the nominal value given by [7]. An explanation could be the lab findings by [2] that space conditions substantially affect *E*.

Another observation was that the building operators asked occupants not to adjust the in-floor diffuser settings due to the effects on zone air distribution via the zone VAV boxes (occupant adjustability being one of the putative benefits of UFAD).

The scope of the study was too limited to be definitive but it does indicate the need for more extensive field studies of the many UFAD configurations to better understand performance.

ACKNOWLEDGEMENTS

The authors express their sincere gratitude to the staff of the Alberta Health Services and the University of Calgary for accommodating the measurements. Kasian Architecture provided

interior furnishing plans. William Fisk and Douglas Sullivan of Lawrence Berkeley National Laboratory kindly provided advice and other assistance. The Natural Sciences Engineering and Research Council of Canada and the University of Calgary provided financial support. .

REFERENCES

1. Satish, S., Mendell M. J., Shekhar K., Hotchi T., Sullivan D., Streufert S. and Fisk W. J. Is CO_2 an indoor pollutant? Direct effects of low-to-moderate CO_2 concentrations on human decision-making performance. Env. health persp 120(12): 1671–1677, 2012.
2. Lee, K.S., Jiang, Z. and Chen, Q. Air distribution effectiveness with stratified air distribution systems. ASHRAE Trans. 115 (2) 322-328, 2009.
3. Bauman, F. and Daly A. Underfloor air distribution design guide. Atlanta: ASHRAE, 2003.
4. Woods, J.E. What real-world experience says about the UFAD alternative. http://www.doas-radiant.psu.edu/Woods_UFAD.pdf Last accessed 2012 April 20. 2004.
5. ASHRAE. Standard 62.1 Ventilation for acceptable indoor air quality. Atlanta, GA : ASHRAE, 2004
6. Fisk W.J., Faulkner D., Sullivan D.P., et al. Performance of underfloor air distribution in a field setting. Int. J. Vent. 5(3)291-300, 2006.
7. ASHRAE. Standard 62.1, Ventilation for acceptable indoor air quality. Atlanta, GA : ASHRAE, 2010
8. Cubi Montanya E. and Love J.A.. Pollutant removal effectiveness with underfloor air distribution: field study of a ducted variable-flow system. ASHRAE Trans. 117 (2) 759-770, 2011.
9. University of Calgary. http://www.ucalgary.ca/fmd/buildings/child_ development_centre. last accessed April 25, 2013.
10. Ouazia, B., Macdonald, I., Tardif, M. Thompson, A., and Booth, D. (2012) Field study assessment of the performance of displacement air distribution in a Canadian school during the heating season. Int. J. Vent. 11 (1)43-51, 2012.
11. ASHRAE Standard 55. Thermal environmental conditions for human occupancy. Atlanta, GA: ASHRAE, 2010.
12. Schiavon, S., Bauman F., Lee K.H., and Webster T. Development of a simplified cooling load design tool for underfloor air distribution systems. Final Report to CEC PIER Program. CEC Contract No. 500-06-049, July,2010.

MOTIVATING INDIVIDUAL EMISSION CUTS THROUGH DIFFERENT COMMUNICATION PATHWAYS: THE POTENTIAL OF RECIPROCAL INFORMATION FLOWS

D. Dantsiou; M. Sunikka-Blank; K. Steemers.

Department of Architecture, University of Cambridge, 1-5 Scroope Terrace, CB2 1PX, Cambridge, United Kingdom.

ABSTRACT

A significant part of the discourse towards the transition to a low carbon future is dominated by the use of new emerging materials, advanced metering infrastructure and microgeneration technologies. However, it is widely accepted that if the target is an overall demand reduction it won't flow naturally through technological upgrade only but societal engagement and behavioural change has a vital role to play. Towards this two-sided reduction approach, there are promising signs that universities on a global scale take upon actions engaging in activities linked to creating 'greener campus environments' through efficiency investments and information tools. This paper investigates the effect of behavioural change initiatives applied on a two-dimension information and communication model. The 'top-down' information campaigns to motivate voluntary change and 'bottom-up' feedback provided to the users by a real-time workplace tracker system form the two sides of the vertical axis while the flow of information from an individual house level to an institutional work environment is located on the horizontal plane. With the aim to identify the factors that affect willingness to public engagement and future expectations a questionnaire survey was undertaken among university campus users (Hokkaido University, Japan). Consequently, a smaller sample is engaged in order investigate the long-term impact of a real time energy use feedback tool (University of Cambridge, United Kingdom). Results indicated that personal norms were a stronger drive towards energy consciousness compared to social influences. The application of reciprocal feedback appeared to have a noticeable effect on raising awareness but its long-term effect needs to be further studied. The understanding of the interaction between different consumption feedback venues and the type of information needed is implied if a long-term and wide engagement is aimed.

Keywords: behaviour, feedback, social norms, personal norms, interaction, energy demand

INTRODUCTION

The beginning of the twenty-first century has been marked by a significant body of evidence that indicates urgency to act upon climate change and CO_2 emission rate at an international scale [1]. Encouraging individuals to decarbonise their behaviour has been the main focus of several policies and information tools on an international scale aiming to the transition towards a low carbon society. Yet recent research indicates that although there is a widespread awareness of climate change and different information tools are employed, behavioural engagement is still low [2, 3] and in line with a 'value-action' gap where actions do not always meet individuals' attitude due to complex social, psychological and environmental interactions [4]. If awareness-raising tools are to be more effective there is a need for a more realistic view of public knowledge and concern including individuals' evaluation of different information sources, motivations for and barriers to engagement in community actions and consideration of carbon in everyday decision making [5-7].

Currently the debate on behavioral change is heavily tilted towards households although organizational and institutional energy use has a significant part on the carbon emissions with energy used by non-domestic buildings being responsible for approximately two-fifths of the energy related CO_2 emissions in the UK only [8, 9]. There are promising signs that universities on a global scale take upon actions to promote sustainability through their academic agenda and by creating 'greener campus environments' through carbon reduction and behavioural change initiatives associated with their operational aspects. The institutional setting shifts the focus from individual experiences to collective practices where a set of interactions, interdependencies and collective behaviour take place.

To induce change in energy demand patterns, information tools such as real-time energy use displays, smart controls and carbon reduction activities have been employed at a building level while wider scale informational campaigns, regulatory schemes and initiatives have been established from a top-down organisational approach. This paper aims to understand the factors that affect willingness to act environmentally friendly in a workplace environment and investigate the effectiveness of carbon reduction information tools focusing on individual and institutional dimensions. The paper begins with an overview of the Higher Education (HE) sustainability guidelines in Japan looking at the case of a Hokkaido University (HU). It then presents empirical findings from a questionnaire survey on behavioural trends and sustainability perception of the campus users. Finally, it discusses the next research step looking at the effectiveness of a Workspace Footprint Tracker (WFT) energy use feedback project at the University of Cambridge and concludes with the findings and future potential for HE to promote sustainability and behavioural change.

Higher Education sustainability actions in Japan: the case of Hokkaido University informational campaigns

Following the international agreement of the Kyoto protocol, Japan has set an ambitious target of reducing its Green House Gas emission by 25% relative to1990 levels by 2020 and 80% by 2050 [10]. As a result of the Fukushima nuclear accident in March 2011 energy policies have radically sharpened and the government called on universities and other organizations to reduce their electricity consumption by 15% setting mid-term and long tern energy reduction targets [11]. Although universities carry the mission to lead towards a sustainable society the budget for energy and sustainability actions within university campuses is not supported by certain incentives or grants but national universities develop their own policies and produce an annual budget for that purpose. MEXT is expected to issue a holistic guideline on sustainable campuses in 2013 based on the assessment of the existing campuses and their action plans. All the universities will be required to implement the guidelines by 2014 [12].

HU was founded in 1876 and is located in the centre of the city of Sapporo on the northern Japanese island of Hokkaido. It encompasses of 31 schools and currently counts over 18,000 students and 3,917 members of staff and the campus covers an area of 1,776,249 m^2 with a floor area of 739,368 m^2. In HU the Office for Sustainable Campus (OSC) overlooks a variety of programs and initiatives related to Sustainable Development (SD) established between departments and student associations. These initiatives could be categorized in four key groups consisting of the sustainable campus core schemes such as the establishment of the OSC and the set up of an Action Plan for a Sustainable Campus, sustainability programs (e.g. information campaigns), human resource development and education with sustainability related academic activities, leading Sustainability Networks and campus sustainability assessment schemes.

METHOD

Case study building

To understand the energy use behaviour and the effect of the university's environmental campaigns that took place during the previous year towards the sustainability perceptions of HU campus users, a questionnaire survey took place in the Institute of Low Temperature Science during November 2012 (Table 1).

	Main building	**Annex A**
Construction date	1968 (Renovated 2007)	2000
Building type	3 storey building	3 storey building
Number of occupants	126	47
Use	Research offices and labs, administration offices, amphitheatre	Research offices and labs, administration offices
Size	Total floor area: 3,948 m^2	Total floor area: 2,442 m^2
Heating type	Air-conditioning, manually set	Air-conditioning, manually set
Cooling type	Air-conditioning, manually set	Air-conditioning, manually set
Ventilation	Mechanical ventilation	Mechanical ventilation
Photo		

Table 1: Institute of Low Temperature Science building characteristics.

Questionnaire

The questionnaire was categorised in four sub-sections. Initially, a set of questions about age, gender, type of working area, employment time and working schedule were asked to give a background of basic demographics. In the second section, it prompted the building users to comment on the environmental conditions and the comfort levels in their workspace. Following that, the respondents were encouraged to comment on their energy use behaviour. Finally, it focused on their experience with sustainability campaigns in the university campus and attitude towards the issue of energy saving opposed to activity enhancement. A total of 149 questionnaires were distributed in two of the institute's buildings, the main building and the new annex with a total response rate of 68%. The results were analysed using bar-graphs and pie charts in order to identify percentages and main trends.

RESULTS

Demographics

The survey sample was male dominated (66%), with the majority of the participants being students between 20-29 years old (38%) working in office spaces (76%). Almost three quarters of the participants (74%) stated that they have been working in the building for more than a year indicating awareness of the energy reduction campaigns that took place during the past year.

Pro-environmental behaviour and the effect of personal and social norms

Approximately a quarter of the sample (30%) commented on the use of additional heating equipment while a third of the sample stated that it doesn't turn off the heating when leaving the room because it is either set on automatic mode or they are not aware of the way to do it. Interestingly, the building has a manually operated air-conditioning system, which gives the option to adjust and turn on/off the heating. While the rate of responses related to energy saving measures was significantly high (84%) a third of the participants (33%) stated of personal reasons behind their attitude towards energy use reduction with the past and ongoing OSC campaigns following (16% each). The social pressure after the Fukushima accident and the government policies were also considered at a lower extend (11% and 6% respectively). When the campus users where asked whether they prioritize energy saving over activity enhancement a noticeable 42% answered 'maybe' while an equivalent amount of respondents (38%) replied negatively indicating a lack of a certain opinion on the issue and a preference towards activity enhancement.

Campus sustainability campaigns

The low participation rate in campus carbon reduction activities (78%) because of lack of adequate information (38%), time constraints (15%) or other -not stated- reasons (37%) indicates a weakness of the ongoing activities to reach deeply and engage a large amount of the campus users. The difficulty to understand the meaning of the term 'energy reduction activity' was mentioned by some of the respondents along with the need of appointing faculty representatives.

Interest in future participation

The interest in future participation in carbon reduction activities was moderate (38%) however a considerable amount did not gave a straight answer (38%) stating 'maybe' indicating significant space for future action and shift of this opinion towards a positive response.

DISCUSSION

Based on the findings of the HU survey future research centres on the effectiveness of 'bottom-up' tools to facilitate behavioural change through a pilot study at the Gurdon Institute of the University of Cambridge conducted in May 2013. The use of statistical analysis tools (standard deviation, regression analysis) were relationships between different variables (energy use behaviour, demographic characteristics, spatial parameters, type of feedback) is sought, deepens the understanding between the interrelationship of different factors and could lead towards more rigid strategies based on the characteristics of certain groups.

The effectiveness of a behavioural change campaign with the use of a workplace footprint tracker at the University of Cambridge

As a result of the HEFCE's (Higher Education Funding Council for England) carbon reduction requirements the University of Cambridge has set a target for a 34% reduction in its energy related carbon emissions by 2020 against a 2005 baseline [13]. In response to the target the university has approved a Carbon Management Plan in 2010 with the Energy and Carbon Reduction Project (ECRP) aiming to trial different energy saving interventions. Gurdon Institute is a research institute, which constitutes predominantly of labs, a few offices and special equipment rooms. Under the auspices of the ECRP project it was the first pilot site to implement a significant behavioural change programme of user engagement in order to reduce its energy consumption. A WFT online-tool was installed where real-time metering of work-zones (research laboratories and equipment rooms), indoor climate (heating, cooling and ventilation), and services (computer servers, compressed air and vacuum plant) is displayed in carbon emissions (kg CO_2), cost (£) and Kilowatt-hours (KWh). Researchers have full access to the on-line information tool through their computers. A competition between the labs took place from March 2012 till September 2012 with a reward of £1000 to the lab with the most savings. The work-zone energy usage at the beginning of the competition equated to approximately 43% of the Institute's total energy consumption. By the end of September the different work zones had shown a decrease in electrical consumption by 19% (Figure 1). However, by the end of the year the reduction was close to 14% possibly due to a turnover of staff and new equipment added [14].

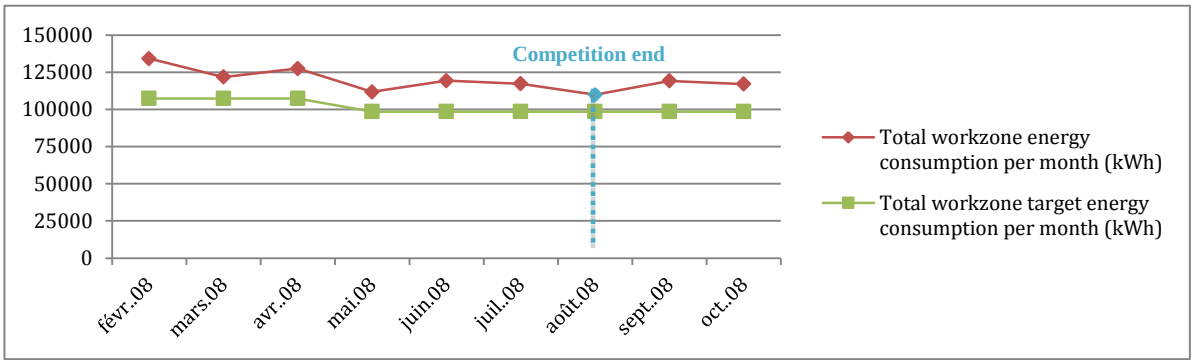

Figure 1: Actual and targeted average work zone energy consumption per month.

A comparative study between the labs that went through a behavioral change campaign in Gurdon Institute and a control group that did not take part aims to assess the lasting observable impact on energy use is planned to explore the synergy between different information and feedback mechanisms (footprint tracker, award, competition), examine the reciprocal information flow between individual house level to an institutional work environment and probe the limitations and motives of passive and active individuals.

CONCLUSION

The findings of the HU survey may have some practical implication for the structure of its future sustainability campaigns as they consist a good indication of the present situation and future potential of enhancing environmental friendly behaviours and participation in joined SD programs. The results indicate a lack of information on the proper use of the building systems and raise questions on how familiar the users are with temperature setting controls. Overall, the campus users highlighted self-motivation drivers to facilitate a behavioural change questioning the long-term effects of sustainability campaigns. The amount of passive participants is outweighed by the ones interested in future participation indicating the

potential of sustainability initiatives as long as the right communication strategies are implemented. There is considerable potential to drive sustainability activities and innovation emerging from within the HE sector, therefore, the sustainability strategies followed should be assessed and taken on board as key challenges and issues for the universities in line with their mission of shaping a better future.

ACKNOWLEDGEMENTS

Partial funding for this work came from the European Commission through the 7th Framework Program within the Marie Curie Actions IRSES-International Research Staff Exchange Scheme. The support of the Office for Sustainable Campus at Hokkaido University and the Environmental office at the University of Cambridge are gratefully acknowledged.

REFERENCES

1. IPCC, *Climate change 2007: Mitigation of Climate Change*, in *Contribution of Working Group III to the Fourth Assessment Report of the Intergovernmental Panel on Climate Change*, B. Metz, et al., Editors. Cambridge, UK, 2007
2. Whitmarsh, L., G. Seyfang, and S. O' Neill, *Public engagement with carbon and climate change: To what extent is the public 'carbon capable'?* Global Environmental Change. 21: p. 56-65, 2011
3. Kollmuss, A. and J. Agyeman, *Mind the gap: Why do people act environmentally and what are the barriers to pro-environmental behaviour?* Environmental Education Research. 8(3): p. 239-260, 2002
4. Stern, P., Towards a coherent theory of environmentally significant behaviour. Journal of social issues. 56: p. 407-424, 2000
5. Darby, S., Social learning and public policy: lessons from an energy-conscious village. Energy Policy. 34: p. 2929-2940, 2006
6. Borgstede, C. and A. Biel, Pro-Environmental Behaviour: Situational barriers and concern for the good at stake. Goteborg Psycological Reports. 32(No.1), 2002
7. Ockwell, D., S. O'Neill, and L. Whitmarsh, Behavioural insights: motivating individual emissions cuts through communication, in Routledge handbook of climate change and society. C. Lever-Tracy, Editor, Routledge: Great Britain. p. 341-350, 2010
8. HM Government, *The Carbon Plan: Delivering our low carbon future*. D.E.C.C., London UK, 2011
9. Schweber, L. and R. Leiringer, *Beyond the technical: a snapshot of energy and buildings research.* Building Research and Information. 40(4): p. 481-492, 2012
10. Takahashi, Y., Mid and Long Term Roadmap for Global Warming Countermeasures, in LCS RNet Second Annual Meeting2010, Ministry of Environment: Berlin.
11. Sunikka-Blank, M. and Y. Iwafune, Sustainable building in Japan - Observations on a market transformation policy. Environmental Policy and Governance. 21: p. 351-363, 2011
12. MEXT, *Guide to the creation of a sustainable masterplan*, Higher Education Bureau, Japan, 2011.
13. University of Cambridge, *Carbon Management Plan 2010-2020*. Cambridge, UK, 2010
14. Gurdon Institute, Introducing Behaviour Change Towards Energy Use: Strategies undertaken as a University ECRP pilot department, University of Cambridge, UK, 2012

COMBINED EFFECTS OF OCCUPANT BEHAVIOUR PATTERN AND BUILDING STRUCTURE ON THERMAL COMFORT

A. Drakou; A.Tsangrassoulis

Dept. of Architecture, School of Engineering, University of Thessaly, 38334 Volos, Pedion Areos, Greece

ABSTRACT

Considerable differences between energy simulation estimates and real energy consumption have been noticed, partly because of the occupant behaviour and its simplified pattern used for simulations. Thus, different regional behavioural patterns could, hinder the applicability of certain architectural and environmental strategies. The present study explores the relationship between the Greek behavioural pattern in residences, derived from a questionnaire survey, and different construction techniques of a typical apartment (naturally ventilated, conventional construction i.e. concrete post and beam construction with cement plastered and brick in-fill walls) located in Athens during summer. Greek residents interact significantly with the building shell during summer, in their effort to maintain comfort. Diverse behavioural patterns simulated indicate a variation of approximately 10% at the discomfort hours for a typical construction. The question raised, and addressed at this study, is whether different construction techniques of the typical flat may have a significant influence on the thermal behaviour of the apartment, for the specific behavioural pattern. The study uses dynamic thermal simulation (DesignBuilder) parametric analysis in order to predict the thermal performance of the apartment, for different construction techniques and a specific behavioural pattern. The variation on the construction examined, include envelopes with low thermal mass, high thermal mass walls with appropriate insulation and typical Greek construction of multi-family multi-story buildings, all in accordance with the new Greek Regulation for Buildings Energy Performance. Other influential factors as orientation, shading and the size of the external surfaces have also been implemented in the parametric analysis. The results indicate that for the specific behavioural pattern and building typology, the effect of various construction techniques on the thermal comfort is limited.

Keywords: occupant behaviour, residential, thermal mass, building simulation, comfort

INTRODUCTION

Under the scope of energy saving in building sector, the optimization of energy performance and thermal comfort of buildings has been of primary concern and consequently led to the development of low-energy building standards that have spread rapidly. These standards are characterized by lightweight constructions with low thermal transmittance envelope, usually by applying considerable thickness of insulation, ensuring thus minimum heat loss. Originated in rather heating dominated climates, where the reduction of heating demand is crucial, the concept of a thermally resistant envelope acting as a barrier to the harsh outdoor climatic conditions, ensure thermal comfort to the building's users throughout the year. Along with mechanical ventilation for the maintenance of appropriate indoor air quality, heat losses from window opening are avoided and both the building envelope and the user adopt a static, easily predictable, behaviour which facilitates energy saving. In the case of temperate climates, this concept of lightweight, super-insulated envelope raises concerns about its efficacy to address overheating phenomena during cooling period.

Vernacular architecture in Greece is identified with thick stone walls of high thermal mass and small windows, along with a dynamic behaviour of the user, who interacts with the building shell in order to satisfy its comfort needs to the changing outdoor climate conditions. There is a tendency, therefore, to believe that a significant amount of thermal mass can absorb the heat surplus from solar and internal heat gains, decreasing thus peak temperature and consequently reducing cooling load. An analysis of the literature shows that there are many conflicting opinions on the influence of the thermal inertia of residential buildings on their thermal behaviour and energy performance. In warm climates, thermal mass can reduce the cooling load to a maximum of 30%, but this percentage varies across a range of climates and occupancy/gains [1-3]. Thermal mass on its own does not decrease the cooling load. Only the appropriate combination of insulation and thermal mass can have a slight positive effect on cooling demand [4, 5]. The impact of thermal inertia on the annual cooling demand can be either an increase or decrease depending on the diurnal variations of the outdoor conditions and the intermittent use of active cooling systems, while the decrease of thermal capacity can lead to a significant increase on the peak cooling demand to a maximum of 65% [6].

The position of the insulating material plays also a significant role on the effectiveness of thermal inertia, offering significant reduction in annual cooling load, in hot climates [6,7], when it is placed on the external side of the wall, allowing the thermal mass to be in direct contact with the indoor environment. On the contrary, in tropical climates, internal insulation seems to have a better thermal performance during night time, thus being more cost-effective [8, 9]. It is worth noting that thermal mass can, usually, effectively reduce the indoor peak temperature during daytime, but at night the lower external temperatures would cool a lightweight structure more quickly. Therefore, it is possible that a lightweight structure with optimum orientation, shading and ventilation strategy perform thermally better than the isolated use of high thermal mass [4]. The main positive effect of thermal mass, according to the studies, is the normalization of internal temperature swing [3, 5, 10] and not the decrease of annual cooling load [3, 6, 11]. For high temperatures though, the coupling of high thermal mass with night ventilation and proper solar protection shows better performance [11].

Despite the numerous studies regarding the influence of high thermal mass on the energy and thermal performance of buildings, Greek Regulation for Buildings Energy Performance [12] specify maximum thermal transmittance, according to the climate zone, but not thermal properties of the opaque elements of the building envelope. Typical contemporary apartment buildings are still characterized by heavyweight construction, but the constantly growing problem of overheating has significantly increased the use of mechanical cooling systems [13, 14]. A questionnaire survey indicated significant interaction of Greek residents with the building shell during summer, in their effort to maintain comfort [13]. The simulation of predominant behavioural patterns derived from the survey, in a typical apartment indicated a variation of approximately 10% at the discomfort hours between different behavioural patterns [15]. The question raised, and aiming to address at this study, is whether different construction techniques of the typical flat may have a significant influence on the thermal behaviour of the apartment, for this specific behavioural pattern.

METHODOLOGY AND CASE STUDY

Dynamic thermal simulation (DesignBuilder) was used in order to predict the thermal performance of a typical, naturally ventilated apartment ($73m^2$) located in Athens, for different construction techniques and a specific behavioural pattern, during summer period (1June – 31 August). The building is well protected by other buildings to the south and north (i.e. these walls, the floor and the ceiling were considered as adiabatic) with east/west facing openings, shaded by large balconies. Cross ventilation was possible along the axis of East-

West. The apartment building is a conventional Greek construction i.e. concrete post and beam construction with cement plastered and brick in-fill walls. In order to determine the influence of internal thermal inertia on the apartment's thermal performance three types of walls were developed characterized by the same values of thermal transmittance (U-values), according to the new Energy Regulation [12] for the climatic zone B, but with different values of internal heat capacity (table 1). W1-as built represents the typical wall construction in Greece. The occupancy pattern and the internal gains from electrical equipment were derived from the occupants of the flat (2 working adults and 2 school-age children). All the openings of the flat are fully glazed sliding doors. The opening of the sliding doors in the model and the use of the cooling system were exclusively regulated by the schedules derived from the survey (in conjunction with the occupancy pattern) and not by the internal or external temperature (an airflow network model has been used). The percentage of the sliding doors opening was set to 50% which was the maximum feasible opening. A split AC unit (only cooling, no fresh air) was placed at the living room and the cooling set-point was set to 25^{o}C in line with the responses of the majority of the respondents. The internal doors of the flat remain constantly open, even when cooling system is in use, allowing the movement of the air between rooms. Other influential factors as orientation, shading and the size of the external surfaces have also been implemented in the parametric analysis. The most typical behavioural pattern [13] that relate to the frequency of use of the openings, the night ventilation and mechanical cooling were used for the simulations (table 2).

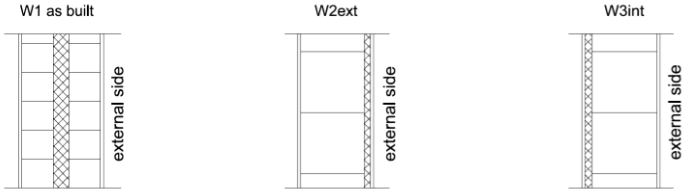

description	double brick fill in insulation	solid masonry (orthoblok) with external insulation	solid masonry (orthoblok) with internal insulation
wall thickness (cm)	28	25	25
insulation	expanded polystyrene (5cm)	expanded polystyrene (2c m)	expanded polystyrene (2cm)
Wall thermal transmittance (W/m2K)	0,5	0,5	0,5
Wall internal heat capacity (KJ/m2K) (according to EN13790)	137.184	57.984	15.204

Table 1. Characteristics of building external wall typologies studied.

Pattern	Open windows	Shading use	Mechanical cooling
B	21:00-09:00, 18:00-19:00	15:00-19:00	uses AC 14:00-17:00 / cooling setpoint 25oC

Table 2. Occupant pattern used for simulations.

DISCUSSION

The simulations analysis started using the main, according to the survey [13], occupant patterns (A. no active cooling, B. active cooling during noon, C. active cooling during night) for the three different types of external wall construction. As no difference was observed at the results between behavioural patterns, the analysis was restricted to the most representative [13] pattern (B) (table 2) that incorporates active cooling. Operative temperature's profiles for the living room show same mean, max, min and standard deviation (σ) values for all types of

external walls. This similarity attributed to high ventilation rate due to the long time that windows are open and due to the use of active cooling. For this reason, the parametric analysis continued with an extreme modification, assuming no ventilation (closed windows). It has to be mentioned at this point that the effect of thermal inertia is being evident when a combination of design parameters is applied. The absent of ventilation, the south-north orientation instead of west-east and the conversion of adiabatic walls to external (with the corresponding wall type construction) did not differentiate the results. A slight increase (max 0.5^{o}C) at the mean and maximum operative temperature is noticed for the wall with internal insulation, when shading is not considered and all walls are external (fig. 2b). This temperature difference increases and reaches the 1.2^{o}C when the floor is considered to be in contact with air (representing first floor in an apartment building with pilotis) (fig. 3).

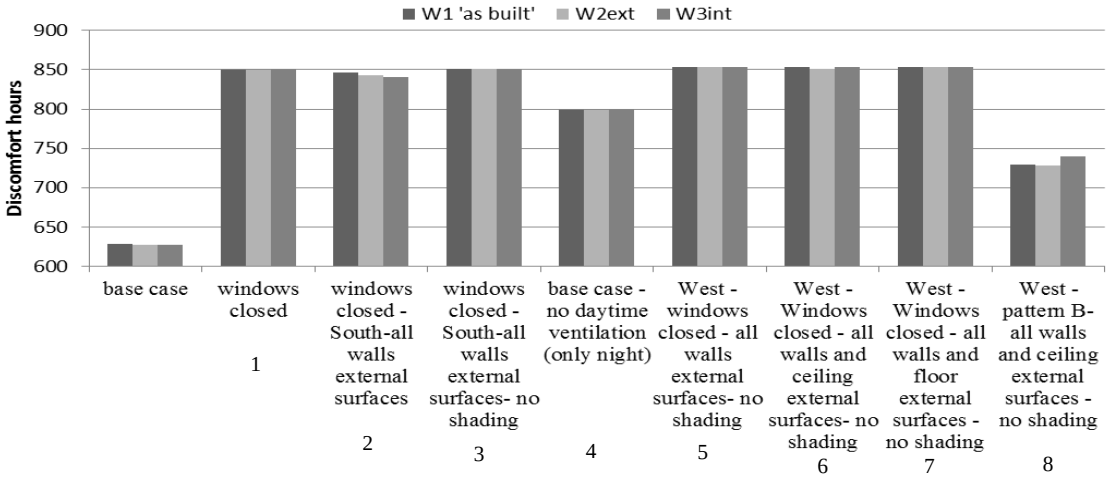

Figure 1. Discomfort hours for different parameters applied for the period 1June-31 August.

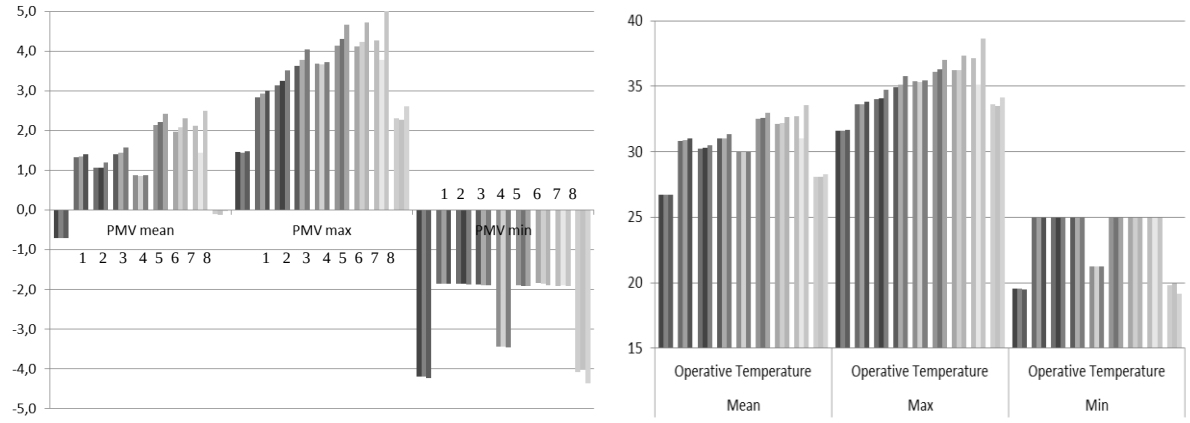

Figure 2 a) Fanger PMV and b) temperature mean, max and min values for different parameters applied for the period 1 June-31 August (order of walls:W1 'as built',W2,W3).

Maximum difference of 3.1^{o}C of mean operative temperature between the internal and external position of the insulation is observed when the orientation is west-east, no shading and ventilation is applied and the walls and ceiling are external surfaces (fig. 3). Fig. 3 presents the internal operative temperatures at the living room during a typical summer week for different wall types for this case. The operative temperature seems to follow a similar pattern for the three wall types, but the use of internal insulation has a negative effect as it leads to an up to 2^{o}C and 3.2^{o}C constant increase in the operative temperature compared to the typical and high thermal mass wall construction respectively.

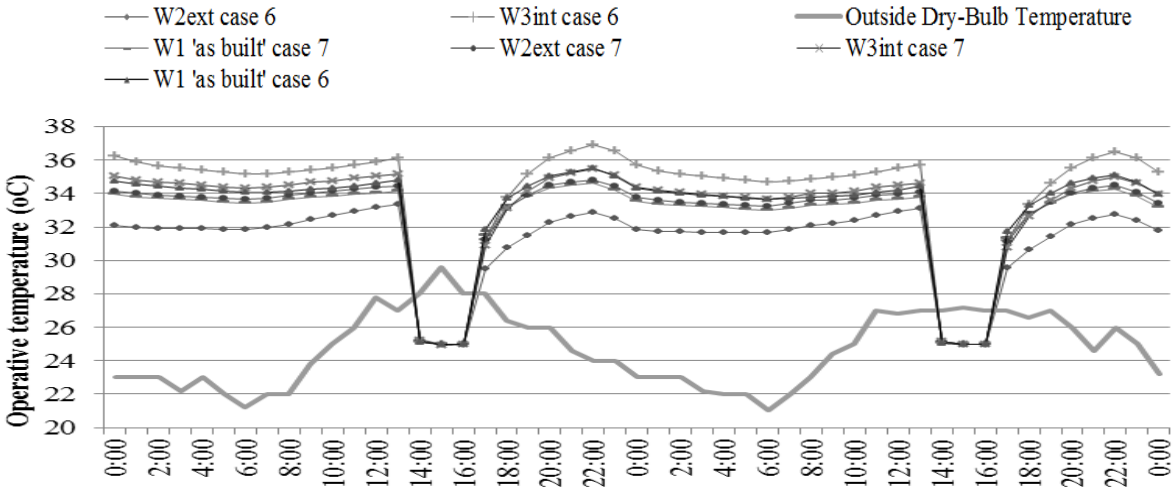

Figure 3. Operative temperatures at the living room for two days during typical summer week for different construction types.

PMV values (mean and maximum) also present differentiation between the wall types, in favour of high thermal mass wall. The amount of the discomfort hours, though, is not affected as ventilation is not considered in this case, so the absolute value of internal temperature is very high. Operative temperature reaches comfort levels only when active cooling is in use (14:00-17:00).When ventilation is applied in line with the occupant behavioural pattern B, the temperature difference between the wall types significantly decreases and the effect of thermal inertia becomes negligible (fig. 4). Low thermal mass wall still presents the slightly worse performance with the highest peak temperatures.

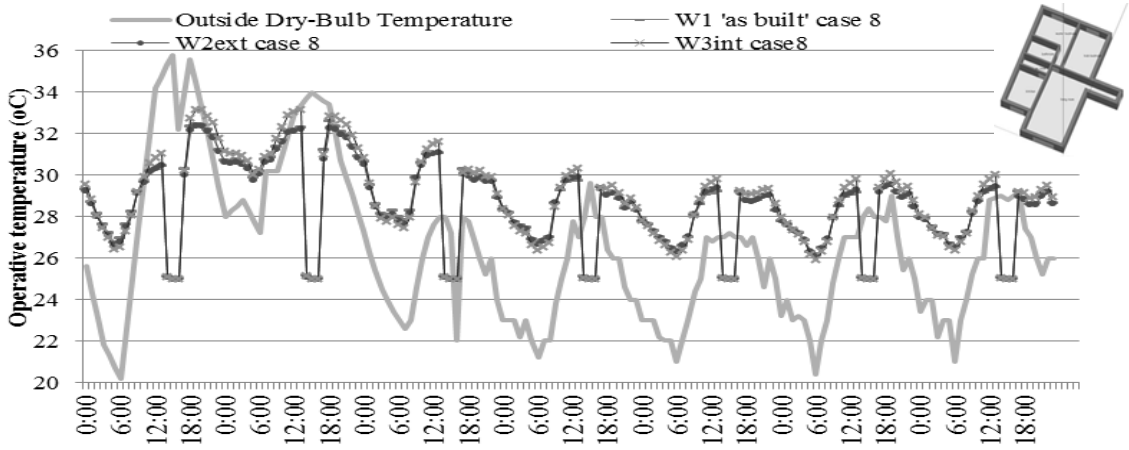

Figure 4: Operative temperatures at the living room for a typical summer week for different construction types case 8 (walls and ceiling external surfaces, pattern B).

CONCLUSIONS

A parametric analysis through dynamic simulations carried out in order to identify the effect of occupant behaviour and building structure on thermal comfort in a typical apartment during summer. Three wall configurations were set with equal thermal transmittance but different internal heat capacity. The results highlight that thermal inertia on its own is not able to define the level of thermal comfort. For most of the parameters, and their combination of them, applied at the simulations, operative temperatures' profiles, PMV index and discomfort hours present a remarkable similarity. Even when thermal mass was coupled with night ventilation,

a passive mean generally believed to exploit positive effects of thermal inertia, only a negligible decrease of 0.2^{o}C on the peak operative temperature was noticed. The maximum decrease on temperature was observed when the orientation was west-east, no shading and ventilation was applied, the walls and ceiling were external surfaces and the cooling system was used during noon. The influence of thermal inertia, in the present study, can be noticed only at lowering peak temperatures when a combination of parameters is applied.

ACKNOWLEDGEMENTS
The authors wish to thank Bodossakis Foundation for funding support.

REFERENCES

1. Yang, L. & Li, Y. Cooling load reduction by using thermal mass and night ventilation. *Energy and Buildings* **40,** 2052–2058 (2008).
2. Aste, N., Angelotti, A. & Buzzetti, M. The influence of the external walls thermal inertia on the energy performance of well insulated buildings. *Energy and Buildings* **41,** 1181–1187 (2009).
3. Flores Larsen, S., Filippín, C. & González, S. Study of the energy consumption of a massive free-running building in the Argentinean northwest through monitoring and thermal simulation. *Energy and Buildings* **47,** 341–352 (2012).
4. Bojic, M., Yik, F., Wan, K. & Burnett, J. Influence of envelope and partition characteristics on the space cooling of high-rise residential buildings in Hong Kong. *Building and Environment* **37,** 347 – 355 (2002).
5. Kendrick, C., Ogden, R., Wang, X. & Baiche, B. Thermal mass in new build UK housing: A comparison of structural systems in a future weather scenario. *Energy and Buildings* **48,** 40–49 (2012).
6. Bojić, M. & Yik, F. Cooling energy evaluation for high-rise residential buildings in Hong Kong. *Energy and Buildings* **37,** 345–351 (2005).
7. Kossecka, E. & Kosny, J. Influence of insulation configuration on heating and cooling loads in a continuously used building. *Energy and Buildings* **34,** 321–331 (2002).
8. Chiraratananon, S. & Hien, V. D. Thermal performance and cost effectiveness of massive walls under thai climate. *Energy and Buildings* **43,** 1655–1662 (2011).
9. Tummu, P., Chirarattananon, S., Hien, V. D., Chaiwiwatworakul, P. & Rakkwamsuk, P. Thermal performance of insulated walls enclosing residential spaces in Thailand. *Energy and Buildings* **61,** 323–332 (2013).
10. Karlsson, J., Wadsö, L. & Öberg, M. A conceptual model that simulates the influence of thermal inertia in building structures. *Energy and Buildings* **60,** 146–151 (2013).
11. Tuohy, P., McElroy, L. & Johnstone, C. Thermal mass, insulation and ventilation in sustainable housing-An investigation across climate and occupancy, 2005.
12. Technical Chamber of Greece, Energy Performance of Builings Directive – Technical Guidelines - T.O.T.E.E. 20701-1/2010 -Guidelines on the evaluation of the energy performance of buildings, Athens, 2010 (in Greek).
13. Drakou, A., Tsangrassoulis, A. "Exploring occupant behaviour in Greek residences during summer", Healthy Buildings 2012, 10th International conference, 8-12 July, Brisbane, Queensland, Australia
14. Plan of Action of Energy Performance. In the frames of Directive 2006/32/EC Athens, June 2008.
15. A. Drakou, A. Tsangrassoulis. "Analysis of the Greek behavioural pattern in residences and its effect on thermal simulation estimates", PLEA2012-28th Conference, Opportunities, Limits&Needs Towards an environmentally responsible architecture, Lima, Peru, 7-9 November 2012

BEHAVIOURAL NUDGES TOWARDS DOMESTIC ENERGY EFFICIENCY: OCCUPANT COMFORT AND THE LIMITS FOR SAVINGS FROM USER FEEDBACK PROGRAMS

A. Gillich[1]; M. Sunikka-Blank

University of Cambridge, Architecture Department, 1-5 Scroope Terrace, Cambridge, CB2 1PX, UK

ABSTRACT

Energy efficiency in dwellings is playing an increasing role in government strategies to mitigate carbon dioxide emissions. While significant savings are possible through retrofits, recent work is increasingly highlighting the role of behaviour in domestic energy use. There is a considerable body of literature reviewing the impacts of different kinds of feedback on energy consumption. These include providing customers their energy use, live updates through smart-meter displays, providing information on methods of conserving energy, neighbour comparisons, goal setting, and structured commitments. The effect sizes range from 0 to 20%, with usual savings between 5 and 12%, though noting that methodological issues cloud direct comparisons amongst studies.

Past work has highlighted the potential for 'nudges' to help influence choices through mechanisms such as social norms and default selection. The impact of feedback on energy use has been explored in a series of studies typically using small sample sizes and focusing on select population subsets. Some larger studies across more diverse populations demonstrate the challenges of bringing such programs to scale.

This paper presents a comparative review of past feedback studies. Typically, the effect size diminishes with increasing sample size, suggesting limitations on the potential to extrapolate behaviour change campaigns to larger scale programs. This paper reviews some of the causes and implications for this, and considers the role that occupant comfort plays in the potential for information and feedback to influence behaviour. While there is no doubt that there is significant potential for energy savings through behaviour change, the path towards achieving this contains significant methodological hurdles. While user feedback programs may offer low cost energy savings, the expectations for the performance and scale of such programs should be carefully managed.

Keywords: Behaviour change, social norms, user feedback, occupant comfort.

INTRODUCTION

Energy efficiency in dwellings is playing an increasing role in government strategies to mitigate carbon dioxide emissions. As the efficiency of our building stock improves, occupant behaviour plays an increasing role in our energy consumption. This is seemingly at odds with increasing expectations for comfort. The past decades have seen considerable investigation into the ways that feedback can influence energy use behaviour. These works frequently use small (N<1000) case studies to demonstrate the potential for savings between 10-20%, however larger studies often exhibit smaller effect sizes. This work will explore the relationship between effect size and sample size and argue that while there is undoubtedly much potential for savings through improved feedback, the ways in which to bring small pilot programs to scale are not straightforward and should be met with managed expectations.

Behaviour, Comfort, and Energy Conservation

The field of behavioural science is being increasingly applied to energy use. There is a well developed literature on the impacts of behaviour on energy use in dwellings [1]. While the proportion of energy use that may be attributed to occupant behaviour varies up to 33% [2] or higher based on a number of factors, the broad implication is clear: any attempts to maximise energy efficiency in housing must take account for occupant behaviour.

For decades environmental economists and sociologists have been concerned with the link between changing comfort expectations and the need for energy conservation [3]. Some have argued that historically diverse standards of comfort are converging around certain norms (eg. 21-22˚C), including increasingly high consumption westernised lifestyles [4]. Surveys of UK homes indicate a steady increase in average temperatures, with living rooms often heated above the standard 21-22˚C [4][5]. Shove [6] goes on to suggest that adhering to comfort standards such as ASHRAE commits society to unsustainable patterns of energy usage. Some call for the use of adaptive comfort models in the future, which take a more relaxed approach to defining comfort [4]. However, there is no denying that the present comfort paradigms are at odds with efforts to mitigate domestic carbon emissions through behaviour change.

The Role of Feedback

There is a considerable body of literature reviewing the impacts of feedback on energy consumption. Effect sizes range from 0 to 20%, with usual savings between 5 and 12% [7][8]. Social norms and behavioural nudges are a frequently used tool in feedback programs as they have been shown to increase the persuasive power of messaging [9][10].

Feedback programs have employed a wide range different messaging techniques including indirect feedback through enhanced billing, direct feedback through real-time in home displays, the provision of energy saving advice and information, neighbour comparisons, goal setting, and structured commitments. Another class of feedback includes bi-directional information or interactive interfaces such as website and smartphone apps. [11]

Reviews of past feedback programs frequently highlight that the methodological distinctions between programs limit the extent to which direct comparisons can be made amongst them. As noted by Darby [12], in addition to variations in feedback type and frequency, studies contain a range of sample sizes, housing types, and additional interventions. However, despite the hurdles, several themes are consistently identified as successful program features such as frequent feedback given over longer time periods, provide appliance specific breakdowns where possible, present information clearly, and use computational and interactive tools [8].

Impact of Sample Size

Numerous review studies consisting mostly of programs with smaller sample sizes (N<1000) have documented effect sizes around 5-12% [7]. Smaller studies often optimistically project that larger savings are possible by multiplying their effect sizes by a wider population, however evidence suggests that scaling up pilot programs is non-trivial. For example, OPower represents one of the most common instances of a feedback program being brought to scale, with sample sizes around the United States in excess of 78,000. The effect sizes documented by OPower range from 1.1-2.8% [13].

While many have noted the trend of decreasing effect size with increasing sample size, the observation rarely receives much focus. Ehrhardt et al. [11] commented in their review of 57 feedback studies that the more diverse and representative sample of households may suggest larger-scale feedback programs are more likely to experience modest savings. They further

noted that their assertion was far from conclusive, calling for further research in the area. As a growing number of utilities and governments attempt to incorporate feedback and information programs to their energy efficiency strategies [14], it is important to consider both the hurdles and the limitations in expanding feedback programs to a larger scale.

METHOD AND ANALYSIS

The past decade has seen several review papers collate the primary feedback studies and sift out common features for their success. This paper looks at the results of four major review papers produced in the past seven years: Darby's [7] review of 38 feedback programs, Faruqui et al [15] review of 12 utility pilot programs, the Ehrhardt-Martinez et al [11] review of 57 primary studies, and finally the Foster [16] review of 9 larger scale programs. These reviews were chosen as they are frequently cited works, they cover a large range of feedback programs, and a broad spectrum of sample sizes. The four review papers cover a total of 116 individual feedback programs that have operated from 1976 to the present. After removing duplicates, and studies that could not easily be simplified to a single effect and sample size, there remained 67 feedback programs in the sample.

These 67 studies contain considerable methodological differences such as feedback types, frequencies, and associated technologies. In addition, some studies measured their savings against a control group, while others compared their results to the pre-study period. Studies variably included gas, electricity, or both. Where studies included multiple treatment groups, a weighted average of the effect size was used. This work attempted to control for these variables by perturbing each one and plotting the resulting change. The departures from the trends given in Figure 1 were negligible.

In addition to these factors, there were several further forms of variation amongst studies that were beyond the control of this paper. Darby [7] noted that the effect size could also be influenced by the situation, with homes in more extreme weather conditions or having otherwise higher utility bills being more sensitive to feedback. Most, but not all studies indicated weather correction in their recorded sample size. Finally, each study used a different methodology to account for free-ridership and spill-over from simultaneous initiatives such as weatherisation. Some did not control for free-ridership at all. This work attempted to compensate for this lack of control by considering a large number of studies and looking at the general trends, thus limiting the influence of the methodological distinctions of any individual study. Indeed, a sensitivity analysis showed that the decision to include or omit any individual study had little impact on the overall trend.

The scatter plot shown in Figure 1 gives the distribution of the effect size versus the log of the sample size. As expected, the distribution is somewhat diffuse due to the previously mentioned methodological differences among studies. The R^2 value of 0.07 indicates that the fit of the logarithmic trend-line is poor. Because this is not a statistically robust fit, the R^2 value varies slightly when excluding individual studies with differing methodologies, however the shape and approximate slope of the trend-line remained unchanged. This therefore supports the commonly held belief that increasing sample size correlates with a reduction in the effect size for a feedback program.

A notable exception, which stands among the only large scale studies to defy the correlation in Figure 1, is the Northern Ireland case with a sample size of 45,000 and an effect size of 19%. The study covered a natural experiment in 2002 [17], in which homeowners received upgrade prepayment meters that offered instantaneous feedback and allowed them to monitor their energy use. The previous prepayment meter did not indicate energy use. A number of factors make this case difficult to repeat. The utility rates were among the highest in the UK,

and due to the nature of their antiquated prepayment meters, they had a relatively high starting point from which to make savings with the new keypad prepayment meters.

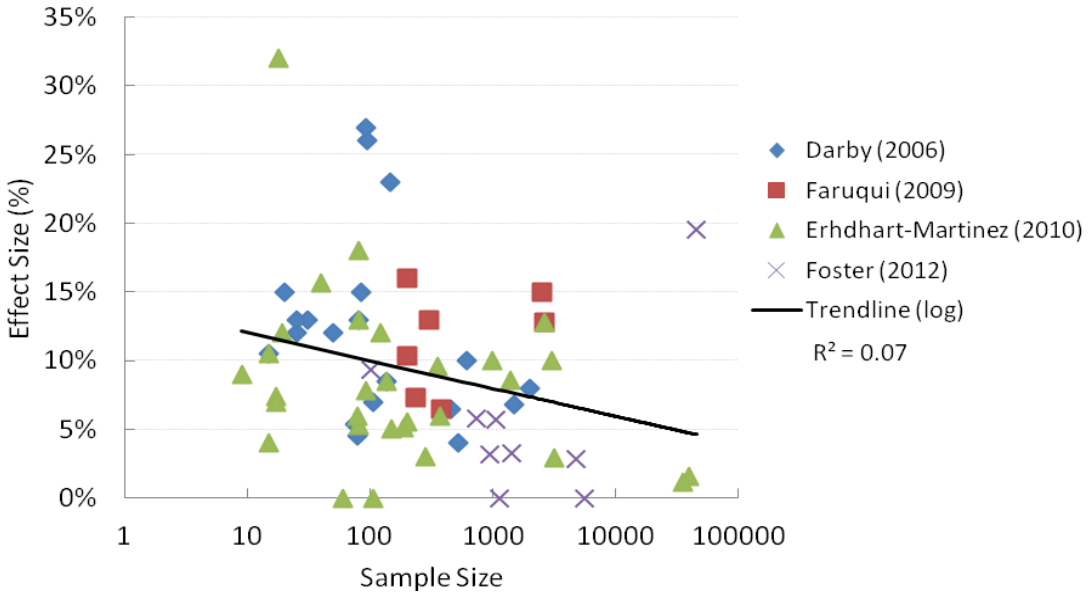

Figure 1: Scatter plot of 67 feedback studies, effect size versus log of sample size.

DISCUSSION

There are a number of possible explanations for the fact that increasing sample size correlates with a reduction in the effect size for a feedback program. Some of these will now be discussed in further detail.

It is highly likely that smaller studies exhibit a form of selection bias in creating their samples. In conducting this review, it was observed that many programs called for volunteers in order to create their sample group. It stands to reason that smaller studies are more likely to call for volunteers than larger studies, which frequently assign participants from a pre-existing group (eg. a randomised sample from a utility database). In their analysis of a feedback program in Chicago, EPRI [18] found that 10% or less of the population was likely to respond to dynamic pricing and real-time feedback treatments. The authors hypothesised that this low figure may have been in part due to the 'opt-out' design of the program, meaning that customers were enrolled without their consent and given the option leave the program. This suggests that programs that have the luxury of requesting volunteers will be more likely to have participants that are more motivated to respond to the proposed feedback.

There is strong consensus in the literature that frequent feedback is more effective than rarer feedback. Benders *et al.* [19] considered the issue of scalability in their study, noting that mass marketing campaigns are less effective than personalised messaging. The smaller studies reviewed in this paper more frequently reported offering personalised attention, even individual attention to program participants. However, frequent and personalised communication is clearly more labour intensive and costly to bring to scale. Benders *et al.* therefore identified computational tools to help address this, such as websites that can be easily adjusted. Web interfaces have the advantage of offering bi-directional communication, further enhancing the potential for useful feedback to reach participants. Another effective example of this is the Green Button campaign hosted by the US Department of Energy [20]. Note that such solutions are only available to online customers, but with increasing access to broadband and the proliferation of smart phones, online feedback tools are very promising.

A final issue in bringing feedback programs to scale is the inevitable diversity of the homeowners in terms of behaviour, motivation, and comfort expectations. Smaller studies are far more likely to find a homogeneous population that is receptive to the feedback. Opinion Dynamics [21] conducted a segmentation analysis (N=752) in California in which they used detailed surveys to create an attitudes and behaviour cluster analysis model. This model grouped respondents into five behavioural classes based on their energy use decision making habits and the types of messaging to which they would likely be responsive. They found that 39-54% of respondents could be classified in groups that were unlikely to sacrifice personal comfort for energy savings. Respondents also differed greatly in the type of messaging and feedback to which they would likely be responsive. The larger the sample size, the more likely participants will cover a range of behavioural categories such as those described by Opinion Dynamics. Efforts to bring feedback programs to scale must acknowledge this, and find means of diversifying their messaging and calibrating it to their target audience.

CONCLUSIONS

Despite the considerable number of feedback studies over the past several decades, there remain some very important questions to address about how to maximise the potential for energy savings through behaviour change. Feedback programs have consistently shown their efficacy at small scale pilot programs, but as more and more utilities and government programs attempt to implement feedback programs at scale, great care must be taken in order to replicate the level of savings seen with small sample sizes.

Despite the methodological limitations, this work attempted to confirm the commonly held view that sample size is inversely proportional to effect size. It then offered a perspective on possible reasons for this correlation. Feedback programs should mind the way in which they select their sample populations, noting that volunteers are likely to be more receptive to feedback. Frequent, personal feedback is more effective but is difficult to execute cost effectively at a large scale. Programs should look to online tools to aid in this process.

Finally, the population diversity is likely to increase with sample size, and a program is increasingly likely to encounter people that value comfort over energy savings. At the same time as occupants are demanding greater comfort, governments are increasingly calling for savings through behaviour change and trying to achieve this through nudges and feedback programs. Effort should be made to understand the target demographics of large scale feedback programs and create calibrated messaging to which they are likely to be responsive. While there is much potential for low cost savings in this way without sacrificing comfort, the path for bringing pilot programs to scale requires further consideration.

REFERENCES

1. *Behavioral Approaches to Residential Energy Conservation.* Seligman, Clive, Darley, John M. and Becker, Lawrence. 1978, Energy and Buildings, pp. 1:325-337.
2. *Movers and Stayers: The Resident's Contribution to Variation across Houses in Energy Consumption for Space Heating.* Sonderegger, Robert C. 1978, Energy and Buildings, pp. 1:313-324.
3. *Comfort and Energy Conservation: A need for Reconciliation?* Cooper, Ian. 1982, Energy and Buildings, pp. 83-87.
4. Chappells, Heather and Shove, Elizabeth. Comfort: A review of philosophies and paradigms. March 2004.
5. Walters, G.A, Kempson, I. and Shorrock, L.D. *Domestic Energy Fact File.* BRE, 2000.

6. Shove, E. Comfort, cleanliness and convenience: the social organisation of normality. Oxford, Berg. : s.n., 2003.

7. Darby, Sarah. *The Effectiveness of Feedback on Energy Consumption.* Oxford, UK : Oxford Environmental Change Institute, 2006. Working Paper - DEFRA Review.

8. *Feedback on Household Electricity Consumption: a tool for saving energy?* Fischer, Corinna. 2008, Energy Efficiency, pp. 1:79-104.

9. *A Focus Theory on Normative Conduct: Recycling the Concept of Norms to Reduce Littering in Public Places.* Cialdini, Robert B., Reno, Raymond, R. and Kallgren, Carl A. 1990, Journal of Personality and Social Psychology, pp. Vol 58, No 6, 1015-1026.

10. *Changing Behavior With Normative Feedback Interventions: A Field Experiment on Curbside Recycling.* Schultz, W. P. 1998, Basic and Applied Social Psychology, pp. 21 [1]. Pgs 25-36.

11. Ehrhardt-Martinez, K, Donnelly, Kat and Laitner, John. *Advanced Metering Initiatives and Residential Feedback Programs: A Meta-Review for Household Electricity Savings Opportunities.* s.l. : American Council for an Energy-Efficient Economy [ACEEE], 2010.

12. *Making it obvious: Designing feedback into energy consumption.* Darby, Sarah. Naples, Italy : Italian Association of Energy Economists, 2000. Proceedings of 2nd International Conference on Energy Efficiency in Household Appliances and Lighting.

13. *Social Norms and Energy Conservation.* Allcott, Hunt. 2009, Working paper, Massachusetts Institute of Technology [MIT], Cambridge, MA].

14. Mahone, Amber and Haley, Ben. *Overview of Residential Energy Feedback and Behavior-Based Energy Efficiency.* San Francisco, CA : Energy and Environmental Economics, Inc., 2011. Consumer Information and Behaviour Working Group of the State and Local Energy Efficiency Action Network.

15. *The Impact of Informational Feedback on Energy Consumption - A Survey of Experimental Evidence.* Faruqui, Ahmad, Sergici, Sanem and Sharif, Ahmed. 2009, Social Science Research Network.

16. Foster, Ben and Mazur-Stommen, Susan. *Results from Recent Real-Time Feedback Studies.* Washington, DC : ACEEE, 2012. Report B122.

17. Gans, Will, Alberini, Anna and Longo, Alberto. *Smart Meter Devices and the Effect of Feedback on Residential Electric Consumption: Evidence from a Natural Experiment in Northern Ireland.* Zurich : Swiss Federal Institute of Technology, 2011. WP No.78.

18. EPRI. *The Effect on Electricity Consumption of the Commonwealth Edison CustomerApplications Program: Phase 2 Final Analysis.* Palo Alto, CA : Electric Power Research Institute, 2011. Technical Report.

19. *New approaches for household energy conservation—In search of personal household energy budgets and energy reduction options.* Benders, Rene M.J., et al. 2006, Energy Policy, pp. 3612-3622.

20. DOE. Green Button - Energy.gov. [Online] 2013. [Cited: 29 04 2013.] http://energy.gov/data/green-button.

21. Opinion Dynamics. *Market Segmentation Findings.* s.l. : Memorandum prepared for the California Public Utilities Commission., 2009.

A NEW VENTILATION CONTROL STRATEGY FOR OFFICE BUILDINGS

X. Lü; T. Lu; M.Viljanen

Department of Civil and Structural Engineering, School of Engineering, Aalto University, P.O. Box 12100, Espoo, Finland

ABSTRACT

Buildings have a significant effect on energy use and the environment, accounting for a large amount of energy consumption and carbon dioxide (CO_2) emissions. A large portion of the energy in office buildings is contributed to space heating and ventilation. Proper ventilation is, therefore, essential for maintaining a good indoor environment and minimizing energy consumption. Currently, CO_2-based demand controlled ventilation (DCV) control is used widely and considered as an economical means to achieve the best balance between indoor air quality and energy consumption. It is especially useful for office buildings. Many practical approaches are available for implementing CO_2-based DCV, with proportional and exponential controls being the strategies most often cited. However, most of these methods need trial and error tuning, which poses a major challenge in practice. To update the current CO_2-based DCV strategies, this paper presents a new and more flexible approach to extending the previous strategy designed for sports buildings. Comparison with conventional CO_2-based DCV control algorithms shows its superiority to conventional strategies.

Keywords: ventilation control, demand-controlled ventilation, energy saving, office buildings

INTRODUCTION

Buildings have a significant effect on energy use and the environment, accounting for 40-50% of total energy consumption and carbon dioxide (CO_2) emissions in EU countries. A large portion of energy usage in office buildings is contributed to space heating and ventilation. Ventilation, on the other hand, is one of the most important contributing factors to indoor air quality (IAQ). Proper ventilation is, therefore, essential for maintaining a good indoor environment and minimizing energy consumption. Various strategies, ranging from simple to complex, have been proposed to reduce energy consumption and to keep good IAQ. CO_2 – based demand-controlled ventilation (DCV) is probably the best known one [1]. It is especially useful for office buildings. Congradc and Kulic [2] used genetic algorithms to optimize the return damper position such that indoor CO2 concentration can be kept close to the desired level as possible and at the same time the lowest value of the valve (the lowest energetic use) can be accomplished. Pavlovas [3] provided a case study over a Swedish multifamily apartment aiming at evaluating the demand-controlled ventilation system with different strategies. Mysen et al. [4] inspected one hundred and fifty-seven Norwegian classrooms to analyze the energy use over there different ventilation systems: Constant Air Volume (CAV), CO2 sensor based demand-controlled system (DCV-CO2) and infrared occupancy sensor based demand-controlled system (DCV-IR).

For control algorithms of CO_2-based DCV, proportional control is one of the most applied methods. It modulates ventilation between a lower set point of indoor CO_2 and an upper set point that represents the equilibrium concentration of CO_2 corresponding to the target per-person ventilation rate of a space [1]. The potential energy saving for this method, however, is affected by the factor how closely the actual design ventilation rate achieves the ventilation

required for the actual occupancy in the space. Such trial and error tuning poses a major challenge in practice. In this paper, we propose new control strategy to address the current challenge of control algorithms. The new strategy extends the previous one designed for sports buildings [5, 6]. It is simple, economical and flexible which can be used as an alternative for conventional CO_2 DCV control algorithms.

METHOD

The Model

To illustrate, we assume that the office building has a single-zoned room (sports hall, see below) and indoor air is well mixed. For a mechanically-ventilated space, the CO_2 concentration is modelled:

$$V\frac{dC}{dt} = Q(C_o - C(t)) + G(t) \quad (1)$$

where
t = time
V=space volume
C(t)=indoor CO_2 concentration
Q=volumetric airflow rate (fresh air) into (and out of)
C_o=outdoor CO_2 concentration
G(t)=CO_2 generation rate

For constant Q, C_o and G(t) , we have

$$C(t) = C_o + \frac{G(t)}{Q} + (C(0) - C_o - \frac{G(t)}{Q})e^{-It} \quad (2)$$

where

C(0)=initial indoor CO_2 concentration

I=Q/V, air change rate

Note that if the CO_2 generate rate is constant for a sufficient time, the last term on the right side of Eq. (2) converges to zero, and the equation can be rewritten as:

$$C_{eq} = C_o + \frac{G}{Q} \quad (3)$$

where C_{eq} is called as the equilibrium CO_2 concentration.

In CO_2-based control approach, C_{eq} is taken from a predefined CO_2 level, G is the design generation rate, Q is the required design ventilation rate for the space. In ASHRAE 62–2007 [7], the minimum requirement for the outdoor air ventilation rate is provided based on the number of occupants.

The Proposed Control Strategy

The sports training hall is used as a test office room to demonstrate the proposed control strategy. We assume that open hours are made up of some training sessions (business or occupied period) and breaks (unoccupied period). A typical timeframe is illustrated in Figure 1.

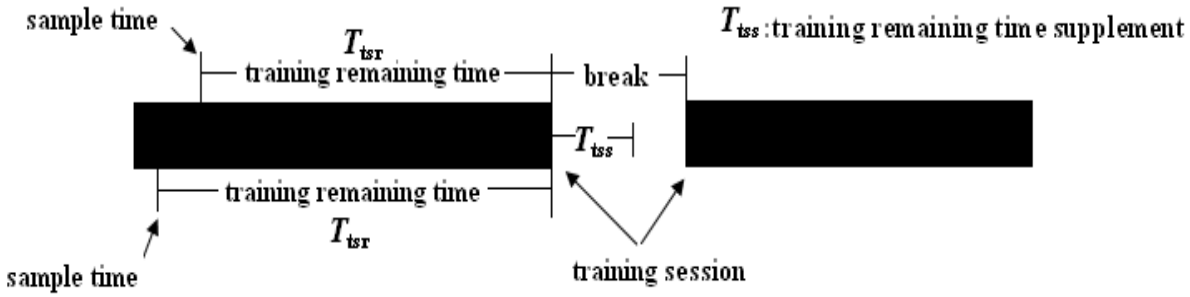

Figure 1: Timeframe for the test office.

Here, *sample time* is defined as the time for reading indoor CO_2 concentration from the sensor. *Sample interval* is defined as the time difference between two sample times. *Training remaining time* (T_{tsr}) is the time period between the *sample time* and the end time of a training session. *Training remaining time supplement* (T_{tss}) is a supplement time period which can be any value (e.g. 10 minutes).

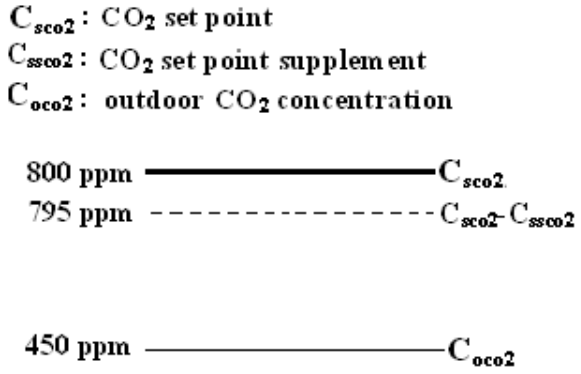

Figure 2: Illustration of CO_2 set point and CO_2 set point supplement.

The basic idea is to use T_{tss} (training remaining time supplement) to extend T_{tsr} (training remaining time) in case the indoor CO_2 concentration exceeds the CO_2 set point at the end of a training session. *CO_2 set point supplement* ($C_{ssco2,}$ Figure 2) acts as in a similar fashion as T_{tss}, except that it is used to lower the CO_2 set point to prevent the indoor CO_2 concentration from exceeding the CO_2 set point. The new method can be described as follows:

1. If sample time is in a break, set the base ventilation as the ventilation rate.
2. If sample time is in a training session, the method goes through the following steps:
   Step 1: Estimate the number of occupants by directly solving Eq. (1);

Step 2: Calculate the minimum requirement for the outdoor air ventilation rate based on Eq. (4). This step ensures the minimum ventilation requirement of outside air by industry standards, such as ASHRAE 62-2007.
Step 3: Calculate the ventilation rate via Eq. (2) by setting: C(0)=measured indoor CO_2 concentration at the sample time, G=estimated from Eq. (1), t= T_{tsr} + T_{tss}, and C(t)= C_{sco2} (CO_2 set point) - C_{ssco2}.
Step 4: Select the maximum value from calculated ventilation rates in Steps 2 and 3 as the building/space ventilation rate.

Note that for more complicated cases, Eqs. (1) can be further enhanced by two zone or multizone model [8]. The implementation of the new strategy can be done flexibly in many ways. Details can be found in [5].

RESULTS

Experiments

These experiments were conducted over a sports training center in Finland. Data were obtained using both simulated and experimental CO_2 generation rates in Matlab. The information about the sports training center is as followed:

Opening hours:	7 a.m. to 23:00 p.m.
Volume:	17220 m^3
Design capacity:	80 persons
Design parameter for minimum requirement of outdoor air:	8 dm^3/person

The base ventilation rate and the maximum possible ventilation were set as 0.26 m^3/s and 3.48 m^3/s respectively based on the actual ventilation system. The outdoor CO_2 concentration was set as 450 ppm (constant) and CO_2 set point as 800 ppm. The sample interval was 5 minutes. As a benchmark, proportional control algorithm [18] was also implemented.

Simulation Results

Figure 3 and Table 1 show the comparison results.

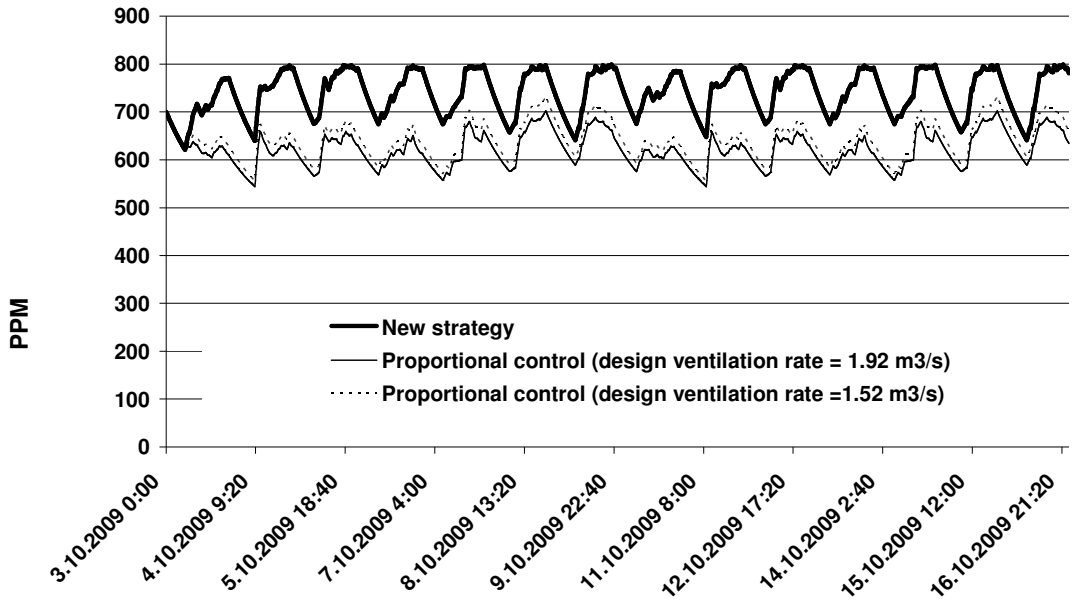

Figure 3: Comparison of simulated indoor CO_2 concentrations between the new strategy and the proportional control.

Control approach	Average ventilation rate (m^3/s)	Average CO_2 concentration during opening hours (7 a.m. – 23 p.m.)
Proportional control (1.92 m^3/s)[a]	0.72	628 ppm
Proportional control (1.52 m^3/s)[a]	0.65	648 ppm
New strategy	0.43	749 ppm

Table 1: Comparisons of average ventilation rates between new strategy and proportional control.

The results clearly show that even though the proportional control algorithm was assigned with a very ideal design ventilation rate (i.e.1.52 m3/s), the indoor CO_2 concentration is under 700 ppm most of the times, which is far away from the CO_2 set point – 800 ppm. As a consequence, the space is often over ventilated although the minimum ventilation rate of outdoor air can be satisfied based on the industry standards. In contrast, the newly developed strategy controlled CO_2 concentration is much closer to the CO_2 set point. This phenomenon is more strongly manifested in training dense periods (or occupied periods) where the indoor CO_2 concentration is mostly controlled between 770 ppm and 800 ppm (results not shown here due to the space limitation).

CONCLUSION

A novel and simple CO_2 DCV strategy was developed for office buildings and sport training was used as an illustration to demonstrate the strategy. The results were verified by simulations using both simulated and experimental CO_2 generation rates and show that the estimated indoor CO_2 concentrations are much closer to the CO_2 set point than the commonly

used proportional control approach. The new strategy improves upon conventional control approaches with many new features, of which important features were, for example, 1) dynamically determines ventilation rate; 2) simpler and easier to be implemented; 3) more flexibly to be extended. It is worth mentioning that the new strategy is applicable for not only buildings where opening hours are scheduled but also other kinds of commercial buildings.

ACKNOWLEDGEMENTS

We are grateful to the Academy of Finland for financial support.

REFERENCES

1. Schell, MB. Turner, SC., Shim, RO.: Application of CO_2-based demand-controlled ventilation using ASHRAE standard 62: optimizing energy use and ventilation, ASHRAE Transactions, Vol 104, pp1213-1225, 1998.
2. Congradac, V., Kulic, F.: HVAC system optimization with CO2 concentration control using genetic algorithms, Energy and Buildings, Vol 41, pp571-577, 2009.
3. Pavlovas, V.: Demand controlled ventilation a case study for existing Swedish multifamily buildings, Energy and Buildings, Vol 36, pp1029-1034, 2004.
4. Mysen, M., Berntsen, S., Nafstad, P., Schild, PG.: Occupancy density and benefits of demand-controlled ventilation in Norwegian primary schools, Energy and Buildings, Vol 37, pp1234-1240, 2005.
5. Lü, X., Lu, T., Viljanen, M., Kibert, CJ.: A new method for controlling CO_2 in buildings with unscheduled opening hours, Energy and Buildings, Vol 59, pp161-170, 2013.
6. Lu, T., Lü, X., Viljanen, M..: A novel demanded-control ventilation strategy for CO2 control and energy saving in mechanically-ventilated buildings, Energy and Buildings, Vol 43, pp2499–2508, 2011.
7. ASHRAE Standard 62-2007, Ventilation for Acceptable Indoor Air Conditioning Engineers, Atlanta, GA, 2007.
8. D2 Finnish code of building regulations, Indoor climate and ventilation of buildings, Regulations and Guidelines, Ministry of the Environment, Helsinki, 2003.

LEARNING FROM OUR EXPERIMENTS: MONITORED ENVIRONMENTAL PERFORMANCE OF LOW ENERGY BUILDINGS IN SCOTLAND

T Sharpe, D Shearer

Mackintosh Environmental Architecture Research Unit, GSA, 167 Renfrew Street, Glasgow G3 6RQ

ABSTRACT

This paper reports on six Technology Strategy Board funded projects that are examining the performance of a range of new build low energy houses throughout Scotland. These are two-year monitored projects that capture quantitative data on energy consumption and environmental conditions including air quality, but also qualitative data through interviews and surveys with occupants and designers. The projects (n=26) have a number of varying characteristics, including different types of construction and design intention, including some Passivhaus, and more mainstream social housing. The paper will examine and compare early observations of comparative performance in respect of air quality. Factors include occupancy and ventilation behaviours, but also include room volume, openings, and mechanical systems. The study identifies trends in terms of high temperatures and CO_2 levels, particularly in bedrooms overnight.

Keywords: Indoor Air Quality, CO2, Occupancy, Behaviour, Comfort, Health, Ventilation

INTRODUCTION

The increasing importance of climate change has led to governments establishing targets for carbon reduction [1]. The primary mechanism for achieving these targets has been increasingly stringent requirements for energy performance [2]. This in turn has led to the adoption of new designs, materials and technologies for buildings that seek to reduce energy consumption. However it is increasingly apparent that there can be significant performance gaps between design intentions and actual performance of buildings and this is increasingly well-evidenced [3], [4], [5], [6].

The main focus of primary legislation is on energy and carbon performance, but there is also increasing concern about other areas of environmental performance, particularly Indoor Air Quality (IAQ) and overheating [7]. [8]. As well as being causes for concern in their own right [9], these issues can also undermine energy strategies, for example overheating being controlled by liberal window opening, leading to increased energy consumption.

To investigate these questions the UK Technology Strategy Board has funded a 4-year £8m programme of Building Performance Evaluation for both domestic and non-domestic buildings across the UK. MEARU is engaged in 6 domestic projects in Scotland, which include detailed monitoring of environmental conditions (including air quality) and energy consumption (including sub-metered energy) over a 2-year period. This is contextualised with a review of construction, testing of fabric performance and gathering of qualitative data from residents about their patterns of behaviour and occupancy. This paper will discuss a broad comparative analysis of the initial results and identify key issues and areas for deeper investigation.

METHOD

The projects being monitored are in 6 different geographic locations across Scotland: Inverness IN (n=8), Livingston LI (n=2), Lockerbie LO (n=4), Barrhead BA (n=3), Glasgow GL (n=6) and Dunoon DU (n=3) Total n=30. The general form and construction of the dwellings is summarised in Table 1. Additional information is provide for bedrooms – room volume, Trickle vents, Occupants, Window opening, and Time Weighted Average (11pm – 7am) CO_2 levels.

									Bedrooms				
Loc	Ref	Const Type	Type	MVHR	Bed	Air Perm	GIFA (m^2)	Heating	Vol	TrV	Occ	WO	TWA
BA	*27MP*	*TF*	*H MT*	*No*	*2*	*4.25*	*93.9*	*Gas CH*	*31.23*	*Yes*	*2A*	*N*	*1888.80*
BA	*29MP*	*M*	*F GF*	*No*	*2*	*2.88*	*75.8*	*Gas CH*	*31.50*	*Yes*	*1A*	*Y*	*1124.44*
BA	*37MP*	*TF*	*H ET*	*No*	*2*	*4.98*	*75.4*	*Gas CH*	*30.34*	*Yes*	*2A*	*N*	*2101.49*
LO	**BC**	**TF**	**H SD**	**Yes**	**2**	**2.42**	**87.3**	**MVHR**	**33.68**	**No**	**1A**	**N**	**n/a**
LO	**CC**	**TF**	**H SD**	**Yes**	**2**	**2.14**	**87.3**	**MVHR**	**33.68**	**No**	**1A**	**N**	**762.98**
LO	**HC**	**TF**	**H SD**	**Yes**	**3**	**2.72**	**102.8**	**MVHR**	**35.76**	**No**	**1C**	**N**	**1111.24**
LO	**OC**	**TF**	**H SD**	**Yes**	**3**	**2.41**	**102.8**	**MVHR**	**35.76**	**No**	**1C**	**N**	**1073.33**
DU	P5	CPTF	H SD	No	3	4.04	113.6	ECH	30.77	Yes	1A	N	1852.98
DU	P14	CPTF	H SD	No	3	4.29	113.6	Elec CH	30.77	Yes	1A	N	872.84
DU	**P15**	**CPTF**	**H SD**	**Yes**	**2**	**0.96**	**103.4**	**ASHP**	**37.85**	**No**	**1A**	**Y**	**913.65**
IN	3BS	TF	H ET	No	3	3.82	109.0	Gas CH	28.08	Yes	2A	N	1457.70
IN	4BS	TF	H MT	No	3	4.21	109.0	Gas CH	28.08	Yes	2A	N	n/a
IN	6BS	TF/M	F GF	No	2	5.71	76.00	CB CH	23.30	Yes	2A	N	701.30
IN	7BS	TF/M	F GF	No	2	4.53	76.00	CB CH	21.86	Yes	2A	N	1335.12
IN	4BG	TF	H SD	No	3	5.82	90.00	Gas CH	28.70	Yes	1A	N	1501.86
IN	5BG	TF	H SD	No	3	6.07	90.00	Gas CH	28.70	Yes	2A	N	1457.70
IN	9BB	TC	F GF	No	1	5.93	52.00	ECH	28.32	Yes	1A	Y	701.30
IN	11BB	TC	F TF	No	1	6.00	52.00	ECH	28.32	Yes	2A	N	n/a
GL	M02	M	F GF	No	2	3.61	67.57	CB CH	26.04	Yes	2A	N	n/a
GL	M03	M	F GF	No	1	7.91	72.15	CB CH	21.60	Yes	1A	N	3638.50
GL	M22	TF	F MF	No	1	4.59	67.57	CB CH	27.00	Yes	1A	N	1762.20
GL	*S02*	*TF*	*F TF*	*No*	*1*	*n/a*	*49.53*	*CB CH*	*21.60*	*Yes*	*1A*	*Y*	*735.97*
GL	*S17*	*M*	*F GF*	*No*	*2*	*10.39*	*49.53*	*CB CH*	*35.14*	*Yes*	*1A*	*Y*	*1044.27*
GL	*S32*	*TF*	*F TF*	*No*	*2*	*7.59*	*75.50*	*CB CH*	*35.14*	*Yes*	*2A*	*Y*	*818.79*
LI	*25BC*	*TF*	*H MT*	*No*	*3*	*3.71*	*106*	*Gas CH*	*27.40*	*Yes*	*1A*	*N*	*1239.84*
LI	*26BC*	*TF*	*H ET*	*No*	*3*	*3.73*	*105.9*	*Gas CH*	*27.40*	*Yes*	*1A*	*N*	*1318.12*

TF=Timber Frame, M=Masonry, CPTF=Closed panel Timber Frame, TC=Timber Cassette H=House, F=Flat: MT=Mid Terrace, ET=End Terrace, GF=Ground Floor, MF=Mid Floor, TF=Top Floor, SD=Semi-detached; CH=Central Heating, CB=Communal Boiler, ST=Solar Thermal, EI=Electric Immersion. *Italics*=elderly/disabled occupants, **Bold**=Passivhaus

Table 1:Key construction, heating and bedroom occupancy data.

This paper provides an overview of the comparative environmental performance of these houses during a 2-week period between 25 Feb 2013 and 10 Mar 2013, taken in the context of a longer monitoring programme and is representative of the use and overall performance of these houses.

AIR PERMEABILITY

Air permeability figures are within design expectations, but result ranges from 0.955 $m^3/m^2.h$ in P15 to 10.39 $m^3/m^2.h$ in S17. This latter figure is the only one that fails to meet the

Building Standard recommendation in force at the time of construction (2010 Scottish Building Standards) of 10 m³/m².h and all but 5 meet the current requirement of 7 m³/m².h and the average is 4.59 m³/m².h. The Passivhaus projects (P15, CC, OC, BC and HC) are the best performers and average at 2.45 m³/m².h, but it is noted that the levels are all above the Passivhaus requirement of 0.6 m³/m².h. In the case of the Lockerbie houses, original airtightness met this value and there has been some deterioration over time. They remain within the recommended figure of 3-5 m³/m².h for MVHR systems [10]. Outwith these projects there is no obvious pattern associated with construction, for example flats in Glasgow having figures at opposite ends of the spectrum. Nevertheless a reasonable standard of air-tightness is present across the sample and suggests that standards in general are improving.

TEMPERATURE

Mean temperatures for living and bedrooms over this period are shown in Figure 1. There is a difference of 8.19°C across the range (excluding MO2 which was unoccupied during this period) but 88% of dwellings having mean living room temperatures above 21°C and 50% of properties having a mean above 23°C. These demand temperatures are above design assumptions, but higher temperatures may reasonable or desirable in those houses occupied by disabled or elderly users (n=8). However relatively high temperatures are observed across the house types. Causes can include unintentional heating due to poor heating controls, oversizing of heating systems or uncontrolled incidental gains; or they may be due to occupants raised expectations or requirements of comfort.

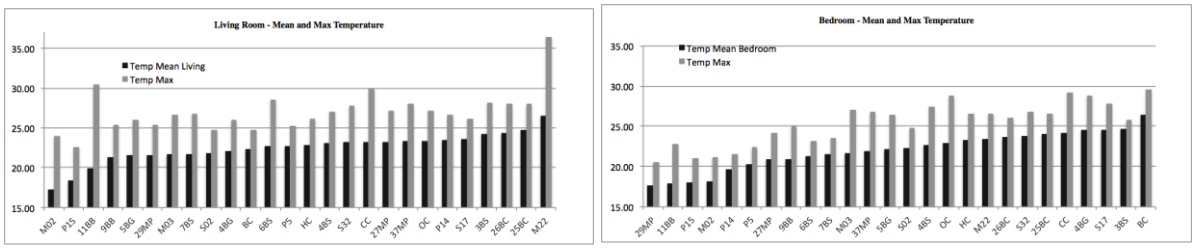

Figure 1: Left - Living room Mean and Maximum: Right - Master Bedroom Mean and Maximum temperature

Mean bedroom temperatures are also consistently high, with 70% of houses having mean temperatures above 21°C and 42% having a mean of over 23°C. The average mean in living rooms was 21.86°C and bedrooms 22.48°C.

CO_2 LEVELS

In these studies CO_2 is being monitored as a useful indicator of 'bad company' with regard to IAQ [11]. Key differences in ventilation strategies are those dwellings relying on natural ventilation (mechanical extract ventilation from kitchens and bathrooms, n=21) and those with MVHR system (n=5).

Mean CO_2 levels are shown in Figure 2 for both living rooms and bedrooms. Bedrooms are of particular interest as they are the spaces where occupants spend the longest uninterrupted time and with the least changes in occupancy. The ventilation strategy that is established when occupants go to bed tends to prevail overnight and provides a reasonably stable condition in which to observe the effects of ventilation.

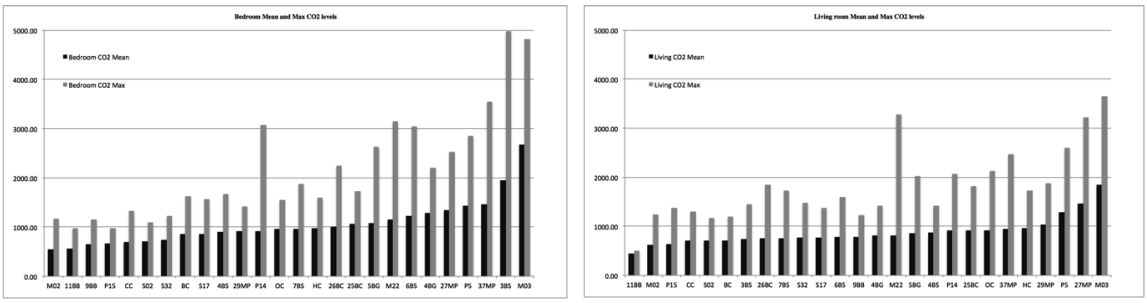

Figure 2: Left - Bedroom, mean and max CO_2 levels; Right – Living room, mean and max CO_2 levels

Levels were found to be above 1000ppm in at least half of the bedrooms, with peak levels in almost all cases well above 1000ppm, typically 1500-3000ppm but in some cases as high as 5000ppm. Comparing mean levels of CO_2 in bedrooms and living rooms indicates that in almost all cases bedroom levels exceed those in living rooms and this difference becomes more marked at mean values rise.

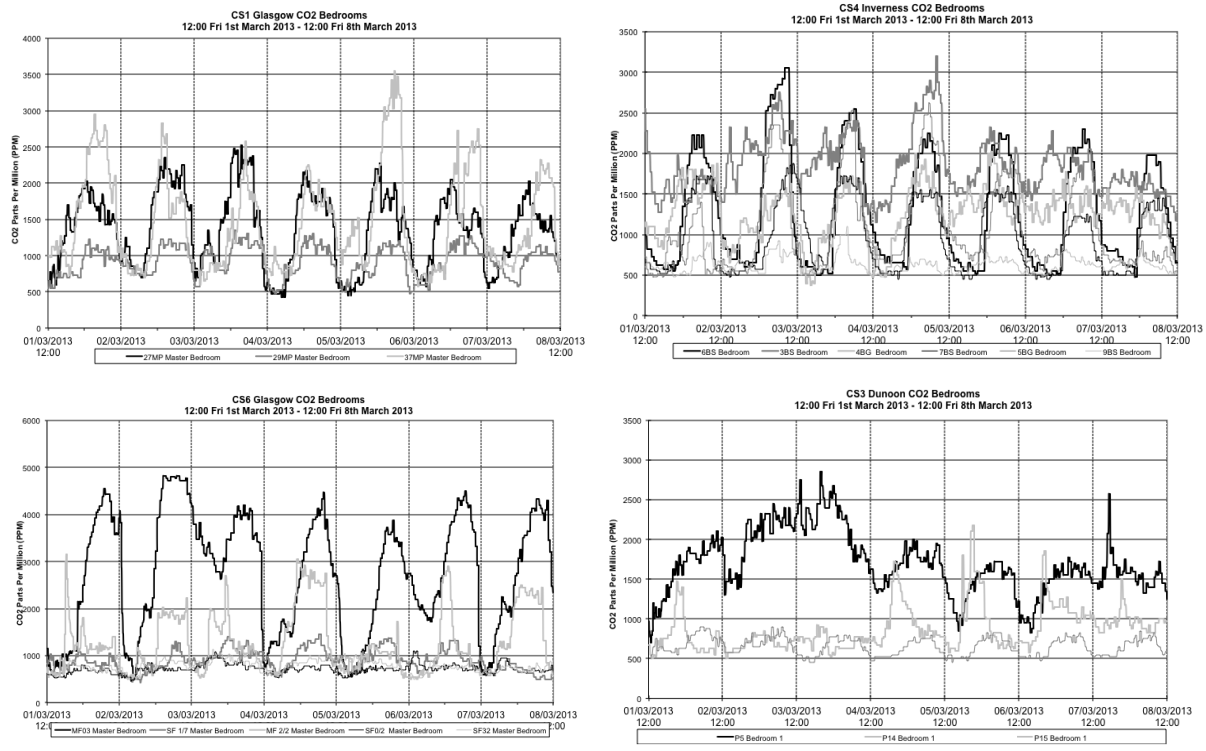

Figure 3: Typical diurnal CO_2 levels Barrhead (top left); Inverness (top right); Glasgow (bottom left); Dunoon (bottom right).

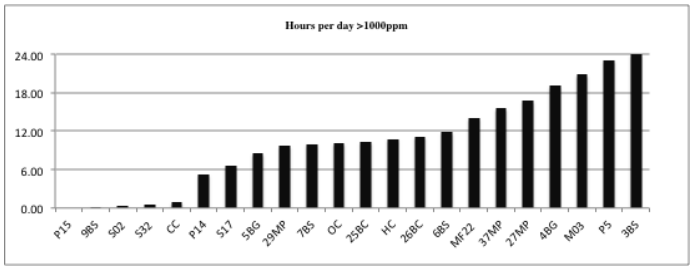

Figure 4: Bedroom exposure to CO2 – Hours per day >1000ppm

Examining CO_2 levels in bedrooms over a three-day period reveals a consistent diurnal pattern that can be observed over the entire monitoring period to date (Figure 3). The degree

of exposure to CO_2 levels is shown in Figure 4, which indicates 70% of bedrooms having exposure to CO_2 above 1000ppm for more than 7 hours a day.

DISCUSSION

The high temperatures and general trend of CO_2 levels, especially in bedrooms may be the result of several conditions. Aside from the use of MVHR systems, several factors are relevant. These include the room volume, number of occupants, night ventilation regime (door, window or trickle vent opening). In some case IAQ is less problematic due either to reduced occupancy or more frequent window opening habits. This is illustrated in 29MP, which contains a single occupant and opens windows at night, also leading to the low mean bedroom temperatures, as compared with 27MP and 37MP, which have double occupancy. Urban context can also be important. The houses in Glasgow are in an urban setting, near to a busy road. M03, which has very high CO_2 levels, is on the ground floor adjacent to this road and rarely opens windows, and the couple also have child who sleeps in the same room. Levels of CO_2 in houses with MVHR systems were not as intense as in those relying on trickle ventilation but periods of CO_2 above 1000ppm were seen at night in OC and HC. Continuously high CO2 levels were seen in some properties. This may be due to continual occupancy due to elderly or disabled occupation, use of bedrooms as workspaces, shift work and in one case a new-born baby.

For those bedrooms relying on trickle ventilation alone (where windows were kept closed n=12) CO_2 levels were noticeably higher, with an occupied mean peak of 2317ppm and an occupied time weighted average of 1834ppm measured between 11pm and 7am. All these bedrooms are characterised by a rapid increase in CO_2 on first occupancy then levelling out presumably due to the background ventilation characteristics. There is no clear pattern emerging from locations or types of construction.

Overheating is also an issue across the dwellings particularly given that average external temperature in this period varied from 3.8^{o}C in Inverness to 7.3^{o}C in Livingston. There is also emerging evidence of overheating due to uncontrolled residual gains. For example, in the Dormont houses the domestic hot water pipework is largely uninsulated, and this appears to be contributing to significant heat gains in the houses, particularly in the upstairs bedrooms where temperatures are typically 3^{o}C higher than downstairs.

CONCLUSION

Comparison of these projects reveals a range of levels of performance and two significant trends are seen. Firstly there are consistently high temperatures observed in the majority of the dwellings, both in the living spaces, but also the bedrooms. This level of demand is leading to a gap between design prediction and actual consumption in terms of both energy use and environmental quality. It would seem that the notion of a bedroom as a cooler space, used infrequently, is outdated. It is suggested that heat delivered into a thermally efficient envelope - particularly where volumes are small - is easily transferred to other spaces such as bedrooms through thermal stratification. This suggests a need for much closer control of heat delivery and that incidental gains may take on much greater importance in low energy dwellings.

The second observation is a tendency toward poor ventilation levels, particularly in bedrooms. For the most part the bedrooms rely on trickle ventilation. Those houses with MVHR systems performed at the better end of the spectrum, and generally did not result in the peak conditions observed in other properties, but were not exempt from poor IAQ and were equivalent to those houses known to keep bedroom windows open at night.

The major concern is for spaces that rely on trickle ventilation as the sole 'planned' ventilation strategy. When considered as a discrete volume, an occupied apartment will require a substantially greater ventilation rate than can be provided solely by trickle ventilators with a free vent area of 12000mm^2. This will be compounded by occlusion from curtains or blinds and the habitual closing of controllable vents. Further research is being conducted to gather more detailed information on ventilation habits and attitudes as the work progresses.

REFERENCES

1. Climate Change Act 2008 (c.27). HMSO, London, 2008
2. HM Government : The Building Regulations 2010 Conservation of fuel and power Approved Document l1A ISBN 978 1 85946 324 6, 2010
3. Thompson, P., Bootland, J. : GHA Monitoring Programme 2009-11: Technical Report Results from Phase 1: Post-construction Testing of a Sample of Highly Sustainable New Homes, Good Homes Alliance, available: http://www.goodhomes.org.uk/downloads/ members/gha-monitoring-report-approved.pdf [accessed 10 Apr 2013], 2011
4. Cutland Consulting : Low and Zero Carbon Homes: Understanding the Performance Challenge, NHBC Foundation NF41, available: http://www.nhbcfoundation.org /Researchpublications/tabid/339/Default.aspx [accessed 26 Mar 2013], 2012
5. Green Construction Board Buildings Working Group : The Performance Gap: Causes & Solutions: http://www.greenconstructionboard.org /index.php/resources/performance-gap [accessed May 2013], 2012
6. Gill, Z. M., M. I. Tierney, I. M. Pegg, and N. Allan. : "Measured Energy and Water Performance of an Aspiring Low Energy/Carbon Affordable Housing Site in the UK." Energy and Buildings 43 (1): 117–125, 2011
7. Crump D, Dengel A, Swainson M : Indoor Air Quality in Highly Energy Efficient Homes – a Review. IHS BRE Press, Watford, England, 2009
8. Davis I, Harvey V. : Zero Carbon: what does it mean to homeowners and housebuilders? NHBC Foundation report, NF9, 2008
9. Carrer, Fanetti, Forastiere, Holcatova, Molhave, Sundell, Viegi, Simoni. : ENVIE Co-ordination action on indoor air quality and health effects. WP1 Final Report – Health effects. www.envie-iaq.eu, 2009
10. Banfill, P,; Simpson, S; Gillott, M; White, J. : The potential for energy saving in existing solid wall dwellings through mechanical ventilation and heat recovery. Energy efficiency first: foundations of a low-carbon society: Proceedings of ECEEE 2011 summer study on energy efficiency.. p. 1401-1412, 2011
11. Porteous, C. D. A. : Ch. 8 'Sensing a Low-CO2 Historic Future', in Chemistry, Emission Control, Radioactive Pollution and Indoor Air Quality, Ed. Micolas A. Mazzeo, Intech, Rijeka, Croatia, pp216-217 in 213-246, 2011

REVIEWING OVERHEATING ASSESSMENT IN THE CONTEXT OF HEALTH RISK – A DEMONSTRATION OF THE EFFECTS OF RETROFIT IN FUTURE CLIMATES

W. Victoria Lee; Koen Steemers

Department of Architecture and WHO Collaborating Centre, University of Cambridge, 1-5 Scroope Terrace, Cambridge, CB2 1PX, United Kingdom

ABSTRACT

Record high temperatures and deadly heat waves in the past decade have prompted an increasing global concern with overheating in buildings. With the problem escalating in light of climate change, there is a need to expand the existing comfort-based overheating assessment approach to account for thermal health risks. Specifically, this calls for means to measure not only the occurrence and severity but also the *exposure duration* of overheating, as epidemiological studies have found additional mortality risk to be associated with the length of heat exposure. Since overheating also affects places with a short cooling season like the UK, it is important to ensure that winter energy-saving retrofits do not unintentionally exacerbate overheating risks in the summer. Using a simulation case study on the effect of cavity wall insulation in a typical London dwelling, this paper illustrates how the examination of overheating duration via *continuously overheated intervals (COI)* may complement existing approach and contribute towards the investigation of thermal health. An analysis of the indoor operative temperature against BSEN15251's adaptive upper limits was conducted first via a suite of three criteria that are representative of the comfort-based approach. The same data then were analysed via the COI approach. For demonstration purposes, a south-facing bedroom was selected to show the comparison of the unfilled and insulated cavity walls for two occupant groups (typical and vulnerable) under five climate scenarios and two thermal adaptability assumptions.

The results suggest that if our current thermal adaptability does not extend into the warmer climates, the bedroom will become overheated for the vulnerable occupants in the near future regardless of the retrofit. The insulation, however, does incur slightly higher risks. Specifically, the elevated risk would come in the form of more continuously overheated intervals of all lengths, during which the temperature consistently remains above the limits acceptable for the vulnerable occupants. Even if we assume that our adaptability will continue into the warmer climates, the results show that future climate patterns may still be too challenging for the vulnerable occupants to keep pace. On the whole, the overheating situation has proved to be complex even within the limited scope of this simulation study. Overheating risk assessment, therefore, warrants detailed examination beyond a binary judgement. Further probing with respect to exposure duration is especially essential in order to make the assessment relevant in the context of thermal health risks.

Keywords: overheating risks, thermal health, exposure duration, insulation, climate change

INTRODUCTION

Increasing occurrences of record high temperatures, hot spells, and deadly heat waves in recent years have warranted a growing global concern with heat-related health consequences. The problem is expected to escalate as the IPCC has predicted a worldwide increase in the frequency and magnitude of warm daily temperature extremes as well as a rise in overall mean temperature [1]. But the deleterious effect of heat is also far-reaching, occurring even in high-latitude places with relatively cool summers like the UK. In fact, an analysis of the daily death records from 1993-2003 has found mortality risks attributable to heat exposure in all regions of England and Wales [2]. As the primary thermal concern for dwellings in places with a short cooling season like

the UK is to keep warm, it becomes particularly important to ensure that winter energy-saving renovations do not unintentionally exacerbate overheating risks in the summer.

While overheating risk assessment has become part of the routine thermal performance evaluation in buildings, the state of being overheated is almost always defined with respect to thermal comfort and not thermal health. In fact, very little is known of the direct health impact of an overheated *indoor* environment despite a dedicated field of epidemiological studies investigating heat-related morbidity and mortality based on the *outdoor* environment [3]. Although one might expect heat-related health consequences to be preceded by thermal discomfort and hence would be captured by existing comfort-based assessment methods, a health-oriented approach is still necessary for two reasons.

First, most existing assessment approaches centre around establishing a boundary of thermal acceptability and using it to make a binary judgement on whether a space is overheated or not. This is useful for guiding building designs and sizing cooling equipment but imparts little information on what happens, for instance *how* overheating unfolds, beyond or even within that boundary. Second, overheating may affect comfort and health differently. While people may be more likely to experience thermal discomfort due to short hot periods because they would not have had the chance to adapt psychologically or behaviourally yet, they can be overwhelmed physiologically by prolonged heat exposure without active awareness of it such as while sleeping at night [3]. This means that in order to quantify overheating risks in ways relevant to health, the *duration* of being exposed to an overheated environment should be considered in addition to the occurrence and severity of that overheated environment. In fact, research has shown that not only does prolonged overheating contribute *additional* mortality risks on top of simply being overheated, but those risks also increase proportionally with the *length* of exposure [4]. Using a simulation case study on the effect of cavity wall insulation in a typical London dwelling in five climate scenarios, this paper illustrates how the examination of overheating *duration* may contribute additional information that are useful to the investigation of thermal health.

METHOD

A typical three-storey London mid-terraced dwelling of the age band 1967-1975 and unfilled cavity masonry external wall was digitally modelled and dynamically simulated in IES-VE. Physical building attributes were based on information available from the English Housing Survey (EHS) 2010 Housing Stock Data [5]. It is assumed that the dwelling has glazing on the south (~12m^2) and north (~10m^2) facades and is surrounded by other terraced dwellings of equal heights. Additional details required for simulation were determined at the authors' discretion, with values and assumptions taken from or calculated according to SAP 2009 and CIBSE Guide A [6, 7]. The dwelling is assumed to operate in free-running mode during the non-heating season (May-September, henceforth referred to as 'summer'), allowing windows to open for natural ventilation whenever the recommended temperature for bedrooms in the summer (23˚C) was exceeded [8].

The dwelling was modelled in its as-built form (with unfilled cavity external walls, 1.6 W/m^{2}k) and in its retrofitted form (with insulated cavity external walls, 0.5 W/m^{2}k). Both forms were then simulated under the current (1961-1990) and four future climate scenarios for London Heathrow: 2030 A1B, 2050 A1B, 2080 A1B, and 2080 A1FI by using the design summer year (DSY) weather files downloaded from the PROMETHEUS Project website [8]. Files used for the future climates all represent the 50th percentile of external temperature under the medium (A1B) or high (A1FI) emission scenarios. Naturally, the future climate may be warmer or cooler than as presented in these weather files. Similarly, there may be different levels and types of insulation to achieve a retrofitted external wall U-value that is lower or higher than the one in this study. Sensitivity analysis investigating these issues will be addressed separately; the present paper aims to highlight an *additional* approach to overheating risk assessment and will focus on how two

representative forms of unfilled and insulated cavity walls compare in alleviating or exacerbating the overheating situation under selected climatic scenarios.

After simulations, the hourly operative temperatures ($\mathbf{T_{op}}$) for the summer season of all bedrooms and the living room in the dwelling were then evaluated. For demonstration purposes this paper will only discuss the results of a south-facing bedroom on the first floor occupied by one adult. The data were first analysed via a suite of three criteria (Table 1) that are proposed by the CIBSE Overheating Task Force based on the British/European Standard (BSEN15251) [9]. A space is deemed overheated if two out of three criteria are violated. In order to assess if a violation has occurred, two additional pieces of information are required: (1) the occupancy schedule of the room, and (2) an upper limit temperature ($\mathbf{T_{limit}}$) to evaluate each hourly data against. In effect, $\mathbf{T_{limit}}$ is not a static threshold, but rather an adaptive upper limit that changes daily and is calculated based on the running mean of the outside temperature and the chosen category of expectation as outlined in BSEN15251 [10]. In the present study, two types of occupants – typical and vulnerable – were considered. It is assumed that the typical occupants would occupy the room only during the night (10pm-7am), while vulnerable occupants would occupy the room almost constantly. Vulnerable occupants also have a stricter $\mathbf{T_{limit}}$ that corresponds to BSEN15251's Category I (highest level of expectation) and is always 2K *lower* than the $\mathbf{T_{limit}}$ for the typical occupants, which corresponds to BSEN15251's Category III (moderate level of expectation for existing buildings). All subsequent discussion refers to these two types of occupants, with the emphasis on the vulnerable occupants, namely young children and elderly persons, who are most at risk of heat-related morbidity and mortality [2].

Criterion 1	No more than 3% of total occupied hours during May-September exceeds T_{limit}
Criterion 2	Daily sum of degrees over T_{limit} at each occupied hour does not exceed 6 degree-hours (K-hr)
Criterion 3	T_{op} at any time when occupied does not exceed T_{limit} + 4K

Table 1: Suite of three overheating criteria proposed by the CIBSE Overheating Task Force [9].

In addition to the assessment done via the suite of three criteria (Table 1), the data were also analysed in terms of continuously overheated intervals (COI), a way of probing the data further that was first introduced by the authors in [11]. Essentially this entails parsing the hours where $\mathbf{T_{op}}$ exceeds $\mathbf{T_{limit}}$ into intervals during which the exceedance occurs *consecutively*. In other words, instead of having a *single* number to represent the total number of hours where $\mathbf{T_{op}}$ exceeds $\mathbf{T_{limit}}$ over the entire summer, the COI approach will render *several* intervals, or stretches of time, within each $\mathbf{T_{op}}$ is *continuously* above $\mathbf{T_{limit}}$.

As $\mathbf{T_{limit}}$ varies with the outside temperature, it stands to reason that $\mathbf{T_{limit}}$ should be calculated independently for each of the five climate scenarios. However, because the equations used to calculate $\mathbf{T_{limit}}$ were developed based on field data gathered in the *current* climate, it is not clear if their range of applicability extends to future climatic patterns, especially given the uncertainties associated with future climates [10]. To investigate this issue, the present study considers two poles of assumptions: (1) occupants' adaptability as we understand it in the current climate does not extend to future climates, therefore overheating in all scenarios are evaluated using $\mathbf{T_{limit}}$ calculated based on the current climate; (2) occupant's adaptability continues into the future climates, therefore $\mathbf{T_{limit}}$ is calculated separately for each of the five climate scenarios. The reality is probably between these two poles.

To summarise the present study: overheating risk is assessed via two approaches - a suite of three criteria that addresses overheating occurrence and severity, and the continuously overheated interval (COI) approach that addresses overheating duration. The results for the unfilled cavity walls are compared against those for the insulated cavity walls for two occupant groups under five climate scenarios and two adaptive assumptions.

RESULTS AND DISCUSSION

As mentioned above, the suite of three criteria facilitates a binary judgement: a space is deemed overheated when two out of the three criteria have been violated. As shown in Fig. 1A, assuming occupants do not continue to adapt in the same way as they do now in the future, both unfilled and insulated cavity constructions become overheated for the vulnerable occupants by 2030, but remain acceptable for typical occupants. On the other hand, under the assumption that the occupants' adaptability continues into the future climates (Fig. 1B), the bedroom only becomes overheated for the vulnerable occupants in 2080 high emission scenario (A1FI). But the fact that the room still becomes unacceptable suggests that even in the best case scenario where occupants adapt to higher temperatures in the same manner as they would currently (which intuition would suggest otherwise as people's adaptability cannot possibly extend indefinitely, especially not for the vulnerable population), their adaptability still cannot keep pace with the changing climate.

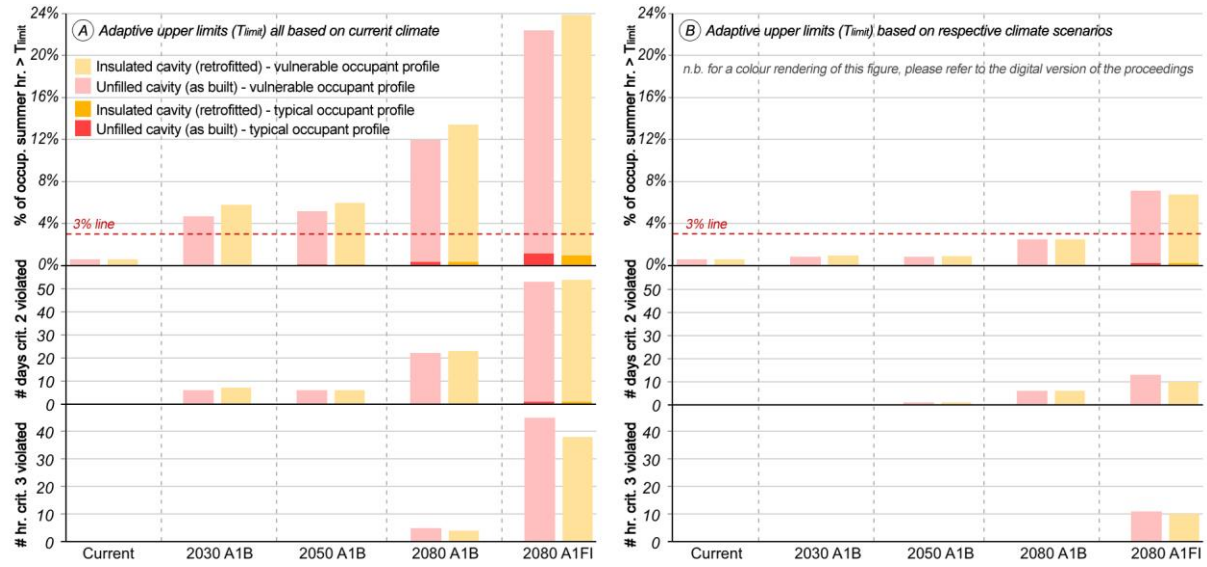

Figure 1: Results from assessment done via a suite of three criteria for the entire summer.

For both adaptive assumptions, whether the cavity wall remains in its as-built (unfilled) state or is retrofitted with insulation seems to only make a small amount of difference, but what little difference they have warrants a closer examination. Under the assumption that the occupants' adaptability remains applicable only to the current climate, the results suggest that adding the cavity insulation would produce more hours where $\mathbf{T_{limit}}$ is exceeded, but doing so seems to slightly reduce the number of instances where $\mathbf{T_{limit}}$ is specifically exceeded by more than 4K. However, under the assumption that occupants' adaptability continues into the future climates, leaving the cavity wall unfilled seems to fare slightly worse in all three criteria.

A closer look at criterion 1 was done to see if a different pattern might emerge when inspected in finer temporal resolutions (by month, week, etc.), as illustrated in Fig. 2 where it is assumed that the occupants' adaptability does not continue into the future climates. When inspected by the summer in its entirety (Fig. 2A), the criterion is not violated for the vulnerable occupants in the current climate. However, the criterion is close to being breached when inspected by individual months (Fig. 2B) and is outright violated when inspected by individual weeks (Fig. 2C). Similar trends are found in all future climate scenarios, with higher percentage of hours exceeding $\mathbf{T_{limit}}$ as the resolution becomes finer, such that criterion 1 becomes violated even for the typical occupants in the 2080 A1B and A1FI scenarios. Furthermore, the difference between unfilled and insulated cavity walls becomes more distinct in certain months and weeks, with the insulation producing more overheated hours in several weeks. Most importantly, the inspection at finer temporal resolution shows that overheated hours tend to occur in clusters, further justifying a continuously

overheated interval (COI) approach. Fig. 3 shows the results from the assessment done using this approach for the vulnerable occupants for the entire summer season.

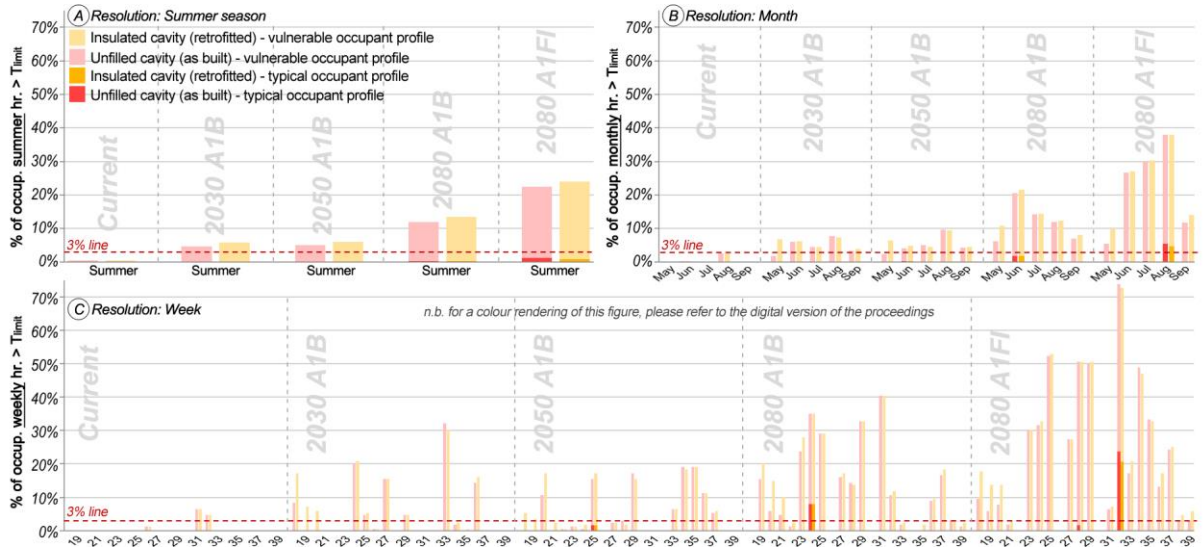

Figure 2: Results from assessment done via criterion 1 by temporal resolution.

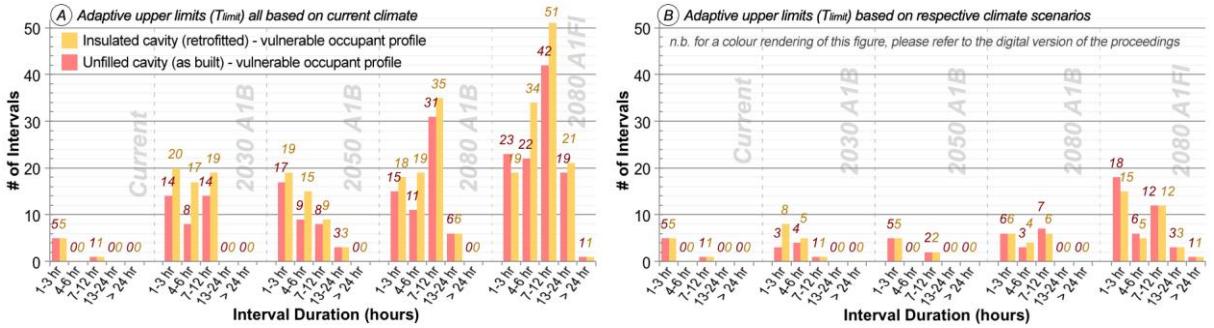

Figure 3: Results from assessment done via the continuously overheated interval approach.

The analysis by COI echoes the findings from the assessment done via the suite of three criteria and shows, for the most part, increasing number of intervals in every duration length with increasing climate change. Additionally, under the assumption that the occupants' adaptability does not continue into the future climates (Fig. 3A), the COI analysis is able to highlight the difference incurred by insulation that formerly could have been made pronounced only by weekly, not seasonal, inspection (Fig. 2C). Furthermore, it becomes easier to compare among the different climate scenarios. While insulating the cavity made no difference in terms of the number of COI or their durations in the current climate, in all future climates the retrofit consistently incurred more COIs, especially those that lasts 4-6 hours straight. More importantly, the COI approach is able to tease out the difference between 2030 A1B and 2050 A1B. While the assessment done using the suite of three criteria gives very similar results for these two climates scenarios (Fig. 1), the COI approach shows that the overheating situation in 2050 indeed differs from that of 2030. Under the 2050 A1B scenario there is slightly less shorter intervals but this apparent improvement is negated by more longer intervals that lasts 13-24 hours straight, a trend that becomes more pronounced in both 2080 A1B and A1FI scenarios. The difference between unfilled and insulated cavity walls is less clear under the assumption that the occupants' adaptability continues into the future climates (Fig. 3B). However, the COI approach also echoes what was seen in Fig. 1B, such that future climates are likely to overwhelm the vulnerable occupants with longer lasting COIs even when assuming the ideal adaptive scenario.

CONCLUSION

Within the limited scope of the present study, the results suggest that while cavity wall insulation retrofit is known to have thermal and energy-saving benefits in the winter, it can also lead to an elevated level of summertime overheating risks in the near future if our current thermal adaptability does not extend into the future. Specifically, the elevated risk would come in the form of more continuously overheated intervals during which $\mathbf{T_{op}}$ remains above $\mathbf{T_{limit}}$ for prolonged periods. This increase in the duration of overheating will add to the thermal health concern especially for the vulnerable occupants who are more sensitive to heat, spend longer times in the bedroom, and arguably have less adaptive opportunity or capability. Therefore, any strategy for thermal insulation must be complemented with effective passive cooling countermeasures. The results also show that even if we assume that we will continue to adapt in warmer climates in the same way as we do currently, future climate patterns may still be too challenging for the vulnerable occupants to keep pace in both as-built (unfilled) and retrofitted (insulated) cavity wall dwellings. More importantly, this paper has demonstrated that the overheating situation can be complex and its assessment warrants detailed examination beyond a binary judgement especially in the context of future climates, which have their own inherent uncertainties. By probing the data further and analysing it from an alternative perspective that emphasises duration, we may be able to gain additional insight into the way overheating unfolds that is more representative of the occupants' experience in real time and more relevant to their thermal health.

REFERENCES

1. IPCC. Managing the Risks of Extreme Events and Disasters to Advance Climate Change Adaptation. Cambridge University Press, Cambridge, UK. 2012.
2. Hajat S, Kovats RS, Lachowycz K. Heat-related and cold-related deaths in England and Wales: who is at risk? Occup Environ Med. 2007; 64(2):93-100.
3. Anderson M, Carmichael C, Murray V, Dengel A, Swainson M. Defining indoor heat thresholds for health in the UK. Perspect Public Health. July 2012.
4. Rocklov J, Ebi K, Forsberg B. Mortality related to temperature and persistent extreme temperatures: a study of cause-specific and age-stratified mortality. Occup Environ Med. 2011; 68(7):531-536.
5. DCLG. English Housing Survey, 2010: Housing Stock Data [computer file]. 2nd Edition. Colchester, Essex: UK Data Archive [distributor]. Downloaded 28th September 2012.
6. BRE. The Government's Standard Assessment Procedure for Energy Rating of Dwellings 2009 edition incorporating RdSAP 2009 (SAP 2009 version 9.90). 2010.
7. CIBSE. Guide A: Environmental Design. The Chartered Institution of Building Services Engineers, London. 2006.
8. Eames M, Kershaw T, Coley D. On the creation of future probabilistic design weather years from UKCP09. Build Serv Eng Res Technol. 2011; 32(2):127-142.
9. Spires B. How to assess overheating: key design issues – The new TM on overheating. CIBSE Summertime Overheating Conference 2011, London. CIBSE. 2011.
10. British Standards. BS EN 15251: Indoor environmental input parameters for design and assessment of energy performance of buildings addressing indoor air quality, thermal environment, lighting and acoustics. 2007.
11. Lee WV, Steemers K. Beyond benchmark: accounting for exposure duration in overheating risk assessment method - A London mid-terraced dwelling case study. CIBSE Technical Symposium 2013, Liverpool. CIBSE. 2013.

ASSESSMENT OF AERODYNAMIC DISCOMFORT IN OUTDOOR PUBLIC SPACES. CASE OF STUDY: CITY 800 HOMES - BOUZAREAH IN ALGIERS, ALGERIA

MESTOUL Djamel, BENSALEM Rafik, DAOUDI Nadia

Laboratory architecture and environment LAE- EPAU, École Polytechnique d'Architecture et d'Urbanisme-EPAU, Beaulieu El Harrach, 16200, Algiers

ABSTRACT

This paper concerns the study of the discomfort related to the wind effect in outdoor public spaces, in particular the mechanical discomfort resulting from disturbed wind flow (venturi effect) and its impact on the level of pedestrian perception and assessment of public space outside related at its use. The reduction of mechanical discomfort of wind in public spaces obeys today to the characterization of two factors; on the one hand we find the physical parameters of the threshold of exceeded velocity limit (5m/s in general) and the frequency period expressed in percentage (%) [1]. On the second hand we deal with human activities such as walking, standing and finally sitting in various places (terrace coffee, park, roadway, etc). These two factors are today considered as the only factors being able to define the quality of aerodynamic comfort in outdoor space [2]. Our present work stresses on the importance of other factors in the assessment of wind discomfort in outdoor public space in particular. These factors are sometimes of an objective order related to the physical environment, and sometimes of a subjective order linked to the user of this environment. Taking into account the sum of these factors and their concomitance in the study of the process of interaction enables us to better apprehend the influence of the discomfort due to the wind effects on the space's psychology (level of appreciation and degree of use). The results of this paper illustrate the influence of the building arrangement (venture shape) in increasing wind speeds. The obtained results could be the first step in pedestrians comfort assessing.

Keywords: Urban design, outdoor microclimate, wind, pedestrian comfort, behaviour, Venturi

1. BACKROUND

Our current research deals with the outdoor discomfort caused by airflow phenomenon generated by housing developments layout. The study of this phenomenon, first identified in the 60s, gave birth to a specific discipline, urban ventilation [2]. Given the complexity of its physical and the costs of ventilation studies to be developed on the subject, only the most prestigious projects, have until recently, been considered.

Today it is recognized that the generalization of these studies is necessary because of the enormous implications of these phenomenon in the quality of life found in the urban public space [3].

Furthermore many examples illustrate the discomfort or aerodynamic disfunctioning due to the absence of any consideration of this factor in urban development morphologies, (café terraces located in the open air, the downstream areas of large buildings height, including skyscrapers, etc..) [3].

When we arrive to the Algerian case, this concern is absent in the planners debates, and marginal in people's eyes? How much inconvenience it can be tolerated and what point can it harm the lived in a neighborhood? These are the key questions we tried to answer through this research considering certain assumptions:

- The urban form of the provision of its built masses, by their morphology and their orientation relative to the direction of prevailing winds can generate aerodynamic disturbance at the pedestrian level.
- Some aerodynamic disturbances such as mechanical discomfort may be "limited" to certain activities and practices in the public outdoor space.

To validate the assumptions cited above, we will try to evaluate:

- The extent to which specific urban configurations associated with the presence of the wind can be detrimental to the daily comfort of users of public space.
- The degree of ventilation comfort in outdoor public space and its impact on the appreciation and use of this space.

2. METHOD

Our present research studies the aerodynamic discomfort in a case of study whose configuration shaped frame venturi generating an aerodynamic events, creates dissatisfaction upon the overall comfort found in the living environment.

Leading our work in an interdisciplinary approach, we will first try to identify the presence and influence of an aerodynamic phenomenon from measures of climatic parameters. Characteristics such as excessive turbulence and overspeed should be the indicators of this anomaly. Once this phenomenon assessed, the discomfort will be evaluated through a psychosocial survey of the inhabitants of this city (case of Stady). Several successors to influence the assessment of the embarrassment parameters will be tested. These parameters are obtained on the basis of a prior pre-survey. The survey will eventually come to establish a cross data on these parameters.

Roughly we have chosen for pooling analysis of the physics goals (microclimate variations on, wind, relative humidity and temperature) that accompany the resulting aerodynamic events, and to assess the impact on population of subjective perspective (perception, evaluation, behavior, spatial practices ... etc..).

a. Case studies

In most of our Algerian cities, our urban planning (neighborhoods, towns ... etc..) outdoor public space seems to be devoid of any prior study sketch that takes into account the aerodynamic given phenomenon and the resulting aerodynamic discomfort. Discomfort is generated from multiple events resulting from the aerodynamic interaction of urban form with the incident wind.

Such aspect is growing and is clearly negative. In our case the morphology of the built environment appears to contribute to the amplification of the aerodynamic turbulence leaving amplify increased aerodynamic discomfort at pedestrian level. Our case study is a housing layout, of 800 homes located in Bouzareah, Algiers suburbs. It highlights the status of an aerodynamic dysfunction that is the subject of our present research. Fig.1

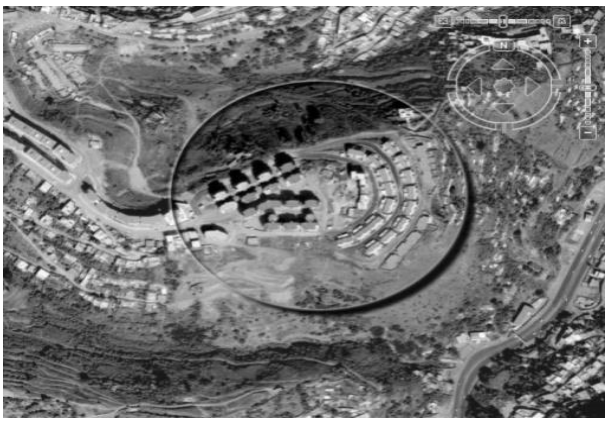

Figure 1: Location map of the case study (city CNEP 800 units- Bouzereah- Algiers.

b. In-situ measurements.

The measurement campaigns that we have conducted on-site lead to collect of meteorological data: air temperature, relative humidity and wind (speed and direction), as these weather factors are essentials for the identification conditions of ventilation comfort.

Figure 2: the venturi shape formed by the master plan of the case study.

We summarize the objectives of the measure in-situ through the following two points:

1. First, we performed a first measurement campaign to determine the local climate of the study site, and this through the comparison of in situ data with those of the reference station ONM[1] located at the airport in Dar el Beida, located in the suburbs of Algiers.

2. Secondly, we focused our attention on the behavior of the wind and its variations in terms of speed, direction and turbulence following a few specific points in the ground plane. The choice of these points was determined by reference to a particular arrangement of masses built which suggests the existence of a venturi effect responsible for the aerodynamic anomaly. Fig.3

Figure 3: Location of station B on the street, (2 m above the ground)

Measurement campaigns were carried out through a series of micro meteorological stations HOBO type consisting across a cup anemometer and a measuring device for the temperature and humidity.

- For the second companion measure, carried out in July, covering a week of action. It consisted, as we have already noted, in characterizing the behavior of the wind on a definite ground plan funnel specific area which leads us to believe the presence of a Venturi effect responsible for the acceleration of the incident wind in a direction from the point V2 to the point V1. Fig. 5

We install it for three micro-stations along the point V1, V2, and B. The two points V1, V2, used for comparison in terms of speed of air flow moving in the V1V2 vector (direction of the prevailing after our first companion measures wind), while point B is used as an indicator the local wind because of its location at a height (h> 20m). Fig. 5

Figure 5: the location of the stations in the second partner of measurement.

[1] ONM : Office national de la météorologie (weather center) http://www.meteo.dz/

c. Analysis of measurement data of weather companions

- Speed and magnitude of the wind

Following these results, we find out that the wind speed at the point V2 is significantly greater than that in V1 and point B, and the numerical results (Tab.1) shows the results clearly distinguished in terms of maximum and average wind speed.

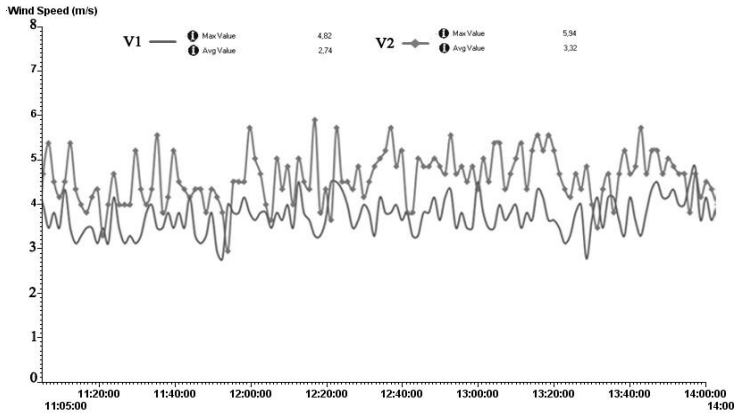

Graph 1: Average speed of the air flow along the stations V1, V2, and B.

Thus in terms of average amplitudes of air velocity, are in the range of 2m/s in the point B, 1.5 m/s and 3m/s, respectively for the point V1 and V2. This amplitude demonstrates the restless nature of the air flow in the point V2, synonymous with high turbulence recorded at this station.

Station Location	Wind Maximum Speed (m/s)	Wind Average speed (m/s)
Point V1	4.82	2.74
Point V2	5.94	3.32
Point B	4.45	1.48

Table 01: Numerical results of speed (max and min) wind in station V1, V2, and B.

- Direction and frequency speeds of wind

In terms of direction: B station we record more than three wind directions, a significant speed and frequency comparing two directions at V1 and only a single direction at V2 station. Fig.6

This is explained by the fact that the point B being the highest (h=24m) intercepts all winds present in the lower atmospheric layer (ABL), unlike the V1 and V2 stations by location 1.5 m from ground between buildings are protected from certain directions and finally report that little direction (one or two). Fig.6

Figure 6: Wind rose for stations V1, V2 and B.

However, between V1 and V2 station, there is still a second direction at the station disappears V1 V2 station, while both stations are practically at the same height (1.5 m above the ground). Between the station and the V1 V2 we are witnessing the emergence of a new class of speed, it is the 5-6m / s (green) with a percentage of 17.1%. This can be explained by the fact that the airflow arriving at the station V2 undergoes confinement by the arrangement of buildings funnel it confers a higher speed and a more stable direction.

The wind was therefore accelerated during its passage from a point V1V2, due to the tapered shape formed by two rows of buildings that reduce the flow area causing the increase of its velocity in that known Venturi effect

d. User's survey

We investigated 92 people in total. Data collection with questionnaire took place during the period from January to mid-February. The duration of the interview was about 20 to 30 minutes for each interviewed. Through this survey are both factors that may amplify this nuisance aerodynamic and the nature of the discomfort (Action thermal, dynamic action, noise, insecurity) that will be investigated events.

3. DISCUSSION OF MAIN RESULTS OF THE RESEARCH.

The general dissatisfaction and immediate vis-à-vis the *aerodynamic discomfort* is implicit in the feelings associated with it: disturbed, very disturbed, scared… etc, resulting different mechanical, thermal and acoustic nuisance. Graph1

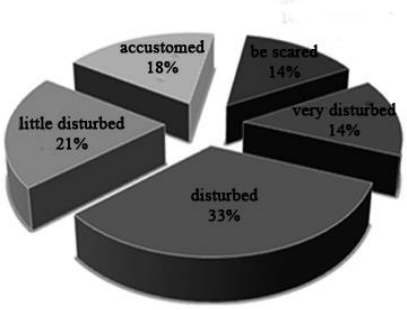

Graph1: Trend of users in the sensation induced disturbance of aerodynamic discomfort

Mechanical disturbance was the most restrictive for users of public outdoor space. This is due to the magnitude of induced damage that is felt on both physiological plans and use of space:

In outdoor space, the mechanical impediment appears to act on the physiology of users under the action of a mechanical force to fight [4].

Increasing wind speeds can interfere with people's activities by affecting people's balance, by increasing the energy required for walking and by affecting performance, walking, hair, clothes etc. [5]. Mechanical discomfort seems to influence the use of public space, because of its influence limited to the performance of certain practices in this area. The magnitude of this effect is observed through the declining in the attendance to the public space and the neglect of certain optional type activities, such as reading a newspaper, enjoying the sunshine, etc).

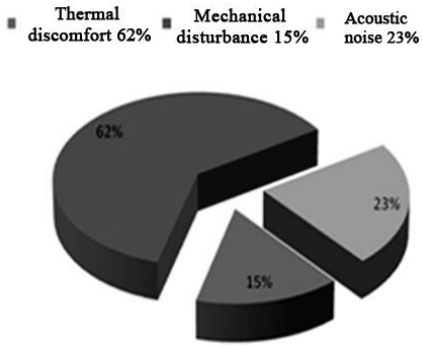

Graph2: Trend of users in the assessment of air flow increasing..

The mechanism of influence of mechanical discomfort depends on the following factors:

- The degree of sensation of the mechanical discomfort depends essentially on the degree of availability on the site.
- The degree of sensation of mechanical discomfort depends primarily on personal characteristics such as age and gender.

4. CONCLUSIONS

This paper concerns the study of the discomfort related to the wind effect in outdoor public spaces, in particular the mechanical discomfort resulting from disturbed wind flow (venturi effect) and its impact on the level of pedestrian perception and assessment of public space outside related at its use.

The wind flow at ground level around buildings is the result of complex interaction between the wind (mean vertical speed gradient, turbulence) and the buildings themselves (shapes, sizes, position etc.). The more or less arbitrary setting of the buildings can create zones of over speed and vortices in the passages, playgrounds, open spaces etc, and lead to very unpleasant wind effect on people's comfort

The level of assessment relative to aerodynamic discomfort can be identified both from the users' behavior and through the changes they make to their physical environment [6]. We have detected that adaptation action adopts three levels:

- The level of *physical control*
- The level of *behavioral control*
- The level of *environmental stress*

Wind effects on people can be the cause of uncomfortable or even dangerous conditions. A sudden increase of wind speed to 15m/s or more can be sufficient to bring people out of balance [4].

In General, adaptation to mechanical disturbance seems to be subject to two parameters, namely:

- The degree of *attendance*
- The type of *activity*

Finally, in terms of expectations for environmental improvement of the quality of outdoor public space and quality of microclimatic environments, this depends on the *vocation of the place.*

This research has identified the magnitude of the influence of aerodynamics discomfort in the perception and use of public outdoor space. It highlights the importance for a thorough preliminary study of aerodynamic events design phase of outdoor public spaces.

5. REFERENCES

1. BOTTEMA, M. (1992), Wind climate and urban geometry. Rapport n° 92.63K, technische universiteit eindhoven, faculteit bouwkunde, vakgroep fago, decembre1992.
2. GANDEMER, J. and GUYOT, A. (1981), La protection contre le vent, aérodynamique des brise-vent et conseils pratiques. CSTB Nantes, groupe abc, 1981. Diffusion CSTB.
3. ADOLPHE, L. and al. (2002), SAGACités – Chapitre A-4 : Synthèse bibliographique, La perception des ambiances urbaines et le confort dans les espaces extérieurs.
4. MURAKAMI, S. and Wind effects on pedestrians: New criteria based on outdoor observation of over 2000 persons, Proc. 5th Int.Conf. On Wind Engineering, Fort Collins, Colorado (1980)
5. ESCOURROU, G. (1981), Climat et environnement - Les facteurs locaux du climat. MASSON Collection géographique, Paris 1981
6. LEVY-LEBOYER, C. (1980), Psychologie et environnement ». Collection Le psychologue. Ed. PUF. France

DETECTING TEMPERATURE SET-POINT PROFILES FROM SIMPLIFIED USER FEEDBACK: RESULTS OF A FIELD TEST

M. Adolph[1], N. Kopmann[1], R. Streblow[1]; D. Müller[1]

[1]*E.ON Energy Research Center, Institute for Energy Efficient Buildings and Indoor Climate, RWTH Aachen University*
Mathieustraße 10, 52074 Aachen, Germany
madolph@eonerc.rwth-aachen.de

ABSTRACT

In this paper we present an algorithm to create temperature profiles from a simplified user feedback to save energy and increase user comfort. The algorithm was tested in a field test.

Optimizing the heat supply of a building should start with determining the right temperature set-point. Thus, we developed an adaptive algorithm that is able to learn the users preferred temperature profiles from a simplified feedback. We have shown by simulations that the algorithm is capable of creating temperature profiles and satisfying the users thermal comfort while simultaneously reducing the energy demand by approximately 10 %.

Scope of this paper is a field test we conducted for further verification of the concept and real life testing. We decided to focus on the values we believe to be crucial for a wide deployment of the system: Keeping the thermal comfort of the user (or even improving it), and using a very simple user interface without any need for setup. As there were no old energy consumption data available we omitted an energy demand analysis. We measured temperatures, humidity and CO_2 concentration in every room for several days before installing the adaptive system to create a "base line" of the occupants current used temperature setpoints. After the installation of the algorithm we continued these measurements.

As thermal comfort is highly subjective we used a survey to ask the participants for their perceived thermal comfort and the usability of the system. From this information we improved the algorithm and re-tested the algorithm with the same users. The new algorithm allowed for faster adaptation to the user's demand while simultaneously improving the user's thermal comfort.

Keywords: temperature profile, thermal comfort, adaptive algorithm, field test

2 INTRODUCTION

To minimize energy demand of buildings, many different approaches have been used. But in all their variety they mostly assume one thing: The set-point set in the system is the correct set-point. But with regards to the works on how people interact with their thermostatic valve, it must be doubted that this is always true [1, 2, 3].

To create temperature set-point profiles from a simple user feedback, we developed an al-

gorithm at the Institute of Energy Efficient Buildings and Indoor Climate. The algorithm is expected to adapt to the user's needs but also to reduce the temperature while the user is absent. We used refined versions of the algorithm described in [4]. Primary objective was to make the algorithm easy to use thus making it accessible for all members of society. While the system showed good results in simulations with energy savings of up to 10 %, the validity of this result is constraint. One reason is the usage of a fixed time-schedule for user presence and another reason is how we decided if the simulated user would give feedback to the system. Thus, we conducted a field test in several apartments to verify the algorithm in a real life environment.

3 METHOD

3.1 The field test

The field test was conducted between December 2012 and April 2013 in the city of Aachen. Initially three apartments were equipped with the adaptive algorithm in December. Starting from February 2013 we gradually expanded the field test to 7 apartments. The field test included retired persons, young families and employed persons. From this we expected different values concerning time spent at home, comfort temperature and variability of daily schedule.

The installation consists of a thermostatic valve, a push button to give feedback and a multi-sensor measuring temperature, relative humidity and CO_2-concentration for every room. All components communicate wireless with a laptop, which runs a LabView program sending and receiving data from all devices. The adaptive algorithm is written in Python and called from within LabView. The installation of the field test was done by ourselves in the apartments of the participants. This included the configuration of the wireless devices.

The user's satisfaction and their opinions towards the adaptive system was accessed with a questionnaire at the end of the field test.

3.2 The adaptive Algorithm

For the adaptive algorithm temperature profiles are created for every room. They consist of 144 time-steps per day for 7 days a week. The system runs in a loop, meaning that after seven days the profile from day 1 is used again. 21 °C is used as initial temperature for every time-step and every room. The adaptive algorithm uses a simple approach to adapt these temperature profiles to the user:

- If the user gives the feedback "too cold" the temperature is raised for the current time-step and several time-steps adjacent to this time-step.
- If the user gives the feedback "too warm" the temperature is lowered for the current time-step and several time-steps adjacent to this time-step.
- If the user does not give any feedback there is a probability that the temperature set-point will be lowered for the current time-step and several time-steps adjacent to this time-step. This is further on called a "random reduction" of the temperature set-point.

We used two different versions of the algorithm. The first version was a refined version of the algorithm described in [4]. The algorithm now borrows from an optimization algorithm

called simulated annealing.

The second algorithm gives more weight to the user feedback by introducing a probability manipulator. In the first algorithm the probability of random reduction would be the same at every time-step. In the second algorithm an "too cold" feedback would result in a reduced probability of a random reduction for the next time-steps.

4 RESULTS

In this section we will present "lessons learnt" from the field test which led to changes in the adaptive algorithm, but are mainly based on communicative feedback from the users instead of measured data. In the second part we'll analyze the gathered profile data. We'll conclude with the results of the questionnaires.

4.1 Lessons Learnt

The probability for a random reduction was the same as the one used previously in simulations, as they led to good results with regards to adaptation speed and thermal comfort. But in the field-test we had to realize that the chosen probability parameters for a random reduction were too aggressive. Especially after users requested higher temperatures there was a high risk that the set-point would be reduced within the next 30 minutes again, resulting in thermal discomfort.

This problem was addressed with a smaller probability for a random reduction, resulting in another problem: Most people expect their sleeping room to be cooler than the rest of the apartment or even unheated. As the default temperature was 21 °C the sleeping room tended to be uncomfortably warm for the first days of the adaptive cycle as the algorithm did not reduce the temperature fast enough by itself. We resolved that problem with a time dependent initial temperature: Between 10:00 pm and 6:00 am the initial temperature was reduced to 18 °C instead of 21 °C. We were able to return to a constant initial temperature with version 2 of the algorithm.

We also noticed that people started to care more about their room temperature after we installed the adaptive system. Before the field test room temperature seemed to be a minor concern, but with the field test running they cared more about room temperature, even using their own thermometers to check our measurements.

4.2 Comparison of the two algorithms

Figure 1 shows the evolution of the temperature profiles the day after starting the algorithm. Red arrows pointing upwards indicate a user complaint "too cold", blue arrows pointing downward indicate a user complaint "too warm" (there are only two of them in figure 1(b) around 3:30 am). Dashed orange arrows pointing downward indicate a random reduction. The dashed line shows the initial temperature profile the algorithm used as the day begun, the green line is the result of the temperature profile in the evening.

Every change in the set-point has an effect on the set-points several time-steps adjacent to that time-step. This can be observed especially for the "too cold" feedback. The random reduction initiated some time-steps before is completely overwritten by that feedback (see for example figure 1(b) at 9:00 am).

The result of version 1 of the algorithm shows more spikes and the user gave 2.5 times more often the feedback "too cold" compared to algorithm 2. The effect of the Probability

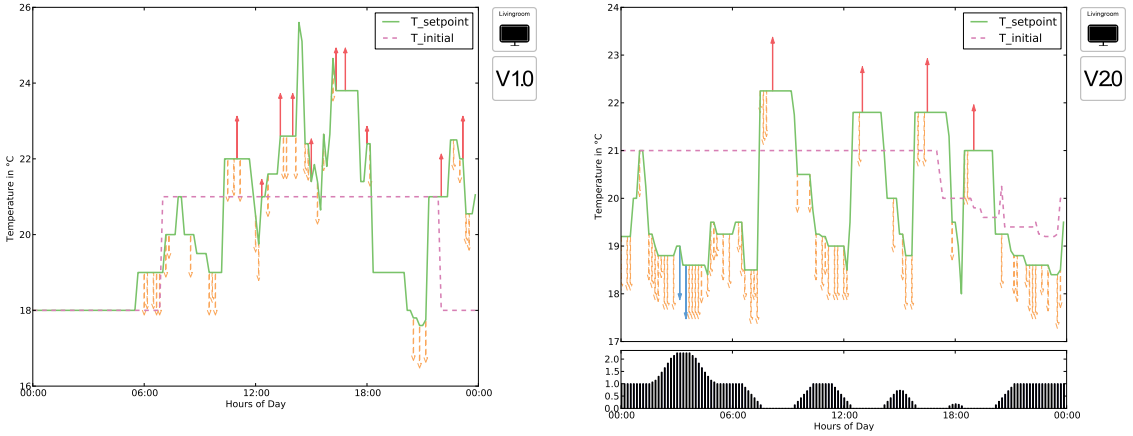

(a) Version 1 of the algorithm

(b) Version 2 of the algorithm

Figure 1: Comparison of the two algorithms and the influence of the higher probabilities for a reduction of the temperature setpoint.

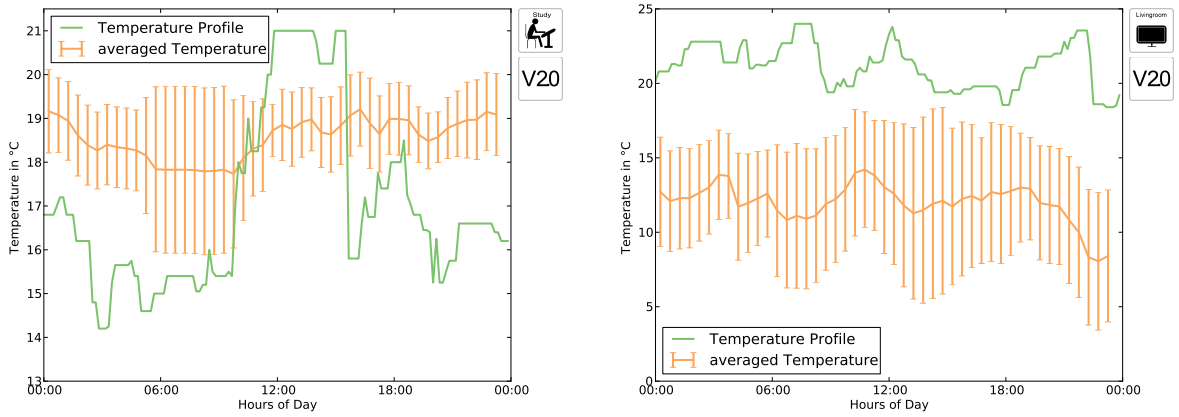

(a) Flat 1, small family with child, father works from home

(b) Flat 2, single person, at home over the day

Figure 2: Mean indoor temperature without the adaptive algorithm compared to the suggested temperature profile at the end of the adaptive cycle.

Manipulator in the second algorithm (lower plot in figure 1(b)) can be observed: in the morning the feedback "too warm" is given two times resulting in an increased probability of random reduction. Later on the feedback "too cold" is given, leading to an increase in room temperature which is stable for some time as the probability for a random reduction is down to zero. At times with no feedback given, algorithm 2 is much faster to reduce the temperature setpoint.[1]

Figure 2 shows in orange the mean room temperature sampled over several days when the apartment was operated with the old thermostatic valves. The bars indicate one standard deviation of the mean value. The green line shows the result of the algorithm approximately two weeks after starting the algorithm for that room. In both cases we show results of algorithm 2. Figure 2(a) shows the study of a small family were the father

[1]The spike in figure 1(b) at 1:00 am is a result of a problem between LabView and Python which sometimes occurred. The result is that the set-point reduction was not incorporated into the profile.

works at home. Before using the algorithm the room temperature was between 18 °C and 20 °C over the whole day. After using the algorithm the room temperature was increased for the time between 10:00 am and 3:00 pm with a smaller peak following between 4:00 pm and 8:00 pm. At night the temperature is reduced to 15 °C to 16 °C.

Figure 2(b) shows a different result: Shown is the combined living and sleeping room of a person who is at home over the day. The mean temperature is in the range between 10 °C to 15 °C. On installation of the field test we did not notice the room being that cold. But the temperature sensor for the bathroom reported similar temperatures and the user complained that with his old thermostatic valves the room would not warm up, so he was forced to wear a jacket even inside his apartment. We could not determine if this was the result of a wrong usage of the thermostatic valve or a failure in the heating system. But with our system installed, the user was able to increase the temperature set-point and also the room temperature to more comfortable temperatures at around 21 °C.

4.3 Results of the user questionnaires

As the number of persons who answered the questionnaires is small, we can not give statistical analysis of the results but will report the major findings.

With regards to the old thermostatic valves most participants reported that they were not satisfied with the control of the room temperature. Most participants reported that they felt sometimes too cold, the room being too warm was only reported once. They generally reported that they interact on a daily basis with their thermostatic valve.

Regarding the adaptive system all participants answered that the system was easy or very easy to use and that the behaviour of the system was comprehensible. Most people had the feeling that the system understood their demands and implemented them. Most of them stated, that the system toke several days to adapt to their demands and that this time-span was acceptable. Having much less control of the heating system was reported as often as having much more control of the heating system with the new algorithm.

Concerning the thermal comfort people reported that they were not more often cold than with the old system. Several people reported an increase in thermal comfort.

60 % of the participants would recommend the system, 20 % were undetermined and 20 % would not recommend the system. On a scale from 1 to 5 the system was rated 2.6 on average with 1 being the best possible rating. 60 % preferred the new system, 40 % the old system. When asked how much money they would be willing to pay for the adaptive system per room the most common answer was below 50 Euro.

5 DISCUSSION

Although algorithm 2 works better in creating temperature profiles, the profiles are still were volatile. Possibly the user feedback should get influence on more time steps after the feedback occurred. Especially for figure 1(b) one could argue that for the last three feedbacks the random reduction does not make sense with regards to energy savings and thermal comfort. To address this issue we apply a post-processing algorithm at the end of every day, combining those spikes to one plateau.

Energy savings depend strongly on the user's behaviour prior to installation of the system. While the result in the study will probably lead the a decreased energy demand (figure 2(a)) the new temperature profile in the one-room apartment will not only in-

crease energy demand but also thermal comfort (figure 2(b)).

According to the answers in the questionnaires we fully achieved our goal of an easy to use system. Also the behaviour of the system was noticed as comprehensible what we also expect to be very important concerning user acceptance. The fact that the same amount of people stated they had less control of their heating system as people reported they had more control over their heating system than before shows that reception of such a system is very different. People feeling in less control were more satisfied with their old thermostatic valves. Anyway, the feeling of being in less control must definitely be addressed as we consider this as crucial for acceptance. That 60 % would recommend the system is a good result, although an average rating of 2.6 leaves room for improvements.

That people cared more about room temperature after starting the field test could result in a bias on their ratings on thermal comfort, because they were much more aware of thermal discomfort. Right now we don't see any approach to access this bias.

6 CONCLUSION AND FUTURE WORK

With the field test we could show that the adaptive algorithm to create temperature set-point profiles works also in a real-world environment. The system achieved its goal of being easy to use. With regards to thermal comfort the algorithm yields acceptable results although it could be further improved.

With the acquired results we'll further refine the algorithm and do simulations with an improved thermal model for the user and a more volatile time schedule according to the suggestions made in [5].

We would also like to include features as detection of a longer absence, resulting in an apartment-wide lower temperature set-point. Additionally we want to improve our method how one profile can be improved by the profiles from the days ahead.

7 ACKNOWLEDGEMENT

Grateful acknowledgement is made for financial support by BMWi (German Federal Ministry of Economics and Technology), promotional reference 0327387D.

REFERENCES

1. Lindén, A.-L., Carlsson-Kanyama, A., and Eriksson, B.: Efficient and inefficient aspects of residential energy behaviour: What are the policy instruments for change? *Energy Policy*, 34:1918–1927, 2006.
2. Peffer, T., Pritoni, M., Meier, A., Aragon, C., and Perry, D.: How people use thermostats in homes: A review. *Building and Environment*, 46:2529–2541, 2011.
3. Carlsson-Kanyama, A. and Lindén, A.-L.: Energy efficiency in residences - challenges for women and men in the north. *Energy Policy*, 35(4):2163 – 2172, 2007.
4. Adolph, M., Kopmann, N., Lupulescu, B., and Müller, D.: Adaptive control strategies for single room heating. *Energy and Buildings*, 2013.
5. Page, J., Robinson, D., Morel, N., and Scartezzini, J.-L.: A generalised stochastic model for the simulation of occupant presence. *Energy and Buildings*, 40:83–98, 2008.

EFFECTS OF INDOOR ENVIRONMENTAL QUALITY IN SCHOOLS ON STUDENT PERFORMANCE AND WELL BEING

E. Cochran; K. Magnuson; N. Papi Reddy; A.Kolosky, R. Srivastava

Carnegie Mellon University, 5000 Forbes Avenue, Pittsburgh, PA 15213, USA

ABSTRACT

School districts throughout the country seek measures to improve test scores, reduce school absenteeism, improve Indoor Environmental Quality (IEQ), and respond to shrinking Facility Management and teacher salary budgets. There is a need to identify key building investments that will provide the highest benefits to children, teachers, and the community. Many schools lack proper building features and controls to maximize day-lighting. Furthermore, many schools have gone to great lengths to block daylight partially or completely; this is contradictory to their original design to maximize day-lighting. The research examined existing school facilities in two US cities; New York, NY and Pittsburgh, PA.

185 built environment characteristics were identified in one of three categories: Physical Conditions, Occupant variables, and Indoor Environmental Quality (IEQ) variables and their relationship with seven (7) health and performance metrics: suspension rates, student absenteeism, weight, asthma, and academic performance. Fourth grade standardized test scores for Math, English Language Arts (ELA), and Science for multiple school years were used to establish academic performance. The research findings focus specifically on the benefits of day-lighting in elementary schools. Eight (8) physical conditions were identified as daylight and views variables; Building Shape, Building Orientation, Building Depth, Proximity of Adjacent Property, Window to Wall Ratio, Window Type, Window Exterior Guard Type, and Shading Device types.

Among the numerous benefits of providing daylit and well maintained schools are higher test scores through retrofitting of school facilities, reduced utility bills, an increased community image and perception, improved teacher retention, and improved health and well-being of the school's occupants. This effort is part of an on-going effort of the Energy Efficient Buildings (EEB) Hub to improve energy efficiency in buildings and promote regional economic growth and job creation.

Keywords: schools, indoor environmental quality, day-light, energy efficiency

INTRODUCTION

For about 1/5 of the United States, over 1,200 hours every year are spent in a school building. Schools are four times more densely occupied than offices.[1] In 2010, nearly 50 million students attended public elementary and secondary schools. Additionally, the public school system employed about 3.3 million individuals (teachers, principals, librarians, etc.).[2]

Poor building conditions influence teacher retention and student test scores. One major aspect of nearly every building, day-lighting, has been shown to improve these conditions, having tremendous benefits over electric lighting in terms of human health, student performance, and additionally, building energy use. Schools are most intensely used during the hours when the sun is shining, yet up to 40% of their electricity use goes towards powering artificial illumination.[3] Over 90% of classrooms are artificially lit even when rooms are unoccupied, wasting both energy and funds. Annually, America's schools spend over $6 billion on energy, more than on textbooks and computers combined.[4] School building conditions affect

teacher effectiveness, morale, and retention. A decrease in teacher performance can have a negative impact on their ability to deliver instructional material. When teachers are dissatisfied with their school environment, they might consider changing schools or leaving the profession entirely. It is necessary to improve the quality of the environment in which our students learn and our teachers work so that equal opportunities for student success and optimal scenarios for teacher effectiveness are created.

METHOD

The analysis was based on school facilities and neighborhoods in one dense urban city and one mid-sized urban city; New York City (NYC), NY and Pittsburgh, PA. Through a multiple level selection process, 120 schools were identified with similar race, sex, and income demographics as well as similar student teacher ratios. Schools designated as private, specialized and special were excluded from the database. One hundred eighty five physical variables were identified as potentially impacting student health and performance. The identification was based on, interviews with Educational Professionals and Facility Managers, site visits, literature reviews, and multiple local, state and federal agencies. Of those 185 variables, eight (8) physical conditions were identified as daylight and views variables; Building Shape, Building Orientation, Building Depth, Proximity of Adjacent Property, Window to Wall Ratio, Window Type, Window Exterior Guard Type, and Shading Device types. Each variable condition was identified for 120 schools using various coding methods to quantify qualitative data. As an example, 120 schools were identified and classified into one of 16 basic architectural layout designs. Each designation was identified with a custom coding variable and included in the research school database. ANOVA, Chi-Square tests, and Regression statistical analysis methods were conducted in SPSS, Minitab, and R to identify the relationships between the physical variables and the health and performance outcomes.

In an effort to focus on the built environment attributes that most impacted student health and performance, High Schools (HS) and Middle Schools (MS) were removed from the dataset. HS and MS students contain an increased number of confounding factors and childhood developmental variables that impact their health and performance. Additionally, elementary school students are more likely to spend the majority of their time in one to two classrooms throughout the day. This stationary tendency reduces confounding factors and increase the possibility to draw conclusions that link their environment to health and performance metrics.

Student performance was accessed based on results of state standardized tests for multiple school years. Based on the 2007 New York State Public Schools Report Card, state wide testing was available for select grades. Math and ELA testing begins in the 3rd grade, however, Science testing begins in the 4th grade and Social Studies was only tested in the 8th grade. Additionally, class size availability was available for two grades, 8th and 10th. The report also includes various state-wide statistics such as suspension, absenteeism, teacher turnover, and graduation rates.[5] Based on available NY State data and the goal to focus on physical environmental characteristics that are linked to student health and performance, fourth grade tests scores were utilized to access student performance.

School test scores are typically identified as the number and the percent of students whose score meets the requirements at one of four levels. Since Level 3 is the minimum required to meet proficiency, built environmental characteristics were evaluated based on their relationship to the percentage of students at a particular schools 4th grade level whose scores were at levels 3 or 4.

Similar research was conducted for Pittsburgh, Pennsylvania City Schools. Visits were made to each school in the district to collect visual information for analysis. The key data sets collected were concerned were 8 types of daylight obstruction which included blocked high windows, blocked view windows, metal mesh on windows, no/low visibility glazing, low glazing area, ideal orientation, and window blocked with material i.e. paper. Likewise, extensive compilations and analysis were performed of the U.S. Commercial Building Energy Consumption Survey (CBECS) detailing the primary use of fuel energy.

CURRENT SCHOOL CONDITIONS

The analysis showed tremendous energy efficient and day-lighting retrofit opportunities. Three-quarters of America's existing schools were built before 1970. Larger, older cities have greater numbers of older schools. In Pittsburgh, PA, around 70% of schools were built before 1945. Older schools are well-suited for sustainable renovations—particularly for improving day-lighting. Sadly, poorly planned renovation decisions, first-cost decision making, lack of whole-building energy considerations, and deferred maintenance over the decades have put many of these buildings in a condition that only vaguely resembles that of their original design logic and aesthetic splendor. Today many windows are covered, restricting daylight from entering mostly or entirely. In fact, the research analysis of CBECS data identified that most schools reported only 0-10% of their building area utilizes daylight.[6] This is a missed opportunity to reduce utility bills since lighting energy loads represent the second largest site energy load and the largest source energy load for schools and offices in the Northeastern U.S.

Both NYC and Pittsburgh contain many schools buildings with long facades facing east and west. In the NYC dataset, almost 62% of the schools contain a long axis in the East-West direction, or contain building floor plans with no dominate orientation. The combination of low sun angles and lack of exterior shading devices can cause significant glare. To control glare, many schools utilize opaque shades that block sunlight and view, therefore rooms with large windows may have reduced daylight and view access due to the shading devices. Schools in both cities with ample day-lighting opportunities were found to have multiple additional methods of daylight obstruction such as metal meshes, dense security screens or blocking the windows entirely.

IMPACTS ON HEALTH, PERFORMANCE, AND ENERGY

In 1999, the *Condition of America's Public School Facilities* found that nearly three quarters of school facilities at that time were in need of 'repairs, renovations or modernization in order to reach *good* condition.'[7] A 1995 report by the General Accounting Office stated that 25,000 public schools need extensive repair and replacement, concluding that the air is 'unfit to breathe' in roughly 15,000 schools.[8]

In many NYC schools, students are not proficient in English, Math, Science, and Social Studies, barley reaching a 50% passing rate. Given the implicit goal of improving every student's performance, it becomes extremely necessary to address the many issues causing students to not perform below optimal level. Day-light access and quality has the potential to impact student learning. Multiple Heschong-Mahone Group's studies identify significant correlations between day-lighting and student performance. Their research found that students with the most day-lighting in their classrooms progressed 20 percent faster on math tests and 26 percent [faster] on reading tests in one year than those with the least amount of day-lighting in their classrooms.[9] 'Similarly, students in classrooms with the largest

window areas were found to progress 15 percent faster in math and 23 percent faster in reading.'[10] Access to daylight can affect human Visual System, the Circadian System, and biological systems. These human systems and understanding their impacts are vitally important for students in a learning environment, and both are highly affected by daylight.[11]

Of the physical variables analyzed for their relationship to health, performance and energy outcomes, building enclosure design, layout, and condition variables were identified as some of the strongest relationships. In Pittsburgh, PA renovated school buildings consumed on average 30% less gas compared with existing buildings and buildings that received additions and buildings with narrow floor plates consumed on average 17% less electricity. Schools with East-West axis (predominate windows on the north and south facades) consumed on average 28% less electricity and those with roof insulation consumed on average almost 10% less gas compared with those without insulation. Naturally ventilated schools (includes schools with functioning operable windows) consumed on average 21% less electricity. Finally, schools integrated with a Building Automation System (BAS) consumed on average 9% less gas.[12,13]

In addition to energy performance impacts, daylight and view variables also showed strong associations to academic performance. Results of multiple regression analyses identified strong relationships between day-lighting variables and academic performance. In particular the window conditions and 4^{th} grade math test scores identified a statistically significant association ($p \leq .05$). Improving daylight can also help minimize teacher turnover rates and reduce student and teacher absences. In terms of building geometry, finger building layouts provide the greatest opportunity for day-lighting classrooms in medium to large school buildings. In the NYC study group, on average, they also provided the lowest teacher turnover rates for both new and experienced teachers. The finger plan layout maximizes day-lighting while at the same time minimizes acoustical problems because of the division of classrooms into separate wings. This geometry design (given proper solar orientation) can be associated with reduced teacher turnover rates and a subsequent increase in student performance.

In addition to building orientation, layout and window condition, window to wall ratios also impact day-lighting access. The results of the NYC schools identified a weak relationship between fenestration percentage and academic performance. NYC schools with 30% fenestration showed the lowest teacher turnover, however it was not statistically significant. This could be attributed to the age, condition of buildings, and the ability to control glare in the school buildings with greater than 50% fenestration values. It is also possible that at 30% fenestration, teachers are able to balance thermal comfort desires, control glare, and have less acoustical intrusions than at 50% fenestration.

SOLUTIONS/RETROFITS

From 2000 to 2008, school construction annual spending averaged $20 billion. 2012 spending is projected at $10 billion.[14] Many Facility Managers are faced with shrinking budgets and rising energy costs and increased building population. They are seeking innovative methods to provide suitable school facilities with limited funds. When it comes to day-lighting and schools, almost every school has room to make improvements. The key components to proper design or retrofit of schools is based on eight key day-lighting features: building shape, building orientation, building depth, proximity of adjacent properties, window to wall ratio, window type, window exterior guard type, and shading devices are major factors in determining the extent to which day-lighting can be used, and these factors can be

manipulated to improve day-lighting in existing schools. Every school is unique, so improving day-lighting will depend on starting condition; however, there are definite trends in how daylight has been blocked or compromised that are unique to different architectural generations of schools.

For improving pre-World War II schools, a key aspect is adjusting possible retrofits that have occurred that are minimizing the sustainable potentials of the classrooms. Many of these classrooms have large portions being covered by the ceiling. Adjusting the ceilings to allow full access to the windows to let in ample daylight as well as provide views to the outside. If certain portions of the ceiling still need to be dropped down, slopping the ceiling upwards near the windows to allow the full height to be open is an ideal solution.

For any era of school an important aspect of day-lighting classrooms is not only the window area (including height and width), but the classroom depth as additional light reflection devices such as light shelves might be necessary to bounce light all the way into the space. Light shelves can also be designed to bounce light into the space through the use of white ceilings as well as be used to block the harsh solar gains of the summer yet allowing those ideal gains in the winter reducing the loads of the HVAC equipment. These light shelves are integral for new schools were large windows that are present in older schools are not as present. Additionally, providing skylights and light wells is a recommended solution for schools with deep floor plates. Skylights provide day-lighting to the building core and reduce electricity loads. Maximizing what daylight is available is the key to retrofitting schools. Room organization also impacts daylight and other factors. Appropriate wall, partition, window, and furniture organization can increase the spacious feeling of a room, provide additional open space for various activities, and reduce eye and voice strain. By not blocking windows, daylight can be more evenly distributed within the space.

CONCLUSION

Day-lighting schools can help free up funds for education materials like textbooks and computers. Lighting energy is the largest quantity of source energy and the second largest consumer of site energy, behind heating. Day-lighting can help reduce heating loads as properly designed windows can bring in solar gains in the winter. Advanced retrofit integrated solutions can help reduce energy consumption and improve IEQ. Integrating overhangs and light shelves can help block direct solar gains in the summer reducing cooling loads while still allowing beneficial solar gains in the winter. Operable windows can increase ventilation while decreasing reliance on mechanical equipment. Utilizing natural day-light means less electrical lighting is needed.

The benefits of daylight inside of a building in the realms of human health, productivity, and energy are so numerous. Health, academic performance, and teacher retention can all be impacted by access to daylight the subsequent quality from views, glare quality, acoustics, and window condition. In a building type which houses our world’s most susceptible minds and bodies, we should be doing everything we can to provide every physical and psychological advantage possible.

ACKNOWLEDGMENTS

This material is based upon work supported by the Energy Efficient Buildings Hub (EEB Hub), an energy innovation hub sponsored by the U.S. Department of Energy under Award Number DE-EE0004261.

REFERENCES

1. New Jersey Work Environmental Council. (2002). Heathly Schools in New Jersey. Preventing Hazards to Students, School Employees, and Construction Workers.
2. U.S. Department of Education, National Center for Education Statistics. (2012). Numbers and Types of Public Elementary and Secondary Schools From the Common Core of Data: School Year 2010–11 (No. NCES 2012). Retrieved from http://nces.ed.gov/pubs2012/2012325.pdf
3. CHPS, Inc. (2006). Best Practices Manual, 2006 Edition (Vol. Volume II:Design for High Performance Schools). California Criteria for High Performance Schools. Retrieved from http://www.chps.net/dev/Drupal/node/288
4. Goggio Borgeson, M., & Zimring, M. U.S. Department of Energy, Lawrence Berkeley National Laboratory. (2013). Financing Energy Upgrades for K-12 School Districts: A Guide to Tapping into Funding improvements. Retrieved from website: http://emp.lnl.gov/sites/all/files/lbnl-6133e.pdf
5. NYSED. (2006-07). Office of Information and Reporting Services. Retrieved February 2009, from New York State Public Schools Report Card http://www.emsc.nysed.gov/irts/reportcard/.
6. CBECS Public Use Microdata
7. National Center for Education Statistics. (2000, June 21). Condition of America's Public School Facilities: 1999. Retrieved June 3, 2012, from http://nces.ed.gov/pubsearch/pubsinfo.asp?pubid=2000032
8. United States General Accounting Office. (1995). SCHOOL FACILITIES: Condition of America's Schools (Report to Congressional Requesters No. GAO/HEHS-95-61). Washington, D.C.: prepared by the Health, Education and Human Services Division.
9. Heschong-Mahone Group. (1999). Daylighting in Schools: An Investigation into the Relationship between Daylighting and Human Performance. (Detailed Report). Retrieved from http://www.eric.ed.gov/PDFS/ED444337.pdf
10. Cooper, Kenneth, K. 'Study says natural classroom lighting can aid achievement.' Washington Post, November 26, 1999: A14.
11. Sinofsky, F.G., & Knirck, E.R. (1981). Chose the right color for your learning style. Instructional Innovator, 26(3), 17-19.
12. Loftness, V., Aziz, A., Lam, K. P., Lee, S., Cochran, E., Park, J., & Srivastava, R. U.S. Department of Energy, Energy Efficient Building Hub. (2012).State of the art enclosure technologies and interated systems for 50% energy savings in existing commercial buildings. Retrieved from EEB Hub website: http://www.eebhub.org/media/files/report-Q4-3-1-4BP-1-Building-661-SOA-Progress-Report-v4a.pdf
13. Gunasingh, Aziz, Loftness, & Cochran. (2011). Renovating Schools to High Performance Facilities: An Energy Efficiency Guide to Pittsburgh Public Schools. Pittsburgh: Carnegie Mellon University.
14. Abramson, P. (2012). *2012 Annual School Construction Report.* School Planning & Management. Planning 4 Education. Retrieved from http://www.peterli.com/spm/pdfs/SchoolConstructionReport2012.pdf

VISUAL CONDITION IN UNIVERSITY: AN EXPERIMENTAL PERFORMANCE EVALUATION ACTIVITY

V. Dessì; M. Fianchini

Politecnico of Milano, DAStU dept., Via Bonardi 3, 20133 Milan

ABSTRACT

The paper presents the outcomes of an experimental evaluation of the environmental quality in the university classrooms. This activity is part of the "Sustainable Campus" research project of the Politecnico di Milano and of the Università degli Studi, aimed to develop new action lines to improve global sustainability in these universities and in their neighbourhood.

The main goal of the research work was to define and to test simplified multicriteria methodologies to evaluate the use adequacy of the classrooms, with a particular focus on natural and artificial lighting conditions, as they were neglected in all the past works of adaptation and/or retrofit. First it was defined an evaluation procedure and applied over a sample building. This was based on the comparison between performance requirements and real conditions. They have been verified by inspections, behavioural observations and by simplified simulations of the visual performance conditions. In particular, the intensity and the way of use during the didactic activities, the equipments and their locations and the overhead lighting were evaluated in various classrooms with different shape and orientation.

The lighting conditions have been evaluated on the desks or the worktable in each classroom, according with the lighting levels requirements for the different activities in the work environments, set in the European Standard UNI EN 12464-1. Comparing the outcomes of the various analysis, some critical states were found and mapped. On this base the main improvement goals were established and then some solutions – alternative and/o complementary among them- were outlined in particular concerning the equipment, the internal layout and the lighting.

Keywords: Building performance evaluation, Visual conditions, Lighting

INTRODUCTION

Universities are multifunctional facilities, with a large variety of activities, each of which periodically changes the operating modes and consequently the way of occupying the available space. As a consequence, buildings are often adapted, to meet single needs or solve sectional problems, with no control on the effects on all activities, and rather with the risk of worsening the usability, the comfort, the resources saving. In order to handle problems arising from the ever-changing requirements and modes of use, some experimental evaluation of the global quality of university buildings have already been developed at the Politecnico di Milano, according to the methods of the post-occupancy evaluation, [1, 2] with particular attention to the fitness for purpose [3].

In June 2011, the Politecnico of Milan joined the International Sustainable Campus Network (ISCN), trough a plan called "Campus Città Studi", with the aim of making the whole university neighbourhood a model area in Milan, as regards to life quality and environmental sustainability. The plan pursues the goal of experimenting innovation by scientific research, of promoting changes in life style and of getting more liveable spaces. One of the plan themes is "Environment" and among its topic there is the increase of the environmental comfort in outdoor and indoor spaces of the Politecnico. This appeared a key opportunity both to keep on

with the experimental research on multicriteria evaluation methods of university buildings, in accordance with the goals of exploitation the available resources and of global sustainability, and to go more in depth with the natural and artificial lighting conditions, since they are particularly important in didactic activity, as well as they have been neglected in all the past works of adaptation and/or retrofit. The experimental activity has been carried out on the "Edificio Nord", that's one of the six oldest buildings (1927) of the present seat of the Politecnico di Milano. It has a quadrangular court plan, with a ring distribution by arcades on the ground floor and by a corridor on the first floor. Most of the interiors are in the west and east sides, along the external fronts, while in the north and south sides, originally there were two auditorium classrooms, extended in the courtyard. Over time, several transformations of the lay-out and of the use of the interiors have been undertaken and in the east side a new floor was added; at present, several functions (such as classrooms, offices and many services or facilities) have there place. Referring to the didactic areas, only the north auditorium classroom has been preserved as it was in shape and furnishing, while the south one has been divided in three flat classrooms (one in the ground level and two in the upper one); all the other classrooms are in the east side: they are equipped for lectures on the first floor, and for workshop activities at the upper one.

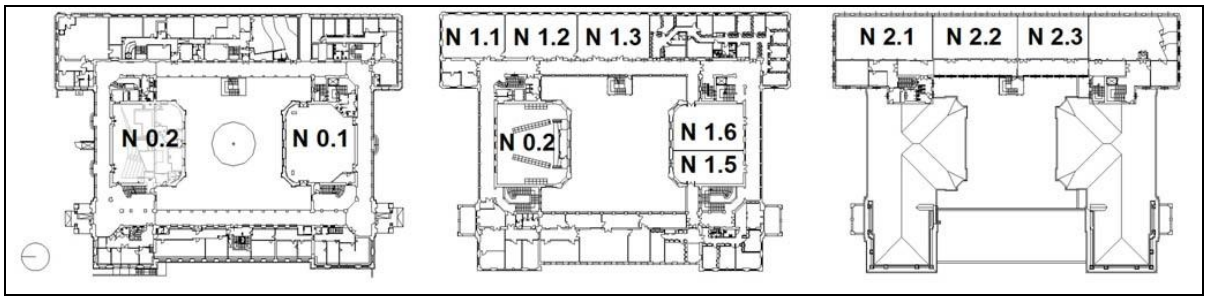

Figure 1. Edificio Nord in Piazza Leonardo da Vinci, Campus Leonardo – Plants

METHOD

The research work was to define a simplified multi-criteria methodology of evaluation able to provide a picture of the whole condition in use, to be put as a basis for developing adaptation design solutions, to better use the resources of the whole building and to increase suitability and visual comfort in the classrooms. According to POE method, the evaluation outcome comes from different analytical activities, depending on technical, functional and behavioural criteria. So, performance requirements, collected from different sources (such as technical codes, regulations and standard, client objectives, “good practices”, etc.), have been compared both with real conditions,(verified by inspections, short interviews, behavioural observations), and with the visual performances by simplified simulations.

In order to draw up the picture of the conditions in use, the present functions of the whole building have been mapped and its decay state, so as the compliance with mandatory technical rules have been verified. Further analysis have been carried out on the classrooms, where shape, fixtures and fittings and seating capacity have been surveyed, so as the natural lighting and ventilation devices and the equipment available, too. In addition, at the aim to record way and intensity of use, in each of them, activities in progress and behaviours have been observed with the support of check-lists and maps, in the second semester, four times a day, for a week from 28 May to 1 June 2012.

In order to bring out the critical issues about the actual conditions of use, the collected data have been elaborated referring both to the single classrooms, and to groups with similar shape, location and purpose. Afterwards they have been compared and integrated with the

analysis on the visual performance, with the goal of outlining design and project ideas for global improvement.

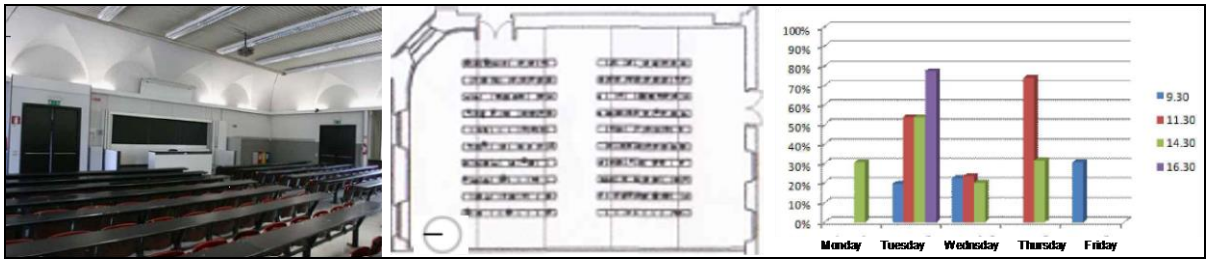

Figure 2: Classroom N.1.6, map of occupation , intensity of weekly use

Considering the visual performance evaluation, we took on those indicated in the European standard UNI EN 12464-1 (lighting in the working spaces) [4] related to the fulfillment of three basic needs:

- visual performance (working people are able to carry out their visual works even in difficult situations and for a longer periods)
- visual comfort (the comfort sensation indirectly contributes to improve the productivity)
- safety

The most commonly used calculation methods are consistent with the choice of the lighting system as function of the use destination and the visual tasks in the analysed space. They are based on the space characteristics, the surfaces reflection coefficients, the selected lighting appliances and the lighting requirements. The main objective of the method is to determine the number and the lamps distribution in order to define the suitable condition for the task. To sum up we report in the table 1 the data of the standard UNI EN 12464-1 related to the school buildings.

Type of interior, task or activity	**Em (lx)**	**UGR_L**	**Ra**	**Notes**
Classrooms	300	19	80	Lighting should be controllable (never under 200 lx)
Lecture hall	500	19	80	
Technical drawing rooms	750	19	80	
Black board	500	19	80	Prevent specular reflection
Computer practice rooms (menu driven)	300	19	80	See lighting of workstation with display screen Equipment

Table 1: Overview of tasks in a classroom together with the requirements for the illuminances according to the European standard UNI EN 12464-1. Em is the minimum required average illuminance (i.e. maintained illuminance) per task;UGR is the upper limit for direct glare. Ra is the lower limit for the colour rendition index

We considered 500 lx as general requirement, since the technical drawing isn't made by hand anymore, but through cad tools.

For the simulations the free software Dialx was used. Light planners are allowed to solve any planning task, considering natural and artificial lighting. The software is the creation of an industrial consortium for the development of a constantly updated light planning tool to meet the changing requirements of light planners all over the world. Luminaire manufacturers have the opportunity to present their products individually on this independent platform. In 2010

this software counted 135 DIALx partners that present their luminaire data in DIALx platform.

The geometric configuration was define in the programme for each single classroom, as well as the internal and external windows position and dimension, and the desks position. In the end the light bulbs system (2x54 watt and 4x 18 watt) and their position were defined.

Every single classroom was analysed in two different time periods of the year- may and December- since they are the most crowded moments of the two semesters. Four moments of the day and different lighting conditions: diffuse natural light (cover sky) and natural and artificial light at the same time. Not considering the kind of furniture in the classroom, all the evaluations are based on the possibility for the classroom to be used for drawing, writing and reading in the blackboard . All these activities have high lighting requirements. By comparing the outcomes of the different analysis, a framework of the general conditions was obtained. Taking into account the multiplicity of the issues, improvement design solutions were proposed on the basis of the defined framework with the aim to give answers at the same time to different questions.

RESULTS

The analysis of the features and of the use conditions of the classrooms has highlighted that:

- all classrooms are regularly used every day in both the morning and afternoon, however, the number of seats occupied is much less than that available; this is especially true in those fitted with fixed rows of writing ledges and tip-up chairs, which have from 110 to 380 seats, but only in 20% of cases surveyed were present more than 99 students (maximum number of occupant for a classroom with a single doorway) and almost in 50% of cases they were less than 60;
- classrooms with fixed furnishing are used for 2 to 4 hour lessons and exercises, by means of the blackboard and sometimes of the projector;
- in the classrooms with movable drafting tables (N.2.1, N.2.2, N.2.3), full day architectural workshops are held, by teachers' lectures, reviews o drafts, work in groups or single, etc;
- several classrooms have shape and fittings layout inadequate, referring to ventilation and natural lighting, to visibility of blackboard or screen, to easily of movement and use, to accessibility of disables; more than all, this concerns the auditorium classroom (N.0.2) and those in the south side (N.0.1, N.0.5, N.0.6), where the lamps are almost ever lit and the external doors left open during the lessons;
- students seem to be conditioned in choosing where to take place in the classroom, mainly by the visibility of the screen or blackboard and by the position of electrical sockets for laptops; then by the difficulty in getting to the central or higher seats in the fixed rows; only at last by the windows location or the natural light level;
- in the east side are placed the classrooms with the best shape and natural lighting conditions, and that is evidenced by the fact that the lamps are often kept off during activities; however, this area does not appear adequately exploited, due to the partial occupation by administration offices and by a darkened multimedia classroom.

Interesting aspects were came to light from the luminous performance simulations of the classrooms:

- first is the data concerning the natural light that is never sufficient. especially due to to the windows position it’s impossible to guarantee homogeneous conditions. Openings are in effects located along only one side of the space;
- through the artificial lighting it’s possible to reach good luminous conditions but not for every single desk and in both simulated seasons;

- Bby observing the simulation results we decided to focus on the winter condition rather than on the spring season. If the lighting conditions are satisfied for the winter condition even more so they will be in the spring season;
- regarding the auditorium classroom (N0.2), on two floors high,the natural light coming from the students' shoulders is completely insufficient. Nevertheless even the existing punctual artificial lighting is completely unsatisfactory;
- in the three classrooms located in the south body of the building, the natural lighting is in both seasons not adequate, while the lighting appliance in 5 rows, perpendicular to the students' positions (7 rows in the upper floor) is adequate, i.e. homogenously distributed and over the 500 lx for all the desks;
- regarding the classrooms block in the first floor facing east we should do some specification that justify some difference in the lighting behaviour of the classrooms. First, the angle classroom N1.1 has two groups of windows in the north and east sides. Nevertheless the natural light is never completely sufficient. Combining it with the artificial light it's possible to have homogeneous conditions with 500 lx in all the desks;
- the classroom N1.2, slightly wider, with openings along the east side, isn't adequately and homogenously illuminated. lighting up through artificial light 500 lx are reached especially along the east side till the middle of the desks, in spring, while in winter only the desks in the centre are adequately lighted;
- the classroom N1.3, smaller than the previous one, presents a different position of the desks . The openings are in rear of the students and the light system is in two rows perpendicular to the desks. The simulated conditions define a strong non homogeneous situation: in the last positions, close to the windows, satisfactory conditions can be reach, at least in spring, although the shadows produced by the students themselves on the desk are not considered in the simulations. Not satisfactory is the condition in winter. By using the artificial lighting it's possible to get good conditions only in the centre of the desks rows;
- at the last floor the drawing classrooms are similar between them in dimension and internal distribution. As we already seen in the N1.1, also the N2.1 has groups of windows in two sides . Especially by using artificial lighting homogeneous and sufficient visual conditions are reached both in winter and spring;
- in the other two classrooms N2.2 and N2.3 we found that conditions aren't so homogeneous. In this classrooms we can have a completely satisfactory situation only in spring, while in winter we can have only about the 80% of the desks in good conditions especially in correspondence to the lighting system.

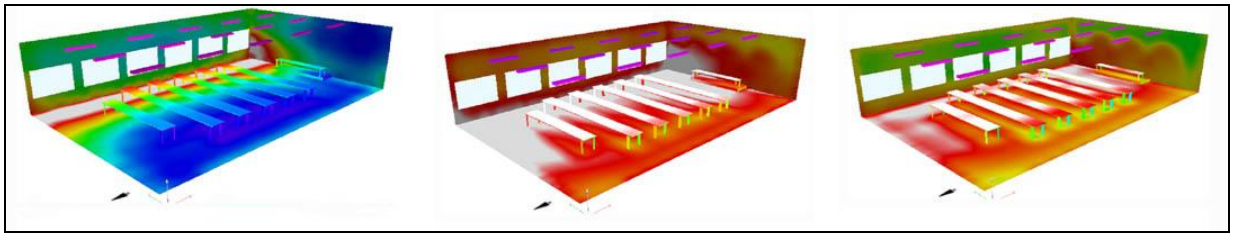

Figure 3. Example of simulation of lighting conditions. Natural lighting in May, natural and artificial lighting in May and December

DISCUSSION

By the results of the evaluation some proposals for action can be outlined, regarding different aspects and with different level of impact on the building:

- in consideration of their low global performances and of the large excess of seats compared to the real use, it seems appropriate to modify the layout of the classrooms in the south side (N.0.1, N1.5, N1.6), reducing the width, and to rearrange the fittings disposal, in order to enhance natural lighting and ventilation and to improve the movement and visibility of the blackboard conditions;
- at the top floors classrooms (N1.5, N1.6, N2.1, N2.2, N.2.3) it is possible to enhance natural light resource, by introducing tubular skylights from roof to ceiling [5];
- darkening curtains need to be replaced by other systems of regulation of natural light (such as Venetian blind), in order to diversify the dark conditions and, at the same time, to allow the natural ventilation in the warm season;
- with regard to artificial lighting, due to the differences of lighting conditions on the work surfaces in the different classrooms, it is necessary to improve the distribution of the equipment, in order to increase the light, where necessary, and in general to ensure operational flexibility, to suit lighting conditions as needs change;
- due to the need of preserving its original fittings and feature, the auditorium classroom (N.0.2) would need a specific project to solve the large set of problems for its use; otherwise it would be better not to use it anymore for daily activities.

CONCLUSION

The experimental activity has provided a first level of interesting results, but partly conflicting. In fact, despite technical standard requires lighting levels of 500 lx in the classrooms and these are never satisfied only by natural light, in the spring days with bright sky, students seem to work adequately with artificial light off. As a consequence, a second stage of research has just been planned, with a comparison between lighting performances from simulations and from on-site measurements, in order to validate the simulation outcomes and to gauge the evaluation model. Thanks to this, it will also be possible to assess more effectively different design solutions, sketching different future scenarios.

ACKNOWLEDGEMENTS

We are grateful to Giancarlo Gagucas for his collaboration in surveying and in elaborating the simulations of lighting performances.

REFERENCES

1. Preiser, W. F. E., Rabinowitz, H. Z., White, E. T. : Post-occupancy evaluation, Van Nostrand Reinhold, New York, 1988
2. Preiser, W. F. E., Vischer, J. C.: Assessing Building Performance, Routledge, 2005
3. Fianchini, M. : Fitness for purpose: a performance evaluation methodology for the management of university buildings, in Facilities, vol 25 n° 3 / 4, pp. 137- 146, Emerald Group Publishing Limited, 2007
4. UNI EN 12464-1: Illuminazione dei luoghi di lavoro. Parte 1: Luoghi di lavoro interni. 2003
5. Rogora, A., Locatelli, A.: L'illuminazione canalizzata in architettura. Simone editore, Napoli, 2008

ROLE AND IMPACT OF ISLAMIC VALUES ON URBAN SUSTAINABLE BEHAVIOUR IN THE ARAB WORLD

Wasel Elgayar

Institute of Architecture and Planning, University of Liechtenstein, Fürst-Franz-Josef-Strasse, 9490 Vaduz , Liechtenstein

INTRODUCTION

Industrialized and developing countries, countries in economic transition, small island states, in fact all nations need to improve their understanding of sustainable development and environmental approaches. This preoccupation is not found in post-revolutionary (2011 – 2013) Arab political discourse. Due to the strong expectations for economic improvement of the young people and to the rising role of religious bodies in political power play, interest in sustainable development and the environment is not a fruit of the Arab spring. It is therefore important and urgent to place sustainability on the agenda of this rapidly changing region.

My study is intended to be a contribution to the scientific understanding of the role and impact of Islamic religious values on architecture and urban sustainable behaviour and development. In particular, it seeks to assess if and how religiosity in the Islamic setting relates to knowledge and behaviour about urban sustainable development and practice favourable to enhancing sustainability. Along the way, the study will possibly contribute to the process of rebuilding devastated and damaged cities in Libya and other war-ravaged Arab countries in a sustainable way.

The phenomena of religious values in the Arab world, and their increasing importance is clearly perceived in the media. At the same time, study of energy use in this part of the world, famous for producing fossil fuels, is becoming more relevant. The link between the two is largely unknown. Many reservations might be held about the sustainability of behaviour in Arab cities and these reservations led me to this investigation which attempts to find out how religious values and urban sustainable behaviour relate to each other.

METHOD

Making use of a small and diverse group that represent as much as possible all different backgrounds of the urban society under investigation, I am using case study methods: "*Often, case studies employ a variety of data collection techniques – archival data, interviews, questionnaires, observations, etc. Unlike questionnaires and interviews when the case researched is the respondent and so a possibly large number of cases are researched for statistical significance, in a case study the case itself is the particular occurrence of the topic of research*" (Fellows and Liu. 2008, p 158). Data collection can be performed using different methods and various instruments: interviews, questionnaires, behavioural models, culturally-specific interpretations, global information system overlay.

Fellows and Liu have already established that trust and confidence are important considerations in data collection, pointing out that with sensitive data, more trust in the researcher is required by the provider (Fellows *et al* p 29). Collecting reliable data is an important first step for accurately describing users' behaviours. But analysing these data correctly is also important and this is where in my research on the link between religiosity and sustainable behaviour, the proposed research will seek to investigate.

Also it supports the reliability, validity and accuracy of the finding and the conclusion of the research. However, in my research on the impact of religious values on urban sustainable behaviour, there will be a balance among the participants to ensure variety and correctly broad

data generated according to background, role played in the local community, city authorities, and society as a whole. There will be a positive identification of religious leaders to be interviewed. A balance in the choice of participants from government, tribal leaders and religious figures, general inhabitants and the representatives of most vulnerable groups will be verified by an independent assessor.

During the whole process, the research will try to make sure that all the concerned parties will be involved (municipality, general inhabitants, vulnerable inhabitants themselves, energy companies, civil society). In some cases "key informants" will be chosen to go deeper into aspects of the case study as much as possible – for example to identify any specific influences of a religion and geographical background on the way their lives evolve in the city.

Online networks now play a significant role in many people's life not just socially but also professionally all over the world. They have become a recognised and important source for research. In the Arab world, online social networks played and are still playing a key role in the Arab political awakening and the Libyan uprising is an example of this. Many Arabs, not just young people, have an online account and are active online. This is going to assist the present research when it comes to data collection, in terms of time, cost, and security and most importantly for credibility and reliability. In a post-conflict environment, people may have the tendency to be reserved in face to face interviews, while being more frank and open online, even for those who are using their real names. Therefore, online social networks will be important for data collection and analysis in my research. However, Internet could be a source of data and online surveys can be established to capture data quickly and easily. While it is hard not to use online research as a source of data in 2013, and while Internet in the Middle East and North Africa region is becoming more accessible, one cannot rely on it alone as a source of data. It could however be a helpful in increasing research capacity by broadening sources of information and in terms of finding participants, keeping in touch with them during the research, as well as collecting, sharing and analysing data and finally for sharing and learning among research peers.

After collecting all the data following the mixed methods approaches as mentioned above, qualitative data on religiosity (religious values, practices and behaviour) will be separated from and compared to the data related to urban sustainable behaviour (for example energy use, recycling).

DISCUSSION

When the present doctoral study was conceived, its research design proposal was generally focused on the role and impact of culture and religion on sustainability in the Arab and Muslim cities. As my reading about sustainability and religion advanced, Islam emerged as the most relevant context to be understood. At the same time, the necessity to narrow down towards a question that would be both measurable and answerable drove me from the general question about impact of culture and religion on sustainability to one more precisely identifying the contribution of Islam to urban sustainable development. Now at this stage, the question has further evolved to ask what are the effects and impacts of Islamic religious values on urban sustainable behaviour in the Arab world. Some might argue that this question still needs to evolve, be narrowed and more focused.

The theory of sustainability started to climb the global agenda in the 1970s. Then in 1987 sustainable development took on an international and public dimension with the release of the Brundtland Commission (World Commission on Environment and Development) Report. This led the UN to take its idea of "Our Common Future" and theory of environment and sustainable development into serious consideration, kicking off the series of international conferences. Incidentally, the vice-chair of the Commission and four of its twenty members

were from Arab or Muslim countries. But there were also some practical actions, with a good example being the publication of a plan focused on education for sustainable development by the United Nations Educational, Scientific and Cultural Organization (UNESCO) and with the World Environment Day theme "Green Cities … Plan for the Planet!" by the United Nations Environment Programme (UNEP).

As the world is becoming smaller and smaller, global and local become debatable terms. What was once considered as local and what had been considered global become interchangeable. In the globalization process there are certain concepts that can no longer stand alone in just one of these categories: immigration, integration, nationalism, global warming, human rights, gender and sexual politics, and of course sustainable development. Most of these concepts have become both local and global issues that need local and global approaches and cooperation.

Today we cannot talk about sustainability and sustainable development without taking in to account or at least referring to The Millennium Development Goals MDGs as they represent the world agreement and the global hope for a sustainable better future for all. The deadline set for the MDGs is 2015, and while not all the goals will be met, the world should stick to the agreement and not give up on the hope. The difficulties experienced in setting the goals were cultural as well as technical, and the same factors also interfere with the attainment of the goals. One sign of good hope is the Rio+20 Conference, which set one of its sustainable development themes as: *" ... integration and a balanced consideration of social, economic and environmental goals and objectives in both public and private decision-making."*

Following on from Rio+20, it was agreed that the ensuing sustainable development goals would be: Universally applicable to all countries while taking into account different national realities, capacities and levels of development and respecting national policies and priorities.

Taking this into account, Prof. Peter Droege mention in his "Beyond Sustainability" that some countries start promoting renewable energy and sustainable development in projects and "eco-villages" as an expression of this applicability in our own time. It is pointed out that the World Bank, the United Nations and bilateral development organizations also slowly start to embrace renewable settlement policies. "*Fears among some leaders that a change in energy infrastructure may risk the pace, direction and nature of development*" (Droege 2011). In Droege's theories or approaches we see the importance of advocacy for political change from a project approach to a programme approach.

The role of local communities is very important in the success or failure of a project or of urban design. Jonathan Barnett explained this in his book "City Design" (2011), where he recommends that the public and the local community leaders should have a say and be involved during all the steps and the phases of the project of the urban design and made to feel part of it. From the cultural point of view the local communities should have a say in the city design in order to guarantee the sustainability of the design as it is they who are going to use and run the city. So if the designer did not take into consideration the local culture, and maybe habits and even the words used to express needs, this may lead to the failure of the design. If the design was forced on the local communities, seen sometimes in developing countries including in the Middle East, as in the collapsing housing estates of Cairo, the design is not going to be sustainable.

In some UN reports describing research and studies, a big role is attributed in developing countries to the design of the city not just from the environmental point of view, but also in the social sense. Quality of life and safety in the city has to be taken in to account. This includes from the gender perspective of women as well as for the promotion of young people and disabled people, in terms of access and barrier free design, transport, and infrastructure. Even UN-Habitat created a logo that promotes a safe city design and the motto "a safe city is

a just city – a just city is a safe city". This motivates us to take into consideration the local users of the city, their traditions concerning urban design, as well as their beliefs, as much as the theory behind design. All this is to make urban design as sustainable as possible.

The city's form, and the beliefs of its population have to be understood together. This is a very important key, especially if we would like to take global ideas into account and apply them to the local context, for example in the Arab world. If we have a look at the UN, some of the results of conferences are useful when it comes to understanding sustainability worldwide, however UN reports and publication are often unhelpful because they create a technocratic language. This is a good way to create a special group of sustainability theorists, but it is unlikely to help the current situation of the city to evolve.

The influence of culture and religion on architecture and urban planning is not new and history is full of examples of that, but nowadays through globalization we are overwhelmed by it. For example the world's airports and shopping malls look very like each other so the moment you are in one you no longer know where you are except by looking hard for some tiny details. In what are called the developing or transition countries we see badly maintained buildings especially in the public places within cities. Sometime it is due to economic reasons but most often it is due to what might be called "forced architecture and urban planning". Therefore, to achieve desired sustainability, we must "rephrase" the universal concepts (human rights ones or modern urban planning principles) so that these concepts harmonise with language, culture and beliefs – the reality on the ground – and are understandable to the poorest and most vulnerable, who might not understood the special "technocratic" language of global reports.

It is possible to see in the literature, that there are strong practical arguments in favour of understanding the role of culture and beliefs and therefore of giving serious consideration to religion in relation to sustainability in architecture and planning. Interestingly, this is something that the Catholic Church has studied. Making complicated matters (concerning faith) understandable to local communities is a process that the Vatican calls "inculturation".

As the type of questions about a research question would naturally be very specific, here in the present case, these specific questions for clarification include: *"does the level of a person's education, their sex, age and income level influence their sustainable behaviour?"* and *"how could this behaviour be led by religious values?"*

Given the historical and geopolitical realities of Middle east and north Africa which have impacted upon religious values and practice, we need also to ask a longer string of questions: "*is behaviour concerning sustainability and religiosity influenced by immigrant background, dual nationality through parents, other birth nationalities or by naturalisation*?" and "*is behaviour influenced by time spent living or studying abroad or otherwise by having been raised in another country or culture*?"

It would certainly appear that religion maintains influence over general education in the Arab Muslim world. We must therefore consider what is the likelihood of it being open to integration of education for sustainable development, and ask if religious figures and leaders play a role in sustainable education and what role they have when it comes to understanding and promoting sustainability? And finally, at the level of personal psychology and learning we need to assess if and how an individual might develop his or her religious or cultural values in a way which could lead to sustainable behaviour.

My doctoral study is intended to be a contribution to the scientific understanding of the role and impact of religion on architecture and urbanism in promoting sustainability. It assesses if and how religiosity in an Islamic setting relates to knowledge about urban sustainable development and to practices that enhance sustainability.

In particular, a link between Islamic religious values and urban sustainable behaviour will be sought. At the same time, the study may contribute to rebuilding of devastated Libyan cities in a sustainable way by introducing a new socio-cultural dimension to reconstruction planning.

To make this significant, it will make use of positive and negative lessons that have been learnt from previous pro-poor and poverty reduction strategies (many undertaken by the United Nations agencies, government programmes and NGOs) in the Arab cities. Previous regional experience can be used to ensure that rebuilt Libyan cities are just and safe and most importantly sustainable.

Changes in population size and structure of some cities in the last few decades have occurred in ways that can best be understood from the culture and religion point of view. The role of local communities is very important in the success or failure of a project or of urban design. While the influence of culture and religion on architecture and urban planning is not new and history is full of examples, one of the biggest problems that the research might face is that of denial. In that part of the world being ashamed of a problem is itself a big obstacle.

Practically speaking, there is a lack of a sufficient database in most of the Arab countries concerning urban sustainable development issues, including energy use. Little experience and education is to be found in local communities about urban sustainable development. Lack of urban planning over many years, and absence of sustainable development policies combine with corruption and nepotism in the region.

The public and local community leaders should be involved during all the steps and the phases of the project. Yet the region is not one where such consultative processes are applied. From the cultural point of view the local communities should nonetheless have a say in the urban design in order to guarantee its sustainability as it is they who are going to use and run the city – we would hope applying their religious values to the process.

Another obstacle is that no one really can predict how the Arab revolutions and the awakening will evolve. There is a "wait and see" attitude on the part of many big actors in the region.

Moving around in conflict or post-conflict countries is nonetheless prone to unfortunate limitations due to unexploded ordnance bombs and mines and other hazards.

Despite whatever might be the result of the research, the aim is not to solve the problem or change behaviour. Rather, it aims for a better understanding of the phenomena and coming up with a possible finding. It may open the door for more questions and research on the subject. This could be a very successful research in itself. The idea is to find out what how and why without necessarily finding a solution or judging the phenomena or the situation.

CONCLUSION

The world is urbanizing faster than current city design practices can sustain, while at the same time climate change has introduced a new dynamism into what once appeared to be a stable environment. But with effective city design more important than ever, there are controversies and uncertainties about the best way to manage unprecedented urban growth and change.

Renewable energy might be our only solution to save our only planet and our common future. Now it is clear that sustainable urban development has to be tried, internationally, regionally and also most importantly locally.

As I have mentioned, sustainable development and the protection of the environment are not yet fruits of the Arab spring. It is therefore important and urgent to place sustainability on the agenda of this rapidly changing region. In Droege's theories or approaches we see the importance of advocacy for political change. My research on the effects and impacts of Islamic religious values on urban sustainable behaviour in the Arab world will hopefully

acquire the messages needed for such advocacy and help make the link between religious values and urban sustainable behaviour. It is my hope that such research on the role of Islamic values in urban sustainable behaviour, will establish if there is a link between religiosity and sustainable behaviour in the Arab cities.

Challenges remain, including lack of capacity, knowledge, skills and lack of experience and education in local communities and professional groups concerning sustainable urban development. In a developing country these issues can be a barrier to the adoption of new technologies or sustainable management of natural resources. Many developing countries, for example, do not have the scientific and institutional capacity to understand the consequences of climate change and the means for reducing, or adapting to, its damaging effects. As mentioned earlier there are even fears among some leaders that a change in energy infrastructure may risk the pace, direction and nature of development. Or of their own ability to create wealth and exercise authority.

Despite whatever might be the result of the research, the aim is not to solve a problem or change behaviour. Rather, it aims for a better understanding of the phenomena and coming up with a possible finding. It may open the door for more questions and research on the subject. This could be a very successful research in itself.

REFERENCES

Barnett, Jonathan (2011): City design. Modernist, traditional, green, and systems perspectives. Abingdon, Oxon, New York, NY: Routledge.

Brundtland, Gro Harlem (1987): Report of the World Commission on environment and development. "our common future.". New York: United Nations.

Farr, Douglas (2008): Sustainable urbanism. Urban design with nature. Hoboken, N.J: Wiley (A Wiley book on sustainable design).

Gardner, Gary T. (2006): Inspiring progress. Religions' contributions to sustainable development. New York: W.W. Norton ("A Worldwatch book"--Cover).

Green Cities … Plan for the Planet (2005): United Nations Environment Programme.

Peter Droege (2002): Renewable Energy and the City.

Peter Droege, (2011): 'Beyond Sustainability: Architecture in the Renewable City. In Crysler, C. Greig, Stephen Cairns and Hilde Heynen. Eds. Sage Handbook of Architectural Theory. Thousand Oaks, CA and London: Sage Publications, Chapter 33

Richard Gale (2002): Religion, planning and the city: The spatial politics of ethnic minority.

United Nations Conference on Sustainable Development (2012): The Future We Want - outcome document of Rio+20: •United Nations Conference on Sustainable Development.

United Nations Educational, Scientific and Cultural Organisation: Building Sustainable, Inclusive and Creative Cities: (UNESCO).

Fellows, Richard; Liu, Anita (2008): Research methods for construction. 3rd ed. Oxford: Wiley-Blackwell.

Groat, Linda N.; Wang, David (2002): Architectural research methods. New York: J. Wiley.

Psarra, Sophia (2009): Architecture and narrative. The formation of space and cultural meaning. Milton Park, Abingdon, Oxon, New York, NY: Routledge.

Roman Banzer & Peter Staub (2012): Writing Archtiecture. University of Liechtenstein.

Simons, Helen (2009): Case study research in practice. Los Angeles, London: SAGE.

Yasser Mahgoub (2009): Architectural Research Methods. Available online at http://www.academia.edu/1733899/Architectural_Research_Methods_-_, updated on 2013, checked on 2013.

REDUCED ORDER MODELLING OF THE THERMAL BEHAVIOUR OF AN OFFICE SPACE

M. Geron[1], R.F.D. Monaghan[2]; M M. Keane[1]

[1] *Civil engineering Department, National University of Ireland, Galway*
[2] *Mechanical Engineering Department, National University of Ireland, Galway*

ABSTRACT

Reduced Order Models (ROMs) have proven to be a valid and efficient approach to model the thermal behaviour of building zones. The main issues associated with the use of zonal/lumped models are how to (1) divide the domain (lumps) and (2) evaluate the parameters which characterise the lump-to-lump exchange of energy and momentum. The object of this research is to develop a methodology for the generation of ROMs from CFD models. The lumps of the ROM and their average property values are automatically extracted from the CFD models through user defined constraints. This methodology has been applied to validated CFD models of a zone of the Environmental Research Institute (ERI) Building in University College Cork (UCC). The ROM predicts temperature distribution in the domain with an average error lower than 2%. It is computationally efficient with an execution time of 3.45 seconds. Future steps in this research will be the development of the procedure to automatically extract the parameters which define lump-to-lump energy and momentum exchange. At the moment these parameters are evaluated through the minimisation of a cost function. The ROMs will also be utilised to predict the transient thermal behaviour of the building zone.

Keywords: CFD, Reduced order models

INTRODUCTION

The availability of low cost wireless sensors to measure temperature, velocity and humidity in building zones is changing the way in which thermal comfort in office spaces can be addressed. The possibility to have several sensors in a room and the ease of their deployment can assist in achieving a deeper understanding of room temperature profiles and in developing and validating thermal models for energy saving strategies or user comfort policies. Computational Fluid Dynamic (CFD) simulations have been successfully utilised to analyse thermal behaviour and user comfort of office space [1, 2, 3] in combination with wireless sensor networks [4]. Nevertheless CFD simulations are computationally expensive, especially if unsteady simulations are required or if they are to be used in conjunction with Building Management Systems (BMS) for operational strategies. For these scenarios the development of reduced order models (ROMs) can be a valid alternative.

ROMs can be distinguished into two categories[5]: (1) state space models in which the problem is divided into input and output, and (2) distributed parameter models [6, 7]. In the category of state space models it is possible to allocate the Compact Thermal Models (CTMs) successfully utilised in the field of electronic components [8, 9, 10], Flow Network Models (FNMs) [11] and lumped and zonal models in building sector [12, 13, 14]. The main issue which arises from the development of zonal/lumped models is that the

decision on how to divide the domain (lumps) is left to the experience of the researcher. The researcher will also utilise empirical data or correlations to evaluate the parameters which characterise lump-to-lump energy or fluid exchange.

The object of this research is to develop a holistic methodology for the generation of ROMs from CFD. The lumps will be automatically extracted from the CFD models through user defined constraints. Lump-to-lump interactions (e.g. mass flow rate, convection coefficients) will also be extracted from the simulation.

The development of this methodology consisted of three stages. Stage 1: collection of experimental data are. Wireless sensors, deployed in a zone of the Environmental Research Institute (ERI) Building in University College Cork (UCC), record temperature, velocity and humidity values of the room. Stage 2: the data are utilised to generate and validate steady state CFD simulations. Stage 3: a lumped model (CTM) of the room, is developed from the CFD simulations. The automatic extraction technique is not fully developed yet thus parameters which characterise the energy exchange between zones are evaluated from the CFD or in the ROMs through the minimisation of a cost function minimisation. The commercial package SINDA/FLUINT [15, 16] is utilised to solve the ROMs. Their accuracy of the ROM will be assessed by comparison with CFD simulations and experimental data.

METHOD

The research activity framework comprises three main phases. In the first phase an iterative process is used for the design and deployment of wireless sensor network (WSN) in a building zone. Preliminary CFD simulations are generated to individuate optimal wireless sensor deployment. CFD simulations are then validated against the WSN data. In the second phase the validated steady state CFD simulations are post processed to generate the ROMs. Lumped parameters are automatically extracted according to user defined constrains on temperature, velocities and/or relative humidity. Lump to lump connector characteristics will also be automatically extracted. Average values for temperature, velocities and humidity for each lump and characteristic connectors will then been prepared for the ROMs solver (SINDA/FLUINT). In the third phase steady state results from the ROM will be compared with the CFD values to assess the accuracy of the ROMs. Consequently unsteady ROMs model will be run and possibly integrated with BMS for building operational strategies.

MODELS

Experimental set up

The location for the study is a north facing room in the ERI Building, shown in figure 1 which has dimensions 5.2x5.6x2.9m. The room is heated by two "Dimplex SmartRad" fan convectors. Two windows, electronically controlled, are also present with maximum aperture of 20°. Furniture comprises of five desks and chairs, and shelf units. No additional heating/momentum sources are present (i.e. computers and people). A set of 38 temperature (TelosB) and 4 anemometers (4 hobo) are used for experimental measurements. The anemometers were positioned in front of the opened windows to evaluate the normal component to the opening and on top of the fan assisted convectors. The temperature sensors were deployed at three different levels: Ceiling (2.65m above floor),

User (1m above floor) and Floor (0.2m above floor) as shown in Figure 1. Ten sensors were dispersed at floor level, 20 sensors at user level and 5 at ceiling level. Three different boundary conditions were analysed and deemed as the most influential: the convectors, the windows and the door. The convectors have been studied only at full regime. The windows have been considered open at an angle of 20°. The door has been considered closed or fully opened at 90°.

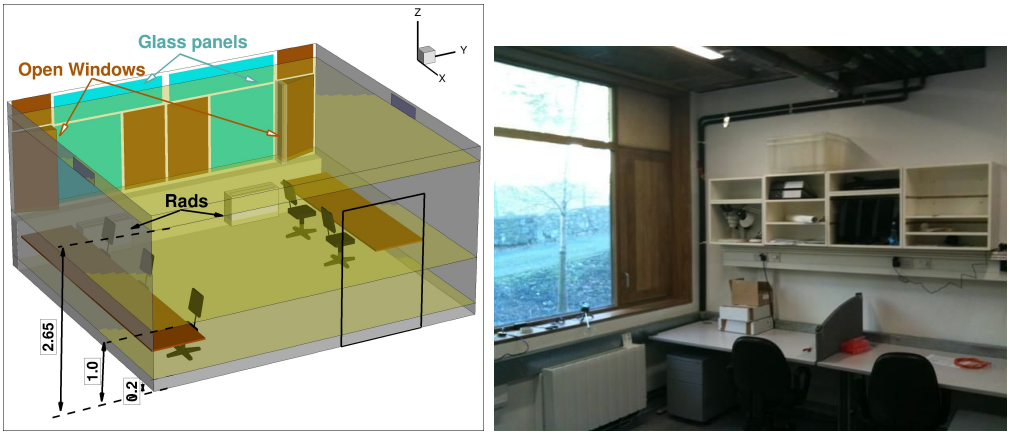

Figure 1: Numerical and physical domain

CFD model

CFD models have been developed to generate a database of test cases. For all simulations, steady state Reynolds Average Navier-Stokes (RANS) equations have been solved coupled with the RNG k-ϵ turbulence model and with air modelled as an incompressible ideal gas. The domain has been discretized using a structured grid to give 1,572,165 cells (115x147x93). Constant temperature boundary conditions have been utilised for the ceiling and the floor, with all other objects considered adiabatic. The glass panels have an overall heat transfer coefficient of $U = 1W/m^2K$. The door, when opened, has been modelled as a zone of constant pressure. The two convectors have been modelled considering two surfaces: an inlet surface, where velocity and temperature were imposed and an outlet surface where an extraction mass flow rate was imposed. Opened windows were also modelled as inlet surfaces.

Reduced Order Model

The number and type of lumps for the ROM are evaluated by post processing the CFD simulations through user defined constraints for temperature. At present, lumps have been defined on the three previously defined levels: Floor, User and Ceiling. The output of the post processing procedure and the lump model generated in SINDA/FLUINT are shown in figure 2. The parameters which characterise the lump-to-lump connectors were obtained in post-processing through the minimisation of a cost function $C = \sqrt{\sum_{i=1}^{Ntot} \left(T_{i_{Lump}} - T_{i_{CFD}}\right)^2}$

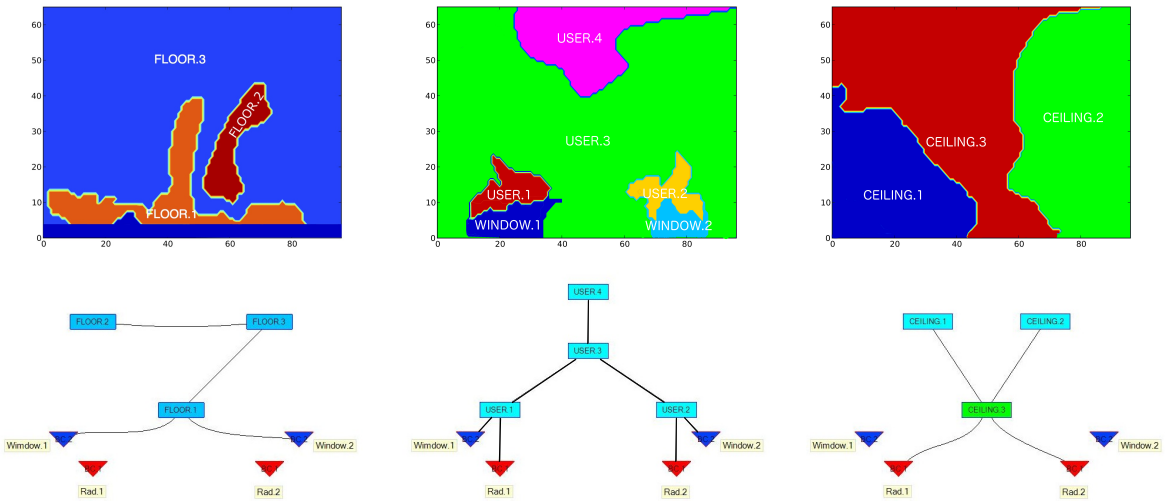

Figure 2: Example of result for for post processing procedure of CFD simulations

RESULTS

Validated CFD simulations and ROMs

CFD results have been qualitatively analysed and compared with experimental data as shown in figure 3. Experiments were run for 6 hours and were deemed at steady state when 10-minute temperature variation was ¡1%. At steady state average values were found for the 35 sensors. In figure 3 b) the comparison between temperature predicted and average temperature recorded has been reported for the test case simulating windows opened and convectors at full power. The good agreement shown between experimental and numerical data shows that the CFD simulations can be confidently used to generate and optimise ROMs.

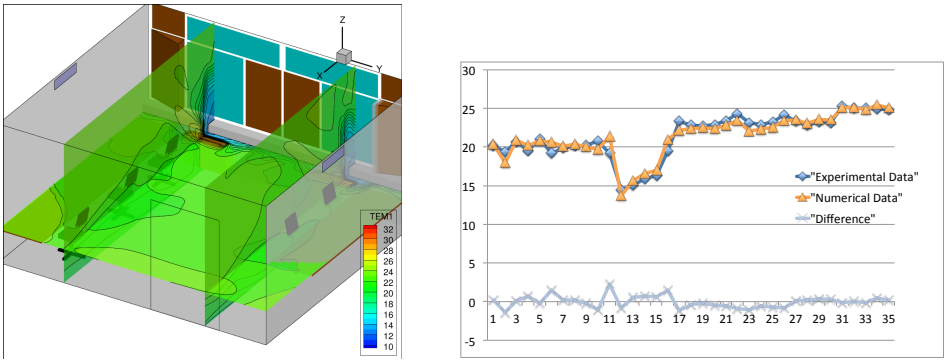

a) Temp contours b) Temp comparison

Figure 3: Temperature contours on three different planes and comparison with experimental data

The ROM was solved utilising SINDA/FLUINT, an equation solver for CTFM with capability to solve optimisation processes. This capability was utilised to evaluate thermal parameters which were not extracted from the CFD simulations. The results obtained from the ROM are compared versus the average values evaluated for each lump from the CFD simulation and are reported in table 1. In the table the percentage error has been defined as $\%err = \frac{(T_{ROM} - T_{CFD}}{T_{CFD} - T_{rads}}$ where T_{rads} is the air temperate from the fan assisted

radiators. The table shows the temperature predictions of the ROM are close to the values extrapolated from the CFD simulation with a maximum error of -4.93% for USER.4 lump, and average error of 1.95%. The computational efficiency of the ROM is highlighted by the running time of the ROM (3.42sec) versus that of the CFD model (5hours).

Plane	Lump	T_{ROM}	T_{CFD}	% Error
FLOOR	1	20.15	20.65	2.05
	2	21.99	21.48	-2.17
	3	22.65	22.1	-2.40
USER	1	24.95	24.82	-0.64
	2	24.01	23.83	-0.85
	3	23.46	23	-2.09
	4	22.65	23.7	-4.93
CEILING	1	26.08	25.8	-1.46
	2	25.01	25.3	-1.47
	3	24.62	24.9	1.39

Table 1: Comparison temperature prediction ROM and CFD

DISCUSSION

ROMs have proven to be a valid and efficient numerical approach to model the thermal behaviour of building zones. The main issues associated with the use of zonal/lumped models are how to (1) divide the domain (lumps) and (2) evaluate the parameters which characterise the lump-to-lump exchange of energy and momentum. This decision is usually left to the researcher who will utilise his/her experience to divide the domain and empirical data or correlations to evaluate lump-to-lump exchanges. The object of this research is to develop a methodology for the generation of ROMs from CFD models. The lumps of the ROM and their average property values are automatically extracted from the CFD models through user defined constraints. At this stage the parameters which characterise energy and momentum exchange are evaluated through an optimisation procedure. It is foreseen that more parameters (e.g. mass flow rate, heat transfer coefficients) will also be extracted from CFD models. The ROM extracted with this procedure accurately predicts the temperature distribution in the zone with an average difference with the CFD model lower than 0.4^oC. The ROM is also computationally efficient (3.4 sec) allowing its possible integration with BMS. Future development of this procedure will allow the extraction from the CFD model of the lump to lump energy and momentum exchange parameters. The overall aim will be to develop a ROM of the room which is able to accurately predict the transient thermal behaviour of the office space under different set of boundary conditions.

ACKNOWLEDGEMENTS

The authors wish to acknowledge the support of Science Foundation Ireland under the 06-SRC-I1091 ITOBO project in funding work reported in this paper.

REFERENCES

1. Chiang, W., Wang, C., and Huang, J.: Evaluation of cooling ceiling and mechanical ventilation systems on thermal comfort using CFD study in an office for subtropical

region. *Building and enviroment*, 48:113–127, 2011.

2. Catalina, T., Virgone, J., and Kuznik, F.: Evaluation of thermal comfort using combined CFD and experimentation study in a test room equipped with a cooling ceiling. *Building and environment*, 44(8):1740–1750, 2009.
3. Hajdukiewicz, M., Geron, M., and Keane, M. M. M.: Formal calibration methodology for CFD models of naturally ventilated indoor environments. *Building and Environment*, 59:290–302, Aug. 2012.
4. Wang, X., Wang, X., Xing, G., Chen, J., Lin, C.-X., and Chen, Y.: Towards optimal sensor placement for hot server detection in data centers. *2011 31st International Conference on Distributed Computing Systems*, pages 899–908, 2011.
5. Shapiro, B.: Creating compact models of complex electronic systems: an overview and suggested use of existing model reduction and experimental system identification tools. *IEEE Transactions on Components and Packaging Technologies*, 26:165–172, Mar. 2003.
6. Rambo, J. and Joshi, Y.: Reduced-order modeling of turbulent forced convection with parametric conditions. *International journal of heat and mass transfer*, 50:539–551, 2007.
7. Cardoso, M. and Durlofsky, L.: Linearized reduced-order models for subsurface flow simulation. *Journal of Computational Physics*, 229(3):681—-700, 2010.
8. Lasance, C., Vinke, H., Rosten, H., and Weiner, K. L.: A novel approach for the thermal characterization of electronic parts. pages 1–9, 1995.
9. Bosch, E. G. T. and Sabry, M. N.: Thermal compact models for electronic systems. pages 21–29, 2002.
10. Sabry, M.-N.: High-precision compact-thermal models. *IEEE Transactions on Components and Packaging Technologies*, 28(4):623–629, Dec. 2005.
11. Miana, M., Cortes, C., Pelegay, J. L., Valdes, J. R., Putz, T., Moczala, M., and Cortés, C.: Transient Thermal Network Modeling Applied to Multiscale Systems. Part I: Definition and Validation. *IEEE Transactions on Advanced Packaging*, 33(4):924–937, Nov. 2010.
12. Musy, M., Wurtz, E., and Sergent, A.: Buildings air-flow simulations: automatically-generated zonal models. *Proceedings of Building Simulation*, pages 593–600, 2001.
13. Griffith, B. and Chen, Q. Y.: A Momentum-Zonal Model for Predicting Zone Airflow and Temperature Distributions to Enhance Building Load and Energy Simulations. *HVAC&R Research*, 9(3):309–325, July 2003.
14. Beausoleil-Morrison, I. *The adaptive coupling of heat and air flow modelling within dynamic whole-building simulation*. PhD thesis, 2000.
15. Cullimore, B., Ring, S., and Johnson, D. General Purpose Thermal/Fluid Network Analyzer V5.5, Oct. 2011.
16. Cullimore, B., Beer, C., and Johnson, D.: Propulsion applications of the NASA standard general purpose thermohydraulic analyzer. *AIAA*, (3723), 2000.

OPTIMISATION STRATEGIES FOR CONTINUOUS MONITORING OF DENSELY SENSED BUILDINGS

A.Hryshchenko[1]; K.Menzel[2]; S.Sirr[3]. B.Cahill[4]

1: Research assistant, IRUSE, University College Cork, Ireland. a.hryshchenko@ucc.ie

2: Professor, Head of IRUSE Group, University College Cork, Ireland. k.menzel@ucc.ie

3: Research assistant, IRUSE, University College Cork, Ireland. s.sirr@umail.ucc.ie

4: Research assistant, IRUSE, University College Cork, Ireland. b.cahill@ucc.ie

ABSTRACT

Continuous Commissioning (CC®) of buildings is a rapidly growing sector within facility management services linked with a long-term demand for efficient tools and strategies directed onto acceptable tenant comfort, reduced energy consumption and cost of buildings maintenance.

Continuous building monitoring techniques are used to provide the best possible level of detail for the analysis of building energy performance. Additional software/hardware installations can be required to provide effective building commissioning and monitoring. However in many cases, when this process is initiated, these additional installations (e.g. sensors, sub-meters, actuators etc.) can exceed the capabilities of the current Building Management System (BMS). Furthermore, there are difficulties in predicting building occupancy trends which very often do not correlate with the expected energy demand when buildings are in use or operation.

This paper is based on the ongoing work and interim results of "ITOBO" project [1] and "CAMPUS 21" project [2], both focusing on the energy-efficient operation of buildings and spaces.

The management experience of the authors combined with the research partners' expertise from multiple sectors, such as Construction & Facilities Management, Building Services Systems Manufacturers, energy research centres and Energy Providers. Two buildings of the campus of University College Cork, Ireland are used as a case studies to demonstrate the process of BMS commissioning, data collection and evaluation. These are the Environmental Research Institute (ERI) and the Civil and Environmental Engineering (CEE) both of which are educational buildings of contrasting ages. The objectives of this paper, based on a series of experiments, are to:

- Describe the continual monitoring algorithm outside of the trademarked CC® description;
- Display the identification methods of various faulty operations in the HVAC system by analysis of collected data – ERI example;
- Establish an understanding of the relationship between sensor density and sensing accuracy for a single physical parameter at a spatial and temporal level – CEE example;
- Outline the possible energy saving measures for the HVAC systems commissioned.

It is expected that the "ITOBO" and "CAMPUS 21" experimental results can be used to provide automated feedback to the Building Management System which can then be further used to improve HVAC control and efficiency.

Keywords: Continuous Commissioning; Building Control; Energy Efficiency; BMS

INTRODUCTION

The energy consumed during the operational phase of a building is one of the major contributors to increasing energy use in Europe. Typically it comprises space conditioning (heating and cooling), lighting, heating of water, and running various appliances. Increasing the efficiency of energy use will have a significant impact on European energy consumption, and consequently reduce carbon dioxide production as well as reduced dependency on imported energy and improved environmental conditions. New operational and maintenance management strategies need to be developed in order to enable the intelligent and efficient use of the energy consumed.

Further new technologies and the liberalisation of the energy market across the EU greatly expand the range of energy service providers, as well as associated industries and services, e.g. smart meters developers, Facility Management and Energy Commissioning companies, Neighbourhood Management System (NMS) providers etc. This is a trend that is set to continue, thus the adoption of a sophisticated Building Management Systems (BMS) and Energy Management Systems (EMS) as a systematic process for continually improving energy performance is crucial in monitoring and controlling building performance.

Effective management of energy use in buildings makes perfect business sense - it cuts the costs, decreases greenhouse gas emissions (for associated restrictions and penalty costs etc.), reduces exposure to volatile energy prices and improves company's image if this is commercial property. However many companies are reluctant to focus on energy management or to invest in energy efficiency measures as they cannot accurately quantify the maintenance costs of their facilities. Nevertheless, there are many good examples which can prove that a systematic approach to managing energy performance can be successfully combined with the priorities and requirements of many companies [3]. Figure 1 below shows how energy consumption behaves over time when a company occasionally implements commissioning actions in response to maintenance and/or rising energy costs, versus implementation of continual facilities' commissioning. Energy consumption will continue to cycle and go out of control if an organisation does not manage its energy use on a regular basis and doesn't make building's commissioning a part of normal scheduled business operations.

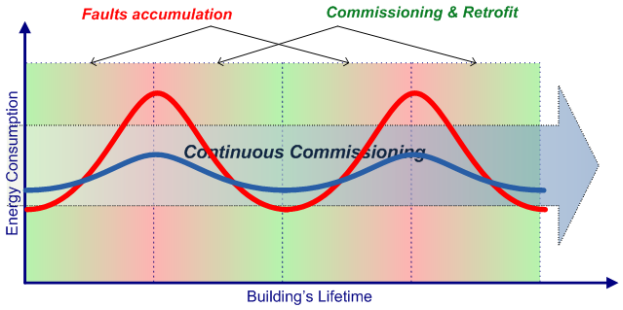

Figure 1: "Ad hoc" VS "Continual Commissioning" approaches to building energy management

An essential part of a BMS efficiency for energy management is its monitoring capabilities. Quality data that is collected and correctly evaluated helps to highlight the possible areas for operational improvements more effectively. Analysing historical data, on a regular basis, further assists BMS operators to track changes in building functionality and occupant energy-related behaviour over the longer periods, improving their ability to react accordingly.

Maintaining building BMS systems can require significant efforts for the building management team. The performance of a BMS can be significantly reduced due to improper/incompatible equipment installation, degradation and failures, or even inappropriate

settings of operational sequences. Usually building maintenance staff can be alerted to mechanical malfunctions through alarms when certain parameters exceeds a pre-set limits. In theory this can be set to occur prior to a malfunction being critical, thus enabling maintenance personnel to act on time and repair the damage before system fails. However, in reality the majority of these minor events are often postponed. These negligible faults, mistakes and mismatches in operational schedules then simply accumulate over time. This leads to situation where the facility manager makes often ad-hoc alterations to the BMS settings that adversely affect the building's energy efficiency, and it's deteriorating over time.

All of the facts presented above, as well as the results of multiple research projects and energy-related literature developed over the last decade, have only confirmed to buildings owners and facilities managers that most of their buildings do not function at their maximum performance level, consuming extra energy and operational expenses. Possible reduction of the building maintenance costs is just one incentive for employing a program for regular commissioning processes (can be named as On-going Commissioning, Continual Monitoring, or Continuous Commissioning (CC®) [4]).

METHOD

Continual BMS monitoring, especially in densely sensed buildings, is one such on-going commissioning process incorporating specific diagnostic tools for gathering energy-related data. It is used for energy benchmarking, data acquisition and following analysis and BMS optimisation. This includes analysis of the BMS alarms and faults information, as well as information and alarms of missed/censored data. Figure 2 below represents the data-related steps of ongoing BMS commissioning.

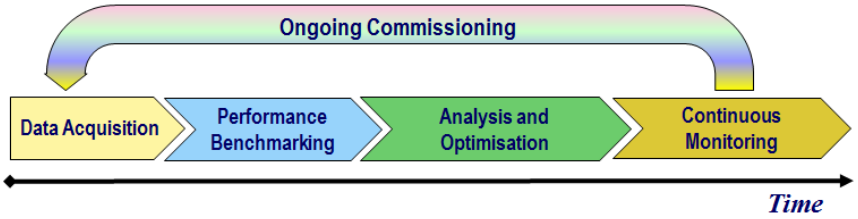

Figure 2: Data-related steps of ongoing BMS commissioning

Closely and continually working with incoming data will:

- provide energy managers with information about the current status of systems' operations,
- leading to how to adjust these systems,
- aiming to maintain or increase their efficiency.

Collection of building information, from architectural and mechanical drawings, specifications of equipment, BMS schedules and operational sequences, is the first step of the process for commissioning specialists. Benchmarking, in our case, is a process of comparing the actual recorded building energy performance data with guides of performance from a large number of reference buildings in the same region. This comparison can show if the commissioned building performs worse, similar to, or better than comparable buildings. Typically building performance benchmarking requires the development of sensible Key Performance Indicators (KPIs), which also can be called as Energy Performance Indicators (EnPI) in connection with an Energy Management System within buildings. These KPIs should be simple, understandable, measurable, objective, boundary containing, verifiable and sensible for the use case figures.

We should also differentiate between two types of these key figures, Absolute and Relative. An Absolute Key figures, for example, could be a total water consumption [m³], total natural gas consumption [m³], total number of employees, total energy consumption of lighting [kWh], total energy consumption of heating [kWh], total costs of gas and water [€] etc.

The Relative Key figures are developed by referencing these Absolute Key figures with reference values, e.g. energy consumption per m², employees per produced piece, energy consumption per employee etc. These KPIs should be extendable and scalable for different use cases and reflecting the needs of different stakeholders.

RESEARCH BUILDINGS DESCRIPTION

As described this study focuses on the ERI and CEE buildings located on the main campus of University College Cork, Ireland. Figure 3 below.

Figure 3. ERI (left) and CEE (right) buildings on the UCC campus

The ERI building is the most densely sensed building on the UCC campus and operates as a "Living Laboratory". Building performance data from the CYLON BMS system is provided by more than 180 wired sensors doing 13 different types of measurements, including indoor environment and outdoor weather conditions, along with integrated actuators and sub-meters. This building features many energy systems including solar collectors (SC, evacuated tube & flat plate) for pre-heating of the Domestic Hot Water (DHW); geothermal (88 kW Heat Pump with aquifer open loop); cooling and air handling (6 heat pumps (2.2 kW) for cold rooms, 4 AHUs for Labs (incl. heat recovery) and a gas fired boiler (163 kW) as back-up for the other systems.

The CEE building is a three story structure with solid 500 mm redbrick walls and 30 mm external roughcast plaster. The building consists of large lecture halls, computer labs, offices and corridors. Heat energy is supplied to the CEE Building from the main campus steam distribution network. The steam from the network, , enters the CEE Building by means of a heat exchanger in the plant room on the ground floor. [5] BMS-controlled thermostatic radiator valves (TRV) are in place on all radiators in the CEE building.

RESULTS

Currently, the energy consumption and production data aggregated from the sites described above is very detailed. Discussed below are the 2012 natural gas consumption data trend plus the data (gathered from integrated heat meter) reflecting energy saved by the solar and geothermal systems. The following figures will graphically show the energy consumptions and savings, allowing qualitative KPIs development, benchmarking, data analysis and buildings' optimisation.

Data analysis results - ERI building

When assessing the contribution the solar array makes to overall DHW demand in the ERI building, it was necessary first to analyse the diffuse solar radiation levels for the year 2012.

By using data classification techniques, the average monthly diffuse solar radiation values were analysed as shown in Figure 4 below.

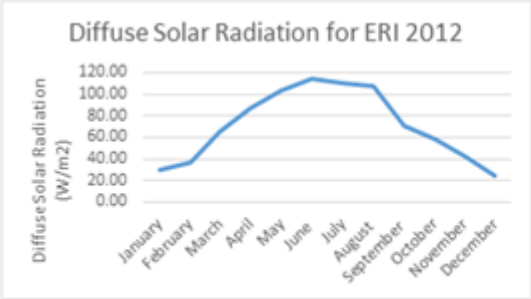

Figure 4. Diffuse Solar Radiation measured on roof of ERI, 2012

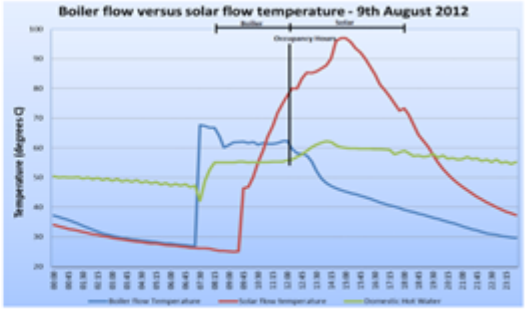

Figure 5. Boiler, solar flow and domestic hot water temperatures, ERI 2012

Using manual data mining analysis techniques, such as data classification and association, it was possible to examine the DHW system performance, so the 9th August 2012 was selected as a good example to demonstrate (Figure 5) within associated occupancy hours of the ERI building. This analysis uncovered an error in the BMS scheduling where the boiler starts early in the day and therefore negates any potential contribution from the solar collectors. This was found to be the case for the majority of the days analysed where high solar radiation could have reduced the need for boiler use. If boiler's schedule will be changed to start 4 hours later it will save up to 80m^3 of natural gas per similar day. For the year 2012 the estimated potential savings equals to 5.7% of the overall gas consumption, or 5.5 tons less of CO_2 emission plus reduced operation of the boiler means longer equipment lifecycles.

This also demonstrates a demand for automated commissioning software tools to highlight days with expected higher solar radiance, so boiler scheduling adjustments could be done automatically for the following day. The overall performance of the DHW system could be further improved by continually checking the data available from a various sensors and heat meters available in order to set the BMS scheduling more efficiently.

Data analysis results - CEE building

In order to establish an understanding of the relationship between sensor density and sensing accuracy for a single physical parameter (air temperature, °C) at a spatial and temporal level, the CEE109 (Computer Laboratory) was taken for analysis. This room is occupied from Monday to Sunday, between the hours of 08.00 and 22.00; however, occupancy levels vary greatly within this time period. There are two temperature sensors installed in this room. Sensor 1 is located next to the access door, and Sensor 2 is located close to the radiator.

Figure 6. CEE109 Sensor Placement

For the purpose of this analysis, these two sensors' readings were taken as the extreme temperatures in the room. Sensor 1 reads the minimum temperature in the room, while sensor 2 reads the maximum. The difference in readings varies in 2-3°C. This is significant difference, which can cause disruption to BMS operation. An interpolation technique was applied to get the mean of these two data entries, from the week January 7th to 13th (Saturday to Friday) as example.

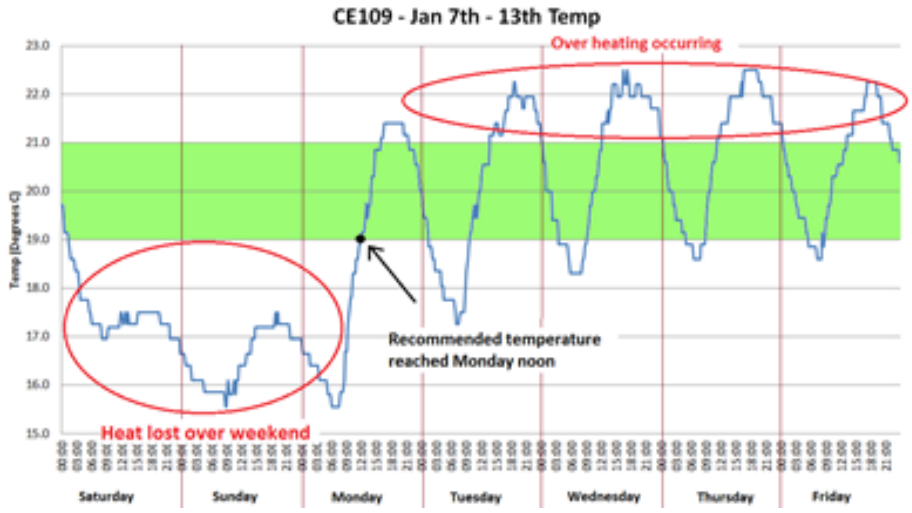

Figure 7. Interpolated temperature readings within the room CEE109

The thermal comfort analysis was based on CIBSE "Guide A" recommended operating temperatures for the four different room types analysed. It is clear that significant amount of heat was lost through infiltration and fabric losses over the weekend period, when the building was not being heated. This is due to the building being an older structure, when building standards were nowhere near as stringent as they are now. Improved insulation of the external walls would reduce the heat lost over the weekend. Correct positioning of sensing devises is important for adequate control procedures and BMS scheduling.

CONCLUSION

On-going/Continuous building and BMS commissioning, in common sense understanding, is a normal process of planned check-ups and maintenance procedures directed on maintaining buildings at their maximum performance level. The aim of this paper was to highlight the importance of regular attention from building energy manager to BMS and its operational processes through precise analysis of incoming data for development of reliable conclusions and consequences. Freedom in terminology will also provide more flexibility in selection of specific software tools, equipment and operations, as well as in adoption of the unique for each building commissioning techniques. It is great though that a well-known and experienced organisation such as Energy Systems Laboratory (ESL) is promoting same ideas.

REFERENCES

1. ITOBO research project, http://www.zuse.ucc.ie/itobo/
2. Campus 21 research project, http://campus21-project.eu/index.php/en/
3. N. H. Petra Lackner, "Step by step guidance for the implementation of energy management," Austrian Energy Agency, 2007
4. The Energy Systems Laboratory, Continuous Commissioning® developers, http://esl.tamu.edu/continuous-commissioning
5. Campus 21 Deliverable 2.1 "Gap Analysis of Existing Monitoring Concepts & Systems", pp. 12-19

THE PERCEPTION OF LIGHT AFFECTED BY COLOUR SURFACES IN INDOOR SPACES

J. López; H. Coch; A. Isalgué; C. Alonso; A. Aguilar

Architecture & Energy. Barcelona School of Architecture. UPC.

Av. Diagonal, 649, 7th floor 08028 Barcelona

ABSTRACT

Visual comfort in indoor spaces depends on the amount and quality of light available and also on space characteristics. One of the most influential aspects is the colour of surfaces defining a space. Each colour has a reflectance coefficient resulting from how much light is reflected back from the coloured surface. However, from the observer's point of view, there are other factors that may affect visual perception of a space painted with colours. Some of them are psychological and depend on the background of the observer while other factors are physiological and are strongly connected to the sense of sight. According to this theory, architectural spaces could take advantage of the benefits of colour to improve visual responses for users.

In this paper, we present a case study in which three coloured spaces with different lighting conditions were assessed by a sample of observers. At the same time, luminance and illuminance measurements were taken so as to compare these values with light perceived in the spaces. The results of this field work show the influence that colour has on the perception of light in three-dimensional spaces and contribute to the study of colour in architecture.

Keywords: architecture, colour, visual comfort, light

INTRODUCTION

Dealing with visual comfort implies keeping in mind features of light and space configuration. Although attention is usually focused on light, space characteristics are vital to the visual response. One of the most important characteristics is the colour used on surfaces shaping a space. As a physical phenomenon, colour is a consequence of interaction between the reflecting properties of materials and the nature of incidental light. However, we can also explain colour from a perception standpoint, connected to psychological factors such as culture, age or education, and to physiological factors as well. These are influenced by the human visual system which shows a different degree of sensitivity based on light wavelength and objects. According to the photopic V (λ) and scotopic V' (λ) human response curve [1], maximum sensitivity corresponds to 555 and 505 nm, respectively. In photopic vision, this value is perceived as a greenish yellow.

In consequence, under the same lighting conditions, spaces can be perceived in a different way depending on the colours they are painted. On the one hand, the physical value which represents the amount of light returned by surfaces is luminance. It depends on incidental light and the reflection index of the colour. On the other hand, it has been noted that surfaces with the same luminance value but different colours are actually seen as having different brightness. In fact, brightness is the subjective perception of luminance [2]. Several studies have been done in the field of brightness and colour, but most of them compare small samples of colour among them as well as in contrast to a lighter or darker background [3].

Nevertheless, from the point of view of architectural spaces, which corresponds to a three-dimensional experience, little research has been conducted.

The aim of this study is to compare the physical phenomenon of colour and light with the human perception of it in order to determine if they coincide. As colour and brightness are the main parts of the theory of light and space in architecture [4], the results of the study can be applied to architecture, especially in the field of interior design where using colour can enhance perception of light in spaces.

METHOD

With this purpose in mind, three spaces were built in a controlled set. The set was appropriate because there was room enough to move in front of the spaces as well as because lighting conditions could be adjusted. The spaces, A, B and C, were of the same dimensions; 2m wide, 1.5m deep and 3m high, with no ceiling, as we see in Figure 1 and Figure 2.

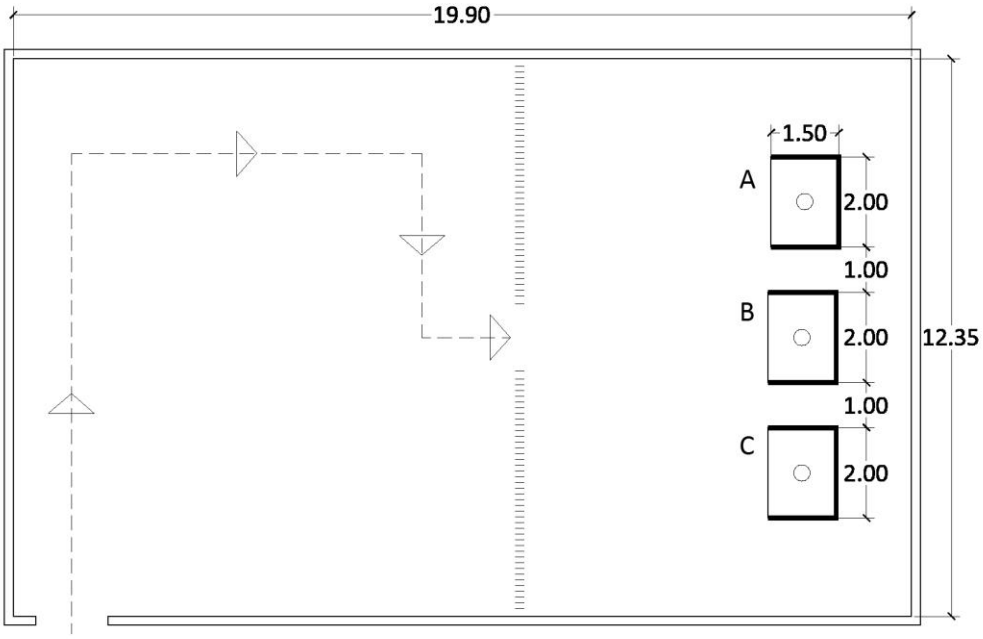

Figure 1: Plan of the set and Spaces A, B, C.

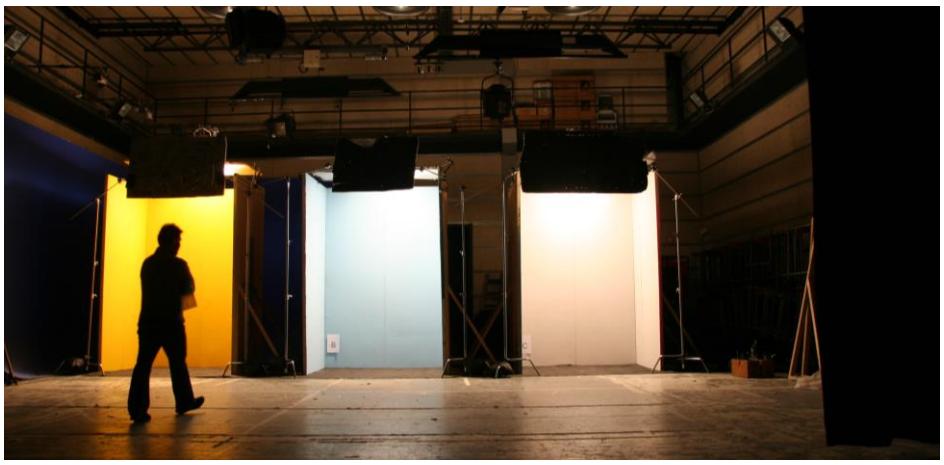

Figure 2: Front view of the set and spaces A, B, C

Each space was painted in a different colour: yellow (NCS S 1070-Y10R) for space A, blue (NCS S 1030-B) for space B, and grey (NCS S 1500-N) for space C. The choice started with a bright yellow because it is associated with a sensation of lightness. Besides, its wavelength is close to the point of highest sensitivity in the eye, according to the human response curve. The purpose was to compare an intense yellow with a grey with the same reflection index and with a slightly darker blue. The reflection index of each colour was calculated from the measurements of luminance and illuminance taken later on in the experiment. The equation (1) was used based on the assumption that all the surfaces were Lambertian. As a result, the experimental reflection indexes for each colour are: 0.64 for A (yellow), 0.50 for B (blue) and 0.66 for C (grey).

$$E \cdot r = \pi \cdot L \quad (1)$$

In order to compare the colours, two lighting arrangements were staged, combining two intensities of light; a starting intensity (I_1) and a modified intensity (I_2) which was half of the previous by means of a neutral filter. To these ends, the lighting fixtures were positioned in order to provide an illuminance level of approximately 900 lux at ground level for I_1. Using a filter, the intensity was reduced to I_2, becoming about 450 lux. A combination of both intensities led to the design of two lighting arrangements: in Arrangement 1, all the spaces had the same intensity (I_1), while in Arrangement 2 the intensity in Space A was reduced (I_2) and spaces B and C remained with I_1. The same lighting fixtures were used in each space: a Quars halogen lamp (2000W) in zenithal position filtered with a 50% Diffuser Frame so as to provide a diffuse and even light. A white board was placed in the upper part of the front side of each space to diffuse light and hide the lamps. The colour temperature and the lamps remained the same during the experiment.

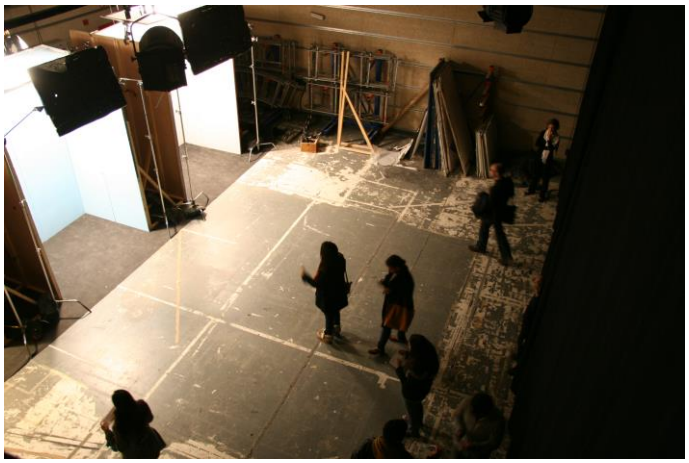

Figure 3: Observer assessment

The spaces were assessed by a sample of observers (Figure 3). A total of 25 participants took part in the test, 9 males and 16 females, from 18 to 39 years old, with an average age of 25. All of them had normal vision with the exception of one, who had Daltonism. The participants were all students with basic knowledge of lighting. They were organised in groups of 3-5 that entered the set twice, each with a different lighting arrangement, and answered some questions about the perception of light. All the groups had a 15 minute gap between Arrangement 1 and 2. On entering the set, they were asked two questions: which space seemed to be lighter and which seemed to be darker. Furthermore, they had to estimate the difference of light in the spaces as “almost equal”, “slightly different” or “very different”.

Apart from the observer assessment, physical measurements were taken in each arrangement. While the measurements give quantitative data, the assessment offers a qualitative evaluation [5]. The measured parameters were illuminance and luminance. Illuminance was measured at ground level and in the middle of each vertical surface, 1.5m from the ground, half width. Luminance was measured in the middle of each vertical surface as well. The instruments used were a Konica Minolta LS-110 luminance meter and a Lutron lux meter.

RESULTS

The results of the measurements are divided into illuminance and luminance values. The first results were used to establish intensities in the lighting arrangements by placing the lighting fixtures and filters, as well as to calculate the reflection index of the colours. The luminance measurements were used as physical and objective data to assess the amount of light coming from vertical surfaces, although other studies take different parameters into consideration [3, 6]. Given that the observers could move freely throughout the set, an average value of luminance was considered to be most suitable. The value for each space resulted from the mean of luminance in the vertical surfaces. The results are shown in the tables and graphs below:

Luminance (cd/m^2)	**Space A**	**Space B**	**Space C**
Arrangement 1	124.0	109.0	149.7
Arrangement 2	65.5	109.0	149.7

Table 1: Average wall luminance values at 1.5m from ground level (cd/m^2) in each space, Arrangement 1 and Arrangement 2

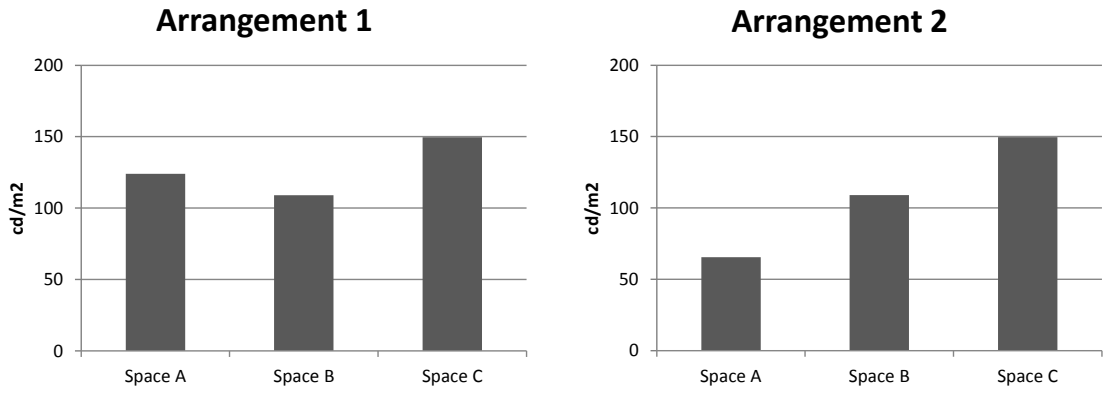

Figure 4: Average wall luminance values at 1.5m from ground level (cd/m^2) in each space, Arrangement 1 and Arrangement 2

Although the lighting conditions in Arrangement 1 were the same for all spaces, the measurements show that luminances are not equal, due to different reflection indexes in the colours. In the second arrangement, when darkening Space A, the measurements show that Space C is clearly the lightest and Space A is obviously the darkest.

The observer assessment comes in two parts. The first part contains the answers to questions about the quantity of light perceived in each space (Figure 5); the second part presents the degree of difference perceived in terms of light (Table 2). In the first part, there is a graph for each lighting arrangement showing the answer percentage. The answers are divided into three blocks, one for each space, containing two columns. The first column corresponds to answers

about the brighter space and the second column shows answers to question about the darker space.

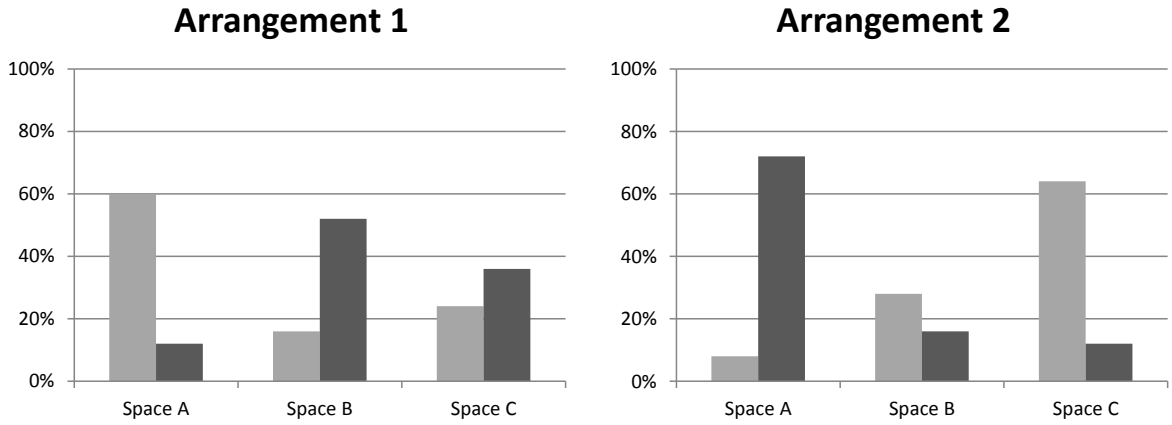

Figure 5: Graphs showing the percentage of responses in Arrangement 1 and Arrangement 2 to the questions: -Which space seems lighter? (light grey columns) -Which space seems darker? (dark grey columns)

In the second part of the results the observers estimated the degree of difference in perception of light in the spaces. It was important to highlight to what extent observers perceived differences in terms of light, because evaluating if this was easily perceived or not was significant. The answers are divided into three categories for each arrangement.

	Answers		
	Almost equal	**Slightly different**	**Very different**
Arrangement 1	44 %	56 %	0 %
Arrangement 2	48 %	48 %	4 %

Table 2: Percentage of answers to the question about the degree of difference in the perception of light in the spaces, Arrangement 1 and Arrangement 2.

DISCUSSION AND CONCLUSIONS

Once the measurements and the observer assessment were completed, the results obtained in both procedures could be compared. First of all, we see that the overall result of observer opinions in Arrangement 1 does not coincide with the measurements, while in Arrangement 2 it does. The assessment in Arrangement 1 concerns yellow and grey, which have a similar reflection index but do not give the same sensation to observers.

As mentioned above, the lighting conditions in Arrangement 1 were equal in all spaces. In Table 1 we see that the highest value of luminance was measured in Space C (149.7cd/m^2) while the lowest was in Space B (109cd/m^2). Space A is in the middle, with 124cd/m^2. Comparing these values with the observer assessment, we find that the majority of observers perceived Space A as the brightest instead of C. In regards to the darker space, opinions coincided with the measurements. The luminance is similar, but if we compare the values, Space C is 1.37 times lighter than B and 1.2 times lighter than A, which is not a big difference. According to the observer opinions (Table 2), none of them found the spaces "very different"; the opinions were divided between "almost equal" and "slightly different". This corresponds to reality, because the measurements didn't show prominent differences.

The results in Arrangement 2 are different. Here, the highest luminance value corresponds to Space C (149.7cd/m^2), while the lowest corresponds to Space A (65.5cd/m^2). The observer assessment coincided with the results, but not with the degree of difference perceived. If we compare the luminance values, we see that Space C is 2.28 times lighter than A, which means that the difference is noticeable. If we look at the observer assessment in Table 2, only 4% of observers perceived light in the spaces as "very different", while 48% thought they were "almost equal". The remaining 48% perceived them as "slightly different". In this case, although Space C is much lighter than A, observers minimise the difference. It makes it clear that, from the observers' point of view, yellow and grey do not offer the same sensation in terms of light.

We came to the conclusion that even though yellow and grey had the same reflection index, the surfaces painted with these colours offered a different sensation of light. While under the same lighting conditions the grey space looked dull and dark, the yellow space seemed brighter. What's more, when the yellow space was darkened it was perceived as darker but to a lesser extent than what the measurements showed.

These results can be taken into account when designing a building, because the perception of light in buildings is vital to visual comfort. The design of interiors could take advantage of the fact that some colours offer more sensation of light than others under the same lighting conditions. This doesn't mean that some colours should be banned or considered obligatory; it means that an intelligent use of colour may help to highlight some parts of a space and improve visual comfort for users. The use of colour goes beyond a choice based on reflection index, tastes or fashions.

ACKNOWLEDGEMENTS

The authors would like to thank the *Escola Superior de Cinema i Audiovisuals de Catalunya* (ESCAC) for providing the spaces where the field work was performed. We also want to thank ESCAC staff, the ESCAC Art Direction students and the *Architecture, Energy and Environment Master* students for their help during preparation of the study and for carrying out the assessments.

REFERENCES

1. Wyszecki, G. Stiles W.S.: Color Science: Concepts and Methods, Quantitative Data and Formulae. John Wiley & Sons Inc, New York, 1982
2. Lam, W.: Perception and lighting as formgivers for architecture. McGraw-Hill Book, New York, 1977
3. Cuttle, C.: Brightness, lightness, and providing 'a preconceived appearance to the interior'. Lighting Res. Technol. 36,3, pp. 201-216, 2004
4. Michel, Lou: Light: the shape of space: designing with space and light. John Wiley & Sons Inc, New York, 1995
5. Hopkinson, R.G. Kay J.D.: The lighting of buildings. Faber and Faber, London, 1972
6. Cuttle, C: Towards the third stage of the lighting profession. Lighting Res. Technol. 42, pp. 73-93, 2010

ASSESSING HEAT-RELATED THERMAL DISCOMFORT AND INDOOR POLLUTANT EXPOSURE RISK IN PURPOSE-BUILT FLATS IN AN URBAN AREA

A. Mavrogianni[1]; M. Davies[1]; J. Taylor[1]; E. Oikonomou[2]; R. Raslan[1]; P. Biddulph[1,2]; P. Das[1]; B. Jones[1]; C. Shrubsole[1]

1: The Bartlett School of Graduate Studies, University College London, Central House, 14 Upper Woburn Place, London WC1H 0NN

2: UCL Energy Institute, University College London, Central House, 14 Upper Woburn Place, London WC1H 0NN

ABSTRACT

The projected climate change-induced rise in external temperatures is expected to lead to an increase of excess heat-related health risks. The comfort and health impacts associated with a warming climate for city dwellers, in particular, is of increasing concern due to interconnected phenomena, such as the urban heat island, social deprivation and synergistic effects of heat waves and outdoor air pollution. Among the most severely affected are expected to be the elderly, the chronically ill and the socially deprived population groups of the inner cities. Whilst there has been a wealth of studies to date investigating the health effects of outdoor weather and pollution, the impact of indoor environment exposure is poorly understood. Furthermore, the majority of existing indoor environment modelling studies assume 'standard occupancy' profiles, which may be markedly different to the lifestyle of elderly, more vulnerable individuals. This paper presents preliminary results of an investigation of the summertime indoor overheating risk and air pollutant levels in three of the commonest purpose-built flat typologies in England (1965-1974 high-rise, 1965-1974 low-rise and post-1990 low-rise flats) using the dynamic and multizone thermal, airflow and contaminant transport analysis software EnergyPlus. The internal heat and indoor pollutant generation was estimated using the underlying assumption that the spaces were heavily occupied during the daytime (elderly occupants and/or occupants with mobility issues), taking into account window opening restrictions in urban environments. It was shown that indoor overheating risk is higher in mid and top floor flats and that temperatures generally decreased following the energy efficient retrofit of properties. $PM_{2.5}$ infiltration was found to be higher in top floor flats, and in flats with a larger exposed external façade to internal volume ratio. The findings of this study aim to enhance our understanding of indoor environment quality in dwellings occupied by vulnerable individuals and could have broader implications for urban public health policy and retrofit practice in social housing.

Keywords: urban, housing, climate change, overheating, indoor air quality, pollutants

INTRODUCTION

Inadvertent climate modifications due to anthropogenic greenhouse gas emissions and heat island effects are expected to pose significant challenges to the health and wellbeing of populations worldwide [1]. The projected climate change-induced rise in external ambient temperatures is expected to lead to an increase of excess heat-related morbidity and mortality. Recent extreme heat events, such as the record-breaking heat waves in Northern Europe in 2003 and 2006, in Russia in 2010 and across the US states and Canada in 2011 have caused both deaths and economic losses. According to climate modelling work, the frequency and

severity of such heat episodes will have doubled by the middle of the century [2]. Epidemiological evidence from the 2003 and 2006 European heat waves shows the worst affected population groups were the elderly and the chronically ill. Social isolation is also considered an appreciable confounding risk factor [3].

The existing building stock and infrastructure of heating-dominated countries are not well suited to hot weather. In addition, the energy efficient retrofit of existing homes in order to achieve carbon emission targets will lead to increased levels of air tightness and insulation, an unintended consequence of which is likely to be indoor overheating risk [4]. Of rising concern is the comfort and health impacts associated with a warming climate for the inhabitants of urban buildings, in particular: Heat island effects combined with potential synergistic effects with outdoor air pollution and social deprivation could render inner city populations increasingly vulnerable. Previous epidemiological studies have indicated that the mortality risk during the Paris 2003 heat wave was higher in top floor flats that provide little protection from extreme heat, older or highly insulated dwellings [5]. In low-income settings, vulnerable individuals are also unlikely to be able to afford the purchase of an active cooling system or have frequent access to cooler spaces. Furthermore, the potential for night ventilative cooling through window opening may be restricted in urban neighbourhoods due to security, noise and pollution concerns, elevated outdoor temperatures and single-sided façades not allowing cross ventilation.

It is recognised that a well-established relationship exists between high external temperatures and heat-related mortality risk for different cities at the population level [6]. However, the heterogeneity of building fabric characteristics may affect the distribution of vulnerability across a city as there will be a wide distribution of indoor temperatures at any given outdoor temperature. Whilst there has been a wealth of literature examining the relationship between external temperature and mortality, little attention has been paid to the potential impact of indoor thermal conditions on health during a heat wave [7]. Given that populations in mid- and high-latitude countries tend to spend the majority of their time indoors this is a research question of significant importance. Notably, the majority of existing indoor environment modelling studies assume ‘standard occupancy’ profiles [8], such as this of a working family with children, which may be markedly different to the lifestyle of more vulnerable, elderly people (e.g. bed-ridden individuals). Furthermore, few studies in the past have attempted a combined assessment of climate change on both indoor air quality and thermal conditions.

This paper seeks to assess the indoor overheating and air pollutant exposure risk of vulnerable individuals in purpose-built blocks of flats in an urban location during a warm summer for two different occupancy behaviour scenarios (temperature-dependent ventilation with and without window opening restrictions that may apply to urban environments), utilising a set of representative dwelling typologies and dynamic thermal and airflow simulation.

METHOD

Generation of English purpose-built flat archetypes

This study entailed the simulation of the indoor overheating and air pollutant risk levels under warm summer conditions in the three commonest purpose-built flat typologies in England: (a) 1965-1974 high rise, (b) 1965-1974 low-rise and (c) post-1990 low-rise block of flats, with estimated frequency of occurrence in the stock 0.8%, 2.7% and 3.2%, respectively. The generation of the dwelling internal layouts is based on existing literature on British residential architecture of different periods and builds on previous archetype development work [9, 10], in conjunction with more recent statistical analysis of the English Housing Survey (EHS) 2010-11 datasets [11]. The modelled archetypes are illustrated in Figure 1 (a, b1 and c1).

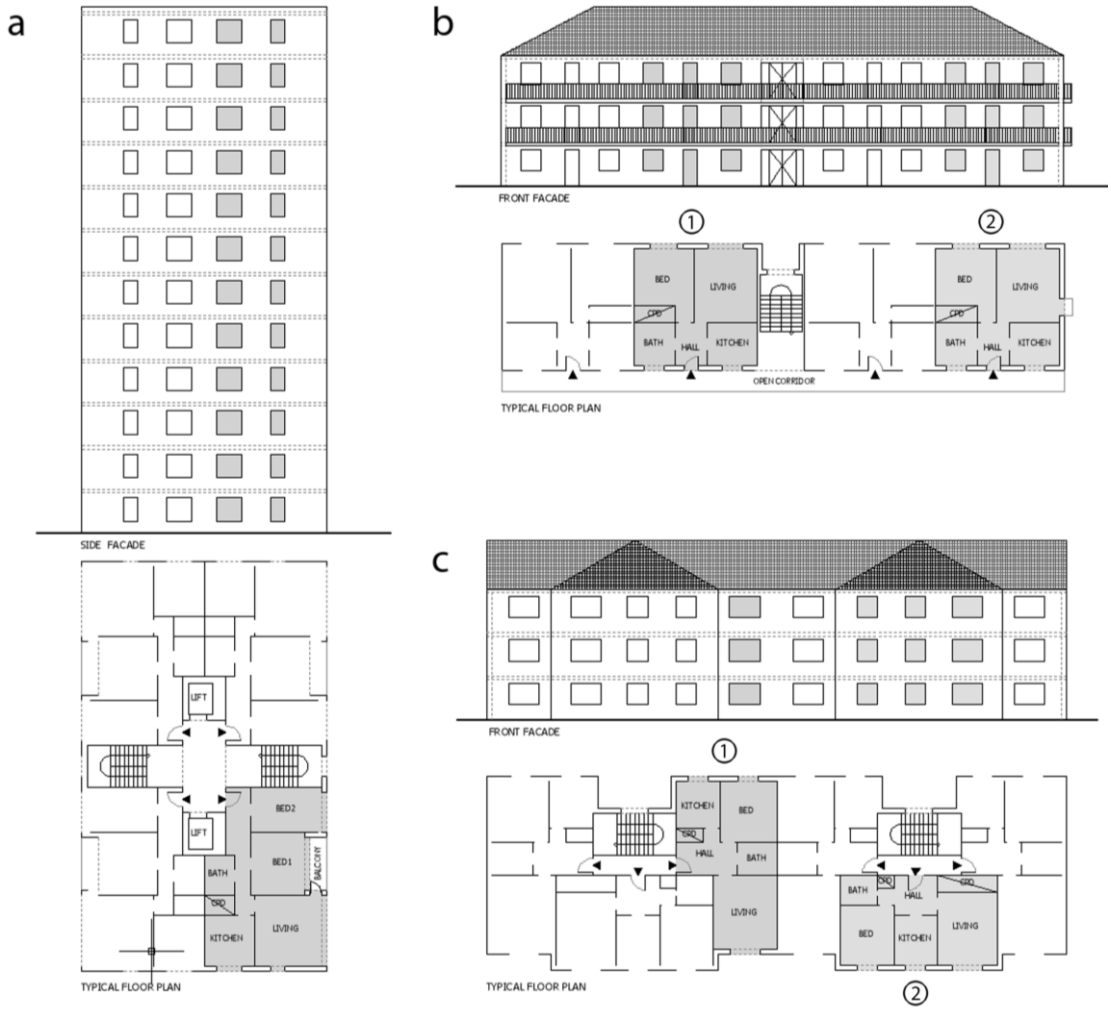

Figure 1: Modelled dwelling archetypes.

Modelling of indoor temperature

The archetypes presented above were modelled employing the widely used and extensively validated dynamic thermal simulation software package EnergyPlus v. 3.1.0 [12]. Typical construction elements were assumed based on the construction age band of each archetype and the corresponding EHS data (Table 1). The modelling involved all combinations of:

- two building fabric efficiency levels (Table 1),
- three floor levels (ground, mid and top floor),
- four building orientations (0^o, 90^o, 180^o and 270^o), and
- two occupant-controlled window opening scenarios ('sensible' window opening as a function of indoor and outdoor air temperature vs. windows closed due to restrictions related to the surrounding urban environment and/or limited occupant mobility, Table 2).

This led to 144 EnergyPlus simulations in total. Dwellings were modelled as constantly occupied by an elderly couple, with the living room occupied between 8 am to 8 pm and the master bedroom (bedroom 1 where there are more than one bedrooms, Figure 1) between 9 pm and 7 am. Internal doors were assumed to be open. The methodology underlying the estimation of internal heat gains is described in detail elsewhere [9, 10]. Simulations were carried out using the standardised CIBSE London Design Summer Year (DSY) weather file [13], commonly used to represent warm summer conditions under the current climate.

	External wall	Ground floor	Roof	Windows	Air tightness
1965-1974 current	Cavity 1.60 W/m^{2}K	Solid concrete 1.20 W/m^{2}K	Concrete tiles 3.10 W/m^{2}K	Double glazing 2.65 W/m^{2}K	11.5 m^3/m^{2}h @ 50 Pa
1965-1974 retrofitted	Cavity 0.50 W/m^{2}K	Solid concrete 0.50 W/m^{2}K	Concrete tiles 3.10 W/m^{2}K	Triple glazing 1.35 W/m^{2}K	5.0 m^3/m^{2}h @ 50 Pa
Post-1990 current	Cavity 0.45 W/m^{2}K	Solid concrete 0.45 W/m^{2}K	Concrete tiles 1.50 W/m^{2}K	Double glazing 2.65 W/m^{2}K	5.0 m^3/m^{2}h @ 50 Pa
Post-1990 retrofitted	Cavity 0.35 W/m^{2}K	Solid concrete 0.25 W/m^{2}K	Concrete tiles 0.15 W/m^{2}K	Triple glazing 1.35 W/m^{2}K	5.0 m^3/m^{2}h @ 50 Pa

Table 1: Summary of EnergyPlus building fabric modelling input assumptions.

Scenario	Window control settings
1	Windows open in the living room and master bedroom when the internal operative temperature rises above the CIBSE summertime upper thermal comfort standards (25 ^{o}C and 23 ^{o}C, respectively) [14] and close if the external temperature lies above the internal
2	Windows always remain closed due to security, pollution or noise concerns and/or occupant mobility issues

Table 2: Summary of EnergyPlus window opening scenarios.

Modelling of indoor air pollutant concentration

In addition to thermal modelling, EnergyPlus was used to simulate the infiltration of $PM_{2.5}$ from the outdoor environment into the indoors for Scenario 1 using the generic contaminant model and airflow network algorithms in EnergyPlus v. 8.0.0 [12]. Air infiltration was modelled through the permeability of the building envelope, taken to be 11.5 m^3/m^{2}h @ 50 Pa for unretrofitted pre-1990 cavity walls or 5 m^3/m^{2}h @ 50 Pa for 'best-practice' retrofitted and post-1990 dwellings [15]. Simulations were carried out for all four orientations for flats at ground level and on the top floor. Doors and windows were modelled as per scenario 1 (Table 2). Only $PM_{2.5}$ infiltration from the outdoor environment was considered, with no internal sources modelled (assuming internally generated $PM_{2.5}$ are effectively removed by an extract fan); a constant outdoor $PM_{2.5}$ concentration of 13 µg/m^3 was modelled, which is the average $PM_{2.5}$ concentration for London [16]. $PM_{2.5}$ was considered to have a deposition velocity of 0.00005 m/s [17]. The results were output for each room, and the total average indoor/outdoor (I/O) concentrations for the dwellings calculated for the simulation period.

RESULTS

Overall indoor overheating results were unsurprisingly higher for Scenario 2 (windows closed). Under this worst case scenario, the worst performing dwelling type in terms of mean temperature was found to be the mid floor followed by the top floor 1965-1974 high-rise flat. Temperature fluctuations in top floor flats were, however, higher with peak temperatures often higher than those observed in other flats. Lowest temperatures were obtained for the 1965-1974 low-rise ground floor flat. The increased insulation levels and air tightness were found to be overall beneficial: For instance, in the mid floor flat of the high-rise block (one of the worst performing types), the retrofit decreased the mean summer temperature in the south-east facing living room by 1.2 ^{o}C (from 29.0 to 27.8 ^{o}C) and the maximum temperature by 1.8 ^{o}C (from 37.5 to 35.7 ^{o}C). As illustrated in Figure 2, floor level is a critical factor for indoor overheating risk. Temperatures in ground floor flats remain significantly lower and more stable compared to upper floors, whereas higher fluctuations are observed in the much more

exposed top floors. The average indoor/outdoor $PM_{2.5}$ ratios for Scenario 1 for the different dwelling types, both pre- and post-retrofit, can be seen in Figure 3. Retrofitting was found to slightly increase the average I/O ratios in ground floor dwellings due to the increased need to open windows when internal temperatures rose above thresholds, thus causing spikes in $PM_{2.5}$ levels. In top floor dwellings, high I/O ratios were due to frequent window openings due to internal temperatures exceeding the threshold. In addition, increased wind pressures against the façade of top floor flats meant that the more permeable non-retrofitted flats had higher I/O ratios despite slightly less frequent window openings. The worst performing dwelling was the non-retrofitted 1965-74 high-rise top floor flat.

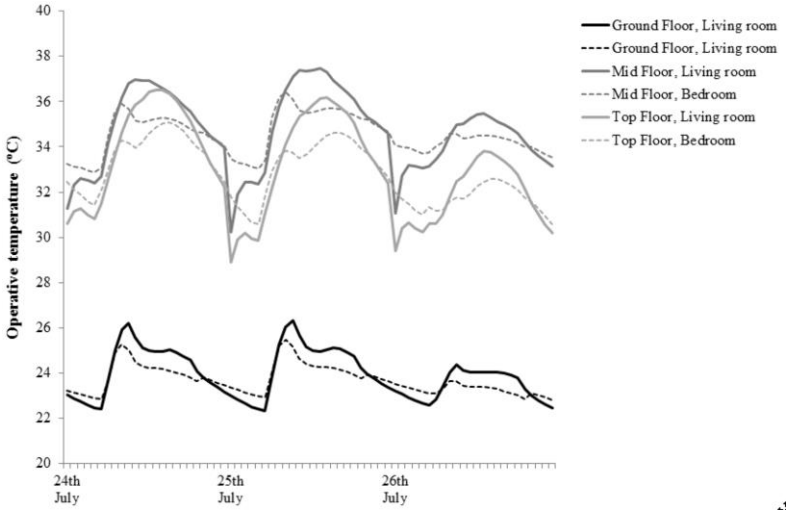

Figure 2. Temperature in the 1965-74 high-rise flats (warmest 3-day period, Scenario 2).

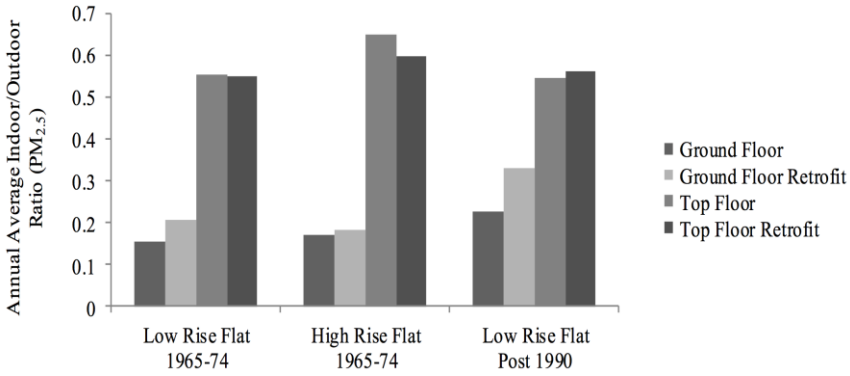

Figure 3. Mean indoor/outdoor $PM_{2.5}$ concentration level ratios (Scenario 1).

DISCUSSION

In accordance with the existing epidemiological literature from past extreme heat wave events, overheating risk was found to be more pronounced on higher floors. Lower and more stable temperatures were observed in ground floor flats, potentially due to the thermal inertia of the ground. The wind pressures experienced by top floor flats meant that the I/O $PM_{2.5}$ ratios were higher than those for the ground floor flats. Differences in the I/O $PM_{2.5}$ ratios were also strongly affected by the ratio of the externally exposed façade surface area to the internal volume of the dwelling. A potential public health strategy could, thus, be to identify vulnerable households and relocate them to lower risk properties. Whilst energy efficient retrofit may be generally beneficial for indoor overheating risk, it may not suffice in isolation; combined shading and intelligent ventilation measures may be required to keep indoor

thermal conditions within the thermal comfort zone. Retrofits that increase air tightness should incorporate appropriate ventilation systems in order to maintain indoor air quality. The results of the pollution infiltration modelling indicate that retrofitting the dwelling by reducing the permeability of the building fabric can have the co-benefit of reducing ingress of external pollutants indoors, provided the risk of overheating does not cause occupants to open their windows often. This study has not addressed stack effects between building floors or pollutants generated indoors. Future work will examine the balance between indoor and outdoor pollutant sources. The results of coupled thermal and air pollution models can provide insight into how building properties and temperature-dependent occupant behaviour may affect indoor air quality; this relationship is in need of further investigation.

ACKNOWLEDGEMENTS

The 'Air Pollution and WEather-related Health Impacts' (AWESOME) project is funded by a Natural Environment Research Council (NERC) grant (NE/I007938/1).

REFERENCES

1. Grimmond S. Urbanization and global environmental change: Local effects of urban warming. The Geographical Journal 2007;173:83–8.
2. Meehl GA, Tebaldi C. More intense, more frequent, and longer lasting heat waves in the 21st century. Science 2004;305:994–7.
3. Kovats RS, Hajat S. Heat stress and public health: a critical review. Annual Review of Public Health 2008;29:41–55.
4. Davies M, Oreszczyn T. The unintended consequences of decarbonising the built environment: A UK case study. Energy and Buildings 2012;46:80–5.
5. Vandentorren S, Bretin P, Zeghnoun A, Mandereau-Bruno L, Croisier A, Cochet C, et al. August 2003 heat wave in France: risk factors for death of elderly people living at home. European Journal of Public Health 2006;16:583–91.
6. McMichael AJ, Wilkinson P, Kovats RS, Pattenden S, Hajat S, Armstrong B, et al. International study of temperature, heat and urban mortality: the "ISOTHURM" project. International Journal of Epidemiology 2008;37:1121–31.
7. Anderson M, Carmichael C, Murray V, Dengel A, Swainson M. Defining indoor heat thresholds for health in the UK. Perspectives in Public Health 2012:1–7.
8. DCLG. Investigation into overheating in homes, Literature review. London, UK: 2012.
9. Oikonomou E, Davies M, Mavrogianni A, Biddulph P, Wilkinson P, Kolokotroni M. Modelling the relative importance of the urban heat island and the thermal quality of dwellings for overheating in London. Building and Environment 2012;57:223–38.
10. Mavrogianni A, Wilkinson P, Davies M, Biddulph P, Oikonomou E. Building characteristics as determinants of propensity to high indoor summer temperatures in London dwellings. Building and Environment 2012;55:117–30.
11. DCLG. English housing survey (EHS) 2010-11. London, UK: 2013.
12. US DoE EERE. EnergyPlus energy simulation software v. 3.1.0 and v. 8.0.0 2013.
13. CIBSE. Current CIBSE TRY/DSY hourly weather data set. London, UK: 2013.
14. CIBSE. Guide A: Environmental design. London, UK: 2006.
15. Stephen R. BRE IP 1/00, Airtightness in UK dwellings. Watford, UK: 2012.
16. Shrubsole C, Ridley I, Biddulph P, Milner J, Vardoulakis S, Ucci M, et al. Indoor PM2.5 exposure in London's domestic stock: Modelling current and future exposures following energy efficient refurbishment. Atmospheric Environment 2012;62:336–43.
17. Thornburg J, Ensor DS, Rodes CE, Lawless PA, Sparks LE, Mosley RB. Penetration of Particles into Buildings and Associated Physical Factors. Part I: Model Development and Computer Simulations. Aerosol Science and Technology 2001;34:284-296.

STUDY ON INDOOR THERMAL COMFORT IN THE RESIDENTIAL BUILDINGS OF LIEGE, BELGIUM

Manoj Kumar Singh[a], Sadhan Mahapatra[b], Jacques Teller[a]

[a] *Faculté des Sciences Appliquées, Department ArGEnCo, Local Environment Management and Analysis(LEMA), Université de Liège, Chemin des Chevreuils, 1 - 4000 Liège, Belgium*
E-mail: mksinghtu@gmail.com

[b] *Department of Energy, Tezpur University, Tezpur 784028, Assam, India*

ABSTRACT

A detailed study on the building stock of Liege urban area (Belgium) has been conducted during 2011-2012. The study is focused on historic buildings, which were constructed before 1945 and represents a very significant share (68.33%) of Liege building stock. In the Walloon region, the average heating energy consumption per year of the building stock is 408 kWh/m^2 and the average heating energy consumption per year stands at 340 kWh/m^2 for Liege. Hence, it is important to study existing buildings to improve the energy efficiency as well as thermal comfort standards. It is also important to understand the behaviour of these buildings and the preferred indoor thermal environment of the occupants. Keeping this in mind, the indoor thermal environment has been monitored for ten residential buildings followed by detailed interaction with the occupants to record their preference and expectations about indoor thermal comfort. It was found from the analysis that the fluctuations in the temperature of living room and bedroom with respect to outdoor conditions are a function of occupant's age, type of heating system and fuel used. It is also found that the average energy expenditure was very high in these buildings. The study further identifies specific areas that need to be taken into consideration in order to improve the thermal comfort and energy efficiency. It put forth the argument that to improve the energy efficiency of occupied houses, occupant's preference and expectations on thermal comfort needs to be considered for designing sustainable solutions towards improving energy efficiency.

Keywords: Building stock, Energy efficiency, Energy Performance Building Directive, Liege

INTRODUCTION

Thermal performance of built environment and preferred indoor environment by the occupants play a critical role in the energy consumption of buildings [1,2]. Indoor thermal environment is a function of occupant's thermal preference and expectations. These are governed by the sensitivity of the occupant to the existing indoor climate [1-4]. This factor also determines the extent and level of control occupants want to keep on built environment to feel comfortable. A high sensitivity of occupants towards indoor thermal environment usually means less adaptation and high energy consumption [1]. The availability and accessibility to energy is directly linked to indoor thermal comfort [1]. Green house gas emission due to heating of buildings is the second largest contributor and responsible for 21.8% of total emissions in Belgium [5-7].The energy consumption and subsequent CO_2 emissions increased substantially with the growth of the building sector [8, 9]. The research reported in this article is based on the assumption that indoor thermal environment of historical houses does not meet the thermal comfort standards and energy efficiency levels. Hence, it is a priority to address the issue of energy efficiency and thermal comfort in these historical houses. In this study, it has been tried to explore the relationship between persisting indoor environment conditions, indoor thermal comfort, occupant's expectation and house characteristics. It is argued that

comfort and adaptation are complementary to each other and one cannot ignore adaptive approach strategies in comfort studies and retrofitting strategies.

Liege city is in Walloon region of Belgium and also know as economic capital of the region. In Liege, 68.33% of buildings are constructed before 1945 [9]. Buildings constructed before 1945 falls into five different typologies, namely Maison Modeste (Modest house), Maison Moyenne (Average house), Maison De Maitre (House), Maison Historique (Historic house) and Maison apartments (Apartment house). These typologies have distinct height and width, window features and built-up area. *General Socio-economic survey 2001* and *Housing quality survey 2006* studies revels the characteristics of historical buildings of Liege. Most importantly 80.5% of buildings do not have insulated walls and 50% have no roof insulation. It is also observed that windows of 60% of buildings are fully insulated with double glazing, 18% have partially insulated glazing and 22% does not have any insulated glazing. This is reflected in the heating energy consumption per year as it varies from 383 kWh/m^2 (for building constructed before 1863) to 127 kWh/m^2 (building constructed between 2001-2012) [9].

METHODOLOGY

Historical residential buildings were constructed with materials and technology when building energy efficiency was not a major issue. Hence, it is important to look into these buildings to improve the energy efficiency as well as their thermal comfort standards. Previous studies on Liege building stock provide the initial understanding to design and carry out this work. In this study indoor thermal conditions of ten residential buildings of Liege, all built before 1945, have been monitored. This monitoring has been combined with a detailed interview of occupants to record their preference and expectations about indoor thermal environment (closed questionnaire). Monitoring of indoor conditions in these ten buildings was carried out during the winter season (November 2011 to February 2012), when the heating system was on in most houses. This monitoring includes the measurements of temperature (inside and outside house), relative humidity (inside and outside house) and illumination level (inside and outside house). The selected houses for this study were kept under normal operation throughout the monitoring period. HOBO-U12 data loggers were installed in the living room, bedroom of these selected houses. The comfort survey questionnaire designed in such a way that it addresses the objective of the study as well as provides enough specific and subjective information for analysis.

DETAILS OF MONITORED HOUSES

Table 1 provides the type, construction period and main characteristics of the ten houses monitored during this study. It can be observed from this table that most houses are over 100 years old. All the houses are terraced (exposed to air from two sides). It is also observed from Table 1 that most houses have relatively old heating system and use natural gas as fuel. The absence of wall insulation and the low performances of the heating system are responsible for high heating energy consumption in these houses. Table 2 presents the reasons of occupant's discomfort in these houses. The preferred adaptive action to regulate indoor temperature in winter is presented in Table 3. Table 4 presents the indoor and outdoor temperatures profile and comfort status in the monitored houses. It can be observed from Table 4 that the living room temperature is always higher than the one in the bedroom and the difference between these temperatures can be quite high. It is found from the recorded temperature data that the decay in the temperature of living room is rapid compared to bedroom in all these houses. In case of house number 4 we observe that living room temperature is lower than bedroom because during the monitoring period renovation work was being carried out in the living room. So frequent opening of doors and windows lead high infiltration of air and low

temperature in living room. This implies that the living room is losing more heat in winter months. Hence, it can be concluded that the living room must be given due consideration during the renovation. Table 4 also represents outdoor mean temperature with occupant's detail and comfort status in these houses. It is observed from Table 4 that the occupant of house number 2 and 5 are comfortable with the house indoor thermal environment. It is found that the temperatures in both these houses are well maintained though the effect of low outdoor temperature in the month of February on indoor temperature is visible. This phenomenon was common in all monitored houses. It can also be concluded that in these houses radiant temperature asymmetry is quite prominent due to the presence of non insulated walls and large glazing areas [10]. This conclusion is supported by the high indoor clothing level of occupants and temperature corresponding to thermal sensation vote. It can be concluded from Table 2, 3 and 4 that the heating systems in the houses are not working effectively. This problem is related to the presence of non insulated walls and large glazed area on front and rear facades of the houses. It can also be concluded that the glazing is an important cause of discomfort in winter (cold sensation) [10].

Table 1 Monitored houses detail

House number	Typology and year of construction	House arrangement	Insulation (wall and roof)	Fuel used and age of heating system (years)	Ownership of house and category of income
1	Maison De Maitre (1919-1945)	Terraced	No, No	Fuel oil (Mazout), >15	Owner, Average
2	Maison De Maitre (1875-1918)	Terraced	Yes, Yes	Natural gas, <15	Owner, High
3	Maison De Maitre (1875-1918)	Terraced	No, Yes	Natural gas, >15	Owner, Average
4	Maison Modeste (1875-1918)	Terraced	Yes, Yes	Natural gas, <5	Owner, Average
5	Maison Moyenne (1875-1918)	Terraced	No, Yes	Fuel oil (Mazout), >15	Owner, High
6	Maison Moyenne (1875-1918)	Terraced	No, Yes	Natural gas, <5	Rent, Average
7	Apartments (1919-1945)	Terraced	No, No	Natural gas, <15	Rent, Low
8	Maison Modeste (1875-1918)	Terraced	No, Yes	Natural gas, >15	Owner, Average
9	Maison Moyenne (1875-1918)	Terraced	No, Yes	Natural gas, <10	Owner, Average
10	Maison Moyenne (1875-1918)	Terraced	Yes, Yes	Natural gas, <5	Owner, Average
Category of income (Euros/year): 20,000 ≤ low; 20,001< average ≤ 30000; High > 30,001					

Table 2 Occupants response towards discomfort in the house

Reason of discomfort	Low lighting level	Low temp in winter	High temp in summer	Sudden temp fluctuation	Difficulty in regulating temp in the house	Cold sensation from glazing	High air infiltration	Sudden cooling of living/ bedroom
Votes	2	5	1	----	4	7	1	1

Table 3 Preferred adjustments to regulate indoor environment in winter

Reason of discomfort	Closing window	Opening window	Switching on room heaters	Switching off room heaters	Moving window curtains	Switching on lights	Switching off light	Use of portable room heater
Votes	6	1	9	2	6	1	1	5

Table 4 Temperature profile and comfort status in monitored houses

House number	Mean indoor temperature (^{0}C)		Mean outdoor temperature (^{0}C)	Clo	Temperature corresponding to TSV (^{0}C)	Overall comfort*	Thermal sensation vote (TSV)	Met (20 min before voting)
	Bed	Living						
1	16.76	17.23	4.87	0.86	12.5	b	-2	2.4
2	18.56	22.00	3.03	1.11	21.8	a	2	1.6
3	11.17	13.16	3.82	1.1	13.4	b	-1	2.4
4	14.19	13.92	3.92	1.01	12.8	b	-1	1.2
5	14.34	18.16	5.74	1.01	15.4	a	0	2.4
6	17.16	19.06	5.46	0.31	19.6	b	1	2.4
7	14.37	15.96	6.08	0.56	13.2	b	-2	1.6
8	13.90	20.57	4.94	1.04	16.9	e	2	1.6
9	15.06	19.39	4.96	1.19	18.4	b	0	1.6
10	17.70	17.77	6.51	1.19	17.6	b	0	1.6

**Overall Comfort rating of house by occupant: Very comfortable (a); Moderately comfortable (b); Slightly comfortable (c); Slightly uncomfortable (d); Moderately uncomfortable (e); Very Uncomfortable (f)*

ANALYSIS

Indoor thermal conditions of ten residential buildings of Liege have been monitored. For space reasons, the results of only two houses (house number 8 and 9) are presented in this paper. The layout and temperature profile of house 8 during monitoring period is presented in Figure 1A and 1B. The front and rear façades of this house are exposed to ambient without any shading. The house is oriented in North-East and South-West direction (front façade facing North-East). Windows of this house has got mixed glazing fitted with internal and external movable blinds. This house has manually controlled local heating system (convectors). The orientation of house is such that the front façade never receives sunlight throughout the year. The maximum temperatures of living room and bedroom reached 29.5^{0}C and 26.5^{0}C respectively during the monitoring period. These temperatures are quite high for comfortable indoor environment with typical winter clothing (*clo*) value. It is observed that the minimum temperatures of living room and bedroom are fluctuating less than maximum temperatures. For a particular outdoor temperature fluctuation, there is a corresponding fluctuation in living room and bedroom temperature of less magnitude with a time lag. This time lag smoothen the effect of sudden outdoor temperature fluctuation and this is due to the thermal inertia of the building. The average temperature of living room and bedroom had shown a swing of 18.5-24^{0}C and 9-18.5^{0}C respectively. This temperature variation is too large, especially in the bedroom. This is due to poor temperature control and distribution. Occupants have reported that the indoor lighting level is low and uncomfortable. The energy consumption in this house is reasonably high and stands at 22000 kWh (4000 kWh electricity and 18000 kWh equivalents for natural gas) in the year 2011.

Figure 2A and 2B represents the layout and temperature profile of house 9. This house is oriented in North-East and South-West direction (front façade facing North-East). Windows of this house have mixed glazing (single and double) fitted with internal and external movable blinds. The house went through major renovation in the form of (i) changed glazing, (ii) added insulation to roof, (iii) installed/changed room heaters and (iv) installation of new boilers. The occupants reported discomfort in the house due to difficulty in regulating indoor temperature (they also use portable heaters) and cold sensation from the window. The use of portable heaters suggests that there is a non uniform temperature distribution in the living space. The daily average temperatures for various rooms and outdoor temperature for the monitoring period is presented in Table 4. It is observed from figure 2B that the daily average temperature of living room and bedroom are maintained at different levels (temperature difference

between living room and bedroom is almost constant) throughout the monitoring period. The daily average temperature profile of this house suggests that swing of temperature in living room and bedroom is maintained well within 1-1.5^{0}C. It may be noted that minimum temperature is important to study because it not only defines the comfort but also effects on the heating energy consumption. The lighting level is below the acceptable level both in the bed room and living room. The energy consumption for the year 2011 is 19299 kWh (2474 kWh electricity and 16825 kWh equivalents to natural gas).

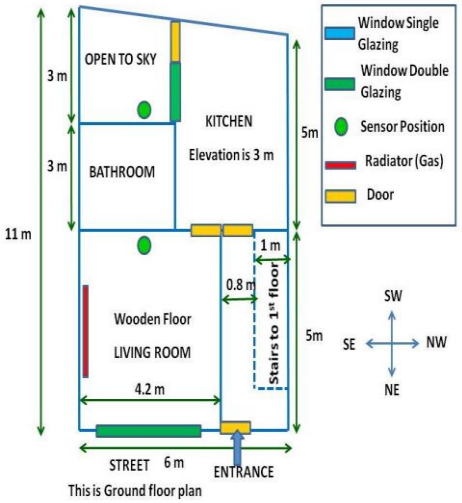

Figure 1A Layout of house number 8

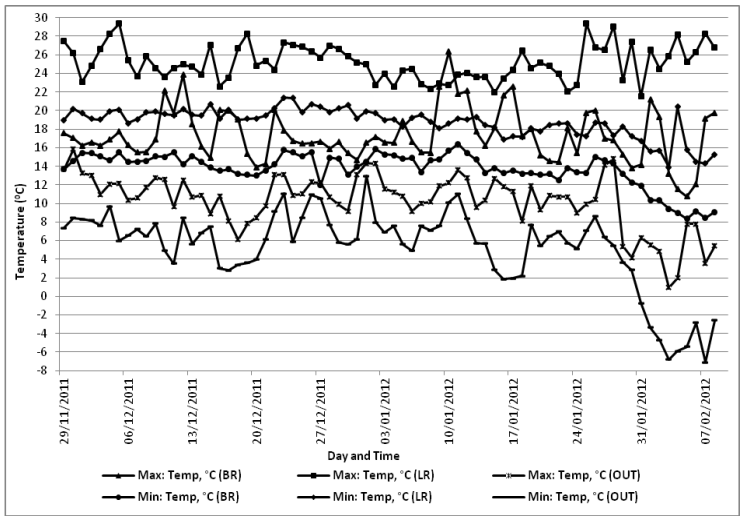

Figure 1B Indoor temperature profile of house 8 with manual control

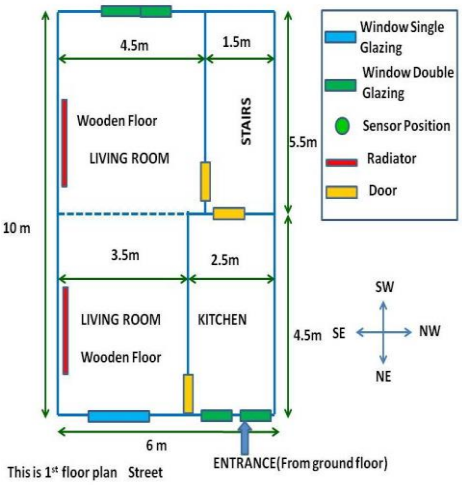

Figure 2A Layout of house number 9

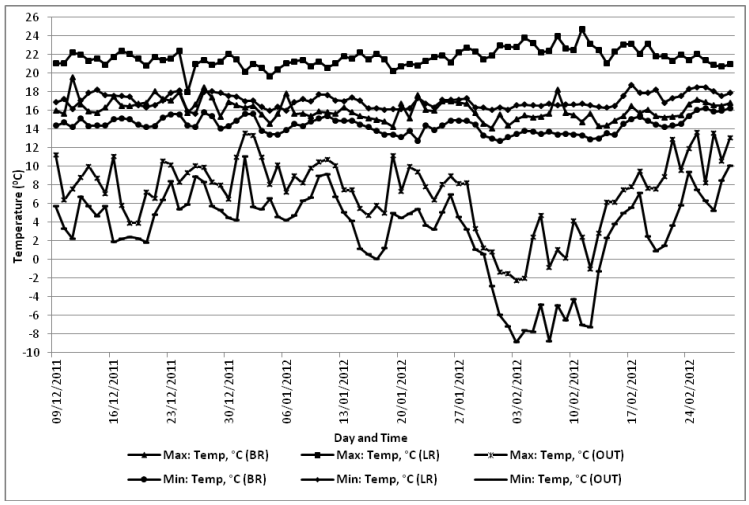

Figure 2B Indoor temperature profile of house 9 with automatic control

CONCLUSION

The building structure is a continuous evolving process to address the thermal comfort of the occupants at the changing micro-climate of a region. The houses considered for the detailed analysis shows that the house composition and occupant's behaviour inside the house greatly affects the functioning and indoor environments. It is found from the study that occupant's adaptation on indoor thermal environment regulates the functioning of the house and consequently the energy consumption and over all energy efficiency of the house. It is found that though the selected houses have similar built-up area, insulation, similar glazing but there

is an important difference in energy consumptions. The reason behind this can be attributed to the building structure and especially its insulation, the heating system, but also the family composition and occupant's expectation of thermal environment. The study further stress that occupants somehow compensate the difficulty to maintain constant and comfortable thermal conditions throughout the house and all over the time, by adjusting temperatures differently in different rooms of the houses at different time of the day. Such a strategy, quite usual in most houses, may be more significant in historic houses like the ones studied in the present research. Thermal as well as energy performance study of any building provides a deep understanding on the complex functioning of building and its possible effects on the environment. Hence, it is necessary to apply an integrated approach by considering the above parameters to achieve the sustainable building design.

ACKNOWLEDGEMENTS

The first author gratefully acknowledges the financial support received in the form of postdoctoral research grant from University of Liege to carry out the work.

REFERENCES

[1] Singh MK., Mahapatra S., Atreya SK., Givoni B. Thermal monitoring and indoor temperature modeling in vernacular buildings of North-East India, Energy and Buildings 2010; 42(10): 1610 -1618

[2] de Meester T., Marique AF., De Herde A., Reiter S. Impact of occupants behaviours on residential heating consumption for detached houses in a temperate climate in the northern part of Europe, Energy and Buildings 2013 (57), 313-323

[3] Reiter S., Marique AF. Towards low energy cities: A case study of the urban area of Liege, Journal of International Ecology 2012; 16(6), 829-838

[4] Energy Annual Statistics 2010: 2011 Edition, Eurostat Statistical Books, Office for Official Publications of the European Communities, Luxembourg, 2011

[5] Salat S. Energy loads, CO2 emissions and building stocks: Morphologies, typologies, energy systems and behaviour, Building Research and Information 2009; 37(5-6), 598-609

[6] Bradley PE., Kohler N. Methodology for the survival analysis of urban building stocks, Building Research and Information 2007; 35 (5), 529-542.

[7] Carvalho M. da G. EU energy and climate change strategy, Energy 2012; 40 (1), 19-22.

[8] Anisimova N. The capability to reduce primary energy demand in EU housing, Energy and Buildings 2011; 43(10), 2747 - 2751

[9] Dujardin S., Marique AF., Teller J., et al. Spatial planning as a driver of change in mobility and residential energy consumption, Energy Buildings (2013), doi.org/10.1016/j.enbuild.2012.10.059

[10] Huizenga C., Zhang H., Mattelaer P., Yu T., Arens EA., Lyons,P. Window performance for human thermal comfort, CBE, University of Californis, Berkeley, 2006.

INTEGRATED INDOOR ENVIRONMENTAL QUALITY ASSESSMENT FOR OCCUPANT COMFORT AND PRODUCTIVITY: FROM DATA ACQUISITION TO VISUALIZATION

Tsung-Hsien Wang [1]; Jihyun Park [2]; Andrew Witt [3]

1: School of Architecture, University of Sheffield, Western Bank Sheffield S10 2TN, UK

2: School of Architecture, Carnegie Mellon University, Pittsburgh, PA 15213, USA

3: Research and Development Team, Gehry Technologies, Los Angeles, CA 90066, USA

ABSTRACT

Indoor environmental quality (IEQ) of buildings can have a strong influence on occupants' productivity and health. Post occupancy evaluation (POE) and associated processes are often the first step in assessing IEQ, which includes visual quality, thermal quality, air quality, acoustic quality, etc. In general, these field measurements are time-consuming and labour-intensive. To present measured results, one efficacious approach is to overlay field data with building floor plans or building system drawings. This approach enables the visualisation of the built environment performance in a more apprehensible fashion.

The current practice of mapping measured data with existing building components is manual, and there is a lack of flexibility of accommodating time-series building performance measurements. In this paper, we propose an integrated process to support IEQ assessments in an automated fashion, which enables field data synchronization and mapping for integrated building performance visualisation.

For demonstration, we conducted a lighting quality measurement on two selected subjects, one unoccupied (core and shell) LEED gold certified building and an occupied office building in Los Angeles, California, USA. The outcomes are presented to show how measured performance data can be updated with the associated building elements for integrated visualisation. Advantages and limitations of this approach for improving the workflow of IEQ are also discussed.

Keywords: Indoor environmental quality; post occupancy evaluation; visual quality assessment; data acquisition and visualization

INTRODUCTION

Post occupancy evaluation (POE) is one of the most important approaches to reducing energy consumption and enhancing indoor environmental quality (IEQ). One notable advantage is that POE helps identify building performance gaps and potential improvements based on the existing built environment context [2, 6].

POE processes include (1) collecting IEQ indices of thermal, air, visual, and acoustic conditions, (2) comparing measured IEQ data with recommendation levels such as ASHRAE standards [1] and the IESNA handbook [2] and (3) providing environmental quality report (EQR) with comprehensive analyses for IEQ, occupant comfort, and ongoing energy savings [4]. These processes also generate critical indicators to improve energy consumption and user satisfaction by fine-tuning existing building systems. However, the processes of conducting POE from building performance data acquisition to post-evaluation data visualization are usually very labour intensive [5].

The tools used in POE include plan analysis, monitoring of IEQ conditions, observations and user-satisfaction surveys. The main purpose of these tools is to help understand interrelations among building IEQ conditions, occupants and the operational building systems [5]. During the evaluation processes, IEQ data collected from numerous devices are, in most cases, presented in distinctive format. The non-unified data representation imposes a lot of efforts for the post-evaluation analyses.

To improve the workflow from POE data acquisition to post-evaluation analyses, we propose an integrated IEQ assessment approach, in which time-series data is updated automatically via a cloud-based platform. This approach affords seamless data aggregation and automates the data integration with associated building geometry.

Given an integrated workflow, POE data can be managed and synchronized in real time. This proposed workflow aims to improve the current POE processes, and in turn provides more immediate post-evaluation visualization. Figure 1 illustrates the integrated workflow consisting of (1) data acquisition, (2) data processing and mapping, (3) visualization. Data acquisition includes acquiring technical attributes of building systems, climate information, and measured IEQ data. Data processing and mapping automate the integration of measured field data with corresponding building geometry. Visualization generates various forms of graphical output.

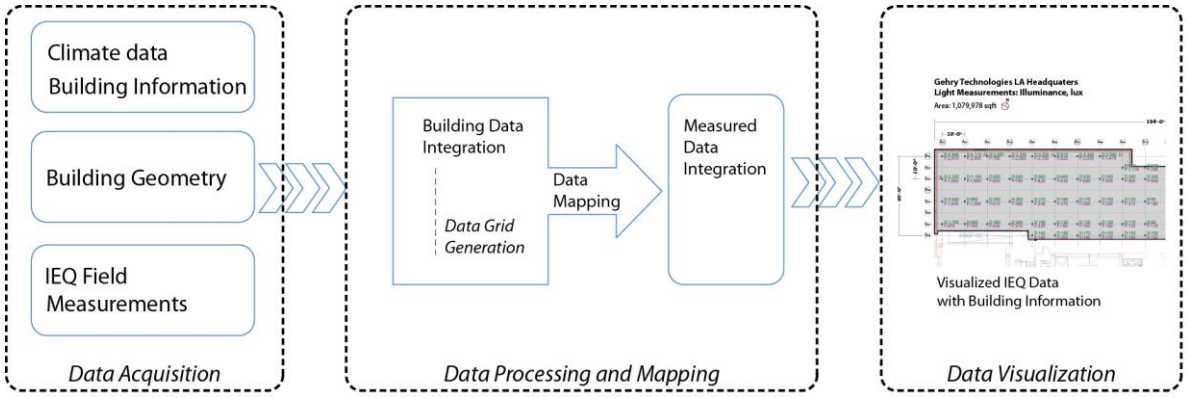

Figure 1 Structure of data acquisition and visualization for IEQ assessment

INTEGRATED IEQ ASSESSMENT WORKFLOW

Data Acquisition

We use visual quality analyses as the pilot study to demonstrate the integrated IEQ assessment workflow. A lighting quality study was conducted in an unoccupied office (core and shell), in Los Angeles, California, USA (Figure 2). The purpose of using an un-occupied space is to take POE in advance to ensure future indoor environmental quality. One potential application could be for improving performance simulation with real environmental data.

At the basic level, spot measurements are taken via a regular grid system to cover entire surface. Typically the spacing between measurement points is set to one-fourth the spacing between luminaires. The height of these points depends on where the primary task is performed. For instance in most office spaces, the task is found at the desk level and thus points will be measured at 0.76 meters (2.5') above the floor. For some spaces where the primary task is walking, the measurements might be taken at floor level [1].

Figure 2: Unoccupied office building for measurement. (Left) Exterior appearance; (Right) Interior space

For our visual quality field measurement, OMEGA HHLM-2 digital light meter was utilized for illuminance level. To investigate possible glare issues of the space, HDR (High Dynamic Range) photography was utilized to evaluate the luminance level. iPAD tablet is used for data recording. Collected field data are then streamlined to the cloud-based platform using prescribed data format. Total 372 points were measured at both desk and floor levels in the morning (10:30 am- 12:00 pm) and afternoon (3:30 pm -5:00 pm). Figure 3 shows three luminance fisheye images captured at the same location in the space.

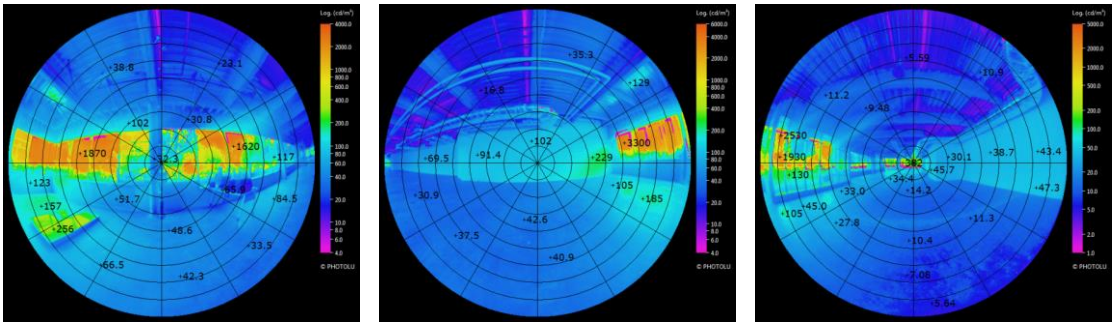

Figure 3 Luminance fish eye images

Data Retrieval and Mapping

In this section, we first describe how data are streamlined via a cloud-based environment, followed by the computational processes that enable post-evaluation data analyses. For the demonstration purpose, we utilize multiple platforms for data synchronization, mapping and analyses. The objective is to demonstrate the feasibility of cross-platform interoperation via cloud. For the data manipulation, we use DropBox [8], which provides hosting services for easy file storage and management. For instance, data stored in the cloud can be accessed via a uniform resource locator (URL—served as a distinct web address for information retrieval). With these URLs, a computational procedure was implemented with customized components using Grasshopper in Rhinoceros 3D [9, 10]. Figure 4 illustrates the snippet of the proposed generative process. In this process, we reconstruct the parametric relationships linking measured field data with associated building geometric elements. The structured parametric relationships allow us to explore various types of analyses and generate graphical outputs in real time. The generative workflow follows a left-to-right fashion.

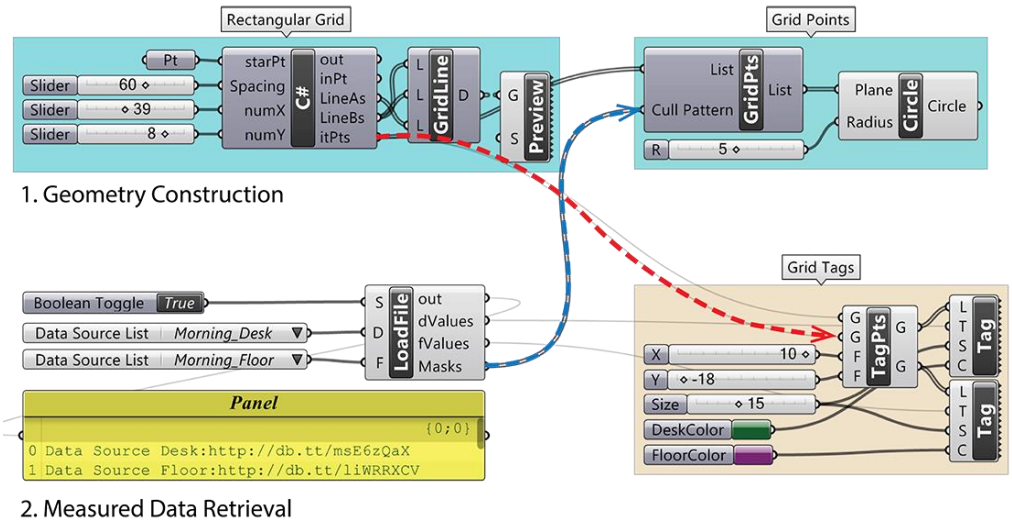

Figure 4 The computational workflow of mapping measured data with associated geometric components in Grasshopper, Rhinoceros 3D

Data Visualisation

In this section, we demonstrated the potential of the proposed integrated IEQ assessment approach for graphical data visualisation. Figure 5 illustrates measured illuminance data superimposed on the building floor plan. With the access to the files stored in cloud, a series of integrated floor plans with associated illuminance levels can be generated automatically. To better represent these numeric data in a more comprehensible manner, we also employ a carpet plot style to colour floor areas in relation to the their illuminance levels respectively, as shown in Figure 6 and Figure 7.

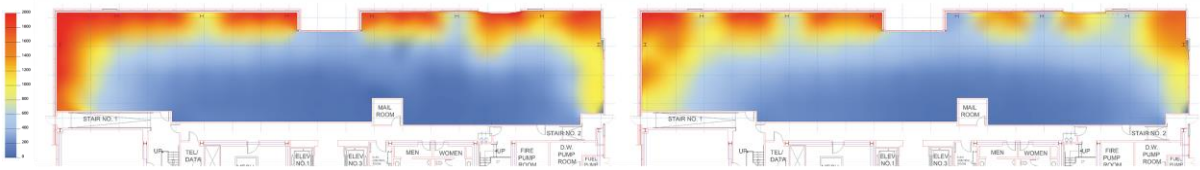

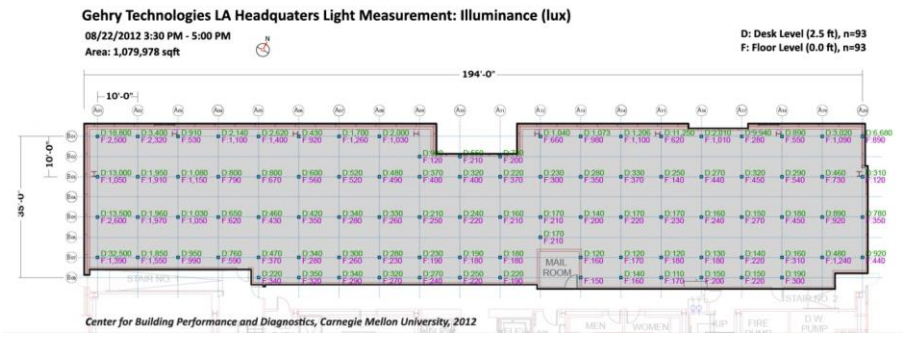

Figure 5 Illuminace measurement data application

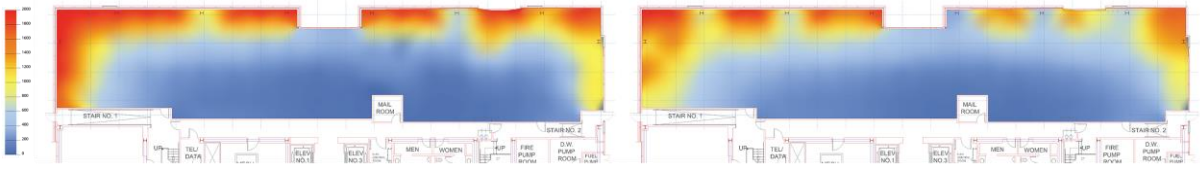

Figure 6 Illuminance desk level (left) and floor level(right), morning (10:30 am - 12:00 pm)

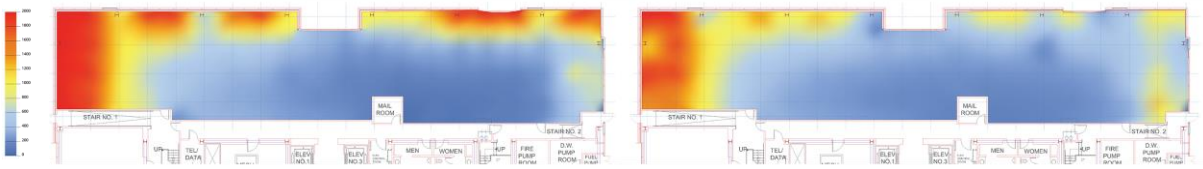

Figure 7 Illuminance desk level (left) and floor level(right), afternoon (3:30 pm - 5:00 pm)

In addition, measured illuminance levels of this study were also provided to the simulation team to re-calibrate the lighting model using LBNL's Radiance simulation tool [7]For this collaboration, cloud plays the same role in agile data storage and synchronization, which allows fluid cross-platform integration. For the practical reason in this paper, we focus on the integrated workflow from data acquisition to post-evaluation visualisation. The graphical output from measured illuminance levels provides critical visual cues for instant building operational improvements within the existing built environment context; for instance, lighting quality of areas with 16,000 lux or more along the perimeter can be hugely improved by implementing blinds or light redirection devices to reduce excessive glare while maintaining optimal views. These areas can be easily identified by those shaded in red in above

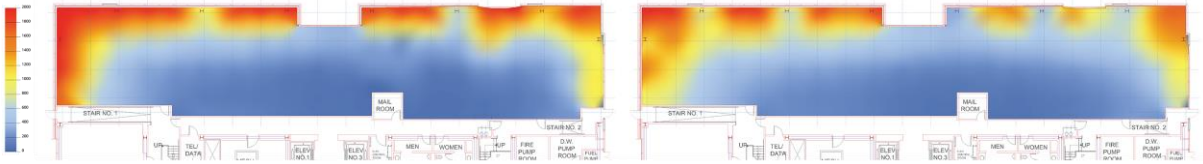

Figure 6 and

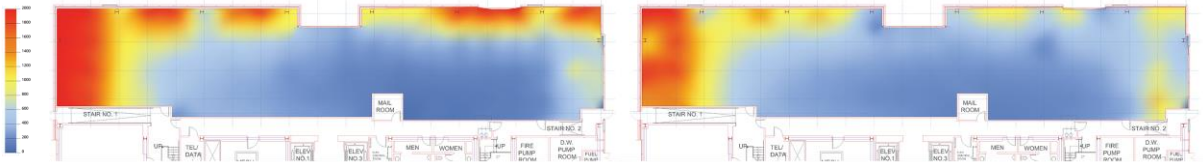

Figure 7.

CONCLUSION AND DISCUSSION

IEQ measurements provide invaluable insights into both physical and operational attributes of building systems, which contribute to overall energy use in the built environment. These measurements also help to quantify the impacts on user satisfaction in relation to indoor visual quality, air quality, thermal quality, acoustic quality, spatial quality, and building integrity. The combined analytical data delineate a holistic view of how a building actually performs.

In this paper, we propose an integrated IEQ assessment approach to better support data acquisition, management and analyses. The proposed approach utilizes cloud as a platform for data storage and synchronization. This enables a seamless workflow for POE researchers to automate data collection. Meanwhile, with an easy access to cloud services, a computational procedure was also presented. The implemented prototype demonstrated how cloud data could be retrieved and re-constructed parametrically for quick visual representation, which allows designers, IEQ investigators, building owners, and facility managers to identify potential problems in the built environments. This proposed workflow is expected to support POE processes in a more efficient and effective manner.

For the future work, the implication of data captured on the field can play an important role in fine-tuning building performance simulation. One potentially interesting application is to investigate how this workflow can assist, for instance, lighting simulation with the real-time environ-

mental inputs for instant lighting analyses. Similarly, the real-time environmental feedbacks can also be utilized to improve the operational controls to achieve better lighting performance.

ACKNOWLEDGEMENT

This material is based upon work supported by the Energy Efficient Buildings (EEB) Hub, an energy innovation hub sponsored by the Department of Energy under Award Number DE-EE0004261.

REFERENCES

1. ASHRAE. (2010). *Performance Measurement Protocols for Commercial Buildings*: American Society of Heating, Refrigerating and Air Conditioning Engineers
2. IESNA (2011) Lighting Handbook 10th edition: Illuminating Engineering Society of North America
3. Loftness, V., Aziz, A., Choi, J., Kampschroer, K., Powell, K., Atkinson, M., & Heerwagen, J. (2009). The value of post-occupancy evaluation for building occupants and facility managers. *Intelligent Buildings International, 1*(4), 249-268. doi: 10.3763/inbi.2009.SI04
4. Loftness, V., Aziz, A., Park, J., & Cochran, E. (2011). *Case Study for the David L. Lawrence Convention Center: Post Occupancy Evaluation* (Builidng in Operatoin study ed.). : Green Building Alliance.
5. Meir, I. A., Garb, Y., Jiao, D., & Cicelsky, A. (2009). Post-occupancy evaluation: an inevitable step toward sustainability. *Advances in building energy research, 3*(1), 189-219.
6. Preiser, W. F. E., & Vischer, J. C. (2005). *Assessing Building Performance*. Routledge
7. The RADIANCE lighting simulation and rendering system, http://radsite.lbl.gov/radiance/ [Last accessed on April 30, 2013]
8. Dropbox, A hosting services for cloud storage and synchronization, http://www.dropbox.com/ [Last accessed on April 30, 2013.
9. Rhinoceros 3D, 3D modeling tools for designers, http://www.rhino3d.com/ [Last accessed on April 30, 2013.
10. Grasshopper, A visual programming environment for design exploration in Rhinoceros 3D, http://www.grasshopper3d.com/ [Last accessed on April 30, 2013].

Advanced Building Control Systems

SHORT-TERM THERMAL AND ELECTRIC LOAD FORECASTING IN BUILDINGS

S.F. Fux; M.J. Benz; A. Ashouri; L. Guzzella

Institute for Dynamic Systems and Control, ETH Zürich, Sonneggstrasse 3, 8092 Zürich

ABSTRACT

Increasing environmental awareness and energy costs encourage the increase of the contribution of renewable energy sources (RES) to the energy supply of buildings. However, the integration of RES and energy storage systems introduces significant challenges for the energy management system (EMS) of complex building energy systems. An energy management strategy based on fixed control rules may fail to efficiently operate such systems. These circumstances raise the need to apply advanced control strategies. A promising approach is model predictive control (MPC), which allows the consideration of the expected dynamic system behavior as well as of forecasts of the loads and of the renewable energy generated. Obviously, the performance of an MPC-based EMS crucially depends on the accuracy of the load forecasts.

The goal of this paper is to compare the capabilities of neural networks (NNs) and of the least squares support vector machine (LS-SVM) in forecasting the hourly thermal and electric load of buildings. Two short-term load forecasting algorithms are evaluated which treat every hour of the day separately by an individual forecasting model. Additionally, the algorithms also distinguish between working days, weekends and holidays. In order to adapt to changing load patterns, the algorithms use the sliding window training approach. Both algorithms are tested using the measured thermal and electric load data of a large office building and of a small building which houses a kindergarten.

In the tests conducted, in general, the forecasting algorithm based on the LS-SVM shows a better performance than the forecasting algorithm based on NNs. In addition, the LS-SVM involves fewer free parameters to be determined than a NN, which makes the former easier to apply.

The results reported further indicate that the accurate forecasting of the load of a small building is the more challenging task compared to the load forecasting of a large office building. Furthermore, using a training window size of more than 20 days does not significantly improve the performance of the algorithms examined.

Keywords: short-term load forecasting, neural networks, least squares support vector machine

INTRODUCTION

Due to sustainability concerns, fossil energy sources in the energy supply of buildings are increasingly being substituted by renewable energy sources (RES). However, if RES and energy storage devices are added to conventional building energy systems, the complexity of the complete system increases considerably. An energy management strategy based on fixed control rules may fail to efficiently operate such a complex energy system [1]. These circumstances raise the need to introduce advanced control strategies. A promising approach is model predictive control (MPC), which is based on solving at each sampling interval a constrained optimal control problem for the current state of the system. Thus, MPC allows the consideration of the expected dynamic system behavior as well as of forecasts of the loads

and of the renewable energy generated. Obviously, accurate load forecasts are essential for the successful performance of an MPC-based energy management system (EMS).

Typically, an MPC-based EMS requires load forecasts with a prediction horizon of up to a few days, which in the literature is often referred to as short-term load forecasting (STLF). Especially for the forecasting of the electric load of large territories, various approaches have been proposed for that purpose [2]. In general, these approaches are divided into two categories [3]. Classical approaches include methods such as time series models, regression models and techniques based on Kalman filtering. Newer approaches apply methods from the research field of artificial and computational intelligence such as artificial neural networks, fuzzy inference and fuzzy-neural models, expert systems, and support vector machines (SVMs). Although there is a large volume of literature on this topic, almost no applications of STLF to the thermal and electric loads of buildings have been reported [4]. Forrester and Wepfer [5], for instance, proposed a method based on multiple linear regression to provide forecasts of the energy demand of a large, commercial building. Dhar et al. [6] applied a Fourier series model to predict the hourly heating and cooling energy use in commercial buildings. Several researchers studied neural networks (NNs) to develop a building STLF algorithm [7, 8, 9]. Hou and Lian [10] studied in their work the feasibility and applicability of the SVM for the specific case of building load forecasting. In [4], the performances of an autoregressive model, an autoregressive integrated moving average (ARIMA) model, a NN and a Bayesian model for the forecasting of the electric load of an air-conditioned non-residential building are examined.

In this paper, two building STLF algorithms providing hourly load forecasts are presented and evaluated. The first algorithm is based on NNs and the second one uses least squares SVM (LS-SVM) regression models. The performances of the two building STLF algorithms are tested using the measured thermal and electric load data of a large office building and of a small building which houses a kindergarten.

INTRODUCTION TO NEURAL NETWORKS AND LEAST SQUARES SUPPORT VECTOR MACHINE

This section provides a brief introduction to NNs and the LS-SVM.

Neural Networks

NNs have received much attention in the field of STLF [11]. They mimic the behavior of the human brain in order to provide an approximation of the nonlinear relationship between input and output variables [8]. The basic unit of a NN is the artificial neuron, which receives information through a number of input nodes, processes it internally, and outputs a response [11]. Typically, the neurons in a NN are organized in layers. For more information about NNs, the interested reader is referred to, e.g., [12].

Least Squares Support Vector Machine

LS-SVM, as proposed by Suykens and Vandewalle [13], is an algorithm based on the standard SVM method developed by Vapnik [14] for classification and regression. The basic idea of the standard SVM method applied for regression is to map the original input vectors into a feature space with higher dimensionality using a nonlinear mapping function, and then to perform a linear regression in the feature space [14]. Instead of using inequality constraints as in SVM regression, the LS-SVM uses equality constraints and a least squares error term to determine the weight vector and the bias of the regression model. Therefore, training the LS-SVM regression model is equivalent to solving a set of linear equations instead of solving a quadratic programming problem as in SVM regression [13].

BUILDING STLF ALGORITHMS PROPOSED

In this work, the load forecasting problem is regarded as being equivalent to describing the relationship between the load and the factors most likely to influence it. Since the electric and thermal loads of a building strongly depend on the activity in the building, it is proposed to distinguish between working days, weekends and holidays, and therefore, to treat each day type individually. This approach avoids much of the non-linearity of the forecasting process [4]. Furthermore, on days of the same day type, building loads typically exhibit a similar daily pattern. Hence, the building STLF algorithms evaluated in this work treat each hour of the day separately by an individual forecasting model, so that a total amount of 24 different models have to be trained for each day type. The variables chosen as input variables of the individual hour-by-hour models are the ambient air temperature and the vertical solar radiation on the south-east and south-west oriented facades of the building in the corresponding hour. A variety of methods exists to describe the relationship between these input variables selected and the load. In this work, the NN model and the LS-SVM model are tested for that purpose. In order to adapt to changing load patterns, the models are trained with the sliding window approach, i.e., as soon as new measurement data is available it is added to the training data set and the oldest data is removed. In doing so, the size of the training data set is kept constant [8].

EXPERIMENTAL RESULTS

To test the building STLF algorithms proposed, the electric and thermal (including domestic hot water) load data of two different buildings are used. These buildings are located next to each other on the Science City Hönggerberg campus of the ETH Zürich. The first building is a large office building built in 2008. It is equipped with a heating, ventilation, and air conditioning (HVAC) system. The second building is a small one which houses a kindergarten. Both buildings have a south-east and a south-west oriented facade. The two buildings are shown in Fig. 1. Figure 2 depicts the hourly electric and thermal loads of these buildings on January 29, 2013.

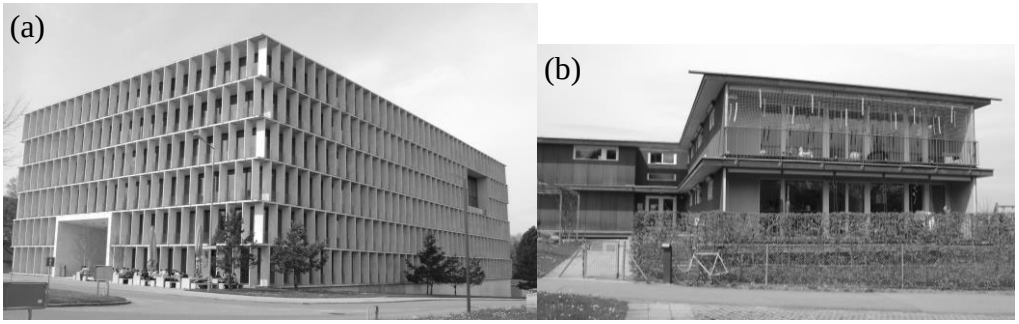

Figure 1: The two test buildings: An office building (left) and a kindergarten building (right).

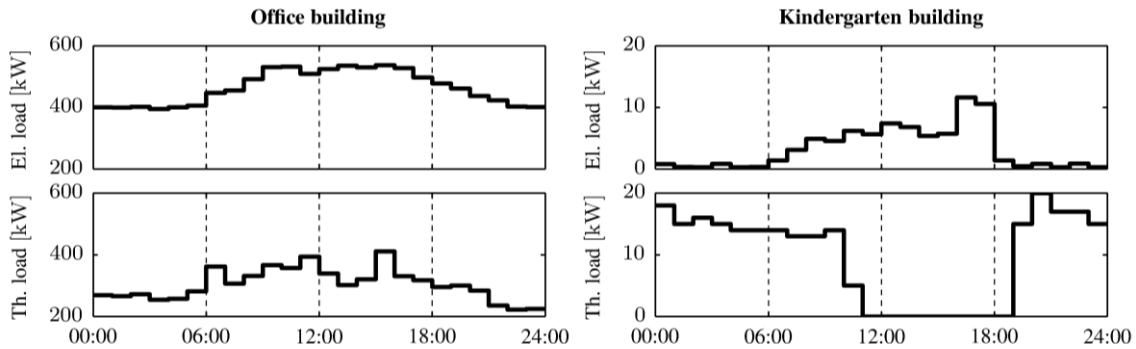

Figure 2: The hourly electric and thermal loads of the test buildings on January 29, 2013.

A weather station located in the neighboring village provides measurement data of the ambient temperature and the global horizontal solar radiation. The Erbs et al. correlation [15] for the estimation of the diffuse component of the horizontal solar radiation and the Perez et al. sky model [16] are used to compute the vertical solar radiation on the building facades from the horizontally measured global solar radiation data. The training of the hour-by-hour models is performed using these measurement data of the input variables. However, the load forecasts are generated using COSMO-2 and COSMO-7 weather forecasts provided by the Swiss national weather and climate service [17].

To test both building STLF algorithms, one-day-ahead forecasts generated at midnight are used. The training data is always updated before a new forecast is generated. Three different training window sizes are examined: 20, 50 and 100 days of the same day type. The analyses are performed using data acquired in the period November 2011 – March 2013, whereas in this work only the results for working days are presented.

The building STLF algorithms evaluated are implemented in MATLAB. The results for the hour-by-hour models based on NNs are obtained using the MATLAB Neural Network Toolbox which applies a feedforward NN [18]. The NNs are trained using the Levenberg-Marquardt backpropagation algorithm. Both, NNs with one hidden layer with two neurons and NNs with one hidden layer with four neurons were examined. Since the NNs with two hidden neurons performed better, only these results are reported. The hour-by-hour models based on the LS-SVM model are implemented using the LS-SVMlab toolbox [19]. The radial basis function is chosen as the kernel function.

The accuracy of the load forecasts are measured by the root mean square error (RMSE) and the coefficient of variation of the RMSE (CV-RMSE), which are computed as

$$RMSE = \sqrt{1/N \sum_{i=1}^{N} (y_i - \hat{y}_i)^2} \quad , \qquad CV - RMSE = \frac{\sqrt{1/N \sum_{i=1}^{N} (y_i - \hat{y}_i)^2}}{1/N \sum_{i=1}^{N} y_i} \quad , \qquad (1)$$

where y_i is the real value, $\hat{y}_i$ is the value forecasted, and N represents the number of samples in the data set.

The results of both building STLF algorithms in the case of the office building are depicted in Fig. 3, whereas Fig. 4 shows the results for the kindergarten building. In general, the LS-SVM-based STLF algorithm performs better than the NN-based STLF algorithm. It is also noticeable that the CV-RMSE values of both the electric and thermal load forecasts are significant larger for the kindergarten building than for the office building. Obviously, the load forecasts for a large office building can be generated more accurately since its load profiles are less sensitive to the behavior of individual occupants.

The performances reported further show that for both buildings the accuracy of the electric load forecasts is slightly improved by increasing the size of the training window. On the other hand, the accuracy of the thermal load forecasts decreases with increasing training window size. The reason is that the thermal load of both buildings varies much more with the season than the electric load. Therefore, in the case of a large training window size, the training data contains data from another season deteriorating the training of the models.

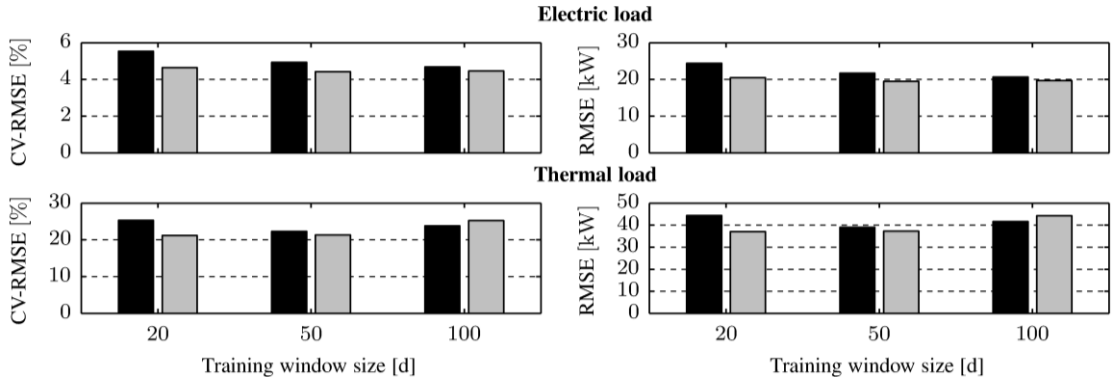

Figure 3: Performances of the NN-based STLF algorithm (black) and the LS-SVM-based STLF algorithm (gray) in the case of the office building.

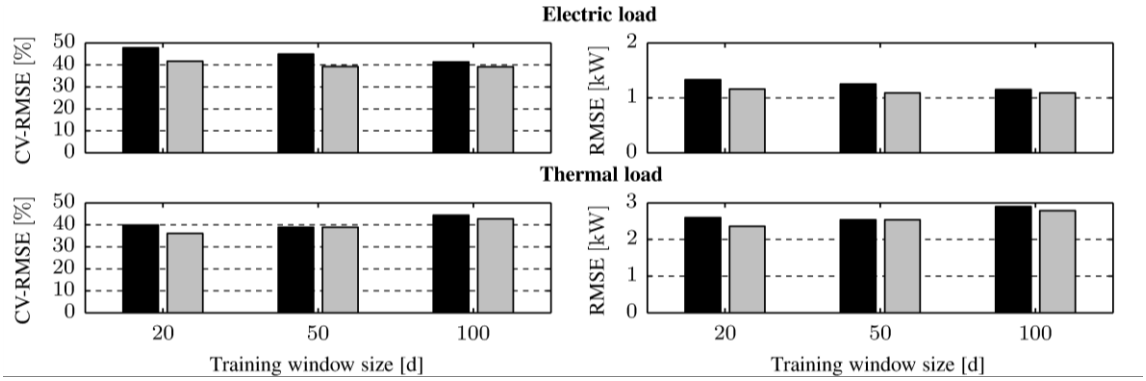

Figure 4: Performances of the NN-based STLF algorithm (black) and the LS-SVM-based STLF algorithm (gray) in the case of the kindergarten building.

CONCLUSION

In this paper, the capabilities of neural networks and of the least squares support vector machine in thermal and electric load forecasting in buildings are examined and compared. The following conclusions are drawn from the tests conducted using the measured thermal and electric load data of a large office building and of a small kindergarten building:

- The least squares support vector machine performs better than neural networks in building load forecasting.
- The least squares support vector machine involves fewer free parameters than a NN. This circumstance makes the application of the forecasting algorithm based on the least squares support vector machine easier compared to the forecasting algorithm based on neural networks.
- Compared to the large office building, the accurate load forecasting of a small building is a more difficult task.
- Using training window sizes of more than 20 days provides no significant benefit.

Future research will focus on the systematic selection of the input variables of the hour-by-hour models.

REFERENCES

1. S.F. Fux: Optimal energy management and component sizing of a stand-alone building energy system. PhD thesis, ETH Zürich, 2013, Diss. ETH No. 21036.

2. A.K. Alfares, M. Nazeeruddin: Electric load forecasting: literature survey and classification of methods. International Journal of Systems Science, Vol. 33, pp 23-34, 2002.
3. E. Kyriakides and M. Polycarpou: Short term electric load forecasting: A tutorial. In K. Chen and L. Wang, editors, Trends in Neural Computation, Studies in Computational Intelligence, Vol. 35, Chapter 16, pp 391-418, Springer, 2007.
4. Y.K. Penya, C.E. Borges, D. Agote, I. Fernandez: Short-term load forecasting in air-conditioned non-residential buildings. IEEE International Symposium on Industrial Electronics, pp 1359-1364, Gdańsk, Poland, 2011.
5. J.R. Forrester, W.J. Wepfer: Formulation of a load prediction algorithm for a large commercial building. ASHRAE Transactions, Vol. 90, pp 536-551, 1984.
6. A. Dhar, T.A. Reddy, D.E. Claridge: A Fourier series model to predict hourly heating and cooling energy use in commercial buildings with outdoor temperature as the only weather variable. Journal of Solar Energy Engineering, Vol. 121, pp 47-53, 1999.
7. P.A. González, J.M. Zamarreño: Prediction of hourly energy consumption in buildings based on a feedback artificial neural network. Energy and Buildings, Vol. 37, pp 595-601, 2005.
8. J. Yang, H. Rivard, R. Zmeureanu: On-line building energy prediction using adaptive artificial neural networks. Energy and Buildings, Vol. 37, pp 1250-1259, 2005.
9. S. Karatasou, M. Santamouris, V. Geros: Modeling and predicting building's energy use with artificial neural networks: methods and results. Energy and Buildings, Vol. 38, pp 949-958, 2006.
10. Z. Hou, Z. Lian: An application of support vector machines in cooling load prediction. International Workshop on Intelligent Systems and Applications, pp 1-4, 2009.
11. H.S. Hippert, C.E. Pedreira, R.C. Souza: Neural networks for short-term load forecasting: a review and evaluation. IEEE Transactions on Power Systems, Vol. 16, pp 44-55, 2001.
12. S. Haykin: Neural Networks: A Comprehensive Foundation. Prentice Hall, 3rd edition, 2007.
13. J.A.K. Suykens, J. Vandewalle: Least squares support vector machine classifiers. Neural Processing Letters, Vol. 9, pp 293-300, 1999.
14. V. Vapnik: The Nature of Statistical Learning Theory. Springer, 1995.
15. D.G. Erbs, S.A. Klein, J.A. Duffie: Estimation of the diffuse radiation fraction for hourly, daily, and monthly-average global radiation. Solar Energy, Vol. 28, pp 293-302, 1982.
16. P. Perez, P. Ineichen, R. Seals, J. Michalsky, R. Stewart: Modeling daylight availability and irradiance components from direct and global irradiance. Solar Energy, Vol. 44, pp 271-289, 1990.
17. MeteoSwiss: http://www.meteosuisse.admin.ch/web/en/weather/models/forecasts.html. last accessed April 25, 2013.
18. M. Beagle, M. Hagan, H. Demuth: Matlab Neural Network toolbox User's Guide. The Mathworks Inc., 2010.
19. K. De Brabanter, P. Karsmakers, F. Ojeda, C. Alzate, J. De Brabanter, K. Pelckmans, B. De Moor, J. Vandewalle, J.A.K Suykens: LS-SVMlab Toolbox User's Guide version 1.8. KU Leuven, 2011.

TOWARDS RELIABLE STOCHASTIC DATA-DRIVEN MODELS APPLIED TO THE ENERGY SAVING IN BUILDINGS

A.Ridi[1,2], N.Zarkadis[3], G.Bovet[1,4], N.Morel[3], J.Hennebert[1,2]

[1] *University of Applied Sciences Western Switzerland (HES-SO), Fribourg, Switzerland*
[2] *University of Fribourg, Department of Informatics, Fribourg, Switzerland*
[3] *Laboratoire d'Energie Solaire et de Physique du Bâtiment (LESO-PB), Ecole Polytechnique Fédérale de Lausanne (EPFL), Lausanne, Switzerland*
[4] *Telecom ParisTech ENST, Paris, France*

ABSTRACT

We aim at the elaboration of Information Systems able to optimize energy consumption in buildings while preserving human comfort. Our focus is in the use of state-based stochastic modeling applied to temporal signals acquired from heterogeneous sources such as distributed sensors, weather web services, calendar information and user triggered events. Our general scientific objectives are: (1) global instead of local optimization of building automation sub-systems (heating, ventilation, cooling, solar shadings, electric lightings), (2) generalization to unseen building configuration or usage through self-learning data-driven algorithms and (3) inclusion of stochastic state-based modeling to better cope with seasonal and building activity patterns. We leverage on state-based models such as Hidden Markov Models (HMMs) to be able to capture the spatial (states) and temporal (sequence of states) characteristics of the signals. We envision several application layers as per the intrinsic nature of the signals to be modeled. We also envision room-level systems able to leverage on a set of distributed sensors (temperature, presence, electricity consumption, etc.). A typical example of room-level system is to infer room occupancy information or activities done in the rooms as a function of time. Finally, building-level systems can be composed to infer global usage and to propose optimization strategies for the building as a whole. In our approach, each layer may be fed by the output of the previous layers.

More specifically in this paper, we report on the design, conception and validation of several machine learning applications. We present three different applications of state-based modeling. In the first case we report on the identification of consumer appliances through an analysis of their electric loads. In the second case we perform the activity recognition task, representing human activities through state-based models. The third case concerns the season prediction using building data, building characteristic parameters and meteorological data.

Keywords: State-based modeling, Gaussian Mixture Models (GMMs), Hidden Markov Models (HMMs)

1. INTRODUCTION

In developed countries, the buildings energy demand represents one of the major source of consumption. As a matter of fact, the energy consumption of buildings in EU and USA

is comprised between 20% and 40% of the total energy consumption, above industry and transportation. Systems like heating, ventilation, air conditioning (HVAC) represent the major source of consumption in buildings, reaching about an half of the consumption. Also electric lighting and consumer appliances represent an important part. In offices for example, HVAC, lighting and appliances, reach together about 85% of the total energy consumption [1]. Interestingly, HVAC systems represent one forth of total energy consumption in developed countries and an increase of these values is anticipated. This is mainly due to growth in population, increasing demand for building services and comfort levels.

Better controlling and automation procedures are therefore needed to optimize the energy consumption in buildings. A typical approach is to use mathematical models that are derived from a priori knowledge about the physics of the building. The approach we follow in our research is to use data driven approaches that involve mathematical equations not derived from physical processes but learnt from the analysis of time series data. Such approaches present several advantages. First, data-driven techniques and self-learning algorithms do not require a comprehension of the underlying physical process. Second, new or unseen building configuration can be handled as soon as observation data are available, making the installation of such systems easier. Third, the models will be able to handle not only the physics of the building but also the patterns of user behaviours.

In most applications the specific building physics are not directly examined. However when they are, they bring some added value, as in the case of the season variable described below in Section 2. Data-driven techniques typically need a large amount of data, because they use statistical properties of a data time series for characterizing the behaviour of a specific system. Data-driven techniques have been the subject of recent research and many projects can be found in the literature [2].

In our approach, we focus on a layered architecture of systems based on state-based models able to capture the temporal and spatial nature of the signals that correspond to modes of use of the building, house or equipment. More specifically, we propose to model these signals with state-based stochastic approaches such as Gaussian Mixture Models (GMMs) and Hidden Markov Models (HMMs). Such models allow detecting automatically probable states linked to modes of use that will, in turn, be used as input for the parameterization of smart control algorithms. The Figure 1 illustrates our approach.

More specifically in this paper, we report on the design, conception and validation of several machine learning applications corresponding to the different levels illustrated in Figure 1. These applications aim at showing the interest of the new data-driven modeling of occupancy-related characteristics of buildings. The concepts can be included in advanced control algorithms and allow at the same time to reduce the energy consumption and to improve the user comfort and the adaptation to user requirements.

The next Section give more details about the different applications that have been developed in this context. Section 3 presents results and discussions.

2. METHOD

In this Section we present three different state-based applications: electricity signature identification, human activity recognition and seasonal modeling.

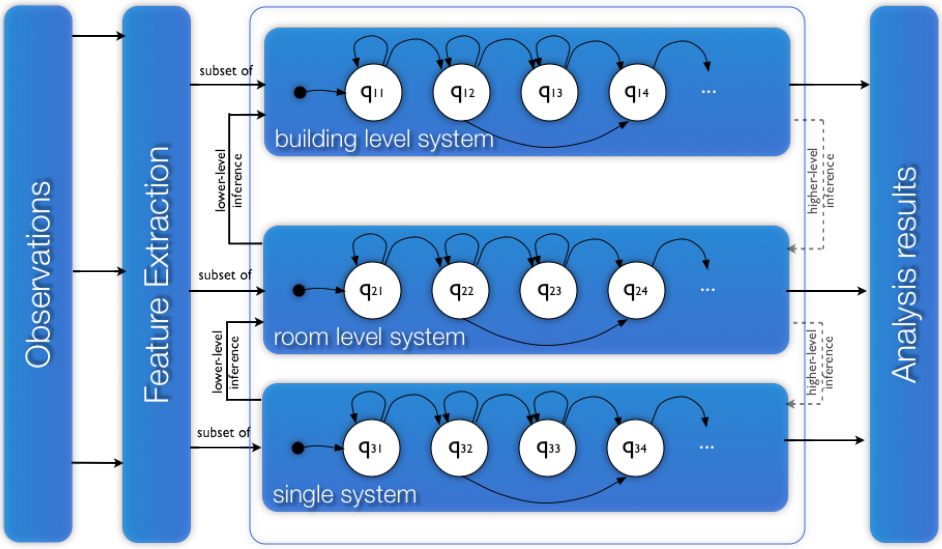

Figure 1: State based modelling.

Electric signature identification

The first application is in the domain of automatic analysis of electricity load in households. The system is based on low-cost smart-plugs measuring every 10 seconds the appliance consumption and producing time series of electric measurements. For the evaluation of the algorithms, we use a database of electric trace *Appliance Consumption Signature Fribourg 1* that includes two acquisition sessions of one hour for 100 appliances spread uniformly into 10 categories [3]. The scientific question here is about the feasibility of modeling, in a data-driven way, the load of single appliance and their automatic identification with generative models such as GMMs and HMMs. As features input of the model, we compute a sequence of vectors using a sliding window procedure on top of the time series. More details about the modelling scheme are provided in [4] and [5]. We applied the two evaluation protocols proposed in [3] to benchmark our models. In the first, called *intersession*, the train set is constituted by instances of the first session, while the testing by those of the second session. Using this paradigm, all the testing signatures come from appliances already seen in the training phase. In the second protocol, called *unseen instance*, the classifiers work with instances coming from appliances not seen before and a 10-cross fold procedure is used to smooth the results. This protocol potentially reveals the system capability of generalizing to new brands or models.

Human activity recognition

In this second application, we show the potential of automatic activity recognition using temporal data captured from presence sensors. In our work, we propose to use HMMs to recognize such human activities. The states in the HMMs are related to the activities and to the expected locations of the activities. The signals we use are asynchronous sensor events from which we sample a sequence of feature vectors spaced in time with a constant interval. Each state includes transition probabilities representing the transitions between states and the corresonding probability to go from one state to the other. Each state also models the probability density function of observing a single feature vector in a given state, i.e. the emission probabilities. Regarding the HMM topologies, we use two types

of states, one for the stable parts of the signals, one for the less-stable parts of the signals (see figure 2a). Using this paradigm, we considered as *unstable* the transition areas, e.g. the corridors or the doors. In the (*stable*) areas, e.g. the kitchen for cooking or the bedroom for sleeping, the transition probabilities are computed through the training and their values depend on the nature of the activities. An evaluation benchmark, results and discussions are presented in Section 3.

Season modelling

In a third application, we introduce a new model of season prediction based on state-based models such as HMMs able to detect more finely the change of seasons from meteorological data. When implementing an advanced control scheme for building services, typically heating, cooling, ventilation (HVAC) and solar shadings, for instance using Fuzzy Logic, a variable "season" (typically represented as a fuzzy variable) represents a good method to fit the behaviour of the control system to the weather conditions. A simple definition, for instance based only on calendar or on outside temperature, is not satisfactory, since building characteristics and use should also be considered.

For the purpose of the season definition, we involve the signals from HVAC, window opening, window blinds, external and internal temperature and solar irradiation. We also use a separate module to calculate the building's time constant (a simple 2-node model) which we include as parameter in our observation vector.

We consider that the "season" variable can have the value of the following 3 states (figure 2b):

- Heating season which is defined when heating is required to avoid that the inside temperature is getting lower than the optimal comfort temperature.
- Cooling season when cooling is needed, either with mechanical cooling or by measures such as passive night cooling or protection against passive solar gains.
- Intermediate season (mid-season) which is normally the most critical season. During this season the building might need sometimes heating and sometimes cooling.

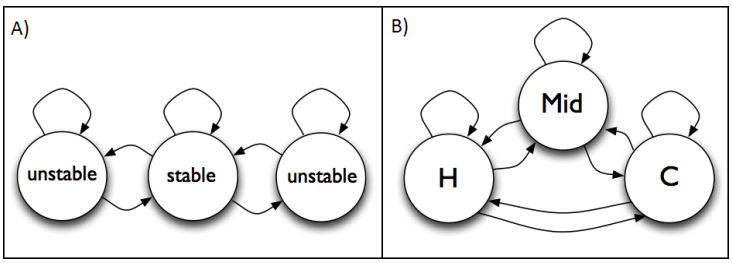

Figure 2: Two different state based modelling: A) Example of model for activity recognition with three states. Such topology is used for modelling Relaxing, Working, Sleeping, Out of Home, Going from Bed to Toilet. B) The three possible states of the ergodic variable "season" and the possible transitions from one state to the next: Heating season (H), cooling season (C) and intermediate season (Mid).

3. RESULTS AND DISCUSSION

Electricity signature identification

In order to evaluate the state-based model performances, two classifiers have been compared, namely k-Nearest Neighbor (k-NN) and GMM systems. Using the *intersession* protocol, we achieved respectively 88% and 93.8% correct category identification [5], while using the *unseen instance* protocol we achieved respectively 57% and 74% correct category identification [6]. Clearly the first protocol achieved better results than the second, given that in the latter case instances coming by appliances never seen before have to be classified. For evaluating the state-based model we used GMM, but we envisage to use the HMMs, which should be particularly suitable for electrical signatures of appliances, which in most cases are state-based machines.

Human activity recognition

We evaluated the proposed models using the WSU CASAS dataset [7]. The raw data is recorded from 31 motion sensors, 4 temperature sensors and 4 door sensors, from which we use the motion and door sensors. In the observation vector we added the time information computed through a 24h cyclic function in order to make it more suitable for the analysis. Among the activities labeled in this dataset, we selected those having an adequate number of data sequences, in order to have a sufficiently large balanced dataset: *Meal Preparation, Relaxing, Eating, Working, Sleeping, Going from Bed to Toilet, Out of Home.* The total time of data recording was 8 months for one person living dayly in a smart home and receiving visits on a regular basis. After several tuning, we measured an overall accuracy using a leave-one out procedure of 98.9% for the HMM presented in Section 2.

Season model

We developed and evaluated the proposed season prediction model using data recorded over a long period of time at the LESO-PB experimental building which is located in EPFL campus near Ecublens and Lausanne. The observation vector consisted of the signals of 8 actuators and sensors from a single-occupant office room including ambient and indoor temperatures, window states (open/closed), external blinds position and solar irradiation values. Hidden states (heating, cooling and intermediate season) are considered ergodic (any transition between various states is possible; see Figure 2b). We verify the developed model against the heating power: we consider the use of heating as an indication for the heating season. Results demonstrated that season was correctly identified with an accuracy of 69% to 91%. Higher accuracy is observed when identifying heating or cooling seasons, while it drops significantly for the intermediate season. This is expected behaviour as intermediate season is not a crisp state and it is far more hard to define and thus to correctly identify. Also, the absence of active cooling in LESO building adds a further difficulty in the validation of our model (it would have provided us with an indication of the cooling season).

4. CONCLUSION AND OUTLOOK

In this paper we showed different applications of state-base modeling in a smart building context. The underlying motivation is to build more precise models to better model and control the energy usage in buildings. In the first application we showed the possibility

to automatically recognize appliance from their electric signatures. When the appliances are known to the database used to build the models, the identification accuracy can be up to 93.8%. The second application is about the use of HMM for the recognition of human activities in smart environments. Quite high accuracy rates have been measured, up to 98.9%. This performance is however to take cautiously as the procedure uses a large number of presence sensors and as the benchmark involves only one person. The third application is about season modelling where the developed HMM model predicted correctly the season with an accuracy of 69% to 91%. As expected, cooling and heating season prediction is more accurate than that of the intermediate season.

As a further step to our research, we aim to demonstrate in practice the interest of the new data-driven modelling of occupancy-related characteristics of buildings. We plan to carry out simulations as well as real life experiments where these concepts will be included in advanced control algorithms and allow at the same time to reduce the energy consumption and to improve the user comfort and the adaptation to user requirements.

ACKNOWLEDGEMENTS

This work was supported by the research grant of the Hasler Foundation project GreenMod.

REFERENCES

1. Pérez-Lombard, L., Ortiz, J., and Pout, C.: A review on buildings energy consumption information. *Energy and Building*, 40:394–398, 2008.

2. Chan, M., Estève, D., Escriba, C., and Campo, E.: A review of smart homes: Present state and future challenges. *Computer Methods and Programs in Biomedicine*, 91:55–81, 2008.

3. Gisler, C., Ridi, A., Zufferey, D., Khaled, O. A., and Hennebert, J.: Appliance consumption signature database and recognition test protocols. In *Proceedings of the 8th Internation Workshop on Systems, Signal Processing and their Applications (Wosspa '13), to appear*, 2013.

4. Zufferey, D., Gisler, C., Khaled, O. A., and Hennebert, J.: Machine learning approaches for electric appliance classification.

5. Ridi, A., Gisler, C., and Hennebert, J.: Automatic identification of electrical appliances using smart plugs. In *Proceedings of the 8th Internation Workshop on Systems, Signal Processing and their Applications (Wosspa '13), to appear*, 2013.

6. Ridi, A., Gisler, C., and Hennebert, J.: Unseen appliances identification. In *Proceedings of the International Joint Conference on Pervasive and Ubiquitous Computing (UbiComp '13), submitted*, 2013.

7. Cook, D.: Learning setting-generalized activity models for smart spaces. *IEEE Intelligent Systems*, 27:32–38, Jan 2012.

TOWARDS LCA OF BUILDING AUTOMATION AND CONTROL SYSTEMS IN ZERO EMISSION BUILDINGS – MEASUREMENTS OF AUXILIARY ENERGY TO OPERATE A KNX BUS-SYSTEM

Jens Tønnesen; Vojislav Novakovic

Department of Energy and Process Engineering, Norwegian University of Science and technology (NTNU), Kolbjorn Hejes vei 1b, NO-7491 Trondheim, Norway

ABSTRACT

The demands for both thermal comfort and reduced energy consumption in buildings have become a major driving force for the increased use of advanced building automation and control systems (BACS). In the on-going development of Zero Emission Buildings (ZEBs), it seems to be a common understanding that such systems are needed in order to save energy and reach the zero emission goals [4], and that energy consumption for their operation is negligible compared to the building needs and the energy saving potential BACS causes.

However, sensors and actuators in automation and control systems require electricity to operate, and both the environmental impact related to this operation, and the manufacturing and maintenance of electronic components (including wiring) is not well understood in a Life Cycle Assessment (LCA) perspective, even though different standards give framework and methods for energy calculations [5-9] and LCA [10-13] of buildings. These standards unfortunately do not include or suggest default values for the auxiliary energy from different levels of BACS. Usually, in building simulation, these values are only assumed to be a part of a fixed internal gain, e.g. as in the Norwegian passive house standard [14], with no further considerations on the actual operating energy or the environmental impact it represents.

In this paper, auxiliary energy to operate a KNX-bus system for a planned passive house office building with demand control on room/zone level, is measured in a laboratory test. For typical room zones, as for a single office and a meeting room, the electrical standby power counts for respectively 0.91 and 2.00 kWh/m^2·y solely for operating the automatic system on room level. E.g., based on the electricity mix UCPTE, components needed to achieve automatic zone control equals 2.86 and 6.28 kWh/m^2·y of non-renewable primary energy ($PEF_{non\text{-}ren}$). For the whole building; 0.85 kWh/m^2·y and $PEF_{non\text{-}ren}$ = 2.67 kWh/m^2·y. Other PEF production factors will give different results which can have decisive implications on the development of the ZEB concept and the use of BACS in future buildings. The auxiliary energy for BACS should therefore be included when conducting energy simulations and evaluations of the environmental performance of Zero Emission Buildings.

Keywords: Auxiliary energy, KNX, light control, LCA, ZEB, office building, BACS

INTRODUCTION

Building automation and control systems are getting more advanced, and there exists a large amount of different products and standards. The most significant world wide open standards for building automation are BACnet, LonWorks and EIB/KNX [15].

The objective of this study is to gain better knowledge of electricity consumption and the environmental impact related to building automation and control systems (on zone/room level) in Zero Energy/Emission Buildings (ZEBs), or in general; buildings with very low energy demand for lighting, heating, cooling and ventilation and where the energy saving potential (absolute value in kWh) by using BACS efficiency factors [9], is limited compared to existing buildings due to passive measures like extra insulation and airtight envelope.

METHOD

The case office building: In Trondheim, Norway, a new University Hospital Building is currently under construction. The building project aims to achieve the Norwegian passive house standard [14]. The building has 17350 m^2 heated floor area[1]. Except from the hospital area, this building can be defined as an office building.

Building automation and control system on room level: A KNX-bus system [16] will be used for individual zone control in the typical office areas. A total of 2324 KNX components are expected to be installed. In addition approx. 2050 lighting fixtures will use DALI light control system in some areas which will be connected to the KNX-bus via gateways. The building services systems, like ventilation plants, have their own automation and control system, often based on BACnet [17]. This type of standard is more suited to control advanced processes with rapid changes. Technical Building Management systems will be used in the building, but only the KNX-bus system and Dali light control system on room level are addressed in this work.

Equipment for electrical measurement: To measure the power and energy consumption from the KNX-components, the following equipment from National Instruments Corp is used to sample the data: NI 9225 (300 V_{rms}), NI 9229/9239 (±60/±10 V) and NI 9227 (5 A_{rms}). The sampled data is analysed with the LabVIEW 2012 software, and the inbuilt Electrical Power Suite. Based on 50 kHz samples on voltage (V) and current (A) the following values were calculated and averaged over 10 seconds before written to file for further analysis: V_{rms}, A_{rms}, real power [W], apparent power [VA], reactive power [VAR] and power factor ($\cos\varphi$). The measurements presented in the result chapter are mean values of real power [W].

Measurement in laboratory test and in an existing office building: Measurements on individual components were conducted in a laboratory test. The control functions were programmed in line with the plans for the office building. The KNX power supply had 13 of 64 possible KNX components attached[2]. The DALI Gateway had 1 lighting fixture (1 ballast), of 64 possible. The power supply for the tested VAV actuator motor was based on 24 V AC.

To examine the electrical energy conversion efficiency for the power supplies under normal conditions, measurements were also conducted on 8 KNX power supplies and 4 DALI Gateways in an existing 2300 m^2 office building (mainly office landscapes/open-plan offices) with zone control. In total 358 KNX components and 168 Dali lighting fixtures/ballasts were connected.

RESULTS

Automation components for typical rooms/zones in the case office building: Five typical room types with different levels of zone control equipment are identified. These are: 1) single office, 2) office landscape, 3) meeting room, 4) advanced office landscape (classroom/ library/conference room) and 5) corridor. In the case office building, the room sizes and zone control equipment will vary to some extent, but the specific automation functions in the 5 typical zones corresponds to BACS efficiency class A [9]. Table 1 gives an overview of planned equipment to achieve the zone control function, and an estimate of the necessary number of components for a typical room size.

[1] 6650 m^2 for hospital area and 10700 m^2 for office building (including technical areas).

[2] The KNX Association recommends 20% surplus capacity in order to meet possible future rebuilding.

Room type	Planed and estimated amount of zone control equipment in case office building
Single office	~10 m^2, 1 person. 1 Multilight with 1 slave lighting fixture, 1 ballast each. This slave ballast with low standby loss. Individual room-temperature control and presence- and constant light detector inbuilt in the Multilight. 1 motorized radiator valve. Multivent (on/off ventilation damper with 1 motor). 1 motorized screen (solar shading) for 1 window with manual override (wall switch or inbuilt in the Multilight).
Office landscape	~35 m^2, 4 persons. 2 Multilight with 2 slave lighting fixtures. Room-temperature control and presence- and constant light detector in the Multilight. 2 motorized radiator valves (one under each window for future flexibility). 1 Multivent with 3 levels (2 VAV-motors). 2 motorized screen (no manual override).
Meeting room	~35 m^2, 10+ persons. 8 Dali lighting fixtures. 1 combined CO_2 and temperature sensor with controller. Presence detector. 2 modulating VAV's with power supply. 2 motorized radiator valves. 1 wall switch for light dimming and screen override. 3 motorized screens.
Advanced landscape	~300 m^2. 24 Dali lighting fixtures. 4 CO_2 and temperature sensors (one in each corner) with room controllers. 6 presence- and constant light detectors. 4 motorized radiator valves. 20 Multivent on/off dampers. 30 motorized screens.
Corridor	~40 m^2 (length of 16 m). 6 Dali lighting fixtures. 1 presence- and constant light detector. Temperature sensor with room control. 2 motorized radiator valves. 2 motorized screens (for windows in each end of the corridor). Constant ventilation.

Table 1: Planned equipment to achieve zone control function (BACS energy efficiency class A) in the case office building

In single offices and office landscapes, the tailor-made Multilight and Multivent will be implemented. Multilight is a lighting fixture with inbuilt temperature sensor, PID controller, presence- and constant light detector on one "monoblock" KNX-bus-coupling unit. MultiVent is an on/off ventilation damper with one motor. In addition KNX power supplies, line couplers, Dali Gateways and shared equipment like 2-4 brightness sensors on each façade are needed for the total automation function[3]. A 230 V AC outlet/plug and a KNX window frame switch to control the radiator as well as the VAV-unit are considered to be installed, but this is not decided upon yet, and is therefore not included in the measurements.

Measurements on component level in laboratory test: Figure 1 illustrates components needed to achieve zone control function in a typical meeting room and single office. The numbers (1 – 22) in the figure point out where the measurements are conducted, and are representative for all the components that will be utilized in the building.

The total power output on the bus-line is 2.34 W with 13 different KNX components attached. This gives an average standby power of 0.18 W per component. However, the switch mode transformer in the power supply needs 5.80 W to operate (see figure 1,①②). This gives a transformer electrical efficiency of only 40%. Taking this into account, the real demand is 0.47 W per component. The ballast loss for the Dali light fixture is measured to 0.45 W with the light switched off. This value is low compared to other studies, see e.g. [18].

The power supplies for the KNX-bus, the VAV actuator motor and the Dali Gateway had poor electrical energy conversion efficiencies (respectively 40, 12.5 and 5.6%) in this laboratory test. This will be better in a real building with more components attached.

For most of the measured sensor components, it is hardly possible to measure variations between standby and operation. For actuator components like radiator valves, screens/blinds and VAV-motors, the total yearly energy need will be a function of climate variations and occupancy pattern. Occupancy pattern in office buildings are treated in [19] and can, e.g. be used to estimate number of changes in VAV-damper position.

[3] In addition 149 Multilight, 395 Multivent and 6 modulating VAV will be used in the building. For further details about the different components, contact the first author (jens.tonnesen@ntnu.no).

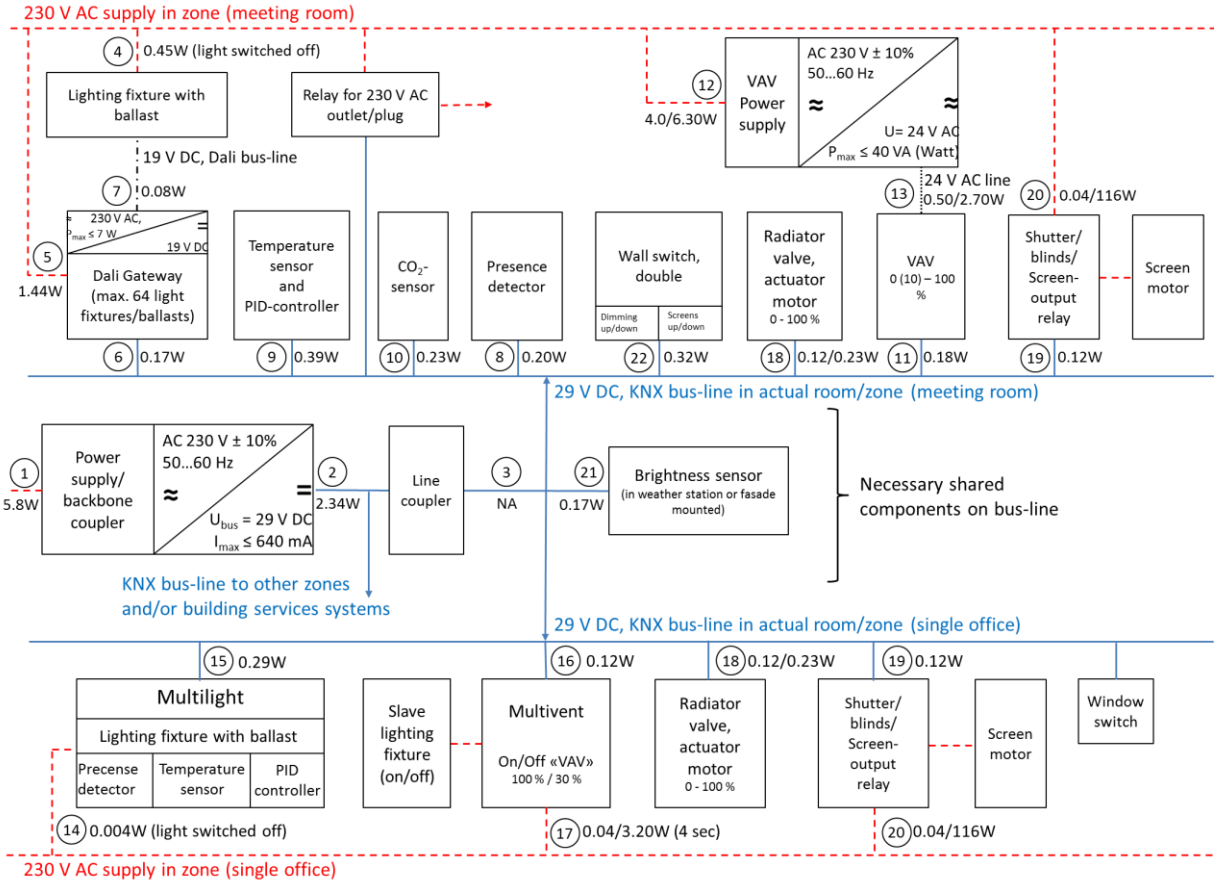

Figure 1: KNX-equipment used for zone control in the laboratory test, illustrating a meeting room and a single office. The standby and operational power is marked beside the number. E.g. for the radiator valve motor (18), the standby power is 0.12 W and 0.23 W is used during operation.

Measurements on KNX Power supplies and Dali Gateways in an existing office building: In the existing office building, the average electrical standby power for the 8 KNX Power supplies was measured to 11.7 W and the power delivered to the KNX bus was 7.96 W with a power factor (cosφ) of 0.86. This equals 68% average electrical efficiency for the power supplies with an average of 0.26 W per KNX component. The average power includes operational energy for the radiator valves on the KNX bus-line. However, energy consumption for operating the radiator valve is low compared to its standby power. The average electrical standby power for the 4 Dali Gateways was measured to 2.84 W, and 0.56 W was delivered on the Dali bus-line. This gives an average of 0.07 W per Dali lighting fixture ballast with an electrical efficiency of 20% (with a range from 5 – 35 %).

The authors of this paper recommend using 0.3 W per KNX-component and 0.1 W per lighting fixture ballast connected to Dali Gateways as default values for average electrical standby power in KNX bus-systems. In addition the ballast losses must be taken into account, in this case minimum 0.45 W are recommended with lights switched off (see figure 1,④).

A rough estimate of operational energy for the 430 screens in the case office building indicates 0.7 – 1.1 kWh/y per screen motor depending on the façade orientation and climate. For the VAV-damper, it could be expected about 4000 changes per year in an average office building [19]. With an estimated value of 15 - 30 sec per change of damper position, this indicate 0.05 – 0.1 kWh/y per VAV-motor (modulating VAV).

Primary energy and CO_2-equivalents for different room-zones: Derived from Table 1 and the measurements, Table 2 give the total standby power, electricity consumption, primary energy and CO_2-eqvivalents for BACS on room level in the case office building.

		Unit	Single office (10 m²)	Office landscape (35 m²)	Meeting room (35 m²)	Advanced landscape (300 m²)	Corridor (40 m²)	Entire building (17350 m²)
Electricity	Standby power	[W]	1.04	1.91	8.90	35.6	4.74	1865
		[W/m²]	0.10	0.05	0.25	0.12	0.12	0.11
	Consumption[4]	[kWh/m²·y]	**0.91**	**0.48**	**2.00**	**0.96**	**0.89**	**0.83**
"EU-mix" (UCPTE) [5]	PEF_{tot} (3.31)	[kWh/m²·y]	3.01	1.59	6.62	3.18	2.95	2.75
	$PEF_{non\text{-}ren}$ (3.14)	[kWh/m²·y]	2.86	1.51	6.28	3.01	2.79	2.61
	$CO_{2\text{-}eq}$ (617)	[g/m²·y]	561	296	1234	592	549	512
NORDEL electricity mix [20]	PEF_{tot} (2.21)	[kWh/m²·y]	2.01	1.06	4.42	2.12	1.97	1.83
	$PEF_{non\text{-}ren}$ (1.48)	[kWh/m²·y]	1.35	0.71	2.96	1.42	1.32	1.23
	$CO_{2\text{-}eq}$ (189)	[g/m²·y]	172	91	378	181	168	157
ZEB[5] [21, 22]	PEF_{tot} (NA)	[kWh/m²·y]	NA	NA	NA	NA	NA	NA
	$PEF_{non\text{-}ren}$ (NA)	[kWh/m²·y]	NA	NA	NA	NA	NA	NA
	$CO_{2\text{-}eq}$ (132)	[g/m²·y]	120	63	264	127	117	110

Table 2: Electricity consumption, primary energy (total and non-renewable) and CO_2-eq for automation components in the 5 different room-zones + estimate for the entire case building.

DISCUSSION

Defining default values for auxiliary energy for BACS in the standards will help the development of ZEBs through better energy simulation and thereby more reliable LCA of buildings including building services systems. In addition Table 2 demonstrates that choices of electricity production systems will provide completely different values for both primary energy and CO_2-equivalents. This should be kept in mind when comparing different BACS in the development of ZEBs.

The different KNX components communicate with telegrams on a single twisted pair bus-line, and require 29 V DC power supply to operate. This high voltage (compared to the 3V microchips normally require) allows for stable communication on a 1000 m bus-line. Normally, KNX components are placed close to each other and the power supply. This illustrates the possibility for more energy efficient components and bus-systems operating on lower voltages. Standby power should furthermore be avoided by, e.g. night-time cut-off.

Wireless building automation based on batteries or energy harvesting technologies are emerging [23, 24], but in practice these systems are still associated with some problems. Especially in concrete buildings, the wireless signal might be obstructed by heavy walls and need to communicate through series of components, which causes increased energy use and thus more frequent battery changes.

The use of automatic systems in buildings clearly has potential to save thermal and electrical energy, but in ZEBs it can prove counterproductive in a life cycle perspective. The authors of Internet-of-Things [25], points out that energy required to operate, e.g. wireless sensors and

[4] The ballast losses are calculated with light switched off 75% per year (6570 h/y). Other components 8760 h/y.

[5] Best case scenario, 2010 – 2070, from «The Research Centre on Zero Emission Buildings», www.zeb.no

network in smart buildings most likely will increase exponentially. To meet this development, the number of components, or their energy consumption, must be dramatically decreased unless novel energy harvesting techniques and/or better battery technologies are developed.

ACKNOWLEDGEMENTS

The authors acknowledge the support from the Research Council of Norway and partners through the Research Centre on Zero Emission Buildings. A special thanks to YIT AS and Åge Sjåvik for useful discussions and assembly of the laboratory test, and Kjetil Johansen (Nordic Semiconductors) for valuable help in understanding energy efficient microelectronic.

REFERENCES

1. HOBNET (Holistic Platform Design for Smart Buildings on the Future Internet). Available from: http://www.hobnet-project.eu/.
2. Smart IPV6 Building. Available from: http://www.smartipv6building.org/.
3. OptiControl (Use of weather and occupancy forecasts for optimal building climate control). Available from: http://www.opticontrol.ethz.ch/.
4. Kolokotsa, D., et al., A roadmap towards intelligent net zero- and positive-energy buildings. Solar Energy, 2011. 85(12): p. 3067-3084.
5. CEN, EN 15603:2008. Energy performance of buildings - Overall energy use and definitions of energy ratings, 2008, European committee for standardization (CEN): Brussels.
6. CEN, EN ISO 13790:2008. Energy performance of buildings - Calculation of energy use for space heating and cooling, 2008, European committee for standardization (CEN): Brussels.
7. CEN, EN 15316. Heating systems in buildings - Method for calculation of system energy requirements and system efficiencies - Part 1: General, 2007, European committee for standardization (CEN): Brussels.
8. CEN, En 15241:2007. Ventilation for buildings - Calculation methods for energy losses due to ventilation and infiltration in buildings, 2007, European committee for standardization (CEN): Brussels.
9. EN 15232: 2012, Energy performance of buildings - Impact of Building Automation Control and Building Management, 2012, European Committee for Standardization (CEN): Brussels.
10. ISO, ISO 14040:2006. Environmental management - Life cycle assessment - Principles and framework, 2006, The International Organization for Standardization: Geneva, Switzerland.
11. ISO, ISO 15392:2008. Sustainability in building construction - General principles, 2008, The International Organization for Standardization: Geneva, Switzerland.
12. CEN, EN 15978:2011. Sustainability of construction work - Assessment of environmental performance of buildings - Calculation method, 2011, European committee for standardization (CEN): Brussels.
13. CEN, EN 15643-1:2010. Sustainability of construction works - Sustainability assessment of buildings - Part 1: General framework, 2010, European committee for standardization (CEN): Brussels.
14. NS 3701:2012, Criteria for passive houses and low energy buildings - Non-residential buildings, 2012, Standard Norge: Oslo.
15. Kastner, W., et al., Communication Systems for Building Automation and Control. Proceedings of the IEEE, 2005. 93(6): p. 1178-1203.
16. The KNX Association. Available from: http://www.knx.org/.
17. ASHRAE BACnet. Available from: http://www.bacnet.org.
18. Roisin, B., et al., Lighting energy savings in offices using different control systems and their real consumption. Energy and Buildings, 2008. 40(4): p. 514-523.
19. Halvarsson, J., Occupancy pattern in office buildings: consequences for HVAC system design and operation. Vol. 2012:37. 2012, Trondheim: Norges teknisk-naturvitenskapelige universitet.
20. PRé-Consultants, SimaPro version 7.3.3. (Electricity, low voltage, supply mix, NORDIC 2007-2011)
21. Graabak, I. and N. Feilberg, CO2 emissions in different scenarios of electricity generation in Europe, 2011, TR A7058, SINTEF Energy Research: Trondheim, Norway.
22. Dokka, T.H., Proposal for CO2-factor for electricity and outline of a full ZEB-definition, 2011, The research centre on Zero Emission Buildings, Norwegian University of Science and Technology: Trondheim, Norway.
23. Reinisch, C., et al. Wireless Technologies in Home and Building Automation. Industrial Informatics, 2007 5th IEEE International Conference on. 2007.
24. vom Boegel, G., F. Meyer, and M. Kemmerling. Batteryless sensors in building automation by use of wireless Energy Harvesting in Wireless Systems (IDAACS-SWS), 2012 IEEE 1st International Symposium
25. Vermesan, O. and P. Friess, Internet of things: Global technological and societal trends2011, Aalborg: River Publishers.

THE HUMAN BEHAVIOR: A TRACKING SYSTEM TO FOLLOW THE HUMAN OCCUPANCY

Timilehin Labeodan, Rik Maaijen, Wim Zeiler

University of Technology Eindhoven Eindhoven, Netherlands w.zeiler@bwk.te.nl

ABSTRACT

Various control strategies have been adopted to improve energy efficiency in commercial office buildings, particularly the alignment of energy consumption for space conditioning and lighting patterns with human occupancy. Considerable uncertainty however exists in these patterns but advancement in information and communication technology(ICT) has made it possible to reduce these uncertainties. More fine-grained building occupants information can now be gotten in real-time for dynamic demand-driven space lighting and conditioning controls. In this paper the performance of one of such technologies; radio frequency identification (RFID) system is accessed in the determination of human occupancy and location from experiments carried out in a typical office building in the Netherlands. The correlation between energy use by office appliance and human occupancy was also investigated. Furthermore, steps that could be taken to improve energy consumption for comfort through a demand-driven process control strategy are identified.

Keywords: RFID, energy, occupancy

INTRODUCTION

Energy consumption for space conditioning and lighting loads (L-HVAC- Light, Heat, Ventilation and Air Conditioning) together account for 70% of all energy consumed in a typical office building[1]. Current building energy management systems (BEMS) used in commercial office buildings typically operate control settings dictated according to assumed schedules that are disconnected from actual space occupancy[2][3]. Human presence and behaviour in buildings have been shown to have significant impact on space heating, cooling, ventilation, lighting, appliances, and building controls[5], however human occupancy information was not until very recently considered in buildings energy performance analysis[4].

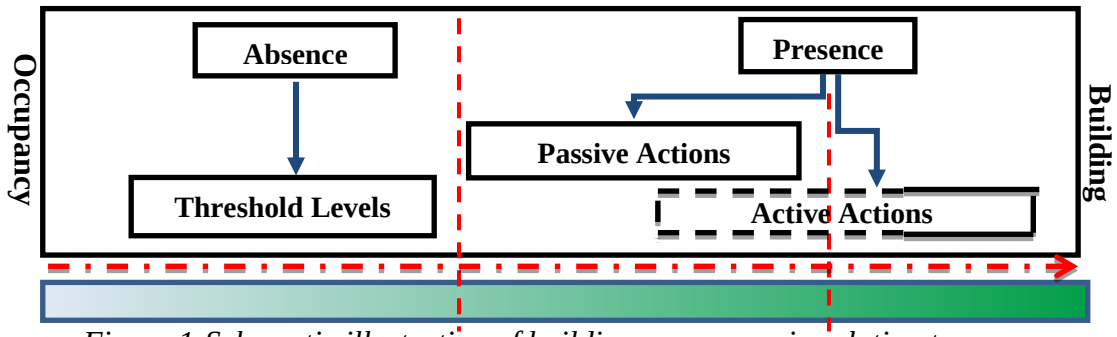

Figure 1:Schematic illustration of building occupancy in relation to energy

Human occupancy is stochastic in nature and as shown in Fig.1 above has both passive and active effect on a buildings energy use. Passive actions, the mere presence of occupant(s) in a building affects energy consumption but is dependent on activity, number of occupants and internal gains[5]. In the same vein, active actions of occupant(s), operation of windows, shades and radiators also have significant effects on a buildings energy consumption [6]. A variety of models have been developed from technologies such as neural network, fuzzy-logic, markov chain and direct logical inference from sensor data[7] for scheduling occupancy

in BEMS. Considerable uncertainty does however exists in these models[6]. Building occupancy is difficult to simply infer solely from building function and type as there are high tendencies for a buildings usage to change with time and occupants might over time display varying patterns of presence thus automatically altering the predicted occupancy model [6][8]. Advancement in ICT has however made it possible to reduce these uncertainties. More fine-grained real-time building occupancy information can now be ubiquitously obtained and connected to the BEMS for demand-driven control hence improving energy efficiency. In subsequent sections of this paper, we present results from experiments conducted in a typical office building in the Netherlands using one of such technologies; RFID to obtain real-time human occupancy information and correlation between energy use by appliance.

BACKGROUND

Occupancy detection systems in general can be classified based on the measurement technology as; motion detection systems, CO_2 detection systems, visible light detection systems, acoustic detection systems, radio frequency detection systems. Alternatively, classification based on functions and methods can also be made as shown in Table 1.

Table 1:Occupancy Detection Systems

Measurement Technology	**SENSOR**	**Function**		**Method**		
		Indiviualized	Non Individaulized	Terminal Based	Non Terminal Based	WSN
Motion[10,12]	PIR,ultrasonic		✓		✓	✓
CO_2 [11]	NDIR		✓		✓	✓
Acoustics[10]	Microphone		✓		✓	✓
Visible light[13]	Camera	✓	✓		✓	✓
RF signals[11,14,15, 16]	WLAN,RFID, GPS, UWB Ultrasonic	✓	✓	✓		✓

Pyroelectric infrared (PIR) and ultrasonic motion sensors as stand-alone and hybrid nodes are widely used in buildings for occupancy detection [9], particularly for control of lighting systems, while this technology has the inherent advantage of non-terminal based methods, extendibility, non-intrusiveness, easy deployment and cost [10], it gives only binary information and stationary occupants are often not detected [11]. CO_2 detection systems however provides better but indirect measure of actual occupancy, it is often used in combination with PIR and acoustic Sensors [12]. CO_2 sensors have a slow response time, are also influenced by other surrounding physical phenomena such as outdoor air quality and ventilation rate [11]. Though advancement in wireless sensor network (WSN) technologies has extended the range as well as usability of the above mentioned detection systems in various environment mostly residential [10][7], it is still difficult to implement individualized functions capable of identifying and providing coordinates for multiple occupants which is the norm in office buildings [11].

Vision based detection systems are capable of both individualized and non-individualized functions [13]. Though capable of detecting multiple occupants, privacy, difficulty in providing occupants coordinates information and computational complexity are limitations that however prevents its wide implementation [11].

Radio Frequency (RF) systems (WLAN,UWB, indoor GPS, RFID,GSM) on the other hand are able to provide occupants coordinates to a higher degree of accuracy than all other detection systems by using tags with appropriate receivers/tags from which the location of tagged users can be conceptually determined and continuously tracked through a number of nodes (access points, receivers, readers, etc.) deployed at fixed positions indoors and

connected to a central processor/server [14]. In choosing the appropriate RF measurement technology, a number of selection criteria such as; cost of deployment, required accuracy, resource requirement , computational complexity, privacy, type of environment and effects on energy consumption have to be considered [15]. Wireless local area Networks (WLAN) systems have a very low infrastructure and deployment costs, but considerable high localization uncertainty [16]. Ultra-Wide Band (UWB) systems offer a good compromise with sub-meter tracking but considerable high deployment cost [14]. Indoor Global positioning systems (GPS) also have a very low position uncertainty however its deployment cost is high [14]. RFID systems however have intermediate deployment cost as well as moderate accuracy [11] hence its preference for use in this study.

Table 2:Selection Criteria applied to indoor Localization(Adapted from 15)

	Cost	Accuracy	Environment	Energy
Indoor GPS[14]	✗✗	✓✓	✓	✓✗
RFID[11]	✓	✓	✓✓	✓✓
WLAN[14]	✓	✓	✓✓	✓
UWB[14]	✗✗	✓✓	✓✓	✓

✓✓ - GOOD, ✓- MODERATE, ✓✗- FAIR ✗✗-POOR

METHODOLOGY

For real-time human occupancy detection, a wireless network comprising of RFID tags and readers with the following components; static nodes, mobile nodes, receiver and a (cloud) server for data collection were installed on the 3rd floor of the case study building. The RSSI technique embedded in active RFID technology was used in determining the coordinates of occupants from meshes created around the office floor. The case study office floor is made up of an open-plan flexible office setup with 29 workspaces, 5 cell offices, 3 meeting rooms and a lounge. The workspaces are separated by closed bookcases a common feature in most office buildings in the Netherlands.The floor has 11 thermal zones, 3 of which are in the open-plan workspace. In the meeting rooms, open-plan spaces and cell offices high efficiency artificial fluorescent lightings in reflective luminaires with no motion sensors are installed. The artificial lighting in the open-plan workspaces are centrally operated while that in the cell offices are locally operated. The lighting is turned on between 8AM and 8PM (12hours) during weekdays and the temperature in all thermal zones on the floor is maintained at 22°C (winter) with the ability to change the set point by ± 1.5 °C. For measurement of the electricity use by appliances, a power logger was installed at every desk and on other points of interest (printer, coffee machines). In total fifteen power loggers were installed for logging the active power of plugged appliances.
A total of 16* employees randomly selected and making up 80% of employees designated to work on the case study floor participated in the experiment.

RESULTS

Floor Occupancy

The mean floor occupancy for the duration of the experiment as shown in Fig.2a was below 50% with the occupancy pattern varying each day of the week. Highest floor occupancy as shown in fig. 2b during working hours(7am-7pm) was recorded on Tuesday and the lowest was recorded on Thursday. Participants were at their workspace 64% of the time when present on the floor as shown in Fig. 3, 6% of the time at locations such as meeting rooms and printing areas while for the remaining 30% of the time participants were at other informal locations on the office floor.

**Though 18 employees participated, only data from 16 participants was used in this study*

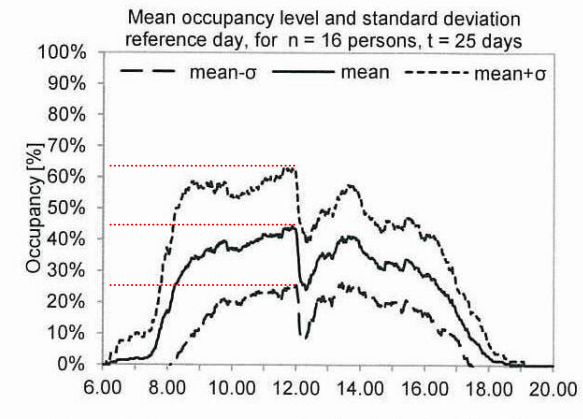

Figure 2[a]:Mean occupancy level

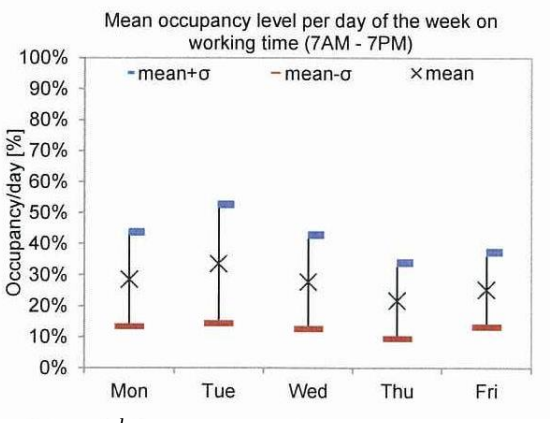

Figure 2[b]:Mean occupancy per weekday

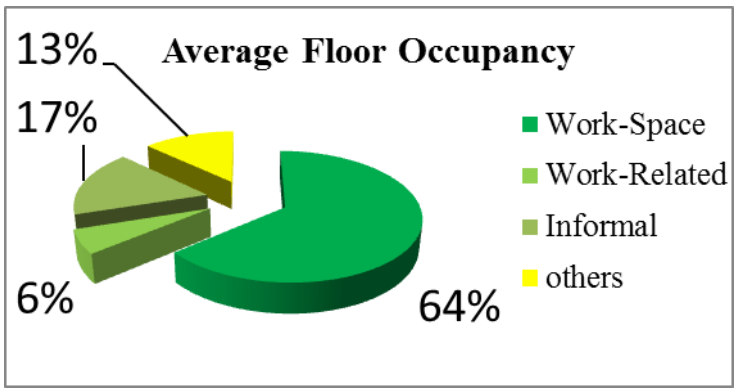

Figure 3: Occupancy distribution on test floor

Correlation between appliance use and human occupancy

Comparison between average occupancy profile and use of electrical appliances for the duration of the study revealed a strong correlation with a determination coefficient of 0.94 see Fig 4. On the workspace level, comprising mostly work appliances (personal computers) the correlation was weak see Fig 5.

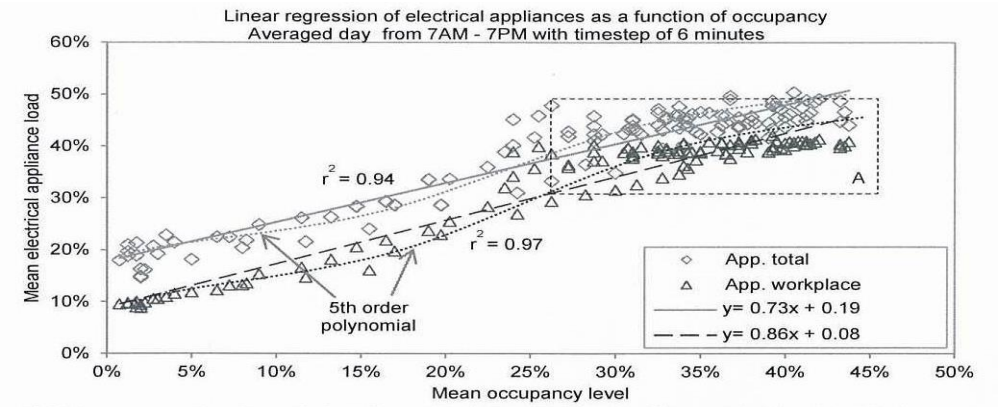

Figure 4: Linear regression of use of all appliances) and electrical appliances on workplace level as a function of mean occupancy level on floor level

It was observed that during lunch and coffee breaks, appliance energy usage on the workspace showed no significant change despite the absence of large percentage of participants from their workspaces at the time. This collaborates with the weak correlation between energy use by appliance and occupancy on the workspace level.

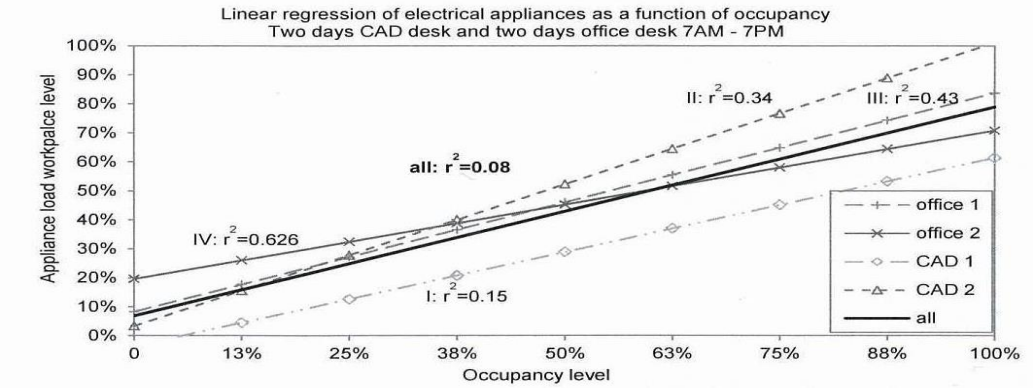

Figure 5: Linear regression for the use of electrical appliances on workplace level as a function of the occupancy level for two reference days

DISCUSSION

Presence Detection Accuracy

18 employees participated in this study through the complete duration. The accuracy of the RFID occupancy detection system was compared against the ground truth, times when participants registered presence at their workspaces during the course of the study. This was found to be 85% as against 100% in some other studies [11] in which user behaviour in the use of tags was not considered. Participants were randomly chosen to be tagged and no incentive was given for been tagged. There were therefore times in the course of the study that some participants were present on the floor but without tags. Also, faulty tags resulted in the exclusion of data from 2 participants. Though a representation of a typical Dutch office building, as no two workplaces as exactly the same [16], these results cannot be generalized for use in other office buildings [6].

CONCLUSION/FUTURE WORK

Opportunity to Improved Efficiency

It was one of the objectives of this study to identify opportunities to improve energy efficiency in the case study building, particularly in the use of HVAC and lighting systems for subsequent retrofitting. Being a typical office building, the HVAC and lighting systems are totally disconnected from human occupancy resulting in inefficient use of energy. The control strategy in use is dictated based on assumed occupied and unoccupied periods with no consideration for times during working hours when the floor is unoccupied. Most rooms on the floor were maintained at the same thermal comfort level despite no human occupancy during the duration of the study. Optimal use of daylight as shown from various studies [2] could also improve energy savings as against the current strategy which is based on assumed occupancy profiles.

The positive correlation between occupancy rate and electricity use on the floor presents the opportunity for worthwhile energy savings. Implementing control strategies dictated based on human presence in rooms on the building floor would significantly improve the buildings energy efficiency. At the moment further research is ongoing to implement a demand-driven multi-agent control strategy which would align HVAC and lighting systems use with occupancy.

ACKNOWLEDGEMENT

The employees of Royal Haskoning DHV B.V. Rotterdam Netherlands are gratefully acknowledged for their supporting through the duration of this study.

REFERENCES

1. Lakshmi V. T., Sunil K. G., Dipanjan C., 'Softgreen : Towards energy management of green office buildings with soft sensors', COMSNETS conference proceedings, 2012.
2. Klein L., Kwak J. , Kavulya G., Jazizadeh F., Becerik-Gerber B., Varakantham P., Tambe M., 'Coordinating occupant behaviour for building energy and comfort management using multi-agent systems', Automation and Construction Vol. 22, pp:525-536, 2012.
3. Martani C., Lee D., Robinson P., Britter R., Ratti C., 'ENERNET: studying the dynamic relationship between building occupancy and energy consumption', Energy and Buildings Vol. 47, pp: 584-591, 2012.
4. Zeiler W., Boxem G., Maaijen R., 'Wireless sensor technology to optimize the occupant's dynamic demand pattern within the building', ICEBO conference proceedings, 2012.
5. Page J., Robinson D., Morel N., Scartezzini J.L., 'A generalized stochastic model for the simulation of occupant presence', Energy and Buildings Vol. 40(2), pp: 83-98, 2007.
6. Oldewurtel F., Sturzenegger D., Moraro M., 'Importance of occupancy information for building climate control', Applied Energy Vol. 101, pp: 521-532, 2013.
7. Mahdavi A., 'The human dimension of building performance simulation', Building Simulation, IBPSA conference proceedings, 2011.
8. Nguyen T. A., Aiello M., 'Energy intelligent buildings based on user activity: A survey', Energy and Buildings Vol. 56, pp: 244-257, 2013.
9. Kwok S. K., Lee E.W., 'A study of the importance of occupancy to building cooling load in prediction by intelligent approach', Energy conversion and management Vol. 22, pp: 2555-2564, 2011.
10. Melfi R., Rosenblum B.,Nordman B., Christensen K., 'Measuring building occupancy using existing network infrastructure' IGCC conference proceedings, 2011.
11. Lee S., Ha K., Lee K., 'A pyroelectric infrared sensor-based indoor location-aware system for the smart home', IEEE Transaction on consumer electronics Vol. 52(4), 2006.
12. Li N., Calis G., Becerik-Gerber B., 'Measuring and monitoring occupancy with an RFID based system for demand-driven HVAC operations', Automation in Construction, Vol. 24, pp: 89-99, 2012.
13. Dong B., Andrews B., 'Sensor-based occupancy behavioural pattern recognition for energy and comfort management in intelligent buildings', IBPSA conference Proceedings, 2009.
14. Erickon L. V., Achleitner S., Cerpa A., 'Power–efficient occupancy-based energy management system', IPSN conference proceedings, 2013.
15. Khoury H.M., Kamat V. R., 'Evaluation of position tracking technologies for user localization in indoor construction environments' Automation in Construction Vol.18, pp: 444-457, 2009.
16. Bruintjes M., Kokkeler A. B., Karagiannis G., Smit G. J., 'Survey of energy efficient tracking and localization techniques in buildings using optical and wireless communication media'. Available from: http://caes.ewi.utwente.nl [Accessed: 25th April 2013]
17. Harle R. K., Hopper A., 'The potential for location-aware power management', UbiComp conference proceedings, 2008.

WEB-OF-THINGS GATEWAYS FOR KNX AND ENOCEAN NETWORKS

Gérôme Bovet[1,2]; Jean Hennebert[2,3]

[1]*LTCI, Telecom ParisTech, 46 rue Barrault, 75013 Paris, France*
[2]*CoSI, HES-SO//Fribourg, Bd. de Pérolles 80, 1700 Fribourg, Switzerland*
[3]*DIUF, University of Fribourg, Bd. de Pérolles 90, 1700 Fribourg, Switzerland*

ABSTRACT

Smart buildings tend to democratize both in new and renovated constructions aiming at minimizing energy consumption and maximizing comfort. They rely on dedicated networks of sensors and actuators orchestrated by management systems. Those systems tend to migrate from simple reactive control to complex predictive systems using self-learning algorithms requiring access to history data. The underlying building networks are often heterogeneous, leading to complex software systems having to implement all the available protocols and resulting in low system integration and heavy maintenance efforts. Typical building networks offer no common standardized application layer for building applications. This is not only true for data access but also for functionality discovery. They base on specific protocols for each technology, that are requiring expert knowledge when building software applications on top of them. The emerging Web-of-Things (WoT) framework, using well-known technologies like HTTP and RESTful APIs to offer a simple and homogeneous application layer must be considered as a strong candidate for standardization purposes. In this work, we defend the position that the WoT framework is an excellent candidate to elaborate next generation BMS systems, mainly due to the simplicity and universality of the telecommunication and application protocols. Further to this, we investigate the possibility to implement a gateway allowing access to devices connected to KNX and EnOcean networks in a Web-of-Things manner. By taking advantage of the bests practices of the WoT, we show the possibility of a fast integration of KNX in every control system. The elaboration of WoT gateways for EnOcean network presents further challenges that are described in the paper, essentially due to optimization of the underlying communication protocol.

Keywords: Smart Buildings, Web-of-Things, RESTful, KNX, EnOcean, Gateways

INTRODUCTION

In recent years, building management systems (BMS) have become very common in various types of buildings, such as offices, manufactures or even private households. Motivated by raising energy costs and by the importance of the comfort, complex management strategies have been developed. Modern BMS include many kinds of sensing and actuating devices, managing the HVAC (Heating, Ventilation and Air Conditioning), the lightening, doors opening, windows and blinds control, and also security access systems. Buildings have become "smart" and are now including complete information systems using dedicated building management networks for communication, as for example KNX, BACnet, or LonWorks. KNX is actually the most used network in Europe. Another emerging standard for interconnecting sensors and actuators in buildings is EnOcean, principally

based on energy harvesting wireless technologies. Unfortunately, such building management networks do not offer a standardised way to interact with devices connected to them from an application point of view. Due to this, it becomes difficult to build BMS combining multiple networks. This situation can be found in buildings where the network should evolve with new devices that are not compatible with the actual one, or where extending the wiring is not feasible because of physical constraints [1]. This is leading to heterogeneous building management networks. While it exists gateways encapsulating the specific telegrams of the building management network in IP packets, there is actually no standard at the application level, resulting in the BMS having to understand and to implement every network protocol.

Looking now at Internet and Web technologies, so called Web services are nowadays widespread, able to make heterogeneous information systems (IS) interoperable. They are platform independent and use well-known standards for structured data exchange. The Simple Object Access Protocol (SOAP) is an example of Web service protocol specification relying on Extensible Markup Language (XML) for its message format and Hypertext Transfer Protocol (HTTP) for message negotiation and transmission. Unfortunately SOAP is not well suited for accessing sensors and actuators that present severe constraints in terms of memory and computing capacities. On the other hands, so-called Internet Of Things (IoT) paradigms are now emerging to qualify small IP based communicating devices. The latest development of IoT includes applications layers defining somehow how programming interfaces can be elaborated on top of the HTTP protocol. This extension of IoT principles is called Web-of-Things (WoT), offering new ways for accessing things in a resource-oriented architecture (ROA) [3].

Trying to ease the development of applications using KNX devices has been explored in different works. A first attempt was realized with the BCU SDK [4], which consists of a script generating C++ classes representing devices capabilities. A more Web oriented approach has been realized in [5]. The principle was to expose KNX functionalities as Web services by using the oBIX (Open Building Information Exchange) standard, which is a special XML schema for representing building data and operations. Unfortunately, oBIX is not at all widespread in BMS, probably because of its relatively complex XML schema. In addition to this, the proposed implementation does not allow an easy integration of the gateway in an existing environment, requiring an important configuration effort for large networks.

THE WEB-OF-THINGS

The Web-of-Things framework fills the gap left by the Internet-of-Things regarding the application layer [2]. It is leveraging on well-accepted standards of the Web to build Application Programming Interfaces (APIs) to things. In this framework, things are representing resources identified by URLs and manageable using the verbs of the HTTP protocol to form the so-called RESTful APIs. In the WoT, every capability or property of a device is considered as a resource. For example, a temperature sensor could return the measured value both in Celsius and in Fahrenheit. More precisely, some resources can allow multiple operations as read and write. So, we first need to be able to identify and address those resources in a simple way before we can interact with them. This is realized by using URLs in the same way as for retrieving Web pages on servers. An advantage of this approach is in its hierarchical way to organize resources reflecting the physical world. This principle is

shown in figure 1. For accessing the Celsius temperature value, one would use the following URL: *http://<DOMAIN>:<PORT>/generic-nodes/1/sensors/temperature/celsius*.

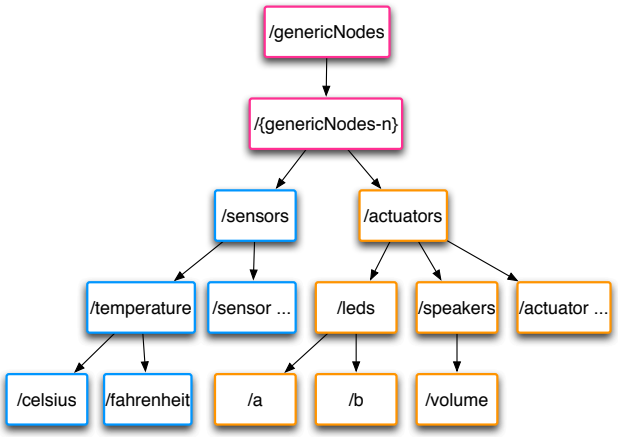

Figure 1: Resource hierarchy example of an abstract node

The domain part of the URL also allows to be hierarchically structured to match a virtual abstract structure or a real physical organization. In the case of buildings, URLs can give insights on the location of devices inside the organization by decomposing it into sub-domains according to buildings, floors and rooms. For communicating with endpoints, RESTful APIs are really the communication and application layers in the WoT by leveraging the HTTP protocol. Unlike SOAP, HTTP is used as application protocol and not only for transport. REST has several advantages over SOAP by having less overhead and being resource oriented, which fits naturally with physical objects. With the WoT paradigm, every object or thing is embedding a Web server exposing an API for acting with its sensing, actuating and configuration capabilities. Those services are located through the URLs as explained previously. The interaction with the resources is achieved by sending HTTP requests containing a so-called HTTP verb that can be one as follows: GET, POST, PUT and DELETE. These verbs reflect actions that can be performed on resources. The GET is for retrieving information (e.g. read a sensor's value) and POST to modify information (e.g. actuating a relay) on a resource. They are in the context of WoT the most used ones.

MAPPINGS TO RESTFUL APIS

As previously outlined with WoT paradigms, every object is expected to embed a REST server offering an API located through URLs for interaction. Unfortunately this approach can not be applied as such to most building networks. Devices connected to KNX or EnOcean network have no IP address and therefore will not be accessible by using URLs. A way of filling this gap is to propose a gateway exposing devices functionalities in the form of RESTful APIs. The gateway will hide the complexity of the building networks and allow clients to interact with attached devices in a Web-of-Things manner. In other words, the devices will appear to other participants of the WoT as they would be embedding the API on themselves.

From KNX

KNX describes device capabilities in terms of datapoints (communication endpoints of devices, standardized data type and size) that are located inside group objects involved in group communications between producers and consumers, basing on a multicast approach. All this information is stored inside the ETS archive file coming from the ETS configuration software. This archive contains several XML files describing the topology of the network, device datapoints and all related group objects including addresses. In order for the gateway to work with a more appropriate and smaller file, a XSL transformation is performed when the archive is loaded to filter unnecessary information. From the resulting XML file, we are now able to map KNX group endpoints to REST services. The URL of each group object is composed as follows: http://<GROUP_NAME>.<LOCATION>. <ORGANIZATION_DOMAIN>/<DATAPOINT>. Here is an example when applying this scheme for an archive file issuing from the KNX network of the EPFL's LESO building for controlling lighting: *http://light..office005.ground.leso/dpt_switch*. By emitting an HTTP GET request, one will read the actual status of the light (on or off), while a HTTP POST will allow to turn it on or off according to the payload data.

From EnOcean

Altough EnOcean is very easy to install and configure by simply pairing devices, the mapping to REST services is more complicated than KNX. This is due to the fact that the EnOcean network is not configured or managed by a central application as ETS. The pairing of devices to form groups is done by users putting actuators in a teach-in mode, while triggering a learn telegram on sensors that have to drive the actuator. All the knowledge is stored inside the devices and there exists no possibility to retrieve it from the devices. As a consequence of this, it is not possible to automate the mapping of the EnOcean network. The user has to reproduce the configuration inside the gateway through a Web interface. However the gateway can automatically detect unknown sensors having sent a learn telegram. The user can edit the related information, set the device type, add actuators and eventually associate them together to build groups. At the time of writing this paper, only the reading of values has been explored. Unlike KNX, EnOcean sensors are not addressable so that it is not possible to read the actual value. To bypass this problematic, the gateway will respond to a read request with the latest value sent by the sensor. The URL for each sensor is composed as follows: http://<SENSOR_NAME>.<LOCATION>. <ORGANIZATION_DOMAIN>/<SHORTCUT>. The shortcut designates the data to read, as EnOcean sensors can report various kind of data like temperature, humidity in one telegram. Shortcuts are defined in the EnOcean Equipment Profile (EEP) specification. EEP are similar to KNX endpoints. Here is an example of an URL mapping to a temperature and humidity sensor: *http://air.office005.ground.leso/tmp*.

Common functionalities

For each gateway, the REST APIs are extended with common functionalities, especially thought for reactive and proactive BMS. The first extension is the discovery of groups and device capabilities. Clients can do GET request on URLs only pointing to a location. The gateway will answer with all sub-locations or devices available in the specified location. One can also ask about the available datapoints/shortcuts for a specific device by putting the .../* placeholder at the end of the URL.

The notification paradigm is used to inform clients as soon as a value of a sensor changes.

This is achieved by a client registering on a resource and furnishing the callback that have to be called by the gateway. One has to put the *.../[un]register* keyword at the end of an URL pointing to an endpoint (e.g. *http://air.office005.ground.leso/tmp/register*).

At last, and specific for proactive BMS, clients can announce their need for storing history data on the gateway, and retrieve it later. For doing this, a client will interact with the *.../storage* sub-resource of an endpoint. It can then decide to add or remove the storage by putting the *add/remove* keywords and indicating the history size in days in the payload (e.g. *http://air.office005.ground.leso/tmp/storage/add*). Clients have then two ways for retrieving the history data. The first is by indicating the number of days one wants to go back in the history with the URL: *.../storage?days=X*. The second one is by specifying a period of time with a start and end date as follows: *.../storage?from=X&to=Y*.

IMPLEMENTATION AND EVALUATION

We implemented both gateways on a Raspberry Pi Model B micro-controller with 512MB of memory. This tiny computer offers several ports like RJ45, HDMI and two USB. For the KNX gateway, our implementation relies on the *Calimero 2.0* Java library, providing classes and methods for KNXnet/IP tunnel communications, and datapoint object representation. The Web part of our application is composed of a Java servlet running on a *Jetty* server, known for being lightweight and optimized for constrained devices. The database is running on MySQL. As shown in figure 2, we base our implementation for KNX on several logical modules shared in different scenarios of use. The first one is the configuration of the gateway, where the administrator will provide all the necessary information for proper running. Once configured, the gateway enters in its normal operation where it can serve requests for manipulating group objects. The architecture and working of the EnOcean gateway is very similar as for KNX.

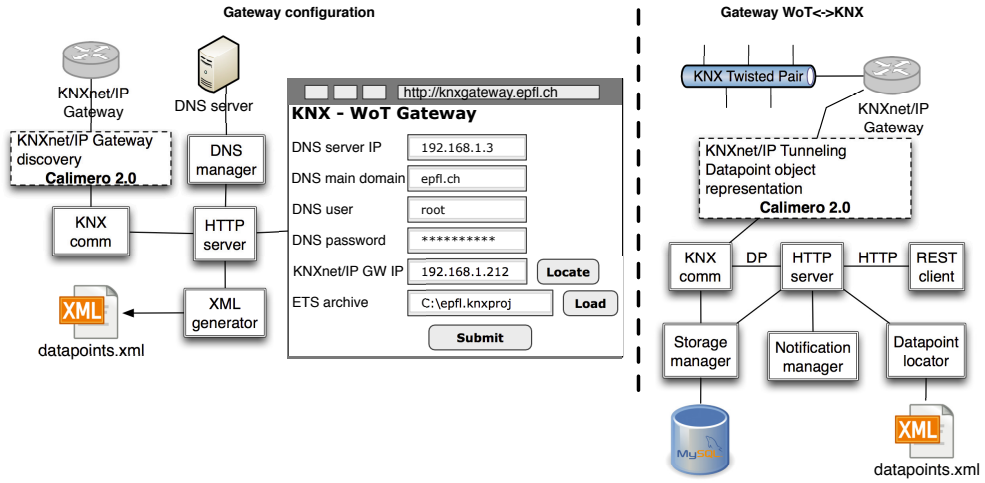

Figure 2: Overall KNX-WoT gateway architecture illustrating the logical modules for two scenarios: gateway configuration (left part) and gateway normal operation (right part).

At the time of writing this paper, the EnOcean gateway not yet being terminated, only the KNX one has been evaluated. We proceeded two categories of evaluations: relative to performance and the usability of the gateway. We evaluated the performance of the KNX gateway with the network of the LESO building composed of 265 devices distributed in 765 groups. Table 1 shows the results we obtained, and that can be considered as

totally acceptable for such an installation. At last, three developers tested the ease of integration of KNX using our gateway. Their feedback was very positive by admitting that our gateway offering RESTful APIs allows to significantly reduce the development time of an application as it would be the case if they would need to implement the KNX protocol.

Measure type	Result
Maximum HTTP requests per second	45
Maximum simultaneous HTTP requests	620
Average event reaction time	33 [ms]

Table 1: Gateway performance measured on a KNX installation running 265 devices

CONCLUSION

Inspired by Web-of-Things paradigms, we explored the feasibility and benefits of using well-known web standards like HTTP and RESTful APIs to interface KNX/EnOcean networks and building management systems. We proposed an architecture for a KNX-WoT gateway that has been validated through an implementation on a low-cost Raspberry Pi and validated on a realistic KNX configuration. Positive feedbacks were also returned by developers of building management systems thanks to the simplicity of use of WoT APIs. Generally speaking, we believe that WoT approaches are good candidates to facilitate the integration of heterogeneous networks. We also believe that building management systems will have to dialogue with various networks in a near future as new technologies are emerging, such as for example EnOcean. Our future works will cover security aspects of the gateway through authentication and encryption of data to prevent misuse.

ACKNOWLEDGEMENTS

This work was supported by the research grant Green-Mod of the Hasler Foundation and the research grant EE-WoT of the HES-SO.

REFERENCES

1. G. Bovet and J. Hennebert. The web-of-things conquering smart buildings. volume 10s/2012, pages 15–19. ElectroSuisse, 2012.
2. D. Guinard. *A Web of Things Application Architecture – Integrating the Real-World into the Web*. PhD thesis, ETHZ, 2011.
3. D. Guinard, V. Trifa, F. Mattern, and E. Wilde. From the internet of things to the web of things : Resource oriented architecture and best practices. In D. Uckelmann, M. Harrison, and F. Michahelles, editors, *Architecting the Internet of Things*, pages 97–129. Springer Berlin Heidelberg, 2011.
4. W. Kastner, G. Neugschwandtner, and M. Kögler. An open approach to eib/knx software development. In *Fieldbus Systems and their Applications*, pages 255–262, 2005.
5. M. Neugschwandtner, G. Neugschwandtner, and W. Kastner. Web services in building automation: Mapping knx to obix. In *Proc. of the 5th IEEE International Conference on Industrial Informatics*, volume 1, pages 87–92, 2007.

A BUILDING ENERGY MANAGEMENT SYSTEM BASED ON DISTRIBUTED MODEL PREDICTIVE CONTROL

A. Lefort[1,2], H. Guéguen[1], R. Bourdais[1]; G. Ansanay-Alex[2]

[1]*Hybrid System Control Team, SUPELEC - IETR, Avenue de la Boulaie - CS 47601, F-35576 Cesson-Svign Cedex, France antoine.lefort, herve.gueguen, romain.bourdais@supelec.fr*
[2]*Energy and Environment Department, CSTB, 84 Avenue Jean Jaurès, Champs-sur-Marne, 77447 Marne-la-Vallée Cedex 2, France*

ABSTRACT

The electrical system is under a hard constraint: production and consumption must be equal. The production has to integrate non-controllable energy resources and to consider variability of local productions. Energy demand is still increasing with larger variability. While buildings are one of the most important energy consumers, they can also be considered as important actors in this problem. Indeed, they have various storage capacities at their disposal : thermal storage, hot-water tank and also electrical battery. The emergence of information and communication technologies (ICT) in the building integrates them as important consumer-actor players in smart-grid. They have the potential to shift, to reduce or even to store [1]. But to ensure their efficiency, it is necessary to develop building energy management (BEM) systems which can interact with the grid and control the building and its systems [2].

In this paper, a BEM system based on distributed predictive control is proposed. The idea is to schedule the actions of the various controllable systems to minimize the energy cost while maintaining the occupant comfort and systems constraints. This scheduling is based on the knowledge of the future data profiles as well as the future cost of energy. The cost reduction is ensured by means of the building storage capacities and by shifting the house consumption periods if the future price is high. Each building is different from another, because of its construction, its systems and its occupants. Consequently, BEM systems have to be modular. This point is ensured by its distributed architecture: one agent is dedicated to each controllable system, and a coordinator agent ensures an optimized global behavior.
Keywords: Building Energy Management, Distributed Model Predictive Control, Load Shedding, Peak Reduction

METHOD

Nowadays, the interest to develop a control for building is to give it the ability to shift or erase its grid consumptions in order to save money and/or reduce its consumption. All this, while ensuring the occupant comfort and system constraints. For that, it is necessary to integrate all the controllable building systems in a BEM system which disposes of a global view.

System formulation

The proposed method is based on a system view of the building installation. It considers that each building system has its own objective and constraints to satisfy. For example, a heating system can be seen as a producer unit, with capacities constraints, which has to ensure the thermal comfort on the building. From a control point of view it is defined as:

Problem 1 Heating System problem :

$$\text{minimize } J = \int_0^H C(t).P_{hp}(t)dt \qquad (1)$$

with respect to $\forall t \in \mathbb{R}$

$$\begin{aligned} Q_{hp}(t) &= \eta P_{hp}(t) \\ \dot{T}_{ambiant}(t) &= f(T_{ambiant}(t), Q_{hp}(t), B_d D(t)) \\ \underline{P_{hp}} \leq P_{hp}(t) &\leq \overline{P_{hp}} \\ \underline{T} \leq T_{ambiant}(t) &\leq \overline{T} \end{aligned} \qquad (2)$$

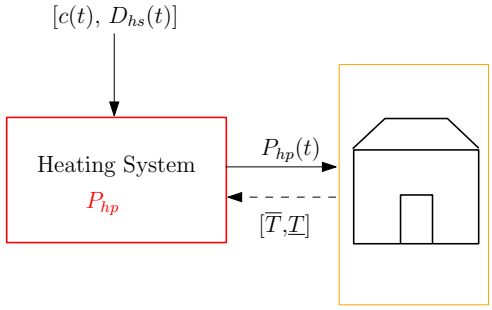

Figure 1: System view example.

where $C(t)$ depends on the control objective. Here, it is supposed to be the time varying energy price. $Q_{hp}(t)$ is the thermal heating power provide through the heating system $P_{hp}(t)$, $T_{ambiant}(t)$ is the internal building temperature, $D(t)$ is the uncontrollable thermal gain variable, f is the thermal dynamics coefficients function while $\underline{T}$, $\overline{T}$, $\underline{P_{hp}}$ and $\overline{P_{hp}}$ are the temperature and power limits.
From this system view, we define a MPC problem in order to optimize the system consumption during the day.

MPC problem formulation

The model predictive control approach refers to a class of control algorithms that compute a sequence of control moves based on an explicit prediction of outputs within some future horizon.
It consists in solving an optimal control problem, on a finite time horizon knowing the system dynamic models and constraints on states and control variables. Figure 2 sums up the MPC control principle.
Thereby, considering an horizon H, all the equations are discretized at a sampling time T, which is an integer divider of the receding horizon such as $N = \frac{H}{T}$. This leads to define the MPC problem formulation of the example Problem 1.

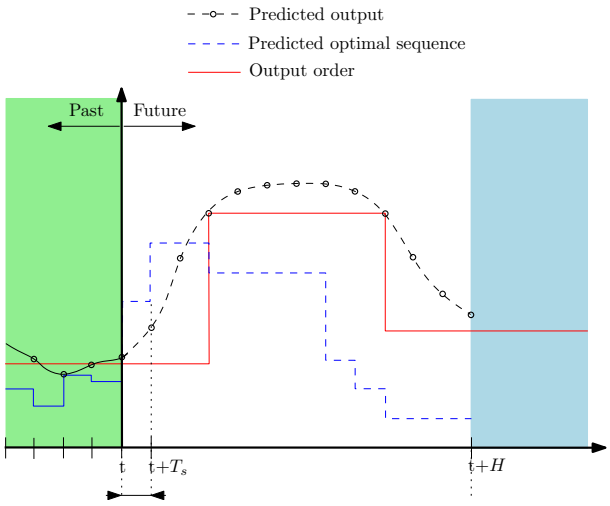

Figure 2: Principle of model predictive control

Problem 2 Heating System MPC problem :
At a time $t = k.T$, given:

- $T_{ambiant}(t)$: the current states of the system
- $D_{hs,T}$ and C_T : the uncontrollable variables and the time varying price at the instant

$[t, t+H]$ such as $D_{hs,T}(k) = D_{hs}(t+k.T)$ with $k \in \{0, \ldots, N-1\}$.

and known f_T the discretized dynamics coefficients function of the systems at the sampling time T.
The optimization problem is:

$$\min_{\mathbf{P_{hp}}(0,\ldots,N-1)} J = \sum_{j=0}^{N-1} c(j).\mathbf{P_{hp}}(j) \tag{3}$$

with respect to $\forall k \in \{0, \ldots, N-1\}$:

$$\begin{aligned} Q_{hp}(k) &= \eta \mathbf{P_{hp}}(k) \\ T_{ambiant}(k+1) &= f_T(T_{ambiant}(k), Q_{hp}(k), D_{hs,T}(k)) \\ \underline{P_{hp}} \leq P_{hp}(k) &\leq \overline{P_{hp}} \\ \underline{T} \leq T_{ambiant}(k) &\leq \overline{T} \end{aligned} \tag{4}$$

with $T_{ambiant}(0) = T_{ambiant}(t)$.

Solving the problem provides, at each sampling time T, the command vector $\mathbf{P^*_{hp}}(0, \ldots, N-1)$. Only the first column $\mathbf{P^*_{hp}}(0)$ is sent to the process.
The MPC method enables to anticipate high price period or production period or better systems efficiencies periods. Thus, and thanks to the building storages capacities (walls inertia, batteries, water storage tank, ...), the BEM MPC leads to a shifting strategy [3].

BEM problem

In order to optimize the whole building consumption and to take into account the several interactions between the systems, we formulate the building optimization problem by gathering together all the building installations. Using the previous system view the building optimization problem is formalized as follows:

Problem 3 BEM MPC problem :
The optimization problem is:

$$\min_{\mathbf{U}} J = \sum_{j=0}^{N-1} C(j).\mathbf{U}(j) \tag{5}$$

with respect to $\forall k \in \{0, \ldots, N-1\}$:

$$\begin{array}{ccccccc} E_1 u_1(k) & & & & & = & f_1(k) \\ & \ddots & & & & \vdots & \\ & & E_i u_i(k) & & & = & f_i(k) \\ & & & \ddots & & \vdots & \\ & & & & E_n u_n(k) & = & f_{n_s}(k) \\ A_1 u_1(k) + & \ldots & A_i u_i(k) & \ldots & + A_n u_{n_s}(k) & = & M(k) \end{array} \tag{6}$$

$$
\begin{aligned}
0 \leq h_1 u_1(k) &\leq b_1^{up}(k) \\
&\vdots \\
0 \leq h_i u_i(k) &\leq b_i^{up}(k) \\
&\vdots \\
0 \leq h_n u_{n_s}(k) &\leq b_{n_s}^{up}(k)
\end{aligned}
\tag{7}
$$

such as, E_i, f_i, h_i and b_i^{up} are the dynamics coefficients and constraints $\forall i \in [1, \ldots, n_s]$, A_i refer to the global coefficients and M the global constraints, n_s corresponds to the number of installations.

This (block-angular) problem is effectively solved by the Dantzig-Wolfe method (see [4] for details). This distributed resolution method is exact (gives an optimal solution) and enables to bring modularity to the BEM system control structure (see Figure 3).
Each sub-system is independent, it has its own objective and constraints, and is only connected to the coordinator. The latter has to ensure the global building objective and common constraint.

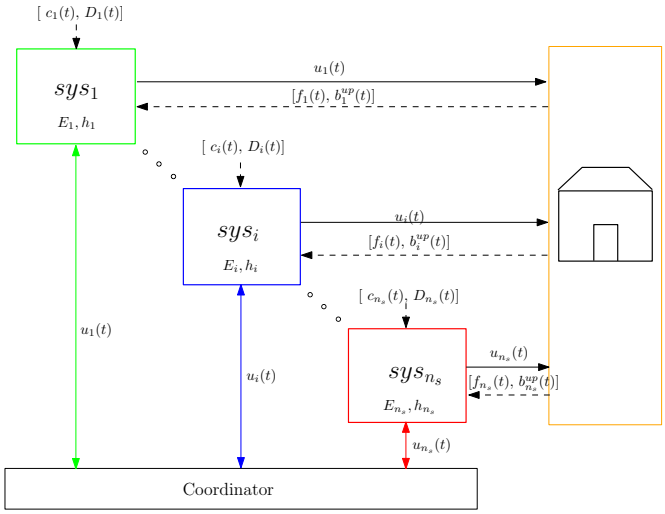

Figure 3: Global system view

The modularity aspect is linked to the system integration. We can note that if we add, delete or modify a system, the concerned system only has to be treated and linked to the coordinator.

SIMULATIONS AND RESULTS

In order to evaluate the adaptability and the efficiency of the proposed BEM control, it has been implemented, in simulation, on two buildings; from one thing the house A, a very inert residential house with very low thermal losses,composed principally of hydraulic radiators, an heat pump (air/water) and a solar water panel combined to a hot water sanitary storage tank; and from another, a high insulated house B with less inertia than the the house A, composed of electrical radiators, a battery, an electrical solar panel and an electric hot water sanitary storage tank.
The simulation scenarii have been performed with disturbances on the data predictions

Daily period (hour)	0 ...	6 ...	13 ...	15 ...	17 ...	19 ...	22 ...
Prices values period	LP	HP	LP	HP	CPP	HP	LP

Table 1: Prices profiles, LP is the Low Price period (0.09€/kWh), HP is the High Price period (0.11€/kWh) and CPP the Critical-Peak Pricing period (0.21€/kWh).

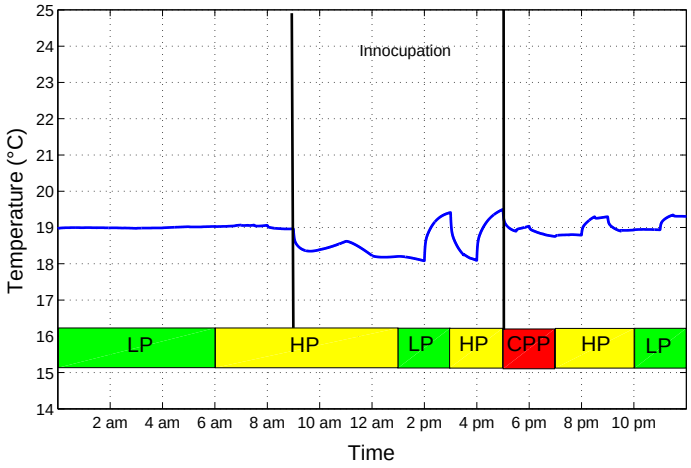

Figure 4: Internal air temperature of the house A regulation

profiles, and the simulation models of the process are not the ones implemented in the controllers but are from the SIMBAD library, a Matlab-Simulink toolbox, dedicated to the building behavior, developed by the CSTB. The temperature set point is set to 19 °C during the occupation period and is free during the inoccupation period.
In this article, we proposed to evaluate the BEMS behavior of the two buildings in response to electricity tariffs profiles.

The simulations results highlight two different strategies. The internal temperature regulation does not vary a lot in the house A (see Figure 4). This is due to its strong inertia and its small heating capacities. Moreover, without electricity storage, the house A regulation is seen as a smoothing strategy even if the hot water tanks are warmed during the LP period.

But, the house B strategy is different. The BEM regulation leads to decrease the temperature until 16 °C during inoccupation period (Figure 5). This is due to its smaller thermal inertia. Moreover, thanks to the battery, the house B changes its heating electrical source and so decreases its impact/consumption on the electrical network. It notes, on figure 6, that the BEM control anticipates the HP periods storing energy in the different systems during the LP period. This leads to shift the building grid consumption. The tariff profile acts as a load shedding strategy.

CONCLUSION

This study proposed an adaptable BEM structure to optimize the energy consumption of residential houses. The modularity is brought by a systemic view combined with a distributed resolution approachs using Dantzig-Wolfe method. For this article, this BEM system architecture, based on MPC, is implemented on two different residential houses.

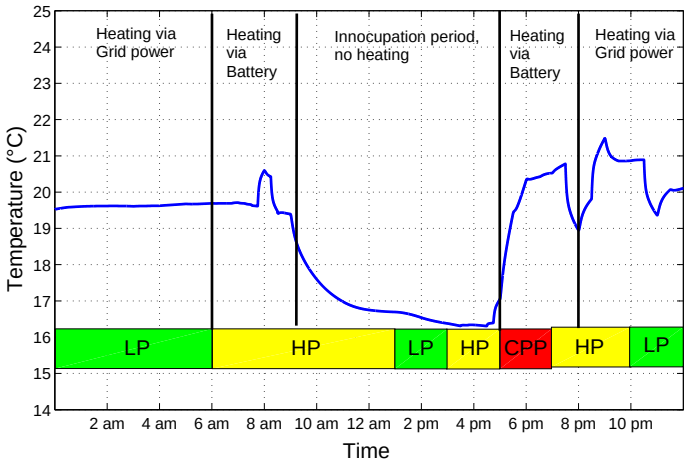

Figure 5: Internal air temperature of the house B regulation

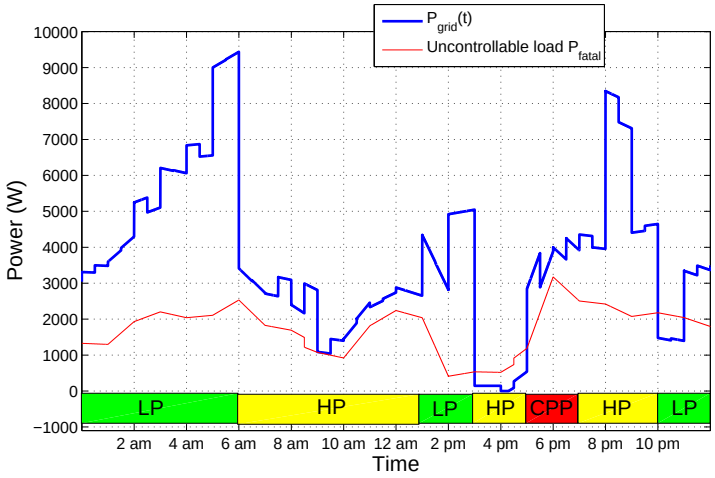

Figure 6: Electrical power consumption P_{grid} from the grid of the house B

The study highlights that the control performance strongly depends on the building characteristics. For a high insulated house with slow dynamic systems, the optimal control results in smoothing of the load, whereas, for a less insulated house with faster dynamic systems, it results in a more reactive control which shifts the peak load consumption.

References

[1] "Le "smart grid" au sein des logements: maitrise de l'énergie et effacement de pointe," tech. rep., Industries du Génie Numérique, Energétique et sécuritaire, 2011.

[2] S.-K. K. S. Heinen, D. Elzinga and Y. Ikeda, "Impact of smart grid technologies on peak load to 2050," tech. rep., International Energy Agency, 2011.

[3] A. Lefort, R. Bourdais, G. Ansanay-Alex, and H. Guéguen, "Hierarchical control method aplied to energy management of a residential house," *Energy and Buildings*, vol. 64, pp. 53–61, 2013.

[4] G. B. Dantzig and P. Wolfe, "Decomposition principle for linear programs," *Operation Research*, vol. 8, pp. 101–11, 1960.

NEUROBAT: A SELF-LEARNING, MODEL-PREDICTIVE HEATING CONTROL ALGORITHM FOR RESIDENTIAL BUILDINGS

D. Lindelöf[1]; A. Guillemin[1]

[1]*Neurobat AG, Industriestrasse 135, 9200 Gossau,* info@neurobat.net

ABSTRACT

We have developed a model-predictive control technology that optimizes the water flow temperature used for heating single-family houses, or small heating zones embedded in larger buildings. Unlike most commercial heating controllers, which typically compute a flow temperature as a function of the (possibly filtered) outdoor temperature, our system forecasts the local climate conditions and achieves near-optimal indoor comfort at reduced energy cost. The algorithm requires no prior parameterization thanks to its adaptive, i.e. self-learning, building model. By regularly sampling the indoor and outdoor conditions, the building model can, after approximately two weeks of operation, forecast the indoor temperature for the next 24 hours and for any given heating schedule with a better than 0.1 degree standard error.

Experimental tests during the 2012–2013 heating season have demonstrated potential energy savings of up to 35%, depending on the type of building. Furthermore, these savings do not compromise the thermal comfort; indeed, we show that the indoor comfort is in most cases improved.

The products that implement our technology are not heating controllers per se; rather, they are add-on modules to an existing heating controller, providing optimal values for the flow temperature as a service to the host controller. Depending on the host controller's capabilities, this optimal flow temperature might be communicated directly (through a building communication bus) or indirectly (via manipulation of the outdoor temperature measured by the host controller).

Keywords: heating controller, model-predictive control, self-learning algorithms

2 THE NEUROBAT TECHNOLOGY

NEUROBAT is a model-predictive control technology derived from several research projects at EPFL [1, 2]. It consists of algorithms that will calculate the exact flow temperature required to bring and keep a building zone to a given indoor temperature setpoint. Continuous measurements of indoor, outdoor and flow temperatures, and of the solar irradiance, lets us build a thermal model of the building under control. This self-learning model requires no prior parameterization and converges to stability in about two weeks.

The algorithm will also build a mathematical model of the local weather conditions, which lets it predict with reasonable accuracy the outdoor temperature and solar irradiance up to 24 hours in advance.

Given the model of the building, and the local weather forecast, the system will then use heuristic algorithms to calculate the optimal heating scenario for the next 24 hours, and

Figure 1: Left: the Ruswil test site. Right: the NIQ installed in Ruswil.

provide this value to the host heating controller. Exactly how this information is provided depends on the capabilities of the heating controller and is beyond the scope of this note.

3 METHODOLOGY

We have fitted 8 buildings in Switzerland with NIQ, an add-on controller that implements our technology and is suitable for legacy heating-curve based heating controllers. It works by shifting the outdoor temperature "seen" by the original heating controller, in such a way as to obtain the optimal flow temperature calculated by the algorithms. The exact control algorithm for the flow temperature is outside the scope of this note.

Of these 8 buildings, 1 turned out to be equipped with a heating controller unsuitable for NIQ. 2 were large 12-appartment buildings in Brigg, on which we did not expect (nor achieve) significant energy savings. 1 is the home of one of our employees which is used for testing new features, not for assessing energy savings.

We have also fitted NBM, a more advanced implementation of the technology, on the north aisle of the CSEM headquarters in Neuchâtel (the so-called JD1 site).

To assess the performance of our technology, we have designed the following experiment:

- The heating season lasts from November 1st, 2012 to March 30th, 2013.
- A given test site will alternate between the NEUROBAT controller and the reference controller.
- The testing period is subdivided in periods of two weeks.
- Each two-week period is randomly allocated to either the reference controller or to NEUROBAT, is such a way that each controller runs for approximatively the same number of weeks.
- For each week, we record the heating energy (through dedicated heat counters).
- Every 5 minutes we record the indoor temperature, the outdoor temperature, the solar irradiance and the flow temperature. Weeks with incomplete data are rejected.

4 DATA ANALYSIS

To avoid needless repetition, we will describe the data analysis only for one site. All the other sites' data have been analyzed in a similar fashion. We choose as our example site the Ruswil site, a single-family, three-story building not far from Lucerne (see Figure 1).

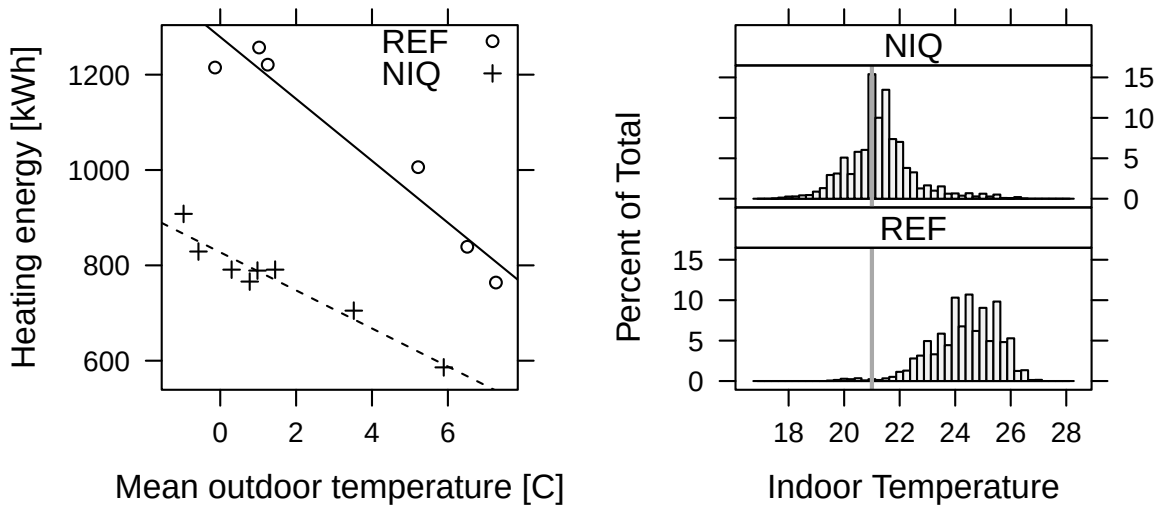

Figure 2: Left: plot of weekly heating energy against average outdoor temperature for the Ruswil site. Each dot represents one week and its shape shows which controller was running that week. Right: histograms of indoor temperatures recorded on the Ruswil site, according to which controller was running. The reference line shows the indoor temperature setpoint.

On the left of Figure 2 we show the relationship between the weekly heating energy and the average outdoor temperature during that week, with a linear best fit going through the data points. On the right we show histograms of the indoor temperature according to which controller was running, with a reference line showing the indoor temperature setpoint chosen by the user (i.e. 21 degrees).

The thermal behavior of a small zone can, to a first approximation, be modeled as two thermal nodes: one representing the indoor temperature, with its thermal capacity; and another representing the outdoor temperature. An equivalent thermal conductivity links these two nodes. For a given time period "sufficiently" long (typically more than one day), one therefore expects the following to be approximately true:

$$E = \alpha \times \overline{t_{\text{out}}} + \beta$$

where E is the heating energy required during that period, $\overline{t_{\text{out}}}$ is the average outdoor temperature during that period, and α and β are coefficients that will, in general, depend on the building's thermal characteristics. In particular, if $E = 0$ then $t_{\text{base}} = -\frac{\beta}{\alpha}$ is the so-called *baseline temperature*, i.e. the outdoor temperature above which the building requires no more heating.

We therefore fit a linear model of the heating energy as a function of the average outdoor temperature, with different slopes and intercepts for each controller. Table 1 shows the estimated coefficients with their standard errors.

The fit is excellent (residual standard error 43.45 on 10 d.f., p-value 6.7e-14, $R^2 > 0.99$). All coefficients are different from zero at the 5% confidence level. Adding more terms to the model does not significantly improve the fit. The intercepts (i.e. the β coefficient) estimate the heating energy required by the building at 0 degrees average outdoor temperature.

Controller	α	β
REF	-65 ± 6	1279 ± 28
NIQ	-40 ± 11	827 ± 18

Table 1: Linear coefficients estimated on the Ruswil site.

Here the value for NEUROBAT is about 35% lower than for the reference controller.

The α coefficient estimates how much extra heating energy is required for each degree less outdoor temperature. The value for our controller is lower in magnitude than for the reference controller, meaning that our controller will require less extra energy for lower temperatures than the reference controller.

Now that we have a suitable model linking the weekly heating energy with the outdoor temperature, we can estimate the energy savings by the following method which we call the *NBS* method:

1. Fit separate models for the reference controller and the NEUROBAT controller.
2. With the reference controller's model, predict how much heating energy would have been used with that heating season's data if only the reference controller had been running.
3. Do the same thing with the NEUROBAT model.
4. Compute the relative difference.

The advantage of this method is that it is completely parameterless. In particular, we make no assumption regarding the building's so-called baseline temperature (i.e., the outdoor temperature above which no heating energy is required. This parameter is needed by, for example, the so-called *degree day* method). It also provides an answer to a very simple question: "How much energy would I have saved this season if I had been running NEUROBAT instead of my old controller?"

Here Ruswil would have used 17.3 MWh with the reference controller but only 11.3 MWh with our controller, i.e. a relative saving of about 35%.

How well does our system keep a comfortable indoor temperature? The right side of Figure 2 shows that our controller is much better than the reference (open-loop) controller at keeping a satisfactory average indoor temperature. The mean indoor temperature is 24.4 ± 1.2 degrees for the reference controller, but 21.3 ± 1.2 degrees for the NEUROBAT controller. NEUROBAT is therefore not only better at keeping the indoor temperature close to the setpoint of 21 degrees, it also reduces the variance of the indoor temperature.

We now show the same plots as in Figure 2, but this time for all the test sites. Plots of energy against mean outdoor temperature are shown in Figure 3, and histograms of indoor temperature are shown in Figure 4. Summary statistics are given in Table 2.

5 DISCUSSION

Our controller achieves significant energy savings (up to 35%) at all sites, except for the Fey single-family home. We later found out that the owner of that house had set the temperature setpoint on the NIQ controller to its maximum value (26 degrees), a value which the existing heat pump was never quite able to honor. Our controller was therefore

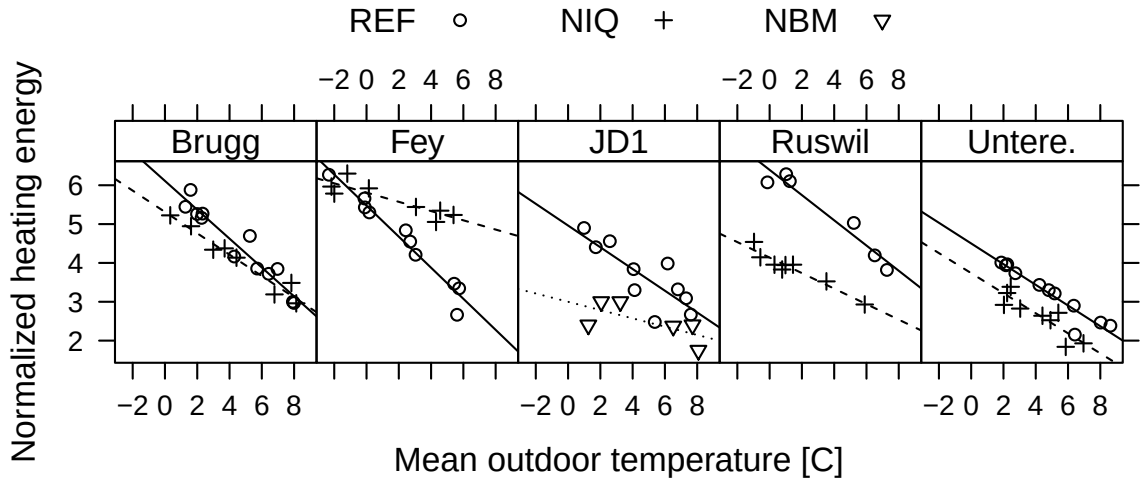

Figure 3: Plots of weekly heating energy against mean weekly outdoor temperature, for all test sites. The heating energy has been divided by each site's approximate heating area to have the same scale.

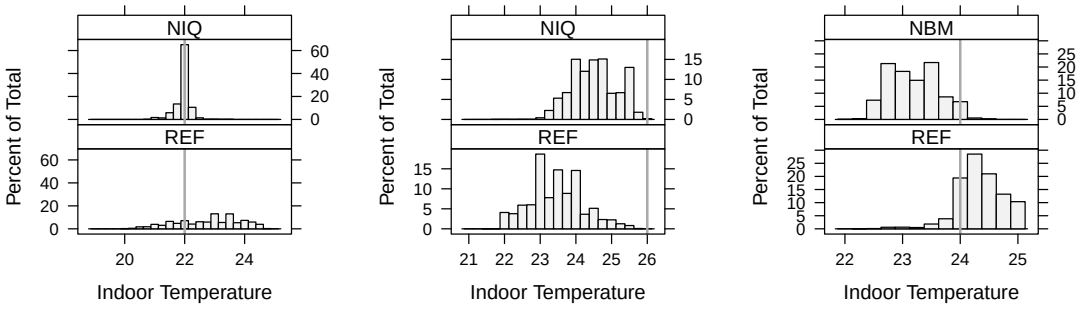

(a) Brugg

(b) Fey

(c) JD1

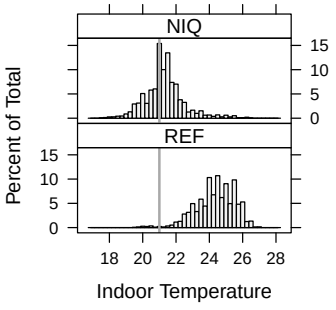

(d) Ruswil

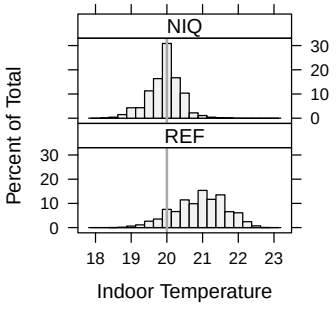

(e) Unterengstringen

Figure 4: Indoor temperature histograms for all test sites. The reference line shows the indoor temperature setpoint.

Site	Ref. energy [MWh]	NB energy [MWh]	Savings
Brugg	18.4	17.9	8%
Fey	18.1	22.1	NA
JD1	73.3	50.1	32%
Ruswil	17.3	11.3	35%
Unterengstringen	14.2	11.0	23%

(a) Heating energy comparison.

Site	Setpoint [C]	Ref. controller	NB controller
Brugg	22	22.8 ± 1.1	22.0 ± 0.2
Fey	26	23.4 ± 0.8	24.5 ± 0.7
JD1	24	24.3 ± 0.4	23.2 ± 0.4
Ruswil	21	24.1 ± 1.3	21.3 ± 1.2
Unterengstringen	20	20.9 ± 0.7	19.9 ± 0.4

(b) Indoor temperature comparison. The third and fourth column give the mean and sample standard deviation.

Table 2: Summary statistics on all test sites.

continuously fighting against the reference controller, who kept an indoor temperature more than 2 degrees lower than the setpoint. We therefore believe that this site's results are not representative.

The indoor temperature has been kept or improved on all sites, none as spectacularly as at Brugg. The worst performance is on the JD1 site, which can be explained by the site being office rooms on five floors of an administrative building. Furthermore, the algorithm running there is an older version; we believe significant improvements can be obtained once we update that site.

We are, overall, very satisfied with the results of this heating season and are confident that this technology can help significantly reduce the energy bill coming from space heating in residential homes.

References

[1] Morel, N.: Neurobat: a Predictive and Adaptive Heating Control System Using Artificial Neural Networks. International Journal of Solar Energy, vol. 21, 2001.

[2] Bauer, M.: Gestion Biomimétique de l'Energie dans le Bâtiment. EPFL Thesis nr. 1792, 1998.

DEVELOPMENT AND TEST OF AN INTELLIGENT WEB-BASED FUNCTIONALITY CHECK FOR SOLAR HEATING SYSTEMS

Sandra Stettler[1]; Bruno Schläpfer[2]; Roger Ruch[3]; André Salathé[3]; Peter Wiesner[3]; Franz Koch[3]; Werner Gut[4]; Thomas Schlegel[5]

1: Egon AG, General Wille-Str. 59, CH-8706 Feldmeilen; energie@egonline.ch; www.egonline.ch

2: Ernst Schweizer AG, Metallbau, Geschäftsbereich Sonnenenergie, Bahnhofplatz 11, CH-8908 Hedingen, info@schweizer-metallbau.ch; www.schweizer-metallbau.ch

3: Industrielle Werke Basel, Margarethenstrasse 40, CH-4002 Basel, info@iwb.ch; www.iwb.ch

4: Steca Elektronik GmbH, Mammostrasse 1, D-87700 Memmingen, info@steca.com; www.stecasolar.com

5: Meteotest, Fabrikstrasse 14, CH-3012 Bern, office@meteotest.ch; www.meteotest.ch

ABSTRACT

Several field studies showed, that up to 1/3rd of the solar thermal systems in Switzerland are substantially less effective than predicted or do not work at all. So far, no effective and well-priced devices exist, which visualise and analyse the solar energy produced by solar thermal systems. In this project we develop a web-based functionality check using measurement data from the solar controller. With the aid of this functionality check, the efficiency of solar thermal systems shall be increased.

The development process started in December 2012 and will be finished in autumn 2013. Until spring 2014, the functionality check will be tested in a field test with 10 solar thermal systems. The project team consists of 5 companies that are experienced as energy engineers, web-programmers, solar system owners, system providers, service staff and manufacturers of controllers and collectors.

The goals of this team are:

- assure an ideal system operation
- support service and trouble-shooting of solar thermal systems
- communicate and visualise the successful operation of the solar systems

The function principle is quite simple: There exist solar controllers on the market that can measure and store all relevant system data e.g. in 1 minute intervals. These data sets are uploaded periodically to a web portal where the intelligent functionality check is hosted. This web portal offers individual functions for system owners, service staff and manufacturers. It visualises the energy production of the system as well as the other measurement data sets. It performs a detailed operating analysis of solar circuit, storages, stagnation, pumps, volume flow and power. The results of these analyses are available for the service staff and give them significant hints for optimising and trouble-shooting the solar systems.

The web-based intelligent functionality check is tested during 12 months of field test with 10 solar thermal systems. Afterwards, the web-portal will also be made available for companies outside the project team.

Keywords: advanced control tool; solar heating systems; innovative solar controller; intelligent analysis algorithms; concurrent meteorological data; online information exchange

INTRODUCTION

Our Motivation: Increase the efficiency of solar thermal systems

Solar thermal collectors can provide a substantial part of the heating energy of a building. But the owners of solar systems are mostly unaware of the amount of solar energy produced daily on their roof. So far, no effective and well-priced devices exist, which visualise and analyse the solar energy produced by solar thermal systems. Such a device is important for the owners, manufacturers and service-providers of solar thermal systems:

- Several field studies showed, that up to 1/3rd of the solar thermal systems in Switzerland are substantially less effective than predicted or do not work at all. With an intelligent functionality-check the operational reliability of solar systems would be enhanced. Amortisation time of the systems could be reduced thanks to higher productivity.
- For photovoltaic systems it is a standard to visualize and control the solar electricity production with data loggers and web portals. This transparency makes photovoltaic systems more attractive to potential customers than solar thermal systems.
- To place a solar thermal system into operation is a difficult task, especially if no information about the actual operating conditions exists. And trouble-shooting gets a time-consuming try and error work if no measurement data are available.

Our Project Team: a strong consortium of engineers, solar system owners and the industry

Thus, five companies have started a common project to develop and test an intelligent web-based functionality-check for solar thermal systems. These companies are:

- Egon AG: An energy engineer office with experience in the development of web-based monitoring and control systems for energy consumption and production.
- Ernst Schweizer AG, Metallbau: One of the main manufacturers of solar thermal collectors in Switzerland. Ernst Schweizer AG also sells complete solar thermal systems, puts them into operation and provides trouble-shooting.
- Industrielle Werke Basel: The energy provider of the city of Basel offers a successful heating contracting. Industrielle Werke Basel owns and operates several hundreds of heating systems for their clients. A substantial part of them is equipped with a solar thermal system.
- Steca Elektronik GmbH: Besides other electronic equipment, Steca Elektronik GmbH manufactures solar thermal controllers. Some of them can store measurement data of all important control points. These data are stored on a SD card or transferred via internet to a web server and thus made available for visualisation and analysis.
- Meteotest: This meteorological office is specialized into web-based meteorological services. An important business segment are services for the solar energy sector.

Besides these five companies, the project is also funded by the SFOE (Swiss Federal Office of Energy).

Our Goals: assure the ideal system operation, support service and trouble-shooting, communicate and visualise the successful operation of solar systems

Together we will develop and test an intelligent web-based functionality check for solar thermal systems. With this check, the following goals shall be reached:

- Assure that the solar thermal systems work properly. Thanks to an ideal regulation of the solar system, the efficiency is enhanced and amortisation time is shortened.
- Support service staff in case of trouble-shooting and putting systems into operation. Thanks to intelligent analyses, the check shall detect failures and potential for optimisation. Early warnings in case of failures prevent from severe long-term damages of the system parts.
- The internet offers multifaceted possibilities to visualise the energy production and successful operation of the system to different user groups: to the service staff and the system owner, but in special formats also to the public, potential customers for solar thermal systems, authorities etc.

METHOD

A Comprehensive Function Principle: Data logging with the existing solar controller; visualisation and data analysis on a web portal with individual functions for system owners, service staff and manufacturers

Main premise for visualisation and analysis of solar thermal systems is the collection of measurement data. This can be performed without any extra costs: Several controller manufacturers (e.g. Steca Elektronik GmbH), offer solar controllers that do not only control the solar thermal system but at the same time store all operating data on a SD card or transmit it via internet to a server of the manufacturer. Typical measurement data are 1-minute values of all relevant temperatures, pumps and switches, often also volume flow and energy production

The measurement data are regularly uploaded to the web-server hosting the functionality check. Additionally, concurrent meteorological data (ambient temperature and solar irradiance) are fetched from weather satellites and nearby weather stations. After each import of measurement data, the measurement values are visualised on the web page and the functionality of the system is checked. The analysis results are made available for the service staff. The web portal also generates yearly PDF-reports for each system, which summarize its energy production and condition.

The development of the web portal started in December 2012 and will be finished in autumn 2013.

12 Months of Field Test with 10 Solar Thermal Systems

The intelligent web-based functionality check is tested until spring 2014 with at least 10 typical solar thermal systems. They are chosen from Industrielle Werke Basel's population of solar thermal systems. All systems will be equipped with a solar controller that can store all operating data in 1-minute intervals. Additionally to the temperatures of the solar collector and the storages, also temperatures of the solar flow and return are measured. To allow for a calculation of the energy production, the volume flow is measured too. Figures 1 to 4 show pictures of some chosen solar systems.

Figure 1: Test system on a flat roof with 36 m^2 collector area. Source: Google Earth

Figure 2: Test system on an inclined roof. Source: Lützelschwab GmbH

Figure 3: Photo of the storage, pump and controllers of a test system. Source: Egon AG

Figure 4: Example of a solar thermal controller. Source: Steca Elektronik GmbH

RESULTS

At the moment (April 2013), the web portal is still in the development phase. Figures 5 and 6 show a few PrintScreens of the actual status of the web portal.

Detailed operating analysis of solar circuit, storages, stagnation, pumps, volume flow and power

All measurement data are aggregated on a daily and monthly basis to provide significant system information for the service staff. Which analyses shall be performed was intensely discussed with service staff for solar thermal systems. Table 1 shows the analyses that are performed for the pump of a simple solar thermal system with just one collector field and one storage. Some of the analysis results have only informative character and are marked as "info". Others detect system failures and are marked as "failure". The analysis methods will be tested and further developed during this project.

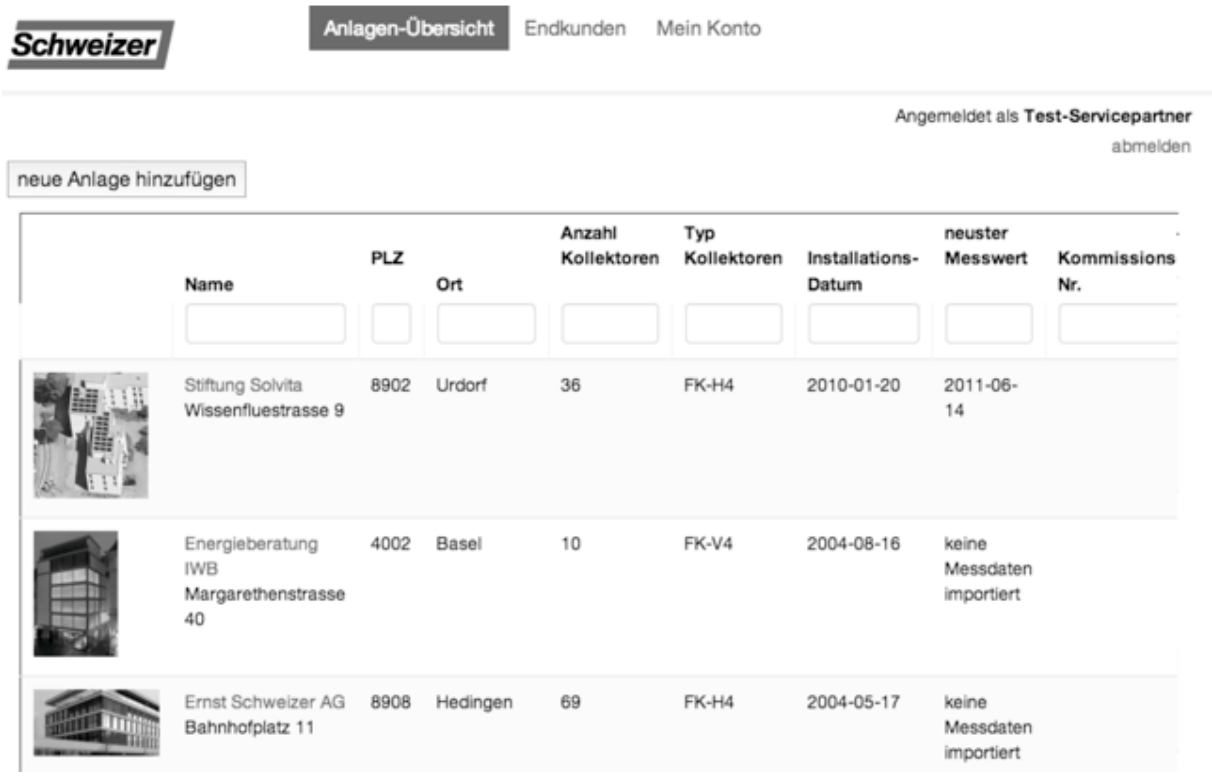

Figure 5: PrintScreen of overview page of the web portal. All solar thermal systems of the logged-in user are presented with photo, name, address and further important information. By clicking on a system, detailed information like measurement data and analysis results can be displayed.

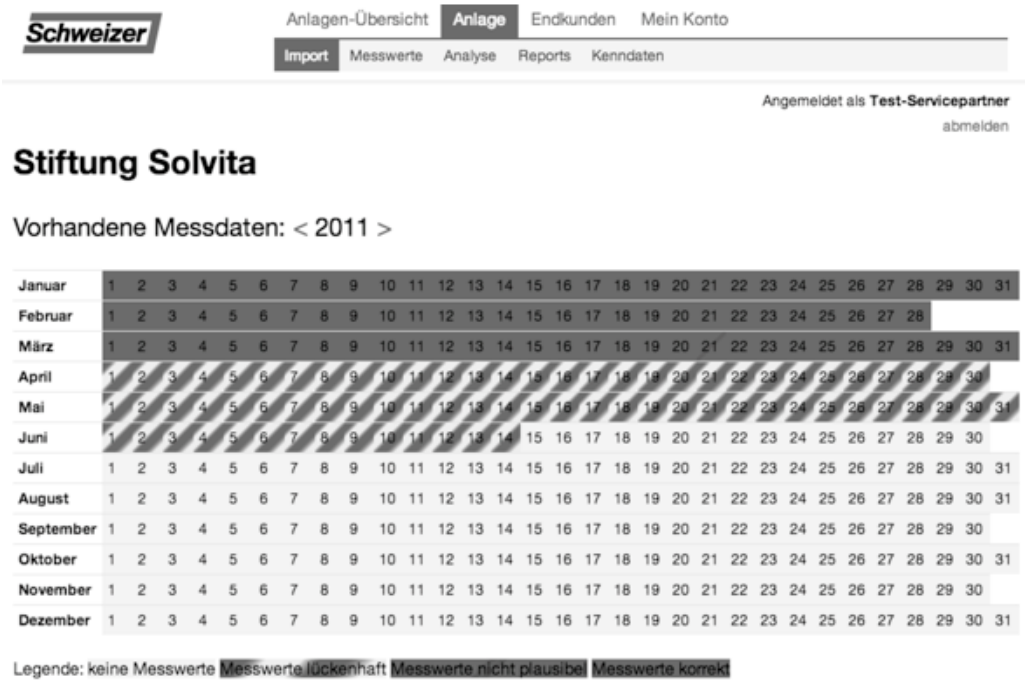

Figure 6: PrintScreen of the "import" page for a chosen solar system called "Stiftung Solvita". At light grey days, no measurement data has been imported yet, at dark grey days measurement data has been imported successfully. At striped days the imported measurement data was not complete. If the imported measurement data would contain non plausible values, such days would be signed with a red cross.

Name	Description	Character
Runtime 100%	Runtime of the pump in hours. Sum of all minutes, during which the pump was 100% (60 seconds) on.	info
Total runtime	Runtime of the pump in hours. Sum of all minutes, during which the pump was on (1 to 60 seconds).	info
Expected runtime	Number of hours, when the irradiance as well as collector and storage temperature indicate that the pump should be on.	info
Pump off despite deltaT	Number of hours during which the pump was off, although storage and collector temperatures indicate that the pump should be on.	failure
Pump on without deltaT	Number of hours during which the pump was on, although the temperature difference between collector and storage was too small to operate the solar system.	failure
Pump on at stagnation	Number of hours during which the pump was on, although the collector temperature exceeded its maximum operating temperature	failure
Pump on when storage full	Number of hours during which the pump was on, although the storage temperature exceeded its maximum temperature.	failure

Table 1: List of the analyses performed for the solar pump of a solar thermal system

A further focus of the tests is the calculation of a reference energy yield based on solar irradiance and ambient temperature with the following formula:

$$Y = A \times R \times \left[I \times \eta_0 \times IAM - a_1 \times \left(\frac{T_F+T_R}{2}\right) - a_2 \times \left(\frac{T_F+T_R}{2}\right)^2 \right] \quad (1)$$

where:
Y = reference yield (Wh)
A = total aperture area of the solar system (m^2)
R = expected runtime (hours)
I = irradiance on collector plane (W/m^2)
η_0 = optical efficiency (-)
IAM = incidence angle modifier (-)
a_1 = 1st order heat loss coefficient ($W/m^2/K$)
a_2 = 2nd order heat loss coefficient ($W/m^2/K^2$)
T_F = temperature of solar flow (K)
T_R = temperature of solar return (K)

The comparison of this reference energy yield with the measured effective yield shall help to detect system failures and to judge the effectiveness of the system.

DISCUSSION & OUTLOOK

The project partners Ernst Schweizer AG and Industrielle Werke Basel will use the intelligent web-based functionality check to improve the efficiency of their solar thermal systems, to simplify service and for trouble-shooting. Through these two companies, the web-based functionality check will also be provided directly to their installers and system owners. Egon AG will provide customized versions of the intelligent web-based functionality check also for other companies.

ADVANCED CONTROL OF ELECTROCHROMIC WINDOWS

N.Zarkadis, N.Morel

Solar Energy and Building Physics Laboratory (LESO-PB), Ecole Polytechnique Fédérale de Lausanne (EPFL), LE 2 200 (Bâtiment/Building: LE), Station 18, CH-1015 Lausanne

ABSTRACT

In our research we use the technology of electrochromic (EC) glazing to maximize the use of daylight and minimize the energy consumption in buildings while preserving visual and thermal comfort of the users. We propose an advanced automatic control of EC windows coupled with an anidolic daylighting system (ADS), blinds and dimmable fluorescent lights. EC windows with a visible transmittance range (Tv) of 0.15 – 0.50 were installed on the southern façade of an office room of the LESO experimental building (EPFL campus in Lausanne, Switzerland). The system is divided in two independent zones: The lower zone is equipped with EC windows and blinds while the upper zone features in addition the ADS, which facilitates the even distribution of daylight across the room. Electric lighting is used only complementary when daylight is not sufficient. Data regarding instantaneous weather conditions, room conditions, as well as user wishes is collected and recorded in the database of the building's central management system (KNX/EIB).

To address visual comfort requirements, a novel sky-scanner approach is implemented into a predictive control strategy to take into account the time the EC glazing requires to switch between different transmission states (up to 15 minutes). For the thermal comfort, we consider a wider time horizon, taking under consideration also the time, day and season. User has always the possibility of manually overriding the automatic control system. Adaptive fuzzy logic algorithms are implemented allowing the system to learn from users' wishes. Simulations showed that the elaborated algorithms for the automatic control of EC windows can provide better thermal and visual comfort conditions when compared to standard glazing coupled with blinds and still exhibit acceptable levels of energy consumption for space heating and electric lighting. Field study results showed that workplane illuminances were mostly kept inside acceptable visual comfort levels (at around 450-1000 lx). Field survey results regarding the acceptance of the system by the users are also presented along with a discussion on the efficacy of an EC windows system to handle glare issues without the use of blinds.

Keywords: electrochromic windows, advanced automatic control, building energy saving, visual and thermal comfort, adaptive and predictive control algorithms, user acceptance

1. INTRODUCTION

The concept of harvesting and using daylight in buildings reflects positively on all three pillars of sustainability: it has a significant energy saving potential; it reduces energy-related costs and it has positive effects on the well-being of building users. Electrochromic (EC) glazing has been commercially available the last few years as an alternative to the combination of standard window glazings with mobile solar shadings (very often discarded by the architects) or to permanently tinted solar protection glazings. EC glazing has the ability of changing dynamically its optical properties and modulating the transmission of visible light and heat solar gains through the window, while maintaining at all times the view towards outside. Several research studies have been carried out during the last few years with regard to the use of EC windows in buildings [1; 2; 3]. In some of these, the visual or thermal comfort

is evaluated through computer simulations or with the use of small-scale models. While this type of research involves an easier setup, is favourable for the study of energy aspects and allows for the execution of different scenarios, it lacks the evaluation of visual or thermal comfort by real persons in real-life situations. In this study we experiment on a full-scale model.

Also, studies carried out until now have essentially considered a manual control of the EC glazing transmission. Some rather elementary automatic control strategies have been investigated, such as the closed loop control based on the measurement of the inside daylighting contribution. Nevertheless, the time characteristics of EC glazing (delayed response of the transmission variation after a command, usually between 5 and 15 minutes) have not been taken into account in these elementary automatic control strategies. In this direction, we developed an optimized control algorithm (which takes account both the energy and the visual comfort aspects), with an innovative short term prediction of incident solar radiation based on a sky-scanner approach and including the user's preferences.

The presented results include an experimental check of the control system on an office room of the LESO Building. This room is equipped completely with EC glazing, both for the lower window and the anidolic daylighting system (ADS). The experimental check has been carried out with real persons, allowing therefore the evaluation of the system by the users. Results of extensive simulations are also presented herein. In these, different control scenarios were tested against a long period of time (one year) and against varying meteorological conditions. The simulations allowed for the comparison of the energy consumption for heating and electric lighting as well as for an estimation of thermal and visual comfort of each case.

2. METHOD

Control algorithm

The developed control algorithm predicts an optimal setting for the EC glazing, the blinds and electric lighting taking into account all the available data on instantaneous weather condition and building state, including data on room occupancy and user wishes/actions, workplane illuminance, internal air temperature. The algorithm predicts this optimal setting at a time horizon corresponding to the EC glazing latency time (5 to 15 minutes). Electric lighting is commissioned only complementary when daylight is not sufficient, while blinds are likewise only employed to protect from glare and/or to avoid overheating when protection from EC windows is not sufficient. A longer time horizon is taken into account for the thermal aspects. Moreover, when the room is occupied priority is given to visual comfort, while if the user is absent the algorithm is optimized for thermal comfort.

To tackle with the issue of the slow switching speed of the EC windows we implemented a predictive algorithm based on image processing of sky images taken by a standard web camera. The camera is placed below the skylight of an office room where it has an almost unobstructed view of the sky. It faces towards the south at a measured angle 'z' from the zenith, making sure the sun trajectory is included in the images taken. A fish-eye lens, capturing the whole sky dome is important and maximizes the prediction window. In this project, no wide angle lens has been used; therefore the prediction window stays at about 5 min. The camera was setup to take automatically images of the sky at fixed time intervals. It was observed that for low or moderate wind speeds the time interval of 1 min is sufficient for the observation of changes in the sky concerning the motion of clouds. However, higher wind speeds require a shorter time interval. The images taken with the camera are stored in the PC and processed in a way that (1) the relative motion of clouds between 2 consecutive images is detected; (2) analysis of the cloud motion using a series of images is performed; (3) the

possibility of clouds to obscure the sun during the next 5 minutes is deducted and passed on to the fuzzy control system [4; 5] so it can issue on time the appropriate commands to the EC windows, blinds and electric lighting.

Simulations

The parametric study allowed for the testing of different control scenarios over a long period of time (one year) and against varying meteorological conditions. Energy consumption for heating and electric lighting as well as estimation of thermal and visual comfort was the output. Simulations were performed using dynamic thermal simulations code that has been developed by LESO laboratory. The code was modified and expanded to include the EC glazing characteristics, the developed control algorithm, electrical lighting features (modules for the calculation of illuminance levels on desktop and energy consumption) and visual and thermal comfort prediction modules. The model used in all simulations was a simplified 13-node model of a South-facing office room similar to the LESO building room where the EC glazing was installed. North, West and East are partition walls adjacent to other offices and the corridor. Ceiling and roof are also adjacent to other offices. The blinds considered are made of textile tissue and they can roll up (completely open) and down (when closed). For the electric light use, the visual and the thermal comfort we consider the presence of a user only during the working hours with a 9-hour daily schedule of 08.00 to 18.00 with a lunch break from 12.00 to 13.00, from Monday to Friday. Window surface was modeled as a single window instead of the coupling of a window with ADS.

The following scenarios of windows of a South-facing office room were compared:
1. Conventional transparent double glazing;
2. Conventional transparent double glazing coupled with blinds and a simple control strategy, depending only on incident solar radiation and season;
3. Solar protection glazing with SHGC=0.38 and Tv=0.50;
4. Solar protection glazing with SHGC=0.12 and Tv=0.15;
5. EC glazing with simple control scheme (same as on 2.);
6. EC glazing with the proposed control algorithm;

Thermal comfort

To calculate thermal comfort, we compare the indoor temperature across the different simulation scenarios. We then analyse thermal comfort using Fanger's model [6]. Using as input for every time step of the simulation the season, the radiant temperature in the room and the room's air temperature, the Predicted Percentages of Dissatisfied (PPD) were generated for every working hour in the year.

Visual comfort estimation

To estimate the visual comfort we build upon the work of Lindeloef regarding the Bayesian optimization of visual comfort [7]. Lindeloef calculates the user's Visual Discomfort Probability (VisDP) as a function of the horizontal workplane illuminance only (no illuminance data was used). Based on his work, we establish the illuminance limits for the VisDP and we evaluate the ability of the simulated case studies to keep the workplane illuminance levels within the ranges which are less likely to cause discomfort to the occupants.

Field measurements and user evaluation

Field tests of the algorithm were not extensive but they allowed for a short check of the elaborated algorithm on the experimental level. Short satisfaction surveys were conducted

with 9 persons who volunteered to spend time inside the office room were the EC glazings are installed. Subjects spent roughly 2 hours in the room (under similar weather conditions for all the persons). They spanned all age groups, both genders (2 female and 7 male) and spent their time doing ordinary desk work (mainly reading from paper, and computer work) facing all possible directions inside the office room (windows, side and back walls).

3. RESULTS

Energy consumption

The results of the simulation study regarding the energy consumption for heating and electric lighting are shown on Figure 1. As expected, standard (clear) glazing permits high solar gains during the winter which results in significantly low energy demand for space heating. In these cases, energy required for electric lighting is also reduced when compared to other cases due to the abundant daylight entering the room (note that LESO building allows important solar gains if no shading is used). However, both cases of standard glazing offer the worst visual and thermal comfort (overheating and extreme illuminance) as seen next.

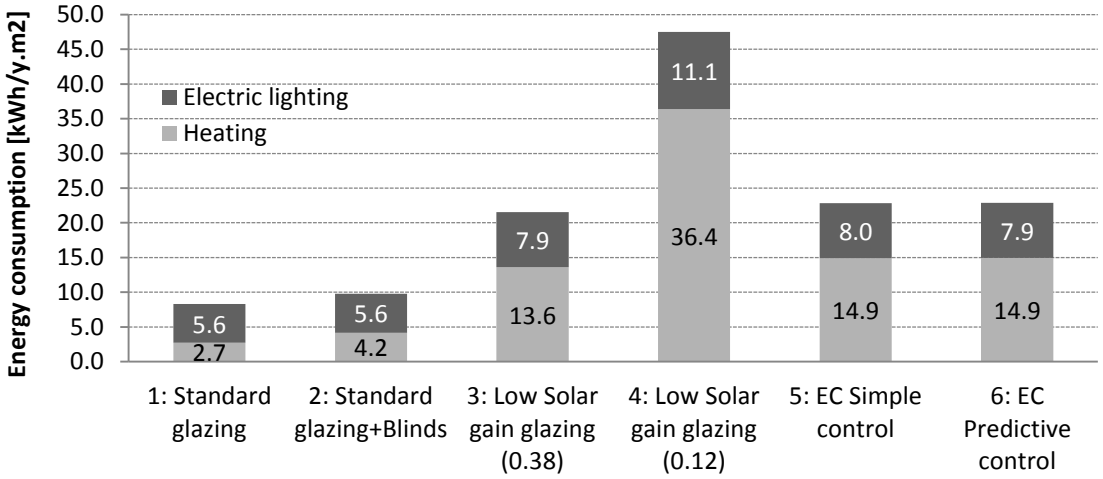

Figure 1: Annual energy demand for space heating and electric lighting for different simulation scenarios

Scenario 4 appears on the other extreme in terms of energy demand. This case features a low solar gain glazing with a very low constant coefficient of solar radiation transmission of 0.12. Solar gains are mostly cut-off and energy demand for heating escalates to over the double in comparison to the other scenarios. Energy demand for electric lighting is also significantly higher (about 40%) when compared to scenarios 3, 5 and 6. This is due to the constant low visible light transmission and the subsequent more frequent use of electric lighting.

The energy demand of the case of low solar gain glazing with a constant coefficient of solar radiation transmission of 0.38 (scenario 3) is comparable to the energy demand by the scenarios 5 and 6 with the EC glazings. It is thus important to compare these 3 scenarios in respect to the predicted visual and thermal comfort they offer.

Thermal comfort

The comparison between all different scenarios (Figure 2) shows clearly that automatically controlled EC windows (scenario 5 and 6) provide the best possible thermal comfort conditions with only a 15.6% of working time during the winter season found outside the thermal comfort limits. Scenario 3 also provides acceptable thermal comfort with 21% of

working time during the winter season lying outside the thermal comfort limits. Standard glazing scenarios provide unacceptably high discomfort conditions. During winter, scenario 4 interestingly enough provides the "perfect" thermal comfort conditions with zero working time being outside comfort conditions. That is of course due to the excessive use of heating energy since almost all solar gains are rejected (See *Energy consumption* above). *Please note that the abnormally elevated discomfort percentages during the heating season are mainly due to the absence of any cooling strategy (even passive).*

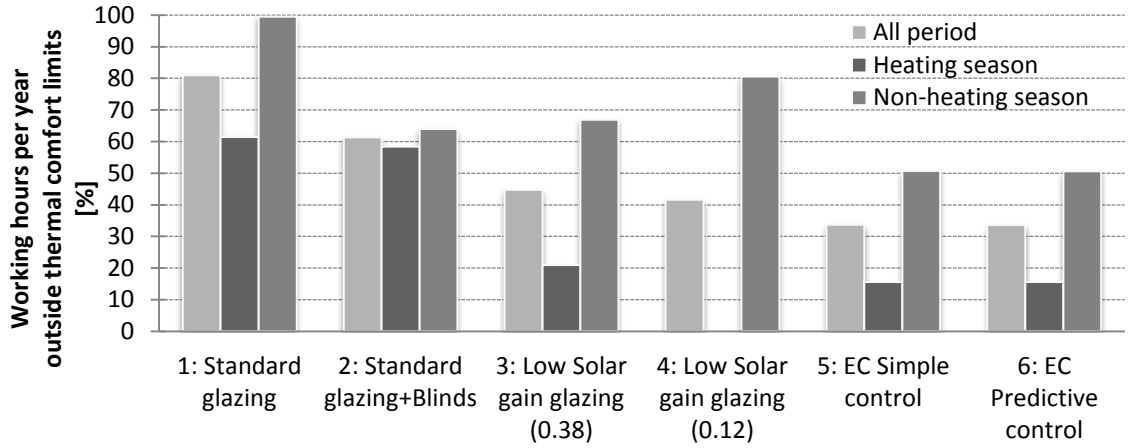

Figure 2: Percentage of working time during the simulation period where temperature is outside comfort limits and the PPD is over 10%, for each of the six considered simulation cases.

Visual comfort

Extreme-case scenario 4 demonstrated the best possible visual performance between the studied cases, followed closely by the EC windows scenarios (5 and 6) and scenario 3, although that is true only for the illuminance ranges corresponding to discomfort probability below 0.35. Scenarios 5 and 6 appear to achieve same levels of visual comfort in this analysis. Nevertheless, a comparison of the 2 scenarios against the same weather conditions and time period, shows that predictive control strategy (scenario 6) maintains workplane illuminance more stable compared to simple control (scenario 5). Workplane illuminance in non-predictive control tends to fluctuate in unison with external irradiance levels.

Field testing and user evaluation

Measured workplane illuminances were kept inside acceptable visual comfort levels (at around 450-1000 lx) most of the time during a day with intermediate sky conditions. Concerning user evaluation, most users were not satisfied by the unnatural colour rendering of the room and/or that of the view when looking outside, especially when the windows were fully tinted (Persian blue colour). Glare issues were also mentioned by half of the persons, which eventually motivated them to use the blinds. This was true in cases that direct sunlight hit the desk and/or the computer monitor. Also, some users expressed the wish for a wider dynamic range of possible transmissions (on both ends). However, most users are willing to oversee any inconveniences or disadvantages of EC windows and they are generally positive when comparing this daylighting system to a standard one (i.e. blinds) mainly due to the unobstructed view that EC windows offer at all times. Users did not express dissatisfaction regarding the control of the EC Windows nor did they seem to consider negatively the slow switching time between different transmission levels.

4. DISCUSSION AND OUTLOOK

Simulations showed that the elaborated algorithms for the automatic control of EC windows can provide better thermal and visual comfort conditions when compared to standard glazing coupled with blinds and still exhibit acceptable levels of energy consumption for space heating and electric lighting. Permanently tinted windows (solar protection windows) with a SHGC=0.38 (the same as the clear state of EC windows) can offer competitive conditions as EC windows, exhibiting slightly worse thermal and visual behaviour, especially during days when solar gains are high (sunny days), which is expected since they cannot modify their transmission and block unwanted solar radiation. Field study results showed that workplane illuminances were mostly kept inside acceptable visual comfort levels, while the user acceptance of the daylight control system is severely impaired by the unnatural colour rendering of the room and of the view when looking outside. As it was expected, glare issues were mentioned by some users and blinds were employed in these occasions. However, most users seem to prefer EC windows to a standard daylight control system such as blinds, mainly due to the unobstructed view that EC windows offer at all times.

As it became evident during the comprehensive parametric study, the developed sky prediction algorithm does not outperform a simpler closed-loop algorithm based on external irradiation when considering energy consumption aspects. In respect to visual comfort, the two control systems perform similarly when analysed for the Visual Discomfort Probability (VisDP). However, under varying intermediate sky conditions predictive control strategy minimizes workplane illuminance fluctuation when compared to simple control and thus, it provides a more stable luminous working environment.

As a further step, we aim to implement extensive field experimentation and an in-depth user survey in order to validate our results.

ACKNOWLEDGEMENTS

The work presented in this article was carried out in the framework of the research project *Automatic control of an electrochromic window* funded by the Swiss Federal Office of Energy (OFEN) and supported by EControl-Glas GmbH & Co.

REFERENCES

1. Lee, E.S., et al. Advancement of Electrochromic Windows. *Lawrence Berkeley National Laboratory.* 2006. LBNL-59821.

2. Baetens, R., Jelle, B.P. and Gustavsen, A. Properties, requirements and possibilities of smart windows for dynamic daylight and solar energy control in buildings: A state-of-the-art review. *Solar Energy Materials and Solar Cells.* 2010, Vol. 94, 2, pp. 87-105.

3. Lee, E.S. and DiBartolomeo, D.L. Application issues for large-area electrochromic windows in commercial buildings. *Solar Energy Materials and Solar Cells.* 2002, Vol. 71, 4, pp. 465-491.

4. Guillemin, A. *Using genetic algorithms to take into account user wishes in an advanced building control system.* PhD thesis no. 2778, EPFL. 2003.

5. Morel, N., et al. Neurobat, a predictive and adaptive heating control system using artificial neural networks. *International journal of sustainable energy.* 2001, Vol. 21, 2, pp. 161-201.

6. Lindeloef, D. *Bayesian optimization of visual comfort.* PhD thesis no. 3918, EPFL. 2007.

7. Fanger, P.O. *Thermal comfort analysis and applications in environmental engineering.* New York : McGraw-Hill, 1970.

OCCUPANT BEHAVIOR AND SCHEDULE PREDICTION BASED ON OFFICE APPLIANCE ENERGY CONSUMPTION DATA MINING

J. Zhao; R. Yun; B. Lasternas; H. Wang; K.P. Lam; A. Aziz; V. Loftness

Center for Building Performance and Diagnostics, School of Architecture
Carnegie Mellon University, Pittsburgh, Pennsylvania, USA 15213

ABSTRACT

Plug load and Heating Ventilation and Air Conditioning (HVAC) systems are the two largest energy consumers in commercial buildings. The use of the 2 systems is closely related to occupant behavior and schedule. It is significant to learn the occupant behavior pattern and predict occupancy schedule for controlling the systems to save energy. A data mining study is performed on the office appliance energy consumption data to predict the individual occupant behavior and the occupancy schedule in an open office space.

An experiment is conducted for 2 weeks by using wireless electric outlet meters. The 5-minute interval electricity consumption data of computers, computer monitors, task lights, and other office appliances are monitored for 6 office workers. Occupant behavior is categorized as "Occupied computer-based work", "Occupied non-computer-based work", "Unoccupied remote work", and "Unoccupied". C4.5 algorithm is used for pattern recognition over the appliance electricity consumption data individually. The average percentage of correct of the 6 individuals is 92.39% using 10-fold cross validation. The occupancy schedule for the space is predicted by using total energy consumption of each subject with Linear Regression algorithm. The correlation coefficient is 0.92 using 10-fold cross validation. The results suggest the models are feasible and can be applied to the plug load and HVAC control systems to reduce energy consumptions.

Keywords: occupant behavior, occupancy schedule, office appliance, electricity data mining

INTRODUCTION

In the U.S., More than 80% of the total site energy in commercial buildings is consumed by office appliance, service equipment and HVAC systems [1]. The use of appliance and HVAC is highly dependent on occupant behavior and schedule, which are difficult to directly control by traditional means. Besides, the standby power of office appliances, known as "phantom load", is often neglected and uncontrollable by occupants. Thus, the need for understanding occupant behavior is essential for reducing plug load.

Several studies have explored methods to predict the occupant behavior and schedule in commercial and residential buildings. Environmental sensors were often used to detect and predict occupant behavior and schedule. Infrared motion, temperature, CO_2, acoustics, and/or light sensor data were used in the studies of [2-7]. Stochastic modeling method was used to predict occupant behavior in [8-11].

The research above has demonstrated the data mining method is capable of predicting occupant behavior and/or schedule for both plug load and HVAC energy saving purpose. However, on the one hand, due to the diversity of human behavior, stochastic modeling may only valid for the tested subjects in the tested location, and on-site sensor data seems to be essential for generalizing the learning method. On the other hand, environmental sensor networks can be costly for installing and maintenance in office buildings. And the robustness of environmental sensors can also influence the prediction result.

In this study, electricity meter data of office appliances are used to predict occupant behavior and schedule, respectively. The presented results show the feasibility of the method in the tested open office.

METHOD

Experiment Setup and Data Processing

The experiment set up in an open office space in the Intelligent Workplace (IW) on the Carnegie Mellon University campus in Pittsburgh, Pennsylvania USA was designed to collect individual office appliance electricity consumption data and record occupant behavior concurrently for 2 weeks. 6 voluntary office workers (4 males and 2 females) age from 24 to 28 years old participated in the experiment.

The metered office appliances include desktop computer, computer monitor(s), task light, speaker, laptop computer, hard drive and personal heater. Plugwise meter/switch devices are used to collect individual office appliance electricity data for each participant [12]. A web-based data collection system is developed by [13] and is modified to collect power consumption data in 5-minute interval for this study. A Matlab program is developed to extract the data from a web-based SQL server and generate a "clean" CSV-format file.

Occupant behavior is classified into 4 categories, (1) "Occupied computer-based work" indicates the occupant is working with the computer actively at his/her bay. (2) "Occupied non-computer-based work" indicates the occupant is at his/her bay, but does not use the computer. The possible activities include paper-based tasks, discussing with colleagues, having lunch, having phone calls and so on. (3) "Unoccupied remote work" suggests the occupant is not at his/her office bay, but is using the desktop computer by remote connection. (4) "Unoccupied" means the occupant is not in his/her office bay and is not working remotely either.

Occupant behavior is recorded for "ground truthing", which should be the "true" result of the prediction that will only be used for training and testing the model for the model building period. The implementation of the trained model would not need this part of experiment. First, a Java program is developed to detect mouse and keyboard activities and record the time that both devices are not used within 5 minutes. Second, a Fitbit Zip™ pedometer is used to indicate whether the occupant is at his/her office bay [14]. Subjects are required to wear the device on his/her wrist for the period of the study. The device contacts the desktop Bluetooth dongle every 9 seconds when it is within a 20 feet (6.09 meter) range from the computer. By reading the 2 pieces of information, the occupant behavior can be recorded and categorized, as shown in Table 1.

	Computer in active mode	**Subject is in the bay**
"Occupied computer-based work"	1	1
"Occupied non-computer-based work"	0	1
"Unoccupied remote work"	1	0
"Unoccupied"	0	0

Table 1: Occupant behavior ground truth labeling.

Individual Occupant Behavior Recognition Method

6 datasets of 4332 instances with 4-6 attributes are trained and tested individually using 10-fold cross validation in Weka program [15]. 3 nominal classification data mining algorithms are considered, including Support Vector Machine (SVM), C4.5, and Locally Weighted

Learning (LWL) [15-17]. 2-tailed paired-T test with the confidence of 0.05 is used for result comparison [15].

Occupancy Schedule Prediction Method

For economic and technical reasons, 2 datasets are compared for occupancy schedule learning. One is sub-metered raw dataset from individual appliances, which has 33 attributes. The other is the aggregated energy consumption data of all the appliances for each subject, which has 6 attributes. The reason for comparing the two datasets is that the less data a method requires the more practical the method will be. In most office spaces, appliance-by-appliance sub-metering data may not be available but subject-by-subject meters are much more economical. 3 numeric regression data mining algorithms –Support Vector Regression (SVR), LWL, and Linear Regression (LR) - are tested by 10-fold cross validation in Weka program. The results are compared by using 2 tailed paired-T test with the confidence of 0.05.

RESULTS

Individual Occupant Behavior Recognition Result

Figure 1 illustrates the ground truth value of all the subjects' behavior schedule in a typical work day. The figure indicates the subjects have diversified working schedules. Sub1 has an earlier and regular office work schedule. Sub 2 works either remotely or without computer. Subs 3, 4, and 5 have similar computer-based work schedules and lunch break schedules. Sub 6 is absence during the tested day.

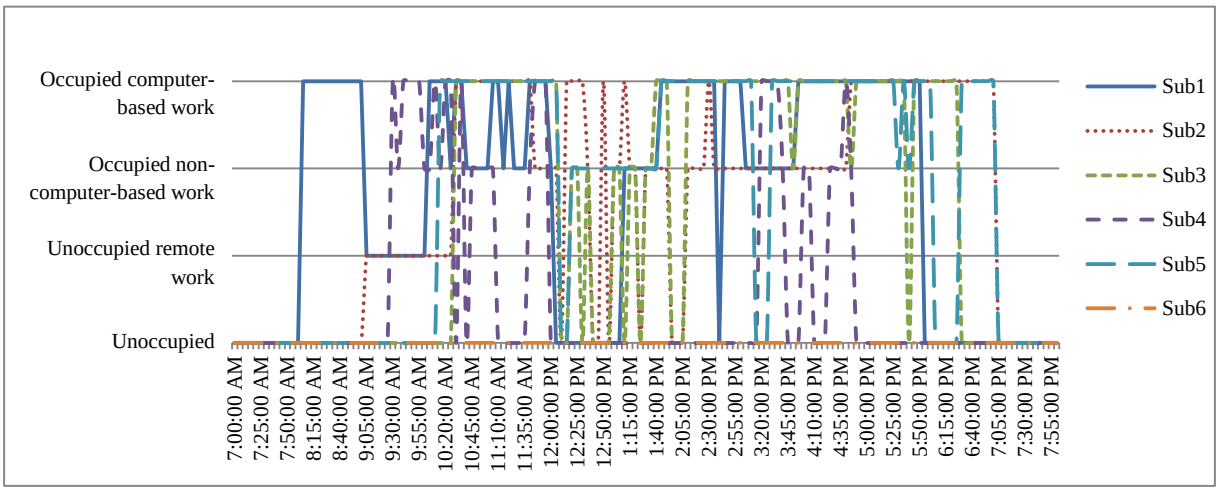

Figure 1: True value of all the subjects' behavior schedule in a typical work day.

Table 2 shows the result of the "percentage of correct" and "kappa statistic" for the 6 datasets using the 3 algorithms [15]. No statistically significant difference among the 3 algorithms is found. Therefore, from the practical point of view, C4.5 can be a suitable candidate to be used in practice. By comparing the 6 subjects, one can see Sub 1 and Sub 6 have highest percentage of correct, but the kappa statistic value for Sub 1 is the highest among all the subjects, while the kappa statistic value for Sub 6 is the lowest among all. The possible explanation is that nominal value of Sub 6 is highly skewed to "unoccupied", which is 89.93% of the entire class value. While other subjects' "unoccupied" class value percentage are 74.51%, 63.73%, 72.46%, 80.77%, and 72.25% for Sub 1 to Sub 5, respectively.

Despite the diversity of the subject behaviors, by using C4.5 algorithm, the average percentage of correct is 92.39%, and the average kappa statistic is 0.68. The overall learning result is satisfactory, although the patterns of each subject are dissimilar.

	SVM	LWL	C4.5
Subject 1	95.96 / 0.87	96.00 / 0.87	96.02 / 0.87
Subject 2	82.06 / 0.61	82.05 / 0.61	84.43 / 0.66
Subject 3	94.92 / 0.85	94.94 / 0.85	94.95 / 0.85
Subject 4	90.65 / 0.62	90.61 / 0.62	92.12 / 0.66
Subject 5	89.26 / 0.71	88.85 / 0.70	89.56 / 0.71
Subject 6	96.69 / 0.04	97.02 / 0.29	97.26 / 0.37

Table 2: Occupant behavior recognition result (percentage of correct / kappa statistic).

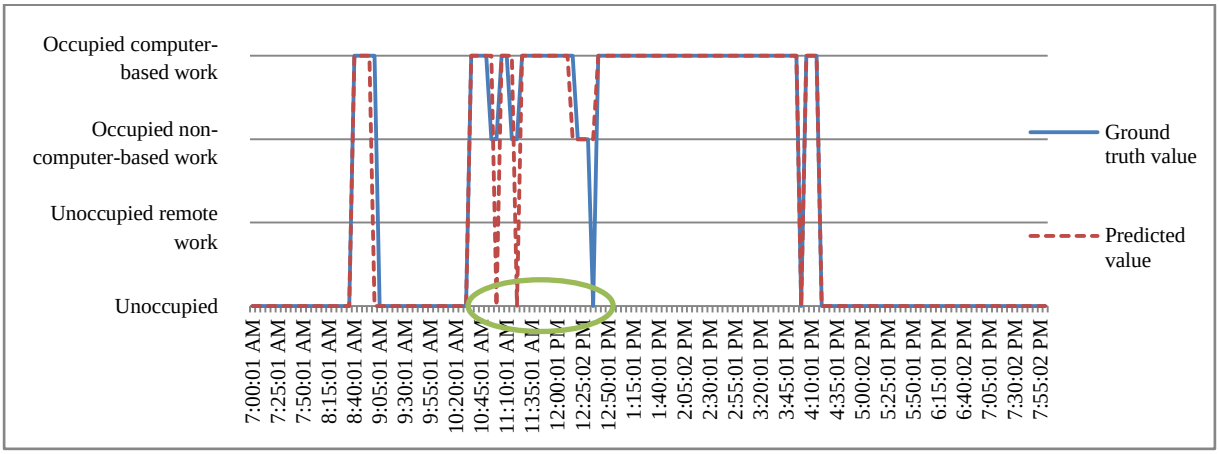

Figure 2: True value and predicted value of Sub 1 in a typical work day.

Figure 2 illustrates the comparison between the ground truth value and predicted value of Sub 1 in a typical work day. The model can predict fairly accurately for occupied computer-based work. However, the model fails to distinguish "occupied non-computer-based work" and "unoccupied" instances in 2 cases, as highlighted in Figure 2. First, from 11:00am to 11:20am, there are several "non-computer-based work" instances, but the model categorized the instances as "unoccupied". When looking at the raw dataset of these instances, the 2 computer monitors were off, due to the "sleep mode" setting of the computer. Given the fact that "computer" and "computer monitor" have high weights on the model, it is expectable the model may make mistakes in this situation. Second, at 12:35pm, the ground truth value is "unoccupied", while the predicted value is "occupied non-computer-based work". Comparing the raw data of electricity meters from 12:20pm to 12:35pm, no significant difference between the first 3 instances and the last one can be found. Thus the authors believe the ground truth value of 12:35pm may be a random error, which may occur when no movement is detected by the Fitbit device for 5 minutes. This error case should rarely happen during the experiment, since the device has an accurate acceleration sensor and the subject is required to wear it on the wrist during the experiment period.

Occupancy Schedule Prediction Result

	SVR	LWL	LR
Dataset by appliances	0.93 / 0.27	0.85 / 0.48	0.93 / 0.28
Dataset by subjects	0.92 / 0.32	0.83 / 0.52	0.92 / 0.33

Table 3: Occupancy schedule prediction result (correlation coefficient / relative absolute error).

2 datasets are trained and tested by using SVR, LWL, and LR algorithms. The correlation coefficient and relative absolute error are shown in Table 3 [16]. No statistically significant

difference is found among the 3 different algorithms and among the 2 datasets. Hence, for predicting occupancy schedule, using LR algorithm over the subject-by-subject electricity meter data can be applicable. Figure 1 shows the comparison between the ground truth value and predicted value of occupancy schedule in a typical work day by using LR algorithm over the dataset by subjects. The relative absolute error is 0.33 for the tested period.

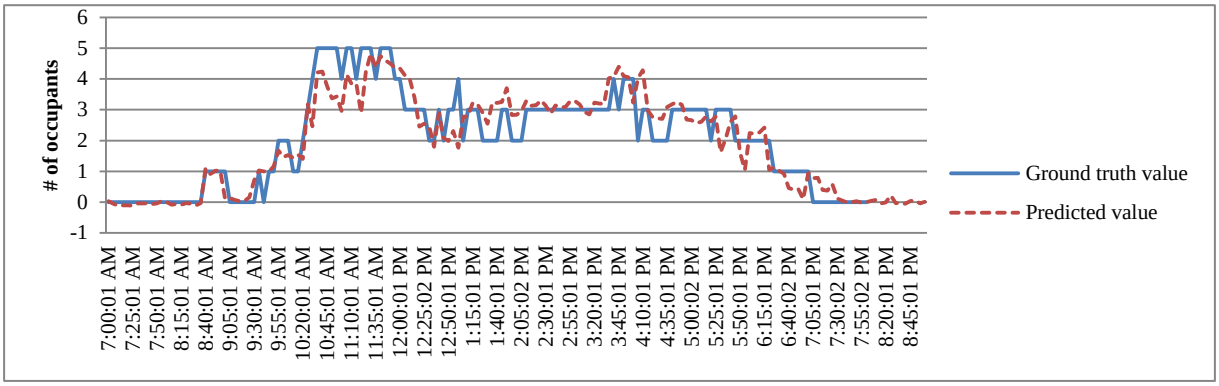

Figure 3 True value and predicted value of occupancy schedule in a typical work day

DISCUSSION

Although the 2 models suffer a similar problem that the information of energy use may not be sufficient for distinguish "non-computer-based work" and "unoccupied" as mentioned in the "RESULT" section. It may not be a problem for HVAC system control in a multi-person zone, but could be a problem for single-person individually controlled HVAC system, in which case, alternative solutions have been tested and implemented to predict single person's schedule [18]. To avoid the error disturbance for appliance control, time step can be increased from 5 minutes to longer time, and the control algorithm should check for status change consistency as well. For instance, only actuate the appliance when the behavior change continues for more than 2 time steps.

Future work will be focused on implementing the two models into the HVAC and plug load control systems and testing the energy saving results and recording the possible occupant behavior change. For predicting occupancy schedules, the model may be applied directly to the offices with similar appliance configuration without conducting ground truthing experiment. Dissimilarly, for individual occupant behavior prediction, more subjects should be tested and compared by using ground truthing method to draw a statistically significant conclusion. Then a more generalized model may be applicable for control purpose.

CONCLUSION

The study proposed a solution to learn and predict occupant behavior and schedule in open office spaces using office appliance electricity meter data. The average percentage of correct of individual behavior recognition is 92.39%. The correlation coefficient of occupancy schedule prediction is 0.92. The results suggest that despite the variation of individual occupant behaviors and schedules, the method is feasible to be used for HVAC and plug load systems control.

ACKNOWLEDGEMENTS

The authors would like to acknowledge DOE Energy Efficient Building Hub (EEB-HUB) (Subtask 6.4) and National Science Foundation-Emerging Frontiers in Research and Innovation (NSF-EFRI) (Subtask 2.2) for funding the study. The authors would also like to acknowledge the 6 volunteers for participating the experiment.

REFERENCES

1. DOE. Commercial Sector Energy Consumption. Building Energy Data Book 2012 March; Available from: http://buildingsdatabook.eren.doe.gov/TableView.aspx?table=3.1.4.
2. Dong, B. and K.P. Lam, Building energy and comfort management through occupant behaviour pattern detection based on a large-scale environmental sensor network. Journal of Building Performance Simulation, 2011. 4(4): p. 359-369.
3. Goldstein, R., et al. Real Time Sensor Based Occupancy Prediction for Model Predictive Control in Buildings. Model predictive control in buildings workshop. 2011. Montreal: IBPSA.
4. Glicksman, L.R. and S. Taub, Thermal and behavioral modeling of occupant-controlled heating, ventilating and air conditioning systems. Energy and Buildings, 1997. 25: p. 243-249.
5. Agarwal, Y., et al. Occupancy-Driven Energy Management for Smart Building Automation. BuildSys 2010. 2010. Zurich, Switzerland: ACM.
6. Wang, C., D. Yan, and Y. Jiang, A novel approach for building occupancy simulation. Building Simulation, 2011. 4: p. 149-167.
7. Zhang, R., et al., Information-theoretic environment features selection for occupancy detection in open office spaces. Building Simulation, 2012. 5: p. 179-189.
8. Page, J., et al., A generalised stochastic model for the simulation of occupant presence. Energy and Buildings, 2008. 40: p. 83-98.
9. Parys, W., D. Saelens, and H. Hens, Coupling of dynamic building simulation with stochastic modelling of occupant behaviour in offices – a review-based integrated methodology. Journal of Building Performance Simulation, 2011. 4(4): p. 339-358.
10. Tabak, V. and B.d. Vries, Methods for the prediction of intermediate activities by office occupants. Building and Environment, 2010. 45: p. 1366-1372.
11. Tanimoto, J., A. Hagishima, and H. Sagara, A methodology for peak energy requirement considering actual variation of occupants' behavior schedules. Building and Environment, 2008. 43: p. 610-619.
12. Plugwise. Circle. 2013; Available from: http://www.plugwise.com/idplugtype-b/circle.
13. Yun, R., et al. Toward the Design of a Dashboard to Promote Environmentally Sustainable Behavior among Office Workers. 8th International Conference, PERSUASIVE 2013. 2013. Sydney, Australia: Springer Berlin Heidelberg.
14. Fitbit. Fitbit Zip. Fitbit 2013; Available from: http://www.fitbit.com/zip/specs.
15. Ian H. Witten, E.F., Mark A. Hall, Data Mining Practical Machine Learning Tools and Techniques - 3rd ed. 2011, Amsterdam: Morgan Kaufmann.
16. Zhao, J. and K.P. Lam, Influential factors analysis on LEED building markets in U.S. East Coast cities by using Support Vector Regression. Sustainable Cities and Society, 2012. 5(0): p. 37-43.
17. Dong, B., C. Chen, and S.E. Lee, Applying support vector machines to predict building energy consumption in the tropics. Energy and Buildings, 2005. 37(5): p. 545-553.
18. Dong, B., Integrated Building Heating, Cooling and Ventilation Control (PhD Dissertation), 2010, Carnegie Mellon University: Pittsburgh.

Urban Ecology and Metabolism

CONTEXTUALIZING THE URBAN METABOLISM OF BRUSSELS: CORRELATION OF RESOURCE USE WITH LOCAL FACTORS

A. Athanassiadis[1,2]; P. Bouillard [2]

1: Aspirant du F.R.S.-FNRS – Research Fellow at Belgian National Fund for Scientific Research

2: Building, Architecture and Town planning – Université Libre de Bruxelles (ULB), Avenue F.D.Roosevelt 50, CP194/02, 1050 Bruxelles, Belgique. Email: arisatha@ulb.ac.be – Tel: +32(2) 650 66 03 – Web: http:// http://batir.ulb.ac.be/people/249

ABSTRACT

To monitor and assess resource use and in order to comprehend its environmental impact -and thus propose adequate policies- urban metabolism and Material Flow Analysis have become tools widely acknowledged and employed. However, due to the high level of aggregation of urban metabolism figures and to the fact that the urban system at stake is often considered as an abstract entity, it becomes hardly unfeasible to use and understand what is hidden behind these results. In fact, urban metabolism studies could be compared to "black boxes". In order to illustrate why the urban metabolism results of Brussels Region are specific to Brussels and not to any other abstract urban system, this paper will identify the causal relations of how and where these material and energetic flows are consumed. Thus, this paper will perform a material and energy balance at a regional scale and in order to contextualize it, it will correlate the results with local factors such as such as socio-economic (demography, income, household size, GINI, …) and territorial organization (density, land use, …) indicators. To do so, energy and material flows were downscaled at municipality level. The outcomes of this paper will be on the one hand to produce the urban metabolism at two different spatial scales and on the other to perform a correlation with local factors identifying which have the highest influence on the consumption of resources.

Keywords: Urban metabolism; correlation; socio-economic and territorial organisation indicators; downscaling; resource use modelling

INTRODUCTION

During the last century, total population quadrupled, the global material use grew 9-fold, the total energy use increased between 10 and 16-fold and the global economic output was estimated to grow more than 20-fold [1]. What is worth considering though is the structural change in the composition of the materials we consume. Indeed, in the last century, construction materials rose by a factor 42, industrial minerals by a factor of 31 and fossil energy carriers materials by a factor of 13 while biomass merely quadrupled [1]. The after war period, was a turning point concerning not only the increase of material use per capita but also towards a shift to mineral economies piling up material stocks with products of higher lifespan. The ever-increasing "weight" of our societies is mainly due to the creation and expansion of urban systems and their respective built environment.

To counter the environmental impacts of our material and energy use, many methodological and accounting tools, policies and directives have emerged. Amongst the few approaches that aim to address material use and thus its consequent impacts in a holistic and systemic way are the Urban Metabolism (UM) and the Material Flow Accounting. Since the first study of UM by Wolman in 1965, a number of comprehensive examinations were carried out around the

world at the scale of the city using top-down approaches based on census, statistical data and consumption patterns. The results of these still few studies are nevertheless very valuable and insightful. For instance, results provide concrete information about resource consumption and stock per capita but also more fundamental findings stating that our cities are linear reactors depending on their hinterlands both for resources and wastes [2].

Towards a more complex Urban Metabolism

As important UM results can be for the environmental assessment of urban systems, they yet present some serious shortcomings. First of all, due to the relative novelty of the field and the scarcity of case studies, UM suffers the absence of a clear and well-funded methodology contrarily to MFA. Another important issue is that due to the dependency on available, reliable and recently updated data (and consequently to the assumptions that each author is taking), UM studies are difficultly comparable between each other. In addition, due to the considerable efforts needed to set up an UM study, this accounting exercise is rarely undertaken more than one time for the same city. This punctual study makes it impossible to trace the evolution of resource consumption and thus assess whether the city at stake is progressing towards a more sustainable state. However, the most important limitation of the majority of current urban metabolism studies is their black box approach, or in other words studies showing only macroscopic (material) inputs and outputs of an urban system with little explanations about their internal mechanisms [3]. Thus, UM fails to grasp, analyse and illustrate the complexity of the interactions between the components of the city, as well as the relation between the urban system itself and its wider environment.

This precise limitation is the starting point of this paper. In fact, this work will attempt to bring forth some causal links between the resource consumption and the socio-economic and territorial organisation reality of the urban system under scope. The relationship between material and energy quantities and local factors will help to contextualize the UM and allow to state why such figures are exclusively valid for one city [4]. To do so, it is necessary to correlate UM results with a large number of variables including demography, income, employment, household size, density, land use, mobility, etc. Nevertheless, at the scale of the city these variables are too aggregated and present the urban system as a homogeneous and static whole. It therefore becomes necessary to downscale and disaggregate them. Accordingly, this research will start by performing an Urban Metabolism analysis for the city/region of Brussels. The latter study will be used to provide figures on absolute and relative consumption of resources. In order to contextualize the previous results, the next section will downscale the UM at a municipality scale and correlate it with local factors.

METHOD, CASE STUDY AND COLLECTION OF DATA

Method

In this study, a classical urban metabolism approach was opted to calculate the material and energy balances over the Eurostat MFA method. Even if this choice, could result to a more difficult comparison of the results, it remains more suited for providing material and energy balance at city and smaller spatial scales. In addition, in the case of European cities, MFA becomes irrelevant as (almost) all materials are imported and none are locally extracted. Finally, the UM approach was chosen in order to incorporate energy and water balances.

Case study

Belgium is divided in three regions, Flanders in the north, Wallonia in the South and Brussels which is enclosed within the Flanders region (see left of Figure 1). The metabolic analysis of

this study is focused on the region and the municipalities of Brussels. It is important to notice at this point, that the city of Brussels as we know it has the particularity of being a region at the same time. This specificity offers a considerable advantage for data collection as the city of Brussels is endowed with precise, available and updated data. However, the limits of Brussels Region do not coincide with the metropolitan area -1st and 2nd commuter zone (illustrated by black concentric boundaries)- which is spreading over the two other regions. Thus, it makes it extremely difficult to have a realistic assessment of Brussels (un)sustainability. Finally, concerning the second part of this paper which will study UM at municipal scale and correlate the results with local factors, let us for the moment precise that Brussels is divided in 19 municipalities.

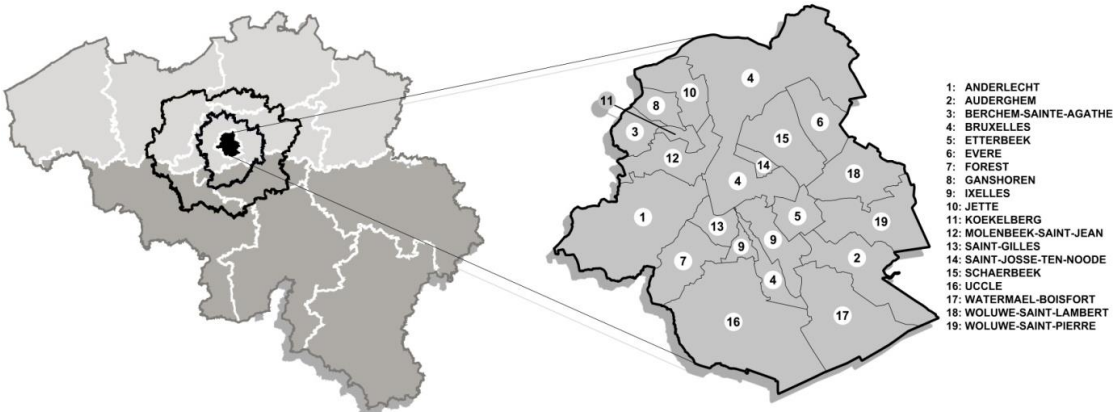

Figure 1: Brussels Capital Region and its 19 municipalities

Collection and calculation

In practice, the data about energy, water, in/out materials, waste, pollution and socio-economic reality were collected in a great number of official reports and statistical data of the Region and of regional companies. However, the material stock was calculated by using GIS data concerning the built environment and material breakdown of buildings, roads and cars (equation 1). Due to the inability of having more precise data for the geometry and function of all buildings, the exact type of all Brussels vehicle fleet, the exact composition of the built environment and their respective material composition, several assumptions had to be made.

$$material\ stock_{total} = weight_{buildings} + weight_{roads} + weight_{cars} \quad (1)$$

First, all vehicles (vehicles, buses, vehicles for transporting goods and motorcycles) were assumed as passenger cars. The material stock of roads is perhaps the most accurate as the exact surface was obtained by GIS cartographic regional data. The material breakdown of roads was based on the work of Stephan [5]. Finally, the estimation of the building stock "weight" was based on a number of assumptions that are summarized in the following equation (2) and inevitably do not reflect the reality. The first assumption was that all buildings in the city were residential (in reality they represent 84% of the buildings). The second assumption was to consider an average height and dwelling area per municipality for all buildings within this municipality. The weight/m² is the last postulate for the calculation of buildings material stock. The former was deduced by taking into account a real and precise material breakdown (including foundations and systems) of an 80m² apartment in a 10 storey building [5].

$$weight_{buildings} = \sum_{mun} number\ of\ buildings_{mun} * average\ number\ of\ stories_{mun} * average\ dwelling\ area_{mun} * weight\ per\ m^2 \quad (2)$$

All in all, due to the facts mentioned previously we have to keep in mind that the material stock presented in the following section is without any doubts underestimated.

RESULTS

The Urban Metabolism of Brussels Capital Region

The results of the material and energy balance of Brussels metabolism as well as general information about the region of the city/region are summarised in Figure 2. In this illustration we can read that Brussels inhabitants consume 24,306 GWh or 21 MWh/cap out of which 42% is natural gas (10,243 GWh), 24% is electricity (5,798 GWh), 12% are petroleum products (2,897), 21% are fuels (5,152 GWh) and 1% is others. The final energy consumption by sector is divided as such: residential 42% (10,127 GWh), tertiary 33% (8,087 GWh), transport 22% (5,474 GWh) and industry merely 3% (618 GWh). The consequence of this energy consumption is the generation of 4,016 kt$C0_2$-equivalents of GHG emissions or 3.5t$C0_2$-equivalents/cap, within which 3,728kt of CO_2 (3.3t/cap). As the region does not produce the great majority of the energy it consumes, an additional amount of GHG is emitted outside of its boundaries.

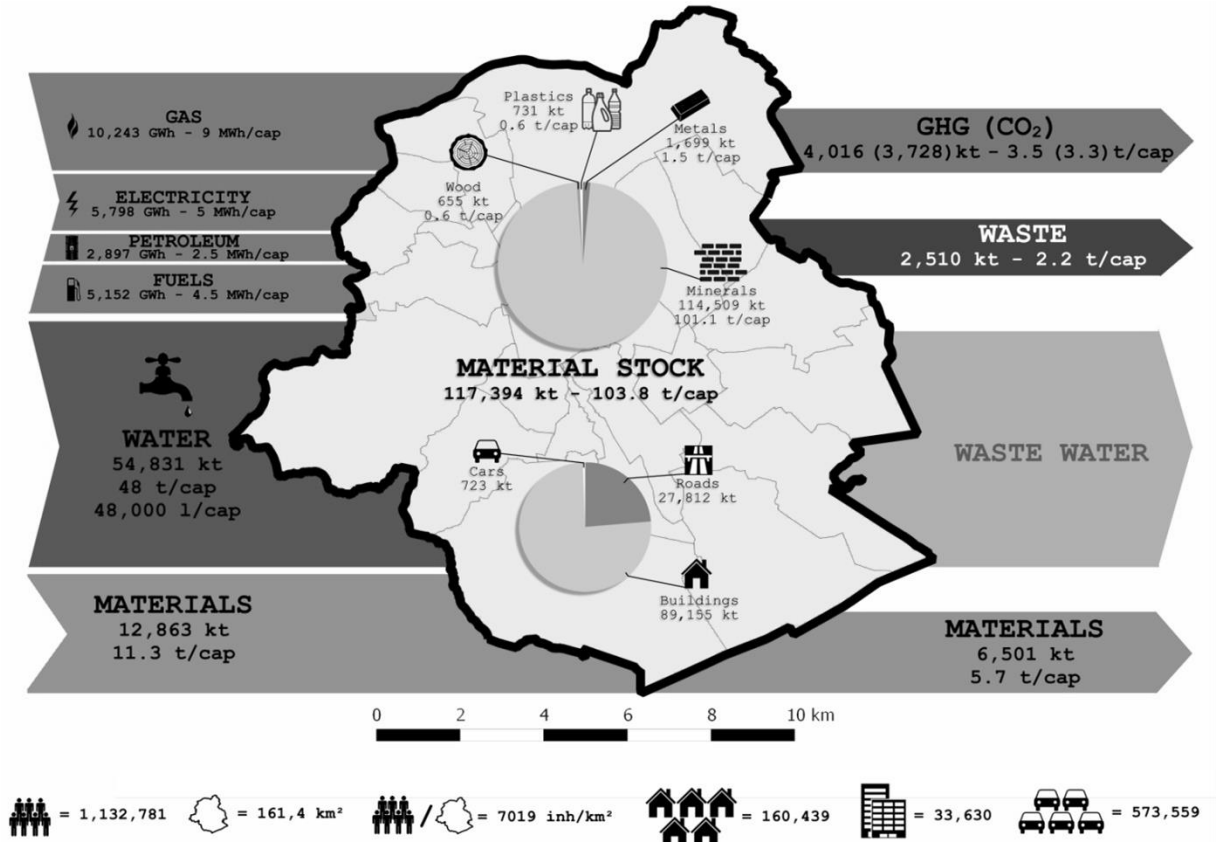

Figure 2: The Urban Metabolism of Brussels Capital Region

Regarding material flows, the city of Brussels requires annually 67,694kt or 60t/cap (which means the rather impressive amount of 163kg per day). Of course, the great majority of the inward material flows are due to water consumption (54,831kt or 48t/cap). "Only" 12,863kt of the materials were imported products out of which 14% were agricultural products, 11% were metallurgy products, 31% were minerals and construction materials, 3% were fertilizers and chemical products and finally 39% were manufactured goods. On the other side, 6,501kt of materials were exported with mineral and construction materials making up for 47%, manufactured goods for 28% and agriculture and food products for 13%. By deducting the

output flows of materials from the input ones the addition to material stock can be estimated to 6,362kt. Another flow coming out of Brussels urban system is waste (2,510kt or 2.2t/cap). The waste flow was subdivided in four main categories namely: municipal waste (23%), excavated soil (25%), construction and demolition waste (31%) and lastly industrial activities waste (21%). Finally, while there is no available data concerning wastewater produced in Brussels we can state that it would be in the same order of magnitude of imported water adding to that a great part of yearly precipitation over Brussels territory.

The last aspect of Brussels metabolism that will be presented here is its material stock. Resulting from the equation (1), Brussels "weighs" 117,394kt and each of its inhabitants weigh a bit more than 100 tons (without taking into account natural elements such as trees, natural soil, etc). This enormous material stock is composed of 97% of minerals (concrete, sand, gravel, glass, plaster, etc) and 3% of steel, wood and plastics. These materials are coming from buildings (76%), roads (23%) and cars (1%).

Correlation of the Urban Metabolism of Brussels municipalities with local factors

To examine whether there is a correlation between resource consumption and local factors, some essential metabolic features such as the final consumption of energy and water as well as the material stock were downscaled at the municipality level. However, flows such as waste, imported and exported materials were not possible to be localised as these figures are typically aggregated at regional scale. In order to keep the UM results as synthetic and concise as possible they are only presented here in cartographic representations. The first row of Figure 3 presents the absolute consumption of energy (gas and electricity) and water as well as the material stock of all 19 municipalities of Brussels region. As it is visible in these maps all resource consumption and the material stock are very highly correlated, yet water and gas consumption present even higher correlation factor (probably due to their further residential use in opposition to electricity). While performing a rapid visual correlation in Figure 3, it might be quite surprising to notice that resource consumption and material stock is not at all correlated with factors such as density, average income or density of office space. However, they are very strongly correlated with the number of buildings per municipality.

To deepen the research of potential relationships between consumption and local factors the correlation was extended to 35 variables including absolute, relative, per capita, per office m² and per m² of built resource consumption (gas, electricity, primary energy, water), absolute and per capita material stock but also socio-economic and territorial organisation indicators (such as average income, unemployment, GINI, household size, number of households, demographic growth, mean age, share of foreigners, density, density of office space, dwelling area, number of buildings, number of cars and share of dwellings built before 1961).

In this extensive analysis, some evident results emerged as mentioned in the immediate visual correlation such as the relationship between resource consumptions themselves but also between resource consumption and the number of buildings and households. One rather surprising correlation is the one between resources consumption and the number cars per municipality. Some other fairly significant associations emerged between individual consumption of water and the GINI coefficient, household size and share of foreigners (consumption of gas/cap was also associated with GINI and household size). In addition, it appeared that there is a relation between resource consumption/m² of built area on the one side and average income, unemployment, demographic growth, mean age, share of foreigners, density, dwelling area and dwellings built before 1961 on the other side. However, in general, most of the rest of relationships are rather dispersed and do not allow us to draw strong conclusions about which exact factors precisely play a crucial role in resource consumption. These fuzzy relations however, allow us to understand the complexity of such endeavour.

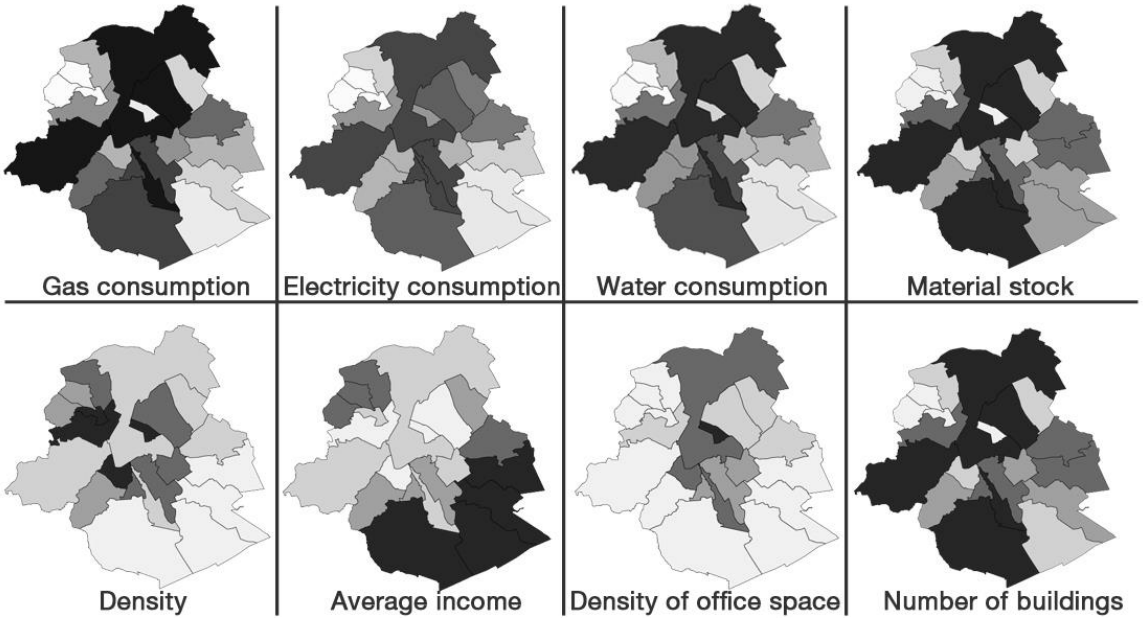

Figure 3: Mapping Urban Metabolism features and local factors at municipality scale.

CONCLUSION AND DISCUSSION

The outcomes of this paper are multiple. First of all, it allows us to see that the aggregated figures of previous UM studies are not homogeneously distributed over the territory under study. Some parts of the city consume more or less for different (socio-economic or spatial planning) reasons. However, the causal relations between local factors and resource consumption are not so evident and this extended analysis allows to set new basis for the UM field and to question some misconceptions and simplifications. In conclusion, in order to refine the previous causal relationships it would be necessary to downscale UM results even further and thus increase significantly the number of correlations. Such research would be necessary in view of creating resource use models based on local factors.

ACKNOWLEDGEMENTS

This project was funded by the Belgian National Fund for Scientific Research (F.R.S.-FNRS).

REFERENCES

1. Krausmann, F., et al.: Growth in global materials use, GDP and population during the 20th century. Ecological Economics Vol 68, No 10, pp 2696-2705, 2009
2. Hendriks, C., et al: Material Flow Analysis: A tool to support environmental policy decision making. Case-studies on the city of Vienna and the Swiss lowlands. Local Environment Vol 5, No 3, pp 311-328, 2000.
3. Akiyama, T: Urban metabolism and sustainability. Available from: http://www.auick.org/database/apc/apc017/apc01701.html.
4. Pincetl, S., Bunje, P., and Holmes, T: An expanded urban metabolism method: Toward a systems approach for assessing urban energy processes and causes. Landscape and Urban Planning, Vol 107, No 3,pp 193-202, 2012.
5. Stephan, A: Towards a comprehensive energy assessment of residential buildings. A multi-scale life cycle energy analysis framework. Ph.D. thesis, Université Libre de Bruxelles and University of Melbourne, Brussels, 2013

TAKING THE STEP TOWARDS NET ZERO ENERGY BUILDINGS – HOW WILL THAT AFFECT THE ENERGY USE FROM A LIFE CYCLE PERSPECTIVE?

Björn Berggren[1]; Monika Hall[2]; Maria Wall[1]

[1]*Lund University, Department of Architecture and Built Environment, Division of Energy and Building Design, Box 118, 221 00 Lund, Sweden.*

[2]*University of Applied Sciences and Arts Northwestern Switzerland, School of Architecture, Civil Engineering and Geomatics, Institute of Energy in Building, St. Jakobs-Strasse 84, CH-4132 Muttenz, Switzerland.*

ABSTRACT

An important measure for climate change mitigation is reduction of energy use in buildings worldwide. There are today a growing number of buildings for which the design principle has been to achieve a Zero Energy Building (ZEB) or Net Zero Energy Building (Net ZEB).

It is today generally assumed, when the energy use of a building is discussed from a lifecycle perspective, that energy use in the operational phase of buildings accounts for 70-90% of energy used during its life cycle. However, a natural consequence is that for Net ZEBs the relative share of energy use related to building operation will decrease. Some might argue that the energy savings achieved related to building operation of a Net ZEB is lower compared to the increased energy use for production, maintenance and demolition.

This study analyzes the change of embodied energy compared to the decrease of the energy use related to building operation; by literature review and detailed analysis of eleven case studies, taking the step from a low energy building to a Net ZEB.

The study shows that taking the step towards Net ZEB is not counterproductive from an LCE perspective. The embodied energy will increase slightly when taking the step from a low-energy building towards Net ZEB balance. However, the energy savings achieved related to building operation exceeds, with great margin, the increased embodied energy.

Based on the literature review; embodied energy exceeds 50% of life cycle energy use when the annual operating energy use, primary energy exceeds 33 kWh/(m^2a) and 45 kWh/(m^2a) for residential and non-residential buildings respectively.

Within the detailed analysis; a rough breakdown of energy demand may be made: 35% embodied energy, 45% plug loads and lighting and 20% for heating, hot water and HVAC.

As embodied energy as a relative share of the total cycle energy use increases, embodied energy should be given more attention in the design of buildings.

Keywords: Life Cycle Energy, Net zero energy building, Embodied energy, Primary energy

INTRODUCTION

Reduced energy consumption is an important strategy for climate change mitigation. Buildings, worldwide, accounts for 40 % of the primary energy use and 24 % of greenhouse gas emissions [1]. As the population of the world grows, the need for buildings increases. Hence, reduced energy consumptions in buildings and increased use of renewable energy are important measures to reduce our energy dependency and generation of greenhouse gases.

Today; a number of buildings exist for which the design principle has been to achieve a Zero Energy Building (ZEB) or Net Zero Energy Building (Net ZEB) [2-6].

There are many different definitions and approaches of the two concepts. In general, the ZEB concept may be described as an autonomous building which does not interact with any external energy supply system (grid) such as district heating network, gas pipe network, electricity grid or likewise. The Net ZEB concept is a building where the weighted supply of energy from the building meets or exceeds the weighted demand and interacts with an energy supply system (grid). Such a building can export energy when the building's system generates a surplus and import energy when the building's system is insufficient to generate the energy required. The scope of the energy balance for the Net ZEB may vary for different concepts but is usually based on an annual balance of primary energy [7].

It is today generally assumed, when the energy use of a building is discussed from a lifecycle perspective, that energy use in the operational phase of buildings accounts for 70-90% of energy used during its life cycle. There are a number of substantiated and extensive studies with results supporting that allegation [8-11]. The studies differ in regard to calculation methodology used to account for the total energy use, Life Cycle Energy (LCE), but they reach similar conclusions which support the statement above. However, a natural consequence is that for Net ZEBs the relative share of energy use related to building operation will decrease.

Sceptics to the Net ZEB concept might argue that the energy savings achieved related to building operation of a Net ZEB is lower compared to the increased energy use for production, maintenance and demolition. A German study [12] concluded that life cycle energy use decreased for each step taken from a building; built according to building regulations, towards the Passive House standard. Taking the step to the ZEB, the life cycle energy use increased.

It may be argued that the German study is inconsistent since the life cycle energy use for the ZEB includes all embodied energy for the building's on-site generation and energy storage systems, whereas the embodied energy of the grid supplying the Passive House with energy is not included in the life cycle energy balance comparison.

The objective of this study is to analyze the change of embodied energy compared to the decrease of the energy use related to building operation; mainly by a literature review, but also by detailed analysis of eleven case studies; taking the step from a low energy building to a Net ZEB.

This paper presents a summary of research [13] which has been largely developed in the context of the joint IEA SHC Task40/ECBCS Annex52: "Towards Net Zero Energy Solar Buildings".

METHOD

The literature review was conducted by reviewing peer-reviewed papers and through a survey among participating researchers of the IEA SHC Task40/ECBCS Annex52 "Towards Net Zero Energy Solar Buildings", asking for case studies where LCE analyses were conducted and for information on country specific strategies for LCE analysis. All data were normalized into kWh/(m^2a). Only data based on primary energy were used, and where all energy use related to building operation was included.

The detailed analysis was conducted for eleven Minergie-A buildings. When this work was set out (July 2011), a total of 11 buildings had applied for Minergie-A certification. Data for the buildings were gathered from the database [14] managed by the Minergie® association.

RESULTS AND DISCUSSION

Within the literature review, a total of 143 case studies were collected [10, 11, 15-28]. Together with the eleven case studies from the Minergie database; a total of 154 cases are used in the analysis. In Figure 1 the relationship between operating energy and life cycle energy is presented for all cases. The relationship between operating energy and life cycle energy is almost linear. This data correspond well with the earlier, highlighted, linear relationship in [10, 11]. The negative values of operating energy occur if the energy supply exceeds the energy demand.

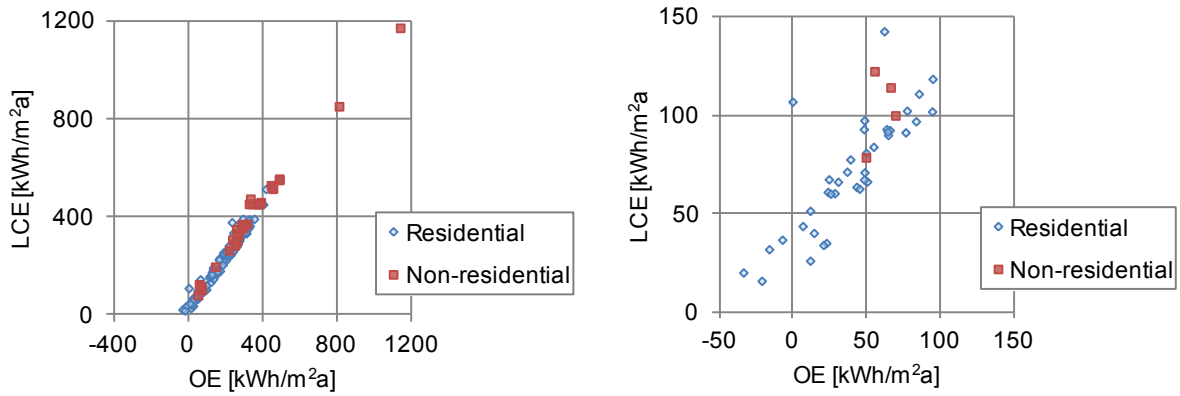

Figure 1: Relationship between operating energy (OE) and life cycle energy (LCE), primary energy. Right: All 154 case studies are included. Left: Case studies with OE < 100 kWh/(m²a) are displayed.

Low energy buildings and Net ZEBs usually requires more material in form of insulation and installations (PV panels, solar thermal collectors, heat pumps etc.). Hence it could be logical to assume that the linear relationship between operating energy and life cycle energy would flatten out. However, the tendency is that the linear relationship is constant. This may be due to that design and construction of low energy buildings and Net ZEBs often has a focus on sustainable material management. It may also be partly due to that newer buildings show a tendency of a lower embodied energy compared to older buildings.

In Figure 2 the relationship between the operating energy and the embodied energy as percentage share of life cycle energy use is presented together with an exponential regression for residential buildings and non-residential buildings. As there are no case studies for non-residential buildings where operating energy≤0 kWh/(m²a), data for a fictitious building have been incorporated.

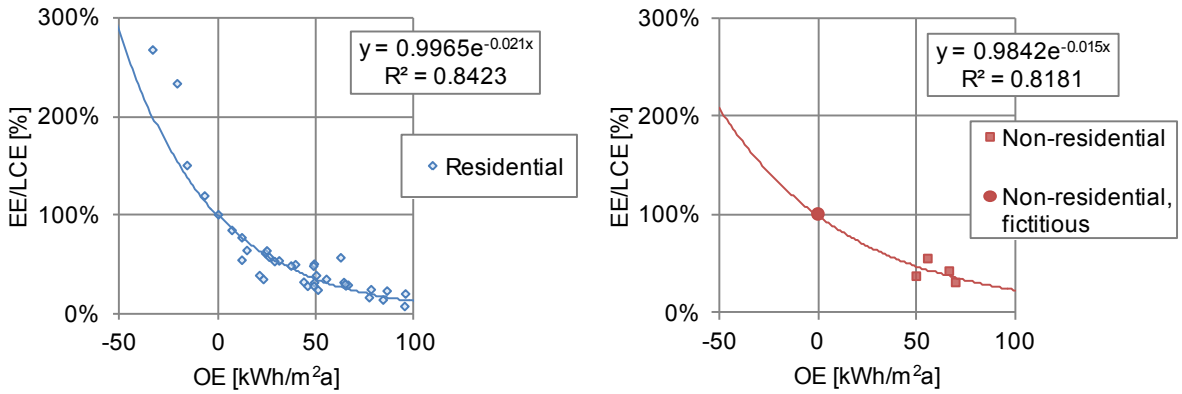

Figure 2: Relationship between operating energy (OE) and life cycle energy (LCE), primary energy. Right: All 154 case studies are included. Left: Case studies with OE < 100 kWh/(m²a) are displayed.

Using the exponential regression formulas, the embodied energy exceeds 50% of life cycle energy use when the annual operating energy use is ≥33 kWh/(m²a) and ≥45 kWh/(m²a) for residential and non-residential buildings respectively. It may occur as strange that embodied energy as a share of life cycle energy exceeds 100% when the operating energy < 0 kWh/(m²a). The effect is due to buildings that annually supply more energy than the annual energy demand, every year generating a surplus and thus reducing the total life cycle energy use.

The detailed distribution of embodied energy and operating energy of the detailed analysis of the eleven Minergie-A buildings is presented in figure 3. 10. For each project, demand and supply related to operating energy and embodied energy is presented. E.g. there is an energy demand to produce PV panels, presented as embodied energy on the demand side in Figure 10 (EE PVs). However, the PV panels also supply energy during building operation, presented as operating energy on the supply side (OE PVs).

Examining the demand for the different cases, the following rough division may be done: 35 % is embodied energy, 45 % is demand for plug loads and lighting and 20% is demand for heating, hot water and mechanical systems.

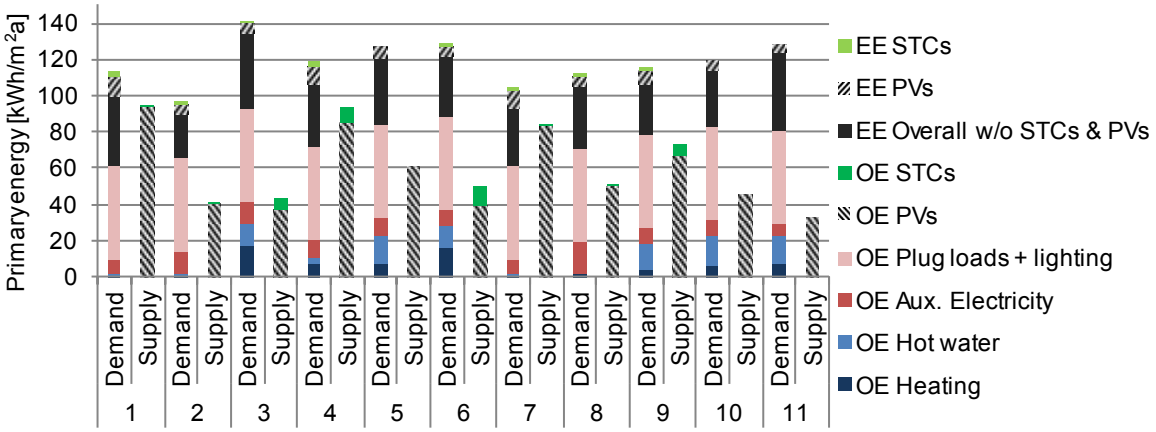

Figure 2: Distribution of operating energy (OE) and embodied energy (EE) by demand and supply in Minergie-A projects (non-renewable primary energy).

CONCLUSIONS

Taking the step towards Net ZEB is not counterproductive from an LCE perspective. The embodied energy will increase slightly when taking the step from a low-energy building towards Net ZEB balance. However, the energy savings achieved related to building operation OE exceeds, with great margin, the increased embodied energy.

Solar thermal collectors, PV panels and heat pumps reduce the operating energy use more than the increase of the embodied energy. Therefore, if a project only has resources to carry out a limited LCE analysis. They should focus on structural elements and building envelope.

ACKNOWLEDGEMENT

This paper presents a summary of the research which has been largely developed in the context of the joint IEA SHC Task40/ECBCS Annex52: *Towards Net Zero Energy Solar Buildings*. The authors wish to thank all the national experts who have contributed.

REFERENCES

1. International Energy Agency (IEA), *Towards Net Zero Energy Solar Buildings*, SHC Task 40/ECBCS Annex 52 IEA, Fact sheet pp. 2, 2011.
2. SHC Task40/ECBCS Annex52 IEA, *Net Zero energy Buildings database*, http://iea40.buildinggreen.com/index.cfm (accessed 10.09.11).
3. Musall, E., et al., Net Zero Energy Solar Buildings: An Overview and Analysis on Worldwide Building Projects, in Eurosun Conference 2010, Graz, 2010. pp. 9.
4. Lenoir, A., F. Garde, and E. Wurtz, *Zero Energy Buildings in France: Overview and Feedback* in ASHRAE Annual Conference 2011, Montreal, 2011. pp. 13.
5. Voss, K. and E. Musall, Net zero energy buildings - International projects of carbon neutrality in building, Birkhauser Verlag, Basel, 2011.
6. Fachinformationszentrum. *Net zero-energy buildings – Map of international projects*. http://www.enob.info/en/net-zero-energy-buildings/map/ (accessed 05.04.12).
7. Marszal, A.J., et al., Zero Energy Building – A review of definitions and calculation methodologies. Energy and Buildings, 2011. 43(4): p. 971-979.
8. Adalberth, K., *Energy use during the life cycle of single-unit dwellings: Examples.* Building and Environment, 1997. 32(4): p. 321-329.
9. Adalberth, K., Energy use in Multi-Family Dwellings during their Life Cycle, Doctoral Thesis, Lund University, 1999.
10. Sartori, I. and A.G. Hestnes, Energy use in the life cycle of conventional and low-energy buildings: A review article. Energy and Buildings, 2007. 39(3): p. 249-257.
11. Ramesh, T., R. Prakash, and K.K. Shukla, *Life cycle energy analysis of buildings: An overview*. Energy and Buildings, 2010. 42(10): p. 1592-1600.
12. Feist, W., Life-cycle energy balances compared: low-energy house, passive house, self-sufficient house, in International Symposium of CIB, 1997. pp. 13.
13. Berggren, B., M. Hall, and M. Wall, *LCE analysis of buildings – Taking the step towards Net Zero Energy Buildings.* Energy and Buildings, 2013. 62(0): p. 381-391.

14. MINERGIE®, *Minergie database*, 2011: Minergie Agentur, CH-4132 Muttenz.

15. Junnila, S., A. Horvath, and A.A. Guggemos, *Life-Cycle Assessment of Office Buildings in Europe and the United States* Journal of Infrastructure Systems, 2006. 12(10): pp. 7.

16. D Carls, Bewertung und Optimierung von ökonomischen und ökologischen Bauwerkslebenszyklen am Beispiel BOB - Balanced Office Building, in Fachbereich Architektur, Bergische Universität Wuppertal: Wuppertal, 2007.

17. D Kugel, Life cycle analyses as an economical and ecological savings potential in building planning and management, in Bauphysik und technische Gebäudeausrüstung, University Wuppertal: Wuppertal, 2007.

18. *CIRCE, ENSLIC BUILDING – energy saving through promotion of life cycle assessment in buildings* http://circe.cps.unizar.es/enslic/texto/d 4-2-circe.pdf (accessed 10.04.12).

19. Schweizer Solarpreis 2007, *Marché international support office*, http://www.solaragentur.ch/dokumente//M-07-10-16%20Marche%20International.pdf (accessed 10.04.12).

20. Swiss Federal Institute of Aquatic Science and Technology. *Forum Chriesbach - Energy*. http://www.eawag.ch/about/nachhaltig/fc/energie/index_EN (accessed 08.04.12).

21. Scheuer, C., G.A. Keoleian, and P. Reppe, Life cycle energy and environmental performance of a new university building: modeling challenges and design implications. Energy and Buildings, 2003. 35(10): p. 1049-1064.

22. Pullen, S.F., *Energy used in the Construction and Operation of Houses.* Architectural Science Review, 2000. 43(2): p. 87-94.

23. Victoria Building Commission, *Energy impacts of different house types in Victoria*, http://www.buildingcommission.com.au/resources/documents/EE_FactSheet_FINAL_18 June06.pdf (accessed 12.09.11).

24. G. Beccali, et al., *Energy and environmental analysis of a mono-familiar Mediterranean house*, in World Sustainable Building Conference - SB08, Melbourne, 2008. pp. 8.

25. Plataforma Arquitectura, *LIMA house*, http://www.plataformaarquitectura.cl/2010/11/12/lima-low-impact-mediterranean-architecture-saas/ (accessed10.04.12).

26. Keoleian, G.A., S. Blanchard, and P. Reppe, *Life-Cycle Energy, Costs, and Strategies for Improving a Single-Family House.* Journal of Industrial Ecology, 2001. 4(2): p. 22.

27. Villa, N., et al., *Life Cycle Assessment (LCA) of buildings applied on an Italian context*, in CleanTech for Sustainable Buildings - From Nano to Urban Scale, Lausanne, 2011. pp. 6.

28. Leckner, M. and R. Zmeureanu, Life cycle cost and energy analysis of a Net Zero Energy House with solar combisystem. Applied Energy, 2011. 88(1): p. 232-241.

LIFE CYCLE IMPACT ASSESSMENT OF RECYCLED CONCRETE AND COMPARISON BETWEEN THREE CONCRETE PRODUCTION SCENARIOS

A. Kleijer; S. Citherlet; B. Perisset

University of Applied Sciences Western Switzerland – HEIG-VD

ABSTRACT

Recycled concrete is now used in many different applications and scientific studies have shown that they have performances similar to concretes which use natural gravel [1, 2]. With the aim to evaluate the environmental impacts of recycled concrete, a life cycle impact assessment (LCIA) has been performed and results compared with those of normal

This study is the result of a project involving the "Claie-aux-Moines (GCM)" gravel mining company and the Canton of Vaud to determine whether the impacts of transporting materials are significant for three different concrete production processes. Two relevant environmental indicators in building environment showed that the recycled concrete have relatively less impacts than normal concrete. This study also demonstrated that the material origin should be taken into account in the LCIA as transport distances have a non-negligible influence on the impacts. These findings suggest that recycled concrete could be an alternative solution to normal concrete as it contributes to reduce environmental impacts of buildings and preserve natural resources by reusing recycled gravel resources.

Keywords: Life cycle impact assessment, recycled, concrete, gravel, transport, construction

INTRODUCTION

The School of Business and Engineering Vaud (HEIG-VD) has been appointed by the Building, Inheritance and Logistics service from the Canton of Vaud and the Claie-aux-Moines gravel mine company (GCM) in Switzerland to perform a LCIA of a recycled concrete called ECOBETON®.

The development of recycled concrete is mainly due to scarcity of natural gravel as a result of political pressures (soil protection) and increase of urban development (construction areas and communication routes). Recycling concrete aggregates reduces the exploitation of raw materials and provides a very interesting secondary material for concrete production.

The GCM gravel site processes all types of gravel either for concrete production or for direct sales. In parallel, the gravel site is used to recover secondary materials to produce new primary material. The site is split into a gravel mine exploitation area and three production areas:

- Natural gravel process (gravel diameters between 4 and 32 mm, sand 0-4 mm and mud);
- Recycled material (bank gravel directly from the mine without sorting, recycled material such as concrete blocks or old tiles);
- Concrete production.

The GCM gravel mine has been producing ECOBETON® (classified and non-classified) for many years. The classified ECOBETON® is according to the EN 206-1:200 standard and

according to the SIA MB 2030 technical book. At the time of this study, there was no recycled concrete dataset available in the international Ecoinvent database v2.2 [3].

There are different types of recycled concrete on the market. In order to evaluate the environmental impacts of their product, GCM decided to conduct a LCIA based on their own production process. For comparison purposes, a LCIA of their normal concrete was also performed.

The objectives of this study are:

- Evaluation of the environmental impacts of recycled concrete produced at GCM and comparison against GCM normal concrete production.
- Comparison of results between three different scenarios with normal and recycled concrete which are transported on construction site and normal concrete which are produced directly on the construction site.

METHODS AND MATERIALS

The methodology applied in this study is compliant with ISO 14'040 and 14'044 standards. All basic data concerning materials and processes to be analysed were obtained directly at the GCM company [4]. This includes raw materials, operating area (gravel mine area, construction area, etc.), type and distance of transport (train, lorry, etc.), type and amount of energy used, co-products, infrastructure and machine used, disposal of waste from process and emissions. The environmental datasets were taken from the Ecoinvent database version 2.2.

System limits

Figure 1 shows the system limits of the concrete production. The required inventory data have been collected at GCM through a variety of sources [5]. To be granted the exploration permit, GCM has prepared an environmental impacts report, which provides the basic data for the LCIA. The lifespan of the gravel site is evaluated at 20 years. By producing secondary materials, the number of years for exploitation can be extended. GCM also holds an annual inventory on which this study is based. Finally, all technical equipment and vehicles have user manuals which give the basic information needed for the study.

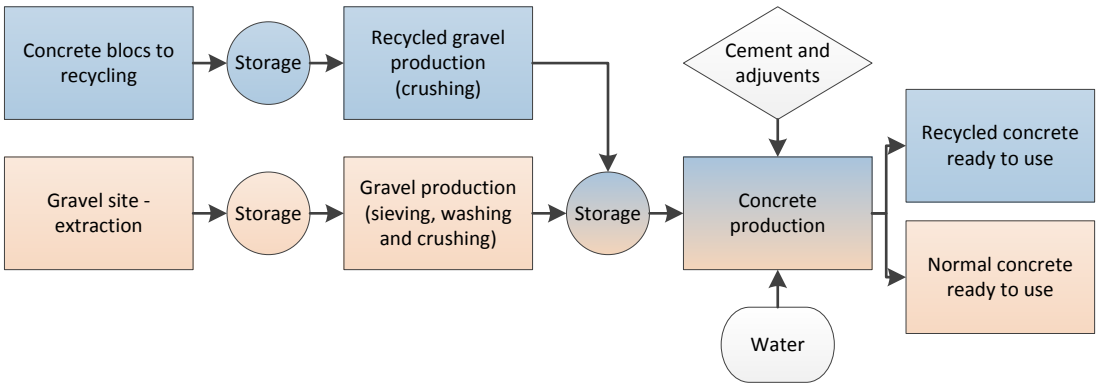

Figure 1 : System limits from the recycled and normal concrete production at GCM

Relevant building environmental indicators

Different indicators can be used to evaluate environmental impacts of a product. In this project, two indicators have been chosen because they are relevant for building materials:

- Cumulative energy demand – total (CED) – accounting for renewable and non-renewable primary energy expressed in MJ-eq.
- Global warming potential (GWP) – accounting for greenhouse gas emissions expressed in kg CO_2-eq.

RECYCLED AND NORMAL CONCRETE – THEORY, CALCULATION AND RESULTS

Gravel site

As the GCM Company wants to have their own datasets, the gravel site has been revaluated in comparison to the Ecoinvent dataset. The same methodology is taken into account, but as the function is different (producing recycled materials) and the site smaller, a new dataset has been created. . It includes buildings, vehicles, technical installations and different areas types (building, ways, vegetation, etc). The gravel site extraction area is not taken into account, in accordance to the Ecoinvent dataset.

The total production of natural gravel during the gravel site lifespan is estimated at 1'560'000 m^3, including bank gravel, round gravel, crushed gravel, sand and mud. The total mass produced is 2'964'000 tons (density of the natural gravel equal 1.9 tons/m^3). Nearly 20% of the bank gravel goes directly to the recycled storage area. The remaining is used to produce:

- Round and crushed gravel (59%),
- Sand (33%),
- Mud (8%) which are « recycled » in the system limits.

For all recycled materials, the total amount corresponds to 1'622'026 tons (density: 1.7 tons/m^3) for 20 years, based on the average results of the annual inventory. The part of recycled gravel we are interested in is the B4-32 with about 96'675 tons for 20 years. The GCM site produces about 8'000 m^3 of recycled concrete each year.

The total weight of the GCM gravel production is about 4'586'026 tons. An allocation (*Table **1***) presents the gravel production that will be used to manufacture the two types of concrete (normal and recycled).

	Mass of material [tons]	**Distribution ratio [%]**
Natural gravel (natural and recycled concrete) - round and crushed gravel and sand	2'377'128	52
Recycled material + bank gravel (for recycled concrete)	2'208'698	48
Total amount of material	4'586'026	100

Table 1 : Distribution of the gravel production between the two groups of products

However, all the inputs data are not on the same allocation rates as in *Table **1***. Some storage areas and machinery are use completely for the natural gravel production.

Gravel round and crushed process

The dataset for production of round and crushed gravel contains the following inputs: resources, gravel mine, infrastructures, exploitation vehicles, installations, energy vectors for process operation, replacement equipment, gravel mining area, storage area and rehabilitation of land. The outputs are the co-products, emissions to air and solid and liquid wastes. In this study, the Ecoinvent dataset "gravel/sand, at mine" was modified so that the inputs and

outputs correspond to the GCM ones. All inputs/outputs are calculated for 1 kg of natural gravel. The main co-products are round and crushed gravel and sand.

Gravel recycled

For this material a new dataset has been created with the following inputs: resources, exploitation vehicles, energy vectors for process operation, equipment replacement and storage area. The outputs are the co-products, emissions to air and liquid wastes. The co-products are recycled gravel (53.6%), recycled sand (43.9%) and steel (2.5%).

The recycled blocks used as secondary materials are considered as resources. The impacts of their transportation from their site of origin (demolished building) to the storage unit are taken into account in the new dataset.

Normal concrete and recycled concrete

The resources inputs used to produce these two types of concrete are different. The rest of the system limits is identical. The real GCM production has been taken into account because the process differs from the one of "normal concrete" in the Ecoinvent dataset. The inputs for 1 m^3 of concrete are: resources, infrastructures, installations, energy vectors for process operation, equipment replacement, storage area and transports. The outputs are heat to the air, rubber waste and sewage.

Data results

The impacts of the GCM products are showed in *Figure 2*.The Ecoinvent v2.2 dataset for the normal concrete is also given for comparison purposes.

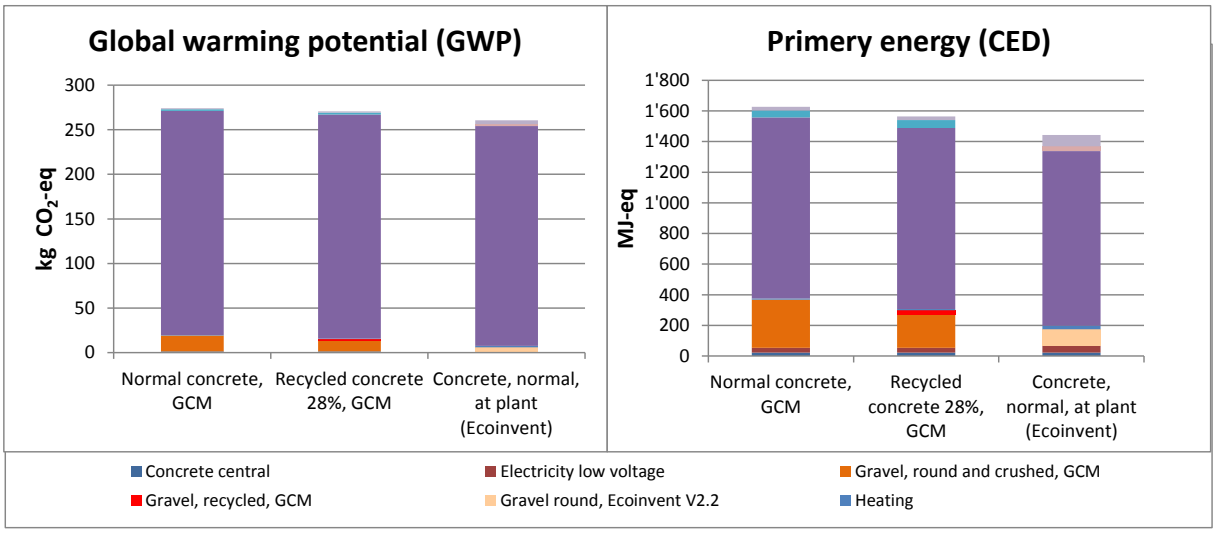

Figure 2 : Impacts for 1 m3 of concrete for the 2 indicators.

It can be seen that recycled concrete has slightly lower impacts than normal concrete with differences of about 2% for GWP and 4.0% for CED. Given that the amount of cement is the same for both concrete types, these differences are due to the recycle gravel that presents three times lower impacts than normal gravel, round and crushed, which is promising. However, differences remain small as impacts from the cement content in the concrete dominate, about 75% for CED and 92% for GWP.

For both indicators, the results from the GCM datasets are close to those of Ecoinvent. The slightly higher impacts are probably due to the higher level of detail of the GCM datasets in

comparison to those of Ecoinvent. Ecoinvent only uses round gravel as primary material, which has lower impacts when compared to crushed gravel. Despite the fact of requiring more transport, no additives are taken into account.

COMPARISON BETWEEN THREE CONCRETE PRODUCTION SCENARIOS – THEORY, CALCULATION AND RESULTS

To put the new datasets into real cases, three scenarios are used to evaluate the effect of the transport:

- Reference scenario: production of recycled concrete, ECOBETON®, at the GCM site and transport to the construction site
- Scenario 1: production of normal concrete at the GCM site and transport to the construction site
- Scenario 2: production of normal concrete at the construction site. All primary materials and the concrete central installation are transported to the construction site.

Methodology

The functional unit of the system is to have "7 m^3 of concrete ready to use on the construction site". The system limits go from the extraction of raw material to the transport of the concrete ready to use on the construction site. The function of each concrete is the same. Concrete is a material with technical features and his implementation is limited in time. The radius of action after manufacturing is at most 25 km.

A reference construction site has been taken 10 km away from the GCM. To perform a sensitivity analysis, four other construction sites have been chosen with distances of 5, 15, 20 and 25 km to the GCM site. For the first two scenarios, the concrete is transported to the construction site by lorry. For scenario 2, all products come from the following production companies: concrete central (Yverdon-les-Bains), cement (Éclepens), additives (Düdingen), gravel (Bretonnière-Switzerland and Pontarlier-France).

Results and discussion

Figure 3 shows the results for the construction site situated 10 km away from GCM. To provide a better comparison between scenarios, all material transportation has been gathered together.

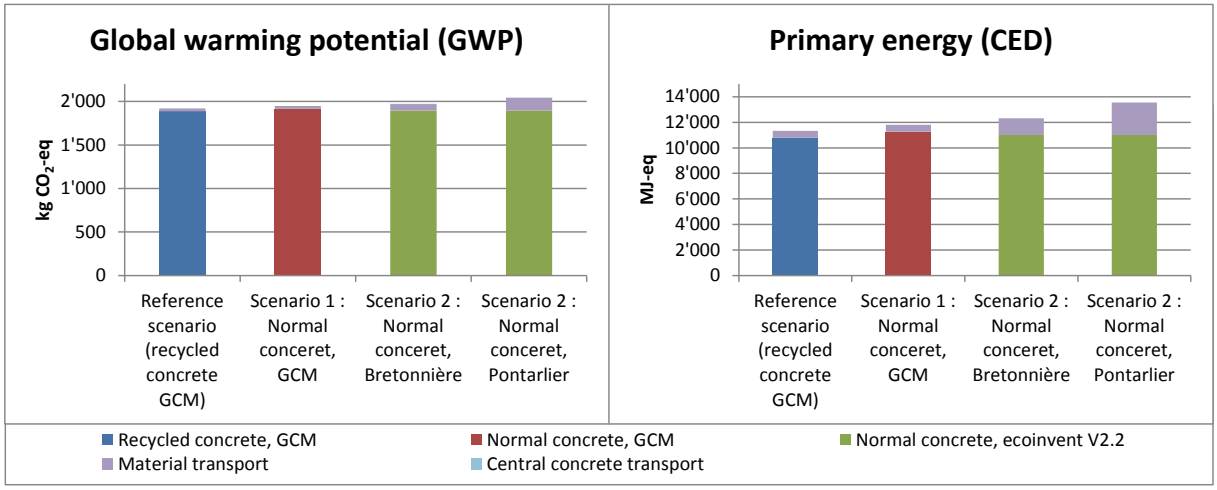

Figure 3 : Impacts for 7 m^3 of concrete ready to use on construction site 10 km away from GCM.

For both indicators, recycle concrete performs better than any other scenario. The same results appear for the other construction site distances (5, 0, 15, 20 and 25 km). The worst case is scenario 2, where the heavy transport of gravel leads to higher transport impacts. Differences between scenarios are less marked for GWP.

The difference with the reference scenario goes from 2.8% and 10.6% more impacts. The difference is mainly due to the transport of the gravel. The latter is heavy to transport and raises the impacts. When taking a construction site between the GCM site and Bretonnière, the difference gets really smaller and at one point the advantage goes to the Bretonnière scenario, unfortunately too far for GCM (more than 25 km). The second scenario with gravel from Pontarlier remains the worst of all.

For the GWP indicator, the differences between the scenarios are less marked, but the reference one stays the best. The results for the reference scenario and the scenario 2 (Bretonnière) give between 0.8% to 7.5% less impacts, depending on the distance of the construction site.

REFERENCES

1. Viviani M. (2011) Mix design for durable recycled concretes, proceedings of the 12th International Conference on Durability of Building Materials and Components, Porto, Portugal.
2. Padmini, A.K., Mathews, M.S., & Ramamurthy, K., 2009, 'Influence of parent concrete on the properties of recycled aggregate concrete', Construction and Building Materials, 23, 829–836
3. ISO 14'040 and 14'044 standards,
4. International database ECOINVENT Version 2.2, Centre for Life cycle Inventories, Dübendorf
5. Documentations of the GCM company : impacts reports, annual company products flow, documents on the vehicles and installations.

CONTRIBUTION TO THE STUDY OF THE IMPACT OF URBAN MORPHOLOGY ON URBAN MICRO CLIMATE AND BUILDING ENERGY LOADS: METHODOLOGY AND PRELIMINARY RESULTS

L. Merlier[1,2]; F. Kuznik[1], G. Rusaouën[1], S. Salat[2].

1: Centre de Thermique de Lyon, UMR 5008, INSA Lyon, 9 rue de la Physique, 69621 Villeurbanne, France.

2: CSTB, Urban Morpholgy Lab, 4 rue du recteur Poincaré, 75 016 Paris, France.

ABSTRACT

Urban micro climate mainly results of complex interactions between sun beams, mesoscale winds and urban objects. Complex heat and mass exchanges occur next to buildings, and define outdoor pedestrian comfort conditions, pollutant exposure, as well as HVAC conditions. The understanding of the impact of urban morphology on the congruent local micro climate is thus of uttermost importance to human health and energy savings. To accurately assess these complex interactions and their applicative implications, numerical investigations seem to be the most relevant technique, enabling systematic and parametric approaches. Nonetheless, few studies simultaneously investigate both urban morphological features at several spatial scales and detailed coupled physical phenomena.

However, recent computational capabilities improvements allow for the modelling of more complex geometrical and physical configurations. Thus, this paper presents a preliminary study based on simulations of the influence of urban morphology on corresponding aeraulic features. CFD simulations are performed on generic urban patterns, corresponding to representative examples extracted from typologies which were built on the base of a morphological analysis of worldwide real urban configurations. The abstraction done when defining these typologies by following a physical point of view is a key point of the approach. Because of their representativeness of real urban patterns, a wide scope of declinations for further urban physics investigations is then allowed.

First comparisons of numerical results obtained for each single building and neighbourhood type, in terms of mean wind flows, highlight the impact of built and empty volumes layouts on ventilation issues. They underline also sensible points relative to the modelling strategy, e.g. the choice of the turbulence model or the near wall treatment. Then, based on those preliminary results, urban configurations as well as physical models would be complexified to reach more realistic and accurate modelling.

Keywords: local micro-climate, urban morphology, generic typologies, CFD simulations.

INTRODUCTION

A city is not only a collection of buildings, but a complex system composed of built volumes and empty spaces. It is their nesting, in combination with the mesoscale climatic conditions, that determines air and energy flows inside. Physical phenomena of concern are mostly related to radiative and convective exchanges. Today, if a single building optimization can be achieved in terms of global shape and technology, less expertise is available to understand and then improve urban patterns. However, considering actual “Sustainable Development” issues, this field needs to be more deeply investigated.

Some studies have been performed to analyse urban micro climate and building energy consumption with regard to urban morphological parameters. Focussing on theoretical typologies, [1] analysed the impact of urban form on building environmental performance through the computing of morphometric and solar accessibility related parameters. [2] also used morphometric descriptions to characterize urban fabric properties, as the shape factor or the passive volume among others, and shows how urbanism and architectural typologies could be linked with energy consumption levels.

Other more detailed coupled radiative / CFD computations have been performed on urban neighbourhoods to assess outdoor conditions or building energy consumptions [3] [4]. They highlight the joint influence of radiative and convective phenomena, and the complexity of such mechanisms. Consequently, traditional meteorological datasets, extracted from airport recordings, and surface exchanges coefficients need to be enhanced when aiming at accurately compute energy transfers in urban contexts. More precise correlations, as proposed by [5] for instance, are yet to be built.

Following quite different approaches, methodologies and spatial scales, all of those investigations question how solar energy and airflows enter, behave and interact with urban objects. Focusing on interactions between urban morphology and urban physics arise two types of questions. First, how to relevantly describe urban and building morphologies in a thermo aeraulic point of view? This issue deals with the identification of suitable parameters and geometrical types based on physical exchanges consideration. Second, how to accurately model the complex thermo aeraulic exchanges occurring in cities? This point is more linked to how to perform quite comprehensive and sufficiently precise numerical simulations.

To investigate such complex phenomena, an analytic methodology has been defined, whose first steps are presented here. This preliminary study on generic urban layouts would then allow for heat transfers integration and geometrical model growing complexity. Thus, this paper begins with the definition of the investigated urban typologies, based on a morphological analysis of real urban patterns. Next, the modelling fundamental hypothesis and the model validation case are presented. Qualitative results in terms of mean wind features are then analysed. Finally, interactions between the investigated urban types and their aeraulic properties, as well as the modelling strategy, are discussed.

DEFINITION OF THE BUILDING AND URBAN BLOCK STUDIED TYPOLOGIES

Focussing on aeraulic aspects, [6] discussed methods linking urban surface morphometric attributes and cities aerodynamic characteristics. A classification of urban patterns with regard to their aerodynamic properties (for pollutant dispersion issues) has been proposed by [7] as well. Its sample is limited to German cities but highlight important geometrical parameters of urban fabric with regard to air flows. Enlarging the scope, and starting with a fairly similar approach as [8], preliminary works and investigations led us to the definition of a generic typology of building shapes and block configurations, on the base of [9]. The book focuses on the relationships between architecture and urban forms typical of the period from last 18^{th} to early 20^{th} centuries, but still existing. Each of the 30 reference urban type is composed of repetitive elements. Focusing on the spatial program and configuration, they show which link could exist between a housing type and the corresponding urban configuration, i.e. the street network and formal properties. An observation is that a housing type should not be associated with just any urban fabric, and reciprocally. This consideration led us to the definition of a first typology of building shapes, whose classification and analysis criteria are only based on objective geometrical considerations: mainly the topology and the three dimensional proportions. For this first study, the regularity and the symmetry of the shapes were kept.

Then, a corresponding typology of urban blocks was deduced. Further investigations could improve this typology with respect to preliminary simulations results, and introduce architectural components as roof shapes, which are known to be important for urban ventilation [10], or other complexity factors at different spatial scales.

As this paper mainly focuses on the methodology, only some elementary, but representative, block case studies belonging to these typologies are shown (Figure 2). More numerous generic building shapes are reviewed (Figure 1).

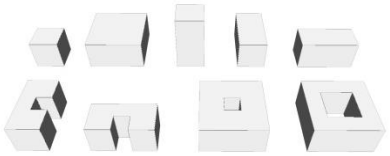

Figure 1: Housing typology (cube, tower, slab, U and courtyard)

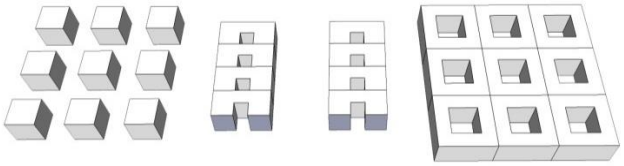

Figure 2: Examples of block configurations (repetitive association of housing types)

FUNDAMENTAL ASSUMPTIONS AND MODEL VALIDATION

Simulations were performed using Ansys Fluent 14.5.The turbulence model was the RANS two equations k-ε realizable one. Standard wall functions (WF) were used to take into account surface roughness. No thermal exchange was modelled yet. Mesh was refined at and next to the smooth walls of obstacles and on the rough floor. Computational methods were at least taken second order upwind.

Prior to simulations, the model validation was realized on an isolated smooth cube (of 8 cm side length) which was simulated in a wind tunnel for a wide range of Reynolds numbers (Re), and then by large eddy simulations (LES) [11]. The tunnel working section was 0.6*0.9*4.5 m^3. The chosen Re case is 18 600, and corresponds to a streamwise velocity (U) magnitude of 3.49 m/s at the cube height (h). A pretty well refined mesh was realized on the obstacle. Due to the floor roughness height of h_0=3 mm, and to the chosen WF formulations, the mesh should be a bit coarser there.

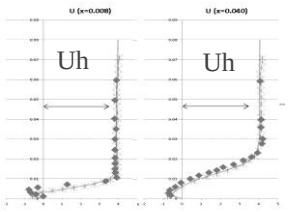

Figure 3: U over the cube for x/h =0.1 and 0.5, ◆ is experiment, ✳ LES and ▬ RANS k-ε.

The reference experiment was modelled following two steps. First simulations aimed at modelling the far-field, knowing the experimental mean U profile at the eventual cube location. Then, assuming that the turbulent boundary layer had been satisfactorily reproduced the mean velocity field around the cube, U and Y velocities (W) profiles above the cube roof and the pressure coefficient on the cube sides were investigated. No fluctuating outputs of turbulence had been examined since the model was performed using the RANS k-ε model. Despite its well known limitations, results were found to be in good agreement with experimental and LES datasets as partially shown in Figure 3.

To verify the Re and the reduction scale independence, two other simulations were performed for the cube case, increasing all the geometrical dimensions by a factor 10 and 100, which correspond to a real building height. Results showed that scatters were weak, except for very high roughness values when modelling the far-field. However, when the far-field was well readjusted, comparisons in terms of U and W profiles over the smooth cube did not show significant scatter in comparison with other models. Hence, following simulations were carried out for the smallest model which was directly confronted to experimental and LES datasets. All of the parametrization of the far-field and of the whole simulation were kept equivalent to investigate the geometrical model influence.

CASE STUDIES: RESULTS AND ANALYSIS

Impact of building shape

Simulations were performed for 9 cases: the cube (l=h and h*2, h=h), the tower (l=h, h= h*2), the slab (l=2h, h=h), the U (l=2*h, hole=h/2, h=h), the courtyard (l=2*h, hole=h/2 or h, h=h). For the slab and the U, two cases were tested: parallel and perpendicular to the mean flow. Some results in terms of mean velocity fields on the XY middle plane (except for the case 3b were it had been moved by 0.02 m to fit the middle of the courtyard) are given in Figure 4.

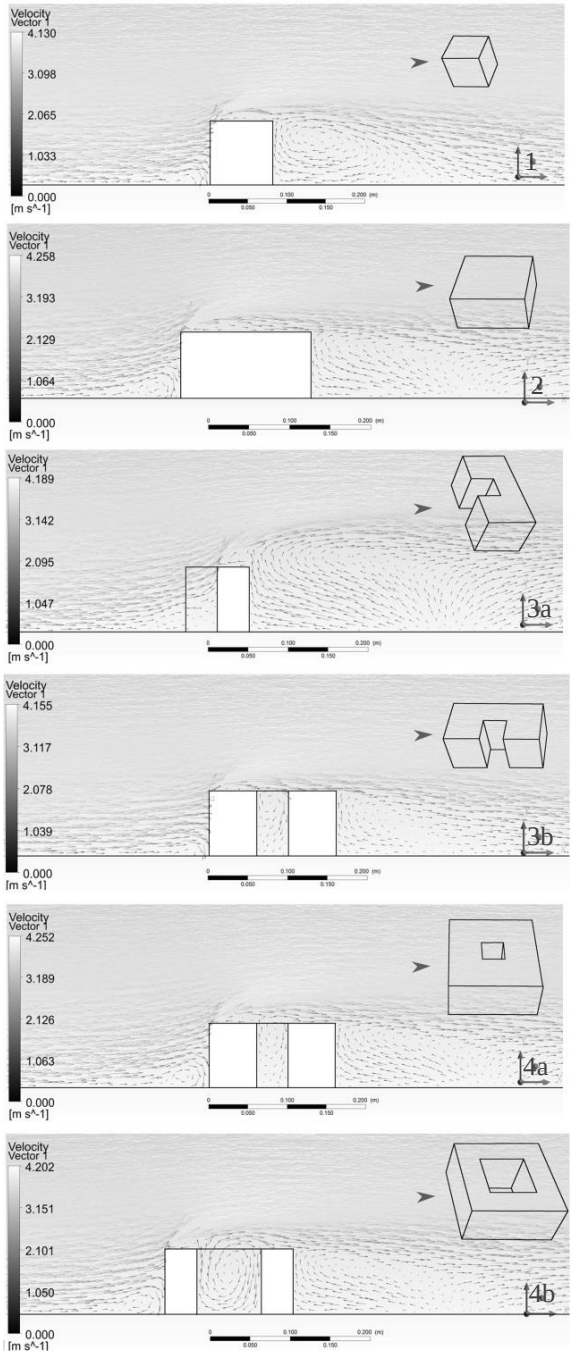

Figure 4: Mean velocity fields for single building case studies.

These results show some common features to all of these cases. At least, three mean wind recirculations always occur. One takes place down just upstream the building, another is at the separation point corresponding to the leading edge of the roof, and the wider, downstream. However, the position and the global shape of the upstream and downstream eddies vary from one case to another. Logically, the downstream vortice centre is higher for higher obstacles (not shown), but its stretch in the slab perpendicular to the mean flow case (not shown) or in the case 3a, is also noticeable. The larger the building, the further the reattachment point is. Moreover, three dimensional recirculations can clearly be observed, especially for the case 3a, where the combination of the building width, of the courtyard and of the corresponding partial thickness reduction, lead to the development of a particular air motion behind the downwind wall. The case 3b, and even more the slab parallel to the mean flow (not shown), show a closer reattachment point than for the cube. This seems to be a tendency for longer buildings. Relatively to the upstream eddy, the larger the building, the bigger the recirculation is.

Hence, those results already show the effective influence of the building relative dimensions, topology and compacity, as well as of the ratio between the empty and the built volumes on the mean flow behaviour in the case of forced convection. Indeed, the size (height, width and thickness), the relative position and the openness of the courtyard lead to different eddy structures, which can notably change the ventilation potential of this semi enclosed air volume.

Impact of the urban block configuration

Simulations were performed for 3 regular cases: an array of 3*3 cubes, two rows of U, and a network of 3*3 courtyard houses. To avoid domain boundary effects on the model, the computational domain width has been extended. The far-field has been readjusted to fit again the experimental profile. Dimensions of obstacles were kept similar as in the last section to allow for an investigation of the surroundings and of the group effects.

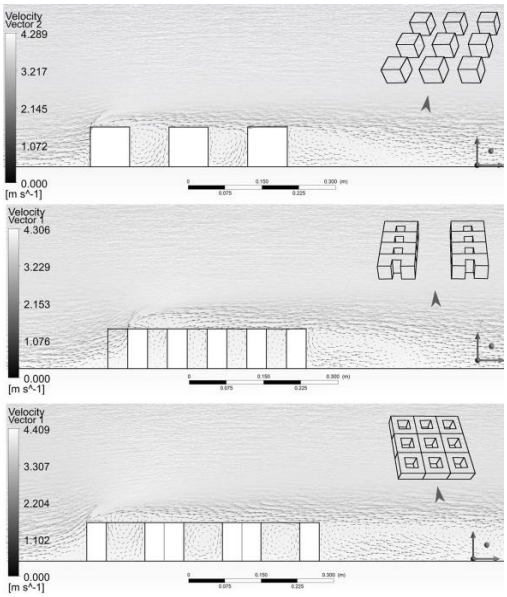

Figure 5: Mean velocity fields for the 3 associated case studies.

Comparisons between mean fields obtained in these cases and the corresponding wind patterns obtained for the elementary volumes clearly show significant differences at roof level and in courtyards, where vortices are however always observable. Those ones vary in shape, strength and position with the distance to the leading edge of the group. If they tend to exceed the roof level at the beginning of the obstacle network, further, they tend to be contained within courtyards. There, fewer exchanges occur with the above mean flow as the roof boundary layer is developed parallel to the roof plane. Especially visible in the third case and due to the geometrical extension and to the obstacles and voids succession, the downstream recirculation shows a horizontal development. The upstream eddy is bigger than in the stand alone building case, certainly because of the increased geometrical model width.

Thus, two kinds of observations could be distinguished from those results. First, it concerns the global group effects, that is to say the built and empty volumes network global impact on upstream and downstream flow features. Second, it deals with flow patterns within the geometrical model, and their attributes with respect to the localisation relatively to the group boundaries. Those features can be explained by the increased dimensions of the geometrical model, by its growing complexity and by the flow adaptation at roof level, which could lead to very different global and local ventilation potential levels.

DISCUSSION, CONCLUSIONS AND PERSPECTIVES

From these preliminary simulations, some tendencies can already be drawn, and confirm the relevancy of such a morphological approach to study urban air and energy flows. Indeed, the influence of the global shape and dimension of built volumes on mean wind fields was observed, as well as the impact of other morphological factors related to empty spaces, which have traditionally a huge social importance. The building compacity and the courtyard geometrical features lead to complex recirculations, whose attributes are very important depending on the regional climatic context. Indeed, even if they have not been modelled yet in our case studies, for lower winds or/and including thermal effects, such outdoor spaces can significantly affect ambient climatic conditions and building energy and ventilation loads, and thus, act as thermal regulators. However, considering an isolated building is not sufficient to understand heat and mass transfers that occur in urban context, because of the great influence of the fetch (history of the flow) and boundary conditions (gradients generated by the surrounding urban built and empty elements), as it was sketched for the multi obstacles configuration examples. Consequently, the identification of urban block patterns which are generally correlated to housing types as well as their more accurate study would contribute to a better urban energy control and city design.

This introductory study also highlights some modelling strategic issues linked to the accuracy of simulations. Indeed, as far as turbulence phenomena and coupled heat transfers are themselves complex, and even more with the urban complexity dimension, micro climatic assessments quickly propagate and amplify uncertainties and errors due to the use of simplified assumptions. The realizable k-ε model, with standard WF, have been used in our preliminary simulations. Nevertheless, this implies the computing of mean values, as well as the modelling of a quasi isotropic turbulence, and the approximation of wall boundary layers with an empirical logarithmic law. The relevance of such choices is discussed and still needs further comparison with experimental data. Thanks to recent advances in computing power, but also of the urban physics expertise, more complex geometrical and numerical models can be used together with more accurate correlations. It deals especially with turbulent features and heat transfers at building outer wall surfaces modelling. Thereby, the next step of this work is to improve the physical modelling to allow for a detailed comprehension of physical phenomena occurring firstly in the generic typologies, and then, in more realistic configurations.

REFERENCES

[1] C. Ratti, D. Raydan, et K. Steemers, « Building form and environmental performance: archetypes, analysis and an arid climate », *Energy and Buildings*, vol. 35, n° 1, p. 49–59, 2003.

[2] S. Salat, « Energy loads, CO2 emissions and building stocks: morphologies, typologies, energy systems and behaviour », *Building Research & Information*, vol. 37, n° 5‑6, p. 598‑609, nov. 2009.

[3] J. Bouyer, C. Inard, et M. Musy, « Microclimatic coupling as a solution to improve building energy simulation in an urban context », *Energy and Buildings*, vol. 43, n° 7, p. 1549–1559, 2011.

[4] Qu, « Three-dimensional modeling of radiative and convective exchanges in the urban atmosphere », Université Paris Est, Paris, 2011.

[5] T. Defraeye, B. Blocken, et J. Carmeliet, « Convective heat transfer coefficients for exterior building surfaces: Existing correlations and CFD modelling », *Energy Conversion and Management*, vol. 52, n° 1, p. 512–522, 2011.

[6] C. S. B. Grimmond et T. R. Oke, « Aerodynamic properties of urban areas derived from analysis of surface form », *Journal of applied meteorology*, n° 38, p. 1262‑1292, 1998.

[7] W. Theurer, « Typical building arrangements for urban air pollution modelling », *Atmospheric Environment*, n° 33, p. 4057‑4066, 1999.

[8] Y. Huang, « Methodology of climatic design of urban district for building energy efficiency », Université de Nantes, Nantes, 2010.

[9] E. Firley et C. Stahl, *The urban housing handbook*. John Wiley & Sons Inc, 2010.

[10] P. Kastner-Klein, R. Berkowicz, et R. Britter, « The influence of street architecture on flow and dispersion in street canyons », *Meteorology and Atmospheric Physics*, vol. 87, n° 1, p. 121–131, 2004.

[11] H. C. Lim, T. G. Thomas, et I. P. Castro, « Flow around a cube in a turbulent boundary layer: LES and experiment », *Journal of wind engineering and industrial aerodynamics*, vol. 97, n° 2, p. 96–109, 2009.

URBAN FABRIC PERFORMANCE IN MEDITERRANEAN CITY: A TYPOLOGY BASED MASS-ENERGY ANALYSIS

Michele Morganti[1]; Anna Pagès-Ramon[2]; Antonio Isalgue[2], Carlo Cecere[1], Helena Coch[2]

1: SOSlab / Sapienza University of Rome, Faculty of Engineering, DICEA Department / Via Eudossiana 18, 00184 Rome, Italy

2: Arquitectura, Energia i Medi Ambient / UPC, School of Architecture / Diagonal, 649, 08028 Barcelona, Spain

ABSTRACT

The link between urban form and building energy demand is a complex balance of morphological, constructive, utilization and climatic factor. Especially in European compact city where existing areas prevail on much more energy-efficient new settlements, it is evident that operative ways to transform efficiently the building stock have to be found. Moreover, it is now widely accepted that urban scale has a first rate importance in the building design process and its correlated energy performance. It has been observed that scaling laws are useful in describing the complex structure of urban systems: modern cities have a "metabolic rate" that approximately follows the living organism scaling laws. Nevertheless, it has not been entirely verified that this connection remains the same while studying the phenomena at the urban and building scale and what kind of relationship between mass and power exists (i.e. energy) depending on typologies and urban form. This study suggests an approach for using mass parameter - representative of built-form - as energy performance evaluation tools on a homogeneous urban texture. Mass is connected to both built-form and technology and these determine, to a great extent, the energy use. In Mediterranean climate, it has been observed that mass has strong relevance on energy demand playing an important role in reducing heating and cooling consumptions. Our work aims at validating this relationship, focusing on widespread urban fabrics of the Mediterranean compact city. Tests on different case studies from Barcelona and Rome (analyzed independently in terms of their energy demands and their masses) are carried out. Mass evaluation is based on calculation of effective mass of built elements. Building energy demand is assessed by modelling on multi space dynamic thermal analysis tool. Results presented and discussed point out that heating and cooling energy demand are related to urban fabrics mass and, starting from typological based analysis, it's possible to estimate it. This work is a broader treatment of a research study about one possible way to comprehend "metabolic rate" scaling law concerning urban fabric. Such knowledge-base could giving hints to conscious and effective built environment transformations towards more efficient conditions.

Keywords: Urban fabric energy performance, Built-form, Building mass, Building energy demand.

INTRODUCTION

In the last few years the EU has introduced Directives and has promoted different studies on the topics of renewable energy, GHG emissions reduction and energy performance in buildings and recently admitted that it's an inevitable need and an opportunity to obtain complete self-sufficiency through renewable energy by this mid-century [1, 2, 3]. In this extremely complex process - where, besides, we notice an urban population growth associated with urban areas expansion - the built environment has a central role, regarding both energy

and emissions (69% global consumptions - 75% GHG emissions overall) both in terms of its reduction possibility [4]. As an example, EU government undertook to reduce CO_2 emissions by 80% by 2050 compared to 1990 levels. It has been estimated that this drop overall implies 95% reduction in the building sector [3]. This goal needs innovative design strategies and technological solutions for new settlements and it requires a simultaneous improvement in energy performance of existing urban fabrics too, in order to reduce global energy demand. Especially in European compact cities of Mediterranean climate - where existing areas prevail on much more energy-efficient new settlements - it becomes crucial to deal with the existing building stock whose housing is the main part and is responsible for 65% of final energy consumption in buildings [5]. Moreover it is now widely accepted that urban scale has a first rate importance in building energy performance: urban form, due to the obvious connection with morphology and building systems, both at the urban and building scale, mostly affects these performances [6]. Our aim is the study of urban fabric energy demand, beginning with building aspects. Estimation of the effects of built-form on mass and energy demand is the main goal of this paper. In Mediterranean climate regions, it has been observed that mass has strong relevance on energy demand, playing an important role in reducing heating and cooling consumptions. This work aims at validating this relationship, focusing on typical urban fabrics. Apart from testing its existence depending on built-form, our aim is to establish some key elements of a knowledge-base for future analysis on conformity with the "metabolic rate" scaling law at urban scale.

BACKGROUND

Despite numerous studies carried out in the last years on the influence of complex environmental interactions occurring in the urban context that allowed to develop methods and techniques for energy simulation at this scale, more research efforts are necessary to comprehend the interaction between built-form typology and energy performance of different urban fabrics. A number of results emerged on the relationship between city textures and energy consumption, proving the accuracy and consistency of different geometrical parameters and the impact of urban geometry on energy [6]. The incidence of built-form features in this interaction has been ascertained at building scale suggesting a typological classification based on chronological, dimensional and morphological factors [7]. Furthermore, under the description of the complex structure of urban systems through scaling laws, it has been observed that modern cities have a metabolic rate (mass-power ratio) that approximately follows the living organism scaling laws [8, 9]. Studying the phenomena at the scale of urban fabric in Mediterranean climate, it has been found that mass plays an important role in reducing energy demand (for heating and cooling) [10]. Once established that mass is a parameter strictly connected to built-form, it can also be the connection between housing types and energy performance. This aspect is even more relevant in the context of European compact city where we can easily find urban fabrics consisting of fundamentally uniform morphological and typological elements.

METHODOLOGY

The methodology of this study focuses on morphological aspects relating to mass and energy performance. Building mass evaluation is based on calculation of effective mass of built elements excluding associated mass due to the construction process, which is not part of the building. Results shown are expressed in metric Tons referring to thermal conditioned areas as specific weight (Tm/m^2). Energy demand was evaluated by modelling on *Lider 1.0* [11] that provides energy demand measured in kWh/m^2year where the considered surface refers to a thermally conditioned area. Thanks to the similar climatic conditions of the cities involved

in this study, it has been possible to take the Mediterranean climate of Barcelona as climate of reference. More details about this procedure could be found in [10].

CASE STUDIES

This study compares nine different conventional housing types located in the metropolitan areas of Barcelona (ES) and Rome (IT) - where we can reasonably assume very similar climate conditions [15]. They represent the basic components of typical urban fabrics built during various historical periods (Fig. 1, Tab. 1). Cases A÷E (Barcelona) are described in [10] while cases F÷I (Rome) are analysed here as follows:

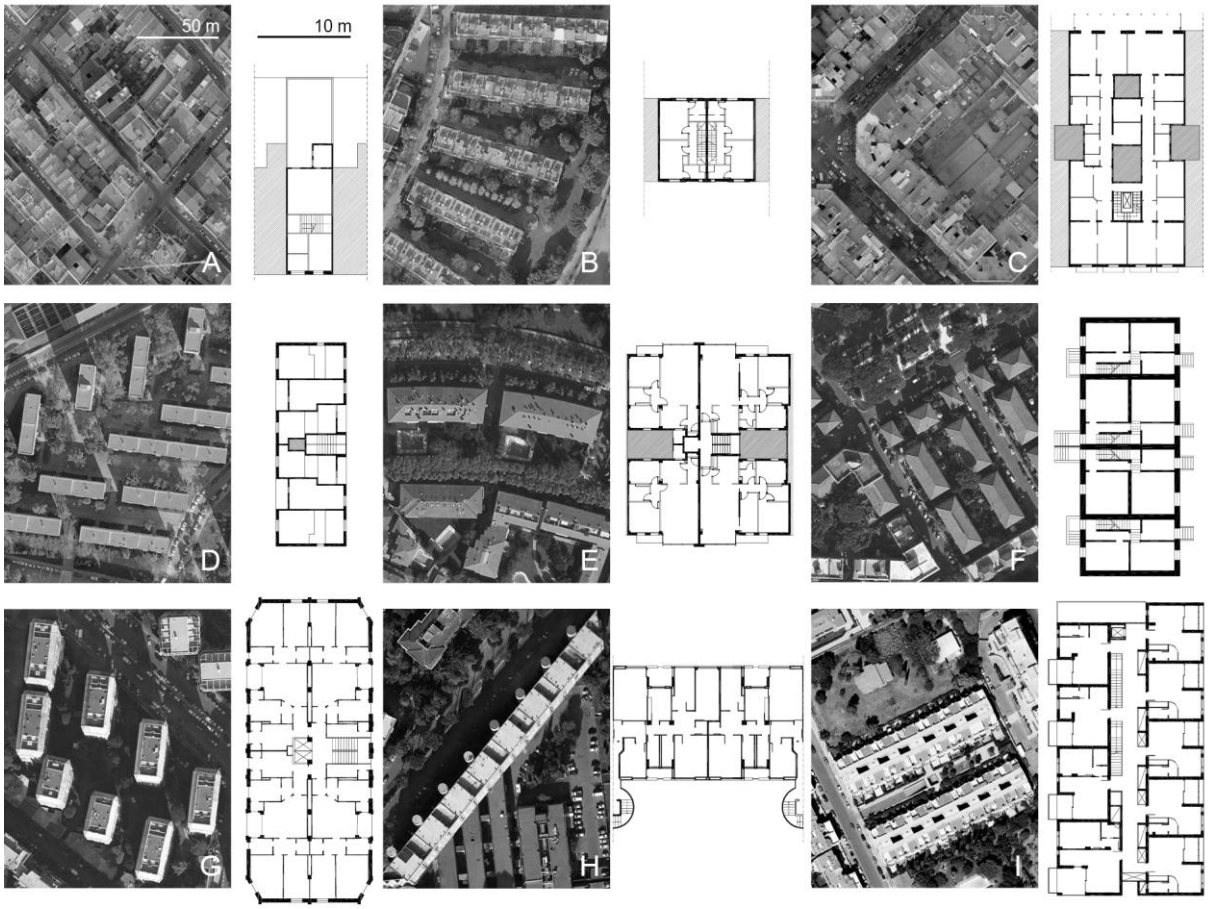

Figure 1: Aerial images and typical plans for case studies (A÷E Barcelona, F÷I Rome).

F - Row house (1920) - Two-level dwelling (plus one basement) with load-bearing walls, above-ground masonry continuous foundations and dry stone drain; vaulted floor at ground level, floors with iron beams and hollow bricks for other level; ventilated hipped roof without thermal insulation.

G - Apartment block (1960) - Nine-level apartment block with basement and floor service on top. The construction system is based on concrete frame, shallow footing and dry stone drain; floors with one-way reinforced concrete slab and ceramic filler blocks; external hollow brick cavity walls and flat roof without thermal insulation.

H - Apartment block (1975) - Seven level apartment block with floor service on top, based on concrete frame construction system and shallow footing; floors made by hollow-core concrete

slab and partially by reinforced concrete slab; external precast concrete wall panels with cavity and flat roof without thermal insulation.

I - Apartment block (2010) - Five level apartment block with basement made up of concrete frame and slab-on-grade foundation and floors with one-way reinforced concrete slab and ceramic filler block; external hollow brick walls with thermal insulated cavity and flat roof thermal insulated.

More detailed descriptions of case studies could be found in [12, 13 and 14].

	Year	Location	Housing type	$H/W_{x,y}$ ratio	GSI*(m2/m2)	FSI**(m2/m2)
A	1900	Barcelona	RH	0.77-1.47	0.45	0.87
B	2000	Barcelona	RH	0.30-1.22	0.16	0.62
C	1900	Barcelona	AB	1.21-2.83	0.49	2.92
D	1960	Barcelona	AB	0.41-1.27	0.13	0.77
E	2000	Barcelona	AB	0.45-0.83	0.37	2.43
F	1920	Rome	RH	0.39-1.02	0.35	1.07
G	1950	Rome	AB	1.08-2.56	0.21	2.35
H	1975	Rome	AB	1.14-1.90	0.13	0.89
I	2010	Rome	AB	0.56-1.11	0.24	1.48

*Table 1: Case studies data. * Coverage: built up area/base land area, ** Building intensity: gross floor area/base land area - RH: row house, AB: apartment block*

RESULTS AND DISCUSSION

Table 2 shows the built mass referring to useful floor area and annual energy demand (heating and cooling). The computation of energy takes into account eight possible orientations whose mean, minimum and maximum values are given in Table 2.

	Housing type	Thermal insulation	Mass (Tm/m^2)	Heating (kWh/m^2y)	Cooling (kWh/m^2y)	Heating and cooling (kWh/m^2year)		
						Average	Min.	Max.
A	RH	No	1.53	86.88	3.22	90.10	86.57	92.12
B	RH	Yes	2.58	21.85	13.32	41.04	33.17	47.01
C	AB	No	1.11	79.33	8.17	87.50	85.48	89.28
D	AB	No	1.24	77.52	5.74	83.26	78.29	89.28
E	AB	Yes	1.65	22.34	11.75	39.64	25.74	47.23
F	RH	No	2.64	67.19	2.95	70.14	66.17	73.50
G	AB	No	1.56	66.19	5.19	71.38	67.36	75.58
H	AB	No	1.69	79.30	6.68	85.98	81.25	90.31
I	AB	Yes	2.96	36.52	10.96	47.48	28.88	56.92

Table 2: Built mass and energy demand. RH: row house; AB: apartment block

In general terms, recent buildings tend to be heavier (in specific weight terms) than those constructed before 1980. The mass of the recent cases (Tm/m^2 of thermal conditioned areas) is greater than old ones, mainly because of mass properties in construction systems based on concrete and also because of more unconditioned spaces in the buildings - especially underground car parks. With regard to energy demand, it is possible to observe a clear distinction between traditional buildings (A, C, D, F, G and H) and recent buildings (B, E and I). The former have no thermal insulation envelopes, while the latter are built according to

thermal regulations that restrict heat transmission coefficient. Recent cases show a mean conditioning energy demand of between 40 and 50 kWh/m^{2}y, while the traditional cases one between 70 and 90 kWh/m^{2}y.

	Housing type	Thermal insulation	Specific Mass (Tm/m^2)	Inverse specific Mass (m^2/Tm)	Heating and cooling (kWh/Tm year)
A	RH	No	1.53	0.65	58.9
B	RH	Yes	2.58	0.39	15.9
C	AB	No	1.11	0.90	78.9
D	AB	No	1.24	0.81	67.0
E	AB	Yes	1.65	0.61	24.1
F	RH	No	2.64	0.38	26.5
G	AB	No	1.56	0.64	45.8
H	AB	No	1.69	0.59	50.9
I	AB	Yes	2.96	0.34	16.0

Table 3: Specific built mass and energy demand. RH: row house; AB: apartment block

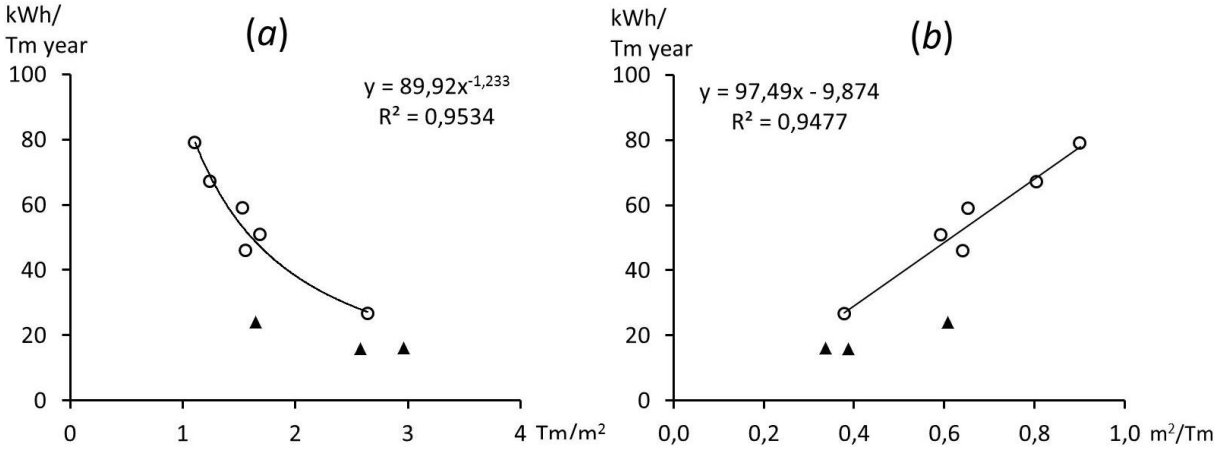

Figure 2 (a) Demand energy versus specific mass. (b) Linear fit of demand energy as a function of inverse specific mass. Empty circles: experimental values of traditional buildings; triangles: experimental values of recent buildings; continuous line: computed fits of traditional buildings.

Table 3 and Figure 2 show the existing tendency between mass properties and building energy demand. Referring to thermally conditioned areas, results point out that mass has strong relevance on energy; for traditional buildings (empty circles), may be approximated by the fitting as formula (1):

$$\boldsymbol{y = 89.92\, x^{-1.233}} \quad (1)$$

where ***y*** represents the energy demand (kWh/Tm year) and ***x*** the built mass (Tm/m^2 of thermal conditioned area) (Fig. 2 (a)). The proximity of the exponent to -1 suggests the trial of a linear fit using the inverse of the specific mass, which is presented in Figure 2 (b). Hence, greater the mass per conditioned square meter of an urban fabric is, less its energy demand for heating and cooling per mass unit is, as in [10]. Recent urban fabrics have heavier building systems (mass per conditioned unit area) and at the same time (because of thermal regulation) they have a lower energy demand. Then the points corresponding to cases built form since 1980 approximately - triangles in Figure 2 - have less energy demand and give different trend than the older buildings. This trend could also depend on the large amount of mass

corresponding to unconditioned spaces such as underground car parks. Moreover Figures 2a and 2b show that greater the mass per conditioned square meter is, more similar is the relation between mass and energy is, in both traditional and recent urban fabrics.

CONCLUSIONS

The analysis carried out in this study confirm that a relation between mass and energy demand (for heating and cooling) of different urban fabrics exists in Mediterranean climate, as we guessed at [10]. Results show a clear tendency of this relationship in buildings built before the introduction of thermal regulations. However, in recent buildings the relation between mass and energy demand, till today it has not been so investigated. Building thermal regulations imposes a minimum performance, which strongly influences energy demand. Moreover, the presence of more unconditioned spaces and basements in contemporary buildings, affects this relation.

REFERENCES

1. EU, P.: Directive 2002/91/EC of the European Parliament and of the Council of 16 December 2002 on the energy performance of buildings. 2002.
2. EU, P. : Directive 2010/31/EU of the European Parliament and of the Council of 19 May 2010 on the energy performance of buildings. 2010.
3. OMA and ECF: Roadmap 2050: A practical guide to a prosperous, low carbon Europe. [online], http://www.roadmap2050.eu/ [accessed 12th April 2012], 2010.
4. IEA, World Energy Outlook 2008. [online], http://www.worldenergyoutlook.org [accessed 12th April 2012], 2008.
5. Market Observatory for Energy: Europe's energy position: markets & supply. Luxembourg, Publications Office of the European Union, 2010.
6. Ratti, C., Baker, N. and Steemers, K.: Energy consumption and urban texture. Energy and Buildings, 37(7), 762-776, 2005.
7. Dascalaki, E. G., *et al.*: Building typologies as a tool for assessing the energy performance of residential buildings. Energy and Buildings, 43(12), 3400-3409, 2011.
8. West, G. B. and Brown, J. H.: Life's Universal Scaling Laws. Physics Today, 57(9), 36-42, 2004.
9. Isalgue, A., Coch, H. and Serra, R.: Scaling laws and the modern city. Physica A: Statistical Mechanics and its Applications, 382(2), 643-649, 2007.
10. Morganti, M., *et al.*: Built-Form, Mass and Energy: Urban fabric performance. Proc. of 28th PLEA Conference, Opportunities, Limits & Needs: Towards an environmentally responsible architecture, Lima, 2012.
11. Ministerio de la Vivienda de España: CTE - Código Técnico de la Edificación. 2006.
12. Cocchioni, C., *et al.*: La casa popolare a Roma: trent'anni di attività del I. C. P. Kappa, Rome, 1984.
13. Todaro, B., *et al.*: Il secondo progetto: interventi sull'abitare pubblico. Prospettive Edizioni, Rome, 2013.
14. Accademia Nazionale di San Luca: Fondo Ridolfi-Frankl-Malagricci. [online], http://www.fondoridolfi.org [accessed April 3rd 2013].
15. See, for instance, data from [online] www.weather.com [accessed April 3rd 2013]

MAPPING THE "TERRITORY-LESS" CITY: A CRITIQUE ON THE ESTABLISHED "AIRPORT CITY" STRUCTURE

A.Athanasopoulos

MPhil in Environmental Design in Architecture Candidate, University of Cambridge, Department of Architecture and University of Cambridge, Churchill College. Churchill College, Storey's Way, CB3 0DS, Cambridge, United Kingdom.

ABSTRACT

"In the UK and the EU, design practise and government policy aim to mitigate the impacts of aviation, but not at the expense of aviation growth. Sustainability should not be taken to mean a realised commitment to environmental impact reduction, but a consideration of environmental and social impacts alongside environmental and financial performance". (Urpham, P. A comparison of sustainability theory with UK and European airports policy and practice. Journal of Environmental Management. 63, 237-248)

The contemporary debate on airport planning and design aligns with the increasingly troubling concerns regarding economic growth and its impact to the natural and built environment. In terms of the city and region's future, under the pressure of both dense urbanisation of metropolitan areas and environmental and social sustainability, prosperity cannot be achieved through the exploitation of transportation growth and transportation inter-connectivity opportunities alone.

In this fragile environment of overlapping or dispersed authority, policy and momentum, "airport cities" emerge as new trade centres and, by attracting a proportion of the area's population to dwell or work within this new platform, they are becoming new urban and regional centres as well, yet of a debatable quality and with no distinct territory or population.

Nevertheless, regardless of the ongoing innovation in the fields of urban theories and construction technology, transportation policies and building regulations have so far failed to fully exploit such an advancement's potential and dilute the controversy over airport design priorities, in respect to both economic development and environmental protection, especially in the scale of the city or the 'airport city'.

As an essential first step towards a more sensible approach, this paper will try to map this "territory-less" platform's elements, and serve as a reference base for a future in-depth research on the establishment and development processes of such a new urban environment.

Key words: Airport city, Kevin Lynch, urban planning, sustainable development

INTRODUCTION

The contemporary debate on airport planning and design aligns with the troubling concerns regarding urban development, economic growth, and the impact to the natural and built environment, especially in terms of the city and region's future under the pressure of dense urbanisation of metropolitan areas and environmental and social sustainability.

It has been proven that transportation networks are of essential importance to the city's evolution. The trend particularly for airports to expand dramatically in area, intensity and variety of activities can significantly affect them very quickly and in very little time.

In this fragile environment of overlapping or dispersed authority, policy and momentum, "airport cities" emerge as new trade centres and, by attracting a proportion of the area's

population to dwell or work within this new platform, they are transforming into a new urban hybrid. Nevertheless, regardless of their obvious advantages in terms of accessibility to transportation networks, concerns about environmental and social instability and degradation still lead to scepticism around this urban structure's quality, territory and population.

By discussing about the city's structure as analysed by Mumford, Lynch and a number of other researchers, this essay will attempt to identify essential characteristics, highlight typological patterns, and map this "territory-less" platform, investigating its urban structure through the comparison of six distinct cases.

In order for the airport city to be recognised as a model of sustainable regional development, its structure must be defined and understood first. Towards that, this study will provide the theoretical background and support the further development of an in-depth field-research.

THE CITY'S STRUCTURE AND ITS SUSTAINABLE DEVELOPMENT

Describing the shift in urban development from the city centre to the periphery, Howard, Kropotkin, Gedes, Soria y Mata, Stein, Wright, Fuller, Soleri, Gruen, Le Corbusier and others proposed various forms of urban development [1,2]. From an *organic* to a *mechanical system,* the city was always perceived as a complex spatial, political and social entity which supports human identity and continuity, avoiding an "aimless and formless" expansion. Regardless of any morphological variations however, they all agreed on the importance of transportation networks and travel patterns in ensuring sufficient links within the region.

Similarly, Kevin Lynch [3] interprets the city as "a multi-purpose organisation, [...], the form of which must be plastic to the purposes and perceptions of its citizens". Focusing on the city's structure he identifies its essential elements: *the path, the edge, the landmark, the nodes, and the regions*, and highlights the importance of people being able to easily understand the space and its characteristics through them.

Analysing further these arguments, several researchers [4,5,6,7,8,9,10,11,12] locate delicate relations between city and region, following the urbanisation's natural life cycle stages "from urbanisation to counter-urbanisation, to re-urbanisation", highlighting the transport-oriented qualities of a polycentric development model. They particularly stress the impact of a community's history to the region's structure, and emphasize the need for establishing the city's development framework within such a scale, presenting several advantages and weaknesses and the importance of local characteristics in promoting sustainable development.

THE ROLE OF AIRPORTS IN THE CITY'S SUSTAINABLE DEVELOPMENT

As nodes of major transportation networks, similarly to train stations, airports are "influencing the growth and shape of the city, through the shift of economic activities from its centre to its periphery" [13]. In a regional scale, highly accessible through a variety of modes, the airport's rail or bus station serves as an interchange station, but usually fails to provide adequate accessibility within its platform. On the other hand, in a decentralised system, Fasone et al. [14] describe the promotion of more flexible mobility patterns. As they and other researchers [13,14,15,16] note however, this development usually happened without a clear planning framework, or as the result of a controversial planning process, causing the rearrangement of local transportation networks, with significant consequences to the form and evolution of the surrounding region.

Due to this "complexity of organisation" accompanying the airport's operation, its area is developing into "a form comparable to that of a city", a new urban hybrid that emerges among other regional centres; something that Güller and Güller [13] explain as: "In terms of

territorial definition, the airport city is, in principle, the more or less dense cluster of operational, airport-related, activities and other commercial or business concerns, on and around the airport platform. However, this cluster is an airport city only if it shows the qualitative features of a city (density, access quality, environment, services)". In the US, this term is used by Kasarda and Lindsay [17] to signify even a broader municipality. Both these research groups clearly describe the importance of a structured land use policy and distribution within or near the airport's area, and understand that the growth of an airport city "is not always inevitable, necessary, or desirable".

These two definitions, however, have two weaknesses, especially when progressing from the business park to the city level identification. The European approach considers essential the *qualitative features of a city*, not mentioning that of a permanent and vivid population, while the American one refers to an actual community, yet to that of the suburban residential enclave; with the reason for that lying probably behind the (un)suitability of the airport's platform as a receptor of residential development, as previously discussed.

Therefore, under the framework of principles established so far to describe the city's structure and evolution, it is difficult to identify the 'airport city's hybrid' as an emerging prototype of contemporary urbanism, substituting already established centres. Even if not a 'city' per se however, handling the airport's area as a distinct form of the built environment brings about some of the clearest practical challenges to achieving the right balance between economic, social and environmental sustainability.

SIX EXAMPLES

Following the previous discussion, six 'airport cities' (Spruce Creek, Berlin-Tempelhof, Denver, Frankfurt, Athens and Helsinki) will be compared, attempting to identify typological patterns, planning characteristics and urban qualities. These examples, even though constitute a small sample, present a variety in characteristics, and their further analysis could provide a valuable insight over elements of urbanity within the airport's platform, often neglected or disregarded, progressing the relevant discussion initiated in the existing literature.

For this comparison, an investigation based on Kevin Lynch's proposed elements of the city (*the path, the edge, the landmark, the nodes, and the regions*) will be attempted. This is an essential first step in the research on this urban hybrid's integration into the city's sustainable evolution. Due to the spatial dispersal of these examples however, the present analysis will be based on satellite images, maps, and the information from relevant authorities. Even though results, as detailed and accurate as possible are presented in the following tables, a future field- research, could supplement the theoretical conclusions, and evaluate and re-adjust them.

Resulting from this comparative examination, it can be argued that all cases show extremely similar path and node patterns and forms, mainly associated with road infrastructure. They also tend to be defined by very sharp external and penetrable internal edges, which also affect the area's segmentation into distinct regions. As for the landmarks, they interestingly seem to be associated with either the road network, or very distinct public buildings and open spaces, the latter only in cases where significant residential levels can be observed as well.

As it appears, a single-use development is often preferred to a mixed-use one, and in almost all cases the airport city is significantly less accessible by public transport than the main airport site. Cultural/Community activities emerge, obviously, only within larger residential areas, while heavy industry is not a preferred use at all, probably due to the high land value. Green areas, in various forms, are unexpectedly common. A relation between the area's size, location and land uses could exist but needs further investigation.

		Spruce Creek	Denver	Tempelhof	Frankfurt	Athens	Helsinki
Airport City		A small community organised around a central airport runway	Suburban residential development far from the airport / planned business park	The airport is built within the city	Commercial park at the edge of the airport's platform	Retail and conference park, built within the airport's platform	Business and retail park at the fringe area between the city and the airport
Path	Main	Airport runway	Main street	Main street	Highway	Highway	Highway
	Secondary	Suburb's streets	Secondary streets	Secondary streets	Secondary streets	Secondary streets	Secondary streets
Edge	Internal	Between the residences and the runway	No hard edges apart from between the main street and back streets	Between the main street and back streets / dense urban block	No distinct edges apart from a light urban block	Between building and parking lot	Secondary streets dividing the area
	External	Green belt	Outer fence	Between the airport building and the city buildings / urban fabric	Highway network	Highway and airport's fence	Highway, forest and airport's fence
Landmark		Runway, commercial area, golf course	School, church, park, golf course, community centre, convenient store	Square, subway station, esplanade	Central roundabout	Central roundabout, individual buildings, chapel, bus stop	Highway exit, forest, individual buildings, museum
Nodes	Main	Airport runway	Main street – side streets crossroads	Main street crossroads and square	Highway exit	Highway exit	Highway interchange and exit
	Secondary	Suburb's streets crossroads	Side streets crossroads	Side streets crossroads	Side streets crossroads	Side streets crossroads	Secondary streets crossroads
Regions		Clear distinction between the residential and commercial / administrative areas	Large uniform residential area with dispersed landmarks	Mixed-use urban fabric with higher densities at local central points	Small uniform area with a slightly different central point	Two distinct sub-areas in the opposite sides of the airport's platform	Uniform business and residential areas with retail development in their periphery

Table 1: Urban characteristics of the airport city

	Spruce Creek	Denver	Tempelhof	Frankfurt	Athens	Helsinki
Airport's land ownership	Private	Public	Public	Mixed	Public	Public
Airport city's land ownership	Private	Private	Mixed	Mixed	Public	Public
Airport's area (mil. m^2)	5.2	137.3	6	11.3	16.8	7.3

Airport city's area (mil. m^2)	5.2	10.5	-*	0.5	0.3	2.8
Airport's distance from traditional centre (km)	8	37	4	12	20	17
Airport city's distance from traditional centre (km)	8	20	4	10	18-22	16
Airport's accessibility	Car	Car, Local and regional bus (+internal underground light rail)	Car, Subway, Local bus	Car, Local and regional bus, Suburban, regional and national train, High-speed rail (+internal light rail)	Car, Local and regional bus, Subway and suburban train (+internal bus service)	Car, Local and regional buses, +High-speed rail (from 2014)
Airport city's accessibility	Car	Car, Local bus	Car, Subway, Local bus	Car, Local bus	Car, Local bus	Car, Local bus
Residential development	Y	Y	Y	N	N	Y
Commercial development	N	N**	Y	Y	Y	Y
Industrial development	N	N**	Y***	N	N	Y****
Green / public areas	Y	Y	Y	Y	N	Y
Cultural/Community facilities	Y	Y	Y	N	N	Y

Table 2: Area accessibility and land uses

*Tempelhof airport is incorporated in Berlin's urban fabric. The airport city's area is not therefore distinct from the city. **Commercial and Industrial uses are developed in nearby locations within other single-use suburban enclaves. ***In parts of the airport's building, heavy machinery factories were operating until some years prior to the airport's closure. ****Light industrial uses are permitted.

DISCUSSION - CONCLUSIONS

The aim of this essay was to map the "territory-less city", the contemporary urban hybrid widely known as "airport city". Its purpose was to investigate the existence of any urban qualities within it, which would explain the arguments regarding its viability as a model for sustainable urban development. Its focus point was on the city's qualities, as an *organic structure of complexity and order*, as described by Kevin Lynch, Lewis Mumford, and others.

In this process, it has been proven that the city's evolution relies on a structural mechanism of correlations, uniquely shaped by each environment's special characteristics. As an integral part of this, transportation networks, and airports in particular, provide the opportunity for significant economic growth, but impose intense stress to the city's environment at the same time, as their recent evolution from simple buildings to urban hybrids implies.

It has been claimed that the sustainable city would be *an environmentally attractive, safe city, of high quality, in which people will want to live* [18], yet the present structure of the airport city is still quite distant from this ideal form. The main weakness of the existing models is the

fact that this new city is a place where no one wants to live, and when it is not, then it retains a form similar to the suburban enclave, alienating it from the urban core and the airport itself.

In order to enlighten the case around this controversial territory, an analysis of six examples was attempted. Even though limited in breadth, it approaches those new urban forms with relevant detail, and proves that, even though of a diverse morphology, most of them do share certain common features, and that in many cases an airport can coexist sustainably with a community, as an integrated part of its urban fabric and structure.

Among all of them, strong similarities can be observed in terms of their paths' characteristics, nodes and hierarchy, as well as of the sharpness of their external edges compared to the penetrability of their internal ones. The latter is probably due to the large uniformity of uses and the less common pattern of segmentation. A relation between the area's size, location, land uses and accessibility by public transport, could exist but needs further investigation. The nature, form and dispersal of landmarks within the area seem to depend on all these factors, in addition to other cultural and economic parameters.

It is therefore understood that, even though in some cases certain principles and characteristics of urbanity can be identified, the diversity in this urban hybrid's form and structure is imposing the clearest practical challenges to identifying it as a city per se, and achieving the right balance between economic, social and environmental sustainability.

REFERENCES

1. Mumford, L.: The city in history: Its origins, its transformations, and its prospects. Penguin Books [1991], first published in the UK by Martin Secker & Warburg Ltd, pp.: 549 – 656, London, 1961
2. Haughton, G., and Hunter, C.: Sustainable Cities. Sustainable Policy and Development Series 7. Regional Studies Association. Jessica Kingsley Publishers Ltd, pp.: 199 – 311, London, 1994
3. Lynch, K.: The image of the city. MIT Press. Camridge, MA & London, UK, 1960
4. Breheny, M.J.: The contradictions of the compact city: Areview. in: Breheny, M.J. (ed.) *Sustainable development and urban form*. European Research in Regional Science 2. Pion Ltd, pp.: 138 – 159, London, 1992
5. Orrskog, L., and Snickars, F.: On the sustainability of urban and regional structures. in: Breheny, M.J. (ed.) *Sustainable development and urban form*. European Research in Regional Science 2. Pion Ltd, pp.: 106 – 121, London, 1992
6. Hall, P.: Urban Development and Research Needs in Europe. CERUM Report 8. Umeå University, 2001
7. Kloosterman, R.C., and Lambregts, B.: Clustering of economic activities in polycentric urban regions: The case of Randstad. Urban Studies. vol.38, no.4, pp.: 717 – 732, 2001
8. Dempsey, N., and Jenks, M.: Future forms of city living. in: Jenks, M., and Dempsey, N. (eds.) *Future forms and design for sustainable cities*. Architectural Press, pp.: 415 – 417, Oxford & Burlignton, 2005
9. Okabe, A.: Towards the spatial sustainability of city-regions: A comparative study of Tokyo and Randstad. in: Jenks, M., and Dempsey, N. (eds.) Future forms and designfor sustainable cities. Architectural Press, pp.: 55 – 70, Oxford & Burlignton, 2005
10. Buxton, M.: Energy, Transport and Urban Form in Australia. in: Williams, K., et al. (eds.) *Achieving sustainable urban form*. E&FN Spon Press, pp.: 54 – 63, London & New York, 2000
11. Newton P.: Urban form and environmental performance. in: Williams, K., et al. (eds.) *Achieving sustainable urban form*. E&FN Spon Press, pp.: 46 – 53, London & New York, 2000
12. Simmonds, D., and Coombe, D.: The transport implications of alternative urban forms. in: Williams, K., et al. (eds.) *Achieving sustainable urban form*. E&FN Spon Press, pp.: 121 – 130, London & New York, 2000
13. Güller, M., and Güller, M.: From Airport to Airport City. Editorial Gustavo Gili, Barcelona, 2003
14. Fasone, V., et al.: Multi-Airport System as a Way of Sustainability for Airport Development: Evidence from an Italian Case Study. Procedia – Social and Behavioral Sciences. Elsevier. vol.53, pp.: 96 – 105, 2012
15. Pestana Barros, C., and Weber, W. L.: Productivity growth and biased technological change in UK airports. Transport Research Part E. Elsevier. vol.45, pp.: 642 – 653, 2009
16. Schlaack, J.: Defining the Airea: Evaluating urban output and forms of interaction between airport and region. in: Knippenberger, U., and Wall, A. (eds.) *Airports in Cities and Regions – Research and practice*. KIT Scientific Publishing, pp.: 113 – 121, Karlsruhe, 2010
17. Kasarda, J. D., and Lindsay, G.: Aerotropolis: The way we'll live next. Allen Lane. London, 2011
18. Banister, D.: Unsustainable Transport. City transport in the new century. Routledge, Abingdon, 2005

THE BEHAVIOUR OF ENERGY BALANCE IN A STREET CANYON, CASE STUDY CITY OF BISKRA.

BOUKHABLA Moufida[1], Pr ALKAMA Djamel[2], Pr. MOUMMI Noureddine[3],

1: *Laboratory LACOMOFA, Department of Architecture, University Mohamed Khidder Biskra. Algeria.*

2: *Laboratory LACOMOFA, Department of Architecture, University Mohamed Khidder Biskra. Algeria.*

3: *Laboratory LGM, Department of Mechanical engineering, University Mohamed Khidder Biskra. Algeria.*

ABSTRACT

This research studies the heat flow exchanged between paving of two different types (concrete and asphalt) and the urban environment in a street canyon. A method which takes into account all fluxes is established. A numerical approach is made in order to assess the modification of energy balance and its impact on air warming according to the geometry of canyon streets. The proposed approach provides assistance in the identification of important parameters resulting in the phenomenon of air warming, which can explain the thermal phase between the ground surface and the urban environment in summer. The extensive sunshine duration and the large mineral surface exposed to direct sunlight combine to generate a large storage of heat during the day and its return at night, which contributes significantly to overheated air during a summer night. This systematic research constitutes a significant step during interventions in the urban fabric or even in new urban developments. The heat flow density is determined by the heat transfer between the urban canopy and the atmosphere. A set of field measurements is performed using "multmeter" equipment to measure the temperature of the under soil: the air temperature and the wind speed using a measuring instrument called "thermo-anemometer with propeller LV 110", the temperature of the ground surface by an instrument called "Infrared Thermometer", the relative humidity through an instrument called "Thermo-hygrometer HD100". The time interval between measurements is two hours. A total of two measuring stations, representing street canyons with two different ground coatings (asphalt and concrete), are chosen in the city of Biskra. Such research is needed to find reliable ways to determine accurately the energy balance in an urban environment in the future. Finally, all of this can contribute to refresh the air and sustainable cities of tomorrow.

Key words: Heat flow, energy balance, numerical approach, air warming.

INTRODUCTION

A primary objective of environmental design in an urban context is the creation of comfortable spaces. The built environment has a significant impact on air warming. We will try to demonstrate clearly in the canyon streets in the city of Biskra the impact of the change in energy balance on air warming.

PROBLEM

In recent years urban climatology focused primarily on air warming. [1]. Heat flux exchanged between the soil and urban environment play an important role through their contributions to this air warming. Various authors have conducted studies on these exchanges. The synthesis of bibliographic work shows that the authors discuss the phenomenon of exchange considering that the daily net radiation is divided between latent heat and sensible heat [2] [3] [4]. To limit air warming in an urban environment, mastery of the energy balance should be a priority. Cities must anticipate this new climate data.

OBJECTIVES

Determine the change in the energy balance where the ground is covered by concrete and asphalt in an urban environment defined by the geometry of the street (canyon shape) and its impact on air warming. This study uses a numerical approach including a monitoring methodology.

The parameters of the energetic balance as follows:

Rn	ENERGY BALANCE	W/m^2
H	Sensible heat flow	W/m^2
LvE	Latent heat flow	W/m^2
G	Heat flow into the soil	W/m^2
$\int$	Heat flow absorbed by vegetation	W/m^2
E	Mass flow of water vapor	W/m^2
h_c	Coefficient of thermal convection	
T_a	Air temperature	K
$T_{surf\ sol}$	Soil surface temperature	K
V_{vent}	Wind speed	m/s
K_E	Coefficient of convective mass transfer	
ρ	Density of air	ρ_{air} = 1.18kg.m^{-3}
c_p	Specific heat of air	c_p =1004J/kg.K
L_V	Latent heat of vaporization of water	L_V = 2.4*10^6 j/kg
M_W	Molar mass of water vapor	M_W =18,01g*mol^{-1}
R	Gas constant	R=8.32j.K-1.mol-1
P_{VS}	The saturation vapor pressure	kPa
P_V	The vapor pressure	kPa
Hr	Relative humidity	%
K	Thermal conductivity of the soil	W/m/K
ΔT	Coldest and Hottest temperature	K
e	Level of ΔT	m

Site Description

This study applies to the city of Biskra, located in an arid region with a warm and dry climate in Algeria. Its arid climate is characterized by significant annual and daily fluctuations between maximum and minimum temperatures. Between the coldest month and the hottest month, the temperature range exceeds 20°C. The daily range for the hot season is around 22°C. Solar radiation is intense about 10h/day. The average relative humidity is 47%, not exceeding 60% in winter. Rainfall is irregular and low (120 mm)

[5]. The measurements of the different climatic parameters were made at two measuring stations (Figure 1). Thermal and physical characteristics of the ground are: rough ground in asphalt,whose thermal conductivity is k=1.90W^{-1}.m-¹.k, the emissivity about 0.90 to 0.98, and the color black; and a rough ground in concrete, whose thermal conductivity is k=1.80W^{-1}.m^{-1}.k, the emissivity varies between 0.71 and 0.90; and the color is greenish gray.

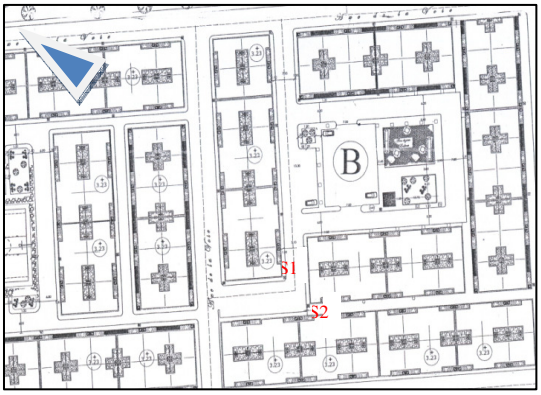

Figure1: The streets where the stations were placed. Source: Author.

Geometric details of each station are shown below (Figure 2).

Station N°1 : Canyon Street H >2W		
View of the station: 	**Geometry and orientation of the station:** 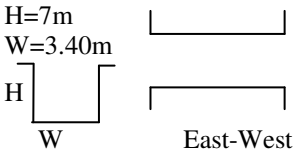	**Type of soil:** asphalt 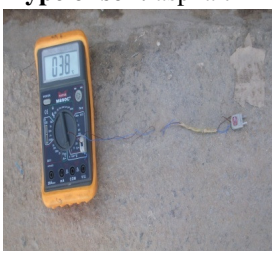
Station N°2: Canyon Street H >2W		
View of the station: 	**Geometry and orientation of the station:** 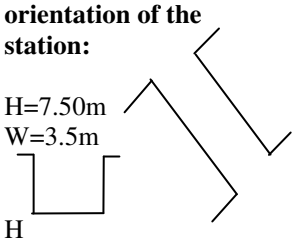	**Type of soil :** concrete 

Figure2: The geometric details of the stations. Source: Author

MONITORING CAMPAIGN AND CLIMATIC CONDITIONS

Studying the effect of energy balance on air warming begins by drilling through the asphalt and concrete and measuring the underground temperature using a measuring instrument called "multmeter", with two accurate sensors to measure the temperatures T1 and T2 and a small handheld portable digital multmeter with LCD display, M890C. The instrument is product conform with the IEC 1010 and the CE certificate. The temperature measurement range is -20°C to 1370°C with an accuracy of ±0.5%, in measuring stations belonging to a similar climatic environment. A campaign pilot was

addressed to determine at what level the fluctuation of temperatures starts according to the ground level in asphalt with a thickness of 7cm, and in concrete with a thickness of 5 cm. A level of 5 cm measures T1 as the coldest temperature, and 10 cm measures T2 as a hottest temperature for asphalt. Then a level of 4 cm measures T1 as a coldest temperature and 8 cm measures T2 as the hottest temperature for concretel. The air temperature and the wind speed are measured using a measuring instrument called "thermo-anemometer with propeller LV 110", the temperature of the ground surface by an instrument called "Infrared Thermometer" and the relative humidity by an instrument called "Thermo-hygrometer HD100" with a capacitive humidity sensor and a temperature sensor integrated.

THE ENERGY BALANCE EVALUATED

A portion of the net energy arriving on the ground is heating it by conduction, another by evaporation of water and another changes the atmosphere by convection. Because our investigation site lacks vegetation, the photochemical processes of chlorophyll assimilation of plants are neglected in our case; therefore the energy balance is defined by the following equation:

$$Rn = H + LvE + G + J \quad (1)$$

The measurements were performed for three hot days under typical conditions of summer on 8, 9 and 10 July 2012 (days included in the overheating zone in the city of Biskra). Assuming that there is a permanent regime; the sensors will be fixed with no changes during the measurement period.

A) SENSIBLE HEAT FLOW H:

This heat flow is calculated by the following equation:

$$H = h_c\,(T_a - T_{surf\,sol}) \quad (2)$$

$$h_c = 0.5 + 1.2\sqrt{v_{vent}} \quad (3)$$

hc is the convective transfer coefficient.

B) LATENT HEAT FLOW LVE:

It is calculated by the relationship of Stefan based on the theory of mass transfer, also called film theory given by:

$$L_vE = \frac{L_v.K_E.M_w}{R.T_a}\left(P_{vs}\left(T_{surf\,sol}\right) - P_v(T_a)\right) \quad (4)$$

$$P_{VS}\,(T) = \exp^{(25{,}5058-(5204{,}9/T))} \quad (5)$$

$$P_V\,(T_a) = Hr\,P_{VS}\,(T_a) \quad (6)$$

The assumption of Louis asks that is:

$$K_E = \frac{h_c}{\rho * c_p} \quad (7)$$

C) CONDUCTIVE HEAT FLOW G:

The heat flow in the soil is defined by Oke by the following equation:

$$G = -K\frac{\delta T}{\delta x} \approx -K\frac{\Delta T}{\frac{\Delta e}{e}} \quad (8)$$

By replacing each quantity in the energy balance equation (1), we can finally write the energy balance as follows:

$$Rn = \frac{L_v.K_E.M_w}{R.Ta}\left(P_{vs}\left(T_{surf\ sol}\right) - P_v(T_a)\right) + h_c.\left(T_a - T_{surf\ sol}\right) + K\frac{\Delta T}{\frac{\Delta e}{e}} \qquad (9)$$

RESULTS AND DISCUSSION

Figures 3 and 4 show that at the two measuring stations, a high correlation exists between the energy balance and latent heat flow determined by evaporation.

A first field measurement result gives value fluctuations between the air temperature, ground temperature and the relative humidity at the measurement stations, as well as the values of the wind speed for day and night periods. It can be seen that for Station N°1 the measured values of air temperature are higher than those recorded in Station N°2 from 08h00 to 20h00 and from 02h00 to 10h00. In Station N°1, it is clearly noticeable that the measured ground temperatures are higher than the air temperatures. The mean value for the ground temperature is 47.6°C, and then comes the air mean temperature with 43.5°C. This can be explained by the fact that the ground surface pavement is of a dark colour with high absorptivity. The soil surface temperatures are remarkably higher for Station N°1 than those for Station N°2, because of its large emissivity due to the presence of asphalt which heats up quickly during day time. For Station N°2, the decrease of wind speed appears from 08h00 to 16h00 and from 20h00 to 08h00. For Station N°1 the observed decrease of wind speed is from 08h00 to 20h0 and from 00h00 to 08h00. The wind speed recorded at Station N°2 became higher than that of Station N°1 after midnight, due to the street orientation (North west-South-east), which is attributed to the hot prevailing winds in summer blowing from SE. Decrease in relative humidity before 16h00 and at night from 00h00 to 04h00 fluctuated between 11% and 23.2% in Station N°1, while the recorded values in Station N°2 for these periods fluctuated between 11.6% and 22.9%. This can be explained by the presence of traffic, air-conditioning systems and ground absorptivity characteristics.

STATION N^{O}.1:

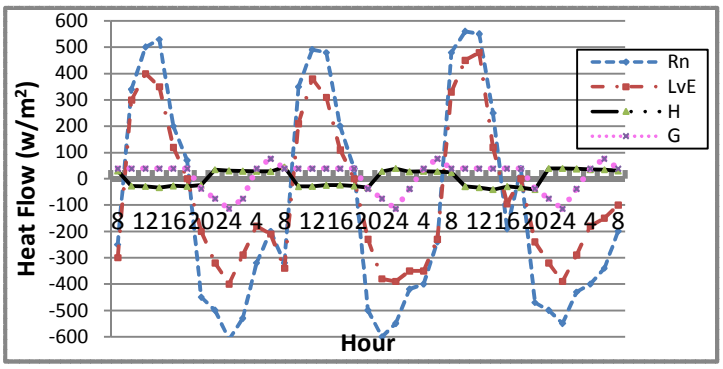

Figure 3: cycle of latent, sensible and conductive heat flow, and energy balance in a canyon street, asphalt ground. Source: The

The extent of the (LvE) is large, which represents more than 80% of the (Rn). Changes in flow between (Rn) and (LvE) indicate that the energy balance (Rn) s significantly with a maximum difference between the two flows equal to 180W/m^2 (at 14h00 during the day time) (Figure 3) . The maximum value of Rn is 564W/m^2. At night time the difference between the two flows equals 220W/m^2 at 22h00. The sensible heat flow (H) is contributed in the presence of the urban heat island. It is powered by both the release of anthropogenic heat and the heat stored in the ground (G). This last allows (H) to stay positive during the night from 20h00 to 08h00.

The energy balance (Rn) and latent heat flow (LvE) can progress: at 14h00 in a canyon street oriented East-West with an asphalt ground cover, LvE reaches a maximum value equal to 480W/m^2 and Rn equal to 564W/m^2 (Figure 3).

STATION N .2:

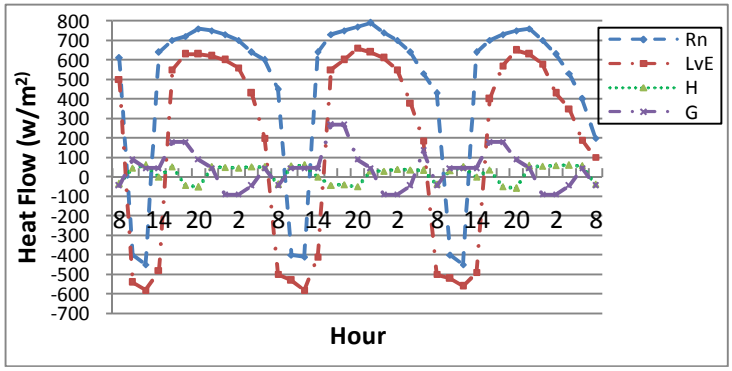

Figure 4: cycle of latent, sensible and conductive heat flow, and energy balance in a canyon street, concrete ground. Source: The author

The influence of the prevailing wind from the North West - South East appears on the energy balance (Rn) and latent heat flow (LvE), from 08h00 to 06h00. (LvE) and (Rn) drop gradually. This wind favoring the rejection of heat in the atmosphere during the night and therefore sensible heat flow (H) becomes positive. In the canyon street with concrete ground, the energy balance reached its maximum value at 16h00 (720W/m^2) during the day. The energy balance is generally increased, the latent heat flow also increased and the extent of the conductive heat flow (G) often delayed especially in the transition to negative values in the early evening from 20h00 until 04h00.

CONCLUSION

This research has a role to perform in the analysis of the extent and the behavior of the energy balance in a canyon street and its impact on thermal fluctuations. This document focuses on field measurements of the temperature of the air, temperature of the ground surface, of relative humidity, the wind speed and the temperature under ground at two levels within two stations situated in canyon streets, which were conducted from 8 to 10 July 2012, at a bi-hourly intervals. At 14h00 in the canyon street oriented East-West and ground covered with asphalt, the latent heat flow (LvE) constitutes 80% of the day flows exchanged within a highly urbanized site. In the canyon street with concrete ground, the energy balance is increased, it reaches its negative values in the morning, from 09h00 until 13h00.

REFERENCES

1. Mestayer P.G., Anquetin S., 1994, *Climatology of cities. In Diffusion and Transport of pollutants in Atmospheric Mesoscale Flow Fields.* A. Gyr F.S. Rys editors, ERCOFTAC Series, Kluwer Academics Press p. 165-189.
2. Saighi M., 2002, Nouveau modèle de transfert hydrique dans le système sol-*plante-atmosphère*, Thèse de Doctorat, Université des sciences et technologies Houari Boumediene-USTHB.
3. Fennessey N.M, Vogel R.M., 1996, Regional model of potential evaporation *And reference evapotranspiration for the northeast USA*, Journal of Hydrology,
4. Eichinger W.E, Nichols J., Prueger J.H., Hipps L.E., 2003, *Like Evaporation estimation in arid environment*, Hydroscience- Engineerin g, Repport N430, University of Iowa.
5. Cote Marc, 2005, *La ville et le désert*, Karthala, Paris.

GIS BASED TOOLS TO ASSESS LOCAL SELF-SUFFICIENCY

Matteo Clementi; Gianni Scudo

Politecnico di Milano, Department of Architecture and Urban Studies, via Bonardi 9, Milan.

ABSTRACT

An analysis and design method to elaborate self-sufficiency urban scenarios is presented, where energy and material flows related to residential sector, food consumption, and private transport have been considered.

The method uses open-source Geographic Information Systems (GIS) and is articulated in the following processing phases:

1) Identify the territorial boundaries defined as local
2) Assessing the Renewable Local Energy Potential - Analysis of contextual conditions and local renewable energy potential.
3) Assessing Local Energy-Matter Demand and Supply for residential, agricultural/food consumption and (marginally) private transport activities. Quantification of aggregated impacts through the environmental impact indicators adopted (GWP100 - CO2eq emissions, NRE / RE MJ non-renewable and renewable primary energy).
4) Assessing local self-sufficiency scenarios based on best practices transfer, filtered on the basis of local factors mapped on the GIS (climate, use, existing buildings shape and technology).

The effectiveness evaluation of good practices is carried out using specific tools, called "user histograms". These are used to verify the choices adopted by calculating the local demand for energy and materials through three specific indicators and related reference thresholds :

- Accounting productive land demand compared with the locally available land.
- Accounting CO_2 emissions per capita, compared with reference value of sustainability (in a range between 1000 and the 2000 kg CO_2 eq/ person*year).
- Accounting primary renewable and non-renewable energy consumption, compared with threshold values, characteristic of the 2000Watt-Society program (1500W coming from renewable sources and 500W from not renewable ones).

The results describe the application of this methodology in the context of a settlement of about 5000 inhabitants in the province of Milan, Albairate. They show how local self-sufficiency can be achieved in the categories of food and energy supply related to residential buildings. The main actions taken into consideration, concern an adequate use of renewable energy in the built environment, interventions on existing buildings to reduce energy consumption in the residential sector and a readjustment of the inhabitants diet towards local low energy productions (i.e. vegetal versus animal proteins).

Keywords: CO_2 accounting, local self-sufficiency, GIS.

METHODOLOGY

The text presents the current state of development of the applicative tools of ELaR, which stands for Ecodynamic Land Register, a methodology to assess different design choices on

the basis of their contribution to achieving self-sufficiency with regard to energy and material flows, in a context defined as local.

ELAR aims to highlight and rethink energy and materials flows which feed people activities through analysis carried out by Geographic Information Systems [1, 2]. It highlights the dynamic relations between energy and matter demand and local renewable potential which should necessarily be maintained in equilibrium in a self-sufficient system. Local demand for energy and materials and the local renewable potential supply are assessed from the information gathered and processed. The local demand for energy and materials analyzes the consumption categories of housing, food and marginally of private transport; data are expressed in terms of general amount referred to the local context or in terms of per capita data.

The collected and processed information is organized in order to enable the transferability of good practices oriented to local sustainable self-sufficiency, and to measure their effectiveness in terms of dweller environmental impacts reduction.

TOOLS

The ELAR methodological approach allows to aggregate the data processed in graphic format easily understandable to local actors (general users, local administration, designers, producers)

The elaboration and communication of the results are provided by two basic tools:
" Resources / impacts geographies."
" User histograms"

RESOURCES/IMPACTS GEOGRAPHIES

Resources and impacts geographies are obtained by collecting on the same territorial information support data on Local Demand of Energy and Matter (LDEM), and on the Renewable Energy Technical Potential (RETP).

Information on Local Demand of Energy and Matter (LDEM) is collected in the form of impact geographies, while information on Renewable Energy Technical Potential (RETP) is collected as resources geographies concerning local supply.

Impacts geographies represent the supply chains of production and consumption through geo-referenced vectors which locate supply chain different nodes. Two different indicators quantify the environmental impacts associated to the different nodes of the supply chain:

- the use of primary non-renewable/renewable energy sources, expressed in MJ equivalent;
- accounting of CO_2 equivalent emissions, expressed in kg of CO_2eq.

Figure 6 shows an example of impact geography related to primary energy accounting, where energy consumption values are graphically represented as colored circles of different sizes.

Resources geographies are obtained by collecting in specific thematic maps quantitative data related to the locally available renewable resources. Once the boundaries of the local context have been defined, this phase of the methodology processes and stores in the same Geographic Information System data concerning local physical and biological/agricultural environment. This data-base provides descriptive information on the climatic conditions (solar potential mapping at different scales [3], pluviometric conditions, windiness, humidity and air temperature throughout the year), on actual land uses, on geo morphological aspects etc..

(Figure 1). The main goal of such a data archive is to provide useful information to identify the current local renewable potential supply and develop possible local sustainable scenarios for good practices transferability.

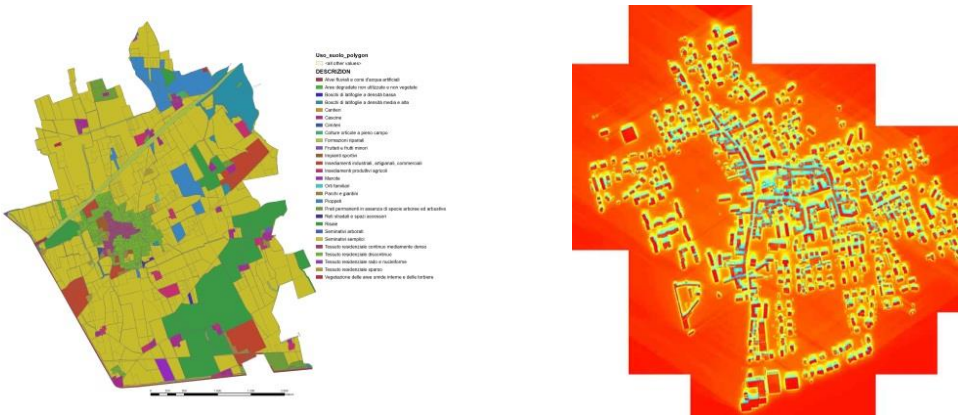

Figure 1: Some maps that make up the resources geographies of Albairate (Lombardy region), to the left a land use map, to the right a solar radiation map.

Good practices transferability depends on the assessment of similarity between territories under analysis and good practices territories. This information, as part of one single Geographic Information System (GIS) can be associated to different portions of land, as example a cadastral land or urban parcel.

The association of such information to geometric particles using GIS, enables identifying the vocational characteristics of each portion of the local territory.

USER HISTOGRAMS

The user histograms build the connecting structure between the information collected in the geographies, in order to check different design choices. They report in terms of per-capita flows energy and matter local demand and relate them with the extension of productive land per-capita. The user histogram general structure can be easily understood looking at the following diagram (Figure 2).

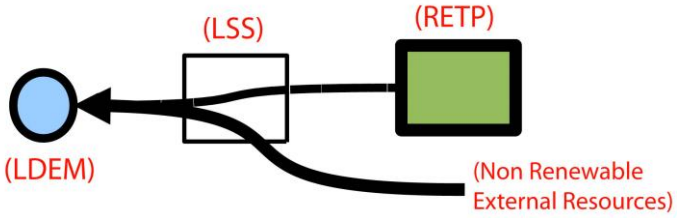

Figure 2: General synthetic structure of a user histogram

As shown by the arrows, the histogram describes energy and matter flows direction from the right to the left. Consequently, the right side of the histogram contains information on the resources supply (RETP Renewable Technical Potential, locally available), where information on local renewable supplies are given. The left side shows information about Local Demand of Energy and Matter (LDEM). The central part houses strategies as possible design choices in between local renewable energy/matter supply and demand (LSS Local Self-sufficiency Scenario). They perform the main function to connect local demand and supply. The image below shows an example of user histogram describing the main components. The extreme left of the graph shows data of energy and matter demand expressed in terms of the indicators

adopted, in this case the CO_2 equivalent emissions. The quantities of energy and materials are aggregated into the consumption categories of housing, food and, marginally, of private transport, to compose the total amount of energy and impact (NRE, GWP 100) per person (on the extreme left) (Figure 4). Such option gives the possibility to compare the data with reference threshold values per person (15800MJ of primary non-renewable energy per year as sustainability goal suggested by the 2000W Society program, and between 1000 and 2000 kg of CO_2 equivalent emissions per year) [4].

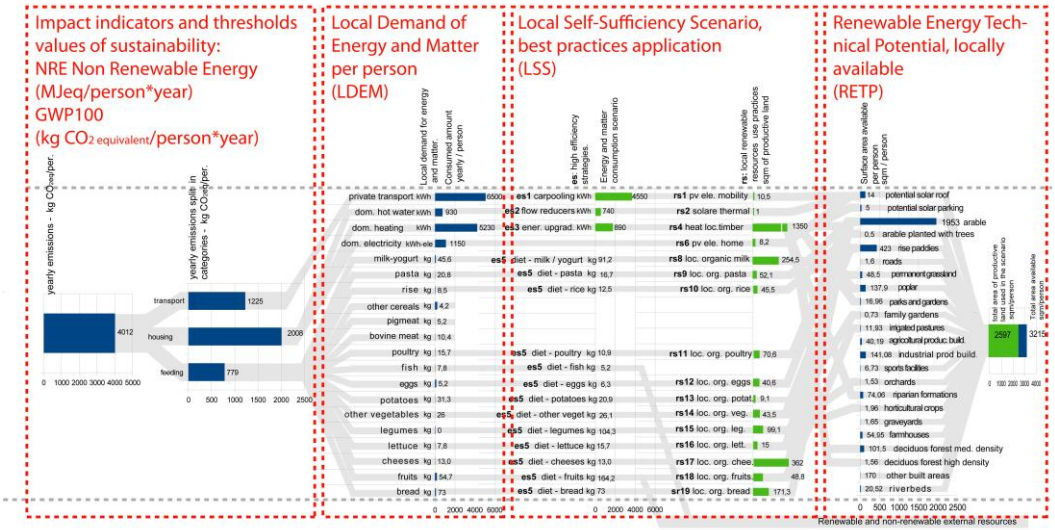

Figure 3: Example of user histogram describing the main components

The right part of the graph represents the local renewable supply, it shows the extension of the productive surfaces in the local context, expressed in square meters per person (Figure 5). The productive surfaces are intended to be the productive portions of land for agriculture and forestry, as well as the built-up portions that show relevant features such as high solar vocation surfaces.

The far right part of the histogram brings together the extensions of productive land per capita identifying the amount of productive land available. The different colors of blue and green refer to the extension of productive land available per person (in blue) and the extension of the available productive land interested by the application of good practices assumed in the scenario (in green) (Figure 5).

The structure of information allows in the design phase to operate a useful and immediate comparison between productive land necessary to local self-sufficiency and land actually available. Such condition of immediate comparison drives the design choices among the good practices, in order to find out the ones more suitable to the real conditions of the territory.

The central part of the histogram is representative of best practices application, and identifies two specific application steps. The first, in the column to the left, refers to strategies to improve efficiency (es), both in terms of energy use and matter consumption. The main function of this phase is to reduce the amount of energy and matter shown in the part related to the current demand (Figure 5, on the left). For example, the main strategies adopted in the case study of Albairate (Figure 4, 5, 6) concern the energetic upgrading of the building envelope, the adoption of low animal proteins diet and the spread of carpooling practices. The second application step, in the column to the right, refers to the application of good practices on renewable energy use (rs), with the purpose to mediate between the energy and matter

reduced demand and the potential renewable supply (Figure 5, central column). The data shown in the histograms translate the amount of energy expressed by the demand, in the amount of productive land required in order to compare the result with the quantity of locally available productive surface per person (Figure 5, right column).

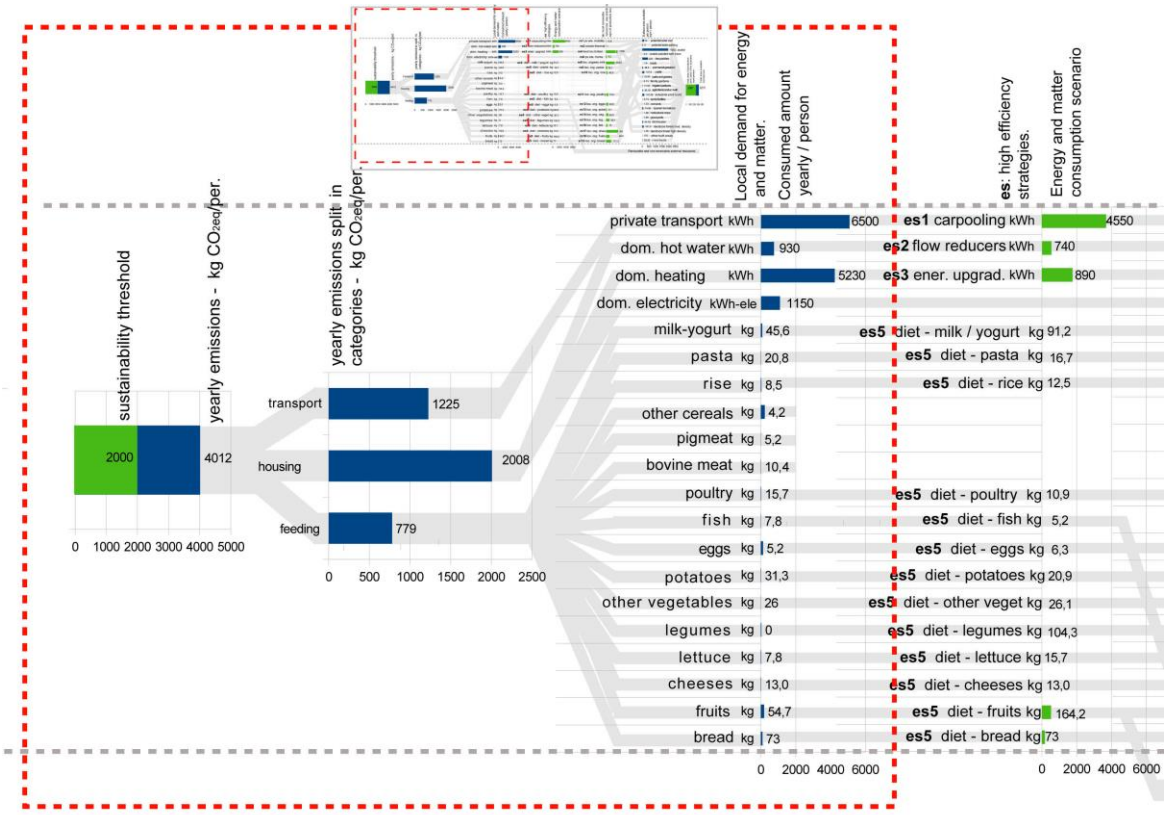

Figure 4: Part of the user histogram concerning Local Demand of Energy and Matter (LDEM), Albairate (Lombardy region)

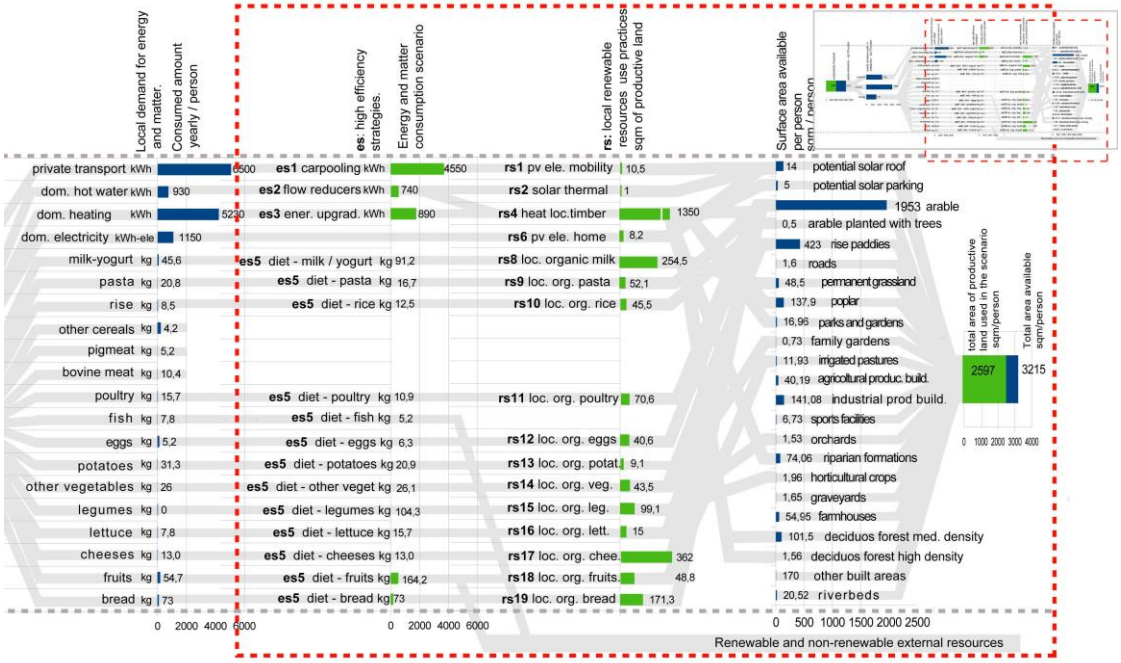

Figure 5: Part of the user histogram concerning the strategies adopted in the proposed Local Self-sufficiency Scenario (LSS), Albairate

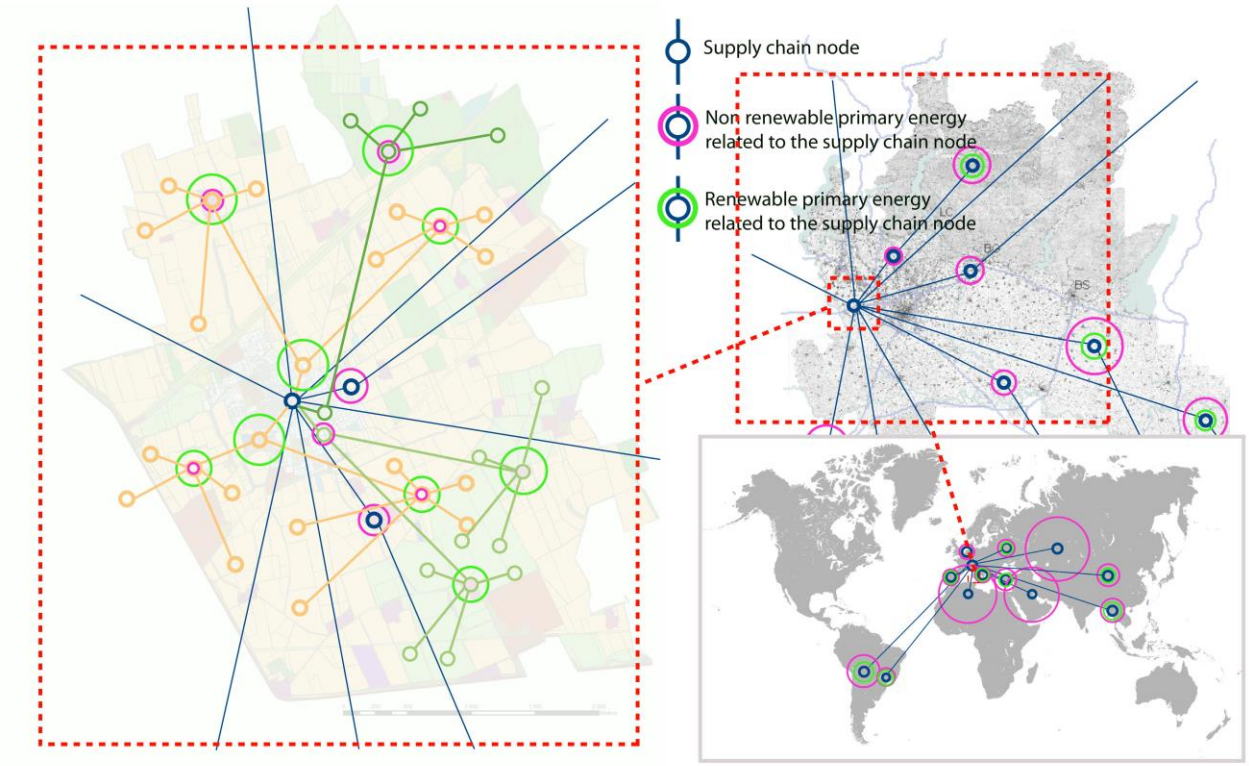

Figure 6: Extract from the impact geographies concerning the adoption of good practice on local supply chain of bread (sr19) inside di LSS, Albairate

CONCLUSION

The GIS based tool was tested in the context of the Albairate region to assess local self sufficiency. The data presented in the resulting histogram (Figures 4, 5) claim that the local territory can sustain local demand using 2600m^2 of productive land. Among the main practices to be adopted the following emerged: electric mobility powered by grid connected photovoltaics, changing the diet of the inhabitants (see previous "es" strategies description) and energy requirements reduction of dwellings by approximately 80%. Future developments concern the online publication of a good practices database so as to allow a better fruition and an easy implementation of data by the users.

We wish to thank Paola Caputo (Politecnico di Milano) for the support given in the data collection concerning the good practices database.

REFERENCES

1. Clementi, M. : ELaR, Ecodynamic Land Register. A proposal to assess the "strong sustainability" of design alternatives according to the local context conditions, in World Renewable Energy Congress X and Exhibition - Conference, Proceedings, pag. 861/866, Glasgow, 2008.
2. Clementi, M., Scudo G. : Ecodynamic Land Register - Current development level of the tool in Renewables in a changing climate. From nano to urban scale. CISBAT 2009- Conference Proceedings, Editor EPFL, pag.415/420, Lausanne, 2009.
3. Clementi, M., Scudo, G. : Solar radiation mapping at the micro-urban scale using GIS, in PALENC2010, Passive and Low Energy Cooling for the Built Environment - Conference Proceedings, Athens, 2010.

Semadeni, M. et al., : Steps Towards a 2000 Watt-Society, 2002. http://efficientpowersupplies.epri.com/pages/Steps_towards_a_2000_WattSociety.pdf

DYNAMIC CONSUMPTION EVOLUTION OF BUILDING MATERIALS IN THE HOUSING SECTOR IN THE NETHERLANDS: TOWARDS A MATERIAL METABOLISM?

Icibaci, L. M. [1]; Timmeren, A. van [2]; Brezet, H. [1]

1: *Technical University of Delft Faculty of Industrial Design Department of Design for Sustainability Landbergstraat 15 2628 CE Delft, The Netherlands* 1

2: *Technical University of Delft Faculty of Architecture Department of Urbanism Julianalaan 134 2628 BL Delft, The Netherlands* 2

ABSTRACT

The Netherlands has moved a long way from a landfill to a waste processing society. In 2008 the European Waste Framework Directive signalized the wish to step up on the material hierarchy. This paper is based upon investigating how this process could take place and includes a renewed look on the 'urban metabolism' and the role of environmental technology, urban ecology and environment behavior focus for the field, focusing on material flows. Relevant aspects continue transformation, economic-technological innovation before, during and after design and construction.

Industrial ecology principles have shown to be powerful tools to track economic and environmental characteristics connected to specific flows. To step up on the material hierarchy towards waste prevention it will be necessary a more qualitative evaluation of the building industry related waste flows, which both the government and the companies involved in the industry should be prepared. Moreover even for a "recycling" based society as the Netherlands aims to become, there are challenges in specifying consumption trends and connecting national material accounting to product consumption. How to plan future capacity in an integrated system is a challenge for the waste management chain that has to be in tune with fluctuations of consumption trends in early stages. This paper has investigated dynamic consumption evolution of building materials in the housing sector through Domestic Material Consumption, waste accounting and dynamic stocks. The results show that traditional waste accounting does not bring enough relevance to evaluate waste prevention based on quantitative analyzes. Finally, an unprecedented qualification of material flows shows to be necessary to classify materials not only for waste prevention measures but for a drastic improvement in the material recycling chains, waste treatment and at last design of new products.

Keywords: material metabolism, waste hierarchy, accounting flows, dynamic housing stock

INTRODUCTION

According to de Bree (2005)[1] the Dutch overall waste industry is young and has rapidly become a large-scale operation. The most important changes of the Dutch waste industry in recent years include scale increase, consolidation / vertical integration, the formation of multi-utilities and the entrance of other European waste companies. In addition, the liberalization of the European energy industry has had an important influence on the Dutch waste industry. Waste prevention has to be included one way or another in such structure, formed mainly by large-scale players. Within this context, the government position has been to create policy structure that defines what needs to be avoided in accordance with European rules. In this

group the focus will be mainly on landfill, incineration and export of waste. Within this framework private companies will have to formulate the management of waste themselves including technology, logistics and costs. With this background, the government has also abstained from other "controlling" forms, which includes further improvements of waste accounting flows. Nonetheless without a clear and consistent evaluation of the development of waste flows the long term effects of such policy structure is questionable in regard to building capacity for future waste treatment, assessment of environment impacts and setting goals to improve waste management.

With the attempt to step up in the waste hierarchy treatment, different ways to process waste are needed rather than incineration, and a better measurement of waste flows is necessary. In this regard, a quantitative and qualitative evaluation of the waste flows, building stock and consumption trends are crucial for future waste treatment building capacity, design guidelines of new products and building systems and consequently a more clear environment assessment of waste production. This qualitative accounting has to include, besides volume, a better characterization of waste that ideally connects large-scale waste flows to the accounting of products including physical evaluation.

For a small country as the Netherlands, building waste, has critical effects in the carrying capacity to provide adequate treatment; more so with the increase of import waste bans raised by neighbor countries, such as Germany imposed in 2005. In a report published in 1999[2], the Netherlands was the only EU member state that expressed concerns that the supply of Construction & Demolition (C&D)-derived aggregates may one day match the construction industry's capacity to substitute them for primary aggregates. The same report includes the observation that the rush towards full recycling treatment should not disregard that full substitution of primary aggregates by secondary material may never match equivalent quality. Hence, the importance of improving accounting systems also illuminates related consumption of material flows by increasing and opens possibilities to substitute primary resources.

METHOD

One of the measures to implement in the waste hierarchy according to the European Waste Framework is to avoid recycling through the reusability of components and materials that are included as waste prevention resolution. Within this context this study evaluates the proportion of materials that are potentially reusable within construction waste in the housing segment and the prognostics through time. According to these materials, the study investigated 3 different levels of data:

i. The consumption trend to evaluate if materials combined with component design and building systems would be more prone to be reused in the future according to technology and management structures.

ii. The evolution of the building stock as a reservoir of present and future reusable materials.

iii. The development of waste production to assess the volume and speed which these flows occur, including the ways the extraction of these materials happen at this phase of the building life.

Within these three datasets the material types were described according both to the current national accounting systems and to information acquired from the private sector.

RESULTS

I. Consumption

For the purpose of this paper, consumption trends will be described instead of absolute numbers. Information on consumption of building materials described in this study was derived from private industry but with the exception of cement based products, the data is very inconsistent and when available it was not easily shared by sources. There is also disaggregated information available at the national accounting system, but not entirely available for the public. The information is organized by goods (e.g. triplex, clay brick) and by the industry types that consumes and supply goods. Most of the existent data is classified by monetary value rather than volume and in both cases dated within an average of 10 years. The classification does not prioritize between residential and non-residential consumption rates, instead within industry (e.g. construction materials, site preparation, construction installation). Steel consumption is available since 2000 and has been mostly stable until 2009 followed by drop in 2010 as most of the construction sector developments decreased. Rate of wood consumption was the most challenging to estimate, mostly due to lack of cooperation within the wood chain and in general it has seen a slight growth within the same time frame of the other products mentioned. Currently the government is compiling new datasets with the goal to assess national economic performance, although not national reserves through the environmental perspective, neither future waste production.

According to current building deconstruction technology available and the context of the market demand for reusable materials, the list of materials was selected as being the best candidates for reuse. The evolution of recent building material consumption trends indicates that the new housing stock is more concrete intense than constructions before the 1950's; more precisely at the structural level, floor structure and roof tiles. These components will be better candidates for *downcycling* or recycling if new technologies prove to be feasible. For roof structure, wood remains to be the primary material used in the housing sector. For framing of windows and doors wood based production still dominates compared to plastic components such as PVC. Consumption of ceramic components has steadily decreased with exception of external façade, which still has the largest share of ceramic-based products. Plastic products are in volume represented by pipes and frames with the largest share being PVC products. There is an important growth among insulation materials. The consumption of materials is also divided into products for new construction and products for renovation works. The latter group has been re-shaping the building material manufacturing and in the future regarded as the largest consumption activity.

II. Building stock

The forecast for building waste is generally problematic as demolition rates are based on assumed life span of buildings. Reasons for demolishing buildings are also not entirely understood, but construction year, building typology, tenure and building methods have been pointed to be partially define demolition trends (Hoogers et al, 2004; INTRON and RIGO, 2006). The concept of life span of buildings needs further research. Kohler and Hassler (2010) mention that such estimations in Germany have assumed average life span of 50 years resulting in 2% demolition rate when in practice the demolition rate was in average 0,5% while in the Netherlands the average life span is considered to be 90 to 120 years (Itard et al 2008; Van Nunen, 2010). Very little is known about demolition dynamics and even less about renovation cycles, where in the Netherlands demolition represents only partially the total building stock while renovation projects have a large participation in the waste production of the housing sector as well. Renovation until recently was not regarded as significant but has

increasing importance in the housing stock dynamics in most of mature urban centers and northern Europe.

According to TNO[3] (Koops, 2005) within the period 1990-2001, nearly 120,000 homes were removed and over 1 million new homes were added to the stock. He concludes by saying that "demolition is a small phenomenon that occurs spatially very uneven", and suggests that demolition often occurs in areas with large-scale concentration of inexpensive buildings.

Deriving data from INTRON and RIGO[5] it is estimated that within a period of 8 years 1995-2003 in the Netherlands there were 7 new houses built for every 1 demolished. Between 2004 and 2011, however, the ratio was 3,7 new houses for 1 demolished. The reduction of demolition and construction of new buildings is a current trend indicating that C&D waste flows in the housing segment are not only defined by demolition, but also largely affected by renovation cycles; which is still a poorly measured phenomenon. Despite the decreasing ratio between demolition and new construction, there has been an absolute increase of demolition rates from 0,17% in 2000 to 0,25% in 2008.

For this study the housing stock was divided according to construction year and typology. By comparing previous housing stock reports, it was possible to identify which housing groups were more prone to be demolished. Highest demolition rates were from gallery flats before 1964, terraced houses before 1964, and semi- detached from the same period all mostly from the social housing segment. The type of classification defines the quantities and quality of the material composition in the stock. A more detailed description of materials has been made according each group and then compared to the recovered material rates derived from demolition companies. The results show that different materials and different amounts of materials will be recovered from different building groups. The general average recovery rate among products will range from 30% to 70% (interviews with different demolition companies). The proportion of these materials present today in the housing stock was in this paper exemplified by one group of buildings (free standing, terraced, semi-detached and duplex before 1964), representing 29.2% of the total existing housing stock. Recoverable materials: 4,232,161 tons of wood (roof structure, floor & frames); 17,052,149 tons of ceramic (roof tile and brick façade[1]); 979 ext. doors; 9600 int. doors; 1199 wash basin; 1460 wcs. Interviewed demolition companies also extract different products from housing stock as lamps, balcony fences, staircase handrails, kitchen systems as cabinets, mirrors, handles, sockets, etc. that have not been included in this calculation.

III. Waste production

Today, development of C&D waste production is periodically published by two major sources of information: by the Agentschap NL (NL Agency, Ministry of Economic Affairs) and the National Registration Centre for Waste (LMA). Reporting of waste is dependent on the company that disposes the waste, which in most cases is a transportation company, either private or public. There is not a clear relation between the waste generator and ownership of waste in waste registration (Koppert et al, 2010)[4]. Even though currently the code description for waste registration at the LMA is based on the Euralcode system, previous code(s) systems are at times still used to classify waste. Regular accounting using this new coding system is more consistent since 2002 with improvements made in 2008 describing construction and demolition waste by material type and origin which LMA aggregated into three categories: building, infrastructure and utility; while the Agentschap database uses 14 different

[1] Recoverable façade bricks today are mainly extracted from constructions dated until 1930s that more often employed lime based mortar rather than cement based mortar, which increase deconstruction of these bricks.

categories. Hence, one barrier is that not all companies register their waste properly according to the Euralcode. At times companies may mismatch material categories, which will influence at final waste accounting. Another issue confronted is double accounting. The waste will be accounted by the transportation companies and at times also by the waste processing companies.

The accuracy of the data provided as a total is therefore still questionable since not all disposals need to be reported (*e.g.* small businesses do not have to register waste and processed waste that is classified under a different Euralcode). The lack of "control" that reinforces the registration practice allows companies to by-pass registration of " unknown" waste derived from demolition and construction (Afvalbeheer, 2011).

Currently the National Demolition Association in the Netherlands (VERAS) works with a set of forms which demolition companies are asked to complete. These forms are actual inventories done in two phases before and after demolition as an evaluation of the material flows content in the project to be demolished. This documentation is essential as part of tenders offered by these companies in large-scale demolition projects. Nonetheless, there is no official requirement that this documentation is submitted. These documents are however precious source of information about waste production (from source) and possible assessment for the entire building stock when comparing waste production with building typologies and construction year.

The overall evolution of waste streams shows that cement-based products have progressively substituted consumption of ceramic products. Internal walls, roof tiles and floor systems are the best cases that evolved from this substitution. Nonetheless, waste fractions are still evolving according to older fraction of the stock. A consistent database for ceramic-based products in C&D waste stream started in 2002 and its volume has slightly decreased in absolute numbers. Wood streams have drastically increased in the same period, while all metals can be considered as relatively stable since 2002; plastics presents a surprising continuous decline, which is a very small percentage from the current consumption rate. Total C&D waste production has increased from 1995 to 2009, stony fraction waste production has a very similar evolution. Housing demolition rates in the same period have increased in the same period, which coincides with the evolution of total C&D waste production and stony fraction waste production.

DISCUSSION

There are several benefits when integrating an accounting system in these three levels as described in this paper: the input of materials, the analyses of stock and output as waste production over time. It has been shown that it is possible to connect these scales (primary resource consumption to product) and evaluate which products are, or will be, critical to waste production and consequently treatment. This type of information can give feedback to product development, building design and waste treatment solutions that could better process certain waste flows. Such initiative of tracking materials from waste back to material consumption, product manufacture and back to waste production is part of a new trend seen in both recycling industry in the Netherlands and partially in small scale micro business deconstruction and recover of materials for retail previous recycling. Without such qualitative analyses fractions of waste that today are being incinerated or generally *downcycled* could be upgraded in the waste hierarchy as *upcycle* and reuse. In the Netherlands here is already an existent structure in the accounting national systems that could be improved in order to make this integration happen. Savings in data assessment as prevention measures may lead to future higher expenditures in repairing long term consequences both at the primary extraction

material level and at the waste production and treatment level. The case of quick and large scale implementation of incinerating plants around the country in the past showed that with lack of more detail information waste treatment solutions are leveled from the minimum standards while technology and consumer behavior evolves resulting in technological *lock-in* effects, or have to be long term support of outdated solutions instead of shifting to better ones.

The liberalization of the waste market should not hinder the legitimacy of a centralized national accounting system based on compulsory waste registration flows and reinforcement of measures that are today voluntary or "ungoverned".

CONCLUSION

The findings from this research concluded that there is already an existing structure in the Netherlands able to organize the information of construction and demolition waste production that can support integrated material metabolism bringing large advances in waste management and qualitative improvement of material consumption. Nonetheless, this structure is not yet effectively applied, the organization of the data is not easily comprehensive and the data sharing is not public available. Despite the progress made of waste flows accounting since 1995, towards standardization of accounting methods in the Netherlands and in Europe tracking material flows through codes and origin, there are still challenges in evaluating the development of waste production as constant changes occur in the classification of material flows, origin, and waste registration. In three different levels (input, stocks and output), an existent effective structure able to improve the evaluation of waste production was found that could directly support waste treatment improvements, environmental assessments extending to evaluation of product development and construction systems and the a review of the entire construction mechanism that is currently intertwined to the final material choices.

REFERENCES

1. de Bree, M. A.: Waste and Innovation. How waste companies and government can interact to stimulate innovation in the Dutch waste industry. Delft, 2005.
2. Symons Group Ltd.: Priority Waste Streams Programme. Project Group to the European Commission on the C&DW, 1999.
3. Koops, M.: Sloop en nieuwbouw in Nederlandse stadswijken; ontwikkelingen en effecten. Delft, 2005.
4. Koppert, H.: Environmental protection expenditures in the building industry Final report Statistics Netherlands
5. Hofstra, U.:Scenariostudie Bsa-Granulaten aanbod en afzet van 2005 tot 2025. Delft, 2006.

HOW TO GIVE AN ADDED VALUE TO URBAN ENERGY DATA: TWO COMPLEMENTARY APPROACHES

F. Roduit[1]; G. Blanc[2]; G. Cherix[3].

1: Project Manager, CREM, 1920 Martigny Switzerland

2: Project Manager, CREM, 1920 Martigny Switzerland

3: Director, CREM, 1920 Martigny Switzerland

ABSTRACT

Cities will play a major role to achieve the energy-climate objectives adopted by the European Union, and its member states. Many have adopted ambitious objectives and elaborate associated operational strategies: increasing energy efficiency, reducing CO2 emissions and increasing renewable energy production. The achievement of such objectives implies that cities dispose of reliable energy-climate data, ensuring that local authorities are able to control their energy consumptions and productions, thus able to develop concrete strategies, and measure the effect of the implementation of these strategies.

Two approaches of energy data collection and valorisation are presented, with two complementary aims consisting of urban energy flows monitoring and energy planning. In the first approach, we consider the city as a global and unique consumer. The data must be derived from actual and dynamic measurements, in order to benchmark with reliability the effect of actions undertaken by the city. Consumption data are aggregated by services and by sectors, and then plotted on a flow diagram incorporating energy conversion processes at the city-scale. In the second approach, we consider the city as a set of different consumers. Calculation of heat and electrical consumptions and needs of each territorial element such as building is made through the use of several statistical models. The potential of local renewable energy resources is determined based on resources availability, regulations and technological models. Geo-referencing all of these data provides a multi-scale vision of the energy situation. Furthermore, the simulation of several future scenarios allows to represent and to analyse the local energy situation with different temporalities.

The global approach of energy data collection and valorisation, aiming at "energy flow monitoring", has established a first draft of an urban energy information system called SIEU, while the multi-scale approach lead to the development of the PlanETer energy planning tool. The latter, designed for local decision-makers, has been tested in over 10 municipalities allowing us to complete and validate our method and scientific approach. The use of this tool has helped to launch major projects related to the energy supply and consumption of territories.

Keywords: Urban data management, energy flow monitoring, infrastructures and networks, synergies between consumptions and resources, regional energy strategy and planning, GIS tool.

INTRODUCTION

In order to define and implement most efficiently their energy policies, cities need to know the specific characteristics of their territory in terms of energy needs, consumptions, production and resources. This implies that they will have to collect a large amount of data, structure them and make them "available"; they will then feed tools that help decision making

through relevant indicators. Monitoring and planning tools represent two examples of such data valorisation. Since the objectives of these two later are clearly distinct, the methodological and technological approaches used to collect, process and represent data are also different. However, it is relevant to put these two data treatment approaches in parallel, not only to present their specificities, but also to identify points of convergence, with the perspective of developing global tools integrating the two approaches.

METHOD

Monitoring approach

Frameworks having already been suggested to represent urban energy flows [1, 2], the main challenge consists on making the monitoring reliable, in order to benchmark as accurately as possible the actions undertaken by municipalities; it is thus essential to dispose of multi-energy data based on current and dynamic measurements [3]. The objective is therefore to identify and implement the most appropriate approaches to obtain high quality data. It has been identified that the consumption data can be collected through multiple sources:

- Automated measurements at the final consumer level. These can be done by smart-meters (for electricity, gas and district heating consumption), sensors (for solar thermal consumption) and gauges (for fuel tank level).
- Import of existing databases. Actors that can provide local data consumption are variable: utilities (electricity, gas, district heating), oil and wood suppliers, companies specialized in the oil supply logistics for housing, local municipalities, departmental and national services.
- Recording and transmission of information by the final consumer, through occasional surveys (mail, phone, mail), online questionnaires, or energy social networks.
- Assessment of consumption, based on installed systems (boiler power, solar panel surfaces), through the identification of needs, or through the extrapolation of regional statistics.

The quality of these collection methods and of the data gathered is then analysed through performance criteria to select methods that best meet the specifications of the monitoring approach. These criteria are: the compatibility with the specific requirements of the approach (dynamic representation of the energy situation and evolution); the quality and reliability of methods, measurement systems and data collected; the methods and measurement systems implementation potential (simplicity and speed of implementation, acceptance, ...); the human and material costs.

Planning approach

The success of sustainable energy planning depends on the ability of local decision-makers to integrate a number of complex and dissociated elements which are exclusively dependent to the concerned territory. The main challenge is to bring these elements together giving decision-makers an overview focused on added-value in terms of energetic and sustainability aspects. Up until now, geographic information systems (gis) were mainly used to inventory and to evaluate the potential of renewable energy resources in specific case study [4, 5, 6]. With our approach of energy planning, the use of a geodatabase enables not only to evaluate local energy resources but also local energy demands and possible synergies between them. Our energy planning approach is based on the following steps:

- Evaluation and geo-referencing of local renewable energy resources potential mainly based on resources availability, regulations, technological models and existing energy network infrastructures.
- Calculation and geo-referencing of heat and electrical consumptions and needs of each building made through the use of several statistical models related to federal and regional building registers for household, industry and services. The statistical model is continuously updated with real values if available and provided by local energy distributors.
- Estimation and geo-referencing of future heat and electrical consumption depending on possible future scenarios mainly based on time horizon, rate of new or renovated building, stricter energy policies and climate objectives.
- Evaluation and geo-referencing of possible synergies between energy resources and demands at different geographical scale from the building itself to the city as a whole.
- Analyse and geo-referencing of technical and economic opportunities, which take in account the local synergies and constraints. Design of the energy system.

RESULTS AND DISCUSSION

Monitoring approach

This approach has resulted in a first draft of an urban energy information system, called SIEU. The first component of SIEU represents the energy production and consumption flow diagram, incorporating conversion processes at the city-scale. Consumption data are aggregated by services, such as electricity, heating / cooling and transport, and by sector, such as building, transport and industry. The second component contains sets of indicators representing the overall performance of the city as well as their evolution in terms of energy consumption, greenhouse gas emissions, and quality of supply. These energy indicators are furthermore complemented by the display of demographic, socio-economic and weather indicators. The data collection methods were evaluated according to their performance (reliability, quality, cost, etc). The results are summarized in figure 1. In this figure, the width of discs refers to the compatibility of the method with the specifications of SIEU, and the darkness represents the overall application potential considering the different criteria.

The main conclusions of the evaluation are the following, for the most relevant methods:

- Consumptions databases that already exist, belonging to utilities, municipalities or private companies, reveal a very high application potential for SIEU. However, if existing, they are not necessarily available or usable in the state: their use requires the establishment of strong multi-stakeholder collaborations, but also data mining operations to translate data into useful information.
- Telemetry based methods also have a strong potential for SIEU: high quality data can be obtained (frequency, accuracy, granularity) on actual consumption. However, both for economic and social acceptance reasons, these meters can hardly be deployed exclusively in the perspective of the establishment of a SIEU; the aim can therefore be to exploit meters installed by local actors (energy suppliers).
- Data collection through online questionnaires or energy social networks may be useful: data can be obtained quickly, easily, at low cost, and for specific consumption. This method enables to collect all data in the same format which no measurement systems allows (e.g. kerosene). However, the approach can only be used in support of the first two

approaches, since the data are of low quality (low frequency of update, risks of error) and the reliability of the approach, its implementation (acceptance) and long term use (the user could give up) are not guaranteed.

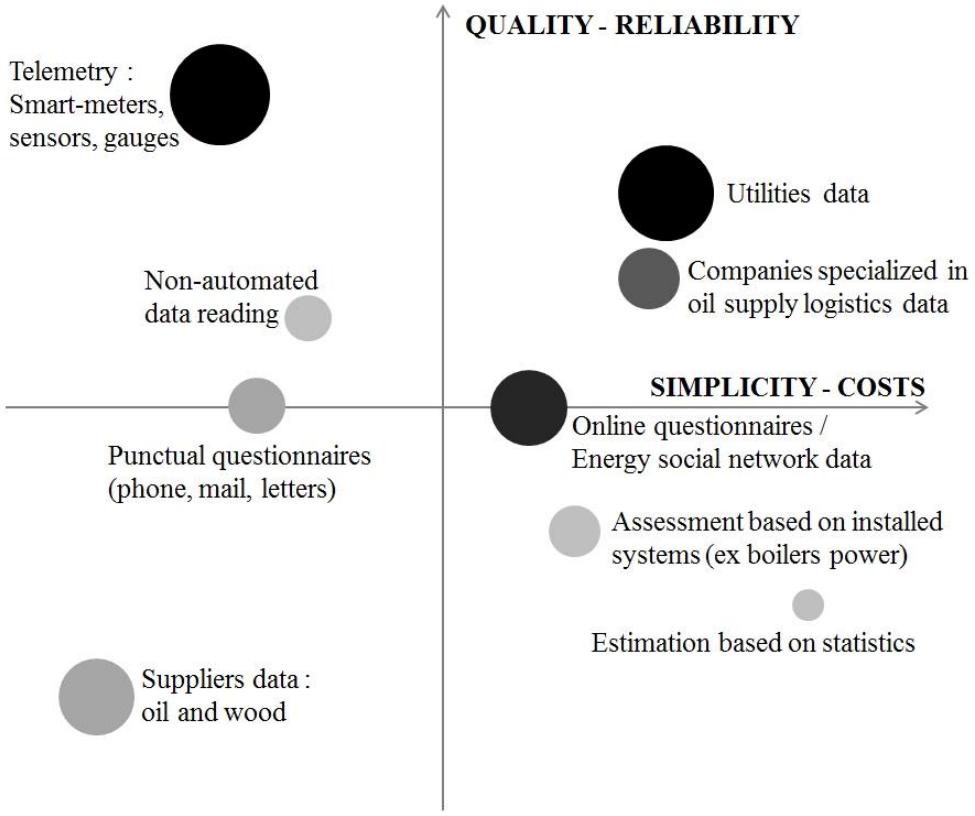

Figure 1: Evaluation of data collection methods

Planning approach

This approach as resulted in the development of a new GIS- tool for regional energy planning, called PlanETer. To give more accuracy to this planning approach, the developed GIS-tool was tested in more than 10 Swiss pilot cities. These cities differ from one to another by their size, their natural resources availability, and their energy need. This variety offers a solid background to develop and validate our methodology, which can be reproducible in other urban area. The developed geodatabase enable us to give detailed answers to their energy planning territory related questions. Is district heating an energy- and cost-effective solution for my region? Which buildings should be connected? What is the required temperature level? How many geothermal probes should I install, where and at which depth? What is the return of investment I could expect? The answers based on our GIS-tool were convincing and highly considered by local authorities. One example, amongst many others, is the launch by one of the pilot municipality of a 100% renewable district heating project.

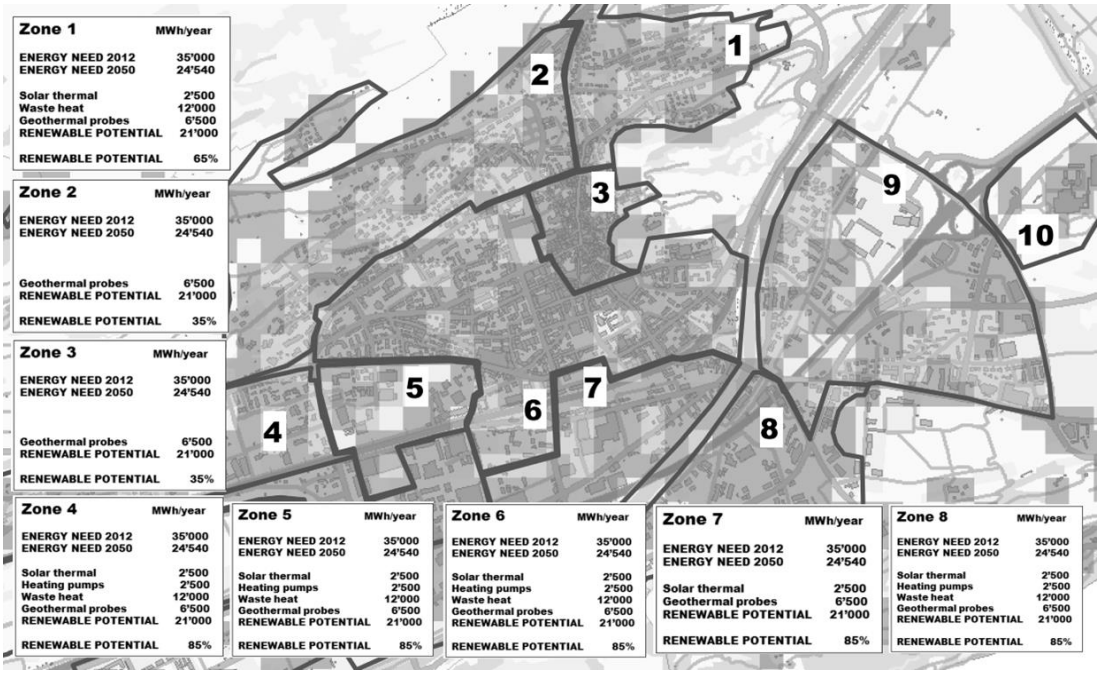

Fig. 2 : Synergies between energy resources and future energy needs on specific areas of a city with 30'000 inh.

CONCLUSION

Cities around the globe want to control their energy costs, to take advantage of their local energy resources, to reduce their carbon footprint. Since 2008, more than 4'000 European cities has set themselves ambitious goals by signing the Covenant of Mayors[1]. On one hand, it's an enormous difficulty for cities to get reliable, structured and sufficient energy data of their territory. On the other hand, energy management is driven and impacted by many local actors, such as municipalities, energy providers, consumers and urban planners. Furthermore, they all have different approaches and responsibilities on this common thematic, mainly based on their own professional competencies, abilities and specific objectives.

In this context, the challenge consists on the development of a unique and multifunctional information system, based on reliable and dynamic urban energy data, which enables all actors to reach their objectives but also to interact with each other's. Such a development requires an intense collaboration between the local actors, particularly in terms of data sharing. This implies to overcome information transfer barriers such as the problems of acceptance and protection of data. For this, economic and social gains leading to promote and sustain the exchange of data should be identified. From an economic perspective, new business models, especially based on the use of ICT infrastructure, must be found to enable stakeholders to generate mutual benefits through the sharing and valorisation of data. On the other hand, one should also integrate the final consumer in the development and operational stages of energy services, rather than leaving him at the end of the energy chain. The objective is to identify his real needs in terms of energy information and, on this basis, to establish an energy data sharing that would benefit to all.

The resulting multi-partners information system, fed by reliable and dynamic multi-energies data, will then be an appropriate tool leading to a more efficient energy management at the city level.

[1] Signatories of the Covenant of Mayors voluntarily commit to increase energy efficiency by 20% and the use of renewable energy sources by 20% and to reduce their CO_2 emissions by 20% on their territories by 2020.

REFERENCES

1. Chapuis A., Cherix G., Capezzali M., Püttgen H. B., Finger M.: A Conceptual Framework for Energy Planning and CO_2 Emission Counting in Urban Area. Proc. of the 9th Conference on Applied Infrastructure Research (INFRADAY), Berlin, 8-9 October 2010
2. Kim S. A., Shin D., Yoon C., Seibert T., Walz S. P.: Integrated energy monitoring and visualization system for Smart Green City development: Designing a spatial information integrated energy monitoring model in the context of massive data management on a web based platform. Automation in Construction, Vol 22, pp 51-59, March 2012
3. Keirstead J., Jennings M., Sivakumar A.: A review of urban energy system models: Approaches, challenges and opportunities. Renewable and Sustainable Energy Reviews, Vol 16, Issue 6, pp 3847-3866, August 2012
4. Van Hoesen, J., Letender S.: Evaluating potential renewable energy resources in Poultney, Vermont: A GIS-based approach to supporting rural community energy planning. Renewable Journal, Vol. 35, Is. 9, pp. 2114-2122, Sept 2010
5. Athanasios A-D., Biberacherb M., Dominguezc J.: Methods and tools to evaluate the availability of renewable energy sources. Renewable and Sustainable Energy Reviews, Vol. 15, Is. 2, pp. 1182-1200, Feb 2011
6. Piguet P., Blunier P., Lepage L., Mayer A., Ouzilou O.: A new energy and natural resources investigation method: Geneva case studies. Cities, Vol. 28, Is. 6, pp. 567-575, Dec 2011

THE MODEL OF THE RESILIENT CITY BETWEEN THE TRADITIONAL AND MODERN MODEL - THE WATER CYCLE

Giovanna Saporiti[1]; Carlos Girón[2]; Cynthia Echave[3]; Albert Cuchì[1].

1: Politecnico di Milano, Dip DAStU, via Bonardi 3 - 20133 Milano

2: Universitat Pompeu Fabra, Barcelona, Dip. Humanidades, Ramon Trias Fargas, 25-27 08005 Barcelona

3: Agencia de Ecologia Urbana de Barcelona, C. Escar 1, 3 · 08039 Barcelona

4: Universitat Politècnica de Catalunya, Dip. Construccions Arquitectòniques I, C. Pere Serra, 1-15, 08190 Sant Cugat del Vallès

ABSTRACT

The study is focused in the relationship between water and the urban form specifically in pre and post industrial Milan.

Resilience is not an absolute capacity of the ecosystem but a reply to a determinate traumatic event. It is linked to the city and to the lack or alteration of the flows that feed it. This means that it is necessary to model a resilient city.

Milan is the case study: its evolution from the traditional to the post-industrial model. The elements of crisis are deeped in the analysis of water cycle. It is not a casual choice because water is one of the fundamental elements in human life, one of the deepest matrixes of the human teachings. This character is recognized in the traditional model that is the one of a resilient city in full harmony with the surrounding environment. In this city water plays a decisive role. It is the element that shapes and structures the urban form -surface and groundwater. It is the key element for modelling the urban form and defining of the quality of the anthropized space. In the modern age, in the Western world, water was used as an element for aesthetic embellishment, not as a functional one.

Therefore, starting from the traditional urban layout related to its hydrography, the hypothesis is that there was an unsustainable change because of the industrial age. This is necessary to identify characters of urban resilience in order to evaluate the resilient level in the water cycle of the current city. This is made with the analysis of some strategies that have been already developed.

The case study is Milan that was named water city for its abundance of good quality water. The urban morphology evolution is based on the drinking water supply, how water is collected, as energy source and also as a nutrient for cultivated land.

Keywords: urban resilience, water cycle, urban morphology

INTRODUCTION

From the definition of urban resilience as «(...) the whole of adaptive capacities of a urban system when facing stress factors and particularly climatic change phenomena and energetic lack» (UNEP, 2005), a resilient neo-ecosystem is able to «absorb shocks and/or perturbation without suffering relevant alterations in its functional organization, in its structure and in the characteristics of its identity» (UNEP, 2005).

Therefore the concepts of resilience and sufficiency are tightly linked so we can understand which is the dimensional limit of the analysed neo-ecosystem. As a matter of fact, the important element of sufficiency is de capacity of using only the necessary quantity of elements so welfare is guaranteed for the individual and the territory he inhabits. As Sachs

says «meanwhile efficiency means doing things in the right way, sufficiency is equivalent to doing what is fair» (Sachs, 2007). The concept of sufficiency is linked with «the fair measure seen as an equal system and as the art of life» (Sachs, 2007) and also with a «new way of interacting with goods and services» (Sachs, 2007), this not only regarding the quantity and the efficiency of technology, but mostly the quality of life and the decrease of the charge in the natural capital. It is sure that the efficiency in the use of resources remains an essential element in the discussion, but this efficiency must be together with a sufficiency perspective regarding the natural and social capital.

This capacity, typical of the natural ecosystems and now lost in those that are man-made, can be focalized and discussed in the analysis of the relationship between water and the urban form, most of all if it is analysed in the relations between the pre and post industrial model and the elements that led to the crisis of the traditional model.

Water is a main element of the urban metabolism not only as part of the essential properties for the survivorship of humans and vegetables, but as a critical element for the metabolism of the city influencing in as source of energy and as vital nutrient. Is this way water has been always a fundamental vector of modelling and balance of the urban form.

METHOD

Milan and the crisis of the traditional model

Milan is located in the middle of a plain and it is very rich from the hydrographical point of view because of the abundant ground water and also for the proximity to numerous rivers that arrive from the Alps to the Po Valley. The pre-industrial Milan, as a matter of fact, profited from good quality water supplying without too much complications. Almost every block had a well, private or public, that warrantied the access to a high quantity of **potable water** even for domestic use. The potable water public fountains arrived later to the city. The first one is located in Fontana Square, built by Piermarini in the second half of the 700 century with the same supplying system of the public and private wells that already existed.

Rainwater helps to preserve the nutritional balance of the cultivated land. The first works of sewerage are from the imperial era. The emissary channel of the network followed the course of what today is Torino Street ending in the Carrobbio. With the dawn of the Roman Empire we have to wait until the end of the Middle Age to see how channelling sewage projects were resumed, but not as organic and efficient as the roman ones. This was caused by the absence of a general plan that led to the realization of conducts that tried to solve the contingent and specific problems of every single street for then carrying the water to the antique defence channels: Seveso and the intern pit. In any way this conducts were only used for meteorological water. The “problem” of the disposal of black water and the use of organic wastes and excrements for agriculture was easily resolved. In fact, from the first roman expansion, the city was equipped with a lot of channels and pits realized for transportation, defence, agriculture, sewage water and, later un time, for the production of energy. Some of them drew the water from near rivers (Seveso and Olona mainly), other ones from the naviglio of the Martesana that entered Milan form north and, as the name of intern Fossa, flowed along most part of the urban perimeter. In its way collected the private and public discharges delivering them later in the Vettabbia channel that was uncovered. The houses nearby the channels had to build the underground discharge conducts for wastewater and latrines mandatorily; meanwhile in the intern zones without looking out the channels had a black wells system.

The morphology and hydrography of the Lombard territory facilitated the creation of mills so that they could profit water **energy**. As a matter of fact, in the Middle Age we can find numerous mills in the Lombard territory that were a fantastic instrument of control for the

authorities upon surrounding territories. However the apex of development of the mill activity is dated in the XVII century.

Post-industrial Milan

With the Industrial Revolution the water demand grows exponentially and so it does the pollution of this good. The population in the 1881 census was 321.000 habitants. That's why the city was forced to take actions as the construction of the sewerage network and one aqueduct.

The potable water supplying changed radically with the Industrial Revolution not only because of the quantity needed, but also because of the demand of a hygienic control substantially diverse. The choice was to build deeper wells that reached the groundwater in order to warrantee the purity and sanity of the **drinking water**. At the beginning of 1889 the first pumping plant was built –called Arena– and it started its service at the end of the same year. To regularize the water delivery pressure two great storage tanks were build in proportion: one of steal in 1893 and the second one in 1903 of reinforced concrete. These ones were placed inside the towers of the Sforzesco castell. The success of this system determined the technical setting of Milan's aqueduct.

As for the draining of **meteorological water** it was until 1868 when the first real project of modern sewerage was presented in the town council. This one included a widespread network, but an unorganized one, of 123 channels partially covered and partially uncovered with a longitude of 153 km. A "mixed system" is adopted that collected in a unique conduct the meteorological waters and the wastewaters. In 1884, with the expansion of the Beruto plan, it was possible to deal with the problem of the sewer network in a more organic way in the expansion areas. The new network of conducts, that choses the "mixed system" anyway, was determined by the morphological structure of the city and led with his evolution to the formation of a system "in terraces". Therefore, there were done concentric zones related to the central core of the city in decreasing proportion and served each one with its own and autonomous collector located in the intern zone (diagram). In this expansive phase they bet again for the biologic natural depuration of the campaigns irrigated south of the city. Only in 2001 they were realized three poles of depuration (San Rocco, Nosedo and Peschiera Borromeo).

The Industrial Revolution involved a radical change in the relationship between water and **energy**. As we already said water is energy, the cycle of water, in deed, allows us to maintain biotic balance saving a lot of energy. In particular, with the introduction of coal and new machines that made the development process more efficient and fast, Milan at the end of 1800 decides to build the first thermoelectric central in Europe. Italy, generally speaking, is a country with a lack of fossil fuels so the technicians of the Italian Society of Electricity, in 1884 when it was born, decided to push the studies related to the hydroelectric production of energy. From that moment in Lombardy will continue in that direction. The number of centrals built continues to grow specially during the wars that did not allowed the coal importation. Between 1966 and 1967 the hydroelectric energy covers almost the 50% of the national requirements.

The crucial element of this change was the conviction that one city with such water wealth in the underground and in the surrounding territory could not do anything else that profiting the new technologies and the new materials available for industrial development, for creating a modern image, that wants to disclaim its evolution as city of water. The element of the crisis resides in the same objective that has persecuted, and stills do, the post-industrial city: the idea of a development that today only adds the adjective sustainable creating a profound antithesis.

What do we understand indeed as (un)sustainable development? What is development and what does it entails? To answer these questions is helpful to reed a passage from *Scritti corsari* that seems that was written today and give us light about some contradictions.

«There are two words that frequently come back in our conversations: on the contrary, they are the keywords of our speeches. These two words are "development" and "progress". Are they synonyms? Or, if they aren't synonyms, do they indicate two different moments of the same phenomenon? Or do they indicate two different phenomena that are integrate with each other? Or, even, do they suggest two only partially similar and synchronic phenomena? Finally, do they indicate two phenomena that are opposed between them and which only appear to coincide and complement themselves» (Siti, 1999). In fact Pier Paolo Pasolini specifies that «the progress is an ideal (social and political) notion but the development is a pragmatic and economic fact» (Siti, 1999).

Starting with this definition, the sustainable model that is called to solve the post-industrial crisis, is only partially effective. In fact, to manage a change of the model, it is necessary to consider the transmission of natural capital. It is feasible introducing the possibility of losing natural resources but acquiring the ability to compensate with other one that has the same function.

«(…) A self-sufficient system that is truly homogeneous and where the climatic fluctuations are reasonably limited, a complex adaptive system» (Holling, 73) is a model that can be opposed to neo-ecosystems contemporaries model. It is a dynamic, sensitive to external changes and unexpected changes system and it is focused on the connections between them, and between the species of the system and the external environment with the specific components of the system.

RESULTS

A resilient neo-ecosystem «tents to keep an integrity of functions during a impairment» (Common, Stagl, 2008). This resilient system is able to work with species that modify its function or replace some of other one. This means that a resilient system can be composed of species that tend to zero during the shock and return to a normal activity after waiting a time. Therefore resilience is a system property and not a property of its components.

The resilient capacity depends on the shock and on the evaluation of the primary productivity of the system and the recovery time.

Major threats of the urban neo-ecosystem			
Climate change		**Welfare state**	
Scope of impact	**Threat**	**Scope of impact**	**Threat**
Energetic model Water management model Material management model	Resource depletion because of greenhouse	Equipment Home	Provision of basic services low (education, health, home)
Territorial occupancy model Biodiversity Species protection	Biodiversity loss	Public space Urban mobility	Loss of urban space quality
		Activities Population Economy Participation	Low social cohesion

Table 1: Relation between threats of neo-ecosystem and impacts.

The second step is to specify the elements of urban resilience that depend on its scope of impact respect water cycle. It emphasizes that water cycle is linked to the urban metabolism, the territory occupancy, the biodiversity, the urban form and space and welfare.

Urban neo-ecosystem components	Elements of the resilience linked to the climate change	Elements of the resilience linked to the welfare state
Physic structure	Adapting to a model of efficiency and passive capacity of the urban form (buildings and open space)	Ecological urban planning
Processes	Measures to improve the efficiency of the urban metabolism	Ability to self organization (social and economy activities)
	Dematerialization of the resource management	
	Urban biodiversity conservation	
Society	Awareness Reduced demands	Habitability of urban space Awareness Individual's relationship with the (rural and urban) environment

Table 2: synthesis of the resilient elements

Therefore, a resilient system has three basic features: diversity of the elements of neo-ecosystem, modularity and feedback capacity.

A resilient system is, in fact, characterized by a diversity of elements capable of reacting in different ways to different challenges. Overall, ecologists think that the diversity of elements in the resilient system is key because a complex ecosystem has a proper number of species and connexions of the food chain. Complexity does not depend only on the stability of the system. In fact, as Common and Stagl explain, if a shock impacts the key specie, it is not always a loss of resilience. For example, if the function of the key specie x is to disseminate seeds, the system can be composed by other species able to do the same function. This means that a system with another specie able to do this function may react to the shock without collapsing. Its starting organization can change and continue to work, although not without modifying itself.

It is modular because the components of the group are well connected to each other inside and they can create a community able to isolate themselves during a shock. The modularity is a typical feature of computer networks. It evaluates the network division into modules (community). A module works independently from the contribution of the others modules. Increasing modularity, therefore, the collaboration between the different modules is stimulated, but the dependency between them is eliminated. Finally, a resilient system is characterized by a good feedback. It is the ability to store the obtained results and uses them to modify the characteristics of the system. It involves the cause-effect chain and allows the system to perceive the consequences of their actions in a short time and so it is able to activate a solution.

The feedback capacity brings out the fundamental problem of our times: globalization and the loss of an overview at a global scale able to evaluate our territory and to keep it productive. Speaking about the water cycle, the productivity challenge of the surrounding area is closely linked to modern sewerage system. From on side the organic matter can be used as fertilizer and from the other one urban rainwater can runoff and carry nutrients to farmland. Therefore it would be necessary to specify at a neighbourhood scale to recover and use these nutritional elements. It allows rediscovering the use of underground water and sewerage system to improve the permeability of urban areas, because water can be functional to the process described.

Finally, the modularity is directly linked with the concept of dimensional limit, explained above. We cannot think to look for effective solutions only for small cities that maintain an

important link with the countryside or important waterways. Therefore this approach attempts to work at a neighbourhood scale to redefine the urban form so that green and water are not only a decorative supplement that needs constant and expensive maintenance, but elements that shape this change.

DISCUSSION

The traditional model is the one of resilient neo-ecosystem and it cannot be reproduced in the contemporary model because of its technological, social and economic changes. Therefore a comparative analysis between the urban morphology of the modern city and traditional city is required to define and evaluate the elements of resilience and to propose improvement strategies of water cycle at the urban scale.

The resilient concept is connected to the *ascendenza* (Ulanowicz 1986) that is a quantitative attribute of the ecosystem and, especially, a natural condition of it. It is the product of two elements: the information contained in ecological network and the data transmitted by the system. It includes the evaluation of the complexity of the elements of the system and its relations with environment. The interesting thing in the approach of Ulanowicz is the focus on the system organization and dimension. So each system can grow without limits. Its limit is the self organization habitat that is able not to «make difficult but rather facilitate food production, water supply, climate protection, protection of private and collective property organization of social relations and aesthetic satisfaction of each one» (Friedman 2009).

This definition of habitat by Friedman is based on the idea of «critical group» (Friedman 2009). It is connected to capacities, biologically determined by man, for wich «each structure of a group has a limited size (…) able to react fast to attacks from outside» (Friedman 2009).

Therefore the concept of physic limit of an urban sprawl is reflected in some problems of the urban grow of Milan. Surely the modern city exceeded this limit because it has created a clear separation between the city and its territory. Therefore, speaking about the diversity of components, it is important to implement and protect the variety of sources of supply abundant in the city and that we discussed above.

The first one is rainwater, its collection, its ability to transport and channel organic matter and nutrients, not only to the countryside -now too far away from the urban centre- but also to the parks and brownfield sites. They can be converted into gardens or green areas that can be a link between the built-up and the surrounding area.

The second one is the channels network that can be used for transporting materials and nutrients and that, with water sources inside the city and green spaces, can help to mitigate the urban microclimate, especially in the summer.

And finally the *fontanili* can contribute to the drainage and agricultural development of the Lombardy territory. Furthermore they can be used to produce energy, using the many mills in Lombardy or the hydroelectric power plants.

REFERENCES

1. Bovesin de la Riva De magnalibus Mediolani, Libri Scheiwiller, Milano.
2. Basilico G., Negri G., Sandri M.: Architettura d'acqua per la bonifica e l'irrigazione, Electa, Milano, 1990.
3. Common M., Stagl s.: Introducción a la Economía Ecológica, Barcelona, Editorial Reverté, S.A., 2008.
4. Friedman Y.: , Torino, Bollati Boringhieri Editore s.r.l., 2009.
5. Holling, C.: Resiliente and stability of ecological systems. Annual Rewievs , 1973.
6. Magnaghi, A.: Il progetto locale, Torino, Bollati Boringhieri Editore s.r.l., 2010.
7. Malara E.: Mikano città porto. Origin difensiva e trasformazione funzionale del naviglio interno, Mediaset, 1996
8. Odum, E. P.: Basi di ecología, (L. Nobile, Trad.) Padova, Piccin Nuova Librería, 1988.
9. Sachs, A.C. & Santarius, T.: Per un futuro equo. Conflitti sulle risorse e giustizia globale. Milano, Feltrinelli, 2007
10. Sporcinelli A.: Storia sociale dell'acqua, Mondadori, Milano, 1998.
11. UNEP: Climate change. The role of the cities. Nairobi, 2005.

THE SMART NODE: A SOCIAL URBAN NETWORK AS A CONCEPT FOR SMART CITIES OF TOMORROW

A. Scognamiglio[1]; M. Annunziato[2]; R. Cosenza[3]; R. Germano[3]; G. A. Lagnese[3]; C. Meloni[2]

1: ENEA, UTTP FOTO, largo Enrico Fermi 1, 80055 Portici, Italy

2: ENEA, UTTEI, Casaccia, via Anguillarese 301, 00123 Santa Maria di Galeria, Italy

3: 4M Engineering, via Ilioneo 25, 80124 Napoli, Italy

ABSTRACT

Smart Cities are a very important topic that researchers, politicians and planners are facing nowadays. Due to the necessary multidisciplinary approach, still today the smart city definition is not univocally given, and this gives us food for thinking.

What is a smart city in reality, and how can the concepts that it implies transform into benefits for the social life of a city community? To answer these questions ENEA is participating in several research programs. Among these, the European Energy Research Alliance (EERA) - Joint Program Smart Cities that was launched in 2011, which investigates the highly complex structure of a future smart energy system on an urban level by applying innovative solutions in an interdisciplinary manner based on a clear long-term research strategy. Furthermore, in the framework of a national funding program (City 2.0) ENEA is experimenting at the scale of a medium town with the development of a proper model of smart city, which focuses on the social dimension.

An interdisciplinary team (researchers, architects and engineers) is working on the design of what we call a *Social Urban Network* (SUN), which will find an iconic tangible expression (the contact point between the community and the city) in an interactive micro-architecture named *Smart Node*. The *SUN* is a co-ordinated system of interventions that develops both in the digital scene (web, social network, etc.) and in the real scene (interactive installation, social events). The aim is enhancing the development and wholeness of the social capital (the stock of competencies, knowledge, social and personality attributes, including creativity, embodied in the ability to perform labor so as to produce economic value) of the social network of the community. If in general a *SUN* might focus on several topics (welfare, health, relationship between the citizen and the public administration, etc.), the one ENEA is developing focuses on *cultural processes*. The *Smart Node* is an iconic and technological object, with a dimension that encompasses both city elements and people (micro-architecture), able to represent the idea of connectivity for people. In particular, by being a space where people can meet each other, and integrating interactive output and interaction devices such as touch screens, beams, and other interactive technologies, it will represent for people a node where information can be shared and exchanged. This way, the social capital of the city can thrive thanks to the possibility of introducing creative contents and sharing them with the community.

The ambition of the project is placing the first prototype of the *Smart Node* in L'Aquila, a city whose historical centre was greatly destroyed by an earthquake in 2009, to help city and citizens to re-set up a common sense of identity.

Keywords: smart city, smart community, interactive architecture

INTRODUCTION AND APPROACH

In order to experiment with Smart City concepts and models, ENEA decided to work on a specific reality in Italy, L'Aquila, where the need of improving the "city performance" is very high, due to a natural catastrophe occurred in 2009.

L'Aquila is a medium size town (about 66000 inhabitants), located in the region Abruzzi (Central Italy). Famous in the past thanks to its architectural and historical heritage, the city historical city centre was widely destroyed by an earthquake in 2009. Since that date many buildings have been secured by means of scaffoldings and several different kinds of structure. To preserve the citizens security, the inner part of the historical city centre has been designated a so-called "red zone", where the access is not allowed (Figure 1). People who used to live in the city centre have been living in "new towns" placed out of the inner city for five years now, with a consequent progressive loss of identity of the city itself .

Figure 1: Historical city centre of L'Aquila before and after the 2009 earthquake

This condition of "emptiness" of the city centre has several implications on the relationship between the citizens and the city. Some of them are ascribable to concrete evidence of a discomfort (e. g. difficult or impossible accessibility of private and public buildings), some others are more ascribable to a social dimension (e. g. lack of a "centre" where it is possible to have a social life). Despite the works in progress, it is unlikely that a kind of "new L'Aquila", preserving its traditional and strong identity, can be built in the near to medium term. The "suspended", "uncertain" condition in which the city is today seems to be more permanent than temporary, and looks like an image for the psychological condition of the citizens themselves.

All these premises seem to suggest that L'Aquila can be a good domain where to experiment with Smart City concepts, just because there is an urgency to re-build not only the functional city, but also the sense of the city itself. In such a situation, any reconstruction, to be "sustainable" should take into account the buildings, but, also, services for citizens, the social wholeness and the cultural heritage preservation.

In order to structure a possible reference model that the reconstruction might follow, ENEA is experimenting with a *Smart Ring*, a specific application of the Smart City.

The *Smart Ring* is conceived as the main core of the Smart City, a connection point of both utilities and citizens. It is a system of different interventions related to the integration of urban networks, controlled and managed by a centralized City Control Room, where all the data coming from the city's monitoring system are collected. The single interventions that have been conceived and are under construction/development are coherent with the *Historical City Centre Reconstruction Plan*, approved by the Municipality of L'Aquila. In particular: public mobility and info-mobility; intelligent public lighting; buildings energy diagnostics and analysis; environmental monitoring; last but non least, a *Social Urban Network.*

THE SOCIAL URBAN NETWORK AS A POSSIBLE MODEL OF DEVELOPMENT FOR A SMART CITY

The *SUN* is an experiment with a Smart Community aimed to strengthen the sense of wholeness through the collective production of contributes related to the cultural heritage and to the cultural processes of the city. The general goals of the project are: enhancing the social capital of the community in L'Aquila; moving the society from a digital dimension to a hybrid/physical one; overcoming the social dismemberment due to the effects of the earthquake; re-building a cultural identity, by bridging over the past and the future; contributing to re-build the city from the social capital.

To enrich and to build-up the cultural processes we focused on two main aspects: strengthening the identity of the community (history, memory, cultural material heritage and immaterial identity heritage); supporting the creative act as a continuous element of construction of the cultural heritage, as well as having an impact on the social sharing and wholeness. Having set these premises, the SUN can be seen as an aggregator of experiences, and as an incubator of the social processes that take place in the city, aimed to strengthen the social wholeness.

From a methodological point of view, the structure of the SUN is articulated in several tools, performing different functions (Figure 2).

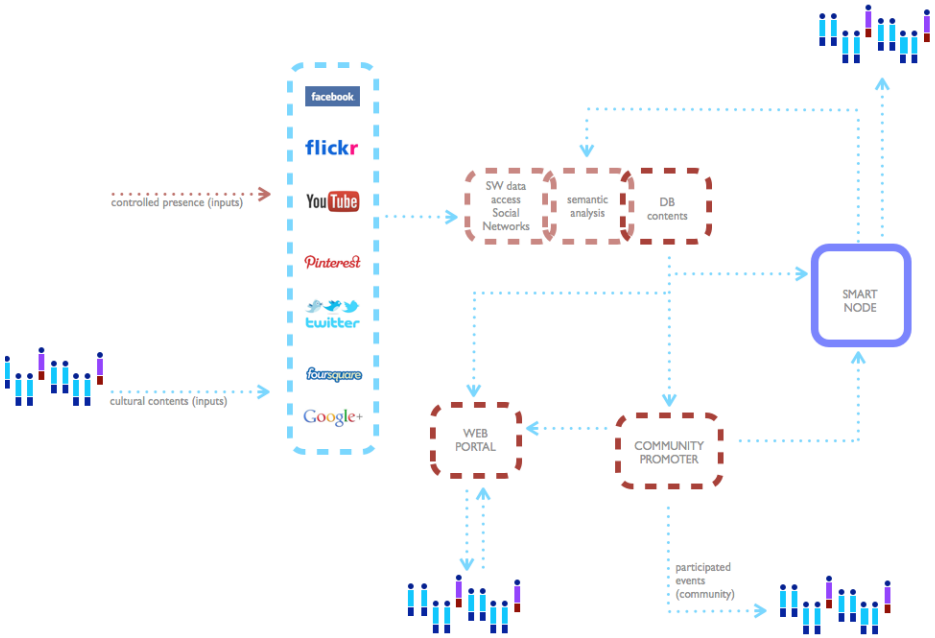

Figure 2: The Social Urban Network (SUN) functional structure

The first tool of the SUN is the Social Network. We will ensure a structured presence on the main social networks where citizens insert cultural contents.

The second tool works on the cultural contents collected in the social networks. After a contents analysis done by means of a semantic analysis system, the cultural contents are classified and stored in a "contents database". The semantic analysis system selects indicators related to the social exchange that happens in the social networks, with regard to cultural heritage, creative contents, the community experience and membership, emotional states (emotional city, discomfort, etc.). These indicators will be built up on the social network

model (web theory), and from them the attempt is trying to characterise a possible evolution of the connectivity features (intensity of connections, web model, possible presence of hubs on specific topics).

Some of the indicators will be visualised on a web portal. The web portal helps in explaining and showing the content of the project, in creating galleries of creative contributes; in sharing a kind of picture of the community, based on the most communicative indicators of the semantic analysis. The main aim of the web portal is, therefore, showing a structured representation of the city of L'Aquila.

The whole system of the SUN is supervised by a Community Promoter (CP), a person who is very much familiar with the city of L'Aquila (may be from cultural city associations). The CP is the entertainer of the Social Network and of the cultural processes; at the same time the CP can manage information coming from the database, both easing and filtering actions. The contents will be managed so as to work as inputs for the web portal and/or for the *Smart Node*, being presented to the public through output tools (e. g. videos, projections, etc.). The CP can also organize events for the community to focus on the most interesting contents proposed by the community.

The whole project has a physical representation in the shape of a *Smart Node*. It is an interactive micro-architecture that works as a kind of window for sharing creative contents collected in the database, as well as some contents that can be chosen either by the CP or by the community itself (the citizens can vote their favourite contents). More creative contents sent by the semantic database could be shown in the *Smart Node*.

THE SMART NODE

The Smart Node is shaped in the form of three different spatial domains, made out of three identically sized tube-shaped cells, named "tubes". They are arranged around a central void, so as to be placed at the same distance from each other; the whole system can be seen as made out of three tubes, connected by means of an open air space (Figure 3).

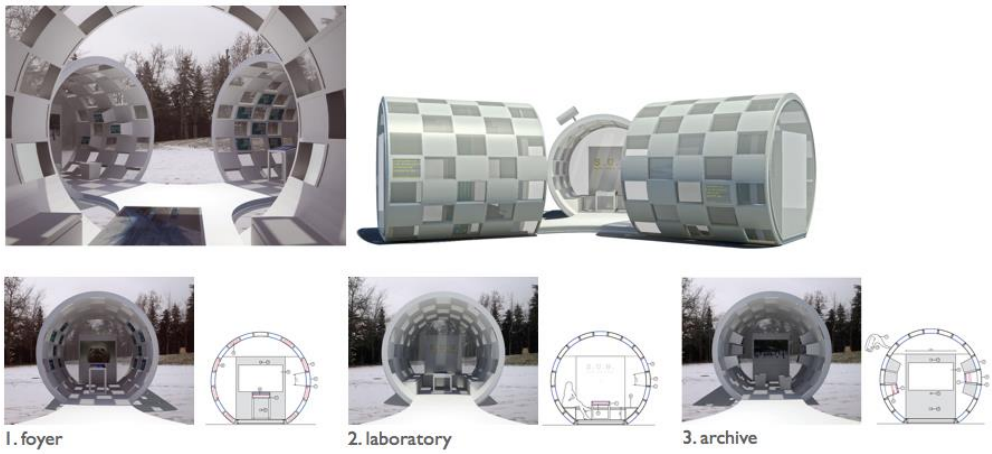

Figure 3: The Smart Node. The main parts (cells) are: an open air space; a foyer, a laboratory, an archive.

The three tubes perform different functions. The first one, the *foyer*, is a welcoming space, where people can meet each other, getting informed on the cultural processes of the city and sharing information. It is a kind of home page of the system SUN, that shows its contents,

aims, and approach. The second one, the *laboratory*, is a space devoted to creating and elaborating proper contents (e. g. videos, pictures, installations, etc.). Here people can go and insert the contents that the CP will analyse and, if indicated, promote and share with the community, either by means of the web or/and by the output devices of the Smart Node. The third tube, the *archive,* is the space devoted to collecting materials that people can access.

The *open air space*, in between the three tubes, plays a communicative role as well as the other parts of the system, since on its skin, thanks to visualization devices, there are traces of not-filtered activities coming from the social networks (e. g. tweets).

More in detail, the tubes are equipped with different technological system and furniture; the approach to the use of technology is primordial and playful at the same time.

In the *foyer*, a continuos seat along the wall welcomes the visitor/s, who can watch the display on the wall, which visualizes information, or can interact with the touch screen integrated into the small table in the centre. This touch screen is the interface for accessing the information on the SUN and on the cultural processes of the city.

In the *laboratory* some interactive monitors hang over the walls. On the deep end wall there is a space with an interactive board. Touch screen monitors connected to computers are integrated in the circular wall as well. They are available for those performative activities that do not require a big display (such as writings or audio recordings). Here, in the laboratory, it is supposed that people enter one by one, or in small groups, so as to perform a creative activity with a certain degree of intimacy. Audio-video materials, as well as graphic-painting digital works can be produced and recorded here, thanks to the technological equipment of the room. Appropriate software will be available for the public to help in their creative interactive actions. All the contents created, elaborated and recorded here, are sent to the CP, who selects the ones suitable to be showed and shared with the community through the web portal or the smart node itself.

The *archive* is the space where all the materials that the SUN produces are collected and preserved, to be accessible to the public. Close to the entrance there is a bookstand that integrates an interactive monitor, from which it is possible to control and to select the outputs of the other monitors integrated in the deep end wall and into the circular walls.

The outdoor space is a communicative/exhibitive space itself. In the external skin of each single tube there are LEDs displays that visualize messages coming from the social networks, from the web community, or from the SUN. A beamer, placed upon one of the tubes, can project images on the walls of the surrounding buildings, or on the ground. The idea is that the creative contents that people insert in the smart node can be shared with the community through the smart node itself. This kind of functioning enables a physical relationship between the digital city and the real one. The Smart Node is a small architecture that people can use, and a technological device at the same time, that can collect inputs from the community and give them back to the community as cultural contents after a controlled process managed in the framework of the SUN. Sensors and webcams placed on the Smart Node, work as security devices and support interactive actions in the community: for instance sounds, lights, images, can be produced by the smart node when someone is stepping close to it.

PRELIMINARY RESULTS AND CONCLUSIONS

A multidisciplinary team has been working on a proposal for the development of a real experience of smart city, to help a city almost destroyed by an earthquake to re-build its social identity and to enhance its social capital.

Together with ENEA researchers, architects and engineers have been working on the Smart Node design (4M Engineering). At the same time an analysis of the social networks has been carried out by a group of researchers in Clinic Psychology (University of Chieti) to understand how to design the SUN so as to enhance the social capital of the city of L'Aquila. Researchers and professionals experienced in the field of social media (the Vortex) have been working to understand how the SUN had to work in order to enhance the cultural processes. We consider the experience we made as a good starting point for experimenting with smart citiy concepts, that very often suffer from different disciplinary approaches as well as from the use of different languages. The development of the SUN, and of the Smart Node are occasions to verify possible trans-disciplinary approaches to smart city.

We consider the experimentation in L'Aquila as a validation of our approach and tools. In particular we would like to verify that both the technological and methodological tools are appropriate for the project goals; the tools we develop are appropriate to be used correctly by the social operators; the project is effective in terms of citizens involvement (quality and level), and its effects on the social network.

Right now the project of the SUN, and the project of the Smart Node are completed, and we are discussing with local administrators to better understand how to realize them in reality in L'Aquila.

REFERENCES

1. http://www.eera-set.eu/index.php?index=30 (accessed 22/04/2013).
2. Giffinger, R., Kraman, H., Fertner, C., Kalasek, R., Pichler-Milanovic, N., & Meiers, E.: Smart cities - Ranking of European medium-sized cities, Vienna, Centre of Regional Science, 2008
3. Hollands, R., G., Will the real smart city please, stand up?, City, 12 (3).
4. Putnam R: The prosperous community: social capital and public life, The American Prospect, 13 (1995), 65-78, 1993.

AUTHOR INDEX

AUTHOR INDEX

E

F

G

H

N

O

P

Q

R

S

T

V

W

X

Y

Z

ACKNOWLEDGEMENTS

CISBAT 2013 would not have been possible without the efficient contribution of the secretariat of the Solar Energy and Building Physics Laboratory as well as that of our scientific and technical staff.

Our scientific partners from Cambridge University and the Massachusetts Institute of Technology as well as the members of the international scientific committee and the session chairs have enthusiastically supported the conference and ensured its quality. We would like to express our sincere thanks for the time and effort they have spent to make it a success.

CISBAT can only exist thanks to the patronage of the Swiss Federal Office of Energy. We are grateful for their continuing support.

We also owe sincere thanks to the Zeno Karl Schindler Foundation, whose financial support was vital for the conference.

Finally, we cordially thank all speakers, authors and participants who have brought CISBAT 2013 to life.

Prof. Dr J.-L. Scartezzini

Chairman of CISBAT 2013

Head of EPFL Solar Energy and Building Physics Laboratory